D1,2 - 10400

Труды XVIII Международной конференции по физике высоких энергий

Тбилиси, июль 1976 г.

ТОМ I

VOL. I

Proceedings of the XVIII International Conference on High Energy Physics

Tbilisi, July 1976

Dubna 1977

QC 770
.IN83
1976
V.1

Advisory Committee

N.N.Bogolubov
M.Conversi
H.Falk-Vairant
E.Goldwasser
B.P.Gregory
H.Harari
V.D.Kupradze
E.K.Kharadze
F.E.Low
M.A.Markov
W.Paul
L.D.Soloviev
G.H.Stafford
Gyo Takeda
A.N.Tavkhelidze
I.N.Vekua
A.K.Wroblewski

Organizing Committee

N.N.Bogolubov - Chairman
V.P.Dzhelepov - Vice-Chairman
A.N.Tavkhelidze - Vice-Chairman
V.G.Kadyshevsky - Scientific Secretary

N.S.Amaglobeli
E.L.Andronikashvili
A.Ts.Amatuni
A.M.Baldin
D.I.Blokhintsev
G.A.Chilashvili
O.I.Chkhikvishvili
I.V.Chuvilo
E.L.Feinberg
O.I.Kavtiashvili
V.N.Kachibaya
V.F.Kuleshov
M.A.Markov
E.M.Nikitin
B.M.Pontecorvo
R.G.Salukvadze
A.N.Skrinsky
L.D.Soloviev
O.I.Sumbaev
I.G.Timerbulatov
A.A.Vasiliev
V.A.Vasiliev
D.V.Volkov
V.A.Yarba
G.P.Zedginidze

The Editorial Board

N.N.Bogolubov
V.P.Dzhelepov
V.G.Kadyshevsky
G.I.Kolerov
V.R.Sarantseva
A.N.Sissakian
A.N.Tavkhelidze
V.I.Zhuravlev

I.I. 8568 6.10.77 8 52 руб Ub/4 me

FOREWORD

The XVIII International Conference on High Energy Physics was held at Tbilisi State University, Tbilisi, USSR, from 15 to 21 July 1976. The Conference was organized by the USSR Academy of Sciences, the USSR State Committee for Utilization of Atomic Energy, and the Academy of Sciences of the Georgian Soviet Socialist Republic under the sponsorship of the International Union of Pure and Applied Physics and with the active participation of the Joint Institute for Nuclear Research and Tbilisi State University.

Over 1200 papers which covered almost all major themes in high energy physics were submitted to the Conference. The full list of contributions as well as the list of participants are given in the end of the second volume of these Proceedings.

The contributions presented at the Conference were summarized with the help of discussion leaders in mini-reports and invited talks given at 24 parallel sessions. The most principal topics were reviewed by rapporteurs at 15 plenary sessions. The main aim of such an organization was to create a representation of the elementary particle physics development in the period after the London Conference.

The Organizing Committee has recommended to include into Proceedings all rapporteur's, mini-reports and invited talks that had been received by December 15 1976. The Table of Contents is given at the beginning of each volume. The Editorial Board was aimed to make the Proceedings available within a short time following the Conference. Therefore the collection is printed by direct reproduction from the original typescripts and we apologize to authors and readers for any errors.

It is a pleasure for the Editorial Board to thank all discussion leaders, speakers and scientific secretaries whose cooperation in preparing these Proceedings had made it possible.

Joint Institute for Nuclear Research,
Dubna, December 1976

The Editorial Board

Contents of vol. I

PAGE

SECTIONS A

DETAILED CONTENTS V

A1. PARALLEL SESSION ON BINARY AND LOW MULTIPLICITY REACTIONS A1-1
Discussion Leaders: V.A.Tsarev and S.V.Mukhin

PLENARY REPORT ON BINARY AND LOW MULTIPLICITY REACTIONS A1-27
A.B.Kaidalov

A2. PARALLEL SESSION ON MULTI-PARTICLE PRODUCTION AND INCLUSIVE REACTIONS A2-1
Discussion Leaders: Yu.A.Budagov and V.I.Savrin

PLENARY REPORT ON MULTI-PARTICLE AND INCLUSIVE REACTIONS A2-42
P.V.Chliapnikov

A3. PARALLEL SESSION ON MECHANISMS OF MULTI-PARTICLE PRODUCTION PROCESSES A3-1
Discussion Leaders: N.S.Amaglobeli and A.N.Sissakian

PLENARY REPORT ON MECHANISMS OF MULTIPLE PRODUCTION PROCESSES A3-31
I.M.Dremin

A4. PARALLEL SESSION ON LARGE TRANSVERSE MOMENTUM PHENOMENA A4-1
Discussion Leader: L.A.Slepchenko

PLENARY REPORT ON LARGE TRANSVERSE MOMENTUM HADRONIC PROCESSES A4-23
P.Darriulat

A5. PARALLEL SESSION ON THEORY OF STRONG INTERACTIONS AT HIGH ENERGIES A5-1
Discussion Leader: A.A.Anselm

PLENARY REPORT ON HIGH ENERGY THEORY OF STRONG INTERACTIONS A5-34
V.A.Matveev

A6. PARALLEL SESSION ON HADRON-NUCLEAR INTERACTIONS A6-1
Discussion Leader: A.M.Baldin

A7. PARALLEL SESSION ON ELECTROMAGNETIC INTERACTIONS OF HADRONS A7-1
Discussion Leader: R.N.Faustov

SECTIONS C

C1. PARALLEL SESSION ON MESON SPECTROSCOPY C1
Discussion Leaders: S.A.Bunyatov and M.V.Terent'ev

C2. PARALLEL SESSION ON BARYON SPECTROSCOPY C30
Discussion Leaders: M.D.Shafranov and M.V.Terent'ev

PLENARY REPORT ON MESON AND BARYON SPECTROSCOPY C45
K.Lanius

C3. PARALLEL SESSION ON INTERACTION MECHANISM IN THE RESONANCE REGION C83
Discussion Leader: A.Ts.Amatuni

C4. PARALLEL SESSION ON COMPOSITE MODELS AND RELATIVISTIC BOUND STATES C99
Discussion Leader: P.N.Bogolubov

PLENARY REPORT ON COMPOSITE MODELS OF HADRONS AND RELATIVISTIC BOUND STATES C129
A.T.Filippov

SECTIONS A

CONTENTS

A1. PARALLEL SESSION ON BINARY AND LOW MULTIPLICITY REACTIONS

Discussion Leaders — V.A.Tsarev, S.V.Mukhin
Scientific Secretaries — I.M.Sitnik, N.P.Zotov, K.G.Boreskov, L.A.Ponomarev

Fine structure of the diffraction peak	V.A.Tsarev	A1-1
High mass diffraction excitation of protons on protons and deutrons	S.V.Mukhin	A1-3
Nucleon diffraction dissociation (experiment)	Yu.Kamyshkov	A1-7
Spin dependence studies with the ZGS polarized proton beam	A.B.Wicklund	A1-11
Baryon exchange in 12 GeV/c π^-p interactions	D.H.Stork	A1-14
Small momentum transfer antiproton charge exchange scattering on protons at 30 GeV/c	D.B.Kakauridze	A1-17
The measurement of nucleon-nucleus inelastic cross sections at energies higher than those of accelerators	V.I.Yakovlev	A1-18
The theory of the Pomeron with $\alpha > 1$ and the Froissaron dynamics	K.A.Ter-Martirosyan	A1-20
The description of the low multiplicity reactions	L.A.Ponomarev	A1-24
PLENARY REPORT ON BINARY AND LOW MULTIPLICITY REACTIONS	A.B.Kaidalov	A1-27

A2. PARALLEL SESSION ON MULTI-PARTICLE PRODUCTION AND INCLUSIVE REACTIONS

Discussion Leaders — Yu.A.Budagov, V.I.Savrin
Scientific Secretaries — N.N.Melnikova, L.A.Tikhonova, E.P.Kistenev, A.K.Likhoded

New results from Fermilab on hadron production in inclusive hadron-hadron interactions	E.W.Beier	A2-1
Multi-Particle production in $\bar{p}p$ -interactions	I.M.Gramenitsky	A2-3
Inclusive resonance production and two-particle correlations in π^-p -interactions at 40 GeV/c	V.G.Grishin	A2-6
Inclusive particle and resonance production	P.Schmid	A2-9
Associated correlation effects in π^-p interactions at 40 GeV/c	Yu.V.Thevzadze	A2-13
Investigation of some inclusive distributions of Λ°-hyperons and K_1° -mesons in π^-C^{12}-interactions at 40 GeV/c	N.S.Amaglobeli	A2-15
Two-particle correlations	E.P.Kistenev	A2-17
Recent results on 32 GeV/c $K^\pm p$ and $\bar{p}p$ interactions in the Mirabelle bubble chamber	R.Barloutaud	A2-21
Experimental data on determination of interaction range dimension. Identity effects	M.I.Podgoretsky	A2-27
Multiple production above 10^{14}eV	N.N.Roinishvili	A2-30
Inclusive reactions at medium energies	W.Kittel	A2-32
Inclusive π° and γ -production in pion-proton interactions at 5 GeV	Yu.A.Budagov	A2-34
Net charge distribution in rapidity and transverse momentum for semi-inclusive π^-p interactions at 11.2 GeV/c	S.P.Ratti	A2-37
A search for new neutral particles produced in highly inelastic π^+ proton collisions at 10.5 GeV/c	J.R.Elliott	A2-39
PLENARY REPORT ON MULTI-PARTICLE AND INCLUSIVE REACTIONS	P.V.Chliapnikov	A2-42

A3. PARALLEL SESSION ON MULTI-PARTICLE PRODUCTION PROCESSES

Discussion Leaders — N.S.Amaglobeli, A.N.Sissakian
Scientific Secretaries — V.K.Mitrjushkin, I.V.Andreyjev, A.S.Potupa, E.V.Shuryak

Statistical and hydrodynamical theories of multiple production . . . . . E.V.Shuryak A3-1
Recent developments in multiperipheral models . . . . . C. De Tar A3-4
Manycomponent description of inclusive and semiinclusive processes . . . . . A.N.Sissakian A3-10
Overlapping independent emission in the fragmentation region . . . . . J.Benecke A3-12
Inclusive approach to particle production . . . . . A.Białas A3-15
Correlations in multiple production and clusters . . . . . G.H.Thomas A3-19
Jet and fireball structure of multi-hadron processes . . . . . V.P.Shelest A3-23
Multiparticle production in the Pomeron theory with $\alpha(0)>1$ . . . . . B.Z.Kopeliovich A3-26
Multiparticle correlations and identical particle effects in the independent cluster emission model . . . . . J.Ranft A3-28

PLENARY REPORT ON MECHANISMS OF MULTIPLE PRODUCTION PROCESSES . . . . . I.M.Dremin A3-31

A4. PARALLEL SESSION ON LARGE TRANSVERSE MOMENTUM PHENOMENA

Discussion Leader — L.A.Slepchenko
Scientific Secretaries — D.Vesztergombi, E.A.Kochetov, S.V.Russakov, A.V.Radyushkin

Recent results on single particle high production at FNAL . . . . . M.J.Shochet A4-1
Correlations in collisions with a high-$p_\perp$ particle produced . . . . . R.Sosnowski A4-3
Large transverse momentum photons from high energy proton-proton collisions . . . . . G.Vesztergombi A4-6
Recent developments in the theory of large transverse momentum processes . . . . . S.J.Brodsky A4-9
High transverse momentum processes in composite models . . . . . A.N.Tavkhelidze A4-11
Large p_T inclusive distributions in composite models . . . . . L.A.Slepchenko A4-13
Dynamics of high momentum transfer processes . . . . . A.V.Efremov A4-15
Urbaryon model and large transverse momentum physics . . . . . T.Matsuoka A4-18
The hadron production at large transverse momentum and the parton interaction . . . . . E.M.Levin A4-19

PLENARY REPORT ON LARGE TRANSVERSE MOMENTUM HADRONIC PROCESSES . . . . . P.Darriulat A4-23

A5. PARALLEL SESSION ON THEORY OF STRONG INTERACTIONS AT HIGH ENERGIES

Discussion Leader — A.A.Anselm
Scientific Secretaries — A.A.Arkhipov, N.V.Krasnikov, K.G.Chetyrkin, M.A.Smondyrev

The fundamental length as a key to physics at very high energies . . . . . V.G.Kadyshevsky A5-1
Recent progress in reggeon field theory . . . . . R.L.Sugar A5-3
The Pomeron as a nonrelativistic Goldstone particle . . . . . I.T.Dyatlov A5-6
Theory of the Pomeron with intercept larger than 1 . . . . . D.Amati A5-8

Does u-channel in t-plane influence the behaviour of the forward scattering cross section at high energies? . . . . . M.A.Mestvirishvili A5-11

Analytical form of the Froissart bound at finite energies . . . . . Yu.S.Vernov, M.N.Mnatsakanova A5-14

Description of inclusive reaction scaling properties in terms of density matrix . . . . . V.I.Savrin A5-16

Investigation of the power automodel asymptotic behaviour of the large-angle hadron-hadron scattering . . . . . S.V.Goloskokov A5-19

High energy behaviour of gauge theories . . . . . Tai Tsun Wu A5-23

Multi-Regge processes and the Pomeranchuk singularity in nonabellian gauge theories . . . . . L.N.Lipatov A5-26

Multiparticle Regge poles and their trajectories . . . . . S.G.Matinyan A5-29

Universality of hadron multiplicity in color-gauge theory models . . . . . J.F.Gunion A5-31

PLENARY REPORT ON HIGH ENERGY THEORY OF STRONG INTERACTIONS . . . . . V.A.Matveev A5-34

A6. PARALLEL SESSION ON HADRON-NUCLEAR INTERACTIONS

Discussion Leader — A.M.Baldin
Scientific Secretaries — M.G.Shafranova, P.P.Temnikov, B.S.Yuldashev

Regularities of the scale-invariant interaction of relativistic nuclei . . . . . V.S.Stavinski A6-1

Nuclear scaling . . . . . G.A.Leksin A6-3

Interactions of few-nucleon systems at relativistic energies . . . . . I.P.Zielinski A6-6

A study of the "young" states of particles in p-, d- , and α-nuclei interactions . . . . . L.I.Sarycheva A6-10

Mechanisms of the cumulative hadron production on nuclei . . . . . A.V.Efremov A6-12

Dispersion description of the deuteron . . . . . L.L.Frankfurt A6-16

On spontaneous nuclear transitions into superdense state . . . . . V.P.Martemyanov A6-18

A7. PARALLEL SESSION ON ELECTROMAGNETIC INTERACTIONS OF HADRONS

Discussion Leader — R.N.Faustov
Scientific Secretaries — A.I.Kirillov, S.I.Bilenkaya, R.M.Ibadov, V.M.Budnev, A.F.Pashkov

Elastic and inelastic electron scattering from the deuteron at large momentum transfer . . . . . B.T.Chertok A7-1

The measurement of the nucleon and pion form factors in the region of time-like 4-momentum transfers from $1.5\,F^{-2}$ to $3.0\,F^{-2}$ . . . . . L.L.Nemenov A7-5

Measurement of the pion form factor . . . . . D.Stork A7-8

Phenomenological analysis and the models of the electromagnetic form factors of hadrons . . . . . N.B.Skachkov A7-11

Vector meson-nucleon coupling constants . . . . . G.Höhler A7-15

Effects of the SU(3)-breaking in masses and electromagnetic decays of vector mesons . . . . . S.B.Gerasimov A7-19

The nucleon axial vector form factor from threshold π^+-electroproduction . . . . . P.R.Norton A7-22

Shadowing effect in inelastic electron scattering on ^{12}C and ^{27}Al nuclei at small four momentum transfer . . . . . D.Wegener A7-25

Small-angle Compton scattering on hydrogen and deuterium . . . . . D.Wegener A7-27

Detection of π-μ Coulomb bound states . . . . . M.Schwartz A7-30

SECTIONS C

CONTENTS

C1. PARALLEL SESSION ON MESON SPECTROSCOPY

Discussion Leaders — S.A.Bunyatov, M.V.Terent'ev
Scientific Secretaries — V.B.Vinogradov, M.G.Riskin, G.S.Shabratova, A.E.Shabad

The $\delta(970)$ resonance and other 0^+ effects . . . . . S.O.Holmgren C1

$\eta'(958)$ spin-parity problem . . . . . V.I.Ogievetsky C4

Recent results on the $K\bar{K}$ system and on $\rho-\omega$ interference . . . . . A.B.Wicklund C7

The A_1 meson problem . . . . . M.Markytan C11

Review of $K^*(1400)-K^*(1800)$ $S=1$ meson spectroscopy . . . . . V.P.Kenney C15

New phenomena in the Q-region . . . . . G.Otter C19

The D(1285) and E(1420) mesons . . . . . H.Böttcher C22

A search for exotic mesons $X^{--} \to p\bar{p}\pi^-\pi^-$ in the CERN Omega spectrometer . . . . . A.Rougé C26

Nucleon polarization in the reaction $\pi^- p \to n\pi^+\pi^-$ . . . . . G.Lutz C27

C2. PARALLEL SESSION ON BARYON SPECTROSCOPY

Discussion Leaders — M.D.Shafranov, M.V.Terent'ev
Scientific Secretaries — L.I.Zhuravleva, N.G.Fadeev, V.S.Rumyantsev, H.M.Beshtoev

Resonances and resonance parameters from a πN partial wave analysis between 0.8 and 2.0 GeV/c . . . . . R.E.Cutkosky C30

A π^+ proton partial wave amplitude analysis for $P_{lab.}$ = 1.6 up to 10 GeV/c . . . . . A.W.Hendry C34

Investigation on the nature of enhancements observed in Λp effective mass spectra . . . . . B.A.Shahbazian C35

KN-scattering and the problem of $S=+1$ baryon resonances . . . . . G.Giacomelli C38

Production of baryon resonances in K^-p interactions at 4.2 GeV/c . . . . . E.W.Kittel C40

Ω^- and Ξ^* production in K^-p interactions . . . . . R.Barloutaud C42

PLENARY REPORT ON MESON AND BARYON SPECTROSCOPY . . . . . K.Lanius C45

C3. PARALLEL SESSION ON INTERACTION MECHANISM IN THE RESONANCE REGION

Discussion Leader — A.Ts.Amatuni
Scientific Secretaries — I.G.Aznaurian, S.V.Goloskokov, Yu.A.Kamyshkov, V.I.Kryshkin

Regge amplitudes with crossing and unitarity . . . . . D.Atkinson C83

Hadron physics in quantum chiral theory . . . . . M.K.Volkov C84

Amplitude and phase-shift analysis of the binary reactions in the resonance region . . . . . G.Oades C87

Final states of K^-N reactions . . . . . W.Kittel C89

Recent results from NINA . . . . . J.Allison C90

Photo- and electroproduction of the mesons in the first πN resonance region . . . . . P.V.Sorokin C93

Results on the π and η photoproduction polarization experiments in the energy range 0.7-1.8 GeV . . . . . G.A.Vartapetian C96

C4. PARALLEL SESSION ON COMPOSITE MODELS AND RELATIVISTIC BOUND STATES

Discussion Leader — P.N.Bogolubov
Scientific Secretaries — D.P.Mavlo, N.M.Atakishiyev, I.L.Solovtsov

Models of quark bags and their consequences	P.N.Bogolubov	C99
The Budapest bag model	Julius Kuti	C101
Relativistic effects in the constituent quark model	B.V.Struminsky	C103
Radial excited mesons in the M.I.T. bag model	M.G.Schepkin	C105
The potential and quasipotential models for bound quarks	R.M.Mir-Kasimov	C108
Null-plane quantization and quasipotential equation for composite particles	A.A.Khelashvili	C111
A new particle with the mass M= 1110 MeV and vector meson spectrum in the relativistic model of quark confinement	N.B.Skachkov	C114
Scattering processes in relativistic composite models	A.N.Kvinikhidze	C116
Investigation of the solutions of quasipotential equations	V.Sh.Gogokhia	C118
Local gauge symmetry and confinement in quantum chromodynamics	W.A.Bardeen	C121
Bound and resonant states in the nucleon-antinucleon system	I.S.Shapiro	C122
Bilocal functional approach to dynamical symmetry-breaking	D.Ebert	C125
Hadronization of quark theories and bilocal QED	H.Kleinert	C127
PLENARY REPORT ON COMPOSITE MODELS OF HADRONS AND RELATIVISTIC BOUND STATES	A.T.Filippov	C129

Речь Председателя Государственного комитета по использованию атомной энергии СССР проф. А.М.Петросьянца на открытии конференции

Уважаемый товарищ председатель! Уважаемые товарищи! Дамы и господа!

По хорошей традиции раз в два года ученые-физики многих стран мира, занимающиеся изучением фундаментальных свойств материи, съезжаются на свою главную конференцию, которая проводится поочередно в Соединенных Штатах Америки, одной из стран Западной Европы или в Советском Союзе. Собираются для того, чтобы подвести итоги своей работы и наметить наиболее перспективные направления, поставить задачи на ближайшее и более отдаленное будущее.

Теоретики и экспериментаторы, работающие на том или ином относительно узком участке широкого фронта физики высоких энергий, собираются вместе, чтобы увидеть общую картину микромира в том виде, в каком он вырисовывается сегодня. Конечно, это еще далеко не законченная картина, а скорее всего, лишь эскиз, постоянно меняющийся в каких-то своих деталях.

Нетрудно представить, какие чувства испытывает каждый из вас, талантливых мастеров, рассматривая картину микромира сегодняшнего дня и подводя итоги нынешних достижений.

Вместе с тем я хорошо могу представить себе волнение и тревогу, с которыми ожидают всякий раз ваши научные сообщения и заключения те руководители и организаторы, которые должны оплачивать расходы на сооружение мощных ускорителей и оборудования для проведения новых экспериментов.

Государственный комитет по использованию атомной энергии СССР совместно с Академией наук СССР щедро финансируют и всемерно поддерживают проведение и развитие исследований по физике высоких энергий в Советском Союзе. Вам хорошо известны успехи ученых Института физики высоких энергий в Серпухове, Института теоретической и экспериментальной физики и Физического института имени П.Н.Лебедева в Москве, Физико-технического института им. А.Ф.Иоффе в Ленинграде, научных центров Еревана, Тбилиси, Новосибирска, Алма-Аты и многих других советских физических институтов.

Мировую известность приобрел международный центр - Объединенный институт ядерных исследований в Дубне. Советские физики совместно с учеными социалистических стран ведут большую работу и намечают серьезные планы дальнейшего развития экспериментальной базы для физики высоких энергий.

Наши ученые успешно сотрудничают со своими коллегами из ЦЕРНа, США, Франции, Италии и многих других стран путем проведения совместных исследований как на ускорителях в нашей стране, так и на ускорителях в этих странах.

Пользуясь случаем, я хочу поздравить делегатов ЦЕРНа и всех сотрудников и руководителей этого научного центра с замечательным успехом - вводом в действие протонного синхротрона на 400 ГэВ - и одновременно выразить надежду, что сотрудничество наших ученых с учеными ЦЕРНа будет развиваться и крепнуть так же, как это было после ввода в действие серпуховского ускорителя.

Возвращаясь к тем чувствам, с которыми обычно воспринимаются ваши растущие от конференции к конференции требования и заявки на финансирование и создание новых ускорителей на такие большие энергии, которые теперь уже называют "сверхвысокими", хочу отметить, что и финансирование по своим объемам тоже становится сверхвысоким.

В наше время экспериментальная ядерная физика развивается так бурно, что зачастую ставит в тупик наших талантливых теоретиков. Поневоле вспомнишь, как хорошо было жить в век "неделимого" атома. Но уже в первой трети нашего столетия стали известны первые элементарные частицы. Через небольшой промежуток времени их стало более десяти, а затем их число начало лавинообразно увеличиваться и теперь перевалило за три сотни. Наступил период, когда физики-теоретики и физики-экспериментаторы схватились за голову, ибо при объеме наших нынешних знаний невозможно пока что создать стройную картину микромира. Вот почему ученые требуют сооружения более мощных ускорителей, масштабы которых начинают выходить за рамки материальных возможностей одного государства.

В этой связи нам представляется исключительно важным, чтобы, подводя итоги и намечая новые пути и задачи, вы смогли правильно и критично соразмерить ожидаемые результаты с теми затратами, которые общество в состоянии выделять на физические исследования фундаментальных свойств материи.

Позвольте мне теперь от имени моих коллег из Государственного комитета по использованию атомной энергии СССР и от себя лично пожелать всем вам новых больших творческих успехов и плодотворной работы XVIII Международной конференции по физике высоких энергий.

В заключение я должен сказать, что на сей раз организаторам конференции и всем нам, ее участникам, очень повезло потому, что конференция проходит в Тбилиси - столице Грузинской Советской Социалистической Республики. Грузины - народ исключительно организованный и гостеприимный, и я уверен, что они сделают все необходимое для успешной работы конференции.

Мне хочется также выразить большую признательность правительству Грузинской Советской Социалистической Республики и всем тем товарищам, кто принял на себя нелегкий труд - организовать такой большой и представительный форум, в котором участвуют ученые 38 стран мира.

Благодарю за внимание.

OPENING SPEECH

Prof. A.M.Petrosyants
Chairman of the USSR State Committee
for Utilization of Atomic Energy

Dear Chairman, Dear Comrades, Ladies and Gentlemen,

It has become a tradition for the physicists from many countries of the world who study the fundamental properties of matter to come biannually to their main international conference which in turn is organized in the USA, in one of the West European countries and in the USSR.

They assemble to sum up the results of their investigations and determine the most perspective trends, to outline the problems for the near and more remote future.

Theorists and experimentalists occupied in their own narrow field of high energy physics get together to review the general picture of the microworld in its present-day state.

Of course, this is still a far incomplete picture of the microworld. It is rather a sketch permanently varying in some of its details.

One readily imagines what emotions each of you, gifted masters, feels viewing the modern picture of the microworld, the picture of the present-day achievements.

I can well imagine the anxiety of the leaders and organizers that have to pay the expenses for the construction of accelerators and facilities for new experiments with which they expect each time your scientific publications and conclusions.

The USSR State Committee for Utilization of Atomic Energy together with the USSR Academy of Sciences generously finance and support the investigations and development of high energy physics in the USSR. You are well aware of the success achieved by the physicists of the Institute of High Energy Physics, Serpukhov, the Institute of Theoretical and Experimental Physics and the Lebedev Institute of Physics, Moscow, the Joffe Physical-Technical Institute, Leningrad, by the physicists of the scientific centres of Erevan, Tbilisi, Novosibirsk, Alma-Ata and other numerous Soviet centres of physics.

The Joint Institute for Nuclear Research at Dubna is one of the well-known international scientific centres.At present Soviet scientists together with the scientists of other socialist countries carry out intensive work and outline the plans for further development of the experimental basis for high energy physics. Soviet scientists also collaborate successfully with those of CERN, the USA, France, Italy and many other countries by performing joint investigations both at the accelerator centres in the USSR and in the above-mentioned countries.

I take this opportunity to congratulate the CERN delegates, the scientific staff and the Directorate of CERN on the outstanding success, putting into operation of the 400 GeV proton synchrotron and to express our hope that the collaboration of the Soviet and CERN scientists will develop and strengthen as after the Serpukhov machine began working.

Returning to the emotions with which your requirements and applications for greater funds and construction of new accelerators of extremely high energies now called "very big" are accepted, I would like to remark that a financial backing becomes "very big" too.

In our "atomic" century we are gaining via experiments the knowledge of matter so fast and vigorously that quite often drive our talented theorists to a dead-lock. One cannot but remember the good old time of "the undivided atom". But in the thirties of our century the first elementary particles were discovered. After a short time their number amounted to more than a dozen. Then the number of elementary particles began increasing to avalanches and now it is above three hundred.

A period arrived when physicists-theorists and physicists-experimentalists came to a despair for in our present state with the amount of our up-to-date knowledge it seems impossible to draw a consistent picture of the microworld. That is why physicists demand the construction of still more powerful accelerators. The scale of such accelerators, to be true, exceeds the financial possibilities of a single country.

In this connection we consider it important that you could, when summing up the results and outlining new problems, reasonably and critically commensurate your results with the expenditures a society can permit for the physical investigations of the fundamental properties of matter.

On behalf of my colleagues of the USSR State Committee for Utilization of Atomic Energy and on my own account I wish you new scientific achievements and successful work of the XVIII International Conference on High Energy Physics.

In conclusion I should mention that the Conference organizers and delegates are lucky to be present at a Conference held in the capital of the Georgian Soviet Socialist Republic. Georgians are extremely hospitable people, I am sure they will do their best to make your Conference successful.

I would like to express my gratitude and appreciation to the Government of the Georgian Soviet Socialist Republic, and all those who have taken the burden of the organization of such a representative forum which has convened scientists of 38 countries of the world.

Thank you.

PARALLEL SESSION ON BINARY AND LOW MULTIPLICITY REACTIONS

FINE STRUCTURE OF THE DIFFRACTION PEAK

V.A.Tsarev

P.N.Lebedev Physical Institute, Moscow, USSR

Recent measurements revealed rich structure of the differential cross section and polarization of the elastic hadron-hadron scattering. It is characterized by sequence of breaks, dips and bumps with typical intervals $\Delta t_\ell \gtrsim 1$ (GeV/c)^2 /1/. This ("large-scale") structure is usually assumed to be a manifestation of coherent effects originating from "hadron size" region $\lesssim 1$ Fermi.

The possibility of a small-scale structure with period Δt_s of order of 0.1 (GeV/c)^2 was also discussed theoretically/2,3/. Some experimental indication to this structure is perhaps present (?)/2/ in the ISR data/4/. New data presented at this Conference seem to give quite a clearcut evidence for such structure.

To begin with we show in Fig. 1 elastic proton-proton differential cross section measured at p=60 GeV/c at Serpukhov/5/. Experimental points are plotted with respect to commonly used smooth curve $(d\sigma/dt)_{\Delta V} = A\exp(\ell t + ct^2)$ ("peak with break") and display distinct oscillations with period $\Delta t \sim 0{,}4$ (GeV/c)^2.

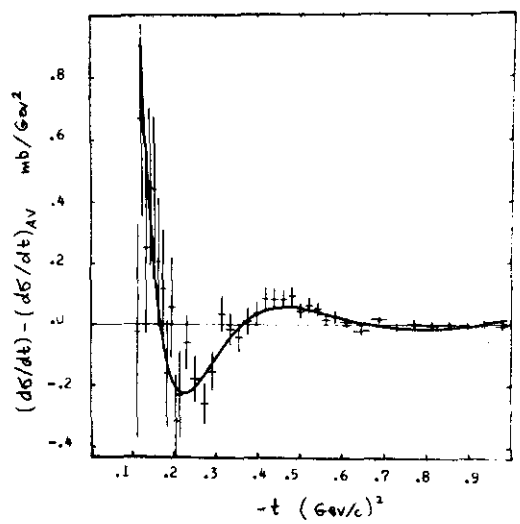


Fig. 1

The questions arise: What is the mechanism responsible for the small-scale oscillations (SSO)? Do they mean the existence of a new hedronic scale $\gg 1$ Fermi? We believe there is no need in any exotic dimensions. In fact SSO-phenomenon has been anticipated/2,3/ on the basis of ordinary scales ($t \sim 4\mu^2$ or $R \sim 1$ Fermi). It may arise simply due to edge effect caused by peripheral processes occurring mainly at impact parameters $\rho \sim 1$ Fermi.

It is instructive to consider an explicit model, but qualitative effect is not very sensitive to details and is model independant.

The main contribution to peripheral part $\Delta T(t)$ of elastic amplitude $T(t)$ is suggested in/3/ as coming from inelastic diffraction which is believed to have peripheral impact parameter profile/6/ (although there may be, of course, another contributions). Deck model with absorption/7/ was used to calculate the profile of diffractive dissociation contribution $\Delta G(\rho)$ into inelastic overlap function $G(\rho)$. Normalizing to diffractive cross section σ_D ($\simeq 6$ mb) the normalization parameter C has been fixed. The resulting profile (Fig. 2) is a "ring" with radius $R \sim \left\{2\ell \ln \frac{\sigma(B+B_1+\ell)}{4\pi\ell^2}\right\}^{1/2} \sim 0{,}9$ Fermi (Here $B \simeq \ell \simeq B_1 \simeq 10$ (GeV/c)$^{-2}$ are slopes of πN, NN scattering cross sections and π -meson vertex and propagator; $\sigma \equiv \sigma_{tot}(NN)$).

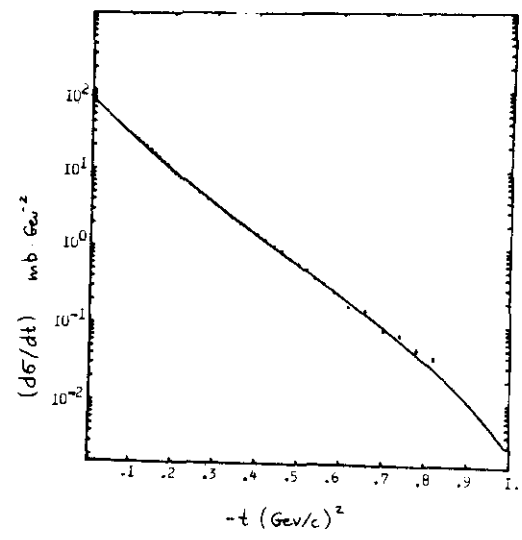


Fig. 2

Neglecting spin-flip and $Re\ T$ contributions the S-channel unitarity gives $T(\rho) = 2i(1 - \sqrt{1 - G(\rho)})$, where $G = G_c + \Delta G$. G_c is a "central" term. Using the fact that $\Delta G(\rho)$ contributes mainly near $\rho \sim 1$ Fermi, where $G(\rho) \ll 1$, one can approximate elastic amplitude as $T(t) \simeq T_c(t) + \Delta T(t)$. $\Delta T(t)$ is the Fourier transform of $\Delta G(\rho)$ and exhibits expected Bessel - like behaviour*)

$$\Delta T(t) \sim i C \exp(at) J_0(R\sqrt{-t})$$

Inelastic diffraction is believed itself to give rise to absorption resulting in alternation of the ΔT sign. In other words the "central term" T_c may be expected to have a simple form if one takes $T = T_c - \Delta T$. Here $T_c(t)$ has a meaning of unabsorbed overlap fuction of true inelastic processes. So, we can consider both versions:

$$\frac{d\sigma}{dt} = \left\{ |T_c(t)|^2 \pm 2 T_c^*(t) \Delta T(t) \right\} + |\Delta T(t)|^2 \quad (1)$$

First of all, it is easy to see that $|\Delta T(t)|^2$ gives rise to SSO (about "averaged" t-dependence) which are nicely confirmed by the data (see curve in Fig.1, $C = 4\ mb^{1/2} GeV^{-1}$, $\alpha = 2{,}5\ (GeV/c)^{-2}$, $R = 5{,}0\ GeV^{-1}$). Furthar, it is the absorptive (minus) sign which was shown by carefull analysis giving proper description of the "peak with break" with "simple" form for $T_c(t)$. Fig. 2 is an illustration with

$$T_c(t) = i C_1 \exp(a_1 t) J_1(R_1\sqrt{-t}) / R_1\sqrt{-t}$$

corresponding to scattering off a disk with rounded edge ($C_1 = 26\ mb^{1/2} Gev^{-1}$, $a_1 = 4.8\ Gev^{-2}$, $R_1 = 4\ Gev^{-1}$).

One can expect the "edge effect" to show up also at large $|t|$ leading to large - and small-scale structure due to $\Delta T(t)$ and $|\Delta T(t)|^2$. SSO have to manifest itself in other elastic reactions and at different energies. Indeed, one could probably find it in SLAC data[7] at 10 GeV/c and some $\pi^{\pm} p$ data at 4–6 GeV/c[8].

*) From t-channel point of view it can be described by complex singularities in j-plane [2,3].

Another place to look for SSO is the high energy nuclear scattering. Here nuclear fragmentation plays the role of dissociation and characteristic scale is determined by nuclear radii. The verification of the SSO hypothesis[2,3] with nuclei has been done at JINR[9] in α-particle beam at p=17.9 GeV/c. The data are summarized in Fig.3 where difference of experimental and Glauber cross sections for $\alpha - C$, $\alpha - Al$ and $\alpha - Cu$ scattering is plotted. At small $|t|$ ($.007 < |t| < .1\ GeV^2$) the data exhibit oscillatory structure (although it

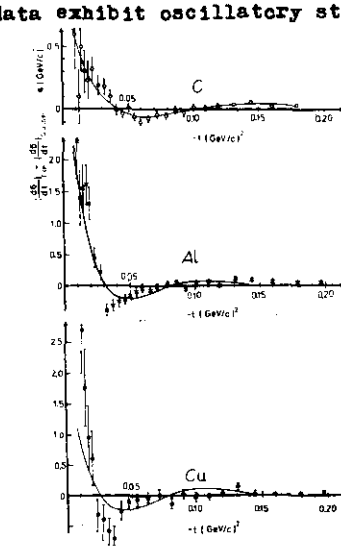


Fig. 3

is not excluded that the effect is introduced by inaccuratness of the Glauber description). Curves in Fig. 3 show the function $A_i J_0^2(R_i\sqrt{-t}) \exp(at) + c_i t + d_i$. The values of R_i found from the fit are of the order of radii of C, Al and Cu.

Detailed study of the nuclear fragmentation is of great interest in the light of present consideration.

We have discussed the model connecting the SSO with existence of peripheral inelastic diffraction. One can also try (especially for nuclei) to relate the SSO to fluctuations of the nuclear matter distribution ("shell effect"). However, as we know, the nuclear shell effects are expected to be shown up rather at large $|t|$ (small ρ) and have much larger period. Anyway one can hope to discriminate between these possibilities experimentally by comparing reactions

with and without diffractive dissociating probe (for instance, hadron-hadron and electron-hadron scattering).

In conclusion we want to emphasize that the SSO phenomenon giving interesting information on s- and t-channel aspects of high energy scattering has to be investigated further in great detail. The energy dependence is of particular interest. If $\sigma_{tot} \sim (\ln s)^{\alpha}$ and elastic slope $B \sim (\ln s)^{\beta}$ we expect

$$\Delta t^{-1} \sim R^2 \sim (\ln s)^{\beta}[(\alpha-\beta)\ln\ln s + C].$$

The data available at present seem to confirm Δt decrease with s increasing.

I am grateful to A.M.Baldin, N.I.Starkov, L.N.Strunev and participants of E.L.Feinberg's seminar for useful discussions.

References

1. A.W.Hendry, Phys.Rev. D10, 2300 (1974). B.Schremp, F.Schremp, Phys.Lett. 55B, 303 (1975).
2. V.A.Tsarev, FNAL-Pub-74-17 (Jan. 1974).
3. N.I.Starkov, V.A.Tsarev, JETP Lett. 23, 403 (1976).
4. G.Barbellini et al., Phys.Lett. 39B, 663 (1972).
5. Y.M.Antipov et al. Paper No 40/A1-40 submitted to this Conference.
6. H.I.Miettinen, Proc. of the EPS Int.Conf. on High Energy Physics, Palermo, 1975.
7. V.A.Tsarev, Phys.Rev. D11, 1864, 1875 (1975).
8. R.K.Carnegie et al. Phys.Lett. 59B, 313 (1975).
9. G.Fox, C.Quigg, Compilation of Elastic Scattering data, UCRL-20001 (1970).
10. V.G.Ableev et al. Paper No 448/A6-5 submitted to this Conference and mini-rapport. talk by P.Zielinski at this Conference.

HIGH MASS DIFFRACTION EXCITATION OF PROTONS ON PROTONS AND DEUTRONS

S.V.Mukhin

Joint Institute for Nuclear Research, Dubna

In this short talk I shall discuss some new results of four papers, submitted to the Conference, on the inclusive processes

$$p + p \longrightarrow X + p$$

and

$$p + d \longrightarrow X + d$$

in the kinematic range $5 \leqslant M_x^2 \leqslant 0.25$ (GeV)^2, $s > 120$ GeV^2 and $t < 0.3$ (GeV/c)^2.

Two of them present the data obtained at Fermilab with deuterium (USSR-USA collaboration)[1] and hydrogen (C-SB collaboration)[2] jet targets. In these experiments the recoil particles from the interactions of an internal beam were detected by the solid-state detector telescopes.

The authors took special care for background corrections which were < 8% for the pd case and $\leqslant$ 2% for pp.

The two others from CERN-ISR present the single-arm spectrometer data obtained with deuteron (CHM-collaboration)[3] and proton (CHLM-collaboration)[4] circulating beams.

The high mass region is the region where the triple Regge phenomenology is expected to apply. Using the generalized optical theorem[5], the inclusive reaction $a + b \longrightarrow c + X$ can be related to three-body scattering amplitudes as shown in Fig. 1 and an invariant double differential cross section can be expressed as

$$s\frac{d^2\sigma}{dt\,dM_x^2}(s,t,M_x^2) = \frac{1}{s}\sum_{i,j,k} G_{i,j,k}(t)\left(\frac{s}{\nu}\right)^{\alpha_i(t)+\alpha_j(t)}\nu^{\alpha_k(0)},$$

where

$$\nu = M_x^2 - t - M_e^2.$$

The term $G_{i,j,k}$ denotes the triple Regge coupling of three Reggeons i, j and k, where the Regge poles i and j with trajectories

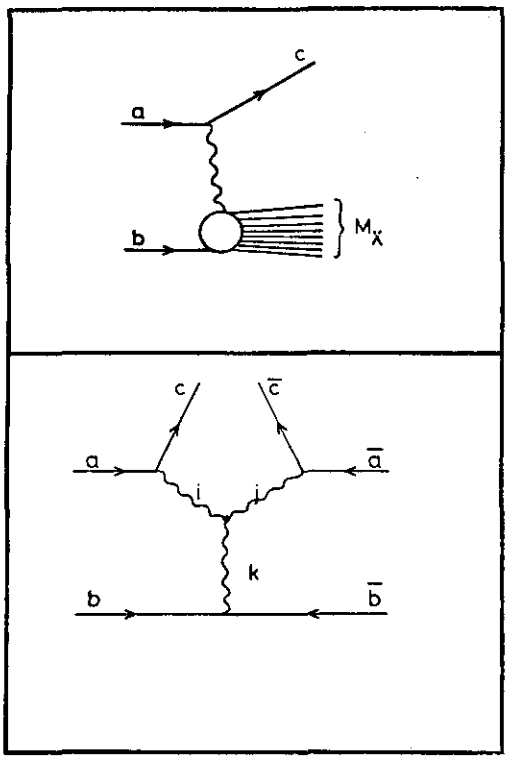


Fig. 1.
The quasi-two-body and associated triple Regge diagrams.

$\alpha_i(t)$, $\alpha_j(t)$, respectively, are exchanged and the Regge pele k with trajectory $\alpha_k(0)$ controls the Reggeon particle total cross section. Table 1 shows the corresponding coefficient of $G_{i,j,k}$ for $d^2G/dt\,dM_x^2$ and $d^2G/dt\,dx$, where $x = p_{\parallel}^{cm}/p_{max}^{cm} \simeq 1 - M_x^2/S$. One can see that the triple Regge terms have different M_x and S dependence and as diffraction (PPP, PPR), non-diffraction ($\pi\pi P$, $\pi\pi R$, RRP, PRR) and interference enes (RPR, RPP) have to dominate in different mass regions.

Since the London Conference it is well-known[6] that in the pure diffraction region $S < M_x^2 < 0.05S\,GeV^2$ at small t-values the mass spectrum falls as $1/M_x^2$ with approximate sealing due to triple Pemeron (PPP) dominance whereas the fits of the data[7] show a significant rele ef the $\pi\pi P$ and $\pi\pi R$ terms as non-PPP backgreund.

The comparison of the pp and pd data in the same kinematic range is at interest as the non-PPP background should be smaller in pd due to the isospin conservation.

Let us look at the new higher statistics data which cover a rather large M_x^2 region to better understand this phenomenon.

Figs. 2 and 3 show the USSR-USA collaberation pd inelastic mass spectrum at t =0.003

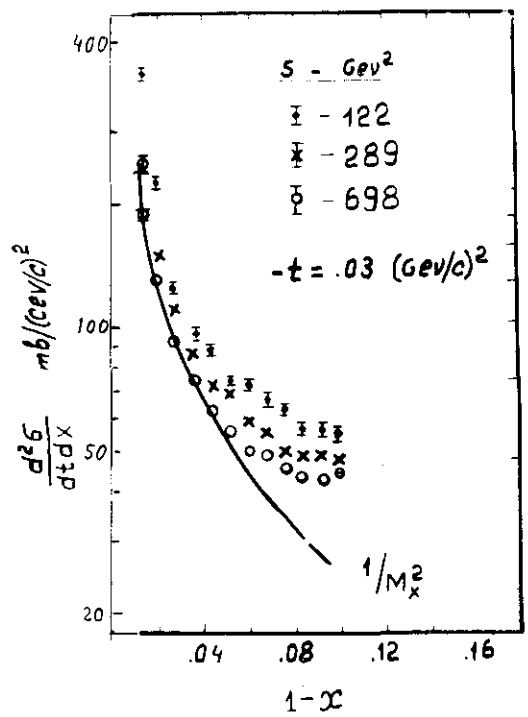


Fig. 2.
The invariant inelastic pd⟶Xd cross section divided by the deuteron coherence facter as a function of 1-X for S=122,289 and 698 GeV^2 at t=0.03 (GeV/c)^2. The curve represents the behaviour adjusted to the high energy data.

and 0.13 (GeV/c)^2. The results are divided by the deuteron coherence factor $F_{cl}(t) = (G_t^{pd}/G_t^{pp})^2 \times exp(-26.4|t| + 62.3t^2)$ in order to compare with the pp data. The energy dependence at $122 \leq S \leq 699$ GeV^2 is quite pronounced at these two values of t. The solid curves represent the $1/M_x^2$ behaviour fixed to be in agreement with the high energy points for $M_x^2/S < 0.05$.

There are clear deviations from this simple behaviour for $M_x^2/S > 0.06$.

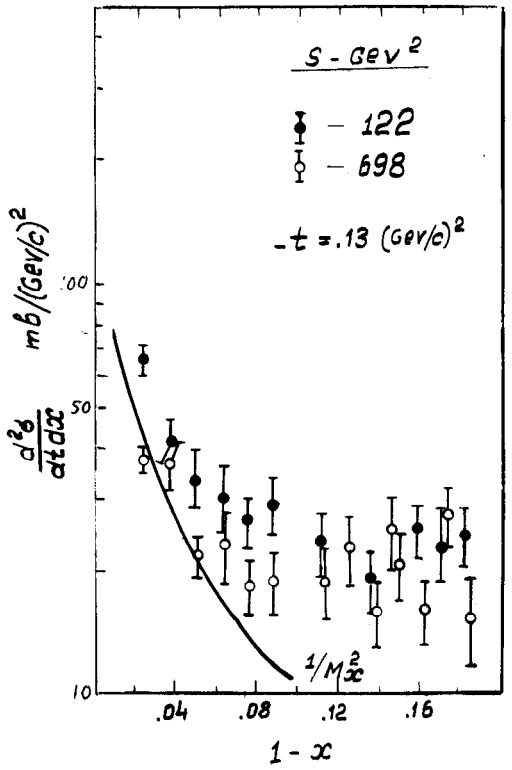


Fig. 3.
The invariant inelastic pd ⟶ Xd cross section divided by the deuteron coherence factor as a function of I-X for S=122 and 689 GeV^2 at t=0.13 (GeV/c)^2. The curve represents the $1/M_x^2$ behaviour adjusted to the high energy data.

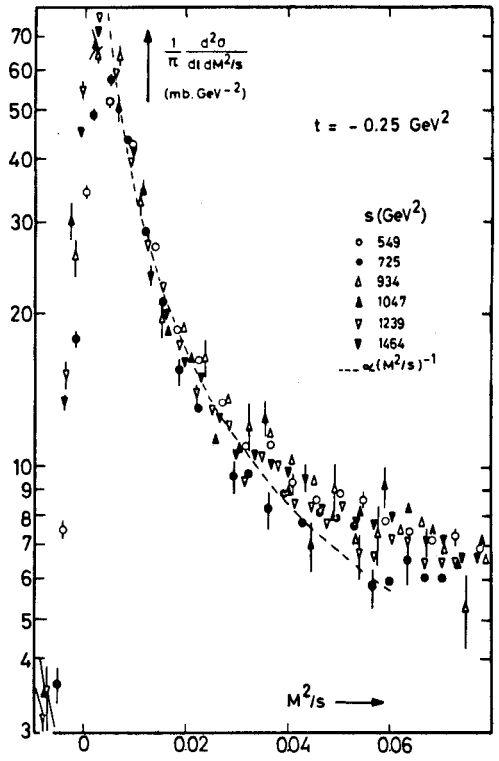


Fig. 4.
The invariant inelastic pp⟶Xp cross section at t=0.25 (GeV/c)^2 as a function of M_x^2/S and S. The dashed line shows the dependence of the form $(Mx^2/S)^{-1}$.

The new CERN ISR p-p data (CHLM collaboration) at $549 \leqslant S \leqslant 1464$ GeV^2 and t=0.25 (GeV/c)^2 in Fig. 4 also show the approximate $1/M_x^2$ mass spectrum dependence up to $M_x^2/S = 0.05$, but they scale well in terms of the variable M_x^2/S.

There arises a good question whether scaling occurs at $S > 600$ GeV^2 or at $t > 0.2$ (GeV/c)^2. Further experimental work is needed to get an answer to this question.

Returning to the region $M_x^2/S > 0.05$, where nondiffractive triple Regge terms have to be valid, I plot the pd (USSR-USA collaboration) and pp (C-SB collaboration) data at the same t values in Fig. 5. Distracting from normalization problems (both results are preliminary) and the difference in S, it is remarkable that the M_x^2 dependence is similar for the pp and pd processes.

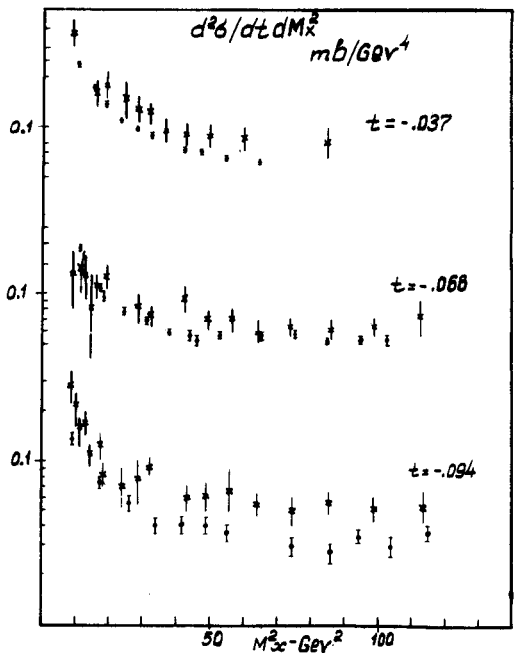


Fig. 5.
The M_x^2 dependence of $d^2\sigma/dt\,dM_x^2$ at fixed t=0.037, 0.068 and 0.094 (GeV/c)^2 for pp⟶Xp (x-points) at $S \cong 940$ GeV^2 and pd⟶Xd (o-points) at S=698 GeV^2.

In fig. 6 we can see CHM collaboration CERN-ISR results for the pp and pd inelastic spectrum at S=2800 GeV^2 and t=0.22 (GeV/c)^2.

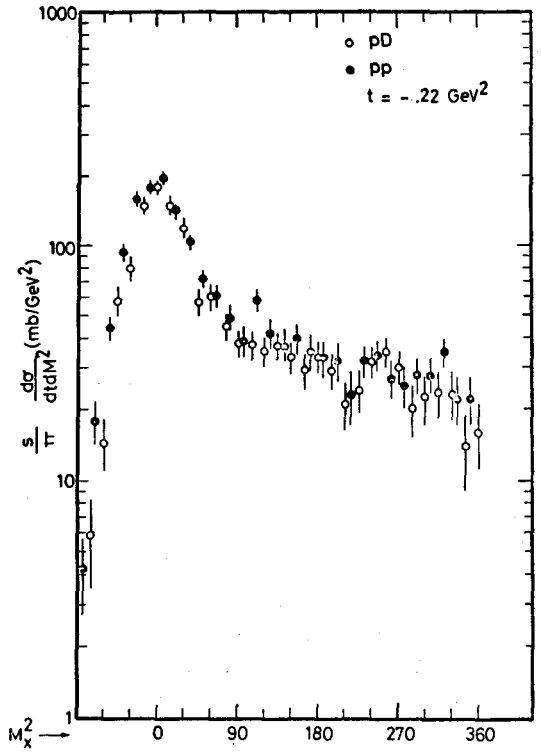


Fig. 6.
The invariant inelastic cross section versus M_x^2 for pp → pX (• -points) and pd→dX (o -points) at S=2800 GeV^2 and t=0.22 (GeV/c)^2. The pp cross section is scaled down by the ratio of the differential elastic cross section.

For comparison the pp → pX spectrum was scaled down by the measured ratio of the differential elastic cross sections for the two reactions. The striking feature of this graph in the resemblance between the pp and pd spectra over the whole M_x^2 range.

It seems there is good experimental evidence for a dominating role of the isospin =0 triple Regge components in exchange processes. In these four papers the authors do not report any deviations from the regular exponential t dependence like turn-overs, dips or breaks for inclusive inelastic pp and pd reactions.

The results of the discussion of the recent high mass inelastic data can be summarized as follows.

1. The triple Pomeron exchange dominates in the pure diffraction mass region $5 \leqslant M_x^2 \leqslant 0.055$ GeV^2.

2. There are deviations from scaling for $S \leqslant 600$ GeV^2 or $t < 0.2$ (GeV/c)^2.

3. The deviation from the $1/M_x^2$ behaviour for $M_x^2/S \gtrsim 0.06$ indicates a significant role of nondiffractive exchanges in this mass region.

4. The similarity at the pp and pd mass spectra shows that the isospin =0 exchange dominates.

5. There are no dips, breaks, turn-overs, etc., in the t-dependence.

I should like to express my gratitude to S.Olsen and D.Gross who helped me in the preparation of this report.

Table 1.

Triple Regge Formulae, where
$\alpha_P(t) = 1.0 + \gamma t$, $\alpha_R(t) = \alpha_0 + \beta t$ and $\alpha_\pi(t) = 0.0 + \delta t$

Triple Regge Term	$d^2\sigma/dt_c dM_x^2$		$d^2\sigma/dt_c dx$	
i j k	Cosmic[a]	Full	Cosmic[a]	Full
P P P	$1/M_x^2$	$\frac{S^{2\gamma t}}{(M_x^2)^{1+2\gamma t}}$	$1/(1-x)$	$\frac{1}{(1-x)^{1+2\gamma t}}$
P R P	$1/(M_x^2\sqrt{s})$	$\frac{S^{\alpha_0+(\beta+\gamma)t-1}}{(M_x^2)^{\alpha_0+(\beta+\gamma)t}}$	$1/(1-x)^{1/2}$	$\frac{1}{(1-x)^{\alpha_0+(\beta+\gamma)t}}$
R R P	$1/S$	$\frac{S^{2\alpha_0+2\beta t-2}}{(M_x^2)^{2\alpha_0+2\beta t-1}}$	1	$\frac{1}{(1-x)^{2\alpha_0+2\beta t-1}}$
P P R	$1/M_x^3$	$\frac{S^{2\gamma t}}{(M_x^2)^{2-\alpha_0+2\gamma t}}$	$\frac{1}{\sqrt{s}(1-x)^{3/2}}$	$\frac{(M_x^2)^{\alpha_0-1/2}}{\sqrt{s}(1-x)^{3/2+2\gamma t}}$
P R R	$1/(M_x^2\sqrt{s})$	$\frac{S^{\alpha_0+(\beta+\gamma)t-1}}{(M_x^2)^{1+(\beta+\gamma)t}}$	$\frac{1}{\sqrt{s}(1-x)}$	$\frac{1}{s^{1-\alpha_0}(1-x)^{1+(\beta+\gamma)t}}$
R R R	$1/(sM_x)$	$\frac{S^{2\alpha_0+2\beta t-2}}{(M_x^2)^{\alpha_0+2\beta t}}$	$\frac{1}{\sqrt{s(1-x)}}$	$\frac{1}{s^{1-\alpha_0}(1-x)^{\alpha_0+2\beta t}}$
π π P	M_x^2/s^2	$\frac{S^{2\delta t-2}}{(M_x^2)^{2\delta t-1}}$	$(1-x)$	$\frac{1}{(1-x)^{2\delta t-1}}$
π π R	M_x/s^2	$\frac{S^{2\delta t-2}}{(M_x^2)^{2\delta t-\alpha_0}}$	$\sqrt{\frac{(1-x)}{s}}$	$\frac{1}{\sqrt{s}(1-x)^{2\delta t-\alpha_0}}$

a) Cosmic is defined by $\gamma = \beta = \delta = 0$, $\alpha_0 = 1/2$

References

1. Y.Akimov et al., Dubna-Fermilab-Rockefeller--Rochester-Arisona (USSR-USA) Collaboration, Proton Excitation to High Mass States on Deuterium, paper No 1262 (A1-171) submitted to this Conference.
2. S.Childress et al., Columbia-Stony Brook Collaboration, Proton-Proton Inelastic Scattering at 0.5 TeV, paper No 829 (A1-169) submitted to this Conference.
3. J.C.M.Armitage et al., CERN-Holland-Manchester Collaboration, High Mass Single Diffraction Excitation in dp $\longrightarrow$ dX at S=2800 GeV^2, paper No 345(A1-170)submitted to this Conference.
4. M.G.Albrow et al., CERN-Holland-Landcaster-Manchester Collaboration, Inelastic Diffraction Scattering at the CERN ISR, paper No 799 (A1-90) submitted to this Conference.
5. A.H.Müller, Phys.Rev., D2, 2963 (1970).
6. See, for instance, Y.Akimov et al., Proton-Deuteron Elastic Scattering and Diffraction Dissociation from 50 to 400 GeV, Rockefeller Univ. preprint COO-2232A-I and contribution to the XVII Intern.Conf. on High Energy Physics, London (1974).
7. R.D.Field, E.C.Fox. Nucl.Phys., B80, 367 (1974).

NUCLEON DIFFRACTION DISSOCIATION (EXPERIMENT)

Yu.Kamyshkov
ITEP, Moscow, USSR

In this paper the present situation in nucleonic diffraction dissociation into $(N\pi)$-system is discussed. New experimental data have come mainly from experiments performed at high energies by electronics technique /1-4/ at Serpukhov, FNAL and ISR with high statistics.

The main features of nucleon diffraction dissociation $N \to N\pi$ observed at intermediate energies (< 30 GeV) are the following. The $(N\pi)^-$ system is preferably produced with low invariant mass. The energy dependence of the reaction is rather weak. The t-distribution shows diffraction - like behaviour ($\sim e^{Bt}$) with the slope B, which depends on the mass of the $(N\pi)^-$ -system. For the nucleon of the system, the cos θ_{GJ} distribution is strongly peaked towards cos θ_{GJ} =+1. Azimuthal φ_s and φ_t distributions are not uniform and hence are not in agreement with S- and t-channel helicity conservation.

1. Manifestation of Baryon-exchange Deck-effect

Fig. 1 shows the angular distribution over cos θ_{GJ} as obtained by Moscow-Karlsruhe-CERN Collaboration/1/ in all experimental phase space (a) and under small M and |t| restrictions (b). One can be sure that the influence of resonance production is considerably weakened by this restrictions.

Forward peak near cos $\theta_{GJ} \sim +1$ can be described as π -exchange Deck-effect (dotted). But quite pronounced backward peak near cos $\theta_{GJ} \sim -1$ is not consistent with π -exchange. This backward peak can be explained by a mechanism which is similar to the Deck one, but involving baryon exchanges instead of pion exchange/9/ (solid).

In fig. 2, one can see that taking into account baryon-exchange Deck graphs' contributions

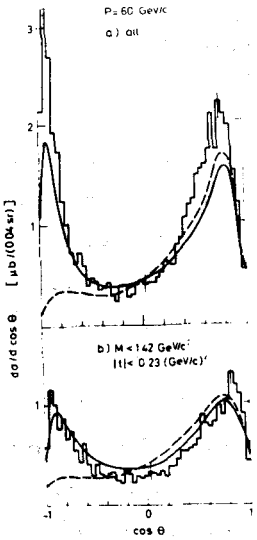


Fig. 1.

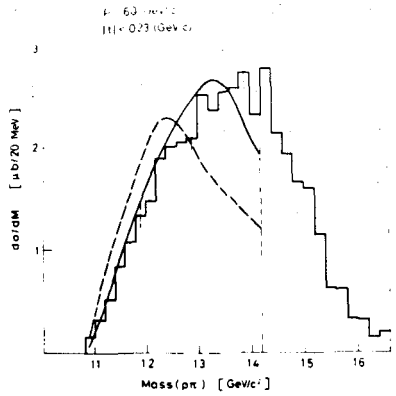


Fig. 2

improves mass spectrum description considerably (π -exchange Deck alone predicts too soft mass spectrum).

The backward peak near cos $\theta_{GJ} \sim -1$ at small M and $|t|$ was also clearly seen in FNAL[2] and ISR[3] experiments. Authors of[2] compared φ_{GJ} -distributions at cos $\theta_{GJ} \sim +1$ and cos $\theta_{GJ} \sim -1$ with reggeized Deck model predictions (fig. 3). They consider the φ_{GJ}-distribution structure to be a manifestation of baryon-exchange Deck-effect.

So we have now at least three arguments for the existence of baryon-exchange Deck mechanism, i.e., backward peak at cos $\theta_{GJ} \sim -1$, mass spectra discription and φ_{GJ} structure.

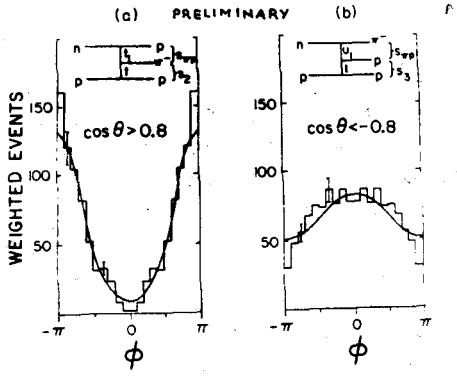


Fig. 3

2. t-distributions. Correlations

The appearence of the structure in $d\sigma/dt$ near $|t| \sim 0.2$ (GeV/c)^2 in DD-processes was recently discussed[2,3,9]. The new data have come from CHOV experiment[3] at ISR the deep in t-distributions has been observed. Fig. 4 (b) shows that for the mass range 1.30-1.35 GeV the deep is most pronounced for the cos $\theta_{GJ} \sim 0$. Fig. 4 (a) presents the t-distributions for $-0.3 < \cos\theta_{GJ} < 0.3$ at different mass intervals. The deep is clearly seen for the masses M < 1.4 GeV and moves to higher $|t|$ values with mass increasing.

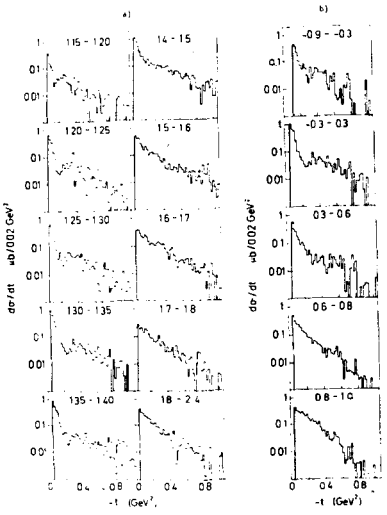


Fig.4

Deck-type model with absorption, perhaps, can interpret the appearence of this structure [9 and ref. therein].

Collection of the data on mass-slope correlation is shown in fig. 5. One can see that in the momentum range 12-1000 GeV/c the shape of

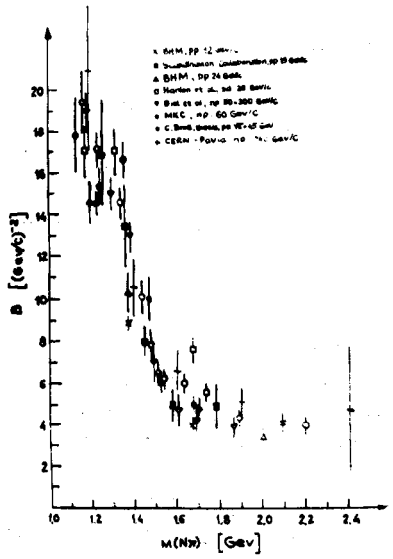


Fig. 5

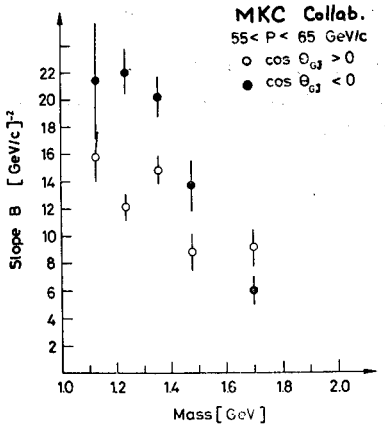


Fig. 6

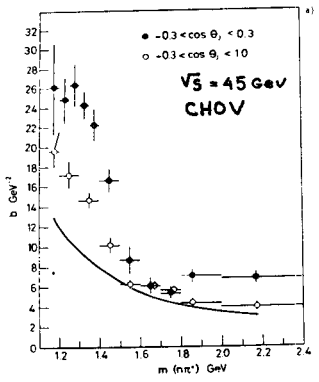


Fig. 7

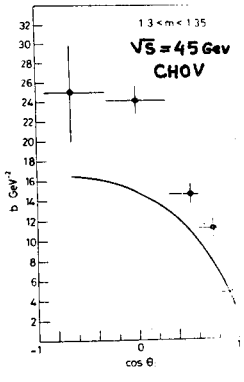


Fig. 8

the function is universal; at small masses the slope is about twice that of NN elastic one and for M≥1.6 GeV is about a factor of 2 less. At small masses (<1.3 GeV) there are some indications to increasing of the slope with the energy, but due to large experimental errors one can hardly say that the energy dependence of the slope in all mass intervals is different from that of elastic scattering. New experimental results[1,2,3] show the existence of the correlation between production and decay of $(N\pi)$ system (fig. 6-8). Theoretical description of the slopes is discussed in[9]. At least partially these correlations can be explained kinematically.

3. Mass spectra and cross sections

In fig. 9 the $(p\pi^-)$ mass distribution for $45 \leq p_n \leq 65$ GeV/c[1] is compared with the corresponding preliminary distribution from the FNAL experiment[2]. Both sets of data are absolutely normalized. The spectra turned out to be almost identical, apart from the mass region around 1.5 GeV.

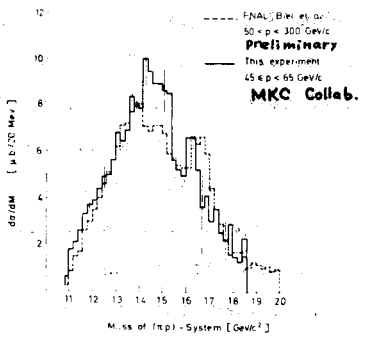


Fig. 9

Fig. 10 shows energy dependence of the cross sections integrated over two low mass intervals for $0.002 < |t| < 1.0$ (GeV/c)^2[1,2,7]. One can see that in the error bars low mass cross sections are energy independent.

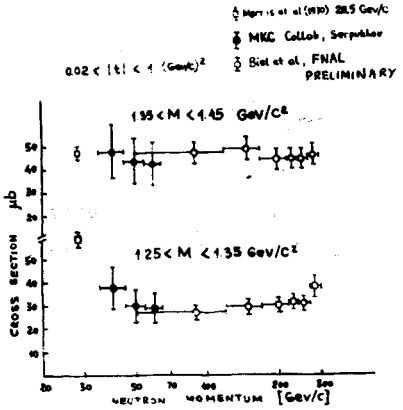


Fig. 10

Mass spectra for Serpukhov and ISR experiments

are presented in fig. 11 under the same phase space distributions. All masses with the exception of the interval near $M \sim 1.5$ Gev display equal cross sections.

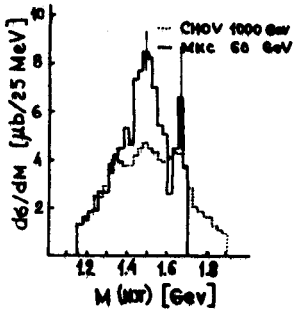


Fig. 11

If high energy diffraction dissociation is dominated by isospin $I = 0$ exhange, cross section for the reactions $pp \to (n\pi^+)p$ and $np \to (p\pi^-)p$ should be equal (total DD pp cross sections have a trivial factor 2). Fig. 12 shows experimental data on total nucleon dissociation cross section in the momentum range from 7 to 1500 GeV/c[1-7]. At ISR energies np and pp channels have equal cross sections within the experimental errors. At the energies above Seprukhov range cross sections seem to be flattened.

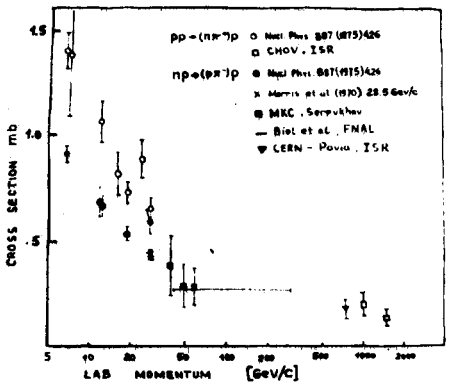


Fig. 12

I wish to thank Prof. V.A.Lyubimov and Dr. L.A.Ponomarev for useful discussions and some essential remarks.

References

1. A.Babaev et al., Paper 29/A1-29.
2. J. Biel et al., Papers 909/A1-8,69/A1-69. T.Ferbel, UR-541 (The University of Rochester, New York 1975). The latest contribution to the Conference contains more detailed analysis of differential cross sections in approximately whole phase space. Data are based on 80000 events.
3. H. de Kerret et al., Paper 65/A1-65. C.Broll, Thesis, Orsay, 1976.
4. CERN-Pavia Collab. Paper 338/A1-102.
5. E.Dahl-Jensen et al., Nuclear Phys., B87, 426 (1975).
6. V.Bakken et al., Paper 74/A1-74.
7. T.W.Morris et al., Comparison of Reactions $pp \to pn\pi^+$ and $pn \to pp\pi^-$ in pp and pd Interactions at 28.5 GeV/c. Paper submitted to the 15-th Int. Conf. on High Energy Phys., Kiev, 1970.
8. D.Denegri et al., Paper 73/A1-73.
9. L.A.Ponomarev. Mini-rapporteur's talk at this Conference.

SPIN DEPENDENCE STUDIES WITH THE ZGS POLARIZED PROTON BEAM

A.B.Wicklund

A.N.L., U S A

We summarize here selected results from recent measurements using the polarized proton beam at the Argonne Z.G.S.

1. Elastic $p_\uparrow p_\uparrow \to pp$ at large $p_\perp$:

Using polarized proton beam and target, the Michigan-A.N.L.-St.Louis collaboration[1] has measured both the polarized target asymmetry A, and the beam-target spin correlation C_{NN} at 6 and 12 GeV/c (Fig.1). What is remarkable

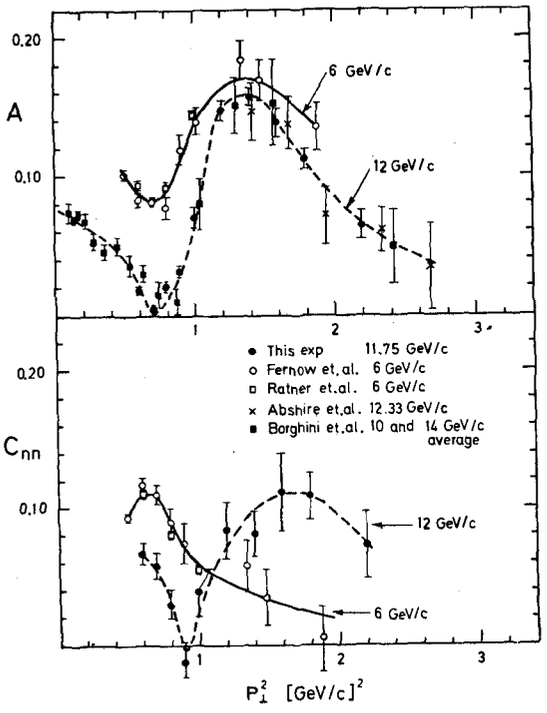


Fig. 1.
The parameters A and C_{NN} measured in $p_\uparrow p_\uparrow \to pp$ at 6 and 12 GeV/c.

is that in the secondary maximum region of $p_\perp^2$ (1 to 2 GeV^2), A is slowly varying with energy while C_{NN} increases considerably going from 6 to 12 GeV/c. Furthermore, C_{NN} develops a sharp dip structure at 12 GeV/c which is not seen at the lower energies. An obvious interpretation is that the spin dependent part of the pp elastic amplitude falls more slowly with energy than the nonflip diffractive component at large $p_\perp^2$. This behaviour is not anticipated by conventional models.

II. Comparison of elastic $p_\uparrow p \to pp$ and $p_\uparrow n \to pn$ polarizations

The effective mass spectrometer (E.M.S) has been used to measure pn elastic asymmetries for the first time above cyclotron energies[2]. From 2 to 6 GeV/c (Fig.2) the pn polarization falls faster with energy than the pp.

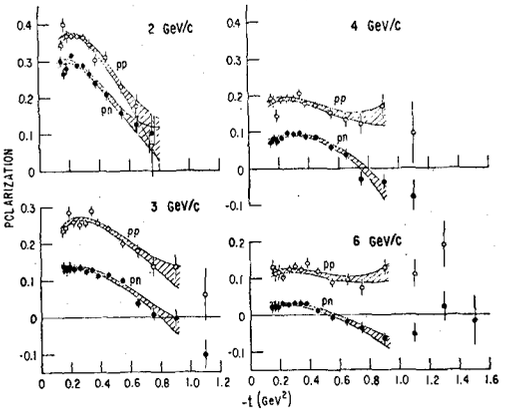


Fig. 2.
The polarization parameters in pp and pn elastic scattering at 2,3,4, and 6 GeV/c.

Since the polarization is given by natural mines-parity exchanges (e.g. ρ, ω, B and A_2 exchange flip amplitudes interfering with the Pomeron), Regge models expect that pp and pn polarizations should seal in the same way with energy. The data shows that the pp and pn polarization tend to approach mirror symmetry as the energy increases, implying that the I=1 exchange flip amplitude falls more slowly with energy then the I=0 term. In fact, the effective Regge trajectory of the I=0 exchange flip amplitude is empirically one unit lower than conventional ω and B trajectories, and the data can be satisfactorily fitted only by introducing ad hoc low-lying trajectories that are not anticipated from meson-baryon reactions.

III. Charge exchange production of N^* and Δ^{++}:

The E.M.S. has been used to study the reactions[3]

$$p_\uparrow p \to p\pi^+ n \text{ (2000000 events)} \quad (1)$$

$$p_\uparrow n \to p\pi^- p \text{ (150000 events)} \quad (2)$$

from 2 to 6 GeV/c. For small $-t$ ($-t < 0.2$ GeV^2) these reactions should be dominated by π exchange and the spin-dependence effects can be compared with polarizations measured (in $\pi^\pm p$ elastic scattering). Fig.3 shows the small -t cross sections for reactions (1) and (2) versus $p\pi^+$

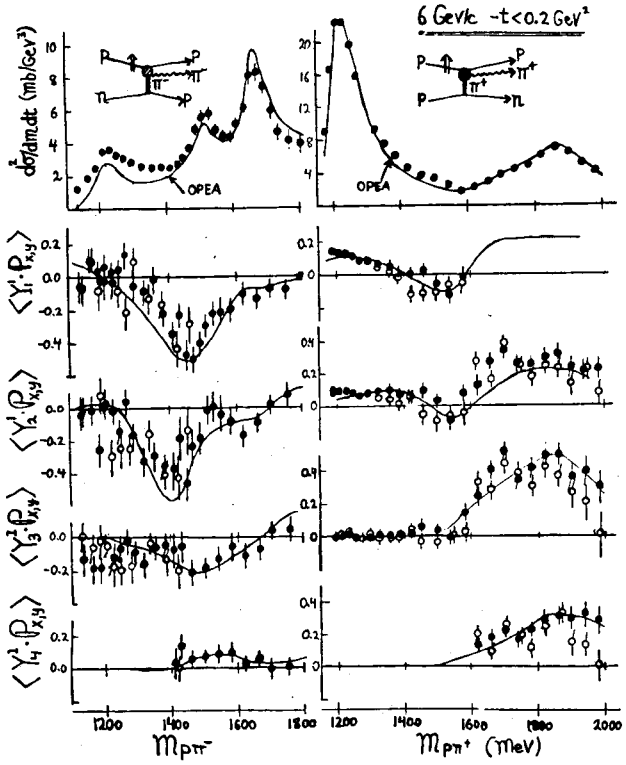


Fig.3.

Cross sections and polarizations versus $p\pi^-$ and $p\pi^+$ masses for reactions $p_\uparrow n \to p\pi^- p$ and $p_\uparrow p \to p\pi^+ n$. The solid points are correlations $\langle \mathrm{Im}\, Y_L^1 \cdot P_x \rangle$; the open points are $\langle \mathrm{Re}\, Y_L^1 \cdot P_y \rangle$, where P_x (P_y) are transverse polarization components in the scattering plane (normal to the scattering plane).

and $p\pi^-$ masses; the correlations of the spin vector with the decay moments Y_L^1 are also shown and compared with absorbed π-exchange calculated with measured elastic phase shifts. Agreement with OPEA is reasonably good.

At larger -t values other mechanisms besides π-exchange become important. Fig. 4 shows unpolarized density matrix elements in the S channel for $p_\uparrow p \to \Delta^{++} n$ at 6 GeV/c. Considerable structure can be seen. The polarized beam asymmetries at 3,4 and 6 GeV/c are also shown; these are substantial (40% for $\sqrt{-t} > 0.5$ GeV/c) and show little if any variation with energy. These asymmetries would arise in Regge models from π-B or ρ-A_2 exchange interference, and would vanish if the exotic $pp \to \Delta n$ amplitudes were purely real.

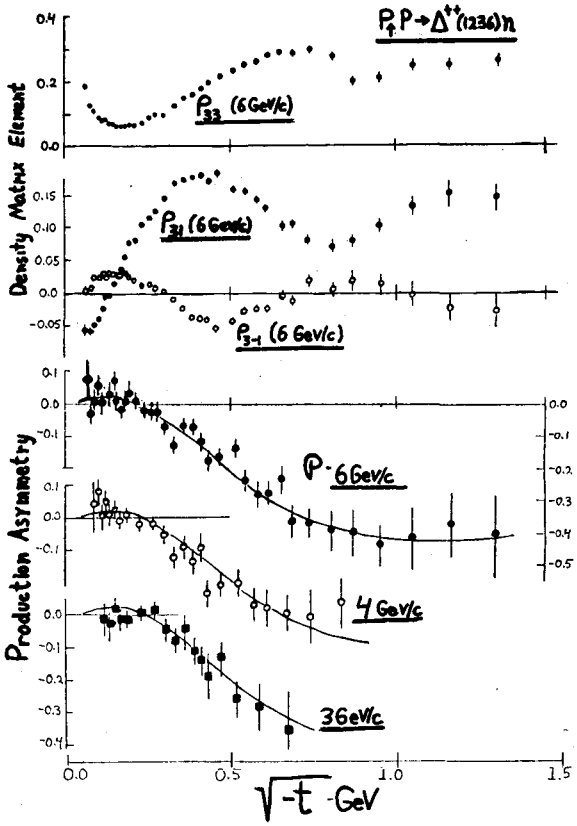


Fig.4.

Density matrix elements at 6 GeV/c and overall polarization asymmetry at 3,4 and 6 GeV/c for $p_\uparrow p \to \Delta^{++} n$.

IV. Inelastic diffraction at 6 GeV/c

The 3-body diffraction dissociation reactions have been measured at 6 GeV/c with hydrogen and deuterium targets[3]:

$$p_\uparrow p \to p\pi^+\pi^-(p) \text{ (500000 events)}, \quad (3)$$

$$p_\uparrow d \to p\pi^+\pi^-(pn) \text{ (250000 events)}. \quad (4)$$

The uncorrected mass spectra are shown in Fig.5 for two different $p_\perp^2$ regions. For $p_\perp^2 < 0.02$ GeV^2 peaks are seen at 1425 and 1660 MeV $p\pi^+\pi^-$ mass.

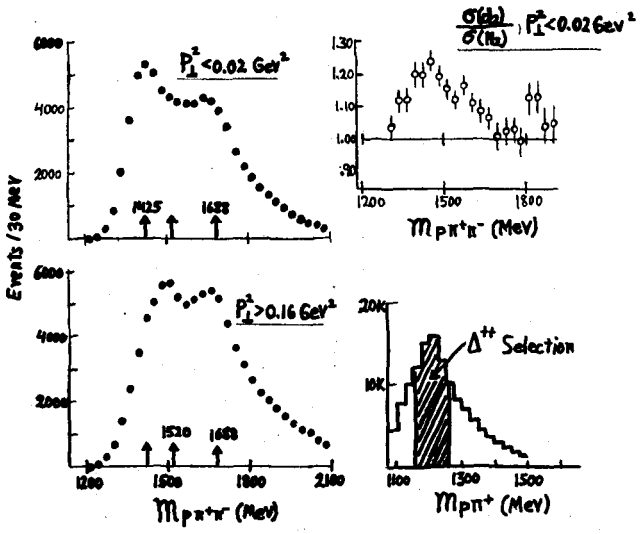


Fig. 5.
$p\pi^+\pi^-$ mass spectra from $p_\perp p \to p\pi^+\pi^- p$ for $p_\perp^2 < 0.02$ and $p_\perp^2 > 0.16$ GeV^2.

For $p_\perp^2 > 0.16$ GeV^2, the low mass peak migrates to 1500 MeV. Comparison of hydrogen and deuterium cross sections for $p_\perp^2 < 0.02$ GeV^2 reveals a considerable coherent contribution off deuterium, which has a $\sim$20% larger cross section per nucleon than hydrogen.

As in the case of π-exchange reactions discussed above, polarization effects can arise in the $\Delta^{++}\pi^-$ system from interference of partial waves having different production or decay phases. In particular, diffractive resonance production (90° production +90° decay phase) can interfere with the large S wave $\Delta\pi$ Deck amplitude (90° production). Since the dominant Deck S wave is $J^P = 3/2^-$, the only known resonant states that can produce polarization are the $J^P = 1/2^+$ and $J^P = 5/2^\pm$ states (the $3/2^-$ N*(1520) has the same J^P as the Deck amplitude and can therefore not produce polarization). The main signature of the $1/2^+$ Roper resonance is that only helicity -1/2 Δ^{++}, S can be produced in the decay $N^*(1470) \to \Delta\pi$. Selecting $p_\perp^2 < 0.12$ GeV^2, the production mechanisms should be simple (i.e. helecity conserving), and should not affect the polarization asymmetries.

The asymmetry is defined as the correlation between the proton spin vector and the $N^* \to \Delta\pi$ decay normal. Fig. 6 shows the asymmetries for helicity 1/2 and 3/2 Δ states for different $\Delta\pi$ mass intervals, plotted against the $N^* \to \Delta\pi$ decay cosine. Large asymmetries are seen for masses below 1600 MeV in the helicity 1/2 state only; the asymmetry in helicity 3/2 Δ production is large only for masses above 1600 MeV where $5/2^\pm$ resonances are important. The fact that the asymmetries are confined to helicity -1/2 Δ states suggests that the dominant interference effect is between the $1/2^+$ Roper resonance and the $3/2^-$ S-wave Deck background. The fitted curves in Fig.6 assume a constant 90° phase difference between these two waves, roughly consistent with the known slow variation with mass of the $1/2^+$ state. The measured asymmetry is consistent with a very small $1/2^+$ cross section ($\sim$5% of Deck) and a +90° phase for the $1/2^+$ production amplitude.

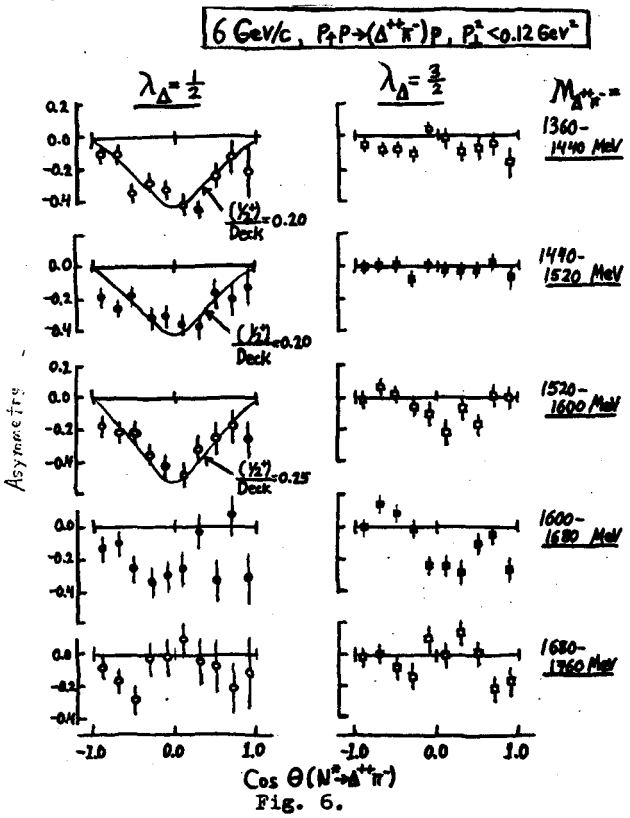


Fig. 6.
Polarization asymmetry for helicity 1/2 and 3/2 Δ states in 5 $\Delta\pi$ mass intervals, plotted against the Gottfried-Jackson $\Delta\pi$ decay cosine.

References

1. K.Abe et al., Measurement of Proton-Proton Elastic Scattering in Pure Initial Spin States at 11.75 Gev/c (Univ. of Mich. preprint submitted to this conference) 1209/A1-162.
2. R.Diebold et al., Measurement of the Proton-Neutron Elastic Scattering Polarization from 2 to 6 GeV/c, paper 1153/A1-153.
3. A.B.Wicklund et al., Study of Inelastic Reactions with a Polarized Proton Beam, paper 61/A1-61.

BARYON EXCHANGE IN 12 GeV/c $\bar{n}p$ INTERACTIONS

M.W.Arenton, W.J.Bacino, J.M.Hauptman, C.F.May, F.D.Rudnick, W.E.Slater, D.H.Stork, H.K.Ticho

University of California, Los Angeles

P.F.Shepard
University of Pittsburgh

R.A.Gearhart
Stanford Linear Accelerator Center
(present by D.H.Stork)

We report preliminary results on the production of boson states B° by baryon exchange in reactions of the type $\bar{n}p \to nB^{\circ}$ at an incident momentum of 12 GeV/c. Baryon exchange has been extensively studied in elastic scattering and charge exchange reactions. However, data on inelastic reactions at energies as high as 12 GeV/c are rare[1,2].

We have carried out this experiment by photographing the SLAC 40" hydrogen bubble chamber operating in its rapid cycling mode on detection of the energetic forward neutron. The trigger apparatus was 5 meters downstream of the chamber. The beam, bent by the bubble chamber magnet, just missed the apparatus.

The first element in the apparatus is an anticounter package of two 1.25 cm. sheets of lead and 2 scintillators to veto charged particles and photons. The remainder of the apparatus is a calorimeter. Interspersed in the front part of the calorimeter are eleven optical spark chambers. By measuring the vertex point of the hadronic shower made by the neutron as well as its production vertex in the bubble chamber the direction of the neutron is established. Events with no other neutral secondaries besides the neutron yield three constraint fits.

The calorimeter is 79 x 79 cm^2 in cross section and has 26 modules. The first 11 of these contain four gap spark chambers with lead plates. Each calorimeter had its own phototube

and a sum pulse from the calorimeter was formed electronically.

The trigger for the experiment was the simple requirement of no count in the anti-counters and a sum pulse greater than a calibrated threshold in the calorimeter. Typical running conditions were 10 expansions per second and 6 pions per pulse. The trigger rate was about 180 per hour. A total of 242,500 triggers were taken. This required 6.5×10^7 expansions of the 40" chamber.

The film was scanned for all event types. About 35,000 2-prong and 30,000 4-prong events were measured on the UCLA measuring system, MOLLY. The neutron interaction vertex in the spark chambers was reconstructed in space with standard deviation of 1.25 cm in transverse position. The measurements were processes through TVGP and SQUAW.

There are a number of corrections to the data. We assign a weight to each event equal to the inverse probability that it caused a trigger. The most important part of this weight is the triggering probability as a function of neutron momentum. We have made a cut excluding events with neutron momentum less than 7 GeV/c. This avoids events whose weight is greater than 5 and eliminates events with recoil mass ≥ 3.1 GeV.

The most fully analyzed data concern the reaction $\pi^- p \to n\pi^-\pi^+$ and we shall concentrate on it. There are 344 samples of this reaction. None of these events are ambiguous with other three constraint hypotheses. The contamination due to reactions with additional missing neutrals is estimated to be at most 10% and is flat in $\pi^-\pi^+$ mass.

Figure 1 shows the mass distribution of the $\pi^-\pi^+$ system. The mass resolution is always substantially smaller than the width of the bins. Peaks at the ρ and f masses are evident. No other structure is evident. Events that appear as a Δ^- peak in the π^-n mass plot are shown

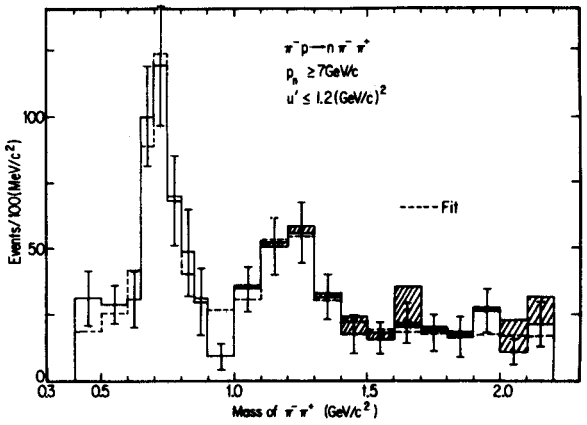


Fig. 1

cross hatched. These Δ^- events were not included in the fit to the mass distributions which was made with Breit-Wigner shapes having energy dependent widths for the ρ and f plus a constant background term.

The bin from .9 to 1.0 GeV/c^2, with only a few events, has an undue influence on the fitting procedure and was rejected. The best fit is shown in Figure 1. It has $\chi^2 = 8.0$ for 13 degrees of freedom.

The parameters of the best fit are $M_\rho = 0.716 \pm 0.007$ GeV, $\Gamma_\rho = 0.128 \pm 0.025$ GeV, $M_f = 1.204 \pm 0.017$ GeV, $\Gamma_f = 0.187 \pm 0.068$ GeV. According to the fit, the data consists of 171 ± 21 ρ's, 118 ± 27 f's and 16.5 ± 2.0 background events per 100 MeV. The widths of the ρ and f are in good agreement with the accepted values. The masses are both lower than the accepted values. This may results from low statistics and an unrealistic background treatment, but it is interesting to speculate that this may be a dynamical effect, particularly since an experiment at 6 GeV/c also finds a low ρ mass[3].

The total cross sections for $0 < u < 1.2$ (GeV/c)^2, where $u' = u_{max} - u$ are 0.61 ± 0.11 μb for ρ's and 0.49 ± 0.13 μb for f's.

The differential cross sections $d\sigma/du'$ for ρ's and f's are shown in Figure 2. We define the ρ mass range to be $0.62 \leq m_\rho \leq 0.90$ GeV and the f mass range $0.90 \leq m_f \leq 1.43$ GeV. No specific background subtraction was made in determining

the differential cross sections since the events outside of the resonant regions show similar U' dependence. However, the absolute scales of the $d\sigma/du'$ plots have been normalized to give the total cross section obtained from fitting the mass plot. The $d\sigma/du'$ distributions are consistent with simple exponentials. Least squares fits to the form $Ae^{xp}(-Bu')$ give $A=1.3\pm0.2$ μb $(GeV/c)^2$, $B=2.0\pm0.4$ $(GeV/c)^{-2}$ for ρ's and $A=1.0\pm0.3$ μb $(Gev/c)^2$, $B=1.9\pm0.4$ $(GeV/c)^{-2}$ for f's.

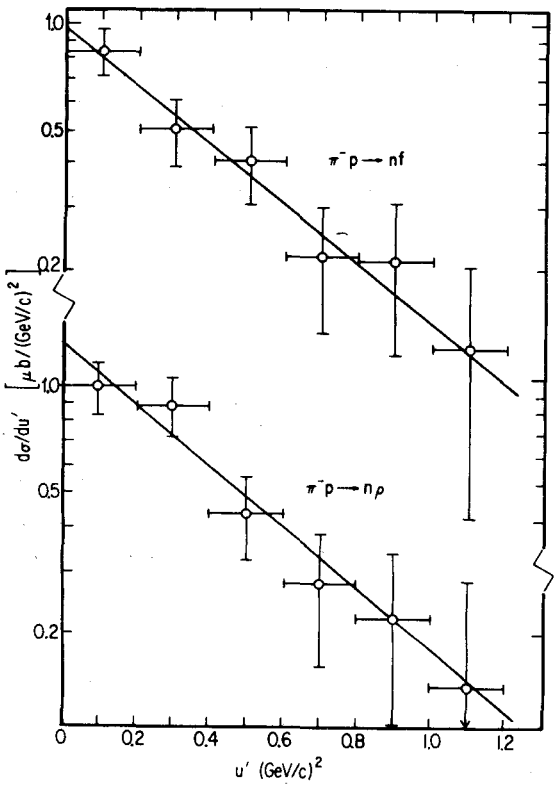


Fig.2

We may compare these results with other experiments at different energies /3-7/. Figure 3 shows the slope B of $d\sigma/du'$ plotted against s for ρ's and f's. Our experiment confirms the shrinkage of the background peaks suggested by the earlier experiments. We find that the slopes are roughly linear in $\ell n(s)$ (ignoring the point of Reference 5 for ρ's) with slope 1.4 ± 0.4 $(GeV/c)^{-2}$ for ρ's and 1.3 ± 0.4 $(GeV/c)^{-2}$ for f's. Figure 4 summarizes the intercept of $d\sigma/du'$ $(u'=0)$ for ρ production. A fit to the form s^{-n}

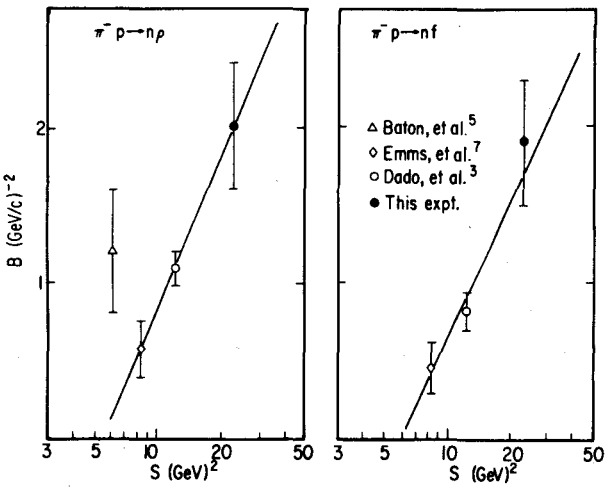


Fig.3

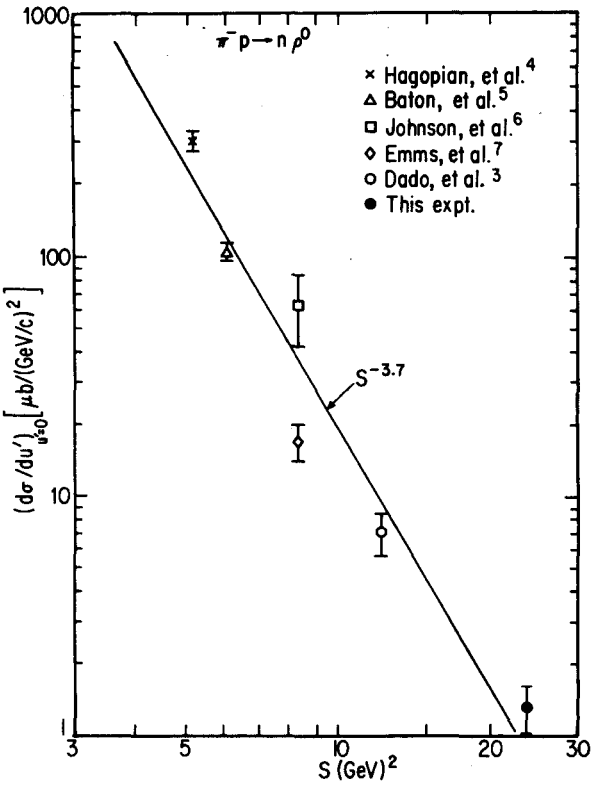


Fig.4

yields $n=3.7\pm0.1$. A fit to s^{-n} for f production in Figure 5 yields $n=3.4\pm0.3$. We note the similar s dependence for both the ρ and f. This result is striking in view of the fact that N exchange is allowed in both ρ and f production whereas exchange is allowed only in ρ production.

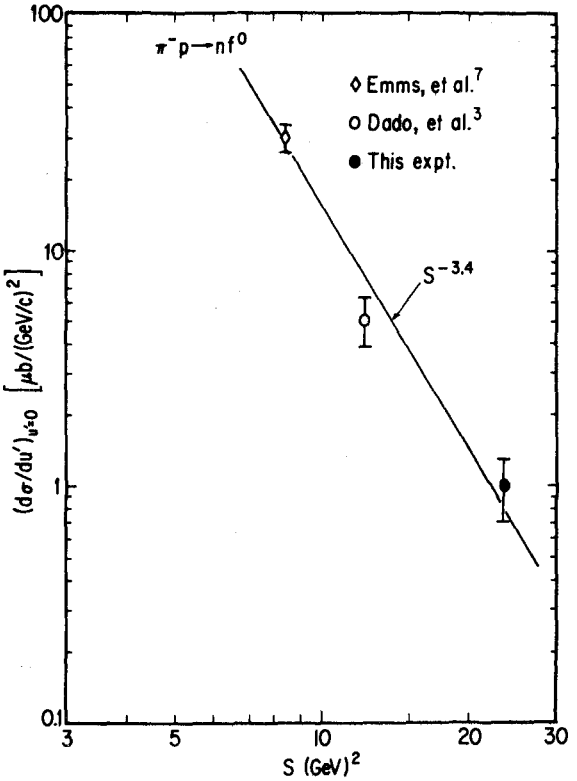


Fig.5

We thank the many people at the Stanford Linear Accelerator Center who have helped to make this experiment possible. We are expecially grateful for the helpful encouragement of Dr. J.Ballam. Gordon Bowden and the 40" bubble chamber crew made the bubble chamber an extraordinary success. Dauna Whitehead and our scanning staff deserve special acknowledgment for their efficient and dedicated work.

References

1. E.W.Anderson et al., Physical Review Letters 22, 102 (1969).
2. E.W.Anderson et al., Physical Review Letters 22, 1390 (1969).
3. S.Dado et al., Physics Letters 50B, 275 (1974).
4. S.Hagopian et al., Physical Review Letters 24, 1445 (1970).
5. J.P.Baton and G.Laurens, Nuclear Physics B21, 551 (1970).
6. P.B.Johnson et al., Physical Review 176, 1651 (1968).
7. M.J.Emms et al., Physics Letters B51, 195 (1974).

SMALL MOMENTUM TRANSFER ANTIPROTON CHARGE EXCHANGE SCATTERING ON PROTONS AT 30 GEV/C

V.V.Isakov, D.B.Kakauridze, G.V.Khaustov, V.E.Pestoev, Yu.D.Prokoshkin, A.V.Startsev

Institute for High Energy Physics, Serpukhov, USSR

The investigation of antiproton charge exchange scattering on protons

$$\bar{p}p \to \bar{n}n \qquad (1)$$

is of great interest both from the point of view of studying the energy dependence of a narrow forward peak at small momentum transfers[1-3] and a detailed study of the structure in the differential cross sections which we observed at $\bar{p}$ = 40 GeV/c[4].

It is also of interest to carry out a simultaneous analysis of reaction (1) abd cross-symmetric process

$$n + p \to p + n \qquad (2)$$

that was experimentally studied in the same energy range[5].

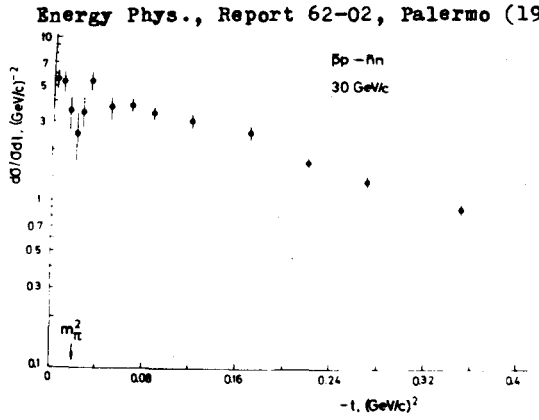
In the present work reaction (1) was investigated with 30 GeV/c antiprotons at the IHEP accelerator. The experimental set-up consisted of the same basic elements as in the earlier experiment[4]: i.e, a system scintillation and threshold Čerenkov counters used to define the beam and identify particles; a liquid hydrogen target, surrounded by a guard counter system which allowed one to suppress effectively charged particles and photons, produced from antiproton interaction in the target; a system of scintillation hodoscope counters used to determine the angle and the point of the incoming particle; a spark detector, consisting of wide-gap spark chambers, alternated by iron plates with a full thickness of 3 collision lengths or 25 radiation lengths. The spark detector was used to identify antineutrons by their nuclear interpretation in the steel plates of the spectrometer. A magnet was introduced between the target and the spark detector to deflect a charged particle beam from the spectrometer. 12 000 events of charge exchange reaction (1) were recorded in the experiment.

The angular distribution for reaction (1) obtained experimentally at p = 30 GeV/c is presented in Fig. 1. The resolution of the set-up over the 4-momentum transfer squared was better than 10^{-3}(GeV/c)^2 at $t \simeq 0$. With the growth of the error became larger: $\Delta t = 0.04\sqrt{-t}$ (in terms of (GeV/c)^2). As is seen from Fig. 1 in the range of momentum transfer $0 \leq t \leq 0.02$ (GeV/c)^2 there is a distinct narrow forward peak in the angular distribution for reaction (1). It is similar to the one observed at lower energies[1-3]. Further on with the inorease of $-t$ one reveals a new structure in the distribution, i.e., after a sharp fall of the cross section at $-t = m_\pi^2$, it starts growing again, passes the maximum at $-t \simeq 0.05$ (GeV/c)^2 and then decreases exponentially with the slope $b \simeq 7$ (GeV/c)$^{-2}$.

Thus the experiment performed by our group, confirmed the existence of a structure at small angles in the angular distribution of reaction (1) at high energies observed at p = 40 GeV/c[4]. The t-position of the dip and the second maximum in the angular distribution of the reactions observed at 30 GeV/c is the same as at 40 GeV/c.

References

1. P.Astbury et al. Phys.Lett., 23, 160 (1966).
2. W.Beush et al. XV Int. Conf. on High Energy Phys., Kiev (1970).
   W.Awood et al. Phys. Rev., 2, 2519 (1970).
3. J.G.Lee et al. Nucl.Phys., B52, 292 (1973).
4. V.N.Bolotov et al. EPS Int. Conf. on High Energy Phys., Report L-61, Palermo (1975).
5. A.Babaev et al. EPD Int. Conf. on High Energy Phys., Report 62-02, Palermo (1975).



Angular distribution for charge exchange reaction (1) at 30 GeV/c.

THE MEASUREMENT OF NUCLEON-NUCLEUS INELASTIC CROSS SECTIONS AT ENERGIES HIGHER THAN THOSE OF ACCELERATORS

R.A.Nam, S.I.Nikolsky, N.I.Starkov, V.A.Tsarev, A.P.Chubenko, V.I.Yakovlev

P.N.Lebedev Physical Institute, Moscow, USSR

The cosmic ray hadrons with 1000-30000 GeV energy were selected by the ionization calorimeter of Tien-Shan EAS complex[1]. If such hadron is not accompanied by an air shower, it is a primary proton passing through the atmosphere without inelastic collisions. The extensive air showers accompanying hadrons were detected by hodoscopic counters and scintillators. There were registered the air showers with a number of electrons at the measurement level (700 g/cm^2) more than $\sim$ 100.

The flux of surviving primary protons $I(E,x)$ is connected with the primary flux $I(E,0)$ by the relation

$$I(E,x) = I(E,0)\exp(-x/\lambda).$$

where $\lambda = A/M\,\sigma_{p\text{-}air}$, $\sigma_{p\text{-}air}$ is the nucleon - air nucleus inelastic cross section, A is the air average atomic weight, M is Avogadro number, the thickness of atmosphere x =700 g/cm^2. The primary energy spectrum of protons is established well up to energy $\sim 10^{12}$ eV [2]. The extrapolation of this spectrum in the energy region 10^{12}-10^{14} eV coincides with the energy spectrum obtained by indirect methods of the extensive air showers[3].

To compare the experimental data and the theoretical extrapolations of the total pp-cross section in high energy region we used different forms of extrapolation.

1. $\sigma_{tot} = 38.4 + 0.5\,\ln^2(s/137)$ mb [4,5]
   $\ell = 12.8$ (Gev/c)^2
2. $\sigma_{tot} = 27.2\,s^{0.06}$ mb [6]
   $\ell = 12.8$ (Gev/c)^2
3. $\sigma_{tot} = 27.1 + 1.78\,\ln s$ mb [7,8]
   $\ell = 10.9 + 0.24\,\ln s$ (Gev/c)^2

4. $\sigma_{tot} = 40.77 + 2.42 \cos(-0.1 + 0.68 \ln s) + 0.05 s^{-0.59}$
$b = 10.9 + 0.1 \ln s - 1.2 \sin(0.6 \ln s)$ $(Gev/c)^2$ /7/

5. $\sigma_{tot} = 73 - 325 / \ln(s/0.11)$ mb
$b = 8.32 + 0.57 \ln s$ $(Gev/c)^2$ /9/

Here b is the slope parameter of elastic pp-scattering differential cross section. We assume that the Glauber theory is applicable to the region of high energies with certain modifications due to inelastic shadowing account taken into consideration.

The comparison of the experimental data to the calculated curves for the different (1-5) dependences of interaction cross section on the energy can be seen in fig.1. Our experimental data for protons with energy 1500-4000 GeV are corrected on the calculated events with small shower accompaniment. This correction is shown

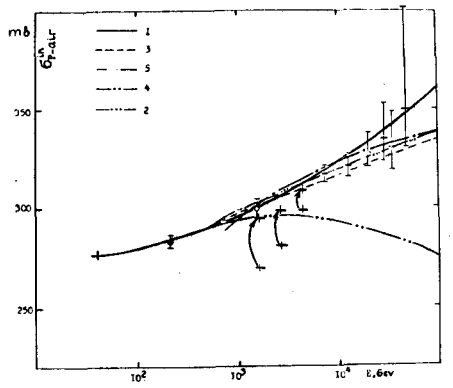


Fig.1

in the figure. Our experiment gives the proton-lead nucleus inelastic collision cross sections for different energies obtained from the distribution of the interaction points in lead absorber of the ionization calorimeter. This data (σ_{p-Pb} =1880±20 mb for $\langle E_p \rangle$ = 4500 GeV) do not contradict to the increase of inelastic collision cross section but this result is less certain than those for air because the different theoretical models are less distinguished in σ_{p-Pb}. The general result of the work is the conclusion about the increase of nucleon- nucleus inelastic collision effective cross section at the energies exceeding those of accelerators. The comparison with calculation shows that most acceptable are models with the σ_{tot} dependence of $\ln^2 s$, $\ln s$ and $s^{0.06}$ type.

References

1. T.P.Amineva, V.S.Aseykin et al. Trudy FIAN, v. 46, 157 (1972).
2. M.J.Ryan et al., Phys.Rev.Lett., v.28, N 5, 985 (1972).
3. S.I.Nikolsky, preprint FIAN No 35 (1970).
4. H.Cheng, J.K.Walker, T.T.Wu, Phys.Lett., 44B, 97 (1973).
5. L.D.Soloviev, A.V.Shelkachev, Yadernaya Fizika v.23, 636 (1976).
6. S.Y.Chu, B.R.Desai et al., preprint OCR-75-03 (1975).
7. N.P.Zotov, N.I. Starkov, V.A.Tsarev. JETP Letters 18, 460 (1973). Kratkie Soobsheniya po Fizike, N 12, 3 (1975).
8. A.J.Buras, J.Dias de Deus, Nucl. Phys. 71B, 481 (1974).
9. R.J.N.Phillps , Proc. Int. Conf. on Element. Particles, Amsterdam (1972).

ТЕОРИЯ ПОМЕРОНА С $\alpha>1$ И ДИНАМИКА ФРУАССАРОНА

К.А.Тер-Мартиросян

Институт теоретической и экспериментальной физики, Москва

Этот краткий обзор основан на работах[1,2,3] группы МФТИ-ИТЭФ-Дубна. Речь идет о теории померона с $\alpha>1$[4,5], удовлетворяющей s и t унитарности и описывающей данные опыта с малыми $p_\perp$. Идея состоит в введении P-траектории $\alpha(t)=1+\Delta+\alpha' t$, вклад которой $M_P \simeq i g_A g_B e^{(\Delta-\alpha' q_\perp^2)\xi_1}$, $\xi_1=\xi-\frac{i\pi}{2}$, $\xi=\ln\frac{s}{2m^2}$, растущий как s^Δ, сокращается в эйкональном ряде

$$M(\xi,q_\perp)\simeq i g_A^\circ g_B^\circ e^{\xi_1\Delta}\sum_{n=1}^{\infty} C_n \frac{(-z)^{n-1}}{n\,n!} e^{-\lambda q_\perp^2/n} \qquad (I)$$

вкладом последовательных перерассеяний (рис.I). Здесь $z=g_A^\circ g_B^\circ e^{\xi_1\Delta}/\lambda$, $\lambda=\alpha'\xi_1+R^2$, $g_A=g_A^\circ \exp(R_A^2 t)$, $R^2=R_A^2+R_B^2$, а $C_n=N_n^A N_n^B/(g_A^\circ g_B^\circ)^n$ – безразмерные коэффициенты. Амплитуду (I), приводящую к наблюдаемому на опыте росту σ_{tot}, переходящему во фруассаровский ход $\sigma_{tot}\sim 2\pi a_0^2\xi^2$ при $\xi \gg 1/\Delta$, будем называть фруассароном(нулевого порядка). В (I) она записана без учета усиленных графиков. Ниже показано, что

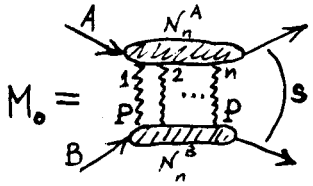


Рис.I.

(а) их учет не приводит к нарушению s-унитарности и (в) фруассарон (I) хорошо описывает все известные сейчас данные опыта.

Анализ удобно проводить в представлении прицельного параметра $\vec{b}$, характеризуя амплитуду функцией профиля рассеяния

$$F(\xi,b)=1-e^{2i\delta(\xi,b)}=\int_0^\infty \frac{2}{i} M(\xi,q_\perp) J_0(bq_\perp) q_\perp\, dq_\perp$$

Вклад померона в этом представлении $F_P=p(\xi,b)$ есть $p=z\,e^{-b^2/4\lambda}$, причем $p=1$ при $\xi>1/\Delta$ при $b=b_0$, где $b_c=a_0\xi-b_c\ln\eta_0\xi$, причем $a_0=2\sqrt{\alpha'\Delta}$, $\beta_c=\sqrt{\alpha'/\Delta}$. Фруассарон (I) имеет в нем форму

$$F_0(\xi,b)=\sum_{n=1}^{\infty}(-1)^{n-1}C_n p^n(\xi/b)/n!\simeq 1-e^{-p(\xi,b)} \qquad (2)$$

отвечающую кривой рис.2. Последнее видно из

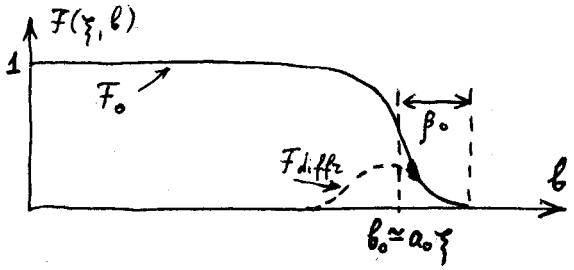


Рис.2.

анализа различных физически разумных приближений: модели эйконала, полагающей $C_n\equiv 1$ и дающей $F_0=1-e^{-p}$, или более аккуратной модели рождения резонансов при перерассеяниях на помероне, дающей $F_0=1-\sum_n B_n e^{-D_n p}$, где B_n и D_n – некоторые коэффициенты, причем $\sum_n B_n=1$ (и $\sum_n B_n D_n=1$). В общей форме: $F_0=E(p)$, где $E\to 1$ при $p\to\infty$ и $E\to p$ при $p<1$, или, как показал Карди[6],

$$F_0(\xi,b)=C_0\,\theta(b_0-b), \qquad (3)$$

если C_n в (2) являются значениями аналитической функции $C_n=C(n)$, не растущей при $n\to\infty$ быстрее экспоненты. Как видно из рассмотренных примеров, должно быть $C_c=C(0)=1$, а θ – функция должна быть "сглажена" на длине $\Delta b\sim\beta_0$.

Отметим, что пороговые особенности (при $t=-q_\perp^2\to 4\mu_\pi^2$) амплитуды немного меняют эти выводы, – в частности, профиль рис.2 на его "хвосте" (при $b\gtrsim a_0\xi$), немного изменяя величины a_0 и β_c. Однако для дальнейшего это не важно, как не важна также и явная форма функции $F_0=E(p)$, которую мы будем брать в простейшем виде $1-e^{-p}$.

Вводя все многомерные взаимодействия

$$\mathcal{L}'=\sum_{n,m}(-i)^{n+m} g_{nm}\frac{\varphi^n\bar{\varphi}^m}{n!m!}$$

и полагая, что вершины $g_{nm}=g(n,m)$ аналитичны в n, m и не растут при $n,m\to\infty$ быстрее экспоненты, получим вклад усиленного

графика рис.3 с двумя "струями" померонов в виде[6]

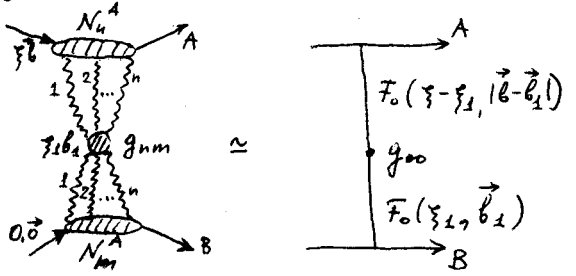


Рис.3.

$$\delta F(\xi,b) = \int \frac{d^2b_1}{4\pi} \int_0^{\xi} F_0(\xi-\xi_1, |\vec{b}-\vec{b}_1|)\, g_{00}\, F_0(\xi_1, b_1)\, d\xi_1,$$

где $g_{00} = g(0,0)$ есть константа размерности $1/см^2$. Точно также, суммируя по числам n_k померонов в каждой померонной "струе", можно определить амплитуду в виде суммы вклада всех усиленных графиков рис.4, построенных на линиях распространения фруассаронов - $F_0(\xi,b)$ и на вершинах g_{00} их взаимодействия. В каждой вершине может сходиться любое их число, причем ее вклад

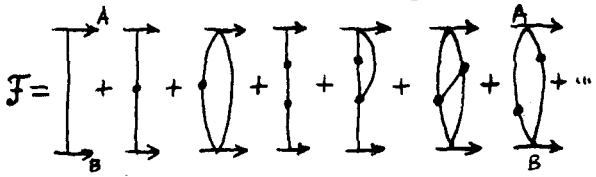


Рис.4.

остается равным g_{00} (этот результат, справедливый[6] при $\xi \to \infty$, такой же, как если бы g_{nm} имело вид $g_{00} G^{n+m}$, где G - некоторая константа). Линии двух или нескольких фруассаронов на рис. 4 не могут оканчиваться в одной точке, если они все начались в одной другой. Если бы $F_0(\xi,b)$ была θ - функцией (3) с резким краем, то вклады графиков рис.4в и рис. 4с (как и рис. 4d и рис.4е) точно взаимно сократились[6]. Фактически это сокращение происходит лишь частично и возникает задача получения вклада $F(\xi,b)$ всех "усиленных" графиков рис.4. Отметим, что этот вклад $\mathcal{F}(\xi,b)$ (точный фруассарон) удовлетворяет уравнению

$$\mathcal{F}(\xi,b) = E(V) \simeq 1 - e^{-V}, \qquad (4)$$

$$V(\xi,b) = \rho(\xi,b) + C(\xi,b) + D(\xi,b), \qquad (5)$$

где $C(\xi,b)$ - есть суммарный вклад всех графиков типа цепочки рис.5, состоящих из звеньев $Z(\xi,b)$, с числом более двух, связанных вдоль t -канала лишь вершинами g_{00}, причем $Z = F(\xi,b) - C(\xi,b)$. Через $D(\xi,b)$ обозначен вклад графиков, "неприводимых" по t- и по s-каналам,- в том смысле, что они не являются ни

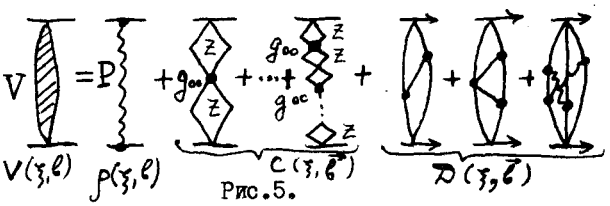


Рис.5.

цепочкой, как $C(\xi,b)$ (в t-канале), ни состоят из эйкональной цепочки, (в s-канале), составленной из других графиков. Примеры указаны на рис.5, они построены из линий точного фруассарона $F(\xi,b)$ и вершин g_{00}, в каждой из которых сходятся не менее трех линий фруассаронов. В $\omega \vec{q}_\perp$-представлении вклад цепочки $C(\xi,b) \to C(\omega,k)$ может быть выражен через точный фруассарон $F(\xi,b) \to \varphi(\omega,k)$

$$C(\omega,k) = g_{00}\,\varphi^2(\omega,k) / (1 + g_{00}\,\varphi(\omega,k)) \qquad (6)$$

Равенства (4)-(6) вместе с представлением $D(\xi,b)$ на основе правил Грибова[7] в виде вклада графиков рис.5 является интегральным уравнением для функции $\varphi(\omega,k) \to F(\xi,b)$.

Так как $C(\xi,k)$ - величина порядка g_{00}, при $g_{00} \to 0$, а $D(\xi,k)$ - порядка g_{00}^2, то при малых g_{00} решение уравнения можно получить методом итераций, полагая в нулевом приближении $g_{00} = 0$, т.е. $F \simeq F_0(\xi,b)$, где F_0 - есть функция (2), (3). При $\omega > a_0 q_\perp$ (когда важна, как можно показать, область $b \ll a\xi$) ей отвечает $\varphi_0(\xi, q_\perp) = (a_0/2)^2 / (\omega^2 + a_0^2 q_\perp^2)^{3/2}$. При подстановке в (6) это приводит к полюсу Редже у $C(\omega,k)$ при $\omega = \omega_0 = (\tilde{g}^{2/3} - a_0^2 q_\perp^2)^{1/2}$, где $\tilde{g} = (a_0/2)^2 g_{00}$. Это дает экспоненциально растущее с ростом ξ, отрицательное $C(\xi,b)$:

$$C(\xi,b) \simeq const\, \theta(b_0 - b)\, exp\left(\tilde{g}^{1/3}(\xi^2 - b^2/a^2)^{1/2}\right).$$

Это значение справедливо при $b < b_0 \simeq a\xi$, при $b > a_0 \xi$ анализ требует учета пороговых особенностей амплитуды и дает аналогичные результаты. Сравнивая это значение $C(\xi,b)$ с вкладом $\rho \sim e^{\xi\Delta - b^2/4\alpha'\xi}$ померона, получаем,

что $|C| < \rho$ в области $\ell < a_0 \xi$ при условии $\tilde{g} = (a_0/2)^2 g_{cc} < \Delta^3$, т.е. при $g_{cc} < \Delta^2/\alpha'$. При этом и $D(\xi, \ell)$ может быть вычислено на основе теории возмущений и по модулю всегда меньше, чем ρ (оно не содержит опасно растущих при $\xi \to \infty$ членов). Поэтому при $g_{cc} < \Delta^2/\alpha'$ уравнение (4)-(6) может быть решено методом итераций и его нулевым приближением, заведомо справедливым при достижимых энергиях является нулевой фруассарон $\mathcal{F} = \mathcal{F}_0(\xi, \ell)$.

Покажем кратко, что эта амплитуда (I)-(2) хорошо описывает все известные сейчас данные опыта для небольших $p_\perp$ (коэффициенты C_n можно брать в виде "квазиэйконала" $C_n \simeq C^{n-1}$ или учитывать возможность рождения резонансов при каждом перерассеянии; от выбора их результаты зависят слабо).

I) Полное сечение σ_{tot} и наклон конуса B определяются согласно (I) формулами

$$\sigma_{tot} = 8\pi \, Re\,[g_A^0 g_B^0 e^{\xi_1 \Delta} f(z)]$$

$$B = 2\, Re\,[(\alpha' \xi_1 + R^2) f_1(z)],$$

где $f(z) = \sum_{n=1}^{\infty} \frac{(-z_1)^{n-1}}{n\,n!}$, $f_1(z) = \sum_n \frac{(-z_1)^{n-1}}{n^2 n!} / f(z)$, $z_1 = C z$. Пренебрегая при $\xi > 1$ малой комплексной фазой функций f и f_1, получим

$$\sigma_{tot}' / \sigma_{tot} \simeq B'/B \simeq \Delta,$$

если $z'/z = 0$, т.е. при $\Delta = \alpha'/(\alpha' \xi + R^2)$, где штрих у σ_{tot} и B означает дифференцирование по ξ. Опыт показывает, что действительно $\sigma_{tot}'/\sigma_{tot} \simeq B'/B \simeq 0.07$ в области Батавии- ISR, где $\xi \simeq \xi_0$, $\xi_0 = 6$. Это соотношение называют геметрическим скейлингом. Таким образом, $\Delta = 0{,}07$, а $\alpha' = (\alpha' \xi_c + R^2)\Delta$, так как $\alpha' \xi_0 + R^2 \simeq B/2 f_1(z) \simeq B/2.4$ ($f_1(z)$ близко к I.I-I.2), а $B \simeq 12$-14, то $\alpha' = 5\Delta \simeq 0.35$ (Гэв/с)$^{-2}$. Так как $\alpha' \xi_c + R^2 = 5$, то $R^2 \simeq 5 - 2.5 \simeq 3$(Гэв/с)$^{-2}$, причем отношение $\sigma_{tot}/B = \mathcal{F}(z)$ определяет величину z, т.е. вычет $g_A^c g_B^c$ померона. Более точные значения Δ, α', R^2 и $\gamma_c = g_A^c g_B^c$ (вместе с параметрами f, ω, ρ, A_2 полюсов, дающих небольшие поправки), соответствующие лучшему описанию эксперимента (рис.6,7,8), указаны в табл. I.

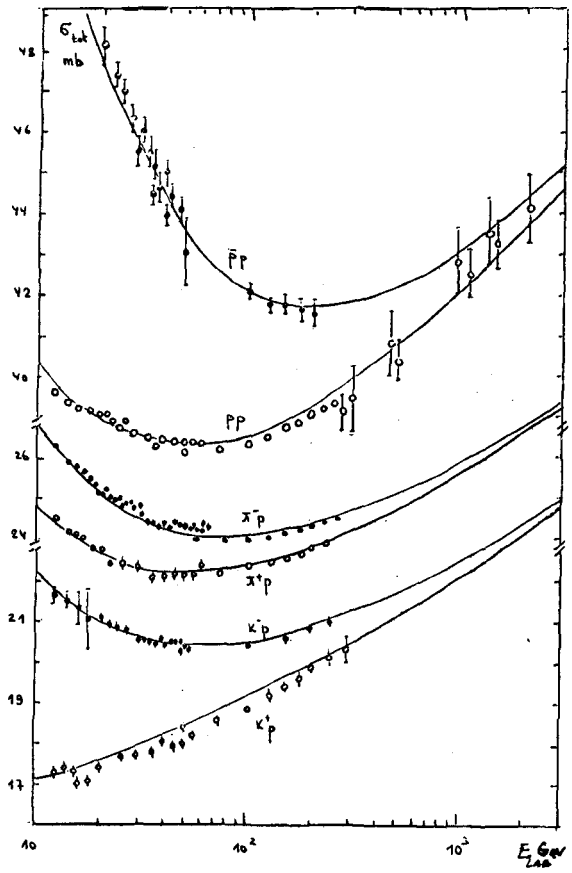


Рис.6.

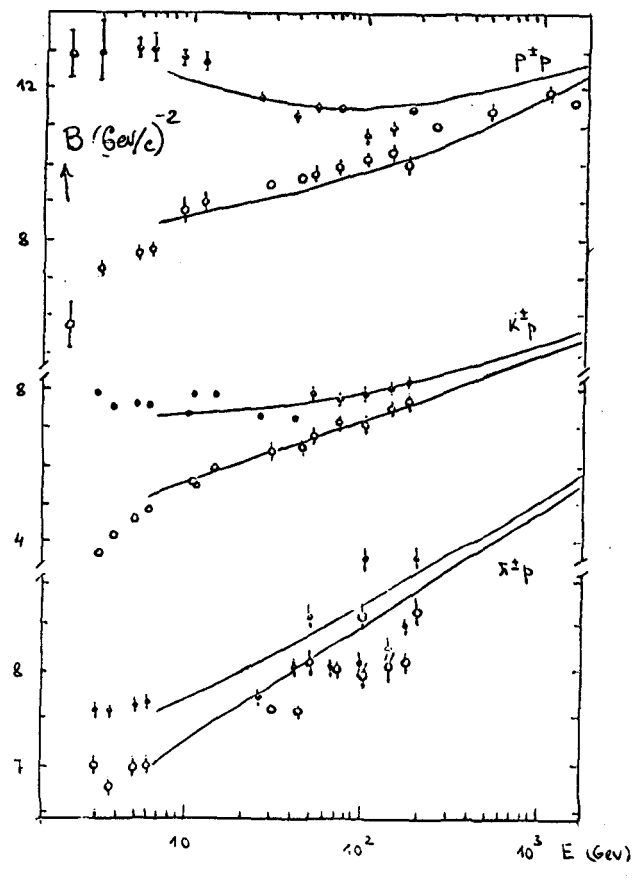


Рис.7.

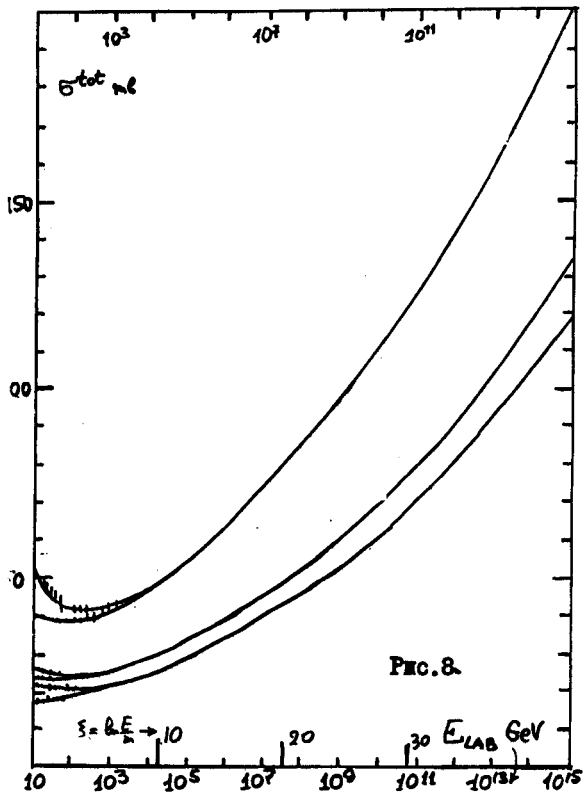


Рис.8.

Таблица I. $g_{NR}(q_\perp^2) = g_A^{(1)} e^{-R_1^2 q_\perp^2} + g_A^{(2)} e^{-R_2^2 q_\perp^2}$

$g_{Aa}(q_\perp^2) = g_{Aa}^0 e^{-R_{Aa}^2 q_\perp^2}$

$a \to$		P	f	ω	ρ	A_2
$\alpha_a(0)$		I.062	0.45	0.43	0.49	0.35
$\alpha_a'(0)$ (Gev/c)$^{-2}$		0.36	0.70	I.00	0.70	0.70
N	$g_N^{(1)}/g_N^{(2)}$	I.26/0.63	2.95	I.87	0.30	0.45
	$R_N^{(1)}/R_N^{(2)}$	2.32/-0.24	I.22	4.65	2.00	I.00
π	g_π^0	I.05	I.I4	-	I.47	-
	R_π^2	0.85	0.50	-	3.I9	-
K	$g_K^{(0)}$	0.9I	0.5I	0.50	0.75	0.60
	R_K^2	0.44	0.30	0.65	2.00	I.00

В рассмотренном варианте теории сечения $\sigma_{tot} \simeq 2\pi R_0^2$, $R_0 = a\xi$ безгранично растут при $s \to \infty$ (рис.8), показывая универсальный ход в области $\xi\Delta > 1$, для $E_{lab} \simeq 10^8$–10^{10} Гэв, где они имеют огромные значения $\sigma_{tot} \sim 100$ мбн, при этом σ_{el} также растет, $\sigma_{el} \simeq \pi R_0^2$, достигая $1/2\,\sigma_{tot}$.

2) Для описания хода $d\sigma/dt$ (рис.9) в области не очень малых t ($|t| \lesssim 1$ Gev) померонную вершину нуклона пришлось представить в виде суммы двух экспонент.

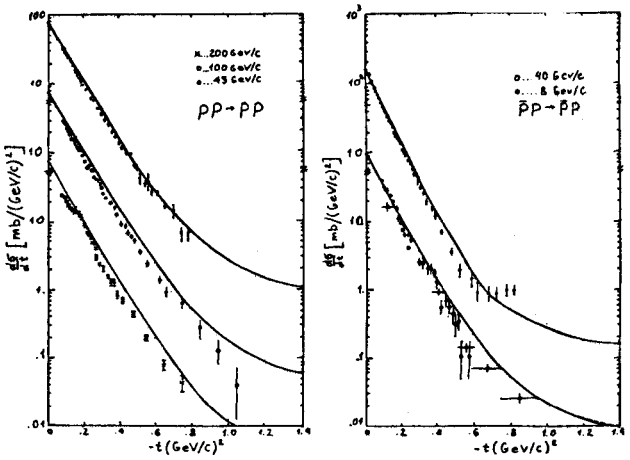


Рис.9.

3) Амплитуда процесса диффракционного рождения частиц $\mathcal{F}_{diffr} \simeq \rho(\xi, t)\, e^{-\rho(\xi t)}$ определяется кривой типа пунктира на рис.2, а его сечение отвечает площади кольца $\sigma_{diffr} \simeq 2\pi\beta_0 R_0$, т.е. должно расти при $s \to \infty$ как $\xi \simeq \ln(s/2M^2)$.

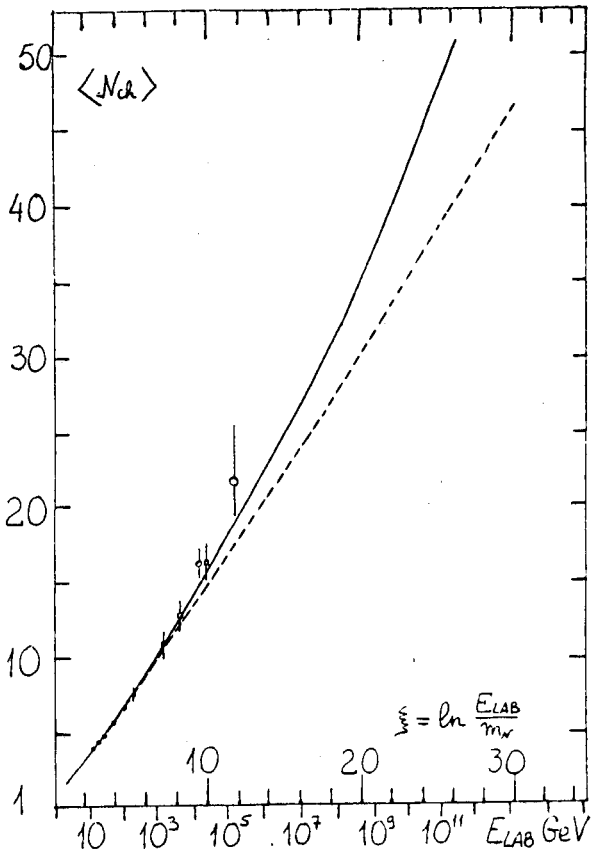


Рис.10.

4) Инклюзивное сечение $d\sigma_{incl}/dy$ и средняя множественность (рис.10) должны расти

при $S \to \infty$ по степенному закону $\sim S^{\Delta}$ — как среднее число померонов в эйкональном ряду (I)-(2).

Литература

1. M.S.Dubovikov, K.A.Ter-Martirosyan. Preprint ITEP-37, Moscow, 1976.
2. M.S.Dubovikov, B.Z.Kopeliovich, L.I.Lapidus, K.A.Ter-Martirosyan. Preprint JINR D2-9789, Dubna, 1976.
   B.Z.Kopeliovich, L.I.Lapidus, Preprint JINR, E2-9537, Dubna, 1976.
3. A.M.Lapidus, V.I.Lison, K.A.Ter-Matritosyan, P.E.Volkovitsky. Preprint ITEP 115, Moscow, 1976.
4. H.Cheng, T.T.Wu. Phys.Rev.Lett. 24, 1456, 1970.
5. A.Capella, J.Thank Tran Wan, J.Kaplan. Preprint LPTHE, Leningrad, 75/12.
6. J.L.Cardy. Nucl.Phys., B75, 413 (1974).
7. В.Н.Грибов. ЖЭТФ 53, 654 (1967).

THE DESCRIPTION OF THE LOW MULTIPLICITY REACTIONS

L.A.Ponomarev

ITEP, Moscow, USSR

I will consider briefly the theoretical description of the diffractive dissociation (DD) data in the reactions

$$a + N \to a + (N\pi), \qquad (1)$$

$$\pi^{\pm} p \to \pi^{\pm}(\Delta^{++}\pi^{-}),\ \pi^{+}p \to (\pi^{+}p^{c})p. \qquad (2)$$

As for reaction (1), the different theoretical approaches may be classified by means of Feynman graphs in Figs. 1–4.

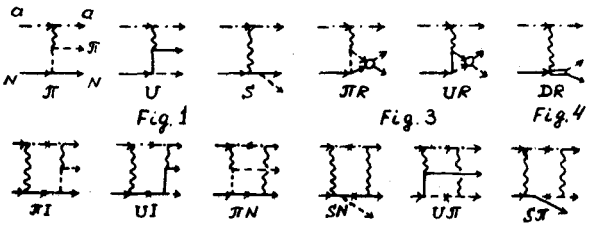


Fig. 1 Fig. 3 Fig. 4

Fig. 2

The wavy, dotted and unbroken lines correspond to the reggeon (as a rule to the pomeron), pion and nucleon accordingly. Fig. 1 contains the pion pole graph and U-channel and S-channel nucleon graphs; Fig. 2 contains rescattering graphs in onshell approximation; and Fig. 4 contains the graph which corresponds to the direct production of the resonances.

The whole amplitude containing all the mechanisms in Figs.1–4 has not been considered in the papers contributed to the Conference. But the majority of them was discussed in different papers.

The complete set of the variables is the following: M is the mass of the excited system, t is the momentum transfer to the excited system, z_t and φ_t are the cosine of the polar angle and the azimuthal angle in Gottfried-Jackson frame.

Let us consider amplitude which corresponds to the ordinary Deck mechanism and is used in the article[1]. First Deck model with reggeized pion exchange was considered by Berger[2].

The analogous model was suggested in ITEP[3].

I want to emphasize the following deficiency of this description:

a) The maximum in the mass distribution is very near to the threshold.

b) The break in the t-distribution in the region $-t \simeq 0.2 \div 0.4$ GeV^2 is absent.

c) The theoretical curves for angle distributions show no bump in the region $z_t \simeq -1$ and distribution is too asymmetrical.

Two distributions from ref.[1] are shown in Fig. 5 for example. The natural next step in

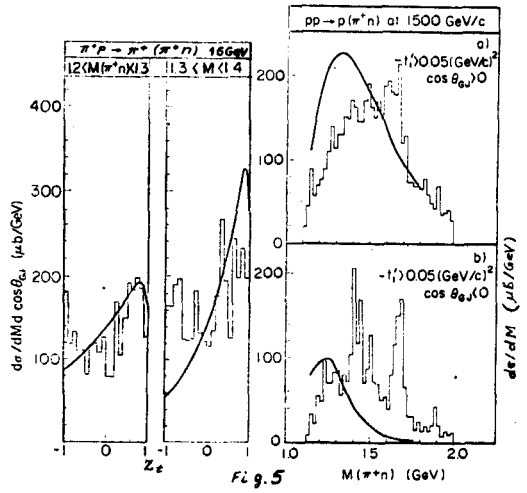
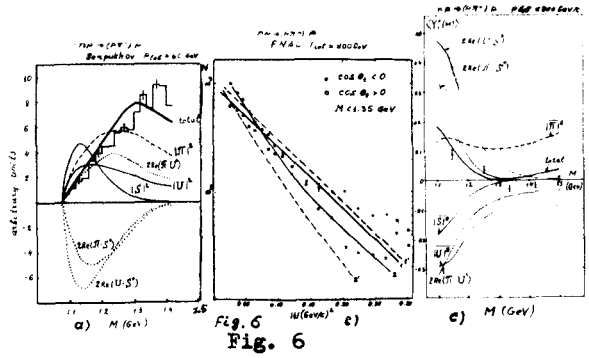


Fig. 5

the development of the DD theory is the model with all pole graphs in Fig. 1. This model without off-shell corrections was qualitatively considered in ref.[4]. In this work it was shown analytically that the differential cross section $d^3\sigma/(ds_1\,dt_1\,dt_2)$ has zero in low M and low $|t|$ region. The data (see Fig. 8a) confirm this conclusion. But our quentitative calculations in this model (see curve 2 in Fig. 8a) do not confirm this qualitative consideration. Fig. 8a shows that the theoretical cross section 3–4 times exceeds the data. To decrease the theoretical result for the absolute value of the cross section we considered this model with off-shell corrections[5]. Some distributions from this paper are displayed in Fig. 6. The conclusions from this work are:

a) The maximum from the mass distribution shifts to the high mass region in the coincidence with data. In the low mass region $M<1.3$ GeV there is large destructive interference of π and $(U+S)$ amplitudes.

b) The cross-over effect is obtained taking into account total amplitude $\pi+U+S$ only.


Fig. 6

c) It is necessary to use nucleon graphs to describe the maximum in distribution in the region $z_t \simeq -1$ and small mass of the excited system.

d) In spite of the naive expectation[7,8] in the model with spin taken into account the second bump in φ_t-distribution ($z_t \simeq -1$, $\varphi_t \simeq \pi$) is absent. This result was obtained in paper[9] in the analogous model.

e) But the absolute value of the cross section in the model keeps to exceed the data in this model.

The problem with absolute normalization may be solved by means of the rescattering graphs in Figs.2,3. First this is the model in which the amplitude without baryon exchange is considered and which was obtained by Tsarev[10] and later by Berger and Pirilä[11]. In paper[12] the model was developed which contains the amplitudes π, $\pi I + \pi N$, πK and DR with reggeized pion exchange. The comparison of this model with the data[13] is shown in Fig. 7.

The coincidence of the theory with the data is satisfactory at this energy (P_{lab}=16 GeV/c). In paper[14] the amplitude was considered which contains the amplitudes π, U, πI and UI. The off-shell correction was taken into consideration by means of the phenomenological form-factors. The coincidence of the theory and the

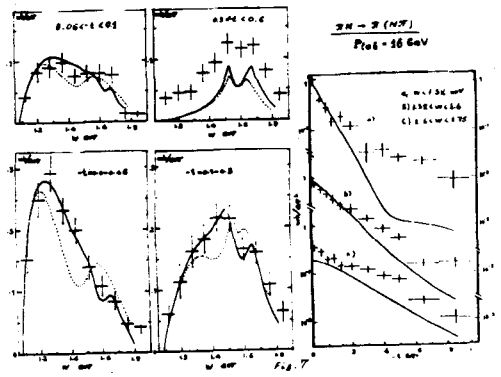


Fig. 7

data at high energies is not satisfactory. The main lack of this model is the absence of the S-channel nucleon graph and the interference terms which are rather large[5].

Let us consider the model with the amplitude $T = \pi + U + S + 2\pi I$. Factor 2 corresponds to the calculation of the amplitude πN, so $\pi I \simeq \pi N$. We can expect that the region of the applicability of our formulas is $x_t \geq 0$ (we do not consider amplitudes UI and SN) and the region of the low mass of the excited system (we do not consider amplitudes R, UR and DR). As for amplitudes $U\pi$ and $S\pi$ the estimate shows that its contribution is small. We do not consider off-shell correction in our model, so our model has no free parameters. Figures 8-9 contain the comparison of the model with ISR data[15,16]. The dotted curves in Fig. 8 correspond to the different amplitudes.

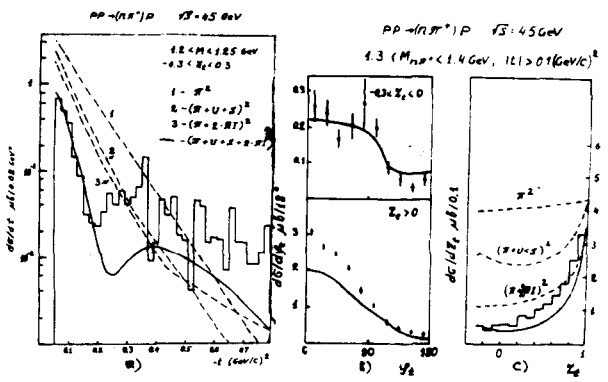


Fig. 8

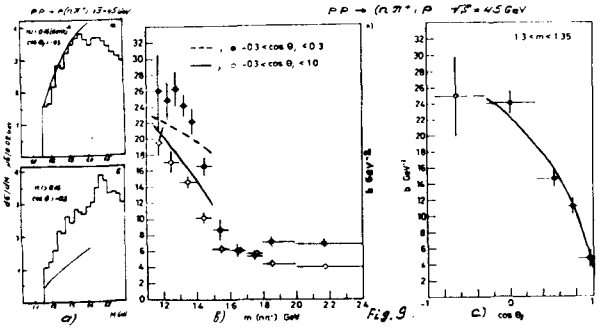


Fig. 9

Fig. 8 shows that: the absorption amplitude πI and amplitude $(U+S)$ have the same sign; the dip in $d\sigma/dt$ distribution in the region $|t| \simeq 0.2$ (Fig. 8a) may be explained only by means of the total amplitude and connects with interference term $\pi I(U+S)$.

Now I will consider briefly the reactions $\pi^+ p \to (\pi^+ \rho^0) p$ and $\pi^\pm p \to \pi^\pm (\Delta^{++} \pi^-)$. The qualitative analysis which was performed by Berger[1] predicts large contribution of u-channel graphs into these reactions (ρ exchange into $\pi^+ p \to (\pi^+ \rho^0)$ and Δ exchange into $\pi^\pm p \to \pi^\pm (\Delta^{++} \pi^-)$). But quantitative description of this reaction in the framework of the reggeized one-pion exchange model[1] shows that latter do not exceed 20%.

Conclusions:

1) There is large contribution of the different mechanisms (pion and nucleon exchange and absorption) and the interference terms in DD processes $aN \to a(N\pi)$.

2) The whole description of all phenomena in DD processes now is absent.

3) But the many characteristic features of the DD processes can be described in the simple models.

4) The contribution of the u-channel graphs into the processes $\pi^\pm p \to \pi^\pm (\Delta^{++} \pi^-)$ (Δ^{++} exchange) and $\pi^+ p \to \pi^+ \rho^0 p$ (ρ exchange) does not exceed 20%.

References

1. T.Hirose, K.Kanai and T.Kobayashi, Paper 406/A1-110, submitted to this conference.
2. E.L.Berger, Phys.Rev.Lett., 21, 701, 1968.
3. K.G.Boreskov, et al. Yad.Fiz. 15, 361, 1972.
4. F.Hayot, A.Morel, A.Stantoro and M.Souza, Paper 1211/A1-164, submitted to this conference.
5. L.A.Ponomarev, Paper 33/A1-33, submitted to this conference.
6. Babaev et al. Paper 28/A1-28, submitted to this conference.
7. J.Biel et al., paper submitted to the Palermo conference, 1975.
8. H.I.Miettinen, Plenary Session Talk on the Conference on High Energy Physics, Palermo, 1975.
9. A.Minaka, H.Sumiyoshi, M.Uehara, paper 371/A1-86, submitted to this conference.
10. V.Tsarev, Phys.Rev. D11, 1864, 1975.
11. E.L.Berger and P.Pirila, Phys.Rev., D12, 3448, 1975.
12. M.Uehara, Paper 68/A1-68, submitted to this conference.
13. H.Grassler et al. Nucl.Phys., B95, 1, 1975.
14. H.R.Gerhold, W.Majerotto, Paper 393/A1-111, submitted to this conference.
15. C.Broll, Thesis, Orsay, 1976.
16. H. de Kerret et al. Paper 65/A1-65, submitted to this conference.
17. E.L.Berger, paper 1006/A1-145, submitted to this conference, Argonne preprint ANL-HEP--PR-75-06.
18. A.N.Kamalov, L.A.Ponomarev. Papers 32/A1-32 and 1038/A1-93, submitted to this conference and ITEP preprints ITEP-8, ITEP-75, 1976.

PLENARY REPORT

BINARY AND LOW MULTIPLICITY REACTIONS

A.B.Kaidalov

ITEP, Moscow, USSR

I. Introduction

Investigation of elastic, quasi two-body and low multiplicity reactions is one of the main sources of information on the mechanism of strong interaction at high energies.

Many interesting results in this field have been obtained since the time of the London Conference. New measurements of total cross sections, real parts of forward elastic amplitudes, differential cross sections of elastic reactions in large t-interval are performed and new interesting effects are found. Sections II and III are devoted to the discussion of these results. New information on the spin effects in the elastic NN-scattering is also discussed in Section III.

Theoretical approaches to the description of two-body reactions at high energies are reviewed in Section IV.

Experimental investigations of inelastic binary reactions revealed new (sometimes puzzling) features of these processes. Charge exchange reactions and two-body resonance production are considered in Section V.

In the past few years considerable progress has been achieved in the investigation of inelastic diffractive reactions. Section VI is devoted to the discussion of new results in this field.

Nearly one hundred and seventy experimental and theoretical papers, devoted to the study of binary and low multiplicity reactions, were submitted to this Conference. Because of the limited size of this report I'll discuss only some of the new experimental results, general features, which follow from the data and shortly mention on their theoretical interpretation. I wish to appologize to all those authors whose results will be out of scope of this report.

II. Total Cross Sections and Real Parts of the Forward Elastic Amplitudes

New data on the total cross section of pp-interaction in the ISR energy range[1] are submitted to the Conference. It is well known that the substantial rise of $\sigma_{pp}^{(tot)}$ was found in the previous measurements at ISR[2]. The previous results depend on the value of luminosity L, which was measured independently. New results are obtained with increased precision ($\pm 0.6\%$) by two methods. This gives the possibility to measure $\sigma_{pp}^{(tot)}$ in a way independent of L. These results are shown in fig. 1. The new points are

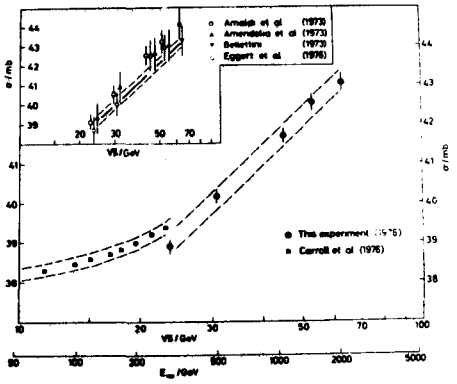


Fig. 1. $\sigma_{pp}^{(tot)}$ from paper[1] together with previous measurements[2] and FNAL data[3]. The broken lines represent the estimated scale error[1].

within the errors in an agreement with the previous data of ISR, though the new values of $\sigma_{pp}^{(tot)}$ at the highest ISR energies are systematically lower than the existed points. There is also some difference at the lowest ISR energy with the results from FNAL[3].

These measurements together with the previous results on the total cross sections of hadron-hadron interactions from FNAL[3] and Serpukhov[4] confirm the rise of all the $\sigma^{(tot)}$ at very high energies. On the other hand all the differences of particle and antiparticle total cross sections have the power law decrease with energy[3,4] in an agreement with Pomeranchuk theorem. It is of interest also to consider the energy dependences of the definite combinations of $\sigma^{(tot)}$, which correspond to the definite quantum numbers in t-channel (ρ, ω, A_2). For example

$$\Delta\sigma_{\omega}^{KN} = \frac{1}{4}\left[\left(\sigma_{K^-p}^{(tot)} - \sigma_{K^+p}^{(tot)}\right) + \left(\sigma_{K^-n}^{(tot)} - \sigma_{K^+n}^{(tot)}\right)\right]. \qquad (1)$$

The values of $\Delta\sigma_{\omega}^{NN}$, $\Delta\sigma_{\omega}^{KN}$ and $\Delta\sigma_{\rho}^{\pi N}$ are shown in fig. 2. Note the universality of the $\Delta\sigma_i$ behaviour, - the energy dependences of the contributions with the given quantum numbers are the same for different reactions. Thus for the parametrization $\Delta\sigma_i = A/p_L^{1-\alpha_i}$ the value of α_ω in NN($\bar{N}N$) interactions is $\alpha_{\omega}^{NN} = 0.435 \pm 0.02$ and $\alpha_{\omega}^{KN} = 0.45 \pm 0.03$. The values $\alpha_{\rho}^{\pi N} = 0.56 \pm 0.02$, $\alpha_{\rho}^{KN} = 0.55 \pm 0.12$, $\alpha_{\rho}^{NN} = 0.5 \pm 0.2$ are also equal within errors (α_ρ seems to be different from α_ω). It should be taken into account, that α_i are the intercepts of "effective" trajectories, which in general do not coincide with trajectories of Regge poles (because of the presence of Regge cuts). In the framework of the absorption model α_i^{eff} depend on energy (this does not contradict to the experimental data, which possibly indicate to some decrease of α_i^{eff} as energy increases) and at present energies $\alpha_i^{eff} - \alpha_i^{Pole} \sim 0.1$. So the energy dependences of $\Delta\sigma_i$ show, that absorptive effects have universal character and $\alpha_{\rho}^{Pole} - \alpha_{\omega}^{Pole} = 0.1 \div 0.15$.

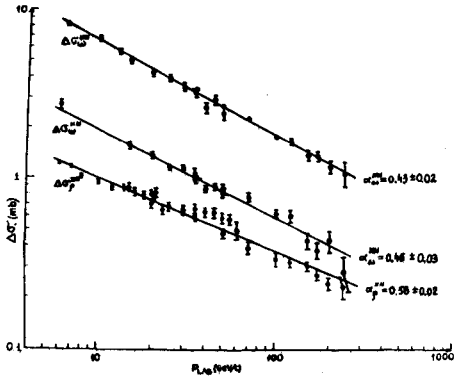
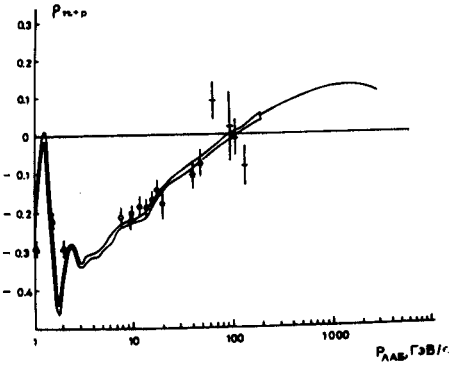
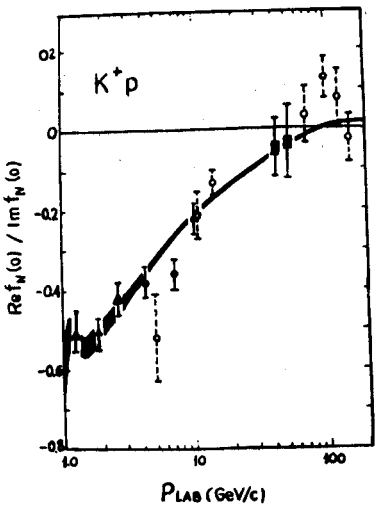


Fig. 2. $\Delta\sigma_{\omega}^{NN}$, $\Delta\sigma_{\omega}^{KN}$ and $\Delta\sigma_{\rho}^{\pi N}$ as functions of energy.

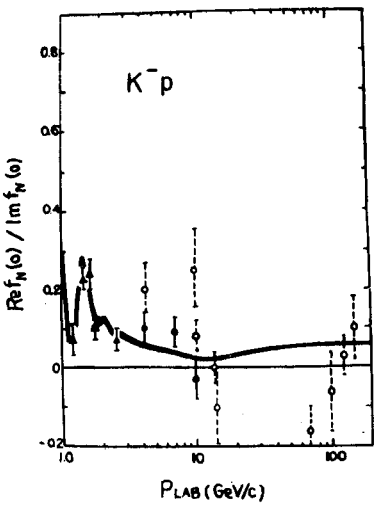
The results of the new measurements of the real parts of the forward elastic pp, $\bar{p}p$, π^+p, K^+p -scattering are submitted to this Conference[5,6]. They are shown in fig. 3a)-d) together with the other new results[7,8].



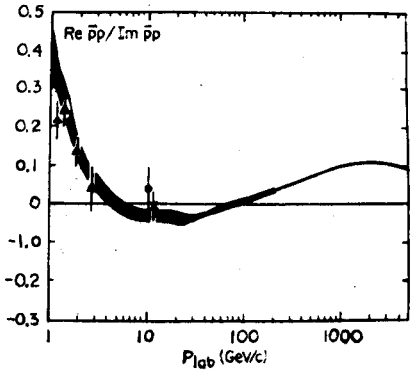
a)



b)



c)



d)

Fig. 3. $\varrho = Re\,T(s,0)/Im\,T(s,0)$ for π^+p - a), K^+p - b), K^-p - c) and $\bar{p}p$ - d). Figures taken from ref.[5-7].

Previous information on the values of $\varrho = Re\,T(s,0)/Im\,T(s,0)$ for the reactions $K^\pm p$ and $\bar{p}p$ was very limited and rather contradictory. Functions ϱ in $\pi^\pm p$ and $K^\pm p$ -scattering probably change sign and become positive at energies $E_L \approx 100$ GeV. In K^-p -soattering ϱ is positive already at low energies. The predictions of dispersion relations are also shown in fig. 3. They are in good agreement with the new experimental data.

III. Elastic Scattering at Non-Zero Angles

In the past two years experimental information on the processes of elastic $\pi^\pm p$, $K^\pm p$, pp, np and $\bar{p}p$ -scattering at high energies substantially increased[9-20] (especially in the region of $|t| > 1$ GeV^2).

Energy dependence of a diffraction slope b is shown in fig. 4 for different elastic reactions. Let us note, that the rise of the slope at $t = -0.2$ GeV^2 in pp-soattering is weaker than at $|t| < 0.1$ GeV^2 ($\alpha'(t=-0.2) = 0.13 \pm 0.02$[17] and $\alpha'(t\approx 0) = 0.278 \pm 0.024$[21]). It is well known, that there is a substantial change of slope at $t \approx -0.15$ GeV^2 in elastic pp -scattering at ISR[22]. New very accurate measurements at SLAC[12] have shown that the same structure exists in pp -scattering at energy 10 GeV. Interesting t-dependence of slopes was observed also

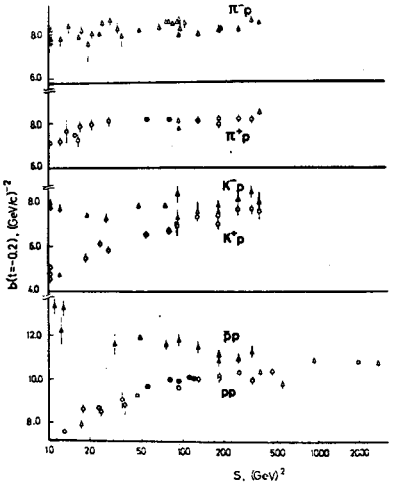


Fig. 4. The energy dependence of diffraction slope b (at $t = -0.2$). Figure taken from ref./17/.

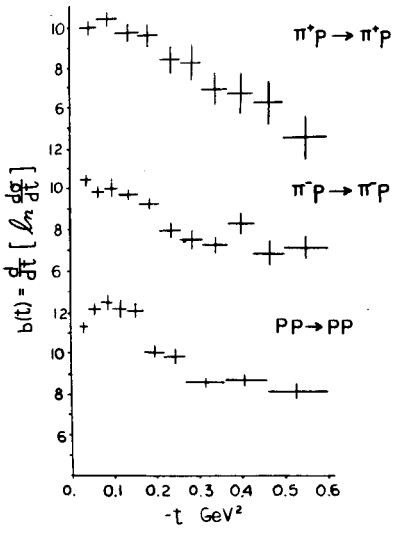


Fig. 5. The t-dependence of slopes of elastic π^+p, π^-p and pp-scattering at 200 GeV/c. Figure taken from ref./20/.

in other elastic reactions/12/. The t-dependence of slopes in $\pi^\pm p$ and pp-elastic scattering has been obtained in a high statistics experiment at 200 GeV/20/ - fig. 5. The first time the decrease of the pp-slope is observed at very small values of t. This result is important for theoretical understanding of the structure of the diffraction cone.

Another interesting effect, - small oscillation of the differential cross section of elastic pp-scattering in the diffraction peak region, was observed at 60 GeV in Serpukhov/17/. The differential cross section was fitted by the smooth curve $\left(\frac{d\sigma}{dt}\right)_{fit} = \left(\frac{d\sigma}{dt}\right)_{t=0} \exp(bt+ct^2)$ x/. The difference $\frac{d\sigma}{dt} - \left(\frac{d\sigma}{dt}\right)_{fit}$ shown in fig. 6a, indicates to the existenoe of small oscillation with the period of ~ 0.4 GeV^2 and the scale of $\approx(0.05 \div 0.1)\frac{d\sigma}{dt}$.

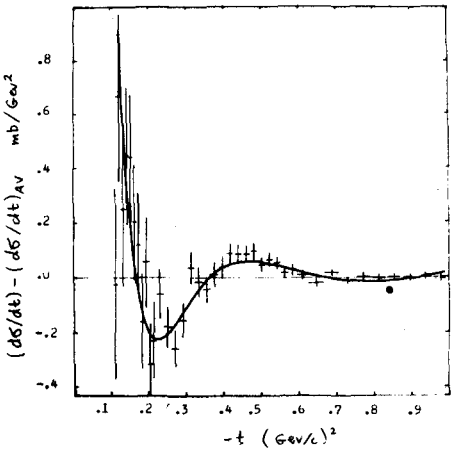
Analogous phenomenon was observed also in the processes of the elastic α-nuclei scattering in Dubna at 18 GeV/c/23/, fig. 6b)-d). Here the period of oscillation is much smaller. It means that the effect depends strongly on the radius of the system. The curves in fig. 6 are the calculations based on a simple theoretical model/24/, which predicted the existence of these oscillations (see below).

The energy dependence of elastic cross seotions at larger $|t|$ values is shown in fig. 7. The differential cross seotions of π^-p and K^+p-scattering at fixed t-values practically do not depend on energy at $E_L \geq 30$ GeV. The cross sections of pp-scattering at fixed $|t| \geq 1.2$ GeV^2 have minima in the FNAL energy range. Let us note that the elastic np-differential cross sections, measured in Serpukhov/15/ in the region $|t| < 1$ GeV^2 coincide with $d\sigma_{pp}/dt$ at the same energies, however there is clear difference in magnitude and energy dependence of $\frac{d\sigma}{dt}$ for these reactions at $|t| > 1$GeV xx/, - see fig.7c). If this observation will be confirmed by measurements of $d\sigma_{np}/dt$ at higher energies it will change the usual view, that the behaviour of $d\sigma_{NN}/dt$ in this t-range is determined by the exchange of the states with $I_t = 0$ only.

The results of the new measurements of the elastic pp-scattering at ISR in the large $|t|$ region are submitted to this Conference by CHOV group/19/. The data are obtained at $\sqrt{s} = 53$ GeV and up to $|t| \approx 9$ GeV^2, - fig. 8. The cross section has the well known minimum at $t=-(1.34\pm$

x/Other types of parametrization were also used.

xx/At lower energies $d\sigma/dt$ of np-and pp-scattering are equal within errors.



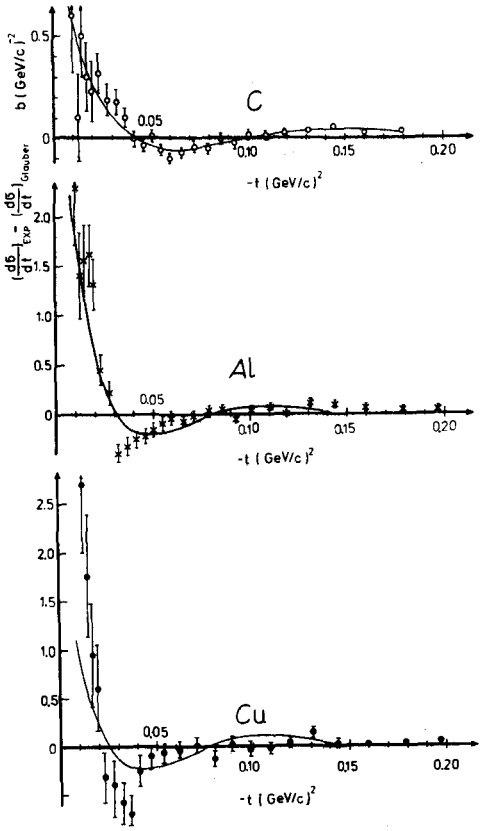
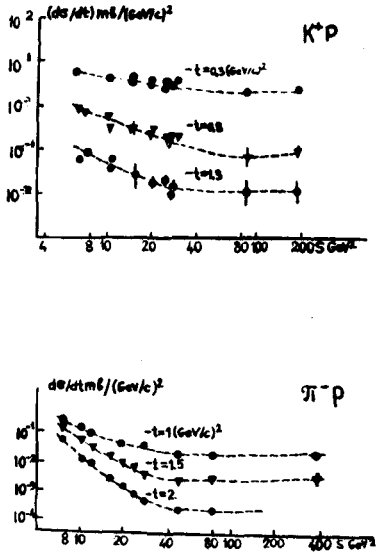


Fig. 6. The value of $d\sigma/dt - (d\sigma/dt)_{fit}$ a) in the elastic pp-scattering at 60 GeV/c[17], b),c) and d) in dA elastic scattering at 18 GeV/c[23]. Theoretical curves are from ref.[24].



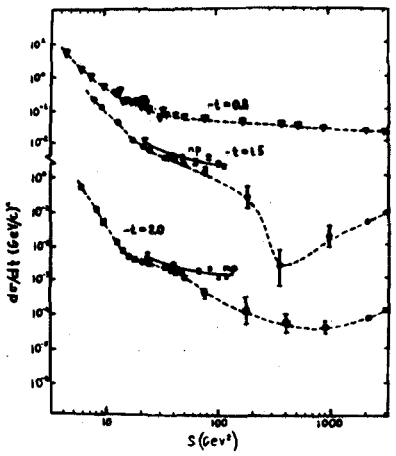


Fig. 7. Energy dependence of π^-p, K^+p and pp elastic scattering at fixed values of t. Figure taken from ref.[16], np-data[15,25]. The curves are drawn to guide the eye.

$\pm 0.02)$GeV^2, but no further minimum or change of slope is observed between 2 and 6.5 GeV^2. This result rules out a number of theoretical models, which predict the minimum of $d\sigma/dt$ in this t-range.

Spin effects in the elastic NN-scattering (and quasi two-body processes) have been studied recently in Argonne[26-29] using polarized proton

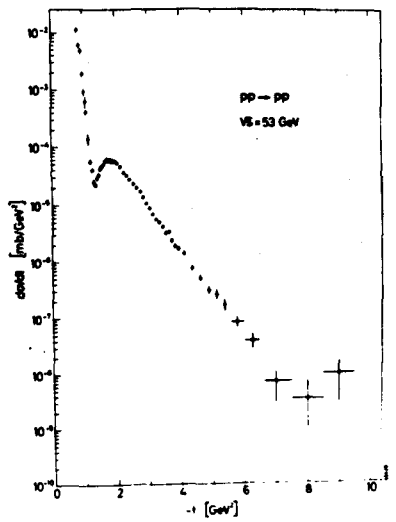


Fig. 8. Differential cross section of elastic pp -scattering at large t and $\sqrt{s}$ = 53 GeV. Figure taken from ref./19/.

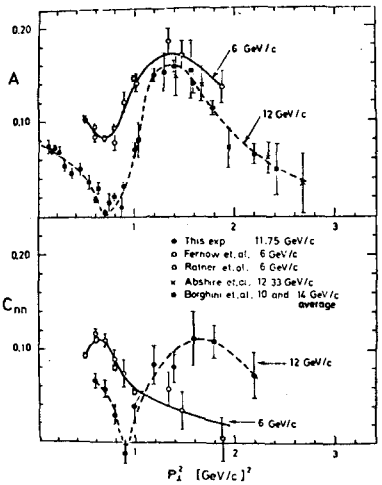


Fig. 9. Parameters A and C_{nn} for pp -elastic scattering. The curves are lines to guide the eye. Figure taken from ref./26/.

beam. The differential cross sections of the elastic pp-scattering in different spin states are measured up to an energy 11.75 GeV and the spin correlation parameter C_{nn} is determined, fig. 9. It is interesting, that in the region $|t| > 1$ GeV^2 spin effects are rather large and the parameter C_{nn} has peculiar energy dependence, - it decreases with S at $|t| < 1$ GeV^2 and increases at $|t| > 1$ GeV^2. Polarization in this last region has weak energy dependence. These phenomena are not yet explained theoretically and indicate also that the structure of NN-scattering in large $|t|$ region is more complicated, than it was previously believed.

IV. Theoretical Models

Theoretical models, used for the description of binary reactions, are based usually either on t-channel picture of the process, - the exchange in t-channel by the states with definite quantum numbers (Regge poles), or S-channel picture, - geometrical properties of the scattering or S-channel unitarity. This separation on t-channel and S-channel approaches is certainly rather arbitrary. In fact the models, which combine the features of both approaches are usually the most successful in the description of experiment. One of such examples is the absorptive Regge model/29-34/, where absorptive rescatterings in S-channel are applied to the Regge pole exchange in t-channel. The resulting amplitudes in this model have many properties, which are typical for "geometrical" models/34,35/.

The nature of Pomeranchuk singularity is the main problem for all theoretical approaches.

a) The parametrizations of elastic amplitudes.

The various phenomenological parametrization of amplitudes/34,36-38/ have been proposed for the description of elastic scattering at high energies. In the model/34/, for example, the following parametrization is used

$$T(s,t) = is\left[R_c^2 A_c e^{a_c t}\frac{J_1(R_c\sqrt{-t})}{R_c\sqrt{-t}} + R_e^2 A_e e^{B_e t} J_0(R_e\sqrt{-t})\right] \quad (2)$$

where $R_c^2 = R_{c0}^2 + R_{c1}^2(\ln s - i\pi/2)$, $R_e^2 = R_{e0}^2 + R_{e1}^2(\ln s - i\pi/2)$.

The first term in formula (2) corresponds to the "central" part of the amplitude (in the impact parameter space), and the second term to the "peripheral" or "edge" part. This parametrization gives good description of elastic processes at high energies/34/. The peripheral part in formula (2) is usually connected with the contribution of inelastic diffraction. Its

interference with central part leads to the change of slopes with t and it's square, - to the small oscillations of $d\sigma/dt$ [24]. The simple parametrization of amplitudes, which asymptotically leads to Froissart behaviour, is proposed in papers [36]. The model predicts negative value of the polarization in pp-scattering at energies larger than 200 GeV.

The assumption that Pomeron is the double pole was used for the description of elastic pp-scattering in the framework of dual approach [37,38].

Let us note that the different parametrizations of amplitudes, which differ strongly at $s\to\infty$ give a reasonable description of available experimental data on total cross sections, differential cross sections and polarizations of elastic scattering.

b) Regge Theory.

The Gribov's reggeon graphs theory [39] is the most successive approach to the problem of Pomeranchuk singularity. It gives the possibility to consider from unified point of view both binary and multiparticle processes. The question of intercept of "bare" Pomeranchuk pole $\alpha_0^P(0)$ is very significant for Regge theory. If the value of $\Delta\equiv\alpha_0^P(0)-1$ is equal to $\Delta_{crit}=\frac{\gamma_{PPP}^2}{4\alpha'_P}\ln\frac{4\alpha'_P}{\gamma_{PPP}^2}$ where γ_{PPP} is the triple Pomeron vertex, then the selfconsistent solution at $s\to\infty$ exists [40,41]. The variants of the theory with $\Delta>\Delta_{crit}$ were investigated recently [42,43]. The interest to the case $\Delta>\Delta_{crit}$ is connected mainly with two reasons: i) there are no arguments for $\alpha_0^P(0)$ to be exactly at the critical value, ii) present estimates of the $\gamma_{PPP}(0)$ from triple-Regge analysis of inclusive spectra give for Δ_{crit} the value $\approx 10^{-2}$. This shift of the bare pole is too small to explain the observed rise of the total cross sections in the framework of standard[x] approach [44]. But for $\Delta\approx 0.1$ it is possible to obtain a good description of the experimental data on the total cross sections and elastic processes in the diffractive cone region [43,44,46,47].

The hypothesis that the intercept of the Pomeranchuk pole is larger than unity and that it's eikonalization leads asymptotically to Froissart behaviour of scattering amplitudes was proposed several years ago by Cheng and Wu [48]. The most difficult problem for this approach is the question of consistency of the solution with it's iterations in t-channel and with t-channel unitarity. The first steps to the solution of this problem were made in papers [43], where the general set of reggeon graphs (fig. 10), which includes n to m Pomeron transitions, was considered under the assumption of analyticity in n,m first used by Cardy [49].

The input element in such approach is the amplitude of Fig. 10a), which corresponds to the iterations of Pomeranchuk pole in s-channel. It was shown, that the resulting system of equations

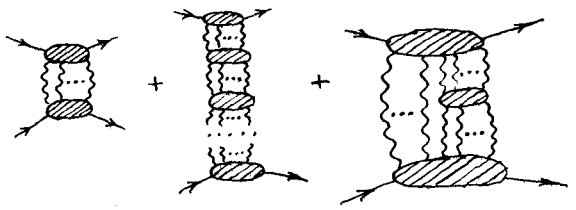


Fig. 10. Reggeon graphs considered in ref. [43].

has the selfconsistent solution (under some restrictions on the parameters of the theory), corresponding as $s\to\infty$ to the Froissart type behaviour of scattering amplitudes, - scattering on a black (or grey) disc with the radius $R\sim\ln s$. The asymptotic behaviour of scattering amplitudes in the framework of reggeon field theory with $\Delta>\Delta_{crit}$ and triple Pomeron interaction was investigated in ref. [42]. The solution again corresponds to the Froissart asymptotical regime. So it is natural to suggest that this regime is typical for a large class of Reggeon models with $\Delta>\Delta_{crit}$.

[x] In the framework of reggeon diagram approach the asymptotic formulae, which do not take into account a number of "threshold" effects, are usually used. It was shown in ref. [45], that it is possible to explain the rise of the total cross sections even in the case $\Delta=\Delta_{crit}$ taking into account these effects.

If one takes into account eikonal diagrams with the Pomeranchuk pole above one, then the elastic scattering amplitude has the well known form

$$T(s,t) = 8\pi s \int \frac{e^{2i\delta_R(s,b)} - 1}{2i} e^{i\vec{q}\vec{b}} \frac{d^2b}{2\pi}, \qquad (3)$$

$$\delta_R(s,b) = \frac{g_R(0)\,\eta(\alpha_R(0))\,(s/s_0)^{\Delta}}{16\pi R^2(s)} \exp\left(-\frac{b^2}{4R^2(s)}\right), \qquad (4)$$

where $\eta(\alpha_R(0)) = \frac{1+e^{-i\pi\alpha_R(0)}}{\sin\pi\alpha_R(0)}$, $R^2(s) = R_0^2 + \alpha_R'(0)(\ln s/s_0 - i\pi/2)$.

In contrast to the parametrization, proposed in ref.[48], the slope of Pomeranchuk trajectory α_R' is taken into account in formula (4). Because of this the value of $\delta_R(s,0) \simeq iC(1+\Delta\ln\frac{s}{s_0})/(1+\frac{\alpha_R'(0)}{R_0^2}\ln\frac{s}{s_0})$ practically does not depend on energy ($\Delta \approx \alpha_R'(0)/R_0^2$) at available energies[43] and the approximate geometrical scaling[50] takes place.

c) Geometrical Models

The geometrical and optical models were extensively investigated in recent years. After the successful application of the hypothesis of geometrical scaling to pp-scattering at ISR energies[50] it was used for the description of other processes[51-55]. This hypothesis was generalized in order to take into account secondary exchanges[52,54,55] and real parts of amplitudes[55].

The ratios $\sigma^{(el)}(s)/\sigma^{(tot)}(s)$ and $B(s)/\sigma^{(tot)}(s)$ are different for πp, Kp and pp scattering. So it is clear that not only radii, but also opacities are different in these reactions. It was shown[52,55] that the best agreement with experiment was achieved, if the function $\delta(b/R(s))$ (not $f(b/R(s))$ or $G_{in}(b/R(s))$), obtained from pp-scattering, was multiplied by the constant factor dependent on the reaction - see fig. 11.

The ratios $B(s)/\sigma^{(tot)}(s)$ for particle and antiparticle scattering are very close (fig. 12). So it was supposed in papers[35,52,55] that the whole difference between the reactions of elastic AB and $\bar{A}B$ scattering is related to the difference of interaction radii. In the framework of such models the amplitudes of secondary exchanges (ρ,ω) in impact parameter (b) space are closely related to the b-space distribution

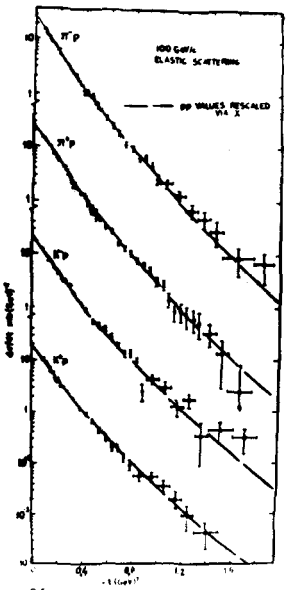


Fig. 11. Differential cross sections of $\pi^{\pm}p$, $K^{\pm}p$ scattering at 100 GeV and their description in the geometrical scaling model. Figure taken from ref.[50].

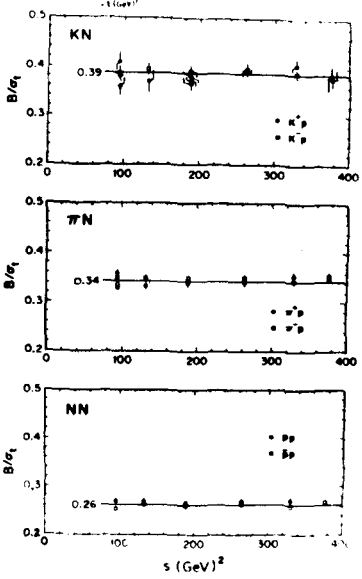


Fig. 12. Ratios $B(s)/\sigma^{(tot)}(s)$ for different elastic processes. Figure taken from ref.[50].

of the main (Pomeron) term and have the peripheral shapes[54,55]. As the functions $R_{AB(\bar{A}B)}$ depend on s, then due to the analyticity and crossing they have to contain some small imaginary parts. This approach gives a good description of elastic processes in a large energy range with a small number of free parameters[55]. In the framework of this model the differential cross section of elastic pp-scattering at the point of the minimum is proportional to the square of the real part of the amplitude at $t = 0$[55]

$$\frac{d\sigma/dt|_{t=t_{min}}}{d\sigma/dt|_{t=0}} \sim \frac{\varrho^2}{1+\varrho^2}. \qquad (5)$$

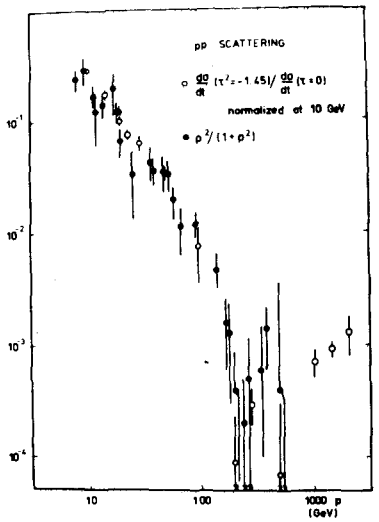


Fig. 13. The relation between $d\sigma_{pp}/dt|_{t=t_{min}}$ and $\varrho^2/(1+\varrho^2)$. Figure taken from ref./55/.

This relation agrees with experimental data (fig. 13) and relates the very pronounced dip in $d\sigma_{pp}/dt$ observed at $E_L = 200$ GeV/10/ with vanishing of ϱ in the same energy range.

The hypothesis of "b-universality" in the framework of geometrical approach leads to a simple systematics of helicity amplitudes/56,57/. The model, based on the b-universality and Regge approach, - "Reggeometry"/56/ describes successfully large class of two body processes, including meson-baryon backward scattering.

The assumption of the peripheral character of b-space distributions and of b-universality was used also for the description of inelastic diffractive processes/58-60/. The characteristic structures in t-distributions of the diffraction dissociation of nucleon (see below) actually point out to the peripheral character of these reactions. The account of absorption in the framework of Regge model for inelastic diffractive processes also leads to the peripheral b-space distributions/61,62/ (though b-universality is not valid in this model).

V. Inelastic Binary Reactions

The charge exchange reactions $\pi^-p\to\pi^0n$, $\pi^-p\to\eta n$, $\pi^-p\to\eta' n$ provide the most detailed information on the properties of the secondary (ϱ and A_2) exchanges.

The reactions $\pi^-p\to\eta n$ and $\pi^-p\to\eta' n$ [x] were studied recently in a large energy interval/63-67/. The following characteristic features of these processes are established:

a) There is a pronounced minimum in the $d\sigma/dt$ of $\pi^-p\to\eta^0 n$ at $t\to 0$, which points out to the dominant role of the spin-flip amplitude. The minimum is practically absent in the reaction $\pi^-p\to\eta' n$ /65/.

b) The effective A_2-trajectory is well determined and up to $|t|\sim 1$ GeV^2 is described by the straight line $\alpha^{eff}_{A_2}(t) = (0.426\pm0.007) + (.737\pm0.026)t$ /64/. A_2-intercept is certainly lower, than $\alpha^{eff}_{\varrho}(0)$. There is an indication to the strong curvature in A_2-trajectory at $|t|\gtrsim 1$ GeV^2.

c) There is a break at $|t|\sim 1.2$ GeV^2 in the t-dependence of the reaction $\pi^-p\to\eta^0 n$ - fig. 14 (the result is obtained in the high statistics experiment at Serpukhov at 40 GeV/c/66/). It is interesting to note, that the slope of $d\sigma/dt$ in

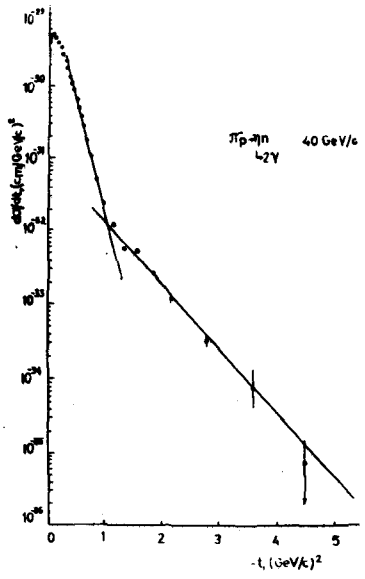


Fig. 14. Differential cross section of the reaction $\pi^-p\to\eta^0 n$ at 40 GeV/66/.

large $|t|$-region is close to one of pp-elastic scattering in the same $|t|$-range (see Sect. III), so both the phenomena may be of the same nature.

---

[x] The final results of the study of the reaction $\pi^-p\to\pi^0 n$ at FNAL energy range are discussed in the talk of A.V.Tollestrup at this Conference/63/.

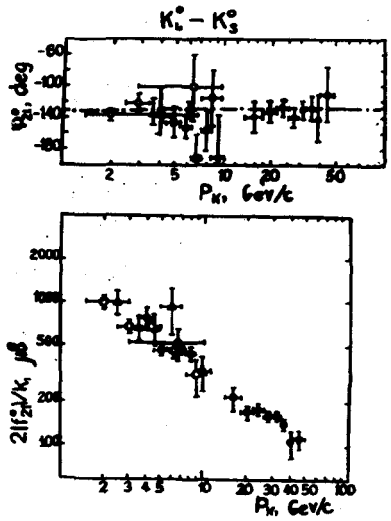


Fig. 15. Energy dependence of the phase and modulus of the amplitude of K_L^0-K_S^0 regeneration. The curve is the prediction of the model[70]. Figure taken from ref.[68].

The final results on the K_L^0-K_S^0 -regeneration on hydrogen and deuterium in the energy interval 10-50 GeV/c[68,69] show, that the modulus of the amplitude $|f_{21}|/k$ decreases with energy as $p^{-0.50\pm0.15}$ (for protons) and the phase is practically energy independent and is equal to $\varphi_{21} = -132\pm5^0$, - see fig.15. So these results are in agreement with Pomeranchuk theorem and the predictions of the models, which take into account ω, ϱ -poles and associated Regge cuts[70]. The differences of the total cross sections of $(\bar{K}^0p - K^0p)$ interaction and $(\bar{K}^0d - K^0d)$, determined from these experiments are in good agreement with the results of the measurements $(\sigma^{(tot)}_{K^-n} - \sigma^{(tot)}_{K^+n})$ and $(\sigma^{(tot)}_{K^-d} - \sigma^{(tot)}_{K^+d})$.

New interesting results on the nucleon charge exchange reactions $pn \to np$ and $\bar{p}p \to \bar{n}n$ at high energies have been obtained in the past two years[71-74]. The investigations of the reaction $pn \to np$ at $p_L \lesssim 30$ GeV/c showed, that $d\sigma/dt \sim 1/p_L^2$ and $\alpha_{eff}(t) \approx 0$ in the region $|t| < 1$ GeV^2. This result can be connected with the dominant role of the π-Regge pole and $(\pi\rho)$-cut at small t, while ϱ and A_2-exchanges are important at larger $|t|$ values. The models[34,75] predict the change in the energy behaviour at $p_L > 30$ GeV, due to the gradual increase with energy of the relative weight of ϱ and A_2-contributions.

This qualitative prediction of Regge approach is oonfirmed by the recent experimental data from Serpukhov[71] and FNAL[72], - at highest energies ($p_L \gtrsim 100$ GeV) and small $|t|$ $d\sigma/dt \sim 1/p_L$ $(\alpha_{eff} \approx 0.5)$. The quantitative agreement of the data with the predictions of the models[34,75] can hardly be considered as satisfactory[76].

Sharp minimum at $t = -\mu_\pi^2$ in the differential cross section of the reaction $\bar{p}p \to \bar{n}n$ has been found previously at energy 40 GeV[73]. The existence of the dip is confirmed by the new data of the same group at 30 GeV[74] - fig. 16.

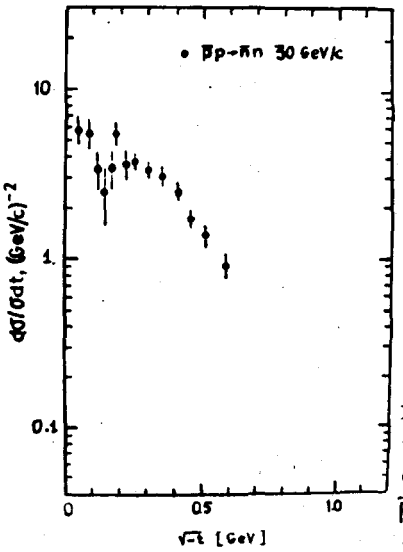


Fig. 16. Differential cross section of the reaction $\bar{p}p \to \bar{n}n$ at 30 GeV[74].

Theoretical models, mentioned above prediot the minimum in $d\sigma/dt$ at $t = -\mu_\pi^2$, but its depth and the form of $d\sigma/dt$ at small $|t|$ do not agree with the experimental data. It was pointed out in ref.[77], that this disagreement may lead to the important consequences for the theoretical approaches to the binary reactions. Further investigations of this question are needed.

The number of interesting investigations of quasi-two-body reactions is submitted to this Conference[78-95]. The detailed study of the polarizations and spin-density matrices of the produced particles and resonances and careful amplitude analysis of some reactions revealed many interesting properties of these processes. I'll briefly discuss some of them.

a) Parameters of the effective Regge-trajectories are universal, i.e., they do not depend

on the processes, from which they were determined. For example effective ϱ-trajectory, found from the reaction $\pi^+p \to \pi^0\Delta^{++}(1236)$ and ϱ-A_2 -trajectory from $\pi^+p \to \eta\Delta^{++}(1236)$ and $K^+p \to K^0\Delta^{++}(1236)$ are in good agreement with the values, found in $\pi^-p \to \pi^0 n$, $\pi^-p \to \eta n$ - fig. 17.

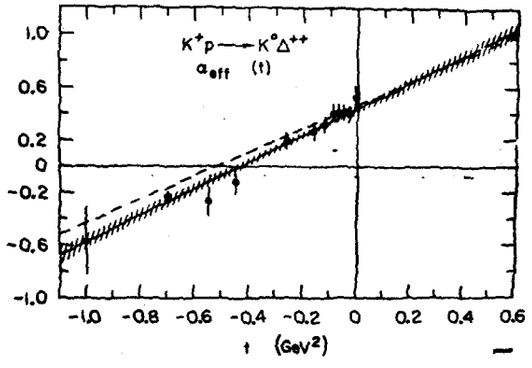


Fig. 17. Effective ϱ-A_2 -trajectory from the reaction $K^+p \to K^0\Delta^{++}$. Figure taken from ref./80/.

b) Pion Regge pole is a dominant exchange (in the reactions where it is allowed by quantum numbers) in the region of small $|t| \lesssim 0.2$ GeV^2 and intermediate energies $E \lesssim 30$ GeV. It, probably, has the same slope (~ 1 GeV^{-2}) as the other Regge-trajectories/96,97,81,95/. Amplitude analysis of the reactions $K^-p \to (K^-\pi^+)n$, $K^+p \to (K^+\pi^-)\Delta^{++}$ /81/ and $\pi^+p \to (\pi^+\pi^-)\Delta^{++}$ /91/ shows, that the contributions of the states with "natural" quantum numbers in t-channel (ϱ, A_2) are important at $|t| \gtrsim 0.3$ GeV^2 for the production of resonances with small masses ($K^*(890)$, ϱ). As the mass of the produced system increases the relative weight of these contributions as well as of $(\pi\varrho)$-cut decreases.

The first data on the quasi two-body (non-diffractive) reaction $pp \to n\Delta^{++}$ at ISR energies are submitted to this Conference by CHOV-group/93/. It decreases rapidly with energy (as $1/p^{1.94\pm0.03}$ up to $\sqrt{s} = 23$ GeV) in agreement with the dominant contribution of π-exchange. There is an indication to the slower decrease with S at highest energies. This is, possibly, connected with manifestation of ϱ , A_2-exchanges.

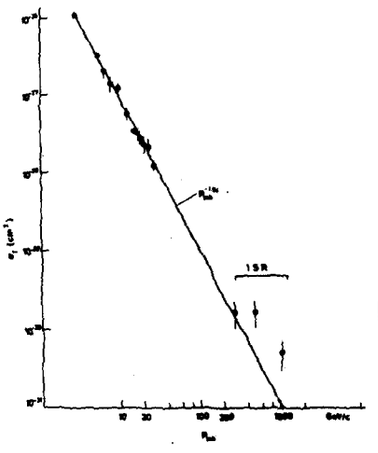


Fig. 18. The cross section of the reaction $pp \to n\Delta^{++}$ as a function of energy. Figure taken from ref./93/.

c) The existence of the exchanges with quantum numbers $\sigma P = -1$, $\sigma G(-1)^I = +1$ (σ -signature) was clearly demonstrated in high statistics experiments, - study of $\pi^-p \to \omega n$ at 6 GeV/88/ and $\pi^-p \to \varrho^0 n$ on a polarized target at 17 GeV/94/. The question of the existence of such trajectories ($\mathcal{L}$ with $\sigma=+, P=-, G=+, I=1$/98/ and A_1 with $\sigma=-$, $P=+$, $G=-$, $I=1$) is of importance for classification of particles and resonances. These results can be also explained in terms of Regge-cuts (πA_2 , $\pi\varrho$)/99/. The investigation of the energy dependence of these effects is needed to clarify the situation.

d) The predictions of the hypothesis of strong exchange degeneracy (SED) or dual diagrams are often in a clear contradiction with experimental data/83,84/ (see also/57/). For example polarizations in the reactions $\pi^+p \to K^+\Sigma^+$, $K^-p \to \pi^-\Sigma^+$/87/ which should be equal to zero, if SED is valid, reach the maximum values $|P| \approx 1$.

e) The predictions of simple additive quark model are usually in a reasonable agreement with experimental data/83,85,90/. (The deviations from quark model predictions are seen in some cases. For example in the decay angular distribution of Δ^{++} in the reaction $K^+p \to K^0\Delta^{++}$ /85/ in region of small $|t|$).

VI. Inelastic Diffractive Processes

In recent years our knowledge of inelastic diffraction was greatly improved[x] due to considerable extension of the energy range, accessible for experimental investigation and high accuracy of the data.

1). Exclusive diffractive reactions

The results of the investigation of a number of exclusive reactions with small number of particles in final states, - $NN \to N(N\pi)$ /101-105/, $\pi N \to \pi(N\pi)$ /106-108/, $K^-p \to K^-(n\pi^+)$ /113/, $\pi^\pm p \to \pi^\pm\pi^+\pi^- p$ /109/, $pp \to pp\pi^+\pi^-$ /110,111/, $\bar{p}p \to \bar{p}p\pi^+\pi^-$ /112/, $K^\pm p \to K^\pm\pi^+\pi^- p$ /113-116/ give rather complete picture of the properties of diffraction dissociation:

a) Weak energy dependence (see for example fig 19).

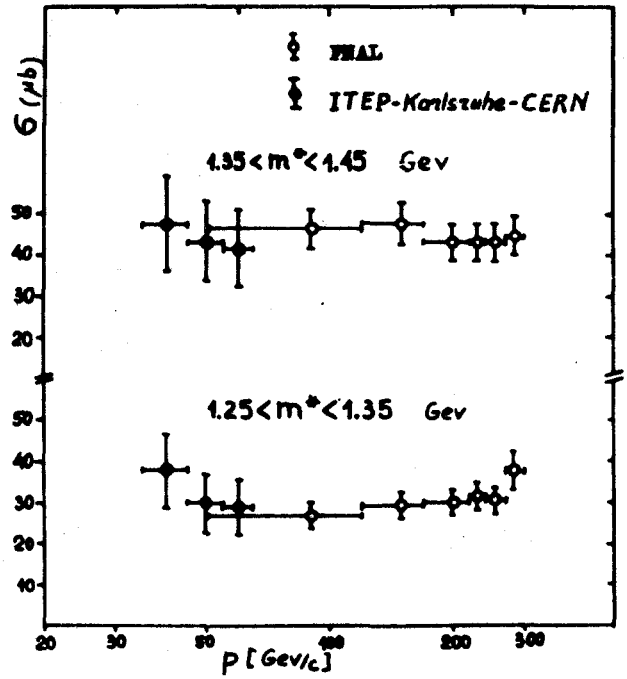


Fig. 19. Energy dependence of $d^2\sigma/dM^2dt$ of the reaction $np \to (p\pi^-)p$ /102,103/.

It is very interesting to study, whether there is a rise of $d\sigma/dM^2dt|_{t=0}$ with energy, as predicted by some theoretical models/43,48/ which describe the increase of $\sigma^{(tot)}$ (Let us note, that the increase of $d\sigma/dt$ for inelastic diffraction can happen even at higher energies, than for elastic scattering. The early rise is expected to be in the reaction $K^+p \to K^+(n\pi^+)$).

b) The mass-spectra of diffractively produced systems are concentrated in a region of rather small masses ($M \lesssim 2$ GeV). Their form depends weakly on initial energy and the type of colliding particles (see fig. 20). In the threshold region of $N\pi$-system ($M \lesssim 1.4$ GeV) the forms of the mass-spectra are determined mainly by the Drell-Hiida-Deek (DHD)-type diagrams - fig. 21a)-c) (see papers/119-123/ and the talk by L.A.Ponomarev/118/). At higher masses the contributions of resonances at M = 1.5, 1.68 and (possibly) at 2.1 GeV/c are important/101-108,113,117/. Approximate factorisation takes place.

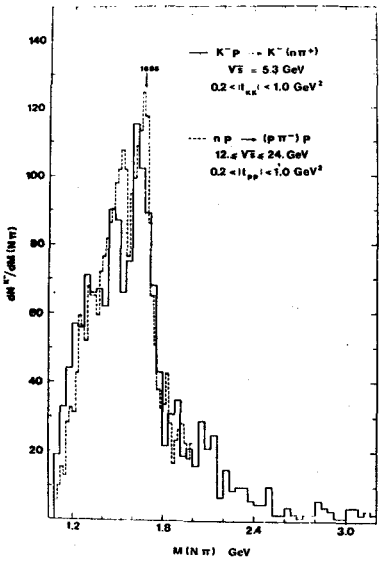


Fig. 20. The comparison of $N\pi$ - mass distributions in $K^-p \to K^-n\pi^+$ /113/ and $np \to (p\pi^-)p$ /103/. Figure taken from ref./113/

c) The momentum transfer t distributions depend strongly on mass of the produced system (slope-mass correlations). The strong dependence of the slope on the polar angle $\cos\theta_J$ (in the Gottfried-Jackson system) of the diffractively produced nucleon in the reaction $NN \to (N\pi)N$ - see fig. 22, - was discussed recently/95-97,101,112/. These correlations are partly explained by the pion exchange diagram of fig. 21a) (dashed curves in fig. 22), but much better agreement with experiment is obtained if all the diagrams

x/ Detailed discussion of some questions of the diffraction dissociation, which will be only shortly mentioned in my report, can be found in a number of reviews on this subject/100/.

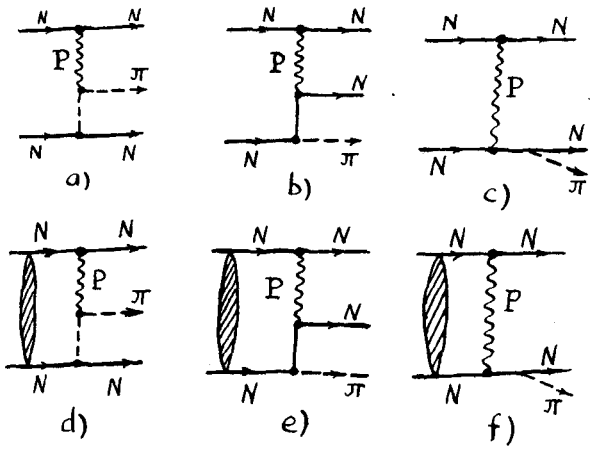


Fig. 21. The diagrams of DHD-model, -a)-c), and absorptive corrections to them -d)-f).

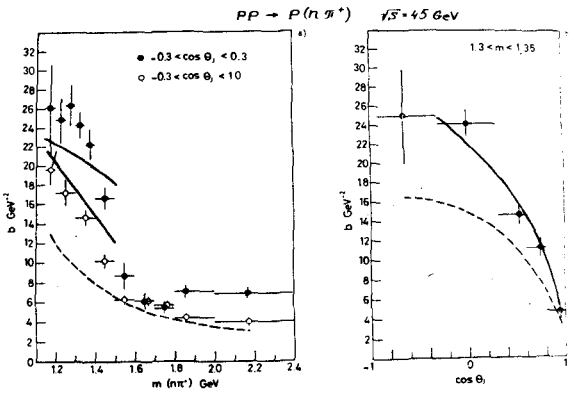


Fig. 22. The dependence of the slope b in the reaction $pp \to p(n\pi^+)$ on $M_{n\pi^+}$ and $\cos\theta_J$ /101/. The dashed curves are the results of calculations in pion Deck model. - fig. 21a). The full curves are obtained with the account of the other graphs of fig. 21 (see ref./118/).

of fig. 21 are taken into account (full curves in fig. 22/118/).

In the region of small masses of $N\pi$ and $N\pi\pi$ - systems there are dips and breaks in t-distributions. These structures depend both on mass and $\cos\theta_J$ /101,103,117/, - see for example fig.23. The dip is the most clearly seen in the region $M < 1.35$ GeV and $\cos\theta_J \approx 0$. In the framework of DHD-model such t-dependence can be reproduced only if the absorptive corrections fig.21d)-f) to the diagrams of fig. 21a)-c) are considered/118/. The structures in t-distributions

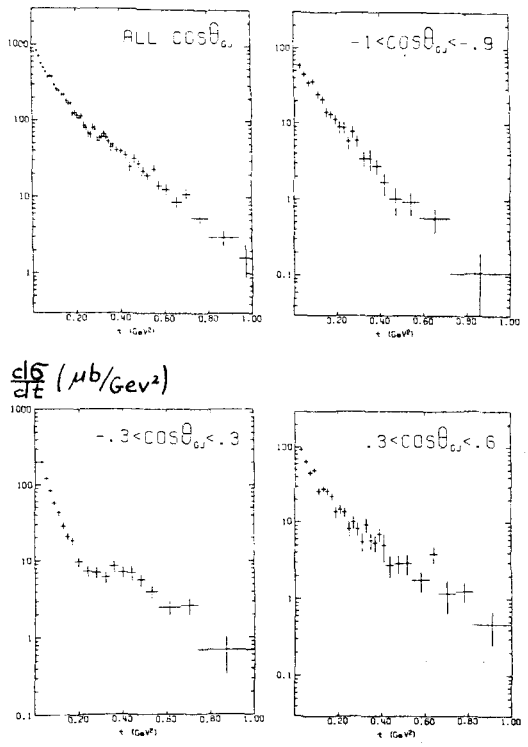


Fig. 23. The $d\sigma/dt$ in the reaction $np \to (p\pi^-)p$ for $1.35 < M_{p\pi^-} < 1.55$ GeV and different intervals of $\cos\theta_J$ /103/.

under the diffractive dissociation of nucleon are usually interpreted as a manifestation of a peripheral character of the amplitudes of inelastic diffraction in impact parameter space. But it should be noted, that there is no evidence for such a structure in the diffraction dissociation of K-mesons in the reaction $Kp \to (K\pi\pi)p$ /113/. The amplitude analysis of $(K\pi\pi)$ system/114/ shows, that there are slope-mass correlation for the diffractively produced states with given quantum numbers. These results contradict to the hypothesis of b-universality for diffractive reactions.

d) The backward peak in $\cos\theta_J$ distributions is observed in the reactions $NN \to (N\pi)N$ at high energies/101-103,117/ - fig. 24. The fact, that the peak is seen also in the region of small masses of $N\pi$-system ($M_{N\pi} < 1.4$ GeV), where the contribution of resonances is small, indicates to the important role of the nucleon exchange (fig. 21b) in the amplitudes of the

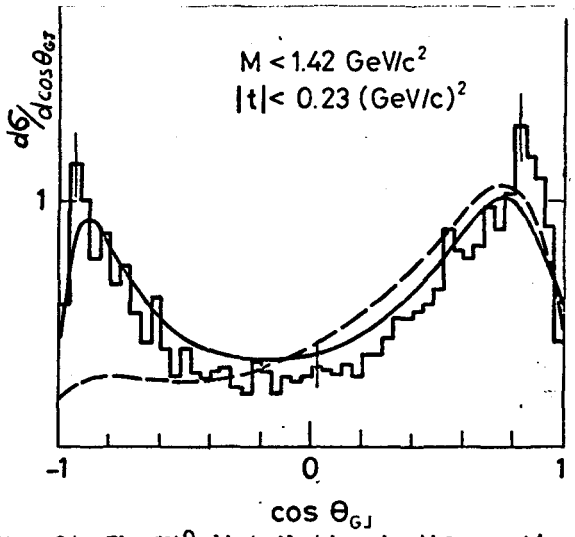


Fig. 24. The $\cos\theta_J$ distribution in the reaction $np\to(p\pi^-)p$ at 60 GeV and $M_{p\pi^-}<1.35$ GeV/102/.

diffraction dissociation of nucleon. The theoretical analysis of these reactions in the framework of DHD-model/118-123/ shows that not only t- and u-channel diagrams of fig. 21a), b) but also S-channel graph, - fig. 21c) should be taken into account in order to describe the main features of the experimental data.

e) It follows from the investigations of the azimuthal angular distributions that in the inelastic diffractive processes in general the helicity is not conserved neither in t- nor in S-channel. The DHD-models reproduce the main trends of the φ-dependence/118/.

f) The Morrison rule is violated. The amplitude analysis of the reaction $\pi N\to\pi(\pi N)$ at 16 GeV/c/106/ has shown that at low masses of πN -system the $J^P=1/2^-$ (S-wave) is diffractively produced[x/].

All these results demonstrate that the exclusive diffractive processes have very rich and interesting structure. Theoretical understanding of the correlation effects, seen in experiment, is far from being complete. The best results are obtained in the framework of DHD-model which takes into account a coherent sum of all the diagrams of fig. 21 with proper spin dependence.

9. Inclusive Diffractive Processes

The inclusive diffractive production of hadrons at high energies was investigated in past few years by many experimental groups/124-135/. The interest to these reactions is connected mainly with the discovery of the diffractive production of the high mass hadronic systems. This phenomenon is usually interpreted in terms of triple-Pomeron interaction. The phenomenological analysis allows to determine the effective triple-Pomeron coupling/136-142/, which is important for the Regge approach to high energy scattering.

I shall briefly discuss some properties of inclusive processes at high energies in the diffractive region $(M^2/s\ll 1)$.

a) The invariant inclusive cross section $\rho=Ed^3\sigma/d^3p$ of the reaction $pp\to pX$ does not depend on energy s at fixed value of x $(1-x\approx M^2/s)$ at $s>500$ GeV^2 /124/ - so within the errors of 5 - 10% scaling takes place. In the region of small $|t|$ and $x\to 1$ the spectra have pronounced peak, which is consistent with the behaviour $\rho\sim\frac{1}{1-x}$ (see fig. 25), expected for the triple-Pomeron interaction.

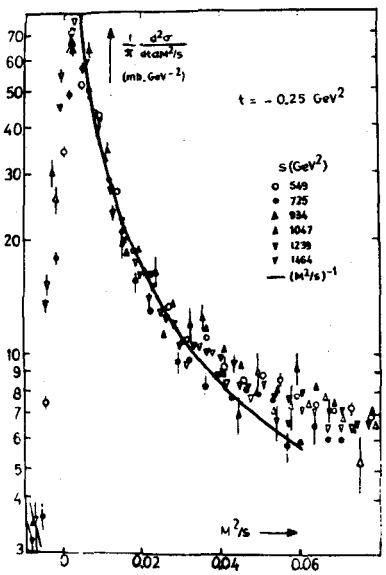


Fig. 25. The function $\rho=Ed^3\sigma/d^3p$ of the processes $pp\to pX$ at high energies. Figure taken from ref./124/.

[x/] The authors of ref./106/ used an interesting method of amplitude analysis, - the study of the interference between $I_t=0$ (diffractive) and $I_t=1$ (ρ) components in order to determine unambiguously the quantum numbers of πN -system.

b) In the region $1-x > 0.05$ there is a substantial contribution of the secondary exchanges, which leads to the slower decrease of S as $(1-x)$ increases. New data on the reaction $pd \to Xd$ are obtained at ISR with the help of deuteron beam[126] and at FNAL[125]. The spectra in this reaction have the shape, which is very similar to the one in the process $pp \to Xp$, fig. 26. (The cross section of $pp \to pX$ in fig. 26 is

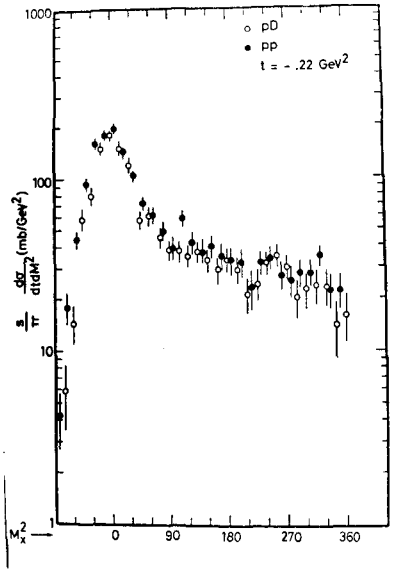


Fig. 26. The spectra in the reactions $pd \to Xd$ and $pp \to Xp$ at ISR[126].

scaled down by the measured ratio of the differential elastic cross sections). This observation can be interpreted[126] as the smallness of the contributions of exchanges with $I=1$ (which are absent in the case of the reaction $pd \to Xd$)[x].

c) The slope of t-distributions decreases with M^2 at $M^2 < 10$ GeV^2. In the region $M^2 \geq 10$ GeV^2 the slope practically does not depend on M.

d) The total cross section of inelastic diffraction σ_D rises with energy, because of the mass of the system, which can be produced diffractively, increases with S ($M^2 = \alpha S$, $\alpha \ll 1$). It is interesting to answer the question – whether the rise of σ_D can explain the rise of $\sigma_{inel}^{(tot)}$ in the ISR-energy range? The data

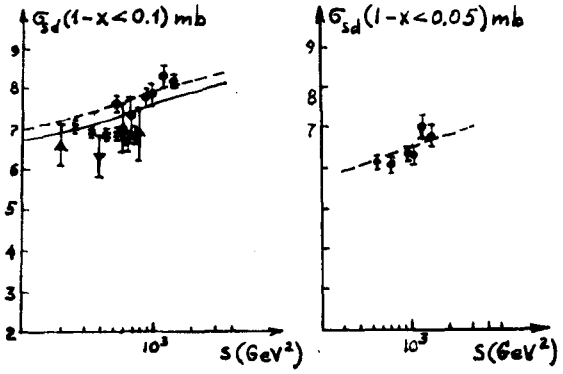


Fig. 27. The energy dependence of the cross section in the diffractive region. The curvature in t-dependence of high mass diffraction is taken into account in theoretical calculation (full curve), the same curvature is assumed to be present in low mass ($M^2 \leq 4$ GeV^2) -dashed curve.

on the energy dependence of the inclusive cross section of the process $pp \to Xp$ in the diffractive region[124] and theoretical calculations, based on the triple-Regge phenomenology, are shown in fig. 27. Both the theoretical calculation and experimental results show that the increase of σ_D in the ISR energy range is insufficient to explain all the rise of $\sigma_{inel}^{(tot)}$.

e) The processes of double diffraction excitation both in inclusive and exclusive channels were investigated recently[134,135,143,144]. These experiments demonstrated the validity of factorization in the region of $|t| < 0.5$ GeV^2. The most precise test of factorization in the double diffractive processes has been performed in ref.[135]. The reactions $pp \to pX$, $pp \to (p\pi^+\pi^-)X$ and $pp \to (\Lambda^0 K^+)X$ have been measured (X – can be either proton or some hadronic state) in the diffractive region ($1-x < 0.1$). If factorization is valid, then the ratios $R_i = \frac{d\sigma/dt(pp \to ip)}{d\sigma/dt(pp \to iX)}$ where $i = p, (p\pi^+\pi^-), (\Lambda^0 K^+)$ should be equal. It follows from fig. 28, that factorization takes place at $|t| < 0.5$. At larger values of $|t|$ there is apparent breakdown of factorization. It is interesting to note that in an agreement with factorization the mean slope of t-dependence in double dissociation processes is very small, $b = (2.2 \pm 0.2)$ GeV^{-2}[135].

[x] This statement should be taken with caution, because the spectra were compared at the same value of S, but it is more reasonable from theoretical point of view to compare the functions $d^2\sigma/dtdM^2$ at the same energy E_{LAB}.

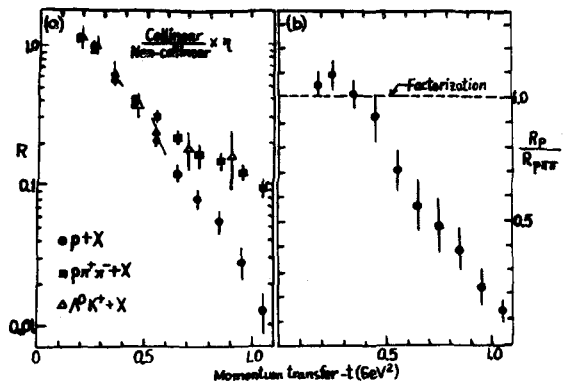


Fig. 28. Test of the factorization in the processes of double diffractive excitation. Figure taken from ref./135/.

3. Double Pomeron Exchange

The very high energies available now make possible the experimental investigation of a completely new class of diffractive processes, namely double Pomeron exchange reactions (DPE). The existence of DPE mechanism of particle production - fig. 29a) - is very natural from t-channel point of view. In the framework of Regge theory the cross section of inclusive processes $pp \to pXp$ in the DPE-region of phase space ($1-x_1, 1-x_2 \ll 1$; two large rapidity gaps, - fig. 29b)) is connected with the new quantity -

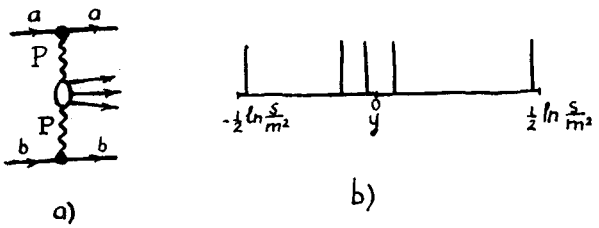


Fig. 29. a) The diagram of DPE, b) rapidity distribution of final particles, corresponding to DPE.

the total cross section of Pomeron-Pomeron interaction. The behaviour of PP-interaction (especially at small $|t_i|$ region) is of great importance for existing theoretical approaches to the scattering of hadrons at very high energies (see for example/145/).

The experimental information on the DPE/110,111,146-150/ is still rather fragmentary.

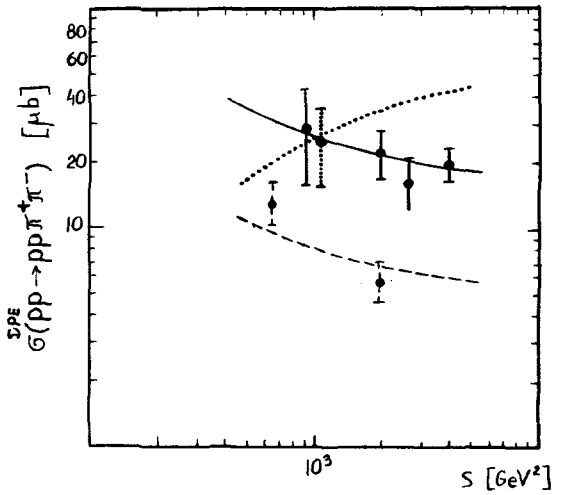


Fig. 30. The contribution of DPE to the cross section of the reaction $pp \to pp\pi^+\pi^-$. The theoretical calculation (full curves) take into account the "background" contribution and kinematical cuts of the experiments/145/.

The cross sections of DPE reactions are very small. The results of the recent experiments, performed at ISR, on the study of DPE in the reaction $pp \to pp\pi^+\pi^-$ are shown in fig. 30. Theoretical calculations/145/ are also shown in this figure. It follows from fig. 30 that: a) the absolute values of the cross sections, as well as their energy dependences, are strongly influenced by the experimental cuts, b) existing data are in an agreement with theoretical expectations. It should be noted that the "background" contribution, which is due to the "tail" of the single diffraction dissociation or in other words due to the secondary exchanges is important even in the conditions of the experiments at ISR-energies. The unambiguous evidence for DPE can result only from a detailed analysis of the energy dependence of the differential cross sections at fixed mass of the produced system/145/. More work in this direction is needed to establish reliably existence of DPE.

VII. Summary and Conclusions

1. The investigation of the total cross sections of hadronic interactions and elastic scattering at very high energies demonstrated

that the results, which follow from the basic properties of theory, dispersion relations and asymptotic theorems are in an agreement with experiment.

2. The change in the behaviour of $\sigma^{(tot)}$ and $\rho = Re T(s,0)/Im T(s,0)$ at $E \sim 100$ GeV points out that we are in a "threshold" of asymptotic region. Current theoretical models show, that the energies, where "true" asymptotic behaviour is valid, are much higher.

3. New effects are seen (probably) in elastic scattering:

a) The decrease of the pp-slope with t as $t \to 0$.

b) Small oscillations of $d\sigma/dt$ in the region of diffraction cone.

c) The increase of spin-spin correlations with energy.

d) Inequality of $d\sigma_{pn}/dt$ and $d\sigma_{pp}/dt$ at $|t| > 1$ GeV^2 and $E_{Lab} > 30$ GeV.

e) There is only one pronounced dip (at $|t| \approx$ $\approx$ 1.3GeV^2) in $d\sigma/dt$ of pp-scattering at very high energy and $|t| < 6.5$ GeV^2.

4. The nature of Pomeranchuk singularity is the main problem for theoretical approaches to high energy scattering. The models with Froissart-type asymptotic behaviour of amplitudes are on the firmer theoretical basis now and can be considered as good candidates for the description of diffraction at $S \to \infty$. Due to smallness of the $\Delta = \alpha_P(0) - 1$ the Pomeranchuk pole is still the main contribution to amplitudes at present energies.

5. Effective Regge-trajectories for secondary exchanges are universal.

6. Geometrical approaches are useful in the phenomenological analysis of two-body reactions.

7. New level is achieved in the investigation of exclusive diffraction production of particles. Interesting correlations are observed. Theoretical models reproduce some characteristic features of the data.

8. Approximate factorization takes place in diffractive processes.

9. Double Pomeron exchange is the new phenomenon and its further investigation may give new insight into properties of diffraction.

Acknowledgements

I would like to thank K.G.Boreskov, Yu.Kamyshkov, V.A.Lyubimov, L.A.Ponomarev, Yu.D.Prokoshkin, K.A.Ter-Martirosyan, P.Shelein, V.A.Tsarev, A.B.Wicklund and N.P.Zotov for valuable discussions and K.G.Boreskov for help in preparing this report.

References

1. G.Belletini et al. Conference paper. No. 1157/A1-5.
2. U.Amaldi et al. Phys.Lett., 44B, 112 (1973). S.R.Amendolia et al. Phys.Lett., 44B, 119 (1973).
3. A.S.Carrol et al. Phys.Lett., 61B, 303 (1976).
4. S.P.Denisov et al. Phys.Lett., 36B, 415 (1971); 36B, 528 (1971); Nucl.Phys., 65B, 1 (1973).
5. V.D.Apokin et al. Conference paper No. 42/A1-42.
6. R.K.Carnegie et al. Phys.Lett., 59B, 308 (1975) and Conference paper No. 290/A1-105.
7. P.Jenni et al. Nucl.Phys., B94, 1 (1975). P.Baillon et al. Nucl.Phys., B105, 365 (1976). P.Baillon et al. CERN Preprint 76-1.
8. C.Ankenbrandt et al. FERMI LAB-Conf-75/61 EXP.
9. D.S.Ayres et al. Phys.Rev.Lett., 35m 1195 (1975).
10. C.W.Akerlof et al. Phys.Rev.Lett., 35, 1406 (1975).
11. C.Baglin et al. Nucl.Phys., B98, 365 (1975).
12. R.K.Carnegie et al. Phys.Lett., 59B, 313 (1975) and Conference paper No. 266/A1-120.
13. G.Brandenburg et al. Conference paper No. 267/A1-81.
14. R.K.Carnegie et al. Conference paper No. 721/A1-124.
15. V.Bohmer et al. Nucl.Phys., B91, 266 (1975).
16. K.Bruneton et al. Conference paper No. 817/A1-123.
17. Yu.M.Antipov et al. Conference paper No. 40/A1-40.
18. N.Kwak et al. Phys.Lett., 58B, 233 (1975).
19. H. de Kerret et al. Conference paper No. 75/A1-75.

20. C.Ankenbrandt et al. Conference paper No. 1242/A1- 167.
21. V.Bartenev et al. Phys.Rev.Lett., 31, 1088 (1973).
22. G.Barbiellini et al. Phys.Lett., B39, 663 (1972).
23. V.G.Ableev et al. Conference paper No. 448/A6-5.
24. N.I.Starkov, V.A.Tsarev. JETP Letters, 23, 403 (1976); and the Talk at this Conf.
25. J.Engler et al. Nucl.Phys., B62, 160 (1973).
26. K.Abe et al. Conference paper No.1209/A1-162.
27. A.B.Wicklund et al. Paper No. 61/A1-61. and invited talk at this Conference.
28. R.Diebold et al. Phys.Rev.Lett., 35, 632 (1975) and Conference paper No. 1153/A1-153.
29. R.C.Arnold. Phys.Rev., 153, 1523 (1967).
30. G.Cohen-Tannoudji, A.Morel, Ph.Salin. Nuovo Cim., 55A, 412 (1968).
31. F.S.Henvey, G.L.Kane, J.Pumplin, M.H.Ross. Phys.Rev., 182, 1579 (1969).
32. K.A.Ter-Martirosyan. Yad. Fiz., 10, 1047 (1969).
33. A.B.Kaidalov, B.M.Karnakov. Phys.Lett., 29B, 372, 376 (1969).
34. G.L.Kane and A.Seidl. Reviews of Modern Phys., 48, 309 (1976).
35. A.B.Kaidalov. Yad.Fiz., 16, 401 (1972).
36. L.D.Soloviev. JETP Letters, 18, 455 (1973); 19, 185 (1974).
L.D.Soloviev, A.V.Shchelkachev. Conference paper No. 45/A1-45.
37. A.I.Bugrij et al. Lett.Nuovo Cim., 6, 577 (1973) and A.I.Bugrij et al. Conference paper No. 14/A1-14.
38. A.N.Wall et al. Conference paper No. 17/A1-17.
39. V.N.Gribov. JETP, 53, 654 (1967).
40. A.A.Migdal, A.M.Polyakov, K.A.Ter-Martirosyan. Phys.Lett., 48B, 239 (1974); JETP, 67, 848 (1974).
41. H.D.I.Abarbanel, J.B.Bronzan. Phys.Lett., 48B, 345 (1974); Phys.Rev., D9, 2397 (1974).
42. D.Amati, L.Caneschi, R.Jengo. Nucl.Phys., B101, 397 (1975).
V.Allessandrini, D.Amati, R.Jengo. CERN Preprint TH.2089 (1975).
D.Amati et al. CERN Preprint TH.2152 (1976).
43. M.S.Dubovikov, K.A.Ter-Martirosyan. Preprint ITEP-37, Moscow (1976) and Conference paper No. 23/A1-23.
B.Z.Kopeliovich, L.I.Lapidus. JINR, E2-9537, Dubna (1976).
M.S.Dubovikov et al. Conference paper No. 814/A1-134.
44. A.Capella, J.Kaplan. Phys.Lett., 52B, 448 (1974). A.Capella, J.Kaplan and J.Tranh Thanh Van. Nucl.Phys., B97, 493 (1975).
45. A.Capella, A.Kaidalov. CERN Preprint TH.2151 (1976).
46. P.D.Collins et al. Phys.Lett., 47B, 171 (1973); Nucl.Phys., B80, 135 (1974); B83, 241 (1974).
47. P.E.Volkovitskii, A.M.Lapidus, K.A.Ter-Martirosyan. Conference paper No. 24/A1-24.
48. H.Cheng, T.T.Wu. Phys.Rev.Lett., 24, 1456 (1970).
H.Cheng, J.K.Walker, T.T.Wu. Phys.Lett., 44B, 97 (1973) and Conference paper No. 284/A1-116.
49. J.L.Cardy. Nucl.Phys., B75, 413 (1974).
50. J.Dias de Deus. Nucl.Phys., B59, 231 (1973). A.J.Buras, J.Dias de Deus. Nucl.Phys., B71, 481 (1974).
51. W.Grein, P.Kroll. Phys.Lett., 58B, 79 (1975).
52. V.Barger, J.Luthe, R.J.N.Phillips. Nucl. Phys., B88, 237 (1975).
V.Barger, R.J.N.Phillips. Preprint RL-75-176 and Conference paper No. 310/A1-93.
53. J.Fröyland. Phys.Lett., 58B, 317 (1975); 60B, 87 (1975).
54. J.P.Ader, R.Peschanski and R.Lacaze. CERN Preprint TH 2112 (1976).
55. J.Dias de Deus, P.Kroll. Conference papers No. 388/A1-80, 389/A1-79.
56. J.P.Ader et al. Nuovo Cim., 27A, 385 (1975). J.P.Ader, Nucl.Phys., B98, 154 (1975).
57. F.Schrempp, B.Schrempp. Rapporteur Talk at the International Conference on High Energy Physics, Palermo, CERN Preprint TH.2054.
58. G.L.Kane. Acta Phys.Polon., B3, 845 (1973).
59. N.Sakai, J.N.J.White. Nucl.Phys., B59, 511 (1973).
60. S.Humble. Nucl.Phys., B86, 285 (1975).
61. V.Tsarev. Phys.Rev., 11D, 1864, 1875 (1975).
62. E.L.Berger, P.Pirila. Preprint ANL-HEP-PR-75-27 (1975); and Conference paper No. 56/A1-56.
63. A.V.Barnes, D.J.Millema, A.V.Tollestrup et al. Conference paper No. 967/A1-128 and invited talk of A.V.Tollestrup at this Conference.
64. M.H.Shaevitz et al. Phys.Rev.Lett., 60B, 117 (1975) and Conference paper No. 405/A1-99.
65. K.W.Edwards et al. Conference paper No. 403/A1-101.
66. W.D.Apel et al. Conference paper No. 1164/A1-67.
67. O.I.Dahl et al. Conference paper No. 968/A1-129.
68. V.K.Birulev et al. Conference paper No. 18/A1-18.
69. K.F.Albrecht et al. Conference paper No. 12/A1-12.
70. V.I.Lisin et al. Nucl.Phys., B40, 298 (1972).

71. A.Babaev et al. CERN Preprint (1975).
72. H.R.Barton et al. Conference paper No. 1234/A1- 165.
73. V.N.Bolotov et al. EPS International Conference on High Energy Physics, rep. L-61 Palermo (1975).
74. V.V.Isakov et al. Conference paper No. 39/A1-39.
75. K.G.Boreskov, S.T.Sukhorukov, K.A.Ter-Martirosyan. Yad.Fiz., 21, 825 (1975).
76. A.Bouqet et al. Conference papers No. 797/A1-88, 798/A1-89.
77. E.Leader. Phys.Lett., 60B, 290 (1976).
78. J.N.Carney et al. Conference paper No. 62/A1-62.
79. D.C.Colley et al. Conference paper No. 881/A1-137.
80. G.W.Brandenburg et al. Conference paper No. 288/A1-105.
81. G.W.Brandenburg et al. Conference paper No. 282/A1-119, and Phys.Lett., 59B, 405 (1975).
P.Estabrooks et al. Phys.Lett., 60B, 473 (1976); SLAC PUB 1730.
82. B.Chaurand et al. Conference paper No. 70/A1-70.
83. M.Aguilar-Benitez et al. Conference paper No. 294/A1-87.
84. Amsterdam-CERN-Nijmegen-Oxford Collab. Conf. paper No. 300/A1-133.
85. - " - No. 293/A1-140.
86. - " - No. 298/A1-141.
87. - " - No. 301/A1-127.
88. M.H.Shaevitz et al. Phys.Rev.Lett., 36, 8 (1976) and Conference paper No. 404/A1-100.
89. R.Honecker et al. Conference paper No. 48/A1-48.
90. H.Grässler et al. Conference paper No. 49/A1-49.
91. Aachen-Berlin-Bonn-CERN Coll.Conference paper No. 51/A1-51.
92. M.W.Arenton et al. Conference paper No. 794/A1-112.
93. N.Kwak et al. Conference paper No. 76/A1-76.
94. H.Becker et al. Conference paper No. 795/A1-132.
95. V.N.Bolotov et al. Conference paper No. 44/A1-44.
96. K.G.Boreskov, A.B.Kaidalov, L.A.Ponomarev. Preprint ITEP-950 (1972).
97. P.Estabrooks, A.D.Martin. Phys.Lett., 42B, 229 (1972).
98. A.C.Irving. Nucl.Phys., B105, 491 (1976).
99. N.N.Achasov et al. Conference paper No. 4/A1-4.
100. G.Goggi. CERN Preprint (1975).
M.Derrick. ANL-HEP-CP-75-52.
D.W.G.S.Leith. SLAC-PUB-1646 (1975).
H.I.Miettinen. Preprint CERN TH.2072 (1975).
A.B.Kaidalov, V.A.Khoze. Preprint LIYF-193 (1975).
101. H. de Kerret et al. Conference paper No. 65/A1-65.
102. A.I.Babaev et al. Conference paper No. 29/A1-29.
103. J.Biel et al. Conference papers No. 909/A1-8, 69/A1-69.
104. CERN-Pavia-Zurich Collab., Conference paper No. 338/A1-102.
105. V.Bakken et al. Conference paper No. 74/A1-74.
106. Aachen-Berlin-Bonn-CERN Collab. Conference paper No. 52/A1-52.
107. J.Ballam et al. Conference paper No. 1260/A1-143.
108. V.Kistiakowsky et al. Conference paper No. 742/A1-113.
109. Aachen-Berlin-Bonn-CERN-Cracow-Heidelberg Collab., Conference paper No. 1156/A1-157.
110. M.Della Negra et al. Conference paper No. 128/A1-85.
111. H. de Kerret et al. Conference paper No. 77/A1-77.
112. France-Soviet Union and CERN-Soviet Union Collab. Conference paper No. 1036/A1-142.
113. Saclay-Ecole Polytechnique-Rutherford Collab. Conference papers No. 72/A1-72, 73/A1-73.
114. R.K.Carnegie et al. Conference paper No. 287/A1-117.
115. Brussels - CERN - Mons - Serpukhov Collab. Conference paper No. 46/A1-46.
116. France-Soviet Union and CERN-Soviet Union Collab. Conference papers No. 38/A1-38, 1165/A1-121.
117. Yu. Kamyshkov. Talk at this Conference.
118. L.A.Ponomarev. Talk at this Conference and Conference paper No. 32/A1-32, 34/A1-34, 1038/A1-94.
119. F.Hayot et al. Conference paper No. 1211/A1-164.
120. M.Uehara. Conference paper No. 68/A1-68.
121. A.Minaka et al. Conference paper No. 371/A1-86.
122. T.Hirose et al. Conference paper No. 406/A1-110.
123. H.R.Gerhold, W.Majerotto. Conference paper No. 393/A1-111.
124. M.G.Albrow et al. Nucl.Phys., B72, 376 (1976) and Conference paper No. 799/A1-90.
125. Yu.Akimov et al. Phys.Rev.Lett., 35, 763 (1975) and talk by S.V.Mukhin at this Conference.
126. J.C.M.Armitage et al. Conference paper No. 345/A2-74.

127. R.D.Schamberger et al. Phys.Rev.Lett., 34, 1121 (1975); and preprint
128. J.M.Chapman et al. Phys.Rev.Lett., 32, 257 (1974).
129. S.J.Barish et al. Phys.Rev.Lett., 31, 1080 (1973).
130. F.T.Dao et al. Phys.Lett., 45B, 399 (1973).
131. ACGHT Collab., Nucl.Phys., B79, 1 (1974).
132. Rutgers-Imperial College Collab. Phys.Rev. Lett., 31, 1527, 1530 (1973).
133. M.G.Albrow et al. Nucl.Phys., B102, 275 (1976).
134. R.Webb et al. Phys.Lett., 55B, 331, 336 (1975).
135. W.Lockman et al. Conference paper No. 1210/A1-163.
136. A.B.Kaidalov et al. JETP Letters, 17, 626 (1973); Phys.Lett., B45, 493 (1973).
137. A.Capella. Phys.Rev., D8, 2047 (1973).
138. D.P.Roy, R.G.Roberts. Nucl.Phys., 77B, 240 (1974).
139. R.D.Field, G.C.Fox. Nucl.Phys., B80, 367 (1974).
140. A.B.Kaidalov, K.A.Ter-Martirosyan. Nucl. Phys., B75, 471 (1974).
141. Yu.M.Kazarinov et al. JINR, E2-9218, Dubna (1975) and Conference paper No. 1015/A1-151.
142. T.Inami, R.G.Roberts. RL-75-025.
143. L.Baksay et al. Phys.Lett., 53B, 484; 55B, 491 (1975).
144. M.Cavalli-Sforza et al. Nuovo Cimento Lett., 14, 345, 353, 359 (1975).
145. A.B.Kaidalov. Theoretical Introduction to Double Pomeron Exchange. In the Summary of the 18th ISR Discussion Meeting between Experimentalists and Theorists. CERN/TH.
146. L.Baksay et al. Phys.Lett., 61B, 89 (1976).
147. D.Denegri et al. Nucl.Phys., B98, 189 (1975).
148. M.Derrick et al. Phys.Rev.Lett., 32, 80 (1974).
149. B.Musgrave. ANL-HEP-CP-75-31.
150. L.A.Didenko et al. Conference paper No. 6/A1-6.

PARALLEL SESSION ON MULTI-PARTICLE PRODUCTION AND INCLUSIVE REACTIONS

NEW RESULTS FROM FERMILAB ON HADRON PRODUCTION IN INCLUSIVE HADRON-HADRON INTERACTIONS

E.W.Beier
University of Pensylvania, U.S.A.

In this report I will discuss recent results from FNAL from three experiments on single particle inclusive hadron-hadron interactions. All the experiments measure the cross sections for the reactions

$$a + p \rightarrow c + X \ ,$$

where a and c are charged hadrons $(\pi^{\pm}, K^{\pm}, p^{\pm})$ and X represents undetected particles.

A Fermilab-Northeastern-Northern-Illinois collaboration[1] has studied the processes

$$pp \rightarrow \begin{Bmatrix} \pi^{\pm} \\ K^{\pm} \end{Bmatrix} + X$$

at incident momenta of 200 and 400 GeV/c. The spectrometer utilizes two half quadrupoles and multiwire proportional chambers to measure the momentum and angle of the secondary particle, and scintillation and Cherenkov counters to measure the secondary particle type. The kinematic region covered by the spectrometer is

$$-1.0 \leq X_{\parallel} \leq 0$$
$$0.3 \leq p_{\perp} \leq 1.0 \ \text{GeV/c} \ .$$

The objective of the experiment is to measure the single particle invariant cross section, $E\frac{d^3\sigma}{d^3p}$ at fixed S and especially at large X, and to study the S dependence at large X.

The cross sections for π^+ and π^- production by 200 and 400 GeV/c protons is shown in Fig.1a as a function of the radial scaling variable $X_R = (X_{\parallel}^2 + X_{\perp}^2)$ at fixed $P_{\perp} = 0.5$ GeV/c. The absolute normalization of this preliminary result is not yet available, but the relative normalization is correct to ±10 per cent. In fig.1b the ratio of these cross sections at 200 and 400 GeV/c is displayed. Although the cross sections vary by almost four decades over the range of X_R, it is seen that scaling holds to about ±10 per cent up to $X_R \simeq$ ≃ 0.9. The authors report further that for $K^{\pm}$ production scaling is valid to within ± 20 per cent to $X_R \simeq 0.8$.

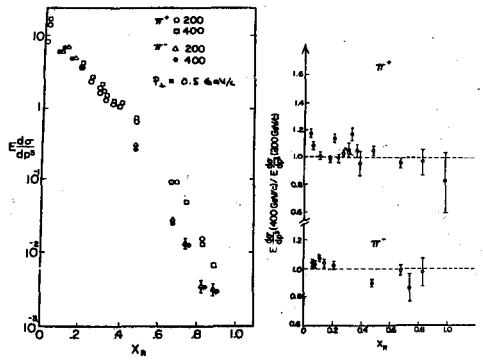


Fig.1a,b

The University of Pennsylvania group[2] with which I am associated has measured the cross sections for the reactions

$$\begin{Bmatrix} \pi^{\pm} \\ K^{\pm} \\ p^{\pm} \end{Bmatrix} + p \rightarrow \begin{Bmatrix} \pi^{\pm} \\ K^{\pm} \\ p^{\pm} \end{Bmatrix} + X$$

as a function of S over a fixed region of phase space in the fragmentation region of the target proton. The spectrometer consists of a small dipole magnet and multiwire proportional chambers to measure the momentum and angle of the secondary particle and scintillation and Cherenkov counters to measure the particle type. The spectrometer measures particles in fixed angle and momentum intervals in the laboratory corresponding approximately to $p_{\perp} \simeq 0.3$ GeV/c and $y_{LAB} \simeq 0.6$, 0.4 and 0.2 for produced π, K and p respectively. Incident momenta of 4.6, 8, 10, 12, 15, 20 and 24 GeV/c were measured at Brookhaven and incident momenta of 150 and 250 GeV/c were measured at Fermilab.

The objective of the experiment is to fit the measured cross sections to the form $A + BS^{1/2}$ or $A + BS^{-1/2} + CS^{-1}$ as suggested by Mueller-Regge theory, and then to extrapolate to $S^{-1/2} = 0$ to test the factorization of the Pomeron trajectory. Pomeron factorization requires that for incident particle types a and a':

$$\frac{E\frac{d^3\sigma}{d^3p}(ab \rightarrow c)}{E\frac{d^3\sigma}{d^3p}(a'b \rightarrow c)} \underset{S \rightarrow \infty}{=} \frac{\sigma_{tot}(ab)}{\sigma_{tot}(a'b)} \ .$$

The measured cross sections, integrated over the acceptance of the spectrometer, are shown for π^-, π^+, K^+ and p production in Fig.2.

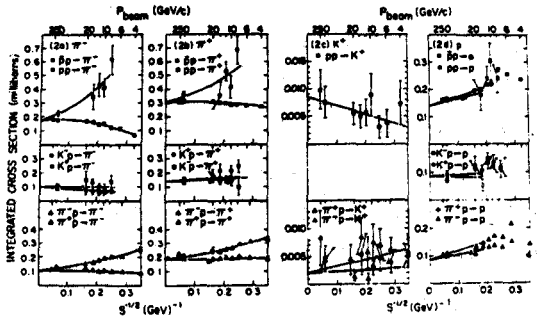


Fig. 2

The ratios of the intercepts at $S^{-1/2}=0$ are given in Table 1 where the quantity $\Delta\sigma$ is the invariant cross section integrated over the spectrometer acceptance. We conclude from Table 1 that Pomeron factorization holds quite well.

Table 1

	Particle type $C=\pi^-$	$C=\pi^+$	$C=p$	$\sigma_{tot}(aC)/\sigma_{tot}(a'C)$ Diffractive part
$\frac{\Delta\sigma(\bar{p}p\to C)}{\Delta\sigma(pp\to C)}$	0.63±0.03	0.62±0.03	0.62±0.03	0.61±0.03
$\frac{\Delta\sigma(Kp\to C)}{\Delta\sigma(pp\to C)}$	0.60±0.06	0.45±0.04	0.61±0.08	0.53±0.02

The Fermilab single Arm Spectrometer[3] Group has measured inelastic diffractive scattering in conjunction with their measurements of elastic scattering. The reaction studied is $a+p\to a+X$, where $a=\pi^{\pm},K^{\pm}$ and $p^{\pm}$. The high resolution spectrometer covered the kinematic range

$$0.7\le x_{\parallel}\le 1.0$$

$$0.05\le|t|\le 0.7$$

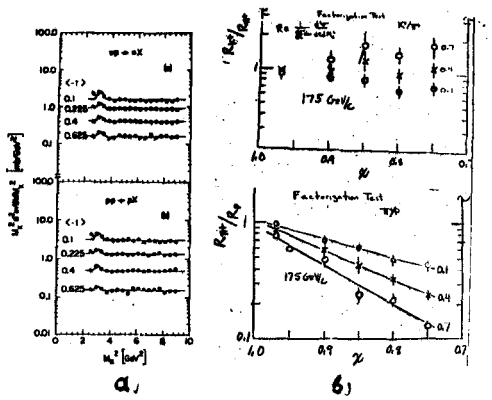
and the incident momenta ranged from 50 to 175 GeV/c.

This experiment has tested scaling by comparing the invariant cross sections for $pp\to pX$ at 70 and 175 GeV/c as a function of $x_{\parallel}$ at $|t|=0.3$. Over the range $0.75\le x_{\parallel}\le 0.97$ they find that scaling holds at a level of sensitivity of 10 per cent.

At high energy and X near unity, Regge theory suggests that the process $a+p\to a+X$ is dominated by Pomeron exchange, leading to the relation

$$M_X^2\frac{d^2\sigma}{dt\,dM_X^2}=\frac{1}{16\pi S_0^2}\left|\beta_{aa\mathbb{P}}(t)\right|^2\sigma_{tot}^{\mathbb{P}p}(M_X^2,t)$$

where M_X is the mass of the system X, $S_0=1$ GeV^2 is the Regge scale factor, $\beta_{aa\mathbb{P}}$ is the coupling between the incident hadron a and the exchanged Pomeron, and $\sigma_{tot}^{\mathbb{P}p}(M_X^2,t)$ is the Pomeron-proton total cross section. At large M_X^2 $\sigma_{tot}^{\mathbb{P}p}$ should become independent of M_X^2, and the expression above should thus be independent of M_X^2. Figure 3a shows the quantity $M_X^2\frac{d^2\sigma}{dt\,dM_X^2}$ plotted as a function of M_X^2 for πp and pp scattering at different average values of t and with data at 140 and 175 GeV/c combined. One observes resonance production at $M_X\sim1600$ MeV/c and no dependence on M_X^2 between 4 and 9 (GeV/c^2)^2.



a) b)

Fig. 3

Using the same phenomenology, the elastic differential cross section $a+p\to a+p$ can be written

$$\left.\frac{d\sigma}{dt}\right|_{elast}=\frac{1}{16\pi S_0^4}\left|\beta_{aa\mathbb{P}}(t)\right|^2\left|\beta_{pp\mathbb{P}}(t)\right|^2.$$

The implied factorization of the Regge residues requires that

$$R=\frac{M_X^2\frac{d^2\sigma}{dt\,dM_X^2}}{\left.\frac{d\sigma}{dt}\right|_{elast}}=\frac{\sigma_{tot}^{\mathbb{P}p}(M_X^2,t)}{\sqrt{16\pi\left(\frac{d\sigma}{dt}\right)_{pp\to pp}}}$$

be independent of incident particle type [6]. In Fig.3b R_{K^+}/R_{π^+} and R_{π^-}/R_{p} are plotted as a function of x for $-t$ =0.1; 0.4 and 0.7. One observes that as $x \to 1$, factorization holds for all particle types and values of t, but for x significantly different from 1 the ratio depends significantly on particle type and t. For the mass range $4 \leq M_x^2 \leq 9$ $(GeV/c^2)^2$, or $0.975 \leq x \leq 0.995$, the triple Regge formalism adequately describes the high energy data, and the "Pomeron-proton" total cross section

$$\sigma_{tot}^{Pp}(t) = 2.9 \exp(-1.04t + 0.35t^2)\ mb$$

is obtained. Defining the triple Pomeron coupling constant at t=0, by

$$\tau_c = \sqrt{\sigma_{tot}^{pp}} \cdot \frac{M_x^2 \frac{d^2\sigma}{dt dM_x^2}}{\frac{d\sigma}{dt}\Big|_{elast.}}$$

the values of τ_c for all six particle types are in statistical agreement. The average value of τ_0 obtained from the $\pi^{\pm}$ and p data is $\langle\tau_0\rangle = 0.80 \pm 0.03\ GeV^{-1}$.

References

1. R.Kammerud et al. 285/A2-53.
2. E.W.Beier et al. 402/A2-58.
3. Fermilab Single Arm. Spectrometer Group "Inelastic Diffractive Scattering at Fermilab. Energies" to be published.

МНОЖЕСТВЕННОЕ РОЖДЕНИЕ ЧАСТИЦ В $\bar{P}P$ -ВЗАИМОДЕЙСТВИЯХ

И.М.Граменицкий

ОИЯИ, Дубна

Одной из важных характеристик неупругих взаимодействий являются топологические сечения и параметры, характеризующие множественность. Топологические сечения для $\bar{p}p$-взаимодействий известны вплоть до импульса 100 ГэВ/с. Зависимость средней множественности $\langle n_{ch}\rangle$ от энергии при $P_{лаб} \geq 5$ ГэВ/с хорошо описывается соотношением вида $\langle n_{ch}\rangle = (0{,}69 \pm 0{,}19) + (1{,}05 \pm 0{,}05) \ln s$ /1/. Меньше информации о поведении $\langle n_{ch}\rangle$ имеется для $\bar{p}n$ -взаимодействий, однако, существующие данные свидетельствуют о том, что $\langle n_{ch}\rangle_{\bar{p}n} < \langle n_{ch}\rangle_{\bar{p}p}$ (рис.I)/2/.

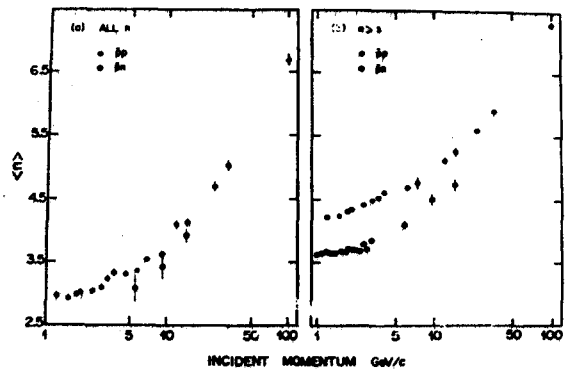


Рис.I

Исследование корреляционных явлений может дать информацию о механизме взаимодействия. Анализ корреляций по множественности заряженных частиц, вылетающих в переднюю и заднюю полусферы, дает оценку сечения дифракционной диссоциации. Распределение по множественности "вперед-назад"/3,4/ определяется как $P(n_f, n_b) = \sigma(n_f, n_b)/\sigma_{in}$, где n_f и n_b - число частиц в передней и задней полусферах, соответственно. Разделив это дискретное распределение на четную (n_f, n_b - четные) и нечетную (n_f, n_b -нечетные) части, можно приближенно оценить нижний предел сечения дифракционной диссоциации $\sigma_d/\sigma_{in} = P_{odd} - P_{even}$.

Для $\bar{p}p$ -взаимодействий при 22,4 ГэВ/с[5] при дополнительных предположениях, вытекающих из простой двухкомпонентной модели, получено $\sigma_M/\sigma_{in} = 0,11\pm0,03$, что согласуется с ранее полученными данными по анализу спектра недостающих масс[6]. Зависимость среднего заряда $\langle Q \rangle = (n_+ - n_-)/n_{tot}$ для передней и задней полусферы как функция p_T для двух интервалов быстрот при 22,4 ГэВ/с[7] представлена на рис.2. Можно

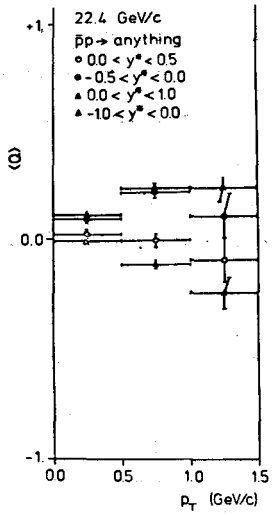


Рис.2

видеть, что наблюдается увеличение (уменьшение) с p_T среднего заряда в задней (передней) полусферах. Аналогичный эффект наблюдается также для pp- и πp -взаимодействий, причем увеличение зарядовой асимметрии с ростом p_T в $\bar{p}p$- больше, чем в pp- и меньше, чем в $\pi^- p$ -взаимодействиях.

Изучение двухчастичных корреляций при 22,4 ГэВ/с[8] проводилось с помощью корреляционной функции $C(y_1, y_2)$, представленной в виде разложения по полуинклюзивным процессам

$$C^{ij}(y_1,y_2)=\sum \omega_N C^{ij}_N(y_1,y_2)+\sum \omega_N(\rho^i_N(y_1)-\rho^j_N(y_1)) \times (\rho^i_N(y_2)-\rho^j_N(y_2)), \quad (1)$$

где $C^{ij}_N(y_1,y_2)$ - корреляционная функция для событий с данной множественностью N:

$$C^{ij}_N(y_1,y_2)=\rho^{ij}_N(y_1,y_2)-\frac{n^i-\delta_{ij}}{n}\rho^i_N(y_1)\rho^j_N(y_2) \quad (2)$$

и $\omega_N=\sigma_N/\Sigma\sigma_N$, $\rho_N(y)=\frac{1}{\sigma_N}d\sigma_N/dy$, n^i - число частиц сорта i.

Разложение (I) позволяет оценить верхний предел суммарных короткодействующих корреляций $C^{ij}_{SR}=\sum\omega_N C^{ij}_N(y_1,y_2)$. Корреляционная функция $C(y_1, y_2)$, изображенная на рис.3, в зависимости от $y_1=y_2$ имеет ярко выраженный пик при $y_1=y_2=0$, который, однако, связан с суперпозицией состояний с различным числом частиц. Корреляционная функция C_{SR}, показанная на том же рисунке, также имеет пик при $y_1=y_2=0$, но существенно меньшей величины. Там же для сравнения приведены данные для pp при 69 ГэВ/с (кресты) и K^-p при 32 ГэВ/с (точки). Возможно, что наблюдаемый в C_{SR} эффект связан с кинематическими корреляциями.

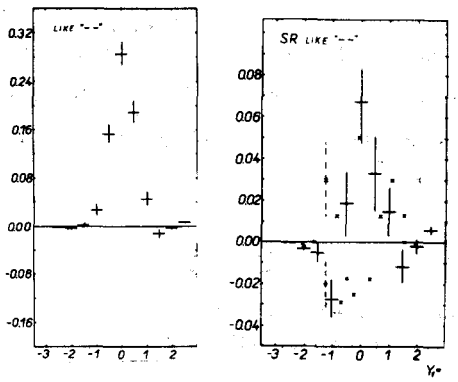


Рис.3

Азимутальные корреляции исследовались для реакций $\bar{p}p \to 2\pi^+2\pi^-$, $2\pi^+2\pi^-\pi^0$ и $2\pi^+2\pi^-(m\pi^0)$ при 5,7 ГэВ/с[9]. В распределениях по азимутальному углу $\varphi=\arccos[(p_{x1}p_{x2})/|p_{t1}||p_{t2}|]$ пар пионов одинакового и разного знака наблюдается заметное различие, особенно при уменьшении разности продольных и поперечных импульсов (рис.4). Аналогичный эффект, значительно ярче выраженный, наблюдается также при 22,4 ГэВ/с в инклюзивных реакциях[10]. Коэффициент асимметрии для тождественных и нетождественных пар равен $B_L=0,002\pm0,02$ и $B_{uL}=0,140\pm0,01$, соответственно. Наблюдаемый эффект может быть связан с влиянием интерференции в парах тождественных частиц.

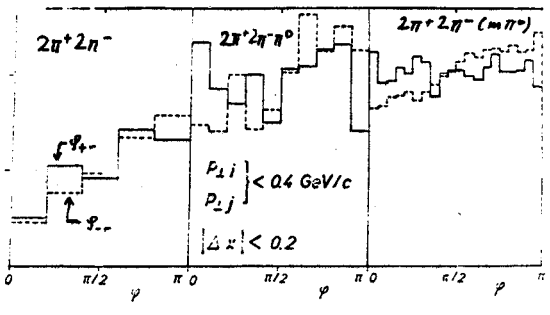


Рис.4

Выделение эксклюзивных каналов, в том числе аннигиляционных, легко осуществляемое при сравнительно небольших энергиях, становится крайне затруднительным при импульсах $p \gtrsim 10$ ГэВ/с. В работе[II] приведены данные по оценке сечений различных каналов в $\bar{p}p$-взаимодействиях при 9,I ГэВ/с. Особое внимание в работе уделено разделению неоднозначных событий и выделению аннигиляционного канала. Последнее особенно трудно в связи с большим количеством нейтральных частиц, возникающих при аннигиляции. Для определения доли событий с разным числом нейтральных частиц применялся метод подгонки распределений по квадрату недостающей массы.

В результате анализа были определены сечения различных каналов реакций. Полное сечение аннигиляции в пионы оказалось равным I3,2±0,5 мбн при σ_{tot} = 57,5±73 мбн. Были определены также сечения рождения резонансов ρ^0, ω^0 и изобары Δ^{++} $(\bar{\Delta}^{++})$. Инклюзивные сечения рождения ρ^0 и Δ^{++} приведены в табл.I.

Таблица I

Конечное состояние	ρ^0+...	ρ^0 + пионы	Δ^{++}+...
Сечение (мбн)	7,0±I,0	6,5±I,5	5,35±0,I4

Можно видеть, что относительный вклад ρ-мезонов в аннигиляционном канале очень велик.

Сечение процесса $\bar{p}p \to \Delta^{++}\bar{\Delta}^{++}$ равно 0,9±0,I мбн, т.е. составляет 35% от сечения реакции $\bar{p}p \to \bar{p}p\pi^+\pi^-$. Следует отметить, что эта доля падает с энергией и при 32 ГэВ/с составляет $\sim$ I5%/I2/.

Определение сечения рождения K^0-, Λ -$\bar{\Lambda}$ и π^0-мезонов исследовалось при импульсах 4,6, 9,I, I2, 22,4 и 32 ГэВ/с/I3-I5/.

Инклюзивные сечения рождения этих частиц приведены в табл.2.

Таблица 2

P (ГэЬ/с)	4,6	9,I	I2	22,4	32
$K^0+\bar{K}^0$	3,8± 0,I8	4,4± 0,26	4,08± 0,I2	4,48± 0,4	6,I± 0,6
Λ	0,6I± 0,05	0,3I± 0,I	0,I7± 0,08	I,23± 0,I8	I,6± 0,2
$\bar{\Lambda}$			I,03± 0,06	0,92± 0,I5	I,4± 0,2
π^0	73±3	78±4		59±4	68±5

Были построены инвариантные сечения для инклюзивных процессов с рождением V^0-частиц. Инвариантная функция $F(x)$ для реакции $\bar{p}p \to \Lambda + X$ при разных энергиях приведена на рис.5. Ошибки

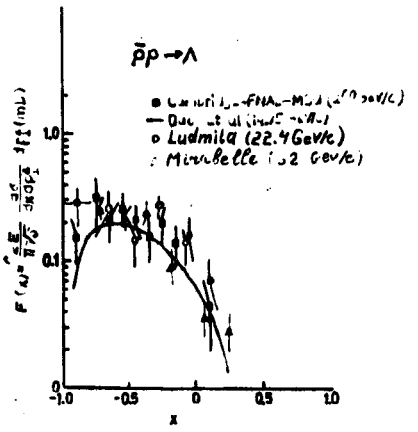


Рис.5

в полученных данных слишком велики, чтобы сделать определенные выводы об энергетической зависимости $F(x)$.

Литература

1. L.N.Abesalashvili et al. Phys.Lett.,52B,236 (1974).
2. H.Braun et al. Submitted paper to the Conference. 376/2A-95.
3. D.R.Suider. ANL/IHEP 7326 (1973).
4. H.Grassler et al. Nucl.Phys., B90 461 (1975).
5. E.G.Boos et al. Submitted paper to the Conference. 201/2A - 25.

6. E.G.Boos et al. Preprint JINR, E1-9781,Dubna, 1976.
7. E.G.Boos et al. Submitted paper to the Conference 903/A4 - 8.
8. E.G.Boos et al. Submitted paper to the Conference 161/A2 - 9 .
9. H.W.Atherton et al. Submitted paper to the Conference 400/2A - 60.
10. E.G.Boos et al. Submitted paper to the Conference 686/2A - 64.
11. P.S.Gregory et al. Submitted paper to the Conference 683/2A - 102.
12. M.A.Jabiol et al. Submitted paper to the Conference 1036/A1 - 9 .
13. M.T.Kegan et al. Submitted paper to the Conference 682/2A - 63.
14. O.Bertrand et al. Submitted paper to the Conference 722/2A - 67.
15. J.Manton et al. Submitted paper to the Conference 1035/2A - 90.

ИНКЛЮЗИВНОЕ ОБРАЗОВАНИЕ РЕЗОНАНСОВ И ДВУХЧАСТИЧНЫЕ КОРРЕЛЯЦИИ В $\pi^- N$-ВЗАИМОДЕЙСТВИЯХ ПРИ p = 40 ГЭВ/С

В.Г.Гришин
Объединенный институт ядерных исследований, Дубна

В настоящем докладе представлена часть результатов по исследованию инклюзивного рождения резонансов и двухчастичных корреляций вторичных частиц в $\pi^- p$-взаимодействиях при p = 40 ГэВ/с, полученные большой группой физиков ОИЯИ и институтов стран-участниц ОИЯИ[1-4]. Основное внимание в докладе будет уделено вопросу определения вероятности образования ρ^0-мезонов и изменению наших представлений о двухчастичных азимутальных корреляциях вторичных пионов с учетом рождения резонансов. Экспериментальный материал, около 11000 неупругих $\pi^- p$-взаимодействий, был получен с помощью двухметровой пропановой пузырьковой камеры, облученной на серпуховском ускорителе.

I. Сечение рождения ρ^0-мезонов в $\pi^- p$-взаимодействиях, определенное общепринятым методом по спектру эффективных масс $(\pi^+\pi^-)$-мезонов

Основным источником информации о рождении ρ^0-мезонов является спектр эффективных масс пар $\pi^+\pi^-$-мезонов. На рис. I приведено инклю-

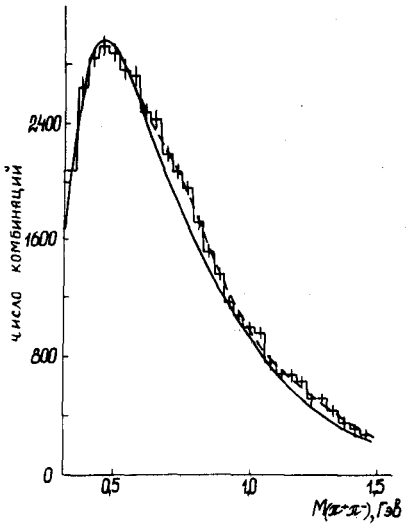


Рис. I

зивное распределение $M(\pi^+\pi^-)$ для π^-p-взаимодействий при p = 40 ГэВ/с. Сплошная линия - фоновая кривая и пунктирная - аппроксимирующая функция:

$$F(M)=(1-\alpha_\rho-\beta_f)\,\Phi(M)+$$
$$+\alpha_\rho\,Б.В._\rho(M)+\beta_f\,Б.В._f(M),$$

где α_ρ и β_f - относительные вклады резонансов $\rho^0\to\pi^+\pi^-$ и $f\to\pi^+\pi^-$, $\Phi(M)$ - фоновое распределение, нормированное на единицу. Функции Брейта-Вигнера (Б.В.) брались при M_0 = 770 МэВ, Γ_0 = 150 МэВ, l = 1 для ρ^0-мезона и 1270 МэВ, 170 МэВ, l = 2 для f-мезона. Мы также учитывали искажение функций Б.В. из-за экспериментальных погрешностей в измерении $M(\pi^+\pi^-)$. Правильность учета этих погрешностей была проверена по распределению $M(K_1^0)$, которое было определено по распадным $\pi^\pm$-мезонам в этом же эксперименте[1].

Фоновая кривая $\Phi(M)$ бралась в виде

$$\Phi(M)=K(M_1)^\alpha\exp(-bM_1+cM_1^2),$$

где $M_1=M(\pi^+\pi^-)-2m_\pi$, K - нормировочный коэффициент и a, b, c - подбираемые параметры.

В результате такого анализа было получено, что

$$\sigma(\rho^0)=(5{,}8\pm1{,}4)\ \text{мбн}.$$

В этом случае доля π^+-мезонов, образованных при распаде $\rho^0\to\pi^+\pi^-$ от всех π^+-мезонов, составляет $\approx(15\pm4)\%$ и практически не меняется в интервале 16-200 ГэВ для π^-p-взаимодействий.

Однако следует отметить, что при $E\gtrsim20$ ГэВ "сигнал" от ρ^0-мезона в спектрах $M(\pi^+\pi^-)$ составляет всего лишь (10÷20)%. Поэтому от выбора фоновой кривой, особенно в области резонанса, существенно зависит величина сечения $\sigma(\rho^0)$. В связи с этим мы исследовали влияние учета отражения распада $\omega\to\pi^+\pi^-\pi^0$ на определение величины $\sigma(\rho^0)$.

2. Учет влияния образования ω-мезонов на спектр $M(\pi^+\pi^-)$ и определение сечений рождения ρ^0- и ω-мезонов

В случае образования ω-мезонов продукты их распадов $\omega\to\pi^+\pi^-\pi^0$ дают вклад в спектр $M(\pi^+\pi^-)$ в интервале масс от $2m_\pi$ до $(m_\omega-m_{\pi^0})$, т.е. вблизи ρ^0-резонанса. Учет распадных пар $(\pi^+\pi^-)$ от ω-мезонов приводит к следующему виду аппроксимирующей функции:

$$F(M)=(1-\alpha_\rho-\beta_f-\gamma_\omega)\,\Phi(M)+\alpha_\rho\,Б.В._\rho(M)+$$
$$+\beta_f\,Б.В._f(M)+\gamma_\omega\,\omega_\omega(M),$$

где $\omega_\omega(M)$ была вычислена с учетом матричного элемента распада $\omega\to3\pi$. В результате аппроксимации экспериментального спектра $M(\pi^+\pi^-)$ функцией $F(M)$ было получено: $\sigma(\rho^0)$ = 13,3±1,4 мбн, $\sigma(\omega)$ = 10,0±1,1 мбн и $\sigma(f)$ = 1,3±0,8 мбн при $\overline{\chi^2}$ = 1,37. В этом случае доля π^+-мезонов, образованных в результате распадов $\rho^0\to\pi^+\pi^-$ и $\omega\to\pi^+\pi^-\pi^0$ от всех вторичных π^+, составляет $\Delta\approx(50\pm5)\%$! Если предположить, что $\sigma(\rho^+)=0{,}5\,\sigma(\rho^0)$, и учесть образование Δ^{++}-изобары ($\sigma\approx1$ мбн) и f-мезонов, то $\Delta\approx70\%$!

Таким образом, проведенное исследование показывает, что заметное рождение ω^0-мезонов может существенно изменить полученные ранее данные по $\sigma(\rho^0)$. В связи с этим мы попытались оценить $\sigma(\omega)$ по спектрам эффективных масс $(\pi^+\pi^-\pi^0)$-систем, где π^0-мезоны восстанавливались по эффективной массе двух гамма-квантов, зарегистрированных в пропановой пузырьковой камере. Однако статистика невелика ($\approx$ 700 π^0-мезонов), и поэтому отсюда можно сделать лишь качественное заключение, что $\sigma(\omega)$ = (4÷10) мбн.

Таким образом, традиционный метод определения сечений образования резонансов при $E\gtrsim20$ ГэВ из-за большого числа "ложных" комбинаций становится неэффективным. Он, по-видимому, дает только нижнюю границу $\sigma(\rho^0)$.

3. Азимутальные корреляции

Изучение двухчастичных азимутальных корреляций в π^-p-взаимодействиях при p = 40 ГэВ/с показало, что коэффициент асимметрии

$$B=[N(\varphi\gtrsim\pi/2)-N(\varphi<\pi/2)]/N_{tot}.$$

может быть тем параметром, который позволит определять сечения рождения резонансов в инклюзивных процессах при высоких энергиях. ($N(\varphi\gtrsim\pi/2)$ - число пар пионов с углом $\varphi\gtrsim\pi/2$). На рис. 2

приведены зависимости B от $M(\pi\pi)$ при различных ограничениях на разность быстрот и модулей поперечных импульсов пионов. Из рисунка видно,

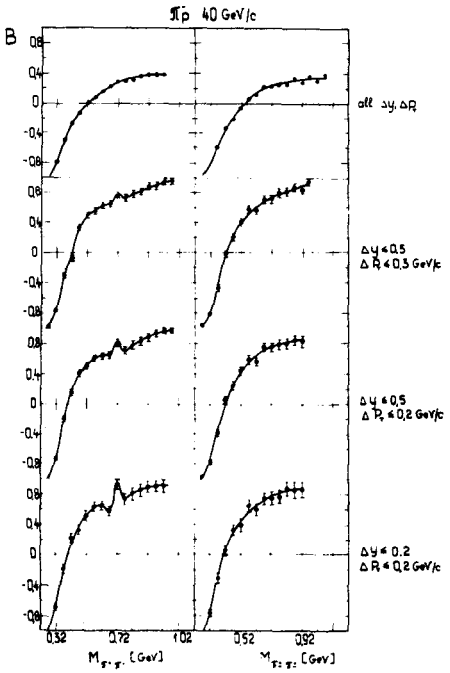


Рис.2

что при $\Delta y \leq 0{,}2$ и $\Delta P_\perp \leq 0{,}2$ ГэВ/с для $\pi^+\pi^-$-пар имеется четкий сигнал, связанный с ρ^0-мезоном. В то же время, в распределениях по $M(\pi^\pm\pi^\pm)$ при тех же ограничениях он отсутствует. Таким образом, параметр $B(M(\pi\pi))$ является более чувствительным индикатором резонансов, чем традиционное распределение по $M(\pi\pi)$.

В последние годы было обнаружено различие в поведении $dN/d\varphi$ для тождественных и разных пар пионов. Оно часто связывается с эффектом тождественности. Однако учет рождения резонансов может существенно уменьшить это различие. На рис. 3 приведены отношения вероятностей образования $(\pi^\pm\pi^\pm)$-пар к $(\pi^+\pi^-)$-парам. На рис. 4 построены те же распределения, но при этом были исключены пары $(\pi^+\pi^-)$-мезонов с $M = M(\rho^0) \pm 80$ МэВ. Как видно, различие в поведении $dN/d\varphi$ практически исчезло.

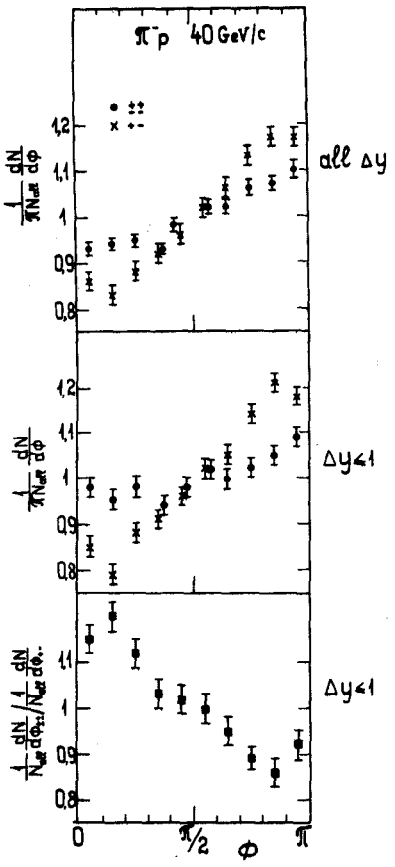


Рис.3

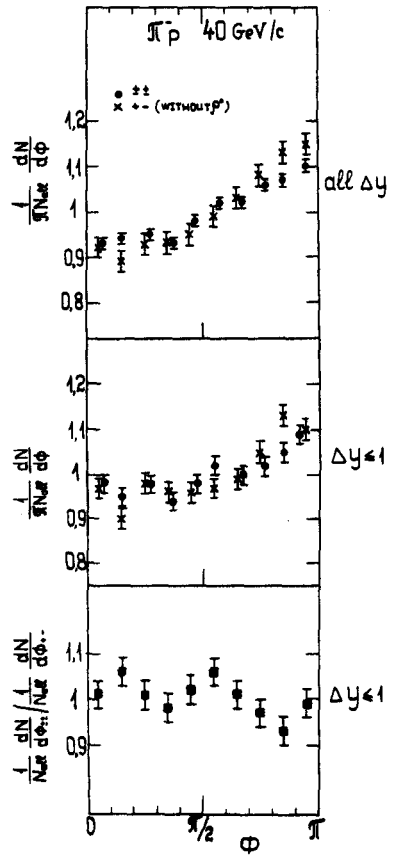


Рис.4

Литература

1. Н.Ангелов, К.П.Вишневская, В.Г.Гришин и др. Препринт ОИЯИ, I-9536, Дубна, 1976.
2. Н.Ангелов, К.П.Вишневская, В.Г.Гришин и др. "Исследование рождения резонансов в π^-p - взаимодействиях при 40 ГэВ/с". Доклад, представленный на XVШ Международную конференцию по физике высоких энергий (Тбилиси, I5-2I июля, 1976).
3. Н.Ангелов, К.П.Вишневская, В.Г.Гришин и др. "Исследование эффектов тождественности и влияния рождения ρ^0-мезонов на корреляции частиц в π^-p -взаимодействиях при p =40 ГэВ/с". Доклад, представленный на XVШ Международную конференцию по физике высоких энергий (Тбилиси, I5-2I июля, 1976).
4. Н.Ангелов, К.П.Вишневская, В.Г.Гришин и др. "Изучение двухчастичных корреляций гамма-квантов и заряженных частиц в π^-p-взаимодействиях при p = 40 ГэВ/с". Доклад, представленный на XVШ Международную конференцию по физике высоких энергий (Тбилиси, I5-2I июля, 1976).

INCLUSIVE PARTICLE AND RESONANCE PRODUCTION

Aachen-Berlin-Bonn-CERN-Cracow-London-Vienna-Warsaw Collaboration

P.Schmid

CERN, Geneva, Switzerland

This talk summarises work on inclusive resonance production done by the Aachen-Berlin-Bonn-CERN-Cracow-London-Vienna-Warsaw Collaboration during the past year [1]. It is based on about 1.1 million events coming from the following bubble chamber experiments: π^+p at 8, 16 and 23 GeV/c, π^-p at 16 GeV/c and K^-p at 10 and 16 GeV/c. The resonances ρ^0, f, η, ω, K^*_{890}, K^*_{1420}, Δ^{++} and Σ^-_{1385} are studied. Results are presented on

- separation of fragmentation and central production of secondary particles;
- universality of transverse momentum spectra;
- direct particle production and contributions from resonance decays.

The energy dependence of total production cross sections of resonances is discussed separately by P. Chliapnikov at this Conference.

SEPARATION OF FRAGMENTATION AND CENTRAL PRODUCTION OF SECONDARY PARTICLES

Longitudinal momentum spectra of ρ^0 production in π^+p and π^-p interactions at 16 GeV/c are very similar. They differ, however, from the corresponding spectra in pp interactions at 24 GeV/c as seen in fig. 1.

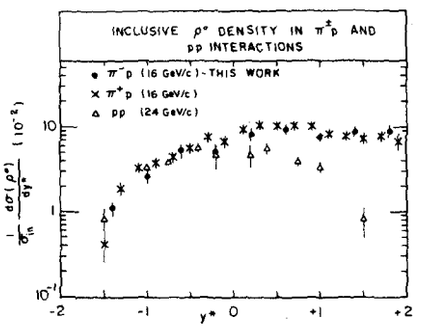


Fig.1- Comparison of the c.m. rapidity distribution of ρ^0 in 16 GeV/c π^-p interactions with the same in 16 GeV/c π^+p (1b) and 24 GeV/c pp interactions (6).

Whereas the spectra coincide for $y < 0$, ρ production is much stronger in the forward direction for πp than it is for pp interactions. The difference can be interpreted as being due to different beam fragmentation. A quantitative estimate of beam fragmentation and central components can be obtained by comparing invariant cross sections for ρ^0 production in π^+p with K^*_{890} production in K^-p interactions at 16 GeV/c (fig. 2). As K^*_{890} is mainly produced by kaon fragmentation, the difference of the two spectra may be considered as an estimate of the central component of ρ production. Using the cross sections

$$\sigma_{\rho^0}(\pi^+p) = 4.7 \pm 0.4 \text{ mb}$$

$$\sigma_{K^{*0}}(K^-p) = 3.3 \pm 0.4 \text{ mb}$$

at 16 GeV/t the following estimates have been obtained I[b)

$$\sigma^F_{K^{*0}} = \sigma^F_{\rho^0} = 3.1 \pm 0.4 \text{ mb}$$

$$\sigma^C_{\rho^0} = 1.6 \pm 0.5 \text{ mb}$$

$$\sigma^C_{K^{*0}} = 0.2 \text{ mb}$$

where F and C stand for fragmentation and central production, respectively. These estimates are consistent with the interpretation of fig. 1 as given above.

Similarly spectra for the production of Σ^+_{1385} and Σ^-_{1385} may be compared in K^-p interactions at 16 GeV/c (fig. 3). If Σ^+ and Σ^- are produced by a "central" process, they should have the same cross section, as the total charge of the initial state is zero.

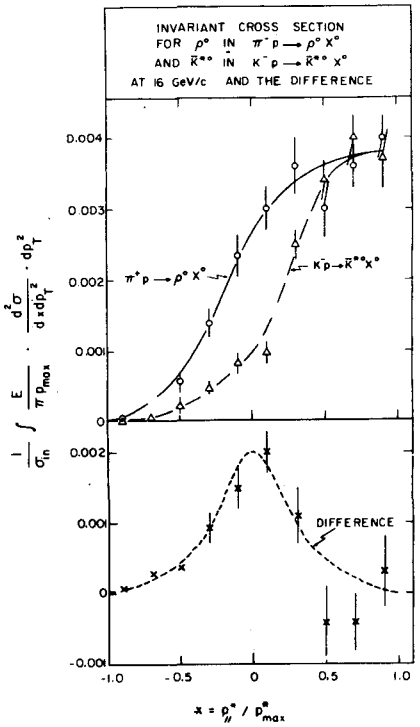


Fig.2 Comparison of the invariant x-distributions of ρ^0 in π^-p and K^{*0}_{890} in K^-p interactions at 16 GeV/c (Ib)

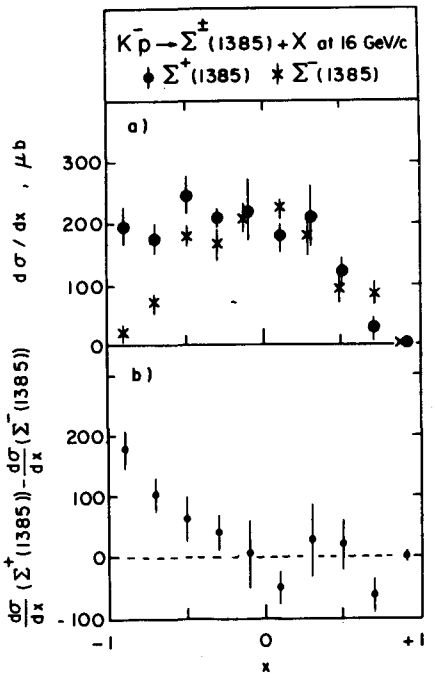


Fig.3 Comparison of $d\sigma / dx$ for $\Sigma^+(1385)$ and $\Sigma^-(1385)$ production at 16 GeV/c K^-p interaction (Ie).

In the proton fragmentation region Σ^- production should be small as it requires double charge exchange, whereas Σ^+ production is allowed. Indeed the difference of two spectra is very suggestive of a fragmentation component. With the cross sections $\sigma_{\Sigma^{*+}}(K^-p) = 0.41 \pm 0.05$ mb and $\sigma_{\Sigma^{*-}}(K^-p) = 0.27 \pm 0.04$ mb at 10 GeV/c (Ie) one arrives at fragmentation and central components of

$$\sigma^{F}_{\Sigma^*} = 0.14 \pm 0.07 \text{ mb}$$
$$\sigma^{C}_{\Sigma^*} = 0.27 \pm 0.04 \text{ mb}$$

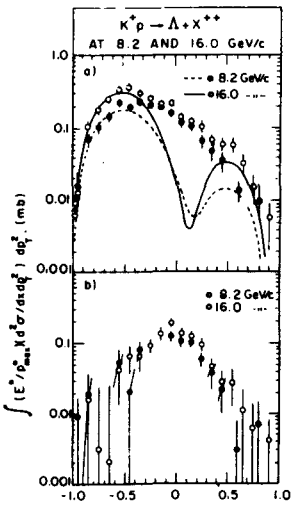


Fig.4 a) Invariant x distribution for Δproduction K^+p interactions at 8.2 GeV. The curves represent fits of triple Regge expressions to the fragmentation regions.
b) Difference between data and fragmentation components of fig.4(a) representing the central component of Δproduction.

A different technique has been used by the Birmingham- Brussels-CERN- Mons Collaboration to separate fragmentation and central production of Δ's in K^+p interactions at 8 and 16 GeV/c (2). Contributions from beam and target fragmentation have been obtained by fitting triple-Regge expressions to the distributions of large |x| and by extrapolating them to small |x| (Fig.4(a)). The central component of Σ production is obtained by subtracting the sum of the two fragmentation components from the overall spectrum (Fig.4(b)).

2. UNIVERSALITY OF TRANSVERSE SPECTRA

Inclusive p_T^2 distributions of produced particles have been found to depend on the mass of the particle (3). Spectra for heavy particles are approximately exponential between $p_T^2 = 0$ and 2 (GeV/c). For ligth particles like pions and kaons the spectra have a much steeper slope at small p_T^2 which gradually decreases to about the same slope as for heavy particles above p_T^2 1 (GeV/c). Apart from some structure at very small p_T^2, resonances turn out to have spectra with an exponential fall-off out to about 2(GeV/c)^2 with slopes similar to the ones of heavy particles. Some resonance spectra are shown in Fig.5(a,b,c) and compared to spectra of pions and kaons, respectively.

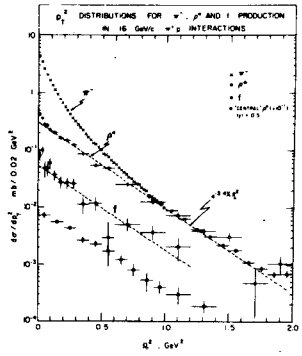
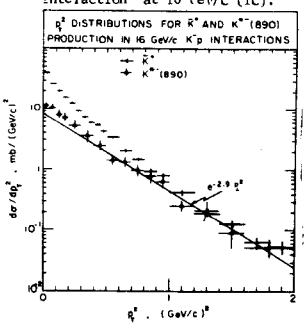
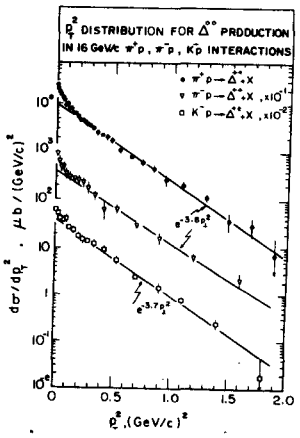


Fig.5 p_T^2 distributions for

a) π^-, ρ^0 and f production in π^-p interaction at 16 GeV/c (Ia).



b) K^0 and K^{*-}_{890} production in K^-p interaction at 16 GeV/c (Ic).



c) Δ^{++} production in π^+p, π^-p and K^-p inetraction at 16 GeV/c (Id).

A surprisingly similar slope is found for all resonances studied inclusively independant of the initial state over a large range of lab. momenta (6 - 200 GeV/c, see Table I). Moreover the same slope is found for "quasi"-inclusive $p_\perp^2$ distributions of η and ω production [1f] (fig. 6).

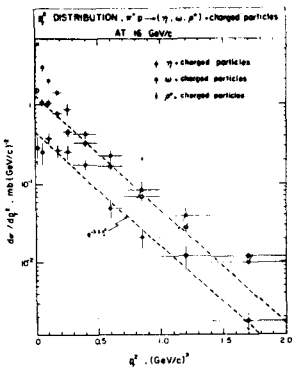


Fig. 6 $p_\perp^2$ distributions for the inclusive reactions

$\pi^+ p \to (\eta, \omega, \rho^o)$ + charged particles at 16 GeV/c [1f].

TABLE I

Slopes of $p_\perp^2$ distributions for inclusive resonance production.

Resonance Produced	Initial State	Incident Momentum (GeV/c)	Slope of $d\sigma/dp_\perp^2$ $(GeV/c)^{-2}$	Reference
ρ^o	$\pi^+ p$	6	3.9 ± 0.4	[5]
		16	3.45 ± 0.1	[1a]
		22	3.0 ± 0.6	[5]
	$\pi^- p$	16	2.95 ± 0.2	[1b]
	pp	12	3.6 ± 0.4	[6]
		24	3.6 ± 0.4	[6]
		147	2.7 ± 0.5	[7]
		205	3.0 ± 1.0	[8]
f^o	$\pi^+ p$	16	3.45 ± 0.3	[1a]
ω	$\pi^+ p$	16	3.3 ± 0.15	[1f]
	pp	12	3.4 ± 0.2	[6]
		24	3.7 ± 0.3	[6]
η	$\pi^+ p$	16	3.3 ± 0.3	[1f]
K^{*-}_{890}	$K^- p$	16	2.9 ± 0.2	[1c]
$\bar{K}^{*o}_{890}$	$K^- p$	16	3.15 ± 0.2	[1c]
K^{*+}_{890}	pp	12	3.4 ± 0.4	[6]
		24	2.8 ± 0.3	[6]
Δ^{++}	$\pi^+ p$	16	3.6 ± 0.2	[1d]
	$\pi^- p$	16	3.6 ± 0.2	
	$K^- p$	16	3.7 ± 0.2	
Σ^+_{1385}	$\pi^+ p$	16	3.6 ± 0.15	[9]
	$K^- p$	4.2	3.7 ± 0.2	[10]
		10	3.4 ± 0.3	[9]
		16	3.4 ± 0.25	[9]
Σ^-_{1385}	$\pi^+ p$	16	3.8 ± 0.5	[9]
	$K^- p$	4.2	3.9 ± 0.3	[10]
		10	3.3 ± 0.4	[9]
		16	2.9 ± 0.3	[9]

This combined evidence leads to the conjecture of universality of the slope of $p_\perp^2$ spectra of directly produced particles. "Second order" effects like

- systematic differences of slopes for certain beams or produced particles

or

- a slow decrease of slopes with increasing energy cannot be established with presently available data.

Slope universality will be used in the following as a method of estimating production cross sections.

The first example concerns η and ω production in $\pi^+ p$ interactions at 16 GeV/c [1f]. With bubble chamber data these resonances can only be observed when all other particles in the final state are charged (or observed V^os). To compare them to ρ production, ρs should be studied in similar "quasi"-inclusive reactions, i.e. produced with charged particles only. The ratio of the production cross section in the $p_\perp^2$ range where all three resonances have exponential distributions with almost identical slopes is found to be

$$\eta : \omega : \rho = 0.3 : 0.8 : 1.$$

Based on slope universality and on the similarity of x and y distributions [1f], these ratios are assumed to be true also for the fully inclusive case and the following cross sections for η and ω production are obtained:

$$\sigma_\eta = 1.5 \pm 0.3 \text{ mb}$$

$$\sigma_\omega = 4.0 \pm 0.6 \text{ mb}$$

3. DIRECT PARTICLE PRODUCTION AND CONTRIBUTIONS FROM RESONANCE DECAYS

As cross sections for resonance production are large, many of the final particles observed are in fact decay products. With some plausible assumptions [1h] it is straightforward to calculate the contribution of the important resonances, the cross sections of which have been measured at 16 GeV/c, to the final particle yield (Table II). Almost half of the production cross section of the particles listed in Table II can be accounted for by known resonances. As possible contributions from broad or high mass resonances are difficult to measure, the numbers obtained can be used to get upper bounds for the frection of directly produced particles.

TABLE II

Particle	% from resonance		in interaction
K^n	∿ 45%	K^*_{890}	$K^- p$
	3%	K^*_{1420}	
Λ	∿ 40%†	Σ_{1385}	$K^- p$, $\pi^+ p$
π^-	∿ 25%	ρ^o, ρ^-	$\pi^+ p$
	2.5%	f	
	15%	ω	
	2%	η	
	∿ 45%		

† This percentage holds for true Λs, i.e. after subtracting Σ^os from the observed Λ yield.

An experimental technique has been developed to establish differential spectra of decay products which can then be subtracted from the overall particle spectra. Such an analysis has been done for negative pions produced in $\pi^+ p$ interactions and for neutral kaons in $K^- p$ interactions both at 16 GeV/c [1g]. As expected from pure kinematics, fig. 7(a) shows that decay pions are

the more peaknd at small $p_\perp^2$ the smaller the Q-value of the resonance and the heavier the mass recoiling against the pion. Summing up the contributions of all meson resonances studied (fig. 7(b)), the particular form of the $p_\perp^2$ spectrum of pions can well be reproduced. Because of the heavy recoiling mass, pions coming from baryon resonances are expected to contribute even more to the peak at small $p_\perp^2$.

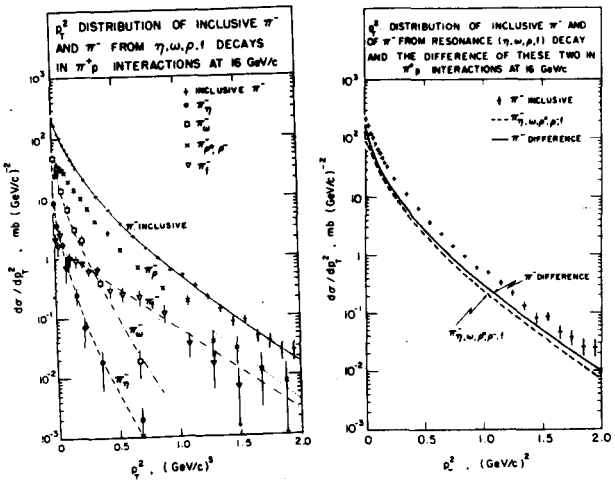


Fig. 7 $p_\perp^2$ distributions of π^- production in π^+p interaction at 16 GeV/c [1f].

a) Inclusive π^- distribution and spectra of π^-s coming from η, ω, ρ and f resonances

b) Inclusive π^- distributions, sum of all π^-s from (η, ω, ρ, f) decay (broken line) and difference of the two distributions (full line).

Having shown that pions at small $p_\perp^2$ mainly come from resonance decays, one can try to get another upper bound on direct pion production using the conjecture of slope universality. As seen in fig. 4(a) the $p_\perp^2$ spectrum of pions is compatible with the exponential ρ spectrum above $p_\perp^2 \sim 0.8$ GeV^2 where decay-pions are expected to play a less important role. Extrapolating the exponential spectrum at large $p_\perp^2$ down to $p_\perp^2 = 0$, one obtains an upper bound for direct pion production of 20% of the total pion yield. Taking into account the large $p_\perp^2$ tail of decay-pions one arrives at a best estimate of about 10%. In Table III we compare the production cross cross sections for meson resonances and the estimate for directly produced pions with quark model predictions by Anisovitch and Shekhler [4]. Although the predictions are only valid for a large number of produced quarks, i.e. high energies, the quantitative agreement between data and predictions is surprisingly good for resonances not containing strange quarks. The predictions for ϕ and η production, however, are off by one order of magnitude which may indicate some dynamical mechanism like the Zweig-Iizuka rule for suppressing these states.

TABLE III

Comparison of particle ratios in 16 GeV/c π^+p interactions with quark model predictions [4].

PARTICLE RATIO	QUARK MODEL PREDICTION	"EXPERIMENTAL" RESULT
ω/ρ	1	0.8 ± 0.2
η/ω	11/18 = 0.14	0.39 ± 0.03
π^-_D/ρ^0	1/3 = 0.33	∼ 0.5 - 1.0
π^-_0/ρ^-_{ALL}	1/14 = 0.07	< 0.5 best estimate ∼ 0.1
ϕ/ρ^0	1/9 = 0.11	< 0.025
η'/η	19/11 = 1.7	∼ 0.05 - 0.10

I would like to thank the Birmingham-Brussels-CERN-Mons Collaboration for allowing me to include unpublished results. I am especially grateful to Drs. V. T. Cocconi, M. J. Counihan, H. G. Kirk, P. K. Malhotra, F. Mandl, B. R. O. Morrison and H. Saarikko for their assistance in preparing this talk.

REFERENCES

[1a] M. Deutschmann et al., Nucl. Phys. B103 (1976) 426.

[1b] J. Bartke et al., Nucl. Phys., B107 (1976) 93.

[1c] Inclusive Production of $\bar{K}^*(890)$ and $\bar{K}^*(1420)$ in K^-p Interactions at 10 and 16 GeV/c, Aachen-Berlin-CERN-London-Vienna Collaboration, H. G. Kirk et al., CERN/EP/PHYS 76-13.

[1d] Inclusive $\Delta^{++}(1236)$ Production in π^+p, π^-p and K^-p Interactions at 16 GeV/c, Aachen-Berlin-Bonn-CERN-Cracow-Heidelberg-London-Vienna-Warsaw Collaboration.

[1e] Inclusive Production of $\Sigma^\pm(1385)$ in K^-p Interactions at 10 and 16 GeV/c, Aachen-Berlin-CERN-London-Vienna Collaboration.

[1f] Eta and Omega Meson Production in Medium Energy π^+p and K^-p Collisions, Aachen-Berlin-Bonn-CERN-Cracow-London-Vienna-Warsaw Collaboracion, CERN/EP/PHYS 76-28.

[1g] A Study of Indirect Pion Production in π^+p Interactions at 16 GeV/c, Aachen-Berlin-Bonn-CERN-Cracow-Heidelberg-Warsaw Collaboration, CERN/EP/PHYS 76-27.

[1h] Inclusive Yields and Transverse Spectra of the Mesons Comparison with the Quark Model and the Problem of "Direct" Pion Production, Aachen-Berlin-Bonn-CERN-Cracow-London-Vienna-Warsaw Collaboration, CERN/EP/PHYS 76-30.

[2] The Reactions $K^+p \to \Lambda X^{++}$ and $K^+p \to \bar{\Lambda} X^{++}$ at Incident Moments of 8.2 and 16 GeV/c, Birmingham-Brussels-CERN-Mons Collaboration, P. V. Chliapnikev et al., CERN/EP/PHYS 76-11.

[3] See a.g. Experimental Review of Strong Interactions at High Energy, D. R. O. Morrison, Lectures at the Fifth Hawaii Topical Conference in Particle Physics, 1973.

[4] V. V. Anisovitch and V. M. Shekhter, Nucl. Phys. B (73) 455.

[5] H. A. Gordon et al., Phys. Letters 34B (75) 284.

[6] V. Blobel et al., Phys. Letters 48B (74) 73.

[7] D. Fong et al., Phys. Letters 60B (75) 124.

[8] R. Singer et al., Phys. Letters 60B (76) 385.

[9] Aachen-Berlin-Bonn-CERN-Cracow-London-Vienna-Warsaw Collaboration, F. Mandl, private communication.

[10] Study of $\Sigma^\pm(1385)$ Inclusive Production in K^-p Interactions at 4.2 GeV/c, Amsterdam-CERN-Nijmegen-Oxford Collaboration, CERN/EP/PHYS 76-23.

ASSOCIATED CORRELATION EFFECTS IN π^-p-INTERACTIONS AT 40 GeV/c

L.N.Abesalashvili, N.S.Amaglobeli, N.K.Koutsidi, T.G.Makharadze, R.G.Salukvadze, L.A.Slepchenko, Yu.V.Thevzadze, M.S.Chargeishvili

High Energy Nuclear Physics Problem Laboratory, Tbilisi St.University, USSR

Results of an experimental study of semi-inclusive reactions in π^-p interactions at 40 GeV/c are presented in this paper. The work was done within the framework of the 2-m JINR propane bubble chamber international collaboration[1]. The results reported are based on the analysis of ~10400 inelastic interactions. Data processing was described elsewhere[2].

The distribution of an associated multiplicity as a function of transverse momentum of the trigger $\pi^\pm$-meson from reaction

$$\pi^-p \to \pi^\pm + (n-1)_{ch} + \ldots \qquad (1)$$

is shown in fig.1. Data from π^-n-collisions (on quasi-free neutrons of the carbon nucleus) are also given for comparison.

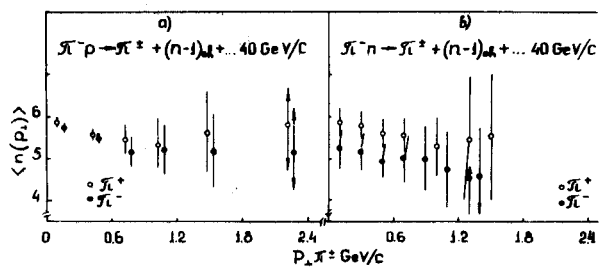


Fig.1.The associated charged multiplicity as a function of transverse momentum of the trigger $\pi^\pm$-mesons.

A weak dependence of the associated multiplicity on $p_\perp$ is seen for low $p_\perp$ region ($p_\perp \leq 0.5$ GeV/c), whereas $\langle n(p_\perp)\rangle$ is nearly constant for higher $p_\perp$. The experimental results were approximated by the expression

$$\langle n(p_\perp)\rangle = a + b/p_\perp \qquad (2)$$

deduced within the framework of the diffraction excitation model for semi-inclusive reactions[3,4]. Small values of parameter b (e.g, for π^--mesons $b = 0.08 \pm 0.02$) point a rather weak correlations between n and $p_\perp$.

However it turns out that such behaviour of the $\langle n(p_\perp)\rangle$ is the result of averaging over some different dynamical effects that manifest themselves in different phase-space regions; that we see in fig.2, where the associated multiplicity dependence on $p_\perp$ is shown for different kinematical regions of trigger $\pi^\pm$-mesons. Note

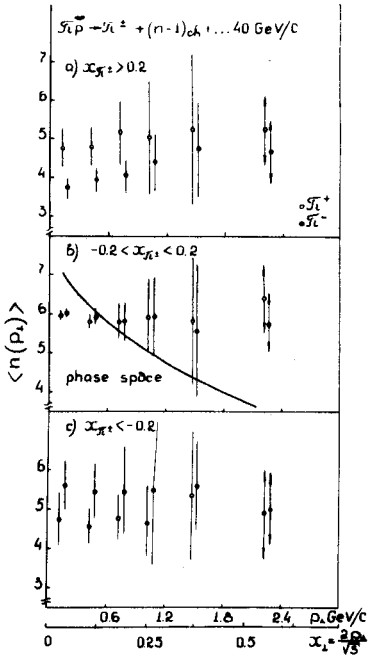


Fig.2. The same dependence in different phase space regions of the trigger particle.

the following main features: i) the $\langle n(p_\perp)\rangle$ values in fragmentation regions - fig.2a) and 2c) are lower than in the central region - fig.2b) because of the diffraction-type mechanisms of the particle production; II) an approximate constancy of the $\langle n(p_\perp)\rangle$- e.g.,in the central region - is the result of the influence of the process dynamics - the fact clearly seen when comparing the experimental data with Monte-Carlo generated events[5]- curve in the fig.2b); III) the associated multiplicity for the trigger π^--mesons from beam fragmentation region shows tendency to increase.

Further analysis of the $\langle n(p_\perp)\rangle$for fast π^--mesons reveals that particles produced in the central region are responsible for this rise of the $\langle n(p_\perp)\rangle$ - fig.3b).

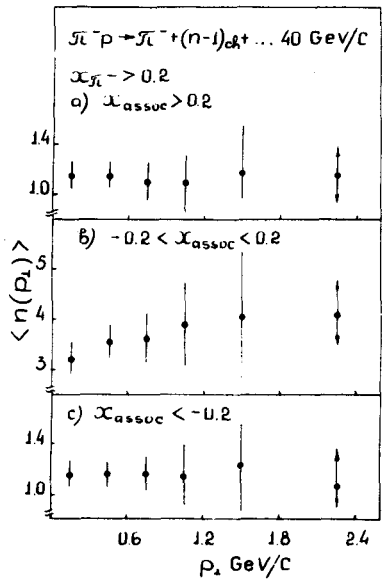


Fig.3. The same dependence for trigger π^- in the beam fragmentation region; associated particles in different phase space regions.

So in this case we can't explain the rise of the $\langle n(p_\perp) \rangle$ for forward emitted π^--mesons by means of the model of beam particle excitation in the course of its interaction with the target hadron constituents[6].

When taking two subsets of associated particles: those having the same direction of the $\vec{p}_\perp$ as the trigger particle and the ones with the opposite direction, the different behaviour of the $\langle n(p_\perp) \rangle$ is seen - fig.4. Whereas the associated multiplicity decreases in the same hemisphere it has a tendency to rise in the opposite one - while correlations of a kinematical origin produce a fall of the $\langle n(p_\perp) \rangle$ in both hemispheres-curves in the fig.4.

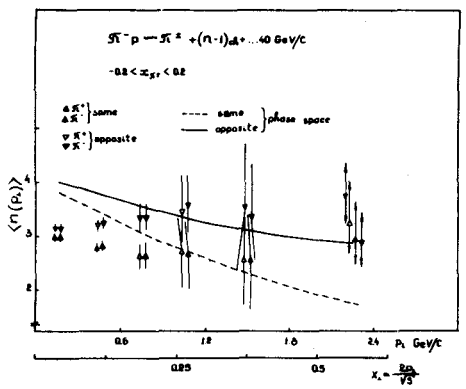


Fig.4. The same dependence for $\pi^\pm$-mesons from the central region in the same and opposite hemispheres.

We have studied further the dependence of the average transverse momentum of associated particles on the value of $p_\perp$ of the trigger particle. Our data show an increase in the $\langle p_\perp \rangle_{ass}$ with the increase in the $p_{\perp\,trig}$ value- fig.5 - which is well approximated by a linear dependence

$$\langle p_\perp \rangle_{ass} = a_1 + b_1 \cdot p_{\perp\,trig} \qquad (3)$$

(e.g. for π^+-mesons $\chi^2/N = 5.86$, $a_1 = 0.354 \pm 0.001$, $b_1 = 0.028 \pm 0.003$).

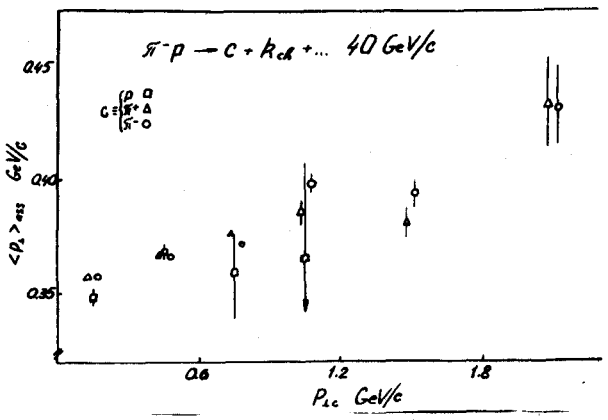


Fig.5. The average transverse momentum of associated particles as a function of the $p_\perp$ of the trigger particle.

When analysing the average associated $p_\perp$ in different azimuthal cones we see that in the cones with opening angle $\varphi > 90^\circ$ $\langle p_\perp \rangle_{ass}$ increases when increasing $p_\perp$ of the trigger the more the closer is φ to 180° - fig.6. However $\langle p_\perp \rangle_{ass}$ increases also for particles in the narrow cone on the same side ($\varphi < 30^\circ$), whereas it decreases in two other cones. It agrees rather well with the big correlations observed at the ISR for high $p_\perp$ particles in the cases of $\varphi \approx 0^\circ$ and $\varphi \approx 180^\circ$[7].

Note in conclusion that the results reported here point at the associated productions of particles with $p_\perp$ greater than the average one and the data do not contradict "jet-type" models.

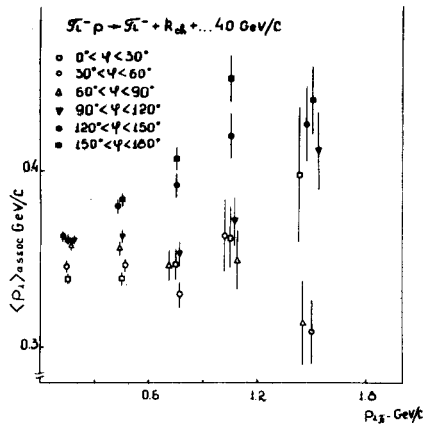


Fig.6. The same dependence in different azimuthal cones for the trigger π^--meson.

The authors are grateful to the staff of the 2-metre chamber international collaboration and to the group of physicists and laboratory assistants of the High Energy Nuclear Physics Problem Laboratory of the Tbilisi State University.

Referenoes

1. Nguen Din Ty, V.N.Penev et al. JINR, 13-5942, Dubna, 1973.
2. A.N.Abdurakhimov, N.S.Angelov et al. JINR, 1-6967, Dubna, 1973.
3. L.N.Abesalashvili, N.S.Amaglobeli et al.Sov. J.of Nucl.Phys., 23, 782 (1976); JINR, 1-9406, Dubna, 1975.
4. J.S.Darbaidze, L.A.Slepchenko. Bull. of the Acad. of Sci.Georg. SSR, 79, 61 (1975).
5. S.N.Komarova, G.I.Kopylov et al. JINR, 1-8501, Dubna, 1974.
6. L.J.Gutay, A.T.Laasen et al. Lett.al Nuovo Cim., 16, 49 (1976).
7. F.W.Busser et al. Phys.Lett., 51B, 306 (1974); Nucl.Phys., B106, 1 (1976).

INVESTIGATION OF SOME INCLUSIVE DISTRIBUTIONS OF Λ^0-HYPERONS AND K^0_1-MESONS IN $\pi^- C^{12}$ INTERACTIONS AT 40 GEV/C

L.N.Abesalashvili, N.S.Amaglobeli, L.T.Akhobadze, D.V.Gersamia, M.A.Dasaeva, T.L.Kchvachadze, N.S.Koutsidi, R.G.Salukvadze, Yu.Thevzadze, M.S.Chargeishvili

Tbilisi State University, USSR

In this paper we present results on the investigation of some inclusive spectra of Λ^0-hyperons and K^0_1-mesons produced in $\pi^- C$ and $\pi^- C^{12}$ interactions at 40 GeV/c. (Symbol $\pi^- C$ applies to the π^--meson interactions with carbon without accounting pion interactions with quasifree nucleons).

As an experimental material for physical investigation were used events selected from the films of 2m JINR propane chamber, obtained in π^--meson beam at the Serpukhov accelerator. Questions concerning the measuring of πp-events and section definition of their production are considered in papers[1] and[2]. Distributions for $\pi^- C$ and $\pi^- C^{12}$ interactions are compared with corresponding distributions for $\pi^- p$ collisions.

Momentum Characteristics of Λ^0-Hyperons and K^0_1-Mesons

In Fig.I normalised momentum distributions of Λ^0 and K^0_1 partioles are presented for $\pi^- C^{12}$, $\pi^- C$ and $\pi^- p$ interactions. Comparison of distributions for πp and πC collisions makes it possible to examine the influence of nucleus over the considered distributions. It may be seen that in πC interactions the part of slow particles is slightly higher and there is a tendency of decreasing the number of particles with maximal momenta. An average momenta of Λ^0 and K^0_1-particles in πC interactions are less than in πp collisions (see Table I). Momentum distributions of Λ^0 and K^0_1-particles for πC^{12} interactions within the range of errors coincide with corresponding distributions for πp collisions.

In Table I the average characteristics of Λ^0-hyperons and K^0_1-mesons produced in πp, πC and πC^{12} interactions are given.

Table 1

		$\langle p_{lab} \rangle$	$\langle p_{lab} \rangle$	$\langle p_\perp \rangle$	B	χ^2/N
$\pi^- p$	Λ^0	3,67±0,22	3,58±0,22	0,489± 0,016	3,21±0,57	2,4/5
	K_1^0	5,43±0,20	5,38±0,20	0,452±0,012	4,19±0,47	1,7/6
$\pi^- C$	Λ^0	3,36±0,18	3,26±0,18	0,490±0,014	3,49±0,43	2,3/5
	K_1^0	4,68±0,16	4,48±0,15	0,465±0,010	3,68±0,38	7,2/6
$\pi^- C^{12}$	Λ^0	3,52±0,13	3,43±0,13	0,478±0,010	3,71±0,39	3,3/5
	K_1^0	5,01±0,12	4,90±0,11	0,469±0,007	3,28±0,42	8,3/6

In Table I one may see that in $\pi^- C$ interactions meanly slower neutral strange particles are produced than in pion-nucleon interactions. The average values of transverse momenta of Λ^0-hyperons in $\pi^- C^{12}$, $\pi^- C$ and $\pi^- p$ collisions coinside. One may say the same of K_1^0-mesons transverse momenta. These facts show that transverse momenta do not depend on the nature of colliding particles.

One-Particle Inclusive Distributions of Λ^0 Hyperons and K_1^0-Mesons

The behaviour of normalized invariant differential sections $\frac{E\, d^2\sigma}{dp_\parallel\, dp_\perp^2}$ in lab.system for Λ^0-hyperons and K_1^0-mesons from $\pi^- C^{12}$, $\pi^- C$, $\pi^- p$ interactions was investigated. Integration by square of transverse and longitudinal momentum leads to the functions.

$$H_1(p_\parallel) = \frac{1}{\sigma_{in}} \int \frac{E\, d^2\sigma}{dp_\parallel\, dp_\perp^2} dp_\perp^2$$

$$H_2(p_\perp^2) = \frac{1}{\sigma_{in}} \int E\, d^2\sigma / dp_\parallel\, dp_\perp^2\, dp_\parallel$$

Functions $H_1(p_\parallel)$ for Λ^0-hyperons and K_1^0-mesons in lab.system of coordinates are given in Fig.2. For comparison the relations of these values are given too:

$$R = \frac{H_1(p_\parallel)_{\pi^- C}}{H_1(p_\parallel)_{\pi^- p}}$$

It may be seen that $H_1(p_\parallel)$ for $\pi^- C$ and $\pi^- p$ interactions slightly differs in the region of low value of longitudinal momentum in the case of Λ^0-hyperons and K_1^0-mesons as well. Our experimental distributions by square of transverse momentum in $\pi^- p$, $\pi^- C$ and $\pi^- C^{12}$ interactions up to 1 $(GeV/c)^2$ are shown in Fig.3. (One may see that functions $H_2(p_\perp^2)$ for Λ^0 and K_1^0 particles in $\pi^- C^{12}$, $\pi^- C$ and $\pi^- p$ collisions coinside within the range of errors. Functions $H_2(p_\perp^2)$ for Λ^0-hyperons and K_1^0-mesons in the given interactions were fitted by the exponent of the form $H_2(p_\perp^2) = A e^{-B p_\perp^2}$.

The results of fitting are given in Table I. Coefficient B is the same for $H_2^{\Lambda^0}(p_\perp^2)$ and $H_2^{K^0}(p_\perp^2)$.

From the comparison of different distributions of Λ^0-hyperons and K_1^0-mesons from $\pi^- p$ and $\pi^- C$ interactions one may conclude that carbon nucleus unsubstentially change the momentum and angle characteristics of Λ^0 and K_1^0-particles. The influence of carbon nucleus is observed as a displacement of momentum spectra of Λ^0 and K_1^0 particles to the smaller values. Secondary interactions in Carbon nucleus play, apparently, unimportant role in the production of Λ^0 and K_1^0-particles.

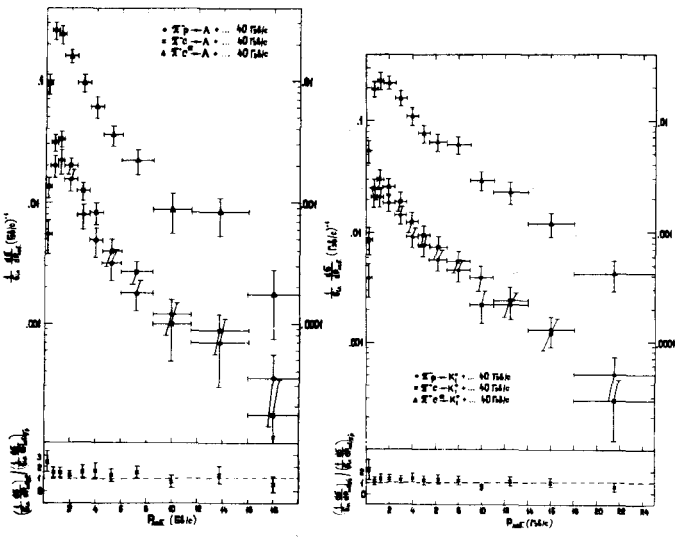


Fig.1.

Normalized momentum distribution of Λ^0 hyperon and K_1^0-mesons in lab. system.

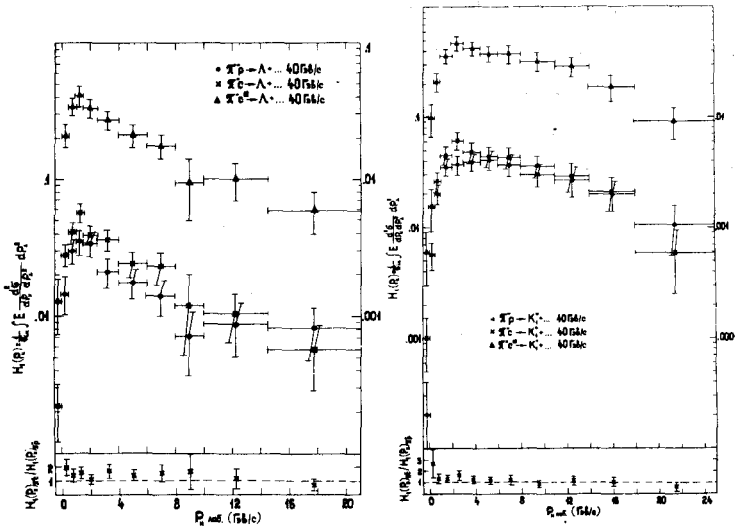


Fig.2.

Distribution of the function $H_1(P_{II})$ to P_{II} for Λ^0 -hyperons and K^0_1- mesons.

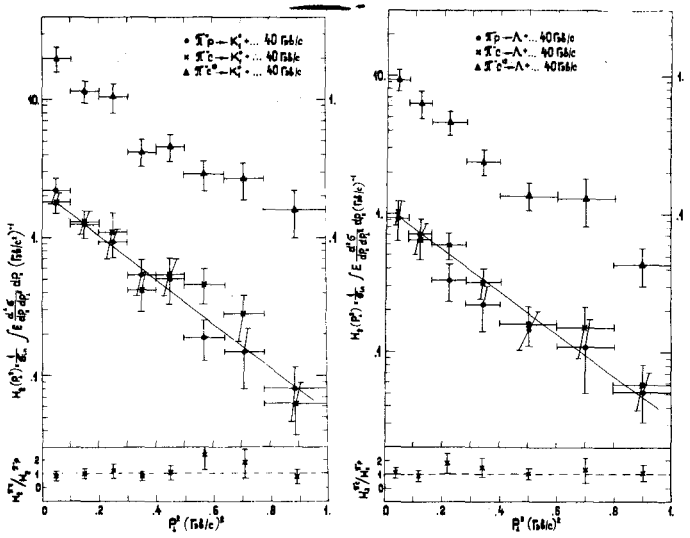


Fig.3.

Dependence of the function $H_2(P^2)$ on P^2 for Λ^c-hyperons and K^0_1-mesons.
Straight line - the result of approximation of experimental data from interactions.

References

1. Budapest-Bucharest-Dubna-Cracow-Hanoi-Sofia-Tashkent-Tbilisi-Ulan Bator- Collaboration. JINR P1-7267, Dubna,1973; Journal of Nucl. Phys.(USSR),17,1251(1973);Nucl.Phys.,B79,57 (1974).
2. N.Angelov, C.P.Vishnevskaia,V.G.Grishin et al. JINR,P1-9209,Dubna,1975; Nucl.Phys.,(USSR), (in print).

TWO-PARTICLE CORRELATIONS

E.P.Kistenev

IHEP, Serpukhov, USSR

Progress in correlation studies reached in recent years makes it obvious that a real understanding of the phenomena responsible for the structure observed in correlations is impossible without precise separation of the production mechanisms playing a dominant role in different regions of the phase space. For this reason this talk will be devoted mainly to those results which provide information about the interplay between the correlations and production dynamics.

1. Longitudinal Correlations in the Central Region

The correlations are usually studied in terms of correlation functions. The most popular definitions are the following:

$$C_n^{ij}(\vec{P}_1,\vec{P}_2)=\frac{1}{n^i(n^i-\delta^{ij})}\rho_n^{ij}(\vec{P}_1,\vec{P}_2)-\frac{1}{n^i n^j}\rho_n^i(\vec{P}_1)\rho_n^j(\vec{P}_2),$$

$$R_n^{ij}(\vec{P}_1,\vec{P}_2)=C_n^{ij}(\vec{P}_1,\vec{P}_2)\Big/\left(\frac{1}{n^i n^j}\rho_n^i(\vec{P}_1)\rho_n^j(\vec{P}_2)\right),$$

where $\rho_n(\vec{P})=\frac{1}{\sigma_n}\frac{d\sigma_n}{d\vec{P}}$, $\rho_n^{ij}(P_1,P_2)=\frac{1}{\sigma_n}\frac{d\sigma_n}{d\vec{P}_1 d\vec{P}_2}$ are one and two particle densities, i, j - types of the particles in the pair.

The inclusive correlation function can be defined in a similar way and rewritten in terms of the components of semiinclusive processes

$$C_n^{ij}(\vec{P}_1,\vec{P}_2)=\sum_n \omega_n C_n^{ij}(\vec{P}_1,\vec{P}_2)+\sum_n \omega_n(\rho^i(\vec{P}_1)-\rho_n^i(\vec{P}_1))(\rho^j(\vec{P}_2)-\rho_n^j(\vec{P}_2)),$$

where $\omega_n=\sigma_n/\sigma_{inel}$.

The first term in this equation is the sum of the semiinclusive correlation functions taken with the weights proportional to the topological cross sections.The second term is a crossing term which originates from the mixing of the semiinclusive spectra depending on the multiplicity.The last term does not contain any information about the dynamical correlations among the produced particles[1].

The semiinclusive correlations are presented to the conference for $\pi^- p$ [2-6], pp [7], $\bar{p}p$ [8] and ph [9] interactions in the energy range 5–400 GeV/c. General structure of such correlations is illustrated in fig. 1 where the values of the semiinclusive correlation functions $C_n^*(y_1, y_2)$ are plotted against the $\frac{1}{2}(y_1 - y_2)$ for a fixed value of $\frac{1}{2}(y_1 + y_2) = 0$ [7] (y_1 and y_2 – rapidities of the particles in pair).

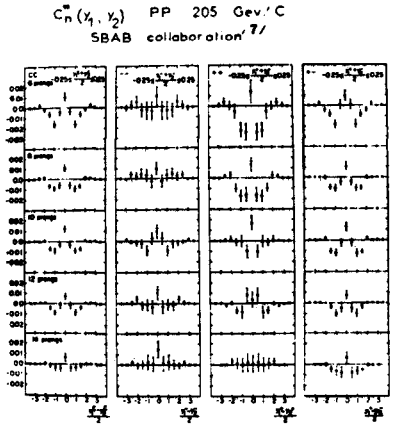


Fig. 1

a) The observed correlations are of short range and the function $C_n^*(y_1, y_2)$ decreases sharply from its value at $y_1 = y_2 = 0$.

b) The values in the central bin are of compatible size for all the charge combinations.

In the framework of the simple cluster emission model the shape of the semiinclusive correlation function can be parametrized in the form [10]

$$C_n^*(y_1, y_2) = \frac{\langle K(K-1)\rangle}{\langle K\rangle_{(n-1)}} \left(\rho(y_1, y_2) - \frac{1}{n(n-1)} \rho_n(y_1)\rho_n(y_2) \right),$$

where K – is the cluster multiplicity, $\rho(y_1, y_2)$ – two particle density within the cluster. New data of SBAB collaboration [7] support the conclusion from PSB experiment [11] that the clusters are entities with multiplicity independent characteristics. As seen from data of fig. 2 where the values of $\langle K(K-1)\rangle / \langle K\rangle$ are functions of the scaled multiplicity $n/\langle n\rangle$ the multiplicity distribution within a cluster is broader than a δ -function ($\langle K(K-1)\rangle / \langle K\rangle = K_0 - 1$) and narrower than a Poisson-like distribution ($\langle K(K-1)\rangle / \langle K\rangle \simeq \langle K\rangle (n-1)/\langle n\rangle$). The small values of $\langle K(K-1)\rangle / \langle K\rangle$ in the figure imply an average number of charged particles $\langle K\rangle \leq 2$ which means that well known resonances, such as vector or tensor bosons could play a dominant role in the picture observed.

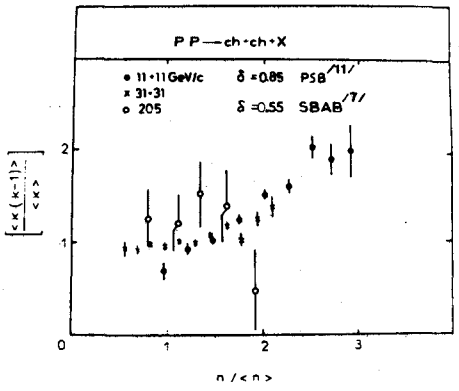


Fig. 2

The effect of ρ^0 -production on longitudinal correlations was investigated by the BFGMOP collaboration in $\pi^- p$ interactions at 11.2 GeV/c [6] (fig. 3).

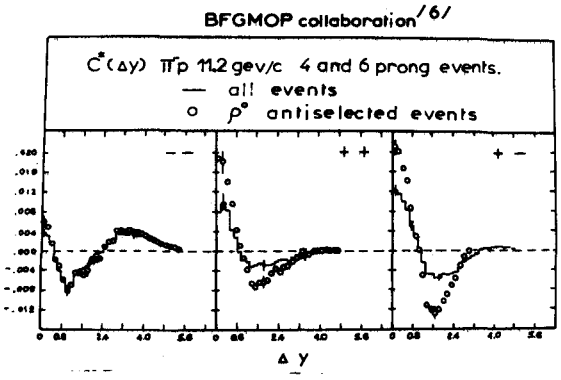


Fig. 3

The ρ^0 -meson leads to the effect of forcing apart the π -pairs reducing the short range correlations in $\pi^+\pi^+$ and $\pi^-\pi^-$ systems. This conclusion coincides with a prediction made by E. Levin and M. Ryskin in the context of multiperipheral model considering the alignment of the resonances in the final state [12].

The French-Soviet Union pp -collaboration at 69 GeV/c previously reported the existence of the maxima in semiinclusive correlation function $C_n^*(y_1 = y_2)$ at $y_1 = y_2 = \pm 1$ for both

$\pi^-\pi^-$ and $\pi^+\pi^-$ combinations[13]. The corresponding data are now available also in pp interactions at 205 GeV/c[7], K^-p at 32 GeV/c[14] and $\bar{p}p$ at 22.4 GeV/c[8]. The compilation of the proton data for multiplicity $n=10$ is shown in fig. 4. Positive correlations are present

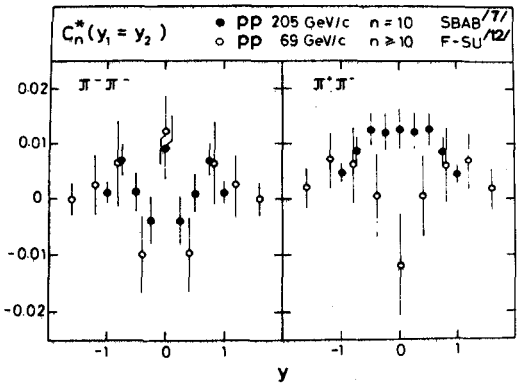


Fig. 4

in all data. The same structure as at 69 GeV/c is seen in the 205 GeV/c data for $\pi^-\pi^-$ pairs. One of the possible explanation for the maxima in $C_n^*(y_1=y_2)$ at $y_1=y_2=2$ could be the anisotropy of the resonance decay if they are produced in aligned state. The central maximum at $y_1=y_2=0$ can be a manifestation of the second order interference effect (see for example the minirapporteur talk of M. Podgoretsky at this conference).

The data for $\pi^+\pi^-$ combinations are contradictory, The dip at $y_1=y_2=0$ seen in the 69 GeV/c data is absent at 205 GeV/c. More precise data are still needed to study this effect in detail.

2. Joint Angular-Momentum Correlations

The existence of the angular correlations can be partly explained by the negative sign in the right-hand part of the corresponding inclusive sum rule which can be written for identical particles as follows

$$\int (\vec{P}_{t_1}\vec{P}_{t_2})\rho(\vec{P}_1,\vec{P}_2)\frac{d^3P_1}{E_1}\frac{d^3P_2}{E_2} = -\int P_t^2\rho(\vec{P})\frac{d^3P}{E}$$

which means that wide open pairs are favoured over narrow ones.

Compilation of the data for azimuthal asymmetry defined as $B=[N(\varphi>\frac{\pi}{2})-N(\varphi<\frac{\pi}{2})]/N_{tot}$ is shown in fig.5[6] (φ is the opening angle in transverse momentum plane).

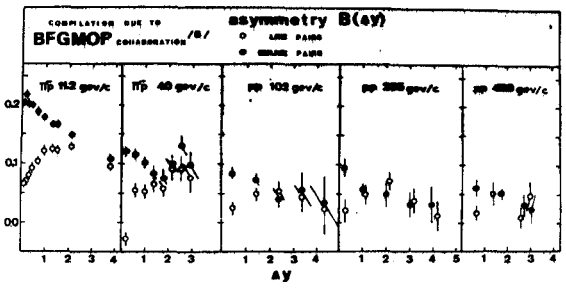


Fig. 5

Comparison for the different energies and initial states suggests that at least for small values of the rapidity difference Δy the asymmetry B for like and unlike particles have consistently a similar behaviour. Higher multiplicity and consequently more neutral particles results in a decrease of asymmetry with energy as is seen from this figure.

The constructive interference which exists in the pairs of like particles[15] can explain the difference between the azimuthal correlations for like and unlike pairs only in the threshold region $M_{\pi\pi}\simeq 2m_\pi$ where the energy-momentum vectors of the particles in pair are almost equal. Outside this region the resonance production can contribute to the observed difference in the correlations. The corresponding data are now available from a number of experiments. Fig. 6 shows the results obtained in π^-p experiments at 40 GeV/c[16](a) and 11.2 GeV/c[6] (b).

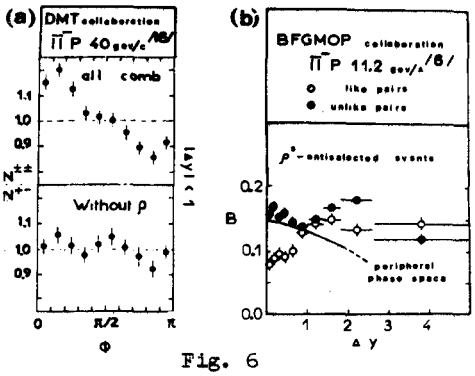


Fig. 6

When ρ -like combinations are excluded from the data no clear distinction between the distributions of the opening angle in transverse momentum plane for like and unlike pion pairs is left in π^-p data at 40 GeV/c[16](fig.6a).

The elimination of the events with a $\pi^+\pi^-$ couple in the ρ-region from the total sample makes the experimental data for unlike pairs consistent within the errors with statistical model prediction (fig. 6b). The situation is different for like pairs where the decrease of the asymmetry at small Δy still exists

Let us summarize now the conclusions of these two sections.

The data presented to the conference support the existence of the positive short-range correlations in rapidity space for both like and unlike charge combinations. The dependence of the semiinclusive correlation function on Δy can be parametrized in the framework of the independent cluster emission model with cluster multiplicity $\langle K \rangle \leq 2$ which means that the resonances could play a dominant role in the longitudinal correlations, even if no quantitative connection has yet been established.

The angular correlations observed in the $\pi\pi$ systems are mainly of the kinematical origin. The difference between the like and unlike charge pairs apart from the threshold region where the interference effects could be essential can be explained by the resonance production.

References

1. V.V.Ammosov et al. French-Soviet Union Collaboration, preprint IHEP M-16, Serpukhov, 1975.
2. Notre Dame-Duke-Canada-Iowa-Maryland-Michigan Collaboration, conference paper 1023/A2-103.
3. I.Ya.Chasnikov et al. Alma-Ata, USSR, conference paper 166/A2-4.
4. N.Angelov et al. JINR, Dubna conference paper 157/A2-12.
5. Dubna-Košice-Minsk-Tbilisi Collaboration, conference paper 810/A2-79.
6. Bologna-Firenze-Genova-Milano-Oxford-Pavia Collaboration, conference paper 1202/A2-160.
7. Stony Brook-Argonne-Batavia Collaboration, conference paper 738/A2-106.
8. Alma-Ata-Dubna-Helsinki-Košice-Moscow-Prague Collaboration, conference paper 161/A2-9.
9. Strasbourg-Rehovot Collaboration, conference paper 375/A2-38.
10. E.L.Berger. Nucl.Phys., B85, 61 (1975).
11. S.R.Amendolia et al. Nuovo Cim., 31, 17 (1976).
12. E.M.Levin, M.G.Ryskin, conference paper 83/A3-3.
13. V.V.Ammosov et al. French-Soviet Union Collaboration, preprint IHEP M-21, Serpukhov, 1975.
14. V.V.Babintsev et al. French-Soviet Union and CERN-Soviet Union Collaboration, preprint IHEP M-24, Serpukhov, 1975.
15. G.I.Kopylov, M.I.Podgoretsly. JINR, Dubna, conference paper 1007/A2-120.
16. Dubna-Moscow-Tbilisi Collaboration, conference paper 205/A2-108.

RECENT RESULTS ON 32 GEV/C $K^{\pm}p$ AND $\bar{p}p$ INTERACTIONS IN THE MIRABELLEE BUBBLE CHAMBER

Presented by R.Barloutaud, DPhPE,CEV-Saclay, France

This report is intended to be a summary of the recent results obtained by the France-Soviet Union and CERN-Soviet Union Collaborations* with the 4.6 m. MIRABELLE hydrogen bubble chamber exposed at the Serpukhov accelerator to RF separated K^+, K^- and $\bar{p}$ beams at 32 GeV/c. These results are based on the analysis of 100K, 80K and 12K pictures of K^+, K^- and $\bar{p}$ experiments respectively.

All events including V^0 and e^+e^- pairs have been doubly scanned, measured on manual or automatic devices and submitted to 4C kinematical fits. Therefore, both inclusive and exclusive studies have been carried out on these samples. Four communications[1-4] for the K^+p , five for the K^-p [5-9] and two for the $\bar{p}p$[10-11] experiments were reported.

In this brief sketch of the results given in these papers, the data on the similar final states obtained with the different beams will be presented together allowing a useful comparison between the K^+p, K^-p and $\bar{p}p$ interactions.

I. INCLUSIVE STUDIES

1.1. Particle Multiplicities

The π^0 average multiplicity $\langle n_{\pi^0} \rangle$ assumed to be equal to $\langle n_\gamma \rangle / 2$ is almost identical in the three experiment (1.89±0.05),(1.96±0.05) and (1.80±0.15) for K^+p, K^-p and $\bar{p}p$ interactions respectively as well as its topological dependence shown in fig.1. The shape of the $\langle n_{\pi^0} \rangle$ dependence is also quite compatible with the results obtained in $\pi^{\pm}p$ and pp interactions[12]. In the Kp experiment the average multiplicity of each type of produced particle has been evaluated by using the equations of charge, strangeness and baryonic number conservation and some general hypothesis on the production of K^0, K^+ and antibaryons. In particular, the average multiplicity of π^+ and π^- are found to be quite compatible with the π^0 multiplicity ($\langle n_{\pi^+} \rangle$ = =1.87±0.07, $\langle n_{\pi^-} \rangle$=1.96±0.10). The multiplicity distribution of π^+ and π^- has also been derived. It is presented in fig.2 and differs significantly from the charged particle multiplicity distribution since more than 20% of these particles

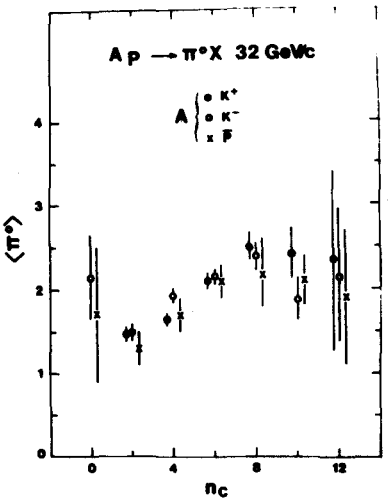


Fig.1. π^0 average multiplicity as a function of the charged topology.

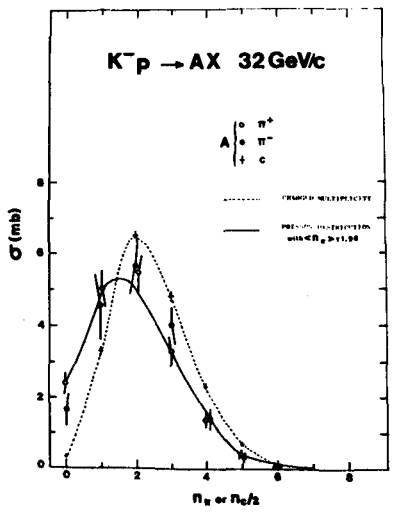


Fig.2. $\pi^{\pm}$ cross section as a function of the $\pi^{\pm}$ multiplicity and topological cross section (dashed curve). The full curve is a Poisson distribution.

* The laboratories involved in the Collaborations are: Bruxelles, Mons, Paris, Saclay and Serpukhov for the K^+p experiment; Aachen,Berlin, CERN, Saclay, Serpukhov and Vienna for the K^-p experiment; Bruxelles, Mons, Saclay and Serpukhov for the $\bar{p}p$-experiment.

are not pions. The dispersion D and the correlation coefficient f_2 have been determined for π^+, π^- and π^o multiplicity distributions; in the π^o case, the average value of the number of produced $\gamma\gamma$ pairs has been used. A general agreement is found within the experimental errors between these coefficients for $\pi^\pm$ and π^o. In particular, f_2 is compatible with zero for $\pi^\pm$ and π^o, and the $\pi^\pm$ distributions are compatible with a Poisson distribution as seen in figure 2.

1.2. Associated Charged Multiplicities in K^-p Interactions

The average charged particle multiplicity $\langle n_x \rangle$ of the system X associated to π^+, π^- (for $x_\pi \leq 0$, K^n, Λ and identified protons ($p_p < 1.2$ GeV/c) has been calculated as a function of M_x^2. Below $M_x^2 \simeq 40$ GeV^2, i.e. mainly in the fragmentation region of the incident particle, the M_x^2 dependence of $\langle n_x \rangle$ is well described by the logarithmic law $\langle n_x \rangle = \alpha + \beta \ln M_x^2$ with a coefficient β which is about the same as the one describing the dependence of the total multiplicity in the K^-p interaction. Above 40 GeV^2 the β coefficient increases strongly especially for $\pi^\pm$ and K^n inclusive reactions, indicating that the values of $\langle n_x \rangle$ found in the central region are larger than expected by the law describing the S dependence of the charged multiplicity. A similar phenomenon has been seen also in K^+p interactions /13/.

1.3. $K^n = K^o + \bar{K}^o$ Production

The inclusive cross sections for the reactions

$$A + p \rightarrow K^n + X$$

are (7.6±0.2), (9.8±0.25) and (6.3±0.6) mb for $A = K^+$, K^- and $\bar{p}$ respectively. Their comparison with lower energy data shows a small increase for $K^\pm p$ interactions and a more rapid rise for $\bar{p}p$ interactions. Using the cross sections for the reactions $K^-p \rightarrow \Lambda K^n + X$ and $K^\pm p \rightarrow K^n K^n + X$ and some simple hypothesis on the K and $\bar{K}$ charge distributions among the possible final states, the percentage K^c/K^n $\left(\bar{K}^o/K^n\right)$ in $K^+(K^-)p$ interactions has been evaluated to be 10% (13%). As it is impossible to separate accurately the two strangeness components of the K^n, this value has to be kept in mind before interpreting quantitatively the K^n production properties in $K^\pm p$ interactions.

The invariant cross section for K^n produotions are presented as a function of X in fig.3.

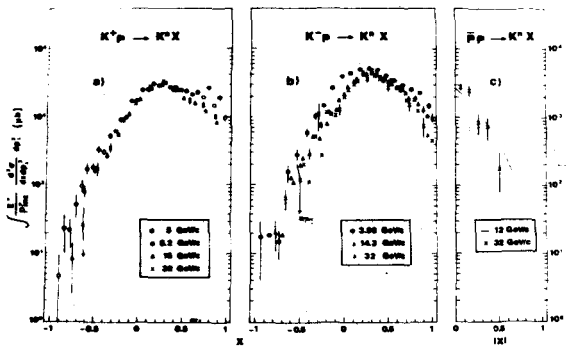


Fig.3. Invariant cross section as a function of X .

These distributions are quite similar for K^+p and K^-p interactions and they do not show any strong variation with the data obtained at 16 or 14.3 GeV/c. In the $\bar{p}p$ interactions in which the symmetrical K^n distribution has been folded around X=0 the errors are still too large to draw any firm conclusion.

A systematic study of the approach to scaling in K^+p interactions has led to the following conclusions:

a) in the K^+ fragmentation region, no energy variation is found between 16 and 32 GeV/c for all sets of inclusive variables;

b) scaling is not observed in the proton fragmentation region where its approach is described by an S^{-1} behaviour, suggesting the contribution of ϕ exchange (strangeness annihilation);

c) in the central region the decrease of the structure function found at low energy is not observed between 16 and 32 GeV/c (see fig.4).

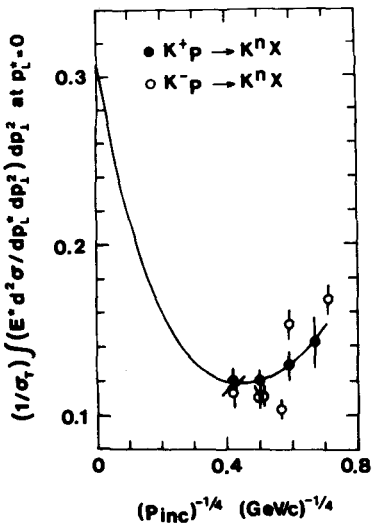


Fig.4. Invariant cross sections at $X=0$ normalized to the total cross section, as a function of $(P_{inc})^{-1/4}$.

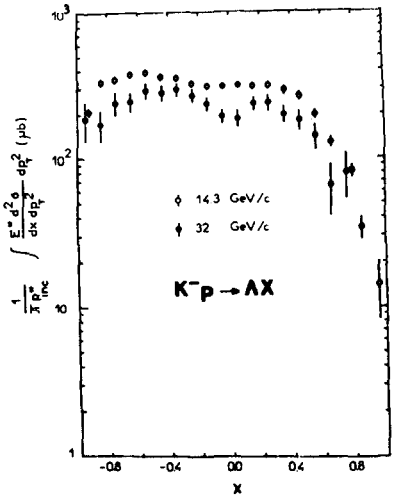


Fig.5. Invariant cross section as a function of x .

The same behaviour is found in K^-p interactions. A general fit of the structure function to all K^+p available experimental data in the interval $|x| < 0.1$ to a double Regge model including PR ($s^{-1/4}$ dependence) and RR ($s^{-1/2}$ dependence) terms is also shown (curve of fig.4); it predicts a rise of the structure function at $X=0$ above ~ 30 GeV/c and its asymptotic value.

1.4. Λ Production

The inclusive production cross section for Λ (and Σ^0) amounts to (0.8 ± 0.08), (2.35 ± 0.08) and (1.7 ± 0.3) mb in K^+p , K^-p and $\bar{p}p$ interactions respectively. A strong increase with incident momentum of the K^+p and $\bar{p}p$ cross sections is observed, while for K^-p there is a definite flattening in the decrease found at lower energy.

In K^-p interactions where the Λ are copiously produced a detailed analysis has been done of the different processes contributing to their production. In particular, the dip which develops near $X=0$ at 32 GeV/c in the invariant cross section (fig.5) can be qualitatively explained by the simultaneous decrease of the hypercharge annihilation processes ($K^-p \to \Lambda + n\pi$) which has a rather flat X dependence, and the increase of two other processes. The firts one, ($K^-p \to \Lambda K\bar{K} + X$) occurs mainly in the proton fragmentation region; from the $K^-p \to \Lambda K^n + X$ cross section it is found to contribute to about 50% of the whole Λ cross section. The second one ($K^-p \to \Lambda N\bar{N} + X$) plays a role in the $X>0$ region. Its relative intensity is estimated from the $K^-p \to \Lambda + p + X$ cross section derived from the events where a Λ and an identified proton are found; it amounts to $\sim$ 13% of the total cross section. This leaves only 37% for the contribution of the hypercharge annihilation, for which the cross section decreases with incident momentum as $P_{inc}^{-0.7}$ between 4 and 32 GeV/c.

1.5. $K^{*\pm}_{890}$ Production

The production of K^{*+}_{890} and K^{*-}_{890} resonances is very important in the K^+p and K^-p -interactions respectively. It is visible on fig.6 where the $K^n\pi^+$ and $K^n\pi^-$ mass distributions are shown. These distributions fitted with a Breit-Wigner function and a suitable background have led to the

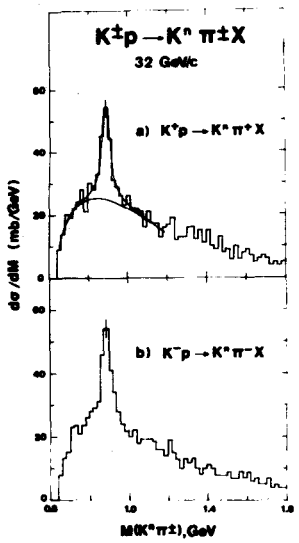


Fig.6. Invariant mass distributions.

following cross sections: $\sigma(K^{*+})$ =(3.4±0.4)mb and $\sigma(K^{*-})$ =(3.9±0.5) mb. Taking into account the proportion of $\bar{K}^0(K^0)$ previously found in $K^+p(K^-p)$ interactions, this means that about one third of the $K^0(\bar{K}^0)$ come from the $K^{*+}(K^{*-})$ decays. Comparing these data with lower energy ones one does not see any obvious energy dependence, although the variation could be compatible with that observed for $K^0(\bar{K}^0)$. The structure functions which have been calculated as a function of x (fig.7) are comparable for K^{*+} and K^{*-} and do not display (for K^{*-}) any significant energy dependence when compared to 10 and 14.3 GeV/c data. Finally the density matrix of these vector

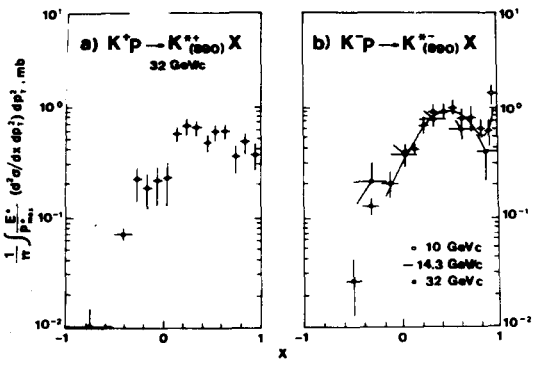


Fig.7. Invariant cross section as a function of x.

resonances have been calculated in the $K^{\pm}$ fragmentation region in the G.J.frame. They show a small amount of alignment and lead to a proportion of ~ 70% of unnatural parity exchange between the incident $K^{\pm}$ and the $K^{*\pm}$ in the region on $M_x^2/s < 0.5$ and $|t_{K K^*}| < 1$ GeV^2.

II. EXCLUSIVE STUDIES

2.1. $K^{\pm}p$ Elastic Scattering

Results have been presented at this Conference on K^-p elastic scattering: the total cross section (2.54±0.10 mb) and the differential cross section are in very good agreement with the data obtained in a counter experiment (14) at 25 and 40 GeV/c. The fig.8 presents the differential cross section; the full line is a fit

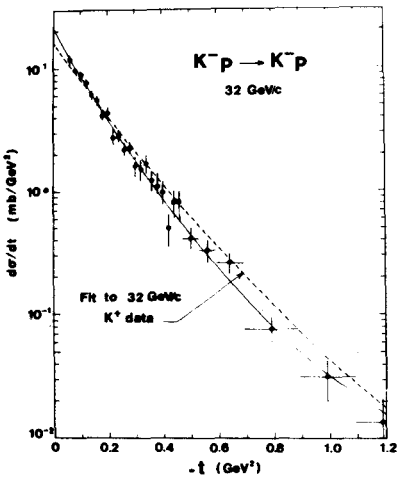


Fig.8. Differential cross section $d\sigma/dt$ for K^-p elastic scattering; the full curve is a Ae^{Bt+Ct^2} fit to the data, and the dashed curve is the fit to K^+p elastic scattering at 32 GeV/c[15].

to Ae^{Bt+Ct^2}. The dashed curve is the fit obtained in the K^+p elastic scattering at 32 GeV/c (15). A first cross over between the two fitted distributions is found at $|t_0|$=(0.16±0.05) GeV^2, which is in agreement with the values found at lower energy (16) and recently in the 50-175 GeV energy range (17). A second cross over located around 1.2 GeV^2 and also reported at 14 GeV (16) can also be guessed from the 32 GeV/c data.

2.2. Reactions $Ap \to Ap + n(\pi^+\pi^-)$ where $A = K^+, K^-, \bar{p}$

The cross sections of these reactions have been measured, they are summarized in table.1. The energy dependence of the four-body reactions $(n=1)$ shows a steeper decrease for K^+ and $\bar{p}$ incident particles than for K^-, which can be explained by a larger amount of 3 and 2 body non diffractive processes (as $K^*\Delta^{++}$ or $\overline{\Delta^{++}}\Delta^{++}$) present in these final states. The general behaviour of the outgoing particles is illustrated in 4,6 and 8 body reactions in fig.9, where the

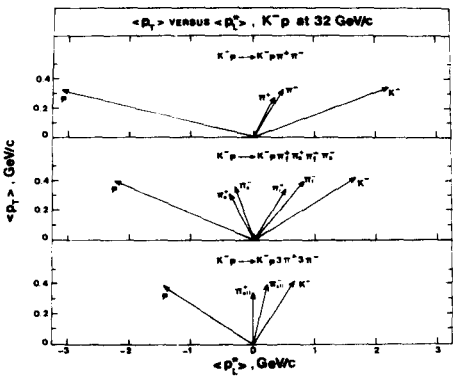


Fig.9. Average direction in the C.M.system of the particles emitted in 4,6 and 8 body reactions.

average C.M. directions is indicated for each kind of particle. The leading effect of p and K^- is, as expected, strongly reduced when the number of pions increases.

2.3. Diffraction Dissociation in 4 Body Reactions

A simple way to present the clustering effects in the four body reactions is to plot the π^+ C.M. rapidity versus the π^- C.M.rapidity as done in fig.10 for the K^+, K^- and $\bar{p}$ reactions. The populations of the sectors where y_{π^+} has the same sign as y_{π^-} is larger than that of the two other sectors especially in $K^-p\,\pi^+\pi^-$ final state where the $K^-\pi^+\pi^-$ and the $p\pi^+\pi^-$ threshold enhan-

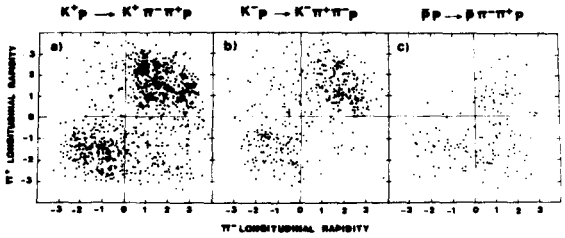


Fig.10. Scattered plot of the y_{π^+} versus y_{π^-} C.M. rapidity in the 4 body reactions.

cements dominate the reaction. In $K^+p\,\pi^+\pi^-$ and $\bar{p}p\,\pi^+\pi^-$ final states, the sectors $y_{\pi^-} > 0$ and $y_{\pi^+} < 0$ have still an important population which is dominated by non-diffractive production of Δ^{++} and K^{*0}_{890}, Δ^{++} and $\overline{\Delta^{++}}$ respectively. The cross sections of the $K^\pm\pi^+\pi^-(Q^\pm)$ and $p\pi^+\pi^-$ diffractive enhancements defined as $M_{K^\pm\pi^+\pi^-} < 1{,}5$ GeV and $M_{p\pi^+\pi^-} < 2.5$ GeV are presented in table II. The ratios of these cross sections to the elastic $K^\pm p$ and $\bar{p}p$ ones, given also in table II, are equal within experimental errors in agreement with the factorization requirements.

2.4. Principal Axis Analysis in the Reactions $K^+p \to K^+p\pi^+\pi^-$ and $K^+p \to K^+p\,2\pi^+2\pi^-$

An analysis of these two reactions has been carried out by this method. The distributions of $\cos\alpha$, where α is the generalized scattering angle defined in the principal axis formalism, have a slope, for the 4 and 6 body reactions of (205 ± 10) and (175 ± 25), which is comparable to that obtained in elastic scattering at 32 GeV/c (195 ± 9). Moreover for these two reactions the outgoing particles are concentrated around a principal plane revealing a certain amount of planarity. Although these observations are difficult to interpret quantitatively, it is interesting to see that some alignment subsists in the 6 body event at this energy.

I would like to thank Dr. P.Granet for the important part he took in the preparation of this report.

Table I

Cross sections in mb for the reactions $K^{\pm}p \to K^{\pm}p + n(\pi^+\pi^-)$ and $\bar{p}p \to \bar{p}p + n(\pi^+\pi^-)$

	K^+p	K^-p	$\bar{p}p$
n=1	0.62±0.05	0.61±0.04	1.40±0.12
n=2	0.15±0.01	0.14±0.01	0.33±0.06
n=3	0.050±0.006	0.060±0.008	0.14±0.04

Table II

Cross sections and ratios σ/σ_{el} for the diffractive enhancements defined as $M_{K\pi\pi} < 1.5$ GeV and $M_{p\pi\pi} < 2.5$ GeV in 4 body reactions

Final state	pQ^+ $\hookrightarrow K^+\pi^+\pi^-$	pQ^- $\hookrightarrow K^-\pi^+\pi^-$	$N^{*+}K^+$ $\hookrightarrow p\pi^+\pi^-$	$N^{*+}K^-$ $\hookrightarrow p\pi^+\pi^-$	$N^{*+}\bar{p}$ $\hookrightarrow p\pi^+\pi^-$
	230±20	235±20	160±20	177±20	480±80
	(9±1)%	(9.6±1)%	(6.7±1.3)%	(7.0±1.5)%	(5.8±1)%

References

1. P.V.Chliapnikov et al.Study of Inclusive Reaction $K^+p \to K^h + X$ at 32 GeV/c. 1167/A2-127.
2. M.De Beer et al. Inclusive K^{*+}_{890} Production in K^+p Interactions at 32 GeV/c.1168/A2-128.
3. J.Saudraix et al. General Features of the Reaction $K^+p \to K^+p\pi^+\pi^-$ at 32 GeV/c.1165/A1-121.
4. I.V.Ajienko et al. An Analysis of K^+pInteractions at 32 GeV/c in Terms of "Principal Axis" Variables.1162/A1-50.
5. C.Cochet et al. Particle Multiplicities in K^-p Interactions at 32 GeV/c.1034/A2-89.
6. V.V.Babintsev et al. A Study of the Associated Multiplicities in K^-p Interactions at 32 GeV/c. 204/A2-35.
7. Yu.J.Arestov et al. Study of Λ Production Processes in K^-p Interactions at 32 GeV/c.207/A2-37.
8. U.Gensch et al. Inclusive Resonance Production in K^-p Interactions at 32 GeV/c.206/A2-36.
9. A.Givernaud et al. Cross Features of the Dominant Exclusive Reactions in K^-p Interactions at 32 GeV/c.38/A1-37.
10. J.Hanton et al.Inclusive Production of Strange Particles and π^0_s in $\bar{p}p$ Interactions at 32 GeV GeV/c. 1035/A2-90.
11. M.A.Jabłol et al. Cross Sections and General Features of the 4C Channels in $\bar{p}p$ Interactions at 32 GeV/c.1036/A1-9.
12. F.T.Dao and J.Whitmore. P.L.46B(1973)252.
13. France-Soviet Union and CERN-Soviet Union Collaboration,to be published in Nuclear Physics.
14. Y.M.Antipov et al. N.P.B57(1973)333.
15. Y.Cranet et al.P.L.62B(1976)350.
16. G.Brandenburg et al. P.L.58B(1975)367.
17. R.L.Anderson et al. Fermilab preprint 76/47.

ЭКСПЕРИМЕНТАЛЬНЫЕ ДАННЫЕ ОБ ИЗМЕРЕНИИ РАЗМЕРОВ ОБЛАСТИ ВЗАИМОДЕЙСТВИЯ. ЭФФЕКТ ТОЖДЕСТВЕННОСТИ

М.И.Подгорецкий
Объединенный институт ядерных исследований, Дубна

I. Экспериментальные работы, представленные на конференцию, вместе с опубликованными ранее, содержат информацию о взаимодействиях $\pi^{\pm}p, \pi^{-}C, pp, \bar{p}p$ и $\bar{p}n$ в интервале импульсов от I до 200 ГэВ/с.

Возможность корреляционного измерения размеров источника впервые была продемонстрирована в связи с т.н. эффектом G GLP (см. /I/ и последующие экспериментальные работы; на конференции - доклады /2-4/. Однако принципиальные основы корреляционного метода в его современном понимании разработаны в течение последних пяти лет /5-8/. Основная идея, взятая из астрономии /6,9/, имеет своим исходным пунктом классические работы Г.С.Горелика /I0,II/, установившего наличие интерференционных свойств света, испускаемого независимыми источниками. Применительно к пионам эта идея достаточно широко обсуждена в указанной выше литературе. Речь идет о бозе-симметризации амплитуды регистрации двух тождественных пионов, испущенных в разные моменты времени и из разных мест излучающего объема. В результате возникают интерференционные корреляции, повышающие вероятность регистрации тождественных пионов с близкими импульсами.

Соответствующие формулы модельно зависимы, но имеют общую структуру. Если, например, источники "включаются" одновременно и расположены на поверхности сферы радиуса R, а их время жизни $\tau \gg R/c$, то вероятность наблюдения пионов с импульсами $\vec{p}_1$ и $\vec{p}_2$

$$W = W_0(1+\Delta), \quad \Delta = \frac{[2J_1(q_\perp R)/q_\perp R]^2}{1+(q_0\tau)^2} \simeq \frac{\exp[-\frac{1}{4}q_\perp^2 R^2]}{1+(q_0\tau)^2}. \quad (I)$$

Здесь $q_0 = E_1 - E_2$, $\vec{q} = \vec{p}_1 - \vec{p}_2$, $\vec{q}_\perp$ - проекция $\vec{q}$ на плоскость, перпендикулярную $\vec{p} = \frac{\vec{p}_1 + \vec{p}_2}{2}$. Множитель W_0 соответствует фоновому распределению без интерференции. Обычно для экспериментального определения W_0 используют пары $\pi^+\pi^-$, хотя такой выбор требует еще специального обсуждения.

Наблюдая корреляции пар $\pi^+\pi^+$ и $\pi^-\pi^-$, можно с помощью (I) измерить параметры R и τ. Можно также определить форму излучающей области, если сопоставить результаты для пар, вылетающих в разных направлениях.

В общем случае физический смысл величины τ довольно сложен. Она слагается из среднего времени жизни источников τ_1, разброса моментов "включения" источников τ_2 и "продольного времени" $\tau_3 = \frac{R}{V}$, где V - скорость отбираемых пионов.

При современном состоянии эксперимента можно надеяться измерить только некоторую комбинированную эффективную величину τ. В отношении величины R следует подчеркнуть, что она связана с расстоянием между источниками, поставляющими тождественные пионы с близкими импульсами. В статистических схемах это совпадает с полными размерами излучающей области, но в мультипериферических моделях R, вероятно, характеризует расстояние между соседними узлами диаграмм. Заметим еще, что если пионы рождаются не непосредственно, а в результате распада достаточно долгоживущих резонансов, величины R и τ определяются пробегом и временем жизни этих резонансов.

Высказывались опасения, что $\pi\pi$-взаимодействия в конечном состоянии могут существенно исказить нарисованную картину. Оценки, проведенные в /2I/, показали, что это не так.

2. Экспериментальные результаты получены в работах /2,I2-I8/, где приведены спектры $q_\perp$ для различных значений q_0 и спектры q_0 для различных значений $q_\perp$. Параметры R и τ измерялись путем сопоставления двумерных распределений по $q_\perp$ и q_0 с выражениями типа (I); фоном в большинстве случаев служили пары $\pi^+\pi^-$. На рис. I и 2 приведены для примера некоторые из полученных распределений (рис. I из /2/, рис. 2 из /I8/). Из совокупности указанных работ с несомненностью следует как само существование интерференционных корреляций тождественных частиц, так и двумерный характер этого эффекта.

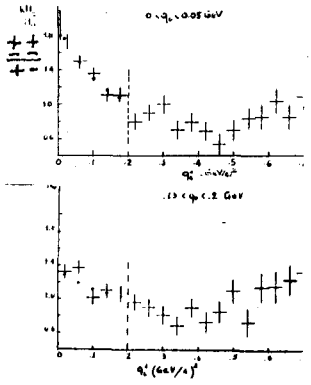


Рис. I

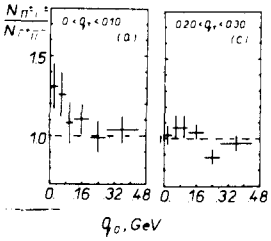


Рис. 2

В таблице дана сводка полученных результатов. По ряду обстоятельств их следует пока что считать предварительными. Отметим, в частности, что в большинстве случаев отношение $\frac{W(0,0)}{W(\infty,\infty)} < 2$, т.е. не согласуется с формулами типа (I). Это может быть связано со многими

Таблица

№ работы	Реакция	Импульс, ГэВ/с	R, Фм	$c\tau$, Фм
/2/	$\bar{p}n \to 3\pi^-2\pi^+n$	I,0÷I,6	$I,29\pm0,06$	$I,47^{+0,18}_{-0,16}$
/I2/	$K^+p \to K^+p2\pi^+2\pi^-$	8,25	$0,8\pm0,08$	$\sim I,0$
/I3/	$pp \to p\pi\pi\ldots$, $n_c \geq 6$	28,5	$I,3\pm0,I$	$0,3\div0,4$
/I4/	$\pi^\pm p \to \pi^\pm p2\pi^+2\pi^- \to \pi^\pm p3\pi^+3\pi^-$	4÷25	$I,0^{+0,4}_{-0,2}$	$0,7^{+0,6}_{-0,3}$
/I5/	$\pi^-p \to \pi\pi\ldots$, $n_c \geq 6$ $\pi^-C \to \pi\pi\ldots$, $n_c \geq 6$	40	$I,3\pm0,3$ $5,I\pm I,5$	$0,5\pm0,4$ $2,0\pm2,2$
/I6/	$\pi^-p \to p2\pi^+3\pi^-X^0 \to p2\pi^+3\pi^- \to n3\pi^+3\pi^-$	II,2	$I,04\pm0,I$	$0,4I\pm0,I5$
/I7/	$\pi^-C \to p\pi^-\pi^-\pi^+\ldots$	3,7	$2,6\pm I,2$	$0,76\pm0,47$
/I8/	$\bar{p}p \to \pi\pi\ldots$, $n_c \geq 6$	22,4	$3,I\pm0,4$	$3,3\pm I,4$

причинами; не исключено, что существенную роль играют особенности использованного фона. Для пар $\pi^+\pi^-$ интерференционные корреляции отсутствуют в рамках простейших статистических моделей, но они могут иметь место для мультипериферических схем и даже для таких статистических моделей, в которых мезоны образуются в результате распада промежуточных резонансов. Это может понизить отношение $W(0,0)/W(\infty,\infty)$ и несколько изменить параметры R и τ. Из сказанного ясна важность специального изучения и сопоставления различных способов конструирования фона /I2, I5, I7/. Не исключено, что в некоторых случаях окажется целесообразным применять процедуры "перемешивания" вторичных частиц, описанные в /I9/.

Во всех работах величина τ оказалась довольно малой ($c\tau \lesssim R$). Поскольку одна из компонент τ имеет чисто геометрическую природу /6, I9/, истинное время жизни еще меньше, что плохо согласуется с наивными статистическими представлениями. Следует, впрочем, иметь в виду, что измеряемое значение τ зависит от скорости источника. Кроме того, ошибки в определении энергии также могут привести к фиктивному уменьшению величины τ.

Из работ /I4-I6/, по-видимому, следует, что в $\pi^\pm p$ -взаимодействиях при $n_c \geq 6$ величина $R \sim 1$ Фм и мало зависит от знака и энергии первичных частиц в интервале от 4 до 40 ГэВ/с. Интересно, что такое же значение R получено также для взаимодействий K^+p при 8,25 ГэВ/с /I2/ и pp при 28,5 ГэВ/с /I3/. Иначе ведут себя аннигиляционные процессы. При импульсе (I÷I,6) ГэВ/с величина R примерно такая же, как для πp- и pp -взаимодействий /2/. Однако с увеличением энергии R сильно растет /I8/. Вместе с тем параметры удара в процессах с аннигиляцией, по-видимому, в несколько раз меньше, чем в процессах без аннигиляции /20/. Причины этих различий пока что неизвестны.

Следует подчеркнуть, что "корреляционные размеры" не должны обязательно совпадать с размерами, определяемыми из анализа поперечных импульсов вторичных частиц или с помощью данных по упругому рассеянию. В каждом из этих случаев мы получаем информацию о различных сторонах сильных взаимодействий. Поэтому все указанные подходы надо считать не конкурирующими, а дополняющими друг друга.

С связи с исследованиями в области релятивистской ядерной физики интересны корреляции тождественных частиц, образующихся во взаимодействиях с участием ядер. В настоящее время известны такие результаты по $\pi\pi$ -корреляциям в π^-C -взаимодействиях при 3,7 ГэВ/с /I7/ и 40 ГэВ/с /I5/. В обеих работах отмечается сильное увеличение R по сравнению с πp -взаимодействиями. Интересно было бы выяснить, как

ведут себя $\pi^-\pi^-$-корреляции (а также корреляции между быстрыми протонами) при переходе к более тяжелым ядрам.

Выше уже отмечалось, что корреляционный анализ, в принципе, позволяет получить представление о форме излучающей области. Такие попытки были предприняты при изучении $\pi^\pm p$ -взаимодействий[14] и $\bar{p}p$ -взаимодействий[15]. В обеих работах получены указания на отступления от сферы, однако в первом случае речь идет об эллипсоиде, сжатом в направлении движения первичных частиц, а во втором случае - о вытянутом эллипсоиде. Дальнейшее изучение этого вопроса представляет несомненный интерес.

Корреляции тождественных частиц имеют, по-видимому, непосредственное отношение к азимутальным корреляциям и к корреляциям поперечных импульсов, но этот вопрос выходит за рамки моей темы. Недостаток времени не позволяет также обсудить методы определения параметра удара и сопоставить их с корреляционным методом.

Итоговый вывод таков: изучение корреляций тождественных частиц может дать новые важные сведения о свойствах сильных взаимодействий, если удастся существенно повысить точность экспериментальных данных. Вероятно, это обстоятельство потребует более широкого использования электронных методик, хотя пузырьковые камеры тоже не сказали еще здесь своего последнего слова.

Литература

I. G.Goldhaber, S.Goldhaber et al., Phys.Rev., 120, 300 (1960).
2. G.Borreani, F.Marchetto et al., 112/A2-66.
3. N.N.Biswas, J.M.Bishop et al. 1022/A2-107.
4. A.Quareni-Vigundelli, G.Di Caporiacco et al., 1202/A2-132.
5. В.Г.Гришин, Г.И.Копылов, М.И.Подгорецкий. ЯФ, I3, III6 (I97I).
6. Г.И.Копылов, М.И.Подгорецкий. ЖЭТФ, 69, 414 (I975); см. также литературу, цитированную в этой статье.
7. E.V.Shuryak. Phys.Lett., 44B, 387 (1973).
8. G.Cocconi. Phys.Lett., 49B, 459 (1974).
9. R.Hanbury Brown, R.Q.Twiss. Phil.Mag., 45, 663 (1954).
I0. Г.С.Горелик. ДАН СССР, 58, 45 (I947).
II. Г.С.Горелик. ДАН СССР, 83, 549 (I952).
I2. F.Grard, V.P.Henry et al. Nucl.Phys., 102B, 221 (1976).
I3. J.Canter, F.T.Dao et al. BNL-20516 (1975).
I4. M.Deutschmann, R.Honecker et al. Nucl.Phys., 103 B, 198 (1976).
I5. N.Angelov, L.A.Didenko et al. 205/A2-108.
I6. E.Calligarich, G.Cecchet et al. Lett. Nuovo Cim., 16, 129 (1976).
I7. Ю.Д.Баюков, В.Б.Гаврилов и др. ИТЭФ-70 (I976).
I8. А.А.Локтионов, М.С.Такибаев и др. I60/A2-I0.
I9. G.I.Kopylov, M.I.Podgoretsky. Commun. JINR, E2-9285, Dubna, 1975.
20. H.Braun, P.Fischer et al. 377/A2-109.
2I. Г.И.Копылов. 939/A2-II9.

MULTIPLE PRODUCTION ABOVE 10^{14} eV

N.N.Roinishvili
Institute of Physics of the Academy of Sciences of GSSR, Tbilisi

1. Introduction

There are 5 contributions presented to the Conference concerning multiple production above 10^{14} eV.

i. The main problem discussed in all of them is the following. Are the experimental data at very high energy ($\sim 10^{15}$ eV) in agreement with extrapolations of data obtained at the accelerators ($\sim 10^{12}$ eV)?

In most of them the answer is more or less, but negative.

ii. All the papers presented used an indirect method of evaluating results.

As it is at present impossible to investigate individual hadron-hadron interactions their arguments are based on properties of nuclear-electromagnetic cascades (NEC) induced by a high energy hadron in the atmosphere or in solid substance.

iii. Depending on lower energy limit of detected particles two kinds of phenomena are observed.

1. Extensive air showres (EAS) are NEC at the age when they are almost in equilibrium of their development. Main component of EAS are electrons, muons and hadrons, the number of which is about 10^5-10^6. Suitable arrangement for their detection covers km^2. Threshold energy $E_{th} \sim 1$MeV.

2. γ and hadron families are young NEC in which a number of first step of generations is detected. Main component of the families are photons, electrons and hadrons. Suitable arrangements are the so-called x-ray emultion chambers ($E_{th} \sim$ (1-2) TeV).

2. EAS Results

EAS data are analysed in two contributions, presented by Moscow State University[1] and the English-Polish group[2].

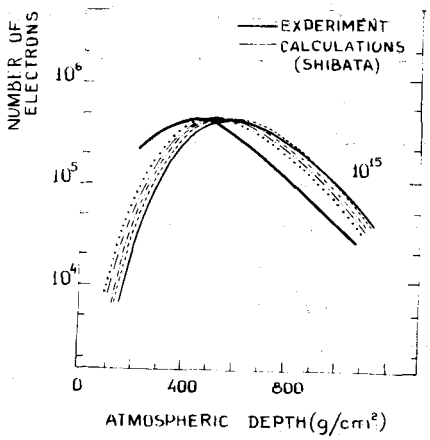


Fig.1 shows the average cascade curve of EAS at 10^{15} eV[2]. Full line denotes experimental data, dotted lines, various extrapolations of accelerator data.

As is seen, EAS develops more rapidly than it is expected.

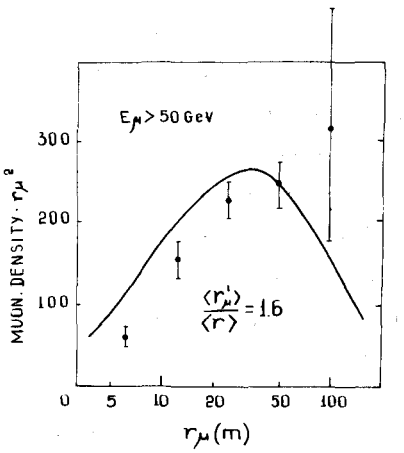


Fig.2.(MSU result, presented by the English-Polish group) Lateral distribution of the high energy muons. The figure proves that the fast development of EAS relates to the hadronic component as well.

Another piece of information comes from correlations between various components of EAS[1].

The authors of both the contributions are analysing a number of possible reasons of such disagreement:

change of chemical composition of primary cosmic ray,

increase of nucleon-antinucleon pair production and others.

They came to the conclusion that the best explanation is based on the assumption: the

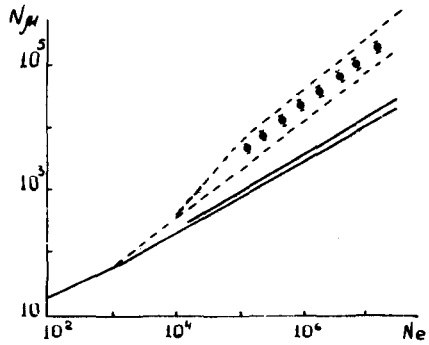


Fig.3. Multiplicity of muons in showers with given number of electrons is by an order of magnitude higher than expeoted.

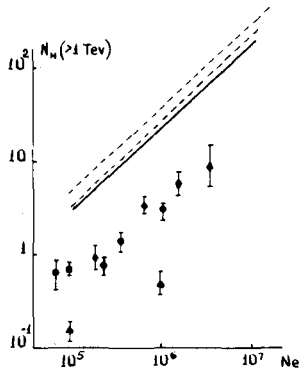


Fig.4. Multiplicity of hadrons is by an order of magnitude lower than expected.

average multiplicity increases as $\langle n \rangle \sim E^{1/4}$ or even more rapidly above 10^{14} eV.

3. Families Results

During the last three years 7 Soviet and 2 Polish institutes exposed x-ray emulsion chambers with total area ~ 1000 m^2 in Pamir mountains (Pamir collaboration)[3]. Two reports concerning the work are presented. The experimental one is based on analyses of 230 families with total energy $\Sigma E \geq 30$ TeV ($E_0 \gg 10^{14}$ eV). The second report presents NEC calculations of checked various models having inclusive spectra like that obtained on the accelerators[4].

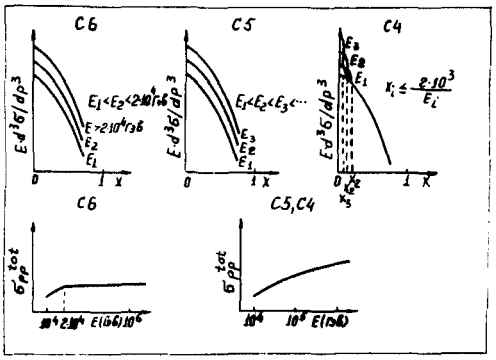


Fig.5 shows a typical property of used models.

In C6 σ_{tot} rise only till 10^{14} eV. According to it inclusive spectra of pions change in the whole region of x from 0 to 1.

In C5 and C4 $\sigma_{tot} = (3.6 \ln E_0 + 40.7)$ mb

In C5 inclusive spectra changed as in C6, and in C4 only the pionisation region violates the scaling.

It is shown in the report that the flux of hadrons and photons obtained by Pamir collaboration can be explained better by C4 model.

The most direct result is presented in the experimental paper of Pamir collaboration[3] (Fig.6). It is integral distribution of f' variable normalised to one family. f' is an analog of x-variables for nuclear electronic cascade. It is the fraction to total energy carried out by given photons $f' = E/\Sigma' E$. In this analysis f'_{min} is independent of $\Sigma' E$ and equal to 0.04.

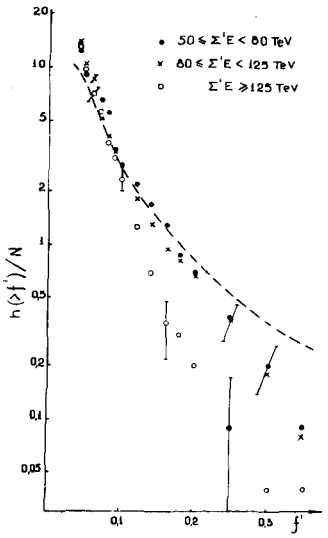


Fig.6

It can be shown that if scaling holds in fragmentation region then f' spectra do not depend on the ΣE.

As one can see from Fig.6, starting from 10^{14} eV f' spectra indicate that it is not the fact. Unfortunately, statistics is still poor. In the nearest future better statistics will be available in Pamir experiment.

§4. Results Obtained by NEC in Solid Substances

The serious change of elementary act at 10^{14} eV is presented by Lebedev Physical Institute[5]. By means of ionization calorimeter in Tian Shan mountains, the authors were studying NEC properties in lead. They observed that

i. The fraction of the energy of primary hadron transferred to π^0 ($K_{\pi^0} \simeq 17\%$) is independent of the energy until 30 TeV.

ii. An attenuation length which at lower energy is equal to $3\lambda_{int}$ sharply increases at $E \sim 10^{14}$ eV (Fig.7).

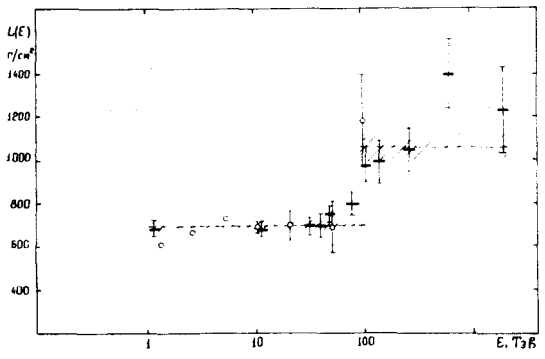


Fig.7

One of the simplest explanation of the result is the production of a new unstable particle with $\sigma_{in}(or K)$ 2 or 3 times less than σ_{in}^{hh} (or K^{hh}).

References

Papers contributed to the conference.

1. S.N.Vernov et al. 778/A2-110.
2. J.Olejniczak et al. 194/A2-29.
3. V.K.Budilov et al. 169/A2-1.
4. A.M.Dunaevsky et al. 803/A2-84.
5. V.P.Pavljuchenko et al. 168/A2-2.

INCLUSIVE REACTIONS AT MEDIUM ENERGIES

W.Kittel

University of Nijmegen, Netherlands

Two interesting questions studied in inclusive reactions at medium energies are those of inclusive resonance production and strange baryon production. The first has been treated by P.Schmid[1], so I can concentrate on strange baryon production.

At medium energies, the inclusive $K^-p \to \Lambda^c X^c$ cross section decreases like about $P_{LAB}^{-0,5}$, while the $K^-p \to K^0\Lambda^c$ cross section increases slightly[2]. The $\pi^-p \to \Lambda^0 X^0$ structure function shows approximate scaling for $X \gtrsim -0.8$ between 5 and 205 GeV/c, while it grows by a factor 3 at $X \simeq 0$ for $\pi^-p \to \bar{K}^0 X^0$ in the same energy range[3].

A high statistics measurement of the Λ^0 polarization P in $K^-p \to \Lambda^0$ + pions at 4.2 GeV/c[4] shows (fig.1) that P is positive for $X \lesssim -0.5$

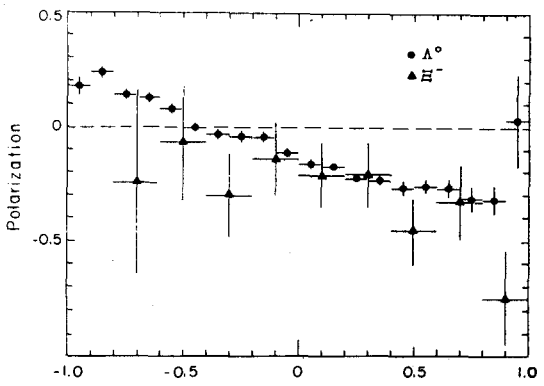


Fig.1. Polarization of the Λ^0 and Ξ^- from $K^-p \to \Lambda^0 X^0$ and $K^-p \to \Xi^- X^+$ at 4.2 GeV/c. and negative above in this reaction. From comparison to higher energies[5] we deduce that P decreases with energy for $X \lesssim -0.5$ while it is constant for $X \gtrsim -0.5$. The Ξ^- polarization from $K^-p \to \Xi^- X^+$ at 4.2 GeV/c[6] is given in the same figure. It compares well with that of the Λ^0 in the region where the Ξ^- structure function is large ($X \gtrsim -0.5$).

On the other hand, the polarization of Λ^0's produced in $\pi^-p \to \Lambda^0 X^0$ at 8 GeV/c[7] vanishes for $0 < X \leq 0.6$ and rises to $P=1$ for $X \to 1$. In $\bar{p}p \to \Lambda^0 X^0$ studied at 5.7 GeV/c[4] the Λ^0 polarization is small or negative for $X < 0$; a similar behaviour is found for Λ^0's from $K^-p \to \Lambda^0 + K\bar{K} +$

pions at 4.2 GeV[4]. These observations are in qualitative agreement with the similarities or differences of the triple-Regge diagrams possibly contributing to the above reactions.

Quantitative results can be obtained for the effective trajectories in triple-Regge diagrams, even at energies where the conditions for the triple-Regge expansion are not satisfied. In agreement with the observed polarization, the p-trajectory was shown to dominate $K^- \xrightarrow{p} \Lambda^0$ beam fragmentation at 4.2 GeV/c[8]. For $p \xrightarrow{K^-} \Lambda^0$ target fragmentation at 4.2 GeV/c the effective trajectory lies between the K and K^* trajectory[8], for $K^+ \xrightarrow{p} \Lambda^0$ at 8.2 and 16 GeV/c[9] the data are consistent with the K trajectory (fig.2).

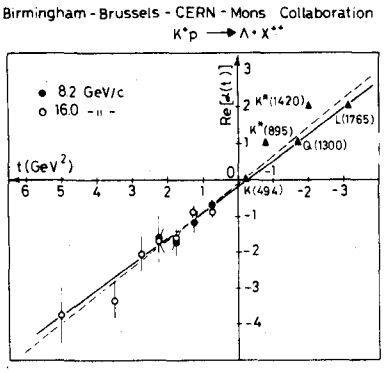


Fig.2. Effective trajectory points for $K^+p \to \Lambda^0 X^{++}$ target fragmentation. The dashed line is a fit through the data at 8.2 and 16.0 GeV/c, the solid line is the trajectory drawn through the K, Q and L positions.

At medium energies, the mass distribution of X is dominated by resonance production. This can be described by the triple-Regge expansion only in an average sense[10]. For target fragmentation $p \xrightarrow{K^-} \Lambda^0$ at 4.2 GeV/c, the off-shell forward $K\bar{K}$ and $K^*\bar{K}$ scattering amplitude is written as a sum of Veneziano four-point amplitudes plus diffractive terms[11]. Leaving 11 coupling constants as free parameters gives the fit to the m_X distribution shown in fig.3 for various t intervals. Five of these eleven couplings determine the target fragmentation $p \xrightarrow{K^-} \Sigma^+$. The m_X distribution for this reaction is reproduced without further fitting, also for various t intervals.

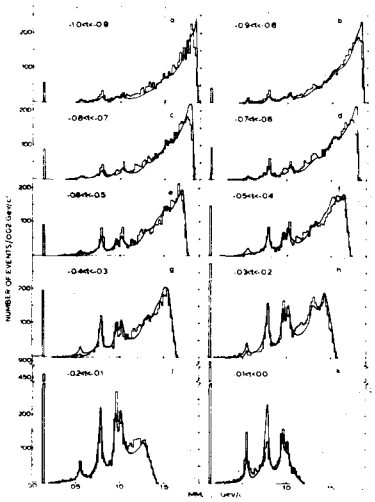


Fig.3. Missing mass produced against the Λ^0 in $K^-p \to \Lambda^0 X^0$ target fragmentation at 4.2 GeV/c for ten $t_{p\Lambda}$ intervals between -1,0 and 0,0 GeV^2. The curves are from the fit described in the text.

The inclusive Σ (1385) cross section falls for $\Sigma^+(1385)$ production at medium energies and is constant for $\Sigma^-(1385)$ production[12]. While $\Sigma^-(1385)$ is predominantly produced around $X=0$, $\Sigma^+(1385)$ has a leading particle peak around $X \simeq -0.8$, in particular at 4.2 GeV/c. The decay distribution of $\Sigma^+(1385)$ is in agreement with prediction of the additive quark model.

References

1. P.Schmid."Inclusive Part. and Resonance Speotra - an Attempt to Separate Directly Produced Particles from Decay Products" Invited talk in this session.
2. ANL-Brussels-Kansas-Michigan-Tufts Collaboration, B.Musgrave et al. "Inclusive V^0-Production in K^-p Interaotion at 6.5 GeV/c". Paper 366/A2-59.
3. Dubna-Tbilisi-Kosice-Erevan-Minsk-Collaboration, Yu.A.Budagov et al."Inclusive Λ^0 and K^0-Production in π^-p and π^-C Interactions at 5 GeV/c". Paper 811 / A2-82.
4. Amsterdam-CERN-Nijmegen-Oxford Collaboration "Study of Λ -Polarization in 4.2 GeV/c K^-p and 5.7 GeV/c $\bar{p}p$ Interactions. Paper 272/A2-50.
5. I.Bartsch et al. Nucl.Phys., B40, 103 (1972); S.U.Chung et al. Phys.Rev., D11, 1010 (1975); M.Abramowicz et al. Nucl.Phys., B105, 222 (1976).
6. Amsterdam-CERN-Nijmegen-Oxford Collaboration "A Study of Inclusive Ξ^- Production from K^-p Interactions at 4.2 GeV/c" paper 276/A2-51.

7. Freiburg-Saclay-Zurich Collaboration, "Preliminary Results on Incl. Forward Λ -Production in $\pi^{\pm}p$ and $K^{-}p$ Interactions at 8 and 12 GeV/c" Paper at this Conference.
8. R.Blokzijl et al. Nucl.Phys., B48, 401 (1975).
9. CERN-Birmingham-Brussels-Mons Collaboration, P.V.Chliapnikov et al. "The Reactions $K^{+}p \to \Lambda X^{++}$ and $K^{+}p \to \bar{\Lambda} X^{++}$ at Incident Momenta of 8.2 and 16.0 GeV/c", paper 1060/A2-75.
10. Chan Hong-Mo, H.I.Miettinen and R.G.Roberts. Nucl.Phys., B54, 411 (1973).
11. Amsterdam-CERN-Nijmegen-Oxford Collaboration, R.Blokzijl et al. Dual Analysis of Target Fragmentation in $K^{-}p \to \Lambda X$ and $K^{-}p \to \Sigma^{\mp} X$ at 4.2 GeV/c" paper 279/A2-78.
12. Aachen-Berlin-CERN-London-Vienna Collaboration, "Inclusive Production of $\Sigma^{\pm}(1385)$ in $K^{-}p$ Interactions at 10 and 16 GeV/c", paper 144/A2-111.
I.D.Aljolhin et al. "$\Sigma^{*}(1385)$ and K^{*} Resonance Production in $\pi^{-}p$ Interactions at 4.35 and 4.85 GeV/c", paper 190/A2-23.
Amsterdam-CERN-Nijmegen-Oxford Collaboration, "Study of $\Sigma^{\pm}(1385)$ Inclusive Production in $K^{-}p$ Interactions at 4,2 GeV/c", paper 278/A2-52.

INCLUSIVE π^{0} AND γ PRODUCTION IN PION-PROTON INTERACTIONS AT 5 GEV

Yu.A.Budagov, L.Šándor

JINR, Dubna

One meter JINR propane bubble chamber collaboration (Dubna-Košice-Tbilisi-Yerevan-Minsk) studied the inclusive neutral particle production $(\pi^{0}, \gamma, \Lambda^{0}, K^{0})$ in 5 GeV pion-nucleon interactions. Some results are presented in this report and compared with high energy experimental data.

Previously we have measured the cross sections of many different exclusive reactions $-\pi^{-}p \to (0,2,4)$ charged particles + $(1,2,3,4,5)\pi^{0}$ and $\pi^{-}p \to (0,2,4)$ charged particles + $(\geq 1\gamma^{0}) + (\geq 1\pi^{0})$. Together with the data of other groups they form almost a complete set of 5 GeV $\pi^{-}p$ -scattering partial cross sections[1]. This allowed one to obtain new data on the multiparticle production.

The π^{0} multiplicity distribution at 5 GeV is close to Poisson form with $f_2^{\omega} = -0.07 \pm 0.10$; at 40 GeV this distribution becomes wider[2].

The analysis of the total multiplicity $n = n_{+} + n_{-} + n_{0} + 1$ distribution for the reaction $\pi^{-}p \to n_{+}\pi^{+} + n_{-}\pi^{-} + n_{0}\pi^{0} + N$ at our energy and at 10, 16, 40 GeV (other groups measurements) shows[3] that the logarithm of the integrated probability of $\geq n$ particle production $F(n)$ is a linear function of the reduced multiplicity squared: $F(n) \sim (n-2)^2$ (see Fig.1).

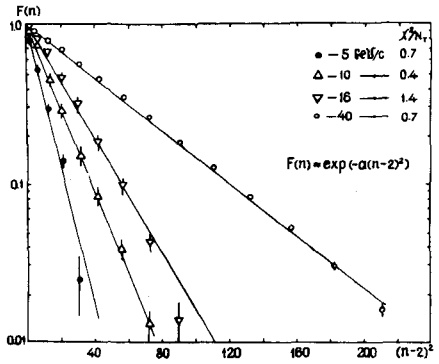


Fig. 1

The multiplicity distribution for the "newly produced" particles $n' = n - \alpha$ (α - the average number of leading particles[4]) in 5-40 GeV interval follows the KNO-scaling (Fig.2). With $\alpha = 2$ the universal function $\psi(z' = n'/\langle n' \rangle$ has the form $\psi(z') = \frac{\pi}{2} z' \exp\left(-\frac{\pi}{4} z'^2\right)$

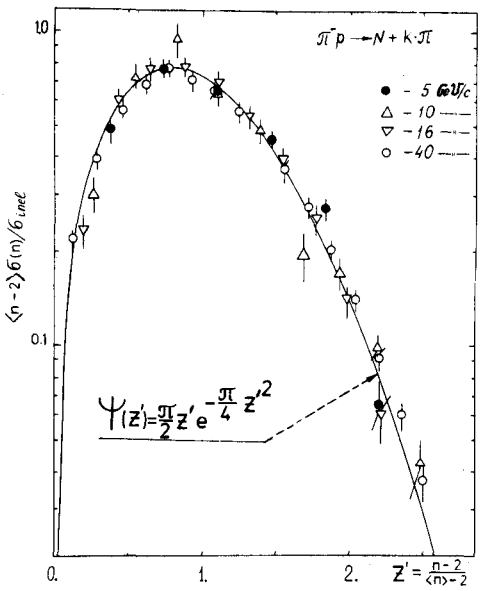


Fig. 2

This function with $\alpha = 0.7$ describes satisfactory also the charged-particle multiplicity distributions for the πp, Kp and pp -interactions above 20 GeV[5].

The analysis of the correlations in the yields of π^0-s and charged secondaries for 5-205 GeV $\pi^- p$ collisions gave the following results[6]. The dependence $\langle n_0 \rangle_{n_-} = f(n_-)$ is satisfactorily described by linear function $f(n_-) = a + b n_-$. The values of the b parameter are the same within error limits for the $\pi^- p$ and pp interactions in the whole energy interval studied.

Fig.3 represents the correlation integrals f_2^{--} and f_2^{0-} as a function of incident momentum. The approximating function $f_2^{--} = 0.86 - 1.15 \ln S + 0.16 (\ln S)^2$ is shown by the full line. The dashed line corresponds to the relation $f^{0-} = f_2^{--} + \frac{1}{2}\langle n_- \rangle$.

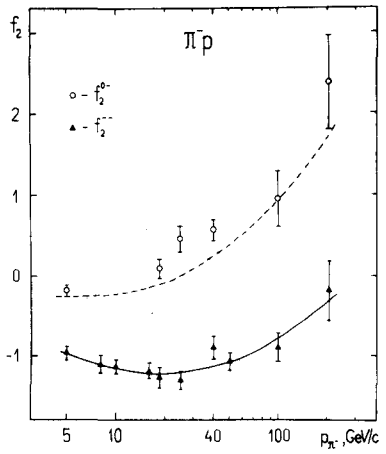


Fig. 3

The deviation from the dependence $f_2 \sim \ln S$ gives evidence to a noticeable contribution of the long-range correlations. The experimental data agree with the relation $f_2^{0-} = f_2^{--} + \frac{1}{2}\langle n_- \rangle$; within the Regge-Mueller approach it shows that the contribution of diagrams with isospin $I \geq 2$ exchange is small.

The study of the scaling properties of the semi-inclusive π^0 cross sections for 5-205 GeV/c $\pi^- p$ scattering[7] shows that for the momentum range $p_{\pi^-} < 40$ GeV/c the Dao-Whitmore relation $\langle n \rangle \sigma_n(x^0)/\langle n_0 \rangle \sigma_{in} \to \Phi(z = \frac{n}{\langle n \rangle})$ is not valid (n - the charged-particle multiplicity). At the same time there is an obvious similarity of the $\langle n \rangle \sigma_n(x^0)/\langle n_0 \rangle \sigma_{in}$ distributions in the whole energy interval studied. We have noticed that the variety of the experimental data may be regularized if one introduces the scale transformation $z_1 = z + \frac{\beta}{\langle n \rangle_2}$ with β=const. It gives the universal description for the whole experimental results available.

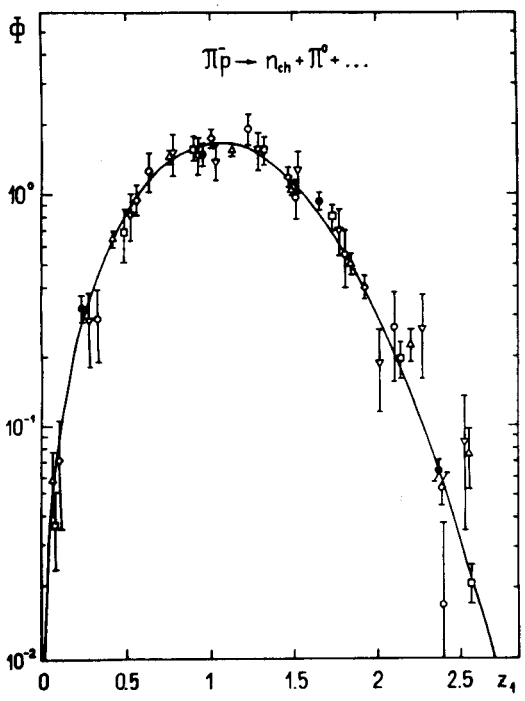


Fig. 4

In Fig.4 the values of $\langle h \rangle \sigma_n(\pi^0)/\langle n_s \rangle \sigma_{in}$ for 5 GeV - ●, 18.5 GeV - ◇, 25 GeV - □, 40 GeV - △, 100 GeV - ○ and 205 GeV - ▽ $\pi^- p$ collisions as a function of new variable z_1 are plotted. Solid line - approximating function $\varphi(z_1) = a_0 z_1 \exp(a_1 z_1 + a_2 z_1^2)$

If the proposed energy dependence should be valid at higher energies too, the result obtained may be interpreted as the quantitative description of the approach to asymptotics for the $\langle h \rangle \sigma_n(\pi^0)/\langle n_s \rangle \sigma_{in}$ distribution.

We have measured the differential cross section

$$\frac{E^*}{\pi p^*_{max}} \frac{d^2\sigma}{dx\, dp_\perp^2} = f(x, p_\perp)$$

for the reaction $\pi^- p \to \gamma + \ldots$ at 5 GeV/c in a large range of x and $p_\perp$ using the statistics of ≈ 10000 γ-quanta[8]. The results are given in Fig.5.

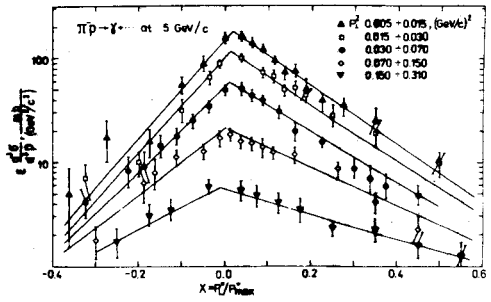


Fig. 5

The experimental data are satisfactorily approximated by the function $f(x,p_\perp) = a_1 \exp(-B|x| + a_4 p_\perp)$, $B = a_2 \exp(-a_3 p_\perp^2)$; where a_i are the free parameters. The function $f(x,p_\perp)$ does not factorize with respect to x and $p_\perp$ at energy of 5 GeV.

We have shown earlier[9] that the differential cross sections $\int E \frac{d^2\sigma}{d^3p} dp_\perp^2$ of the reaction $\pi^- p \to \gamma + \ldots$ are energy independent a) in the central region for 5-100 GeV interval and b) in both fragmentation regions for 5-40 GeV primary energy interval.

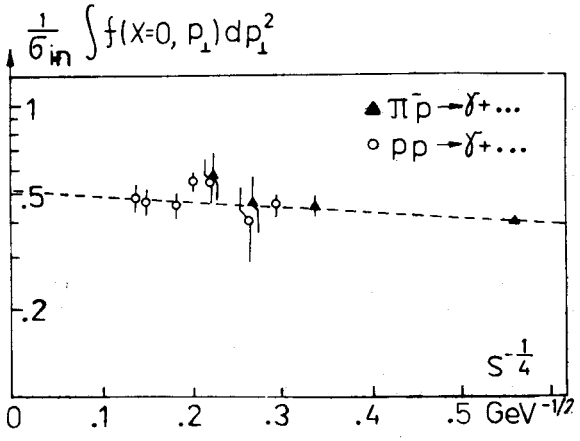


Fig. 6

Fig.6 represents the normalized differential cross sections $\frac{1}{\sigma_{in}} \int f(x=0, p_\perp) dp_\perp^2$ for γ-production in the momentum range of incoming particles (π^- and p) from 5 to 1500 GeV/c. The straight line is a handdrawn one. The essential feature of this picture is a significant difference

from the analogous dependence for charged particle production.

References

1. N.S.Amaglobeli et al. JINR, E1-9817, Dubna, 1976.
2. N.Angelov, V.G.Grishin, P.Kerachev.Yad.Fiz., 21, (1975) 1298.
3. N.S.Amaglobeli et al. JINR, E1-9820, Dubna, 1976.
4. A.J.Buras, J.Dias de Deus, R.Møller. Phys. Lett., 47B (1973) 251; A.Bassetto, J.Dias de Deus. Lett. Nuovo Cim., 9 (1974) 525.
5. N.S.Amaglobeli et al. JINR, P1-9847, Dubna, 1976.
6. Yu.A.Budagov et al. Paper 810/A2-110 presented to this Conference; to be published in Czech.Journ.Phys.B.
7. Yu.A.Budagov et al.JINR, E1-9501,Dubna,1976.
8. N.S.Amaglobeli et al.JINR,E1-9854,Dubna,1976.
9. N.S.Amaglobeli et al. Yad.Fiz.,22 (1975) 1269.

NET CHARGE DISTRIBUTION IN RAPIDITY AND TRANSVERSE MOMENTUM FOR SEMI-INCLUSIVE π^-P INTERACTIONS AT 11.2 GEV/C

(Bologna, Firenze, Genova, Milano, Oxford, Pavia Collaboration)

S.P.Ratti* - Instituto di Fisica Nucleare and Sezione I.N.F.N. - Pavia (Italy)

We present an analysis of the net charge density distributions in π^-p collisions at 11.2 GeV/c, studying how electric charge gets distributed, for different topologies, as a function of rapidity Y and transverse momentum p_T. Following the notations of previous papers[1,2] we define:

$$\rho_n^{(\vec{p})} = \frac{1}{N^{(n)}} \left\{ \frac{dN^{(+)}(\vec{p})}{d\vec{p}} - \frac{dN^{(-)}(\vec{p})}{d\vec{p}} \right\} = \rho_n^{(+)}(\vec{p}) - \rho_n^{(-)}(\vec{p}), \quad (1)$$

where n is the topology, $dN^{(+,-)}(\vec{p})/d\vec{p}$ is the number of positive (negative) particles produced in a given interval of any kinematical variable $\vec{p}$ (in our case; Y and p_T) and N^n is the total number of events of a given topology.

The experimental data have been collected in a~850.000 picture exposure of the CERN 2m HBC exposed at the CERN PS to a π^- beam of 11.2 GeV/c. A total of 49593 two prongs, 107173 four prongs and 36656 six prongs is used. When necessary, proton tracks have been identified with a method developed by our collaboration[3,4].

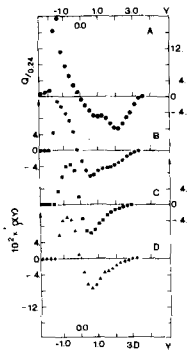


Fig.1. Charge density distributions $\rho(Y)$: A) two prongs; B) four prongs; C) six prongs; D) cut four prongs $t' > 0.4$ (GeV/c)^2.

* Co-authors are: R.Attendoli, E.Calligarich, G.Cecchet, R.Dolfini, L.Mapelli (Pavia); A.Quareni-Vignudelli (Bologna); S.Berti, A.M.Cartacci (Firenze); G.Tomasini, U.Trevisan (Genova); G.Costa, L.Perini (Milano); D.Radojicic, G.Thompson (Oxford).

The charge density distributions in rapidity $\rho(Y)$ are shown in figs. 1a,b,c. The data show structures which were not clearly seen in previous similar analyses[1,2,5]. The sharp peak in positive charge excess at $Y \simeq -1.3$ in two prongs becomes, with increasing topology, broader and smaller. For six prongs, the position of the maximum shifts at $Y \simeq -0.7$. In the region of $Y > 0$, an interesting effect is present in two and four prongs but not in six prongs. In figs.1a and 1b, two minima are visible around $Y_1 \simeq 0.8$ and $Y_2 \simeq 2.4$. The contributions to the two accumulations are however of different importance. In fig.1a the excess at Y_1 is $\rho_1 \simeq 5\%$ and at Y_2 is $\rho_2 \simeq 8\%$, while the opposite occurs in fig.1b. The charge excess in six prong at Y_1 (fig.1c) is $\rho_1 \simeq 8\%$. A similar behaviour could be seen in ref.(1) for $\pi\bar{p}$ data, but there the topologies were added and, as a result, the effect is smeared out.



Fig.2. Charge density distributions $\rho(p_T)$; A) two prongs; B) four prongs; C) six prongs; D) cut four prongs $t' > 0.4$ (GeV/c)2.

The distributions of $\rho(p_T)$ are shown in figs.2a,b,c. Again, they display topology dependent structures (positive excess at small p_T in two and four prongs, no positive excess in two prongs for $p_T \geq 0.4$ GeV/c).

In figs.3a,b,c the distributions of the charge density $\rho(Y, p_T)$ are shown by means of equal-level curves: $10^2 \times \rho(Y, p_T) = 0.0;\ 0.4;\ 0.8;\ \ldots$ in units [Q] (0.08 GeV/c x 0.24). The structures, whose presence was detected in figs.1a,b, become clear and separated. On the line of the most probable transverse momentum ($p_T \simeq 0.25$ GeV/c), peaks in charge excess are well visible. The position of the positive charge excess for six prongs at a smaller $|Y|$ (fig.3c) is due to the multiplicity and to the presence of the massive nucleon. The splitting of the accumulation in p_T, is a consequence of the following facts; the p_T distributions are slightly different for protons and for negative pions[6,7]; the total negative charge $Q = -3$ is large in six prongs; the position in Y of the positive excess in six prongs is much nearer to $Y = 0$ than in two and four prongs[6]. In figs. 3a and 3b, the positive excess ($\simeq$ 0.8%) has similar extension and the same position. The relative importance of the two negative excesses for $Y > 0$ (e.g. at the level of $\simeq$ -0.8%) is clearly seen from the figures.

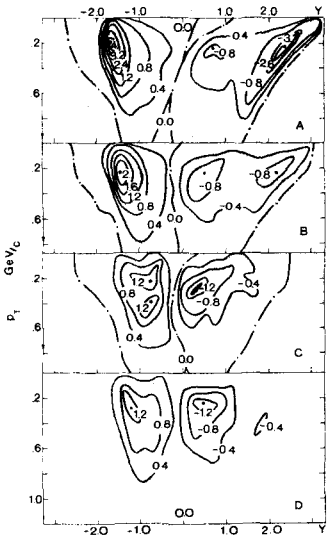


Fig. 3. Charge distributions $\rho(Y, p_T)$. Equal-level curves; A) two prongs; B) four prongs; C) six prongs; D) cut four prongs $t' > 0.4$ (GeV/c)^2.

An appealing explanation of the observed complex structures is the leading particle effect and/or diffraction dissociation, present in two and four prongs, but not in six prongs, at our energy.

To investigate this point we have performed several cuts and selections on both two and four prong events. For the sake of brevity, we show how a very simple cut on four prongs supports this explanation. In fact, by selecting $t' > 0.4$ (GeV/c)^2 (where $t' = t'_{beam,(3\pi)^-}$) all distributions of the four prong events are reduced identically to those of the six prong topology (apart from the splitting in p_T of the positive excess).

For cut four prong events $\rho(Y)$ is shown in fig.1d; $\rho(p_T)$ in fig.2d and $\rho(Y, p_T)$ in fig.3d. The cut antiselects about 40% of the four prongs (61670 events surviving). The negative excess at Y_2 disappears both in fig.1d and in fig.3d; the positive excess at small p_T in fig.2d is absent and the figures can be directly superimposed to figs.1c,3c and 2c respectively. A similar procedure can be applied to the two prong events.

References

1. U.Idschok et al. Nuclear Phys. B67,93(1973).
2. T.Ferbel.U. of R. preprint COO-3065-91 (1974).
3. A.Forino et al.Nuovo Cimento 31A,696(1976).
4. A.Quareni-Vignudelli et al.Paper submitted to this Conference.
5. E.K.Kladnitskaya et al. Paper n.163 to this Conference.
6. P.Borzatta et al. Nuovo Cimento 15A,45(1973).
7. e.g. see R.Slansky. Physics Reports 11C,100 (1974).

A SEARCH FOR NEW NEUTRAL PARTICLES PRODUCED IN HIGHLY INELASTIC π^+ PROTON COLLISIONS AT 10.5 GEV/C

J.R.Elliott, L.R.Fortney, A.T.Goshaw, J.W.Lamsa, J.S.Loos, W.J.Robertson, W.D.Walker, W.M.Yeager
Physics Department, Duke University, Durham, North Carolina 27706

C.R.Sun, S.Dhar
Physics Department, State University of New York, Albany, New York 12222

In recent years, detailed inclusive studies have been made of the charged particle spectrum coming from high energy hadronic interactions. In contrast, many simple but basic properties of the neutral particle spectrum still remain unexplored. We have done an experiment which makes an analysis of the neutral particle spectrum coming from 10.5 GeV/c π^+ proton interactions in which a large fraction of the available energy goes into neutrals. The experiment is designed to determine if all the energy carried away by neutral particles can be accounted for by photons, K^0's, Λ^0's and neutrons. It uses the 4π solid angle detection properties of a bubble chamber and has two distinct advantages over most other neutral particle searches. First, it is sensitive to new neutral particles produced in multineutral final states (in contrast to missing mass experiments). In addition, it does not rely upon any particular decay characteristics of the neutral particle.

The data were taken from an exposure of the SLAC 82'' bubble chamber filled with a hydrogen-neon mixture (30 molar percent neon) and exposed to a 10.5 GeV/c π^+ beam. We select 2 and 4 prong events with one identified proton and net-charge +2. This event sample consists of both neon and hydrogen interactions with about 65% of the events being free proton collisions. These are dominated by the processes

$$\pi^+ p \longrightarrow \pi^+ p + \text{(neutrals)}$$
$$\longrightarrow \pi^+ p \pi^+ \pi^- + \text{(neutrals)}.$$

The event distribution as a function of the lon-

gitudinal laboratory momentum of the neutrals is shown in Fig.1. Most of this neutral momentum is carried away by gamma rays coming from π^0 and η^0 decays. For the purpose of this study, we will group all short lived sources of gamma rays into one category and measure their total contribution to the neutral momentum spectrum. This is done from the gamma ray pair production in the hydrogen-neon liquid (the average gamma detection efficiency is 25%). The next most important contribution to the neutral momentum comes from K^0 production. We measure this from the $K^0_S \to \pi^+\pi^-$ decay (detection efficiency 75%) properly corrected for neutral and K^0_L decays (3). The average number of gamma rays is 3.79 per event and of $(K^0_S + K^0_L)$'s is 0.18 per event.

The results of a longitudinal momentum balance are plotted in Figure 2 and tabulated in Table 1. The events have been divided into three

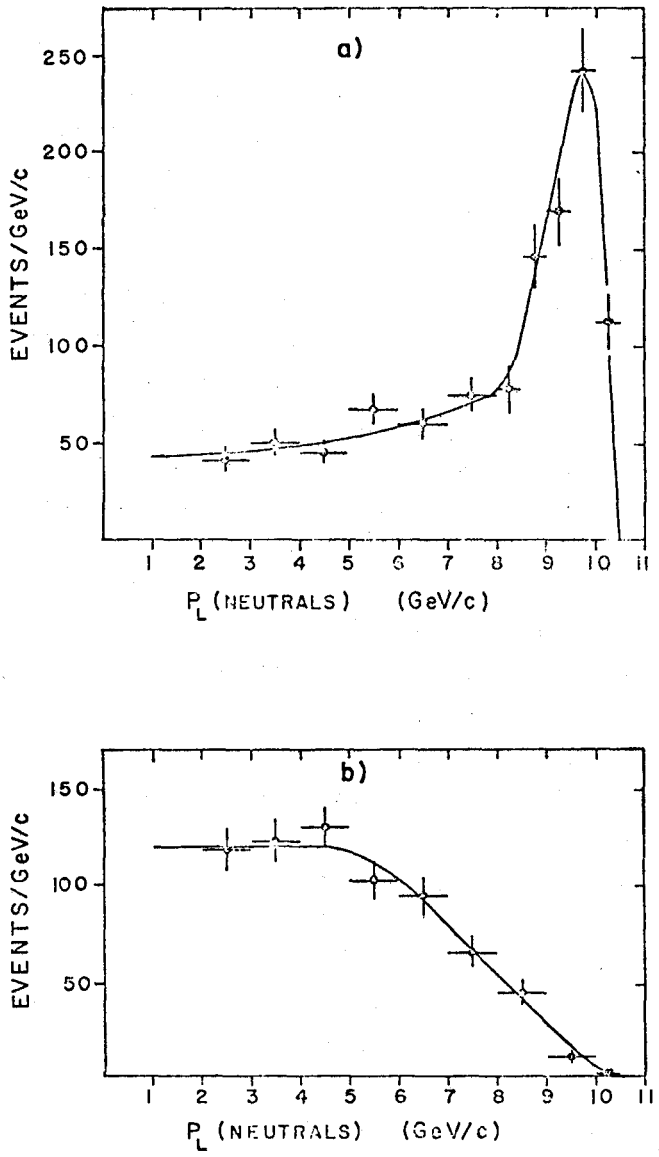


Fig.1. Event distributions as a function of the longitudinal momentum carried by all neutral particles. a) $\pi^+ p \to \pi^+ p$ + (neutrals); b) $\pi^+ p \to \pi^+ p\, \pi^+\pi^-$ + (neutrals).

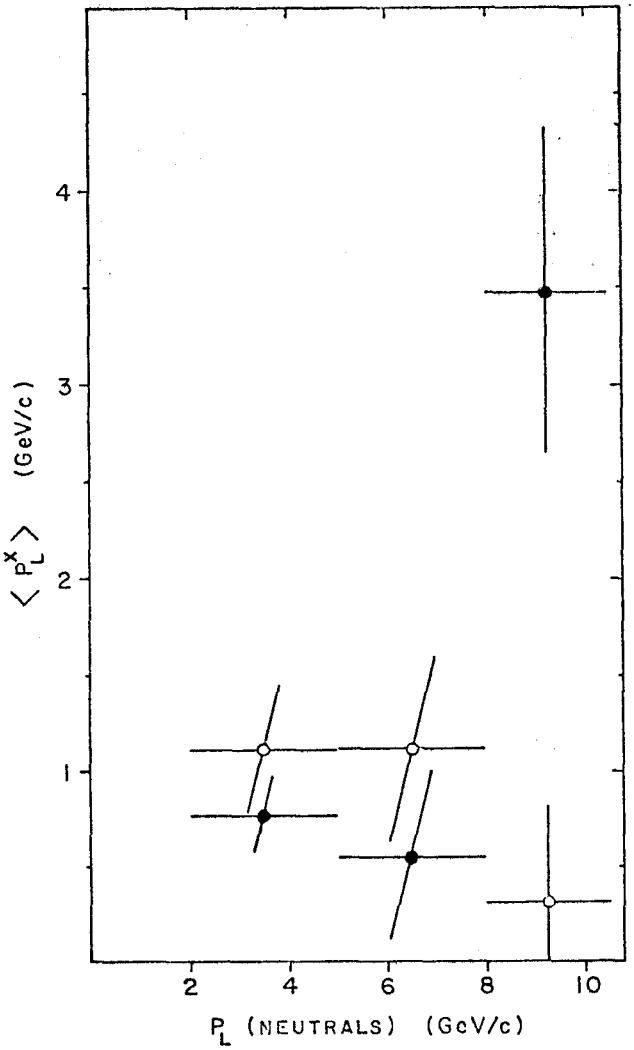


Fig.2. Neutral longitudinal momentum carried by particles other than K^0's and γ's as a function of the longitudinal momentum carried by all neutrals. Open circles $\pi^+ p \to \pi^+ p$ + (neutrals). Solid circles $\pi^+ p \to \pi^+ p\, \pi^+\pi^-$ + (neutrals).

neutral momentum regions and the neutral momentum that cannot be accounted for γ's and K^0's, $\langle p_L^x \rangle$, is plotted separately for two prongs (open circles) and four prongs (solid circles). Some structure is indicated and the overall missing neutral momentum is (0.83±0.27) GeV/c per event. This must be accounted for by neutrons unless some unexpected neutral particle is produced.

The requirement of an identified proton eliminates single neutron production from the free proton interactions, but $n\bar{n}$ pair production is possible. The neon interactions included in our event sample can, in addition, produce one or more target fragmentation neutrons. The momentum carried away by neutrons has been measured from their secondary hadronic interactions in the hydrogen-neon liquid. A total of 46 neutral hadronic stars were observed, of which 23 are predicted to come from K^0 interactions as calculated from the measured $K_S^0 \to \pi^+\pi^-$ spectrum. After subtracting the contribution of the K^0's, and assuming that all the remaining neutral stars are caused by neutrons, we find that the average longitudinal momentum carried by neutrons, $\langle p_L^n \rangle$, is (0.30±0.09) GeV/c per event. Table 1 shows the contribution of neutrons to the neutral momentum in each event category. Finally, the last two columns of the table give the momentum carried away by any neutral particle other than γ's, K^0's, Λ^0's, or neutrons.

Of the six event categories presented in Table 1, only one shows a possibly significant momentum imbalance. The $\pi^+ p \to \pi^+ p\, \pi^+\pi^-$ events with neutral momentum over 8 GeV/c have a missing momentum of (2.9±1.0) GeV/c per event. However a significance of 2.9 standard deviations does not establish a new effect although it does define an event category that should be studied further. Averaged over all the events in our data we find that the momentum carried away by any new neutral particle is limited to (0.53±0.28) GeV/c per event. This is within a subset of all $\pi^+ p$ collisions which is especially sensitive to neutral particle production (over 50% of the collision energy goes into neutrals). Expressing this result relative to all inelastic two and four prongs implies that momentum balances to (3±2)%. Therefore, on the level of a few percent, there is no "energy crisis" in these hadronic interactions.

In conclusion, we find that the neutral particle spectrum produced in 10.5 GeV/c $\pi^+ p$-interactions can be explained in terms of neutrons, Λ^0's, K^0's and photons. Any additional neutral particles produced carry less than 5% of the available momentum.

Table 1

Reaction		$\langle p_L^x \rangle$	$\langle p_L^{neutrons} \rangle$	Missing Neutral Momentum	
Charged Tracks	p_L (neutrals) GeV/c	GeV/c/event	GeV/c/event	GeV/c/event	% of total Momentum
$p\pi^+$	2 to 5	1.11 ± 0.37	0.57 ± 0.23	0.54 ± 0.43	5 ± 4
	5 to 8	1.12 ± 0.52	0.04 ± 0.16	1.08 ± 0.54	10 ± 5
	8 to 11	0.32 ± 0.56	0.02 ± 0.21	0.30 ± 0.60	3 ± 6
$p\pi^+\pi^+\pi^-$	2 to 5	0.78 ± 0.26	0.26 ± 0.10	0.52 ± 0.28	5 ± 3
	5 to 8	0.56 ± 0.51	0.77 ± 0.24	-0.21 ± 0.56	-2 ± 5
	8 to 11	3.48 ± 0.85	0.60 ± 0.56	2.88 ± 1.02	27 ± 10
All data	2 to 11	0.83 ± 0.27	0.30 ± 0.09	0.53 ± 0.28	5 ± 3

PLENARY REPORT

MULTIPARTICLE AND INCLUSIVE REACTIONS

P.V. Chliapnikov

Institute for High Energy Physics, Serpukhov, USSR

An enormous amount of experimental and theoretical results have been obtained within the last few years in the field of multiparticle production. Global description of multiparticle final states in terms of only a few variables in the framework of inclusive approach suggested by Logunov and co-workers (1967)[1], the first experimental evidence for scaling in hadron induced reactions (1969)[2,3], the theoretical formulation of the limiting fragmentation hypothesis (LFH) by Yang and co-workers (1969)[4] and of scaling by Feynman (1969)[5] and all subsequent development have been extremely successful in enlarging our knowledge of hadronic processes at high energies.

Detailed discussions of the available data have been the object of many thorough reviews (see, for example[6-11]) where a host of very important results have been collected. Many of the new interesting results have been covered in the invited and mini-rapporteur's talks in the A2-session of this conference. In my embarassing position where I can but describe, with some personal prejudices (and my inability to understand everything), only a small part of the imposing results presented in about 130 submitted contributions, I shall concentrate your attention on the following subjects:

1. Total inclusive cross sections
2. The approach to scaling in the fragmentation and central regions.
3. Inclusive resonance production
   - total cross sections
   - differential cross sections
   - mechanisms.
4. Two-particle correlations
   - angular correlations
   - space structure of events.

1. Total inclusive cross sections

Present results on the energy dependence of the total inclusive π^+, π^- and π° cross sections $\sigma_\pi = \langle n_\pi \rangle \sigma_{inel}$ in inelastic hadron collisions are compiled in fig.1. The increase of the pion cross sections for pp data above 50 GeV/c is compatible with logs dependence. The cross section ratio $\sigma(\pi^-)/\sigma(\pi^+)$ changes slowly from the value of 0.74 ± 0.02 at 69 GeV/c[12] up to 0.80 ± 0.08 at 303 GeV/c[11] (see Table 1). The ratio $\sigma(\pi^\circ)/\sigma(\pi^+)$ is 0.94 ± 0.02 at 69 GeV/c[12] and 1.01 ± 0.10 at 303 GeV/c[11]. It is of interest to note that $\sigma(\pi^+) \approx \sigma(\pi^-) \approx \sigma(\pi^\circ)$ for K^-p interactions up to 32 GeV/c. The energy dependence of the pion cross sections in reactions induced by the different beam particles seems to be similar to that for pp

collisions. The charge conservation, leading particle effect and the contribution of the annihilation channels in $\bar{p}p$ reactions explain some differences observed at low energies.

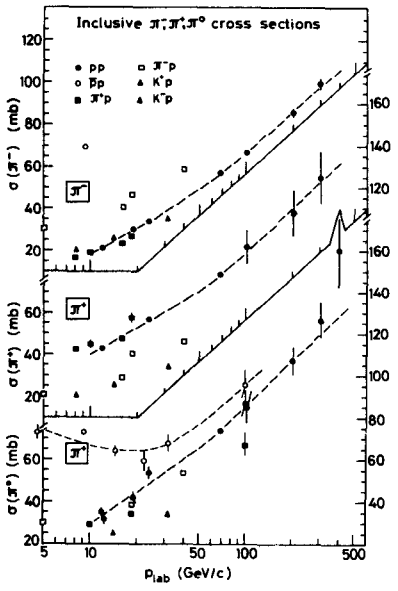


Fig.1. Inclusive π^-, π^+ and π° production cross sections as a function of incident momentum (compilation of published data; new data: K^-p 32 GeV/c[15]; $\bar{p}p$ 32 GeV/c[16], 22.4 GeV/c[17], 9.1 and 4.6 GeV/c[18,19]; π^-p 5 GeV/c[20]); the lines are to guide the eye.

Table 1

Total inclusive cross section (in mb) for π^+, π^- and π° in pp and Kp interactions at highest energies

	pp				K^-p	
P_{LAB} GeV/c	69[12]	100[11]	205[11,14]	303[11,13]	14.3[8]	32[15]
$\sigma(\pi^+)$	78.5 ± 1.3	91.8 ± 9.2	108 ± 11	125 ± 13	25.6 ± 0.8	33.6 ± 1.3
$\sigma(\pi^-)$	57.5 ± 0.6	66.9 ± 1.3	86 ± 2	99.5 ± 3	25.9 ± 1.5	35.3 ± 1.8
$\sigma(\pi^\circ)$	74.0 ± 1.5	85 ± 8	107 ± 7	126.5 ± 9	27.2 ± 1.0	35.3 ± 0.8

Neutral strange particle production cross sections are shown in figs.2 and 3 for $K^n(K^\circ/\bar{K}^\circ)$, Λ and $\bar{\Lambda}$. The K^n cross section rises by about a factor of 10 for pp interactions between 12 GeV/c and the highest FNAL energies. For π^-p interactions, the increase of the K^n production is consistent with logs dependence through all energy range up to the highest beam momentum of 205 GeV/c[23]. In $\bar{p}p$ collisions the K^n cross section is systematically higher than in pp interactions and rises as fast as in pp collisions through the Serpukhov-Fermilab energy range[16,17,21].

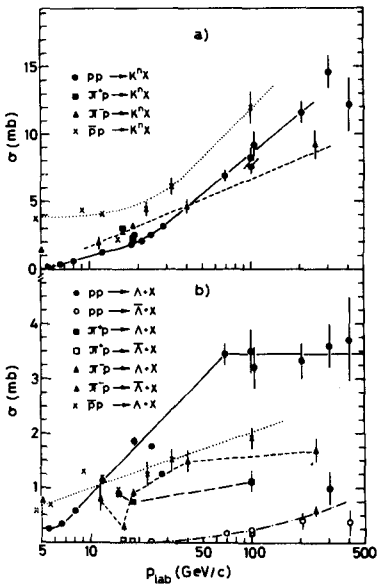


Fig.2. Inclusive K^n, Λ and $\bar{\Lambda}$ production cross sections as a function of incident momentum for $p^\pm p$, $\pi^\pm p$ interactions (compilation of published data; new data: $\bar{p}p$ 32 GeV/c[16], 22.4 GeV/c[17], 12 GeV/c[22], 9.1 and 4.6 GeV/c[18]; π^-p 205 GeV/c[23], 5 GeV/c[24]); the lines are to guide the eye.

The Λ production cross section rises between 5 and 50 GeV/c in pp collisions, but shows little energy dependence above 69 GeV/c. It is about two times higher in pp interactions than in $\bar{p}p$ and $\pi^\pm p$ collisions in the Serpukhov-Fermilab energy range, as it should be expected if the Λ production is dominated by the proton fragmentation. The dominance of the fragmentation process over that of $\Lambda\bar{\Lambda}$ pair production explains also a small energy variation of the

Λ cross section through the FNAL energy range. The $\bar{\Lambda}$ production is small, but exhibits a rapid increase with energy above 69 GeV/c in a striking similarity with $\bar{p}$ production.

In fig.3 the neutral strange particle cross sections for 32 GeV/c $K^{\pm}p$ interactions obtained by the France-USSR and CERN-USSR Collaborations[15,25] are compared with the corresponding data at lower energies.

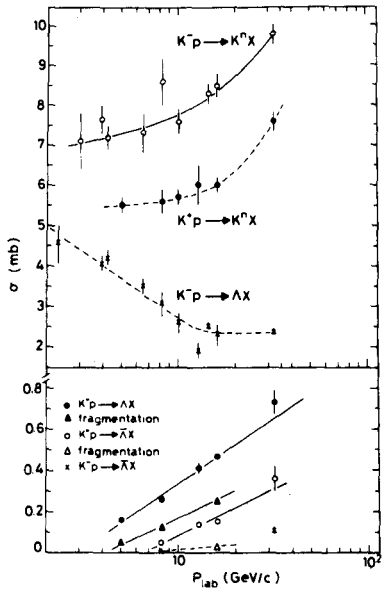


Fig.3. Inclusive K^0, Λ and $\bar{\Lambda}$ production cross sections as a function of incident momentum for $K^{\pm}p$ interactions (compilation of published data; new data: K^+p 32 GeV/c[25], 16, 8.2 and 5 GeV/c[26]; K^-p 32 GeV/c[15], 16 and 10 GeV/c[27], 6.5 GeV/c[28]); also are shown contributions of the Λ and $\bar{\Lambda}$ fragmentation cross sections in K^+p interactions (ref.[26]); the lines are to guide the eye.

One observes a significant rise of the K^0 production cross section for both the K^+p and the K^-p interactions ($\Delta\sigma \approx 1.5$ mb) between 16 and 32 GeV/c . This increase may be at least partly attributed to a higher K^0K^0 pair production: $\sigma(K^0K^0) = 1.1\pm0.1$ mb and 1.68 ± 0.24 mb in K^+p[25] and K^-p[15] interactions at 32 GeV/c, respectively. It is of interest to note that a significant amount of the K^+K^- pair production has also been observed in the exclusive channels in K^+p interactions at 32 GeV/c[29]. Similar effect was found by the France-USSR and CERN-USSR Collaborations in 32 GeV/c K^-p collisions[30]:

$$\frac{\sigma(K^-p \to K^-pK^+K^-\pi^+\pi^-)}{\sigma(K^-p \to K^-p2\pi^+2\pi^-)} = 0.18\pm0.05;$$

$$\frac{\sigma(K^-p \to K^-pK^+K^-2\pi^+2\pi^-)}{\sigma(K^-p \to K^-p3\pi^+3\pi^-)} = 0.55\pm0.21 .$$

The energy dependence of the Λ and $\bar{\Lambda}$ production in K^+p collisions resembles in character that observed in pp interactions at similar energy range; the data are well described by the logs dependence. In K^-p interactions, the Λ production cross section falls with energy at low incident momenta, but seems to be fairly constant between 10 and 32 GeV/c. The decrease of cross sections at low energies is explained by the falling contribution of the strangeness annihilation process in virtual K^-K^+ scattering in the reaction $K^-p \to \Lambda$+ pions. As energy increases, other mechanisms of the Λ production such as $K^-p \to K\bar{K}$ + pions, become more important (fig.4).

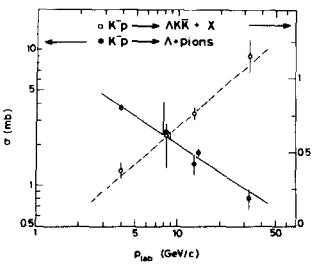


Fig.4. Energy dependence of the Λ production cross sections in the strangeness annihilation process $K^-p \to \Lambda$ + pions (left hand scale) and in the reaction $K^-p \to \Lambda K\bar{K}$ + X (right hand scale)(from ref.[31]).

This results in approximately energy independent cross sections at 10-32 GeV/c incident momentum

range. From the present trend of data, one may expect that Λ production in K^-p interactions will start to increase at higher energies.

2.1 The approach to scaling in the fragmentation region

The approach to scaling in the target fragmentation region has been extensively discussed during the past two years[7,8,32-34]. However the conclusions differ, thus reflecting the lack of the high statistics data in this phase space region at the highest energies. Indeed most of the π data measured at the CERN ISR are confined to $p_T > 0.4$ GeV/c or $y_{LAB} > 0$ while the bubble chamber data are integrated over transverse momenta because of the poor statistics.

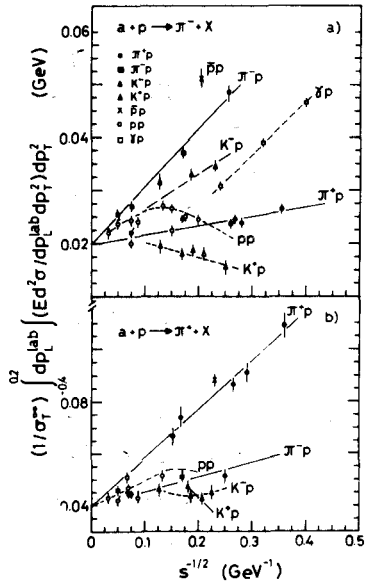


Fig.5. The approach to scaling in the proton fragmentation region for inclusive $\pi^\pm$ production (from ref.[34] with some added published data).

Fig.5 summarizes the present situation with respect to the factorization and the approach to scaling in proton fragmentation into $\pi^\pm$ as measured in the bubble chamber experiments. The hypothesis of limiting fragmentation[4] is not valid in the whole available energy range. However the data at highest energy suggest, that a scaling limit may exist, that it is being approached from above and that the factorization may hold in the limit of infinite energy.

More specifically, for reactions with no exoticity combination (ab, $ab\bar{c}$, $b\bar{c}$, $a\bar{c}$) such as $\pi^\pm p \to \pi^\pm X$, $K^-p \to \pi^- X$, $\gamma p \to \pi^- X$ (and most probably $\bar{p}p \to \pi^\pm X$), one observes a strong energy variation in entire energy range consistent with the Mueller-Regge predictions[35,36] based on the generalized optical theorem[37,38]:

$$E\frac{d^3\sigma}{d^3p} = f(s,p_L,p_T^2) =$$

$$= A(p_L,p_T^2) + \sum_R B_R(p_L,p_T^2)s^{\alpha_R(0)-1} \qquad (2.1.1)$$

where the $\alpha_R(0)$ are the intercepts of the exchange Regge trajectories. For reactions where at least one of the ab, $ab\bar{c}$, or $a\bar{c}$ combinations is exotic (Table 2), the situation is not as straightforward.

Table 2

Exoticity of various combinations for the reaction a + b → c + anything

Reaction	ab	$ab\bar{c}$	$a\bar{c}$	$b\bar{c}$
$pp \to \pi^- X$	Exotic	Exotic		
$\pi^+p \to \pi^- X$		Exotic	Exotic	
$K^+p \to \pi^- X$	Exotic	Exotic	Exotic	
$pp \to \pi^+ X$	Exotic	Exotic		
$\pi^-p \to \pi^+ X$			Exotic	
$K^+p \to \pi^+ X$	Exotic	Exotic		
$K^-p \to \pi^+ X$			Exotic	

For these reactions the energy variation is much less pronounced but still exists even in the Serpukhov-Fermilab energy range, where it amounts to 10-20% . It appears[34] that the rise from threshold, which is seen for $pp \to \pi^\pm X$ and $K^+p \to \pi^- X$ reactions and is indicated for $K^+p \to \pi^+ X$ reactions, is related to (ab) being an exotic combination. For these reactions, as

cross sections are increasing, the prediction (2.1.1) can not be applied. The reactions $\pi^+p \to \pi^-X$, $\pi^-p \to \pi^+X$ (and perhaps, $K^-p \to \pi^+X$), which show a systematic but small energy variation and which are characterized by having $(a\bar{c})$ exotic, are again consistent with an energy dependence predicted by (2.1.1).

It is of interest to test the above relations between the exoticities of different particle combinations and the energy dependences of the $\pi^\pm$ inclusive cross section in the beam fragmentation region. The study of the reactions $\pi^-p \to \pi^+X$ and $K^-p \to \pi^+X$ with only $(a\bar{c})$ combination being exotic (Table 2) may be of special interest.

The experimental data in the target fragmentation region for heavy particles are quite poor in high energy range. Very qualitative picture of the approach to scaling in proton fragmentation into neutral kaons K^n and Λ is presented in fig.6.

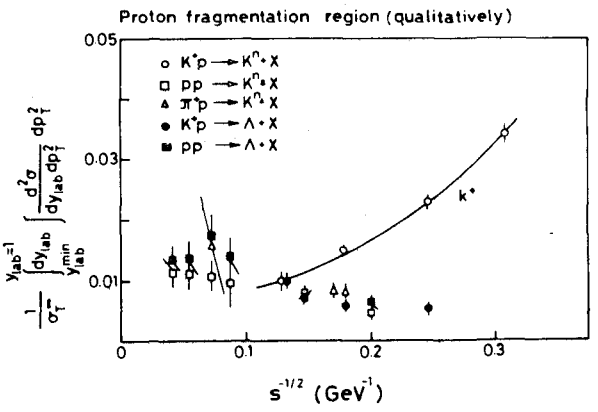


Fig.6. The approach to scaling in the proton fragmentation region for inclusive K^n and Λ production (compilation of published data).

However it is interesting to note that the trend of data is similar to that observed for $\pi^\pm$ production. In particular, the factorization holds in a first approximation, the energy dependence seems to be small in the FNAL energy range and the rise from threshold is observed for all reactions with ab being exotic, apart from $K^+p \to K^n + X$.

The exceptional behaviour of the $K^+p \to K^n + X$ reaction may be related to the presence of the strangeness annihilation process in the virtual K^+Y^{*+} scattering, i.e. the contribution of the f'- Ø exchange, which leads to an s^{-1} behaviour of the structure function (2.1.1)[36,39]. Indeed the data seem to be compatible with such a picture (fig.7(a)) in the target fragmentation region, favouring an s^{-1} dependence.

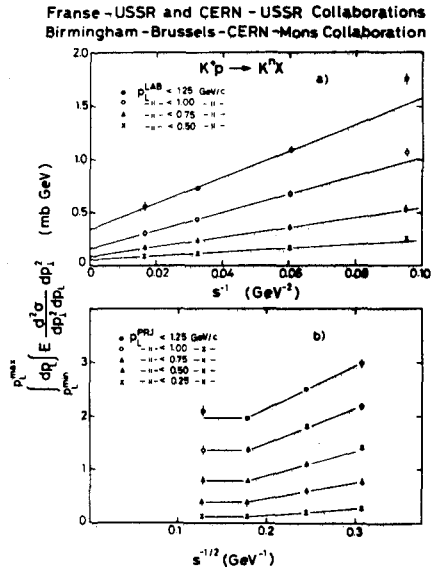


Fig.7. Energy dependence of the structure functions for reaction $K^+p \to K^nX$: (a) in the proton fragmentation region: the lines are fits to the 8.2-32 GeV/c data; (b) in the beam fragmentation region; the lines are to guide the eye (from ref.[25]).

Another interesting experimental observation made by the France-USSR and CERN--USSR Collaboration[25] is the surprising energy dependence of this reaction $K^+p \to K^nX$ in the beam fragmentation and central regions. The cross sections for this reaction in the beam fragmentation region (fig.7(b)) are decreasing with incident momentum between 5

and 16 GeV/c[39] following an $s^{-1/2}$ dependence as predicted by (2.1.1), but practically coincide at 16 and 32 GeV/c. Fig.8 shows this effect in more detail . One indeed observes the scaling of the $d\sigma/d(M^2/s)$ distributions at 16 and 32 GeV/c over the entire range of M^2/s .

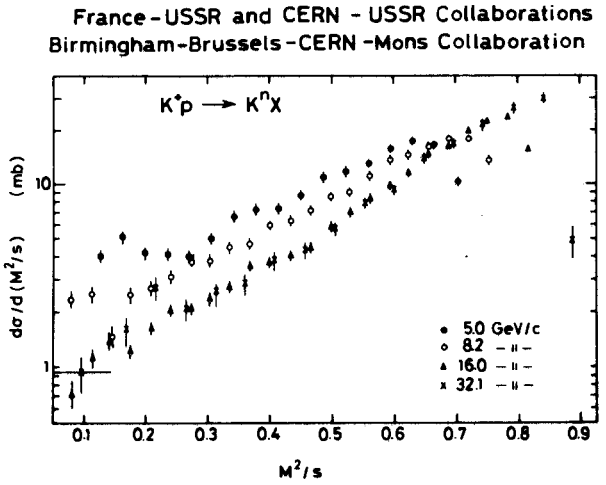


Fig.8. The differential cross section, $d\sigma/d(M^2/s)$, for reaction $K^+p \to K^0X$ (from ref.[25]).

A similar effect has been found for reaction $K^-p \to K^0X$ in the same energy range[40]. It is tempting to explain this surprising behaviour by the higher contribution of the K^0K^0 pair production at 32 GeV/c (see above section). From this one may expect that, at least in the central region, the observation of the early scaling at 16-32 GeV/c incident momentum range is accidental and the K^0 cross section should start to increase at higher energies.

The measurements of the production of $\pi^\pm$, K^+ and protons in $\pi^\pm p$, $K^\pm p$ and $p^\pm p$ interactions from 4 to 250 GeV/c in the target fragmentation region have been made by Pennsylvania group[41], using an electronic detector, in a fixed region of phase space corresponding approximately to $p_T = 0.3$ GeV/c and $y_{LAB} = 0.6$, 0.4 and 0.2 for produced π, K and p, respectively (fig.9).

They have fitted the data to the expression $A + Bs^{-1/2} + Cs^{-1}$ for production of pions in $\pi^\pm p$ and $p^\pm p$ collisions and to the expression $A + Bs^{-1/2}$ for the statistically less significant data.

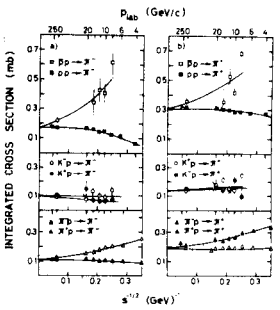


Fig.9. Energy dependence of the invariant cross sections (integrated over the kinematic region $0.3 \leq p^c_{LAB} \leq 0.6$ GeV/c and $60.75° \leq \theta^c_{LAB} + \frac{3.3°}{p^c_{LAB}} \leq 64.25°$) for (a) π^- and (b) π^+ production. The solid lines are fits to $A + Bs^{-1/2}$ and $A + Bs^{-1/2} + Cs^{-1}$.

It seems that at least for the statistically most significant data of the reaction $pp \to \pi^\pm X$, with ab combination being exotic, the cross sections systematically rise to asymptotic limits in contrast to the bubble chamber data (fig.5), where the cross sections rise slowly and then fall to their asymptotic limit (note, however, that the rapidity ranges are different in these two experiments).

Since in the PS-FNAL energy range the central production may contribute substantially to the fragmentation region, the increased precision of the experiments in different regions of phase space is needed for determination of the actual s-dependence of the invariant cross section in the proton fragmentation region. It is of interest to test in detail whether the s-dependence indeed has a form $A + Bs^{-1/2} + Cs^{-1}$. If it does, we have additional reason to believe (besides the facts that the cross sections are rising in the

central region and for reactions $pp \to \pi^{\pm}$ and $pp \to K^{+}X$ the same is true in the fragmentation region) that we do not understand either the singularity structures in the Regge language or the dual properties of the Regge trajectories (or both) in the scope of the simplest dual Regge approach.

The tests of the factorization of the leading Pomeron singularity

$$\frac{Ed^3\sigma\,(ap \to c)/d^3p}{Ed^3\sigma\,(a'p \to c)/d^3p} \underset{s\to\infty}{=} \frac{\sigma_{tot}(ap)}{\sigma_{tot}(a'p)}$$

made by Pennsylvania group[41] by the extrapolation of the fitted s-dependence to $s \to \infty$ (Table 3) show that the results are within the predictions of the naive quark model ($\sigma(\pi p) = \sigma(Kp) = \frac{2}{3}\sigma(pp)$) or the parametrization[42] of the diffractive part of the total cross sections, evaluated at p_{LAB} = 250 GeV/c.

Table 3

Tests of Pomeron Factorization

Cross section ratio	Asymptotic ratio for produced particle c: $c=\pi^-$	$c=\pi^+$	$c=K^+$	$c=p$	Predicted ratio Ref.[42]	Quark model
$\frac{\pi p \to c}{pp \to c}$	0.63±0.03	0.62±0.03	0.25±0.18	0.62±0.03	0.61±0.02	0.67
$\frac{Kp \to c}{pp \to c}$	0.60±0.06	0.45±0.04		0.61±0.08	0.53±0.02	0.67

A similar conclusion is made by the SLAC group[43] which has measured the ratios R of inclusive particle and antiparticle cross sections in $A^{\pm}p \to A^{\pm}X$ reactions (A = π, K, p) at 10 and 14 GeV/c at $|t| < 0.25$ $(GeV/c)^2$. The integration of R over the whole available missing mass range yields $R = 0.96^{\pm}0.04$, $0.90^{\pm}0.02$ and $1.02^{\pm}0.02$ for $K^{\pm}$, $\pi^{\pm}$ and $p^{\pm}$ inelastic scattering, respectively, at 10.4 GeV/c. This indicates that the C = -1 exchanges are very small for these reactions in contrast to the elastic scattering, where the C = -1 exchanges are quite significant at these energies.

In measurements at the CERN ISR of the diffraction exitation processes, $pp \to (p\pi^+\pi^-)+X$, $pp \to p+X$ and $pp \to (\Lambda K^+)+X$ at $\sqrt{s}$ = 53 GeV[44], factorization is shown to be valid to ≈5% for $|t| < 0.5(GeV/c)^2$. For $0.5 < |t| < 1.1(GeV/c)^2$, a pronounced breakdown in factorization is however observed between the elastic and inelastic diffractive cross sections. This can be seen from fig.10 where the ratios of collinear to non-collinear events are plotted vs.momentum transfer for above three reactions.

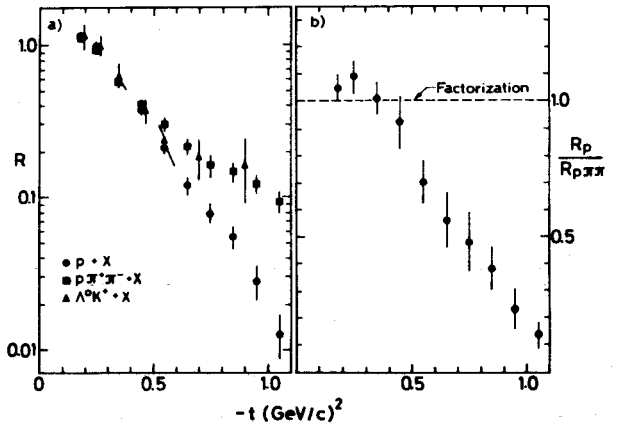


Fig.10. (a) Ratios R_p, $R_{p\pi\pi}$, $R_{\Lambda K}$ of collinear to non-collinear events (corrected for loss of non-collinear events) for reactions $pp \to p + X$, $pp \to p\pi\pi + X$ and $pp \to (\Lambda K^+) + X$ at $\sqrt{s}$ = = 53 GeV vs. momentum transfer; (b) R_p/R_p vs. t (from ref.[44]).

These ratios are related to the differential cross sections of these reactions:

$$R_p = \frac{\varepsilon_p(d\sigma_{el}/dt)}{\varepsilon_p(\frac{1}{2}d\sigma_{SD}/dt)}, \quad R_{p\pi\pi} = \frac{\varepsilon_{p\pi\pi}(\frac{1}{2}d\sigma_{SD}/dt)}{\varepsilon'_{p\pi\pi}(d\sigma_{DD}/dt)},$$

$$R_{\Lambda K} = \frac{\varepsilon_{\Lambda K}(\frac{1}{2}d\sigma_{SD}/dt)}{\varepsilon'_{\Lambda K}(d\sigma_{DD}/dt)}.$$

Factorization requires $\varepsilon_{p\pi\pi} = \varepsilon'_{p\pi\pi}$ and $\varepsilon_{\Lambda K} = \varepsilon'_{\Lambda K}$. All these R parameters are seen to agree with each other for $|t| < 0.5(GeV/c)^2$, but at $|t| > 0.5$ the parameter R_p departs

sharply, demonstrating a breakdown in Pomeron factorization for elastic scattering. The apparently different energy behaviour of the inelastic cross section for reactions $pp \to p(n\pi^+)$ and $pn \to p(p\pi^-)$ as compared to the elastic ones over a broad energy range from 24 GeV up to the ISR energies is also related[125] to the breakdown of a single factorisable t-channel model, which predicts that the elastic and inelastic diffractive amplitudes should have the same energy behaviour $\sim s^{\alpha_P}$.

The experimental values of R_p and $R_{p\pi\pi}$ have been used to extract the absolute differential and total cross sections for single and double diffractive excitation at $\sqrt{s} = 53$ GeV[44]. They were found to be 8.6 ± 0.7 mb and 5.0 ± 0.8 mb, yielding a total elastic and inelastic diffractive cross section of

$$\sigma_{el} + \sigma_{SD} + \sigma_{DD} = 21.3 \pm 1.1 \text{ mb},$$

or $(49.4 \pm 2.5)\%$ of the total cross section at $\sqrt{s} = 53$ GeV. The value of $\sigma_{SD} + \sigma_{DD} = 13.6 \pm 1.1$ mb is considerably larger than it is usually assumed and, in fact, is compatible with saturation of the Pumplin bound[45]

$$\sigma_{diff} \leq \frac{1}{2}\sigma_{tot} - \sigma_{el} .$$

The interesting approach to the behaviour of inclusive cross section in the fragmentation region has been suggested by Logunov and co-workers[46]. Using the Jost-Lehmann-Dyson representation of the spectral function they have shown that the inclusive cross section may be written in the form

$$E\frac{d^3\sigma}{d^3p} = \gamma^{a(q^2,\nu)} F(q^2,\nu) \qquad (2.1.2)$$

with $q^2=(p_a-p_c)^2$, $\nu = 2p_b(p_a-p_c)$ and $\gamma = 2p_b(p_a+p_c)/\nu$. If the spectral function has no singularities, then $a(q^2,\nu) < 0$, otherwise $a(q^2,\nu) > 0$. Fig.11 taken from ref.[47] shows that the function (2.1.2) indeed describes the data, with very small dependence of $a(q^2,\nu)$ and $F(q^2,\nu)$ on ν.

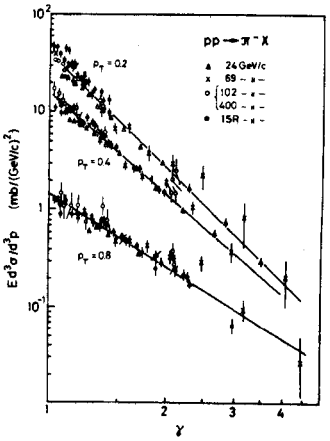


Fig.11. Inclusive cross sections for reaction $pp \to \pi^- X$ as a function of the variable γ; the straight lines are to guide the eye (from ref.[47]).

Besides, $a(q^2,\nu) < 0$ for reactions $pp \to \pi^{\pm} X$ and $a(q^2,\nu) > 0$ for reactions $pp \to pX$[47] and $K^+p \to K^0X$[48] with the strong leading particle effects. For $p_T = 0.4$ GeV/c $\approx \langle p_T \rangle$, $a \approx 3$. This gives $Ed^3\sigma/d^3p \sim (1-x)^3$. The similar x dependence is observed for the structure function $\nu W_2(x)$ for deep inelastic scattering at x=1, thus suggesting an interesting relationship between the behaviour of inclusive reactions in hadron-hadron collisions and the deep inelastic scattering (see also[49]).

Moreover it seems[47] that the invariant cross section is factorisable in the variables γ_1 and γ_2, pertaining to the beam and target fragmentation regions. In the usual variables

$$x_1 = \frac{E + p_L}{\sqrt{s}} = \frac{m_T e^{y}}{\sqrt{s}}, \quad x_2 = \frac{E - p_L}{\sqrt{s}} = \frac{m_T e^{-y}}{\sqrt{s}}$$

this implies

$$E\frac{d^3\sigma}{d^3p} \approx \varphi(m_T) f(x_1) f(x_2) \qquad (2.1.3)$$

where the function $f(x) \sim (1-x)^3$ in pp collisions at $x \to 1$. One of the possible manifestations of eq.(2.1.3), related to the

deep inelastic scattering, is the mechanism of the amalgamation of quarks from the colliding hadrons[50].

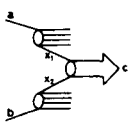


Fig.12. Mechanism of particle production resulting from the amalgamation of quarks from the colliding hadrons.

This analog of the familiar Drell-Yan mechanism for production of lepton pairs in hadron-hadron collisions (fig.12) gives

$$E\frac{d^3\sigma}{d^3p} \approx \frac{A}{m^2} f_q(x_1) f_{\bar{q}}(x_2) \qquad (2.1.4)$$

with $f(x) = \nu W_2(x)$ and

$$x_{1,2} = 1/2((x^2 + 4m^2/s)^{1/2} \pm x) \qquad (2.1.5)$$

From eq.(2.1.4) and (2.1.5) it follows that

$$E\frac{d^3\sigma}{d^3p}_{x\to 1} \approx \frac{A}{m^2} f_q(x) f_{\bar{q}}(\frac{m^2}{sx}) \qquad (2.1.6)$$

$$E\frac{d^3\sigma}{d^3p}_{x\to 0} \approx \frac{A}{m^2} f_q(\frac{m}{s}) f_{\bar{q}}(\frac{m}{\sqrt{s}}) \qquad (2.1.7)$$

Thus this mechanism predicts the different approaches to scaling in the fragmentation and central regions (the energy dependence is defined by the variables m^2/s and $m/\sqrt{s}$ in (2.1.6) and (2.1.7), respectively). Besides, we see that the scale of energy is measured in units of the mass m of the produced particle (or in units of the transverse mass m_T if the transverse momentum is taken into account). Consequently the average multiplicities of the different particles produced in hadron-hadron interactions may follow[51] some universal curve $(1/m_c^2)\varphi(\langle m_T^2\rangle/s)$ as seems to be the case (fig.13), at least in a first approximation. This has also important implications for the yield of particles in the hadron-hadron collisions, since the factor A/m^2 in the eq.(2.1.4) may distort the simple quark counting rules in the naive quark models (see section 3). It is of interest that similar conclusions have been reached in quite different approaches[52,53].

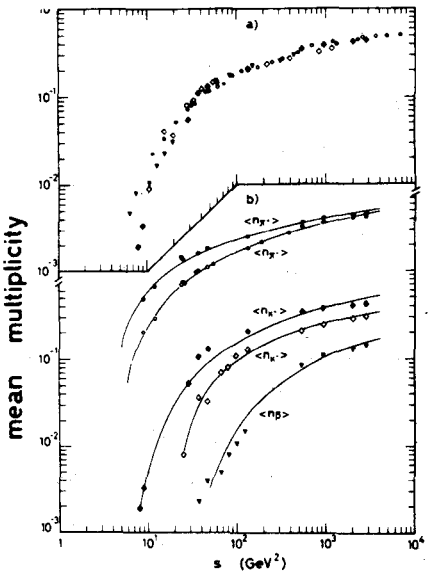


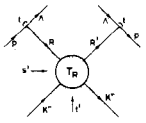
Fig.13. (b) Average multiplicity of $\pi^{\pm}$, $K^{\pm}$ and $\bar{p}$ as a function of s; (a) the same data as in (b) obtained by the simple shifts of the $\pi^{\pm}$, K^- and $\bar{p}$ data to the average multiplicity of the K^+'s; the shifts along the $\langle n\rangle$ axis are in the ratios of the corresponding masses squared (for details see ref.[51]; the data from ref.[54]).

2.2 Triple-Regge region

The inelastic hadron diffraction at high energy has been discussed by Kaidalov in his rapporteur's talk at this Conference. I shall concentrate on some specific reactions in the triple-Regge region.

The inclusive production of Λ, $\bar{\Lambda}$, Ξ^- and $\Sigma^+(1385)$ in the fragmentation regions has been studied in several experiments[26,55-58]. Target fragmentation $p \to \Lambda$ can be associated with the diagram in fig.14 with the exchange Reggeon R represented by the K and $K^*(890)$ trajectories. It has been shown that the triple-Regge model yields an approximate description of fragmentation processes even

when extrapolated to cms energies of a few GeV.



$T_R = T_R^0 + T_R^1$

$\mathrm{Im}\, T_R^0 = 2K' s'^{1/2} \sigma_R$

$T_{K^-}^1 = \beta_K^{\rho\rho}(V_{\rho\rho} + V_{\rho\rho}) + \beta_K^{\omega\omega}(V_{\omega\omega} + V_{\phi\omega})$

$T_{K^{*-}}^1 = \beta_{K^*}^{\rho\rho}(V_{\rho\rho} + V_{\rho\rho}) + \beta_{K^*}^{\omega\omega}(V_{\omega\omega} + V_{\phi\omega}) +$
$+ \beta_{K^*}^{\pi\pi} V_{\pi\pi} + \beta_{K^*}^{\eta\eta} V_{\eta\eta} + \beta_{K^*}^{\chi\chi} V_{\chi\chi}$

σ_R and β_R are the adjustable parameters

V is the Veneziano function

Fig.14. Regge diagram for $p \xrightarrow{K^-} \Lambda$ fragmentation.

Resonances in the M_X^2 channels for nonexotic ($abc\bar{c}$) reactions can be accounted for in the sense of semi-local duality[59]. An interesting attempt to explore more directly a dual description of the reggeon-particle scattering in $K^-p \to \Lambda X$ (and $K^-p \to \Sigma^+ + X$) reaction at 4.2 GeV/c is made by the Amsterdam-CERN-Nijmegen-Oxford Collaboration[55]. They use the usual Regge formula

$$\frac{d^2\sigma}{ds'dt'} = \frac{1}{16k^2 s} \sum_R \frac{\gamma^2_{R\Lambda}}{4\pi} \mathrm{Im}\, T_R(s',0,t) \left(\frac{s-u}{2s'}\right)^{2\alpha_R(t)} \qquad (2.2.1)$$

where $\gamma^2_{R\Lambda}$ is the residual factor, but instead of taking the triple-Regge limit, they describe the RK scattering (fig.14) by introducing four-point function $T_R(s',t',t)$. The amplitude T_R is written as a sum of two terms $T_R = T_R^0 + T_R^1$. The diffractive term T_R^0, which according to two-component duality may be extrapolated to low s', describes a non-resonance background in inclusive distribution. The non-diffractive amplitude T_R^1, which is applied as Veneziano amplitude, explicitly reproduces M_X^2 channel resonances.

Fig.15 shows the experimental $d^2\sigma/dtdM$ distributions for reaction $K^-p \to \Lambda + X$, together with the absolute predictions of the above model. The overall agreement is very good, although one observes a discrepancy in the ρ-ω mass region for the two smallest $|t|$-bins. Similar results were obtained for reaction $K^-p \to \Sigma^+X$. The relative contributions to the integrated cross section evaluated separatly for K and K* exchange are summarized in Table 4.

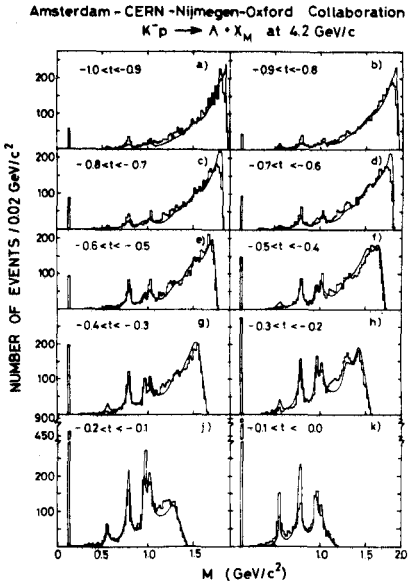


Fig.15. Missing mass distributions in reaction $K^-p \to \Lambda X$ at 4.2 GeV/c for different t-intervals with the absolute predictions of the model (from ref.[55]).

Table 4

Relative contributions of K and K* exchange in the reactions $K^-p \to \Lambda X$ and $K^-p \to \Sigma^+X$ at 4.2 GeV/c for $-t_{p,\Lambda(\Sigma)} < 1\,(\mathrm{GeV/c})^2$

Type of exchange	$K^-p \to \Lambda + X$		$K^-p \to \Sigma^+ + X$	
	σ (mb)	%	σ (mb)	%
Dual part of K exchange	0.11	9	0.01	3
Diffractive part of K exchange	0.33	28	0.16	40
Dual part of K* exchange	0.51	43	0.08	20
Diffractive part of K* exchange	0.23	20	0.15	37

One observes that the ratio of K* exchange to K exchange is 1.7:1 for $K^-p \to \Lambda X$ and 1.3:1 for $K^-p \to \Sigma^+X$, while the ratio of the total contributions from the diffractive and non-diffractive terms is close to unity for $K^-p \to \Lambda X$ and is 3.5 for $K^-p \to \Sigma^+X$.

Similar results were obtained by the Birmingham-Brussels-CERN-MONS Collaboration[26] in the triple-Regge analysis of the reaction $K^+p \to \Lambda X$ at 8.2 and 16 GeV/c in the proton fragmentation region. Here the exoticity of ($abc\bar{c}$) implies the early scaling behaviour which is indeed observed when the threshold effects

are accounted for by introduction of the variable $(M^2 - M_{th}^2)/s$ instead of M^2/s ($M_{th} = 2m_K$ for reaction $K^+p \to \Lambda X$ and $2m_p$ for reaction $K^+p \to \bar{\Lambda} X$). The fit to the triple-Regge formula

$$\frac{d^2\sigma}{d(M^2/s)dt} = \frac{s}{(2p^*)^2} C\exp(-bt)\left(\frac{M^2-M_{th}^2}{s}\right)^{1-2\alpha(t)} \qquad (2.2.2)$$

yields the trajectory $\alpha(t)$ (fig.16) passing close to the mass squared values of the K, Q and L mesons lying between K and K* trajectories.

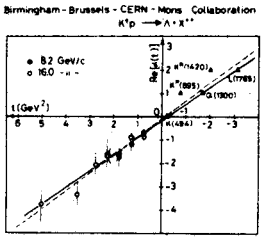


Fig.16. The effective trajectory $\alpha(t)$ resulting from the triple-Regge fit of the reaction $K^+p \to \Lambda X$ at 8.2 and 16 GeV/c; the dashed line corresponds to a simultaneous fit of expression $\alpha(t) = \alpha_0 - \alpha' t$ to combined 8.2 and 16 GeV/c trajectory points; the solid line results from a simultaneous fit of the triple-Regge formula (2.2.2) to the 8.2 and 16 GeV/c data (from ref.[26]).

The beam fragmentation in the reactions $K^+p \to \bar{\Lambda} X$ and $K^+p \to \Lambda X$ is shown to be present although small at the energies of this experiment. Its contribution is evaluated by setting the trajectory parameters in (2.2.2) to the values of N_α and Ξ_α trajectories. Thus one is able to estimate a complete fragmentation contributions to these reactions by integrating distribution functions (2.2.2) over the whole Chew-Low plots. The fragmentation contributions do not account for all of the data. If central production is defined as non-fragmentation production, it can be evaluated by subtracting the distributions predicted by (2.2.2) from the observed distributions. The residual distributions (fig.17) have indeed the characteristics of the central component. It is of interest to apply a similar procedure for other inclusive reactions in order to analyse in detail the central region as it pertains to different incident and inclusive particles.

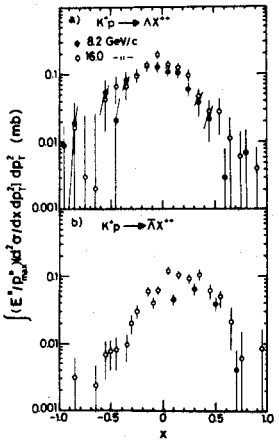


Fig.17. Inclusive distributions for reactions $K^+p \to \Lambda X$ and $K^+p \to \bar{\Lambda} X$ pertaining to the central production (from ref.[26]).

The triple-Regge analysis has also been applied for description of inclusive production of Λ, K^0 and $\bar{\Lambda}$ at small angles in pBe interactions at 300 GeV/c[58]. The results show that the nuclear effects can be ignored in a first approximation and confirm the relevance of the triple-Regge parametrization to inclusive production on the nucleus.

Thus the triple-Regge parametrization successfully describes a large variety of inclusive reactions in a wide energy range. However, the parameters of leading singularities obtained in TR fits should be treated with caution, especially in the cases when the inclusive particle can be the decay product of the resonances. This has been beautifully demonstrated by the Birmingham-Brussels-CERN-Mons-Serpukhov Collaboration[60] in the study of the slow protons in the reaction $K^+p \to pX$ at 16 GeV/c. Fig.18(a) shows that the substantial $\Delta^{++}(1236)$ production strongly

affects the shape of the inclusive spectra and consequently the results of the triple-Regge fit (fig.18(b)). It is seen that after removal of events associated with $\Delta^{++}(1236)$ production, the data are consistent with the dominance of an ffR coupling, although this is not the case for total sample of inclusive protons.

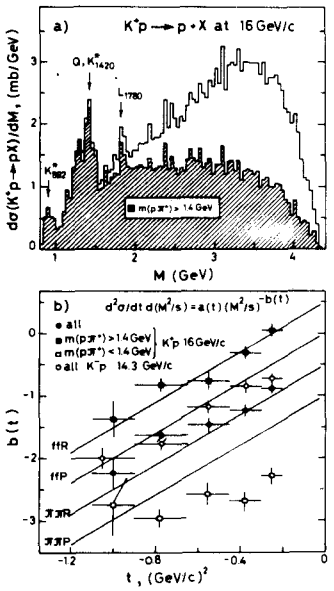


Fig.18. (a) Distribution of the missing mass M to the proton in the reaction $K^+p \rightarrow pX$ at 16 GeV/c. The events with the $\Delta^{++}(1236)$ antiselection ($m(p\pi^+) > 1.4$ GeV) are shaded. (b) The fitted values of b(t) in the triple-Regge fit for reaction $K^+p \rightarrow pX$ at 16 GeV/c for all events, for events with $m(p\pi^+) > 1.4$ GeV and $m(p\pi^+) < 1.4$ GeV. Expected variations of b(t) for several possible triple-Regge couplings are shown as straight lines (from ref./60/).

2.3 The approach to scaling in the central region

The British-Scandinavian-MIT Collaboration (BSM)/61,62/ has extended the measurement of the inclusive $\pi^\pm$, $K^\pm$ and $p^\pm$ production at x=0 over the ISR energy range ($23 \leq \sqrt{s} \leq 63$ GeV) to the small p_T regions: $0.04 \leq p_T \leq 0.4$ GeV/c for $\pi^\pm$, $0.1 \leq p_T \leq 0.3$ GeV/c for $K^\pm$ and $0.1 \leq p_T \leq 0.5$ GeV/c for $p^\pm$. These data together with those at higher values of p_T /63/ are shown in fig.19. The scaling limit is not reached in the central region even at the ISR energies. The average increase of the differential cross section over the ISR energy range amounts to $36\pm2\%$ and $41\pm2\%$ for π^+ and π^-, $52\pm8\%$ and $69\pm8\%$ for K^+ and K^-, $8\pm5\%$ and $84\pm6\%$ for p and $\bar{p}$ in the kinematical region covered by the BSM experiments.

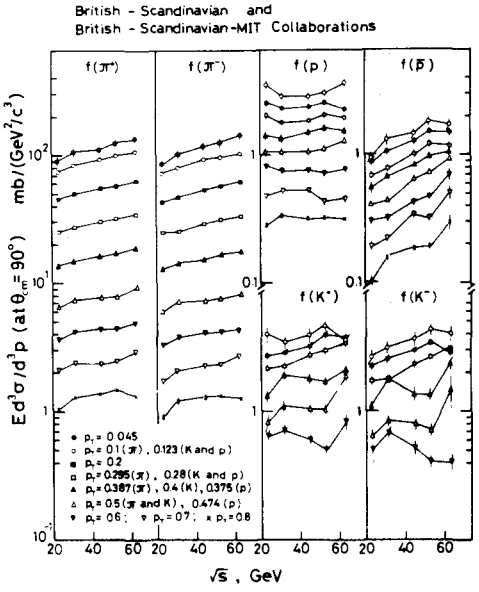


Fig.19. Energy dependence of the invariant inclusive cross section of $\pi^\pm$, $p^\pm$, $K^\pm$ at $\Theta cm = 90°$ for different p_T values at ISR energies ($\sqrt{s}$=23,31,45,53 and 63 GeV) (the data from ref./61-63/).

The particle flux at small p_T is dominated by pions but the fraction of heavier particles, kaons and nucleons, is growing almost linearly with p_T. There is a more pronounces increase with energy in the differential cross sections for $K^\pm$ and $p^\pm$ at higher p_T(fig.20). However the very low p_T pion cross sections seem to increase more at small values of p_T.

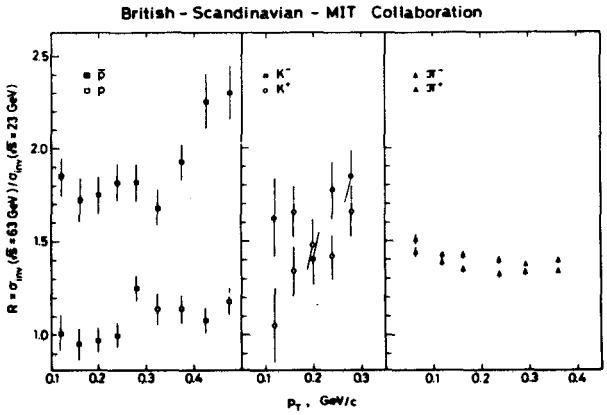


Fig.20. The cross section ratio, $R = \sigma_{inv}(63\ GeV)/\sigma_{inv}(23\ GeV)$, between the invariant differential cross sections of $\pi^{\pm}$, $K^{\pm}$ and $p^{\pm}$ at $\sqrt{s} = 63$ and 23 GeV as a function of p_T (from ref./61,62/).

It is tempting to explain the latter effect by the increase of the resonance production with energy which leads to higher proportion of pions produced from resonance decays at low p_T values (see section 3). The ratio of particle to antiparticle cross sections (fig.21) shows the strongest variation with p_T and s for protons and antiprotons. A large fraction of

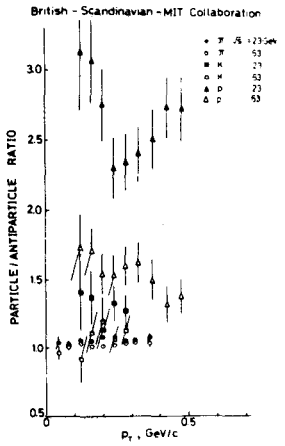


Fig.21. Particle/antiparticle ratio as a function of p_T at $\sqrt{s} = 23$ and 63 GeV (from ref./62/).

protons at the lowest ISR energy and low p_T appears to result from the fragmentation of incoming particles, whereas at larger s and p_T, p and $\bar{p}$ tend to be produced in equal numbers as expected in the central collisions.

A turnover is observed in the invariant inclusive p_T-distributions at low p_T for pions which is consistent with a p_T dependence proportional to $\exp(-Bm_T)$ with $B=7.1\ GeV^{-1}$ for π^+ and $B=7.2\ GeV^{-1}$ for π^-, where m_T is transverse mass ($m_T^2 = p_T^2 + m^2$). The same tendency to flatten off is found for $K^+(B=6.6\ GeV^{-1})$ and $K^-(B=7.09\ GeV^{-1})$, but it is not apparent for p and $\bar{p}$ data.

The significant violation of scaling at x=0 in available energy range may imply either an unlimited increase of invariant inclusive cross section with s as predicted by some theoretical models/64/, or an asymptotically constant cross section. The latter alternative is advocated in the framework of the double-Regge expansion/65,66/, represented graphically in fig.22,

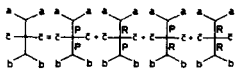


Fig.22. The double-Regge expansion diagram for inclusive reaction $a+b \to c+X$ in the central region. P and R are usual singularities with effective intercepts $\alpha_P=1$ and $\alpha_R=1/2$,

which predicts

$$E\frac{d^3\sigma}{d^3p} = \beta_{PP}(m_T)+s^{-1/4}\left(\sum_R \beta_{RP}(m_T)\right)e^{y/2} +$$

$$+\sum_R \beta_{PR}(m_T)e^{-y/2})+s^{-1/2}\sum_R \beta_{RR}(m_T) \cdot \qquad (2.3.1)$$

The assumption that the separate vertices $\beta_{ij}(m_T)$ are factorizeable gives

$$\beta_{ij}(m_T) = (-1)^{2(\alpha_i+\alpha_j)}\,\delta^a_i\,\delta^b_j\,\phi_{ij}(m_T), \qquad (2.3.2)$$

where the term $(-1)^{2(\alpha_i+\alpha_j)}$ is a conjecture, inspired by the rising cross sections in the central region/66/ (α_i, α_j are the intercepts

$\alpha_P(0)=1$ and $\alpha_R(0)=1/2$ of the Pomeron and Reggeon trajectories). The formulae (2.3.1) and (2.3.2) have several important implications. In particular they predict

i) the existence of the asymptotic plateau in rapidity distribution with the same height $(1/\sigma_T)Ed^3\sigma/d^3p = \phi_{PP}(m_T)$ for particle c and antiparticle $\bar{c}$;

ii) an energy dependence of the average multiplicity for the particles of type c

$$\langle n_c\rangle_{central} = a_c + b_c \ln s + \frac{c_c}{\sqrt{s}} + \frac{d_c \ln s}{\sqrt{s}} \qquad (2.3.3)$$

$$\text{with} \quad b_c = \frac{1}{\sigma_T^{pp}} \int E^* \frac{d^2\sigma}{dp_L^* dp_T^2} dp_T^2 \Big|_{p_L^*=0} = \pi \int \phi_{PP}(m_T) dm_T^2 \qquad (2.3.4)$$

Besides, the expression (2.3.1) relates the energy dependence of inclusive cross section to the shape of rapidity distributions at different energies and through the expression (2.3.2) one is able to relate the inclusive spectra of particle c produced by different incident particles. It has been shown[66-68] that this approach describes the energy dependence of inclusive cross sections and the shape of rapidity distributions in the central region for a number of inclusive reactions. The important result is that the values of the vertex functions β_{RR} and β_{PP} in (2.3.1) are about the same. Therefore one can not neglect the last term when the low energy data are included in the analysis of the energy dependence of inclusive cross sections in the central region.

The compilation of the available high energy data pertaining to the energy dependence of $\pi^{\pm}$ production in the central region is presented in fig.23. The present situation is somewhat different from that expected several years ago[70] (dashed line in fig.23 with b_c = =0.78). The scaling is not yet reached at highest ISR energies. But the data suggest that a scaling limit may exist, that it is being approached from below and that factorization may eventually hold. The double-Regge formalism reproduces the trend of the data up to the highest ISR energies.

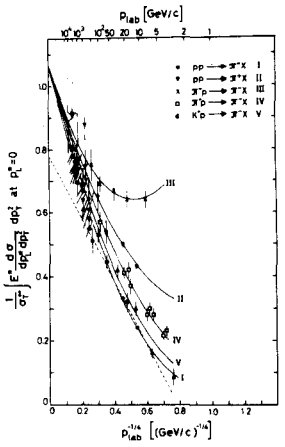


Fig.23. Energy dependence of the invariant inclusive cross sections of $\pi^{\pm}$ in the central region (compilation of published data; new data: $pp \to \pi^{\pm}$ at $\sqrt{s}$=23,31,45,53 and 63 GeV[61]). The curves are the results of the double-Regge fit[66] in (s,m_T,y) space to $pp \to \pi^{\pm}$ data at 12 and 24 GeV/c[69].

The curves I and II in fig.23 represent the results of the fit[66] of formula (2.3.1) to the $pp \to \pi^{\pm}X$ data at 12 and 24 GeV/c in (s,y,m_T) space. The curves IV and V are obtained by using relation (2.3.2) with the values of $\delta_i^{\pi^+}$ and $\delta_i^{K^+}$ known from the analyses of the total cross sections. It is quite surprising that the double-Regge analysis at such low energies (which was made before the high energy data above 100 GeV/c were obtained) provides such promising description of data, apart from some discrepancies for $pp \to \pi^+X$ reaction. For reaction $\pi^-p \to \pi^-X$ with the strong leading particle effect the similar trend is obvious with increasing energy. The energy dependence is quite consistent with that predicted by the formula (2.3.1) when the value of b_c is fixed to be the same as for $pp \to \pi^{\pm}$ reactions (curve III in fig.23).

The situation with respect to an approach to scaling in the central region for $pp \to K_s^0X$ and $K^+p \to K_s^0X$ reactions is summarized in fig.24 .

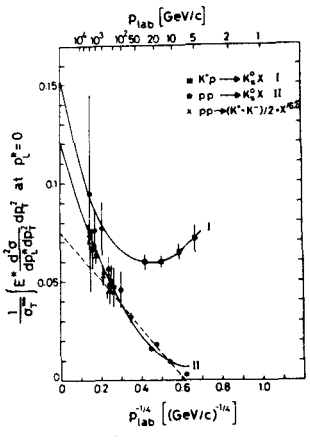


Fig.24.

Energy dependence of the invariant inclusive cross sections of K_s^o for pp and K^+p interactions in the central region (compilation of published data; new data: K^+p 32 GeV/c[25]; pp $\sqrt{s}$ = 23,31,45,53, 63 GeV[62]).

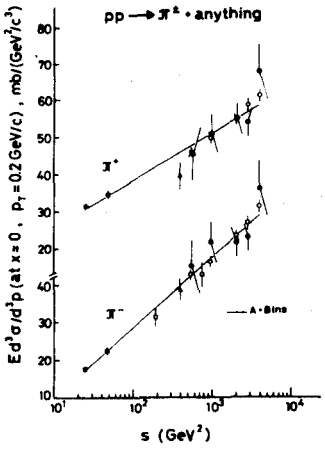


Fig.25.

Energy dependence of the invariant cross section for pp → $\pi^{\pm}$X reactions at x=0 and p_T=0.2 GeV/c (from ref.[61]).

Again the energy dependence of inclusive cross sections for reaction pp → K_s^oX is consistent with the double-Regge picture. The same, with some reservation, can be said about K^+p → K_s^oX reaction, where the RR-term in (2.3.1) is responsible for the falling cross sections in the 5-16 GeV/c incident momentum range[68]. The cross section does not decrease any more between 16 and 32 GeV/c and the double-Regge fit made by the France-USSR and CERN-USSR Collaborations[25] for 5-32 GeV/c data predicts that the cross section should start rising at higher energies. The value of $b_c = 0.152 \pm 0.030$ for this reaction is quite compatible with that for reaction pp → K_s^oX (fig.24). Therefore kaon production in the central region is also consistent with the factorization hypothesis.

Thus, although scaling in the central region is strongly violated at present energies, the available data seem to be consistent with the existence of the asymptotic limit as suggested in the framework of the double-Regge approach. However the compilation made by the British-Scandinavian-MIT Collaboration[61] warns us against possible preconception. The invariant cross sections for pp → $\pi^{\pm}$X reactions at x=0 and p_T=0.2 GeV/c plotted versus s (fig.25), although consistent with double-Regge predictions, are compatible also with logs or $A + Bs^{\alpha}$ ($\alpha > 0$) dependences, i.e with no scaling limit. More precise data are needed to clarify this picture.

In this respect, it is also of great interest to measure the multiplicity moments in the restricted region of the phase space and particularly in the pionization region. According to the theoretical predictions[71], the rise with energy of the moment $\langle n_c n_d \rangle$ for inclusive reaction a+b → c+d + anything may be as fast as $s/\ln^{\alpha} s$ ($\alpha > 0$) in the pionization region. The studies of the associated multiplicities $\langle n(M_X^2) \rangle$ for a number of inclusive reactions a+b → c+X_M have shown that they behave differently in the fragmentation and central regions, exhibiting much steeper M_X^2-dependence in the central region[72-74].

The energy dependence of the inclusive cross sections in the central region (fig.23,24) and relations (2.3.3), (2.3.4) have very important implications for the energy dependence of total charged multiplicity, which should have the same form as (2.3.3) with the coefficient of the logs term entirely determined*)

---

*) The contribution of the fragmentation processes to the average charged particle multiplicity is $\langle n \rangle_{fragm.} = a + \frac{b}{\sqrt{s}}$.

by the central production. From the trend of the data (figs.23,24) it follows that the coefficient of the logs term in (2.3.3) for the average charged multiplicity $\langle n_{ch} \rangle$ is of the order 2.5, i.e higher than usually assumed. Therefore one should be careful in comparing the cosmic ray data on the multiplicities of secondary particles at 10^{12}- 10^{16} eV with the extrapolation of data at lower energies.

However, the data on extensive air showers seem to indicate even much faster growth of the multiplicities of secondary particles at cosmic ray energies[75]. Other data on cosmic rays presented at this conference[76-78] also indicate the deviation from scaling (for details, see ref.[79]). The evidence for deviation from scaling at cosmic ray energies is not, of course, surprising since the strong violation of scaling is already apparent at accelerator energies (figs.23-25). What is important is the degree of scaling violation which may be either compatible with the asymptotically constant cross-sections or imply an unlimited increase of cross sections. We wish to remind that the scale of energy in the central region is $\sqrt{s}$ as compared with s in the fragmentation region. Therefore one may expect quite new phenomena at much higher energies than available at present accelerators. The analysis of secondary cosmic ray propagation in the atmosphere indicates that this indeed happens at 10^{14}- 10^{16} eV. It is clear that the accelerators of new generation with energies $\gtrsim 2$ TeV and with the ISR's are very much needed for quantitative studies of all these interesting phenomena.

3. Inclusive resonance production

At present much attention is given to the study of inclusive resonance production. There are several reasons for this. The main one is the abundant production of resonances, which may account for a considerable fraction of the observed final state particles. Correlation effects in multipion production suggest that many pions result from the decay of higher mass clusters. There is increasing evidence that the observed short range correlations may in fact be due to the resonance production. Moreover the resonances, being the "parent particles", represent more of the primary production features than do the observed particles in which they decay. This is important for the test of various symmetry models and production models. The study of the spin density matrix of the resonance decay provides a unique information on the dynamics of production process. Finally, unexpectedly large direct lepton production measured in nucleon-nucleon interactions adds further interest to the study of meson resonances, which may account for at least a part of the observed effect.

3.1 Inclusive production of meson resonances

The energy dependence of the inclusive ρ° and f cross sections in hadron-hadron collisions is summarized in fig.26. Average multiplicity of the ρ° and the ratio $\langle n(\rho^\circ) \rangle / \langle n(\pi_c) \rangle$ are also shown. Following ref.[83] we define $\langle n(\pi_c) \rangle$ as the mean number of the "created π^-'s", in order to take into account the strong leading particle effect and the influence of the charge conservation: $\langle n(\pi_c) \rangle = \langle n(\pi^-) \rangle - 1$ for $\pi^- p$ interactions and $\langle n(\pi_c) \rangle = \langle n(\pi^-) \rangle$ for other interactions. The data show a clear rise of the $\sigma(\rho^\circ)$, $\sigma(f)$ and $\langle n(\rho^\circ) \rangle$ with increasing energy which is consistent with the lns dependence. The lines drawn in fig.26 (a) and (b) through the experimental points

give

$\sigma(\rho^0)_{pp} \sim 2.4$ mb $\langle n(\rho^0)\rangle_{pp} \sim 0.08$ lnS

$\sigma(\rho^0)_{\pi p} \sim 1.1$ mb $\langle n(\rho^0)\rangle_{\pi p} \sim 0.04$ lnS

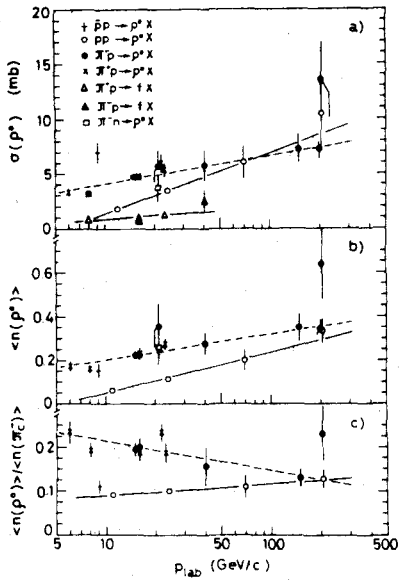


Fig.26. Energy dependence of the ρ^0 and f production (a) inclusive cross section of the ρ^0 and f as a function of p_{LAB}; (b) average multiplicity of the ρ^0 as a function of p_{LAB}; (c) ratio $\langle n(\rho^0)\rangle/\langle n(\pi^-_c)\rangle$ as a function of p_{LAB}; the lines are drown to guide the eye (the compilation of published data; new data: π^-p 200 GeV/c [80], 40 GeV/c [81], 21 GeV/c (π^-p and π^-n from π^-d data) [82], 16 GeV/c [83]; $\bar{p}p$ 9.1 GeV/c [19]).

Thus there is a strong indication that the energy dependence of the ρ^0 production is about twice stronger for pp interactions in the energy range now available. We may attribute this feature to the strong leading particle effect in the charge exchange reactions $\pi^\pm p \to \rho^0 X$ (fig.27).

From the empirical fact that in the region of $x > 0.4$ the x-distributions for reactions $K^-p \to \bar{K}^{*0}(890)X$ and $\pi^-p \to \rho^0 X$ at 16 GeV/c almost coincide [83], it is reasonable to assume that the fragmentation component

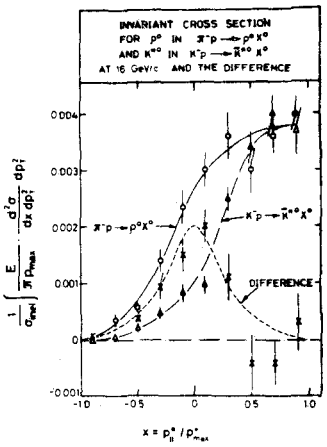


Fig.27. The invariant x distributions of ρ^0 in π^-p interactions and of $\bar{K}^{*0}(890)$ in K^-p interactions at 16 GeV/c and their difference (from ref. [83]).

of the ρ^0 production is equal to the total inclusive $\bar{K}^{*0}(890)$ cross section, since the $\bar{K}^{*0}(890)$ production is dominated by the beam fragmentation. Thus the central ρ^0 production can be evaluated by subtracting the $K^{*0}(890)$ distribution from that of ρ^0. The residual distribution (fig.27) has indeed the characteristics of the central component. From this procedure one may conclude that the fragmentation component of the ρ^0 production in π^-p interactions is dominant at low energies:

$\sigma_{fragm.}(\rho^0) = 3.1 \pm 0.3$ mb,

$\sigma_{centr.}(\rho^0) = 1.6 \pm 0.5$ mb [83]

We have seen earlier that for reactions $\pi^-p \to \pi^-X$ and $K^+p \to K^nX$ where the beam fragmentation is dominant, the energy dependence of the cross sections in the central region is quite different from other reactions (figs.23,24), although it tends to approach the same behaviour as the energy increases. There is a strong reason to believe that the same mechanism is responsible for energy dependence of the ρ^0 production observed in π^-p interactions. Moreover, one may assume that asymptotically, when $\sigma_{centr.}(\rho^0) \gg \sigma_{frag.}(\rho^0)$, the energy dependence of the $\sigma(\rho^0)$ and $\langle n(\rho^0)\rangle$ in $\pi^\pm p$ interactions is the same as in pp interactions.

From these considerations it follows that the ratio $R = \langle n(\rho^0)\rangle / \langle n(\pi)\rangle$ should asymptotically be the same for pp and π^-p interactions and independent of energy. The accuracy of the data does not allow to decide, whether this asymptotic trend is established at present energies (fig.26(c)). The investigation of the energy dependence of the ratio R is crucial for the test of the quark models[84,85]. Anisovich and Shekter predict[84] that asymptotically $R_{\pi p} = R_{pp} = 0.18$ when the main contribution to the meson production comes from the central region. The data at low energies disagree with the equal values of $R_{\pi p}$ and R_{pp}, presumably due to the dominance of the beam fragmentation for reactions $\pi^{\pm}p \to \rho^0 X$. At the highest energies now available, $R_{\pi p} \approx R_{pp}$, but are smaller than predicted. To reduce the value of R in the above quark model one may introduce the short range correlations between constituent quarks (or partons). If the mesonic state of mass M is formed as a bound state of quark and antiquark (with masses m_1 and m_2), then the rapidity difference between them $\Delta y \sim \ln(M^2/(m_1 m_2))$. The probability to find such pair vanishes with the rapidity difference Δy as $\exp(-\alpha \Delta y)$, thus giving the factor $(M^2)^{-\alpha}$ of the SU(6) symmetry breaking. Such considerations[86] lead to the ratios $\rho/\pi = 0.07$, $K/\pi = 0.09$ and $K^*/\pi = 0.10$, if one assumes that $\alpha = 1$, as seems to follow from several theoretical considerations[52,53] (for details see section 2.1).

Fig.28 presents the compilation of data pertaining to the K*(890) production. The K*(890) cross section exhibits a significant rise for pp and πp interactions, but small variation, if any, in $K^{\pm}p$ interactions up to 32 GeV/c. The bulk of the K*(890) production in $K^{\pm}p$ collisions takes place at low

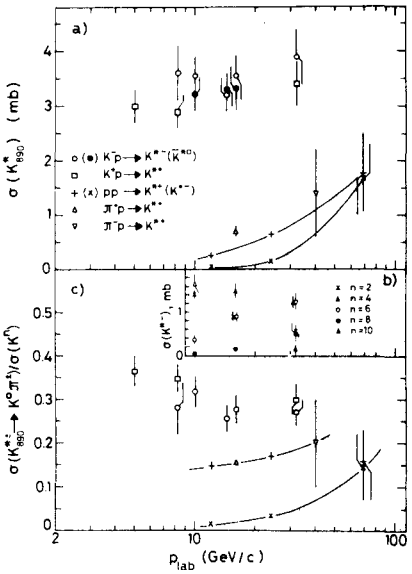


Fig.28. Energy dependence of the $K^*(890)$ production (a) inclusive cross section of the $K^*(890)$ as a function of p_{LAB} ; (c) fraction of the K^n mesons ($K^o + \bar{K}^o$) coming from the $K^{*+}(890)$ or $\bar{K}^{*-}(890)$ decays in $K^{\pm}p$ interactions as a function of p_{LAB} ; insert (b) shows the p_{LAB} dependence of the $\bar{K}^{*-}(890)$ production in K^-p interactions for different final state multiplicities[87] (compilation of published data; new data: K^-p 32 GeV/c[87], 16 and 10 GeV/c[27]; K^+p 32, 8.2 and 5 GeV/c[88]; π^-p 40 GeV/c[81]).

multiplicity events, but the contribution of higher multiplicities increases with energy[27,87]. The $K^*(1420)$ production is small, amounting to about 10% of that of $K^*(890)$. About 50% of all neutral kaons are produced via the decays of $K^*(890)$'s. The K^n and $K^*(890)$ cross sections are larger in K^-p than in K^+p interactions, but their average multiplicities per inelastic event are approximately the same for K^+p and K^-p interactions (fig.29).

Basically the energy behaviour of the K^* cross sections and average multiplicities in $K^{\pm}p$ interactions is quite similar to that of the ρ^0 in $\pi^{\pm}p$ interactions in the same energy range, because masses of these mesons are

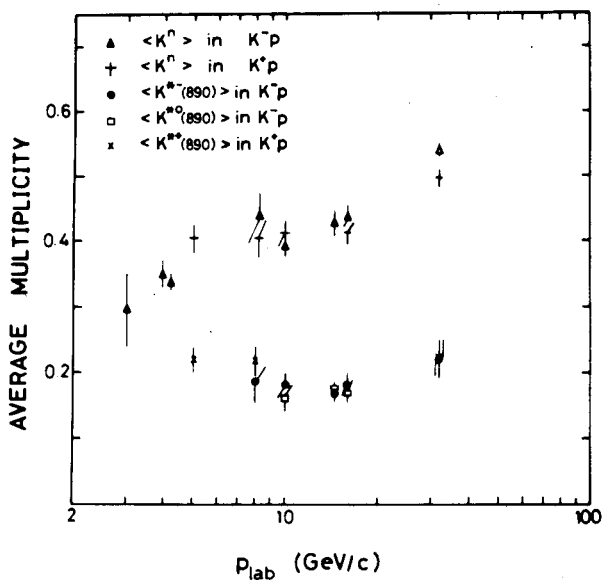


Fig.29. Average multiplicity of the K^n and $K^*(890)$ per inelastic event in K^+p and K^-p interactions (compilation of published data; new data: the same as in fig.28).

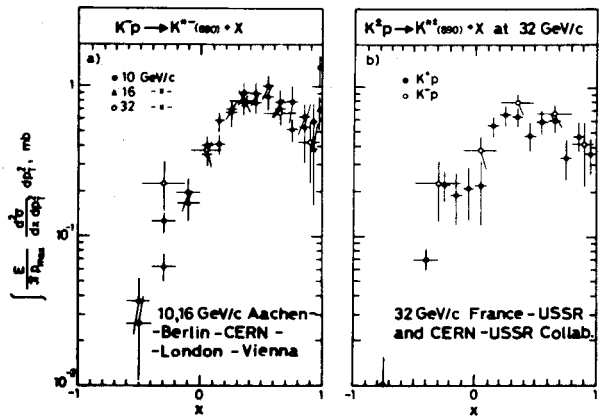


Fig.30. The invariant x distributions for $K^*(890)$ mesons produced in K^-p and K^+p interactions: (a) for reactions $K^-p \to \bar{K}^{*-}(890)X$ at 10, 16[27] and 32 GeV/c[87]; (b) for reactions $K^+p \to K^{*+}(890)X$ and $K^-p \to \bar{K}^{*-}(890)$ at 32 GeV/c[88,87].

comparable and both of them originate dominantly from the beam fragmentation. Indeed most of K^*'s are produced in the forward direction (fig.30), with no evidence for any significant production in the proton fragmentation region and presumably small central production. However, the data of the France-USSR and CERN-USSR Collaborations at 32 GeV/c suggest that the central $K^*(890)$ production has started to increase and would be much higher at the energies of the future BEBC experiments.

We may now compare the average ρ^0 and K^* multiplicities with the predictions of a "non-asymptotic" quark model[89], where an attempt has been made to improve the original quark model predictions[84], using the experimental information on the average particle multiplicities. The model predictions $\langle n(\rho^0)\rangle_{pp} = 0.30+0.15\ln(s/s_0)$, $\langle n(\rho^0)\rangle_{\pi p} = 0.45+0.15\ln(s/s_0)$ ($s_0 \approx 55$ GeV^2) are compared with the experimental data in Table 5.

Table 5

The comparison of the measured vector meson multiplicities in inelastic hadron collisions with the predictions of a "non-asymptotic" quark model[89]

Reaction	P_{LAB} GeV/c	Average multiplicity	
		experiment	prediction
$\pi^-p \to \rho^0 X$	40[81]	0.25 ± 0.06	0.45
	147[90]	0.35 ± 0.06	0.67
	200[80]	0.35 ± 0.04	0.75
$pp \to \rho^0 X$	69[12]	0.20 ± 0.05	0.30
	205[91]	0.33 ± 0.06	0.60
$K^+p \to K^{*+}_{890}X$	32[88]	0.224±0.026	0.41
$K^-p \to \bar{K}^{*-}_{890}X$	32[87]	0.22 ± 0.03	0.41

Since the $K^*(890)$ mesons in $K^\pm p$ interactions are dominantly produced in the fragmentation region, we compare their average multiplicities with the model predictions[89] in the fragmentation region. From Table 5 it is clear that the quark model disagrees with the experimental data at the highest available energies by a factor of 2.

The reaction $K^+p \to K^{*+}(890)$ and $K^-p \to \bar{K}^{*-}(890)X$ may proceed via I=0 and I=1 exchanges with both exchange particles π- B,

ρ - A_2 and ω - f. The spin density matrix elements of the K^* decay (Table 6) show an important contribution of pion exchange at 32 GeV/c, a fact already known at lower energies[92,93].

Table 6

K^*_{890} spin density matrix elements in $K^{\pm}p$ reactions at 32 GeV/c for $|t_{KK}^*| < 1\,(GeV/c)^2$ and $(M_X^2/s) < 0.5$[87,88]

Reaction	ρ_{00}	ρ_{1-1}	$Re\,\rho_{10}$	$\frac{\rho_{00}+\rho_{11}-\rho_{1-1}}{\rho_{11}+\rho_{1-1}}$
$K^+p \to K^{*+}_{890} X$	0.45±0.08	-0.02±0.08	-0.03±0.07	2.9 ± 1.1
$K^-p \to K^{*-}_{890} X$	0.42±0.10	0.07±0.08	-0.07±0.06	1.8 ± 0.6

The ratio of unnatural $\sigma^- = \rho_{00} + \rho_{11} - \rho_{1-1}$ to natural $\sigma^+ = \rho_{11} + \rho_{1-1}$ parity exchange for both K^* helicities ($\lambda = 0$ and 1) implies a higher contribution of the unnatural parity exchange in the region of $|t_{KK}^*| < 1\,(GeV/c)^2$ and $(M^2/s) < 0.5$, although an important part of the K^* production in both reactions proceeds through the natural parity exchange. Within the present accuracy, the inclusive x-distributions of K^*-mesons in K^+p and K^-p interactions are about the same in the shape (fig.30(b) and roughly are in the ratio of the total inelastic K^+p and K^-p cross sections.

In fig.31 and 32 the transverse momentum distributions of $\bar{K}^{*-}(890)$ produced in K^-p interactions and of ρ° and f mesons produced in $\pi^{\pm}p$ interactions are compared with the corresponding p_T^2-distributions of the neutral kaons and pions. We observe a well known fact that the p_T^2-distributions of meson resonances are roughly exponential in shape and have approximately equal slopes at similar energies. The low p_T steep peak for ρ° production in π^-p[83,94] and π^+p[95] interactions comes from the contributions of the quasi-two-body processes (it is not seen for ρ°'s produced

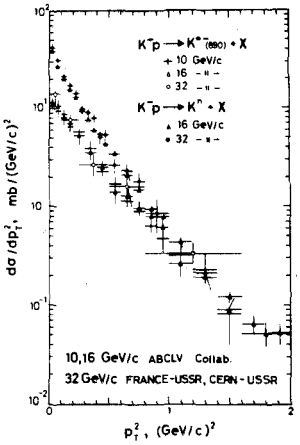


Fig.31. Inclusive p_T^2-distributions for neutral kaons in reaction $K^-p \to K^0X$ and for $\bar{K}^{*-}$'s in reaction $K^-p \to \bar{K}^{*-}(890)+X$ (data from refs.[27,87])

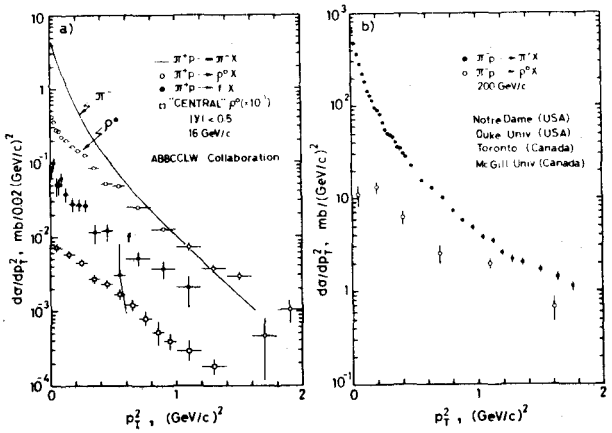


Fig.32. Inclusive p_T^2-distributions (a) for π^-'s, ρ°'s and f's in π^+p interactions at 16 GeV/c[94] and (b) for π^+'s and ρ°'s in π^-p interactions at 200 GeV/c[80].

in central region fig.32(a)) and disappears with the increasing energy (fig.32(b)). The ρ°/π and $K^*(890)/K^0$ ratios are quite small at low p_T^2 region but they are increasing to near unity as p_T^2 increases. This tendency is quite striking for 200 GeV/c where the ρ°/π^+ ratio is about 0.02 for the smallest values of p_T^2. This difference between the meson resonance transverse momentum spectrum and that of pions may be considered as a consequence of the decay kinematics, since many pions are likely to originate from the decays of resonances. It is beautifully demonstrated by the

ABBCCHW Collaboration[96]. The daughter pions originating from the decay of the ω and η resonances produced in a quasi-inclusive reactions

$$\pi^+ p \rightarrow \omega + \text{charged particles} \qquad (3.1.1)$$

$$\pi^+ p \rightarrow \eta + \text{charged particles} \qquad (3.1.2)$$

have much steeper p_T^2-distributions than the corresponding parents, while the p_T^2-distribution of π^-'s from the f decay is very similar to that of the f. The values of the exponential slopes of p_T^2-distributions for η, ω and ρ^0 in quasi-inclusive reactions are the same within errors, and the x-distributions for η and ω in reactions (3.1.1) and (3.1.2) are quite similar to the fully inclusive distributions for ρ^0.

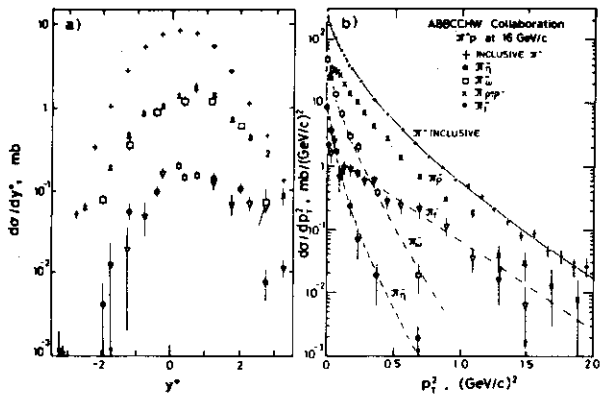


Fig.33. Comparison (a) of the c.m. rapidity distributions of π^-'s from the decays of the η, ω, ρ^0 and f and (b) of the p_T^2-distributions of π^-'s from the decays of the η, ω, $\rho^0+\rho^-$ and f with the corresponding distributions of the inclusive π^-'s in π^+p interactions at 16 GeV/c. The data are normalized to $\sigma(\eta)$ = 1.5 mb, $\sigma(\omega)$ = 4.0 mb, $\sigma(\rho^0)$ = 4.8 mb, $\sigma(\rho^-)$ = 1.6 mb and σ(f) = 0.63 mb (from ref.[96]).

In fig.33 the c.m. rapidity distributions and p_T^2-distributions of the daughter pions from the η, ω, ρ and f decays are compared with one another and with that of the inclusive π^-'s. From the comparison of the rapidity distributions one sees that the indirect pions account for a larger fraction of the inclusive pions in the beam fragmentation region than elsewhere. In the very low p_T^2 region the contribution of the pions from the ω decay seems to be dominant, while at the high p_T region the π^-'s from the ρ and f decay give the most important contribution.

These experimental observations and the analysis of the exclusive channels with η, ω and ρ^0 production have permitted to evaluate the inclusive yields of η, ω and ρ^0 in $\pi^\pm$p interactions at 16 GeV/c[97]:

$$\eta : \omega : \rho^0 = 0.34 : 0.9 : 1$$

with $\sigma(\rho^0) = 4.8 \pm 0.4$ mb, $\sigma(\omega) = 4.0 \pm 0.6$ mb and $\sigma(\eta) = 1.5 \pm 0.3$ mb. These estimates are in agreement with the values of $\omega/\rho^0 = 1.0 \pm 0.2$ and 1.1 ± 0.2 obtained in pp interactions at 12 and 24 GeV/c[98] and the new results from the CERN ISR[99] for reaction pp $\rightarrow$ ppX (X = ρ, ω, f, A_2) in the restricted region of momentum transfers t_{pp1}, t_{pp2} and the rapidity of the central cluster $y_X < 0.8$:

$\sqrt{s}$ (GeV)	(ω/ρ)	$(\omega+\rho)/f$	(A_2/f)	$<-t>$ (GeV^2)
4.9[98]	0.78 ± 0.13	3.3 ± 1.0	–	
6.9[98]	0.66 ± 0.13	0.89 ± 0.15	–	
23.5[99]	0.5 ± 0.25	1.1 ± 0.3	0.7 ± 0.2	0.22 ± 0.05
30.5[99]	0.8 ± 0.5	0.7 ± 0.3	0.8 ± 0.3	0.30 ± 0.07

The ABBCCLVW data[97] also support the results from the CERN ISR, showing the substantial amount of the η production at large transverse momenta[100]. Thus pions from the decays of ρ, ω, η and f alone (σ(f)=0.63 mb) account for nearly 46% of all pions produced in $\pi^\pm$p interactions at 16 GeV/c and this fraction is consistent with being stable in a broad energy range.

The η', ϕ production is suppressed at least at low energy experiments. The inclusive ϕ production amounts to $\sigma(\phi) = 158 \pm 35$ μb with $\phi/\rho^0 = 0.045 \pm 0.012$ in pp interactions at

24 GeV/c[8,10]. In π^+p interactions at 16 GeV/c, $\phi/\rho^0 \leq 2.5\%$ and $\eta'/\eta \approx (5\text{-}10)\%$[97]. The measurement of the ϕ production in π^-Be and K^-Be experiments at 43 GeV/c in Serpukhov[102] by the studying of dimuon $\mu^+\mu^-$ spectra has revealed no ϕ signal in π^-Be interactions, but a very clean ϕ meson signal in K^-Be interactions (fig.34) with $\sigma(K^-Be \to \phi X) = 2.0 \pm 0.5$ mb/nucleus for $x \geq 0.4$. This gives $\sigma(K^-N \to \phi X) = 0.43 \pm 0.11$ mb for $x \geq 0.4$, if one assumes the $A^{2/3}$ dependence of the ϕ production on nucleus. The ratio of the cross sections for ϕ meson production in π^-Be and K^-Be interactions is $(2.1 \pm 1.1)10^{-2}$ for $x \geq 0.4$.

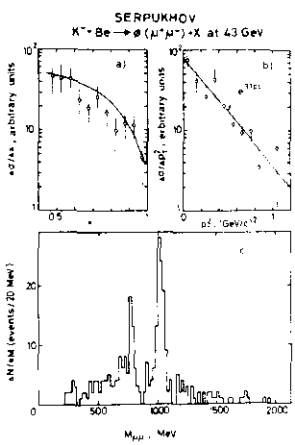


Fig.34. Mass spectrum for dimuons produced in K^-Be interactions at 43 GeV/c and the x and p_T^2-distributions of the ϕ meson (from ref.[101]); the lines in (a) and (b) represent the fits to the (1-x) and $\exp(-Bp_T^2)$ dependences, respectively.

The x-distribution of ϕ-meson (fig.34(a)) is well described by the 1-x dependence as it follows from the Drell-Yan mechanism described above and the dimensional counting[103]. The similar $(1-x)^n$ dependence for spectra of the ρ, ω and ψ is observed by the Boston group[104] in πFe and pFe interactions at 200 and 240 GeV/c. As expected, n=3 and n=1 for $x > 0.5$ in pFe and πFe collisions, respectively.

The supprassion of the ϕ production in πp and pp collisions may be a consequence of Zweig's rule, which states that the two quarks in a meson do not annihilate and the production and decay take place by connected quark diagrams. The applicability of Zweig's rule has been established in a study of the ϕ production in reactions $\bar{p}p \to K^+K^-K^+K^-$ and $\bar{p}p \to K^+K^-\pi^+\pi^-$ at 3.6 GeV/c[105]. In reactions $K^-p \to K^-\omega p$ and $K^-p \to K^-\phi p$ at 14.3 GeV/c[106], the absence of events with low $p\phi$ masses in comparison with low mass enhancement in the $p\omega$ mass spectrum is also a direct consequence of Zweig's rule. The similar conclusion has been made in the study of ϕ and ω production in exclusive reactions in πp, Kp and pp interactions at 10 GeV/c[107]. Thus there is a peculiar situation when the Zweig rule is operative in exclusive reactions, but does not hold good in the case of inclusive ϕ production in pp collisions at 24 GeV/c[101]. In the latter experiment the ϕ production in association with an additionsl pair of strange particles is found to be less strong than the production via the nonstrange component. An interesting suggestion to explain this descrepancy has been made in two papers contributed to this conference[108,109], where one uses a simple ϕ-ψ analogy to postulate a possible existence of the new excited state $P_\lambda^* \to \phi_\chi$.

The suppression of the ϕ and η' production represents still another serious problem for the simple quark models[84,85] as seen from the the comparison of the model predictions with the results of the π^+p experiments at 16 GeV/c[94] (Table 7).

Table 7

Ratios of the inclusive cross sections of non-strange mesons in π^+p interactions at 16 GeV/c[94] and the predictions of a simple quark model[84]

Ratio	Prediction	Experiment
ω/p^0	1	1
η/ω	11/81	0.39 ± 0.03
ϕ/p^0	1/9	0.025
η'/η	19/11	0.05 - 0.10
π_{DIR}/π_{ALL}	1/14	0.5

If one takes into account the suppression factor $(M^2)^{-1}$ for the meson of the mass M, discussed earlier with respect to analogy with the Drell-Yan mechanism, the situation improves, but only slightly.

Since the pions are frequently produced as the resonance decay products one should make a distinction between directly produced pions and those from the decay of other particles. The evaluation of fraction of the directly produced pions, π_{DIR}/π_{ALL}, obtained in above experiment[94] by summing up all the contributions to the total inclusive cross section for $\pi^+p \to \pi^- + X$ from the decays of the various known resonances (Table 7), is also incompatible with the quark model prediction. Another approach to evaluate the π_{DIR}/π_{ALL} ratio uses the fact, that the high p_T^2 region is dominated by the direct pion component. The data indicate that a ρ^o/π_{DIR} ratio is about unity at $p_T > 1$ GeV/c for πp interactions at 16 GeV/c and slightly lower at 200 GeV/c (fig.32), thus leading to $\pi_{DIR}/\pi_{ALL} \approx 0.2\text{-}0.3$. The ratio $\rho^o/\pi_{DIR} = 3$ expected from the number of spin polarization states in quark models seems to be ruled out by the present data within a factor of 3-4. However, if the above ratio π_{DIR}/π_{ALL} is corrected for the contribution of π_{ρ^o} and π_f in the high p_T -region[96], then we obtain $\pi_{DIR}/\pi_{ALL} \approx 0.15$. This result is still incompatible with quark model predictions. It is also difficult to reconcile this very rough estimate with the value of $\pi_{DIR}/\pi_{ALL} \lesssim 0.5$ obtained by summing up the resonance contributions, if the baryon resonance production is not responsible for an appreciable fraction of indirect pions.

3.2 Inclusive production of baryon resonances

Most of available information on baryon resonance inclusive cross sections comes from the studies of the Δ^{++} and Δ^o resonance production in bubble chamber experiments . Therefore the data are confined to the target fragmentation region, where the slow protons can be identified by ionization. The measurement of the inclusive $\Delta^{++}(1236)$ cross section is somewhat arbitrary since the Δ^{++} is a wide resonance and the different procedures are used for evaluation of the background. The overall features of the cross section dependence on energy are summarized in fig.35 .

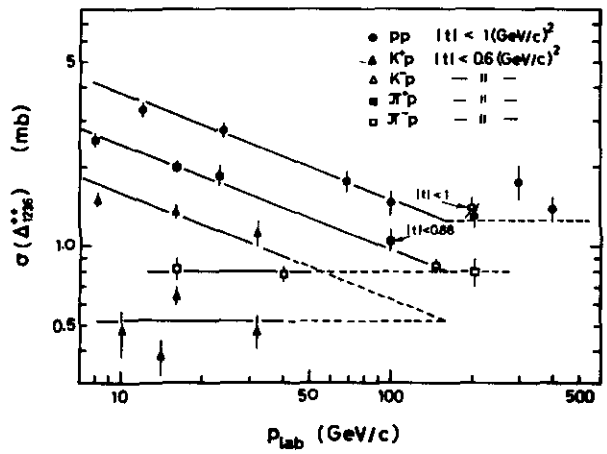


Fig.35. Inclusive $\Delta^{++}(1236)$ production cross section as a function of incident momentum. The Δ^{++} is defined in the $1.12 < M(p\pi^+) < 1.32$ GeV mass band (with some small deviations for some of the data) and for $|t|$-cuts indicated in the fig. The background is, however, evaluated by different methods in different experiments. The Breit-Wigner procedure is used to extract the Δ^{++} cross section in some experiments (compilation of published data; new data: π^-p 200 GeV/c[80], 147 GeV/c[110], 40 GeV/c[81], 16 GeV/c[111]; π^+p 16 GeV/c[111], K^-p 32 GeV/c[87], 16 GeV/c[111]).

For nonexotic ($abc\bar{c}$) pp, π^+p and K^+p reactions, cross sections fall at low incident momenta with about the same rate. The ratios of the inclusive

cross sections for these reactions are compatible with the ratio of the corresponding total inelastic pp, π^+p and K^+p cross sections, thus supporting the factorization.

For pp collisions above 100 GeV/c, the energy dependence of the Δ^{++} production levels off at the value of $\sigma(\Delta^{++}) \approx 1.5$ mb. The study of the Δ^{++} production at the CERN ISR in the range $0 < p_T < 0.7$ GeV/c and $x > 0.6$ has shown[112] that the Δ^{++} cross section is essentially s-independent, $\sigma(\sqrt{s}=23\ \text{GeV})/\sigma(\sqrt{s} = 35\ \text{GeV}) = 1.03 \pm 0.03$, between center of mass energies $\sqrt{s} = 23$ GeV and 35 GeV. In the restricted range of variables ($1.16 < M(p\pi^+) < 1.32$ GeV, $0.86 < x < 0.92$, $0.1 < -t < 0.5\ (\text{GeV/c})^2$), the Δ^{++} production at $\sqrt{s} = 30.4$ GeV in the same experiment is found to be consistent with the dominance of one-pion-exchange and particularly with the Chew-Low equation modified by the Dürr-Pilkuhn form factor. The integration of this equation over all variables yields an s-independent cross section $\sigma(\Delta^{++}) = 4.5$mb for production in both hemispheres. This result is not incompatible with the bubble chamber data above 100 GeV/c, where the application of t-cuts leads to underestimation of real cross sections.

For exotic π^-p and K^-p reactions one expects no energy dependence even at low energies. Within limited statistics the data are consistent with this assumption. This trend is clearly seen for π^-p collisions in a broad energy range (fig.35), where the data are obtained with a similar experimental technique. From the very rough comparison between the trend of data for nonexotic K^+p and π^+p reactions and approximately constant cross sections for exotic K^-p and π^-p reactions, it follows that the energy dependence for K^+p and π^+p reactions should start to level off at FNAL energies above 100 GeV/c, as it does for pp collisions. Of course, the real energy dependence of the Δ^{++} production in reactions initiated by different incident particles at high energy range may be quite different from that obtained by a simple extrapolation of the low energy data. It depends upon the leading exchange mechanisms.

The analyses of the Δ^{++} decay angular distributions and of the Δ^{++} spin matrix elements in a number of experiments have established a strong dominance of one-pion-exchange at low $|t|$-values even at the CERN-ISR energies. Extrapolation to the pion pole using the Chew-Low formula, applied to the reaction $pp \rightarrow \Delta^{++}(1236)X$ at $\sqrt{s}=30.4$ GeV[112], yields $\sigma_{tot}(\pi^-p)$ in the range between 21.1 ± 1.3 mb and 23.7 ± 0.5 mb which is in good agreement with the true value of 24.3 mb. The Chew-Low extrapolation to the pion pole or the application of the Reggeized one-pion-exchange model has permitted to obtain the total $K^\pm\pi^-$ and $\pi^+\pi^-$ cross sections (fig.36) from the studies of reactions $K^\pm p \rightarrow \Delta^{++}X$[113-115], $\pi^-p \rightarrow nX$[116] and $\pi^+n \rightarrow pX$[117].

The $\pi^+\pi^-$ total cross section is observed to fall rapidly from the resonance region to an asymptotic value of about 14-16 mb. The data are consistent with the factorization prediction $\sigma_t(\pi^+\pi^-) \approx \sigma_t(\pi^+p)\sigma_t(\pi^-p)/\sigma_t(pp)$. The $K^+\pi^-$ total cross section measured up to the c.m.energy 3.5 GeV seem to follow the same trend but still exceed slightly the factorization prediction in the energy range available. One may speculate that this is due to the existence of the numerous resonance states in the nonexotic ($K^+\pi^-$) channel. The $K^-\pi^-$ total cross section, in the exotic $K^-\pi^-$ channel, is much smaller than the $K^+\pi^-$ cross section and tends to the asymptotic limit from below. If this trend of the data indicated in fig.36 will persist at higher energies one may expect that the Δ^{++} production cross sections in the target fragmentation region will be

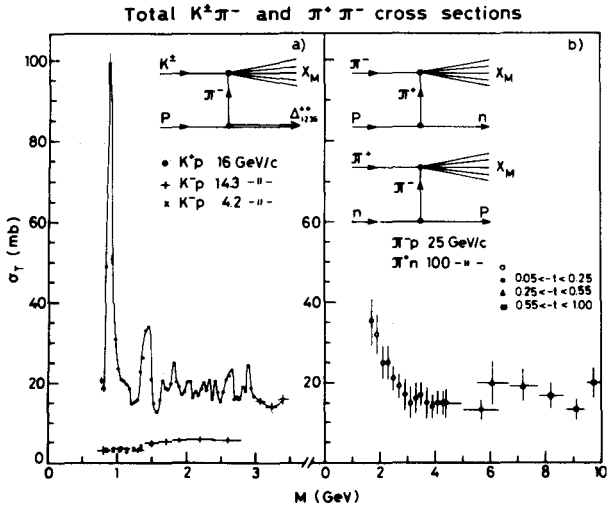


Fig.36. Total $K^+\pi^-$, $K^-\pi^-$ and $\pi^+\pi^-$ cross sections obtained from the analysis of the reactions $K^\pm p \to \Delta^{++}X$, $\pi^- p \to nX$ and $\pi^+ n \to pX$ as a function of X mass (i.e.energy of $K\pi$, $\pi\pi$ systems in their rest frame); the data from ref./113-117/.

equal for K^+p and K^-p and for π^+p and π^-p interactions, respectively, with

$$\sigma_{\Delta^{++}}(pp):\sigma_{\Delta^{++}}(\pi p):\sigma_{\Delta^{++}}(Kp)=\sigma_t(\pi p):\sigma_t(\pi\pi):\sigma_t(K\pi)$$

However the contribution of other isotopic one exchange particles (ϱ,A_2), which could mediate these reactions, and the interference between possible exchanges may eventually lead to a quite different results for all t-region. Besides, the important part of the Δ^{++} cross section comes from the production and subsequent decay of the diffractive systems $p\pi^+\pi^-$ where the triple-Pomeron coupling and factorization of the Pomeron should give somewhat different predictions.

Very little information is available about the Δ° inclusive production. We know that the production of low mass $p\pi^+$ and $p\pi^-$ systems is strongly correlated by the diffractive production of $p\pi^+\pi^-$. Since this diffractive system is generally assumed to be an isospin 1/2 state, there are nine times more $\Delta^{++} \to p\pi^+$ than $\Delta^\circ \to p\pi^-$. This explains the large background under the Δ° peak and makes difficult the study of the Δ° production. However, contrary to what is often stated, I would like to stress that the Δ° inclusive cross section may be quite higher than the value of 1/9 from the Δ^{++} cross section, since the diffractive production of the $p\pi^+\pi^-$ state with I=1/2 is not the unique mechanism of the Δ° production at least at present energies. Specifically in the low |t|-region, where the pion exchange dominates one has the following relations:

$$\frac{\sigma(pp \to \Delta^\circ X)}{\sigma(pp \to \Delta^{++}X)} = \frac{\sigma(\pi^+p)}{3\sigma(\pi^-p)} \qquad (3.2.1)$$

$$\frac{\sigma(\pi^\pm p \to \Delta^\circ X)}{\sigma(\pi^\pm p \to \Delta^{++}X)} = \frac{\sigma(\pi^\pm\pi^+)}{3\sigma(\pi^\pm\pi^-)} \qquad (3.2.2)$$

$$\frac{\sigma(K^\pm p \to \Delta^\circ X)}{\sigma(K^\pm p \to \Delta^{++}X)} = \frac{\sigma(K^\pm\pi^+)}{3\sigma(K^\pm\pi^-)} \qquad (3.2.3)$$

Just for example, the Δ inclusive cross sections are found to be equal to $700\pm100\,\mu b$ for reaction $K^-p \to \Delta^{++}X$ and to $985\pm180\,\mu b$ for reaction $K^-p \to \Delta^\circ X$ at 14.3 GeV/c high statistics experiment/118/. In the same experiment the ratio (3.2.3) for K^-p reaction as well as the ratio $\sigma(K^+p \to \Delta^{++}X)/\sigma(K^-p \to \Delta^\circ X)$ which should be equal to 3 for any isospin 1 meson exchange, have been specifically tested and found to be compatible with the K^-p/113,118/ and K^+p/114,119/ data. Thus the production and decay of the Δ^{++} and Δ° resonances may account for considerable fraction of indirect pions produced in hadron-hadron interactions.

An interesting attempt to separate the Δ^{++} production over the entire kinematic region has been made by ABBCCHLVW Collaboration in $\pi^\pm p$ and K^-p experiments at 16 GeV/c/111/. Table 8 shows, that the total inclusive cross sections of $\Delta^{++}(1236)$ are almost twice as high as those obtained with a mass cut $1.12 < M(p\pi^+) < 1.34$GeV and $|t|<0.6(GeV/c)^2$ (shown in fig.35). The fraction of Δ^{++} production increases with increasing charged multiplicity and

Table 8

Δ^{++} production cross sections and the fraction of produced Δ^{++}'s per inelastic collision at 16 GeV/c for different charged multiplicities[111]

Reaction	σ_{inel} (mb)	Fraction (%)				
		inclusive	2prongs	4prongs	6prongs	8prongs
π^+p	3.39	17.2	6.1	19.6	21.9	23.4
π^-p	1.41	6.6	-	7.5	10.5	18.0
K^-p	1.23	4.4	-	7.7	12.0	13.3

a substantial part (45 + 49%) of the Δ^{++} cross section comes from topologies with more than four prongs.

Because of practical difficulties, there is almost no information about inclusive production of heavier N^{*}'s which presumably decay through a 3-body or cascade processes. Some new information is obtained on strange baryon $\Sigma^{\pm}(1385)$ production in K^-p collisions[57,87,120] (fig.37).

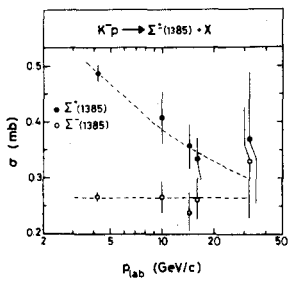


Fig.37. Inclusive $\Sigma^{\pm}(1385)$ production cross sections in K^-p interactions as a function of incident momentum (the data from refs.[57,87,120,121]); the lines are to guide the eye.

The decrease of the $\Sigma^+(1385)$ cross section with energy seems to be similar with that observed earlier for reaction $K^-p \to \Lambda X$ (fig.3). It is falling between 4.2 and 10 GeV/c but then shows the tendency to level off in the 10-32 GeV/c incident momentum range, where the Σ^+ cross section is quite close to the Σ^- cross section which is essentially energy independent. From the invariant x-distributions (fig.38), one sees that Σ^- is produced symmetrically about x=0, thus suggesting a predominance of the central production.

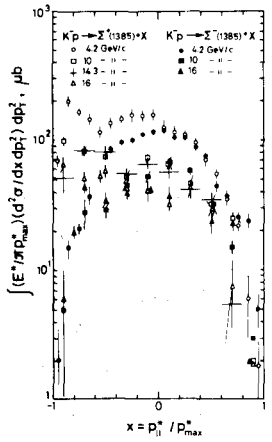


Fig.38 The invariant x-distributions for reaction $K^-p \to \Sigma^{\pm}(1385)X$ (the data from refs.[57,120,121]).

For each energy the Σ^+ and Σ^- distributions are the same in the forward direction, but there is a strong excess of Σ^{+}'s in the backward direction, which can be attributed to a quasi-two-body hypercharge exchange processes with a strong energy dependence. Indeed a triple-Regge analysis of the $\Sigma^+(1385)$ production at 4.2 GeV/c in proton fragmentation region, involving strangeness annihilation at the K^- vertex, has shown[57] that the Regge trajectory responsible for the strangeness annihilation process $K\bar{K} \to$ pions is consistent with the f'- Ø trajectory.

The information provided by the weak Λ-decay in the two step sequence $\Sigma^+(1385) \to \pi^+(\Lambda \to p\pi^-)$ has been used by the Amsterdam-CERN-Nijmegen-Oxford Collaboration[57] for the reconstruction of the complete $\Sigma^+(1385)$ spin density matrix in the reaction $K^-p \to \Sigma^+(1385)X$ at 4.2 GeV/c. Although the errors in the polarization are large due to the uncertainties introduced by the appreciable amount of background, the conclusion is that the $\Sigma^+(1385)$ polarization in the region $|t'_{p\Sigma}| < 0.5 (GeV/c)^2$ is small and compatible with 0, which is in agreement with the predictions[122] of the additive quark model. These results are in remarkable contrast with the recent studies of the inclusive Λ production in reaction $K^-p \to \Lambda X$ where the existence of significant

polarization has been established (see[123] and references therein).

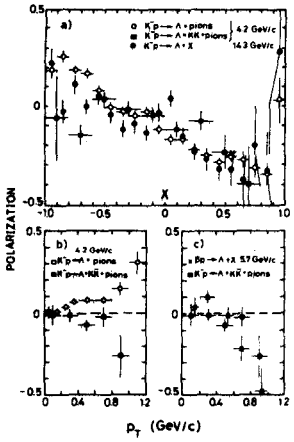


Fig.39. (a) Variation of the Λ polarization $P_\Lambda = \frac{3}{\alpha N} \sum_{i=1}^{N} \vec{q}_i \vec{n}_i$ (usual notations) with x for reactions $K^-p \to \Lambda$ + pions, $K^-p \to \Lambda KK$ + pions at 4.2 GeV/c[123] and $K^-p \to \Lambda$ + anything at 14.3 GeV/c[124]; (b,c) Λ polarisation for reactions $K^-p \to \Lambda$ + pions, $K^-p \to \Lambda + K\bar{K}$ + pions at 4.2 GeV/c and for $\bar{p}p \to \Lambda$ + X at 5.7 GeV/c in the region $-1 < x < -0.2$ as a function of p_T.

Fig.39(a) shows that the Λ polarization in the region $x < -0.5$ exhibits different behaviour for the reactions

$$K^-p \to \Lambda + \text{pions} \qquad (3.2.4)$$

$$K^-p \to \Lambda + K\bar{K} + \text{pions} \qquad (3.2.5)$$

It is positive for reaction (3.2.4), while it is slightly negative for reaction (3.2.5). For events in the target fragmentation region ($-1 < x < -0.2$), a striking difference in the P_Λ with increasing p_T is seen for these two reactions in fig.39(b), whereas the P_Λ for strangeness nonannihilation process (3.2.5) and for $\bar{p}p$ reaction $\bar{p}p \to \Lambda$ + X have a similar dependence (fig.39(c)). The small magnitude of the Λ polarization in proton fragmentation region for $\bar{p}p$ interactions and for K^-p interactions with the off-mass-shell strangeness nonannihilation process $K\bar{K} \to K\bar{K}$ + pions might indicate that the above two processes are dominated by the Pomeron exchange.

4. Two-particle correlations

Many conclusions on the status of two-particle correlations in rapidity space are now completely different from those made at the time of the Aix-en-Provence and London conference. The importance of presenting results in terms of semi-inclusive correlations (shown by the bubble chamber experiments in Serpukhov and Fermilab), of discriminating between particles of different charges and of collecting the reasonable statistics is well understood now and it explains the drop in flow of experimental (but not theoretical) information on this subject.

A simple independent cluster emission model still describes the most salient features of the data. But there is increasing evidence that the copious resonance production may explain to a large extent the short-range effects observed in two-particle correlations. From my personal point of view some of the most significant evidence for such interpretation comes from the stable structure of events in a broad energy range.

Thus the Saclay-Ecole Polytechnique--Rutherford Collaboration[125] has found a striking similarity between the diffractive excitation systems $N \to N\pi$, $N \to N\pi\pi$ and $N \to \Lambda K$ induced by K^- mesons at 14.3 GeV/c and protons at ISR energies.

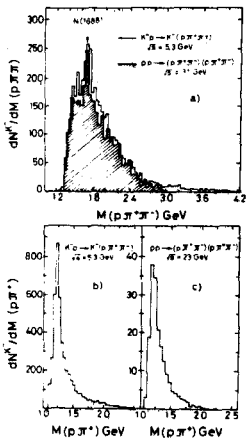


Fig.40. Comparison of $p \to p\pi^+\pi^-$ fragmentation systems in single dissociation process $K^-p \to K^-(p\pi^+\pi^-)$ at 14.3 GeV/c and in double dissociation reaction $pp \to (p\pi^+\pi^-)(p\pi^+\pi^-)$ at 500 GeV/c: (a) $p\pi^+\pi^-$ mass spectra; (b) and (c) $p\pi^+$ subsystem mass spectra (arbitrary units in fig.(c)); from ref.[125].

As an example fig.40 shows that the shapes of the $p\pi^+\pi^-$ and $p\pi^+$ effective mass spectra in reactions $K^-p \to K^-(p\pi^+\pi^-)$ at 14.3 GeV/c and $pp \to (p\pi^+\pi^-)(p\pi^+\pi^-)$ at 500 GeV/c are practically the same, both for resonance components and for overall fragmentation background.

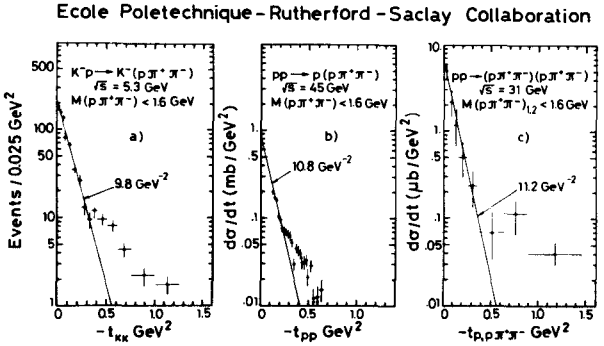


Fig.41. Comparison of production differential cross sections of the low mass diffractive $N\pi\pi$ systems (from re./125/).

The production differential cross sections for three sets of data (fig.41) display a similar behaviour with a break at $|t| \approx 0.3$ GeV^2 and relatively large slopes below the break. The similarities of the invariant mass distributions, decay angular distributions and differential cross sections at c.m.energies differing by an order of magnitude indicate a remarkable energy independence of the diffractive production dynamics over this broad energy range.

The small energy dependence of the correlation function $R(y_1, y_2)$ in the central region over a broad energy range is another important feature of data. The CERN-USSR and France-USSR Collaboration has shown/29/ that the behaviour of the semi-inclusive correlation function

$$G_n^{--}(y_1,y_2) = \left(\frac{d^2\sigma}{dy_1 dy_2}\right)_n - \frac{n-1}{n\sigma_n}\left(\frac{d\sigma}{dy_1}\right)_n\left(\frac{d\sigma}{dy_2}\right)_n$$

for reaction $K^+p \to \pi^-\pi^-X$ is quite similar between 12 and 32 GeV/c. In the study of the energy dependence of two-particle rapidity correlations in the central region for π^-p semi-inclusive reactions between 8 and 360GeV/c the NDDCIMM Collaboration/126/ has presented evidence that the central region correlation maximum grows as logs. The semi-inclusive (--) correlations are smaller and have less s dependence than those for the (+-) pairs, where the logs growth of semi-inclusive correlations is quite strong. The latter fact is consistent with the cluster emission phenomenology, but can be as well explained by the growth of the resonance production.

The only evidence against the resonance interpretation of correlations seems to be a somewhat higher average charged particle multiplicity of "cluster" $\langle k \rangle \approx 2\text{-}3$/127,128/. One should remember, however, that it is a model dependent value and other estimates give $\langle k \rangle \lesssim 2$ (for details see, for example/129/), which is not inconsistent with the resonance interpretation. Besides, the decay of baryon resonances of high masses may result in higher multiplicity of charged particles in a "cluster".

Following is a brief discussion of the experimental data on two-particle correlations presented to this conference, where the main emphasis is made on angular correlations, interference correlations between the like pions and on the spacial structure of interaction region (for more details see the mini-raporteur's talks of Kistenev and Podgoretsky at this conference).

4.1 Angular correlations

Azimuthal correlations are usually studied in terms of the asymmetry parameter $A = (N(\phi_T > \pi/2) - N(\phi_T < \pi/2))/(N(\phi_T > \pi/2) + N(\phi_T < \pi/2))$, where the ϕ_T is the azimuthal angle between the transverse momenta p_{T_1} and p_{T_2} of two particles. In Table 9 the experimental values of A for like and unlike pairs obtained in several experiments/130-133/ are shown.

Table 9

Asymmetry parameters A for like and unlike pion pairs

	$\bar{p}n$ /130/ (1-1.6) GeV/c	π^-p /131/ 11.2 GeV/c	π^-p /132/ 40 GeV/c	pp /133/ 102 GeV/c
$A_{LIKE(L)}$	0.182±0.008	0.1074±0.0008	0.062±0.006	0.040±0.010
$A_{UNLIKE(U)}$	0.335±0.006	0.1764±0.0008	0.106±0.003	0.078±0.010
$A_U - A_L$	0.153±0.009	0.0690±0.0011	0.044±0.007	0.038±0.01
$\frac{A_U - A_L}{A_U + A_L}$	0.296±0.018	0.243±0.004	0.262±0.04	0.322±0.08

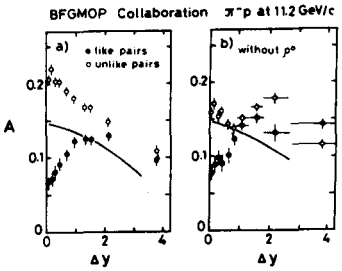


Fig.42. Azimuthal asymmetry parameters for like and unlike pairs in π^-p interactions at 11.2 GeV/c as a function of the rapidity difference $\Delta y = y_1 - y_2$; (a) for all events; (b) after removal of events with a $\pi^+\pi^-$ pair in the ρ° region (from ref./131/).

In fig.42 the parameters A_L, A_U in π^-p experiment at 11.2 GeV/c/131/ are presented as a function of the rapidity difference Δy and compared with the predictions of statistical model. We observe the following important facts. The high multiplicities of neutral particles at higher energies result in decrease of A_L, A_U and $A_U - A_L$ with increasing s, whereas the ratio $(A_U - A_L)/(A_U + A_L)$ is constant within errors. The difference between A_U and A_L is most significant for small rapidity difference. The asymmetry for unlike pairs tends to be compatible with statistical model predictions after removal of events in ρ° mass band, but persists for like pairs. Thus the rise of A_U at small Δy can be interpreted as a consequence of resonance decay, whereas the drop of A_L at small Δy seems to be due to Bose-Einstein symmetrization effect.

Since the resonance production influences the angular asymmetries, it is appropriate to investigate angular correlations between particles in terms of their effective mass M. Indeed, effect of different origins, such as resonances or Bose-Einstein statistics can contribute predominantly at $\Delta y = 0$, while with respect to M these mechanisms could be separated.

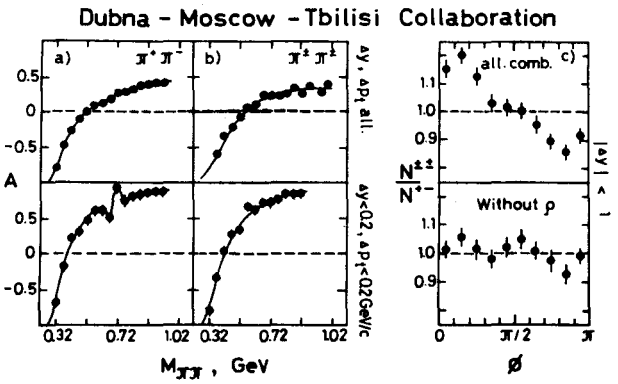


Fig.43. Azimuthal asymmetry parameter A for (a) $\pi^+\pi^-$ and (b) $\pi^\pm\pi^\pm$ pairs as a function of their effective mass M in π^-p interactions at 40 GeV/c; (c) the ratio of the azimuthal distributions for like and unlike pairs for all combinations and after removal of $\pi^+\pi^-$ pairs from the ρ° mass band (from ref./134/).

The Dubna-Moscow-Tbilisi Collaboration/134/ has studied asymmetry parameter A for $\pi^+\pi^-$, $\pi^\pm\pi^\pm$ pairs in π^-p interactions at 40 GeV/c as a function of their mass M (fig.43(a)). A sharp maximum is observed at $M = M_{\rho^\circ}$ for $\pi^+\pi^-$ pairs which is strongest at $\Delta y < 0.2$ and $\Delta p_T^2 < 0.2 (GeV/c)^2$. No difference is seen in the azimuthal distributions for like and unlike pairs (fig.43(c)), when the $\pi^+\pi^-$ pairs from ρ° mass band are removed from the data.

The detailed study of the angular correlations as functions of the effective mass has been made by the Aachen-Berlin-Bonn-CERN-Cracow-Heidelberg-Warsaw Collaboration/135/ in 4 and

6 prong events of π^+p interactions at 16 GeV/c. They present the results in terms of the opening angle ϕ between the three-momenta p_1 and p_2 of particles for pion-pion and proton-pion pairs, which is studied as a function of the two-particle mass M. The mean value of cos ϕ as a function of M for like and unlike charged pions is to a large extent determined by kinematics. However, an influence of the momentum configuration of resonance on the opening angle is striking when for pion pairs the difference

$$d_{\pi\pi}(M) = \langle\cos\phi^{\pi^+\pi^-}\rangle_M - \langle\cos\phi^{\pi^\pm\pi^+}\rangle_M$$

and for proton-pion pairs the difference

$$d_{p\pi}(M) = \langle\cos\phi^{p\pi^+}\rangle_M - \langle\cos\phi^{p\pi^-}\rangle_M$$

is studied as a function of M

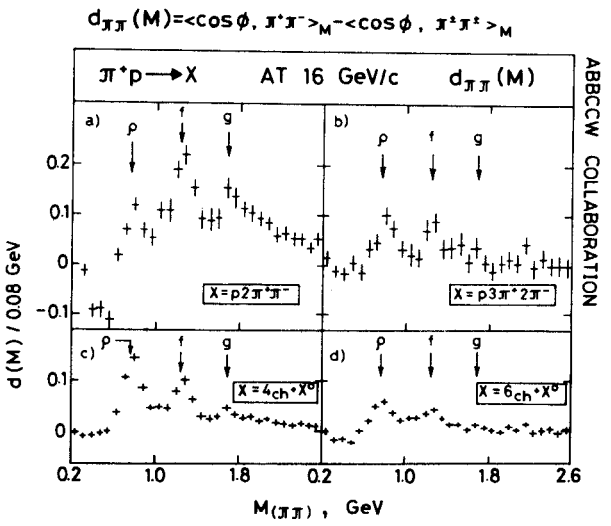


Fig.44. The distribution of the difference in the opening angle ϕ between the three momenta of particles for unlike and like pion pairs as a function of the effective mass M of the pair for (a) $p2\pi^+\pi^-$ final state, (b) $p3\pi^+2\pi^-$ final state, (c) 4-prong events, (d) 6-prong events in π^+p interactions at 16 GeV/c (from ref.[135]).

A clear structures with the resonance signals of ρ^0,f,g mesons (fig.44) and of the $\Delta^{++}(1236)$ and $\Delta^{++}(1890)$ (not shown) are visible. It is of great interest that resonances which are not (or just hardly) seen in the corresponding two-particle mass distributions, such as f,g, and $\Delta^{++}(1890)$, are observed more clearly in d(M) distributions. This is due to an increase of the $\langle\cos\phi\rangle$ caused by resonances, which increase the probability for the longitudinal momenta p_{L1} and p_{L2} to have the same sign and even more so if they are produced peripherally.

Thus it seems reasonable to conclude that the angular correlations are mainly of the kinematical origin. The difference between the like and unlike charged combinations outside the threshold region, where the interference effects could be essential, can be explained by the resonance production.

4.2 Space structure of events

Let us consider now the interference region near the threshold $M \approx 2m_\pi$. The interest to this region is motivated by the possibility to study the dimensions of the region from which pions are emitted. The first indication that it is possible to measure the space-time properties of the interaction region was observed in the angular clustering of identical pions (in terms of the opening angle ϕ) known as GGLP effect[136]. The measurement of the range of the Bose-Einstein correlations in units of pion Compton wave-length as formulated by GGLP has been attempted in π^-p experiment at 200 GeV/c[137]. It was shown that $\pi^+\pi^-$ correlations differ from the $\pi^-\pi^-$ correlations only at small values of $t_{12}=(p_1-p_2)^2$. This difference is accounted for if the range of the Bose-Einstein correlations $R = (1\pm0.25)$ fm.

More recently Kopylov and Podgoretsky[138] (see also[139,140]) have proposed to study the dimensions of the region from which pions are emitted by means of second order interference effects between identical pions. They argue that the interference between identical pions

is constructive at small values of the variables q_o and q_t defined as

$$q_o = E_1 - E_2 \quad \text{and} \quad q_t = \angle(\vec{p}_1 - \vec{p}_2)\vec{xn},$$

where $\vec{n} = (\vec{p}_1+\vec{p}_2)/|\vec{p}_1+\vec{p}_2|$, ($q_t^2 \to M_{\pi\pi}^2 - 4m_\pi^2$ at $q_o \to 0$). The interference effect is measured in terms of ratio

$$\frac{N_L}{N_B} = 1 + \frac{(2J_1(q_tR)/(q_tR))^2}{1 + (\tau q_o)^2}, \qquad (4.2.1)$$

where N_L is the number of pions of equal charge and N_B is background. This expression is obtained[138] in the framework of the statistical Pomeranchuk model, describing the emission of pions from massive point-like centers with the radius of the interaction region R and the lifetime of the pion source τ.

The existence of Kopylov-Podgoretsky effect is firmly established at several experiments[130,141-147]. In all of them (as for example is shown in fig.45) one observes a clear excess of like pion pairs at small values of q_t^2 and q_o, which decreases with increasing q_o and q_t^2 and finally disappears.

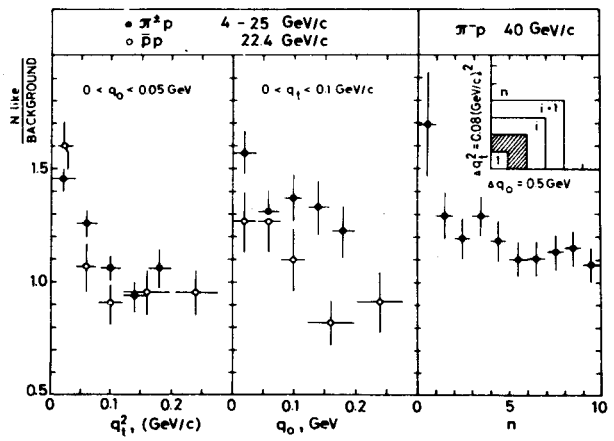


Fig.45. The ratio of the normalized q_t^2 and q_o spectra of like and unlike pions for two intervals of q_o and q_t, respectively, (from ref.[142,145,146]).

The effect of the ρ^o production on the q_t^2 and q_o distributions is negligible in the region of low q_t^2 and q_o, affecting the shape of q_t^2-distribution for unlike pion pairs only around $q_t^2 \approx 0.40(\text{GeV/c})^2$[130]. The estimates of the interaction radius R obtained in several experiments[130,141-147] are compiled in fig.46.

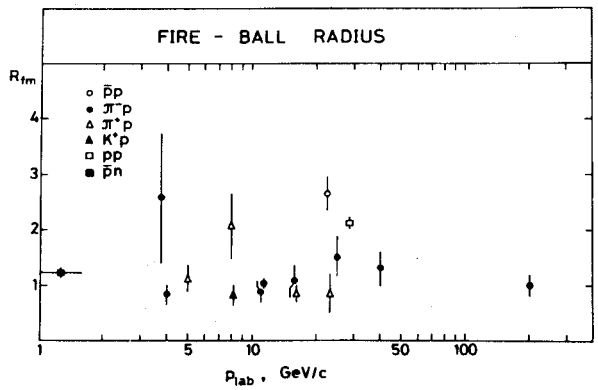


Fig.46. Energy dependence of the interaction (fair-ball) radius; (in refs.[130,141-147] it is obtained from the fits to the Kopylov-Podgoretsky formula (4.2.1), in ref.[137] (π^-p 200 GeV/c) as proposed by GGLP (see text))

R values for meson-proton interactions are all in good agreement, being consistent with the value of R ≈ 1fm, which is quite close to the proton radius. The energy dependence seems to be small within present accuracy. However there is some indication that interaction radius may be different for different types of interaction. Characteristic emission time of the pion source was found to be small in all experiments. But while in some of them $c\tau < R$[142,144,147], in others $c\tau > R$[130,141,146]. This may suggest different interpretations of the parameter $c\tau$[138,140] (see also[148]).

Another possibility of studying the spacial structure of the interaction region has recently emerged from the impact parameter representation of inelastic reactions[149-152]. In the paper[153] the lower bounds b_L for the

root mean square impact parameters

$$\langle b^2 \rangle \geq b_L^2 = \langle \sum_i^n (x_i^2 - r_i^2)/(2p_i^{max2}) \rangle^2 / \langle \sum_{ij}^n x_i x_j \vec{r}_i \vec{r}_j \rangle$$

have been determined for annihilation, production and coherent $\bar{p}$ induced reactions in the 5-15 GeV/c incident momentum range ($\bar{p}p$ 5.7 GeV/c, $\bar{p}d$ 4.72 - 14.6 GeV/c). Here r_i is the transverse momentum of the i-th final-state particle with $x_i = p_i/p_i^{max}$, where p_i^{max} is the maximum allowed p_i value calculated for each kind of particle emitted in the studied reactions. The results indicate that at a given incident momentum, the b_L decreases with the number of final state particles for annihilation and production processes. For the coherent channel $\bar{p}d \to \bar{p}d\pi^+\pi^-$ the b_L decreases with increasing incident momentum as has already been observed[154] in the $pp \to pp\pi^+\pi^-$ and $\pi^-p \to \pi^-p\pi^+\pi^-$ reactions produced diffractively (fig.47).

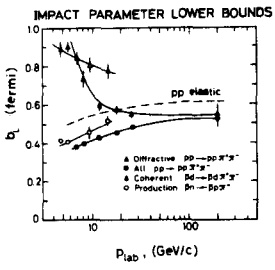


Fig.47. Impact parameter lower bounds b_L for $pp \to pp\pi^+\pi^-$, $\bar{p}d \to \bar{p}d\pi^+\pi^-$ and $\bar{p}n \to \bar{p}p\pi^-$ reactions as a function of incident momentum (data from refs.[153,154]).

The impact parameter bounds for coherent reactions were found to be about 2-3 times larger than for production reactions and even much larger (about 10 times) than for annihilation channels. Thus $\bar{p}p$ annihilation to mesons is more central than the production reactions. This conclusion is in accord with the earlier results[155] and seems to indicate that the simple interpretation of $\bar{p}p$ annihilation as responsible for difference between $\bar{p}p$ and pp interactions has to be abandoned, since elastic scattering data show that this difference is particularly peripheral in impact parameter.

The impact parameter language is intimately connected with the search of the planarity effects in the momentum space, i.e. the alignment of emitted particles in a preferred direction in the transverse plane containing the impact parameter vector. Several methods have been proposed to measure a degree of a possible alignment of the final particles in the transverse plane. In the framework recently developed by Counihan[156] one introduces the principal axis as the direction for which the sum of the squares of the transverse momenta is minimum. The principal axes are defined as the eigenvectors $\vec{z}^{(k)}$ of the matrix

$$Q^{\alpha\beta} = \sum_i^n p_i^\alpha p_i^\beta$$

where the sum includes all final state particles in the event and α and β denote the 3 components of the momentum $\vec{p}_i$. The eigenvalues $\lambda_k = \sum_i (\vec{p}_i \vec{z}^{(k)})^2$ describe the overall shape of the final state in momentum space and are ordered as $\lambda_1 > \lambda_2 > \lambda_3$. Thus defined principal axis system is shown in fig.48.

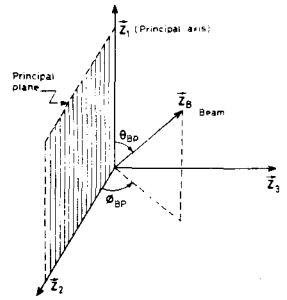


Fig.48. Definition of the principal axis system.

The France-USSR and CERN-USSR Collaborations[157] have indeed observed the alignment of the final state particles and the beam particle in the reactions $K^+p \to K^+p\pi^+\pi^-$ and $K^+p \to K^+p2\pi^+2\pi^-$ at 32 GeV/c in thus defined principal plane. The degree of this alignment seems to be higher than can be expected from the ordering relation ($\lambda_1 > \lambda_2 > \lambda_3$). Even more surprising is the

behaviour of the differential cross sections $d\sigma/d\cos\Theta_{BP}$ and $d\sigma/d\cos\alpha$ in these reactions (α is the generalized scattering angle, see [156]). They are consistent with exponential shape (fig.49) for $\cos\Theta_{BP} > 0.98$ and $\cos\alpha > 0.98$ with the values of the slope:

$B_\alpha = 205 \pm 10$ $\quad B_\Theta = 204 \pm 10$ for $K^+p \to K^+p\pi^+\pi^-$

$B_\alpha = 175 \pm 25$ $\quad B_\Theta = 168 \pm 24$ for $K^+p \to K^+p2\pi^+2\pi^-$

which are quite close to the corresponding value of the slope $B_{el} = 195 \pm 9$ in the exponential parametrization of the $d\sigma/d\cos\Theta$ distribution of elastic K^+p scattering at the same energy.

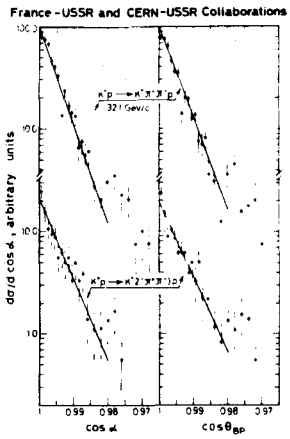


Fig.49. The $d\sigma/d\cos\Theta_{BP}$ and $d\sigma/d\cos\alpha$ distributions in the principal axis system for reactions $K^+p \to K^+p\pi^+\pi^-$ and $K^+p \to K^+p(2\pi^+)(2\pi^-)$ at 32 GeV/c (from ref. [157]). The scattering angle Θ_{BP} is defined in fig.48, the generalized scattering angle α is defined as the angle between the beam direction and the same direction rotated by the matrix $Q^{\alpha\beta}$.

This means that the description of multiparticle final states in principal axis variables is quite similar to that of elastic scattering. One might expect this for $K^+p \to K^+p\pi^+\pi^-$ reaction where the diffractive channels are dominant [158] (indeed, B_α is slightly higher than B_{el}, reflecting the well known fact that the slope of the differential cross section $d\sigma/dt$ is higher for diffractive system than for elastic scattering). However the nearness of B_{el} and B_α for 6 particle state is quite surprising and invites further investigations.

In closing I would like to make a point of some general conclusions which the above presentation leads us to draw.

5. Conclusions

1. Limiting fragmentation hypothesis as formulated by Yang and co-workers is compatible with the present trend of data at the highest accelerator energies within ≈ 10% errors.

2. The Pomeron factorization seems to hold with the same accuracy at low momentum transfers. However for $-t > 0.5(GeV/c)^2$ pronounced breakdown in factorization is indicated between the elastic and inelastic diffraction cross sections.

3. The dramatic violation of scaling is firmly established in the central region. The accelerators of new generation with energies $\gtrsim 2$ TeV and with ISR's are very much needed to choose between two very important alternatives: the existence of asymptotic limit or unlimited rise of cross sections with energy.

4. There is a strong evidence that hadron-hadron reactions are dominated by resonance production. As a consequence the cluster and the short range order correlation effects may be to a large extent explained by resonance production.

Aknowledgements

The author is grateful to the organizing committee of the conference and to the scientific secretaries Drs. E.Kistenev, A.Likhoded, N.Melnikova and L.Tikhonova for their efficient help. He thanks in particular Dr.A.Likhoded for many useful discussions and suggestions.

It is a pleasure to aknowledge the help of Drs. L.Gerdyukov, O.Tchikilev and V.Uvarov in the compilation of data. The author would like to thank Mrs.G.Pavlovskay for efficient preparing of the drawings.

REFERENCES

1. A.A.Logunov, M.A.Mestvirishvili, Nguen Van Hieu, Phys.Letters 25B (1967) 611.
2. Yu.B.Bushnin et al, IHEP-CERN Collaboration, Phys.Letters 29B(1969) 506.
3. D.B.Smith, R.J.Sprafka, J.A.Anderson, Phys.Rev.Letters 23 (1969) 1064.
4. J.Benecke, T.T.Chan, C.N.Yang, E.Yen, Phys.Rev. 188 (1969) 2159.
5. R.P.Feynman, Phys.Rev.Letters 23 (1969)1415.
6. L.Foá, Physics Reports 22C (1975) N1.
7. K.Zalewski, Rapporteur's talk at the XVII-th International Conference on High Energy Physics, London (1974).
8. K.Böckmann, Rapporteur's talk at the Intern. Conf. on High Energy Physics, Palermo (1975).
9. N.A.McCubbin, Rapporteur's talk at the Intern. Conf. on High Energy Physics, Palermo (1975).
10. M.Boggild and T.Ferbel, Ann. Reviews of Nucl. Sci. 24 (1974).
11. J.Whitmore, Phys.Reports 10C (1974) 273.
12. V.V.Ammosov et al, IHEP Report M-26 (1976).
13. A.Sheng et al, Phys.Rev. D11 (1975) 17.
14. K.Yaeger et al, Phys.Rev. D11 (1975) 2405.
15. C.Cochet et al, France-USSR and CERN-USSR Collaboration, paper 1034 (A2-89).
16. J.Hanton et al, France-USSR, CERN-USSR Collaborations, paper 1035 (A2-90).
17. B.V.Batyunya et al, Alma-Ata-Dubna-Helsinki--Moscow-Prague-Kosice Collaboration, paper 159 (A2-11).
18. M.T.Regan et al, Liverpool-Stockholm Collaboration, paper 682 (A2-63).
19. P.S.Gregori et al, Liverpool-Stockholm Collaboration, paper 683 (A2-102).
20. N.S.Amaglobeli et al, Tbilisi-Dubna-Minsk Collaboration, paper 1078 (A2-122).
21. W.W.Neale, Invited talk at the Intern. Conference on High Energy Physics, Palermo (1975).
22. D.Bertrand et al, Brussels-CERN-London--Mons-Orsay Collaboration, paper 722(A2-67).
23. D.Bogert et al, FNAL-Florida Collaboration, paper 199(A2-33).
24. Yu.A.Budagov et al, Dubna-Tbilisi-Kosice--Erevan-Minsk Collaboration, paper 811(A2--82).
25. P.V.Chliapnikov et al, France-USSR, CERN--USSR Collaborations, paper 1167(A2-127).
26. P.V.Chliapnikov et al, Birmingham-Brussels--CERN-Mons Collaboration, paper 1060(A2-75).
27. H.G.Kirk et al, Aachen-Berlin-CERN-London--Vienna Collaboration, paper 695(A2-68).
28. B.Musgrave et al, Argonne-Brussels-Kansas--Michigan-Tufts Univ. Collaboration, paper 366(A2-59).
29. P.V.Chliapnikov, invited talk at the Intern. Conference on High Energy Physics, Palermo (1975).
30. A.Givernaud et al, France-USSR, CERN-USSR Collaborations, paper 1161(A1-10).
31. J.I.Arestov et al, France-USSR, CERN-USSR Collaborations, paper 207(A2-37).
32. R.Stroynowski, Rapporteur's talk at the VI Intern.Colloquium on Multiparticle Reactions, Oxford (1975).
33. T.Ferbel, Proceedings of the Summer Institute on Particle Physics, SLAS REPORT 179, v.II(1974),175.
34. J.Whitmore et al, Phys.Letters 60B(1976)211.
35. Chan Hong-Mo et al, Phys.Rev.Letters 26(1971)672.
36. H.I.Miettinen, Phys.Letters 38B(1972)431.
37. A.H.Mueller, Phys.Rev.D2(1970)2963.
38. O.V.Kancheli, JETP Letters 11(1970)397.
39. G.Ciapetti et al, Nucl.Phys. B89(1975)365.
40. R.Barloutaud, Invited talk at this conference.
41. E.W.Beier et al, Pennsylvania, paper 402(A2-58).
42. R.E.Hendrick et al, Phys.Rev. D11(1975)536.

43. R.K.Garnegie et al, SLAC, paper 289(A2-55).
44. W.Lockman et al, California-Saclay Collaboration, paper 1210 (A1-163).
45. J.Pumplin, Phys.Rev. D8(1973)2899.
46. A.A.Logunov et al, IHEP 74-66,Serpukhov (1974).
47. A.N.Tolstenkov, paper 791(A5-2).
48. P.V.Chliapnikov, IV Intern. Seminar on High Energy Physics Problems, Dubna(1975), 32.
49. P.V.Chliapnikov et al, Phys.Letters 60B (1976)218.
50. J.F.Gunion, Phys.Rev. D11(1975)1796; M.B.Green, M.Jacob, P.V.Landshoff, Nuovo Cimento 29A(1975)123.
51. A.K.Likhoded, A.N.Tolstenkov, IHEP 75-88 (1975) Serpukhov.
52. T.K.Gaisser, F.Halzen, Phys.Rev. D11 (1975)3157.
53. D.Silvers, ibid., 3253 and Nucl.Phys. B106 (1976)95.
54. A.M.Rossi et al, Nucl.Phys. B84(1975)269.
55. K.Blokzijl et al, Amsterdam-CERN-Nijmegen--Oxford Collaboration, paper 279(A2-78).
56. Amsterdam-CERN-Nijmegen-Oxford Collaboration, paper 276(A2-51).
57. Amsterdam-CERN-Nijmegen-Oxford Collaboration, paper 278(A2-52).
58. T.J.Devlin, paper 332(A2-57).
59. A.A.Logunov, L.D.Soloviev, A.N.Tavkhelidze, Phys.Letters 24B(1967)181; P.Freund, Phys.Rev.Letters 20(1968)235; H.Harary, Phys.Rev.Letters 20(1968)1395.
60. I.V.Ajinenko et al, Birmingham-Brussels--CERN-Mons-Serpukhov Collaboration, paper 200(A2-34).
61. K.Guettler et al, British-Scandinavian-MIT Collaboration, paper 114(A2-39).
62. K.Guettler et al, British-Scandinavian-MIT Collaboration, paper 1121(A2-113).
63. B.Apel et al, Nucl.Phys. B100(1975)237.
64. H.Cheng, T.T.Wu, Phys.Letters 45B(1973)367.
65. Chan Hong-Mo et al, Phys.Letters 40B(1972) 406.
66. M.N.Kobrinsky, A.K.Likhoded, A.N.Tolstenkov, Yad.Fiz. 20(1974)775; A.K.Likhoded, A.N.Tolstenkov, IHEP Preprint 74-51(1974).
67. R.Windmolders et al, Yad.Fiz. 22(1975)1014.
68. P.V.Chliapnikov et al, Nucl.Phys.B97(1975)1.
69. V.Blobel et al, Nucl.Phys. B69(1974)454.
70. T.Ferbel, Phys.Rev. D8(1973)2321.
71. V.V.Ezhela, A.A.Logunov, M.A.Mestvirishvili, IHEP 72-1(1971) Serpukhov.
72. P.V.Chliapnikov et al, Phys.Letters 52B (1974)375.
73. I.V.Ajinenko et al, IHEP Preprint M-30(1976) Serpukhov.
74. V.V.Babintsev et al, France-Soviet Union and CERN-Soviet Union Collaborations, paper 204 (A2-35).
75. T.Stewart et al, Durham-Lodz Collaboration, paper 194(A2-29).
76. S.N.Vernov et al, paper 778(A2-110).
77. V.P.Pavluchenko et al, paper 169(A2-2).
78. V.K.Budilov et al, "Pamir" Collaboration, paper 169(A2-1).
79. N.N.Roinishvili, minirapporteur's talk at this conference.
80. N.N.Biswas et al, Notre Dame-Duke Univ.--Toronto-McGill Univ. Collaboration, paper 1026(A2-87).
81. N.Angelov et al, Dubna 2 m Propane BC Collaboration, paper 868(A2-86)
82. R.E.Ansorge, Cambridge-Kraców-Warsaw and Davis-Kraców-Seattle-Warsaw Collaborations, paper 1003(A2-73).
83. J.Bartke et al, Aachen-Berlin-Bonn-CERN--Cracow-Heidelberg-Warsaw Collaboration, paper 196(A2-31).
84. V.V.Anisovich, V.M.Shekhter, Nucl.Phys.B55 (1973)455.
85. J.D.Bjorken, G.R.Farrar, Phys.Rev. D9(1974) 1449.
86. A.K.Likhoded et al, IHEP 76-2 Serpukhov (1976).

87. U.Gensch et al, France-USSR, CERN-USSR Collaborations, paper 206(A2-36).
88. M.De Beer et al, France-USSR, CERN-USSR Collaborations, paper 1168(A2-128).
89. V.V.Anisovich, M.N.Kobrinsky, V.I.Povsun, paper 85(A3-5).
90. D.Fong et al, Phys.Letters 60B(1975)124.
91. R.Singer et al, Phys.Letters 60B(1976)385.
92. P.V.Chliapnikov et al, Nucl.Phys. B37(1972) 336.
93. K.Paler et al, Nucl.Phys. B96(1975)1.
94. Aachen-Berlin-Bonn-CERN-Cracow-London--Vienna-Warsaw Collaboration, paper 663 (A2-105).
95. M.Deutschmann et al, Nucl.Phys.B103(1976)426
96. Aachen-Berlin-Bonn-CERN-Cracow-Heidelberg--Warsaw Collaboration, paper 664(A2-104).
97. Aachen-Berlin-Bonn-CERN-Cracow-London--Vienna-Warsaw Collaboration, paper 186 (A2-27).
98. V.Blobel et al, Phys.Letters 48B(1974)73; Nucl.Phys. B69(1974)237; Preprint Bonn HE 76-9(1976).
99. J.C.M.Armitage et al, CHM Collaboration, paper 347(A2-72).
100. F.W.Büsser et al, Phys.Letters 55B(1975)232
101. V.Blobel et al, Phys.Letters 59B (1975)88.
102. Yu.M.Antipov et al, IHEP 76-42 Serpukhov (1976).
103. V.Matveev, R.Muradyan, A.Tavkhelidze, Lett.Nuovo Cimento 7(1973)719.
104. M.L.Mallary et al, Northeastern Univ., paper 138(N1-18).
105. R.A.Donald et al, Phys.Letters 61B(1976)210
106. Rutherford-Ecole Polytechnique-Saclay Collaboration, paper 71(A1-70).
107. R.Baldi et al, Geneva Univ., paper 728 (A1-135).
108. V.G.Kartvelishvili et al, paper 631(N3-14)
109. S.D.Ellis, M.B.Einhorn, C.Quigg, paper 953 (N3-35).
110. D.Brick et al, 30-inch-bubble chamber--proportional-wire-chamber hybrid spectrometer Collaboration, paper 1050 (A2-88).
111. Aachen-Berlin-Bonn-CERN-Cracow-Heidelberg--London-Vienna-Warsaw Collaboration, paper 198(A2-32).
112. W.Lockman et al, Univ.California-Aachen--CERN Collaboration, paper 1201(A2-108).
113. M.Bardadin-Otwinowska et al, Nucl.Phys.B72 (1974)1.
114. P.V.Chliapnikov et al, Nucl.Phys. B91 (1975)413; Phys.Letters 55B(1975)237.
115. H.Voorthuis et al, Amsterdam-CERN-Nijmegen--Oxford Collaboration, paper 277(C3-24).
116. W.J.Robertson et al, Phys.Rev.D7(1973)2554.
117. J.Hanlon et al, FERMILAB-PUB-76/28-EXP (1976).
118. M.Bardadin-Otwinowska et al, paper submitted to the International Conf. on Elementary Particles, Palermo (Italy)1975.
119. P.V.Chliapnikov et al, Nucl.Phys. B105 (1976)510.
120. Aachen-Berlin-CERN-London-Vienna Collaboration, paper 144(A2-111).
121. M.Bardadin-Otwinowska et al, Nucl.Phys. B98(1975)418.
122. P.Gizbert-Studnicki, A.Golemo, Lett.al Nuovo Cimento IV(1970)473.
123. Amsterdam-CERN-Nijmegen-Oxford Collaboration, paper 272(A2-50).
124. H.Abramowicz et al, Nucl.Phys.B105(1976) 222.
125. D.Denegri et al, Saclay-Ecole Polytechnique -Rutherford Collaboration, paper 73(A1-72).
126. V.P.Kenney et al, Notre Dame-Durham-Canada--Iowa-Maryland-Michigan Collaboration, paper 1023(A2-103).
127. C.B.Chiu, K.-H.Wang, papers 357(A3-24) and 358(A3-25).
128. A.M.Gershkovich, I.M.Dremin, Reports on Physics, FIAN N1(1976)1.
129. P.Darriulat, Rapporteur's talk at the VI Intern. Colloquim on Multiparticle Reactions, Oxford(1975).

130. G.Borreani et al, Torino, paper 112(A2-66).
131. A.Quareni-Vigundelli et al, Bologna-Firenze-Genova-Milano-Oxford-Pavia Collaboration, paper 1202(A2-117).
132. Alma-Ata-Bucharest-Budapest-Cracow-Dubna-Hanoi-Moscow-Sofia-Tashkent-Tbilisi--Ulan Bator-Warsaw Collaboration, Phys. Letters 48B(1974)277; G.Ranft et al, Nucl.Phys. B86(1975)63.
133. G.Bromberg et al, Phys.Rev. D9(1974)3100.
134. N.Angelov et al, Dubna-Moscow-Tbilisi Collaboration, paper 205 (A2-6)
135. Aachen-Barlin-Bonn-CERN-Cracow-Heidelberg--Warsaw Collaboration, paper 1070(C2-53).
136. G.Goldhaber, S.Goldhaber, W.Lee, A.Pais. Phys.Rev.120(1960)300.
137. N.N.Biswas et al, Notre Dame-Duke Univ.--Toronto-Monreal Collaboration paper 1022 (A2-107).
138. G.I.Kopylov and M.I.Podgoretsky, Yad.Phys. 15(1972)392; 18(1973)656; 19(1974)434; G.I.Kopylov, Phys.Letters 50B(1974)472.
139. E.V.Shuryak, Phys.Letters 44B(1973)387.
140. G.Cocconi, Phys.Letters 49B(1974)459.
141. F.Grard et al, Nucl.Phys. B102(1976)221.
142. M.Deutschmann et al, Nucl.Phys.B103(1976) 198 and paper 197(A2-24).
143. J.Canter et al, Preprint BNL-20516(1975).
144. Y.D.Bayukov et al, Preprint ITEP(1976) Moscow.
145. N.Angelov et al, Dubna-Moscow-Tbilisi Collaboration, paper 205(A2-106).
146. V.V.Filippova et al, Alma Ata-Dubna--Helsinki-Kosice-Moscow-Prague Collaboration, paper 160(A2-10).
147. A.Calligarich et al, Pavia-Bologna-Firenze--Genova-Milano-Oxford Collaboration, paper 1090(A2-114).
148. G.I.Kopylov and M.I.Podgoretsky, paper 1007(A2-120).
149. V.G.Grishin, V.I.Ogievetski, Nucl.Phys.18 (1960)516.
150. M.I.Shirokov, JETP 42(1962)173.
151. A.A.Logunov, Nguen Van Hieu, Theor.Mat. Phys. 1(1969)375.
152. B.R.Webber, Phys.Letters 49B(1974)474.
153. H.Braun et al, Strasbourg, paper 377 (A2-109).
154. B.R.Webber, D.M.Chew, M.J.Counihan, H.Yuta, Nucl.Phys. B97(1975)317.
155. G.Warren et al, Nucl.Phys.B97(1975)381.
156. M.J.Counihan, Phys.Letters 59B(1975)367.
157. I.V.Ajinenko et al, France-USSR and CERN-USSR Collaborations, paper 1162 (A1-49).
158. J.Saudraix et al, France-USSR and CERN-USSR Collaborations, paper 1165 (A1-120).

PARALLEL SESSION ON MECHANISMS OF MULTI-PARTICLE PRODUCTION PROCESSES

STATISTICAL AND HYDRODYNAMICAL THEORIES OF MULTIPLE PRODUCTION

E.V.Shuryak

Institute of Nuclear Physics, Novosibirsk, USSR

The applications of statistical methods-thermo-[1] and hydrodynamics[2] to multiple production of hadrons already at fifties become rather developed theory[3-8]. Recently this approach causes new wave of interest when it was realized[6-9] that data from large acoelerators are in agreement with them (see also reviews[10-13]). The aim of this report is to review its recent applications to hadron-hadron collisions. Other interesting topics: low energy reactions like e^+e^- and $p\bar{p}$ annihilation; collisions with nuolei; principal questions of statistical theory, statistical bootstrap, etc., - are not discussed because of the lack of time.

According to this theory inelastic collision passes three stages: a) <u>initial</u>, at which system is mixed and excited; b) <u>hydrodynamical</u>, at which isoentropy expansion takes place; c) <u>final</u>, at whioh real seoondaries are formed. Our discussion proceed backwards, from c) to a), from more to less clear phenomena.

<u>Final stage</u>, as was noted by Pomeranchuk[1], corresponds to low temperature $T \sim m_\pi$. The hadronic matter is similar to ideal gas, so calculations are simple. The main conclusions are 1) for all kinds of particles $p_\perp$ distribution is thermal; $\frac{d\mathcal{E}}{dp_\perp^2} \sim \exp\left(-\frac{M_\perp}{T}\right)$; $M_\perp^2 = p_\perp^2 + m^2$. Data support this for π, K, $\bar{p}$[14,15], ρ, ψ[16], 2) the composition of partioles can be calculated, the data agree with them for $K, \bar{p}$[14,15] $\bar{d}$, $\overline{He_3}$[14], etc.

From this one can conclude that at final stage thermodynamical equilibrium really takes place. This conclusion may have separate meaning, for example as an addition to parton model, which does not discuss final state interaction.

<u>At hydrodynamical stage</u> motion is determined by local energy-momentum conservation $\frac{\partial T^{ik}}{\partial x^k} = 0$; $T_{ik} = (\mathcal{E}+p) u_i u_k - g_{ik} p$; p-pressure; $\mathcal{E}$ - energy density; u_i - 4-velocity. One needs only to determine equation of state, which usually is taken as $p = c^2 \mathcal{E}$[4] with $c^2 = \text{const}$. Landau choosed $c^2 = \frac{1}{3}$, as for ideal gas. The account for interaction by Beth-Uhlenbeck method gives $c^2 = c_1 2$[15]. According to[15] this method can only be used for $T \lesssim 1$ GeV, but in[16] an attempt is made to use it for $T \gg 1$ GeV, the result is again $c^2 = 0.2$. Quite other conclusion $\mathcal{E} \sim T^2$ or $c = 1$ is made in[17] on the basis of degenerate quark gas model. But in quark-antiquark mixture chemical potential $\mu = 0$ and Fermi-degeneracy is not possible, so the true result is $c^2 = 1/3$.

The solution of equations gives explicit form of inclusive spectrum. Various authors account for the following effects;

	4a	4b	6	7	8	9	17
1. Non one-dimensional corrections	+	-	+	-	+	-	+
2. Arbitrary	-	+	+	-	-	+	+
3. Thermal motion	+	+	+	-	-	+	+
4. Leading partioles	-	-	-	-	-	-	+

The theoretical accuracy is not better than 20-30%.

Results do not differ much and their conclusions are:

1) Central region grows with energy, violating scaling. This result is essentially confirmed by new data[18] according to which π^- spectrum grows to 41±2% in ISR energy region.

2) The shape of spectrum in central region is approximately gaussian; $\frac{d\mathcal{E}}{dy} \sim \exp\left(-\frac{y^2}{2L}\right)$. This prediction is in good agreement with all data below ISR energy; but in this energy region the situation is not yet clear for data are not very consistent, see Fig. 1[17].

Dependence of the parameter L (gaussian width) on energy is shown in Fig. 2[13].

Note, that L_π and L_K, $L_{\bar{p}}$ differs in energy independent constant caused by different thermal velocities.

3) At finite X spectrum deviates from scaling very little and slowly decreases[7,9,19], see Fig. 3[9].

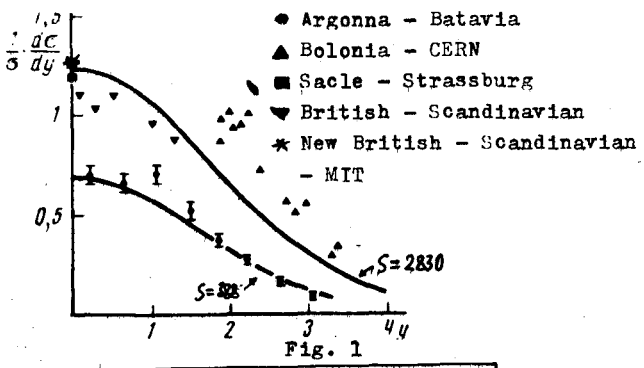


Fig. 1

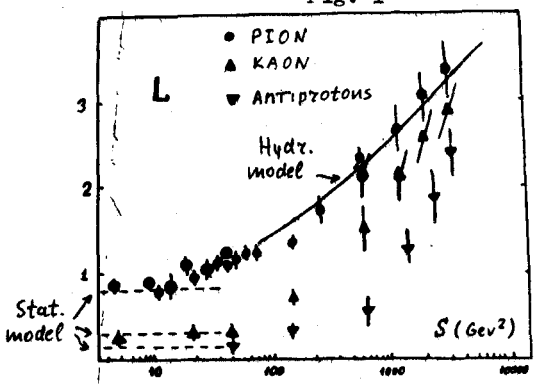


Fig. 2

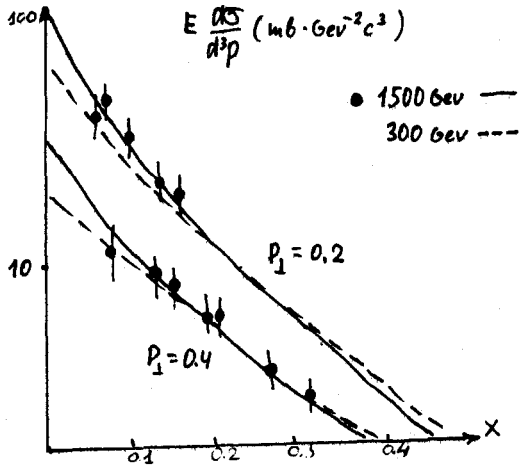


Fig. 3

4) Transverse motion leads to some growth of the average $p_\perp$ with energy as $s^{1/14}$/4/. In/20/ close estimates $s^{1/12}$ are obtained, but the wrong conclusion (due to misprint) is made that it oontradicts to data. In fact, the agreement is very reasonable, see Fig. 4.

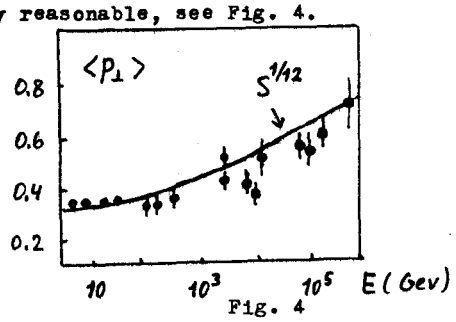


Fig. 4

We know very little about the initial stage. The conclusions above are based on Fermi-Landau initial conditions with zero collective velocity. If the initial rapidity distribution is flat, as in parton model, than this scaling solution satisfies also the hydrodynamical equations. This fact, known already by Landau, has been rediscovered recently/96,21/. Spectra are not sensitive to initial conditions, which are not therefore easy to study.

More direct investigations of the initial state is connected with large $p_\perp$ phenomena. In/15,22-24/ it is proposed to explain them by the evaporation at stage when temperature is higher than final one. In/15/ heavy particle growth is connected with this; in/23/ energy dependence of large $p_\perp$ spectra are fitted and the parameter of the equation of state c^2 = = 0.20±0.01 is found. In/24/ the evaporation during the expansion is considered which leads to a different parametrization. In/25/ the same mechanism is applied for the explanation of "cumulative" meson production on nuclei/26/. It is not yet clear in what $p_\perp$ region this mechanism is essential, probably 1÷3 GeV/c, while at higher $p_\perp$ "hard" collisions dominate. But we may in any case conclude, that the probability of such evaporation is small. In this connection direct photon and lepton productions/27/ are of particular interest, for they can go out from the system freely.

Let us discuss briefly the weak points of this theory. Some arguments against it are 1) there exist leading particles, which are not mixed at initial stage; 2) Data on deep inelastic lepton scattering reveal pointlike constituents (quarks), which hardly can be "stopped" in the collision. 3) Strong nonstatistioal fluotuations are observed. For example, relative multiplicity dispersion $\mathcal{D}/\langle n\rangle$ does not decrease with $\langle n\rangle$, but remains constant. The possible answer/28/ is that valent quarks indeed "go through" and form leading particles, while neutral glue (carrying

another half of the total momentum) interact and form multibody system, which can be described by this theory. The nonstatistical fluctuations are then caused by the leading particles. Very nice multiplicity distribution was found in such model[17].

The other important question is: Why the evaporation is so small? Landau's answer is that particles are closed in by strong interaction. If so, why equation of state is similar to that of ideal gas? Possible answer is that colored objects are confined, while inside the "bag" (29) they are almost free. Another explanation is that Fermi-Landau initial conditions do not exist at all, and hydrodynamical equations become valid at larger time and space values. It may be caused by quantum effects[30], viscosity[5], "parton like" initial conditions[21], etc.

Finally, the applicability condition of thermo- and hydrodynamics is not still clear. In[31--33] attempts are made to connect kinetic equations with field theory, but much more work in this direction is needed to reach final conclusions.

In conclusion of the report I may say, that predictions of hydrodynamical theory, and among them those made more then 20 years ago, are in good agreement with data. In the same time, its main assumptions still have no firm theoretical ground.

References

1. E.Fermi. Progress Theor. Phys., 5, 570 (1950); I.Ya.Pomeranchuk. Doklady Akad. Nauk., 78, 889 (1951).
2. L.D.Landau. Izv.Akad.Nauk, ser. fiz., 17, 51 (1953); S.Z.Belenky, L.D.Landau. Usp. Fiz. Nauk., 56, 309 (1955).
3. I.L.Rosental, D.S.Chernavsky. Usp. Fiz. Nauk, 52, 185 (1954).
4. G.A.Mileckin JETP, 35, 1185 (1958); Proc. of Int. Conf. on Cosmic Rays, Moscow, 1, 220 (1966).
5. E.L.Feinberg. Trudy FIAN, 29, 155 (1965).
6. E.V.Shuryak. Multiple Production in High Energy Collisions. Preprint, Novosibirsk, 1971; Sov. J. of Nucl.Phys., 16, 395 (1972).
7. P.N.Carruthers, Minh Duong-van. Phys.Lett., 42B, 597 (1972).
8. E.N.Daibog, Yu.P.Nikitin, I.L.Rosental. Sov. J.Nucl.Phys., 16, 1314 (1972).
9. F.Cooper, B.Schonberg. Phys.Rev.Lett., 30, 880 (1973).
1 F.Cooper, G.Frye. Phys.Rev., D10, 186 (1974).
10. E.L.Feinberg. Statistical and Hydrodynamical Models of Multiple Production. Preprint of Lebedev Phys.Inst., Moscow, 1973.
11. I.L.Rosental. Usp. Fiz. Nauk, 116, 271 (1975).
12. F.Cooper. Landau's Hydrodynamical Model of Particle Production. Preprint 74-1346, Los-Alamos, 1974.
13. E.V.Shuryak. High Energy Multiple Production of Hadrons and Landau Hydrodynamical Theory. Preprint, Novosibirsk, 1-75, 1975.
14. I.N.Sissakian, E.L.Feinberg, D.S.Chernavsky. JETP, 52, 545 (1967). E.L.Feinberg. Usp. Fiz.Nauk, 114, 539 (1971); Phys.Rep., 56, 1972.
15. E.V.Shuryak. Final State Interaction and Composition of Secondaries. Novosibirsk, 1973; Sov. J. of Nucl.Phys., 20, 549 (1974).
16. T.F.Hoang. Phys.Rev., 13D, 1881 (1976).
17. O.V.Zhirov, E.V.Shuryak. Sov. J.Nucl.Phys., 21, 861 (1975).
18. L.L.Enkowsky, A.A.Trushevsky. Rep. 90/A3-10; A.T.Bugrij, A.A.Trushevsky. Rep. 89/A3-9.
19. E.I.Daibog, Yu.R.Nikitin, I.L.Rosental. Izv.Akad.Nauk, ser. fiz., 37, 1396 (1973).
20. M.Shaichain, M.Satz, E.Suhonen. Phys.Lett., 50B, 362 (1974); Rep. 927/A3-40.
21. C.B.Chiu, E.C.G.Sadarshan, K.M.Wang. Phys. Rev., 12D, 902 (1975).
22. J.J.Dumont, L.Heiko. Univ. of Brussels. Preprint IIME-74.1.
23. M.I.Gorenstein, V.P.Shelest, G.M.Zinoviev. Phys.Lett., 60B, 203 (1976), Rep. 610/A3-76.
24. C.B.Chiu, Kuo-Hsing Wang. Phys.Rev., 12D, 2725 (1975), Rep. 355/A3-23.
25. E.V.Shuryak. Rep. 97/A3-17.
26. A.M.Baldin et al. Sov. J.Nucl.Phys., 20, 1201 (1974).
27. E.L.Feinberg. Izv. Akad.Nauk, ser. fiz., 26, 622 (1962), 34, 1987 (1970); Preprint TH-2156, CERN (1976).
28. S.Pokorski, L. van Hove. Acta Phys.Polon., B5, 229 (1974). Nucl.Phys., B86, 243 (1975).
29. A.Chodos et al. Phys.Rev., D9, 3471 (1974).
30. J.Nowakowski, F.Cooper. Phys.Rev., D9, 771 (1974).
31. P.Carruthers, F.Zachariaren. Part. and Field. Proc. of Willansbaurg Meeting of American Phys.Soc., 1975.

32. F.Cooper, D.H.Sharp. Phys.Rev., D12, 1123 (1975).
33. V.Canuto, I.Lodenguai, P.Olesen. Nordita Prepr., 1975.

RECENT DEVELOPMENTS IN MULTIPERIPHERAL MODELS

Carleton De Tar

Laboratory for Nuclear Science and Physics Department, Massachusetts Institute of Technology, Cambridge, Massachustts 02139, USA

1. Introduction

Once we have agreed that multiperipheral models do a reasonably good job, as far as models of high energy interactions go, in accounting for the broad features of hadronic multiple production in the region of small transverse momenta, the basic residual problem still remains; experiments do not provide and, practically speaking, cannot provide all of the detailed information required in order to select out of the myriad of possible formulations of the multiperipheral model[1-5], the correct ones. Allow me for the purposes of this talk to refer to this as the "uniqueness problem".

There are at least three directions which lead us away from this uniqueness problem. The first is at the phenomenological end - one constructs over-simplified models with only enough complexity so as to satisfy the data approximately. Thus a model of particle production with simple Lorentz-invariant longitudinal phase space (independent emission model) can be used to account for the observed approximate scaling and approximate central plateau in inclusive reactions. Such a model does not account for two-particle correlations, but a model in the same spirit has replaced it which does, namely the independent cluster emission model[6]. In keeping with the effort to avoid cluttering models with details that are not uniquely constrained by experiment is the search for measurable quantities which provide more nearly direct tests of the production mechanism, for example, the two-particle correlation function, the "charge transfer" between production hemispheres[7] and more recently the rapidity gap distribution[8] and the fluctuation measure of Slansky[9].

The second effort to avoid the uniqueness problem involves invoking theoretical constraints which limit the theoretical flexibility of the model. For example it is useful to impose constraints of unitarity on production amplitudes[4,10,11]. The topological expansion and related approaches[12-14] seek to draw together a unified description of the strong interactions and thereby to limit the choice of production mechanisms.

The third and ultimate solution may someday be provided by the quark-gluon models or string models. Having an explicit and constructive model of the strong interactions would undoubtedly answer many of the questions of multiple production.

2. How Big are Clusters?

The recent interest in the role of clusters in multiple production is a good illustration of the phenomenological problems facing multiperipheral models. Experimental measurements of short-range correlations in two-particle inclusive reactions[15] inspired efforts at accounting for them through the notion that produced particles are emitted in clusters[6,7,16]. The meaning of cluster depends, of course, on the model in question. Clusters can be incorporated into more elaborate description of multiple production[3-5]. This is necessary when discussing specific exclusive processes. However, I shall confine my attention to the cruder, but much simpler, independent cluster, emission models[6,8] and the broad question of how large clusters must be in this model. This is important since if most events have only two or three clusters, one wonders whether the multiperipheral model has much to do with the emitted hadrons.

A good example of an independent cluster emission model is that of Berger and Fox[5]. It has the following ingredients:

(a) The clusters are produced uniformly in rapidity according to a Poisson multiplicity distribution.

(b) The clusters decay isotropically in their rest frames with a Gaussian dependence on momentum.

(c) The multiplicity distribution of particles in the cluster is constant up to a maximum number and then zero for higher numbers.

(d) Some effort is made to take diffractive production into account.

They fit data on particle multiplcities and single and two-particle inclusive rapidity distributions above 50 GeV/c and conclude that an average per cluster of four pions of all charges is called for. Other analyses give similar results[6,17].

Recently there has been an interesting discussion about the significance of these results. The question was raised whether it is possible to determine the existence and size of clusters in the data independently of extraneous assumptions, such as whether the number of clusters obeys a Poisson distribution or that many clusters are produced in the central region. To make this point is a vivid way, suppose we assume that each cluster decays into exactly K_{ch} charged particles, no more, no fewer. Then if the number of clusters obeys a Poisson distribution, the value of K_{ch} is rigorously determined by fitting the overall charged particle multiplicity distribution. A value K_{ch} of about 2 works fairly well. One might expect that some vestige this undesirable effect would remain if the cluster decay were made to be somewhat more flexible.

If clusters are really present, we should be able to tell from the particle production spectra. If the particles show distinct non-random groupings in rapidity event by event there would be no debate about their existence or size. Unfortunately, they don't, at least in the non-diffractive component, and so one seeks some statistical measure of clustering. The most

traditional measure of clustering is the two-particle correlation function, defined in terms of the one-particle and two-particle inclusive cross sections as

$$C(y_1, y_2) = \frac{1}{\sigma} \frac{d^2\sigma}{dy_1 dy_2} - \frac{1}{\sigma^2} \frac{d\sigma}{dy_1} \frac{d\sigma}{dy_2} \quad (1)$$

In the independent cluster emission model[6] the correlation function in the central region has the form

$$C(y_1, y_2) = \frac{\langle K(K-1)\rangle}{\langle K\rangle} \cdot \left(\frac{1}{\sigma} \frac{d\sigma}{dy}\right)_{y\simeq 0} \cdot G(y_1 - y_2), \quad (2)$$

where G is a gaussian distribution normalized to unity and K is the number of particles emitted in a single cluster decay. The averages $\langle K\rangle$ and $\langle K(K-1)\rangle$ are taken with respect to the single cluster decay distribution. This form for $C(y_1, y_2)$ has been used[7] to determine $\langle K_{ch}\rangle \simeq 2{,}5$. The expression (2) is based on the assumption that a large number of clusters are produced uniformly in the central region. It does not apply to diffractive events in a straightforward fashion.

Morel and Plaut and Berger[14] have proposed avoiding complications due to diffraction by using the semi-inclusive data instead. They argue that higher multiplicity events are less apt to be diffractive. They derive formulae similar to (2) for the semi-inclusive function $C_n(y_1, y_2)$, which were adapted to a phenomenological analysis of ISR data by Eggert et al. and S.R.Amendolia et al.[17] with the result that $\langle K_{ch}\rangle = 2.2 \pm 0.2$ and 2.0 ± 0.1 respectively.

Assuming that many clusters are produced in the central region may be begging the question about the size of the clusters, however. What if only three or four clusters are produced? With proper constraints of energy and momentum conservation included, would Eq. (2) still be reliable? In an effort to free themselves from extraneous assumptions about cluster production, Ludlam and Slansky[9] have proposed a statistical measure of fluctuation which is to be applied to events with a fixed number of observed particles n. The particle rapidities are measured. A quantity $n_L(y) - n_R(y)$ is defined which gives the difference between the number of particles with rapidities to the left of y and to the right of y. The left-right fluctuation density is then defined as

$$K_n = \frac{3}{2n} \int dy \cdot p(y) \left\{ \langle [n_L(y) - n_R(y)]^2 \rangle - \langle [n_L(y) - n_R(y)] \rangle^2 \right\} \quad (3)$$

where $p(y)$ is the semi-inclusive cross section $\frac{d\sigma_n(y)}{dy}$ normalized to unit area. If particle emission is independent, but weighted according to $p(y)$, then $K_n = 1$. However, energy and momentum conservation introduces kinematical correlations which cause deviations from randomness. Ludlam and Slansky use a model which does not begin with a Poisson distribution in the number of clusters, and which emphasizes energy momentum conservation. A comparison of their results with experimental measurements of K_n at 205 and 303 GeV/c pp collisions shows that an average of at least 4 charged particles per cluster is called for (see Fig. 1) or a total of 6 including neutrals. Thus they would conclude that there are only two clusters on average at Fermilab energies.

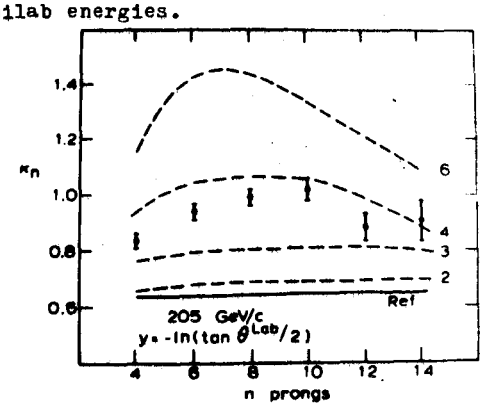


Fig. 1. Figure from Ludlam et al. Ref.[20]. Average fluctuation measure vs. number of charged particles in an event in pp collisions at 205 GeV/c. Dashed curves are calculated using an independent cluster emission model for an average of 6, 4 and 2 charged particles per cluster. The solid curve marked "Ref." is for independent emission (no clustering). Error bars on data points are statistical.

Another recently proposed measure relating to cluster size in the independent cluster emission model is the rapidity gap distribu-

tion[8]. Quigg, Pirilä, and Thomas fit the probability $P(\tau)$ in Fermilab data of finding a gap of length τ in rapidity with a model in which clusters have an average of two charged particles per cluster. However Ludlam et al. claim that this measure is not very sensitive to cluster size. They fit the 200 GeV data with their model and a cluster size of up to 6 hadron of all charges per cluster, i.e., 4 charged hadrons[20] (see Fig. 2).

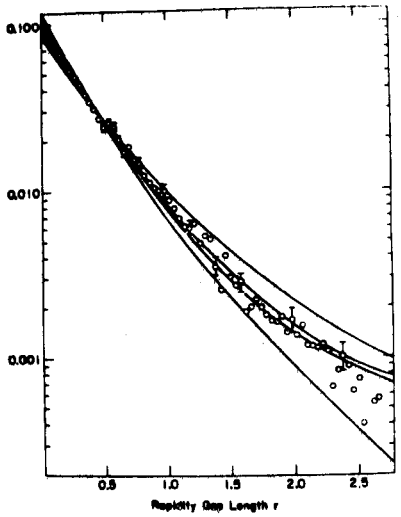


Fig. 2. Figure from Ludlam and Slansky, Ref.[9]. Distribution of rapidity gaps vs. gap interval. Data from the ANL-Fermilab-Stony Brook collaboration (205 GeV/c). The solid curves are calculated from an independent cluster emission model with 1, 3.2, 6.0 and 8.0 particles (including neutrals) per cluster, in order of increasing steepness of the model curves.

Arneodo and Plaut[30] claim that the results of Ludlam and Slansky change if a leading particle is introduced explicitly and conclude that clusters are smaller.

Thus the existence of clusters is certainly agreed upon, but if we want to determine their size directly from rapidity distributions, the result so far depends on what one assumes about how they are produced. Clearly there is a uniqueness problem here that need to be settled.

3. The Topological Expansion

Theoretical work toward a unified picture of strong interactions has also led to some novel developments in multiperipheral models and Regge pole theory. Some years ago Veneziano[21] proposed a topological expansion for scattering amplitudes based on duality diagrams[22,23] which were associated with amplitudes that satisfied some duality feature. This idea has been taken up by several authors[12-14] and applied to a multiperipheral approach to particle production. In the hands of Chew and Rosenzweig[12] one is asked to imagine a lowest order planar S-matrix with properties that were inspired by the dual resonance model in the three approximation:

(a) Regge poles are present in exchange degenerate families but no Regge cuts or Pomeron.

(b) Resonances of finite width are present and they are dual to the Regge poles.

These features are postulated, although we are urged to believe they could be derived rigorously from a well-defined set of bootstrap equations called planar S-matrix theory, which differs from ordinary S-matrix theory in that certain contributions to unitarity are excluded. Each successive correction to planar unitarity is to be obtained by relaxing step-by-step the restrictions on unitary. The key application to the multiperipheral model appears in generating the cylinder in the four-body amplitude from the unitarity sum over twisted planar graphs[21,24,25]. At this level one sees[26,27]

(a) Breaking of exchange degeneracy

(b) Violation of the Iizuka-Okubo-Zweig rule[28].

Indeed in the $I=0$ channel exchange degeneracy is broken in a rather remarkable way. The planar f-meson trajectory is elevated and the planar ω-trajectory is lowered with respect to the ρ-trajectory. But in the most straightforward analysis there is only <u>one</u> high lying vacuum trajectory[29]. This contradicts the traditional wisdom that two trajectories are needed[22,31]. Iterations to higher order in-

volving the two-pomeron cut might well suffice to split the vacuum singularity.

What is most striking about the approach of Stevens, Chew and Rosenzweig[27] is that they propose as a consequence a major reassessment of the traditional view of the vacuum channel. First they note that at energies up to 30 GeV/c, total cross sections can be fit quite well with only one vacuum trajectory[32]. In Fig. 3 their fit is reproduced with $\alpha_{f-p} = 0.96$ and with $\alpha_{f'} = 0.31$. But, one naturally asks, what about at Serpukhov, NAL and ISR energies? Their second observation answers this and appears to be very anti-Regge pole. They note that as more massive quark degrees

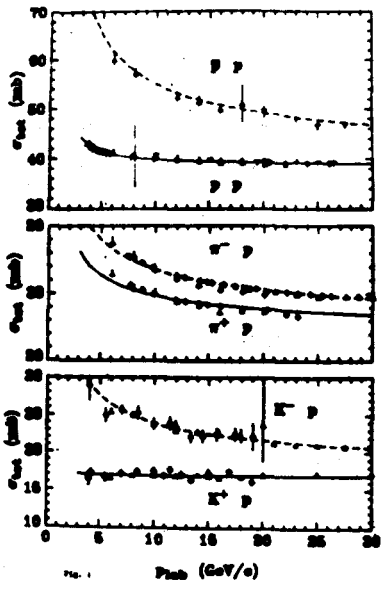


Fig. 3. Figure from Chew, Rosenzweig, and Stevens, Ref.[27]. Regge pole fit to total cross sections in a model with the f and P trajectories equated. Intercepts are $\alpha_{f-p} = 0.96$, $\alpha_{f'} = 0.31$. Data from ten sources, cited in Ref.[27].

of freedom are excited, including baryon production, one might expect threshold effects to keep the cross section from falling[30]. This was the same mechanism that was invoked a few years ago in an attempt to explain the rising total pp cross section at the ISR[33], not without some criticism[34]. In the multiperipheral model these thresholds generate complex poles in the J-plane, which are associated with oscillating cross sections. No oscillations have yet been observed, though perhaps we are seeing only the upswing so far. But traditional Regge phenomenologists may find it frustrating to have to deal with a set of poles which must be repositioned depending on the energy range which is to be fit. Perhaps they would be satisfied if future work in this field provides a well defined prescription for what they should use at what energy.

The identification of the Pomeron and f has been criticized by Quigg and Rabinovici[35] who find that a two-pole fit works very well at energies from 6 to 300 GeV. They remind us that the combination of cross sections

$$L = 2(\epsilon_{K^+p} + \epsilon_{K^-p}) - (\epsilon_{\pi^+p} + \epsilon_{\pi^-p})$$

in the quark language is the total cross section for ϕN scattering with ϕ ideally mixed, so should have only pomeron exchange in the Harari-Rosner scheme[22]. The combination L is nicely fit to the pure power law $s^{\alpha-1}$ with $\alpha = 1.0755$. The single vacuum trajectory model of Chew and Rosenzweig taken literally predicts a slow decrease at energies below 30 GeV/c, an indication of a systematic error in their fit; but they and Stevens argue that the quantity L is most sensitive to the opening of thresholds for strange particles[27]. In their model

$$L \sim \sin\theta^+ \cdot s^{\alpha_f - 1}$$

where θ^+ is also s-dependent and rises from 0 to 20° after strangeness is excited.

Thus we are asked to choose between the more traditional Harari-Freund picture of two vacuum singularities or the more novel approach of Chew and collaborators which makes a genuine effort to deal not merely with four-body amplitudes, but in a more profound way, with multiple production processes which are related to them through unitarity. Perhaps it would not be such a great loss to see some of our traditional prejudices reorganized, if in exchange we obtained a more unified understanding of the strong interactions.

Informative discussions with R.Slansky and J.Dash are gratefully acknowledged.

REFERENCES

1. Chan Hong-Mo, J.Łoskiewicz, and W.W.M.Allison, Nuovo Cimento, 57A, 93 (1968).
2. K.G.Boreskov, A.B.Kaidalov, L.A.Ponomarev. Yad.Fiz., 17, 1285 (1972), (Sov.J.Nucl. Phys., 17, 669 (1973)); ITEP preprint No. 92 (1973) and references cited therein.
3. E.M.Levin, M.G.Ryskin. Leningrad preprint 76-225 (1976) and references cited therein.
4. E.I.Volkov, I.M.Dremin, A.M.Dunaevskii, I.I.Royzen, and D.S.Chernavskii. Yad.Fiz., 20, 149 (1974) (Sov. J.Nucl.Phys., 20, 78 (1975)) and references cited therein.
5. I.F.Ginzburg and L.I.Perlovsky. Novosibirsk preprint TP-84 (1975).
6. For a reasonably complete list of references to the independent cluster emission model, see Berger, Ref./19/ and Dremin and Dunaevskii, Ref./11/.
7. See, for example, the discussion by K.Zalewski in Proc. XVII Conf. on High Energy Physics, London, 1974, ed. J.R.Smith (Rutherford Laboratory, Chilton, England, 1974), p. 1-93.
8. C.Quigg, P.Pirilä, and G.H.Thomas. Phys. Rev.Lett., 34, 290 (1975). P.Pirilä and G.H.Thomas. Phys.Rev., D11, 2532 (1975); Nucl.Phys., B86, 526 (1975). A.Krzywicki, G.H.Thomas, and C.Quigg. Phys.Lett., 57B, 369 (1975). D.R.Snider. Phys.Rev., D11, 140 (1975).
9. T.Ludlam and R.Slansky. Phys.Rev., D12, 65 (1975); Phys.Rev., D12, 59 (1975); Phys. Rev.Lett., 35, 127 (1975).
10. G.F.Chew and A.Pignotti. Phys.Rev., 176, 2112 (1968).
11. I.M.Dremin and A.M.Dunaevskii. Phys.Rep., C18, 159 (1975).
12. G.F.Chew and C.Rosenzweig. Phys.Lett., 58B, 93 (1975); Phys.Rev., D12, 3907 (1975). C.Rosenzweig, in VIth Int. Colloquium on Multiparticle Reactions, Oxford, 1975. Rutherford Laboratory report RL 75-143, p. 475.
13. P.Aurenche, Ng Sing Wai, J.E.Paton, Tsou Sheung Tsun, Chan Hong-Mo, A.Gula, T.Inami, and R.G.Roberts. Rutherford preprint RL-75-084 (1975) and references therein.
14. C.Schmid and C.Sorensen. Nucl.Phys., B96, 209 (1975). C.Schmid, in Proc. VIth Int. Colloquium on Multiparticle Reactions, Oxford, July 1975, ed. Chan Hong-Mo, R.Phillips, and R.Roberts. Rutherford report RL-75-143, p. 509.
15. H.Dibon et al. Phys.Lett., 44B, 313 (1973). S.R.Amendolia et al., Phys.Lett., 48B, 359 (1974).
16. W.Ko, p. 1-73, and G.Thomas, p. 1-83, in Proceedings cited in Ref./7/. P.Darriulat, p. 1, in Proceedings cited in Ref./14/.
17. K.Eggert et al. Aachen-CERN-Heidelberg-Munich Collaboration. Nucl.Phys., B86, 201 (1975). S.R.Amendolia et al. (Pisa-Stony Brook Collaboration), Nuovo Cimento, 31A, 17 (1976).
18. R.Slansky. Phys.Rep., 11C, 99 (1974).
19. E.L.Berger. Nucl.Phys., B85, 61 (1975). See also A.Morel and G.Plaut. Nucl.Phys., B78, 541 (1974).
20. T.Ludlam, R.Slansky, J.Slaughter, F.T.Dao, J.Lach, E.Malamud, J.Schivell, R.Poster, R.Engelmann, T.Kafka, and M.Pratap. Phys. Lett., 48B, 449 (1974).
21. G.Veneziano. Phys.Lett., 52B, 220 (1974); Nucl.Phys., B74, 365 (1974); Phys.Lett., 43B, 413 (1973).
22. H.Harari. Phys.Rev.Lett., 22, 563 (1969). J.Rosner. Phys.Rev.Lett., 22, 689 (1969).
23. Chan Hong-Mo and J.E.Paton. Phys.Lett., 46B, 228 (1973).
24. Huan Lee. Phys.Rev.Lett., 30, 719 (1973).
25. M.Ciafaloni, G.Marchesini, and G.Veneziano. Nucl.Phys., B98, 418, 472 (1975).
26. C.Schmid, D.M.Webber, and C.Sorensen. ETH Zürich preprint (January 1976).
27. P.R.Stevens, G.F.Chew, C.Rosenzweig. "The Pomeron-f Identity and Hadronic Total Cross Sections at Moderate Energy", Caltech report CALT-68-541 (1975).
28. I.Iizuka. Progr. Theor.Phys., 35, 1061 (1966). S.Okubo. Phys.Lett., 5, 165 (1963). S.Zweig (unpublished).
29. This result has also been urged by L.A.P.Balazs. Phys.Lett., 61B, 187 (1976). However different assumptions about the J-plane singularities represented by the cylinder graph lead to the traditional two-vacuum pole result. See S.S.Pinsky and D.R.Snider. Phys.Rev., D13, 1470 (1976) and J.W.Dash, Ref./30/.
30. A.Arneodo and G.Plant. Nucl.Phys., B107, 262 (1976).
31. P.G.O.Freund. Phys.Rev.Lett.,20,235 (1968).
32. N.F.Bali and J.W.Dash. Phys.Lett., 51B, 99 (1974); Phys.Rev., D10, 2102 (1974).
33. T.K.Gaisser and C.-I.Tan.Phys.Rev.,D8, 3881 (1973). M.Suzuki. Nucl.Phys., B64, 486 (1973). G.F.Chew and J.Koplik.Nucl.Phys., B79, 365 (1974); Nucl.Phys., B81, 93 (1974). D.Sivers and F. von Hippel.Phys.Rev., D9, 830 (1974).
34. M.B.Einhorn and S.Nussinov. Phys.Rev., D9, 3032 (1974).
35. C.Quigg and E.Rabinovici.Phys.Rev., D13, 2525 (1976).

MANYCOMPONENT DESCRIPTION OF INCLUSIVE AND SEMI-INCLUSIVE PROCESSES

A.N.Sissakian

Joint Institute for Nuclear Research, Dubna

I. What is Manycomponent Description?

A hypothesis that secondaries are not of the same origin, but are produced due to two or more different mechanisms is one of the interesting ideas in phenomenology of multiparticle production. The schemes and models based on this hypothesis are called manycomponent description.

The efforts to combine two extreme approaches have served as a starting point of such a trend.

The first one proceeds from the fact that the production of secondaries is due to the fragmentation of the colliding objects. The secondaries of this type possess information about a colliding hadron and a target particle. These are "grateful" particles as they remember their "parents". We call such an approach a diffraction excitation (DE).

The second one considers "ungrateful" secondaries which do not remember their "parents". Schemes based on the idea of independent emission of particles (IE) or their definite associations (clusters, resonances, etc.) can be referred to such a category.

It is natural to combine two extreme approaches since even a number of simple characteristics can hardly be explained if one keeps to simple positions.

For instance, even topological cross sections obtained at Serpukhov, Batavia, ISR accelerators deviate from the predictions of the schemes with IE on DE only.

Note that these extreme approaches are sometimes classified in the language of the correlations of secondaries. The approach DE is specified by strong long range correlations, and IE is either the absence of correlations or the existence of weak short range ones.

II. The Way of the Manycomponent Description

It should be mentioned that the idea to separate the contributions of different mechanisms to multiparticle cross sections was initiated by A.A. Logunov et al. (see, e.g. review [1]).

Different realizations of multicomponent description were proposed in a number of papers[2-6] during 1971-73.

a) The two-component model:

This model is one of the most clear realizations of the idea we are interested in.

It is based on the multiplicity distribution which can be written as the sum:

$$\sigma_n = \alpha\sigma_n^{(1)} + \beta\sigma_n^{(2)}. \qquad (1)$$

The first term (or component) in this formula corresponds to the approach DE and the second one to IE. It is assumed that these mechanisms work in different acts of the interaction.

Using the two-component model one may succeed in describing the multiplicity distribution in the interval from 20 GeV to 200 GeV. The increase of the second correlation parameter $f_2 = \langle n\rangle^2 - \langle n(n-1)\rangle$ specifing this model is in good agreement with experiment. The "play" of two components results in a weak dip between the components which can be verified experimentally at higher energies (~1500 GeV).

However, the topological cross sections at the energies higher or equal to 200 GeV and the deviation of the predictions of this model from experimental data on high correlation moments should be considered in a more complicated way [7,8].

b) The model of two mechanisms.

Let us consider now the manycomponent description of the multiparticle production which can be realized using the phenomenological model of two mechanisms (TMP-model). The model was first proposed at Dubna[9,11] as a concrete phenomenological scheme based on the consideration of the quantum field theoretical (QFT) models in straightline-paths and eikonal approximations[10]. Owing to an interest in the charged-neutral correlations this model is worth-mentioning. Note that the straightline-path method allows one to obtain from QFT the leading particle effects and boundness of transverse momentum.

The TMP-model starts from the idea about the existence of the two following mechanisms of the secondaries production:

i. There exist the leading particles which can dissociate with local conservation of isospin;

ii. In the interaction process hadron associations are also produced in a statistically independent way, and they decay into pions.

In this model the probability of cluster production at given dissociation channels of the leading particles has the form:

$$W^{ij}_{n_1 n_2 \ldots} = \alpha_i \beta_j \, P_{n_1}(\langle n_1\rangle) \cdot P_{n_2}(\langle n_2\rangle) \ldots \qquad (2)$$

α_i β_j - are the probabilities of the dissociation channels, $n_k(\langle n_k\rangle)$ are the numbers (average numbers) of associations produced independently.

One can clearly see that the TMP-model leads to the distribution over a number of secondary particles which has the form of the superposition of the Poisson factors. Manycomponent character of the

distribution arises as a result of the summation of formula (2) over a number of possible dissociation channels of the leading particles.

Such a scheme gives a good description of the topological cross sections, it represents correctly the basic features of the charged-neutral correlations and allows to study the dependence of these correlation on the number and mass of clusters.

There is a number of new investigations in this field. For instance, Biebl, Klein and Nahuhauer[12] obtained positive charged-neutral correlations in the framework of the correlated jet model where independent π-meson and ρ-resonance production was considered taking into account the total isospin conservation.

I should like also to note that the old schemes are reconstructed in accordance with manycomponent ideology. In order to explain experimental data on charged distributions and correlation dependancies in multi-Regge scheme, the assumption is used about the necessity of considering diagrams with a large number of showers (or clusters) at high energies[13]. This is also equivalent to the multicomponent structure of distributions over multiplicity. Unfortunately, it is impossible to obtain in the framework of these schemes the fine structure of charged-neutral correlations. For instance, a decrease of charged-neutral correlation curve at large n, as well as a number of other characteristics is well described in the model of the independent cluster emission by S.Pokorski and L. Van Hove [14], if one takes into account the energy momentum conservation law (see contributed paper by R.Kirshner [15]).

I mention only the paper by J.Benecke, A.Bialas and S.Pokorsky[16] which comprises many interesting consequences in the framework of the idea about the multicomponent strusture of spectra.

III. New Applications of the Manycomponent Description

Manycomponent representation became highly useful when analysing the inclusive distributions in the process $e^+ e^- \to$ hadrons.

M.Gorenshtein, G.Zinoviev and V.Petrov[17] developed the two-component model in which the fast partons are described by the parton distribution function and the region of wee x by the fireball mechanism. An interesting property of this model is that both mechanisms work simultaneously in each individual act of the e^+e^- annihilation. This fact results in a number of consequences which agree with experiment. Manycomponent description was also used when studying the semi-inclusive spectra.

In paper [18] we established the validity of the following "automodelity" law for the behaviour of the semi-inclusive cross section:

$$\langle n(\vec{p})\rangle \frac{d\sigma_n}{d\vec{p}} \Big/ \frac{d\sigma^{incl.}}{d\vec{p}} = \psi(n/\langle n(\vec{p})\rangle).$$

This relation does not start from the assumption of the Feynman scaling and provides a good agreement with experiment [11,19].

Note, however, that to study the distributions in a wide interval p, one should consider a manycomponent description. It requires a simultaneous account of soft particles and production of jets (hadronic associations).

Let us consider a simple model[11] with the two-component structure: (see also ref.[20])

$$\frac{d\sigma^{(n)}}{d\vec{p}} \sim \frac{d\sigma_n^{(1)}}{d\vec{p}} + \frac{d\sigma_n^{(2)}}{d\vec{p}}.$$

If one chooses the components with the following behaviour:

$$\frac{d\sigma^{(1)}}{d\vec{p}} \sim \downarrow a(\vec{p}) e^{-np} \qquad \frac{d\sigma^{(2)}}{d\vec{p}} \sim \downarrow b(\vec{p})^{-p/n}$$

then the average associated multiplicities have the form

$$\langle n^{(1)}\rangle \sim \frac{I}{p}, \quad \langle n^{(2)}\rangle \sim p.$$

We see that the components correspond to the behaviour of the associated multiplicity in the same and opposite hemispheres.

It is interesting to note that such a two-component scheme with strong correlations between n and p satisfies the above mentioned "automodelity" law. Obviously, this is an indication to its universality.

A number of papers submitted to the conference is devoted to the field theoretical validity of the contributions of different mechanisms [21-23].

In particular, one can succeed in obtaining the "automodel" solution of the equation of the renormalization groups within the method of the renormalization groups [22]. The method allows one to consider the deviation from the "automodelity" law of semi-inclusive spectra.

IY. C o n c l u s i o n

In conclusion I should like to note that the idea of the manycomponent description which first arose as an attempt to combine the approaches of diffractive excitations and of independent emission while being developed became more profound.

At present, this idea is a convenient way to describe the processes of multiparticle production for which a number of mechanisms (which are not only DE and IE) is responsible. In the language of the manycomponent description, one can study the

role of these mechanisms and their contributions to different regions of the phase space volume and different energy intervals.

R e f e r e n c e s

I. A.A.Logunov,M.A.Mestvirishvili,CERN TH-I707, Geneva (I973).
2. K.Wilson,CLNS-I3I,Cornell(I97I)
3. C.Quigg,J.D.Jackson, NAL-THY-93,Batavia(I972), C.Quigg,Lectures at Summer School,McGill Univ., ITP-SB-73-42.
4. S.P.Kuleshov,V.A.Matveev,A.N.Sissakian,IRB-TP-72-3,Zagreb(I972); Fizika 5,67(Zagreb); V.G.Grishin,S.P.Kuleshov,V.A.Matveev,A.N.Sissakian,G.Jancso,preprint JINR E2-6596,Dubna(I972)
5. K.Fiałkowski,H.Miettenen,Phys.Lett.,43B,pII(I973)
6. H.Harari,E.Rabinovici, Phys.Lett.,43B,49(I973)
7. L.A.Slepchenko,preprint JINR P2-7042,Dubna(I973)
8. N.K.Dushutin, V.M.Maltsev,JINR P2-7676,Dubna(I974)
9. V.G.Grishin,S.P.Kuleshov,V.A.Matveev,A.N.Sissakian,G.Jancso,Nuovo Cim.Lett.,8,590(I973); N.S.Amaglobeli,V.K.Mitrushkin,A.N.Sissakian, L.A.Slepchenko,E.T.Tsivtsivadze, contributed paper A3-I044.
I0. S.P.Kuleshov,V.A.Matveev,A.N.Sissakian,M.A. Smondyrev,A.N.Tavkhelidze.Particles and Nucleus,v.5,part I,p.3(i974); A.N.Sissakian. Lectures given at JINR-CERN School on Physics,Alushta(I975),JINR E2-8825.
II. A.N.Sissakian,L.A.Slepchenko,JINR DI,2-9224, Dubna(I975); contributed paper A3-I099.
I2. K.J.Biebl et al.,contributed paper A3-I38.
I3.Ju.Arestov,R.M.Suljaev.Preprint IHEP(I975)
I4. S.Pokorski,L.Van Hove.Preprint CERN(I975)
I5. R.Kirschner,contributed paper A3-674.
I6. J.Benecke,A.Białas,S.Pokorsky,contributed paper A3-708.
I7. M.I.Gorenshtein et al.contributed paper A3-92
I8. V.A.Matveev,A.N.Sissakian,L.A.Slepchenko,contributed paper A3-II30;Preprint JINR P2-8670 (I975).
I9. L.Abesalashvili et al.Preprint JINR I-9406 (I975)
20. J.L.Alonso,A.C.D.Wright,Phys.Rev.DI2,776(I975)
2I. A.N.Kvinikhidze,A.N.Sissakian,L.A.Slepchenko, A.N.Tavkhelidze.Contributed paper A4-I08I.
22. J.Z.Darbaidze,N.V.Mahaldiani,A.N.Sissakian,L.A. Slepchenko, contributed paper A4-II38.
23. E.M.Ilgenfritz,contributed paper A3-398.

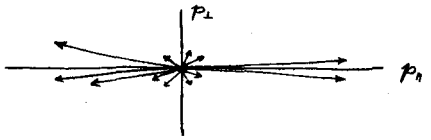
Overlapping Independent Emission in the Fragmentation Region

J. Benecke

Max-Planck-Institut für Physik und Astrophysik, Munich (Fed.Rep.Germany)

1. Introduction

In these days of jets I am concerned here with the old-fashioned ones,



the ones at small $p_\perp$ in hadronic collisions ($p_\parallel$ is in the direction of the incident hadrons in the cms). The central region of particle production, which is also indicated in the above sketch, seems to be the same for the case of high-$p_\perp$ jets (current-induced or quark-induced) as well as for low-$p_\perp$ hadron-induced jets. Also the transverse momentum distribution (transverse with respect to the jet axis) seems to be roughly the same for all of these cases. But as the momenta along the respective jet axes get large, there are characteristic differences in the longitudinal spectra of hadrons: the small-$p_\perp$ jets, as sketched above, are unique in the sense that they contain the leading particle effect and the diffractive peak.

The leading particle spectrum and also forward-backward correlations at high energies are related in a simple way to the multiplicity distribution. This is shown in refs. [1] and [2], on which my raport is based largeley. I am going to describe the inclusive spectra along the $p_\parallel$-axis as power laws

$$(1-|x|)^\lambda , \qquad x = 2p_\parallel/\sqrt{s}.$$

This resembles the case of high-$p_\perp$ jets, where the exponent is determined by quark counting rules [3]. But in our case, the power λ is a variable rather than a fixed number, and will be integrated over.

Our description arises from a generalization of the Bremsstrahlung model [4] which I want to call "overlapping independent emission". The Bremsstrahlung analogy is suggested to us by the observation of

(i) soft pion production [x],

$$\frac{dN}{dx} = \frac{\lambda}{x} \qquad \text{for small } x, \qquad (1)$$

and

(ii) the leading particle effect,

$$\langle x_{proton} \rangle = 0.5$$

in pp collisions, which says that the proton looses on the average only half its energy in the collision.

The concept of cluster production accounts for short range y-correlations: the objects emitted via Bremsstrahlung are understood to be clusters (of mostly pions) with average transverse mass $\sqrt{m^2 + \langle p_\perp^2 \rangle} \approx 1.2$ GeV/c^2. Their multiplicity distribution for a fixed value of λ is a Poisson distribution, as in any independent emission picture; its mean value is $\bar{n}(\lambda) = \lambda \ln s$.

The experimentally observed multiplicity distribution is known, however, to deviate from Poisson and to show Koba-Nielsen-Olesen scaling, i.e.

$$\bar{n} \frac{\sigma_n}{\sigma} = \Psi\left(\frac{n}{\bar{n}}\right), \qquad \bar{n} \text{ large},$$

with a universal function Ψ which does not explicitly depend on energy. We want to take KNO scaling seriously by assuming that Ψ retains an essentially energy-independent width at asymptotic energies. If this is the case, the multiplicity distribution reveals the presence of long range y-correlations among clusters. In the following, I am going to exploit the information on long range correlations

[x] For the report at hand, I want to disregard the rising central plateau at $x = 0$, as observed recently at the ISR. Presently the variation of the plateau height with energy at rapidities $y \neq 0$ is unknown.

which is contained in the multiplicity distribution in order to calculate inclusive one- and two-particle spectra and also multiplicity correlations.

2. Leading particle spectrum

First we consider the leading particle spectrum $\frac{1}{\sigma}\frac{d\sigma}{dx}$, i.e. the proton spectrum in pp $\rightarrow$ pX. For a given value of λ in equ. (1), Stodolsky has shown [4] that the energy loss spectrum of the radiating proton is

$$\frac{1}{\sigma(\lambda)}\frac{d\sigma(\lambda)}{dx} = \lambda\,(1-|x|)^{\lambda-1} . \qquad (2)$$

As explained in ref. [1], our generalization of Bremsstrahlung consists in a weighted integration of equ. (2) over λ, where the KNO function $\psi(\lambda)$ is taken as the weight. This gives

$$\frac{1}{\sigma}\frac{d\sigma}{dx} = \int_0^\infty d\lambda\ \psi(\lambda)\ \lambda\ (1-|x|)^{\lambda-1} . \qquad (3)$$

From the normalization of $\psi(\lambda)$, $\int_0^\infty d\lambda\ \psi(\lambda) = \int_0^\infty d\lambda\ \lambda\,\psi(\lambda) = 1$, we get for the mean multiplicity of clusters

$$\bar{n} = \ln\frac{s}{s_0} .$$

This formula gives an order of magnitude fit to the experimentally observed mean multiplicity of charged secondaries if each cluster contains on the average two charged particles. The proton spectrum, as calculated from (3), is approximately flat from x = 0 to x = 0.9 and rises steeply for x > 0.9. Its peak-plateau structure fits the experimental spectrum, as shown in fig. 1.

3. Interpretation of λ

There are two obvious possibilities for the physical interpretation of the parameter λ which plays the role of a "radiation strength" and, in each Poissonian component, equals the density of clusters (in rapidity):

(a) λ may be related to the impact parameter (geometrical model) [5], or

(b) λ may be related to the variety of Regge trajectories $\alpha_i(t)$, since in the triple-Regge model one has

$$E\frac{d\sigma}{d^3p} \sim \sum_i (1-|x|)^{1-2\alpha_i(t)} .$$

(A difficulty for the triple-Regge model will be discussed in section 7).

4. Inclusive two-particle spectra

Some of the inclusive two-particle spectra in our model are listed in the following table.

	opposite hemispheres	same hemisphere
pp	$\lambda^2(1-\lvert x_B\rvert)^{\lambda-1}(1-x_F)^{\lambda-1}$	—
pc	$\lambda^2(1-\lvert x_B\rvert)^{\lambda-1}(1-\xi)^{\lambda}$	$\lambda^2(1-x-\xi)^{\lambda-1}\,\Theta(1-x-\xi)$

($x_B < 0$, $x_F > 0$; $x, \xi > 0$)

Each entry is to be multiplied by $\psi(\lambda)$ and integrated over λ. The phase space element for protons (p) is dx, and for clusters (c) it is $d\xi/|\xi|$ ($\xi = \frac{2p_L}{\sqrt{s}}$ for a cluster). The derivation of $\frac{|\xi|}{\sigma}\frac{d\sigma}{d\xi\,dx}(x,\xi x)$ parallels that of Stodolsky's calculation for the leading particle energy loss. Since

$$\int_0^{1-\xi} dx\ \lambda^2\,(1-x-\xi)^{\lambda-1} = \lambda\,(1-\xi)^{\lambda} ,$$

the inclusive cluster spectrum is given by

$$\frac{|\xi|}{\sigma}\frac{d\sigma}{d\xi} = \int_0^\infty d\lambda\ \psi(\lambda)\ \lambda\ (1-|\xi|)^{\lambda} . \qquad (4)$$

This spectrum is shown in fig. 2. For practical purposes, it can be approximated by $(1-|\xi|)$.

Next we consider the correlation ratio for two back-to-back protons,

$$R_{pp}(x_B, x_F) = \frac{\sigma\,\frac{d\sigma}{dx_B\,dx_F}}{\frac{d\sigma}{dx_B}\frac{d\sigma}{dx_F}} - 1 . \qquad (5)$$

The result of our model calculation is shown in fig. 3 for the symmetrical case, $-x_B = x_F \equiv x$. This plot leads us to expect fairly strong positive correlations of long range at ISR energies. I want to stress that this violation of factorization for the inclusive spectrum is predicted to be asymptotic. I.e., in our model, R does not vanish as $s \rightarrow \infty$. Preliminary data on $R_{pp}(-x, x) + 1$ at $0.94 \leq x \leq 0.96$, as a function of s, are reproduced in fig. 4. It should be noted that these data points are at certain fixed values t_1 and t_2 of the four-momentum transfers to the protons. Our prediction of $R_{pp}(-x, x) + 1 = 1.5$ at $x = 0.95$ and its energy-independence is seen to be satisfied rather well, provided the integration over the t's does not change the value of R drastically.

5. Multiplicity Correlations

Let us now turn to forward-backward multiplicity correlations. It is customary to express them by the quantity $\bar{n}_F(n_B)$, i.e. the average number of clusters in the forward hemisphere when the number of clusters in the backward hemisphere is fixed to be n_B. For independent emission with a fixed value of λ one gets $\bar{n}_F(n_B) = \lambda\,\bar{n}/2$, i.e. no correlation. Taking the appropriate average over λ by weighting with the KNO function one finds the curves shown in fig. 5, as explained in ref. [2]. The curves correspond to three different values of the mean number $\bar{n}$ of clusters (or three different values of the primary energy). One sees that the correlations are quite appreciable already at low $\bar{n}$. Asymptotically, for $\bar{n} \rightarrow \infty$, n_B fixed, we obtain

$$\bar{n}_F(n_B) = n_B + 1 + \alpha$$

if $\psi(\lambda) \propto \lambda^\alpha$ near $\lambda = 0$. Preliminary data at $\sqrt{s} = 22$ and 53 GeV from the Aachen-CERN-Heidelberg-Munich Streamer Chamber Collaboration agree very well with our expectation. (Note that $\bar{n} = 5$ corresponds to a mean multiplicity of charged secondaries $\bar{n}_{ch} \approx 10$.) In particular, it should be noted that the experimental slope for $\bar{n}_F(n_B)$ increases with rising $\sqrt{s}$. The predicted forward-backward multiplicity correlations may be affected by fluctuations caused by the cluster decay. But the decay can only provide short-range correlations, and they can be neglected in the asymptotic limit.

6. Picture of long-range correlations

The experimental confirmation of our results on $R_{pp}(-x, x)$ and $\bar{n}_F(n_B)$ leads us to the following suggestion: Long-range inclusive correlations in rapidity y or in x exist and are fully determined by the information contained in the overall multiplicity distribution. The deviation from factorization is expected to persist at higher energies. In the framework of our model, the ISR data on $R_{pp}(-x, x)$ and $\bar{n}_F(n_B)$ indicate that the KNO function $\psi(\frac{n}{\bar{n}})$ retains an essentially energy-independent width at very high energies.

7. Inclusive pion spectrum

My last point is to discuss the inclusive pion spectrum $\frac{x}{\sigma}\frac{d\sigma}{dx}$ for $x > 0$. As mentioned earlier, the cluster spectrum is to a good approximation given by

$$x\,\frac{dN_c(x)}{dx} = 1 - x . \qquad (6)$$

The clusters "decay" into mostly pions. The resulting pion spectrum is determined by a parent-child relation,

$$x\,\frac{dN_\pi(x)}{dx} = \int_0^1 \frac{dz}{z}\ \frac{\frac{x}{z}\,dN_c(\frac{x}{z})}{d(\frac{x}{z})}\ g(z) . \qquad (7)$$

Here

$$g(z) = z\,\frac{dN_{\pi/c}}{dz} , \qquad z = p_\pi/p_c ,$$

is the decay spectrum for pions from a single cluster with large momentum p_c (the direction of the pion momentum p_π is then approximately the same as that of p_c). Equ. (7) arises from folding the decay spectrum g(z) into the cluster spectrum $xdN_c(x)/dx$ [6]. Under the assumption that the cluster decays according to three-body phase space, we find

$$g(z) \sim z\,(1-z) . \qquad (8)$$

The choice (8) for g(z) is supported by recent inclusive spectra from $e^+e^- \rightarrow$ hadrons. The SPEAR data at $E_{cm} = 4.8$ and 7.4 GeV show the formation of two jets [7] and give longitudinal spectra of the form

$$s\,\frac{d\sigma}{dx} \sim \frac{1-x}{x} , \qquad x = \frac{2p_L}{E_{cm}} > 0.2 .$$

Here, p_L is the momentum component of a charged hadron parallel to the jet axis. The translation of this result to our case of hadronic small-$p_\perp$ jets is as follows: the process $e^+e^- \rightarrow$ hadrons is thought as being mediated by $e^+e^- \rightarrow q+\bar{q}$, and each quark is equated to a cluster.

Inserting (6) and (8) into (7), we find

$$x\frac{dN_\pi(x)}{dx} = \frac{x}{\sigma}\frac{d\sigma_\pi}{dx} \sim (1-x)^3 \quad \text{as } x\to 1. \qquad (9)$$

Experimental π^- spectra at PS energies and at the ISR are plotted in fig. 6. The agreement is satisfactory; for the ISR data, one has to assume that the integration over $p_\perp$ does not change the power of (1-x) by much.

Since I mentioned earlier that our parameter λ may correspond to Regge trajectories $\alpha_i(t)$, I should point out a difficulty for the triple-Regge description which arises from fig. 6b: The power of (1-x) in $\frac{E}{\sigma}\frac{d\sigma_\pi}{d^3p}$ should vary with $p_\perp^2$, since $-t \approx p_\perp^2$ at small angles. The ISR data, on the contrary, can be fitted to a power 3.5 independent of $p_\perp$ ($p_\perp$ = 0.55 and 0.85 GeV/c, i.e., $-t$ = 0.30 and 0.72 GeV/c^2).

References

[1] J. Benecke, A. Białas and E.H. de Groot, Phys.Lett. 57B (1975) 447.

[2] J. Benecke, A. Białas and S. Pokorski, Nucl.Phys. B110 (1976) 488. Contributed paper A3 # 47.

[3] R. Blankenbecler and S.J. Brodsky, Phys. Rev. D10 (1974) 2973. J. Gunion, Phys.Rev. D10 (1974) 242.

[4] L. Stodolsky, Phys.Rev.Lett. 28 (1972) 60.

[5] S. Barshay, Phys.Lett. 59B (1975) 63, and references quoted therein.

[6] See, e.g., J.D. Bjorken, Acta Phys. Polonica B5 (1974) 893, where the appropriate relation for high-$p_\perp$ processes is given.

[7] G. Hanson, Proceed. of the VIIth International Colloquium on Multiparticle Reactions, Munich 1976.

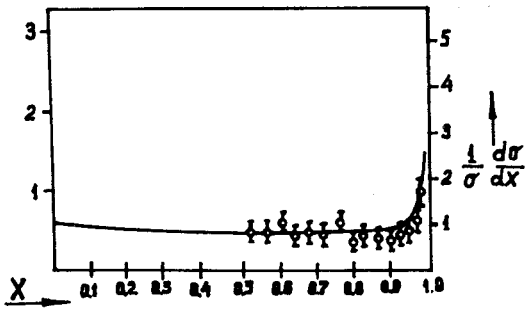


Fig. 1: Leading proton spectrum in pp collisions, calculated from equ. (3). The data are at 405 GeV/c, J.W. Chapman et al. (Michigan-Rochester Collaboration), Phys.Rev. Lett. 32 (1974) 257. For details see ref. [1].

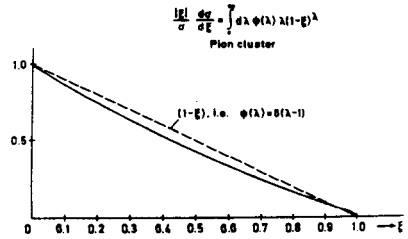


Fig. 2: Cluster spectrum in pp collisions, calculated from equ. (4).

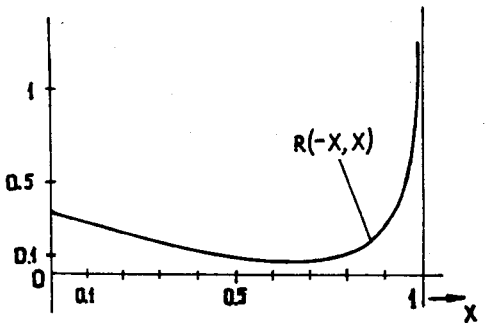


Fig. 3: Correlation ratio $R(x_B, x_F)$ for symmetrical leading particles, $-x_B = x_F \equiv x$.

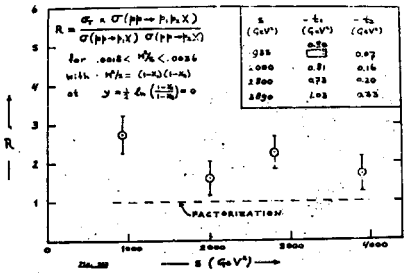


Fig. 4: Data on R(-x, x) +1 as a function of s, from the CERN-Holland-Manchester Collaboration, reported in M. Jacob, ISR Discussion Meeting # 18, CERN 1976. Each data point represents an average over the x-interval 0.94 ≤ x ≤ 0.95. Note that the four-momentum transfers t_1, t_2 to the two proton have fixed values.

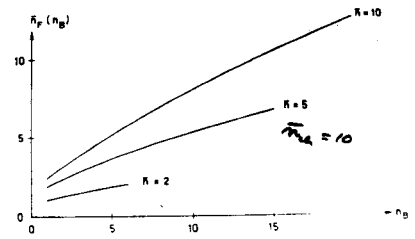


Fig. 5: Average multiplicity of clusters in the forward cms-hemisphere plotted versus the number of clusters in the backward hemisphere. Different curves correspond to different values for the average total multiplicity of clusters.

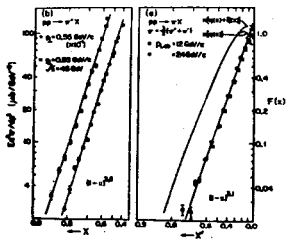


Fig. 6a: Experimental π^- spectrum $F(x') = \frac{1}{\sigma}\int d^2p_\perp E\frac{d^3\sigma}{d^3p}$ for $pp\to\pi X$, $x' = (p_\pi / p_{\pi,\max})_{cms}$. Data from V. Blobel et al. (Bonn-Hamburg-Munich Collaboration), Nucl.Phys. B69 (1974) 454.

b: Invariant π^- spectrum $E\frac{d\sigma}{d^3p}$ for $pp\to\pi^+X$ from the CERN-Holland-Lancaster-Manchester Collaboration, J.C. Sens (private communication).

INCLUSIVE APPROACH TO PARTICLE PRODUCTION

A.Białas
Institute of Physics, Jagellonian University
and Institute of Nuclear Physics,
Krakow, Poland

My task is to review briefly problems which arised in recent years in studies of inclusive spectra. Since the available space is very limited, I was obliged to make severe cuts in selecting the material for this report, and I decided to present out only some general remarks. More detailed discussion of many particular aspects of inclusive distributions are discussed in other talks presented in this Session.

Several different theoretical languages are now available for description of inclusive spectra: Mueller-Regge description[1], Gribov field theory[2], multiperipheral approach[3], bremsstrahlung analogy[4], parton model[5] - to list only the most popular ones. They are rather different in physical content and in phraseology. It is interesting to observe, however, that there is one fundamental idea which is common to all of them: it is always assumed that the basic underlying mechanism of particle production satisfies strong short-range order[6], i.e., the spectra have two properties:

(a) Feynman scaling[7] of single-particle spectra and

(b) no long-range correlations in multiparticle spectra.

This property is formulated very differently in different languages listed above. Nevertheless it is present in all of them and therefore it is natural to discuss it independently of particular models.

Few years ago the hope was expressed that also the observed inclusive spectra should show the property of short-range order. We know that this is not the case. Indeed, already first experiments at NAL showed that multiplicity distribution does not resemble Poisson distribution - thus long range correlations must be present. This is illustrated in Figure 1 where the Wroblewski[8] plot is presented showing linear dependence of dispersion versus average multiplicity, characteristic of the KNO scaling[9]. In the recent years also violation of

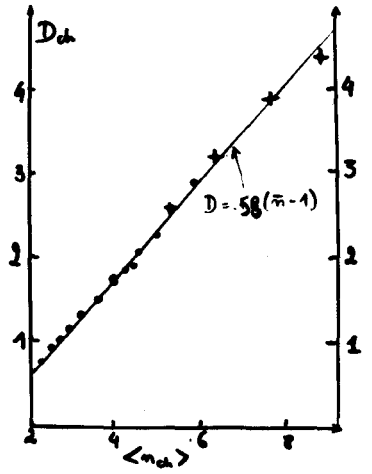


Fig. 1. Dispersion vs average multiplicity plot.

Feynman scaling in the central region, first observed by Michejda[10] was definitely established[11,12]. This is illustrated in Figure 2, where the invariant inclusive 90° cross sections for the processes $pp \to \pi^{\pm}$ + anything are plotted versus c.m. energy of the collision.

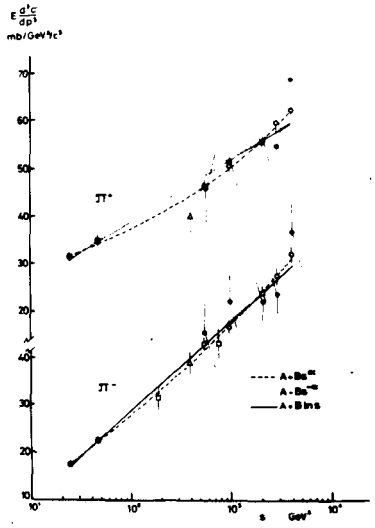


Fig. 2. Invariant cross section at 90° vs total c.m. energy. Compilation from Ref.[12].

The same feature is presented in Figure 3, taken from ref.[13], where it is shown that the data scale in relative rapidity $\tilde{z} = \frac{y}{Y}$ rather than in y.

Thus the problem arises for the theory: how to explain this contradiction with strong short-

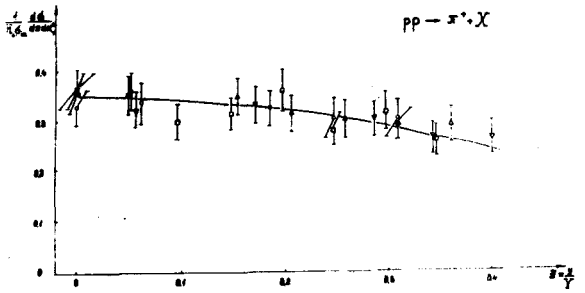


Fig. 3. Cross section for the prooess $pp \to \pi^+ +$ + anything showing evidenoe for Z-scaling (Ref.[13]).

range order hypothesis. In other words: in any model the reason must be found to justify correotions to the elementary produotion mechanism. These oorreotions should be large enough to ohange drastioally short range order property of the spectra and thus bring them to agreement with experiment.

The simplest way is to rejeot short range order idea altogether. This is done, e.g., in hydrodynamioal model which was discussed at this Session by Dr.Shuryak[14]. It was shown by Frøyland[15] in the paper submitted to this Conferenoe that indeed hydrodynamical model can explain the 90° inclusive spectra, provided proper aocount is taken of the hadronic profile function.

In the more popular conservative approach short order property is kept as a first approximation. The physioal motivation for the deviation from it is twofold:

(a) Hadrons are oomposite objeots

Consequently, the observed spectrum is likely to be superposition of many different elementary processes (which may arise, e.g., from interaction of different kind and/or number of constituents). As a result the long-range correlations should appear.

(b) The interaction responsible for partiole production is strong

It follows that any elementary mechanism must imply rescattering (unitariry) corrections which change the observed spectra. There are two kinds of such corrections: (i) elastic scattering and diffraotion dissociation appear as shadow effects and (ii) elementary processes absorb each other.

I like to emphasize that these are both very physical reasons which are found to oocur. In fact, were they not observed, a reason should be found for explanation of such a phenomenon.

The reader should get impression that these two effects are unrelated. Just the contrary - they substantially influenoe each other. For example, the appearance of diffraction dissociation adds one more component to the inclusive spectrum. On the other hand - the size of unitarity oorreotions dramatically depends on hadron structure.

Let me now come to more specific discussion of the progress achieved recently along these lines.

Multicomponent Approach

In the multicomponent approaoh[16,17] it is assumed that the observed spectra are incoherent superpositions of many different components. In phenomenological applications, the crucial point is to determine weights with which different components enter the distribution. It was pointed out in Ref.[18] that this weight is simply related to the KNO scaling. Thus once the KNO function is determined, many other distributions can be predicted, in particular long range correlations, leading partiole spectrum, correlations between leading and produced particles and forward-backward correlations[18,19]. I am very brief on this problem since it is discussed in detail by Max Beneoke in his report[20]. I would like to emphasize, however this new development increased greatly the predictive power of the multicomponent approach and transformed it into a useful tool for quantitative analysis of inclusive data.

Diffraction Dissociation

This effect of unitarity is the earliest to identify experimentally. Since it is covered in another Session, I will restrict myself to two remarks.

(i) The effect is large. This was particularly emphasized by work of Ref.[21] and[22], where it was shown the existing data are rather close to the unitarity bound[23]. This point is further supported by contribution to this Conference by UCLA-Saclay coll.[24], who measured the diffractive dissociation at ISR and claim that in pp collisions $\sigma_{el}+\sigma_{diff.} \approx \frac{1}{2}\sigma_{tot.}$ i.e., the unitarity bound is saturated.

(ii) From the analysis of structure of absorption which may lead to such a behaviour[22] it follows that nucleon in the collision process appears sometimes black and sometimes nonabsorbing at all. The grey disc observed in analysis of elastic data is the result of averaging over this complicated structure. The most naive (and exciting) interpretation of this result is that nucleon consists of few small (point?) constituents. A particular example of such a behaviour was observed in quark-glue model[25,26].

Absorptive Corrections

The hope here is that by studying unitarity effects it will be possible to understand energy dependence of total cross sections and inclusive spectra.

There are two problems: (i) how to estimate theoretically the absorptive corrections to inclusive spectra and (ii) how to fit experimental data.

It seems to me that the main conclusions from the analysis of theoretical models is that the simple eikonal picture[27] is probably the best approximation. The characteristic feature of eikonal models is that although the total cross section is absorbed, the single particle spectrum is not. This situation is illustrated in Figure 4, which shows that in eikonal picture the inclusive particle density is proportional

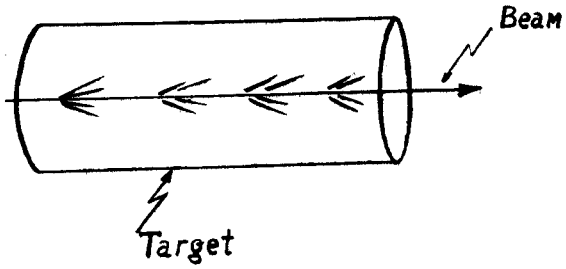


Fig. 4. Eikonal picture of particle production.

to "effective thickness" Ω of the target and, consequently, there is no shadowing. It was shown for very general class of theories that such a picture correctly summarizes the theoretical situation[28,29].

Thus in the phenomenological description of the data, the problem arises whether it is possible to describe the energy dependence of both the total cross section and single particle inclusive spectrum by the same effective thickness Ω. This is not so trivial because the effective thickness as measured from elastic cross section does not seem to rise in the small b - region[30]. On the other hand, the rise of Ω at large impact parameters is unlikely to produce large increase of multiplicity. The solution to this apparent discrepancy may be again the internal structure of the proton. Indeed, if it is made of some small well-separated objects (as indicated by results of refs.[22] and[26]) then the effective target thickness in individual collision may be large and growing with energy, whereas the average target thickness, which is measured in elastic scattering may be approximately energy independent.

Another approach was proposed in Ref.[31]. The authors indicated that energy and momentum conservation can destroy the simple eikonal picture at finite energies. Their analysis indicates that the corrections are going in the right direction, i.e., they are likely to explain the data.

I would like to summarize all this in the following points.

(i) The data show strong disagreement with short-range order picture which is fundamental for most of the existing descriptions of inclusive spectra. Thus modifications must be found.

(ii) There are two physical effects which should be taken care of and which give hopes to restore the agreement with data: (a) compositeness of the hadrons and (b) unitarity corrections.

(iii) The existing data on diffraction dissociation and cross section rise seem to indicate that hadrons are made of well-separated objects of rather small dimensions.

References

1. A.H.Mueller. Phys.Rev., D2, 2963 (1970).
2. V.Gribov. Soviet Phys. JETP, 26, 414 (1968).
3. P.Amati, S.Fubini and A.Stanghellini. Nuovo Cim., 26, 896 (1962).
4. L.Stodolsky. Phys.Rev.Lett., 28, 60 (1972).
5. R.Feynman. Photon-Hadron Interactions, Benjamin, 1972.
6. A.Krzywicki. Nucl.Phys., B58, 633 (1973).
7. R.Feynman. High Energy Collisions, Stony Brook Conference (1964), Gordon and Breach, N.Y.,London, Paris, p. 237.
8. A.Wroblewski. Acta Phys.Pol., B4, 857 (1973).
9. Z.Koba, H.B.Nielsen and P.Olesen. Nucl. Phys., B40, 317 (1972).
10. L.Michejda. Nucl.Phys., B35. 287 (1971).
11. B.Alper et al. Nucl.Phys., B100,237 (1972).
12. K.Guettler et al. British-Scandinavian-MIT collaboration. CERN preprint (1976).
13. A.S.Potupa, V.V.Skadorov and A.S.Fridman. Pis'ma JETP, 23, 546 (1976) and private communication from Dr.Potupa.
14. E.Shuryak. Contribution to this Conference.
15. J.Frøyland. Paper No. A3-67 submitted to this Conference.
16. A.Białas, K.Fialkowski and Z.Zalewski. Nucl.Phys., B48, 237 (1972).
17. A.Białas. Invited talk at Pavia meeting (1973).
18. J.Benecke, A.Bialas, E.H. De Goot. Phys. Lett., 57B, 447 (1975).
19. J.Benecke, A.Białas, S.Pokorski. Paper No. A3-47 submitted to this Conference and Munich preprint.
20. J.Benecke. Report at this Conference.
21. L.Caneschi et al. Phys.Lett., 56B, 359 (1975).
22. K.Fialkowski and H.I.Miettinen. Nucl.Phys., B103, 247 (1976).
23. J.Pumplin. Phys.Rev., D8, 2899 (1973).
24. UCLA-Saclay collaboration, W.Lockman et al. Paper presented to this Conference, UCLA-1104.
25. S.Pokorski and L.Van Hove. Acta Phys. Pol., B5, 229 (1974). Nucl.Phys., B86, 243 (1974).
26. L. Van Hove and K.Fialkowski. CERN preprint TH 2123.
27. See, e.g., A.Białas and W.Czyz. Phys.Lett., 51B, 179 (1974).
28. V.Abramovsky, V.Gribov, O.Kanchelli. Yad. Fiz., 18, 595 (1971).
29. References for later work can be found in M.Ciafaloni and G.Marchesini. CERN preprint TH 2146 submitted to this Conference.
30. See e.g., U.Amaldi. Report at Air-cu-Prorcuca Conference (1973).
31. A.Capella and A.Kaidalov. CERN Preprint TH 2151.

CORRELATIONS IN MULTIPLE PRODUCTION AND CLUSTERS

G.H.Thomas
Argonne National Laboratory, Argonne, Illinois, 60439, U.S.A.

At the time of the London Conference, there were several interesting puzzles: 1) The Mueller-Regge model description of the small rapidity distance behaviour of the $\pi^{\pm}\pi^{-}$ correlation functions was not satisfactory. If one thought the small separation behaviour should be the extrapolation of the predicted large separation behaviour, then $\pi^{-}\pi^{-}$ (being oxotic) would have a shorter correlation length than $\pi^{+}\pi^{-}$. 2) The fraction of the $\pi\pi$ correlation due to resonance production was not known, in particular that due to ρ for FNAL and ISR data. 3) The fraction of the $\pi^{-}\pi^{-}$ correlation due to Bose-Einstein statistics was unknown. 4) The simplest explanation of all the available data was in terms of a cluster description. However several features of these clusters were not determined, such as their typical charges, their mass and their mean multiplicity. Most significant was our lack of knowledge of the underlying meaning of the cluster description.

By the time of this conference, some progress has been made on all of these points. 1) The low sub-energy behaviour of the $\pi^{\pm}\pi^{-}$ correlations is consistent with the Mueller-Regge description. 2) Several groups have measured the inclusive ρ production cross-section, which is about 10% of the total $\pi^{+}\pi^{-}$ correlation. We don't yet know for sure the origin of the remaining part, but one would expect 3 and 4 body resonances to make an important contribution. 3)There is a growing belief that a Bose-Einstein effect is seen in the inclusive data.I will present some of this evidence and argue that it is not greater than about a 20% effect in $\pi^{-}\pi^{-}$.4)Finally,about clusters there still seems to be no firm experimental answer to whether they are new objects, or manifestations of known resonances and production mechanisms. Whatever they are, there is evidence now about some of their characteristics. I personally believe they come in both neutral and charged varieties and decay on average into 2 charged particles. This is consistent with having mainly resonance production. There is still however some controversy about these conclusions.

In the time allowed me for this talk, I would like to emphasize the results on the Mueller-Regge picture and on the Bose-Einstein effect (points 1 and 3 above).

The $\pi^{\pm}\pi^{-}$ correlation functions depend on six variables, so they contain much more information than can be seen in any particular one dimensional plot.One should study several types of plots, in addition to the usual rapidity-difference ones[1]. I would like to show now the results[2] of using the dipion mass as one of the variables of the correlation function.

Recall that the correlation function is defined as

$$C_2(p_1,p_2) = \rho_2(p_1,p_2) - \rho_1(p_1)\rho_1(p_2) \quad (1)$$

where the invariant one and two particle normalized inclusive cross sections are

$$\rho_1(p) = \frac{1}{\sigma} E \frac{d\sigma}{d^3p}$$

$$\rho_2(p_1,p_2) = \frac{1}{\sigma} E_1 E_2 \cdot \frac{d\sigma}{d^3p_1 d^3p_2} \quad (2)$$

Here σ will be the inelastic cross section, though other choices could be imagined[2].

To evaluate the dipion mass (M) dependence of (1) we note that for each pair of vectors $\vec{p}_1$, and $\vec{p}_2$ both $C(\vec{p}_1,\vec{p}_2)$ and the variable M are defined. Thus we can sum $C(\vec{p}_1,\vec{p}_2)$ over all of the six dimensional phase space keeping M fixed. One result of doing this is shown in Fig. 1 for both $\pi^{+}\pi^{-}$ and $\pi^{-}\pi^{-}$. For each charge configuration, $C_2(M)$ is shown along with the mass dependences resulting from the separate terms in Eq. (1). Note how nicely ρ_2 joins on to $\rho_1 \otimes \rho_1$, as M increases sufficiently. This is some indication that our choice of σ is a proper choice.

Three main physics points to note about the correlations, reproduced on the same scale in

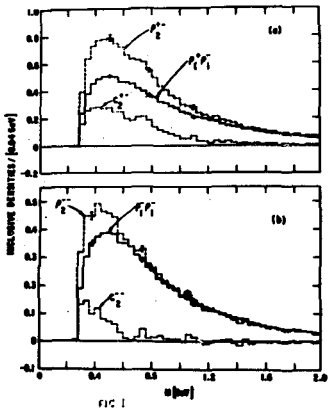


Fig. 1. The data (ref.[2]) here and elsewhere in the paper are from the ANL-FNAL-Stony Brook collaboration, $pp \to \pi^{\pm}\pi^{-}X$ at 205 GeV/c. Displayed as a function of dipion invariant mass are the three distributions ρ_2, $\rho_1 \otimes \rho_1$ and C_2 for (a) $\pi^+\pi^-$ and (b) $\pi^-\pi^-$ pairs.

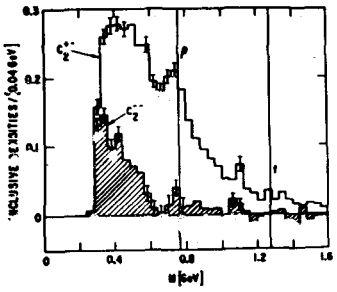


Fig. 2. $C_2(M)$ for $\pi^+\pi^-$ and $\pi^-\pi^-$ are displayed on the same scale. The nominal locations of the ρ ($M=0.76$ GeV) and f ($M=1.27$ GeV) are marked.

Fig. 2, are: 1) $\pi^-\pi^-$ falls faster than $\pi^+\pi^-$ for increasing values of M, 2) The threshold peak in $\pi^+\pi^-$ is at a smaller value of M than in $\pi^+\pi^-$, 3) There is an obvious ρ^0 signal which accounts for about 10% of the total $\pi^+\pi^-$ correlation (there is no noticeable signal at the f).

About the first point, let us recall what the Mueller-Regge description[3] would tell us concerning the M behaviour of $\pi^{\pm}\pi^{-}$ correlations. A certain discontinuity of a 4 particle to 4 particle amplitude (Fig. 3a) gives the correlation function $C_2(p_1,p_2)$. We then assume the π 's are in the central region and that the leading

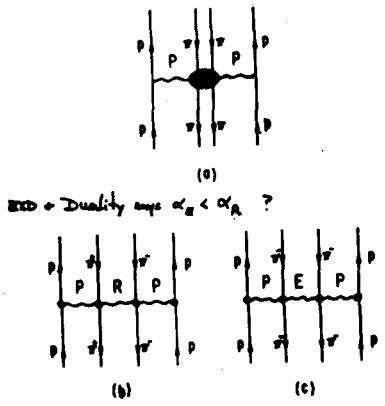


Fig. 3. a) Mueller-Regge diagram for the inclusive reaction $pp \to \pi\pi X$ where the dipion system is produced in the central region of rapidity. b) Mueller-Regge diagram for $pp \to \pi^+\pi^- X$ at large s and large mass M of the $\pi^+\pi^-$ pair. c) Mueller-Regge diagram for $pp \to \pi^-\pi^- X$ at large s and large mass M of the $\pi^-\pi^-$ pair.

graph is double Pomeron exchange as shown. At large mass, one then assumes that the central blob is dominated by exchanges R for $\pi^+\pi^-$ or E for $\pi^-\pi^-$. The leading exchanges R in $\pi^+\pi^-$ are the ρ and f. For $\pi^-\pi^-$ the ρ and f contribute the same magnitudes but the isospin 1 exchange changes sign. This is similar to what happens in $\pi\pi$ scattering. Thus, duality arguments relate the absence of exotic resonances in $\pi^-\pi^-$ to the exact cancellation of the ρ and f trajectories. If a similar phenomena obtains for inclusive $\pi^-\pi^-$ production, the leading exchanges E could have intercept less than the ρ-f trajectories. Of course exchange degeneracy cancellations may not be exact and E could be similar to R but with substantially reduced coupling.

To study this in the data, we remark that $+-$ and $--$ correlation functions are

$$C^{+-}(M) = (M^2)^{\alpha_R - 1} \int \frac{d^3p_1}{E_1} \cdot \frac{d^3p_2}{E_2} \beta_{pR}(m_{T1}) \beta_{pR}(m_{T2}) \quad (4)$$

$$C^{--}(M) = (M^2)^{\alpha_E - 1} \int \frac{d^3p_1}{E_1} \cdot \frac{d^3p_2}{E_2} \beta_{pE}(m_{T1}) \beta_{pE}(m_{T2}).$$

Thus the Regge behaviour is modified by the behaviour of the vertex functions β which depend on the transverse mass. To remove this behaviour in first approximation we note that the single particle contribution to $C(M)$ in (1) has leading behaviour

$$\rho_1 \otimes \rho_1 (M) = \int \frac{d^3p_1}{E_1} \cdot \frac{d^3p_2}{E_2} \beta_{pp}(\omega_{T1}) \cdot \beta_{pp}(\omega_{T2}) \qquad (5)$$

taking double Pomeron exchange for $\rho_1(p)$. If the vertex function β_{pp} is roughly proportional to β_{pR} then $C_2^{+-}(M)/\rho_1^+ \otimes \rho_1^-(M)$ has only a Regge M dependence. This is shown in Fig. 4 where one sees that an effective α of 1/2 is consistent in an average sense with the data. Note that the dotted lines show that the low mass dependence is more consistent with 0.6 and the high mass with 0.35, so the value of 1/2 has an error of about 0.1.

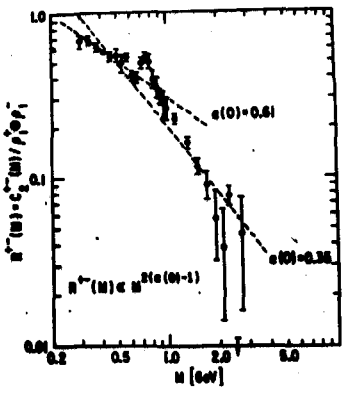


Fig. 4. Mass dependence of $R^{+-}(M) = C^{+-}(M)/\rho^+ \otimes \rho^-(M)$. The straight lines correspond to two choices of α_R in the expression $R^{+-}(M) \sim (M^2)^{\alpha_R - 1}$.

Next, again assuming a rough proportionality between vertex functions, $C^{--}(M)/C^{+-}(M)$ gives the difference between the effective trajectories $(+-)$ and $(--)$ (See Fig. 5). The dotted line represents $\alpha_E - \alpha_R = -1$, which is consistent with the data.

We conclude that this evidence favors the explanation that there is exchange degeneracy

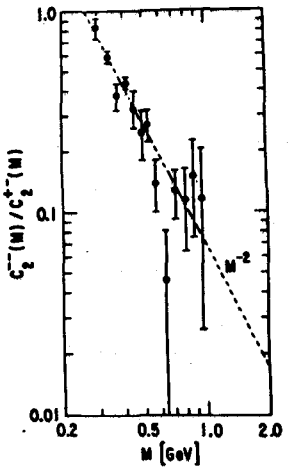


Fig. 5. Mass dependence of $C^{--}(M)/C^{+-}(M)$. Dashed line is proportional to M^{-2} and is not a fit to data.

between the ρ and f such that there is cancellation in the exotic $\pi^-\pi^-$ channel. We find that the effective interoept $\alpha_R \sim 0{,}5$ and $\alpha_E \sim -0{,}5$. Thus $\pi^-\pi^-$ has a shorter range than $\pi^+\pi^-$ /3/. We have also investigated the magnitudes of the vertex ocuplings. There is not time to discuss this analysis /2/, but there are no major surprises.

The next topic I would like to disouss is the difference in the $\pi^-\pi^-$ and $\pi^+\pi^-$ threshold behaviours (Fig. 2). One sees that $\pi^-\pi^-$ peaks earlier than $\pi^+\pi^-$. This is indeed what one might expect for an interferenoe effect due to identical particles /4/. In the region of phase space where the magnitude Δ of the four momentum difference $p_1 - p_2$ is about 1 pion mass (ω_π) or less, there can be constructive interferenoe effeots. This magnitude Δ is related to M by

$$\Delta^2 = -(p_1 - p_2)^2 = M^2 - 4\omega_\pi^2 . \qquad (6)$$

In other words the interference effect extends about m_π above the $\pi\pi$ threshold. Thus the behaviour we see in the data could be attributable to Bose-Einstein statistics, but we note the effect is not large. More than 75% of the $\pi^-\pi^-$ correlation lies outside the region where one expects an interference; in the region where we expect an effect, we see only a slight difference between $(+-)$ and $(--)$.

To study the question of the size of the interference effect better, I have looked at a specific model[5]. The idea is to produce both π and ρ mesons independently. To generate interferences, one constructs the model for amplitudes and then squares the amplitudes keeping all interference terms. The result of such a calculation is shown in Fig. 6. The prominent peak is the ρ resonance used as input, with some slight broadening. The threshold peak

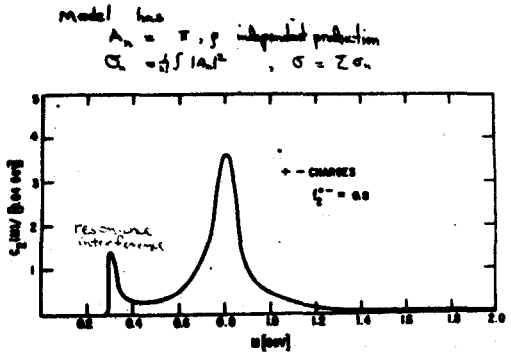


Fig. 6. Model calculation taken from Ref.[5] for $C^{+-}(M)$.

has the Breit-shape and results from coherent interferences between resonances. This coherent interference is present also in $\pi^-\pi^-$ (Fig. 7).

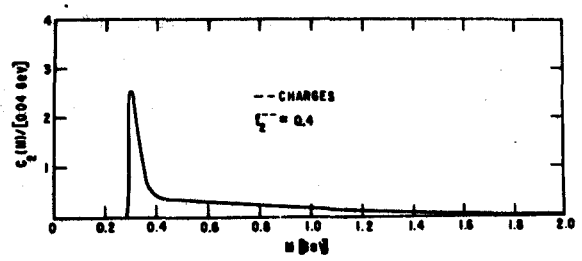


Fig. 7. Model calculation taken from Ref.[5] for $C^{--}(M)$.

The model assumes isospin conservation, so there are peaks both in $\pi^+\pi^-$ and $\pi^-\pi^-$ though the $\pi^-\pi^-$ effect is twice that of $\pi^+\pi^-$.

Of course in this model, ω production as well as other 3 or more particle resonances are left out. What may be believable however is the ratio of the interference cross section (taken to be the area from threshold to about m_π above threshold) to the ρ^0 cross section. In $\pi^-\pi^-$ the ratio is about 1/2 and in $\pi^+\pi^-$, about 1/4. Since the ρ^0 cross section is known, we have a rough estimate of the interference cross section. The result is the prediction that about 20% of f_2^{--} (the area of $C_2^{--}(M)$) could be due to second order interferences and only 4% of f_2^{--} (the area of $C_2^{+-}(M)$).

The conclusion about such second order interference effects is that they might now have been seen in the data. If true, their range is about m_π, and in $\pi^-\pi^-$ the effect is not greater than about 20% f_2^{--}.

The overall conclusion is that the mass variable is very useful for studying questions about the Mueller amplitudes, and for studying coherent interference effects which are expected near threshold. It would be very interesting to see correlations as functions of mass at other energies and for reactions other than that studied here. This would test our conclusions about "Muellerology" and about our conclusions concerning the strengths of coherence effects.

References and Footnotes

1. Several recent papers submitted to this conference advocate two dimensional (rapidity difference Δy and azimuthal angle $\Delta\phi$) plots to obtain this information. See e.g., Ranft, Ranft and Kirschner, Fadeev, Lutov and Nazargulov # 677; Levin, Ryskin, and Troyan # 84.
2. E.L.Berger, R.Singer and G.H,Thomas. Submitted to this conference, to be issued as Argonne preprint ANL/HEP 76-09.
3. Cf. Oh et al. Phys.Lett., 56B, 400 (1975). They look at joint $\Delta y, \Delta\phi$ distributions. When they select $\Delta\phi \simeq 0$ (which by the way samples low mass) they find that the $(--)$ rapidity range is shorter than the $(+-)$.
4. The Bose-Einstein effect implicated here has been discussed in different forms and with different terminology by several authors. Typical terminologies are: a) "Goldhaber" effect, G.Goldhaber, S.Goldhaber, W.Lee and A.Pais. Phys.Rev., 120, 300 (1960);

b) "Second Order Interference" effect, V.G.Grishin , G.I.Kopylov and M.I.Podgoretsky. Yad. Fiz., 13, 1116 (1971) (English Trans.: Sov.J.Nucl.Phys., 13, 638 (1971));
c) Bose or Bose-Einstein statistics, J.Ranft and G.Ranft. Phys.Lett., 57B, 373 (1975).
A more complete list can be found below in Ref./5/.
5. G.H.Thomas, ANL-HEP 76-33.
6. This subject has been treated in greater detail in the mini-rapporteur talk by C.E. De Tar.

JET AND FIREBALL STRUCTURE OF MULTI-HADRON PROCESSES

V.P.Shelest
V.A.Steklov Mathematical Institute, Moscow, U.S.S.R.

The universal transverse momentum bound could be considered as one of the most general features of the multihadron production processes from the experimental point of view. It has been known for hadron-hadron interactions, and now there is evidence for it also in γ -hadron, e -hadron as well as in the e^+e^- -annihilation processes.

Therefore the question arises whether this behaviour (i.e., jet structure) of the multihadron production is indeed universal also theoretically?

Define the jet structure as the emission of secondaries with bounded transverse (p_T) and scale invariant longitudinal momentum (p_L) distributions relative to some jet axis. It is necessary to differentiate between the hadronic jets (where the beam fixes the jet axis) and partonic jets with the directions of flight of the involved constituent(s) determining the jet axis.

There are two main parameters of jets: average transverse momentum of secondaries (determining the jet diameter in the momentum space) $\langle p_T \rangle$ and the average multiplicity of secondaries $\bar{N}(s)$, which corresponds to the particle number content of jets. The situation with these parameters in different multiparticle processes is the following.

Hadron-hadron collisions. Average transverse momentum is definitly bounded - e.g., for π -mesons the figures are:

$$\langle p_T \rangle_\pi \sim 300 - 500 \text{ MeV}.$$

Besides, the transverse momentum inclusive distributions can be written in the universal form

$$\frac{d\sigma}{dp_T^2} \sim e^{-\lambda E_c}; \quad E_c = \sqrt{p_T^2 + m^2}$$

$$\lambda \simeq 6 \div 6.5 \text{ GeV}^{-1} \quad \text{(universal parameter)}$$

and these features hold for both "old" and new particles and for arbitrary 2-particle systems.

As concerns the average multiplicity, the experimental data give

$\bar{N}(s) = c \ln s + const$ ($c \approx 3$, universal parameter)

which follows also from all scaling-type models (dual, multiperipheral, uncorrelated jet model, etc.).

Photoproduction of hadrons. Data computible with the previous case.

Electroproduction of hadrons. Data somewhat ambiguous: there are jets, but $\langle p_T \rangle$ increases. This may be due to the real increase in the jet diameter or to the "sea-gull effect"[1], interpretable rather easily in the two-stage pictures of constituent-type multiple production. Up to $-q^2 \simeq 8$ GeV^2 average multiplicity data here are computible with the two previous cases.

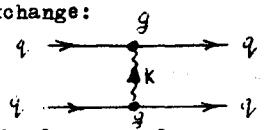
$\bar{N}(s, q^2) \sim \bar{N}(s)$

e^+e^- annihilation. Evidence of jets of hadronic size[2].

Large p_T hadrons production. Evidence of the coplanar, 2-jet structure.

One of the reliable interpretations of the jet universality assumes its direct connection with a universal soft quark-quark interaction[3].

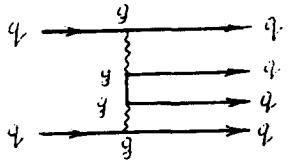
Assume quark-quark interaction through the gluon exchange:



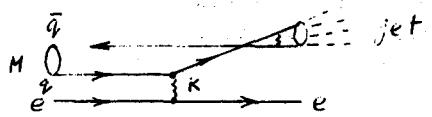
The quark-gluon coupling constant $g(\kappa^2)$ must then be taken large for small κ's (for confinement purposes) and small for large κ's:

$$\lim_{|\kappa^2| \to \infty} g(\kappa^2) = 0$$

which gives the asymptotic freedom of quarks inside the hadron. Then it is clear that for small κ's - that is, for soft interaction of the quarks - the dominating are the higher orders in $g(\kappa^2)$ processes:



Therefore, e.g., for deep inelastic electron-meson scattering the whole process can be separated in the two stages: a) hard (large p_T), weakly coupled electron-quark scattering; and b) soft, strongly coupled quark-quark interaction which, according to the previous conclusion, gives birth to some kind of jet:



Indeed, in the second stage the scattering quark is subject to the confinement force of its spectator companion, and this high-energy interaction must be soft to ensure a large quark-gluon coupling and thus prevent free quarks. In turn the largeness of the coupling provides the asymptotic dominance of multiparticle production in form of a jet (the latter being guaranteed by the softness). As the similar picture can be as well used for meson-meson, baryon-baryon, etc., high-energy scattering, one can consider the soft, high-energy quark-quark scattering as the fundamental mechanism for multiparticle production, predicting the asymptotical universal jet structure.

There is necessary, however, to consider the whole energy range of multiparticle processes. We'll use e^+e^- annihilation into hadrons as a good model for multihadron production mechanisms.

High energy region: (parton model predictions are good)	Main features: a) Scaling of single-particle inclusive distribution[4]. b) Presence of hadron jets; $(1+\cos^2\theta)$ angular dependence[2,5].
Low energy region: (statistical boot strap model predictions are good)	a) No scaling. b) Isotropy in the angular distribution[6].

Therefore, an adequate phenomenological model was proposed to incorporate both descriptions[7,8]

$$\frac{p_c}{\sigma_{tot}(s)} \cdot \frac{d^3\sigma}{d^3p} = F_{fireball} + F_{jet}.$$

The most important distinction of the approach 7 consists in the assumption that both the mechanisms operate simultaneously in every act of e^+e^--annihilation. Thus there must be present the mutual influence of $F_{fireball}$ and F_{jet}.

First of all, the jet influence on the fireball spectrum is to be obtained from the theory in the form of the recoil effect.

Write down the inclusive distribution in the fireball system of rest:

$$F_f'(M,\vec{p}') = Const \cdot M \cdot \exp\left[-\frac{p_c}{T_c}\right]$$

M - fireball mass; T_c - universal temperature ($\simeq 160$ MeV). Then in the oenter of mass system one gets

$$F_f(M,\vec{K};\vec{p}) = Const \cdot M \cdot \exp\left[-\frac{p_\mu u^\mu}{T_c}\right],$$

where u_μ is the four-velocity of the fireball:

$$u_\mu = \left(\frac{1}{(1-v^2)^{1/2}}, \frac{\vec{v}}{(1-v^2)^{1/2}}\right) = \left(\frac{K_0}{M}, \frac{\vec{K}}{M}\right).$$

Inclusive spectrum of secondary hadrons from fireball decay shall then has the form:

$$F_f(M,K,\vec{p}) = Const \cdot M \exp\left[-\frac{p_c (K^2+M^2)^{1/2}}{T_c M}\right] \times$$
$$\times \int \sin\theta^* d\theta^* d\varphi^* (1+\cos^2\theta^*) \exp\left[\frac{\vec{K}\vec{p}}{T_c M}\right],$$

where θ^* is the angle between the jet direction and the e^+e^--collision axis.

Integrating now over the angle between the secondary partide momentum $\vec{p}$ and e^+e^--collision axis, we finally obtain the energy spectrum of secondary hadrons:

$$F_f(M,K,p) = Const \cdot M \exp\left[-\frac{p_c}{T_c(1-v^2)^{1/2}}\right] \cdot \frac{sh\left(\frac{pv}{T_c(1-v^2)^{1/2}}\right)}{\frac{pv}{T_c(1-v^2)^{1/2}}}$$

From this formula one gets different limiting cases.

a) Small q's. $K \simeq 0$. No jets, thus - no recoil.

$$F_f(M,p) = Const \cdot M \cdot \exp\left[-\frac{p_c}{T_c}\right]$$

That is, fireball decay with fixed temperature (T_c) is got.

b) $q \gtrsim 5$ GeV; $K \neq 0$; $p \sim 0$

In this case the energy spectrum has again the fireball-type form, but with different temperature:

$$F_f(M,K,p) \simeq Const \cdot M \cdot \exp\left[-\frac{p_c}{T_1}\right]$$
$$T_1 = T_0 \cdot (1-v^2)^{1/2} < T_c$$

c) $q \gtrsim 5$ GeV; $K \neq 0$; $p \gg T_c$ ($p \simeq p_c$).

Once more the basically fireball-type spectrum is obtained; this time with the temperature larger than the universal T_c :

$$F_f(M,K,p) \simeq Const \cdot M \cdot \frac{(1-v^2)^{1/2}}{pv} \exp\left[-\frac{p_c}{T_2}\right]$$
$$T_2 = T_c \cdot \left(\frac{1+v}{1-v}\right)^{1/2} > T_c.$$

All these results of b) and c) cases form a very good fit to the existing experimental data[7]. The change of the temperature in the fireball-type decay spectra with the account of the recoil effect can be also understood in Doppler-effect terms.

Indeed, at $p \sim 0$ the emission of secondaries goes in a direction opposite to the fireball movement ("red shift"). On the contrary, at large p the emission goes in a direction along the fireball movement ("blue shift").

It could be claimed, therefore, that at $q \sim 3$-4.5 GeV the jet contribution to the inclusive spectrum of secondaries goes mainly through the recoil effect.

But already at $q > 4.5$ GeV this picture is replaced by the <u>two-fireball model</u>, with the moving fireballs imitating the jet structure on the following lines:

a) momenta are aligned with the flight axis,

b) decay spectra show scale-invariant behaviour, <u>if</u> $M_{fireball} \to M_0 = Const$ (Fit gives $M_0 \sim 3$ GeV).

One may then consider at last the total physical high-energy picture of the e^+e^--annihilation: the intermediate photon gives birth to the pair of quarks (or partons) which produces along the excape axis the tail of quark-antiquark states, (this can be regarded, in general, as a string with the initial quark-antiquark pair on its ends). In producing such states the quarks lose their energy (slow down) and in the limit case the initial pair comes almost to a complete stop (pure fireball case). It may be, however, that the initial quarks (or one of them) pick up some quarks, necessary for their screening, out of the tail and thus transform into hadrons (i.e., the string breaks) - and we have the intermediate case of the combination of a jet and a fireball. And, at last,

at rather high energies the string break leads to the two moving fireballs.

This concept, where at high energies there exist not the massive fireballs, but two (or more) bounded in mass fireballs (clusters), is rather similar to the hadron-hadron multicluster picture.

It is amusing to note the curious coincidence of the fireball mass in our picture with the mass of the ψ -particle. This allows one to speculate that the $\psi(3.1)$ gives an essential contribution to the fireball component of e^+e^--annihilation especially as the inclusive distribution resulting from the $\psi(3.1)$ decay is indeed of the fireball type (Ting, 1975).

REFERENCES

1. H.Satz, Y.Zarmi. Lett. al Nuovo Cim., 15, 421 (1976).
2. R.F.Schwitters et al. Phys.Rev.Lett., 35, 1320 (1975).
3. H.Satz. Preprint BI-TP 76/14 (Bielefeld, 1976).
4. J.Bjorken, B.L.Joffe. Preprint SLAC-PUB 1467 (1974).
5. G.Hanson et al. Phys.Rev.Lett., 35, 1609 (1975).
6. R.Baier, J.Engels, H.Satz, K.Schilling. Preprint BI 75/02 (Bielefeld, 1975).
7. M.I.Gorenstein, V.K.Petrov, G.M.Zinovjev. Preprint ITP-76-32E (Kiev, 1976).
8. F.Elvekjaer, F.Steiner. Preprint DESY 75/49 (1975).

MULTIPARTICLE PRODUCTION IN THE POMERON THEORY WITH $\alpha(0) > 1$.

M.S.Dubovikov, Moscow Physical-Technical Inst., Moscow, USSR

B.Z.Kopeliovich, L.I.Lapidus, Joint Institute for Nuclear Research, Dubna

K.A.Ter-Martirosyan, Institute of Theoretical and Experimental Physics, Moscow, USSR

Experimental data on binary reactions at high energies need the Pomeron, which has an intercept above one[1-6]. If $\alpha(0)=1+\Delta$, then the theory is changed drastically when $\xi\Delta \gg 1$, where $\xi = \ln \frac{s}{s_0}$. The hadron scattering at such energies is governed by a new object, a "Froissaron", which is a contribution to the scattering amplitude of unenhanced graph series shown in Fig. 1.

In the impact parameter (b) representation Froissaron contribution to the elastic scattering amplitude has a form of a disk with a radius rising as ξ (if $\xi\Delta \gg 1$):

$$F(\xi, b) = 1 - \exp[-\rho(\xi, b)]. \qquad (1)$$

Here, the eikonal approximation is used and $\rho(\xi,b)$ is a Pomeron pole graph profile function

$$\rho(\xi, b) = z \cdot \exp\left[-\frac{b^2}{4(R^2+\alpha'\xi)}\right], \qquad (2)$$

$$z = \frac{N_A^{(1)} N_B^{(1)}}{R^2+\alpha'\xi} \cdot \exp(\xi\Delta). \qquad (3)$$

We omit here various questions which concern the elastic scattering[4-6], or the theoretical problems of the S -channel unitarity, refs.[7,4-6] (see rep. of K.A.Ter-Martirosyan) and consider only the multiparticle production.

According to the theorem of Abramovsky, Gribov, Kanchely[8] only the pole graph from the series in Fig. 1 gives a contribution to the one particle inclusive spectrum

$$\frac{dc}{dy} = 8\pi \cdot N_A^{(1)} N_B^{(1)} \cdot d \cdot \exp(\xi\Delta)$$

The vertex d is shown in Fig. 2. It is seen from (4) that the inclusive spectrum has a plateau with a height which grows as $\exp(\xi\Delta)$ violating the Feynman scaling. It has been noted previously[8], that expression (4) contradicts the energy conservation sum rule

$$\frac{1}{\sigma_{in}}\cdot\int_0^{\lambda_{3/2}}\exp(y)\cdot\frac{d\sigma}{dy}\,dy<\exp\left(\frac{\xi}{2}\right) \qquad (5)$$

(Here and below we use the c.m. frame). If one chooses the upper limit of integration in (5) very close to the edge of the spectrum $1-2\Delta<\lambda<1$, then inequality (5) is really violated. The solution of this paradox is in fact that AGK cutting rules are valid not in the whole rapidity interval. At the edges of the spectrum the Kanchely-Mueller graph (Fig. 2) does not reflect the contribution of the sum of graphs in Fig. 3 in a proper way. If one takes into account that the incoming energy is divided between Pomerons in Fig. 3 and the effective number of these Pomerons grows as $\frac{\exp(\xi\Delta)}{\xi^2}$, then one finds that expression (4) is valid only in the narrowed rapidity interval $|y|<\frac{\xi}{2}\left(\frac{1}{2}-\Delta\right)$ /4/. So, inequality (5) is fulfilled. The asymptotic form of the inclusive spectrum is shown in Fig. 4.

It is worth noting that at energies available now a large deviation from the described pioture should occur due to the secondary pole contribution. The value of $\xi\gg 10$ is needed for the Reggeon contribution to become negligible in the centre of the inclusive spectrum.

Having (4) one can obtain an expression for the average multiplicity $\langle n\rangle$:

$$\langle n\rangle=(c+d\xi)\cdot\frac{2z}{\varphi(2z)}\underset{\xi\Delta\gg 1}{\approx}2d\frac{N_A^{(1)}N_B^{(1)}}{\alpha'\Delta}\cdot\frac{\exp(\xi\Delta)}{\xi} \qquad (6)$$

where $\varphi(2z)=\int_0^{2z}(1-e^{-\rho})\frac{d\rho}{\rho}$.

At high energies available now $z\approx const$ (this explains the observed geometrical scaling /4-6/), so $\langle n\rangle$ does not deviate from an ordinary linear dependence. Asymptotically it grows exponentially with ξ.

The enhanced graph contribution does not change qualitatively this result. It renormalizes only the values of $\Delta\to\Delta_0=\Delta-g_{11}$ and $d\to d_0=\left(1+\frac{4g_{00}\alpha'}{\Delta_0^2}\right)^2 d$, where g_{00} and g_{11} are the analytical continuation of the g_{mn}-vertex of m-Pomeron transition into n ones[x/].

Now consider briefly the problem of topological cross sections. At accessible energies the experimental data show the existence of the KNO-scaling, which means that /10/

$$\sigma_n=\frac{\sigma_{in}}{\langle n\rangle}\cdot\psi\left(\frac{n}{\langle n\rangle}\right), \qquad (7)$$

where $\psi(x)$ is some energy independent function. If one neglects the fact that energy is divided between produced showers and assumes that each shower has on average ξd -particles, then one finds for $\langle n^q\rangle$ the following expression /6,7/:

$$\langle n^q\rangle=(\xi d)^q\,\Phi_q(2z), \qquad (8)$$

where $\Phi_q(2z)$ is defined in ref. /7/. So, in the modern energy region, where $z\approx const$, the value of $M_q=\frac{\langle n^q\rangle}{\langle n\rangle^q}$ is energy-independent and leads to KNO-scaling with $M_q=\int_0^\infty x^q\psi(x)dx$.

This result remains valid after energy conservation and Poisson distribution on the particle number in showers are taken into account.

As the energy rises, the KNO-scaling should be violated. This can be most easily understood from the fact that at sufficiently high energy ($E\gtrsim 10^8$ GeV), in the multiplicity distribution the Kanchely's oscillations /8/ will emerge. This is a series of maxima, corresponding to different numbers of cut Pomerons in Fig. 3.

As $\alpha(0)>1$, the amplitude of these peaks will rise with energy as $\sqrt{\xi}/K$, where K is the number of peaks. The positions of these maxima correspond to $n=Kd\xi$. There is also a peak arising from diffraction production. It is placed at small multiplicities and has a height rising as ξ.

REFERENCES

1. P.D.B.Collins, F.D.Gault, A.Martin. Phys. Lett., 47B, 171 (1973); Nucl.Phys., B80, 135 (1974); Nucl.Phys., B83, 241 (1974).

x/ Ciafaloni and Marchesini /8/ have obtained in tree approximation that $\langle n\rangle\propto\xi^3$. Their Lagrangian includes the triple Pomeron interaction only. We use the Cardy's type Lagrangian /7/ which contains all multi-Pomeron vertices. It is worth noting also that the described picture is valid only if Pomeron interaction is weak enough /4,6/: $g_{00}<2\Delta_0^2/\alpha'$.

2. A.Capella, J.Thanh Tran Wan, J.Kaplan. Nucl. Phys., B97, 493 (1975).
3. K.G.Boreskov, A.M.Lapidus, K.A.Ter-Martirosyan, P.E.Volkovitsky. Contributed paper A1/24-24.
4. M.S.Dubovikov, K.A.Ter-Martirosyan. Preprint ITEP-37, Moscow, 1976; Contributed paper A1/23-23.
5. B.Z.Kopeliovich, L.I.Lapidus. JETP, 71, 61 (1976); Contributed paper A5/97-48.
6. M.S.Dubovikov, B.Z.Kopeliovich, L.I.Lapidus, K.A.Ter-Martirosyan. JINR, D2-9789, Dubna, 1976; Contributed paper A1/814-133.
7. J.L.Cardy. Nucl.Phys., B75, 413 (1974).
8. V.A.Abramovsky, V.N.Gribov, O.V.Kanchely. Proc. of the 16th Int. Conf. on High Energy Phys., v. 1, p. 389, Yad. Fiz., 18, 595 (1973).
9. M.Ciafaloni, G.Marchesini. Preprint TH. 2146-CERN; Contributed paper A3/925-39.
10. Z.Koba, M.B.Nielsen, P.Olesen. Nucl.Phys., B40, 317 (1972).

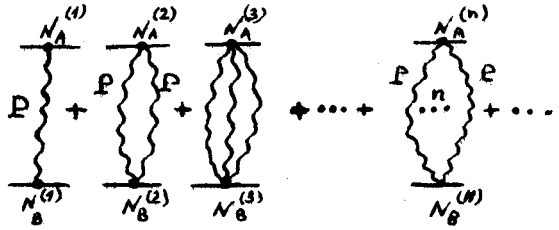


Fig. 1. The unenhanced graph series.

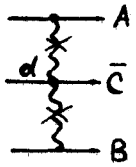


Fig. 2. The Kanchely-Mueller graph.

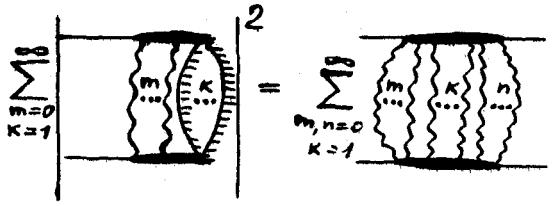


Fig. 3. The cutting of graphs in Fig. 1.

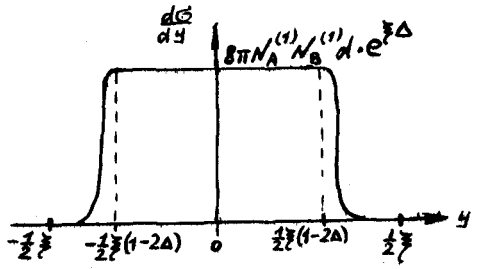


Fig. 4. Asymptotic form of the inclusive spectrum in the central region.

MULTIPARTICLE CORRELATIONS AND IDENTICAL PARTICLE EFFECTS IN THE INDEPENDENT CLUSTER EMISSION MODEL

J.Ranft
Sektion Physik, Karl-Marx-Universität, Leipzig, DDR

A b s t r a c t

In the nucleon approach to phenomenological applications, the model is compared to many different kinds of experimental data. Two recent examples, where this is done using different techniques are discussed. The comparison indicates, that the model is qualitatively consistent with all available data. Our analysis indicates, that identical particle effects due to Bose statistics are present in data on joint rapidity - azimuthal correlations near $\Delta y = \Delta\Phi = 0$. A new approach to this problem is the uncorrelated jet model with Bose statistics by Kripfganz. This model confirms the previous results. Furthermore, taking isospin conservation into account, Bose correlations are predicted in $\pi^+\pi^-$ channels, which should be most easily detectable in the decay of heavy resonances J/ψ.

1. The model and the data

The independent cluster emission model[1] describes the short range correlation in rapidity as due to the uncorrelated production of clusters in the central region. Clusters are produced with limited transverse momentum and flat rapidity distribution. They decay isotropically with an average charged multiplicity $\langle n_{ch} \rangle = 2$ to 2.5. There are neutral as well as charged clusters. Experimental evidence indicates, that some of the clusters are known resonances but there might be also a continuum. Quantum numbers like charge Q, strangeness S and baryon number B seem to be compensated locally in rapidity. Long range correlations are present due to the effect of energy momentum conservation and due to the presence of leading particles[2]. Identical particle effects are explained as due to the effect of Bose statistics[3] and/or due to second order interference[4]. The local compensation of transverse momentum was proposed[5] but no for no-positive evidence was found[6]. Only first attempts have been made so far to connect the dynamics of cluster production with the quark-gluon dynamics of strong interactions[7].

The model has been applied phenomenologically using data on multiparticle production in many different forms, inclusive and semiinclusive single particle distributions and two particle correlations for leading as well as produced particles, multiplicity distributions and multiplicity numbers, neutral charged correlations, rapidity gap distributions, charge distributions and charge transfer correlations, azimuthal correlations in their Φ, y, $p_\perp$, M_{12} dependence, left-right multiplicities, etc.

2. Model building and phenomenology

For phenomenological applications of the model it is important to use all available data as constraints. If only one particular kind of data is used, the danger is, that this data

might be rather unsensitive to some of the properties of the model. Recent examples for phenomenological applications in this spirit are due to Sruevde and Plant[8] and Kirrehner[9].

Arnecdc and Plant[8] investigete the model using Monte Carlo calculations, their input includes: local compensation of charge, charged and neutral clusters with an average charged multiplicity $\langle n_{ch}\rangle \approx 2$, a flat x distribution for leading particles and limited transverse masses of clusters. Rather unclear remains the meaning of their statement, that in the calculation the experimental charged particle distribution is enforced. They calculate rapidity gap distributions, rone and charge transfer distributions and inclusive and semiinclusive rapidity correlations. The model is found tc be consistent with all experimantal data considered.

3. The independent cluster emission model of Kirrohner

Kirrohner[9] formulates his model using generating functional techniques. His input includes: Poisson weights and factorized distributions for produced and leading clusters, exact energy momentum conservation in cluster production, non-trivial mass distributions for central and leading clusters. The clusters decay isotropically, iscspin is conserved in the decay, leading clusters have the quantum numbers of the primary particles. He is able tc calculate multiplicity moments and neutral charged correlations, inclusive and semiinclusive single particle distributions and correlations for leading and produced particles, left-right distributions and gap distributions. Formulating the model in the language of coherent states he calculates the overlap function. He needs clusters decaying into 2 to 2.5 charged particles and finds the model consistent with all experimental data considered.

We indicate shortly, how he proceeds. The starting point is the distribution of 2 leading ($V(p_i')$) and in central ($U(k_i)$) clusters

$$P_L(m|k_1\dots k_m, p_1', p_2') = V(p_1')V(p_2')\,\frac{e^{-\lambda}\lambda^m}{m!}\prod_{i=1}^{m} U(k_i)\cdot\delta\Big(p_1+p_2-p_1'-p_2'-\sum_{(1)} k_i\Big).$$

The generating functional is constructed as follows

$$G_L(\phi,\psi) = \int dp_1' dp_2' \psi(p_1')\psi(p_2')\cdot\sum_m \int\dots\int P(m|k_1,\dots k_m, p_1' p_2')\prod_{i=1}^{m}\Phi(k_i)\,dk_i =$$

$$= \int e^{iQy} dy \int V(p_1')\psi(p_1') e^{ip_1' y} dp_1' \int V(p_2')\psi(p_2') e^{-ip_2' y} dp_2' \int dg\, e^{-igy}\, G_c(g,\phi) \quad (2)$$

with the generating functional for central clusters

$$G_c(Q|\phi) = e^{-\lambda}\int dx\, e^{iQx}\exp\Big[\lambda\int dk\, U(k)\phi(k)\, e^{-ikx}\Big]. \quad (3)$$

For the argument functions ϕ and ψ, the generating functionals for the cluster decay have to be inserted. For many applications it is suffioient to know the generating functionals and their derivatives fer constant argumento, these can be evaluated

$$G_c(1) \sim e^{-\lambda}\,\frac{8\pi^2}{s}\left(\frac{s}{m^2\gamma^2}\right)^{\lambda}\frac{1}{\Gamma(\lambda)}. \quad (4)$$

From the generating functicnal all quantities of phencmenological interest are obtained in analytic form. As an example, the single particle distribution is obtained as

$$f_1(y) = \frac{1}{G_L(1,1)}\cdot\frac{\delta G}{\delta\varphi}\Big|_{\varphi=1} =$$

$$\int\frac{\delta G_L}{\delta\Psi(y,\mu)}\Big|_{\Psi=1}\frac{\delta g_L(y,\mu|\varphi)}{\delta\varphi(y)}\Big|_{\varphi=1} dy\,d\mu + \int\frac{\delta G_L}{\delta\Psi(y,\mu)}\Big|_{\Psi=1}\frac{\delta g_c(y,\mu|\varphi)}{\delta\varphi(y)}\Big|_{\varphi=1} dy\,d\mu \quad (5)$$

The two terms give the contributions from leading and central clusters. g_L and g_c are the generating functionals for the decay of leading and central clusters, μ and y are cluster mass and rapidity.

In Fig. 1 we plot the neutral charged correlation at 205 Gev as calculated by Kirrohner[9]. The curve shows the effect of energy-momentum conservation in his approach.

4. Azimuthal correlations and the effect of Bose statistics

In[3], see also[10] we proposed a procedure tc include the effect of Bose statistics into the independent cluster emission model. It was found that the sharp peak seen around $\phi = 0$ in the azimuthal angle distribution $dN^{\pm\pm}/d\phi$ of identical pion as well as the sharp dip near $\Delta y = 0$ in the azimuthal asymmetr parameter $B^{\pm\pm}(\Delta y)$ plotted versus the rapidity difference Δy is due to Bose correlation. This correlation is also seen in the different behaviour of the asymmetry parameter B for $\pi^+\pi^-$ and $\pi^\pm\pi^\pm$ combinations, when plotted as function of the transverse momentum difference $\Delta p_\perp$ or as function of the average transverse momentum $\langle p_\perp\rangle = \langle p_{\perp 1} + p_{\perp 2}\rangle/2$ of the two pions.

If contributions from large invariant masses M_{12} of the two pions $\pi^+\pi^-$ as well as $\pi^\pm\pi^\pm$ are not excluded experimentally, the differences in the asymmetry parameters B^{+-} and $B^{\pm\pm}$ result partly from resonances. This effect was already calculated in[11] considering a cluster mass distributior it was taken into account in[3] and [10] by using different parameters B_{1F}^{+-} and $B_{1F}^{\pm\pm}$ characterizing single fireball decay. Experimentally it is of advantage to study the Bose correlation excluding contributions from large M_{12} exporimentally for $\pi^+\pi^-$ as well as for $\pi^\pm\pi^\pm$.

Largely free from resonance influence is the joint rapidity -azimuthal $\Delta y - \Delta\phi$ correlation. Data were published by Oh et al.[12] and Biswas et al.[13], see Fig. 2. The analysis of these data was given in[14] and [10]. The correlation R^{--} for identical particles, shown in Fig. 1, exhibits a very steep peak at $\Delta y = 0$ and $\Delta\phi = 0$. The correlation length in rapidity $L^{--} \approx 0.3$ is much shorter then the correlation length in R^{+-} which is characteristic for cluster decay. The peak in the $\pi^+\pi^-$ correlation can not be removed by subtracting resonances, a procedur which influences most by the $\pi^+\pi^-$ channel. From our comparison we conclude that evidance for Bose correlations is found in joint rapidity-azimuthal correlations. However it should be noted, that the effect is small due to the narrowness of the peak. One phenomenological assumption in our approach[3,10,14] was factorization between phase space and Bose effect in the two particle distribution. This factorisation in found in the rigorous treatment of Kripfganz[15].

5. The UJM with Bose statistics of Kripfgans[15]

Kripfgans considers an uncorrelated jet model with exact treatment of Bose statistics and Isospin conservation. The level density for a N particle system with Bose statistics

$$\mathcal{L}_N(Q^2) = \mathrm{Tr}_N\, P^Q P_i^I \qquad (6)$$

where P^Q and P_i^I are the projection operators ensuring energy momentum and isospin conservation, is calculated using the appropriate commutation relations $[a_p, a_{p'}^+] = \delta_{pp'}$. The result, considering only energy momentum conservation was given by Chaichian et al.[16], the full result is due to Kripfgans[17]. Applied to the UJM[15] with a transverse momentum cut off function $f(p_{\perp i}^2)$ the level density (without isospin for the moment) can be written in the form of a cluster decomposition

$$\mathcal{L}_N(Q^2) = \sum_{\{\ell_\mu\}} \delta\Big(N - \sum_\mu \mu\ell_\mu\Big) \cdot \int \delta^4\Big(Q - \sum_\mu \sum_{j_\mu}^{\ell_\mu} n p_{j\mu}\Big) \times$$
$$\times \prod_\mu \frac{1}{\ell_\mu!} \prod_{j_\mu}^{\ell_\mu} d^4p_{j_\mu}\, \frac{B}{N}\, f\big(p_{\perp j_\mu}^2\big) \cdot \delta_+\big(p_{j_\mu}^2 - m^2\big) \qquad (7)$$

The sum goes over all possible combinations of Bose clusters out of particles with identical momenta. In the Boltzmann limit only the term $\ell_1 = N$, $\ell_\mu = 0$ for $\mu \geq 2$ is considered, this is the invariant phase space usually considered in high energy physics. Inclusive single and two particle distributions are obtained from (7) as follows

$$2E \frac{dN}{d^3p} = B\, f(p_\perp^2) \sum_{k=1}^{\infty} \mathcal{L}_{N-k}(Q-kp) \big/ \mathcal{L}_N(Q) \qquad (8)$$

$$2E_1 2E_2 \frac{dN^{\pm\pm}}{d^3p_1 d^3p_2} = B^2 \cdot f(p_{\perp 1}^2)\, f(p_{\perp 2}^2) \sum_{k,k'} \mathcal{L}_{N-k-k'}(Q-kp_1-k'p_2) \big/ \mathcal{L}_N(Q)$$
$$+ B \cdot f(p_{\perp 1}^2) \cdot 2E_1 \cdot \delta^3(p_1 - p_2) \cdot \sum_k (k-1) \cdot \mathcal{L}_{N-k}(Q-kp_1) \big/ \mathcal{L}_N(Q) \qquad (9)$$

The first term of the two particle distribution corresponds to the usual UJM (note however that the correct level density $\mathcal{L}_N$ is used), both particles come from different Bose clusters. In the second term both particles come from the same Bose cluster, this term gives the Bose correlation. For phenomenological proposes we use the usual approximation for the $p_\perp$ and ϕ dependence of phase space and write

$$2E_1 2E_2 \frac{dN^{\pm\pm}}{d^3p_1 d^3p_2} \sim \Big[B^2 f(p_{\perp 1}^2) f(p_{\perp 2}^2) + w_1 f\Big(\frac{(p_{\perp 1}+p_{\perp 2})^2}{2}\Big)\Big] \times$$
$$\times 2E_1 \cdot \delta^3(p_1 - p_2) \cdot \Big(1 - \frac{\vec{p}_{\perp 1}\vec{p}_{\perp 2}}{\langle p_\perp \rangle^2} \cdot \frac{\pi}{2} \cdot e^{+\cdot} \cos\phi\Big) \qquad (10)$$

To (10) a term representing central cluster production might be added if the usual short range correlation is also to be studied. To take account of the finite extension in space of the interaction region the δ function in (10) is replaced by a Gaussian

$$\exp\left(-\frac{(y_1-y_2)^2}{(\Delta y)^2} - \frac{(\vec{p}_{\perp 1} - \vec{p}_{\perp 2})^2}{(\Delta p_\perp)^2}\right) \qquad (11)$$

with parameters $\Delta y \approx 0.3$ to 0.4 and $\Delta p_\perp \approx 0.25$ Gev/c a good agreement with the shape of the peak in the $\Delta y - \Delta\phi$ correlation is obtained, see Fig.2.

6. Isospin correlation leads to Bose correlations of $\pi^+\pi^-$, for instance in J/ψ decay

Considering isospin correlation in (6) Kripfgans[15] obtains also the two particle distribution for $\pi^+\pi^-$ in the form (9), however with a factor $C^{I,i}_{N_+N_-N_0}$ in front of the second term. This factor is related to Cerulus weights. The $C^{I,i}_{N_+N_-N_0}$ alternate in sign for exclusive decays or are small. Therefore, the not-effect in inclusive distributions is expected to be small. In exception is the decay of states with fixed isospin in the initial state. For instance in the decay $J/\psi \to \pi^+\pi^-\pi^0$ the Bose correlation is expected in the $\pi^+\pi^-$ distribution with negative sign.

7. Summary

(i) All presently available data are qualitatively consistent with the model.

(ii) There is evidence for Bose correlations from joint rapidity azimuthal correlation in $\pi^\pm\pi^\pm$ at $\Delta y = \Delta\phi = 0$.

(iii) Due to isospin conservation Bose correlations should also exist in the $\pi^+\pi^-$ channel. This should be most easily detected in the decay $J/\psi \to \pi^+\pi^-\pi^0$. The presence of the Bose correlation in the $\pi^+\pi^-$ channel indicates that Bose correlations[3] and interference correlations[4] are not completely equivalent. The Bose correlation is a dynamical property of the strong interaction itself.

(iv) To exclude resonances and enrich the sample, the Bose correlation should be studied experimentally only at small masses M_{12}.

References

1. J.Ranft, Fortsch.d.Physik 23, 467 (1975) and references given there.
2. J.Benecke, A.Bialas, E.H. de Groot, Phys.Lett. 57B, 447 (1975).
   E.M.Elgenfritz, Helsinki preprint 1976, subm.paper 398.
   J.Benecke, A.Bialas, S.Pokorski. München preprint , 1976.
3. J.Ranft, G.Ranft, Phys.Lett.53B,188 (1974); Nucl.Phys. B92, 207 (1975).
4. G.I.Kopylov, M.I.Podgoretzki, Yad.Fiz. 18,656 (1973).
   E.V.Shuryak, Yad.Fiz. 18, 1302 (1973).
   G.Coccorvi, Phys.Lett. 49B, 459 (1974).
5. A.Krzywicki, Nucl.Phys. B86, 296 (1975).
   D.Weingarten, Phys.Rev. D11, 1924 (1975).
6. J.Ranft, G.Ranft, Leipzig preprint K144-HEP 1514 (1975) subm.paper 679.
   J.Memmev, P.Grassberger, priv.comm. 1976.
7. L.Van Hove, S.Pokorski, CERN preprint TH 1930 (1974).
   J.D.Bjorken, G.R.Farrar, SLAC-preprint SLAC-PUB-1298 (1973).
   W.Ochs California Institute of Technology preprint CALT-68-542 (1976); J.Ranft, G.Ranft, Leipzig preprint KMU-HEP-7603 (1976); subm.paper 678.
8. A.Ameodo, G.Plant, Nice preprint NTH-75/8,NTH 76/3 (1976).
9. R.Kirrohnev, Nucl.Phys. B101, 507 (1975).
   R.Kirrohnev, Leipzig preprint KMU-HEP 7601 (1976), subm.paper, 674: R.Kirrohnev , priv. communication.
10. G.Ranft,J.Ranft,B.Sabau,K.G.Fadeev,A.N.Solomin,Nucl.Phys. B86, 63 (1975); G.Ranft, J,Ranft,R.Kirrohnev,N.G.Fadeev, S.Lutov,R.M.Nazargulov,Leipzig preprint KMU-HEP-7602, subm.paper 677.
11. G.Ranft, J.Ranft, Lett. Nuovo Cim. 10, 485 (1974).
12. B.Y.Oh et al., Phys.Lett. April 1975.
13. N.N.Biswas et al., Phys.Rev. Lett. 35, 1095 (1975).
14. G.Ranft, J.Ranft, Phys.Lett. 57B, 375 (1975).

15. J.Kripfganz, Leipzig preprint KMU-HEP-7607 (1976); contr. paper 399.
16. H.Chaichion, R.Hagedorn, M.Hayashi; Nucl.Phys. B92, 445 (1975).
17. J.Kripfganz, Nucl.Phys. B100, 302 (1975).

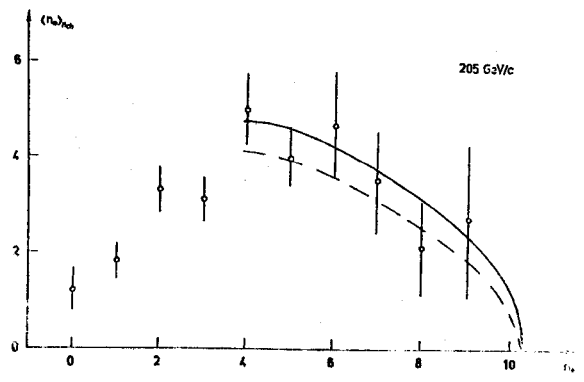


Fig. 1. The associated average neutral multiplicity $< n_0 >_{n_{ch}}$ in pp collisions, at 205 GeV. The curves are calculated by Kirschnev[9].

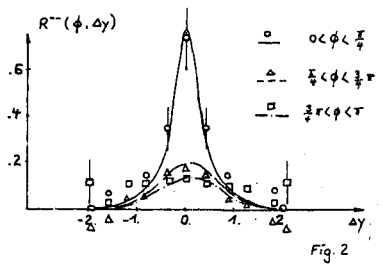


Fig. 2. Divided correlation function R^{--} as function of Δy for different $\Delta\phi$ ranges. The data are due to Bisnas et al.[13]. The curves are calculated by Kripfganz[15] and similarly by Ranft et al.[10].

PLENARY REPORT

MECHANISMS OF MULTIPLE PRODUCTION PROCESSES

I.M.Dremin

FIAN, USSR

1. Introduction

My object is to speak about theoretical approaches to multiple production processes. The variety of the approaches enforces me to start with some classification, this classification being, of course, rather relative.

A large number of models proceeds from the notion about common excited system produced by colliding hadrons. This class of models, including hydrodynamical, statistical, thermodynamical and statistical bootstrap models will be referred to hereafter as H (hydrodynamics) models.

Sometimes the production process is conjectured as due to excitement and decay of two colliding particles, that is two systems are assumed to be formed, originating from two initial hadrons. The fragmentation, bremsstrahlung and inelastic diffraction models are pertained to this F (fragmentation) group.

The largest group of models describes the multiple production process as a result of formation of many excited centers. The typical example is the multiperipheral model (so this group is referred to as M group), which is connected closely with inclusive Regge approach, parton description, independent cluster production model and uncorrelated jet models. An eikonal prescription is used widely to take into account rescattering effects.

An interesting direction is given by the papers where attempt is made to interrelate the mechanism of multiple production with internal structure of particles, that is with their constituents (C-group)-quarks, gluons, etc.

Besides the models there are phenomenological (P group) attempts to connect different features of multiple production.

Experimental data indicate the existence of leading and pionization particles thus giving an

evidence for applications of different models.

The idea of fragmentation can be applied to leading particles. Such particles appear in peripheral blocks of multiperipheral diagrams and they are viewed as being formed by quarks which fly through in constituent picture.

At the same time one can attempt to use statistical approach to the particles in pionization region (to the whole set of these particles or to some subunits which can be produced by multiperipheral or some other mechanism). So as a rule one deals with many-component description of multiple production processes.

There is some periodicity in the development of the theory of multiple production. Approximately once a decade ideas appear influencing considerably the direction of research.

In 1950 Fermi's paper pushed forward the statistical approach which was later developed by Landau as a hydrodynamical theory. In 1960 peripheral diagrams became very popular giving rise to multiperipheral theory. In 1970 the new development to this approach was stimulated by ideas of inclusive description and scaling in the frames of parton and fragmentation models.

As the decade has not yet passed and new theoretical ideas have not been developed I'll confine myself mainly to giving an account of recent developments of approaches mentioned above to show to which extent they can accomodate continuously increasing flow of new experimental data.

II. Statistical and hydrodynamical approach

Experimantal data on inclusive spectra at high energies have raised interest in statistical and hydrodynamical models during recent years. The point is that only these models explain naturally the exponential damping of transverse momenta of produced particles and go away from somewhat monotonous plateau picture for rapidity distributions.

An account of these models was given at many conferences. So, after short introduction, I'll give a review of only those papers, which appeared recently.

The basic assumption of statistical approach to multiple production [1,2] is that the subsystem produced at hadron collision comes quickly to the state of thermodynamical equilibrium due to strong interaction. The three stages can be distinguished.

1. Initial stage of mixing and forming of highly excited system. 2. Hydrodynamical stage of isoentropic expansion. 3. Final stage when system breaks-up into secondary particles.

To describe completely the evolution of the system it is necessary to specify:

1. Energy-momentum conservation. 2. Statistical momentum distribution. 3. State equation. 4. Chemical potential. 5. Initial conditions and break-up prescription.

As a pattern to compare with I'll give a summary of Landau hydrodynamical model. Energy-momentum conservation is given by

$$\partial T_{ik} / \partial x_k = 0 \qquad (1)$$

where

$$T_{ik} = (\varepsilon + p)\, u_i u_k - p g_{ik} \qquad (2)$$

is energy-momentum tensor of ideal relativistic fluid, ε is density of energy, p is the pressure, u_i -four-velocity, $g_{00} = -g_{ii} = 1$.

Pion momentum distribution is given by Bose distribution in an accompanying frame:

$$dN = \frac{g V}{(2\pi)^3} \cdot \frac{d^3 q}{e^{E/T} - 1} \qquad (3)$$

where $E = \sqrt{q^2 + m^2}$ is the energy of the paricle, g is the number of its spin and charge degrees of fredom ($g = 3$ for the pion), T is the temperature and V is the volume of the final state.

State equation is taken in the form

$$p = \varepsilon / 3 \qquad (4)$$

valid for three-dimensional gas of relativistic particles.

Chemical potential is

$$\mu = 0 \qquad (5)$$

So the number of particles is not fixed but have to be determined by equilibrium condition (similarly to the case of the black-body radiation), that is the thermodynamical potential is zero,

$$\varepsilon - TS + p = 0 \qquad (6)$$

(S is the entropy density). From here one can easily obtain that $\varepsilon = \varkappa T^4$.

It is assumed that at the initial moment the hadron system is a disk at rest ($v = 0$ at $t = 0$) the redius of the disk being $\sim \frac{1}{m_\pi}$ and its thickness is $\sim \frac{1}{m_\pi} \cdot \frac{m}{E_0}$ (m_π, m - pion and nucleon, masses, E_0 -CMS energy). The expansion of the system is controlled by eqs. (1.)-(5) and a break-up into free particles occurs when temperature becomes of the order of m_π .

The physical consequences of this picture are well known. The mean multiplicity increases like $s^{1/4}$, the rapidity distribution is well approximated by Gaussian exponent, etc.

The following directions of its development can be noted:

1) attempts to give a more detailed description resembling kinetic approach and closely connected with non-linear Lagrangians of the field theory; 2) incorporating the information on internal structure of colliding particles; 3) revision of the points 3)-5) mentioned above; 4) detailed comparison with experimental data.

In more general kinetic approach[4,5] (leading in some limit to hydrodynamics the Wigner distribution function is used:

$$F(p,R) = \int d^4\xi \, e^{ip\xi} \langle \Psi_{in} | \Phi(R - \tfrac{\xi}{2}) \Phi(R + \tfrac{\xi}{2}) | \Psi_{in} \rangle \qquad (7)$$

where Φ are the field operators, averaging is performed over in-states and Heisenberg picture is used. Accepting Ψ_{in} to be two-particle states and using the relation of unclusive spectra to many-particle amplitudes it is easy to see that the single-particle inclusive spectrum can be expressed in terms of Wigner F -function:

$$2\omega \frac{d^3N}{d^3p} = \frac{(p^2 - \mu^2)^2}{(2\pi)^3} \cdot F(p, q = 0) \qquad (8)$$

At the same time, F -function can be shown to obey the kinetic-type equations with nonlinear term depending on the form of the Lagrangian. In some approximation a transition to hydrodynamical theory can be demonstrated[5]. The connection of nonlinear Lagrangians with hydrodynamical theory parameters was considered many years ago[6]. Now it is suggested to establish this connection in the frame of kinetic approach where Regge-type inclusive description can be incorporated to.

Hydrodynamical theory is usually supposed to give a "macroscopic description" of the extension process as the density of the matter is too strong to say about individual particles. If one accepts a hypothesis of pointlike constituents of hadrons, then it is possible to give[7,8] a treatment of hydrodynamics which suggests that just statistical properties of constituents (but not dynamics of their interaction) are responsible for basic features of the process, such as one-particle distributions, for example.

The presence of phase transition is the characteristic feature of a statistical approach in which the thermodynamical properties of the system are expressed through S-matrix of the particles constituting the system[10,11]. The state equation is different from (4) in this case and has the form $p = \frac{\varepsilon}{5}$ at high energies. Similar picture, with the presence of phase transition, arises when one attempts to use the results of field theory models with symmetry breaking in high energy physics[9].

Let us note that phenomenological attempts to modify the state equation had been undertaken earlier[6,12-16]. In particular the state equation

$$p = c_c^2 \varepsilon \qquad (9)$$

was investigated with arbitrary constant value of C_0. The value of C_0 was connected with a power of nonlinear Lagrangian[6] $C_0^2 = \frac{1}{2n-1}$ for $L_{eff} \approx \lambda \left(\frac{\partial}{\partial x_\mu}\varphi\right)^{2n}$. For this case $p \sim T^{\frac{c_0^2+1}{c_0^2}}$, $S \sim T^{1/c_0^2}$, $\bar{n} = E_{cm}^{(1-c_0^2)/(1+c_0^2)}$.

Calculation[13,14] of C_0 was performed taking into account a set of known resonances. The equations used are the following

$$c_0^2 \equiv \frac{\partial p}{\partial \varepsilon} \; ; \; p = \frac{1}{3}\sum_i \int \frac{d^3q \cdot V g_i}{(2\pi)^3} \frac{q^2}{E_i} \cdot \left[e^{E_i/T} - 1\right]^{-1} \quad (10)$$

$$\varepsilon = \sum_i \int \frac{d^3q \cdot V g_i}{(2\pi)^3} \cdot E_i \cdot \left[e^{E_i/T} - 1\right]^{-1} \quad (11)$$

where sums are taken over resonances. The results are given in Fig.1.

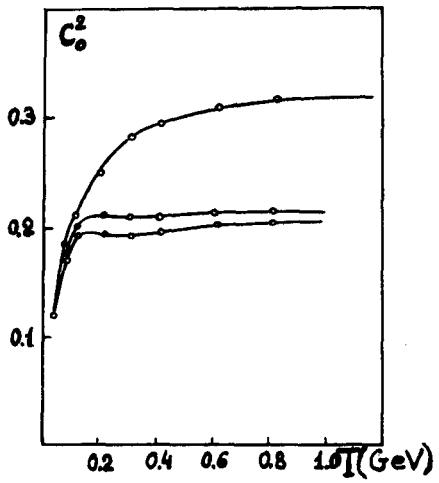


Fig. 1. The T-dependence of C_0^2 [14]. The upper curve was obtained without resonance contribution in (10), (11). The lower curves are for different sets of resonances.

One can see that C_0^2 is close to 1/5 at high temperature. It is interesting to note that comparison with experimental data also suggests the same value for C_0^2 [13,14] in order to obtain the best agreement between theory and experiment.

Quantitative comparison with experiment [13-15, 17-31] will be considered below. Here I wish only to emphasize that one needs to take a special care when selecting a system (or subsystem) to apply a statistical treatment[15]. It is connected mainly with peripheral nature of collisions displaying through appearence of leading particles whose treatment is far from being definite in the frames of statistical approach (compare[12,13]).

At the same time it is the peripheral character of interactions that underlies fragmentation and multiperipheral models.

III. Fragmentation Models

According to fragmentation models[32-37] the inelastic interaction of two hadrons proceeds through excitation of one or both of them whith subsequent decay into many particles. The energy and the angular momentum could be transferred from one hadron to another. Other internal quantum numbers of an excited system coincide with those of its parent hadron.

The formation of two centers of particle emission, each of which reminds its primary hadron, is a distinctive feature of fragmentation models.

Not very much work was done on F-models since 72-74-Conferences. The reason is that even though their particular realizations[36,37] can get a reasonable behaviour of the mean multiplicity

$$\langle n \rangle \sim \int^{\sqrt{s}} \rho(M) n_e(M) dM \sim \int^{\sqrt{s}} M^{-2} M dM \sim \ln s \quad (12)$$

they predict rather strong fluctuations in individual events

$$f_2 = \langle n(n-1) \rangle - \langle n \rangle^2 \sim \int^{\sim\sqrt{s}} \rho(M) n_e^2(M) dM \sim \sqrt{s} \quad (13)$$

Here $\rho(M)$ is the probability of production of an excited state of mass M and $n_e(M)$ is its decay multiplicity.

The missing mass dependence of the associated multiplicity differs in the experiment from the behaviour of $n_e(M)$.

The above-mentioned as well as some other features of the fragmentation model are in favour of the opinion that its particular realizations could be if at all, applied for very restricted

energy region[37], or just asymptotically [36].

Another feature of F -models is the presence of long-range correlations at high energies. Even if one assumes the independent emission of clusters with the rapidity plateau within the bremsstrahlung model[38-40] the long-range correlations of nucleons persist. But such a model is surely quite similar to multiperipheral ones.

The fragmentation ideas combined with reggion exchange are widely used for the description of diffractive dissociation processes which are described in Kaidalov's report.

IV. Multiperipheral Scheme

The production of many centers of particle emission is a general feature of the multiperipheral approach[41-43]. It follows from the main assumption about small transferred momenta. The graph representation of the process is shown in Fig.2. At large enough energies the multiperipheral chain is long and one can use the integral equation for total cross sections[41-43]:

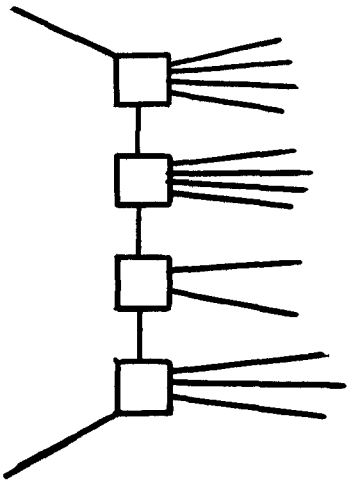


Fig. 2.
The multiperipheral graph.

$$\sigma = \bar{\sigma} + [\bar{\sigma}, \sigma] \qquad (14)$$

where

$$[\bar{\sigma}, \sigma] \approx \frac{1}{16\pi^3 s^2} \int \frac{dK^2 s_1 ds_1 s_2 ds_2}{(K^2+\mu^2)^2} \bar{\sigma}(s_1, K^2)\, \sigma(s_2, K^2) \qquad (15)$$

The function $\bar{\sigma}$ is the total cross-section of all nonperipheral processes plus interference terms of those processes with peripheral ones. Therefore, it can contain the resonance production and elastic diffraction as well as some part of the inelastic processes.

Similar equations could be derived[44] for inclusive spectra (for example, for $F_1 = E\frac{d^3\sigma}{d^3p}$):

$$F_1 = \bar{F}_1 + [\bar{F}_1, \sigma] + [\bar{\sigma}, F_1] \qquad (16)$$

where $\bar{F}_1$ is the single-particle inclusive spectrum of particles produced in non-peripheral processes.

The solution of eq. (16)

$$F_1 = \bar{F}_1 + [\bar{F}_1, \sigma] + [\sigma, \bar{F}_1] + [\sigma, [\bar{F}_1, \sigma]] \qquad (17)$$

consists of the sum of contributions from nonperipheral processes (the first term), from the fragmentation of colliding hadrons (the second and third term) and from the pionization component (the last term) - see Fig. 3.

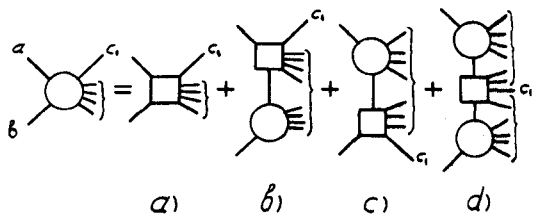


Fig. 3.
Inclusive multiperipheral graphs.

Thus the multiperipheral approach (14), (16) incorporates the multicomponent structure of inelastic processes.

The main advantage of the graphical representation is both in the clear-cut interpretation of inelastic processes and especially in its connection with the main parameters of elastic scattering (as well as with the amplitudes of processes $3 \leftrightarrow 3$ for single-particle inclusive spectra).

The general conclusions of the scheme are well known. Those are the Regge behaviour of

elastic scattering amplitude, the logarithmical increase of the mean multiplicity, scaling and plateau in rapidity distributions, short-range correlations, etc.

Strictly speaking all those predictions are valid at extremely high energies where eqs. (14), (16) can be used, calculations are simpler and the theorist's life is not questioned by experimentalists.

To complete the picture I start from "asymptotical results" and then move to the realistic models, to the role of conservation laws, etc.

The multiperipheral dynamics of t-channel iterations of low-energy interactions produces the elastic shadow scattering described by the reggeon exchange. Replacing the multiperipheral ladder by the reggeon one can use all knowledge of the reggeon properties which is available from two- and quasitwo-particle processes. It is well known[45] that the inclusive spectra in the fragmentation region for the reaction $AB \to C+X$ are described by the formula

$$\frac{d\sigma^{c}_{AB}}{dy} \sim g_B V_{A\tilde{c}}(y)\, \exp\left[(\alpha(0)-1)\,Y\right] \qquad (18)$$

(y is the rapidity, $Y \sim \ln s$). The limiting fragmentation follows from (18) at $\alpha(0)=1$:

$$\frac{d\sigma^{c}_{AB}}{dy} \sim g_B V_{A\tilde{c}}(y) + O(s^{-1/2}) \qquad (19)$$

up to the terms of the order of $s^{-1/2}$.

Pionization region is characterized by:

$$\frac{d\sigma^{c}_{AB}}{dy} \sim g_A g_B V_{\tilde{c}}\, \exp\left[(\alpha(0)-1)\,Y\right], \qquad (20)$$

i.e., by the rapidity plateau for $\alpha(0)=1$:

$$\frac{d\sigma^{c}_{AB}}{dy} \sim g_A g_B V_{\tilde{c}} + O(s^{-1/4}) + O(s^{-1/2}) \qquad (21)$$

up to the terms of the order of $O(s^{-1/4})$ due to non-leading trajectories and of the order of $O(s^{-1/2})$ due to the kinematical bounds[52]. The former terms are positive if the P'-residue is positive as it follows from the behaviour of total cross sections but they could become negative if the cluster production is taken into account[93]. The kinematical terms are always negative.

Let me note that the rapidity plateau is widely used in parton models where a hadron develops the parton ladder with the energy of each subsequent parton being $\sim \lambda = const$ times smaller than the energy of the preceding one.

From eq. (21) one gets the logarithmical increase of mean multiplicity (for $\alpha(0)=1$):

$$\langle n \rangle = \frac{1}{\sigma}\int \frac{d\sigma}{dy}\,dy = a\,Y + b. \qquad (22)$$

Two-particle correlations are given by

$$C_2(y_1,y_2) = \frac{1}{\sigma}\cdot\frac{d^2\sigma}{dy_1 dy_2} - \frac{1}{\sigma^2}\frac{d\sigma}{dy_1}\frac{d\sigma}{dy_2} \sim e^{-\beta|y_1-y_2|} \qquad (23)$$

where $\beta = 1-\alpha_f(0)$, $\alpha_f(0)$ are the Regge-trajectories closest to Pomeron ($\beta = 0{,}5$ if $\alpha_f(0) = 0{,}5$, i.e. there are short-range correlations and β is small if the Regge-cuts close to Pomeron are important, i.e. there is no short-range ordering).

The experimental data about total cross sections initiated the reggeon scheme with Pomeron lying above one[46] in which the different energy behaviour appears for different energy intervals. Since just experiment created this scheme I consider its predictions concerning multiple production processes only in the region of energies now available. Its main results are:

1. Total cross sections increase with energy like

$$\sigma_{tot} \sim e^{\Delta Y} \approx 1 + \Delta Y. \qquad (24)$$

It reminds of the logarithmical law because the value of Δ is small ($\Delta \sim 0.06 \div 0.08$[47]).

2. The inclusive distribution develops a plateau in the central region with

$$\frac{1}{\sigma}\frac{d\sigma}{dy}\Big|_{y=0} \sim const + O(?), \qquad (25)$$

i.e., scaling is valid for the function $\frac{dN}{dy} = \frac{1}{\sigma}\cdot\frac{d\sigma}{dy}$ (but not for $d\sigma/dy$) and the mean multiplicity

$$\langle n\rangle \sim a Y + b \qquad (26)$$

increases logarithmically.

The t -channel bootstrapping of M -models suffers of the problems of S-channel unitarity i.e. the usual question to all of them is how the elastic (absorptive corrections) and inelastic (multiple ladder creation) rescattering influences the final states. This is the so-called Regge-cut problem. Another question is how the Pomeron is renormalized. Both of them are closely connected with the problems of final state interaction.

Self-consistency of the scheme and its asymptotical predictions have been mainly investigated (see, for example, /48/). The AGK cut rules /49/ for inclusive distributions are widely used. Simple (but may be simplified) prescriptions for calculation of rescattering effects in the pionization region can be derived from eikonal approximation/50/ where the number of exchanged reggeons (ladders) is fixed by the elastic scattering phase. (The criterium of its applicability is the presence of well separated leading particles).

The qualitative effects of rescattering are the increase of the dispersion of multiplicity distribution (in comparison with single-ladder results), the growth of the inclusive spectra in the central region, the long-range correlations, etc. In particular, the mean multiplicity $\langle n\rangle$, the dispersion of the multiplicity distribution D_n , the correlation function f_2 , and the normalized two-particle correlation function $R(p_1,p_2)$ are modified in eikonal model when compared with the single-ladder values $\langle\tilde n\rangle$, $\tilde D_n$, $\tilde f_2$:

$$\langle n\rangle = \langle m\rangle\cdot\langle\tilde n\rangle \qquad (27)$$

$$D_n^2 = \langle m\rangle\cdot\tilde D_n^2 + \langle\tilde n\rangle^2\cdot D_m^2 \qquad (28)$$

$$f_2 = \langle m\rangle\cdot\tilde f_2 + \langle\tilde n\rangle^2\cdot D_m^2 \qquad (29)$$

$$R(p_1,p_2) = \frac{1}{\langle m\rangle}\cdot\tilde R(p_1,p_2) + \frac{1}{\langle m\rangle^2}\cdot D_m^2 \qquad (30)$$

where $\langle m\rangle$ and D_m are the mean number of inelastic rescattering processes and the dispersion of its distribution. Such corrections can help to fit experimental data starting from simplest Poisson distribution for a single ladder/5/ and to account for long-range correlations /57/ which occur due to averaging over different possibilities. This is a typical feature of all many-component models and of those cluster models where one has to average different processes. One can diminish this effect by choosing the processes belonging mainly to the same class (for example, the semi-inclusive processes/101/).

It is well known that reggeon cuts make negative contribution to the total cross section, i.e., the interference of different graphs plays an important role. In particular, the rescattering graph shown in Fig. 4 has properties similar to the ones of usual multiperipheral

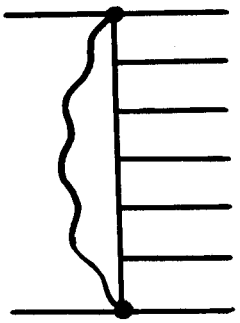


Fig. 4.
The rescattering process .

ladder and, therefore, interferes with it. One can try to take into account this interference just in the framework of the multiperipheral equation (14). The simplest model/53/ predicts that due to the interference the coefficient in front of the integral term (15) should be diminished approximately by σ_{tot}/σ_{in} times. In that case the rescattering processes should not

be considered as contributing to the term $\bar{6}$. This again reminds the many-component models where the contributions of different processes are determined from experimental data[54].

The problem of contributions of different processes is closely related to the nature of exchanges and of blobs in multiperipheral graphs. The nature of t-channel exchange (quantum numbers) can be checked in reactions where t is close to the physical pole ($p \to \pi$ or $p \to K$, etc.)[55a] or by studying the rapidity gaps and cherge transfer[55b].

The nature of blobs of multiperipheral graphs is important for understanding the mechanisms of multiple production and influences the correlation parameters of the processes. There exist the schemes with the exchange and the production of the whole set of resonances[56,57] as well as the schemes with pion exchange and the production of resonances[58-60] or, in addition, of fireballs and elastic diffraction of virtual particles[43,61,62] without which the pion exchange seems to be inadequate[43]. The former and the latter versions should differ in correlations.

The qualitative estimetes were performed in cluster models[63-68]. The plateau in the rapidity distribution of clusters is usually assumed and their decay reminds the decay of resonances (with a δ-symbol in multiplicity distribution) or that of fireballs (Poisson-like). The energy and momentum correlation was incorporated in an approximate way. The main conclusion is that such a model is able to fit experimental data if clusters decay on an average in 3-4 particles.

However the influence of energy-momentum conservation is rather strong at present energies[57,91]. In particulat, it can noticeably change AGK-rules and the form of inclusive spectra. Therefore all preasymptotic formulae should be used cantiously.

Much more reliable and complete calculations with the proper treatment of conservation laws have been performed for multiperipheral cluster model which considers both the resonances and the fireballs[43,62, 76-88]. The Monte-Carlo computer program is used. This is the only model which is able to provide the complete exclusive information about available channels of hadron reactions. It can be considered as "the theoretical bubble chamber" providing the whole set of parameters of all particles including neutrals. It has been successfully compared with experimental data at 40,70 and 200 Gev.

V. Constituent Approach

The multiple production models which try to explain these processes by considering the internal (quark) structure of particles are especially appealing. The interrelation with deep-inelastic lepton-proton processes[69,70] is easily established. These models are still not so well developed as multiperipheral or statistical ones and provide less quantitative results. However they pretend to reveal the internal mechanisms underlying multiple production processes. These models differ mainly by the role played by gluons in production reactions.

The simplest of them is the additive quark model[71,72] which does not take gluons into account. It is assumed[73] that the multiple production process can be described by the graph shown in Fig.5. Such a model explains a number

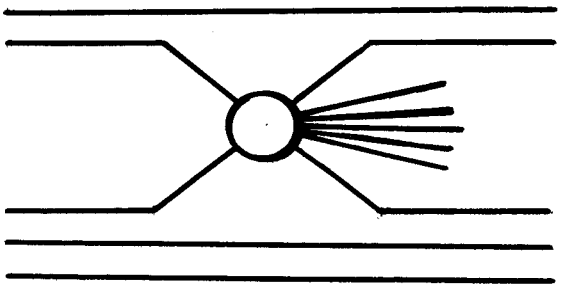


Fig. 5.
The quark graph of the multiple production process.

of typical features of multiple production, in particular, the KNO-scaling[75] (even if there

is no Feynman scaling) and predicts some interesting peculiarities. The decisive predictions stem from the fact that the symmetry (forward-backward) system of secondary particles coincides with the c.m. of two interacting quarks which is not the same, on the average, as the c.m. of colliding hadrons for πN and KN processes. Experiment supports the conclusion about the quark-quark symmetry system (see refs.[74,76]) however the analysis of the asymmetry of individual πN -events shows some discrepancy[81].

This model was used to calculate the relative yields of different particles[77-80] with the assumptions of SU(6) symmetry and of the statistically independent production and redistribution of quarks. Suppressing the production of strange quarks (by the factor of ~ 0.5 compared to usual quarks) it was possible to explain the observed relative abundance of particles of different kind, its energy dependence and its magnitude at large transverse momenta.

There exists an alternative approach[63,82], which relates the pionization components to the gluon-gluon interaction. All the valence quarks remain spectators and go through the interaction region to produce the leading particles with the flat rapidity spectrum in non-diffractive inelastic processes. Such a spectrum is consistent with the steeply decreasing spectrum of quarks, typical of deep-inelastic lepton-proton processes.

A slightly different role is prescribed to gluons if one assumes[83] that during the collision they are transformed into $q\bar{q}$ -pairs which enlarge the quark sea. Afterwards the quarks from the sea are redistributed and from the final particles like in the additive-quark model[77]. The first attempt of the global quantitative description of multiple production has been made within such a quark model[83] with the Monte-Carlo simulation.

The most attractive feature[74,82,83] of quark models is that they show that the unique quark distribution functions in the proton can explain the main features of electromagnetic, weak and strong interactions. Some people argue[84] that the strong quark-quark interaction with the low transferred momentum can also explain the universal jet structure of multiple production processes at high energies.

VI. Comparison with Experiment

Even though each group of the models considered pretends to describe experimental data, however the most extensive quantitative studies have been performed for the hydrodynamical models with the state equation $p \approx 0{,}2\,\varepsilon$ [13,14,20] and for the multiperipheral cluster model[43,62,85,86].

Table I.*)

Experimentally available data	H-models	M-models
I. Total cross sections	-	-
II. Multiplicity		
1) energy dependence of $\langle n \rangle$	+	+
2) distribution and its moments	+	+(?)
3) KNO-scaling	+(?)	+(?)
4) $n_{\pi^c} = F(n_{ch})$	+(?)	+
5) composition	+	-(?)
III. The rapidity spectra		
1) pionization region	+	+(?)
2) fragmentation region	-	+
3) energy dependence	+	+(?)
4) semi-inclusive distribution	-	+
IV. p_T -spectra		
1) low	+( )	+
2) large	+(?)	+(?)
3) semi-inclusive distributions	-	+
V. The pair-mass and transferred momenta distributions	-	+(?)
VI. Correlations		
1) dependence p_T on p_L	+	-
2) azimuthal	-	+
3) two-particle rapidity correlations	-	+
4) many-particle (rapidity intervals)	-	+
5) charge transfer	-	+(?)
VII. Inelastic diffraction	-	+

*) The plus sign means that the good quantitative agreement is claimed by the model. The minus sign is used in the following cases:
1. the theory is unable to predict this characteristics,
2. the results are unsatisfactory,
3. no calculations were performed.
The additional arguments in favour of the plus sign ( ) or against the obtained results (?) are marked in brackets.

Therefore I have chosen these two models which differ strongly in their assumption and methods to compare them and to show how many experimental distributions are described by them (see Table I). The main conlcusion that follows at first glance from the Table is that up to ISR energies the inclusive distributions do not separate definitely the two models. (The latest data about the pionization spectrum in ISR region can be more conclusive). I will discuss mainly those features which can not be easily explained or are most sensitive to the mechanisms of multiple production. I omit many successes of the theoretical schemes.

1. Total Cross Sections

This is the simplest and most precisely known quantity but it is the one which always enforces the theory to change its parameters. H-models do not pretend to calculate total cross sections. M-models use experimental data about the energy behaviour of total cross sections to get some knowledge about the leading trajectory (and about the ones nearest to it) and to choose some parameters of multiple production models.

For example, the energy behaviour (24) in preasymptotical region is determined in reggeon scheme by the parameter Δ the value of which 0.06-0.08 is chosen according to ISR data. The asymptotical behaviour is governed by the law $\ell n^2 s$ where γ is not definitely established but is rather small[47].

The properties of ρ and ρ' -trajectories help in choosing the parameters of the multiperipheral cluster model[43,85].

Eikonal models provide a variety of asymptotical regimes according to the nature of exchanged particles[88] from the constancy $\sigma \sim const$ to the Froissart behaviour ($\sigma \sim \ell n^2 s$).

C -models predict only the ratios of the cross sections for different initial particles. For example, the additive quark model predicts $\sigma_{pp}/\sigma_{\pi p} \approx 3/2$ [72] (the experimental value is $\sim 5/3$).

In conclusion, experiment but not the theory is leading here.

2. Inclusive Single-Particle Spectra

Let me show in the beginning how nicely the rapidity distributions can be fitted in controversial models (see Fig. 6a for H-models and Fig. 6b for M-models).

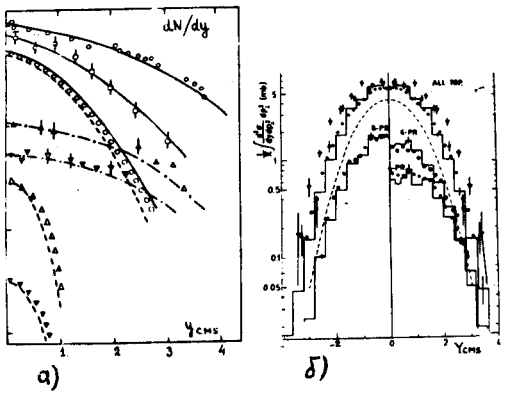


Fig. 6.
The rapidity distributions
a) H-model[13] (points are experimental ones, curves are theoretical ones)
b) M-model[43] (dots are the theoretical results).

Now I am coming to an interesting problem which is imposed on the theory by experimental results[89] about the large increase of inclusive spectra at $x \simeq 0$ in the energy region from $\sqrt{s} = 23$ to 63 GeV (about 40% for pions). It is demonstrated by Fig.2 in [90].

For H-models where scaling is violated ($\langle n \rangle \sim s^{1/4}$) the growth is rather large even though it does not seem very unnatural ($\frac{s^{1/4}}{\sqrt{\ell n s}}$ changes just by 40%). Statistical formulae similar to (3) explained rather well the yields of secondary particles $\pi, K, \bar{p}$ [24,25,28], ρ [28], $d, \bar{T}, He^3$ [24,25]. They predicted the larger increase of the heavier particle production[24,25] (for example, $\langle n_{\bar{p}} \rangle / \langle n_\pi \rangle \sim \langle n_\pi \rangle$ that should be compared with ISR data[89] $1,84/1,4 \approx 1,4$).

The increase of the pionization component

at $x \simeq 0$ imposes extremely severe restrictions on all attempts to revive F-models in this region.

In the reggeon interpretation of M-models one can attempt to use the formulae (21), (25)

$$\frac{1}{\sigma}\frac{d\sigma}{dy}\Big|_{y=0} \sim \begin{cases} 1 - \frac{d}{s^{1/4}} & (31a) \\ 1 - \frac{f}{s^{1/2}} & (31b) \end{cases}$$

depending on whether one attributes the main role to cluster density increase[93] or to kinematical effects[52]. In both the cases the correction terms seem to be too high ($d \approx 2$, $f \approx g$) to be naturally accepted. The break of the curves in Feibel plot is easily seen.

A possible explanation of this effect both by the increase of the number of multiperipheral ladders and by the strong restrictions imposed by conservation laws (of the type[91]) would mean that the simplest reggeon approach fails and one should use large corrections. The growth of the heavy particle production imposes some problems on the multiplicative production of ladders which reduces the increase of heavy particle contribution because the whole process becomes to split into processes with lower energies.

In cluster models with rather wide distribution of cluster masses (i.e., different from resonances) the increase of inclusive spectra can appear if scaling is violated within the cluster, i.e., the product of the mean multiplicity within the cluster K on its production cross section increases[44]. Sometimes the nucleon-antinucleon clusters are blamed for such an increase of inclusive spectra[92]. There are also some phenomenological proposals of new scalings for semi-inclusive[87a] and inclusive[87b] spectra leading to some increase of $\frac{1}{\sigma}\frac{d\sigma}{d^3p}$ (the variables are $\frac{y}{Y}$, $\langle n \rangle x$ or $(p_L/\langle p_L \rangle)_n$).

The experiment shows that neither of the theoretical conditions for early scaling is valid. The conditions are usually formulated as the requirements for some groups of particles to have exotic quantum numbers ($AB, A\bar{C}$ or $AB\bar{C}$) or for the system $A\pi\bar{C}$ to be non-exotic[93].

The transverse momentum distribution is

$$\frac{dN}{dp_\perp^2} \sim \exp\left[-\mu_T/T\right] \qquad (32)$$

where $\mu_T = \sqrt{p_T^2 + m^2}$, describes well with one and the same temperature T experimental data on $\pi, K, \bar{p}$ [24,25,28], p, ψ [27] in H-models for which such a behaviour is quite natural (see eq. (3)). One can notice even a slight difference from Boltzmann distribution (32) due to more correct Bose-Einstein statistics[28]. It is important also for the theoretical calculations of the density of states in relativistic ideal gas in application to H-models[94]. The mean transverse momentum is limited by the temperature T but can increase slightly $p_T \sim s^\gamma \left(\gamma = \frac{1}{12} \div \frac{1}{14}\right)$ at still higher energies[6,29].

At present the field theory and graph (multiperipheral) models can not explain such a behaviour of transverse momenta without additional ad hoc form factors. Nevertheless, the form factors chosen reasonably could supply us with the fits of experiment[43,85] which do not look worse than the previous ones.

In the large transverse momentum region the most popular ones are C-models (see rapporteur's talk of Darriulat). But H-models also pretend to explain the spectrum behaviour in p_T [28,30,31] its energy dependence and the increasing role of heavier particles[28] by the leakage of particles at the earlier stage of the system development. Some additional information about this stage could be obtained from spectra of photons and leptons[95].

The simple resonance ladder in M-models contradicts the experiment because it predicts the decrease of associated multiplicity at higher p_T [56]. Therefore, if one wants to preserve the multiperipheral approach one should consider creation of heavier clusters[43,96]

in the multiperipheral graph. For understanding the mechanisms of multiple production it is important to know how many resonances are produced on an average in each event. However, experimental data are not precise enough (for example the percentage of pions from resonance decay is estimated from 20 to 70% /97-100,81/). The experiments in which the leptons from the resonance decay are detected could, in principle, clear up the situation. The qualitative predicts of the models are as follows. There are many resonances in multiperipheral resonance ladders/56,57/, they produce a pronounced effect in multiperipheral fireball model/43,85/ but few resonances are produced in some versions of quark model/80b/.

3. Correlations and Clusters

The separation of dynamical correlations from purely kinematical ones (due to the energy-momentum conservation) is a difficult task. The widely used functions $C(y_1, y_2)$ and $R(y_1, y_2)$ whose maxima at $X=0$ support the short-range order models with cluster production are not very informative. The semi-inclusive correlations C_n and R_n start from different levels for each n and interfere strongly when combined into inclusive functions C and R. Nevertheless, taking into account these effects it is possible to show that the main conclusion about short-range ordering persists/101,102/. Approximately, $2 \div 3$ charged particles are attributed to each cluster from such a method in independent cluster emission models/68,103,104/. The similar values are obtained from the rapidity gap distribution/105,106/. It is easy to show that for independent emission of clusters decaying into K particles and distributed along the rapidity axis with the constant density ρ the rapidity gaps Δy follow the laws/106,107/:

$$dN/dy \sim exp[-\rho K \Delta y] \text{ at small } \Delta y, \quad (33)$$

$$dN/dy \sim exp[-\rho \Delta y] \text{ at large } \Delta y. \quad (34)$$

Formulae (33), (34) compared with the experimental curves give the above conclusions. However, there was a criticism of such estimations and twice as large values of K were obtained from the fluctuation analysis/108/.

Inclusive distributions of rapidity gaps are not very sensitive to the mechanism of multiple production/62,109/ and are strongly correlated with the mean multiplicity. The more effective way is to investigate the semiinclusive distributions of rapidity intervals/62,107,109,110/ which are determined as intervals between two particles which contain some other particles inside the interval i.e.,

$$\Delta y_{i,K} = y_{i+K+1} - y_i \quad (35)$$

(at $K=0$; $\Delta y_{i,0} \equiv \Delta y$), where i are numbers of particles along the rapidity axis and K is the number of particles inside the interval.

These distributions have maxima moving to lower values of interval length when the role of clusters increases /107/ (Fig. 7). The calculations have shown that the most sensitive ones are the distributions with K of the order of $n/2$ (n is the multiplicity of an event). The comparison with experiment/62,110,111/ was made and these distributions helped to distinguish between the two versions of the multicluster model both of which explained successfully other experimental data.

Let me stress that when studying intervals $\Delta y_{i,K}$ we learn something about many-particle correlations and this way is much simpler than the many-dimensional generalization of functions C and R.

The correlations between the produced clusters and exchanged links could be studied by the rapidity interval method joined with the charge transfer/112,113/. Connection between correlation functions for the processes initiated by different projectiles can be sometimes established using isotopic invariance/114/. The function C can be revived if considered as a

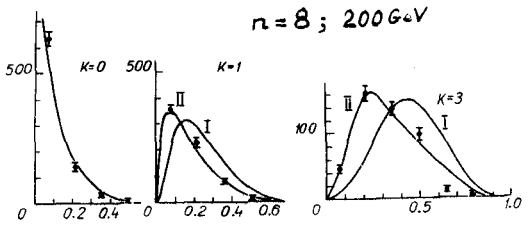


Fig. 7.

The rapidity interval distributions[110]. I - independent particle production; II - independent cluster production.

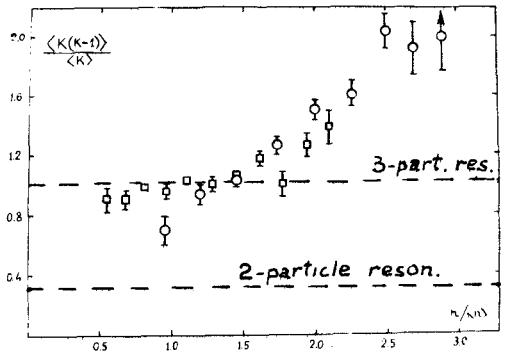


Fig. 8.

The value of $\left[\langle K(K-1)\rangle / \langle K\rangle\right]_n$ as a function of $n/\langle n\rangle$ at energies $\sqrt{s}$ =23÷63 GeV[102]. The levels for the decay of 2- and 3-particle resonances are shown (ρ-like and ω-like ones).

function of mass of pair of particles (see Fig. in[68]).

In conclusion , we should deal with the clusterization phenomenon. If there is anything dynamical besides resonances in the notion of clusters it should be further studied, I'd like to argue in favour of the point of view that some heavier correlated groups of pions are created: 1. the correlated groups contain on an average at least 2÷3 charged particles (for resonances the value 2 is an absolute limit and the value 1, 3÷1.5 is the most probable one), 2. the effective mass of the group varies from 1.5 to 3 GeV which is higher than all prominent boson resonance masses, 3. the charged multiplicity of the cluster decay K increases with n for $n>\langle n\rangle$ i.e., the multiplicity distribution for a cluster is not described by δ-function[101] (fig. 8), 4. the slope of the logarithmical increase of the mean multiplicity is too small for the schemes with resonance production, 5. the strong increase of inclusive production of K and $\bar{p}$ at ISR-energies favours cluster interpretation.

Qualitatively this point of view is supported also by the scaling violation at $X=0$, the belated increase of total cross sections, the high p_T behaviour.

Now I'd like to make the general comment on the comparison of models with experiment. At present we witness the "multiple model production". Any serious model should pass through the complete quantitative comparison with experiment. It implies the huge amount of numerical Monte-Carlo calculations[43,62,83,85,86,115] with some analytical estimates. Sometimes such a widespread comparison is decisive because a model can reproduce some data and fails at other points. It was demonstrated in analysis of multiperipheral cluster models[43,62,85,86,115] and of quark models[83]. We should also propose the criteria to kill models.

Here I tried to discuss those experimental facts and theoretical methods of analysis which discriminate different models and help to choose the most promising objects for the further investigation.

VII. Space-Time Picture

The space-time description of the process could be useful for studying the multiple production. The naive geometrical consideration leads to the Lorentz-contracted disk and to impact larger multiplicities at smaller parameter b. Vice versa, for the simplest multiperipheral ladder one gets the larger multiplicity for the longer ladder.

It is possible to distinguish two pictures in the experiment.

The effective transverse distance ($b_{eff} \sim 1$ fm) typical of the whole set of inelastic processes is determined from the elastic differential cross sections applying the unitarity condition (fig.9). Most peripheral ones are the diffraction dissociation processes /116-119/.

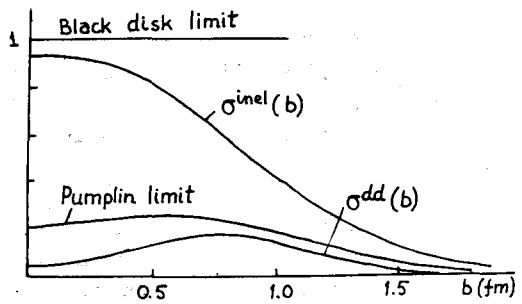


Fig. 9.

The impact parameter structure of total cross section and of inelastic diffraction processes σ_{dd}.

It is possible to estimate the lower limit of the values of b_{eff} for any exclusive channel according to the formula/120-122/:

$$\langle b^2 \rangle = \frac{\left\langle \sum_i \left(x_i^2 - \frac{k_i^2}{2p^2} \right) \right\rangle^2}{\left\langle \sum_{i,j} x_i x_j \vec{k}_i \vec{k}_j \right\rangle} \equiv b_L^2 \qquad (36)$$

where k_i, p - are the momenta of produced and colliding particles.

The results obtained are: 1) b_L decreases 3÷4 times when the multiplicity increases from 4 to 9, i.e., the multiplicity is higher for central interactions, 2) at fixed multiplicity b slowly increases with energy, 3) b_L is larger for inelastic diffraction, 4) b_L is smaller for the strangeness or baryon number exchange processes.

Therefore in such interpretation these result supports the naive geometrical picture rather than the multiperipheral Brownian motion in the transverse plane. It may be related to the fact that multiperipheral logarithms are in general much smaller than residues' contributions. The refinement of eq. (36) is suggested in/122/.

The problem of understanding the effective longitudinal distances is more complicated. When dealing with H-models one uses explicitly a geometrical picture of Lorentz-contracted and expanding volume/1-3,123/. Contracted volume appears also in cylindrical phase space picture (uncorrelated jets)/124/.

At the same time effective longitudinal size and time duration determined by dependence on four momentum squared of incoming particle/125/ appears to be large for electroproduction amplitude/126/, $z_{eff} \sim \frac{E}{m^2}$. Long time interaction can be realized in multiperipheral parton picture with interacting slow partons. In this picture the time of formation of parton ladder /125b,127a/ is of the order of $\frac{E}{m^2}$, whereas at a fixed moment hadron consists of the outer shell, whose form is close to the sphere $\sim \frac{1}{m}$ (slow parton) and internal contracted shells (fast partons), the transversal size being of the order of $\sqrt{R^2 + \alpha' \ell n E}$ at large E's.

The similar picture of long time formation of a "dressed state" was studied earlier in electrodynamics/130/ and it was exploited for interpretation of hadron-nucleus interactions/131,132/.

Let me note that there exists a proposal to consider a hadron as a parton state of length $\sim \frac{E}{m^2}$ /127b/.

A method of studying the space-time region is proposed and used in the experiment/128/. It exploits the second order interference effects (similar to the Hunberry-Brown, Twiss method in astronomy). The experimental results/129/ $R \sim 1$ fm and $c\tau \sim (0.4 \div 0.7)$ fm do not contradict what was expected. However the interpretation of the value of τ and restrictions imposed by the smallness of the relative momentum of two detected pions need further study.

In conclusion, the problem of the space-time description is far from being solved and

must be discussed. Our main hope is to use the hadron-nucleus collisions to clear it up[131,132].

VIII. Extremely High Energies

What can we say about mechanisms of multiple production at still higher energies?

The region of $10^{14} \div 10^{15}$ eV is often thought of as a region where some new phenomena may appear. Which facts from the cosmic ray studies are known?

1. Total cross sections increase slowly (if at all) with energy (Fig. 10).

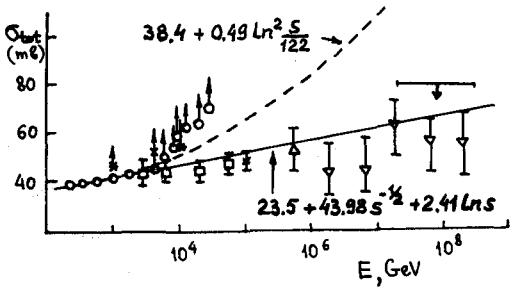


Fig. 10.
The energy dependence of total cross sections at very high energies.

2. The mean multiplicity increases, probably, faster than logarithmically (Fig. 11).

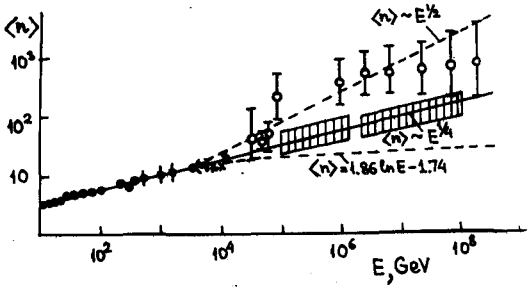


Fig. 11.
The energy behaviour of the mean multiplicity of charged secondaries.

Let me note that at present there is no theoretical scheme which predicts the logarithmic behaviour of total cross sections (but not $\sim \ln^2 s$) and the strong power increase of mean multiplicity (with the high enough power).

3. Scaling for $\frac{E}{\sigma} \frac{d^3\sigma}{d^3p}$ is, probably, violated in the pionization region[133]. As the calculation shows[133b] the data of the experiment "Pamir" in the energy region $10 \div 10^3$ TeV could be fitted best of all if the inclusive distribution $E \frac{d^3N}{d^3p}$ at small $|x|$ increases while it decreases in the fragmentation region. It coincides with the trends observed at ISR.

4. At energies about 10^{14} eV the absorption of the hadronic component of air showers starts decreasing[134-137]. If it is interpreted as the creation of a new highly penetrating component than it should contribute about 25% of hadronic component at energies above 100 TeV.

5. The energy shared in electron-photon component increases compared with the energy of hadronic component in the center of air shower from 0.8 to ~ 1.5 in the energy interval 40-300 TeV. These results were interpreted[134-137] as a consequence of production of some new particles with their subsequent decay into electrons and photons or as a possible associative production of new particles with leptons and photons.

6. There exist some exotic events. The most interesting ones are the events with the production of the large number of particles in the narrow rapidity interval which have been interpreted as the production of very heavy clusters with masses up to 25 GeV/c^2 or as very large p_T -events[138].

I would mention that the clusters with masses 3-4 GeV/c^2 were discussed in cosmic ray physics long ago [139].

And, finally, we may hope that the energy region above 10^{14} eV will persuade us to change our opinion about mechanisms of multiparticle production. The colliding beams 1×1 TeV^2 would just enter into this region.

IX. Conclusions and Perspectives

The experimental data about the increase

of total and inclusive cross sections, the behaviour of the mean multiplicity and correlations at high energies provide a very interesting clue for further development of multiple production theory. Thus I hope that the next Conference will be more definite about the validity of some models.

Now I would like to discuss how the multiple production studies are connected with other problems arising in the neighbouring fields of particle physics.

Surely the interesting relationship is provided by C-models because they are intimately connected with the internal structure of particles. It would be valuable to understand which features of the internal structure are related to the cluster production. Probably, the clusters could result from the non-linear theory of particles and their interactions in a way similar to the transformation of two quantum solitons in N solitons (or two bags into N bags[140]). The problem of kinetics of such solitons is related to the speculations about the so-called young particles[130].

Dynamical description in terms of non-linear Lagrangians is connected with the transport theory and further with the statistical and hydrodynamical approaches. As we have seen one can derive here the form of inclusive spectra and therefore find some correspondence with the reggeon approach to inclusive processes.

By itself the problem of the connection between statistical and dynamical approaches to multiparticle production is a part of more general question of how dynamics transforms in statistics[141]. Surely the observation of statistical behaviour in inelastic processes would be invaluable for particle models.

Non-linear effects can appear in a way similar to that of superconductivity. The state equation of hadronic matter can be very complicated. For instance, such state equations which give rise to phase transitions in hadronic matter, to its superfluid properties, etc., were already exploited. The problem of state equation of hadronic matter is important not only for understanding the hadron-hadron and hadron-nucleus collisions at high energies but it plays a noticeable role in cosmological studies.

In conclusion I would like to say the situation with our understanding of multiparticle production is far from being clear. The capital letters of the reviewed models form the phrase:

"Multiple Production Has Curiour Features".

Still much time is needed to make all of them clear and predictable.

Acknowledgements

I am very grateful to all the authors who contributed to this talk and I appologize for any possible omissions in references. I am indebted to E.L.Feinberg for permanent encouragement, to D.S.Chernavsky for the discussion and to I.V.Andreev for the invaluable help in preparing the talk. My thanks are also to N.S.Amaglobeli, A.N.Sissakian, V.K.Mitrjushkin, A.S.Potupa and E.V.Shuryak for organizing the session.

References

1. E.Fermi, Progr. Theor. Phys. 5, 570 (1950); Phys.Rev. 81, 683 (1951).
2. I.Ya.Pomeranchuk, Doklady Academy of Sciences of USSR 78, 889 (1951).
3. L.D.Landau, Izvestija Acad. of Sciences of USSR 17, 51 (1953).
4. P.Carruthers, F.Zachariasen, Preprint LA-UR--75-375, 1975.
5. F.Cooper, D.H.Sharp, Phys.Rev. D12, 1123 (1975).
6. G.A.Milekhin, Proceedings of Int.Conf. on Cosmic Ray Phys., v.1, 223, 1960.
7. R.C.Hwa, Phys.Rev. D10, 2260 (1974).
8. C.B.Chiu, K.-H.Wang, Phys.Rev. D12, 272 (1975); C.B.Chiu, E.C.G.Sudarshan, K.-H.Wang, Phys. Rev. D12, 902 (1975).
9. S.Eliezer, R.M.Weiner, Phys.Rev. D13, 87 (1976).
10. A.I.Bugrij, A.A.Trushevskii, paper No 89/A3-9.
11. L.L.Enkovskii, A.A.Trushevskii, paper No 90/A3-10.
12. R.Hagedorn, Nuovo Cimento 35, 216 (1965).
13. E.V.Shuryak, Yadern. Fiz. 16, 395 (1972); Prepr. INR-Novosibirsk, 75-4 (1975).
14. O.V.Zhirov, E.V.Shuryak, Yad.Fiz. 21, 861 (1975).
15. E.L.Feinberg, Phys.Rep. 5C, 237 (1972).
16. M.I.Gorenshtein, G.M.Zinoviev, paper No 91/A3-11.
17. P.Carruthers, M.Duong-Van. Phys.Lett., 41B, 593 (1972); Phys.Rev., D8, 859 (1973).
18. F.Cooper, E.Schonberg. Phys.Rev.Lett., 30, 880 (1973).
19. F.Cooper, G.Frye. Phys. Rev., D10, 186 (1974).
20. B.Andersson, G.Jarlskog, G.Damgaard. Ref. TH2133-CERN, 1976.
21. I.L.Rozental. Uspekhi Fiz.Nauk, 116, 271 (1975).
22. C.B.Chiu, K.H.Wang. Phys.Rev., D12, 2715 (1975).
23. J.Ranft. Nucl.Phys., B105, 139 (1976).
24. I.N.Sissakyan, E.L.Feinberg, D.S.Chernavskii, JETP, 52, 545 (1967).
25. E.L.Feinberg. Uspekhi Fiz.Nauk, 104, 539 (1971).
26. E.I.Daibog, Yu.P.Nikitin, I.L.Rozental. Yadern. Fiz., 16, 1314 (1972); Izvestija Academy of Sciences of USSR, 37, 1396 (1973).
27. T.F.Hoang. Phys.Rev., 13D, 1881 (1976).
28. E.V.Shuryak. Yadern. Fiz., 20, 549 (1974); Phys.Lett., 42B, 357 (1972).
29. M.Chaichian, H.Satz, E.Suhonen. Phys.Lett., 50B, 362 (1974).
30. J.J.Dumont, L.Heiko. Univ. of Brussel's preprint IIME-74.1.
31. M.I.Gorenshtein, V.P.Shelest, G.M.Zinoviev. Phys.Lett., 60B, 283 (1976).
32. T.T.Chou, C.N.Yang. Phys.Rev., 170, 1591 (1968).
33. H.Cheng, T.T.Wu. Phys.Rev.Lett., 23, 670 (1969).
34. R.K.Adair. Phys.Rev., 172, 1370 (1968).
35. J.Benecke, T.T.Chou, C.N.Yang, E.Yen. Phys.Rev., 188, 2159 (1969).
36. R.Hwa. Phys.Rev., D1, 1790 (1970); Phys. Rev.Lett., 26, 1143 (1971).
37. M.Jacob, R.Slansky. Phys.Rev., D5, 1847 (1972).
38. J.Benecke, A.Bialas, E.H. de Groot. Phys. Lett., 57B, 447 (1975).
39. L.Stodolsky. Phys.Rev.Lett., 28, 60 (1972).
40. J.Benecke, A.Bialas, S.Pokorski. Preprint MPI/PTh 5/76 (1976); paper No 707/A3-54; J.Benecke, mini-rapporteur talk.
41. D.Amati, A.Stanghellini, S.Fubini. Nuovo Cim., 26, 896 (1962).
42. F.Zachariasen. Phys.Rep., 2C, 1 (1971).
43. I.M.Dremin, A.M.Dunaevskii. Phys.Rep., 18C, 159 (1975).
44. I.M.Dremin, A.M.Dunaevskii. Yad.Fiz., 22, 568 (1975).
45. O.V.Kancheli. Pisma ZETP, 11, 397 (1970); A.Mueller. Phys.Rev., D2, 224, 1963 (1970);
46. P.D.B.Collins, F.D.Gault, A.Martin. Phys. Lett., 47B, 171 (1973); Nucl.Phys., B80, 135 (1974); B83, 241 (1974); A.Capella, J.Thanh Tran Wan, J.Kaplan. Preprint LPTHE 75/12, 1975.
47. M.S.Dubovikov, K.A.Ter-Martirosyan. Preprint ITEP-37, 1976; M.S.Dubovikov, B.Z.Kopeliovich, L.I.Lapidus, K.A.Ter-Martirosyan. Preprint JINR, D2-9789, Dubna, 1976.
48. A.Schwimmer. Ref. TH 2055-CERN, 1975.
49. V.A.Abramovskii, V.N.Grobov, O.V.Kancheli. Yad. Fiz., 18, 595 (1973).
50. I.V.Andreev. Yad. Fiz., 22, 186 (1975).
51. K.A.Ter-Martirosyan. Phys.Lett., 44B, 377 (1973).
52. L. Caneschi. Nucl. Phys., B68, 77 (1974); E.M.Levin, M.G.Ryskin. Yad.Fiz., 19, 904 (1974).
53. I.I.Royzen. Preprint FIAN, No. 39 (1976); paper No. 88/A3-8.
54. A.N.Sissakian, mini-rapporteur talk, paper No. 1044/A3-55, 1099/A3-45.
55. a) I.F.Ginzburg, L.I.Perlovsky, A.M.Vasylev, paper No. 95/A3-15. b) P.Pirila, G.H.Thomas, C.Quigg. Phys.Rev., D12, 92 (1975).
56. E.M.Levin, M.G.Ryskin. Yad.Fiz., 17, 386 (1973); 18, 431 (1973).

57. E.M.Levin, M.G.Ryskin, paper No.83/A3-3.
58. E.L.Berger. Phys.Rev.Lett., 20, 964 (1968); 21, 701 (1968).
59. K.G.Boreskov, A.B.Kaidalov, L.A.Ponomarev et al. Yad.Fiz., 15, 361; 557 (1972); 17, 1285 (1973).
60. D.Griffiths, A.M.Saperstein, D.T.Schnitzer. Phys.Rev., D6, 2546 (1972).
61. I.M.Dremin, I.I.Royzen, R.B.White, D.S.Chernavskii. JETP, 48, 952 (1965).
62. E.I.Volkov, I.M.Dremin, T.I.Kanarek, D.S.Chernavskii. Preprint FIAN No.40 (1976); paper No.87/A3-7.
63. S.Pokorski, L.Van Hove. Acta Phys.Pol., B5, 229 (1974).
64. F.Hayot, F.Henyey, M.Le Bellac. Nucl.Phys., B80, 77 (1974).
65. G.Ranft, J.Ranft. Nuovo Cim.Lett., 10, 485 (1974); R.Kirschner, paper 674/A3-30.
66. J.Meunier, G.Plaut. Nucl.Phys., B87, 74 (1975).
67. C.deTar. Mini-rapporteur talk.
68. G.H.Thomas. Mini-rapporteur talk.
69. R.P.Feynman. Photon-Hadron Interactions, W.A.Benjamin, 1972.
70. J.D.Bjorken, E.A.Paschos, Phys.Rev. 185, 1975 (1969); D1, 3151 (1970).
71. E.M.Levin, L.I.Frankfurt, Pisma JETP 2, 652 (1965).
72. H.J.Lipkin, F.Scherk, Phys.Rev.Lett. 16, 71 (1966).
73. H.Satz, Phys.Lett. 25B, 220 (1967).
74. S.P.K.Tavernier, Nucl.Phys. B105, 241 (1976).
75. G.Eilam, Y.Gell, Phys.Rev. D10, 3634 (1974).
76. M.Deutchmann. Proc. of the Amsterdam Int. Conf. on Elementary Particles, Amsterdam, 1971 (North-Holland, Amsterdam, 1972).
77. V.V.Anisovich, V.M.Shekhter, Nucl.Phys.B55, 433 (1973); V.V.Anisovich, M.N.Kobrinsky, Phys.Lett. 46B, 419 (1973).
78. V.N.Guman, V.M.Shekhter, Nucl.Phys. B99, 523 (1975), INPI Preprint No.216 (1976).
79. B.N.Guman, V.M.Shekhter, Yad.Fiz.22, 1237 (1975).
80. a) V.V.Anisovich, M.N.Kobrinsky, B.H.Povzun, paper No.85/A3-5;
b) A.K.Likhoded, V.A.Petrov, A.N.Tolstenkov, Preprint IPVE, Serpukhov 76-2 (1976).
81. L.A.Didenko, V.S.Murzin, L.I.Sarycheva, L.N.Smirnova, Paper No.7/A2-96.
82. L.Van Hove, S.Pokorski, Nucl.Phys. B86, 243 (1975); L.Van Hove, K.Fialkowski, CERN Preprint TH 2123 (1976).
83. V.Černy, P.Lichard, J.Pisut, paper No. 673/a3-29.
84. H.Satz, paper No.891/A3-38.
85. E.I.Volkov, I.M.Dremin, A.M.Dunaevskii, I.I.Royzen, D.S.Chernavskii, Yad.Fiz. 20, 149 (1974).
86. D.S.Chernavskii, T.I.Kanarek, E.I.Volkov Preprint, P.N.Lebedev Inst. No.54 (1975); E.I.Volkov, T.I.Kanarek, Preprint Lebedev Phys.Inst. No.115 (1975).
87. a) F.T.Dao et al. Phys.Rev.Lett. 33, 389 (1974).
b) A.S.Potupa, V.V.Scadorov, A.S.Fridman, Pisma JETP 23, 546 (1976); papers No.94/A3-14; 804/A3-60. R.J.Yaes, paper No.986/A3-72.
88. I.V.Andreev, Yad.Fiz.14, 837 (1971); Pisma JETP 20, 199 (1974).
89. K.Guettler, B.G.Duff et al. Papers No. 124/A2-39.
90. A.Bialas. Mini-rapporteur talk.
91. A.Capella, A.B.Kaidalov, CERN preprint 2151-TH (1976).
92. T.K.Gaisser, C.I.Tan, Phys.Rev. D8, 3881 (1973); M.Suzuki, Nucl.Phys. B64, 486 (1973); C.B.Chiu, D.M.Tow, Preprint ORO-263 (1976); paper No.359/A3-26; S.T.Jones, Phys.Rev. D11, 692 (1975).
93. a) L.E.Gendenstein, A.B.Kaidalov, D.S.Chernavskii, Pisma JETP 19, 61 (1974);
b) L.E.Gendenstein, Pisma JETP 19, 139 (1974).
94. M.Chaichian, R.Hagedorn, M.Hayashi, Nucl. Phys. B92, 445 (1975).
95. E.L.Feinberg, Izv. Acad. of Science of USSR 26, 622 (1962); 34, 1987 (1970); Preprint TH-2156-CERN, 1976.
96. I.M.Dremin, Yad.Fiz. 18, 617 (1973).
97. F.C.Winkelmann et al. Phys.Lett. 56B, 101 (1975).
98. D.Fong et al. Phys.Lett. 60B, 124 (1975).
99. V.V.Ammosov et al. Preprint IHEP, Serpukhov, M-19 (1975).
100. H.Angelov, V.G.Grishin, paper No.205/A2-6.
101. L.Foa, Phys.Reports 22C, 1 (1975); A.Gula, Nuovo Cim.Lett. 13, 432 (1975); T.T.Gien Nuovo Cim. Lett. 13, 193 (1975).
102. P.Darriulat, Invited talk at VIth Intern. Colloquium on Multiparticle Reactions, Oxford, 1975; S.R.Amendolia,G.Bellettini et al. Nuovo Cim. 31A, 17 (1976).
103. C.Quigg, P.Piriula, G.H.Thomas, Phys.Rev. Lett. 34, 290 (1975).
104. E.Albini, P.Capiluppi, G.Giacomelli, A.M.Rossi, Nuovo Cim., 32A, 101 (1976).
105. A.Krzywicki, C.Quigg, G.H.Thomas, Fermilab-Pub-75/40-THY, 1975.
106. C.B.Chiu, K.-H.Wang, Preprint ORO 3992-232 (1976); Paper No.358/A3-25; N.Murai, Phys. Lett. 56B, 351 (1975).

107. A.M.Gershkovich, I.M.Dremin, Short communications in physics No.1, 7 (1976).
108. T.Ludlam, R.Slansky, Phys.Rev. D12, 59 65 (1975).
109. M.I.Adamovich, N.A.Dobrotin et al. Yad. Fiz. 21, 805 (1975).
110. M.I.Adamovich, M.M.Chernjavskii, I.M.Dremin et al. Nuovo Cim. (to be published); paper No.150/A2-19.
111. I.A.Ivanovskaya, S.I.Lyutov, paper No.162/A2-8.
112. J.Benecke, Proceedings of the 1972 Zakopane Colloquium, p. 429;
T.T.Chou, C.N.Yang, Phys.Rev. D7,1425 (1973);
C.Quigg, G.H.Thomas, Phys.Rev. D7, 2752 (1973);
A.Bialas, Jagellonian Univ., Preprint, 1974; R.Baier, F.Bopp, Preprint Bi-74/06 (1974); C.B.Chiu, K.H.Wang, Preprint ORO-3992-231; paper No.357/A3-24.
113. E.N.Kladnitskaya et al. paper No.163/A2-7.
114. V.L.Lynboshitz, paper No.93/A3-13.
115. A.Arneodo, G.Plaut, Nice preprint, N.TH 75/8 (1975).
116. H.I.Miettinen, CERN Preprint TH 1864 (1974);
117. J.Pumplin, Phys. Rev. D8, 2899 (1973).
N.Sakai, J.N.J.White, Nucl.Phys. B59, 511 (1973).
118. M.I.Shirokov, JETP, 42, 173 (1962).A.A.Logunov,Nguen Van Hieu,Theor.Mat.Phys.,1,375(1969).
119. L.Caneschi, P.Grassberger, H.I.Miettinen, F.Henyey, Phys.Lett. 56B, 359 (1975).
120. B.R.Webber, Phys.Lett. 49B, 474 (1974).
121. P.Bosetti et al., Nucl.Phys. B97, 29 (1975);
B.R.Webber et al., Nucl.Phys. B97, 317 (1975).
122. F.S.Henyey, J.Pumplin, paper No.1137/A3-69.
123. S.Sohlo, G.Wilk, Nuovo Cim.Lett. 13, 375 (1975).
124. I.V.Andreev, I.M.Dremin, Yad.Fiz. 9, 176 (1969).
125. a) V.N.Gribov, B.L.Ioffe, I.Ya.Pomernchuk, Yad.Fiz. 2, 768 (1965);
b) V.N.Gribov, ITEP school lectures, 1973.
126. B.L.Ioffe, Phys.Lett. 30B, 123 (1969).
127. O.V.Kancheli, Pisma JETP a) 18, 465 (1973);
b) 22, 491 (1975); paper No.96/A3-16.
128. G.I.Kopylov, MiI.Podgoretskii, Yad.Fiz. 15, 392 (1972); 18, 656 (1973); 19, 434 (1974); paper No.1007/A2-120.
G.I.Kopylov, Phys.Lett. 50B, 472 (1974);
E.V.Shuryak, Phys.Lett. 44B, 387 (1973);
G.Cocconi, Phys.Lett. 49B, 459 (1974).
129. M.Deutschmann et al. Nucl.Phys. B103, 198 (1976).
130. E.L.Feinberg JETP 50, 202 (1966); in "Problems of Theoretical Physics", p.248,1972.
131. A.I.Demyanov, V.S.Mursin, L.I.Sarycheva, paper No.455/A6-12; Yad.Fiz. 23, 382 (1976).
132. N.N.Nikolaev et al. papers 467,468,470/A5--39-41.
133. a) S.N.Vernov, G.B.Christiansen, N.N.Kalmykov et al. paper No.778/A2-110.
b) A.M.Dunaevskii, A.V.Uryson et al. paper No.803/A2-84.
134. V.S.Aseykin, V.P.Bobova et al. Izvestia Acad. of Sciences of USSR, 38, 998 (1974).
135. S.I.Nikolsky, V.P.Pavluchenko, E.L.Feinberg, V.I.Yakovlev, Lebedev Inst. Preprint No.69 (1975).
136. V.P.Pavluchenko, S.I.Nikolsky, V.I.Yakovlev, paper No.168/A2-2.
137. S.I.Nikolsky, V.I.Yakovlev, Short communications in Phys., No.5 (1976).
138. Japanese-Brasilian Collaboration, Report at Cosmic Ray Conf., München, 1975.
139. M.Miesowicz, in: Progress in Elementary Particles and Cosmic Ray Phys., v.10, eds. J.G.Wilson and S.A.Wonthuysen (North-Holland, Amsterdam, 1971) p.103.
140. F.Low, MIT Preprint CTP 438 (1975).
141. L.Galgani, A.Scotti, Rivista del Nuovo Cim. 2, 189 (1972);
N.M.Pukhov, D.S.Chernavskii, J.Theor. and Math. Phys. (1971), v.7, 219.

PARALLEL SESSION

ON LARGE TRANSVERSE MOMENTUM PHENOMENA

RECENT RESULT ON SINGLE PARTICLE HIGH PRODUCTION AT FNAL

M.J.Shochet

University of Chicago, Chicago, Illinois, USA

We report on two experiments recently performed at Fermilab. The Brookhaven-CAL TECH-LHL /1/ experiment measured high p_T π^0's produced in $\pi^\pm p$ and pp collisions at incident energies of 100 and 200GeV/c. The apparatus is shown in Fig.1. Cerenkov counters in the inoident beam allowed π^+ and p data to be

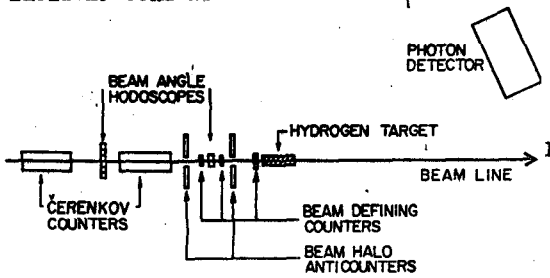


Fig.1.

taken simultaneously. The γ detector (Pb scintillator sandwich) covered a range in θ_{CM} from 50° to 110°. They triggered on high p_T γ's by forming a weighted sum of signals from the scintillators within the γ deteotor. The position resolution ($\sim$ 1mm) as well as energy resolution ($\Delta E/E \sim 0.02 \cdot \sqrt{100\ \mathrm{GeV}/E}$) gave them a very olean π^0 mass peak ($\Delta M^2/M^2 \approx 0.12$) with < 10% background beneath it. The principal objective was to measure $R(A/B)$ the ratio of the invariant cross sections for $Ap \to \pi^0 X$ and $Bp \to \pi^0 X$. In Fig.2 the results are shown.

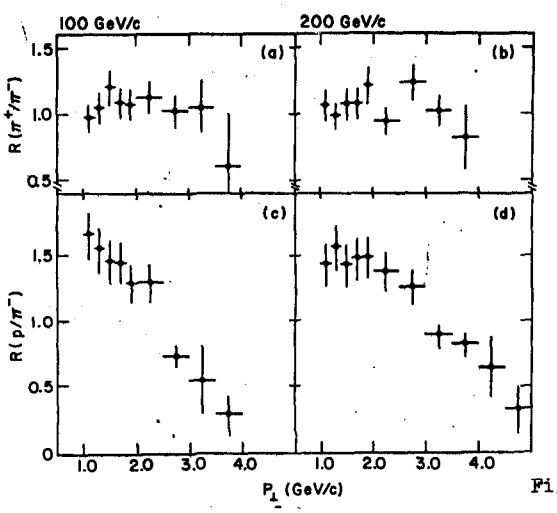


Fig.2.

$R(\pi^+/\pi^-)$ is consistent with 1 over the entire kinematic region covered, while $R(p/\pi^-)$ drops sharply with p_T from a low p_T value of $\sim$ 1.5, the value obtained from simple quark counting. They parameterize the invariant cross section as $(p_T^2 + M^2)^N (1-x_T)^F$ and find $N_p = -5.4 \pm 0.2$, $F_p = 7.1 \pm 0.4$, $M_p^2 = 2.3 \pm 0.3$ GeV^2, $N_\pi = -5.0 \pm 0.1$, $F_\pi = 5.5 \pm 0.3$, $M_\pi^2 = 1.8 \pm 0.2$ GeV^2. Since $N_\pi \approx N_p$ and $M_p^2 \approx M_\pi^2$, $R(p/\pi)$ is a function only of x_T. This is shown in Fig.3.

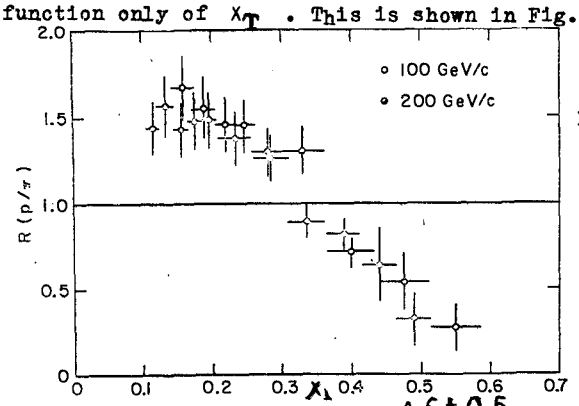


Fig.3.

They find $R(p/\pi) \sim (1-x_T)^{1.6 \pm 0.5}$ consistent with the prediction of the Constituent Interchange Model /2/ (CIM) of 2-4.

The Chioago-Princeton experiment /3/ presented preliminary data on the production of high p_T partioles from 200,300,400 GeV protons incident of H_2, D_2, Be, Ti and W targets. The apparatus consisted of a single arm magnetic spectrometer at $\sim$ 90° in the center of mass which measured particle production in the range $0.8 < p_T < 7$ GeV/c. Two Cerencov counters allowed π, K and p data to be taken simultaneously.

Examples of the A dependence data are shown in Fig.4, which shows that the nuclear target data extrapolate well to D_2. The H_2 data does not fit on these curves, there being an excess of positive pions and a deficit of negative pions. The invariant cross section data (H_2 excluded) are parametrized as A^n, where n can be a function of both p_T and $\sqrt{s}$. Results for π^--production at 400 GeV/c are shown in Fig.5. As observed previously, n increases with p_T from the low p_T value of $\sim 2/3$ to values

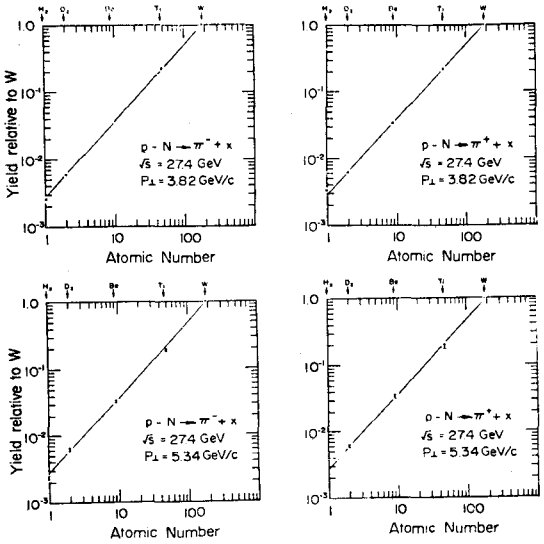


Fig.4.

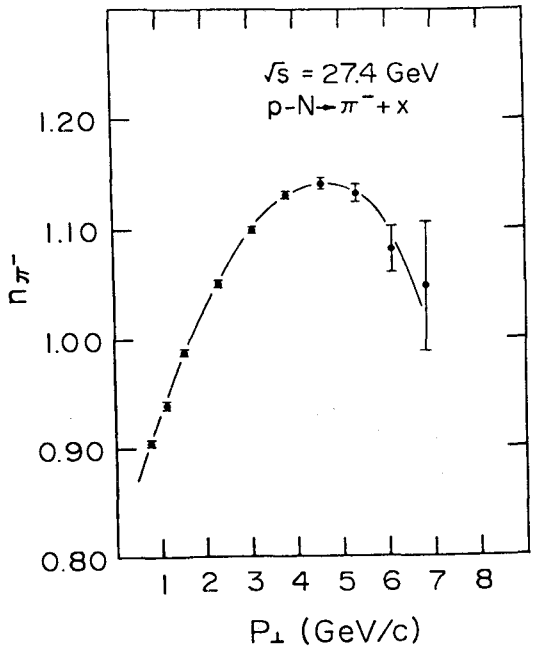


Fig.5.

significantly in excess of 1 at $p_T \sim 4$–5 GeV/c. There is now an indication that n is dropping at very large p_T. Typical particle ratio data are plotted in Fig.6, which shows that with exception of K^-/π^-, the nuclear data extrapolate well through H_2. Fig.7 shows the ratio for H_2 and D_2. While deuterium shows the same slow rise seen with the heavy nuclear targets, the hydrogen data shows rapid rise with the π^+/π^- ratio exceeding 2 at high p_T. If a H_2, D_2 subtraction is made, a naive result is obtained for pn scattering. The π^+/π^- ratio for "n" interactions is seen to be flat or perhaps slightly decreasing.

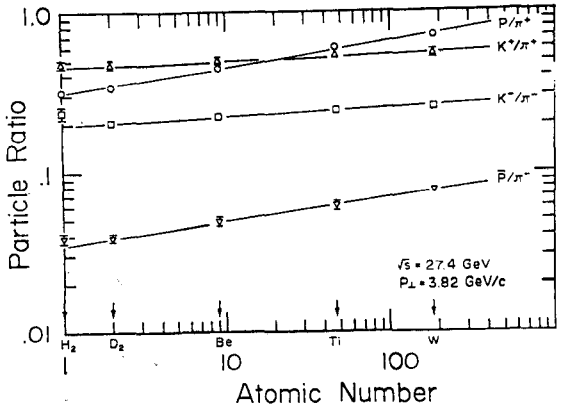


Fig.6.

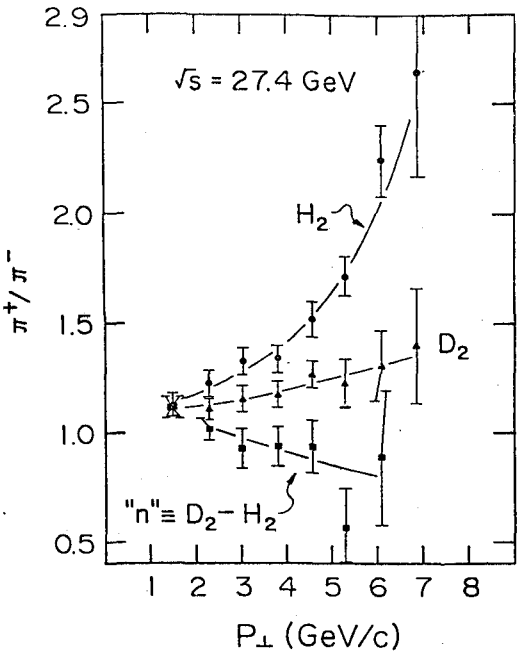


Fig.7.

There are also new results on the energy dependence of high p_T inclusive production in pp interactions. Data have been fit to the form

$$E\frac{d^3\sigma}{dp^3} = A\, p_T^{-n}(1-x_T)^f.$$

An example is shown in Fig.8, where $p_\perp^{8.5} E\frac{d^3\sigma}{dp^3}$ has been plotted vs x_T.

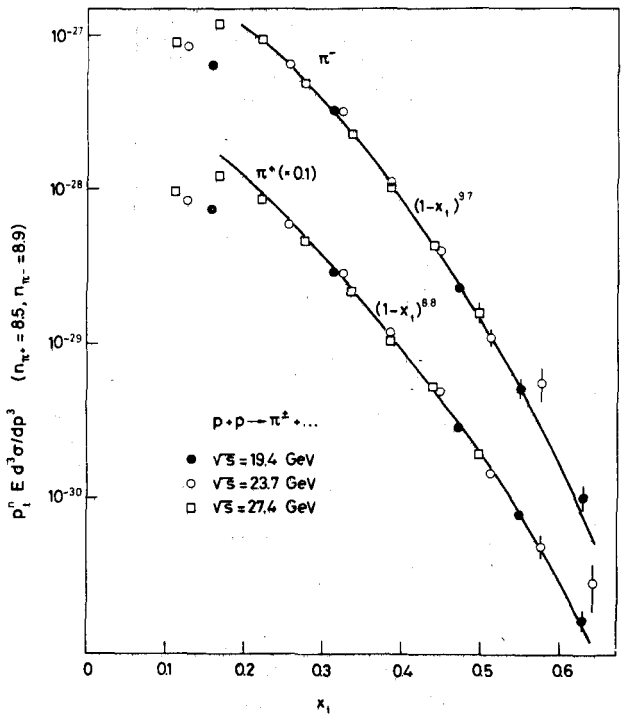


Fig. 8

In the scaling region $x_T > 0.3$ the data from the various energies all fall on the same curve. The results for the various final state particles are tabulated below together with the CIM predictions. The results are in general agreement with the CIM model.

	Data		CIM prediction	
Process	n	f	n	f
$pp \to \pi^+ X$	8.5	8.8	8	9
$pp \to \pi^- X$	8.9	9.3	8	9
$pp \to K^+ X$	8.4	8.8	8	9
$pp \to K^- X$	8.9	11.7	8	11,13
$pp \to p X$	11.7	6.8	12	5
$pp \to \bar{p} X$	11.9	8.0	12	11

Fit to $Ed^3\sigma/dp^3 = A\, p_T^{\,n} (1-x_T)^f$

References

1. G. Donaldson et al. Phys.Rev.Lett., to be published.
2. S.Brodsky, invited talk in this session.
3. L.Kluberg et al. Submitted paper to the Conference 753/A4-17.

CORRELATIONS IN COLLISIONS WITH A HIGH-$p_\perp$ PARTICLE PRODUCED

R. Sosnowski(*)
CERN, Geneva, Switzerland

In order to study the mechanism responsible fer the production of secondaries with large transverse momenta we have to analyse the high-$p_\perp$ collision as completely as possible. The Split Field Magnet detector (SFM) installed at the CERN Intersecting Storage Rings offers such a possibility for high-energy proton-proton collisions. In this review we will discuss the data obtained by three experimental groups which analysed collision at 26 + 26 GeV with a high transverse momentum secondary using the SFM detector.

The CERN group was dealing with the collisions in which a high-$p_\perp$ neutral pion was emitted at 90° c.m. production angle. The analysed sample contained ~ 8000 events [1].

The British-French-Scandinavian Collaboration [2] has studied events with a high-$p_\perp$ charged particle emitted also at 90° c.m. angle. This particle has been identified with a Cerenkov counter as being K, π or a proton. The data are preliminary. The sample analysed so far contains 38 000 events from which 8700 have a charged particle with the transverse momentum above 2 GeV/c.

The CERN-Collège de France-Heidelberg-Karlsruhe Collaboration [3] has presented the data based on about 270 000 events with a charged secondary of transverse momentum bigger than 2 GeV/c. The production angle of high-$p_\perp$ secondaries was equal to about 45° (80 000 events) and about 20° (190 000 events).

It has been found in all three experiments that whenever a high-$p_\perp$ particle is detected the probability to observe another particle(s) emitted roughly in the same direction increases. This is shown in fig. 1 where a clear peak in the rapidity distribution is observed at rapidities close to that of the high-$p_\perp$, triggering particle. In this figure are plotted only those particles which are emitted at azimuthal angles similar to that of the high-$p_\perp$ particle. In the same figure the rapidity distribution for normal events (without a high-$p_\perp$ secondary) is shown as a dashed curve.

The observed excess of secondary particles above the distribution for normal collisions increases with the transverse momentum of secondaries which is shown in fig. 2. It increases also with the transverse momentum of the high-$p_\perp$ particle what can be seen in fig. 3.

However the correlation for same charged particles is weaker than for different charges. This can be seen in fig. 4 where the average multiplicities of particles in the region around a high-$p_\perp$ particle are plotted for different charge combinations of the high-$p_\perp$ and low-$p_\perp$ particles. The average multiplicities are about twice as big for opposite charges than for the same ones. This effect depends weakly on the nature of a high-$p_\perp$ particle. Nevertheless there is an indication that for the same charge the multiplicity associated with a high-$p_\perp$ pion is higher than that associated with a high-$p_\perp$ kaon or a proton (antiproton). One of the possible explanation of this fact could be the Goldhaber effect.

Finally, the excess of particles in the region around the high-$p_\perp$ particle decreases with the increase in the rapidity of the high-$p_\perp$ particle. This is illustrated in fig. 5.

The excess of particles around a high-$p_\perp$ particle is often considered as a manifestation of a jet of hadrons originated, for example, in the hard scattering of two partons. We can then ask what is the distribution of the momentum component perpendicular to the jet axis. The corresponding data are shown in fig. 6. It can be seen that the transverse momentum distribution in respect to the jet axis is similar to that observed in ordinary soft hadron-hadron collisions as expected from the jet concept.

(*) On leave from the Institute for Nuclear Research, Warsaw.

However, we cannot exclude the possibility that the observed excess of particles flying roughly in the direction of the high-$p_\perp$ secondary is due to the resonance production. It may be that the observed high-$p_\perp$ particles are mostly the decay products of known (or unknown) resonances. The discussed SFM experiments show that resonances do exist at high-transverse momenta and a significant number of high-$p_\perp$ secondaries are the decay products of ρ or K (fig. 7).

So far we have discussed the emission of secondaries in roughly the same azimuthal direction as that of the high-$p_\perp$ particle. The SFM detector allows us to study particles in nearly 2π interval of the azimuthal angle. It has been found already before [4] that collisions with a high-$p_\perp$ secondaries exhibit a large excess of particles emitted at the azimuthal direction opposite to that of a high-$p_\perp$ particle (away diraction). This effect has been confirmed and studied extensively by all three SFM experiments. In fig. 8 is shown the rapidity distribution of secondaries emitted in the away azimuthal direction. It can be seen that the excess of the multiplicity in this region covers a wide rapidity interval from -2.5 to 2.5. This excess increases with the transverse momentum of the high-$p_\perp$ particle and is equally strong for negative and positive secondaries. There is no clear dependence of the effect on the nature of the high-$p_\perp$ particle. An interesting question concerning the emission of particles in the azimuthal direction away from the trigger is, whether they form in each collision a collimated bunch of particles-jets. Such a behaviour is suggested by the hard-scattering picture. The data presented by the three experiments discussed here suggest the existence of the correlated groups of particle which balance the most of the transverse momentum of the triggering particles.

In fig. 9 we see a clear demonstration of the short range correlation. Whenever a particle is detected in the "away" direction other particle tend to follow it. The similar correlation is shown in fig. 10. The distribution of the rapidity difference Δy exhibits a maximum at $\Delta y = 0$ which is much stronger than expected for the uncorrelated emission. This correlation is bigger for the high-$p_\perp$ collisions than for normal events. It is also bigger for secondaries with high transverse momenta (see fig. 11).

From the above discussion we see that the jet concept is supported by the data, however, the final proof of the existence of jets remains to be given.

The experimental data show that the higher is the transverse momentum of a triggering particle more numerous are the high-$p_\perp$ particle in the away direction. We can verify whether this effect exhibits a scaling behaviour [5] in the reduced transverse momentum, $x = p_x/p_\perp^t$. The quantity p_x stands here for the transverse momentum component parallel to the transverse momentum of the triggering high-$p_\perp$ particle, $p_\perp^t$. The distribution of the number of particles versus x is shown in fig. 12 for three intervals of $p_\perp^t$. The lack of scaling is evident. However, the lack of scaling in variable x does not mean necessarily the lack of scaling in the longitudinal reduced momentum in jets. This is because the emission angles of away jets covers a wide interval around 90° and often the x variable differs strongly from the longitudinal reduced momentum in jets.

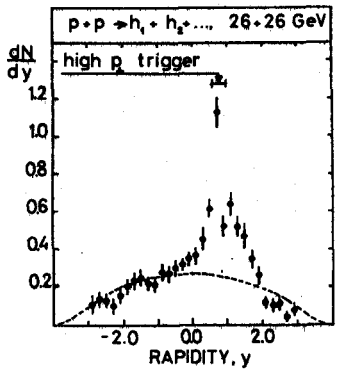


Fig. 1 The rapidity distribution of negative secondaries produced in events triggered on a large $p_\perp$ particle of positive charge with $9 \sim 45^\circ$ and $p_\perp > 2.0$ GeV/c. Only secondaries are entered in the histogram being near in azimuth to the triggering particle, $\Delta\phi = \pm 25^\circ$, and having a transverse momenta $0.5 < p_\perp < 1.0$ GeV/c. The full line represents the equivalent distribution for normal events [3].

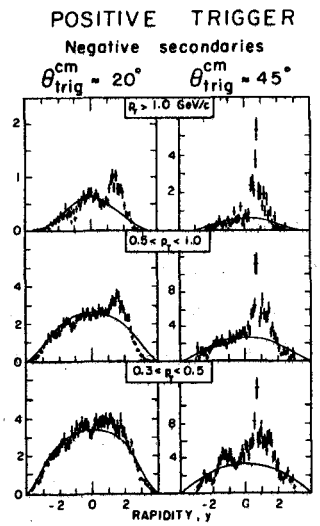


Fig. 2 The same distributions as shown in fig. 1 plotted for different intervals of the transverse momenta of secondaries and for two values of the emission angle of the high-$p_\perp$ particle [3].

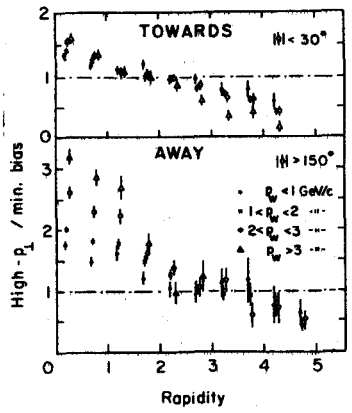


Fig. 3 The ratio of the rapidity distributions for high-$p_\perp$ events to

REFERENCES

[1] P. Darriulat et al., Nuclear Physics B107 (1976) 429.

[2] British-French-Scandinavian-ISR Collaboration, paper A4-899 submitted to this conference.

[3] CERN-Collège de France-Heidelberg-Karlsruhe Collaboration, papers A4-127 and A4-129 submitted to this conference.

[4] See e.g. P. Darriulat, Rapporteurs Talk at the International Conference on High-Energy Physics, Palermo, June 1975.

[5] M. Jacob and P. Landshoff, CERN preprint TH-2182 - CERN.

that for normal (minimum bias) events for the different values of the transverse momenta of a high-$p_\perp$ particle, p_w. The high-$p_\perp$ particles is emitted at $\phi = 0$ [2].

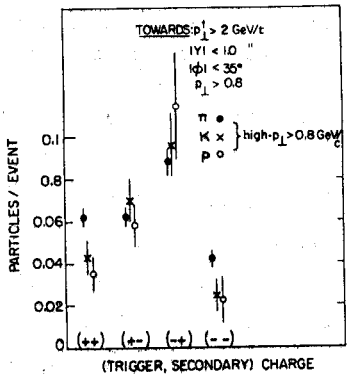


Fig. 4 The average number of secondaries with $p_\perp$ > 0.8 GeV/c emitted around the high-$p_\perp$ particle for four combinations of the charges of the high-$p_\perp$ particla and a secondary [2].

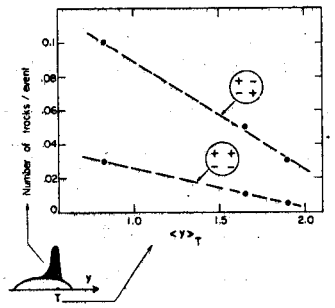


Fig. 5 The increase of chargad multiplicity with respect to normal events in the azimuthal angle region "towards" trigger as a function of the rapidity of the large $p_\perp$ triggering particle. Points on lower line refer to secondaries of the same as the trigger, on upper to those of opposite charge [3].

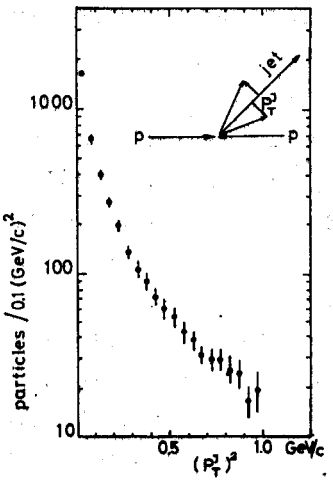


Fig. 6 The transverse momentum squared discribution with respect to the jet axis of particles forming a jet, containing the triggering large $p_\perp$ particle [3].

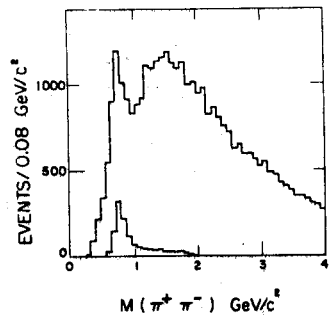


Fig. 7 $\pi^+\pi^-$ invariant mass distribution. The π^- is the high-$p_\perp$ triggering particle emitted at 20° and identified by a Čerenkov counter ($p_\perp(\pi^-)$ > 1.5 GeV/c). An estimation of the ρ^0 signal corresponding to $\rho^0/\pi^- = 1.2$ is ahown.

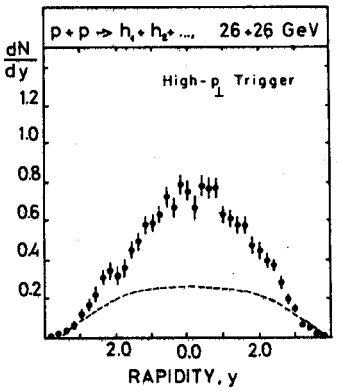


Fig. 8 Same aa fig. 1, but for secondaries in the azimuthal angle region away from the trigger, 140° < φ < 220° [3].

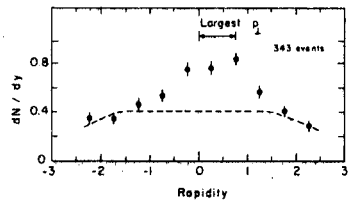


Fig. 9 The rapidity distribution of charged particles away from the 90° high-$p_\perp$ π^0 trigger when the fastest away particle not included in the plot has p_x > 1.2 GeV/c and 0 < y < 0.75 [1].

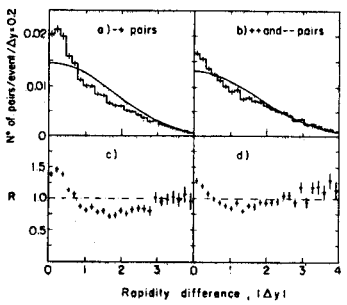


Fig. 10 The distribution of the rapidity difference of pairs of particles (a) with opposite charge and (b) with aame charge produced in

large $p_\perp$ events in the azimuthal angle region away from the trigger (full line). Also shown is the equivalent distribution for uncorrelated pairs obtained by combining secondaries from different events. In both cases only secondaries with $p_\perp > 0.6$ GeV/c were entered. Figs 10(c and d) show a normalized rapidity difference distribution obtained by taking the ratio of the distributions of figs 10(a and b) respectively, to the background distributions of these figures [3]

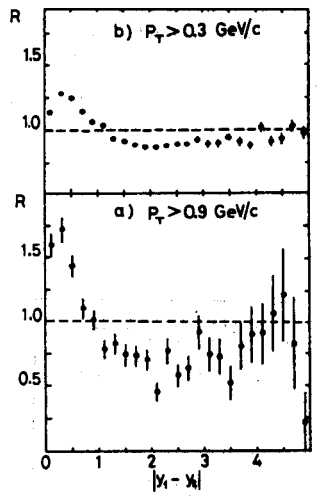


Fig. 11 Normalized rapidity difference for secondaries of opposite charge with $p_\perp > 0.3$ GeV/c (fig. 11 (a)) and $p_\perp > 0.9$ GeV/c (fig. 11 (b)) [3].

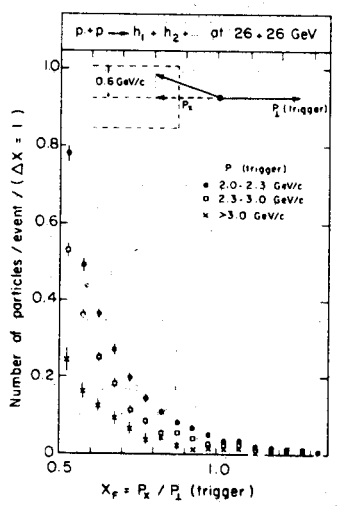


Fig. 12 The distribution of the number of secondaries per event emitted in the away direction versus the reduced transverse momentum $X = p_\perp / p_\perp^t$. Three sets of points correspond to three values of the transverse momentum of the triggering particle. Only particles with the momentum component perpendicular to the trigger plane smaller than 0.6 GeV/c are plotted.

LARGE TRANSVERSE MOMENTUM PHOTONS FROM HIGH ENERGY PROTON-PROTON COLLISIONS

P.Darriulat, P.Dittman, K.Eggert, M.Holder, K.T. Mc Donald, T.Modis, F.L.Navarria, A.Seiden, J.Strauss, G.Vesztergombi, E.G.H.Williams
(presented by G.Vesztergombi (JINR, Dubna))

Large transverse momentum production of photons has been the object of many investigations /1-4/ . However, no systematic investigation concerning the source of the observed photons has been made and it has been generally assumed that they are the products of π^0 or η decays. In order to clarify this situation here we report on a simultaneous measurement of the yields of single photons and of photon pairs produced in proton-proton collisions of total c.m. energies $\sqrt{s} = 45$ and 53 GeV.

The photon detector is a lead glass hodoscope located at 90° production angle in an intersection region of CERN ISR. Its properties and performance have been described in detail in previous publications /5/ . The distance to the beam intersect is 3.62 m, corresponding to a solid angle acceptance of 0.05 sr. To analyse the pattern of energy distribution in the lead glass array, we reduce it to a number of clusters of connected cells with pulse heights significantly above zero. In the following the number of above defined clusters will be referred as number of observed photons. The question of purity of this "photon sample" will be discussed in later paragraphs.

The space around the beams is covered by a large acceptance magnetic spectrometer, the Split Field Magnet Facility, where charged particles produced in association with the lead glass trigger are detected /6/ .

Events were recorded when they simultaneously satisfied two conditions: an energy deposition above an adjustable threshold (usually 1.4 GeV) in the lead glass counter and the detection of at least two charged particles either in the SFM wire chambers or in each of

two scintillation hodoscopes positioned at small angles to the beam lines. The second condition ensures that the detected photons are produced in a genuine beam-beam interaction while it may cause a loss of at most 10% to the inclusive photon spectrum.

The comparison of the measured single photon yield to that expected from π^0 decays involves three operations: the measurement of the yield of ^0S (identified as photon pairs with correct invariant mass), a calculation of the single photon yield expected from π^0 decays seen by the detector (using the measured π^0 cross section) and the measurement of the single photon yield itself.

Applying this method the accurate knowledge of the shape of the energy response curve of the lead glass counter is essential because a single photon detected in the counter usually carries most of the energy of its parent π^0 (87% on the average) while photons from a resolved photon pair carry about half of the π^0 energy. Therefore we performed extensive studies on lead glass calibration, whose details are discussed in our subsequent paper /7/ .

In order to determine the inclusive π^0 spectrum we select a pure sample of $\pi^0 \to \gamma\gamma$ decays by the following selection criteria: we retain only "symmetric pairs" i.e. $\alpha = |E_1 - E_2|/(E_1+E_2) < 0.5$ where E_i represents the measured energy of the photon. We require the distance between the photon impacts to be larger than 27 cm and the invariant mass m of the photon pair to lie within the range $50 < m < 200$ MeV/c^2 . When more than two clusters are detected in the lead glass array (in 8% of the cases) we take the pair with the highest total energy. The background due to wrong pairing is estimated from 3 cluster events to be less than 2%.

Photon conversions in the vacuum pipe and in the material of the SFM detector cause a loss of events which is estimated by Monte Carlo calculations tracking $e^{\pm}$ in the inhomogeneous SFM field to be of 15 $\pm$ 3%.

The resulting invariant cross sections are displayed in figure 1 (open cicles) together with the data of ref. 8 for π^+ (full circles) and π^- (crosses).

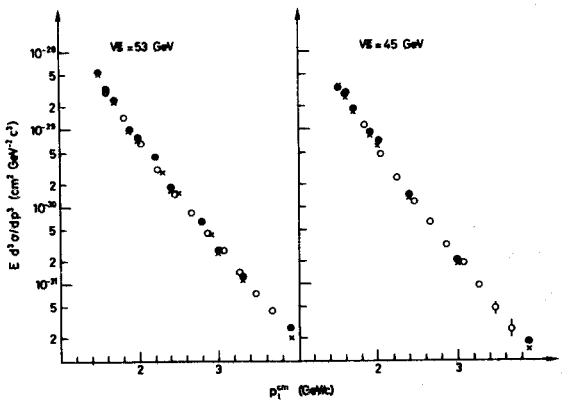


Fig.1

Our results are compatible with the assumption that the π^0 spectrum lies somewhere in between the π^+ and π^- ones.

Selecting single photons we retain those events where a cluster is detected in the lead glass array either alone or, in 2.8% of the cases, accompanied by additional cluster of less than 100 MeV energy. This requirement helps in selecting a pure sample but the loss of single photon events accompanied by an independent cluster must be corrected for. From the rate of occurence of asymmetric ($\alpha > 0.5$) photon pairs we expect this loss to be of the order of 8%.

We also correct for conversions in the material between the interaction region and the lead glass counter. They cause an event loss of 5 to 10% depending upon energy. We compared the observed and calculated fractions of events with a track detected in the SFM wire chambers and pointing to a cluster in the lead glass counter. Electrons and positrons are expected to contribute 1.5% each. In fact we observe 2% positive tracks but a larger fraction, 6% of negative tracks. We tentatively attribute the excess to antiprotons which may

deposit much more than their kinetic energy when they annihilate in the lead glass. This brings up the question of the antineutron contamination, over which we have no direct control since antineutrons leave no track in the SFM wire chambers. For this reason we restrict the range of our analysis to momenta larger than $p_t^{cm} = 2.8$ GeV/c, above which value the contamination of $\bar{p}$ and $\bar{n}$ with $p_t^{lab} = 0.5$ GeV/c is negligible. In this high momentum range we calculate the combination of $\bar{n}$ to be about 11% of the whole single photon yield assuming that $\bar{p}$ and $\bar{n}$ are produced with the same cross section.

Radiative decays of particles other than π^0's also enrich the single photon sample. The largest contribution is expected from $\eta \to \gamma\gamma$ decays, for which the inclusive production cross section has been measured in previous experiments /1,2/. By η decays we can explain 12-13% of the observed single photon spectrum. Radiative decays from other known particles, such as ω and η', are expected to give negligible contribution due to their small branching ratios.

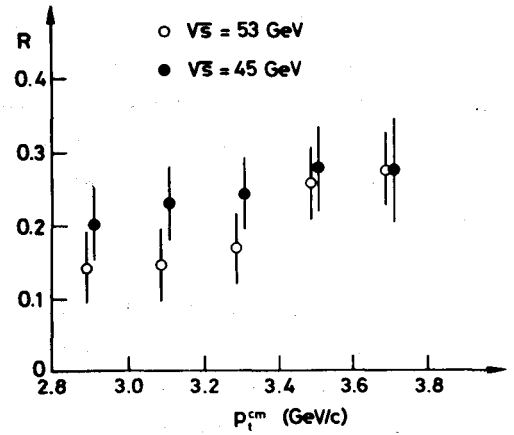


Fig.2.

The ratio between the single photon yield in exoess to that from π^0 and η decays and the π^0 yield itself is displayed in figure 2 in the momentum interval 2.8 GeV/c $< p_t^{cm} <$ 3.8 GeV/c. It typically amounts to 20% for both values of $\sqrt{s}$. To quote an uncertainty on this number we separate that coming from the energy response curve, which amounts to ± 7%, from that coming from all other sources, including statistics, and which amounts to ± 6%.

While this is the first time that a copius production of single photons is mentioned in proton-proton collisions, it had previously been reported in a large p_t photoproduction experiment /9/.

References

1. F.W.Büsser et al. Phys.Lett., 46B, 471 (1973); 471, 51B (1974); 306 and 311, 53B (1974); 212, 55B (1976).
2. K.Eggert et al. Nucl.Phys., B98, 49 (1975).
3. D.C.Carey et al. Phys.Lett., 32, 24 (1974) and 33, 327 (1974).
4. G.Donaldson et al. Phys.Rev.Lett., 36, 1110 (1976).
5. M.Holder et al. Nucl.Inst.Meth., 108, 541 (1973).
6. P.Darriulat et al. Nucl.Phys., B107 (1973).
7. P.Darriulat et al., to be published in Nucl.Phys. B.
8. B.Alper et al. Nucl. Phys., B100, 237 (1975).
9. D.O.Caldwell et al. Phys.Rev.Lett., 33,869 (1974).

RECENT DEVELOPMENTS IN THE THEORY OF LARGE TRANSVERSE MOMENTUM PROCESSES*

Stanley J. Brodsky
Stanford Linear Accelerator Center
Stanford University, Stanford, California 94305

Invited talk presented at the XVIII International Conference
on High Energy Physics
Tbilisi, USSR, 15-21 July 1976

One of the most important questions in hadron dynamics is the understanding of the underlying mechanisms for the production of large transverse momentum particles. The emerging features of the associated particles accompanying a high p_T trigger (jet structure, coplanarity, angular correlations, scaling laws) lend support to an underlying two-body hard scattering mechanism, as outlined by Berman, Bjorken, and Kogut[1] and Bjorken.[2] Although it was natural to hope that the basic large p_T mechanism could be related to elemsntary quark-quark scattering, the new Chicago-Princeton (CP)[3] proton target data at FNAL appear to rule this out. We will briefly review the evidence for this and present a comparison with the predictions of the constituant interchange model (CIM)[4] which postulates that the important subprocesses involve quark-hadron scattering. .

If the parton distribution functions scale, then the large p_T power-law scaling behavior of the inclusive cross section $Ed\sigma/d^3p(A + B \to C + X) \to p_T^{-n} f(x_T, \theta_{c.m.})$ directly determines the fixed $\theta_{c.m.}$ scaling of the underlying hard scattering subprocess - $d\sigma/dt(a + b \to c + d) \to s^{-n} f(\theta_{c.m.})$. The new Chicago-Priaceton data for $pp \to \pi^+ X$ at 200, 300, 400 GeV/c at $\theta_{c.m.} \sim 90^0$ reported at Tbilisi by Shochet,[3] which shows that $n \cong 8.5$ for $0.3 < x_T < 0.7$, greatly extends the scaling behavior ($n \cong 8$) observed at the ISR for $0.1 < x_T < 0.4$, $\sqrt{s} < 57$ GeV.[1] Although the natural scaling behavior predteted for point-like quarks with a scale-invariant interaction is $p_\perp^{-4}$, several authors have proposed scale-breaking modifications to account for the observed behavior.[5] Such modifications of course should also affect the standard parton scaling laws (c.g., for $pp \to \mu^+\mu^- X$ and dimensional counting predictions for form factors). Thie idea now seems intractable in view of the CP data for $pp \to pX$ which scales as $Ed\sigma/d^3p \propto p_T^{-11.7}(1 - x_T)^{6.8}$. The change in p_T power from $n \sim 8$ for meson to $n \sim 12$ for baryon production contradicts the idea of a fixed form for the subprocess. Further, using $qq \to qq$ for $pp \to pX$ requires three powers of the proton structure fuaction $\sim (1-x)^3$, which, together wtth two convolutton integrations, yields a minimum threshold dependence $\sim (1-x_T)^{11}$, in contrast to the $\sim (1-x_T)^7$ dependence obeerved.

The $qq \to qq$ description of large p_T reactions also appears io lead to a difficulty with the scaling behavior of the system on the away side of a 90^0 high p_T pion trigger as measured at the ISR. The quark-fragmentation distribution $\sim (1-x)^m/x$ ($m = 1$ to 2 from SPEAR $e^+e^- \to \pi + X$ data) implies that the p_T of each of the outgoing quarks is 30 to 50% higher than the p_T of the trigger.[6] The observed scaling behavior of the away side system, however, indicates that the recoil jet has an excess of only $\sim 10\%$ of the trigger momentum. This is related to the faot that few additional hadrons are seen along the trigger particle direction, the same side jet often consists of the trigger hadron alone.[1] Even more significantly, the charged particle multiplicity on the towards side is $\langle n_{ch} \rangle \sim .85 \pm .15$, independent of the trigger particle p_T ($2 < p_T < 6$ GeV). In contrasi, in the $qq \to qq$ model one predicts an increase of $\Delta n_{ch} = .4$ (for $m = 1$) over the range $2 < p_T < 6$ GeV. A still mere sensitive test is possible: in the $qq \to qq$ model, the toward eide associated multiplicity is predicted to change significantly as a function of the event-by-event location of the opposite side jet.[7] Such changes are absent in the CIM subprocesses in which the trigger side system is dominated by single particle and resonance production.

In the CIM, one predicts that the leading quark-hadron subprocess for $pp \to \pi X$ is $Mq \to \pi q$ (where M reprssents a limited-mass $q\bar{q}$ state fragmented from one of the nucleons). A $p_\perp^{-8}$ scaling behavior is predicted by the model essentially because of the additional factors $\sim t^{-2}$ from $F_M^2(t)$. The predictions of the CIM are systematized using the dimensional counting rules[8]

$$E\frac{d\sigma}{d^3p} = \sum_{abcd} \frac{f(\epsilon, \theta_{c.m.})}{(p_T^2+m^2)^{n_{active}-2}}$$

where n_{active} is the total number of elementary fields (q, ℓ, γ) in the hard subprocess $a + b \to c + d$, and m^2 ($\lesssim 1$ GeV^2) represents a typical parton mass scale. At the exclusive limit, where $\epsilon \equiv 1 - \sqrt{x_T^2 + x_L^2} \to 0$, $f(\epsilon, \theta_{c.m.}) \to f(\theta_{c.m.})\epsilon^F$; $F = 2n_{spect} - 1$ increases as ths number of "spectator" or "passive" quarks in the hadrons A, B, C tncreases.[9] These rules are based on Born graphs in reaormalizable (scale-invariant) theories and finits Beths-Salpeter hadronic wave functions. Derivations and discussions of spin and kinematic effects are given in Refs. 4, 8, and 9. The quark model requires $n_{active} = 4, 8, 8, \ldots$, and hence predicts the series $p_\perp^{-4}$, $p_\perp^{-8}$, $p_\perp^{-12}, \ldots$ at fixed x_T and $\theta_{c.m.}$.

The leading CIM contrtbution ($Mq \to \pi q$, $n_{active} = 6$, $n_{spec} = 5$) for $pp \to \pi^\pm, K^+X$ leads to the asymptotic prediction $p_\perp^{-8}(1-x_T)^9$. This caa be compared to the fits to the CP measurements, $p_\perp^{-8.5}(1-x_T)^{8.8}$ for $pp \to \pi^+X$, $p_\perp^{-8.9}(1-x_T)^{9.7}$ for $pp \to \pi^-X$, and $p_\perp^{-8.4}(1-x_T)^{8.8}$ for $pp \to K^+X$. (See Table I.) The observed fixed p_T ratio $\pi^-/\pi^+ \sim (1-x_T)$ could be related to the down-to-up quark ratio in the proton structure function or to the effects of resonanca decay. The subprocesses $Mq \to K^-q$ and $q\bar{q} \to K^+K^-$ for K^- production predict the fixed p_T ratio $K^-/K^+ \sim (1-x_T)^4$ and $(1-x_T)^2$, respectively. The CP result for $pp \to K^-X$ is $p_T^{-8.9}(1-x_T)^{11.7}$ or $K^-/K^+ \sim (1-x_T)^3$ at fixed p_T.

The leading subprocesses for proton production $q + qq \to M + p$ and $qB \to qp$ give the predictions $p_\perp^{-12}(1-x_T)^5$ and $p_\perp^{-12}(1-x_T)^7$, respectively, compared to the CP measurement $p_\perp^{-11.7}(1-x_T)^{6.8}$. The $p_\perp^{-8}$ subprocess $q + q \to B + \bar{q}$ (which like $qq \to qq$ requires "double color neutralization" - see below) is ruled out by the data.

The leading CIM subprocess for $\bar{p}$ production[4] with $n_{active} = 6$ is $qM \to qM$ [where the $\bar{p}$ fragments from a large p_T meson state], giving the prediction $p_T^{-8}(1-x_T)^{15}$. The leading $n_{active} = 8$ subprocesses give $p_T^{-12}(1-x_T)^{11}$. The new CP fit[3] is $p_T^{-8.8}(1-x_T)^{14.2}$, indicating that the predicted $n_{active} = 6$ subprocesses give a good rèpresentation ef the $\bar{p}$ data.

Thus the CIM seems to account fer many of the features of the large p_T data - naturally accounting for the meson/baryon power change. Note that all s-wave $q\bar{q}$ resonances contribute roughly equally in $Mq \to M'q$ and one may thus expect appreciable same side associated multiplicity and correlations; multiparticle resonances are required to account for the $\pi^-\pi^-$ same side serrelations. The predicted angular distribution, $d\sigma/dt \sim u^{-1}t^{-3}$, for $qM \to qM$ apparently leads to a reasonable angular correlation for the away side system.[7] (See also R. Baier et al., Ref. 5.)

Many theoretical reasons have been advanced for the suppression of $qq \to qq$. Recent suggestions include (a) the effects of the trigger bias[6] - a $\delta(1-x)$ term gives 20-60 more events than a $(1-x)^m/x$ ($m = 1$ to 2) distribution of the decay jet; (b) small coupling constants and asymptotic freedom effects;[10] (c) the fact that double neutralization of color[11] is required for $qq \to qq$ or $qq \to B\bar{B}$ (and thus double hadron multiplicity[7]); in contrast, the standard parton model lepton processes and the CIM subprocesses all involve single neutralization.

The prediction for $\pi p \to \pi X$ in the CIM has asymptotic terms of the form $p_T^{-8}(1-x_T)^5$, $p_T^{-8}(1-x_T)^7$, and $p_T^{-12}(1-x_T)^3$ for $q\bar{q} \to \pi\bar{M}$, $Mq \to \pi q$, and $q + qq \to \pi + B$, respectively. The "leading-particle" diagram where the incoming meson scatters directly on a quark of the target proton is normalized by the factor $[d\sigma/dt\ (\pi p \to \pi p)]/[d\sigma/dt\ (ep \to ep)]$ to the deep inelastic electron scattering cross section, and is found to be negligible until $x_T \gtrsim 0.7$ at FNAL energies. The recent FNAL data of Donaldson et al.[12] at $p_{lab} = 100$, 200 GeV/c when $x_T < .6$ was fit to the form $(1-x_T)^{5.5\pm0.3}/(p_T^2 + m^2)^{2.5\pm1.1}$ with $m^2 = 1.8$ GeV^2. The CIM predicts the ratio $\sigma(pp \to \pi X)/\sigma(\pi p \to \pi X) \sim (1-x_T)^2$ if p_T^{-12}

terms dominate both reactions in this low energy regime or $(1-x_T)^2$ to $(1-x_T)^4$ depending on which p_T^{-8} terms dominate. The measurements indicate the ratio at fixed p_T is $\sim (1-x_T)^{1.6\pm0.3}$. A much more dramatic effect is predicted for the ratio $\sigma(pp \to \bar{p}X)/\sigma(\pi p \to \bar{p}X) \sim (1-x_T)^6$ since the contributing fusion reaction $q\bar{q} \to B\bar{B}$ is highly sensitive to the projectile antiquark contribution. To summarize, the current pion beam data appear to be consistent with the dominance of the simplest possible subprocesses.

The CIM can predict in detail quantum number flow, correlations of particles associated with large p_T events. Many more experimental tests of the model are required at higher p_T and x_T, including the use of different beams (especially photons). Measurements of quantum number correlations, the distribution of charge, and detailed comparisons with the final states in $e^+e^- \to$ hadrons, $pp \to \mu^+\mu^-X$ are also important.

Jet structure is the underlying link between lepton and hadron processes. Different types of single or multiquark jets (all with total 3 or $\bar{3}$ SU(3) color quantum numbers) are expected in $e^+e^- \to X$ (q and $\bar{q}$ jets), $lp \to lX$ (q and qq jets), $pp \to \mu^+\mu^-X$ (qq and qqqq jets) and $pp \to \pi X$ (q and qq jets for the $qM \to \pi q$ subprocess). Assuming that the multiplicity in the central region is due to the virtual separation of color, the multiplicity can be related in each case to the $e^+e^- \to X$ multiplicity.[7] On the other hand, valence effects can be unraveled by observing the quantum number flow and using the spectator counting rule $dN/dx \sim (1-x)^{2n_{spec}-1}$ in the jet fragmentation region. The form of the forward inclusive cross section and fragmentation probabilities can be predicted for both gluon- and quark-exchange models.[7]

Recent work on dimensional counting includes a field theoretic derivation of the form factor rule[13] $F(t) \sim t^{1-n}$ (modulo anomalous dimension corrections) by Goldberger, Guth, and Soper,[14] and the fixed angle scattering rule[13] $d\sigma/dt \sim s^{2-n}f(t/s)$ by Polyakov.[15] Infinite order modifications in an Abelian gluon model have been recently discussed by Efremov and Radyushkin.[16]

There has also been recent work applying dimensional counting to nuclear systems.[11,17,18]

In the case of the deuteron form factor, one expects on general grounds that $F_D(q^2)$ will fall faster than $F_N^2(q^2/4)$ since each nucleon must change momentum by $\sim q/2$. The underlying six quark structure then predicts[11,17,18] that the reduced form factor $f_D(t) = F_D(t)/F_N^2(t/4)$ will fall like $(1/t)$. This prediction is confirmed by the new measurement at SLAC by B. Chertok's group.[18] This scaling result for $f_D(t)$ reflects an underlying scale-invariant form for the nuclear force once the effects of nucleon structure are removed.[17] (Fig. 1)

ACKNOWLEDGEMENT

The predictions of the constituent interchange model were done in collaboration with R. Blankenbecler and J. Gunion. The manuscript was prepared in collaboration with J. Gunion.

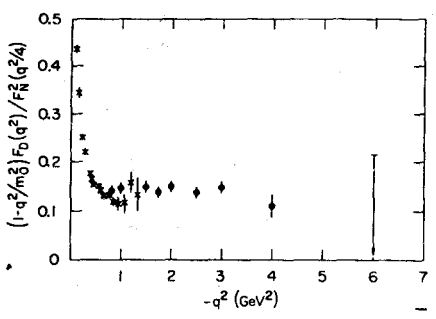


Fig. 1

TABLE I

Scaling Predictions for $E\,d\sigma/d^3p = C\,p_T^{-n}(1-x_T)^F$

Large p_T Process	Leading CIM Subprocess	Predicted n//F	Observed (CP)[3] n//F
$pp \to \pi^+X$	$qM \to q\pi^+$	8//9	8.5//8.8
π^-	$qM \to q\pi^-$	8//9	8.9//9.7
K^+	$qM \to qK^+$	8//9	8.4//8.8
K^-	$qM \to qK^-$	8//13	8.9//11.7
	$q\bar{q} \to K^+K^-$	8//11	
$pp \to pX$	$q(qq) \to Mp$	12//5	11.7//6.8
	$qB \to qp$	12//7	
$pp \to \bar{p}X$	$q\bar{q} \to B\bar{p}$	12//11	8.8//14.2
	$qM \to qM$	8//15	
$\pi p \to \pi X$	$q\bar{q} \to M\pi$	8//5	
	$qM \to q\pi$	8//7	
	$q(qq) \to B\pi$	12//3	
	$\pi q \to \pi q$	8//3	

REFERENCES

1. S. M. Berman, J. D. Bjorken and J. B. Kogut, Phys. Rev. D 4, 3388 (1971). Additional references are reviews given in D. Sivers, S. Brodsky and R. Blankenbecler, Phys. Reports C 23 (1976); P. V. Landshoff, London Conference, 1974; P. Darriullat, XVIIIth Int. Conf. on High Energy Physics, Tbilisi, 1976; and J. Gunion, APS Meeting, Williamsburg, Va., 1974.
2. J. Bjorken, Phys. Rev. D 8, 3098 (1973).
3. M. Schochet et al., XVIIIth Int. Conf. on High Energy Physics, Tbilisi, 1976; J. Cronin, VIIth Int. Colloq. on Multiparticle Reactions, Munich, 1976. The $pp \to \bar{p}X$ fit is from M. Schochet, contributed paper 753/A4-17
4. R. Blankenbecler, S. J. Brodsky and J. F. Gunion, Phys. Letters B 39, 649 (1972); 42, 461 (1973); Phys. Rev. D 12, 3469 (1975). The large p_T work discussed in this paper was done in collaboration with R. Blankenbecler (to be published). The fusion process $q\bar{q} \to M+\bar{M}$ is discussed by P. V. Landshoff and J. C. Polkinghorne, Phys. Rev. D 10, 891 (1974). See also G. Preparata and M. Rossi, CERN preprint TH-2163(1976)
5. R. Field et al., Cal Tech preprint (1976), to be published. R. Hwa, A. J. Spiessbach and M. Teper, University of Oregon preprint (1976), contributed paper 900/A4-22. Levin and M. Ryskin, Yad. Fiz. 18, 1108 (1973). R. Baier et al., University of Biclefeld preprint (1976).
6. S. D. Ellis, M. Jacob and P. V. Landshoff, CERN preprint TH. 2109 (1976).
7. These results are based on the model of S. Brodsky and J. Gunion, UC Davis/SLAC preprint (1976), to be published in Phys. Rev. Letters.
8. S. J. Brodsky and G. R. Farrar, Phys. Rev. Letters 31, 1153 (1973); Phys. Rev. D 11, 1309 (1975).
9. R. Blankenbecler and S. J. Brodsky, Phys. Rev. D 10, 2973 (1974); J. Gunion, ibid., 10, 242 (1974).
10. A. Casher, J. Kogut and L. Susskind, Phys. Rev. D 10, 732 (1974).
11. S. Brodsky, 1975 SLAC Summer Institute, Report No. SLAC-191; Few Body Conference, University of Laval, 1974.
12. G. Donaldson et al., BNL preprint (1976).
13. S. Brodsky and G. Farrar, Ref. 7; V. A. Matveev, R. M. Muradyan and A. N. Tavkhelidze, Lett. Nuovo Cimento 7, 719 (1973).
14. M. Goldberger, A. Guth and D. Soper, Phys. Rev. D 14, 1117 (1976).

15. A. M. Polyakov, Proc. Int. Symposium on Lepton and Photon Interactions at High Energies, Stanford Linear Accelerator Center (1975).

16. A. V. Efremov and A. V. Radyushkin, JINR E2-9717, Dubna (1976), contributed paper I217/A7-52.

17. S. Brodsky and B. Chertok, Phys. Rev. Lett. 37, 269 (1976); and SLAC-PUB-1759, to be published.

18. R. Arnold et al., Phys. Rev. Letters 35, 776 (1975); B. Chertok, XVIIIth Int. Conf. on High Energy Physics, Tbilisi, 1976.

*Work supported by the Energy Research and Development Administration.

HIGH TRANSVERSE MOMENTUM PROCESSES IN COMPOSITE MODELS

A.N.Tavkhelidze

Institute for Nuclear Research, Moscow

It is rather interesting to investigate the high transverse momentum processes in studying the structure of hadrons. Quark counting rules[I] give the following formulas for the e.m.form factors and differential cross-sections of binary reactions:

$$F_A(t) \sim {}^{I}/_{|t|^{n_A-I}}, \qquad {}^{s\to\infty}_{t/s=\text{fixed}} \qquad (I)$$

where $F_A(t)$ is the e.m.form factor and n_A is a valence quark number of a hadron A, respectively.

$$\frac{d\sigma}{dt}^{AB\to CD} \frac{I}{s^{n_A+n_B+n_C+n_D-2}} f^{(z)}_{AB\to CD}, \qquad (2)$$

$$z=\cos\theta=I+{}^{2t}/_{s}.$$

Under some additional assumptions on the topology of the quark diagrams[2,3] the explicit expressions for the structure functions f(z) were obtained. In papers[3,4] contributed to the Conference, it was shown that owing to eqs.(I) and (2) the fit is in a satisfactory agreement with the experiment. In particular, considering the deuterons as a six-quark system, eq.(I) gives for the deuteron the e.m. form factor behaviour like t^{-5} which was supported in a recent SLAC experiment[5]. From this viewpont it is interesting to study the light nuclei form factors as many-quark systems translating the quark-parton models on the relativistic nuclei[6].

Assuming the quark structure of hadrons quark counting rules were generalized for the inclusive reactions in [7,8].

In papers[9,I0] the representation for the inclusive distributions in terms of the generalized density matrix is given in the framework of quantum field theory. Under rather specific assumptions on the density matrix structure one has succeeded to explain some scaling properties of inclusive reactions[I0].

In paper[II] contributed to the Conference and done in collaboration with A.N.Kvinikhidze, A.N.Sissakian and L.A.Slepchenko, in the framework of three-dimensional formalism of quantum field theory the general representation for the inclusive distributions of the high p_T particles was obtained in terms of the hadron structure functions (4). The great attention is paid to an analysis of different approximations leading on the base of these approximations to the quark-parton picture.

In studying the high transverse momentum production processes it is convenient to use the null-plane formulation of quantum field theory[I2-I4].

In this case the role of an energy $P_0 \equiv E$ and three-momenta $\vec{P}$ is played by an "energy" P^- and three-momenta $P \equiv (P^+, \vec{P}_T)$ respectively, where $(P^\pm \equiv P_0 \pm P_3)$.

Denote the state vector of a hadron A as

$$|A\rangle \equiv |P^-\ P, \alpha\rangle$$

$P \equiv (P, P)$ are four-momenta and α are other quantum numbers. Let $\psi_i(x)$ be the fundamental Heisenberg fields of the total Hamiltonian, and $|A\rangle$ be its eigenfunction

$$H^-|A\rangle = P^-|P^-,\ P, \alpha\rangle .$$

In general the hadron A consists of the constituent particles corresponding to the fundamental fields ψ_i (we denote them as a, b, c, ...).

Let us calculate the inclusive cross sections of the hadron C when, in the collision of hadrons A and B, the interaction between the subsystems of constituent particles is taken into account. Using the pole approximation for the many-particle subsystem of the Green functions we obtain for the inclusive distribution (AB → C+X) the following expression:

$$\frac{d\sigma^{AB\to C}}{d^3 p_C / E_C} = \frac{I}{4(2\pi)^2 s} \sum_{A'B'C'} \int (c^+ xy)^{-1} \rho_A^{A'}(\underline{p}, \alpha) \rho_B^{B'}(\underline{q}, \beta) z \cdot$$

$$\rho_C^{C'}(\underline{k}, \gamma) \cdot d^2 p_T d^2 q_T dx\, dy\, \frac{d\underline{k}}{k^+} |T_{A'B'C'D'}|^2\, d\alpha\, d\beta\, d\gamma$$

$$\delta\left(\frac{A^2 - \alpha}{A^+} + \frac{B^2 - \beta}{B^+} + \frac{C^2 - \gamma}{C^+} + \right.$$

$$\left. + \frac{I}{k^+} (s' + t' + u' - c^2 - k^2 - A^{12} - B^{12}) \right) \qquad (3)$$

where $s' = xys$, $t' = {}^{x}/_{z} t$, $u' = {}^{y}/_{z} u$ and $T_{A'B'C'D'}$ is the scattering amplitude of the binary process $A'B' \to C'D'$. The quantities $\rho_A^{A'}$, $\rho_B^{B'}$, $\rho_{C'}^{C}$ are defined in the following way: If A' is the bare quark state then $\rho^{A' \to a}$ and by definition

$$\rho_A^a(\underline{p}, \alpha) \equiv \sum_n c_n \int \delta\left| \alpha - \sum_{e=I}^{n} \frac{(p_e\ x_e\ A_T)^2 + m_e^2}{x_e} \right| A^+ \delta(\underline{A} - \Sigma \underline{p}_e) \cdot$$

$$\cdot \left| \Phi_A^{(n)}(\underline{p}_1 .. \underline{p}_n) \right|^2 \cdot \prod_{e \neq a} x_e\, dx_e\, d^2 p_{Te} \qquad (4)$$

where $\Phi_A^{(n)}(\underline{p}, ... \underline{p})$ is the Fourier-transform of the one time q.p. wave function.

$$\Phi_A^{(n)}(\underline{x}_1 .. \underline{x}_n) \equiv \langle 0 | \psi(x_1) ... \psi(x_n) | A \rangle |_{x_1^+ = ... = x_n^+ = 0}$$

This function satisfies the q.p. equation and the normalization condition

$$\sum_n c_n \int A^+ \delta\left| \underline{A} - \Sigma \underline{p}_e \right| \prod_{e=I}^{n} x_e\, dx_e\, d^2 p_{Te} \left| \Phi_A^{(n)}(\underline{p}_1 .. \underline{p}_n) \right|^2 = I$$

Thus, $\rho_A^a(\underline{p}) \equiv \int d\alpha\ \rho_A^a(\underline{p}, \alpha)$ represents the one-particle distribution and $\rho_A^a\, {}^{d\underline{p}}/_{A^+}$ is the probability for the constituent a to be in a hadron A within the momentum interval $(p, p + dp)$. From the q.p. wave function transformation properties on the null-plane we have

$$\rho_A^a(\underline{p}, \alpha) = \rho_{A^2}^a(p_T - x A_T, x; \alpha)$$

and from the requirement of the transverse momentum boundness for the noninteracting constituents it follows

$$\rho_A^a = \delta(\alpha - p_A^2)\, \delta(p_T - x A_T)\, \rho_A^a(x) \qquad (5)$$

Expression (5) corresponds to the structure function in the quark-parton model, and from eq. (3) we obtain the well-known single-particle distributions.[8]

In the case when $A'B'C'D'$ represent the physical particle states the functions $\rho_A^{A'}$, $\rho_B^{B'}$, $\rho_{C'}^{C}$ are expressed in the similar way to the structure function ρ^a in terms of the one-time q.p. "vertex" functions ^{A} of the form

$$\langle A' | \psi(x_1) ... \psi(x_n) | A \rangle_{x_1^+ = ... = x_n^+ = 0}$$

In general case when requiring the transverse momentum boundness and neglecting the interaction inside the subsystems A, B we can get the following representation for the single-particle distribution of the hadron C:

$$\frac{d\sigma^{AB\to C}}{d^3 p_C / E_C} = \frac{s}{\pi} \int xyz^{-2} \rho_A^{A'}(x)\, \rho_B^{B'}(y)\, \frac{d\sigma^{A'B' \to C'D'}}{dt}$$

$$(s', t', u')\, \rho_{C'}^{C}(z) \delta(s' + t' + u') dx\, dy\, dz \qquad (6)$$

which for the quark states $A'B'C'D'$ goes into the

$$\frac{d\sigma^{AB\to C}}{d^3 p_C / E_C} = \int z^{-2} dz\, \frac{d\tilde{\sigma}^{AB\to C}}{d^3 p' / E'} \cdot \rho_C^C(z) \qquad (7)$$

where $d\tilde{\sigma}^{AB\to C} / d^3 p' / E'$ is the inclusive distribution for a jet production.

The study of the power-law falloff for the inclusive cross-sections and an analysis of the existing experimental data allow us to receive some phenomenological consequences about the hadronic production mechanisms at large p_T[15].

References:

I. V.A.Matveev, R.M.Muradyan and A.N.Tavkhelidze, Lett.Nuovo Cim.7, 719(1973)
S.Brodsky and G.R.Farrar, Phys.Rev.Lett, 31, 1153(1973)

2. V.A.Matveev, R.M.Muradyan and Tavkhelidze, Large angle scattering and the quark structure of the hadrons. JINR E2-8048, Dubna(1974); Proc. of the IV Intern.Seminar on High Energy Physics Problems, JINR D I,2-9224, Dubna(1975)

3. S.V.Goloskokov, S.P.Kuleshov, V.A.Matveev and M.A.Smondyrev, A Study of power automodel asymptotic behaviour of the large angle hadron-hadron scattering, contributed paper A5-4/789.

4. S.J.Brodsky and B.T.Chertok, The deuteron form factor and the short distance behaviour of the nuclear force, contributed paper A5-31/979.

5. R.Arnold et al.Phys.Rev.Lett,35,776(1975).
6. A.M.Baldin.Research Programme with the relativistic nuclei,Proceedings of the 1975 Joint JINR-CERN School of Physics,Alushta,JINR E2-9086,Dubna(1975).
A.M.Baldin et al.contributed papers A6-47/1018,A6-48/1019
7. R.Blankenbecker and S.Brodsky,Phys.Rev.D10,2973(1974); J.Gunion,Phys.Rev.D10,242(1974); D.Sivers,S.Brodsky and R.Blankenbecler,Physics Reports 23C(1976).
8. S.M.Berman,J.D.Bjorken and J.B.Kogut.Phys.Rev,D4,3388, (1971),S.P.Ellis and M.B.Kislinger,Phys.Rev.D9,2027(1974)
9. A.A.Arkhipov,A.A.Logunov and V.I.Savrin,TMF 26(1976); Description of scaling properties of inclusive reactions with density matrix,contributed paper A5-3/790.
10.V.I.Savrin,Description of inclusive reaction scaling properties in terms of density matrix-invited talk at the Conference.
11.A.N.Kvinikhidze,A.N.Sissakian,L.A.Slepchenko and A.N. Tavkhelidze.Large p_T inclusive processes in composite particle approach,contributed paperA4-31/1081; to be published in "Particles and Nucleus",Atomizdat,Moscow(1976)
12. V.P.Garsevanishvili,A.N.Kvinikhidze,V.A.Matveev,A.N.Tavkhelidze and R.N.Faustov,JINR E2-8126,Dubna(1974); S.P.Kuleshov,A.N.Kvinikhidze,V.A.Matveev,A.N.Sissakian and L.A.Slepchenko.JINR E2-8126,Dubna(1974); A.A.Khelshvili,A.N.Kvinikhidze,V.A.Matveev and A.N.Tavkhelidze.JINR D2-9540,Dubna(1976).
13. A.N.Kvinikhidze.Scattering processes in relativistic composite models.Invited talk at the Conference.
14. A.N.Khelashvili. Null-plane quantization and quasipotential equations for composite particles.Invited talk at the Conference; preprint JINR P2-8750,Dubna(1975).
15. L.A.Slepchenko.Large p_T inclusive distributions in composite models.Invited talk at the Conference.

LARGE P_T INCLUSIVE DISTRIBUTIONS IN COMPOSITE MODELS

L.A.Slepchenko
Tbilisi State University

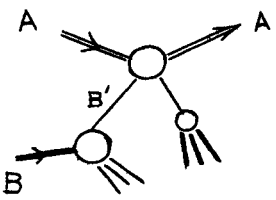
In the paper by A.N.Kvinikhudze,A.N.Sissakian, L.A.Slepchenko,and A.N.Tavkhelidze contributed to the Conference [1], in the framework of three-dimensional formulation of quantum field theory of composite systems the general representation for a production distribution was obtained, which depends crucially on the properties of the constituent quark wave functions and their interaction amplitudes[2,3].

For hadron production at high P_T in the null-plane formalism this approach gives a possibility to estimate the relative importance of the different approximations made in the quark-parton picture [4], and to obtain the distributions for the single-particle, single-jet and two-jet production.

The application of the automodelity principle and quark counting rules[5,6] for the e.m.form factors and exclusive differential cross-sections leads to the quark counting rules for the high P_T hadronic distributions which agree with the results of CIM[7].

Here we list briefly some applications of this approach and we restrict ourselves to the two aspects of the high P_T phenomena: leading particle mechanism and interaction of jets.

i. In case of leading particle production with large transverse momentum, the corresponding single-particle distribution can be represented in the form:



$$\frac{d\sigma^{AB\to A}}{d^3p|E} = \frac{I}{8\pi^2}\sum_b \int dy \quad \rho_B^b(y)\ \delta(t+(s+u)y)\cdot$$
$$\cdot\Big|\sum_a \int S_a^{(n)}(x,(I-x)\cdot\Delta)\frac{dx}{x}\,T_{ab}^{(2)}(s',t')\Big|^2 \qquad (I)$$

where $\sum_a e_a \int S_a(x'(I-x)\Delta)dx = eF_A(t), |t| = \Delta^2$ and $F_A(t)$ is the e.m. form factor.

In general the quantity $S_a(x'(I-x)\Delta_T)$ describes the effects of longitudinal motion[8,9] of the constituent particles(quarks or partons) inside the hadron. In the "static" limit ($x_a \to \mu_a$, $\mu_{\tilde a}$ reduced mass) we have $\sum_a S_a(x,(I-x)\cdot\Delta_T) \to \delta(x-\bar x)F_A(\Delta_T^2)$ and the leading particle distribution at high P_T reduces to the product of deep-inelastic cross section and the square of e.m. form factor of a beam particle.

$$\frac{d\sigma^{AB\to A}}{d^3p|E} \Rightarrow \sum_{ab}\frac{F_A^2(t)}{x}\left(\frac{\widetilde{d\sigma}^{aB\to ax}}{d^3p|E} = \right.$$
$$\left. = \sum_b \rho_B^b(x)\ \frac{d\sigma^{ab\to ab}}{dt'}(s',t',u')\right) \qquad (2)$$

where $x = -\dfrac{t}{M^2 - t}$, $s + t + u \cong M^2$.

Applying the quark counting rules[6] for the e.m. form factors and differential exclusive cross sections for the different allowed subprocesses we receive the values of the power law exponent in accordance with the experimental data on $Ap \to A+x$ ($A=\pi,p$) and the corresponding exclusive limiting ($x_T=1$) values $\frac{d\sigma}{dt}(\pi p \to \pi p)\ s^{-8}$, $\frac{d\sigma}{dt}(pp \to pp)\ s^{-10}$,

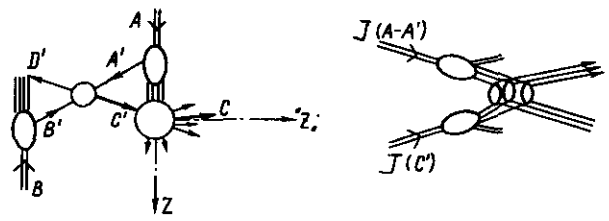
respectively.

The second point we would like to stress here is that for the π-meson production in pp-and πp-collision in addition to the standard central production contribution[7,I] $p_T^{-8}(I-x_T)^9$, this mechanism (2) gives a significant contribution $p_T^{-8}(I-x_T)^7$ to the second (leading) reaction. Thus, for the same p_T power law the ratio is $R(\frac{pp\to\pi}{\pi p\to\pi}) \sim (I-x_T)^2$ which is close to the experimental estimates $F_p - F_\pi = I.6 \pm 0.5$ [I0], and for which the quark fusion mechanism gives too small value of magnitude[II].

ii. Recent experimental data on the high P_T hadron production indicate that the final state events in these processes reveal many interesting features of two-jet structure. Qualitative analysis of these data are extensively discussed in the current theoretical works[I3].

Now we draw attention to the problem of interaction between jets produced in the high P_T experiments(one-along the beam axis,the other-perpendicular to it). Note in this connection the experimental evidence[I4] in particle production on nuclear targets, that can be of great importance in the interaction with nuclei in the high P_T region multiple scattering effects.

Thus, if we describe the high P_T particle production from the two interacting jets in a manner analogous to the usual treatment of nuclear target effects - the problem is reduced to a small angle(fixed t) collision problem in some rotated frame (see also [I5]).



a *б*

Viewed in this, a new frame interaction of two jets can be considered as a coherent process where the multiple rescattering may play a significant role. In the framework of this approach the eikonal solution was obtained which takes into account the longitudinal motion of constituents and their rescattering effects[8,9]. In case of the jet distribution the rising rate of the associated jet multiplicity along and opposite the direction of the trigger particle was estimated[9]. In particular,in some restricted kinematical regions the linear growth $\overline{n}(n_T) \sim p_T$ was obtained which is natural for the coherent and SLPA model considerations[I6]. In addition to the logarithmic p_T- dependence of $\overline{n}^{assoc.}(p_T)$ resulting from the parton and bremsstrahlung model calculations[4,I7], this contribution can be considered as one part of the two-component description of the average multiplicities[I8] in accordance with the 3-component structure of final events[I2] in the high P_T experiments. The study of the atomic number dependence of the large P_T hadronic inclusive spectra is of a special interest.

R e f e r e n c e s:

I. A.N.Kvinihidze, A.N.Sissakian, L.A.Slepchenko,A.N.Tavkhelidze,contributed paper A4-3I/I08I; to be published in "Particles and Nucleus",Atomizdat,Moscow(I976).

2. A.N.Tavkhelidze.High transverse momentum processes in composite models. Invited talk at the Conference.

3. A.N.Kvinikhidze. Scattering processes in relativistic composite models. Invited talk at the Conference.

4. S.M.Berman,J.D.Bjorken,J.B.Kogut,Phys.Rev.D4,3388(I97I). S.P.Ellis and M.B.Kislinger. Phys.Rev.D9,2027(I97I).

5. V.A.Matveev,R.M.Muradyan and A.N.Tavkhelidze,JINR P2-4572,Dubna(I969); E2-6962,Dubna(I97I).

6. V.A.Matveev,R.M.Muradyan and A.N.Tavkhelidze,Lett.Nuovo Cim.7,7I9(I973); S.Brodsky and G.Farrar,Phys,Rev.Lett,3I, II53(I973).

7. R.Blankenbecler and S.Brodsky,Phys.Rev.DI0,2973(I974); J.Gunion,Phys.Rev.DI0,242(I974); D.Sivers,S.Brodsky and R.Blankenbecler,Phys.Reports,23C(I976).

8. A.N.Kvinikhidze and L.A.Slepchenko,Theor.& Math.Phys.24, 54(I975).

9. A.N.Kvinikhidze and L.A.Slepchenko. International School on Actual Problems of Elementary Particle Physics,Sochi, JINR DI,2-8529,Dubna(I975).

I0. G.Donaldson et al.Phys.Rev.Lett,36,III0(I976).

II. B.L.Combridge,Phys.Lett,62B,222(I976).

I2. P.Darriulat et al.Nucl.Phys.B I07(I976); Rapporteur's talk,Palermo(I975); K.Eggert et al.Nucl Phys.B98,49,73 (I975); M.Della Negra et al.Phys.Lett,59B,40I(I975); F.Büsser et al.Nucl.Phys.BI06(I976).

I3. S.D.Ellis,M,Jacob and P.V.Landshoff.CERN TH-20I9,Geneva (I975); CERN TH-2I82,Geneva(I976); J.D.Bjorken.SLAC Summer Inst.of Elementary Particle Physics(I975).

I4. J.W.Cronin et al.Phys.Rev.DII,3I05(I975); SLAC Summer Inst.of Elementary Particle Physics,SLAC-I79(I974); D.A.Antreasyan et al.Contributed paper A4-I7/753.

I5. J.Gasser and W.P.Sukhatme,Univ.of Cambridge,preprint DAMPT 76/3(I976).

I6. V.A.Matveev and A.N.Tavkhelidze,JINR E2-5I4I,Dubna(I970).

I7. A.P.Contogouris,J.P.Holden and E.N.Argyres,Phys.Lett, 5IB,25I(I974); Nucl.Phys.B85,I02(I975); D.Schiff,A.P.Contogouris and J.L.Alonso,Phys.Lett,55B,87(I975);S.P.Kuleshov,V.A.Matveev,A.N.Sissakian,M.A.Smondyrev and A.N.

Particles and Nucleus,v.5,I,Atomizdat,Moscow(I974).

I8. J.L.Alonso and A.C.D.Wright,Phys.Rev.DI2,776(I975); L.J.Gutatv and P.Suranyi,Phys.Rev.D9,250I(I974); V.A.Matveev,A.N.Sissakian and L.A.Slepchenko,JINR,E2-9I05,Dubna(I975); Jadernaya Physika,23,432(I976); A.N.Sissakian and L.A.Slepchenko,Proc.of the IV Int. Seminar on High Energy Physics Problems,JINP DI,2-9224, Dubna(I975); A.N.Sissakian and L.A.Slepchenko. Many component description of the multiple production processes, contributed paper A3-45/I099; A.N.Sissakian.Many component description of inclusive and semi-inclusive processes. Invited talk at the Conference.

DYNAMICS OF HIGH MOMENTUM TRANSFER PROCESSES

A.V.Efremov
JINR, Dubna

Our understanding of this phenomena is based on Field Theory of Quarks interacting through scalar (or pseudoscalar) gluons /1/. It allows one to unify partonology and Quark Counting Power (QCP) rule from one side and reggeology from the other, to understand early scaling in leptohadronic processes and late scaling on p_T in high p_T inclusive hadroproduction.

This approach is based on an algorithm involving the consideration of Feynman diagram asymptotical behaviour and its summation.

TECHNICS: Contribution of any diagram for a given process can be written in α-representation as

$$T \sim \int_0^{\infty} \frac{\prod d\alpha}{\mathcal{D}^2(\alpha)}\, G(\alpha, m, p_i)\, e^{\left[\frac{Q(\alpha, p_i)}{\mathcal{D}(\alpha)} - \sum_\sigma \alpha_\sigma (m_\sigma^2 - i\varepsilon)\right]}$$

Each integration can be split into scale part $|\alpha| < \Lambda^{-1} \ll 1/m^2$ and nonscale part $|\alpha| > \Lambda^{-1}$. Scale regime (SR) of a block V is composed by those terms of contribution in which all $\alpha(\in V) < \Lambda^{-1}$. Note that $\alpha \to 0$ means topologically the contraction of corresponding line into a point.

These are "rules of the game" which are proved for each diagram of perturbation expansion in Euclidean region:

Rule I. SR of V determines the asymptotics with respect to those variables which are "killed" by contraction of V into point.

Figs. 1a,b,d,e,2a,c,3a,c,b,d,e illustrate the connection of different kinematical regions of different processes and small-distance SR blocks V.

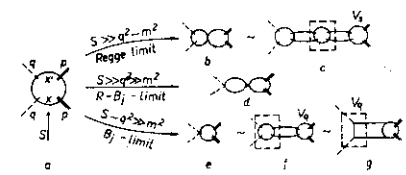


Fig. 1

Rule II. Asymptotics due to SR of V is of the form

$$T \sim S^{\delta_V} \sum_N C_N (\log S/\Lambda)^N + \sum O(S^{\delta_V - 1})$$

where S is a large variable, $\delta_V = (4 - f_V)/2$ is the scale (square momentum) dimension of V, and f_V is a number of external legs of V .

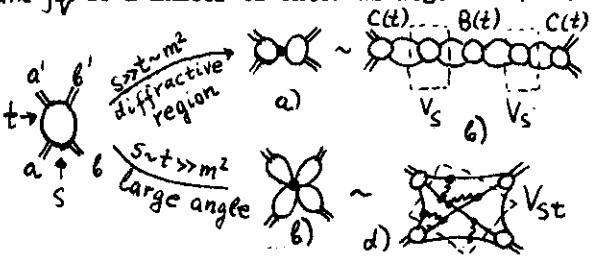


Fig. 2

Note that i) δ_V is just QCP for an amplitude, ii) senior asymptotical term is due to SR of V-blocks with minimal number of external lines. Fig. 1f, 2b,d,3b illustrate the most essential blocks for some chosen cases.

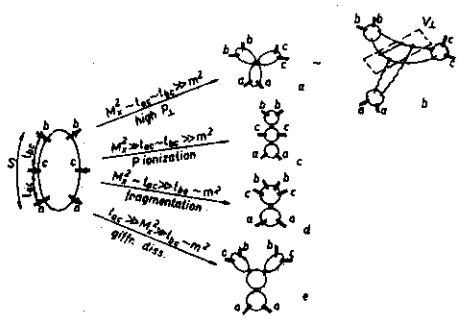


Fig. 3

Rule III. Senior asymptotical term in Mellin transform of T with respect to large momentum variables $S_1, \ldots, S_k \gg t_1, \ldots, t_r$ is

$$T_G(j_1, \ldots, j_k; t_1, \ldots, t_r) = \sum v_V^N(j, \Lambda, g_\Lambda^2)\, f_{G/V}(j, t, \Lambda, g_\Lambda^2)$$

where v_V^N depends only on contracted block V and $f_{G/V}$ is a product of weekly connected parts which rest after the contraction.

This expression is just the analogy of Wilson expansion. It can be shown that in most cases the sum reduces to a single term. (Wide angle scattering Fig.2d is an exclusion).

Application of this rules to deep inelastic scattering, for instance, gives

$$W(j, l) = v_V(j, l, \Lambda, g_\Lambda^2)\, f(j, \Lambda, m^2, g_\Lambda^2)$$

where $W(j,l)$ is double Mellin transform of $\nu W_2(q^2, \omega)$ or $m W_1(q^2, \omega)$. This is equivalent to

$$W(q^2, \omega) = \int_{1/\omega}^{1} dx\, v(q^2, \omega x, \Lambda, g_\Lambda^2)\, F(x, \Lambda, m^2, g_\Lambda^2) + \sum O(1/Q^2)$$

i.e., to modified parton picture /2/ where v is deep inelastic parton formfactor. (This representation is proved also from Wilson expansion /3/ and so it is rigorous result of renormalizable QFT). Analogously, for high p_T production invariant cross section one can obtain:

$$F_{AB \to CX}(S, t, u) = \int_0^1 dx\, dy\, dz\, F_A(x) F_B(y) D_C(z)\, f_{ab \to cx'}(\hat{s}, \hat{t}, \hat{u}) + \sum O(1/S^3)$$

$$\hat{S} = x_y S \; ; \; \hat{t} = \frac{x}{z} t \; ; \; \hat{u} = \frac{x}{z} u$$

Summation of all log. terms is made with the help of Renormalization group. Note that boundary parameter Λ is arbitrary but the leading asymptotical terms in /3/,/4/,/5/ have to be independent on Λ . It is just the basis of RG. This results, for instance, in

$$v_V(q^2/\Lambda, g_\Lambda^2) = \varphi(\bar{g}^2(q^2/\Lambda, g_\Lambda^2)) / \varphi(g_\Lambda^2)$$

where φ is arbitrary function of invariant charge $\bar{g}^2$. The first term of perturbation expansion in $\bar{g}^2$ is $v_V^{(0)} \sim \delta(1 - \omega x)$ (Fig.1g) which is responsible for Bj -scaling, the second one $v_V^{(1)} \sim \bar{g}^2(q^2/\Lambda, g_\Lambda^2) \ln(-q^2/\Lambda)$ breaks it. For high p_T production

$$f^{(0)} \sim \bar{g}^4(p_T^2) \frac{1}{\hat{s}^2} \delta\left(1 + \frac{\hat{t}}{\hat{s}} + \frac{\hat{u}}{\hat{s}}\right)$$

So, we can conclude: i) Parton model and QCP is an approximation of not too high momentum transfer when

$$\bar{g}^2(q^2) \ln(-q^2/\Lambda) \ll 1 ;$$

this assumes that $\bar{g}^2 \ll 1$.

ii) The violation of scaling beyond this region depends on character of charge renormalization and is of the same kind as in Wilson expansion approach.

iii) Scaling (QCP) - term in this region is suppressed by factor $\bar{g}^4$ for high p_T hadroproduction and wide angle elastic scattering, and by factor $\bar{g}^2$ for inclusive lepton production and wide angle electro- and photoproduction. But it is not suppressed for the deep inelastic and electromagnetic form factors /4/ .

iv) Boundary parameter Λ is controlled by hadron masses and can be essential for not too high p_T . (Its effect is similar to that of high $\langle p_T \rangle$ of work /5/).

Let us explain the absence of $\bar{g}^2$ for EM-form factors /4/:

Really,

$$F_{q\bar{q}}(j,t,q^2,j',t') \sim K_L(j,t)\,\frac{\bar{g}^2}{q^2}\,K_R(j',t')$$

(See Fig.4). However, when we come to form factor of $q\bar{q}$ bound state (π , for example)

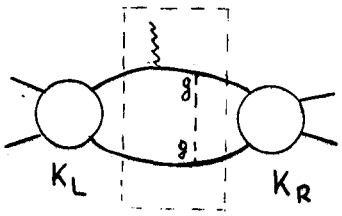


Fig. 4.

$K(j,t) \sim \frac{C(t)}{j-\alpha(t)}$ and $\bar{g}\,C(t)$ is $g_{\pi q\bar{q}}$ effective coupling constant and have to be withdrawn off. Thus, $F_\pi \sim 1/q^2$ without suppressing factor.

References

1. A.V.Efremov.Chechoslovak Journal of Phys., B26, 430 (1976).
2. A.V.Efremov, A.V.Radyushkin, Preprint of JINR, P2-9821 Dubna,1976, paper 1080/B2.
3. A.V.Efremov, A.V.Radyushkin. Preprint JINR P2-9906 Dubna, 1976.
4. A.V.Efremov, A.V.Radyushkin. Preprint JINR E2-9717 Dubna, 1976, paper 1217/A7-52. (submitted to Sovjet Teor.Mat.Fiz.).
5. E.M.Levin, M.G.Ryskin. Preprint LINP-AN 167,Leningrad, 1975, paper 1005/A4-2.

URBARYON MODEL AND LARGE TRANSVERSE MOMENTUM PHYSICS

T.Matsuoka

Nagoya University, Nagoya, Japan

On the basis of urbaryon model we study large p_T two-jet production cross section. It is shown that our calculations of single hadron distributions exhibit power-law scaling. Now we take the following assumptions: (A) Two-jet production mechanism is dominant; (B) The large p_T jets contain the urbaryon composed of the incident hadrons; (C) The subsequent evolution of jets into hadrons is independent of their production.

In our model the urbaryon rearrangement amplitude is expressed by a product of the factors corresponding to urbaryon lines in the urbaryon rearrangement diagram (ref.1). This implies that the countable nature of constituent urbaryons strongly reflects on the amplitude. When applying this amplitude to two-body processes, the amplitude provides the interpolation between Regge-like form and fixed-angle scaling form. Now let us consider the process

$$a+b \to [\ (11)+\ldots] + 2 + 3 + [(41)+\ldots]$$

where (11),... and (41),... stand for the produced clusters and 2 and 3 denote large p_T two jets. The assumption (A) means that $p_{i_T} \sim 0$ for $i = 1.4$. Then two jets 2 and 3 balance their transverse momenta. The assumption (B) leads us to the total amplitude $T = T_1 + T_2$ for the $pp \to (q\bar{q})(q\bar{q})X$, where two $(q\bar{q})$'s represent two jets. The amplitude T_1 corresponds to the diagram shown in Fig.1. T_2 is obtained by the interchange of 2 and 3. This assumption is essential in interpreting the quantum number effect in particle ratios.

Applying our model to the above process, we have

$$\frac{T_i}{S} \sim \frac{\tau_1}{m_1^2}\,\frac{\tau_4}{m_4^2}\,\frac{M_i}{S} \qquad (i=1,2)$$

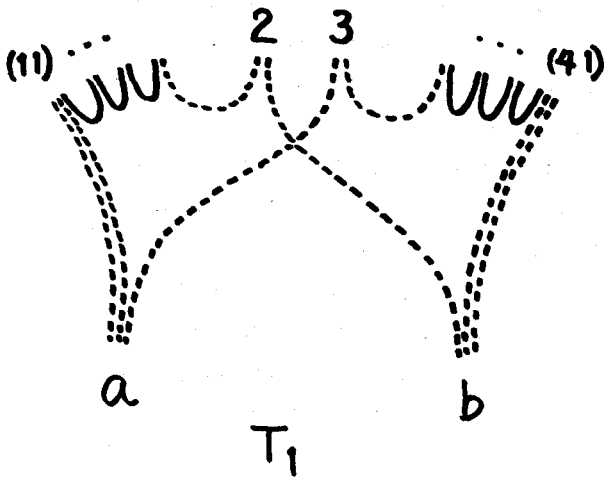


Fig. 1

M_i's represent the product of the factors coming from the dashed lines in Fig.1, while τ_1 and τ_4 from the solid lines. Next we replace $M\,(=M_1+M_2)$ by $\bar{M}$ which is the approximated M postulating that small p_T clusters fall in a line of equal and average rapidity spacing of multi-peripheral chain. Furthermore, employing the unitarity relation for τ_1 and τ_4, we obtain the cross section effectively for the process $a+b \to 1+2+3+4$ where $P_i = \sum_j P_{ij}$ ($i=1,4$). By use of the scaling variables for energies $x_i = 2E_i/\sqrt{s}$ ($i=1,2,3,4$) we have the two-jet production cross section

$$E_2 E_3 \frac{d\sigma^{jet}}{dP_2\,dP_3} = \frac{\sin^2\theta_3}{P_{2T}}\,\Xi(\sqrt{s}, x_2, \theta_2, \theta_3) \cdot \delta(P_{2T} - P_{3T})\,\delta(P_2 - P_3 + \pi)$$

where

$$\Xi = |\bar{M}/s|^2 / (x_1 x_4 \sin\theta_3)^2$$

The calculated single jet spectrum has approximated scaling form

$$E_2 \frac{d\sigma^{jet}}{dP_2} \sim P_{2T}^{-N^{jet}} f^{jet}(x_2, \theta_2)$$

Taking the fragmentation function

$$F(z) = k_0 \delta(1-z) + k_1 \frac{(1-z)^2}{z}\,\theta(1-z) \qquad (3)$$

we have single hadron invariant cross sections. Our calculation can be described in the approximate scaling form

$$E\frac{d\sigma}{dp} \sim p_T^{-N} f(x, \theta)$$

which is shown in Fig.2 and 3. The calculated N approaches to 12 with increasing x. Our results are in good agreement with experiments.

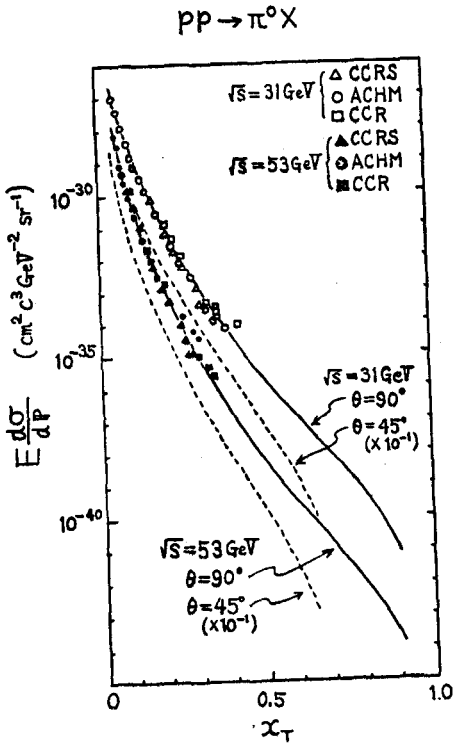


Fig. 2

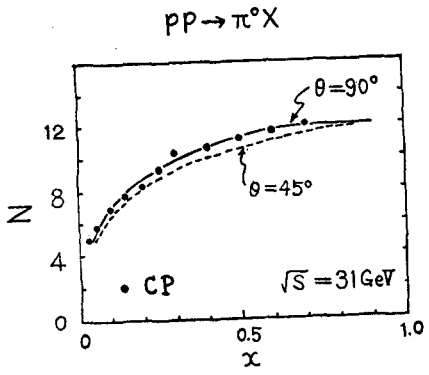


Fig. 3

References

1. Y.Igarashi, T.Matsuoka and S.Sawada. Prog. Theor.Phys., 52, (1974), 618, 986;
The contributed paper to this conference A4-18,19 (896,897).

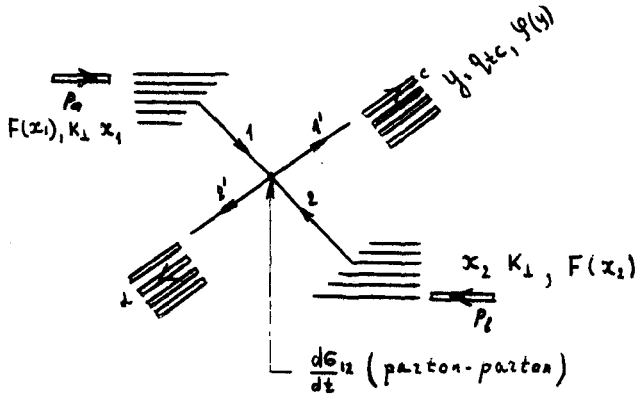
THE HADRON PRODUCTION AT LARGE TRANSVERSE MOMENTUM AND THE PARTON INTERACTION

E.M.Levin, M.G.Ryskin

LINP, Leningrad, USSR

Because of limited space of this report we have to restrict ourselves to a representation of basic ideas and few comments. A more detailed version will be published shortly as a preprint of Leningrad Nuclear Physics Institute.

1. The parton picture for large transverse momentum production:



$$\frac{\omega d\sigma}{d^3q_c} = \int F_a(x_1) F_b(x_2) \frac{d\sigma_{12}}{d^2\vec{K}_{t}}\Big|_{\vec{K}'_{t}=\vec{q}_{tc}/y} \cdot S\delta(x_1x_2S - M^2) \frac{dM^2}{M^2} \delta(\eta_1 - \eta_c) \times$$

$$\times \Phi(y)\frac{dy}{y^2} dx_1 dx_2$$

Fig.1

It is easy to understand that this picture leads to three hadron jets: in the beam direction, toward the trigger particle and at the opposite direction. All these jets have been observed experimentally /1/.

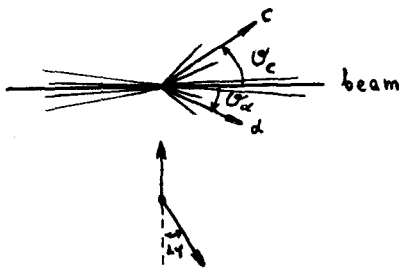


Fig. 2

Such a picture was first suggested by Berman, Bjorken and Kogut /2/ and then was re-discovered and exhaustly discussed in many papers /3/.

II. The parton-parton interaction

The direct information can be obtained from the θ angle distribution for double inclusive process $a+b \to c(q_{tc}) + d(q_{td})$

at $q_{tc} \simeq q_{td} \geq 1.5 \frac{Gev}{c}$ and $\theta_c \neq 90^\circ$ where c is the trigger particle.

Short range-line (in rapidity) parton--parton interaction may be in agreement with the current experimental data. This point we should illustrate by a few qualitative predictions for double inclusive process under the different assumptions.

Assumption	Prediction
1) Parton model (p.m.) with $\frac{d\sigma}{dt}(\text{parton-parton}) = e^{-b\Delta\eta}$	$\theta_c = \theta_d$
Short range interaction in rapidity $\Delta\eta$	
2) PM, $\frac{d\sigma}{dt} \sim const \cdot \Delta\eta$	$\theta_d \sim 90^\circ$ at any θ_c
Long range interaction	
3) Quark-Parton Model collisions of the valence quarks	$\theta_d \sim \pi - \theta_c$

III. The average transverse momentum of a parton inside a hadron.

1. Large q_t hadron production $\langle k_\perp \rangle$ can be extracted from the azimuthal angle distribution for $a+b \to c+d+...$ with the aid of equation

$$\langle tg^2 \Delta\varphi \rangle = \frac{\langle k_\perp^2 \rangle}{k'^2} + \frac{\langle q_\perp^2 \rangle}{2q_{t_c}} + \frac{\langle q^2 \rangle}{2q_{t_d}} \quad (1)$$

$\langle k_\perp \rangle$ is the average transverse momentum of a hadron produced by parton decay). Comparing this equation with experiment we have found /4/ that the $\langle k_\perp \rangle$ value is sufficiently large:

$$\langle k_\perp^2 \rangle = (1.5 \div 2.5)\left(\frac{Gev}{c}\right)^2 \text{ if } \langle q_\perp \rangle \simeq 0.4 \frac{Gev}{c} \quad (6)$$

This large $\langle k_\perp \rangle$ value is in agreement with broad $\Delta\varphi$ distribution observed in many experiments and the same $\langle k_\perp \rangle$ value can be also estimated from the correlation function $\langle F \rangle$ /1/, which is the probability to find the charged particles in large transverse momentum events.

2. The production for leptonic processes.

a) $h+h \to \mu^+\mu^- + ...$. The $\mu^+\mu^-$ production is the direct experiment for measuring $\langle k_\perp \rangle$. Indeed, for large masses $(M^2 >> 4\langle k_\perp^2 \rangle)$ $\langle q_{t_{\mu^+\mu^-}} \rangle = 2\langle k_\perp^2 \rangle$ From experiment /7/ for M equal to 1-3 GeV the $\langle q_{t_{\mu^+\mu^-}} \rangle$ increases from 0.5 to 1.1 GeV/c.

b) $ep \to e + h(y, q_{th}) + ...$ $y = \frac{q_h}{Q/2}$ where Q is the γ -momentum. The value of $\langle q_{t_h} \rangle$ can be calculated from

$$\langle q_{t_h}^2 \rangle = \langle q_\perp^2 \rangle + y^2 \langle k_\perp^2 \rangle$$

So, for $y \to 1$ $\langle q_{t_h} \rangle$ should increase and tend to $\langle k_\perp \rangle$.

3. Hadron collisions without large q_t.

In the PM the slope of pomeron exchange directly relates to $\langle k_\perp \rangle$ /8/ by means of $\alpha' = \frac{1}{2}\frac{1}{\langle k_\perp^2 \rangle}\frac{dn}{d\eta}$ /2/ where $\frac{dn}{d\eta} \sim 1$ is the parton density on the unit rapidity interval. For $dn/d\eta \sim 1$ and $\alpha' = 0.25$ (GeV/c)$^{-2}$ $\langle k_\perp^2 \rangle \sim 2$ (GeV/c)^2. At first sight the large $\langle k_\perp \rangle$ value contradicts to the wellknown fact that the average transverse momentum of a secondary pions in the multiparticle reactions is small ($\sim$ 0.4 GeV/c). In the paper /5/ it was shown that it is incorrect. For simplicity, let us turn to eq. (2) for the hadron production in deep inelastic process. The mean value of $\langle y^2 \rangle$ is $\langle y^2 \rangle = \int \varphi(y) y^2 dy \approx 0.05$, so $\langle q_{t_h}^2 \rangle \approx 0.26$ (GeV/c)^2 if $\langle q_\perp^2 \rangle \approx$

$\approx$ 0.16 (GeV/c)^2 and $\langle k_\perp^2 \rangle = 2\left(\frac{GeV}{c}\right)^2$

In hadron hadron collision each parton should decay in 4–5 pions, and as a result $\langle q_t^2 \rangle_h$ becomes small $(1/4 \div 1/5)\langle k_\perp \rangle$.

IV. How does the new scale $(\sim 1/\langle k_\perp \rangle)$ reveal itself in hadronic scattering at high energy?

We think that the new scale $\sim 1/\langle k_\perp \rangle$ leads us to additive quark-parton model. In this model a hadron consists of three or two valence quark whose size R_q is small up to ultra high energies since $R_q^2 = 1/\langle k_\perp^2 \rangle + \alpha' \ln s$. So, for $s \ll 10^8$ GeV^2; $R_N^2 \gg R_q^2$ and the wee partons from different quarks should not strongly overlap and valence quarks interact as free particles separated in space (see fig.3).

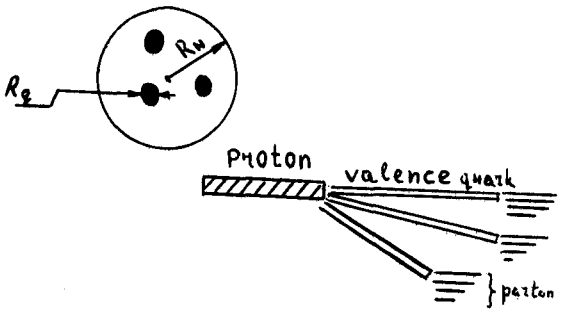


Fig.3

Let us disuss some predictions of the quark-parton model.

1. $\sigma_{tot}(pp)/\sigma_{tot}(\pi p) \simeq 3/2$

$$\frac{f(pp \to c + \ldots)}{f(\pi p \to c + \ldots)} = \frac{3}{2}$$

where $f = \omega_c \, d\sigma/d^3p_c$, is the inclusive cross section.

2. For diffraction dissociation (DD) the slope B should be smaller than for elastic scattering ($d\sigma/dt = A e^{-B|t|}$), more exactly for single DD $B_D \to B_{el}/2 + k_q^2$ and for double DD $B_{DD} \to R_q^2$ at large masses out of the resonance region.

The agreement with the experimental data seems to be good [9].

3. Several numerical estimations under the following assumption $dn/d\eta = 1$ and $d\sigma/dt$ (parton-parton) is the maximal one in wave:

1) $\sigma_{qq} = 16\pi\alpha' = 5$ mb; ($\sigma_{tot}(pp) = 9\sigma_{qq} = 45$ mb); $\sigma_{tot}(\pi p) \simeq 6\sigma_{qq} = 30$mb

2) $\varkappa = \frac{\sigma_{el}}{\sigma_{tot}} \simeq$ 0.18 for pp or 0.24 for π p-interactions;

at ISR $\varkappa(pp) = 0.175 \pm 0.005$ (see ref. [10]).

3) The triple pomeron vertex

$$G_{3P}(0)/\sqrt{\sigma_{tot}(pp)} = 1/30$$

experimental number 1/30 – 1/50 [9].

4. For deep inelastic scattering we predict two scale regions:

(1) $4\langle k_\perp^2 \rangle > Q^2 > 4/R^2$

(2) $Q^2 \gg 4\langle k_\perp^2 \rangle$

In the region I the photon feels only the valence quark as a pointlike particle. So in this region all the deep inelastic processes should be described by the valence quark distributions (see Fig.4).

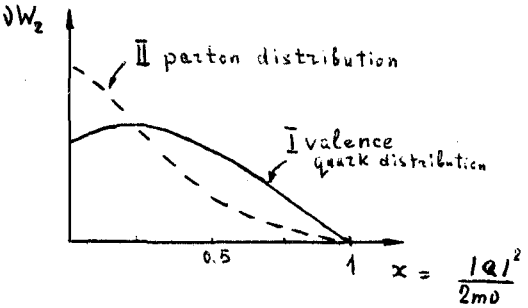


Fig. 4

Only for Q^2 in the region II the photon feels the parton- antiparton sea. So, we predict scale violation. Perhaps, this violation really exists /11/ .

5. It is interesting to suggest that $\sigma_{tot}(qq) \sim \ln^2(Q)$ Such a behaviour has been intensively considered theoretically (12) and we can prove that it does not contradict both to S -channel unitarity and to the parton model. Such a behaviour, perhaps is supported by the fact that all the properties of the jet in beam direction are independent of q_{t_c} value of the hadron c . It is evident for black disk since simultaneously with the sea the ring of two fast partons (1 and 2 on Fig.1) two wee partons are to interact.

References

1. P.Darriulat, Rapporteur talk at the Int. Conf. on High Energy Physics. Palermo, June 1974. Palermo
2. M.Berman, J.B.Bjorken, J.B.Kogut. Phys.Rev. D4, 3388 (1971).
3. D.Sivers, S.J.Brodsky, R.Blankenbecler. Phys.Reports, v.23, C, N 1 (1976). E.M.Levin, M.G.Ryskin, IX Leningrad Winter School, Leningrad 1975, v.1, p.267-366.
4. P.Darriulat et al. CERN D3, FEB. 1976.
5. E.M.Levin, M.G.Ryskin. LNPI-167, 1975, JETP 69, 1537 (1975).
6. R.Sosnovsky. Mini-rapporteur talk at the XVIII Int.Conf. on High Energy Physics. Tbilisi, July 1976.
7. K.J.Anderson et al. Submitted paper 698 B-25.
8. V.N.Gribov. Yad.Fiz., 9, 640 (1969); XVIII Leningrad Winter School, Leningrad, VII, p.5, 1973.
9. G.Gogoi presented at the 10th de Moriond Conf. LNEN/AE-02175, A.B.Kaidalov, V.A.Khoze Talk at Dubna seminar 1975.
10. V.Amaldi et al. Phys.Rev.Lett., 44B, 112, 1973.
11. Sub. p.317/B2-24.
12. J.L.Cardy. Nucl.Phys. B75, 413, 1974; M.S.Dubovikov, K.A.Ter-Martirosyan, ITEP- 37, 1976; E.M.Levin, M.G.Ryskin, Piz'ma JETP (in print).

P L E N A R Y R E P O R T

LARGE TRANSVERSE MOMENTUM HADRONIC PROCESSES

P. Darriulat
CERN, Geneva, Switzerland

I. Introduction

The possible relation between deep inelastic leptoproduction and large transverse momentum (p_T) processes in hadronic collisions was first considered by Berman and Jacob[1] and by Berman, Bjorken and Kogut[2].

Berman and Jacob[1] generalized the relation between the proton form factor and the large $|t|$ behaviour of elastic proton-proton scattering, following the suggestion that electromagnetic and hadronic distributions within a nucleon are the same[3].

Berman, Bjorken and Kogut[2] proposed an explicit quark-parton picture of large p_T production directly inspired from the deep inelastic electron scattering equivalent. According to their model, large p_T production is described by a single binary collision between leading constituents of the colliding hadrons, and the transitions between hadrons and constituents obey the same mechanisms as in deep inelastic electroproduction.

It was in such a context of ideas that three ISR groups[4], while measuring single-particle inclusive cross-sections in the large transverse momentum region, observed much larger yields than was commonly expected from a naive extrapolation of the low p_T exponential behaviour. This demonstrated the feasibility of exploring the large p_T region with existing machines, and immediately triggered off a big experimental effort which is today starting to come to fruition.

Quark-parton ideas have been very successful in motivating such an effort, placing large p_T processes at the heart of strong interaction dynamics, in close contact with its most fundamental aspects. With a good dose of optimism, one might have hoped that large p_T products in a multiparticle final state would carry the relevant kinematic and quantum number contents of the hard-scattered constituents and provide information on their nature and on their interactions, as well as give possible hints toward the understanding of more obscure questions such as the role played by gluons or the puzzle of quark confinement.

Having acknowledged the success of quark-parton ideas in motivating the effort devoted to the field, we are today in a position to give a critical discussion of the experimental data and, free of theoretical prejudice, to analyse the merits of the original motivation.

II. The Event Structure

Experiments observing the structure of the final state in proton-proton collisions producing at least one large transverse momentum particle, have led to the following conclusions:

i) A large fraction of the produced particles are unaffected by the large p_T process. They retain the main properties of "normal" events, where no large p_T particle is produced.

ii) The other products -- with transverse momenta $\vec{p}_T^{\,i}$ -- are correlated to the large p_T particle -- with transverse momentum $\vec{p}_T^{\,0}$. Depending upon the sign of the scalar product $\vec{p}_T^{\,i}\cdot\vec{p}_T^{\,0}$, they can be separated into two groups of "towards movers" ($\vec{p}_T^{\,i}\cdot\vec{p}_T^{\,0} > 0$) and "away movers" ($\vec{p}_T^{\,i}\cdot\vec{p}_T^{\,0} < 0$).

I will first review the experimental evidence favouring such a picture and discuss the properties of each of the three groups (underlying normal event, towards movers, and away movers). I will then present some phenomenological interpretations which have recently been given.

III. The Underlying Normal Event

The pioneer experiment of the Pisa-Stony Brook Collaboration[5], presented two years ago at the London Conference, has led their authors to conjecture that a large p_T event at centre-of-mass energy $\sqrt{s}$ consists of the superposition of a "normal" event at total energy $\sqrt{s} - 2|\vec{p}_T^{\,0}|$ with a set of secondaries including the trigger itself and particles balancing its transverse momentum $\vec{p}_T^{\,0}$.

Further support of this idea is now available.

i) The density of charged particles, and their transverse momentum distribution, in regions of phase space far

Table 1

Trigger			Secondaries			
Type	Polar angle (deg.)	Range of p_T^0 (GeV/c)	Particle identification	Momentum measurement	Azimuthal acceptance (deg.)	Ref.
π^0	90 53	3 to 5	Charged and γ	No	Full	6
π^0	90	$\sim$ 2.5	Charged	Yes	0 ± 27 180 ± 35	7
Positive Negative	20 45	$\sim$ 2.5	Charged	Yes	0 ± 25 180 ± 40	8, 9 10, 11
$p^{\pm}$ $\pi^{\pm}$ $K^{\pm}$	90	> 2	Charged	Yes	0 ± 30 180 ± 30 ±90 ± 15	12
$p^{+}_{\pm}$ $\pi^{\pm}$ $K^{\pm}$	90	1 to 3	Charged	No	Full	13
π^0	90	< 4.5	Charged	No	Full	5

away from the large p_T trigger is approximately the same as in "normal" events. This observation has been made by several groups[5-13] and under various trigger conditions (Table 1). It is particularly meaningful in the azimuthal hemisphere centred on the trigger particle, because the towards movers, in contrast with the away movers, do not occupy a large phase-space domain (Figs. 1 and 2).

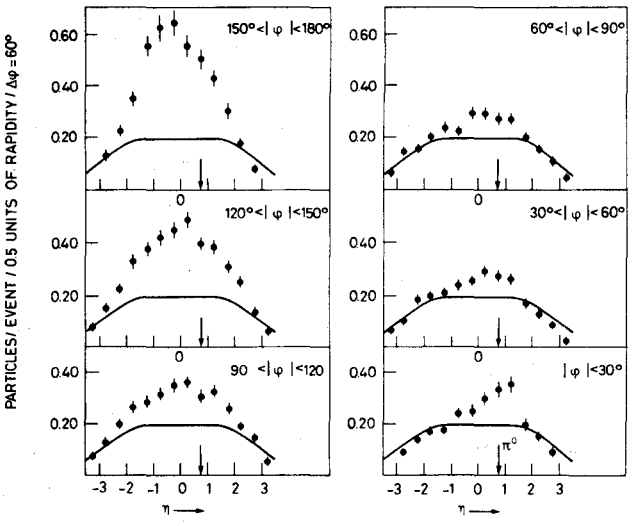


Fig. 1 Rapidity density of charged particles in ISR p-p collisions. The large p_T trigger π^0 is indicated by an arrow (Ref. 6).

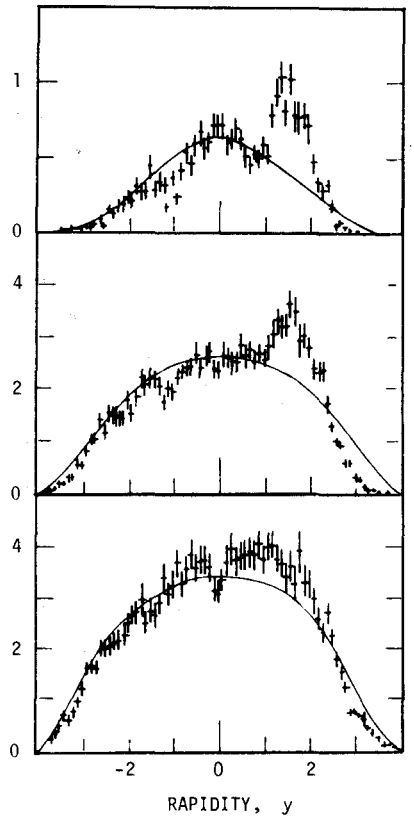


Fig. 2 Rapidity density of negatives with $|p_x|$ = 0.3 to 0.5 GeV/c (lower), 0.5 to 1 GeV/c (middle), more than 1 GeV/c (upper) in an azimuthal wedge around the trigger (large p_T positive at 20°). Data from Ref. 10.

ii) The density of forward ($x_L > 0.5$) positive particles has been measured[8] when a large p_T^0 positive is produced backwards ($-0.5 < x_L < -0.2$). As in "normal" events, they outnumber negatives by a large factor, no significant structure is observed in their azimuthal distribution, and their transverse momentum spectrum is not affected. But their x_L distribution (Fig. 3) shows that the diffraction peak is strongly depressed and that, in addition, the forward density decreases slowly with p_T^0 (Fig. 4). The existence of leading positive particles in large p_T events is a very important piece of information. If it were to persist at higher values of p_T^0 it would suggest that the large p_T process is purely central, with no quantum number flow from the incident hadrons to the large p_T products. More measurements of the particle density and of the charge content in the backward-forward regions are necessary to understand the evolution with p_T^0, and in particular whether the observed decrease is well explained by the lesser available energy $\sqrt{s} - 2|\vec{p}_T^{\,0}|$.

iii) Two-particle rapidity correlations between charged products have been measured in events where a large p_T π^0 is centrally produced. They display the same short-range structure (Fig. 5) amenable to a description in terms of independent cluster formation as in "normal" events, and this with only little dependence upon azimuth.

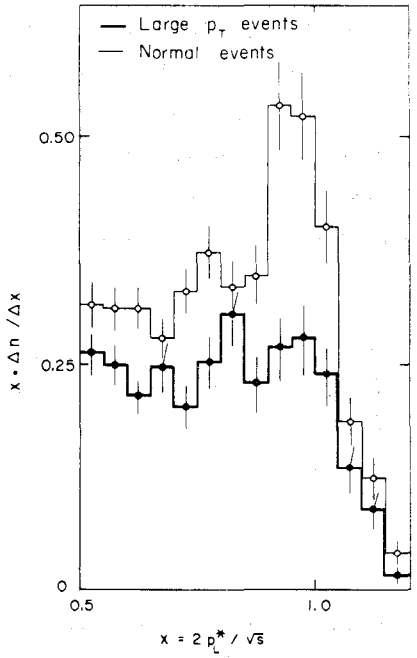


Fig. 3 Leading particles in large p_T events and depression of the diffraction component (from Ref. 8).

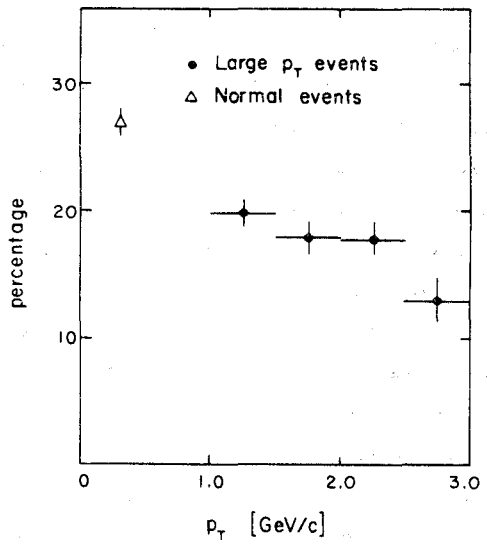


Fig. 4 Percentage of leading particles ($|x_L| > 0.5$) as a function of the trigger p_T (from Ref. 8).

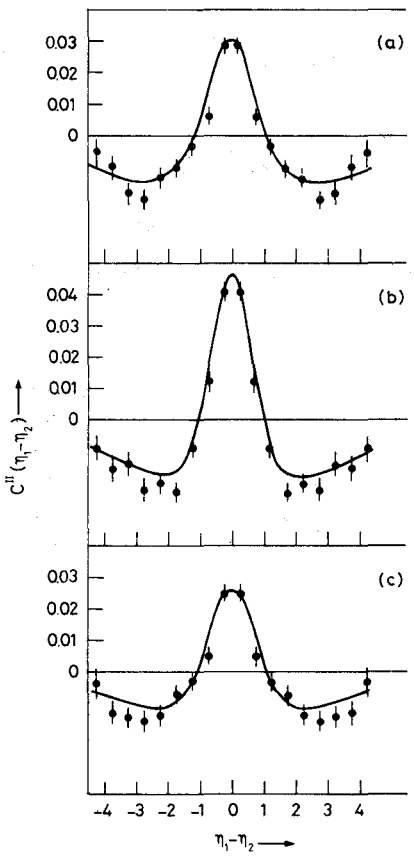


Fig. 5 Average semi-inclusive rapidity correlations in a large p_T event for the full azimuthal range (a), the away hemisphere (b), and the trigger hemisphere (c). From Ref. 10.

IV. The Towards Movers

Momentum correlations between two pions produced alongside one another in the central region have been measured[14,15] and found to be important. When the transverse momentum of one of the pions is larger than 3 GeV/c, that of the other has a distribution broader than in single-particle inclusive spectra, by a factor of 1.2 to 1.3. When expressed in terms of a correlation coefficient at fixed p_T, this corresponds to very large values -- one to two orders of magnitude -- because of the steep fall of the production spectra. Within experimental errors, these correlations are independent of the charge combination in the pion pair, suggesting that two-body decays of low-mass resonances do not play an important role[15] (Fig. 6). Correlation functions are observed to increase slowly with s, and increase more the larger the p_T. This can be expressed in a compact form by noting that the two-pion invariant cross-section for "alongside" production at 90° may be written as[14,15]

$$E_1E_2 \frac{d^6\sigma}{d^3p_1\, d^3p_2} \propto (p_T^1 + p_T^2)^{-n} f(x_T^1 + x_T^2) ,$$

with

$$x_T^{1,2} = 2p_T^{1,2}/\sqrt{s} ,$$

where the exponent n and the function f are very similar to those describing single-particle inclusive spectra (Fig. 7).

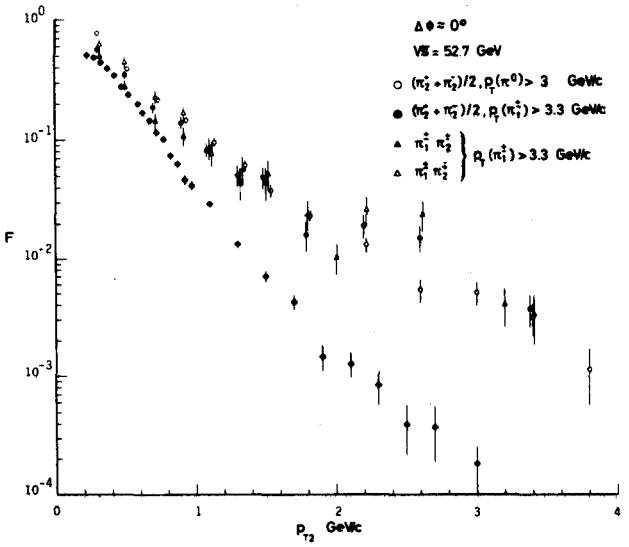


Fig. 6 Momentum correlation function between pions of different charges (towards movers). From Ref. 15.

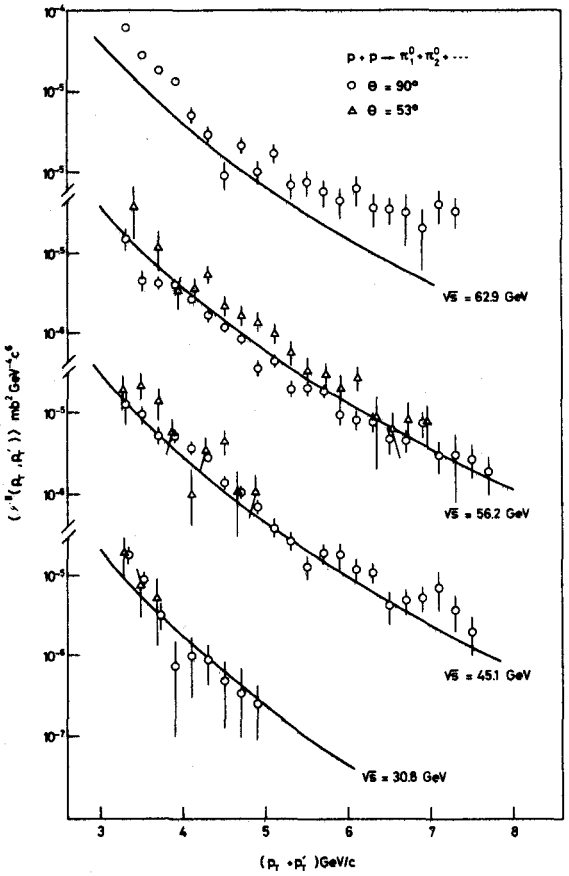


Fig. 7 Invariant cross-sections for production of two alongside π^0's (Ref. 14).

When observed over a wider domain of phase space, towards movers appear to populate a narrow region around the large p_T trigger, well within ±1.5 units of rapidity and ±60° of azimuth. It is possible to estimate their charged particle content by subtracting from the observed density that of "normal" events. This way, 0.85 ± 0.15 charged particles per event are found[6], independent of p_T^0 (Fig. 8).

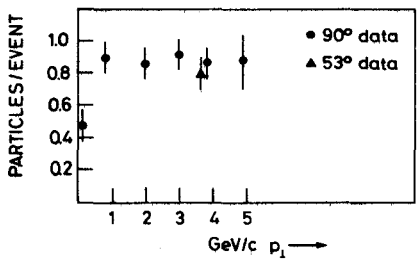


Fig. 8 Population of charged towards movers as a function of p_T of the π^0 trigger (Ref. 6). The point at low p_T corresponds to the cluster structure in normal events.

Measurements in a narrow azimuthal wedge (±30°) around the trigger particle provide cumulative evidence that the towards movers (Fig. 9) have a limited transverse momentum (of the order of 300 MeV/c) with respect to the vector sum of their momenta[7,11,12]. This implies a shrinking of their rapidity distribution when the component of their momentum on that of the trigger increases (Fig. 10), as well as confining to low values their invariant mass with the trigger particle. Searching for structure in the distribution of this invariant mass, some resonance production is indeed observed, but responsible for only part of the correlation among towards movers. Reported resonances[7,12] include $\rho^{\pm} \to \pi^0\pi^{\pm}$ (Fig. 11) -- with a production cross-section

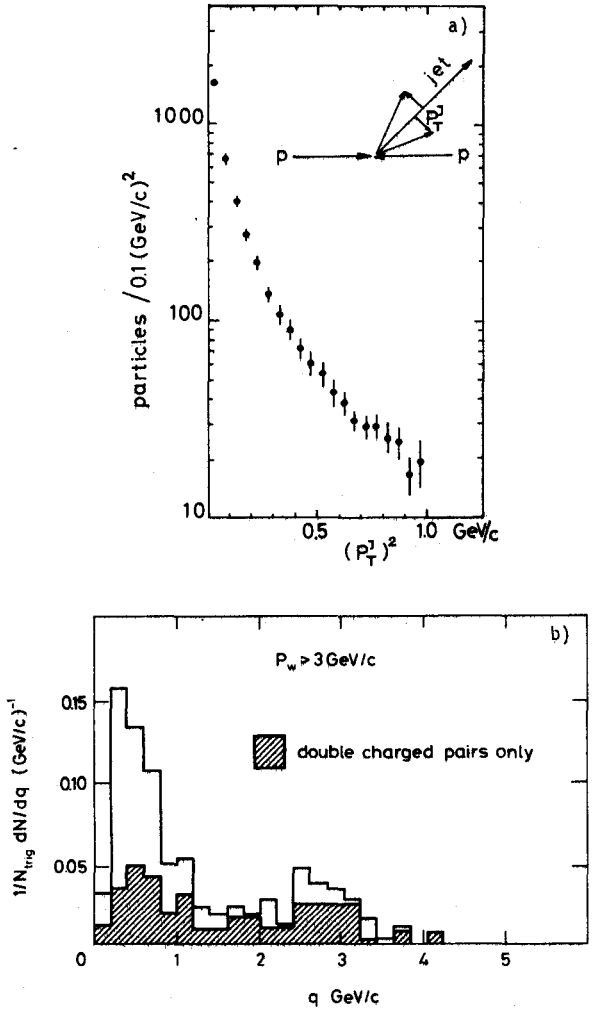


Fig. 9 Transverse momentum distributions along the axis of towards movers:
a) From Ref. 11 (the background of the underlying "normal" event has been subtracted).
b) From Ref. 12 (preliminary data).

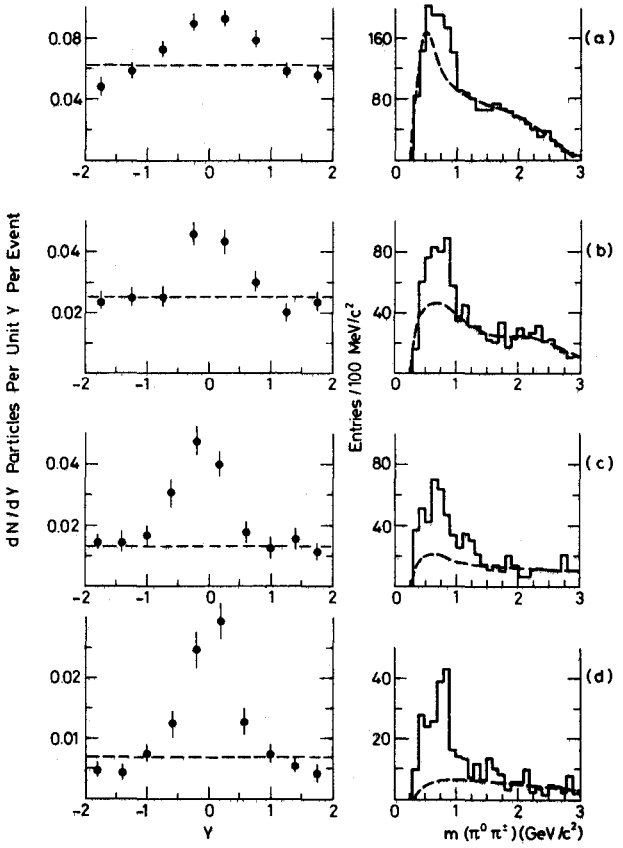


Fig. 10 Rapidity distributions and invariant mass with the π^0 trigger for charged towards movers as a function of their $|p_x|$: a) 0.4 to 0.6 GeV/c; b) 0.6 to 0.8 GeV/c; c) 0.8 to 1.1 GeV/c; d) 1.1 to 1.7 GeV/c. Data from Ref. 7.

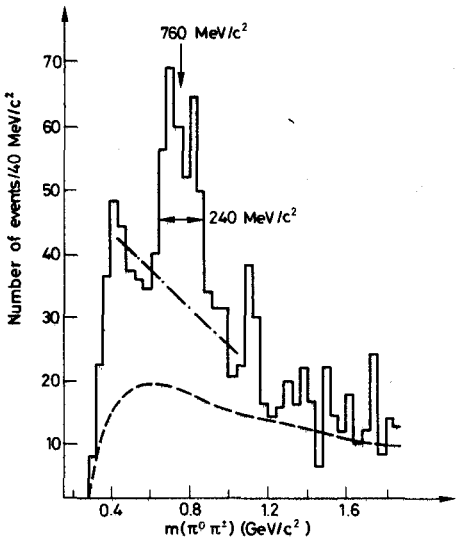


Fig. 11 Charged ρ-meson production in towards movers. Data from Ref. 7.

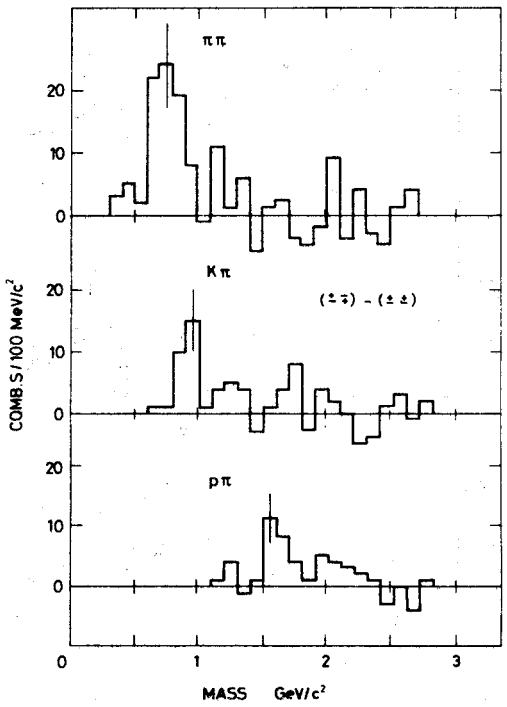


Fig. 12 Invariant mass distribution of towards movers with the large p_T trigger, from Ref. 12. Double charged pairs have been subtracted from neutral pairs.

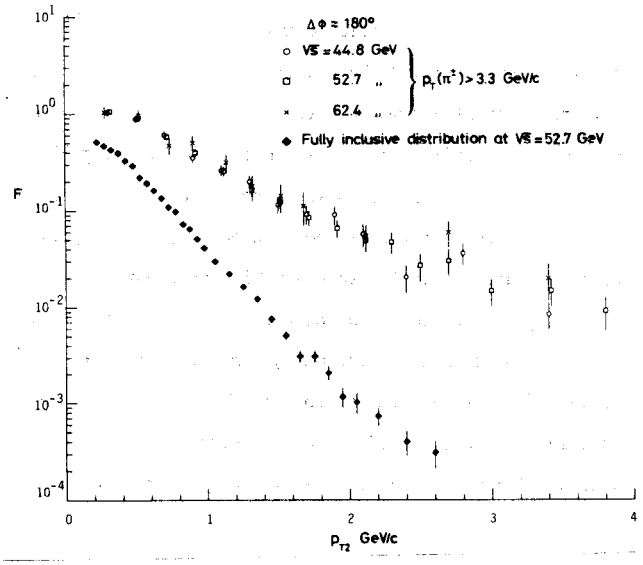


Fig. 13 Momentum correlation function between charged pions for various values of $\sqrt{s}$ (back-to-back configuration). Data from Ref. 15.

around 3.5 GeV/c transverse momentum $\sigma(\rho^{\pm}) = (0.9 \pm 0.2)\sigma(\pi^0)$ -- $\rho^0 \to \pi^+\pi^-$, $K^*(892) \to K^{\pm}\pi^{\mp}$, $N^* \to p\pi$ (Fig. 12). The observation[7] of important three-particle correlations among towards movers brings additional support to the idea that two-body resonance decays do not play a dominant role.

V. The Away Movers

Away movers are at first sight of a different nature in that they cover a wider angular range (Fig. 1) and that their number increases with p_T^0, typically by 0.8 charged particles per GeV/c. These features were already reported in the earlier experiments[5,6] and are now confirmed in more recent measurements[7-13] with the additional information that they depend only little upon the identity of the trigger particle[12,13].

Back-to-back momentum correlations[15] between two pions in the central region are similar to, but even stronger, than those observed in the "alongside" configuration. In particular, they are independent of the charge combination, but, in contrast with the "alongside" case, they do not significantly increase with $\sqrt{s}$ (Fig. 13).

A series of recent experiments[7,11,12], where away movers are momentum-analysed in an azimuthal wedge of ±40° opposite to the trigger, show evidence of strong analogies between the away movers and the towards movers. They indeed suggest that away movers are produced with a small transverse momentum relative to the sum of their momenta, which itself covers a wide rapidity domain from event to event, causing the apparent broad coverage of away movers when observed globally. I now review the various evidences in favour of this interpretation.

i) Some azimuthal confinement of the away movers in the vicinity of the scattering plane (which contains the incident momenta and that of the trigger) has been reported[7]. Defining p_x and p_{out}, the components of the transverse momentum $\vec{p}_T$ of an away mover in and out the scattering plane, the p_{out} distributions are observed to be independent of p_x, in contrast with the situation in "normal" events where p_{out}, on the average, increases with $|p_x|$. The mean value of p_{out} is measured to be 500 MeV/c (Fig. 14).

ii) When studied event by event, away movers are observed to be strongly correlated in rapidity, the stronger the larger p_x. This has been independently reported by three groups[7,11,12] and is illustrated in Figs. 15 to 19.

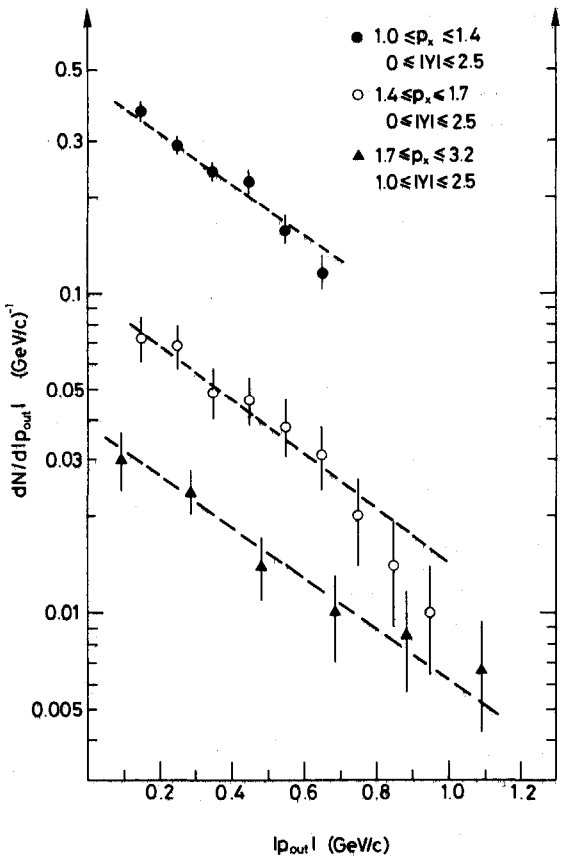


Fig. 14 Distribution in p_{out} of the away movers in different $|p_x|$ intervals. Data from Ref. 7.

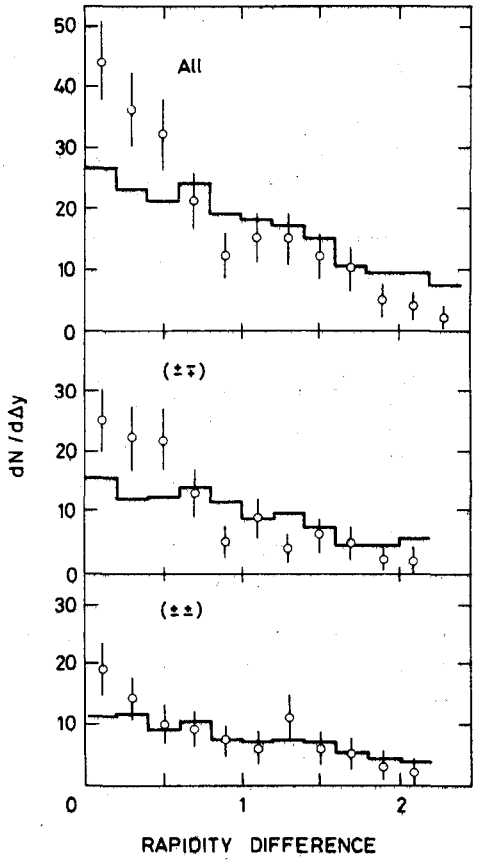


Fig. 16 Rapidity correlation among away movers for different charge combinations. The line indicates the uncorrelated background. Data from Ref. 12.

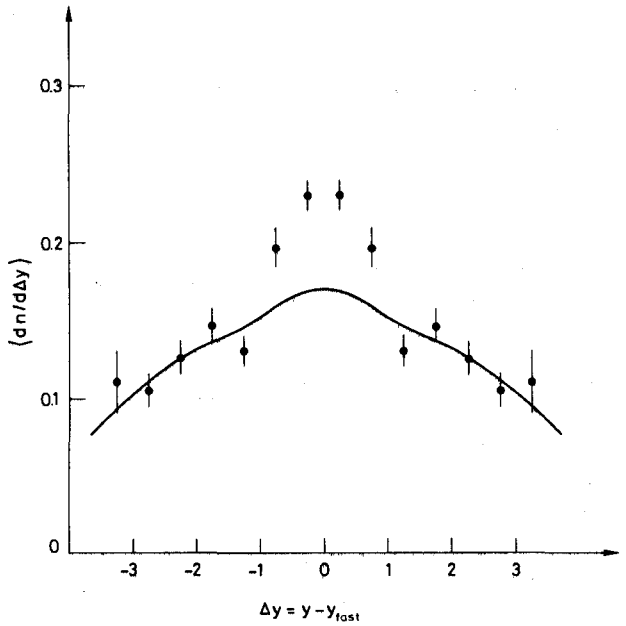


Fig. 15 Rapidity correlation between charged away movers with large $|p_x|$. The line indicates the uncorrelated background. Data from Ref. 7.

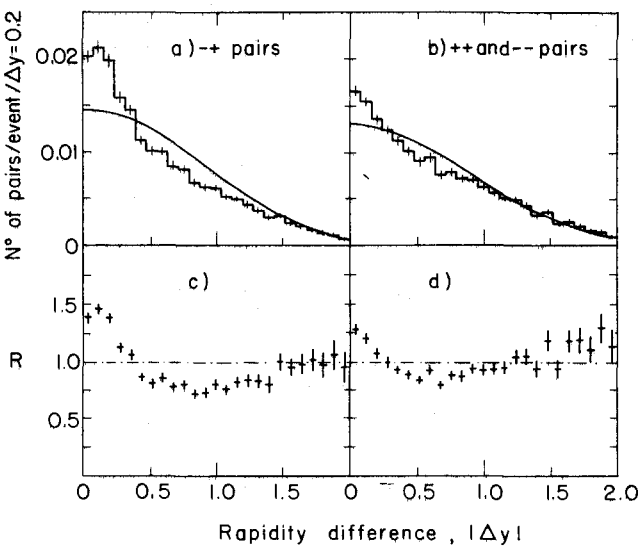


Fig. 17 Rapidity correlation among away movers for different charge combinations. The line indicates the uncorrelated background. Data from Ref. 11.

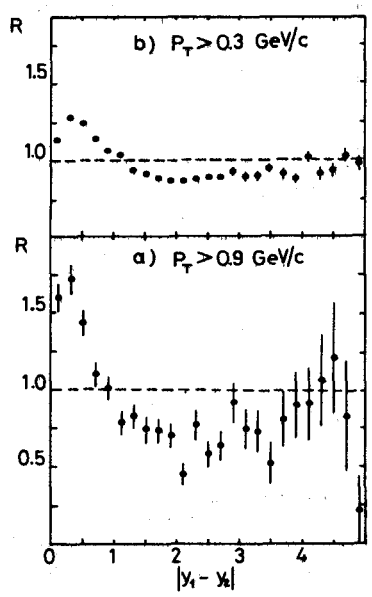


Fig. 18 Rapidity correlation among away movers for two intervals of their transverse momentum. From Ref. 11.

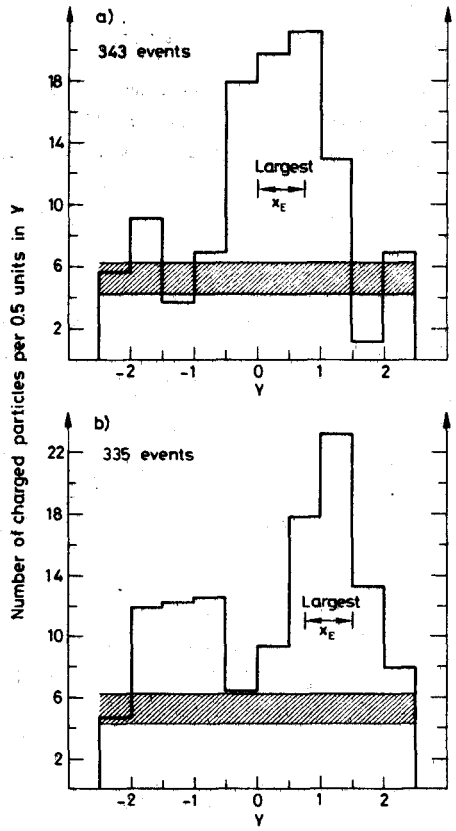


Fig. 19 Rapidity distribution of large p_x away movers when that with the largest p_x (not included in the plot) lies in the regions indicated by the arrows. Data from Ref. 7.

For this result to be significant, it must be compared to the similar correlation observed in "normal" events and commonly described in terms of cluster emission. This has been done[7] for a π^0 trigger at 90°, with $p_T^0 \sim 2.5$ GeV/c, and for secondaries with $|p_x| > 1.2$ GeV/c (Fig. 15). The observed correlation corresponds to an excess of 0.33 ± 0.07 charged particles per event extending over ±0.6 units of rapidity, to be compared with 0.18 ± 0.03 particles per event over ±0.8 units of rapidity in "normal" events. The difference is small but significant and the increase of the correlation with p_x is clearly evidenced (Figs. 18 and 19). Needless to say, higher statistics and larger values of p_T^0 are highly desirable for a better study of the properties of pairs of large p_x away movers. All three experiments report a larger correlation (by a factor of the order of 2) between opposite charge pairs than between same charge pairs (Figs. 16 and 17).

iii) Distributions in p_x [7] are illustrated in Fig. 20. To permit comparison with similar distributions in electroproduction and e^+e^- annihilation experiments, the variable $x_e = |p_x|/p_T^0$ is used rather than p_x. If the trigger itself were the only towards mover, and if the away movers would exactly balance its transverse momentum, the distribution in Fig. 20a would describe the fragmentation of the away movers. But the existence of other towards movers implies that a variable x_e' smaller than x_e should be used instead. This is done in Fig. 20b and shows no significant effect. Note that, on the average, one quarter of the events have at least 40% of the trigger transverse momentum balanced

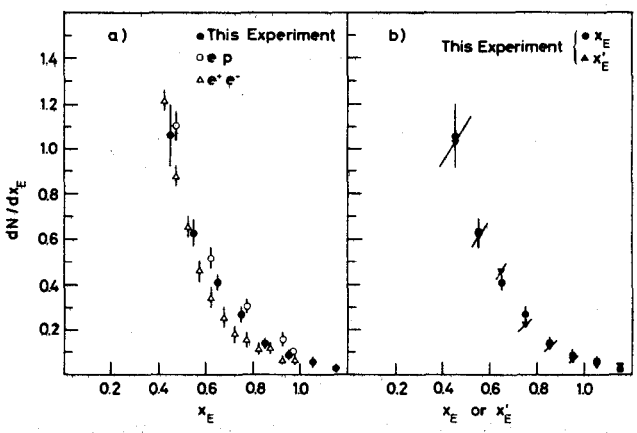


Fig. 20 dN/dx_e distributions for away movers (see text). Data from Ref. 7.

by a single charged particle. The data from Ref. 7 are unfortunately insufficient to study the scaling properties of the p_x distributions, but in the region ($p_x > 1.2$ GeV/c, |rapidity| < 2.5, $|p_{out}| < 840$ MeV/c) the x_e distribution is consistent with being independent of p_T^0 for a 90° π^0 trigger. Preliminary data from Ref. 11, reported by R. Sosnowski at this Conference, however, indicate a substantial scaling violation in the region ($p_x > 1$ GeV/c, $|p_{out}| < 850$ MeV/c) for data taken with a charged particle trigger at 45°. It is premature to draw definite conclusions from these possibly contradictory results.

iv) Most experiments do not show any evidence of correlation between the rapidity of the trigger particle and the mean of that of away movers, as further confirmed by recent data[10]. An exception is, however, worth noting. It comes from an experiment[6] where the secondaries are not momentum-analysed, but where p_T^0 is quite larger than in other data. The trigger is a π^0 at rapidity slightly below 1, and the away movers are observed to have an asymmetric rapidity distribution, with an excess of charged particles (0.50 ± 0.12 charged particles per event in an azimuthal wedge of ±30° opposite to the trigger) towards negative rapidities (Fig. 1).

VI. Phenomenology of the Event Structure

Without going deeper into the study of large p_T processes, and in particular before presenting the vast amount of data concerning single-particle inclusive spectra and their dependence upon quantum numbers, it is useful at this stage to attempt to condense the material of the previous sections into a few characteristic properties.

Let us first comment upon the role played by energy-momentum conservation. In the absence of a precise knowledge of the dynamics to which we should apply the δ-functions expressing energy momentum conservation, the problem is not well defined. Pure phase space, on the other hand, is so far from measured populations that its study is not very informative. As an exercise, having learned the persistence of longitudinal phase space as a dominant dynamical property, we may study the effect of four-momentum conservation on particles produced independently from each other with uncorrelated transverse momentum and rapidity distributions adjusted to best fit single-particle inclusive spectra. The main conclusions are as follows:

i) The transverse momentum of the trigger is balanced by a set of away movers covering a broad angular range, qualitatively similar to what is experimentally observed. However, there are more away movers per GeV/c of p_T^0, each carrying less transverse momentum, than in the observed data.

ii) The away movers are not confined to the trigger plane; namely there is little coupling between momenta collinear to the trigger and momenta at 90° in azimuth.

iii) As expected, not only is there no towards mover, but the particle density on the trigger side decreases slowly with p_T^0.

These remarks give further support to the idea that only a fraction of the particles in the final state takes part in the momentum balance of the large p_T trigger.

To the extent that the towards and away movers are in close relation with the dynamics of the process of large p_T production, it is important to analyse their properties independently of the underlying "normal" event. This is very difficult in the present experimental situation where only a few among the away and towards movers have large enough transverse momenta (say > 1 GeV/c) to be distinguished from the underlying "normal" event, acting as a background. This situation, illustrated in Fig. 21, contrasts with that of e^+e^- annihilation, where there is no

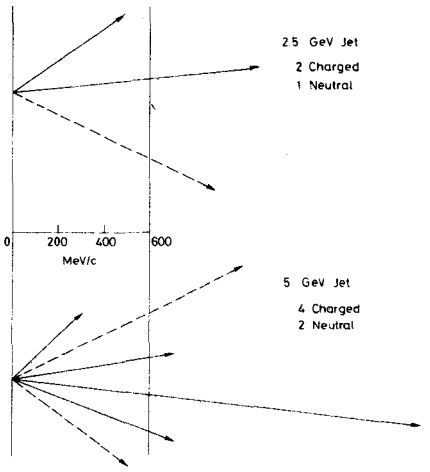


Fig. 21 Scale drawings of typical jets at 90° and "normal" event background. Figure taken from P.V. Landshoff (Ref. 18).

underlying normal event to disturb the analysis of the final hadronic state[16]. A popular and instructive approach[17-22] has been to postulate some simple properties obeyed by the away and towards movers, and to confront their consequences with experimental data. Let us briefly review and comment upon the hypotheses most commonly postulated. To do so we define

$$\vec{P}^T = \sum_{\text{towards movers}} \vec{p} \ ,$$

where the sum includes the trigger particle, and

$$\vec{P}^A = \sum_{\text{away movers}} \vec{p} \ .$$

i) $\vec{P}^T + \vec{P}^A = 0$. This hypothesis implies that the underlying normal event has no transverse movement, which is not directly evidenced (at least in this strong form) from the data. In this context, an important comment by Levin and Ryskin[23] is of relevance. They present cumulative evidence that partons inside hadrons have large transverse momenta, on the average larger than 1 GeV/c. One argument is that the p_{out} distribution[7] presented in a previous section is already quite broad, and corresponds to an even wider transverse momentum distribution for the colliding partons when one accounts for the fact that the observed hadrons carry only a fraction of the momentum of their parent parton. A similar situation is observed in deep inelastic electroproduction[17]. If this were true, the larger p_T trigger particle would most likely be produced in a collision of two partons with abnormally large transverse momenta in its direction and the above hypothesis should be reconsidered.

ii) $$E^A E^T \frac{d^6\sigma}{d^3P^A \, d^3P^T} \approx F(P_T^A) F(P_T^T) \ .$$

This hypothesis of independence upon the rapidities y^A and y^T, and of absence of correlation between these two quantities, is believed to be a good approximation in the central region where single-particle inclusive spectra are observed to have the same property and where, for a fixed direction of $\vec{P}^T$, $\vec{P}^A$ is observed to span a very wide angular range[21].

iii) In the frame where $\vec{P}^A + \vec{P}^T = 0$, let us define the axis J collinear to $\vec{P}^A = -\vec{P}^T$. Away and towards movers have transverse momenta $\vec{p}_T^{\,i}$ with respect to this axis and longitudinal momenta $\vec{p}_L^{\,i}$ along this axis. It is commonly postulated that $\vec{p}_T^{\,i}$ are cut off with an average value of the order of 300 MeV/c and that $\vec{p}_L^{\,i} = x^i \vec{P}^{A,T}$ are distributed according to $x^i \, dN/dx^i = g(x^i)$, where $g(x^i)$ is a smooth function of x^i. This strong hypothesis of Feynman scaling along J is formulated in different manners depending upon the authors. It may be simply postulated[17,18,21], or based on analogy with other processes such as e^+e^- annihilation[19,22] or "normal" hadron-hadron collisions[20].

The remarkably simple hypotheses mentioned above permit quantitative evaluations of the data. For example, when comparing the momentum correlation between the trigger and away movers with that between the trigger and towards movers, we can weigh the relative importance of the wide angular span of $\vec{P}^A$ (which depresses the former) and of the distortion on the towards side due to the fact that we trigger on a single particle (which depresses the latter). The agreement with the data is very impressive in view of the simplicity of the hypotheses made. This does not prove that the above picture is the only possible one, nor that it will resist the confrontation with future data -- with hopefully better statistics and larger transverse momenta. It does, however, put severe constraints on possible interpretations of the data. For example, Ellis, Jacob and Landshoff[18] emphasize the importance of allowing for a small δ-function contribution to $g(x^i)$ in the vicinity of $x^i = 1$ in order to obtain good fits to the data. This implies that the set of away movers has a small probability (at the percent level) to consist of a single particle, but on the towards side, because of the peculiar triggering mode, this rare configuration is very much favoured. They find that a form

$$\frac{g(x_i)}{x_i} \propto \frac{(1 - x_i)^2}{x_i} + 0.016 \, \delta(1 - x_i)$$

gives an adequate description of the data. A meson-like jet, such as predicted by constituent interchange and quark fusion models, is indeed often expected to consist of a single meson, while a quark-like jet cannot fragment in a single hadron without violating triality conservation. J. and G. Ranft[22] account for some scaling violation in the jet fragmentation, as observed in the presumably quark-like e^+e^- jets, and are able to reproduce the experimental situation without the help of a δ-function. The same authors note the impossibility of describing the correlation among towards movers with a function $g(x_i)/x_i$ decreasing

towards $\hat{x}_i = 0$. Such a situation would arise in the case where away and towards movers would consist each of a large p_T, low-mass resonance or cluster, such as observed in "normal" events.

Keeping in mind that there is some amount of speculation in the above picture which needs further experimental confirmation, we may already at this stage discard some of the models which have been proposed to describe large p_T hadronic processes. Single-fireball models[24], where the colliding hadrons fuse in a massive hadronic state which subsequently decays isotropically, and bremsstrahlung models[25], where the incident hadrons experience a hard scattering and radiate neutral vector mesons, do not account for the presence of an underlying "normal" event with longitudinal phase-space dominance, and, as such, are in disagreement with the data. They do, however (especially the latter), give a satisfactory description of single-particle inclusive spectra and of two-particle momentum correlations.

Hard-scattering quark-parton models where a single meson or meson-resonance is produced on one side, such as the constituent interchange model[26] and the quark fusion model[27], find it difficult to understand the properties displayed by towards movers. For these models to survive, towards movers would have to contain resonances with large multiplicity final states to wash out charge correlations in the "alongside" configuration. It is not clear whether such a situation can be reconciled with present experimental evidence, especially with regard to the above comment of Ranft and Ranft[22]. It must, however, be noted that the exactly "alongside" configuration does not favour the observation of resonances, and it is very important for future experiments not only to search for resonances among towards movers but also to produce upper limits for their production cross-section in cases where they are not observed.

Multi-fireball models, such as that developed by Kagiyama and Hirose[28], possess most of the features evidenced in the data. There, one of the clusters in a "normal" event has evolved to a massive excited state, the decay products of which, emitted isotropically in its rest frame, constitute the set of away and towards movers. The fireball must have a sufficiently low multiplicity for energy-momentum conservation within the fireball to take the apparent limitation of $\hat{p}_T^i$, but a large enough temperature to generate towards movers. Whilst it seems that such a compromise is not excluded, a critical quantitative confrontation with all available data is still to be done. In particular, strong angular correlations between $\vec{P}^A$ and $\vec{P}^T$ should apparently be expected in such a picture.

Hard-scattering models, where a binary collision between constituents of the colliding hadrons generates two jets of particles in the final state, are clearly favoured by the data presented in the previous sections. A clear analysis of the experimental situation in these terms has recently been given by Bjorken[17] who also presents several instructive comparisons with leptoproduction and e^+e^- annihilation data.

To progress further in our understanding of large p_T dynamics, it is now time to review the experimental results concerning single-particle inclusive spectra, in particular their scaling properties and their dependence upon quantum numbers.

VII. Single-Particle Inclusive Spectra

Before the Conference, the experimental material on single-particle inclusive spectra, which has been recently reviewed in detail[29], consisted mostly of ISR data[14,15,30] at rather low values of $x_T = 2p_T/\sqrt{s}$ and of FNAL data obtained with proton beams on nuclear targets[31,32]. The main features exhibited by the data may be briefly summarized as follows:

i) Invariant cross-sections decrease steeply with p_T, approximately as $p_T^{-n_{eff}}$, with $n_{eff} \approx 12$. In comparison with this strong dependence upon p_T, that upon $\sqrt{s}$, upon angle, and upon particle type are rather mild.

ii) The dependence upon $\sqrt{s}$ exhibits violation of Feynman scaling, conveniently expressed in the form $E(d^3\sigma/dp^3) \propto p_T^{-n} f(x_T)$, with $n \simeq 8$ in the ISR range. In the FNAL range, when extrapolating the nuclear target data to the p-p case, higher values of n were obtained at large x_T, of the order of 11 for pion production[31].

iii) The dependence upon angle is not significant in the central region. In the forward region it is reasonably well accounted for by replacing x_T by $x_R = (x_T^2 + x_L^2)^{1/2}$ in the formula above[32].

iv) Heavier particles are more copiously produced at larger p_T. When expressed as a function of $m_T = (m^2 + p_T^2)^{1/2}$, m being the mass of the particle produced, all cross-sections are similar, within a factor of 5 or so, for m running all the way from 0.135 to 3.1 GeV/c^2. The π^+/π^- ratio is equal to 1.2, independent of p_T, in the range explored.

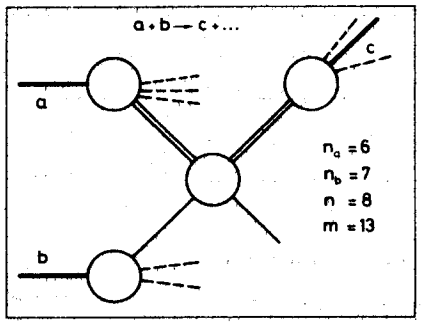


Fig. 22 An illustration of the dimensional counting rules (see text).

These data have been widely analysed and commented upon[29], in the frame of quark-parton models, with the help of the powerful and elegant dimensional counting rules[33] which relate the inclusive cross-section for production of particle c to the number n_a of active quark lines taking part in the hard-scattering process and the number n_p of passive quark lines "wasting" momentum in the hadron ↔ quark transitions (Fig. 22). According to the counting rules, one has, in the central region,

$$E(d^3\sigma/dp^3) \propto (p_T^2 + \mu^2)^{-(n_a-2)} f(x_T)$$

with

$$\lim_{x_T \to 1} f(x_T) = (1 - x_T)^{2n_p-1} .$$

For such arguments to be powerful, they must be confronted with data involving as many particle types as possible, both in the initial and final state, and reaching to large values of x_T, where valence quarks can be expected to play a major role.

Many such data[34,35] are contributed to this Conference from FNAL, evidencing the superiority of fixed target machines in the field of single-particle inclusive cross-sections.

The Chicago-Princeton group[35] have measured invariant cross-sections for the inclusive production of $\pi^\pm$, $K^\pm$, and $p^\pm$ in proton collisions with proton, deuteron, Be, Ti, and W targets. The data on nuclei will be briefly reported in the next section. An important and unexpected result is that they do not extrapolate accurately to the p-p data. In particular, for pion production, the latter are well described by a form $p_T^{-n} f(x_T)$, with n = 8.5 to 8.9, and not 11 as had been previously deduced by extrapolation of nuclear data. The apparent dependence of n upon x_T, which was commonly accepted before the Conference, has now disappeared. All measured cross-sections (Figs. 23 to 26) are amenable to a description of the form

$$E(d^3\sigma/dp^3) \propto p_T^{-n} (1 - x_T)^m$$

in the large x_T region ($x_T > 0.3$). Preliminary fits to the data yield the values of n and m listed in Table 2. The π^+/π^- ratio, in good agreement with ISR data[15], remains at the level of 1.2 to 1.3 in the low x_T region. But above $x_T = 0.3$, where no data exist in the ISR energy range, it abruptly increases and crosses the value of 2 at $x_T = 0.5$. The proton and, even more, the antiproton data, are in significant disagreement with ISR measurements in the same kinematic region[30].

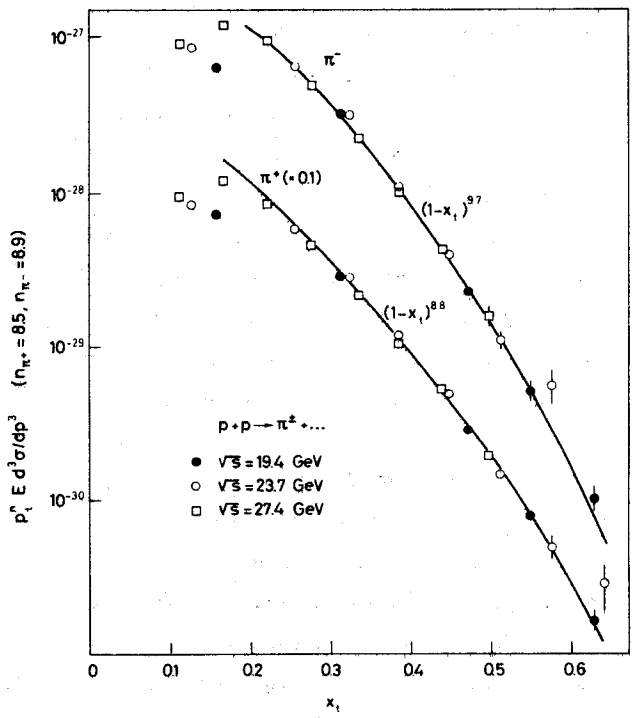


Fig. 23 Scaling in $\pi^\pm$ production in p-p collisions. Data from Ref. 35.

Table 2

Inclusive channel	n	m	Ref.
$p + p \rightarrow \pi^+ + \ldots$	8.5	8.8	35
$p + p \rightarrow \pi^- + \ldots$	8.9	9.7	35
$p + p \rightarrow K^+ + \ldots$	8.4	8.8	35
$p + p \rightarrow K^- + \ldots$	8.9	11.7	35
$p + p \rightarrow p + \ldots$	11.7	6.8	35
$p + p \rightarrow \bar{p} + \ldots$	11.9	8.0	35
$\pi^- + p \rightarrow \pi^0 + \ldots$	-	5.5 ± 0.3	34
$\pi^+ + p \rightarrow \pi^0 + \ldots$	-		34
$p + p \rightarrow \pi^0 + \ldots$	-	7.1 ± 0.4	34

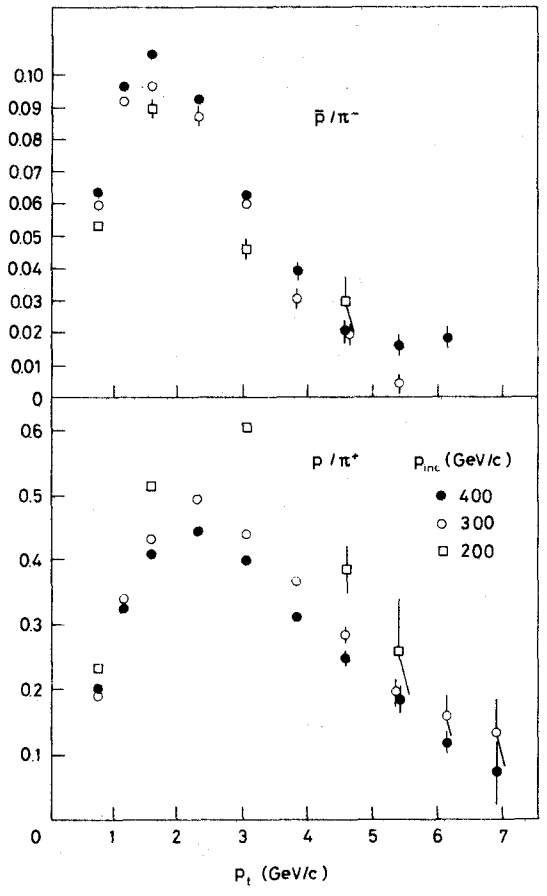


Fig. 24 Antiproton and proton to pion ratios in p-p collisions. Data from Ref. 35.

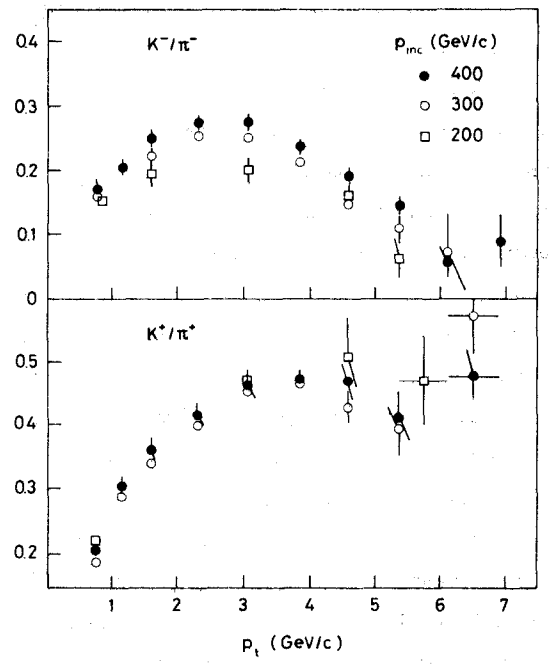


Fig. 25 Kaon to pion ratios in p-p collisions. Data from Ref. 35.

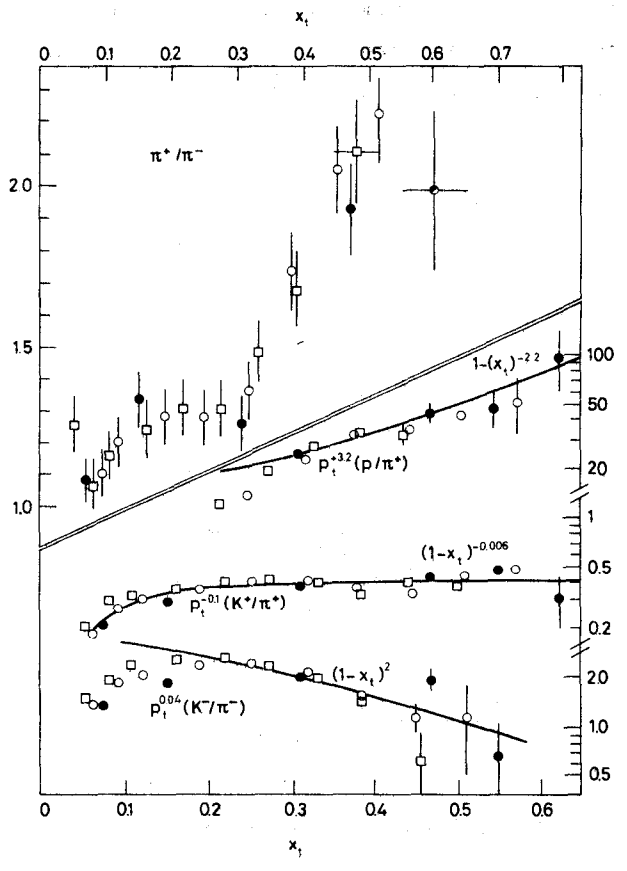


Fig. 26 Particle ratios as a function of x_T in the Chicago-Princeton data (Ref. 35).
Upper figure: π^+/π^- ratio (top and left-hand scales).
Lower figure: p/π^+, $\bar{p}/\pi^-$, K^+/π^+, and K^-/π^- ratios multiplied by the scaling power of p_T.
Lines indicate fits to a form $(1 - x_T)^m$ as indicated on the figure.

The π^+/π^- ratio behaves differently in proton-proton collisions and in proton-deuterium collisions (Fig. 27). This may be interpreted as an indication that the π^+/π^- ratio is roughly equal to 1, independent of p_T, in proton-neutron collisions. Such a conclusion, obtained by simply subtracting the proton value from the deuterium value, may however seem hazardous in the present situation.

The BNL-CalTech-LBL group[34] presents measurements of inclusive π^0 production at 90° from $\pi^\pm$-p and p-p interactions at 100 and 200 GeV/c. They are the first measurements of that kind performed with a meson beam, and will hopefully be followed by a long succession of similar experiments. The lever arm in s is not sufficient to permit a meaningful study of the scaling behaviour of the measured cross-sections. However, the p_T dependences at fixed x_T are observed to be sufficiently similar to study cross-section ratios as a function of x_T. The π^+-p → π^0 + ... and π^--p → π^0 + ... cross-sections are equal within errors over the full p_T,$\sqrt{s}$ range (Fig. 28). The ratio R between the p-p → π^0 + ... and π^--p → π^0 + ... cross-sections is displayed in Fig. 29 as a function of x_T, and varies like $(1 - x_T)^m$ with $m = 1.6 \pm 0.5$. The systematic uncertainty on these ratios, where the numerator and the denominator are measured with the same detector but in different beams and runs, is claimed by the authors to be very small.

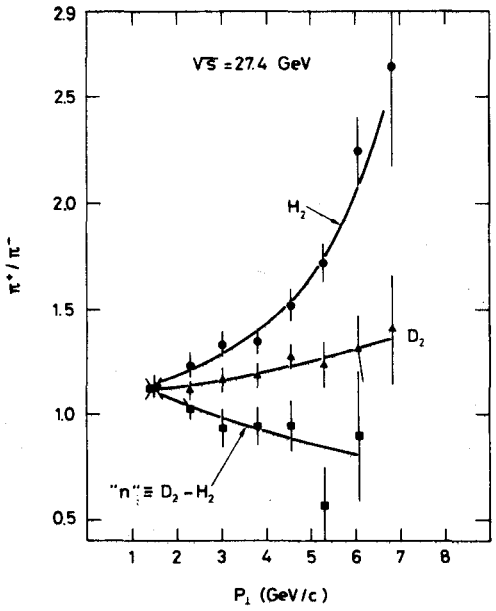


Fig. 27 π^+/π^- ratio in p-p and p-d collisions. From Ref. 35.

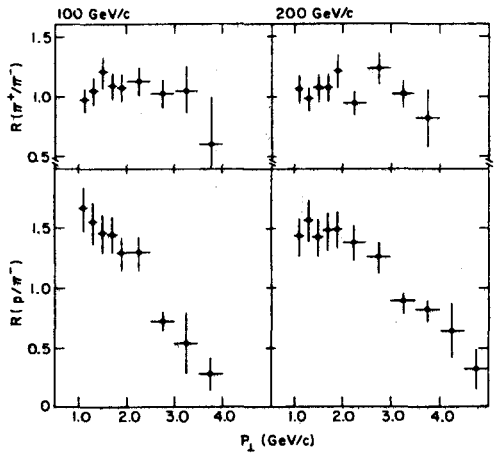


Fig. 28 Ratios between π^+-p → π^0 + ... and π^--p → π^0 + ... (upper figures), and between p-p → π^0 + ... and π^--p → π^0 + ... (lower figures) for two values of $\sqrt{s}$. Data from Ref. 34.

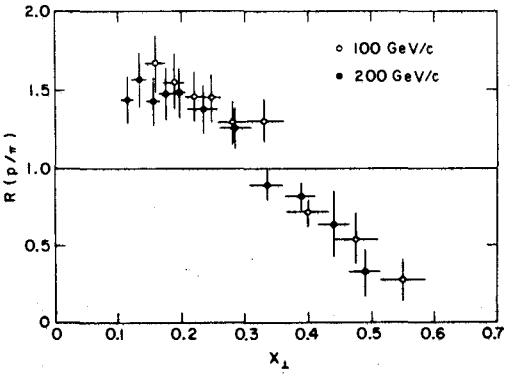


Fig. 29 Ratio between p-p → π^0 + ... and π-p → π^0 + ... as a function of x_T (Ref. 34).

Preliminary data at forward angles (≈ 35°) indicate a similar behaviour.

I conclude this section on single-particle inclusive spectra by briefly mentioning four other contributions to this Conference.

The first one[36] concerns the production of π^0 at 90° in the ISR energy range, and differs from previous measurements in that the π^0 is identified from its $\pi^0 \to \gamma\gamma$ decay mode. In the range $1.6 < p_T < 3.8$ GeV/c the data agree well with $\pi^\pm$ cross-sections[30] within the 20% normalization uncertainty between the two experiments.

The second[37] is a measurement of the charge asymmetry in the central region in $\bar{p}$-p interactions at 22.4 GeV/c incident momentum. The charge asymmetry is observed to occur in the forward and backward directions close to the

central region and to increase with transverse momentum. A similar observation is reported[38] in 16 GeV/c $\pi^{\pm}$-p and 100 GeV/c π^{-}-p interactions by another collaboration, who present in addition[39] a very rich set of data on inclusive production of many resonances which are all observed to have a similar p_T dependence in the larger p_T region.

VIII. Nuclear Effects

The early measurements[31], by the Chicago-Princeton Collaboration, of large p_T inclusive spectra from proton-nucleus collisions had triggered much interest[40] in that the atomic number dependence was observed to behave like A^{α} with $\alpha >> 2/3$, even greater than 1.

The same Collaboration reports on similar measurements[35], but with higher statistics and better control upon systematic uncertainties. In the case of $\pi^{\pm}$ production the power α shows a clear tendency to decrease towards very large values of p_T, after having reached a maximum (slightly above 1.1) at p_T = 4 to 5 GeV/c (Fig. 30).

New data[41] from Serpukhov on large x_T (0.2 to 0.6) inclusive yields at 90° from p-Be and p-Cu collisions (70 GeV/c incident momentum) are presented. The K^+/π^+ and p/π^+ ratios are observed to behave in a similar way to those in the FNAL energy range.

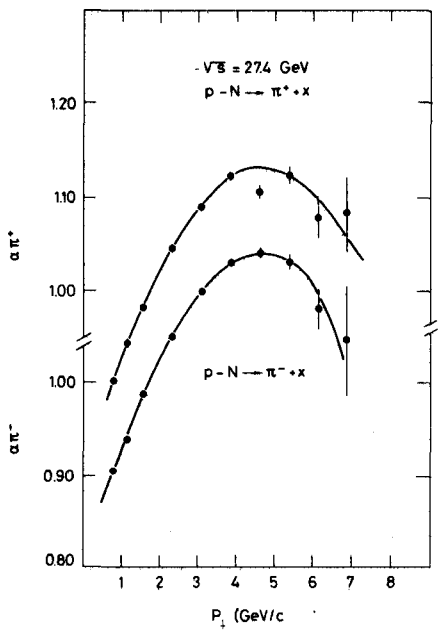


Fig. 30 Atomic number dependence of inclusive $\pi^{\pm}$ production in proton-nucleus collisions (Ref. 35). The exponent α of the atomic number A is displayed as a function of p_T.

IX. More on Models

When considered together, the experimental material on the structure of large p_T events and that on single-particle inclusive spectra sum up to a large amount of information which has generated much activity among theorists. I am not competent to give a critical evaluation of their many contributions to the Conference, and can only extract from their work the points which seem to me relevant for guiding experimentalists in their measurements.

A central question concerns the understanding of the depression of the Berman-Bjorken-Kogut (BBK) diagram[2] (gluon exchange between quarks, Fig. 31a). As is immediately apparent from the dimensional counting rules, this corresponds to n = 4, while the data want $n \approx 8$ (for $p\text{-}p \to \pi + \ldots$). Before the Conference, when n was believed to be different in the ISR and FNAL energy ranges, we might have seen in the data a trend for n to decrease towards larger values of s, and speculate that it might level off at very high energies. This is no longer reasonable. As an illustration of current ideas on the problem, I briefly list a few representative models which have been proposed.

1) The constituent interchange model[26] postulates the depression of the BBK diagram and assumes the dominance of subprocesses involving hadrons as constituents, such as quark-meson scattering (Fig. 31b). Depending upon the (x_T, p_T) domain, several such processes may be at work according to the respective dominance of the p_T^{-n} and $(1 - x_T)^m$ terms. This results in much flexibility built up into the model, which appears to reproduce successfully most of the scaling behaviour of single-particle inclusive distributions. In addition, it offers a natural smooth connection to exclusive processes as well as to low p_T reactions, and provides a good description of form factors. Its most recent developments have been reported by S. Brodsky at this Conference, together with a comparison of its predictions with the new FNAL results presented above. The main merit of this model may be to offer a transparent recipe for immediately deducing from the data which are the dominant subprocesses, and possibly providing some hint towards a better understanding of the dynamics. A recent example is the possible importance of minimum neutralization of quark lines[42].

2) The quark fusion model[27] is of a similar nature (Fig. 31c). The dominant process is postulated to be

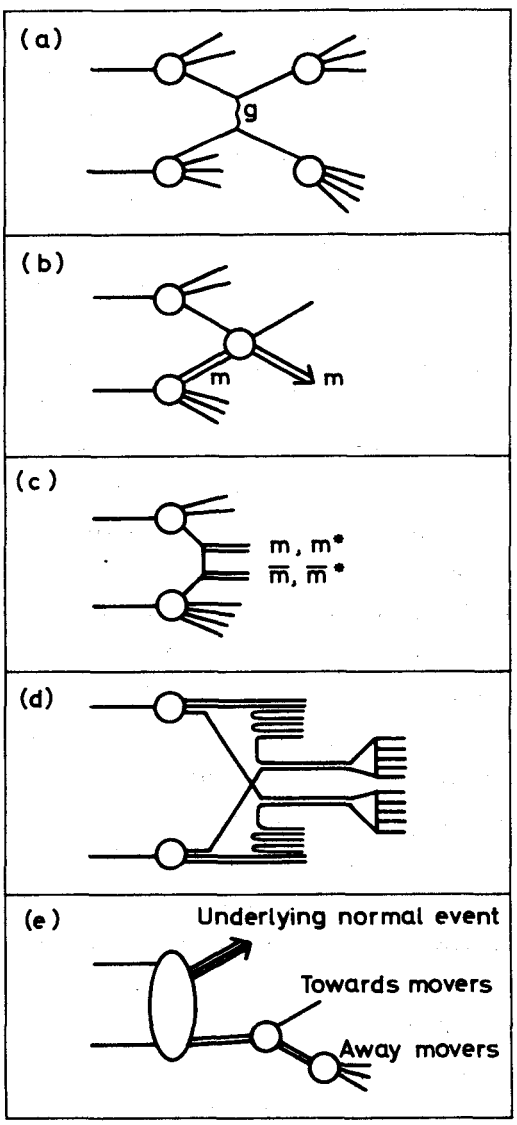


Fig. 31 Some typical diagrams of current parton models (see text).

quark + antiquark → two mesons, which corresponds to n = 8.

As previously mentioned, such models do not account for the production of apparently non-resonant towards movers.

An *ad hoc* modification has recently been proposed[43] by replacing the outgoing mesons by meson-like jets. An interesting consequence[44] is the prediction of a copious single-photon yield (the lesser electromagnetic coupling being compensated by the absence of fragmentation). A recent ISR experiment[36] indeed reports the observation of large p_T photons at 90° ($3 < p_T < 4$ GeV/c) in excess of the $\pi^0 \to \gamma\gamma$ and $\eta \to \gamma\gamma$ contributions. The ratio $R = \sigma(p\text{-}p \to \gamma + \ldots)/\sigma(p\text{-}p \to \pi^0 + \ldots)$ is measured to be (20 ± 10)%, where the error includes several systematic uncertainties (Fig. 32). In the framework of quark fusion models, much effort has been devoted to describing, in a unified manner, high and low p_T processes at all angles[45]. A summary of such work has been given by T. Matsuoka at this Conference. Most features of the data are successfully described by assuming multiperipheral dynamics for the jet fragmentation (Fig. 31d). A feature of the model, which has to be revised, is to predict an increase of n with x_T, similar to what was commonly believed before the Conference.

3) In the massive quark model[19], free quark states are explicitly avoided by setting quark masses to a large value and by strongly damping quark scattering amplitudes at large masses in order to prevent the appearance of on-mass-shell quarks. An n = 4 subprocess is present, but in the FNAL-ISR energy range the dominant subprocess (Fig. 31e) corresponds again to n = 8 for inclusive meson production. A small-mass cluster (towards movers) recoils against a larger mass hadronic state (away movers), which decays with limited transverse momentum and Feynman scaling along its axis. As previously mentioned, this model reproduces well the many aspects of the event structure.

4) Some authors maintain the dominance of the BBK subprocess by introducing a scale at its vertex[23]. A recent comment along this line[46] has been made in relation to the scaling violation apparently observed in deep inelastic leptoproduction. From a description of νW_2 in the form

$$\nu W_2 = f(x)(1 + q^2/\Lambda^2)^{-2}$$

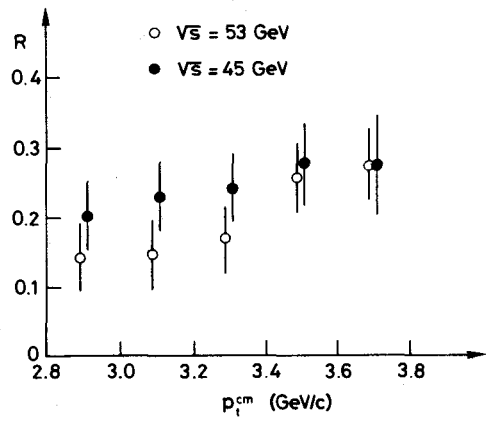


Fig. 32 Ratio between photon and π^0 cross-sections in p-p collisions (the $\pi^0 \to \gamma\gamma$ and $\eta \to \gamma\gamma$ contributions have been subtracted from the photon component). An additional 7% uncertainty must be applied to the data (Ref. 36).

which reproduces the experimental data for $A^2 \approx 50$ (GeV/c)^2, it is possible to infer an effective finite quark size and calculate the modified inclusive cross-sections. It is of course questionable whether such an extrapolation is reasonable, but it results in a beautiful agreement with the pion data.

5) I conclude this list by mentioning the field theoretical approaches[47] which have been reviewed by A.N. Tavkhelidze, A.V. Efremov and L.A. Slepchenko at this Conference. Kvinikhidze et al.[47], starting from field theoretic arguments for composite hadrons, obtain a number of general conclusions which reduce to the usual parton-model results under the more specific assumptions inherent to such models. In particular, they give a general derivation of the dimensional counting rules. Their treatment of the rescattering[48] of the hard scatters in the stream of the passive constituents of the colliding hadrons is of particular interest. Similar ideas have been considered by Gasser and Sukhatme[20] in a purely phenomenological and *ad hoc* manner, with much success in describing the main properties of the event structure.

It is clearly premature and outside my competence to give a critical analysis of the implications of the new FNAL data on current models. The remarkable agreement of the Chicago-Princeton[35] cross-sections with a form $p_T^{-n}(1 - x_T)^m$ over a wide range of $x_T \geq 0.3$ nonetheless indicates that their analysis will be more informative than before. A few simple and possibly naive comments can already be made at this stage.

The data of Donaldson et al.[34] suggest that the presence of an antiquark in the pion wave function is not as important as might have been anticipated, although pions appear to be more efficient than protons at producing π^0's in collisions with protons. If the dominant subprocesses would direclty involve the antiquark from the incident pion, we would naively expect

$$R_\pi = \frac{\pi^+ - p \to \pi^0 + \ldots}{\pi^- - p \to \pi^0 + \ldots} = \frac{1}{2}$$

$$R_p = \frac{\pi^\pm - p \to \pi^0 + \ldots}{p - p \to \pi^0 + \ldots} \propto (1 - x_T)^{-6} .$$

The data rather favour subprocesses where, for example, a pion constituent of the incident pion takes part in the hard scattering, in which case $R_\pi \approx 1$ and $R_p \propto (1 - x_T)^{-2}$. These remarks are not in favour of the quark fusion model.

In the constituent interchange model we expect dominant subprocesses with $n = 8$ for meson production, and $n = 12$ for $p^\pm$ production, in good agreement with experiment. This seems to be difficult to reconcile with quark-quark scattering subprocesses, which would, in addition, predict much higher values of m than experimentally observed in $p^\pm$ production because of the necessity of having a large number of spectators. Another difficulty for quark-quark scattering models, previously noted by Bjorken[17], is the non-equality of the $p/\bar{p}$ and K^+/K^- ratios in p-p collisions. The new data confirm the relation

$$\left(\frac{p}{K^+}\Big/\frac{\bar{p}}{K^-}\right) \approx 4 \quad \text{at } p_T = 3 \text{ GeV} .$$

The observed increase of the π^+/π^- ratio in p-p collisions, up to and possibly above 2, is however a relief for most quark-parton models, which had difficulty in understanding the stable value of 1.2 obtained below $x_T = 0.3$.

Many more measurements are clearly necessary in order to understand the dynamics of large p_T collisions and the respective roles of constituent interchange and quark-quark scattering subprocesses[49], the former being successful at explaining single-particle inclusive spectra, the latter at understanding the global structure of the event. In the guise of a conclusion, we may try to single out some experiments which should shed some light on these questions.

X. Conclusion

Data of the quality of the Chicago-Princeton measurements[35] must be collected on hydrogen at large x_T with various incident beams ($\pi^\pm, K^\pm, \gamma$), looking for $p^\pm$, $\pi^\pm$, and $K^\pm$ inclusive spectra. The accelerators at FNAL, and in the near future at the CERN SPS, are best suited for such studies.

The exact nature of away and towards movers must be further investigated. Their apparent jet structure has to be confirmed in experiments with larger p_T triggers and better statistics to permit detailed studies of the shape and scaling properties of the transverse and longitudinal momentum distributions along the jet axis. In addition, the exact role played by resonances should be understood.

Angular correlations between leading away and towards movers are very informative[49]. Very little is at present known at large enough p_T.

Quantum number flow, both within the set of away and towards movers, and between it and the underlying normal event, are predicted to behave very differently in different models. Their study, at large values of x_T, would give precious information.

The very same studies should be performed with e^+e^- hadronic final states, which are believed to be pure quark-like jets, undisturbed by the cumbersome background of the underlying normal event in hadron-hadron collisions. Much understanding will undoubtedly emerge from a detailed comparison between e^+e^- jets and the final states of large p_T hadronic processes.

Acknowledgements

I am very much indebted to Stan Brodsky for a critical reading of the manuscript and many suggestions for improvements.

I am grateful to Leonid Slepchenko and George Vesztergombi for their constant and friendly help during the Conference.

References

1) S.M. Berman and M. Jacob, Phys. Rev. Letters 25, 1683 (1970).

2) S.M. Berman, J.D. Bjorken and J.B. Kogut, Phys. Rev. D 4, 3388 (1971).

3) T.T. Wu and C.N. Yang, Phys. Rev. 137, B708 (1965).

4) B. Alper et al., Phys. Letters 44B, 521 (1973).
M. Banner et al., Phys. Letters 44B, 537 (1973).
F.W. Büsser et al., Phys. Letters 46B, 471 (1973).

5) G. Finocchiaro et al., Phys. Letters 50B, 396 (1974).

6) K. Eggert et al., Nuclear Phys. B98, 73 (1975).

7) P. Darriulat et al., Nuclear Phys. B107, 429 (1976).

8) M. Della Negra et al., Phys. Letters 59B, 401 (1975).

9) M. Della Negra et al., Nuclear Phys. B104, 365 (1976).

10) M. Della Negra et al., General characteristics of p-p collisions in which a high transverse momentum particle is produced, Paper 127/A4-14 contributed to this Conference.

11) M. Della Negra et al., Study of jet structure in p-p collisions with large transverse momentum secondaries, Paper 129/A4-15 contributed to this Conference.

12) British-Scandinavian-French Collaboration, Preliminary data presented orally at this Conference.

13) B. Alper et al., Multiplicities associated with the production of pions, kaons or protons of high transverse momentum at the ISR, Rutherford Laboratory preprint RL-76-031 (1976).
G. Bellettini et al., Correlation studies of events with a charged hadron at x = 0 in proton-proton collisions at the CERN ISR, Paper 114/A2 contributed to this Conference.

14) K. Eggert et al., Nuclear Phys. B98, 49 (1975).

15) F.W. Büsser et al., Nuclear Phys. B106, 1 (1976).

16) G. Hanson et al., Phys. Rev. Letters 35, 1609 (1975); and, Evidence for jet structure in hadron production by e^+e^- annihilation, Talk delivered at the SLAC Summer Institute on Particle Physics, July 1975.

17) J.D. Bjorken, High p_T dynamics, Lectures delivered at the SLAC Summer Institute on Particle Physics, July 1975.

18) S.D. Ellis, M. Jacob and P.V. Landshoff, Nuclear Phys. B108, 93 (1976).
P.V. Landshoff, Jets in large p_T reactions, Talk presented at the XIth Rencontre de Moriond, Flaine, 1976.

19) G. Preparata and G. Rossi, Looking at hadronic final states at high energies, I. Phenomena at large p_T, CERN preprint TH 2163, 5 May 1976; and, Paper 712/A4-16 contributed to this Conference.

20) J. Gasser and W.P. Sukhatme, The origin of jets, University of Cambridge preprint DAMTP 76/3, January 1976.

21) W. Furmanski and J. Wosiek, Correlations in large p_T processes in parton models, Jagellonian University preprint TPJU 7/76, March 1976; and, Paper 1106/A4-30 contributed to this Conference.
W. Furmanski and J. Wosiek, Parton-parton interaction derived from large p_T data, Jagellonian University preprint TPJU 13/76, June 1976.

22) J. Ranft and G. Ranft, Large transverse momentum correlations on the same hemisphere and realistic jets, Karl-Marx University preprint KMU-HEP 7604, January 1976; Rapidity distributions of large p_T particles and realistic jets, Karl-Marx University preprint KMU-HEP 7610, April 1976; and, Paper 396/A4-24 contributed to this Conference.

23) E.M. Levin and M.G. Ryskin, How large is the average transverse momentum of partons? Is it larger than 1 GeV/c?, Leningrad Nuclear Phys. Inst. preprint No. 167, July 1975; and, Paper 1005/A4-2 contributed to this Conference.
E.M. Levin and M.G. Ryskin, Production of hadrons with large transverse momentum and interaction of partons, Paper 884/A4-1 contributed to this Conference.

24) Meng Ta-Chung, Phys. Rev. D 9, 3062 (1974).
Kwan-Wu Lai and Meng Ta-Chung, Statistical approach to large p_T phenomena in meson-nucleon and nucleon-nucleon collisions, Stony Brook preprint ITP-SB-76-22, March 1976; and, Paper 977/A4-25 contributed to this Conference.

25) A.P. Contogouris, J.P. Holden and E.N. Argyres, Phys. Letters 51B, 251 (1974) and Nuclear Phys. B85, 102 (1975).
D. Schiff, A.P. Contogouris and J.L. Alonso, Phys. Letters 55B, 87 (1975).
A.P. Contogouris, private communication.

26) J.F. Gunion, S.J. Brodsky and R. Blankenbecler, Phys. Letters 39B, 649 (1972); Phys. Rev. D 6, 2652 (1972); Phys. Letters 42B, 461 (1973); Phys. Rev. D 8, 287 (1973).

27) P.V. Landshoff and J.C. Polkinghorne, Phys. Rev. D 8, 4159 (1973); Phys. Letters 45B, 361 (1973); Phys. Rev. D 8, 927 (1973).

28) S. Kagiyama and T. Hirose, Progr. Theor. Phys. 54, 1226 (1975); and, Superconductive fireball model on large p_T phenomena, I, II, and III, Kagoshima Univ. preprints KAGOSHIMA EP-002, 003, and 004 (1976).

29) D. Sivers, S.J. Brodsky and R. Blankenbecler, Phys. Rep. 23C, 1 (1976).

30) B. Alper et al., Nuclear Phys. B87, 19 (1975) and Nuclear Phys. B100, 237 (1975).

31) J.W. Cronin et al., Phys. Rev. D 11, 3105 (1975).

32) D.C. Carey et al., Inclusive π^0 production by high-energy protons, FERMILAB-Pub-75/75-EXP 7100.063, to be published in Phys. Rev.

33) S.J. Brodsky and G.R. Farrar, Phys. Rev. Letters 31, 1153 (1973) and Phys. Rev. D 11, 1309 (1975).
V. Matveev, R. Muradyan and A. Tavkhelidze, Nuovo Cimento Letters 7, 719 (1973).

34) G. Donaldson et al., Phys. Rev. Letters 36, 1110 (1976); and, Inclusive π^0 production at large transverse momentum for $\pi^{\pm}$-p and p-p interactions at 100 and 200 GeV/c, Paper 746/A4-27 contributed to this Conference.

35) D. Antreasyan et al., A precise comparison of hadron production at large p_T in 200, 300, and 400 GeV proton collisions with proton, deuteron, and nuclear targets, Paper 753/A4-17 contributed to this Conference.

36) P. Darriulat et al., Large transverse momentum photons from high-energy proton-proton collisions, Paper 341/A4-28 contributed to this Conference.

37) Alma Ata-Dubna-Helsinki-Košice-Moscow-Prague Collaboration, Charge asymmetry at large p_T in inelastic $\bar{p}$-p reactions at 22.4 GeV/c, Paper 903/A4-8 contributed to this Conference.

38) Aachen-Berlin-Bonn-CERN-Cracow-Heidelberg-Warsaw Collaboration, Studies of events with a secondary of high transverse momentum in 16 GeV/c $\pi^{\pm}$-p and 100 GeV/c π^--p collisions, Paper 898/A4-20 contributed to this Conference.

39) Aachen-Berlin-Bonn-CERN-Cracow-London-Vienna-Warsaw Collaboration, Inclusive yields and transverse spectra of pions and meson resonances and study of "direct" pion production, Paper 905/A4-23 contributed to this Conference.

40) G.B. Alaverdian, A.V. Tarasov and V.V. Uzinsky, Mass number dependence of proton spectra with large transverse momentum in proton-nucleus collisions, Dubna preprint E2-9606 (1976); and, Paper 1014/A6-60 contributed to this Conference.
G.R. Farrar, Phys. Letters B56, 185 (1975).
N.N. Nikolaev and V.I. Zakharov, Parton model and inelastic scattering of leptons and hadrons off nuclei, Moscow, 21 March 1975.

41) S.A. Akimenko et al., A study of relative hadronic yields at large transverse momentum from 70 GeV/c p-nucleus collisions, Paper 1225/A4 contributed to this Conference.

42) S.J. Brodsky, Constituent models and large transverse momentum reactions, SLAC preprint SLAC-PUB-1733, April 1976 (lecture delivered at the 1975 SLAC Summer Institute).

43) B.L. Combridge, Phys. Letters 62B, 222 (1976).

44) C.O. Escobar, Direct production of photons with large transverse momentum in proton-proton collisions, Cambridge preprint DAMTP 76/6 (1976).
G.R. Farrar and S.C. Frautschi, Phys. Rev. Letters 36, 1017 (1976).

45) Y. Kinoshita and K. Kinoshita, Unified description of large and small p_T spectra in p-p collisions at PS and ISR energies, Bielefeld preprint BI-TP 76/5, February 1976.
K. Kinoshita, A model of multiparticle final states in hadronic and current-induced reactions, Bielefeld preprint BI-TP 76/6, March 1976.
T. Matsuoka and S. Sawada, Transverse momentum in the multiple production processes, Paper 896/A4-18 contributed to this Conference.
Y. Igarashi, T. Matsuoka and S. Sawada, Large p_T hadron production and urbaryon rearrangement model, Paper 897/A4-19 contributed to this Conference.
S. Matsuda, Phys. Rev. D 12, 1940 (1975); and, Paper 997/A4-9 contributed to this Conference.
J. Kodaira and S. Matsuda, Progr. Theor. Phys. 55, 770 (1976); and, Paper 998/A4-10 contributed to this Conference.
J. Kodaira and S. Matsuda, Two-way quark cascade and particle ratios in $\gamma + p \to h^{\pm}$ + anything, Kyoto preprint KUNS 325 HE(TH) 75/12; and, Paper 999/A4-11 contributed to this Conference.
J. Kodaira and S. Matsuda, Meson-baryon and baryon-antibaryon ratios in two-way quark cascade model, Kyoto preprint KUNS 341 HE(TH) 76/1; and, Paper 1000/A4-12 contributed to this Conference.

46) R.C. Hwa, A.J. Spiessbach and M.J. Tepper, Connection between scale breaking in deep inelastic processes and large p_T hadronic reactions, Paper 900/A4-22 contributed to this Conference; and, Phys. Rev. Letters 36, 1418 (1976).

47) A.N. Kvinikhidze et al., Production properties at high p_T in a composite particle approach, Paper 1081/A4-31 contributed to this Conference.
A.V. Efremov, Dynamics of processes with large transverse momenta, Paper 894/A4-5 contributed to this Conference.

48) A.N. Kvinikhidze and L.A. Slepchenko, JINR preprint P1,2-8529 (1975), to be published in Nuclear Physics.

49) R. Raitio, Large p_T hadron physics: gluon or quark exchange, Univ. Wisconsin preprint COO-545, April 1976.

PARALLEL SESSION ON THEORY OF STRONG INTERACTIONS AT HIGH ENERGIES

THE FUNDAMENTAL LENGTH AS A KEY TO PHYSICS AT VERY HIGH ENERGIES

A.D.Donkov†, V.G.Kadyshevsky, M.D.Mateev, R.M.Mir-Kasimov

Joint Institute for Nuclear Research, Dubna

Many years ago strong interactions were described by the Yukawa potential. As higher velocities become essential relativistic description of the interactions was necessary. As a result instead of the Yukawa potential one had to use the Feynman propagator:

$$\frac{I}{m^2 - p^2} \quad . \qquad (I)$$

It is important to remark that in (I) a new fundamental constant - the velocity of light c appears.*

In this point a question arises. What will happen if we increase further the energy? Will the propagator modify once more at very high energies and will a new fundamental constant appear in the theory? If it is so this should be crucial in the analysis and understanding of the physics at these energies.

Let us try to answer the question. The propagator (I) can be written as the Fourier transform of the vacuum expectation value of the time-ordered product of two free field operators:

$$F\{<0|T\,\phi(x_1)\,\phi(x_2)|0>\}. \qquad (2)$$

Under the usual locality condition this expression is Lorentz invariant because the sign of the relative time is invariant for timelike intervals:

$$\varepsilon = \frac{t}{|t|} = \text{invar.},\ t=t_1-t_2,\ \text{when } x^2=(x_1-x_2)^2>0. \qquad (3)$$

Let us notice, however, that in the time-ordered product quantities related to higher than Lorentz symmetries are used. Namely the interval x^2 is Casimir operator of the Poincaré group of the fourdimensional momentum space

$$p' = \Lambda p + k \qquad (4)$$

and $\varepsilon=\frac{t}{|t|}$ is additional invariant of its unitary representations when $x^2>0$.

Therefore one can say that the usual properties of x^2, $\frac{t}{|t|}$ and finally of the propagator (2) itself, are closely connected with the Euclidean character of momentum space or more briefly with the Euclidean character of the parallel shifts in this space:

$$\frac{I}{m^2-p^2-i\varepsilon} \longleftrightarrow x^2, \frac{t}{|t|} \longleftrightarrow p'=p+k. \qquad (5)$$

But as the mathematicians teach, there exist noneuclidean geometries with different definitions of the parallel shifts:

$$p' = p \oplus k \qquad (6)$$

(Recall the story of the fifth postulate of Euclid).

Because the transformation (6) is nonlinear it is obvious from dimensional reasoning that a new universal constant ℓ with dimension of length appears. We shall call it fundamental length.

If $p,k \ll \frac{1}{\ell}$, then $p \oplus k \longrightarrow p + k$.

A new question arises: Could the noneuclidean shifts $p \oplus k$ produce a generalization of x^2, invariant $\frac{t}{|t|}$, the corresponding T-product and at last a new propagator substituting the old one at very high energies $|p| \gtrsim \frac{1}{\ell}$?

The answer is positive and is illustrated in the following Table:

Euclidean	Shifts	Noneuclidean
$p'=p+k$		$p'=p \oplus k$
	Lorentz group $p'=\Lambda p$ (common to both)	
$x^2=\begin{cases}=0\\ >0\end{cases}$ cone	Casimir Operator	$x^2=\begin{cases}L(L+3)\\ \text{np cone}\\ -1/9\ -\Lambda^2\end{cases}$
time t is continuous	Time	time n is discrete
$\frac{t}{\lvert t\rvert}$ = invar.		$\frac{n}{\lvert n\rvert}$ = invar.
T_t- product	Time-ordered Product	T_n- product
Propagator: $\frac{I}{m^2 - p^2}$		Propagator: $\frac{\ell^2}{2(\sqrt{I-\ell^2p^2}-\sqrt{I-\ell^2m^2})}$

Later on we shall put also $I^2=I$.

Let us briefly enumerate the properties of the new propagator:

I) The mass of elementary particles is bounded from above i.e. $m^2 \leq I$ (7)

2) At $p^2, m^2 \ll I$

$$\frac{I}{2(\sqrt{1-p^2}-\sqrt{1-m^2})} \longrightarrow \frac{I}{m^2 - p^2}.$$

3) In the timelike region $p^2 \leq I$, which means that the one-photon annihilation cross section vanishes at $p^2 \gtrsim I$ (fig.I)

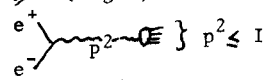
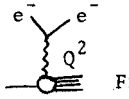


Fig.I

4) In the spacelike region if $|Q^2| \gg I$ the propagator is proportional to $\frac{I}{2|Q|}$ and the cross section decreases with Q^2, slower than usual.



The propagator is $\sim \frac{I}{2|Q|}$

Fig.2

5) The fermion propagator has the form:

$$\frac{I}{\not{p} - (I-\sqrt{I-p^2})\gamma^5 - \mu} \qquad (8)$$

† University of Sofia, Sofia, Bulgaria.

*/ We already put in (I) $\hbar=c=I$.

The γ^5 suggests that parity violation effects should be observed at very high energies and their magnitude should be of the order of $p^2\ell^2$.

Therefore, it is very tempting and natural to identify our fundamental length with Fermi constant

$$\ell \approx \ell_F = \sqrt{\frac{G}{\hbar c}} \approx 6.10^{-17} \text{ cm.} \qquad (9)$$

The introduction of fundamental length ℓ in the theory changes many of its basic relations. For example, series of qualitative predictions could be made on the basis of the new relation between the momentum transfer and interaction distances:

$$r \sim \frac{1}{x_p} , \qquad (10)$$

where

$$ch x_p = 1 + \frac{\vec{p}^2}{2} , \qquad (11)$$

$\vec{p}^2$ being the momentum transfer. If $|\vec{p}| \ll 1$, $r \sim \frac{1}{|\vec{p}|}$. But if $|\vec{p}| \gg 1$, then $r \sim \frac{1}{\ln|\vec{p}|}$. From the last formula one sees that at very high momentum transfers the role of momentum transfer is played by its logarithm

$$\sqrt{t} \to \ln \sqrt{-t} . \qquad (12)$$

In other words one may expect that all the exponent $\sqrt{-t}$ dependences of the standard theory should change in this domain to power dependences. For example:

$$\frac{d\sigma}{dt} \sim a e^{-n\sqrt{-t}} \longrightarrow \frac{a}{(\sqrt{-t})^n} . \qquad (13)$$

The exact calculation confirms this qualitative speculation[1].

The relation (10) is of principal importance, namely distances $r \lesssim \ell$ can not be practically reached (the $\ln(|\vec{p}|)$ in the dominator!). Therefore if $\ell \sim \ell_F$ /see eq.(9)/ the gravitational effects occurring at $r \ll \ell_F$ are irrelevant to particle physics.

In this short talk we sketched some of the implications of quantum field theory with fundamental length. The detailed analysis of the theory can be found in refs./1-5/

Some features of this new quantum field theory are close to the original ideas of M.A.Markov (1940, 1958)[6] concerning the possible formulation of nonlocal field theories. From the other hand, it is close to the more recent field theories on a space-time lattice[7].

In conclusion we would like to stress that reasoning from purely group-theoretical point of view we introduced in quantum field theory a new universal constant and drastically modified the interaction at very high energies (small distances). This can be done in Lorentz and translation invariant way (ref.[4]). Therefore if a fundamental length exists we shall have a completely new physics at very high energies. Reversing the argument - a possible key for understanding the very high energy phenomena is the fundamental length.

References

1. A.D.Donkov, V.G.Kadyshevsky, M.D.Mateev, R.M.Mir-Kasimov, Nonlocal Field Theories, Alushta 1976, Dubna(1976)
2. V.G.Kadyshevsky, JINR-preprint R2-5717, Dubna, 1971.
3. V.G.Kadyshevsky in the book "Problems of Theoretical Physics" dedicated to the memory of I.E.Tamm, Moscow, Nauka, 1972.
4. A.D.Donkov, V.G.Kadyshevsky, M.D.Mateev, R.M.Mir-Kasimov, JINR-preprint E2-6992, Dubna(1973) and JINR-preprint E2-7936, Dubna(1974)
5. V.G.Kadyshevsky, M.D.Mateev and R.M.Mir-Kasimov Preprint JINR E2-8892, Dubna(1975).
6. M.A.Markov, JETP, 10, 1311(1940), Nucl.Phys. 10, 140, (1958), 12, 190(1959).
7. See K.Wilson, mini-rapporteur talk at this Conference.

RECENT PROGRESS IN REGGEON FIELD THEORY

R.L.Sugar

University of California, Santa Barbara, USA

I cannot describe all of the recent work in Reggeon Field Theory (RFT) in the time allotted to me, so I will just discuss a few Topics which I have found particularly interesting. I apologize to those whose work I will have time to cover.

What Gribov did when he invented RFT[1] was to teach us how to systematically evaluate Regge cut contributions to high energy scattering amplitudes. The cuts play a crucial role in processes in which the Pomeron can be exchanged because for small momentum transfers all of the multi-Pomeron branch points are close to each other and to the Pomeron pole. It is essential to take them all into account in order to have a realistic description of diffraction scattering at very high energies.

Two years ago at the Landau conference we heard about the work of Migdal, Polyakov and Ter-Martirosyan [2] and of Abarbanel and Bronzan [3], who showed how renormalization group techniques can be used to sum the multi-Pomeron cut contributions when the Pomeron intercept is exactly equal to one. They obtained a set of scaling laws for high energy scattering amplitudes. For example, they found that the elastic scattering amplitude has the asymptotic form

$$M(s,t) \underset{s\to\infty}{\to} i s\, g_A(t) g_B(t) C_1 (\ln s)^{\eta} F\left[C_2 t (\ln s)^{z}\right] \quad (1)$$

Here η and z are critical indices which are independent of the underlying parameters in the theory such as the triple Pomeron coupling constant. Similarly F is a universal scaling function. The only dependence on the underlying parameters is in the constants C_1 and C_2, and in the couplings of the Pomeron to the external particles g_A and g_B.

The renormalization group analysis which leads to eq. (I) is valid provided the theory has an infra-red stable fixed point. In the original work on the renormalization group[2,3] the theory was studied in $D = 4-\varepsilon$ transverse dimensions, rather than in the physical number $D = 2$. It was shown that for D near 4, i.e., for small ε, the theory does have an infra-red stable fixed point. The critical indices and the scaling function can be expand in a power series in ε and one finds that [2-5]

$$\eta = \frac{\varepsilon}{12}\left[1 + .45\varepsilon + o(\varepsilon^2)\right]$$
$$z = 1 + \frac{\varepsilon}{24}\left[1 + .39\varepsilon + o(\varepsilon^2)\right]. \quad (2)$$

For $D = \varepsilon = 2$ the second order terms in the ε - expansion are of the same magnitude as the first order ones. So, although it is generally believed that the qualitative predictions of the ε - expansion are correct, one does not know what to make of the quantitative predictions.

The situation is even worse if one tries to use the ε - expansion to determine whether the theory has a fixed point in the physical number of dimensions. One can study this problem in a theory with only a bare triple Pomeron coupling constant. Then the theory will have an infra-red stable fixed point provided the Gell-Mann Low β function has a zero with a positive slope. If one computes β to first order in ε and then sets $\varepsilon = 2$, one finds that such a zero exists, but it disappears when the ε^2 term is taken into account [5]. Similarly, if one works directly in two dimensions, there is a zero in the one loop approximation to β but not in the two loop one.

The situation can be clarified by studying the theory for $D = 0$, where it is possible to compute β exactly [6]. One

finds that β does have an infrared stable zero. However, if one makes the loop expansion for β one finds the same pattern as in two dimensions. There is a zero if one stops after an odd number of loops, but not if one stops after an even number. The difficulty is that the perturbation series diverges as one might expect in a non-linear field theory. The perturbation series is an asymptotic expansion for small values of the coupling constant, but it is meaningless in the vicinity of the zero. One can use information from perturbation theory to calculate β accurately in the vicinity of the zero by making use of Pade and Pade-Borel approximants.

The same techniques appear to be applicable in two dimensions. Recently Harrington has calculated β through three loops (seventh order in perturbation theory) for $\mathcal{D} = 2$. The (1,1), (1,2) and (2,1) Pade-Borel approximants obtained from his calculation [6] are shown in Fig.1. The convergence is surprisingly rapid. I believe that this calculation constitutes impressive evidence for the validity of the renormalization group approach to RFT. One can also use the information from the three loop calculation to determine the critical indices. One finds [6]

$$\eta \simeq .22, \quad Z \simeq 1.13. \tag{3}$$

If one believes that scaling laws such as eq. (1) hold, then the next problem is to determine the energy domain in which they are applicable. For a theory with only a bare triple Pomeron coupling constant the energy scale is set by the parameter $\lambda = (\Gamma_0^2/\alpha_0')\ln s$, where Γ_0 is the bare triple Pomeron coupling constant and α_0' is the bare slope parameter. For $\lambda \ll 1$ one can make a perturbation expansion in Γ_0 and for $\lambda \gg 1$ one must sum the perturbation series and obtain the scaling laws. It is difficult to make a precise estimate of the energy at which multi-Pomeron effects will start to become important. Because of the small size of Γ_0, it would appear that one should use perturbation theory at present accelerator energies.

If we are not presently in the asymptotic domain, then we cannot be certain that the intercept of the physical or renormalized Pomeron, $\alpha(0)$ is exactly equal to one. I believe that it is important to consider all possible predictions of the theory. $\alpha(0)=1$ only when the bare intercept, α_0, takes on a certain critical value, α_{0c}. For $\alpha_0 < \alpha_{0c}$, $\alpha(0) < 1$. The data will certainly not allow $\alpha(0)$ to be very much below one, which means that the cuts will still be near the pole for small momentum transfers. They must still be taken into account at all but the highest energies. Under these circumstances it is again possible to use renormalization group to sum the cut contributions. One finds, for example, that the elastic scattering amplitude satisfies a generalized scaling law [8]

$$M(s,t) \underset{\substack{s\to\infty \\ \alpha_0 < \alpha_{0c}}}{\to} i s\, g_A(t)\, g_B(t)\, C_1 (\alpha_{0c} - \alpha_0)^{\frac{1+\eta}{1-K}} \times F'\left[C_2 \ln s\,(\alpha_{0c}-\alpha_0)^{\frac{1}{1-K}},\ C_3 t (\alpha_{0c}-\alpha_0)^{\frac{-Z}{1-K}}\right], \tag{4}$$

η and Z are the same indices encountered in eq. (I). K is a new critical index and F' a generalized scaling function. In the limit $\alpha_0 \to \alpha_{0c}$ eq. (4) goes over smoothly into eq. (I). There are now two dimensionless parameters which set the energy scale: λ and $\mu = [1-\alpha(0)]\ln s$. Again for $\lambda < 1$ one needed take into account only the first few terms in the perturbation series. For $\lambda > 1$ and $\mu < 1$ all the cut contributions must be taken into account and eq. (4) is applicable. In this intermediate energy region it will be difficult to distinguish the subcritical Pomeron from the critical one described by eq. (I). For $\mu > 1$ eq. (4) still holds, but the

pole dominates the cuts and the total cross section decreases like $s^{\alpha(0)-1}$.

Up to this point there is a close parallel between RFT and the problem of second order phase transitions in statistical mechanics. The bare interoept plays a role similar to that of the temperature in statistical mechanics. The analogy can be made more complete by studying correlations among particle produced in the central region [9]. For $\alpha_0 = \alpha_{0c}$ which corresponds to $T = T_c$ in statistical mechanics, one finds that there are long range correlations in rapidity while for $\alpha_0 < \alpha_{0c}$ $(T > T_c)$ there are only short range correlations. The correlation length is $[1-\alpha(0)]^{-1}$. However, for $\mu < 1$ the correlation length is longer than the available rapidity and the results for the suboritical Pomeron are similar to those for the critical one.

Let me now turn to the case of $\alpha_0 > \alpha_{0c}$. It is clear from eq. (4) that the scattering amplitude has a singularity at $\alpha_0 = \alpha_{0c}$. We must ask whether it is possible to continue past this singularity and still obtain a sensible theory. The Green's functions in statistical mechanics also have singularities at $T = T_c$. They arise because the ground state of the system is degenerated for $T < T_c$. One can remove the singularity by introducing an external field which breaks the degeneracy and then smoothly continue past the critical point. It is at this point that the analogy between RFT and statistical mechanics breaks down. Recent work by Amati, Giafaloni, Marshesini, Le Bellac and Parisi [10,11] has shown that the nature of the phase transition in RFT is completely diffirent from the one found in the Ising model. Amati will discuss this work in detail. Let me just state that their final result corresponds to the scattering from a grey disc with a radius which grows like $\ln s$. Amati et al. oonsider a theory in which there is only a bare triple Pomeron coupling. Universality arguments strongly suggest that this is sufficient for studying the high energy, small momentum transfer behaviour when α_0 is at or near its critical value. On the other hand in session AI Ter-Martirosyan discussed the problem of $\alpha_0 > \alpha_{0c}$ in a theory with all possible multi-Pomeron couplings [12]. He finds a black disc with a radius which also grows like $\ln s$. The connection between this work and that of Amati et al. is unclear to me at the present time.

Let me conolude by summarizing the present status of the theory of the Pomeron in RFT. For $\alpha_0 \leq \alpha_{0c}$ the theory is in very good shape. It appears to satisfy both s and t- channel unitarity and to avoid all of the decreases which plagued the simple pole model of the Pomeron. For $\alpha_0 > \alpha_{0c}$ the situation is less clear, partly because the work is more recent. The challenging problem is whether the expanding disc solutions satisfy the multi-particle t-channel unitarity [13].

References

1. V.N.Gribov. Zh.ETP , 53, 654 (1967).
2. A.A.Migdal, A.M.Polyakov and K.A.Ter-Martirosyan. Phys.Lett., 49B, 239 (1974); Zh ETF , 67, 2009 (1974).
3. H.D.I.Abarbanel and J.B.Bronzan. Phys.Lett., 48B, 345 (1974); Phys.Rev., D9, 2391 (1974).
4. M.Baker. Phys.Lett., 51B, 156 (1974).
5. J.B.Bronzan and J.W.Dash. Phys.Rev., D10, 4208 (1974) and D12, 1850 (1975).
6. J.B.Bronzan, J.A.Shapiro and R.L.Sugar, U.C.Santa Barbara preprint TH-4 (1976).
7. S.J.Harrington. University of Washington preprint RLO-1388 -709.
8. H.D.Abarbanel, J.B.Bronzan, A.Schwimmer and R.L.Sugar. Rutgers University preprint.
9. P.Suranyi, Phys.Rev., D12, 2124 (1975); J.L.Cardy and P.Suranyi. U.C.Santa Barbara preprint (1975); M.Giafaloni, G.Marchesini and G.Veneziano. Nucl.Phys., B74, 472 and 493 (1975).
10. D.Amati, M.Le Bellac, G.Marchesini and M.Giafaloni. CERN preprint TH 2157 (1976).

11. D.Amati, G.Marchesini, M.Giafaloni and G.Parisi. CERN preprint TH 2185 (1976).
12. M.S.Dubovskov and K.A.Ter-Martirosyan. ITEP preprint-37 (1976).
13. There has some encouraging recent work on this problem by M.S.Dubovskov (K.A.Ter-Martirosyan - private communication).

THE POMERON AS A NONRELATIVISTIC GOLDSTONE PARTICLE

I.T.Dyatlov
Leningrad Nuclear Physics Institute, USSR

Usually to fit the experimental data the vacuum t-channel is characterized in the compex j-plane by the two poles different disposed at $t=0$: $P(\omega = j-1=0)$ and $P'(\omega=-\Delta<0)$. Only the contribution of P (and its cuts) is important for high energies S while the P'-contribution decreases with energy as $s^{-\Delta}$. If the Pomeron P is located exactly at $\omega=0$ for $t=0$ it becomes an analogue of the nonrelativistic massless excitation. The spectrum of two states in this case is similar to that one coming from the spontaneous symmetry breaking of the simplest nonrelativistic theory with two fields ($O(2)$ symmetrical theory). This situation suggests to suppose that the P and P' speotrum is also originated by the symmetry breaking for the system of vacuum reggeons. The Pomeron appears then as the Goldstone particle.

We can obtain all possible forms of the Lagrangian for such a system [1]. The procedure can be described as follows.

For the Lagrangian of this reggeon system before the breaking we can use a very general O(2)-invariant form with arbitrary number of reggeon operator $\psi_i(\zeta,\vec{\rho}), \psi_i^+(\zeta,\vec{\rho})$ and their derivatives ($i=1$ for P, $i=2$ for P', $\zeta=\ln\frac{s}{s_0}$, $\vec{\rho}$ is an impact vector). Nonhermitian character of reggeon interactions unambiguously chooses the operator with a finite vacuum expectation value

$$\psi_i^+ - \psi_i \to \psi_i^+ - \psi_i + \varphi\,\delta_{i1}. \qquad (1)$$

After the excursion of φ the Lagrangian is required to have the nonrelativistic form without any terms allowing annihilation and creation of reggeons in vacuum $\psi_i, \psi_i^+, \psi_i^{+2}$ ... This requirement provides the system of

equations selecting possible forms for the Lagrangian. Their main properties are

a) they contain only such interactions which leave P massless and stable at $t=0$: all vertices of the P- decay are proportional to the P momentum $\vec{K}$ ($\vec{K} \equiv \vec{K}_\perp$);

b) these forms contain the set of conditions on the different coupling constants (see /2/) which serve to cancel the infrared divergences existing in connection with the massless character of P .

The simplest Lagrangian obtained by this procedure is

$$L = -\frac{1}{2}\left(\psi_i^+ \frac{\partial \psi_i}{\partial \zeta} - \psi_i \frac{\partial \psi_i^+}{\partial \zeta}\right) - \alpha'_P \nabla \psi_i^+ \nabla \psi_i - \Delta \psi_1^+ \psi_1 + \sqrt{\lambda\Delta}\left(\psi_1^+ \psi_i^2 - \psi_1 \psi_i^{+2}\right) + \lambda \psi_i^2 \psi_K^2 . \quad (2)$$

More complicated models enable to describe P and P' with different slopes α'_P and $\alpha'_{P'}$ and so on.

The use of P' in the asymptotic theory (simultaneously with P) can give, of course, only the model description of some qualitative features of the scheme. But it is important that P' provides the theory with the natural energy scale which shows where the real asymptotic begins to work:

$$\Delta \zeta > 1. \quad (3)$$

As P' is located on the Pomeron cut it is really an unstable state decaying into 2P, 3P ... Its properties can be represented by the P' propagator. The approximate equation for it in the simplest case (2) is of the form ($\lambda > 0$)

$$G_{P'}^{(-1)} = \omega + \alpha'_P K^2 + \frac{\Delta}{1 - \gamma(\omega, K^2)};$$

$$\gamma(\omega, K^2) = \frac{\lambda}{4\pi} \ln \frac{2\alpha'_P L}{\omega + \frac{1}{2}\alpha'_P K^2} . \quad (4)$$

The contribution of (4) to σ_{tot} contains not only the positive term decreasing with energy as $s^{-\tilde{\Delta}}$ [x] ($\tilde{\Delta}$ can be different from Δ) but slowly decreasing $\left(\sim \frac{1}{\zeta}\right)$ negative contribution from the cut. This cut contribution to σ_{tot} is proportional to the same experimentally large coefficient $g^2_{P'}$ as the term $s^{-\tilde{\Delta}}$. Moreover the P-loops which form the cuts in the P' - propagator can be considered as coming not immediately from the hadron vertices but after several steps in rapidity (P' - line). There are some experimental evidences that in this case the cut-off momentum L for the reggeon loop is large $(\alpha'_P L \gtrsim 1)$ (all references are in /2/). Thus the P - contribution contains the negative terms of the type

$$-\frac{g^2_{P'}}{\Delta} \frac{\lambda}{\zeta + 1/\alpha'_P L} \quad (5)$$

which is large ($g^2_{P'}$ is large) and strongly depends on ζ $(\alpha'_P L \gtrsim 1)$. This effect could explain, in principle, in more complicated version of the model (2) (even for the constant contribution of the Pomeron) large and fast growth of σ_{tot} at modern energies.

The most interesting effect appears in P' - propagator (4) at $t = -K^2 < 0$. The pole in $G_{P'}$ comes here out of the cut. It is located near the cut at the point

$$x_0 = \omega_0 + \frac{1}{2}\alpha'_P K^2 \approx 2\alpha'_P L \exp\left\{-\frac{\eta}{K^2} - \frac{1}{\zeta}\right\}; \quad (6)$$

$$\eta = \frac{2\Delta}{\lambda \alpha'_P} .$$

Only in the Goldstone P theory we can choose the parameters so that the pole appears in $G_{P'}$ only for $K^2 \neq 0$ and never comes to the region $\omega > 0$.

The contribution of this pole to the scattering amplitude is

$$\sim -\lambda \frac{g^2_{P'}(t)}{\Delta}\left(\frac{\eta}{K^2}\right) \exp\left\{-\frac{\eta}{K^2} - \frac{1}{2}\alpha'_P K^2 \zeta + x_0 \zeta\right\} \quad (7)$$

This contribution has the maximum and the attractive possibility is that the pole (6) plays an important role (together with P and the cut in (4)) in forming the minimum

x) In the simple model (2) these terms are very different from the experimental picture of P.

and the second maximum in hadron elastic cross--sections (pp-elastic scattering). The dependence $exp\{-n/k^2\}$ helps this idea very much. Reasonable choice of model parameters easily allows one to reconcile the qualitative behaviour near the maximum-minimum positions. Of course, the strict quantitative description for such large t ($t \sim$ 1.5-3 GeV^2) strongly depends on the model but the existence of the "Pomeron bound state" is very probable property of the considered scheme.

Papers /1/ and /2/ contain all necessary references.

References

1. I.T.Dyatlov. JETP, 69, 1127 (1975).
2. I.T.Dyatlov. JETP, 70, 374 (1976).

THEORY OF THE POMERON WITH INTERCEPT LARGER THAN 1

D.Amati
CERN, Geneve, Switzerland

What I will tell you is contained in two recent CERN preprints Ref. Th 2152 and 2185. The physicists involved are M.Giafaloni, M.Le Bellac, G.Marchesini, G.Parisi and myself.

I will not disouss the motivation for this research and, neither, the Gribov lagrangian that we adopt for the self interacting pomeron. This is given by

$$\mathcal{L} = \bar{\psi}\partial_y\psi + \alpha'\vec{\nabla}\bar{\psi}\cdot\vec{\nabla}\psi + \mu\bar{\psi}\psi - i\lambda(\bar{\psi}^2\psi + \bar{\psi}\psi^2), \quad (1)$$

where $\mu = \alpha(0) - 1$ and $\psi(y, \vec{b})$ is defined in a space with an (imaginary) time y and a two dimensional space $\vec{b}$. For $\mu < 0$ the perturbative series is meaningful and gives rise to the Gribov calculus. The pomeron propagator is given by

$$D_0(y, \vec{b}) \propto exp\left(\mu y - \frac{\vec{b}^2}{4\alpha' y}\right). \quad (2)$$

For $\mu > 0$ the perturbative series loses its meaning in the sence that every order dominates over the preceding. This is however not true outside of the disc defined by:

$$b = \sqrt{4\mu\alpha'}\, y. \quad (3)$$

Indeed if $b > \sqrt{4\mu\alpha'}\, y$, we see from (2) that D_0 does not explode and one can cheok that higher iterations are even smaller. In other words, for all μ there is a region in $\vec{b}$ space in which-at fixed y - the perturbative expansion of $\mathcal{L}$ as given by (1) is meaningful.

But if we want to understand asymptotic properties of the theory ($y \to \infty$) we will be forced to find nonperturbative solution of it if $\mu > 0$.

We will use a hamiltonian method. The time evolution of the theory is given by e^{-yH} and, therefore, the asymptotic properties will

be controlled by the lower lying eigenstates. To determine them together with their eigenvalues, will be our task.

Let us first remark, that due to the i in front of the trilinear term in (1), H will not be hermitean. However it exists a unitary operator L that transforms H into H^+ i.e.

$$LHL^{-1} = H^+, \quad L\Psi L^{-1} = -\bar{\Psi}^+ . \tag{4}$$

We will introduce a lattice in $\vec{b}$ space (inter-lattice distance a). Then

$$H = \frac{i\lambda}{a}\sum_j \bar{\Psi}_j\left(\bar{\Psi}_j + \Psi_i - \frac{\mu}{i\lambda}\right)\Psi_j - \frac{\alpha'}{a^2}\sum_{(j,\ell)}\bar{\Psi}_j\Psi_\ell , \tag{5}$$

where (j,ℓ) means near neighbours. Our procedure is to first solve the single site dynamics and, then, to introduce the intersite coupling. The single site dynamics was solved in earlier papers (V.Alessandrini, D.Amati and R.Jengo. Nucl.Phys. B108,425 (1976); R.Jengo. Nucl.Phys. B108, 447 (1976); J.Bronsan, J.Shapiro and R.Sugar. Santa Barbara preprint (1976)). The outcoming spectrum has the structure of Fig.1.

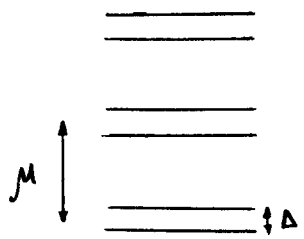


Fig.1

where

$$\Delta \propto e^{\frac{-\mu^2}{4\lambda^2}} \tag{6}$$

If we call χ_0 and χ_1 the eigenfunctions of the two lowest eigenstates we have that the matrix elements of Ψ and $\bar{\Psi}$ in this basis are given by

$$\langle\bar{\Psi}\rangle = \frac{\mu}{i\lambda}\begin{pmatrix} 0 & -1 \\ 0 & 1 \end{pmatrix}, \quad \langle\Psi\rangle = \frac{\mu}{i\lambda}\begin{pmatrix} 0 & 0 \\ 1 & 1 \end{pmatrix}. \tag{7}$$

The lowest lying state is the single site vacuum i.e. [x]

$$\Psi_i \chi_0^i = \bar{\chi}^i \bar{\Psi}_i = 0.$$

We will now introduce the interlattice interaction by keeping at each site only the two lowest lying levels. This approximation is expected to correctly represent the lowest lying levels of the whole system and, in particular, the phase transition. Introducing the representations (7) for the fields we can write the hamiltonian with a spin formalism as:

$$H = \Delta\sum_i (1 - \hat{\sigma}_3^i) + \sum_{(i,j)} J_{ij}\,\frac{1+\vec{\sigma}^i\vec{n}_Q}{2} \cdot \tag{8}$$

$$\cdot\,\frac{1+\vec{\sigma}^j\vec{n}_P}{2}$$

where

$$n_{P,Q} = (\pm 1, -i, -1), \quad J = \sum_{(i,j)} J_{ij} = \alpha'\frac{\mu^2}{\lambda^2} . \tag{9}$$

The spectrum of H looks as fig.2

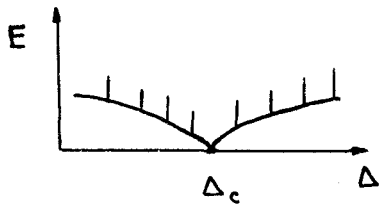


Fig.2

For $\Delta > \Delta_c$ we have a single vacuum $\Phi_0 = \prod_i \chi_0$ and a continuum with a gap that goes to zero as $\Delta \to \Delta_c$. For $\Delta < \Delta_c$ we find two degenerate ground states. One is still Φ_0 , the other Ψ_0 is a negative metric one which is a product of local states only if $\Delta = 0$.

x) The definition of $\bar{\chi}_0$ is $\chi_0^+ L$ where L is the metric operator that appears in eq. (4).

Ψ_0 and Φ_0 are connected by field operator, i.e.

$$(\bar{\Psi}_0\,\bar{\Psi}\,\Phi) = (\bar{\Phi}_0\,\Psi\,\Psi_0) = \frac{\mu}{i\lambda}\,\delta, \qquad (10)$$

where δ is a number that plays the role of the order parameter. The S-matrix can be easily calculated. If the external particles are considered as pomeron sources, located at y_1 and y_2 respectively ($Y = y_2 - y_1$ is the total rapidity) and with structures given by $f(\vec{\ell})$, $g(\vec{B}-\vec{\ell})$ respectively ($\vec{B}$ - total impact parameter), then

$$S = \left(\bar{\Phi}_0\, e^{-i\alpha\sum f_j \Psi_j}\; e^{-yH}\; e^{-i\alpha\sum g_i \bar{\Psi}_i}\; \Phi_0\right) = \qquad (11)$$

$$\underset{\substack{y\to\infty \\ B\ \text{fixed}}}{=} 1 - \left(1 - \exp\left(-\frac{\delta\mu}{\lambda}\int f(\vec{\ell})\,d\vec{\ell}\right)\right)\times\left(1 - \exp\left(-\frac{\delta\mu}{\lambda}\int g(\vec{B}-\vec{\ell})\,d\vec{\ell}\right) + o\left(e^{-\omega t}\right)\right)$$

where ω is the collective excitation frequency (i.e., the continuum of fig.2). Eq. (11) shows an asymptotic scattering amplitude described in terms of a $\vec{B}$ independent positive and factorized opacity. The structure of the spectrum (fig.2) is similar to that of the Ising model - related to a φ^4 - theory - given by eq. (8) but with $n_{\rho} = (\pm 1, 0, 0)$. However the structure of the two lower lying states appearing for $\Delta < \Delta_c$ is very different. Indeed, in the Ising case none of them is the original vacuum; in both of them the fields would have non vanishing expectation values and they would not be connected to each other by field operators (zero non diagonal field matrix element). This last property is the one that determines the spontaneous symmetry breaking of the φ^4 theory ($\varphi \to -\varphi$ symmetry) in the sense that the two vacua, being completely disconnected, define two orthogonal Hilbert spaces any one of them being equally good. In our case, there is only one Hilbert space. The vacuum does not change structure at Δ_c, what happens is that for $\Delta < \Delta_c$ a zero gap state appears. To understand the reason of the vacuum dynamical instability, is better to start from a single dimensional B space and with $\Delta = 0$, where

$$\Psi_0 = \prod_i \chi^i \qquad (12)$$

If we construct a (box) state made up of χ_0^i everywhere but in an interval in which we have χ_1^i (fig.3), i.e., $\prod_{\substack{i<\ell \\ i>m}} \chi_0^i \prod_{\ell\le i\le m} \chi_1^i$

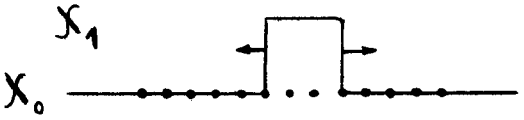


Fig.3

we find that it evolves in time by expanding with a finite velocity. We therefore understand the vacuum instability. If a local field $\bar{\Psi}_i(0)$ operator $\bar{\Psi}_i(0)$ is applied to the vacuum Φ_0, it gives rise at $y = 0$ the state χ_ℓ^i which gives a single site box state which expands therefore with time (y). At infinite y, χ_1 will be excited at all sites and Φ_0 would have gone into Ψ_0. The zero gap state Ψ_0 lies over the vacuum Φ_0 and depletes it dynamically.

The introduction of Δ does not change the picture (as far as $\Delta < \Delta_c$). It is easy to get from these results that $S = 1$ outside the box (also in two-dimensional B space) this being a basic requirement of any reggeon theory. On the other hand, eq. (11) restricted to the also gives rise to total cross section increasing as $(\log s)^2$.

ВЛИЯЕТ ЛИ u-КАНАЛ В t-ПЛОСКОСТИ НА ПОВЕДЕНИЕ ДИФФЕРЕНЦИАЛЬНОГО СЕЧЕНИЯ РАССЕЯНИЯ ВПЕРЕД ПРИ БОЛЬШИХ ЭНЕРГИЯХ?

А.А.Логунов, М.А.Мествиришвили, Г.Л.Рчеулишвили, А.П.Самохин

ИФВЭ, Серпухов

Хорошо известно, что между высокоэнергетическим поведением амплитуды рассеяния и ее особенностями в t-плоскости существует глубокая взаимосвязь.

В данной работе на основе условия унитарности и д.с. по переданному импульсу исследуется вопрос о влиянии t и u-канальных особенностей на поведение амплитуды рассеяния в S-канале в пределе больших энергий. Полученный результат в рамках перечисленных ниже предположений носит строгий характер и не зависит от гипотез частного характера.

Предположение I. Амплитуда упругого рассеяния для физических s ($s \geqslant s_{порог}$) по переменной t или, что удобнее для наших целей, по переменной

$$z = \cos\theta = 1 + \frac{t}{2k^2}$$

допускает д.с. вида

$$F(s,z) = \tilde{G}(s,z) + \tilde{H}(s,z) + \sum_{m=0}^{n-1} \beta_m(s) z^m, \qquad (I)$$

где

$$\tilde{G}(s,z) = \frac{z^n}{\pi} \int_{z_0(s)}^{\infty} \frac{\Delta F(s,z')\, dz'}{(z')^n (z'-z)}, \qquad (2)$$

$$\tilde{H}(s,z) = \frac{z^n}{\pi} \int_{-\infty}^{-z_1(s)} \frac{\Delta F(s,z')\, dz'}{(z')^n (z'-z)}. \qquad (3)$$

Предположение 2. Амплитуда рассеяния $F(s,z)$ в области аналитичности по z при больших физических s удовлетворяет условию

$$|F(s,z)| \leqslant s^N, \qquad (4)$$

где N - некоторое конечное положительное число.

Ниже, для простоты, будет рассматриваться упругое рассеяние π-мезона на скалярном нуклоне, и поэтому входящие в (2) и (3) величины z_0 и z_1 имеют вид:

$z_0 = 1 + \frac{2m_\pi^2}{k^2}$ - определяется t-канальным порогом, $z_1 = \frac{1}{k^2}\left[\sqrt{(k^2+M^2)(k^2+m_\pi^2)} + M\cdot m_\pi\right]$ -определяется u-канальным порогом. Здесь k - величина импульса частиц в системе ц.м., которая связана с s соотношением:

$$k = |\vec{k}| = \frac{1}{2\sqrt{s}}\sqrt{\left[s-(M+m_\pi)^2\right]\left[s-(M-m_\pi)^2\right]} \underset{s\to\infty}{\simeq} \frac{\sqrt{s}}{2}$$

Д.с. такого вида в рамках квантовой теории поля не доказано, но после того, как Мандельстамом было предложено двойное д.с., оно широко используется в теории элементарных частиц.

Очевидно, что функция $\tilde{G}(s,z)$ представляет собой вклад t-канала в амплитуду рассеяния $F(s,z)$ и аналитична во всей z-плоскости с разрезом $[z_0,\infty)$, а функция $\tilde{H}(s,z)$ является вкладом u-канала в амплитуду $F(s,z)$ и аналитична во всей z-плоскости с разрезом $(-\infty,-z_1]$.

Аналитические свойства функций $F(s,z)$, $\tilde{G}(s,z)$ и $\tilde{H}(s,z)$ по переменной z позволяют воспользоваться для них рядами по полиномам Лежандра:

$$F(s,z) = \frac{8\pi\sqrt{s}}{k}\sum_{l=0}^{\infty}(2l+1) f_l(s) P_l(z), \qquad (5)$$

$$\tilde{G}(s,z) = \frac{8\pi\sqrt{s}}{k}\sum_{l=0}^{\infty}(2l+1)\tilde{g}_l(s) P_l(z), \qquad (6)$$

$$\tilde{H}(s,z) = \frac{8\pi\sqrt{s}}{k}\sum_{l=0}^{\infty}(2l+1)\tilde{h}_l(s)(-1)^l P_l(z). \qquad (7)$$

В силу такой нормировки $F(s,z)$ парциальные амплитуды $f_l(s)$ удовлетворяют унитарному ограничению вида:

$$|f_l(s)| \leqslant 1. \qquad (8)$$

Из (I) и (5-7) следует, что если $l \geqslant n$, то

$$f_l(s) = \tilde{g}_l(s) + (-1)^l \tilde{h}_l(s). \qquad (9)$$

Из аналитических свойств $\tilde{G}(s,z)$ и $\tilde{H}(s,z)$ можно легко получить, что коэффициенты разложения $\tilde{g}_l(s)$ и $\tilde{h}_l(s)$ при $|l|\to\infty$ удовлетворяют оценкам:

$$|\tilde{g}_\ell(s)| \leq \text{const}\frac{s^{N+\frac{1}{4}}}{\sqrt{|\ell|}}\exp\left\{-\left(\mathrm{Re}\,\ell+\tfrac{1}{2}\right)\ln\left[x_0+\sqrt{x_0^2-1}\right]\right\},$$

$$|\tilde{h}_\ell(s)| \leq \text{const}\frac{s^{N+\frac{1}{4}}}{\sqrt{|\ell|}}\exp\left\{-\left(\mathrm{Re}\,\ell+\tfrac{1}{2}\right)\ln\left[x_1+\sqrt{x_1^2-1}\right]\right\}.$$

Используя стандартные аналитические свойства по ℓ для функций

$$f^{\pm}(s,\ell)=\tilde{g}_\ell(s) \pm \tilde{h}_\ell(s)$$

и применяя теорему, доказанную в работе Киноситы, Лоеффеля, Мартена (Phys. Rev. , I35, I464 (I964)), можно показать, что в физических точках по ℓ для $\tilde{g}_\ell(s)$ и $\tilde{h}_\ell(s)$ справедлива оценка

$$|\tilde{g}_\ell(s)|, |\tilde{h}_\ell(s)| < d, \qquad (I0)$$

если только

$$\ell \geqslant \ell_0(s)=n+[\text{const}\cdot\ln(\tfrac{s}{s_0})]. \qquad (II)$$

В (I0) d - некоторая не зависящая от s постоянная.

Неравенства (I0) мы будем называть "унитарными" ограничениями для коэффициентов $\tilde{g}_\ell(s)$ и $\tilde{h}_\ell(s)$.

После того, как установлено "унитарное" ограничение (I0), удобно в амплитуде рассеяния произвести некоторую перегруппировку членов и представить ее в виде: $F(s,z)=G(s,z)+H(s,z)+R(s,z)$,

где $$G(s,z)=\frac{8\pi\sqrt{s}}{\kappa}\sum_{\ell=\ell_0+1}^{\infty}(2\ell+1)\tilde{g}_\ell(s)P_\ell(z), \qquad (I2)$$

$$H(s,z)=\frac{8\pi\sqrt{s}}{\kappa}\sum_{\ell=\ell_0+1}(2\ell+1)\tilde{h}_\ell(s)(-1)^\ell P_\ell(z), \qquad (I3)$$

$$R(s,z)=\frac{8\pi\sqrt{s}}{\kappa}\sum_{\ell=0}^{\ell_0}(2\ell+1)f_\ell(s)P_\ell(z). \qquad (I4)$$

Следует отметить, что $G(s,z)$ и $H(s,z)$ от $\tilde{G}(s,z)$ и $\tilde{H}(s,z)$, соответственно, отличаются полиномами по z, и поэтому они на конечном расстоянии в z -плоскости имеют одинаковую аналитическую структуру.

Так как для наших целей достаточно ограничиться конечной областью по z, то оценка вкладов функций G, H и R даст ответ о влиянии ближайших особенностей t и u - каналов на амплитуду рассеяния при $s\to\infty$.

Обозначим через E_δ эллипс с фокусами в точках $\pm I$ и большой полуосью $\delta>1$, где δ - фиксированное число.

Ту область, которая получается из E_δ после выбрасывания сегмента $[-\delta,-x_1]$, обозначим через E_δ^-, а область, которая получается из E_δ выбрасыванием сегмента $[x_0,\delta]$, через E_δ^+.

Можно показать (доказательство мы опускаем), что имеют место оценки:

$$|G(s,z)|_{z\in E_\delta^+} \leqslant A(\delta)\,s^{N_1(\delta)}, \qquad (I5)$$

$$|H(s,z)|_{z\in E_\delta^-} \leqslant B(\delta)\,s^{N_2(\delta)}, \qquad (I6)$$

где $A(\delta)$, $B(\delta)$, $N_1(\delta)$, $N_2(\delta)$ - некоторые конечные постоянные, не зависящие от энергии.

Перейдем теперь к оценкам функций G, H и R в физической области.

В силу условия унитарности и ограничения $|P_\ell(z)|\leqslant 1$ из (I4) непосредственно следует, что

$$|R(s,\cos\theta)| \leqslant \frac{8\pi\sqrt{s}}{\kappa}\sum_{\ell=0}^{\ell_0}(2\ell+1)=\frac{8\pi\sqrt{s}}{\kappa}(\ell_0+1)^2.$$

Учитывая (II), находим:

$$|R(s,\cos\theta)| \underset{s\to\infty}{\leqslant} \text{const}\,\ln^2\left(\frac{s}{s_0}\right). \qquad (I7)$$

Для того, чтобы оценить $|H(s,\cos\theta)|$, мы воспользуемся методом, предложенным в работах В.В.Ежелы, А.А.Логунова и др. (ТМФ 6, 42 (I97I); 9, 3, I53 (I97I); I5, I53 (I973)).

Введем ассоциированную по Борелю к $H(s,z)$ функцию вида: $$\Psi(s,\cos\theta,y)=\frac{8\pi\sqrt{s}}{\kappa}\sum_{\ell=\ell_0+1}^{\infty}(2\ell+1)(-1)^\ell\tilde{h}_\ell(s)P_\ell(\cos\theta)y^\ell. \qquad (I8)$$

Из (I8) очевидно, что

$$\Psi(s,\cos\theta,1)=H(s,\cos\theta). \qquad (I9)$$

Можно доказать, что если $H(s,z)$ аналитична по z в области E_δ^-, то функция $\Psi(s,\cos\theta,y)$ будет аналитической по y в области, изображенной на рис.I

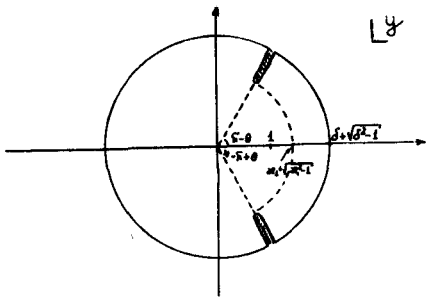


Рис.I.

и представляющей собой круг радиуса $\delta+\sqrt{\delta^2-1}$ с разрезами вдоль лучей (см. рис.I). Положение разрезов зависит от угла рассеяния θ .

Кроме того, может быть доказано, что если $H(s,z)$ удовлетворяет оценке (I6), то $\psi(s,\cos\theta,y)$ также полиномиально ограничена по s в области, указанной на рис.I.

Сделаем следующее построение (рис.2).

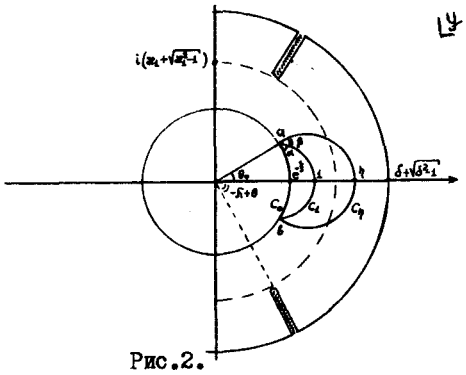


Рис.2.

Проведем круг радиуса $e^{-\xi(s)}$ $(\xi>0)$ с центром в начале. Дугу $a\,b$ этой окружности обозначим через C_0 . Через точки a и b , полярные углы которых есть $\pi-\theta_0$ и $-\pi+\theta_0$, проведем еще следующие дуги окружностей: дугу C_1 , которая проходит через точку $y=1$ и дугу C_η , которая ортогональна к дуге $a\,b$. Обозначим через α угол между дугами C_0 и C_1 , а через β – угол между дугами C_1 и C_η . Очевидно, $\alpha+\beta=\pi/2$ по построению. Область между дугами C_0 и C_η обозначим через B. Заметим, что если $\theta_0>\theta$, то область B полностью находится в области аналитичности функции $\psi(s,\cos\theta,y)$.

Применяя теорему о двух постоянных, можно написать

$$|\psi(s,\cos\theta,1)|\le\Big[\max_{y\in C_0}|\psi(s,\cos\theta,y)|\Big]^{\omega}\Big[\max_{y\in C_\eta}|\psi(s,\cos\theta,y)|\Big]^{1-\omega}. \tag{20}$$

Здесь ω является гармонической мерой области B и равна

$$\omega=\frac{2}{\pi}\beta. \tag{21}$$

На окружности $y\in C_0$ легко найти $\max_{y\in C_0}|\psi|$, если учесть в (I8) "унитарное" ограничение (I0) на коэффициенты $h_\ell(s)$ и неравенство $|P_\ell(\cos\theta)|\le 1$:

$$\max_{y\in C_0}|\psi(s,\cos\theta,y)|\le\frac{8\pi\sqrt{s}}{\kappa}\cdot\frac{d}{th^2(\xi/2)}. \tag{22}$$

Что касается $\max_{y\in C_\eta}|\psi(s,\cos\theta,y)|$, то мы можем использовать полиномиальную ограниченность ψ по s , и из (20) найдем $|H(s,\cos\theta)|=$

$$=|\psi(s,\cos\theta,1)|\le\left(\frac{8\pi\sqrt{s}}{\kappa}\frac{d}{th^2(\xi/2)}\right)\left(\frac{s}{s_0}\right)^{\tilde N(1-\omega)} \tag{23}$$

Из рис.2 видно, что в нашем распоряжении остается параметр $e^{-\xi(s)}$, т.е. радиус дуги C_0 . Если с ростом s, $e^{-\xi(s)}\to 1$, то $\alpha\to 0$ и $\beta\to\pi/2$, поэтому $\omega\to 1$ и в (23) множитель $s^{\tilde N(1-\omega)}$ становится не существенным. Чтобы подавить $s^{\tilde N(1-\omega)}$, достаточно выбрать $\omega\sim 1-1/\ell n(s/s_0)$. Параметр ξ при этом будет определяться из равенства

$$th\left(\frac{\xi}{2}\right)\simeq\frac{const}{\ell n(s/s_0)}.$$

Тогда окончательно находим

$$|H(s,\cos\theta)|=|\psi(s,\cos\theta,1)|_{\theta_0>\theta}\le \tag{24}$$

$$\le const\;\ell n^2(s/s_0).$$

Рассмотрим теперь поведение $\frac{d\sigma}{dt}|_{t=0}$ –

$$\frac{d\sigma}{dt}\Big|_{t=0}=\frac{1}{64\pi s k^2}|F|^2_{\theta=0}=\frac{1}{64\pi s k^2}|G+H+R|^2.$$

Так как экспериментальные данные показывают, что $\frac{d\sigma}{dt}|_{t=0}\ge const\neq 0$, а для R и H справедливы оценки (I7) и (24), видим, что основной вклад при высоких энергиях в $\frac{d\sigma}{dt}|_{t=0}$ вносит только функция $G(s,\cos\theta)$, определяемая особенностями t-канала.

ANALYTICAL FORM OF THE FROISSART BOUND AT FINITE ENERGIES

Yu.S.Vernov
M.N.Mnatsakanova [x]

INR, Moscow, USSR

The work of Indurain [1] initiated investigations of the Froissart bound of finite energies. This study was developed in papers of Common [2], Stewen [3], Roy [4], Blankenbeckler and Sawit [5] and others. However, the most stringent bounds have been obtained only in the numerical form.

It is known [4] that the scattering length a_2 in the t-channel is connected with the amplitude of the elastic scattering in the s-channel in the following form:

$$a_2 = \frac{4}{15\pi}\int_1^\infty \frac{A(s',1)}{s'^3}\,ds'; \quad 4m_\pi^2 = 1. \qquad (1)$$

Here $A(s',1) \equiv \mathrm{Im}\,F(s',1)$, $F(s',1)$ is the amplitude of the elastic scattering, s and t are usual invariant variables. We carry out the calculations for the specific case of the $\pi^\circ\pi^\circ$ scattering. We introduce the following isospin combinations $a_2 = \frac{1}{3}a_2^{(0)} + \frac{2}{3}a_2^{(2)}$; $A(s',1) = \frac{1}{3}A^{(0)}(s',1) + \frac{2}{3}A^{(2)}(s',1)$. From the inequality $A(s',1) \geqslant 0$ the obvious inequality is deduceable

$$a_2 > \frac{4}{15\pi}\int_1^{\nu s} A(s',1)\,ds'/s'^3. \qquad (2)$$

Here s is an arbitrary energy, $\nu > 1$ is an arbitrary number. Making use of the mean-value theorem we obtain

$$A(\bar{s},1) < \frac{15\pi a_2 \nu^2}{2(\nu^2-1)}\,s^2. \qquad (3)$$

Here $\bar{s}$ is some point in the interval $(s, \nu s)$. It is known [4], that given the value $A(\bar{s},1)$ $\max A(\bar{s},0)$ can be realized by choosing the following values of partial amplitudes

$$a_\ell(s) = \begin{cases} 1 & \ell < L \\ \eta & \ell = L+2 \\ 0 & \ell > L+2 \end{cases} \qquad (4)$$

In our case only partial waves with even ℓ are nonvanishing. Hence, when $A(s,0)$ is maximal, then according to eq. (4) we have

$$A(\bar{s},1) = 4\sqrt{\frac{\bar{s}}{\bar{s}-1}}\sum_{\substack{\ell=0 \\ \ell\text{-even}}}^{L}(2\ell+1)P_\ell\left(1+\frac{2}{\bar{s}-1}\right) + (2L+5)\eta\,P_{L+2}\left(1+\frac{2}{\bar{s}-1}\right). \qquad (5)$$

Considering energies for which $s \gg 1$ and using the known formula (see (A.2) in ref.[4]) we obtain

$$A(\bar{s},1) = 4P'_{L+1}\left(1+\frac{2}{\bar{s}}\right) + (2L+5)\eta\,P_{L+2}\left(1+\frac{2}{\bar{s}}\right). \qquad (6)$$

In order to determine L we calculate $P'_{L+1}\left(1+\frac{2}{\bar{s}}\right)$. For this purpose we make use of the following integral representation for $P_\ell(ch\alpha)$ [6]:

$$P_\ell(ch\alpha) = \frac{2}{\pi}\int_0^\alpha \frac{ch(\ell+1/2)\theta}{\sqrt{2ch\alpha - 2ch\theta}}\,d\theta \qquad (7)$$

which by means of the substitution $z = \alpha - \theta$ can be reduced to the form

$$P_\ell(ch\alpha) = I_{\ell+\frac{1}{2}} + I_{\ell-1/2} \qquad (8)$$

where

$$I_{\ell+1/2}(ch\alpha) = \frac{e^{(\ell+\frac{1}{2})\alpha}}{\pi\sqrt{2\,sh\alpha}}\int_0^\alpha \frac{e^{-(\ell+\frac{1}{2})z}}{(sh\,z)^{1/2}}\left(1-th\frac{z}{2}\,cth\alpha\right)^{-1/2}dz.$$

It is easy noticeable that in our case $\alpha < \frac{2}{\sqrt{3}}$. Taking into acoount the condition $\bar{s} \gg 1$ and performing simple manipulations we obtain

$$P'_{L+1}(ch\alpha) = I^*_{L+\frac{3}{2}} + I^*_{-L-\frac{3}{2}} + o(\alpha^2) + o(\alpha^4) \qquad (9)$$

where

---

[x] INP, Moscow State University.

$$I^{*}_{L+3/2} = \frac{L+3/2}{\operatorname{sh}\alpha}\frac{\sqrt{\pi}}{2}\left(1-\frac{\alpha^2}{12}-\frac{\alpha}{4(L+3/2)}\right)\times e^{(L+\frac{3}{2})} \times \int_0^1 e^{-\alpha(L+3/2)x^2}(1-x^2)(1-\frac{x^2}{2})^{-1/2}\,dx .$$

One can show that $o(\alpha^2) > 0$ and that numerically it is significantly smaller than explicitly given terms. We note that, by neglection of positive terms in $\mathcal{P}'_{L+1}(ch\alpha)$ we make only the quantity L larger (see eq. (11) below).

From eq. (9) it follows that at energies of the order of 10 GeV the correction terms with respect to α are small. We will neglect them because errors in determing α_2 are significantly larger than these corrections. We note that they are easily calculable.

We consider the case when $\alpha(L+\frac{3}{2}) \equiv \gamma \geq 1$. Obviously γ is an increasing function of s. The numerical calculations show that the condition $\gamma \geq 1$ for the $\pi^0\pi^0$ scattering is fulfilled already at $s \sim 10\,GeV^2$. Simple but tedious calculations lead to the formula

$$\mathcal{P}'_{L+1}\left(1+\frac{2}{\bar{s}}\right) = \frac{\sqrt{\gamma}\,e^{\gamma}\bar{s}}{4\sqrt{2\pi}}\left(1-\frac{3}{8\gamma}-\frac{5}{16\gamma^2}\right); \qquad (10)$$

$$\gamma = \frac{2(L+3/2)}{\sqrt{\bar{s}}} .$$

On the right hand side of eq. (10) we have neglected the positive terms which are small in comparison with the main terms. The precision of eq. (10) increases with increasing γ, i.e., increasing energy. Returning to ineq.(3) and sibstituting eqs. (6) and (10) into it we obtain the equation for L :

$$\sqrt{\gamma}\,e^{\gamma}\left(1-\frac{3}{8\gamma}-\frac{5}{16\gamma^2}\right) = 30\left(\frac{\pi}{2}\right)^{3/2}\alpha_2 s\frac{v^2}{v^2-1} , \qquad (11)$$

We have omitted the term $(2L+5)\eta\,\mathcal{P}_{L+2}\left(1+\frac{2}{\bar{s}}\right)$ which could lead to some reinforcement of the sought for inequality.

Solving eq. (11) by means of the method of subsequent approximations we obtain

$$\gamma(\bar{s}) = \ln\left(\frac{e\alpha_2 v^2 s}{v^2-1}\right) - \ln\ln\left(\frac{e\alpha_2 v^2 s}{v^2-1}\right)\left(1-\left(2\ln\frac{e\alpha_2 v^2 s}{v^2-1}\right)^{-1}\right) + \frac{3}{8\ln(e\alpha_2 v^2 s/v^2-1)} + \frac{5}{16\ln^2\left(\frac{e\alpha_2 v^2 s}{v^2-1}\right)}; \quad \beta = 30\left(\frac{\pi}{2}\right)^{3/2}. \qquad (12)$$

Formula (12) has been written down with accuracy to the terms which are much smaller than 1. Using the equality

$$\sigma(\bar{s}) = \frac{8\pi}{m_\pi^2 \bar{s}}\sum_{\substack{l=0 \\ l\text{-even}}}^{L+2}(2l+1) , \qquad (13)$$

we obtain with accuracy to the terms $\sim \frac{1}{\sqrt{s}}$ the equality

$$\sigma(\bar{s}) = \frac{\pi}{m_\pi^2}\gamma^2(\bar{s}). \qquad (14)$$

One can improve this bound by estimating on the basis of experimental data the integral in eq. (3) over the interval $(1, s)$. Let us note also that the bound on the cross section in the interval $(s, \sqrt{s})$ depends on its behaviour at energies larger than $\sqrt{s}$.

References

1. F.J.Indirain. Phys.Lett., 313, 368 (1970).
2. A.C.Common. Nuovo Cim., 69A, 115, 1970.
3. A.C.Stewen. Phys.Rev., D7, 2709 (1973).
4. S.M.Roy. Phys.Reports 56, 125, 1972.
5. R.Blankenbeckler and R.Savit. Phys.Rev., D5, 2757, 1972.
6. N.N.Lebedev . The special functions and their applications, Moscow, 1963.

DESCRIPTION OF INCLUSIVE REACTION SCALING PROPERTIES IN TERMS OF DENSITY MATRIX

A.A.Arkhipov, A.A.Logunov, V.I.Savrin
IHEP, Serpukhov, USSR

Description of multiparticle production processes at high energies is complicated by the fact that the number of permitted channels of the reaction is tremendously great and it is a problem to select processes with a fixed number of particles in the final state. In this case one is interested in the momentum distribution for a small number of selected particles getting no information about the remaining secondary hadrons (inclusive reaotions). So it is expedient to introduce a density matrix that would describe the behaviour of these pioked out particles in self-consistent field of all the remaining particles in the final state /1/ .

In the framework of the equal-time formulation of quantum field theory /2,3/ manipartiole wave funotion is introduced in the form: $(2\pi)^3 \delta(\vec{P}_2 + \sum_{i=1}^{n} \vec{K}_i - q_1 - q_2)\Psi_n(\vec{K}_1, \dots \vec{K}_n; t) =$

$$= \sqrt{\frac{2P_2^0\, 2K_1^0 \dots 2K_n^0}{n!\,(2\pi)^{3(n-1)}}} \langle 0|T\{\psi(\vec{P}_2 t)\varphi(\vec{K}_1 t_1)\dots\varphi(\vec{K}_n t_n)\} S \}|\vec{q}_1\vec{q}_2\rangle / \langle 0|S|0\rangle \Big|_{t_1=\dots t} \quad (1)$$

where ψ and φ are operators of nucleon and meson fields and $|\vec{q}_1\vec{q}_2\rangle$ is initial state veotor of meson-nucleon system.

In the quasipotential approach the single-time wave function Ψ_n satisfies the following equation /4-6/ :

$$(E_K - E)\Psi_n(t) = V_{n+1}\Psi_n(t) \quad (2)$$

where $E = q_1^0 + q_2^0$, E_K , and V_{n+1} are kinetic energy and interaction quasipotential of $n+1$ particles. The equation (2) is a relativistic generalization of Schrödinger equation for multiparticle system. Likeness of the quasipotential approach with nonrelativistic quantum mechanics is emphasized by explicit three-dimensional form of the quasipotential equation in contrast to other relativistic equations. Notice that the quasipotential is not equal to a sum of interaction quasipotentials for separate pairs of particles.

We shall construct the density matrix for single-particle inclusive reaction of equal-time wave functions by means of usual rules of quantum mechanics /1/ :

$$\rho_{\vec{c}}(\vec{K}_1, \vec{x}_1|t) = \sum_{n=2}^{\infty} \frac{1}{(n-1)!} \int d\vec{K}_2 \dots d\vec{K}_n\, \delta(\vec{c} + \sum_{i=2}^{n} \vec{K}_i - \vec{q}_1 - \vec{q}_2) \times \Psi_n(\vec{K}_1, \vec{K}_2 \dots \vec{K}_n; t)\, \Psi^*(\vec{x}_1, \vec{K}_2, \vec{K}_n; t) \quad (3)$$

This density matrix describe a behaviour of the picked out meson in the final state of meson-nucleon collision when the summed momentum of this meson and nucleon is fixed and equal $\vec{c}$. The full density operator is defined as superposition over all $\vec{c}$:

$$\rho(t) = \int d\vec{c}\, \rho_{\vec{c}}(t). \quad (4)$$

It is not difficult to see that the diagonal element of the density matrix (4) is related with single-particle inclusive oross section:

$$\lim \rho(\vec{K};\vec{K}|t) = \delta(0)\frac{I}{(2\pi)^2}\frac{d\sigma}{d\vec{K}} \quad (5)$$

where

$$I = 4\sqrt{(q_1 q_2)^2 - \mu^2 m^2}.$$

Starting from the quasipotential equation (2) it is possible to show that the density operator (3) obeys the following equation of the quasipotential type:

$$(E_K - E)\rho_{\vec{c}}(t) - \rho_{\vec{c}}(t)(E_{\vec{x}} - E') = V\rho_{\vec{c}}(t) - \rho_{\vec{c}}(t)V^+, \quad (6)$$

where $E_\kappa = \kappa^\circ + \sqrt{(\bar{c}-\bar{\kappa})^2+m^2}$ and the effective quasipotential is determined by taking an average of maniparticle interaction quasipotentials over all multiparticle wave functions (1). The equation (6) is a relativistic generalization of the equation for density operator in quantum mechanics and in its form coincides with the equation for the density operator of some fictious pure two particle state. However the quasipotential ϑ is not equal to true interaction quasipotential of meson and nucleon but is screened by presence of all the remaining mesons in the final state. In particulary the imaginary part of ϑ is not generally positive.

Solving the equation (6) we obtain with the help of (4) and (5) an expression for inclusive cross section in the fragmentation region $\kappa_\perp \leq \kappa$:

$$2\kappa^\circ \frac{d\sigma}{d\vec{\kappa}} = \frac{(2\pi)^5}{2E^2} \frac{\beta(E^2)}{(2-x)} \Phi(\kappa_\perp, x), \quad x = \frac{2\kappa}{E} \quad (7)$$

It is clear that if inelastic cross section and average multiplicity are slowly changing function $\beta(E^2) = \beta_0 E^2$ where β_0 also slowly varies. Thus we come to radial scaling experimentally observed. Notice that we derived this result from shortrange behaviour of strong interactions and relativistic invariance without using concrete form of the quasipotential ϑ .

In the region of large transverse momenta $\kappa_\perp$ interactions take place mainly at small distances less than nuclear size. So the behaviour of effective quasipotential ϑ at origin plays a significant role. We assume that constituents have point-like character and so the interaction quasipotential is singular. In this case the inclusive cross section has the following form as $x_\perp \to 1$ /7/ :

$$2\kappa^\circ \frac{d\sigma}{d\vec{\kappa}} \cong (2\pi)^5 A \beta_0 \frac{(1-x_\perp)^\nu}{\kappa_\perp^n} \quad (8)$$

where A is a constant, the power index n is determined by quasipotential singularity and ν is related with behaviour at exclusive thresheld.

In this scheme we come to the following interpretation: the initial nucleon is a composite system containing an arbitrary number of mesons. Each constituent (meson) is distributed inside nucleon according to the certain law. The production process is treated as a breakdown of the composite nucleon. It is no problem to extend the scheme for the case of any number of different kinds of particles.

Now we apply the density matrix formalism to the deep inelastic electroproduction of hadrons /8/ . In the one-photon approximation inclusive cross section is reduced to the total cross section of virtual photon absorption. We shall regard the virtual photon as a real particle with mass q^2 . As a result we come to the formula (7) for the inclusive photon-proton scattering where function $\Phi = \Phi(\kappa_\perp, x, \omega')$, $\omega' = 1 - s_q/q^2$. The electroproduction cross section has the following form:

$$2\kappa^\circ \frac{d\sigma}{d\vec{\kappa}} = \frac{(2\pi)^5 \alpha^2 \beta(s_q)}{I\, t^2} \int_e^1 \frac{d\xi}{\xi} \tilde{\Phi}(\xi, \omega') \quad (9)$$

where

$$\tilde{\Phi}(\xi, \omega') = \frac{1}{2-\xi} \int \varkappa_\perp d\varkappa_\perp \Phi(\varkappa_\perp, \xi, \omega') \quad (10)$$

Thus the structure part of the electroproduction cross section depends only on scaling variable ω' . Notice that the formulas obtained here are more general than in parton model. In particular when $\beta(s_q) \sim s_q^{-2}$ and $\tilde{\Phi}(\xi, \omega') = \delta(\xi\omega' - 1) f(\xi)$ we come to the usual parton model /10/ .

Now we consider the general case not restricting ourselves by one-photon approximation. For this purpose we can use directly the formulae (7). Using shortrange character of effective quasipotential we come to the following expression for electroproduction cross

section in deep inelastic region ($S_q \to \infty$, ω' is fixed):

$$2K^0 \frac{d\sigma}{d\vec{K}} = \frac{(2\pi)^5 \beta(s)}{2I(2-x)} \left|T(s_c, t_c)\right|^2 \quad (11)$$

where

$$s_c = \frac{2m^2}{2-x}, \quad x = 1 - s_q/s \quad (12)$$

$$t_c = -\frac{m^2 x(1-x)}{2(2-x)(\omega'-1)} \quad (13)$$

The structure part of the cross section depends only upon two scaling variables x and ω' in accordance with the dimensionality analysis and the autemodelity principle /9/.

We assume now that electron interacts with separate constituents of proton through one-photon exchange so that electron interaction with proton as a whole remains multipheton. Then for the amplitude T describing electron scattering on constituents we have the following standard form:

$$\left|T(s_c, t_c)\right|^2 = \frac{\alpha^2}{t_c(1 - t_c/4m^2)} \Big\{ \quad (14)$$

$$4\left[(s_c - m^2)^2 + t_c s_c\right] \phi_E(t_c) -$$

$$- \frac{t_c}{m^2}\left[(s_c - m^2)^2 + s_c t_c - 2m^2 t_c + \frac{1}{2}t_c^2\right] \phi_M(t_c) \Big\}$$

where ϕ_E and ϕ_M are some structure functions analogies to the squared proton electromagnetic formfactors. We see that these structure functions depend only on one scaling variable

$$\zeta = \frac{x(1-x)}{(2-x)(\omega'-1)} \quad (15)$$

which is a combination of Bjorken's and Feynman's variables. Comparison of this new scaling law with experimental date is shown in Fig.1. The obtained result points to the fact that account of multiphoton exchange in deep inelastic scattering of electron on proton may lead to new scaling law for the cross section of this process.

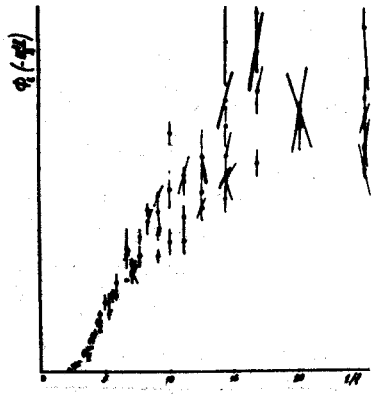


Fig.1

In conclusion the authors would like to express their gratitude to M.A.Mestvirishvili, M.V.Saveliev, N.E.Tyurin and O.A.Khrustalev for useful discussions.

References

1. A.A.Arkhipov, A.A.Logunov, V.I.Savrin. TMF 26, N 3 (1976).
2. A.A.Logunov, V.I.Savrin, N.E.Tyurin, O.A. Khrustalev. TMF, 6, 157, 1971.
3. A.A.Arkhipov, V.I.Savrin. TMF, 16, 328, 1973.
4. A.A.Logunov, A.N.Tavkhelidze. Nuovo Cim., 29, 380, 1973.
5. R.N.Faustov. Nucl.Phys., 75, 669, 1966.
6. V.A.Matveev, R.M.Muradyan, A.N.Tavkhelidze. Preprint JINR P2-3900, Dubna, 1968.
7. A.A.Arkhipov, V.I.Savrin. Preprint IHEP OTF 76-94, 1976.
8. V.I.Savrin. Preprint IHEP OTF 76-47, 1976.
9. V.A.Matveev, R.M.Muradyan, A.N.Tavkhelidze. Commun.JINR P2-4578, Dubna, 1969.
10. R.F.Feynman. "Photon-hadron interactions", Mir, M., 1975.

INVESTIGATION OF THE POWER AUTOMODEL ASYMPTOTIC BEHAVIOUR OF THE LARGE-ANGLE HADRON-HADRON SCATTERING

S.V.Goloskokov, S.P.Kuleshov, V.A.Matveev, M.A.Smondyrev
Joint Institute for Nuclear Research, Dubna

The investigation of the power automodel asymptotic behaviour of the large-angle scattering cross sections is, at present, an important problem of high-energy physics.

Here we consider the power decrease of differential cross sections at large angles in the framework of the Logunov-Tavkhelidze quasipotential approach /1/ .

The power decrease of large-angle differential cross sections discovered in recent experiments /2/

$$\frac{d\sigma}{dt} \sim \frac{1}{s^n} f\left(\frac{t}{s}\right) \qquad (1)$$

was treated on the basis of the principle of automodelity /3/ , i.e., on the basis of the assumption on absence of essential dimensional parameters defining the dynamics of interaction at small distances. By using the dimensional analysis and considerations on the composite nature of particles one may relate the degree n in (1) to the number of elementary constituents of hadrons. For instance, for the binary reaction $a + b \to a + b$ we have $n = 2(n_a + n_b - 1)$, where n_a and n_b are the numbers of elementary constituents (quarks) of hadrons a and b , respectively. In paper /4/ the explicit form of angular dependence of differential cross section of the large-angle high energy scattering has been found for different processes on the basis of the dynamical interpretation of quark diagrams for two-particle scattering amplitudes which results in a generalization of the "quark counting" rules.

On the basis of these investigation results, in papers /5/ the problem was raised concerning the structure of the local two-particle quasipotential which produces, in the case of large-angle two-particle scattering, the behaviour of type (1).

In this report the scattering both of spinless particles and of particles with spin is analysed in a unique way for the quasipotentials obeying the representation

$$\hat{g}(E;\vec{\Delta}^2) = g(E)\int_0^\infty dx\, \hat{\rho}(E;x)\, e^{-x\vec{\Delta}^2}, \quad t = -\vec{\Delta}^2 \qquad (2)$$

and being analytic functions of t in the half-plane $Re\, t \le 0$. In representation (2) $\hat{\rho}(E;x)$ is a matrix defining the nature of interaction at high energies, with a rank dependent on the spin of particles. The main energy dependence in eq. (2) is factorized into $g(E)$ which depends on E by a power low. At x fixed $\hat{\rho}(E;x)$ is assumed to be slowly varying function of energy. Also it is supposed that for the density $\hat{\rho}(E;x)$ there exists the weak limit

$$\lim_{s\to\infty} s^N \hat{\rho}(E; x = z/s) = \hat{\psi}(z) \qquad (3)$$
$$0 < z < \infty , \quad N > 0 .$$

Note that in describing the interaction of particles with spin we use essentially the requirement of γ_5 invariance of the interaction at high energies and large transfer momenta /6/ .

Quasipotentials (2) obeying condition (3) are called analytic. Later we obtain a formal representation for the large-angle high energy elastic scattering amplitude for particles with arbitrary spin within the quasipotential approach. For concrete scattering processes it results in the following asymptotic behaviour of the differential cross section of the high energy large-angle scattering

$$\frac{d\sigma}{dt}(s,t) \sim \left|e^{2i\chi(0)}\right|^2 \frac{1}{s^n} f\left(\frac{t}{s}\right),$$

where $\chi(0)$ is the value of the eikonal scattering phase at zeroth impact parameter. Recall that the eikonal function $\chi(\vec{b})$ defines the behaviour of the scattering amplitude at small angles. Thus, the result obtained allows one to establish certain correlation between asymptotic forms of the scattering amplitude at small and large angles.

Consider the quasipotential equation describing the interaction of particles with spin which is written in general form

$$\hat{G}(E;\vec{p},\vec{k}) = \hat{g}(E;\vec{p}-\vec{k}) + \int d^3\vec{q}\,\hat{g}(E;\vec{p}-\vec{q}) \times \frac{\hat{A}(E;\vec{q})}{E^2(\vec{q})-E^2-i0}\,\hat{G}(E;\vec{q},\vec{k}) \quad (4)$$

where $E=\sqrt{m_1^2+\vec{p}^2}+\sqrt{m_2^2+\vec{p}^2}$ is the total energy of particles in the c.m.s., $E(\vec{q}) = \sqrt{m_1^2+\vec{q}^2} + \sqrt{m_2^2+\vec{q}^2}$, m_1 and m_2 are the masses of the first and second particles, respectively. $\hat{A}(E;\vec{q})$ is a matrix which form depends on the spin of interacting particles. We do not need here the explicit form of $\hat{A}(E;\vec{q})$.

Assuming the quasipotential is given by representation (2) we will solve eq. (4) by iterations

$$\hat{G}(E;\vec{p},\vec{k}) = \sum_{n=0}^{\infty} \hat{G}_{n+1}(E;\vec{p},\vec{k}), \quad \hat{G}_1 = \hat{g}(E;\vec{p}-\vec{k}).$$

On changing variables, $\hat{G}_{n+1}(E;\vec{p},\vec{k})$ can be transformed to the form

$$\hat{G}_{n+1}(E;\vec{p},\vec{k}) = \int\!\!\cdots\!\int dx_1 \ldots dx_n \exp\Big\{t/\sum_{i=1}^{n+1} 1/x_i\Big\}\,\hat{\mathcal{J}}_n(x_1,\ldots,x_{n+1}) \quad (5)$$

where $\hat{\mathcal{J}}_n(x_1,\ldots,x_{n+1})$ is a 3n-dimensional integral. By using representation (5) we analyze the behaviour of the scattering amplitude at high energies and large angles, i.e., in the region $S\to\infty$, $|t|/S = \frac{1}{2}(1-z)$ fixed. In this limit the main contribution, to the asymptotic form of integral (5) comes from the region $1/\sum_i 1/x_i \sim 0$ otherwise we have the decreasing exponential function $\exp\{-|t|/\sum_i 1/x_i\}$. If condition (3) holds, the main contribution to the asymptotic form of (5) can be shown to come from the region where only one of $x_i \sim 0$. In this case we find the following formal expression for the scattering amplitude

$$\hat{G}(E;\vec{p},\vec{k}) = e^{i\hat{\chi}(0)\hat{B}(\vec{p})}\,\hat{g}(E;\vec{p}-\vec{k})\,e^{i\hat{B}(\vec{k})\hat{\chi}(0)} \quad (6)$$

with notations

$$\hat{\chi}(0) = \int_{-\infty}^{\infty} dz\,\frac{\hat{g}(E;\sqrt{z^2+\vec{b}^2})}{g(E)}\Big|_{\vec{b}=0}$$

$$\hat{B}(\vec{p}) = \hat{A}(E;\vec{p})\,\frac{g(E)}{16|\vec{p}|}$$

where $\hat{g}(E;\vec{r})$ is the Fourier transform of quasipotential (2).

Consider now the contribution of exchange forces for the scattering of different particles. The quasipotential is written in the form

$$\hat{V}(E;\vec{p},\vec{k}) = \hat{g}(E;\vec{p},\vec{k}) + \hat{h}(E;\vec{p},\vec{k}). \quad (7)$$

The quasipotentials $\hat{g}$ and $\hat{h}$ are called direct and exchange parts of the quasipotential $\hat{V}$. We assume for $\hat{g}$ representation (2) and for $\hat{h}$ the following representation

$$\hat{h}(E;\vec{p},\vec{k}) = h(E)\int_0^{\infty} dy\,\hat{\sigma}(E;y)\,e^{-y(\vec{p}+\vec{k})^2}. \quad (8)$$

We assume also that the densities $\hat{\rho}$ and $\hat{\sigma}$ obey the weak limits of the type (3) with identical N.

Furthermore, let the scattering amplitude $\hat{T}$ be represented as a sum of two quantities

$$\hat{T} = \hat{G} + \hat{H}. \quad (9)$$

Then inserting (7) and (9) into (4) we arrive at the system of quasipotential equations

$$\hat{G} = \hat{g} + \hat{g}\otimes\hat{G} + \hat{h}\otimes\hat{H} \quad (10)$$

$$\hat{H} = \hat{h} + \hat{h}\otimes\hat{G} + \hat{g}\otimes\hat{H}. \quad (11)$$

For the meson-nucleon scattering the

backward scattering peak is suppressed, i.e.,

$$\left| \frac{\hat{h}(E; |\vec{\Delta}_u| \sim 0)}{\hat{g}(E; |\vec{\Delta}_t| \sim 0)} \right| \to 0 \quad \text{at} \quad E \to \infty .$$

Therefore, when the quasipotentials $\hat{g}$ and $\hat{h}$ obey conditions (2),(8) and (3), the last term in eq. (10) may be neglected. In this way the system of eqs. (10) and (11) becomes uncoupled. The contribution of $\hat{g}$ has been analysed above, next, we consider only the contribution from the exchange part $\hat{h}$.

By using the method developed it can be shown that the main contribution to the asymptotic form of $\hat{H}$ at large $|u| = -(\vec{p}+\vec{k})^2 \sim s$ comes from the region $y \sim 0$. Then

$$\hat{H}(E;\vec{p},\vec{k}) \simeq e^{i\hat{\chi}(0)\hat{B}(\vec{p})}\, \hat{h}(E;\vec{p}+\vec{k})\, e^{i\hat{B}(\vec{k})\hat{\chi}(0)} .$$

Thus, with (6) taken into account, for the scattering of nonidentical particles the total scattering amplitude at large angles has the form

$$\hat{T}(E;\vec{p},\vec{k}) = e^{i\hat{\chi}(0)\hat{B}(\vec{p})}\left[\hat{g}(E;\vec{p}-\vec{k}) + \hat{h}(E;\vec{p}+\vec{k})\right] e^{i\hat{B}(\vec{k})\hat{\chi}(0)} .$$

Now we proceed to calculate the scattering cross sections for concrete processes. First consider the scattering of two identical spinless particles. The quasipotential being a scalar function, with the exchange forces taken into account, is written in form (6), and the scattering amplitude can be represented by (9). With crossing symmetry, we have

$$T(E;\vec{p},\vec{k}) = e^{2i\chi(0)}\left[g(E;t) + g(E;u)\right]$$

and

$$\frac{d\sigma}{dt} \sim \frac{1}{s^2} \left| e^{2i\chi(0)} \right|^2 \left| g(E;t) + g(E;u) \right|^2 .$$

Consider now the scattering of a scalar particle on a spinor one. The quasipotential is taken in the simple γ_5 - invariant form with the densities

$$\hat{\rho}(E;x) = \gamma_0 \tilde{\rho}(E;x),$$

$$\hat{\sigma}(E;x) = \gamma_0 \tilde{\sigma}(E;x) .$$

Passing to the differential cross section

$$\frac{d\sigma}{dt} \sim \frac{1}{s}\sum_{spin} \langle \bar{\psi}(\vec{p})|T|\psi(\vec{k})\rangle \langle \bar{\psi}(\vec{k})|T^+|\psi(\vec{p})\rangle$$

we get

$$\frac{d\sigma}{dt} \sim \frac{(1+z)}{s}\left| e^{2i\tilde{\chi}(0)} \right|^2 \left| \tilde{g}(E;\vec{p}-\vec{k}) + \tilde{h}(E;\vec{p}+\vec{k}) \right|^2$$

Here $\tilde{\chi}$ is eikonal meson-nucleon scattering phase

$$2i\tilde{\chi}(\vec{b}) = -\frac{1}{2ip}\int_{-\infty}^{\infty} dz\, V(E;\sqrt{z^2+\vec{b}^2}) .$$

Analogously, one may consider the large-angle NN scattering. However, in this case we choose the eikonal phase as follows

$$\hat{\chi}(0) = \gamma_0^{(1)}\gamma_0^{(2)}\tilde{\chi}(0)$$

that implies the spin-flip amplitudes are small at high energies and fixed transfer momenta. The quasipotential is taken in the γ_5 - invariant form

$$\hat{V}(s,t) = \gamma_N^{(1)}\gamma^{N(2)} C(s,t) + \gamma_5^{(1)}\gamma_5^{(2)}\gamma_N^{(1)}\gamma^{N(2)} D(s,t) .$$

As its expression is combersome, we omit it here (see /5/).

Now let us give a simple example of the use of the above formulae. Let the densities have zero of a finite order at $x \to 0$. Then one can find the following expressions for the differential cross sections of different processes:

A. For the scalar particles

$$\frac{d\sigma}{dt} \simeq \frac{A}{s^{2N+2}}\left| e^{2i\chi(0)} \right|^2 \left[\frac{1}{(1-z)^m} + \frac{1}{(1+z)^m} \right]^2$$

B. For the meson-nucleon scattering

$$\frac{d\sigma}{dt} \simeq \frac{(1+z)}{s^{2N+2}}\left| e^{2i\chi(0)} \right|^2 \left[\frac{A}{(1-z)^m} + \frac{B}{(1+z)^k} \right]^2$$

C. For the nucleon-nucleon scattering

$$\frac{d\sigma}{dt} \simeq \frac{\left| e^{2i\chi(0)} \right|^2}{s^{2N+2}(1-z^2)^{2m}} \left\{ |\alpha+\beta|^2 \left[(1+z)^{2m+2} + \right. \right.$$

$$+(1-z)^{2m+2}+4\left((1+z)^{m}+(1-z)^{m}\right)^{2}\Big]-$$

$$-2(\alpha\beta^{*}+\beta\alpha^{*})\left[(1+z)^{2m+2}+(1-z)^{2m+2}\right]\Big\}.$$

The parameter in these formulae can be found from comparison with experimental data that has been performed for the $\pi^{\pm}p$ and pp scattering at energies $p_{\perp} \gtrsim 7$ GeV/c and large angles.

The results of calculation are drawn in Figs. 1,2,3 and are in good agreement with experiment.

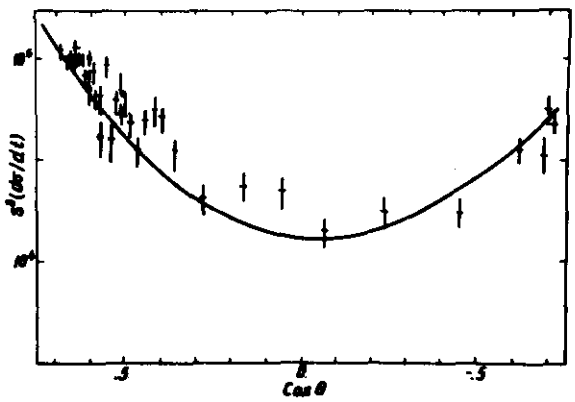


Fig.1. $S^{6}\left(\frac{d\sigma}{dt}\right)$ for $\pi^{+}p$ reaction.

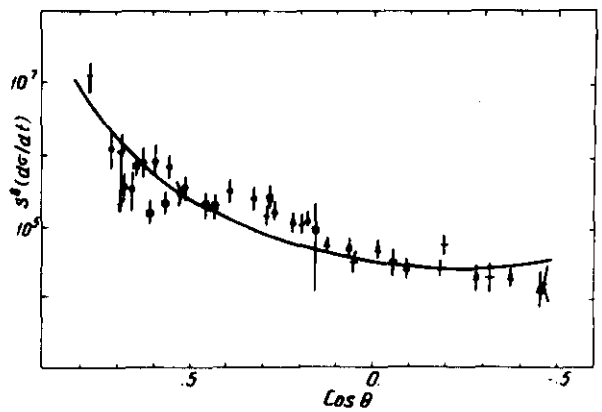


Fig.2. $S^{8}\left(\frac{d\sigma}{dt}\right)$ for $\pi^{-}p$ reaction

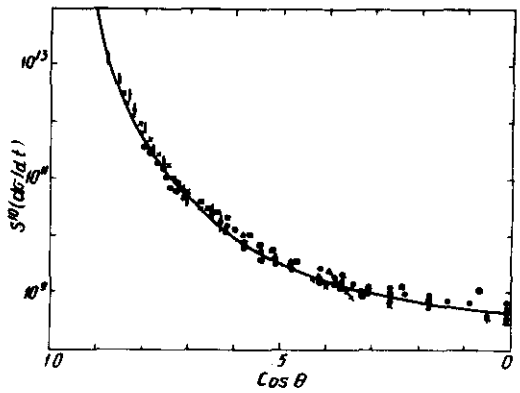


Fig.3. $S^{10}\left(\frac{d\sigma}{dt}\right)$ for pp reaction.

References

1. A.A.Logunov, A.N.Tavkhelidze. Nuovo Cim., 29, 380, 1963.
2. G.Giacomelli. Rapporteur's talk at the XVI Int.Conf. on High Energy Physics, Batavia, 1972.
3. V.A.Matveev, R.M.Muradyan, A.N.Tavkhelidze. Lett. Nuovo Cim., 7, 719, 1973.
4. V.A.Matveev, R.M.Muradyan, A.N.Tavkhelidze. JINR. E2-8048, Dubna. 1974.
5. S.V.Goloskokov, S.P.Kuleshov, V.A.Matveev, M.A.Smondyrev. JINR P2-8211,P2,8337, Dubna, 1974; JINR, P2-9088, Dubna, 1975; JINR, P2-9897, Dubna, 1976.
6. A.A.Logunov, V.A.Meshcheryakov, A.N.Tavkhelidze. Doklady Academii Nauk USSR, 142, 317, 1962.

HIGH ENERGY BEHAVIOUR OF GAUGE THEORIES

Tai Tsun Wu

Harvard University, USA

In this report we discuss the high energy behaviour of gauge field theories with emphasis on its application to hadronic processes at the energies available at ISR and Fermilab. We shall be concerned only with the limit

$$s \to \infty$$

with all transverse momenta fixed. Here as usual s is the square of the center-of-mass energy. We shall disouss the following cases:

1. Abelian gauge theory (electrodynamios);

A. Pomeron exchange

B. Quantum number exchange

2. Non-Abelian gauge theory (Yang-Mills-theory [1]).

The present status in these cases is as follows:

		Result from gauge field theories	Phenomenology and Comparison with experiments
Abelian gauge theories	Pomeron exchange	V	V
	Quantum number exchange	V	
Non-Abelian gauge theories		V	

Here a check mark V means that a good deal of information is now known while a blank space means the almost total absence of useful information. It is clear from this table that an urgent problem is to develop a phenomenology for quantum number exchange on the basis of the high-energy behaviour of gauge theories.

The gauge theories are all studied theoretically on the assumption of summing the leading terms. We emphasize that this is a pure assumption and may well be misleading.

1A. Abelian gauge theory - Pomeron exchange.

The leading contributions in this case come from the tower diagrams. The result was first given by Cheng and Wu [2] for scalar electrodynamics (SED) and slightly later by Frolov, Gribov and Lipatov [3] for QED [4] . In both cases, the result is, give or take a few $\ln s$, $i\, s^{1+A\alpha^2}$

where A is positive, but different for SED and QED. This is the origin of "Pomeron above 1" (or $\alpha(\rho)>1$) extensively discussed at this Conference.

This result is interpreted as the saturation of Froissart bound [5] and applied to hadron physics by Cheng and Wu [6] to predict the infinitely rising total cross sections. Quantitative results are obtained by Cheng, Walker and Wu [7] by an optical model with potential increasing as s increasing (now sometimes referred to as geometrical scaling). Subsequent measurements [8,9] at ISR show that the actual increase in pp cross section is about 50% higher than this first phenomenomogical model. Using the ISR measurements on pp, the parameters of the model are improved [10] and used to predict the total cross sections for $\pi^{\pm} p$, $K^{\pm} p$ and $\bar{p} p$. Fig.1 shows the theoretical prediction together with all the measurements available at that time.

In fig.2-4 we show the comparison of theoretical and experimental [11] total cross sections [12] . We emphasize that in the cases of fig. 3-4 the data were obtained much later than the theoretical prediction and the comparison supports the theme that results from quantum field theory are useful in the understanding of hadron physics.

There are many other theoretical predictions. Those that are verified include the existence of pionization plateau [13] ;

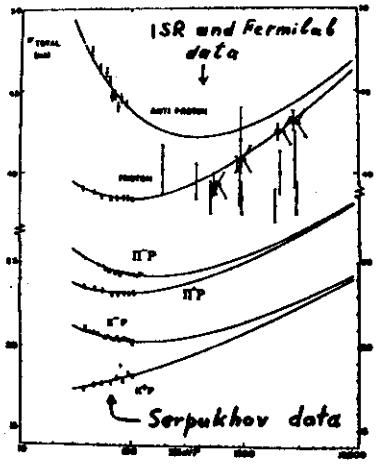


Fig.1. Experimental data from Serpukhov, Fermilab and ISR together with phenomenological results

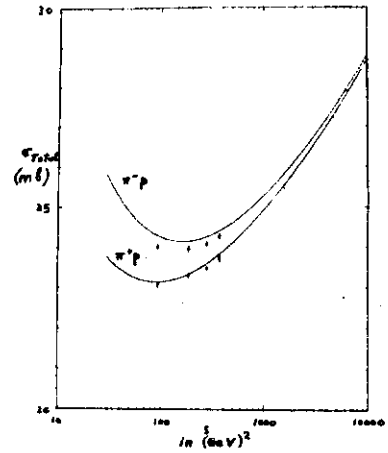


Fig.3. Comparison of theoretical predictions for $\pi^{\pm} p$ total cross sections with later experimental data from Fermilab.

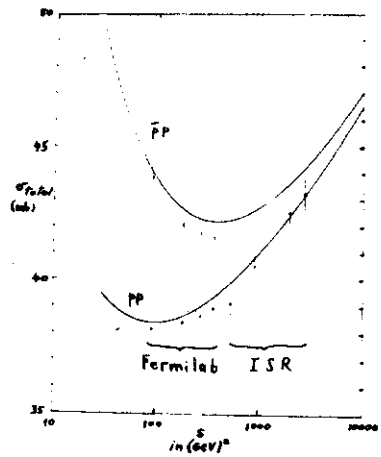


Fig.2. Comparison of theory and experiment for pp and $\bar{p}p$ total cross sections. The ISR data for pp were obtained before theory, while the Fermilab data for $\bar{p}p$ and pp are after theory.

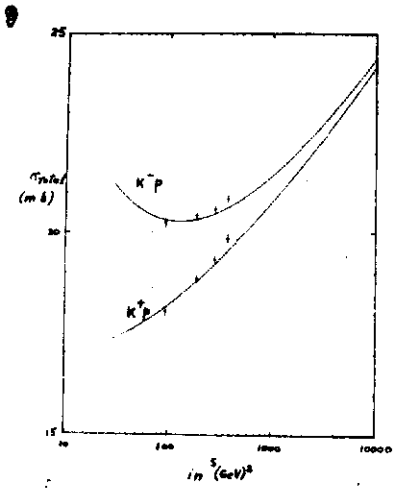


Fig.4. Comparison of theoretical predictions for $K^{\pm} p$ total cross sections with later data from Fermilab.

Real/Imaginary for forward scattering /14/; rising total elastic cross section /6,8/ ; movement of the dip inelastic scattering to smaller momentum transfer /6,15/ ; and most recently the rising pionization plateau discussed this morning by Prof.A.Bialas. Predictions that remain to be tested include the photoproduction of ϕ and diffractive production of ρ^{*} /17/ .

1B. Abelian gauge theory – Quantum number exchange

Fermion exchange in QED was first studied by Gell-Mann et al. [18]. Under the assumption of summing the leading terms their result for the positive signature amplitude is correct, but they missed a sixth-order diagram in the negative-signature amplitude. The corrected result for this negative-signature amplitude shows a fixed cut with a simple pole coming out at a physical value of momentum transfer [19,20]. Therefore there is great similarity between quantum number exchange and Pomeron exchange [19].

2. Non-Abelian gauge theory

The rule of computation for Yang-Mills theory [1] was first given by Faddeev and Popov [21]. To avoid the complicated problem of infrared divergence, we introduce as usual Higg's particles [22]. The calculations are most conveniently carried in the R gauge of 't Hooft [23]. The study of the high energy behaviour was initiated by Nieh and Yao [24], but their result is qualitatively incorrect. The correct result in 6^{th} order comes from about 20 diagrams and was first given by McCoy and Wu [25] and Lipatov [26]. Fadin, Kuraev and Lipatov [27], using an assumption of the multi-Regge form that is explicity verified in the eight order [28], obtains the sum of leading terms for Pomeron exchange. This result for SU(2) is

$$s^{1+g^2(\ln 4)/\pi^2}$$

again a Pomeron above 1. Therefore the similarity between the Abelian and non-Abelian cases is most striking. Fadin and Sherman [29] have treated the case of Fermion exchange in Yang-Mills theory. Both topics will be discussed by Professor Lipatov in the following talk.

I thank Professor A.A. Anselm and K.G. Chetyrkin, M.I.Sakvarelidze, M.A.Smondyrev for their most kind help in preparing this report.

References

1. Chen Ning Yang and Robert L.Mills. Phys.Rev., 96, 191 (1954).
2. H.Cheng and T.T.Wu. Phys.Rev., D1, 467 (1970).
3. G.V.Frolov, V.N.Gribov and L.N.Lipatov. Phys.Lett., 31B, 34 (1970).
4. H.Cheng and T.T.Wu. Phys.Rev., D1, 2775 (1970).
5. M.Froissart. Phys.Rev., 123, 1053 (1961).
6. H.Cheng and T.T.Wu. Phys.Rev.Lett., 24, 1456 (1970).
7. H.Cheng, J.K.Walker and T.T.Wu, contribution to the 16^{th} International Conferenoe on High Energy Physics (1972).
8. U.Amaldi et al. Phys.Lett., 44B, 112 (1973).
9. S.R.Amendolia et al. Phys.Lett., 44B, 119 (1973).
10. H.Cheng, J.K.Walker and T.T.Wu. Phys.Lett., 44B, 97 (1973).
11. A.S.Carroll et al. Phys.Rev.Lett., 33, 928 and 932 (1974).
12. It seems from fig.4 that there is weak evidence that the theory may have underestimated the rate of rise of $K^{\pm} p$ total cross sections.
13. H.Cheng and T.T.Wu. Phys.Rev.Lett., 23, 1311 (1969).
14. Theory: H.Cheng, J.K.Walker and T.T.Wu. Phys.Lett., 44B, 283 (1973); Experiment: Bartenev et al. Phys.Rev.Lett., 31, 1367 (1973).
15. C.Rubbia et al., contribution to the 16^{th} International Conferenoe on High Energy Physics (1972).
16. Theory: H.Cheng and T.T.Wu. Phys.Lett., 45B, 367 (1973); Experiment: British-MIT-Scandinavian collaboration, Phys.Lett., B (to be published).
17. H.Cheng, J.K.Walker and T.T.Wu. Phys.Rev., D11, 68 (1975).
18. M.Gell-Mann et al. Phys.Rev., 133, B145 (1964).
19. B.M.McCoy and T.T.Wu. Phys.Rev.Lett., 35, 1190 (1975).
20. The details are given in B.M.McCoy and T.T.Wu, Phys.Rev. D (Feb. 1976).
21. L.D.Faddeev and V.N.Popov. Phys.Lett., 25, 29 (1967).

22. P.W.Higgns, Phys.Lett., 12, 132 (1964) and Phys.Rev.Lett., 13, 508 (1964); F.Englert and R.Brout. Phys.Rev.Lett., 13, 321 (1964); G.S.Guralnik, C.R.Hager and T.W.B.Kibble. Phys.Rev.Lett., 13, 585 (1964).
23. G.'t Hooft. Nucl.Phys., B35, 167 (1971).
24. H.T.Hieh and Y.P.Yao. Phys.Rev.Lett., 32, 1074 (1974).
25. B.M.McCoy and T.T.Wu. Phys.Rev.Lett., 35, 604 (1975).
26. L.N.Lipatov, preprint LNPI-157 (1975).
27. V.S.Fadin, E.A.Kuraev and L.N.Lipatov. Phys.Lett., 60B, 50 (1975).
28. C.Y.Lo and H.Cheng. Phys.Rev., (1976).
29. V.S.Fadin and V.Sherman, (to be published).

MULTI-REGGE PROCESSES AND THE POMERANCHUK SINGULARITY IN NON ABELIAN GAUGE THEORIES

L.N.Lipatov

Leningrad Nuclear Physics Institute, USSR

1. My talk is based on the results obtained by V.S.Fadin, E.A.Kuraev and muself[1]. I would like to tell you about our calculations of the high energy asymptotics in non-Abelian gauge theories. The papers of other authors on the subject are enumerated in ref.[2] Our final expression for the elastic soattering amplitudes is obtained as a generalization of our results valid up to the eight order of perturbation theory. The result of the tenth order calculation by B.M.McCoy and T.T.Wu [3] coincides with the corresponding term in the perturbative expansion of our final expression and therefore it supports indirectly our oonjecture of a multi-Regge form of production amplitudes.

To study the Pomeranchuk singularity at $j = 1$ in perturbation theory one is obliged to involve vector particles. Renormalizable field models containing vector particles are based on gauge theories. In the simplest gauge theory quantum eleotrodynamics (QED) - the leading j plane singularity turns out to be a fixed branch point at $j = 1 + \frac{11}{32}\pi\alpha^2$ [4]. The violation of the Froissart bound here is a result of the fact that the photon is not reggeized in QED. More realistic models for the strong interaction may be based on the Yang-Mills fields with the Higgs phenomenon. In these theories the vector boson is reggeized as it was shown by many authors by studying several orders of the perturbation theory [2] (the fermion is also reggeized - see ref. [5]).

Therefore the main reason for the violation of the Froissart bound in the leading logarithmic approximation is absent. But our result is a disappointing one: the leading plane singularity turns out to be to the right of the point $j=1$.

2. The field model we have used contains an isotriplet of vector fields with mass M and a scalar isosinglet φ. This model is obtained owing to the Higgs phenomenon from the theory with the Yang-Mills fields interacting with a doublet of scalar particles with negative m^2.

We have calculated the asymptotics of elastic scattering amplitudes in different channels in the kinematical region:

$$s \gg M^2, \quad -t \sim M^2 \tag{Ia}$$

provided that

$$g^2 \ll 1, \quad g^2 \ln \frac{s}{M^2} \sim 1. \tag{Ib}$$

The calculation method is based on using the dispersion relations in s- and t-channels and unitarity conditions. Therefore it is necessary to know inelastic amplitudes $A_{2\to 2+n}$ to find the elastic one. We have verified in lowest orders of the perturbation theory that in the multi-Regge kinematical region the following expression holds for inelastic vector-vector scattering amplitudes:

$$A_{2\to 2+n} = s\,\Gamma^{c_1}_{A\to \mathcal{D}_0} \frac{\left(\frac{s_{12}}{m^2}\right)^{\alpha(t_1)-1}}{t_1-m^2} \gamma^{\mathcal{D}_1}_{c_2c_1} \frac{\left(\frac{s_{23}}{m^2}\right)^{\alpha(t_2)-1}}{t_2-m^2} \cdots \frac{\left(s_{n+1,n+2}/m^2\right)^{\alpha(t_{n+1})-1}}{t_{n+1}-m^2} \Gamma^{c_{n+1}}_{B\to \mathcal{D}_n}, \tag{2}$$

$$s_{i,i+1} \gg m^2, \quad -t_i \sim m^2;$$

where $s_{i,i+1}$ is the squared sum of the energies of the produced particles $\mathcal{D}_i, \mathcal{D}_{i-1}$ in their c.m. system, $c_i = 1,2,3$ are the isotopic states of the virtual vector bosons with mass $\sqrt{t_i}$ and

$$\alpha(t) = 1 + \frac{g^2}{(2\pi)^3}(t-M^2)\int \frac{d^2K}{(K^2+m^2)\left[(q-K)^2-m^2\right]}, \tag{3}$$

$$q^2 = t.$$

For $n = 0$ the relation (2) demonstrates the reggeization of the vector boson $(\alpha(M^2)=1)$. For $n \geqslant 1$ we checked the relation (2) in the Born approximation and by calculating first radiative corrections. In Eq. (2) the vertex functions Γ and γ have the following form:

$$\Gamma^{c_1}_{A\to \mathcal{D}_0} = g\frac{\sqrt{2}}{2}\delta_{Ac_1}\delta_{\lambda_A 3}, \quad \gamma^{\mathcal{D}_1}_{c_2c_1} = \delta_{c_2c_1}\cdot g_m \tag{4a}$$

the case of scalar particle production and

$$\Gamma^{c_1}_{A\to \mathcal{D}_0} = +i\,\varepsilon_{c_1A\mathcal{D}_0}\sqrt{2}\,g\,\alpha_{\lambda_A}\delta_{\lambda_A\mathcal{D}_0}, \quad \alpha_{\lambda_A} = \begin{cases} -1, & \lambda_A = 1,2 \\ -1/2, & \lambda_A = 3 \end{cases} \tag{4b}$$

$$\gamma^{\mathcal{D}_1}_{c_2c_1} = -i\,\varepsilon_{\mathcal{D}_1c_2c_1}\,g\left[-(q_1+q_2) + P_A\left(\frac{P_{\mathcal{D}_1}P_B}{P_AP_B} + \frac{t_1-M^2}{P_{\mathcal{D}_1}P_A}\right) - P_B\left(\frac{P_{\mathcal{D}_1}P_A}{P_BP_A} + \frac{t_2-M^2}{P_{\mathcal{D}_1}P_B}\right)\right]_\mu e^{\lambda_{\mathcal{D}_1}}_\mu$$

in the case of vector meson production. Here $\mathcal{D}_i$ are the isotopic indices of the produced particles and $\lambda_{\mathcal{D}} = 1,2,3$ are their S channel polarizations ($\lambda_{\mathcal{D}} = 3$ corresponds to a longitudinally polarized vector particle).

The multi-Regge region

$$s_{i,i+1} \gg m^2, \quad \prod s_{i,i+1} \sim s, \quad q_i^\perp \sim M \tag{5}$$

gives the main contribution to the s and u channel discontinuities corresponding to $(n+2)$ particle intermediate states. By using the dispersion relation in s channel and by summing contributions from all intermediate states we obtain:

$$f^{A'B'}_{AB}(s,t) = \sum_{T=0,1,2} s \int_{\alpha-i\infty}^{\alpha+i\infty} \frac{d\omega}{i}\left(\frac{s}{m^2}\right)^\omega \frac{(-1)^T - e^{-i\pi\omega}}{\sin\pi\omega} f^T_\omega(t)\,\gamma^{A'B'}_{AB}(T), \quad \gamma^{A'B'}_{AB}(T) = \left[\alpha^2_{\lambda_A}\delta_{\lambda_A\lambda_{A'}}C_T + \delta_{\lambda_A3}\delta_{\lambda_{A'}3}\right]\left[\alpha^2_{\lambda_B}\delta_{\lambda_B\lambda_{B'}}C_T + \frac{\delta_{\lambda_B3}\delta_{\lambda_{B'}3}}{4}\right] \times C^{Tm}_{A'A}\,C^{Tm}_{B'B}, \quad C_T = 2 - \frac{1}{2}T(T+1), \tag{6}$$

$$B_T = -\frac{5}{2} + \frac{3}{4}(T+1)T,$$

where T is the total isospin in the t channel and $C^{Tm}_{A'A}$ are the Clebsch-Gordan coefficients. t-channel partial waves $f^T_\omega(t)$ satisfy the following equation:

$$\left[2+\omega-\alpha(-K^2)-\alpha(-(q-K))\right] f^T_\omega(K,q-K) = \frac{\omega g^2}{-A_Tq^2+B_TM^2} + \left(-A_Tq^2+B_TM^2\right)\frac{g^2}{2\pi^3} \times \int d^2K' \frac{f^T_\omega(K',q-K')}{(K'^2+m^2)((q-K')^2+m^2)} + A_T\frac{g^2}{(2\pi)^3}\left\{\frac{d^2K'\,f^T_\omega(K',q-K')}{(K-K')^2+m^2}\times\left[\frac{K^2+m^2}{K'^2+m^2} + \frac{(q-K)^2+m^2}{(q-K')^2+m^2}\right]\right. \tag{7}$$

The solution of this equation for $T=1$ is

$$f_\omega^T(K,q-K)\Big|_{T=1} = -\frac{\omega g^2}{(q^2+m^2)(\omega+1-\alpha(q^2))} \quad (8)$$

which shows that the assumption (2) is self-consistent: we have a bootstrap scheme in which a multi-Regge equation gives in the j plane the assumed Regge behaviour.

For the cases $T=0$ and $T=2$ Eq. (5) leads to the j plane cut singularities resulting from two reggeized vector meson exchange. In the vacuum channel $T=0$ the Equation can be solved exactly in the region $K_\perp^2 \gg M^2$. The leading j plane singularity turns out to be a square root branch point at $j=1+\frac{2g^2}{\pi^2}\ln 2$. (In the general case of the gauge group $SU(N)$ the branch point is located at $j=1+N\frac{g^2}{\pi^2}\ln 2$).

Thus, the total cross section in the non-Abelian gauge theory increases as a power of s although the cross sections for the produotion of any finite number of particles decrease rapidly with energy owing to the multi-Regge form of inelastic amplitudes (2). The reason for the violation of the Froissart theorem is that the s channel elastic unitarity is not fulfilled in the leading logarithmic approximation (in Eq. (2) the contribution of the vacuum t-channel state should be taken into accoount when $g^2\ln\frac{s}{m^2}\gg 1$).

There is an interesting phenomenon valid in the leading logarithmic approximation. It can be shown that at large $g^2\ln\frac{s}{m^2}\gg 1$ the essential region of integration over $K_\perp^i$ grows with energy. If one modificates Eq. (7) by introducing an invariant charge $g^2(K_\perp^2)=\frac{g^2}{1+g^2\ln\frac{K_\perp^2}{m^2}}$ instead of the renormalized charge g^2 it results in the decay of the fixed branch point into moving poles (their total number is of the order of $1/g^2$) whioh, unfortunately, remain to the right of $j=1$.

It should be stressed that in our leading logarithmic approximation the vacuum singularities emerge as bound stated on only two Reggeons with $T=1$. One can hope. however, that an appropriate Reggeon field theory similar to the Gribov calculus witn Reggeon vertices whioh oan be computated by perturbative methods would lead to a selfconsistent theory compatible with the Froissart restriction.

References

1. V.S.Fadin, E.A.Kuraev, L.N.Lipatov. Phys.Lett., 60B, 50 (1975); JETP, 71, N 9 (1976);
2. H.T.Nieh, Y.P.Yao. Phys.Rev.Lett., 32, 1074 (1974) - the first but incorrect result ; L.N.Lipatov . Preprint LNPI May 1975; Yad. Fiz., 23, 642 (1976); M.M.McCoy, T.T.Wu, Phys.Rev.Lett., 35, 604 (1975); Phys.Rev., 13, 1076 (1976); L.L.Frankfurt, V.S.Sherman. Preprint LNPI, September 1975; Yad.Fiz., 23, 1099 (1976); C.Y.Lo, H.Cheng. Phys.Rev., D13, 1131 (1976); L.Tyburski. Phys.Rev., D13, 1107 (1976).
3. B.M.McCoy, T.T.Wu, unpublished.
4. V.N.Gribov, G.V.Florov, L.N.Lipatov. Phys. Lett., B31, 34 (1970); H.Cheng, T.T.Wu. Phys.Rev.Lett., 24, 1456 (1970).
5. V.S.Fadin, V.S.Sherman. JETP, Pis'ma, 23, 599 (1976).

MULTIPARTICLE REGGE POLES AND THEIR TRAJECTORIES

S.G.Matinyan

Erevan Physics Institute, USSR

This talk is based on the three papers by A.G.Sedrakian and author [1-3].

It became usual to relate to the reggeon a sum of ladder diagrams though the $g\varphi^3$-theory gives its intercept near $j = 1$.

In this connection it always seemed attractive to provide the positive intercept by the inclusion of multiparticle states in the t-channel. Well known Mandelstam diagrams corresponding to multi-particle states in t-channel and giving the branch points in j-plane, of course, are not enough, as they refer to the multiparticle configurations where only "two-body bound" states are present. However, in the theory with attraction it is possible the formation of many-particle bound states. This problem was first considered in the field theory by McCoy and Wu[4]. They showed, that the contribution of fig.1b type diagrams to the asymptotics dominates over the contribution of fig.1a type Mandelstam diagrams corresponding to the reggeon-particle cut.

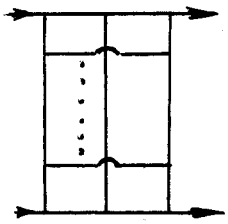


Fig.1a

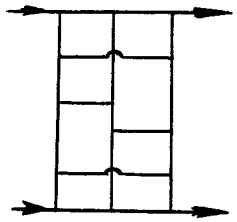


Fig.1b

We generalize here this important result for the case of an arbitrary number of particles in t-channel.

Let there be n_1+n_2 particles in t-channel, of which n_1 emit and n_2 absorb an arbitrary number of particles. Fig.2 gives the example of the considered diagrams.

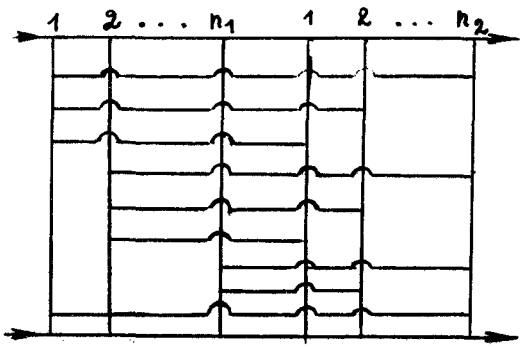


Fig.2

The detailed analysis shows that any line from n_1 group can be connected with any line of the n_2 group, giving thus the additional factor $g^2 \ln \frac{s}{m^2}$. The connections between one group lines are not essential giving the factor $\sim g^2$. Leading logarithmic asymptotics of the diagram of an elastic scattering with $n = n_1+n_2$ particles in the t-channel and L horizontal lines has a form ($\vec{q}$ is the transverse momentum):

$$\frac{-i\,(s/m^2)^{-n+1}}{(L+m_1)!}\, g^{2(L+n)} \left(\ln \frac{s}{m^2}\right)^{L+m_1} \mathcal{K}(\vec{q}),$$

$$\left(m_{1(2)} = \max_{(\min)} (n_1, n_2)\right). \qquad (1)$$

First, consider small $\vec{q}$ values ($|\vec{q}| < n m$). Summing all the topologically different diagrams of the $2(L+n)$ order obtained by means of the rearrangement of horizontal lines as well as of all the possible crossings of vertical lines both within n_1 and n_2 group and the crossings of n_1 group lines with n_2 group ones, and summing over L we find the following asymptotics (for $\vec{q}$ =0):

$$-i\left(\frac{g^2}{m^2}\right)\left[K_0(2\gamma)\right]^{m_2-m_1}\left(\frac{2}{\gamma^2}\right)^{m_1-1}\left(\frac{1}{8\pi^2}\right)^{m_2-1} \times$$

$$\times \left(\frac{s}{m^2}\right)^{\alpha^{(n_1,n_2)}(0)} \delta_{n_1 n_2}, \qquad (2)$$

where

$$\alpha^{(n_1,n_2)}(0) = -n+1+n_1n_2\frac{g^2}{16\pi^2}\left(\frac{\gamma}{m}\right)^2 K_0^2(2\gamma) \quad (3)$$

(γ- is an arbitrary constant connected with our inability to solve n- body problem exactly),

and

$$\delta_{n_1n_2} = \left[1+\exp\left(i\pi\left(-1+\frac{g^2}{16\pi^2}\frac{\gamma^2}{m^2}K_0^2(2\gamma)\right)\right)\right]^{n_1n_2} \quad (4)$$

is a signature factor.

The most essential result here is the appearance in (3) of the term with n_1n_2 factor, which means that, in principle, multiparticle states in t-channel may lead to a positive intercept in the field theory with spinless particles.

Formulae (2)-(4) show that we deal with n_1n_2 effective ladders coalesced along all the length of their ribs. In spite of this coalescence each ladder preserves its individuality as it seem from structure of signature factor.

The singularity (3) is a pole.

For $\vec{q}\neq 0$ $(|\vec{q}| \ll nm)$ we have:

$$\alpha^{(n_1n_2)}(\vec{q}) = -n+1+\frac{g^2}{16\pi^2}\frac{\gamma^2}{m^2}K_0^2(2\gamma)n_1n_2 \quad (5)$$
$$\left[1-\frac{\beta\vec{q}^2\gamma^2}{n^2m^2}\right]$$

where β is constant of order of unity.

For the slope of multiparticle Regge pole trajectory it is easy to obtain:

$$\alpha'^{(n_1,n_2)} = \frac{4n_1n_2}{(n_1+n_2)^2}\alpha'^{(1,1)} \quad (6)$$

where $\alpha'^{(1,1)}$ is the slope for simple ladder with two particles in t-channel.

For $|\vec{q}| \gg nm$ we have:

$$\mathrm{Re}\,\alpha^{(n_1,n_2)}(\vec{q}) \approx -n+1+n_1n_2n^2\times \quad (7)$$
$$\times\frac{g^2}{16\pi^2}\frac{1}{q^2}\ln^2\left(\frac{2|\vec{q}|}{nm}\right).$$

Thus, the observed multiparticle Regge poles realize the Mandelstam conjecture /5/ that multiparticle states in the t-channel is to provide the linearity of Regge trajectories. Figure 3 illustrates this fact.

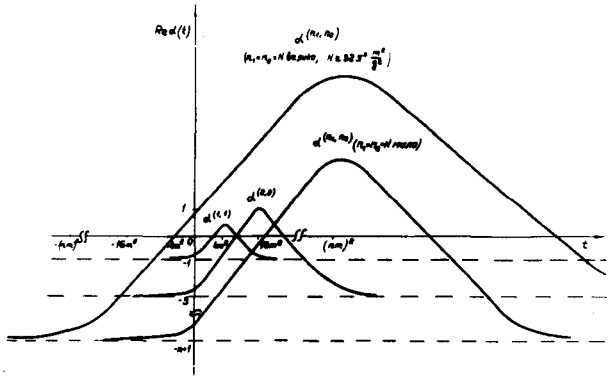


Fig.3

References

1. S.G.Matinyan, A.G.Sedrakeyan. JETP Lett., 23, 588 (1976).
2. S.G.Matinyan, A.G.Sedrakyan. Yadern.Fiz., 25, N 11 (1976).
3. S.G.Matinyan, A.G.Sedrakyan. JETP Lett., 23, 116 (1976).
4. B.M.McCoy, T.T.Wu. Phys.Rev., D12, 546, 578 (1975).
5. S.Mandesltam, (1966) Tokyo Summer Lectures in Theor.Phys., Syokabo, Tokyo and Benjamin, New York (1967).

UNIVERSALITY OF HADRON MULTIPLICITY IN COLOR-GAUGE THEORY MODELS

J.F.Gunion
University of California, Davis, USA

We are accustomed to the idea that in e^+e^- annihilation the final state begins as a fast separating q-$\bar{q}$ pair, and that the final state hadrons are produced in order to prevent the appearance of quark quantum numbers. The multiplicity intuitively must increase as the relative rapidity of the q and $\bar{q}$ increases. This report describes briefly a model in which these ideas can be quantified and extended to other interactions such as deep inelastic and hadron hadron soattering.

First we recall the remarkable multiplicity universality studied by Albini et al./2/. They fit $pp \to X$ average multiplicity by hadron hadron;

$$\langle n \rangle_{pp\to X} = 2.50 + .28 \ln E_r + .53 \ln^2 E_r \equiv f(s_r) \quad (1)$$

where $E_r = \sqrt{s_r} = \sqrt{s} - m_a - m_b = \sqrt{s} - 2m_p$ (Note that a $\ln^2$ term is required to describe the full range of data). They then note that this same function, f, describes multiplicities in many other processes. In particular

e^+e^- annihilation;

$$\langle n \rangle_{e^+e^-\to X} = f(s), \; s = E^2_{CM}; \quad (2)$$

and

deep inelastic;

$$\langle n \rangle_{ep\to e'X} = f(W^2), \; W^2 = 2MV - Q^2 \quad (3)$$

among others.

Secondly we remind the reader that in all these cases, (1)-(3) the produced particles form jets. The collection of particles of limited p_T along the beam target axis in (1) is just as much a jet as similar colleotions observed in (2) and (3). We shall see that both the universality summarized in (1)-(3) and the jet structure is expected in a model where separation of color quantum numbers results in radiation of soft oolored vector gluons, whioh in turn materialize into hadrons /2/.

We begin by abstraoting the basic features of such a model and return to specific details momentarily. The multiplioity in such a model is a funotion of: a) the color quantum #'s of the separating objects; b) the relative rapidity $Y_{12} \approx 2p_1p_2/m_1m_2$ of the objects (labeted 1 and 2)

$$\langle n \rangle = f(\text{color Q \#'s; relative } Y_{12}) \quad (4)$$

Flavour quantum numbers, eto., of the objects which are moving apart are irrelevant. In e^+e^- we know of course that one makes a 3 and $\bar{3}$ of color moving in opposite directions in the oenter of mass. Since $2p_3p_{\bar{3}} = s$ we have

$$\langle n \rangle_{e^+e^-} = f(3\text{-}\bar{3}; s). \quad (5)$$

In deep inelastic soattering the massive photon strikes quark in the incoming color singlet hadron forcing it to separate from the rest of the quarks in the hadron (the collection of which we call the "oore"). If the hadron has momentum p, the struok quark has final momentum $xp+q$ $\left(\omega = \frac{2MV}{Q^2} = \frac{1}{x}\right)$ the oore has momentum $(1-x)p$. Thus we establish immediately after the interaotion a separating 3 and $\bar{3}$ of color with $2p_3p_{\bar{3}} = 2(xp+q)(1-x)p) = W^2$. Hence

$$\langle n \rangle_{ep\to e'X} = f(3\text{-}\bar{3}; W^2) \quad (6)$$

is indepent of Q^2 at fixed W^2 as experimentally varified. Note that we have not needed to refer the "hole"-quark communioation or equality of e^+e^- and hadron plateau

heights in order to derive (6)[3] . Our one assumption is that the 3 or "core" state can be treated as a single radiating particle with a mass near that of the original bound state proton. As the momentum fraction $x \to 0$ the quark probed comes, in general from "sea" multi-$q\bar{q}$ pair states of the struck hadrons Fook space. Thus our core will consist of many quarks but all, we presume, with the same velocity and thus part of coherent state. This assumption may hold in a strong coupling limit but is quite orthogonal to standard multiperipheral approaches to the quark Fock space states. Additional arguments in support of the $x \to 0$ continuation appear in Ref.2.

Turning now to hadron-hadron collisions we may visualize (in the center of mass,e.g.) their interaction as occuring by annihilation of a low momentum quark in one hadron with a low momentum antiquark in the second hadron. Immediately after this annihilation the $\bar{3}$ and 3 cores at the respective hadrons are travelling in opposite directions along the collision axis, with essentially the full momenta of the hadrons. Thus $2p_3 p_{\bar{3}} = s$ and the multiplicity of hadrons will be

$$\langle n \rangle_{HH \to X} = f(3\text{-}\bar{3};\, s) \qquad (7)$$

In the case of hadron scattering it is clear that only $q\bar{q}$ annihilation leads simply to universality of multiplicity. For instance in the Low-Nussinov model of the Pomeron [4] the interaction between incoming hadron color singlets occurs via exchange of a colored (octet) gluon so that the incoming hadrons are transformed into rapidly separating color octets. Simple group theory yields

$$\langle n \rangle_{HH \to X}(\text{gluon exchange}) = f(8\text{-}8;\, s) \simeq \frac{9}{4} f(3\text{-}\bar{3};\, s), \qquad (8)$$

so that at the same s (corrected for mass effects as below (1)) $\langle n \rangle_{HH \to X} \neq \langle n \rangle_{e^+e^- \to X}$ contrary to experiment. In the same model one expects the multiplicity in deep inelastic processes to change by a factor of $\frac{9}{4}$ at fixed W^2 as one goes from the valence dominated region $(x > \frac{1}{2})$, where $3\text{-}\bar{3}$ separation chearly occurs, to the "Pomeron" region $(x < .1)$, in which the gluon exchange (present in HH) should dominate.

Turning now to specific details we wish to calculate the multiplicity of colored gluons radiated from a separating 3 and $\bar{3}$ of color. This problem is entirely analogous to soft photon radiation from separating charges [5] ; if we presume that the n gluon cross section follows a poisson, as in the usual QED soft photon-problem, then we may calculate $\langle n \rangle_{\text{gluons}}$ from lowest order diagrams. The result is (in the c.m. frame with cos angle of gluon w.r.p. to the 3)

$$\langle n \rangle_{\text{gluons}} \propto \int \frac{dK}{K} \int \frac{d\cos\theta\,(\beta_3 + \beta_{\bar{3}})(\cos^2\theta - 1)}{(1 - \beta_3 \cos\theta)^2 (1 + \beta_{\bar{3}} \cos\theta)^2}. \qquad (9)$$

Eq. (9) has two logarithmic singularities; one arises from $\cos\theta = \pm 1$ and the second from the $\frac{dK}{K}$ photon momentum integral. The $d\cos\theta$ integral in fact gives directly the relative $3\bar{3}$ rapidity (i.e. a plateau in $\frac{dn}{dy_{3\bar{3}}}$) while the $\frac{dK}{K}$ integral can cause the plateau to rise as indicated by (1). The result is (for $p_3 p_{\bar{3}} \to \infty$)

$$\langle n \rangle_{\text{gluons}} = \frac{4}{3} \frac{\alpha_s}{\pi} \left\{ \ln \frac{2p_3 p_{\bar{3}}}{m_3 m_{\bar{3}}} \left(\ln \frac{2p_3 p_{\bar{3}}}{K^2_{\min}} + C_1 \right) + C_2 \right\} \qquad (10)$$

where the infrared cutoff $K_{\min}$ is a natural result of the fact that long wave length gluons cannot give rise to color singlet hadrons if $\lambda > R_{\text{hadron}}$. For $\lambda > R_{\text{hadron}}$ all the final hadrons appear to be "neutral" and the gluon coupling vanishes.

We, of course, imagine that the emitted gluons turn into quark-antiquark pairs which

then match up to form hadrons. Thus

$$\langle n \rangle_{hadrons} \approx \langle n \rangle_{gluons} \qquad (11)$$

and by using the fit (1) and the theoretical form (10) we obtain $\alpha_s \approx 0.46$. There are several other interesting features of this theory but we mention only one. Consider the fragmentation regions in hadron hadron collisions. In our approach particles with substantial x_F do not arise from the soft gluon emission subsequent to the $q\bar{q}$ annihilation (which defines the interaction). Rather they are most probably fragments of the fast quark cores which appear immediately after the annihilation. The dimensional counting rules then make a specific prediction for the x_F dependence as $x_F \to 1$. In general

$$F(x_F) \propto q_{H/H_1\,core} \propto (1-x_F)^{2n_s-1} \qquad (12)$$
$$H_1 \to H; H_2$$

where $q_{H/H_1\,core}(x)$ is the probability for the core of H_1 to emit a secondary H with fraction x of its momentum and n_s is the minimal number of spectator quarks left over after the emission. For example consider $pp \to \pi^+ + X$. The minimal core following interaction capable of emitting a π^+ consists of a (pn) quark pair, Upon emitting a π^+ the minimal spectator system is a pair of (nn) quarks. Thus $n_s = 2$ and $F_{p\to\pi^+;p}(x_F) \propto (1-x_F)^3$ independent of t and p_T . Experimentally the power is ≈ 3.5 and is in fact independent of t and p_T . The tripls Pomeron theory does not yield this result in any natural way. Note also that in Low's Pomeron model the pp interaction leaves a minimum of three quarks continuing in opposite directions along the beam target axis. Fragmentation into a π^+ then leaves behind a least 3 spectators for which $F_{p\to\pi^+;p}(x_F) \propto (1-x_F)^5$ a somewhat high power for agreement with existing data.

Thus while no formal field theory has been solved which realizes all of our key assumptions, the basic picture provides both a qualitative and quantitative explanation of all the basic features and relations between hadron production in the full variety of experimentally accessible processes.

References

1. E.Aibini et al. Bologna preprint (1975).
2. The present report is a summary of the papers "Hadron Multiplicity in Color Gauge Theory Models", S.J.Brodsky, J.F.Gunion, VCD-SLAC-preprint (1976) and in preparation.
3. For the standard approach involving such a separation see, for example, J.Bjorken and J.Kogut. Phys.Rev., D8, 1341 (1973).
4. F.E.Low. Phys.Rev., D12, 163 (1975). S.Nussinov. Phys.Rev.Lett., 34, 1286 (1975).
5. For relevant standard infrared photon formulae see, for example, D.R.Yennie Brandeis Summer Lectures in Theoretical Physics, v.1 (1963).

PLENARY REPORT

HIGH ENERGY THEORY OF STRONG INTERACTIONS

V.A.Matveev
Joint Institute for Nuclear Research

Development of strong interaction theory at high energies can be overlooked by following two supplementary directions: surveying the current theoretical approaches and models- on the one hand,and analysing recent experimental results which give us information about the dynamics of strong interaction- on the other hand.This formidable task can be solved only by all the speakers summarizing their efforts in discussions at parallel sessions AI-A5.

The contents of this talk are arranged as follows:

I. General results in QFT
II.Theory of diffraction scattering and the vacuum exchange
III.Regge/quark analysis
IV. High energy scattering in models of QFT
V. Constituent theory of hadron interactions
VI. Power laws
VII. Scaling and similarity laws
VIII. Concluding remarks

I.GENERAL RESULTS IN QFT

I.QFT as a guide to the theory of strong interactions.

The general principles and results of the local QFT are the basis of the most of theoretical constructions and phenomenological analysis in studying strong interaction phenomena at high energies.

One of the most successful methods through the years, was the method of dispersion relations introduced into the QFT by Gell-Mann,Goldberger and Thirring.

In the papers by Bogolubov on the theory of dispersion relations the fundamental idea of scattering amplitude as a unique analytic function of its kinematical variables has been introduced for all the physical channels connected by crossing symmetry relations. This concept proved to be very useful in attempts to understand the existing theoretical schemes and phenomenological approaches as possible approximations to the theory of strong interactions.

Use of the analyticity of amplitudes as functions of momentum transfer related to the short range character of nuclear forces has been particularly fruitful in the study of strong interactions at high energies.

First of all, this has led to the derivation of a number of fundamental asymptotic relations and bounds on the cross sections. This concept has also served as an adequate tool for introducing the Regge ideas to QFT and for developing the quasi-optical picture of the high energy hadron scattering processes.

The most crucial problem of the field theory approach to the theory of strong interactions nowdays is the problem of consistent incorporation of the idea of the composite quark structure of hadrons.

2. Asymptotic bounds and theorems

As is well known, analytic properties of scattering amplitudes in transferred momentum lead to the ultimate relation between high energy behaviour and t-channel singularities. A number of new results have been recently found in that direction.

In the paper by Logunov,Mestvirishvili et al.[1] submitted to this conference, the question has arisen:"Do u-channel singularities in the complex t-plane influence the high energy behaviour of the forward scattering cross sections?" The basic assumptions made in this paper are as follows:

1. Existence of dispersion relations in t at $s > s_{thr.}$ with a finite number of subtractions.
2. Polynomial boundness at large s.

The answer given by the authors is no! Namely,the relative contribution of the u-channel singularities is bounded asymptotically by

$$\left|\frac{T_u(s,\theta=0)}{T_t(s,\theta=0)}\right| \lesssim \frac{\ln^2 s}{s}$$

in the case of the non-decreasing total cross sections.

This result which is based essentially on the dispersion relations and unitarity gives a rigorous extension of the principle of nearest singularity dominance from the high energy behaviour of absorptive part:

$$\mathrm{Im}\, T(s,t=0) = s\,\sigma_{tot.}$$

to the complete amplitude

$$T(s,t=0) = s\,\left(\frac{d\sigma}{dt}\right)^{\frac{1}{2}}_{t=0}.$$

The result has been improved in the work by Rcheulishvili and Samokhin[2] where the more restricted domain of analyticity in the complex Cosθ-plane was considered (see Fig.I).

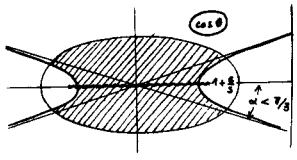


Fig.1.The analyticity domain in CoS -plane as being assumed in the paper[2] (dashed region).

It is argued that scattering in the forward (backward) cones at high energies is determined by singularities which lie in the right(left) half-planes of Cosθ.

Interesting results are found in the recent paper[3] titled as "Why is the diffraction peak a peak?" An attempt is made here to find rigorous and general (as much as possible) answers to a number of questions concerning the asymptotic characteristics of the diffraction peak, namely, whether:

(?) the high energy differential cross section has a maximum exactly in the forward direction;

(??) the slope of the diffraction peak is determined by the absorptive part of scattering amplitude;

(???) the slope parameter is really bounded by $\log^2 s$, etc.

The positive answers to all the questions listed above were found in this paper. Moreover, it was pointed out that the oscillating cross sections are allowed, that the real part of scattering amplitude should not be small and so on.

In two papers by Mnatsakanova and Vernov(jr.)[4] submitted to this conference, a justification of a number of rigorous asymptotic bounds on scattering amplitudes and cross sections is given which are effective on finite energy intervals.

An analysis of analytic properties of scattering amplitudes in local QFT and a review of available axiomatic restrictions on high energy hadron scattering are presented in papers[5].

2. Quasi-local dispersion relations

Evaluation of the real part of a scattering amplitude in terms of an integral over the imaginary part by means of the dispersion relations is a formidable task because of the essentially non-local character of these relations. The quasi-local form of these relations or the derivative analyticity relations have attracted general attention in the last few years[6]. It was found that the DAR provides a simple and effective approximation for the conventional dispersion relations of the real part calculations at high energies if the threshold and resonance effects are unimportant. Moreover, it was proposed to use the DAR as a tool for complete reconstruction of a scattering amplitude from experimental data at asymptotic energies.

In the paper by V.A.Mescheryakov et al.[7] submitted to this conference, another form of quasi-local dispersion relations was presented which is based on the method of uniformization of scattering amplitude at high energies (or UM). It was proposed to use as a uniformization variable the eq.

$$w(\nu)= \frac{I}{\pi} \arcsin\nu = \frac{I}{2} + \frac{i}{\pi}\ln|\nu+\sqrt{\nu^2-I}|,$$

where $\nu=(s-u)/4m$ and $\mu=I$. At $\nu\gg I$, $w(\nu)\sim -\frac{I}{i\pi}(\ln s - i\pi/2)$ which points to complex logarithmic structure of the Riemann surface of a forward scattering amplitude as a function of the energy variable ν.

The function $w(\nu)$ gives a mapping of the whole Riemann surface of a scattering amplitude on the complex w-plane by a system of strips (Fig.2). The image of the physical sheet is the strip: $-\frac{1}{2} < \mathrm{Re}\, w < \frac{1}{2}$. The forward scattering amplitude determined by the formula $\mathrm{Im}F_{\pm} = (\sigma \pm \bar{\sigma})$ has the kinematical poles at $w = n+\frac{1}{2}$, so as $F_{\pm} = f_{\pm}/\sqrt{\nu^2-I} = \frac{f_{\pm}(w)}{i\cos\pi w}$

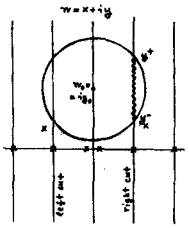


Fig.2. The map of the Riemann surface of the forward scattering amplitude. x - position of poles.

The analyticity and the symmetry relations

$$F_{\pm}(w) = \pm F_{\pm}(-w)$$
$$F^*_{\pm}(w) = -F_{\pm}(w^*)$$

lead to the generalization of DAR:

$$F^*_{\pm}(w) = \mp e^{-2x\frac{d}{dw}} F_{\pm}(w), \quad (w=x+iy).$$

The method has used as a tool for analysis of experimental data. Assume that $F = u+$ if is a holomorphic function within the circle $|w-w_0| \leqslant R$ (see Fig.2) so that $V(x,y)$ is harmonic there, i.e. $\Delta V = (\partial_x^2 + \partial_y^2)V = 0$. By the theory of analytic function[8]

$$F(w) = 2iV\left(\frac{w+w_0}{2}, \frac{w-w_0}{2i}\right) + F^*(w_0).$$

Determining $V(x,y)$ by its decomposition in the convergent (in the circle) series

$$V(x,y) = \sum_{n=I,..} \sum_{m>2n-1} a_m \frac{(-)^{n+I}(m-I)!}{(m+I-2n)!} (y-y_0)^{m+I-2n} \times$$

$$\times \begin{cases} \dfrac{x^{2n-2}}{(2n-2)!} & (\text{for } F_+) \\ \dfrac{x^{2n-I}}{(2n-I)!} & (\text{for } F_-) \end{cases}$$

one gets the decomposition of a forward scattering amplitude in powers of $y(\approx \log s/\pi)$ convergent in some finite interval of energies:

$$y^- \leqslant y \leqslant y^+ \; ; \; y^{\pm} \approx \frac{I}{\pi} \log^2 \nu_{\pm} = y_0 \pm (R^2 - \tfrac{1}{4})^{\frac{1}{2}}.$$

By fitting experimental data on πp, Kp and pp-scattering (with the only parameters $a^{+}_{I,2,3}$ and a^{-}_{I} and $c=F_{-}(iy_0)$) the authors have tested a number of quark relations among the total cross sections. It was found that Lipkin's sum rule

$$^{2}/_{3}\sigma_{tot}(\pi^{-}p)+{}^{1}/_{3}\sigma_{tot}(\pi^{+}p) = {}^{1}/_{2}\sigma_{tot}(K^{+}p)+{}^{1}/_{3}\sigma_{tot}(pp)$$

has to be hold with 3% accuracy from P=10 GeV/c up to 10^3 GeV/c .

T A B L E

Test of Lipkin's sum rule(L and R are the left- and right-hand sides of the relation)

	(L)	(R)
p_z (GeV/c)	L (mb)	R (mb)
200	24.14±0.05	23.69±0.07
400	25.05±0.05	24.45±0.08
600	25.83±0.06	25.13±0.10
800	26.48±0.07	25.71±0.12
1000	27.04±0.08	26.23±0.14
1200	27.54±0.09	26.69±0.16
1400	27.99±0.09	27.10±0.18
1600	28.40±0.10	27.48±0.20
1800	28.78±0.11	27.83±0.21
2000	29.13±0.12	28.15±0.23

Works with 3% accuracy from P=10 up to 10^3GeV/c

II. THEORY OF DIFFRACTION SCATTERING AND THE VACUUM EXCHANGE

I. Models of the fast growth

Five years ago the flattering out of the hadron total cross sections and the growth of σ_{k^+p} with energy have been observed in experiments at IHEP and named "Serpukhov's effect". The foregoing experiments at CERN and FNAL have shown universality of the total cross section energy growth[9].

This effect which is not quite unexpected due to the Froissart theorem known from 1961, did not explain nevetherless, by the popular at that time, the theory of complex angular momenta in its original form. So many different models have appeared, namely: field theory models, quasi-optical models, regge-eikonal models and others, where different approaches in the description of the total cross section energy growth as well as of the whole range of diffraction phenomena were developed.

Notice that a simple and physically lucid description of the cross section energy growth is given in the framework of the hadron scattering quasi-optical picture[10].

It was known for a long time that the energy dependent smooth local quasi-potential allows one to reproduce the main features of the high energy hadron scattering. The polynomial growth of the strength of interaction depending on the energy leads to the maximal energy growth of a total cross section permitted by the s-channel unitarity [11].

In the papers by Khrustalev and Tyurin [12] and Tyurin et al. submitted to this Conference, the quantitative description of the total cross section energy growth as well as of other observable quantities of the high energy πN-scattering was given on the basis of the U-matrix method. The U-matrix is related to the scattering amplitude T by the relativistic one-time dynamical equations

$$T = U + \int_{\text{phase volume of real particles}} U \cdot T \, dw$$

proposed by Logunov, Khrustalev, Savrin and Tyurin in 1970 [13]. By analytic continuation into the t-channel $U \to \tilde{U}$ and using the Regge-pole expansion for $\tilde{U}_{-}$, the authors of the paper [12] developed a method for description of the high energy scattering which allows one to take into account the unitarity in the direct s-channel (by construction). Thus, a good fit to the experimental data is found with polynomially growing $\tilde{U} \sim s^{\alpha}$ where $\alpha > 1$ without contradicting the Froissart theorem (see Fig.3).

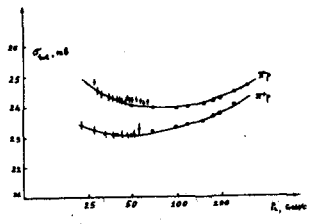


Fig.3. The total cross-section of $\pi^{\pm} p$ scattering in the U-matrix approach.

One of the first detaild analyses of an assumption that the high energy hadron scattering observed at Serpukhov and also at CERN and FNAL realize the maximal energy growth of the scattering amplitudes, was made in the papers by L.D.Soloviev [14] and Soloviev and Schelkachev [15]. The authors introduced there the term "model of the fast growth". Determining the complete scattering amplitude as a sum

$$T = T_{\text{Froissart}} + T_{\text{Regge}} ,$$

where the "Froissart" part at finite energies has the form

$$T_{\text{Froissart}} \sim i \, \delta R^2 \exp(xt/2) \cdot J_1(Rq)/Rq ; \quad q=\sqrt{-t}$$

$$R^2 = \rho^2 + R_0^2(s) ; \quad R_0^2(s) = \frac{I}{M^2} \log^2 s/s_0 ,$$

the authors have found a good description of existing experimental data with the universal energy growth for all the hadronic total cross sections (excluding pp-scattering cross sections)

$$\sigma_{tot} \to 2\pi R_o^2 \simeq c \log^2 s/s_o$$

The fit gives c (0.2 ÷ 0.4)mb or for an effective mass of exchange states M≈(I.3 ÷ 3.0) Gev/c^2 (too high as compared with the pion mass). The authors state that B is too small to be observed at available energies due to the kinematical suppressing the $\log^2 s$ term (see Fig.4 a,b- illustrating the fit)

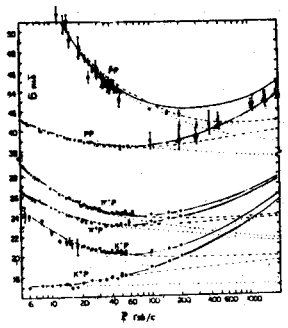


Fig.4a. Total cross sections in the model of "fast growth".

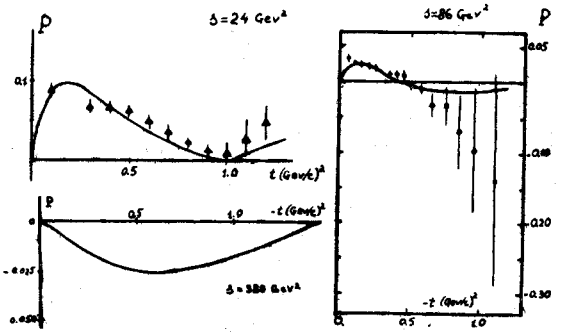


Fig.4b. Polarization in pp-scattering.

An analysis of the high energy hadron scattering in terms of j-plane leading singularity with $\alpha(0) > 1$ was performed in the papers by Dubovikov and Ter-Martirossian[16], Kopeliovich and Lapidus[17] and others[18], who used s-channel unitarization by means of eikonal representation.

2.Nature of the vacuum exchange

Idea of the Regge-poles proved to be very fruitful in the analysis of the high energy hadron reactions. There is a clue of complex problems of the Regge-approach still waiting for their solution. One of them is the nature of the vacuum exchange(the Pomeranchuk singularity). From the time when it was postulated in order to explain the gross features of diffraction scattering,especially the miraculous constancy of total cross sections the term "Pomeron" is still an enigma.

This notion is surrounded by a constellation of different effects, such as: self-consistent j-plane singularity or Reggeon field theory(RFT), critical phenomenon in RFT,Goldstone particle, "cylinder"topology contribution in dual theory, multiparton fluctuations, "bag" model (with colored gluon exchange), "glue balls" and many others [19- 26].

Some of these approaches were discussed at parallel session A5. This rich circle of questions is beyond of scope in our talk and will be discussed by the following speakers(see Kaidalov's talk) Here we only briefly mention some points. In the paper by Sugar et al[20], the Reggeon field theory is studied in zero transverse dimensions,i.e.,at d=0. By means of renormalization group the existence of the infrared stable fixed point is found. It is pointed out that the solution has no bona fide second order phase transition.[21]

In the paper by Dyatlov[24] a theory of the weak-coupled Pomeron as a Goldstone particle was presented. The bound states of two Pomerons are found in this theory which can be useful in explanation of the diffraction peak structure. Unfortunately,this leads to the non-analyticity in transferred momenta at t=0.

The RFT on a lattice for $\alpha(o)>1$ is studied in the paper by Amati et al.[25] Using the low-lying structure of an excitation spectrum the existence of the critical phenomena(second order phase transition) is found which is characterized by the value of α_c more than unity. The final asymptotic picture is that of a grey disc expanding like logs so that the total cross sections grow like $(\log s)^2$, if $\alpha(o)>\alpha_c$. For $\alpha(o)<\alpha_c$ the total cross sections drop as the universe powers of s.

In the paper by Matinyan et al.[26] the Regge-pole singularities associated with the multiparticle states in t-channel are studied and their role in solving the Mandelstam's program of the linear Regge trajectories is discussed.

III.REGGE/QUARK ANALYSIS

I. Regge behaviour vrs.SU_3/quark structure

Merger of the idea of the Regge(power-like) behaviour with the quark constituent theory,dual model and internal symmetries gives an effective tool for analysis of experimental data.

In the last years a considerable attention has been attracted to the study of the energy dependence of hadron scattering versus SU_3/quark structure of the scattering amplitudes.

Differents authors give various results for the dominant power term $s^{\alpha_p(0)}$ (which might be the case either $\alpha_p(0)=I$ or $\alpha_p(0)>I$ or even $\alpha_p(0)<I$) as well as for the SU_3 structure of the Pomeron couplings (different mixtures of the singlet and octet components).

The reason for such wide variations of possible values of the leading singularity position can be illustrated by Fig.5 from the paper [27].

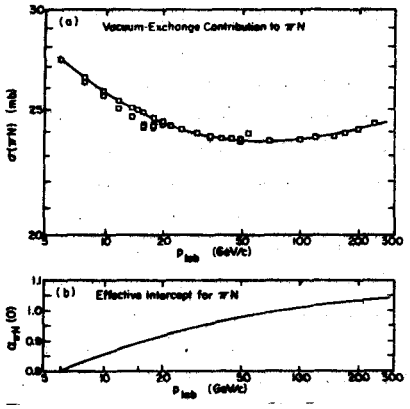


Fig.5(a). The vacuum-exchange contribution to πN total cross sections $\frac{1}{2}(\sigma_t(\pi^+p) + \sigma_t(\pi^-p))$

$\alpha_{\pi N}(0) > I$ at $P_{lab} > 70$ GeV/c .

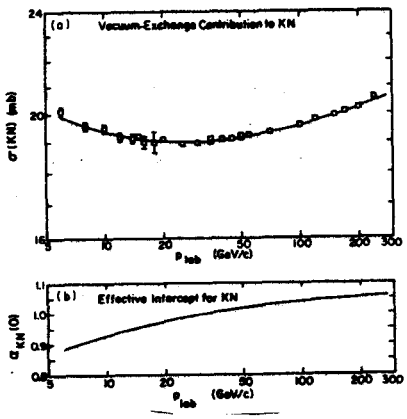


Fig.5(b). The vacuum-exchange contribution to KN total cross sections $\frac{1}{4}[\sigma_t(K^+p)+\sigma_t(K^+n)+\sigma_t(K^-p)+\sigma_t(K^-n)]$

$\alpha_{KN}(0) > I$ at $P_{lab} > 30$ GeV/c .

An effective power of energy dependence is determined by

$$\alpha_{eff}(P_{lab}) = \frac{\partial}{\partial \log p_{lab}} [\mathrm{Im}\, T(P_{lab}, t=0)]$$

which gives different values of $\alpha_p(0)$ for various energy intervals. This is in the qualitative accordance with DAR which relates the effective exponent α_{eff} to the ratio of the imaginary-to-real parts of scattering amplitude, i.e.

$$\alpha_{eff} \approx I + \frac{2}{\pi}\rho(P_{lab}, t=0), \qquad \text{(DAR)}$$

So, α_{eff} exceeds unity where ρ is negative. The detailed analysis shows the dependence of a spectrum of Regge singularities with the vacuum quantum numbers on the assumed SU_3 or quark structure of hadron scattering amplitude.

2. SU_3- structure of the vacuum exchange

One usually describes the vacuum exchange amplitude as the sum of the Pomeron(diffraction) part and the f-pole(resonance-like or dual) part

$$\text{V.E.} = s^{\alpha_p}\hat{p} + s^{\alpha_f}\cdot\hat{f}$$

The SU_3 assignment is determined in the TABLE

	SU_3 - content		
		I	8
Regge terms	p	p_I	p_8
	f	f_I	f_8

Different possibilities for the SU_3-structure and the spectrum of Regge singularities in the vacuum exchange amplitude were considered [27-33]:

* Harari & Freund - P + R(f,f');
* Carlitz, Green, Zee (I97I) - P coupled trough f,f' $\alpha_p(0) = I$;
* Bali, Dash (I974), Chew, Rosenzweig (I975) - $p = f_0$, f'; $\alpha_p(0) \approx 0.85$
* Lipkin (I974) (p_I, p_2) + R, $\alpha_{p_1} \approx I.I3$: $\alpha_{p_2} \approx 0.8$
* Quigg, Rabinovici (I975) $p(\hat{I}+\hat{8}) + f_0$ (ideally mixed) $\alpha_p \approx I.075$
* Others.

No unique solution exists!

We mention here general trend, however. The SU_3 structure of the vacuum exchange depends on the transferred momentum (the Pomeron as a "chameleonic" object [31]).

For t-large and positive, p ideally mixed Regge pole: associated with planar diagrams (in terms of Veneziano's topological expansion [34]). The notion of asymptotic planarity [35] arises related closely to the problem of OZI-rule [36] (Freund, Nambu, I975 [37]).

For t-negative and large enough ($-t \geq 0.5$GeV/c^2) p is dominated by SU_3-singlet. This can be illustrated by Fig.6 from ref. [27], where the singlet (s) and octet(0) components of the non-forward scattering amplitudes for the πp- and Kp-systems are determined by

$$\frac{d\sigma}{dt}(\pi p) \approx |s+20|^2 \approx |s|^2 + 4\mathrm{Re}(s^*0),$$

$$\frac{d\sigma}{dt}(Kp) \approx |s-0|^2 \approx |s|^2 - 2\mathrm{Re}(s^*0).$$

An interesting question arises: at how large t will p be dominated by SU_4-singlet term(if any)? A simple estimation gives the comparatively low value:

$$-t_{cr} \sim \ln \frac{\sigma^2_{tot}(pp)}{\sigma^2_{tot}(p\psi)} / (b_{pp} - b_{p\psi}) \sim 1 \text{ GeV/c}^2!$$

Fig.6 (a)(b) The singlet- octet contributions to $d\sigma/dt$

(a) SU_3 - singlet part of vacuum exchange

(b) $Re(S^*O)/|s|$ octet part

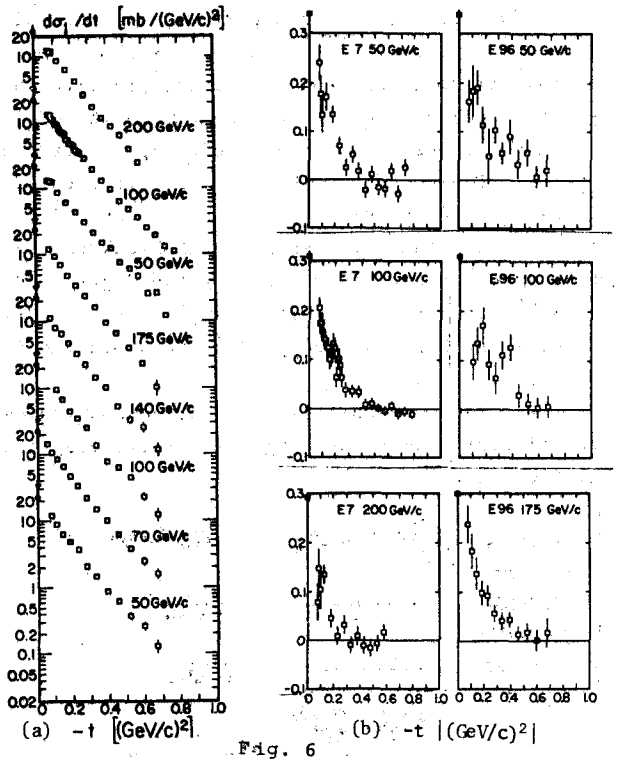


Fig. 6

3. Quark analysis of total cross sections

During the years the quark model was very successful in analysis of regularities in the asymptotic values and variations of the hadron scattering total cross sections. It is now time to ask the following questions:

* Why do some combinations of total cross sections grow, some not?

* Why $\sigma_{tot}(K^+p)$, $\sigma_{tot}(pp)$ and $\sigma_{tot}(\phi p) = 2\sigma_{tot}(Kp) - \sigma_{tot}(\pi p)$, all being pure Pomeronic in two-component duality, have different energy behaviour?

* Why does the Levin-Frankfurt rule [38] $\sigma_{\pi N}/\sigma_{NN} = 2/3$ work only with 10% accuracy and $(\sigma_{\pi N} - \sigma_{KN})$ decreases too slowly?

By the way, it has been noticed in 1971 by Prokoshkin and analysed in details by Denisov et al. [39] on the basis of the Serpukhov experimental data that the ratio

$$R = \frac{2\sigma_{\pi N}}{\sigma_{KN} + \frac{2}{3}\sigma_{NN}} = 1.020 \pm 0.015 \qquad (p_{lab} = 20 \div 60)$$

is consistent with the quark model predictions with much more accuracy than the others.

One of the possible answers to these questions was given by Lipkin who has proposed the three-component picture for the high energy hadron scattering (the first two components for the vaccum exchange, and the third one- for the Regge-pole contribution [40]).

It was assumed that the second vacuum component contributes to πN, KN and NN forward scattering as respectively $2:1:9/2$. Thus, the following sum rule is satisfied:

$$\sigma_{\pi N} = \tfrac{1}{2}\sigma_{KN} + \tfrac{1}{8}\sigma_{NN} \qquad \text{or } R = 1.$$

The model can be formulated in terms of the specific total cross sections $Y_a = \sigma_{a/n_a}$ (per single quark of a projectile for nucleon as a target:

$$Y = \alpha + \beta \cdot n_{\text{non-strange quarks}}$$

Two terms in this expression belong to the first (p_1) and second (p_2) components of the vacuum exchange. In these terms the famous ratio R=1 corresponds to the equidistance rule $Y_\pi - Y_K = Y_N - Y_\pi$. Notice that while the differences $Y_\pi - Y_K$ and $Y_N - Y_\pi$ pick out the second p_2-component, the differences $Y_\phi = 2Y_K - Y_\pi$ and $Y'_\phi = Y_\pi + Y_K - Y_N$ separate the first p_1 - component with an energy dependence different from that of the previous one: p_1 is slowly increasing ($\sigma \sim s^{0.07}$ or powers of log's); p_2 is slowly decreasing ($\sigma \sim s^{-0.2}$).

A number of interesting generalizations was proposed in [41-42]. The simplest is given by $Y = \alpha + \beta n_{\text{non-strange}} + \gamma n_{\text{str.}}$ which leads to the relations between total cross sections of baryons and hyperons:

$$Y_\pi - Y_K = Y_K - Y_\phi = Y_N - Y_{\Sigma/\Lambda} = Y_{\Lambda/\Sigma} - Y_\Xi, \text{ etc.}$$

In the paper by Joynson and Nicolescu [41] submitted to the Conference, the new interesting relation between total cross sections is proposed

$$2\sigma_{\pi^+ p} - \sigma_{\pi^- p} = \frac{7}{16}\sigma_{K^+ p} + \frac{3}{8}\sigma_{pp},$$

which is in a surprising agreement with experimental data (see Fig.7). The authors interpret this by introducing the special form of the second vacuum component for the total cross sections

$$\sigma_{p_2} \sim \frac{1}{n_a n_b} \sum_{i \in a,\, b} y_i^2,$$

where y_i are hypercharges of quarks in the colliding hadrons a and b.

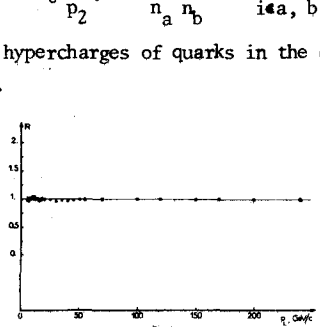


Fig.7. Test of the Joynson - Nicolescu sum-rule. The quantity plotted is

$$R = (2\sigma_{\pi^+ p} - \sigma_{\pi^- p}) / (\tfrac{7}{16}\sigma_{K^+ p} + \tfrac{3}{8}\sigma_{pp}).$$

IV. HIGH ENERGY SCATTERING IN MODELS OF QFT. QED & QCD.

I.QED.

Investigation of the high energy asymptotic behaviour in different models of QFT has a long history.Most of these studies are based on the order-by-order calculations as well as on the non-perturbative methods like path-integral methods which were devoted to the problems of leading singularities and the eikonal approximation.

As was shown by Gribov,Frolov and Lipatov and by Cheng and Wu in I969 in the framework of the massive QED, the main singularity in J-plane is not pole but a fixed branch point above unity,i.e.[43/]

$$T \sim s^{I+g^2 C}, \quad s \sim \infty$$

where $C > 0$ is the main logarithm approximation and different for the scalar and vector variants of QED. The evident contradiction with the Froissart theorem is interpreted as being due to the non-reggeization of the massive photon.

In a series of recent papers [44/] by Cheng and Wu,the asymptotic behaviour of the fermion-exchange processes and the related question of the fermion reggeization are studied in the framework of QED up to the record of I2-th order in coupling constant.[45/]

There are few new results on the eikonal approximation in the models of field theory.[46-49/] The asymptotics of "twisted" graphs(obtained by an interchange of two nucleons in the ladder-type graphs being usually studied in works on the eikonal problem)have been found. This gave rise to an effect of a linkage of large nucleon momenta to the mesons,on the one hand,and to the violation of the simple eikonal formula with Yukawa-type interaction potential-on the other.[46/]The corresponding corrections to an effective high energy potential were calculated which have more singular behaviour in origin that the Yukawa term,e.g. $\sim \log r/r_o$. The relativistic eikonal representation for the scattering on composite particles was studied in papers [48/] by means of the path-integration method.

2. QCD (quantum chromodynamics)

Study of the high energy scattering in non-abelian gauge theories like QCD has recently attracted a great interest.[50/] In a number of papers [5I-64/] the following problems were attacked:

* What is the leading singularity in J-plane?
* Whether the gauge bosons reggeizes?
* Does the large angle elementary fermion scattering pass the point-like scaling?
* Whether there is a sign of the quark confinement in the high energy scattering amplitudes?

The last question is closely related to the whole problem of the infrared mechanism ("infrared slavery") for quark confinement in QCD which was studued in paper [64/]. It was shown by means of the order by order calculations that there is no quark confinement,and the Kinoshita-Lee-Nauenberg theorem[65/] is true in the perturbation theory for both the QED and QCD.

The result of the non-perturbative analysis developed in papers [6I-62/] on the basis of some renormalization group equations still preserve the general belief in quark confinement in the QCD. The most of results on the high energy scattering in the QCD are made by the order by order calculations up to 6-th (or up to the 8-th order [54/]) in coupling constant. The spontaneous breakdown of the gauge group is introduced by the Higgs mechanism [66/] into the 't-Hooft's gauge[68/] (by the Faddeev's and Popov's receipt [67/]) to avoid the infrared problems.

All the necessary elements of Feynman rules to calculate the high energy asymptotic graphs are listed below:

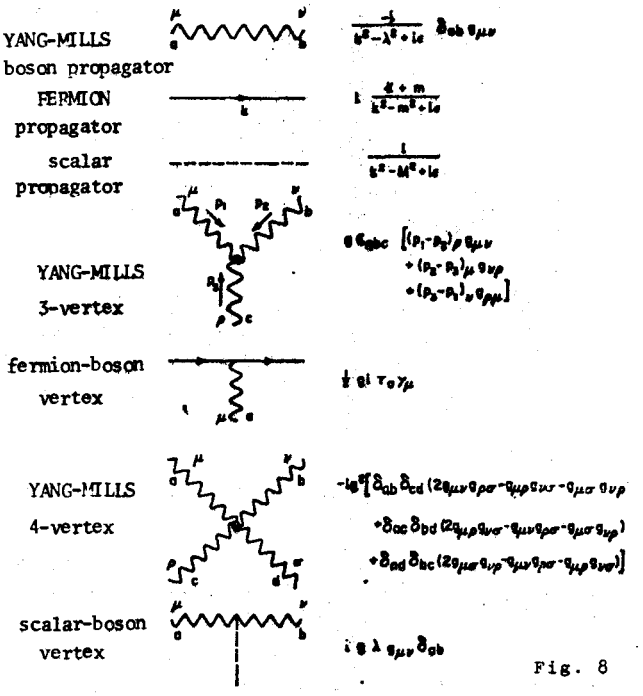


Fig. 8

These include the dimensional coupling of the Higgs scalar with the gauge bosons which goes to zero together with the mass of the vector boson λ (when the symmetry breaking switches off). The results of the calculations for the non-spin - flip amplitudes of the (ff),(fb) and (bb) processes up to the 8-th order can be summarized in the following way:

$$T(\text{non-spin-flip}) = \sum_{i=0,I,\ldots} T_i \Pi^{(i)} c_i$$

Here, T_i are the universal amplitudes with the t-channel isospin "i"; c_i are some normalization factors depending on channels, and $\Pi^{(i)}$ are the (color) isospin projection operators.

$$T_1 = I - g^2(\xi - \frac{i\pi}{2})f_1 + \frac{g^4}{2!}(\xi^2 - i\pi\xi)f_1^2 - \frac{g^6}{3!}(\xi^3 - \frac{3\pi i\xi^2}{2})f_1^3 + \ldots$$

that coincides with the decomposition in the leading log's approximation of the cross-odd Regge term.

$$s^{\alpha-1}(\frac{1-e^{-i\pi\alpha}}{2}), \quad \text{where } \alpha = 1 - g^2 f_1$$

$$f_1 = (\Delta^2+\lambda^2)D = (\Delta^2+\lambda^2)\cdot\int \frac{d^2k_\perp}{(2\pi)^3} \frac{I}{(k_\perp^2+\lambda^2)[(k_\perp-\Delta)^2+\lambda^2]},$$

$$T_0 = \frac{a}{\Delta^2+\frac{5}{4}\lambda^2} + (-\frac{a^2}{\Delta^2+\frac{5}{4}\lambda^2} + 4T)\, g^2\xi + \\ + (\frac{a^3}{\Delta^2+\frac{5}{4}\lambda^2} - 8aT + 4Q)g^4\frac{\xi^2}{2!} + \ldots$$

where $a = (2\Delta^2 + \frac{5}{2}\lambda^2)D$

$$T = \int \frac{d^2k_{1\perp}}{(2\pi)^3}\frac{d^2k_{2\perp}}{(2\pi)^3} \frac{I}{(k_{1\perp}^2+\lambda^2)(k_{2\perp}^2+\lambda^2)[(k_{1\perp}+k_{2\perp}-\Delta)^2+\lambda^2]}$$

$$Q = \int \frac{d^2k_{1\perp}}{(2\pi)^3}\frac{d^2k_{2\perp}}{(2\pi)^3}\frac{d^2k_{3\perp}}{(2\pi)^3} \frac{I}{(k_{1\perp}^2+\lambda^2)(k_{2\perp}^2+\lambda^2)(k_{3\perp}^2+\lambda^2)} \times \\ \times\left\{\frac{}{(k_{1\perp}+k_{2\perp}+k_{3\perp}-\Delta)^2+\lambda^2} + \frac{(q_{1\perp}+q_{3\perp})^2+\lambda^2}{[(k_{1\perp}+k_{2\perp}+k_{3\perp})^2+\lambda^2][(k_{1\perp}+k_{3\perp}+\Delta)^2+\lambda^2]}\right\}$$

This formula coincides with the decomposition of the expression

$$2s^{-a}(D + 2g^2\xi T + 2g^4\xi^2 Q + \ldots)$$

$$T_2 = \frac{b}{\Delta^2+2\lambda^2} + (\frac{b^2}{\Delta^2+2\lambda^2} - 4T)g^2\xi + \\ + (\frac{b^3}{\Delta^2+2\lambda^2} - 8\,b\,T + 8Q)\, g^4\frac{\xi^2}{2!} + \ldots$$

Here, $b = (\Delta^2+2\lambda^2)D$

Summing up the first terms in each perturbation order one gets s^b in violation of unitarity (no reggeization).

In terms of the reggeization properties the results consist of the following:

(color)- isospin in the t-channel	Reggeization
$I_t = I$	Yes
$I_t = 0$	?
$I_t = 2$	No

The problem of reggeization is not completely clear for the case of $I_t = 0$, because the following normalization factors found in the paper [54]

ff: $c_1 = -\frac{g^2}{4m^2}\frac{s}{\Delta^2+\lambda^2}$; $c_0 = 2^{-5}\frac{g^4}{m^2}\, 3\pi i s$;

fb: $c_1 = -\frac{g^2}{m}\frac{s}{\Delta^2+\lambda^2}$; $c_0 = 2^{-2}\frac{g^4}{m}\, i\pi\sqrt{6}s$;

bb: $c_1 = -4g^2\frac{s}{\Delta^2+\lambda^2}$; $c_0 = g^4\, 4\pi i s$; $c_2 = g^4\, i\pi s$;

satisfy the factorization condition

$$c(ff)\cdot c(bb) = c^2(fb)$$

for the channel $I_t=0$ as well as well as for the channel $I_t = I$. However, as it has been found in the paper [55], the leading singularity which belongs to $I_t=0$ turns out to be a square root branch point at $J = 1 + \frac{g^2}{\pi^2}\, 2\ln 2$ (for SU_2- gauge group) and results from two reggeized vector exchange.

This indicates to a violation of the Froissart bound in the main logarithmic approximation in QCD as well as in QED.

Thus, the situation is puzzling. Before answering these questions let us make up the balance:

1. There is a place for the reggeization of basic particles;
2. The "superconvergence" of integrals over the transverse momenta is observed; so, the automatic transverse cutoff in $P_\perp$ appears, and one can think the QCD is a candidate for the theory of strong interactions;
3. The results under study correspond to a non-physical world with the free (non-confined) quarks, antiquarks and gluons.

It seems that all found indications to a quark confinement are illusive, and the whole problem of high energy behaviour in hadronic phase of QCD is still unclear.

In conclusion we shall mention the paper [59] in which some regularities in behaviour of the hadron multiplicities are considered in the framework of QCD. The increase of the hadron multiplycity in the high energy reactions is attributed here to the necessity of confining the quark quantum numbers ("color neutralization").

V. CONSTITUENT THEORY OF THE HADRON INTERACTIONS

1. Dynamical equations in QFT

The constituent picture of the high energy hadron interactions leads to the predictive and consistent theory when combined with a dynamical equation approach in QFT.

The relativistic quasipotential approach was successful in studying the high energy hadron scattering at small and large angles, the form factors of composite particles and many other problems.

There is a number of new results in this direction:

First, I shall mention the density matrix method to describe the multiparticle production processes (see Logunov et al. [70]) which we shall discuss in the following chapter.

Second, there is a development of the null-plane description of composite particles in the framework of the "one-time" quasipotential approach (Tavkhelidze et al.[73]).

In a number of papers[74] the great efforts are made to obtain as much as possible rigorous results on the properties of the n-particle Green functions projected on the null-plane. The spectral and explicit properties of the "two-time" Green functions projected on the null plane are proved. Some of these results were previously found only in the lowest order of the perturbation theory [71-72].

In the paper by Kvinikhidze, Sissakian, Slepchenko and Tavkhelidze [75] submitted to the Conference, the null-plane approach was used in order to obtain a number of general integral representations for the inclusive cross sections which are very useful in the dynamical description of multiparticle production. These results provide the field theoretical grounds for the parton-quark model or constituent- interchange model used by Blanckenbeckler, Brodsky and Gunion to describe the large $P_\perp$ processes[76].

In the paper by Atakishiev, Mir-Kasimov and Nagiev [77] the relativistic Hamiltonian theory with an auxiliary massless spurion field is developed that allows one to exclude all ultraviolet singularities of QFT on the null plane.

The cross-symmetric Bethe-Salpeter equations are studied in the paper by Yaes[78].

2. The Density Matrix Method

The new development of the dynamical approach is made in the paper by Arkhipov, Logunov, Savrin[70] submitted to the Conference, where the method of the density matrix is proposed to describe the multiparticle production processes at high energies

The density matrix of a system of two outcoming nucleons + one additional meson (as an example) is represented by

$$\rho^{(2)}_{\vec{c}}(2,I/2',I') \sim \sum_{\text{others}} T_{2\to 2'+I'+\text{others}}\, T^*_{2\to 2'+I'+\text{others}}$$

as is illustrated in Fig.9:



Fig. 9

Quantum statistical ensemble

The total space momentum of all three particles $\vec{c} = \vec{2} + \vec{I} = \vec{2}' + \vec{I}'$ is fixed in the relativistic invariant one-time description.

The following dynamical equation is true on the general grounds of QFT:

$$(E_k - E)\rho^{(2)}_{\vec{c}}(t) - \rho^{(2)}_{\vec{c}}(t)(E_{k'} - E') = V_{\vec{c}}\,\rho^{(2)}_{\vec{c}}(t) - \rho^{(2)}_{\vec{c}}(t)\,V^+_{\vec{c}}.$$

Here, $V_{\vec{c}}$ is the integral operator of an effective quasipotential for the three-particle system (2+I or 2'+I') affected by screening of the rest part of multiparticle systems:

$$E_k = (m^2 + \vec{p}^2)^{\frac{1}{2}} + (\mu^2 + \vec{k}^2)^{\frac{1}{2}} + |(\vec{c} - \vec{p} - \vec{k})^2 + m^2|^{\frac{1}{2}}$$

The two-particle correlation function is given by

$$\rho^{(2)}(t) = \int d\vec{c}\;\rho^{(2)}_{\vec{c}}(t),$$

and the one-particle distribution function by

$$\rho^{(1)}(t) = \int \rho^{(2)}_{\vec{c}}(t)\; d\vec{c}\; d\vec{p}.$$

The observable inclusive cross section is determined by the adiabatic limit

$$\lim_{\substack{t\to\infty \\ E=E'}} \rho^{(1)}(\vec{k}, \vec{k}/t) = \delta^3(0)\,\frac{I}{(2\pi)^2}\,\frac{d\sigma}{d\vec{k}}$$

where $I = 4\sqrt{(q_1 q_2)^2 - m^2}$ is the initial flux factor.

The authors look for solutions of the eq. for the $\rho^{(2)}$ of the following form

$$\rho^{(2)}_{\vec{c}}(2,I/2',I') \sim \psi_{\vec{c}}(2,I)\cdot\psi_{\vec{c}}(2',I')$$

as the pure three-particle state density matrix. Thus the $\psi_{\vec{c}}(t)$ obeys the quasipotential eq. for the (pseudo) three-particle system

$$(E_k - E)\,\psi_{\vec{c}}(t) = V_{\vec{c}}\,\psi_{\vec{c}}(t)$$

where $V_{\vec{c}}$ takes into account the interaction among three particles screened by other particles in the final states of an inclusive reaction.

$$\frac{d\sigma}{d\vec{k}}(I) \sim \int d\vec{c}\; d\Omega\, |\psi_{\vec{c}}(2,I)|^2$$

The authors have derived the automodel solutions which possess the scaling properties predicted in the Feynman parton model.

Thus, the density matrix method gives a dynamical basis for consistent description of multiparticle reactions in the framework of the constituent models (like Chou-Yang or Van Hove & Pokorski models).

The similar dynamical approach to a multiparticle production has been recently formulated by P. Carruthers and F. Zachariasen[79]. They have shown that the field theoretical description of multiparticle production processes can be cast in a form analogous to the ordinary transport theory where the inclusive differential cross sections are given by integrals of the covariant phase - shift distributions.

VI. POWER LAWS

I. Dimensional Quark Counting for Large Angle Scattering.

Power-like asymptotic behaviour of the large scattering processes and hadron form factors was interpreted in papers[70-72] in terms of the Dimensional Quark Counting (DQC).

As was shown in paper [70], DQC is based on the following general assumptions:

I. Quark structure of hadrons with the confinement.

2. Scale invariance (automodelity) of quark interactions at small distances.

3. Finitness of the quark local densities within hadrons.

In papers[81-83] DQC is derived from a perturbation theory analysis of the renormalized field theoretical models with quarks and gluons as fundamental fields and hadrons as bound states of quarks.

The DQC leads to the following well-known results:

$$F_a(t) \sim \left(\frac{I}{t}\right)^{n_a-I}; \quad \frac{d\sigma}{dt}(ab\to cd) \sim \left(\frac{I}{s}\right)^{n_a+n_b+n_c+n_d-2} \cdot f_{ab\to cd}^{(z=\cos\theta)}(z)$$

where n_a is the minimal number of basic point-like constituents (valent quarks, leptons, etc.).

If one chooses $n_{meson}=2$, $n_{baryon}=3$, $n_{lepton}=I$, he can get

$$F_\pi \sim \frac{I}{t}\text{(monopole)}; \quad F_p \sim \frac{I}{t^2}\text{ (dipole)}; \quad F_e \sim I\text{ (point-like) etc.}$$

and

$$\frac{d\sigma}{dt}(pp\to pp) \sim \frac{d\sigma}{dt}(p\bar{p}\to p\bar{p}) \sim s^{-10},$$

$$\frac{d\sigma}{dt}(\pi p\to \pi p) \sim \frac{d\sigma}{dt}(Kp\to Kp) \sim s^{-8},$$

$$\frac{d\sigma}{dt}(\pi\pi\to\pi\pi) \sim \frac{d\sigma}{dt}(ep\to ep) \sim s^{-6}, \quad \text{etc.}$$

This hierarchy of powers is in a qualitative accordance with observation[83].

In addition to the problem of power-like automodel asymptotics in QFT and justification of DQC the following questions still remain:

* Angular dependence of $d\sigma/dt$;
* Hadron polarization in large angle processes;
* Absolute scales of $d\sigma/dt$, $F(t)$.

The problem of angular dependence of the large angle scattering cross sections was considered in recent papers [84-92].

In paper[84] the generalized DQC has been proposed based on a specific dynamical interpretation of quark diagrams describing the quark rearrangement processes at small distances. The generalized DQC states that an asymptotic contribution to the large angle scattering amplitude is determined by the topology of quark diagram as a homogenious function of the large kinematic variables s, t and u.

The analysis of angular dependence of a number of large binary reactions in terms of the helicity amplitudes, under an additional assumption of the γ_5- invariance was performed in [93].

For the meson-baryon scattering it gives, e.g., the general result which can be written in the following symbolic form:

$$\frac{d\sigma}{dt} \sim \frac{I}{s^2}|f_{tt}|^2 \sim \frac{I}{s^2}\left|\cos\frac{\theta_s}{2}\,\overline{\Sigma\!\!\!\!\!\!\Sigma} + \cos\frac{\theta_u}{2}\,\overline{\Sigma\!\!\!\!\!\!\Sigma}\right|^2$$

where θ_s, θ_u are the scattering angles in the s- and u-channels, respectively, and the asymptotics of two quark diagrams are

$$\overline{\Sigma\!\!\!\!\!\!\Sigma} \sim \frac{I}{st^2}, \quad \overline{\Sigma\!\!\!\!\!\!\Sigma} \sim \frac{I}{ut^2}$$

The Table of results is given below.

TABLE: Angular dependence of the large angle binary reactions.

Reaction	$d\sigma/dt \sim \left(\frac{I}{s}\right)^{2(n_a+n_b-I)} \cdot f(\cos\theta = z)$
$\pi^+p \to \pi^+p$	$s^{-8}\frac{(I+z)}{(I-z)^4}\left\|\beta + \frac{4\alpha}{(I+z)^2}\right\|^2$
$\pi^-p \to \pi^-p$	$s^{-8}\frac{(I+z)}{(I-z)^4}\left\|\alpha + \frac{4\beta}{(I+z)^2}\right\|^2$
$\pi^-p \to \pi^0n$	$s^{-8}\frac{(I+z)}{(I-z)^4}\left\|\frac{\alpha+\beta}{\sqrt{2}}\right\|^2\left(I + \frac{4}{(I+z)^2}\right)^2$
$K^+p \to K^+p$	$s^{-8}\cdot I6\frac{(I+z)}{(I-z^2)^4}$
$K^-p \to K^-p$	$s^{-8}\frac{(I+z)}{(I-z)^4}$
$p\bar{p} \to \pi^+\pi^-$	$s^{-8}\frac{1}{2}\frac{(I+z)}{(I-z)^3}\left\|\alpha + \beta\left(\frac{I-z}{I+z}\right)^2\right\|^2$
$p\bar{p} \to \pi^0\pi^0$	$s^{-8}\frac{1}{2}\frac{(I+z)}{(I-z)^3}\left\|\frac{\alpha-\beta}{\sqrt{2}}\right\|^2\left(I+\left(\frac{I-z}{I+z}\right)^2\right)^2$
$p\bar{p} \to K^+K^-$	$s^{-8}\frac{1}{2}\frac{(I+z)}{(I-z)^3}$
$pp \to pp$	$s^{-10}(I-z^2)^{-6}\{[\alpha(I+z)^2+\beta(I-z)^2)^2 + (z\to -z)] + [\frac{2}{I+z}(\bar{\alpha}(I+z)^2+\bar{\beta}(I-z)^2)^2 + (z\to -z)]\}$
$p\bar{p} \to p\bar{p}$	$s^{-10}\frac{(I-z)^{-6}}{64}\{[4\bar{\alpha}+\bar{\beta}(I-z)^2)^2 + (4\bar{\beta}+\bar{\alpha}(I-z)^2)^2 + [\frac{(I+z)}{2}(4\alpha+\beta(I-z)^2) - \frac{I+z}{I-z}(4\beta+\alpha(I-z)^2)]^2\}$

On the basis of these formulas as well as on the basis of the quasipotential equation with the analytic interaction potentials a new analysis of experimental data has been performed by Kuleshov, Goloskokov,Smondyrev et al. in the paper submitted to the Conference [92] (see Figs.I0,II).The authors have shown that

I. V≈A, or the vector-vector and axial- axial vector couplings in $pp/p\bar{p}$ scattering approximately coincide.

So, only same/opposite helicities couple in the proton/antiproton scattering on the nucleon.

2. The double-quark pair exchange is suppressed by two orders of magnitude as compare with a single-quark model.

This analysis shows that the study of angular dependence can give a rich and important information on the dynamics of large angle scattering and quark processes going at short distances.

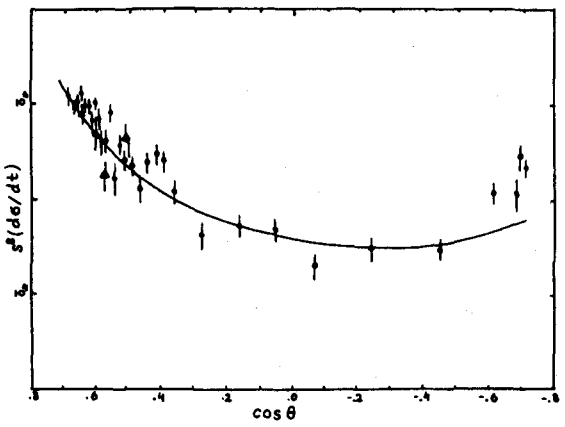


Fig.I0. $s^8 \frac{d\sigma}{dt}$ for $\pi^+ p$ scattering.

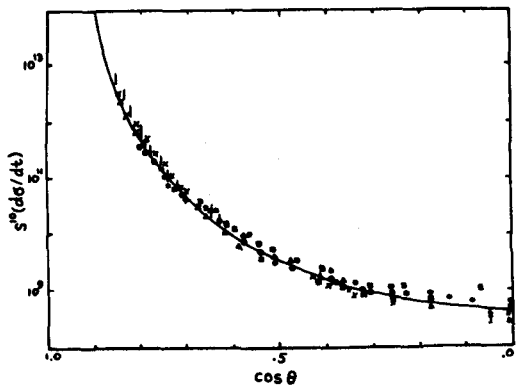


Fig.II. $s^{10} \frac{d\sigma}{dt}$ for pp scattering.

2. Asymptotics of nuclear form factors and structure function.

The dimensional quark counting gives a very simple and direct relationship between asymptotic form of the hadron form factors and complexity of hadrons.

There is an interesting question whether this relationship can be brought into the nuclear physics where fortunately one deals with objects whose complexity varies in wide limits. This question as well as the whole problem of the quark degrees of freedom for nuclei was apparently first arised by A.M.Baldin [94] and discussed in a number of recent papers.

An analysis of recent experimental data on the deuteron electromagnetic form factor as well as the new results of measurements of e^-D elastic and inelastic scattering from q^2=0.8 up to 6.0 GeV^2 were presented by Arnold et al.[97]. An evidence on the absence of the meson exchange currents is found in these experiments accordingly to the quark picture of the processes.

The test of the dimensional quark counting predictions for the form factors of hadrons and a deuteron can be illustrated in Figs.I2,I3 from the paper by Brodsky and Chertok[98].

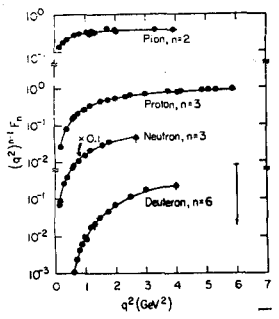


Fig.I2. Test of the Dimensional Quark Counting predictions with the experimental data for the pion (electroproduction data) proton /neutron and elastic deuteron form factors.

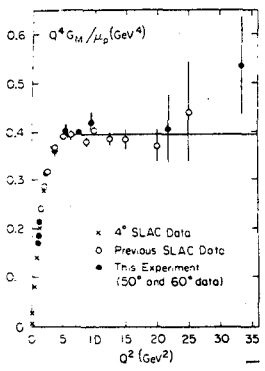


Fig.I3. Comparison of the Dimensional Counting prediction with the SLAC experimental data.

One of the most important problems which have to be understood is the value of the level of "flattening out" of the deuteron form factors.

It seems that this is connected to the relative time which the deuteron spends as a six-quark system (not as a losely bound two-nucleon system). To answer such a question one needs a more sophisticated theory of a nucleus in terms of quark degrees of freedom (like quark bag model of nucleus).

VII SCALING AND SIMILARITY LAWS

I. Automodelity in Strong Interactions

Study of the scaling and similarity properties of strong interactions at high energies is interesting from two points of view. First, it is a question of structure of elementary particles and of interaction dynamics at short distances; second, it is a search for a new energy scale (or fundamental length) which could change (if exists) considerably the picture of strong interactions at superhigh energies.

A great number of papers has appeared as a result of an observation of scaling effects in spectra of secondary particles in the experiments carried out at the Serpukhov accelerator and following the Feynman formulation of scaling phenomena in terms of the quark-parton model[100]. Many interesting experimental and theoretical results were obtained in that direction.

In papers[101] a general approach to the description of scaling and similarity properties has been developed based on the idea of the automodelity.

The term "automodelity", (or "selfsimilarity") itself, belongs to the theory of the gazo-and hydrodynamic phenomena. An analogy of these phenomena to the scaling properties of deep-inelatic processes has been noticed by N.N.Bogolubov in 1969. It is worth to be mentioned, particularly, in connection to the physics of deep-inelastic lepton-hadron scattering, where the character of scaling laws indicates to the analogy with the so-called "point-like explosion" in gazo/hydrodynamics. The scaling regularities in the processes of strong interactions of hadrons at high energies lead to an analogy with the "plane-like" explosion. We emphasize, however, that the analogy with the "plane-like" explosion corresponds only to the processes with bounded momentum transfers, the dynamics of which is determined by the finitness of effective interaction radius of strong interactions [99]. In these processes hadrons look as extended objects with infinitely small longitudinal sizes (due to the Lorentz contaction in a system with infinite momentum, i.e. "$P_z \to \infty$"). This allows one to consider the scaling properties of observable quantities under the transformation (the delatations of the longitudinal scale of momenta) as: $P_z \to \lambda P_z$; $P_\perp \to P_\perp$

A separation of the transverse and longitudinal degrees of freedom in description of the interaction processes at bounded momentum transfers which is specific in this approach, leads to a whole number of scaling laws for the amplitudes and cross sections of inclusive as well as of binary reactions (note results of the Mueller-Kancheli approach and quark-parton model).

The automodelity principle leads, particularly, to the requirement for all the quantities of the type

$$\sigma_{tot},\ \sigma_{el},\ B=(\log\sigma')'_{t=0} \quad \text{etc.}$$

with the same dimensionalty T^2 (in terms of scale of the transverse length T), to have a weak and universal energy dependence on the same footing. This phenomenon known as the law of geometrical scaling is in good accordance with the existing experimental data.

We have noticed in a number of papers[103] that the geometrical scaling laws were effectively mearged with the quark analysis of the hadron interaction total cross sections. It has to be stressed that a weak energy dependence of the transverse length effective scale (say $R^2 \sim \sigma_{tot}$) points to an approximate character of scaling laws related to the similarity transformations,

$$P_\perp \to \lambda P_\perp,\quad P_z \to P_z$$

the separation of the longitudinal and transverse degrees of freedom being suggested for an ideal case.

2. Study of scaling in QFT.

A number of new interesting results was obtained in studying the scaling properties of hadron interactions in the framework of the local QFT. First of all, we shall mention the axiomatic studies of large angle processes which were initiated by the rigorous applications of the Dyson-Lehmann-Jost representation to an investigation of the automodel (scale invariant) asymptotics in the deep inelastic scattering (see Bogolubov, Tavkhelidze and Vladimirov [104].

An extension of this approach to the large $P_\perp$ inclusive reactions on the basis of the DJL-representation was made by Logunov, Mestvirishvili et al. in 1974[105].

The main problems of the axiomatic approach are:

* Consistency of the power-like automodel asymptotics with the general requirements of the local QFT;

** Relations between asymptotic forms in different channels and regions;

*** Connection to the space-time picture of processes.

In the paper by Geyger et al.[106] submitted to the Conference, the results of simultaneous study of three processes (on the basis of the DLJ-representation) are presented:

$p_1 + q_1$ (on shell) $\to p_2 + q_2$ (on shell)

$p_1 + q_1$ (on shell) $\to p_2 + q_2$ (off shell)

$p_1 + q_1$ (off shell) $\to p_2 + q_2$ (off shell)

It is shown that

- on - and off-shell amplitudes can have different asymptotic behaviour at large momenta;
- absorptive and dispersive parts of the amplitudes on-mass shell can have different asymptotics at large angles.

For instance, the automodel (power-like) asymptotics of the process $\gamma(q^2) + p \to \pi/\rho + p$ could have different character at $q^2=0$ and $q^2 \to -\infty$.

The consistent description of scaling properties in terms of the density matrix method was given in paper[70]. Starting from the dynamical equation for a density matrix of a subsystem of particles in final states of the inelastic multiparticle reaction, under rather general assumption on the character of interaction quasipotential, the authors[107] have derived the radial type scaling for the inclusive cross sections. The result is in good agreement with existing experimental data on the inclusive production at high energies[108].

In the paper mentioned above an interesting application of the DM-method to the deep-inelastic scattering is given. The well known Bjorken scaling is found in the one-photon approximation. In general case (for all orders in the coupling constant) the cross section scales in terms of two dimensionless variables are: $\omega = 1 - w^2/q^2$ (Bjorken) and $x = 1 - w^2/s$ (Feynman). In the intermediate case (multiphoton with the one-photon approximation for the scattering on a single "constituent"), the new scaling has been found with the dimensional variable

$$\zeta = \frac{x(1-x)}{(2-x)(\omega-1)}$$

Moreover, it was shown that the DM-method gives a clarification of the correlation between the elastic and inelastic characteristics of particle interactions, as it can be illustrated by the solution

$$\frac{d\sigma}{d\vec{k}_\perp} = c(E)\int d\vec{b}\,\sigma(\vec{b})\,\rho(\vec{b},\vec{k}_\perp)$$

which was found and discussed in the papers by Savrin, Semenov, Tyurin, Khrustalev[109] submitted to the Conference. Here, $d\sigma/d\vec{k}_\perp$ is an inclusive cross section of "soft" mesons, and $\sigma(\vec{b})$ is determined by overlapping of the elastic profiles of initial particles

$$\sigma(\vec{b}) = \int d\vec{b}'\, t_{el}(\vec{b}')\, t^*_{el}(\vec{b}-\vec{b}')$$

and $\rho(\vec{b},\vec{k}_\perp) \sim \int d\vec{\Delta}\, e^{-i\vec{b}\cdot\vec{\Delta}} g(\vec{k}-\vec{\Delta}) \times g(\vec{k}+\vec{\Delta})$,

$g(\vec{k}-\vec{\Delta}) = |\phi_{\vec{k}+\vec{\Delta}}(\vec{k})|^2$ is "a distribution of mesonic constituents" within a screened nucleon with a total momentum $\vec{k}+\vec{\Delta}$.

In the paper by D. Crewther and G.C. Joshi[110] submitted to the Confereence, the scaling properties of the dual resonance model with the Mandelstam analyticity were studied. Non-linear trajectories are used when calculating the scaling functions which are in reasonable agreement with the experiments.

Factorization properties of the exclusive and inclusive cross sections were discussed in papers [111].

The detailed discussion of scaling in the inclusive multiparticle production processes is given in a review talk by Chliapnikov.

SEARCH FOR THE FUNDAMENTAL LENGTH

The success of the most scaling and similarity relations depends on the absence of an energy scale which will be essential at available energies.

What do we expect from the very high energies?

In the invited talk given by Kadyshevsky[112] there is an interesting discussion about the existence of the fundamental length l which should be a key to understand the phenomena at very high energies.

This discussion is based on the version of QFT with a fundamental length[113] which is an alternative to the local QFT in the same sense as the non-Euclidean geometry is a unique alternative to the Euclidean one. Some implications of this theory are listed below:

1. Masses of elementary particles are bounded from above, i.e. $m \leq 1/l$;
2. Modification of the usual uncertainty relation between the momentum transfer q and size of interaction r:
$$r \sim \frac{1}{\log(lq)} \quad \text{instead of} \sim 1/q \;;$$
3. Geometrical interpretation of the power laws such as
$$d\sigma/dt \sim (l^2 s)^{-\nu} f(t/s) \;;$$
4. Parity violation at very high energies $E \gtrsim 1/l$ owing to the modification of the fermion propagator
$$|\not{p} + (1/l - \sqrt{1/l^2 - p^2})\gamma_5 - m|^{-1}$$

$l \sim l_{Fermi} \sim 10^{-17}$ cm?

5. Sharp fall of the $\sigma_{tot}(e^+e^- \to \text{hadrons})$ at $s > 1^{-2}$ and a slower decrease with $Q^2 < 1^{-2}$ of the deep-inelastic e^-p scattering cross sections.

This analysis shows that a search for the fundamental length could be one of the intriguing tasks for super-high energy physics at the accelerators of next generation.

VIII. SOME CONCLUDING REMARKS

I would like to conclude this talk with some remarks. Obviously, the list of interesting questions written below is no way complete and it is based mainly on the author's impressions.

1. Asymptotic energies are not yet reached, e.g. s^α behaviour for the total cross sections with $\alpha > 1$ is allowed by experimental data; polarization in pp-scattering is still non-zero, etc. Apparently, these questions are problems to be studied at the accelerators of next generation.
2. Nature of the vacuum exchange (Pomeranchuk singularity) is still an enigma and waits for its explanation.
3. A close relationship between the t-dependent SU_3-structure of the vacuum exchange and the OZI-rule regularities in the heavy meson decays, apparently, exists. This makes deeper the Regge idea on relationship of high energy behaviour and particle properties with the relevant quantum numbers.
4. Experiments with the high energy hyperon beams and study of $\psi/_J$ -hadron interactions should be very desirable to understand the quark regularities in the total cross sections.
5. Situation with the quark confinement in QCD is still puzzling. Its understanding is important for high energy physics on the whole.
6. Measuring of angular dependence, polarizations and phases of scattering amplitudes of the binary reactions at large angles is important to understand how far are really good predictions of the Dimensional Quark Counting.
7. Quark degrees of freedom seem to be important for a description of nucleus interactions at high energies and large transferred momenta.
8. Presence of the fundamental length or new energy scale could change drastically the picture of particle interactions at extremal energies.

R e f e r e n c e s:

I/ A.A.Logunov,M.A.Mestvirishvili et al.Contributed paper A5-5I/I043.

2. G.L.Rcheulishvili,A.P.Samokhin,contributed paper A5-50/II59.
3. H.Cornille,A.Martin,Nucl.Phys.BI0I,4II(I976).
4. Yu.S.Vernov and M,N.Mnatsakanova,contributed paper A5-7,8/785,786.
5. Yu.M.Lomsadze et al.Contributed paper A5-5,6/787,788; V.Lusur,I.V.Khimich,contributed paper A5-I2/78I.
6. V.Barger.Rapporteur's talk at the XVII-th Inter Conf.on High Energy Physics,London,I974; J.B.Bronzan,G.L.Kane,U.Sukhatme,Phys.Lett.,B49, 272(I974);D.P.Sidhu,U.Sukhatme,Phys.Rev.DII, I35I(I975);U.Sukhatme,G.Kane,R.Blankenbeckler, M.Dave,Phys.Rev.DI2,343I(I975); J.Fisher,P.Kolar,contributed paper A5-52/693; R.Wit,contributed paper A5-33/843.
7. V.Gerdt,V.I.Inozemtsev,V.A.Mescheryakov,contributed paper A5-49/I065.
8. M.A.Lavrent'ev,B.V.Shabat.Methods in the Theory of Functions of Complex Variables,Moscow, I973,p.204.
9. L.D.Soloviev,L.Schelkachev,"Elementary particles & nucleus",6,57I,Dubna(I975);G.Giacomelli, Phys.Reports,23,No 2(I976); J.Lach,preprint FNAL-76/I5 Exp(I976).
10. D.I.Blokhintsev,Nucl.Phys.3I,628(I962);S.P.Alliluev,S.S.Gershtein,A.A.Logunov,Phys.Lett., I8,I95(I965); V.R.Garsevanishvili,V.A.Matveev, L.A.Slepchenko,A.N.Tavkhelidze,Phys.Rev.DI , 849(I97I).
11. A.N.Tavkhelidze.Rapporteur's talk at the XV Intern.Conf.on High Energy Physics in Kiev, (I970).
12. O.A.Khrustalev,N.E.Tyurin,preprint IHEP(I975) N.E.Tyurin et al.Contributed paper I008/AI-I44
13. A.A.Logunov,O.A.Khrustalev,V.Savrin,N.E.Tyurin,Jour.of Math.&Theor.Physics,Moscow,(6,I57, (I97I).
14. L.D.Soloviev,JETP,I8,455(I973).
15. L.D.Soloviev,A.V.Schelkachev,preprint JINR,P2-8230,Dubna(I974).
16. M.S.Dubovikov,K.A.Ter-Martirosyan,preprint ITEP-37,Moscow(I976).
17. B.Z.Kopeliovich,L,I,Lapidus,contributed paper A5-46/907.
18. S.Y.Chu,B.R.Desai,B.C.Shen,Preprint Califor. Inst.of Technol.UCR-75-03(I975);H.Cheng,J.K. Walker,T.T.Wu,Phys.Lett.,44B,97 and 283(I973).
19. V.N.Gribov.Proc.of the XVI-th Intern.Conf.on High Energy Phys.in Batavia,I972.
20. J.B.Bronzan,J.A.Shapiro,R.L.Sugar,contributed paper A5-24/800; R.L.Sugar.Invited talk at the Conference.

21. J.Ellis,R.Savit,CERN report TH-2042(1975); H.D.I.Abarbanel,Revue of Mod.Physics,48,435, (1976).
22. F.E.Low,Phys.Rev.D12,163(1975).
23. H.D.Abarbanel.SLAC-pub.1731(1976).
24. I.T.Dyatlov,contributed paper A5-II/782.
25. D.Amati,M.Le Bellac,G.Marchesini,M.Giaffaloni, contributed paper A5-23/845.
26. S.G.Matinyan,A.G.Sedrakyan,contributed paper A5-34/1010.
27. C.Quigg,E.Rabinovich,Phys.Rev,D.13,2525(1976).
28. H.Harari,Phys.Rev.Lett.,20,1385(1968); P.G.O.Freund,Phys.Rev.Lett.,20,235(1968).
29. R.Carlitz,M.B.Green,A.Zee,Phys.Rev.D4,3439(1971)
30. N.F.Bali,J.Dash,Phys.Rev.D10,2102(1974).
31. G.F.Chew,C.Rosenzweig,Phys.Rev.D13,3907(1976)
32. E.Gotsman,A.Levy,Phys.Rev.D13,3036(1976).
33. A.Hacinliyan,M.Koca,Phys.Rev.D13,1868(1976).
34. G.Veneziano,Nucl.Phys,B74,365(1974);Phys.Lett 52B,220(1974).
35. G.F.Chew,C.Rosenzweig,Phys.Lett,58B,93(1975); C.Schmid and C.Sorensen,Nucl.Phys.B96,209(1975) G.Veneziano,preprint of Kyoto Univ.RIFP-234, Kyoto(1975).
36. G.Zweig,CERN report TH-412/8419,Geneva(1964); S.Okubo,Phys.Lett,5,165(1963);I.Iizuka,K.Okuda,O.Shito,Progress in Theor.Phys.35,1061(1966).
37. P.G.O.Freund,Y.Nambu,Phys.Rev.Lett,34,645(1975).
38. E.M.Levin,L.L.Frankfurt,JETP Letters,2,65(1965). H.J.Lipkin,F.Schock,Phys.Rev.Lett,16,71(1966).
39. Yu.D.Prokoshkin.Talk at the Symposium on High Energy & Elementary Particle Physics,Baku,1973. S.P.Denisov,S.V.Donskov,Yu.P.Gorin et al.Nucl. Phys.B65,1(1974).
40. H.J.Lipkin,Nucl.Phys,B78,381(1974);Phys.Rev. D11,1827(1975).
41. D.Joynson,B.Nicolescu,contributed paper A5-17/849.
42. L.P.Horwitz,D.Sepunaru,contributed paper A5-35/411; M.Koca,contributed paper A5-21/844; E.Gotsman,A.Levy,contributed paper A5-25/851; V.P.Gerdt,V.A.Mescheryakov,JINR P2-9572,Dubna (1976); B.H.Kellett,G.C.Joshi,S.Y.Lo,contributed paper A5-31/993;S.Mavrodiev,contributed paper A5-15/1001.
43. H.Cheng,T.T.Wu,Phys.Rev.Lett,22,666(1969); V.N.Gribov,L.N.Lipatov,G.V.Frolov,Phys.Lett, B31,34(1970).
44. B.H.McCoy,T.T.Wu,Phys.Rev,D13,I-VI papers(1976) V.S.Fadin,B.E.Sherman,contributed paper A5-58/ 531.
45. S.Mandelstam,Phys.Rev,B 949,137(1965);E.Abers, V.L.Teplitz,Phys,Rev,158,1365(1967);M.T.Grisaru,H.Schnitzer,Hung-Shang Tsao,Phys.Rev.D8,(1973)
46. S.P.Kuleshov,V.A.Matveev,A.N.Sissakian,M.A.Smondyrev and A.N.Tavkhelidze,JINR,E2-7041,E2-7720 Dubna(1974).
47. C.Bourrely,J.Soffer,A.Martin,contributed paper A5-44/1150.
48. B.M.Barbashov,V.V.Nesterenko,Journ.of Nucl. Phys.20,218(1976).
49. A.N,Kvinikhidze,L.A.Slepchenko,Journ.of Math. and Theor.Physics,Moscow,24,54(1975); A.N.Kvinikhidze,JINR,P2-6931,Dubna(1973).
50. H.Fritzsch,M,Gell-Mann,in Proceedings of the XVI Intern.Conf.on High Energy Physics,Chicago-Batavia,1972.
51. H.T.Nieh,York-Peng Yao,Phys.Rev.Lett,32,1074, (1974); Phys.Rev.D13,1082(1976).
52. B.M.Coy,T.T.Wu,Phys.Rev,D.12,3257(1975);Phys. Rev.D.13,1076(1976).
53. P.Yeung,Phys.Rev.D.13,2306(1976),contributed paper A5-30/749.
54. C.Y.Lo,Hung Cheng,Phys.Rev,D.13,1131(1976).
55. V.S.Fadin,E.A.Kuraev,L.N.Lipatov,contributed papers A5-56, 61,62.
56. Wu,Yong-shi,Dai Yuan-ben,Scientia Sinica,vol. XIX,65(1976).
57. L.Tybursky,Phys.Lett,59B,49(1975);Phys.Rev.D13, 1107(1976).
58. L.L.Frankfurt,V.E.Sherman,contributed paper A5-57/526.
59. M.T.Grisaru,Phys.Rev,D13,2916(1976).
60. E.C.Poggio,H.R.Quinn,Phys.Rev.D12,3279(1975).
61. J.M.Cornwall,G.Tiktopoulos,USLA/75/TEP/1(1975).
62. P.Carruthers,F.Zachariasen,preprint LA-UR-76-364(1976).
63. L.Tukaszuk,X.Y.Pham,IPNO-TH/75-20,Paris(1975).
64. T.Appelquist,J.Carazzone,Phys.Rev.Lett,33,451, (1975);T.Appelquist,J.Carazzone,H.Kluberg-Stern, M.Roth,preprint Yale-FNAL(1976); E.Poggio,H. Quinn,preprint Harvard Univ.(1976).
65. B.W.Lee.Summary Talk at the Coral Gables Conf. Orbies Scientiae(1976);preprint FNAL 76-20-THY/exp(1976); T.Kinoshita,Journ.Math.Phys.3, 650(1962);T.D.Lee and N.Nauenberg,Phys.Rev. B133,1549(1964).
66. P.W.Higgs,Phys.Lett,12,132(1964).
67. L.D.Faddeev,V.N.Popov,Phys.Lett,25B,29(1967).
68. t'Hooft,Nucl.Phys.B35,167(1971).
69. S.J.Brodsky,J.F.Gunion,contributed paper A5-16/846.
70. A.A.Arkhipov,A.A.Logunov,V.I.Savrin,Journ.of Theor.and Math.Physics,Moscow,26,291(1976); contributed paper A5-3/790.
71. S.Weinberg.Phys.Rev.150,1313(1966).
72. J.Gunion,S.Brodsky,R.Blankenbeckler,Phys.Rev.D8,287 (1973).

73. R.N.Faustov,V.R.Garsevanishvili,A.N.Kvinikhidze,V.A.Matveev,A.N.Tavkhelidze,JINR,E2-8I26, Dubna(I974).
74. A.A.Khelashvili,A.N.Kvinikhidze,V.A.Matveev, A.N.Tavkhelidze,JINR,D2-9540,Dubna(I976);S.P. Kuleshov,A.N.Kvinikhidze et al.JINR,E2-8I28, Dubna(I974).
75. A.N.Kvinikhidze,A.N.Sissakian,L.A.Slepchenko, A.N.Tavkhelidze,contributed paper A4-3I/I08I; A.N.Tavkhelidze.Invited talk at the Conference.
76. J.F.Gunion,S.J.Brodsky,R.Blankenbecler,Phys. Rev.D6,2652(I972);S.Brodsky,R.Blankenbecler, Phys.Rev.DI0,2973(I974).
77. Atakishiev,Mir-Kasimov,Nagiev,contributed paper A5- 6I/443.
78.R.I.Yaes,contributed paper A5-39/I058.
79. P.Carruthers,F.Zachariasen,Phys.Rev.DI3,950, (I976).
80. V.A.Matveev,R.M.Muradyan,A.N.Tavkhelidze,Lett. Nuovo Cim,7,7I9(I973).
8I. S.J.Brodsky,G.R.Farrar,Phys.Rev.Lett,3I,II53 (I973).
82. W.R.Theis,Phys.Lett,42B,246(I972); A.V.Efremov and A.V.Radyushkin,Preprint JINR,E2-97I7,Dubna, I976.
83. P.V.Landshoff,J.C.Polkinghorne,Phys.Lett,44B, 293(I975); S.Brodsky,D.Sivers,R.Blankenbecler Physics Reports,23,No I(I976).
84. V.A.Matveev,R.M.Muradyan,A.N.Tavkhelidze,JINR, E2-8048,Dubna(I974).
85. P.G.O.Freund,S.Nandi,Nuovo Cimento,25A,395, (I975).
86. G.Preparata,CERN TH-I836(I974).
87. K.Kinoshita,Y.Myozyo,Kyushu Univ.Rep.No HE-I0 (I974)
88. B.Pire,SLAC-PUB-I704(I976).
89. T.Uematsu,preprint Kyoto Univ.(I975).
90. A.F.Pashkov,N.B.Skachkov,I.L.Solovtsev,contributed paper A5-9/784.
9I. E.Gotsman,contributed paper A5-I9/737.
92. S.V.Goloskokov,S.P.Kuleshov,V.A.Matveev,M.A. Smondyrev,JINR P2-82II,P2-8337,Dubna(I974); JINR P2-9088,Dubna(I975),see also Invited talk at the Conference.
93. A.A.Logunov,V.A.Mescheryakov,A.N.Tavkhelidze, Doklady Acad.Nauk USSR,I42,3I7(I962).
94. A.M.Baldin, in "High Energy Physics and Nucl. Structure,I975".Ed.by D.E.Nagle et al.(American Institute of Physics,NY,I975).
95. V.A.Matveev,R.M.Muradyan,A.N.Tavkhelidze.Proc. of the Intern.Seminar on Multiparticle processes,Dubna,I975.
96. S.J.Brodsky,G.R.Farrar,Phys.Rev.DII,I309(I975) S.Brodsky,"Few Body Problems in Nuclear and Particle Physics",Les presses de l'univ.Laval Quebec(I975) page 676.
97. R.G.Arnold et al. Phys.Rev.Lett,35,776(I975).
98. S.J.Brodsky,B.T.Chertok,SLAC-PUB-I757(I976). contributed paper A5-I7/846 and 3I-979.
99. S.V.Goloskokov,S.P.Kuleshov,V.A.Matveev,M.A. Smondyrev,V. Teplyakov, JINR,P2-I0I42,Dubna,I976.
I00.R.P.Feynman,Phys.Rev.Lett,23,I4I5(I9669).
I0I. V.A. Matveev,R.Muradyan,A.N.Tavkhelidze,JINR, P2-5443,P2-4824,Dubna(I969); R.M.Muradyan, JINR,P2-6762,Dubna(I972).
I02. A.A.Logunov,Nguen Van Hieu,O.Khrustalev,"Problems of Theor.Physics",Nauka,Moscow(I969)Io7.
I03.V.Barger,R.J.N.Phillips,Phys.Lett,B60,358(I976). J.Dias De Deus,P.Kroll,Phys.Lett,B60,375(I976).
I04.N.N.Bogolubov,A.N.Tavkhelidze,V.S.Vladimirov, JINR,P2-6342,Dubna(I972).
I05.A.A.Logunov,M.A.Mestvirishvili,Nguen Van Hieu, Phys,Lett,25B,6II(I967);A.A.Logunov,M.A.Mestvirishvili,O.A.Khrustalev,Journ.of Math.and Theor.Physics,9,No I-2(I97I).
I06.B.Geyer,Th.Görnitz,D.Robashik,E.Wieczorek,V.A. Matveev,A.N.Tavkhelidze,contributed paper A5-I8/850; P.N.Bogolubov et al.Contributed paper A5-I/792.
I07. V.I.Savrin,preprint IHEP 76-45,(I976).
I08. F.E.Taylor,preprint FNAL/exp 75/90(I975).
I09. V.I.Savrin,S.Y.Semenov,N.E.Tyurin,O.A.Khrustalev,Yadernaya Fizika,2I,I089(I975); V.I.Savrin,S.Y.Semenov,N.E.Tyurin,Yadenaya Fizika, 23,848(I976).
II0. D.Crewthers and G.C.Joshi,contributed paper A5-48/993.
III. A.N.Tolstenkov,contributed paper A5-2/79I; G.C.Joshi,S.Y.Lo,contributed paper A5-40/995; G.C.Joshi,contributed paper A5-4I/990.
II2. V.G.Kadyshevsky.Invited talk at the Conference
II3. A.Donkov,V.G.Kadyshevsky,M.Mateev,R.Mir-Kasimov,preprints JINR E2-6992(I973),E2-7936(I974).

PARALLEL SESSION ON HADRON-NUCLEAR INTERACTIONS

ЗАКОНОМЕРНОСТИ МАСШТАБНО-ИНВАРИАНТНОГО ВЗАИМОДЕЙСТВИЯ РЕЛЯТИВИСТСКИХ ЯДЕР

В.С.Ставинский
ОИЯИ, Дубна

Наши представления о физической природе масштабной инвариантности значительно обогатились в связи с экспериментальным обнаружением кумулятивного ядерного эффекта - при изучении спектров мезонов, рожденных во взаимодействии релятивистских ядер с мишенью, когда энергия мезонов значительно превышает энергию на один нуклон ускоренного ядра. В этой области, кинематически запрещенной для одного столкновения свободных нуклонов ядра, были обнаружены новые закономерности адрон-адронных взаимодействий, предсказанные простой моделью А.М.Балдиным в 1971 году.[1]

Согласно гипотезе ядерного кумулятивного эффекта неупругие взаимодействия с нуклонами сложных составных систем типа атомных ядер описываются суммой масштабно-инвариантных процессов.

Число нуклонов составной системы, участвующих в данном акте взаимодействий, определяется вероятностью попадания N нуклонов в некоторый малый объем (равновероятно по всему объему ядра А).

Таким образом,

$$E\frac{d\sigma}{d\vec{p}}(Am+m\to\pi+X)=C V_A\sum_{N=1}^{A}P_N(N)\,f_N(\vec{x}_N),$$

где C -нормировочная константа и V_A -объем ядра.

Экспериментальная проверка гипотезы была проведена с релятивистскими дейтронами, ускоренными на синхрофазотроне ЛВЭ до энергий порядка 5 Гэв на нуклон. Эксперимент[2] подтвердил гипотезу.

Таким образом, был установлен масштабно-инвариантный характер взаимодействия релятивистских ядер.

В дальнейшем был поставлен эксперимент[3] по детальному изучению инклюзивного процесса при взаимодействии релятивистских ядер

$$A+p(d)\to\pi^{\pm}(p,d,t)+X\ .$$

Были исследованы спектры частиц, вылетающих в направлении "назад" при бомбардировке покоящихся ядер с различными атомными весами, ускоренными протонами либо дейтронами. Энергия, приходящаяся на один нуклон ядра, изменялась от 4 до 8 Гэв. Максимальный перпендикулярный импульс вторичных частиц не превышал 30 Мэв/с. Энергия рожденных частиц от 100 до 1000 Мэв.

В качестве исследуемых мишеней были взяты ядра $p, d, Li^{6,7}, C, Al, Si, Ni^{58,64}, Cu, Sn^{112,118,124}, Sn^{144,154}, W^{182,186}, Pb, U$.

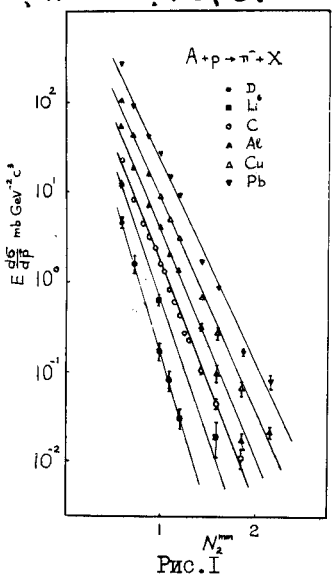


Рис.1

На рис.1 приведены экспериментальные данные[3] по инвариантному сечению инклюзивного рождения мезонов в зависимости от кумулятивного числа $Q = N^{min}$ для разных ядер при импульсе 8,4 Гэв на нуклон.

Полученная экспериментальная информация[3] позволяет отметить следующие закономерности, присущие масштабно-инвариантным взаимодействиям релятивистских ядер.

I. Энергетический спектр рожденных пионов протон-ядерных взаимодействий в системе координат, связанной с фрагментирующим ядром, имеет экспоненциальный (максвелловский) характер

$$E\frac{d\sigma}{d\vec{p}}=a(A)\exp\left\{-T/T_0\right\}.$$

II. Параметр T_0 ($\sim$ 60 Мэв) в пределах точности эксперимента ($\pm$5%) в области кумулятивного мезонообразования не зависит от знака рожденных пионов.

Ш. Параметр $\alpha(A)$ зависит от атомного веса фрагментирующего ядра, причем зависимость инвариантного сечения от атомного веса имеет степенной характер

$$E\frac{d\sigma}{d\vec{p}} = cA^{n(Q)},$$

где показатель степени n имеет специфическую зависимость от порядка кумулятивности $Q \sim T/T^{max}$.

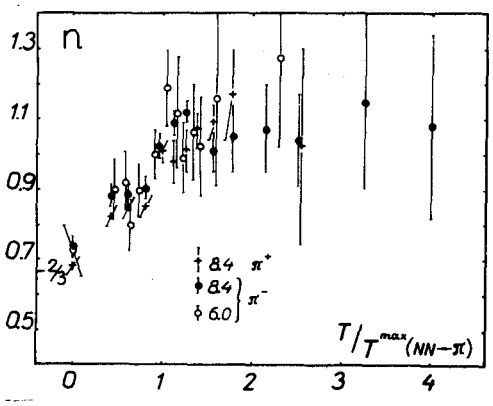


Рис.2а

Рисунок 2а иллюстрирует эту зависимость. В области кумулятивного мезонообразования $\frac{T}{T^{max}} \geq 1$ показатель степени порядка единицы, т.е. кумулятивный эффект имеет объемный характер.

IУ. Экспериментальные данные по инвариантным сечениям образования протонов, дейтронов и трития фитировались зависимостью вида

$$E\frac{d\sigma}{d\vec{p}} = cZ^n$$

для разных энергий вторичных частиц, т.е. при разных порядках кумулятивности. Значения показателя представлены на рисунке 3.

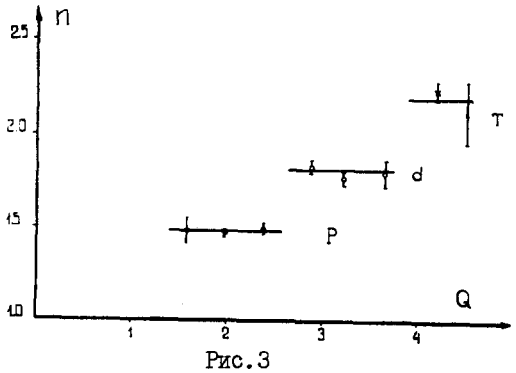
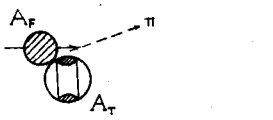


Рис.3

У. Энергетический спектр вылетающих протонов в пион-ядерных взаимодействиях[4] по существу имеет экспоненциальный (максвелловский) характер, причем значение температуры в кумулятивной области ~ 40 Мэв.

УI. Следует отметить единственные на сегодняшний день экспериментальные данные, полученные в Беркли[5] по зависимости инвариантного сечения от атомного веса нефрагментирующего (мишень) ядра в зависимости от порядка кумулятивности. Оказалось (рис.2б), что эта зависимость



$$E\frac{d\sigma}{d\vec{p}} = cA_F^{\alpha_F(Q)}A_T^{\alpha_T(Q)}\exp\{-aQ\}$$

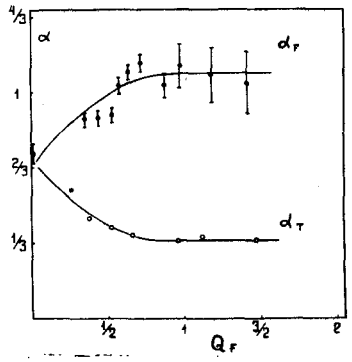


Рис.2б

является "зеркальным" отражением "объемности" кумулятивного мезонообразования.

Таким образом, сечение инклюзивного процесса рождения мезонов можно записать в виде:

$$E\frac{d\sigma}{d\vec{p}} = cA_F A_T^{1/3}\exp\{-T/T_0\}.$$

Для нас сейчас существенно то, что такая характерная А-зависимость возникает в области кинематических переменных рожденных частиц, запрещенной для одного столкновения свободных нуклонов ядер.

В настоящее время можно констатировать, что масштабно-инвариантный характер спектров рожденных частиц в ядерных взаимодействиях наступает гораздо раньше (при энергиях порядка I Гэв) по сравнению с взаимодействием элементарных адронов.

Наибольшее количество экспериментальной информации на сегодняшний день по зависимости от энергии получено по реакции[4], [6], [7]

$$\pi^- + C \to p + X.$$

Авторы цитируемых работ делают вывод о масштаб-

но-инвариантном поведении процесса в интервале импульсов от I,5 до 40 Гэв/с.

При импульсах пионов 2,34 и 3,5[8] Гэв/с; 3,34 Гэв/с[9] исследовалась реакция

$$\pi^- + Xe \to p + X;$$

полученные экспериментальные величины сечений также не зависят от энергии в указанном интервале.

Масштабно-инвариантные свойства были исследованы (Дубна) в реакции образования кумулятивных нейтронов релятивистскими дейтронами[10]

$$d + Al \to n(0^\circ) + X$$

в интервале импульсов дейтронов от 2,5 до I0,2 Гэв/с. В данном процессе скейлинг поступает при 3 Гэв/с.

Следует отметить, что начаты важные исследования кумулятивного рождения частиц в фотон-ядерных взаимодействиях (Ереван)[11].

ЛИТЕРАТУРА

I. А.М.Балдин. Краткие сообщения по физике.№I, стр.35. Сообщение ОИЯИ Р7-5769, Дубна (I97Iг.)

2. А.М.Балдин и др. Сообщение ОИЯИ РI-58I9, Дубна (I97I г.).

3. **A.M.Baldin et.al. Preprint JINR** EI-8054, Дубна (I974 г.). Сообщение ОИЯИ I-8249, Дубна (I974 г.). Препринт ОИЯИ ДI, 2-9224, стр.I76, Дубна (I975).

4. Н.Ангелов и др. Препринт ОИЯИ РI-8566, Дубна (I975).

5. **H.Heckman. Preprint LBL 2052 (1973).**

6. Н.Ангелов и др. ЯФ 22, I026 (I975).

7. С.А.Азимов и др. XУШ Международная конференция по физике высоких энергий, Тбилиси (I976), А6-28.

8. Л.С.Охрименко и др. Препринт ОИЯИ РI-9806, Дубна, I975.

9. Ю.Д.Баюков и др. ЯФ I9, I266 (I974).

I0. А.Абдивалиев и др. Сообщение ОИЯИ I-9924, Дубна, (I976)

II. К.В.Аланакян и др. XУШ Международная конференция по физике высоких энергий, Тбилиси (I976), А6-63.

ЯДЕРНЫЙ СКЕЙЛИНГ

Г.А.Лексин
(ИТЭФ, Москва)

Будем рассматривать глубоконеупругие ядерные реакции, т.е. такие, которые не сводятся к взаимодействию с одним квазисвободным нуклоном. Наглядными примерами таких реакций могут служить реакции типа (I) $a + A \to b + \ldots$ – инклюзивная реакция, где a – любая налетающая частица, A – любое ядро-мишень, b – барион (протон, Λ^0-частица), вылетающий назад в лабораторной системе координат с энергией > 30 МэВ ($p_t^2 > 0{,}I$ ГэВ/с), т.е. с энергией выше энергии испарения; (2) $a + A \to p + p + \ldots + p + X$, где X – нейтральные продукты или часть ядра, – реакция полной или частичной дезинтеграции ядра; (3) $a + A \to b + \ldots$, т.е. как (I), но b – ядра; $d, t \ldots L_i^z \ldots$ Главным образом, будем говорить о реакции (I), сегодня наиболее изученной, но все выводы справедливы вообще для глубоконеупругих реакций, как и для реакций рождения кумулятивных мезонов[1].

Реакция (I) исследовалась под действием протонов, пионов и γ-квантов в диапазоне энергий от 0,5 до 40 ГэВ. Измерялись спектры протонов, вылетающих под углами 90–I80° в л.с. вплоть до импульса I,5 ГэВ/с. Типичные спектры протонов[2,3], вылетающих под углом I37° в л.с. из углерода под действием протонов с энергией I,I5 (нижние точки) и 5,7 ГэВ(верхние точки), показаны на рис. I. Стрелками обозначены максималь-

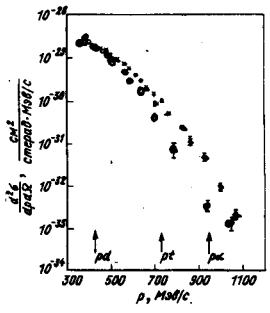


Рис.I

но возможные энергии протонов при столкновении налетающих протонов с ядрами дейтерия, трития и гелия. Если учесть ничтожную величину обратного упругого рассеяния, то видно, что для объяснения наблюдаемых протонов надо привлекать

взаимодействия налетающей частицы более чем с пятью нуклонами ядра.

На рис. 2 показаны те же спектры[4] (точки группируются около нижней прямой), но представленные в виде инвариантной функции $f = \frac{E}{p_t^2}\frac{d^2\sigma}{dpd\Omega}$, где E - полная энергия, а p_t - импульс частицы p. Точки, группирующиеся около верхней прямой, представляют спектр протонов, вылетающих под

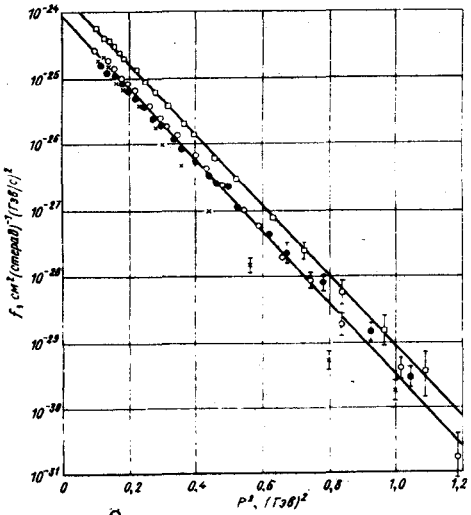


Рис.2

углом 137^0 из ядра меди под действием протонов с энергией 5,7 ГэВ. Приведенные для примера первые данные и многие известные к сегодняшнему дню[5-9] позволяют сделать следующие выводы о нормированной инвариантной функции $\varphi = \frac{f}{\sigma_{tot}^{in}}$ (здесь σ_{tot}^{in} - полное неупругое сечение взаимодействия частицы a и ядра A), описывающей спектры частиц из глубоконеупругих ядерных реакций, начиная с импульсов вторичных частиц выше $p_t > 300$ МэВ/с:

1. $\varphi = Ce^{-T/T_0} \approx Ce^{-Bp_t^2}$, т.е. инвариантная функция имеет экспоненциальный вид.

2. T_0 (или B) $\neq T_0(E_0, a, A)$ т.е. показатель инвариантной функции не зависит от энергии и сорта налетающей частицы и сорта ядра мишени. Рисунок 3, где показана зависимость показателя

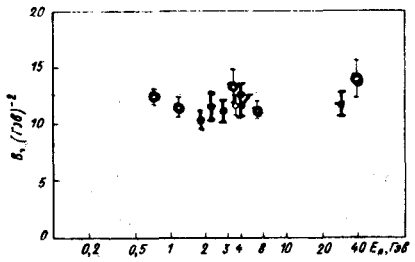


Рис.3

наклона для протонов, испущенных в диапазоне $120-150^0$ из разнообразных ядер (от углерода до свинца) под действием протонов, пионов и γ-квантов с различными энергиями, хорошо демонстрирует утверждение 2. Черными точками указаны новые данные из работ, представленных на конференции[10-12] и новой работы японских авторов[13]. Показанные ошибки только статистические. Рис.4, данные которого получены в одном эксперименте[14], представляет различие в пока-

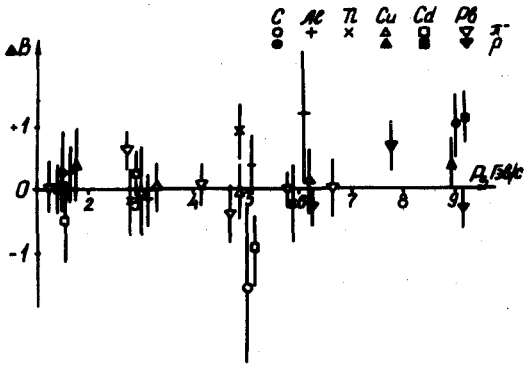


Рис.4

зателях наклона ΔB в зависимости от импульса падающей частицы для первичных протонов и пионов, взаимодействующих с ядрами от C до Pb. Видно, что утверждение 2 выполняется с точностью лучше 10%, начиная с $E_0 \approx 1$ ГэВ.

3. $C \neq C(E_0, a)$, т.е. предэкспоненциальный множитель также не зависит от энергии и сорта налетающей частицы. Если верно утверждение 2, то зависимость величины, прямо пропорциональной C, от E_0 показана на рис. 5 для случая вылета

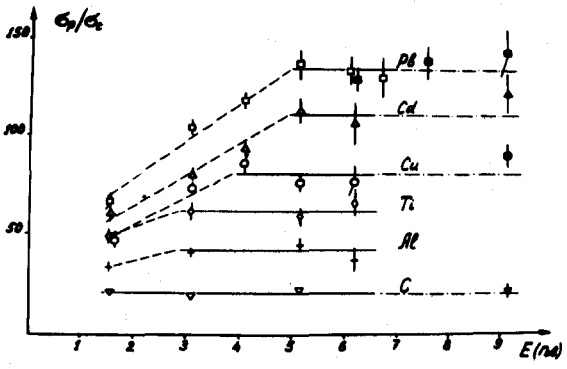


Рис.5

протонов под углом 156° под действием пионов и протонов (темные точки). Видно, что утверждение 3 становится справедливым при тем больших энергиях, чем тяжелее ядро. Грубо говоря, $E_0^{кр} \sim A^{1/3}$.

4. $C \sim A^{1/3}$. Такая зависимость, наблюдаемая ранее [15] для кумулятивных пионов, имеет место и для протонов [16]. Но точнее, $C\sigma_{tot}^{in} = \alpha + \beta A$ [17], как это хорошо видно из рис. 6 для условий рис.5.

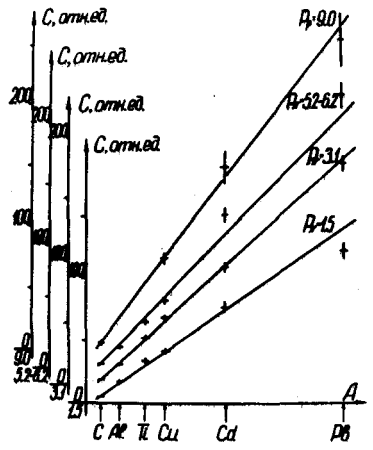


Рис.6

5. Изучение корреляций вторичных частиц в глубоконеупругих ядерных реакциях указывает на независимость в пределах экспериментальных ошибок характеристик вторичных частиц от характеристик лидирующих частиц [7, 8]. Наклон спектров вторичных частиц не зависит или слабо зависит от множественности быстрых частиц в глубоконеупругих реакциях [11,12,17]; другими словами, речь идет о факторизации реакции, о фрагментации мишени.

Не вдаваясь здесь в обсуждения механизма явления, отметим его глубокую аналогию с явлением скейлинга при взаимодействии элементарных частиц, где скейлинг наступает однако при существенно больших энергиях. В силу этой аналогии, связанной, по-видимому, со свойствами взаимодействия со сложными системами, описанное в докладе явление названо ядерным скейлингом. Более подробно свойства ядерного скейлинга и имеющиеся работы рассмотрены в [18].

Литература

1. А.М.Балдин. Препринт ОИЯИ, Р1-5819, Дубна, 1971; ЯФ, 18, 79, 1973.
2. Ю.Д.Бавков и др. Изв. АН СССР, сер.физ., т. 30, №3, 521, 1966.
3. Ю.Д.Бавков и др. ЯФ, 5, 337, 1967.
4. Ю.Д.Бавков и др. ЯФ, 18, 1246, 1973.
5. Ю.Д.Бавков и др. ЯФ, 19, 1266, 1974.
6. Ю.Д.Бавков и др. Письма в ЖЭТФ, 19, 781, 1974.
7. А.В.Арефьев. и др. Письма в ЖЭТФ, 20, 585, 1974.
8. Сотрудничество. Препринт ОИЯИ, Р1-8566, 1975.
9. Ю.А.Будагов и др. Препринт ОИЯИ, Р1-8977, 1975.
10. К.В.Аланакян и др. Доклад этой конф., 510/А6-63, 1976.
11. Л.С.Охрименко и др. Доклад этой конф., 219/А6-19, 1976.
12. М.Г.Горнов и др. Доклад этой конф., 227/А6-54, 1976.
13. T.Hayashino et al. Letter el Nuovo Cim., 16, 71, 1976.
14. Н.А.Бургов и др. Препринт ИТЭФ, 9, 1976.
15. А.М.Балдин и др. ЯФ, 20, 1201, 1974.
16. А.В.Арефьев и др. Препринт ИТЭФ, 56, 1975.
17. Н.А.Бургов и др. Препринт ИТЭФ, 97, 1975.
18. А.В.Арефьев и др. Препринт ИТЭФ, 109, 1975.
19. Г.А.Лексин. Элементарные частицы, в.2, 5, 1975, Атомиздат.

INTERACTIONS OF FEW-NUCLEON SYSTEMS AT RELATIVISTIC ENERGIES

I.P.Zielinski
Institute for Nuclear Research, Warsaw ,Poland

Recently, the acceleration of deuterons, α and heavier ions has been achieved in several proton synchrotrons. I should like to present some results obtained using the deuteron and alfa beams at the Dubna synchrophasotron (accelerating now protons and deuterons up to 10 GeV, alfa's up to 20 GeV and - recently - carbon ions up to 50 GeV).

The results are divided into three sections according to the experimental techniques used.

The first section concerns the interactions of 3.3 GeV/c deuterons and protons using 1 m hydrogen bubble chamber[1]. The use of the deuteron beam provides substantial experimental advantages as compared with the deuterium target experiments, namely the unambigous separation between different channels as well as the possibility to measure the full momentum spectrum of "spectator"-nucleons. The advantages of the method have been described in detail in our paper[2], subsequent results of the study of the $dp \to ppn$ reaction are now being published[3]. Referring to our earlier result[3], we should like to emphasize one experimental finding, namely the large excess of "spectator"-nucleons with momenta above-say-300 MeV/c. Several possible explanations of this observation can be considered, e.g.: Double scattering in the sense of the Glauber model. The existing estimates (see e.g. Alberi et al.[4]) show that this effect is not sufficient for explaining the observation. Nucleon-nucleon final state interaction, recently discussed[4], seems to be also not sufficient. We should like to point out two processes, related to each other, which might be responsible for the effect. Owing to the proximity of the pion pole to the physical region the one pion exchange between the incoming proton and the entire deuteron might be a good approximation for the events with the small momentum transfer, as suggested by Foster et al.[5]. We observe that the angular distribution of two nucleons in their c.m.s. agrees well with that known from $\pi d \to pp$ reaction. Figs.1a and b show the two nucleon mass $Q = M_{eff} - 2M_N$ distribution for $dp \to (pp)n$ charge exchange and $dp \to (pn)p$ charge retention channels for events

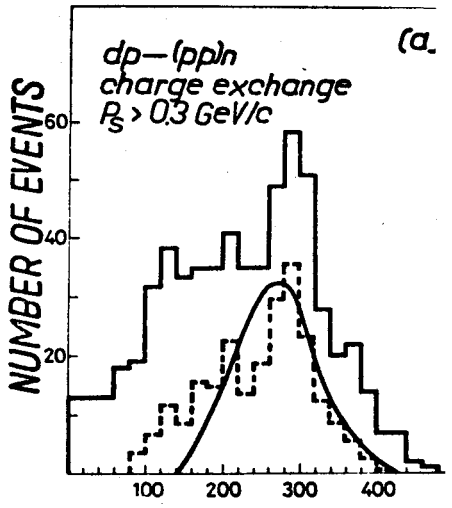


Fig. 1a

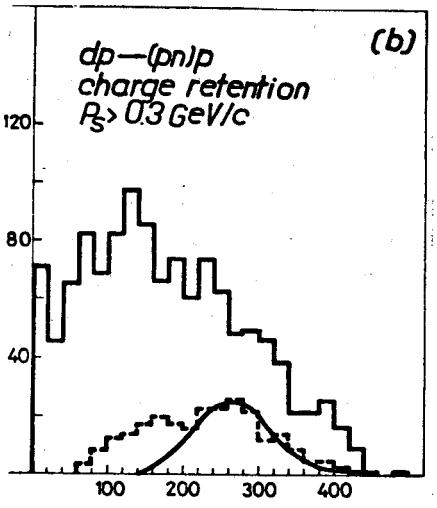


Fig. 1b

with $P_S > 300$ GeV/c. The solid line represent the calculations based on the one pion exchange model. By comparing our data concerning the effective mass and angular distributions in the $\pi^+ d \to pp$ reaction we observe the approximate agreement provided we take into aocount that large two-nucleon masses are attenuated by the kinematical limit. Fig. 1a exhibits an enhancement at $Q \cong 300$ MeV ($\Gamma \cong 50$ MeV) which cor-

responds approximately to the sum of $\Delta(1236)$ and nucleon mass. This suggests the possible role of $\Delta - N$ interaction or $\Delta - N$ resonance for the explanation of the high momentum tail of "spectator"-nucleon momenta.

I should like to mention at the end of this part one of the interesting related results, concerning the relativistic generalization of the deuteron wave function submitted for this Conference by V.R.Garsevanishvili et al. from the Tbilisi State University[6].

In the second sections I should like to present some preliminary results obtained using the recoil measurement technique, developed several years ago in Dubna and used then in Dubna, Serpukhov and Batavia[7]. It consists of the use of the internal beams of particles, the multitraversal of the internal thin target (gas jet or - in this case 0.7-0.8μm polyethylene foil), the recoils being measured using the semiconductor detectors. The experimental apparatus is described in detail in[8].

The first result[9] concerns the very small angle elastic scattering in the energy range 1.75÷4.13 GeV per nucleon. The differential cross section for about half a million events has been obtained in a small $|t|$ region ($0.003 < |t| < 0.05$ GeV^2/c^2). The first results are shown in fig. 2 and Table 1. The differential cross-sections are normalized using the Bethe formula and the Glauber model value for σ_{tot} = 134 mb.

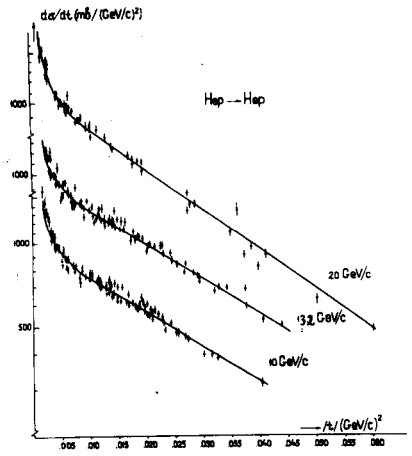


Fig. 2

Table 1

E/nucleon in GeV	b in (GeV/c)$^{-2}$	
1.75	28.1±0.9	-0.22±0.09
2.51	28.6±1.2	-0.23±0.12
4.13	29.8±1.0	-0.34±0.10

The nuclear structure radius has been obtained R_{He} = (1.37±0.02) fm using the Czyz-Lesniak formula[10] and the structure form factor $\exp(-\frac{3}{16}R_{He}^2|t|)$ [11]. This value coincides with the electromagnetic radius obtained from[11]. Due to the experimental method used here, not only the slope parameter b but also the ratio ρ of the real to the imaginary part of the amplitude from the Coulomb-nuclear interference were obtained. Fig. 3 shows the energy dependence of ρ on the energy as calculated by Dumbrajs and Staszel[12] using dispersion relations

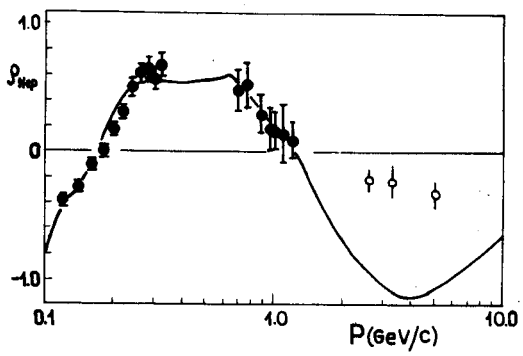


Fig. 3

and the method of conformal mapping. The experimental values of ρ in the helium-proton case are near to the proton-proton case and differ from the theoretical values but it is early to conclude that the dispersion relations are violated in the He-p as the errors in the theoretical curve are large and not well known at present.

The second experiment started recently[13]. It concerns the systematic study of nuclear fragmentation. Figs. 4 and 5 show the resolution of the apparatus (semiconductor detector telescopes are used) and first results.

Now in the 3rd section I would like to present preliminary results by Ableev et al.[14]

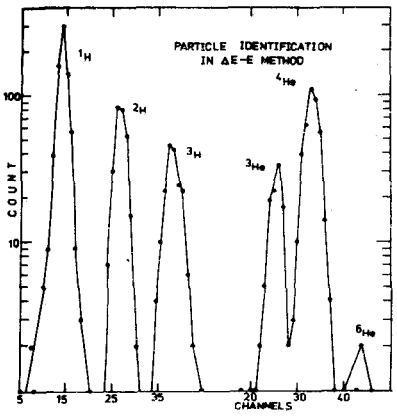


Fig. 4

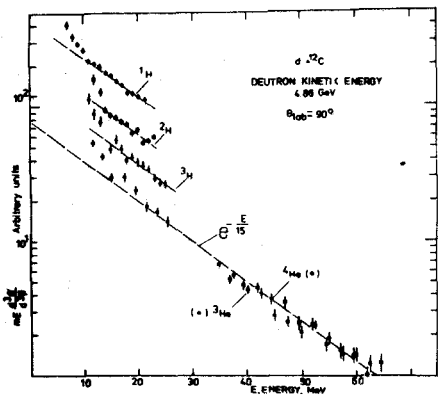


Fig. 5

on "A search for α -particle scattering at 17.9 GeV/c on P, He, C, Al, Cu, Pb". Using a magnetic spectrometer "Alpha"/15/ with multiwire proportional chamber and dE/dx detectors, elastic scattering and reactions with target-nucleus excitations as well as incident α -particle fragmentation processes have been detected with high counting rate and good t-resolution ($\delta p/p \simeq 0.8\%$; $\delta\theta/\theta = 0.8 \cdot 10^{-3}$ rad). Absolute values of $(d\sigma/dt)$ for α -particle scattering at $0.01 \lesssim -t \lesssim 0.2$ $(GeV/c)^{-2}$ are measured (Fig. 6).

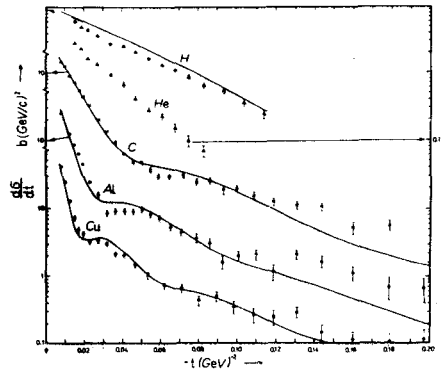


Fig. 6

Preliminary results (Table II) obtained for $(d\sigma/dt)_{t=0}$, B, σ_{tot}, σ_{el} in approximation $(\frac{d\sigma}{dt})_{dA} = A\exp(Bt)$ at $-t \lesssim \frac{4}{B}$ $(GeV/c)^{-2}$ (with additional ct^2 term for $\alpha\alpha$ -scattering) and in approximation $|Re f_{dA}(0)/Im f_{dA}(0)|^2 \ll 1$ are rather consistent with Glauber theory predictions.

Table II

Target	$(d\sigma/dt)_{t=0}$ barn$(GeV/c)^2$	B $(GeV/c)^{-2}$	$R_{dA} = 2\sqrt{B}$ fermi	σ_{tot} barn	σ_{el} barn
H_2	0.910±0.027	32.1±0.8	2.236±0.026	0.133±0.002	0.028
He	7.5±0.7	67.±5.	3.24±0.13	0.382±0.017	0.111
C	33.9±0.8	103.6±1.3	3.982± 0.025	0.814±0.009	0.327
Al	97.±5.	162.6±3.9	5.03±0.06	1.38±0.04	0.59
Cu	288.± 32.	247.±10	6.20±0.13	2.38± 0.13	1.17

However, the authors have observed some deviations of an oscillatory type $\Delta(t) = (d\sigma/dt)_{exp} - (\frac{d\sigma}{dt})_{Th}$ of experimental differential cross sections from Glauber ones for α-C, α-Al, α-Cu scattering (see Fig. 7).

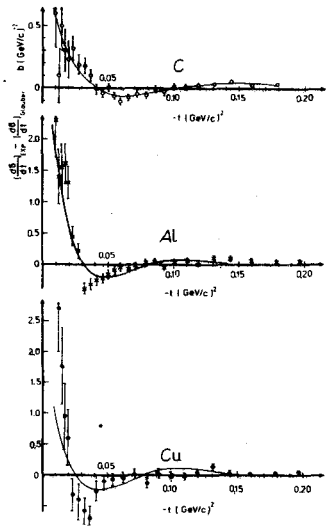


Fig. 7

The calculation of $(\frac{d\sigma}{dt})_{Th}$ was done in the frame of eikonal approximation/17/. In such a representation for differential cross sections one has $(d\sigma/dt)_{Th} = |f(t)|^2 + (d\sigma/dt)_{inel}$, where the coherent scattering amplitude $f(t)$ takes into account the Coulomb effect and the second term accounts for the quasielastic scattering with excitation or break-up of the target nucleus except for meson production. The nucleus was described with nuclear density distribution of the Woods-Saxon type: $\rho = \rho_0/[1+\exp(\frac{R-R_0}{a})]$. All

input parameters from experimental data on eA and NN scattering were used.

Deviations have been fitted (solid line in Fig. 7) by the function[18] $\Delta(t) = a_i + c_i J_0(R_i\sqrt{-t})^2 \exp(kt)$

Fitting results for R_i are of the order of radii of nuclei. The authors would like to mention a possible relationship between the oscillation effect $\Delta(t)$ and a contribution of the peripheral processes. Recently, Tsarev and Starkov[18] derived such oscillations in pp -scattering as a result of contributions into peripherical part of absorption from fragmentation of protons. The authors[14] believe that the observation of an oscillatory behaviour of the differenoe $\Delta(t)$ can be considered as an evidence for the necessity of a more adequate input of peripheral effects to the calculation of the fitting curve $(d\sigma/dt)_{Th}$.

References

1. B.S.Aladashvili, B.B.Badelek, V.V.Glagolev, R.M.Lebedev, M.S.Nioradze, I.S.Saitov, A.Sandacz, T.Siemiarczuk, J.Stepaniak, V.N.Streltsov, P.Zielinski. Dubna-Warsaw-Collaboration, Contributed paper 945/A6-46.
2. B.S.Aladashvili et al. Nucl.Instr. and Meth., 129, 109 (1975).
3. B.S.Aladashvili et al. Nucl.Phys., B86, 461 (1975) and paper in press in Yadernaya Fizika, Nucl.Phys., Journal of Physics G, Acta Physica Polonioa.
4. G.Alberi et al. CERN Report, TH, 1976.
5. R.Poster et al. Phys.Rev.Lett., 33, 1625 (1974).
6. V.R.Garsevanishvili, D.G.Mirianashvili, M.C.Nioradze. JINR, P2-9859, Dubna, 1976 and contribution to this Conference.
7. V.A.Nikitin et al. JETP, 46, 1608 (1964).
8. V.A.Budilov et al. JINR, 13-8898, Dubna, 1975.
9. G.G.Beznogikh, V.A.Budilov, P.Devenski, L.F.Kirillova, N.K.Zhidkov, V.A.Nikitin, P.V.Nomokonov, G.Motz, M.G.Shafranova, W.Skweres, A.Buyak, M.Szawlowski, T.Szczepankowski, V.V.Avdejohikov, V.I.Khachko. Dubna-Leningrad-Warsaw Collaboration, Report No. 451.
10. W.Czyz, L.Lesniak. Phys.Lett., 24B, 227 (1967).
11. R.F.Frosch et al. Phys.Rev., 160, 874 (1967).
12. P.Dumbrajs, M.Staszel. Preprint of the IFTUW No. 25 (1975), Warszawa and Journ. of Phys., G, in press.
13. The same authors as in[9], Report No. 452.
14. V.G.Ableev, S.G.Basiladze, V.A.Bodjagin, Yu.T.Borzukov, A.Filipkowski, L.B.Golovanov, I.V.Khristova, G.L.Mazny, A.A.Nomofilov, N.M.Piskunov, V.N.Sadovnikov, V.I.Skarov, M.N.Shumanov, I.M.Sitnik, L.A.Stepets, A.P.Tsvinev, G.G.Vorobiev, S.A.Zaporozhets, L.S.Zolin. Report JINR No. 448/A6-5 at this Conference.
15. G.Ableev et al. JINR, 13-8967, Dubna, 1975.
16. W.L.Wang. Phys.Lett., 52B, 143 (1974).
17. C.W.Czyz, L.Maximon. Ann. of Phys., 52, 99 (1969).
18. N.I.Starkov, V.A.Tsarev. Lett to JETP, 23, 131 (1975); and Report A1/20 at this Conf.

A STUDY OF THE "YOUNG" STATES OF PARTICLES IN p-, d-, and α-NUCLEI INTERACTIONS

L.I.Sarycheva

Nucl.Phys.Inst., Moscow State University

Introduction

The mechanism of leading particle generation in hadron-nucleus collisions contains the unique information concerning the features of hadronic interaction on a scale of times and distances comparable with nuclear dimensions.

At one time Zatsepin[1] and Feinberg[2] put forward a conception of inelastic collision, in which on incident hadron "sheds" its meson cloud and cannot interact once more until the cloud has been formed again. More recently, an analogous effect was supposed on basis of the parton model[3].

Our previous works[4,5] reported an attempt to directly estimate the efficiency of internuclear interactions from angular and momentum spectra of leading secondaries measured on various nuclei in accelerator experiments.

The object of the report [6,7], submitted to this conference, is to discuss the main points of our method (which represents the "good geometry beam attenuation" method, apllied to the target-nucleus) within the framework of a simple classical model of scattering, that seems to be a close enough approximation to the concerned phenomena.

Model

Imagine the target-nucleus as a spherical droplet of nuclear fluid (of radius $r_A = r_p A^{1/3}$, where r_p is a nucleon radius, and A is atomic number). The cross-section for inelastic (and quasielastic) scattering of a quasi-point projectile on such a nucleus is given by a formula $\sigma_A^{abs} = \pi r_A^2 - f_A$, which fits well the experimental data on absorption cross-section for interaction of different hadrons or light nuclei on various nuclei. The function f_A (nuclear opacity) is determined by

$$f_A = 1 - \frac{1}{\pi r_A} \int_0^{r_A} 2\pi b\, db\, e^{-x(b)\cdot\sigma_0},$$

i.e., depends on a parameter $1/\sigma_0 = \lambda_0$ - mean free path in nuclear fluid. If in first interaction within nucleus a fraction of incident particles is scattered into an interval of angles and momenta $d\omega \cdot dp$, and in repeated interaction (which can be characterized by a scattering length $\lambda_1 = 1/\sigma_1$) leave this interval, then the relative yield of secondaries, scattered into $d\omega dp$ in a interaction

$$R_A = \frac{\beta(\theta,P)_A}{\beta(\theta,P)_p} = \frac{Q_A \cdot f_p}{Q_p \cdot f_A}$$

where $\beta(\theta,P)_A = \frac{1}{\sigma_A} \cdot \frac{d^2\sigma_A}{d\omega \cdot dp}$ is the number of particles observed in macroscopic experiment inside the interval $d\omega \cdot dp$, and

$$Q_A = \frac{1}{\pi r_A^2} \int_0^{r_A} 2\pi b\, db \int_0^{x(b)} e^{-\sigma_0 \xi} \sigma_0 \cdot \xi \cdot d\xi \cdot e^{-\sigma_1 (x-\xi)\cdot \alpha(\theta,P)} d\omega dp$$

depends on a parameter σ_1, since σ_0 can be obtained from the known values of σ_A^{abs}. Thus, the behaviour of R_A measured experimentally, allows estimation of the efficiency of secondary interaction within nucleus. The effective number of collisions on leading particle with nucleons in nucleus (i.e., number of collision along the mean chord in nucleus $\bar{x} = \frac{4}{3} r_A$) in this case can be determined in the relation:

$$\langle \nu \rangle = \left(\frac{\bar{x}}{\lambda_0} - 1 \right) \cdot \frac{\lambda_0}{\lambda_1} .$$

Experimental Results

Fig. 1 illustrates the behaviour of R_A calculated for our model. In the same picture the experimental ratios R_A for leading proton are plotted. These data have been obtained in the paper[6] from the accelerator experiments on pA-collisions at 19,4 ÷ 24 GeV/c[8,9]. The figure shows that secondary protons interact within nucleus substantially less effectively than primaries.

Another work[7], reported to this conference, presents the investigation of the process of conservation and absorption of leading nuclei (deuterons and α-particles) in the nuclear matter. The measurements have been performed in the beam of accelerated nuclei (8,4 GeV/c per charge) from JINR synchrocyclotron, Dubna,

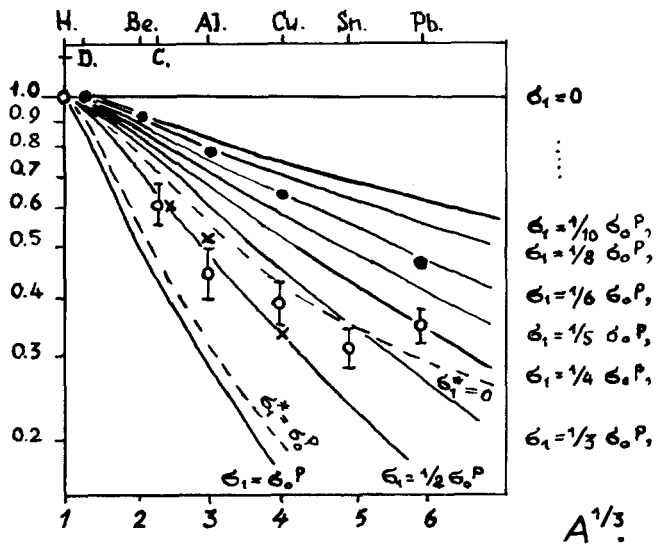


Fig. 1. Relative intensity of secondary particles ($\overset{\circ}{p}, \overset{\circ}{d}, \overset{\circ}{\alpha}$) in the $17 < \theta < 40$ mrad angular and $0.9 > p/p_0 > 0.7$ momentum ranges as a function of target-nucleus size. The curves have been calculated to the classic approximation for two models of particle scattering on nuclei. The dotted curves relate to version 1; the solid curves - to version 2 ($\sigma_0^d = 2\sigma_0^p$).

using single-arm magnetic spectrometer "Alpha"[10], with multiwire proportional chambers as coordinate and scintillators as charge detectors. It was found that in some 1% case of inelastic interactions, deuterons and α-particles did not disintegrate. The efficiency of intranuclear interactions of these "leading" nuclei was estimated for the two alternative models:

1) incident nucleus is a weakly bound system of A nucleons, each of them interact independently, i.e., same manner, as a single nucleon does (dotted line in Fig. 1);

2) nucleus penetrates through the nucleus as a single point-particles (solid line in Fig. 1).

Both the variants lead to a conclusion that the effectivity of secondary nuclei interaction is substantially less than that of primaries (Fig. 1). The same conclusion was made about the behaviour of "young" particle inside a nucleus in the paper[11]. If we choose variant 2), and assume that the propagation of any point-particle is described by the same absorption coefficient σ_0 (or σ_1), then the experimental data for p-, d-, α-particles proves to be consistent with the value of nuclear field regeneration time $\tau_z \approx 0.47 \cdot 10^{-23}$ sec $\sim \hbar/m_\pi$.

Conclusions

1. Our data show that the deuterons and α-particles in the inelastic interactions retain their individuality in some cases, even after loosing from 10 to 30% of their energy and scattering on considerable angles (beyond the diffraction cone). Thus, in analogy with the pA-interactions, the existence of the leading ("conserved") deuterons and α-particles may be postulated.

2. Comparison between the experimental data and the calculations made in terms of simplified models shows that there exists a sufficiently high probability for the 8.4 GeV/c deuterons and the 16.8 GeV/c α-particles to undergo more than one interaction in the same nucleus. The path of a secondary deuteron in nuclear matter proved, however, to exceed the path of the primary deuteron; the ratio σ_0/σ_1 is most probably within 1/3÷1/4.

References

1. G.T.Zatsepin. J.Phys.Soc.of Japan 17, suppl. A-III, 495, 1962.
2. E.L.Feinberg. In col. papers "Problems of Theoretical Physics", Nauka, Moscow, 1972, p. 248.
3. O.V.Kancheli. Pys'ma ZhETF, 18, 465, 1973.
4. V.S.Murzin, L.I.Sarycheva. Sov.Nucl.Phys., 23, 382, 1976.
5. A.I.Demiyanov et al. Proc. 14th Int.Conf. on Cosmic Rays, Munich, 1975, v. 7, p.2522.
6. A.I.Demiyanov, V.S.Murzin, L.I.Sarycheva. Report at the present Conference A6/12-455.
7. L.G.Ableev et al. Report at the present Conference A6/4-447.
8. A.Klovning. et al. Nucl.Phys., B54, 29, 1973.
9. T.Eichten et al. Nucl.Phys., B44, 333, 1972.
10. V.G.Ableev et al. Preprint JINR, 13-8967, Dubna, 1975.
11. V.B.Gavrilov, G.A.Leksin et al. Moscow, Preprint ITEF-2, 1976.

MECHANISMS OF THE CUMULATIVE HADRON PRODUCTION ON NUCLEI

A.V.Efremov
JINR, Dubna, USSR

The cumulative production of hadrons in hadron-nucleus collisions attracts more and more attention both of theorists and of experimentalists. (We use this name for the inclusive production of hadrons beyond the kinematical bound determined by the hadron scattering on a single nucleon of a nucleus). One of the reasons is just the belief that such a mechanism is a common mechanism of the hadron-nucleus interaction rather than of the narrow kinematical region. The astonishing similarity of the A-dependence of high P_t and cumulative production[1,2] and deuteron electromagnetic form factor behaviour supports this point of view.

The cumulative production is characterized by a number of peculiarities:

i) The nuclear scaling[3], i.e., the independence of the invariant cross section of the energy of a projectile;

ii) The power increase of the cross section with atomic number A, the power depending on the energy of a produced hadron (in the nucleus reference frame) and reaching even the value 1.5 - 2 for heavy particles (d,t)[1,4];

iii) The spectrum of produced hadrons falls exponentially with energy, the slope weakly decreasing with A;

iv) The cross section is isotropic at small momenta of the produced hadrons and is backward decreasing at high momenta[5];

v) The pronounced back-to-back correlation of a cumulative and any charged hadron is observed. Figure 1 shows the correlation obtained from $\pi^- C^{12}$ collision at 5 GeV/c.

The proposed mechanisms for explanation of these phenomena can be subdivided into three groups: the Fermi motion inside a nucleus (FM), the multiple scattering with nucleons of a nucleus (MS), and inelastic scattering with

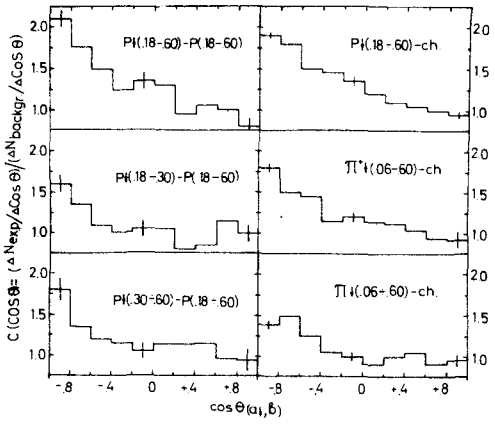


Fig. 1

a coherent "flucton" (CF), i.e., a fluctuation of the nuclear matter inside a nucleus.

The FM consideration is presented in contributions[7-9]. The main problem concerns the high momentum transfer to a nucleon N (fig. 2),

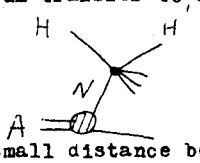


Fig. 2

i.e., the small distance behaviour of the nucleon wave function and the behaviour of the upper block far of the mass shell.

The authors of paper[7] use the specific quantum number and show that only the mass-shell contribution of N is essential. The agreement with the experimental spectrum looks to be satisfactory (fig. 3). However, there are no

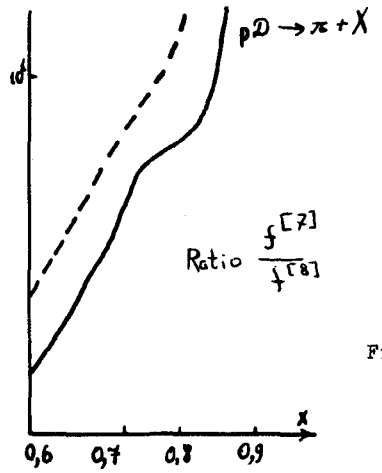


Fig. 3

such specific properties for heavier nuclei[8] and theoretical curves disagree with experiment by 1.5-2 order of magnitude (fig. 4). In addition, FM probably cannot explain the A-de-

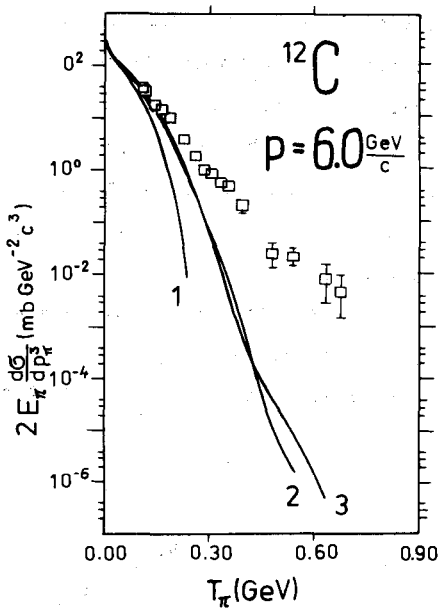


Fig. 4

pendence of the cross section[10] especially, high power for heavy particles ($p^{max}_{Fermi} \sim A^{1/3}$).

The authors of paper[9] propose the quasi-potential approach to this problem using the wave function determined from the disintegration process $pd \to ppn$.

The MS mechanism is more peculiar. It is shown[11] that it can produce nucleons in the region $p \leq 2Am_N/\theta$, where p and θ are the momentum and angle of the produced hadron in the nucleus rest frame. However, for this a great number of rescatterings is required ($n \sim 4 \div 5$), a part of which should have high $p_\perp$ and unavoidably results in breaking of the nuclear scaling. Also the backward nucleons from Al d-scattering[12] is inexpliciable.

Thus, both the FM and MS cannot explain all features i)-v). Nevertheless, sophisticated modifications with a more reasonable description are not excluded. An example of such a modification is a high-frequency term in the nucleus wave function[8]. However, a description of this type seems to be nonadequate to the physical nature of oscillations, i.e., some kind of nuclear correlations. Another modification of this type is the fireball picture of MS[13] when a projectile hits a nucleon producing a fireball which absorbs some other nucleons and decaying produces cumulative hadrons.

The most probable, from our point of view, seems to be the CF mechanism proposed long ago by Blokhintsev[14] for explanation of the d, t, He^4 knock out of heavy nuclei[15] and revived by Baldin for the prediction of cumulative effect[16]. For that reason we dwell on this mechanism in more detail.

If we consider the nucleus as a heavy elementary particle composed of quarks, then it is easy to see that in the usual experimental situation, $M \simeq 12$ GeV (C^{12}), $\varepsilon \simeq 1 \div 2$ GeV, $E \simeq 10$ GeV, $\theta \simeq 180°$, all the invariant variables (fig. 4)

$$s = 2(p_A p_B) = 2ME, \quad t = -2(p_A p_c) = -2M\varepsilon, \quad u = -2(p_B p_c) = -2E(\varepsilon - p_c \cos\theta) \quad (1)$$

are much larger than the hadron mass ($s_0 \simeq 1$ GeV^2), i.e., the same condition holds as in the high-$p_\perp$ inclusive production. This analogy (supported by the Feynman diagram analysis of the type of[17]) leads to the parton mechanism of the cumulative production[18] similar to that of high-$p_\perp$ particles

$$f = \varepsilon \frac{d^3\sigma}{d^3p} = \int dx\,dy\,dz\, F_A(x) F_B(y) D_C(z)\, v(xys, \frac{x}{z}t, \frac{y}{z}u) \quad (2)$$

where F_B, F_A are the numbers of partons with 4-momentum yp_B and xp_A in hadron B and nucleus A, resp., D_C is the number of hadrons C in parton c with 4-momentum p_c/z and the function v is the cross section $ab \to cx$ at small distance

$$v \sim \frac{1}{sxy}\left(\frac{sz^2}{ut}\right)^K \delta\left(1 + \frac{t}{syz} + \frac{u}{sxz} - \frac{s_0}{sxy}\right) \quad (3)$$

$$K = n_a + n_b + n_c - 2$$

In the region where ut/s is not too large and $-t/s = \frac{\varepsilon}{E} \ll 1$ we can choose $D_c(z) \simeq \delta(z-1)$ (trigger bias), $F_B(y) \sim 1/y^{\alpha_B(0)}$.

Let us turn now to the distribution function $F_A(x)$. It can be calculated as a composition of the parton distribution in a nucleon and the nucleon distribution in a nucleus[6,7] (the squared wave function). However, because of the difficulty with the wave function mentioned earlier we prefer a more simple and straightforward arguing.

As the momentum transfer is much higher than the binding energy of the nucleus, the only thing which is important is the coherence of quarks inside the nucleus. This coherence is stated by the emission and absorption of virtual gluon quanta moving near to the light velocity. For the projectile particle those quarks will be coherent which are simultaneously (in the projectile rest frame) inside the shere of radius $r_0 \simeq 1/m_\xi$. In the nucleus rest frame this sphere is stretched along by the γ -factor and when the energy is high enough ($\gamma > R/r_0$) it cuts a "tube" out of the nucleus volume. So, the probability q of one quark to get into the coherence region of another is the ratio of the tube to the nucleus cross section, $q \sim (r_0/R)^2 \ll 1$

It is easy to see that the process on the nucleus as a wholly coherent system is suppressed by the factor q^{3A-1} and more probable is the process on some coherent fluctuations of a smaller number of quarks. In this case/16,18/

$$F_A(x) \sim \sum_n C_{3A}^n q^{n-1} (1-q)^{3A-n} \left(1 - \frac{3A}{n} x\right)^{2(n-n_a)-1} \quad (4)$$

The factor q^{n-1} here suppresses too heavy fluctons and the phase factor $\left(1 - \frac{3A}{n} x\right)$ suppresses too light ones. The substitution of (4) into (3) with the use of the $F_B(y)$ behaviour in the region $y \ll 1$ and summation over n (by the saddle-point method) give ($\varepsilon_\theta \equiv \varepsilon - p\cos\theta$)

$$f \sim \left(\frac{E}{\varepsilon}\right)^{\alpha_p(0)-1} A^{2/3} \frac{\varphi(\varepsilon - p\cos\theta)}{\varepsilon^{k+1}} \exp\left\{-\varepsilon_\theta B\left(\ln \frac{\varepsilon_\theta C}{A^{1/3}}\right)\right\} \quad (5)$$

where φ is a power function of ε_θ, C is a constant parameter and $B(L)$ is the known monotonic function increasing for $L > 0$, $B(0) = 0$, and $B(L) \to L$ for $L \to \infty$. Its concrete form depends on the character of fluctuations, i.e., on the number of quarks which can enter into the coherence volume simultaneously (q-, N- or Δ-groups).

It is easy to see that the expression (5) gives the qualitative description of the cumulative production features i)-v). The nuclear scaling is guaranteed by $\alpha_p(0) \simeq 1$; the cross section increases with A as $A^{(2/3 + 1/3 \langle B/L \rangle \varepsilon_\theta)}$. With increasing mass of the produced particle and with decreasing A the value of $\ln \varepsilon_\theta / A^{1/3}$ and, consequently, the slope B increases. The cross section is isotropic for $p/\xi \ll 1$ and decreases to the backward direction when $p/\xi \simeq 1$; the back-to-back correlation in the lab. reference frame is guaranteed by the mechanism of hard scattering of a light parton of a projectile with a heavy parton of a nucleus.

The quantitative description in the models of this type presented in figs. 6, 7 is given in papers/22/ (with the Fermi-motion correction) and/19/.

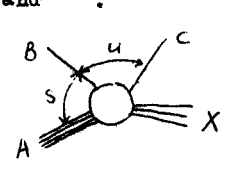


Fig. 5

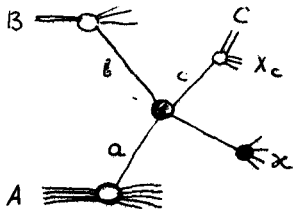


Fig. 6

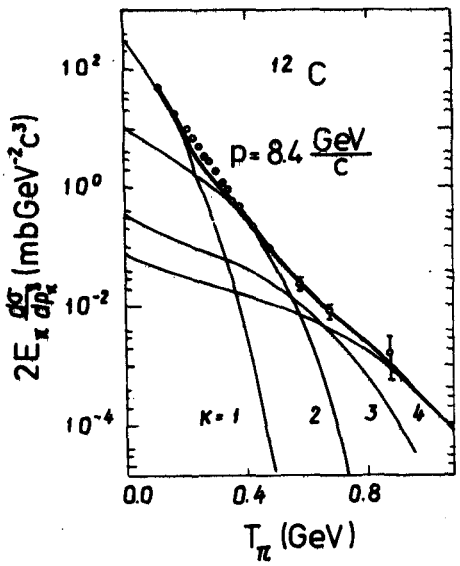


Fig. 7

We have to notice, however, that one of the difficulties of the naive calculation of $F_A(x)$ chosen here is the prediction of the monotonic growth of power $\alpha(\varepsilon_\theta)$ which seems to be not the case experimentally. From this point of view the experimental investigation of the deep inelastic lepton-nucleus scattering in the cumulative region would be especially interesting because it gives the most direct information about this function.

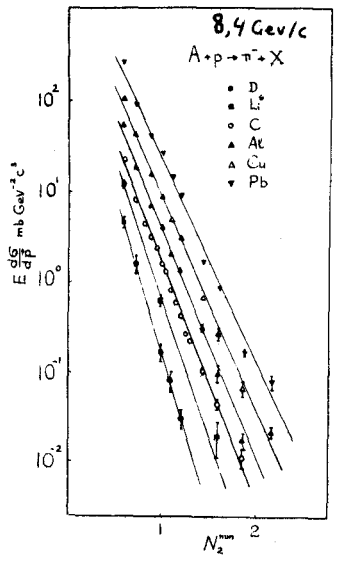


Fig. 8.

References

1. A.M.Baldin et al. Yad.Phys. (Soviet Nuclear Physics), 21, 461 (1975). See also report of V.S.Stavinsky at this Conference.
2. J.W.Cronin et al. Phys.Rev., D11, 3105 (1975).
3. V.B.Gavrilov, G.A.Leksin. Preprint ITEPh-36 (1975), see also Leksin's report at this Conference.
4. A.M.Baldin. JINR Preprint, E1-8858, Dubna, 1975.
5. Yu.A.Budagov et al. JINR Preprint, P1-8977, Dubna, 1975; G.A.Leksin, ITEPh Winter School, 1975 (in Russian).
6. Yu.A.Budagov et al. Contr. 812.
7. E.Frankfurt, M.Strikman, contr. 256.
8. V.Burov, V.Lukjanov, A.Titov. JINR Preprint, P2-9426, P2-9570, Dubna, 1976 (Contr. 889, 888).
9. V.R.Garsevanishvili et al. Contr. 454.
10. J.Blatt, W.Weiskopf. "Theoretical Nuclear Physics". John Wiley&Sons, New York, 1952.
11. V.Kopeliovich. JETP Lett., 23, 348 (1976), contr. 826.
12. L.G.Abdivaliev, contr. 447. Preprint JINR, P1-9924, Dubna, 1976.
13. M.Braun, Yu.Evlashev. Contr. 1109.
14. D.I.Blokhintsev. JETP, 33, 988 (1957).
15. L.S.Ashgirej et al. JETP, 33, 1185 (1957).
16. A.M.Baldin. "Kratkie soobshcheniya po fizike" (Short reports on Physics), no. 1, p.c. "Nauka", 1971.
17. A.V.Efremov. Czechoslovak Journal of Physics, 26, 430 (1976).
18. A.V.Efremov. JINR Preprint, E2-9526, Dubna, 1976; Yad.Fiz., 24, No. 12 (1976); contr. 471.
19. V.S.Stavinsky. JINR Preprint, P2-9528, Dubna, 1976; contr. 1152.
20. V.A.Matveev et al. N.C.Lett., 7, 719 (1971).
21. See for instance R.Blancenbecler, D.Sivers, S.Brodsky. Phys.Rep., 23C, No. 1 (1976).
22. V.Burov et al. Proc. of Int. Conf. on Selected Topics in Nucl. Struct., Dubna, JINR, D-9920 (1976), v. II.

DISPERSION DESCRIPTION OF THE DEUTERON

L.L.Frankfurt, M.I.Strikman
Leningrad Nuclear Physics Institute

1. Everybody knows that nuclei consist of nucleons. At the same time deep inelastic experiments suggest that nucleons consist of quarks. Therefore, to describe short distance effects in nuclei a quark-nuclear theory should be built up which takes into account both these facts.

2. The crucial point is that the distances which are small for nuclear physics are normal for quarks in hadrons. As a result in this transition region all the phenomena should be described both in terms of hadrons and in terms of quarks.

3. Such a description can be achieved on the basis of the space-time picture (STP) of high energy scattering developed by Gribov[1] and Feynman[2]. The importance of taking into account the STP can be demonstrated by the example of the West paradox. West showed that in the conventional form of impulse approximation even at high energies $\sigma_{tot}(\pi d) < \sigma_{tot}(\pi p) + \sigma_{tot}(\pi n)$[3]. It is in contradiction with the STP of the bound state. Really this paradox is due to inclusion of the $N\bar{N}$ pair into the deuteron wave function[4].

4. In analogy with Ref.[1] we shall use the dispersion representation of the amplitude over the deuteron mass[5]. In the dispersion approach (DA) the deuteron consists of real hadrons: NN, $NN\pi$, etc. The low energy NN inelastic processes are dominated by resonance production. Due to the zero isospin of the deuteron the vertex $D \to NN$ dominates at least up to two $\Delta(1240)$ production threshold ($K_N \sim 0.8$ GeV/c). The dispersion representation for the $D \to NN$ vertex function over the deuteron "mass" (i.e., $4(m_N^2 + K^2)$ where K is the momentum of one nucleon) appears to be a straighforward relativistic generalization of the Schrodinger wave function. This becomes obvious in the Infinite Momentum Frame (IMF).[x] Note that the description with $D \to NN$ vertex function can effectively work for much larger $\vec{K}$ due to the quark additivity[4,5].

5. In the deuteron rest frame its wave function has the form:

$$\Phi_\mu(K) = u(K)\sigma_\mu - \frac{w(K)}{\sqrt{2}}\left(\sigma_\mu - \frac{3K_\mu(\sigma K)}{K^2}\right) \quad (1)$$

The normalization condition is $\int (u^2(K) + w^2(K))\, d^3K = 1$. In the impulse approximation and in the Bjorken limit the deep inelastic structure function $F_{2D} \equiv \nu W_{2D}$ has the form:

$$\int \left(F_{2p}\left(\frac{x_D}{\alpha}\right) + F_{2n}\left(\frac{x_D}{\alpha}\right)\right)\left(u^2(K) + w^2(K)\right) d^3K = F_{2D}(x_D) \quad (2)$$

where $\alpha = (1 + K_3/\sqrt{m^2 + K^2})/2$ is the fraction of the deuteron momentum carried by one of the nucleons in IMF. The eq. (2) is the same as in the parton model. The only difference is to include the nucleon structure function. This similarity seems natural owing to duality between the Bjorken-Feynman quark-parton STP and the Gribov STP.

6. The results of calculation F_{2D} based on eq. (2) are presented in the figure. The data are taken from Ref.[6]. For the rough estimate we identify u, w wave functions with the quantum mechanical ones of ref.[7] which reasonably fit the deuteron form factor. Standard fits to

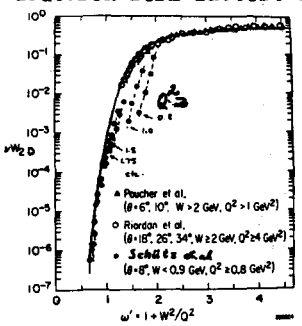


Fig. 1

$F_{2p}(x)$, $F_{2n}(x)$ were used. In the range $0.55 < \omega_D < 1$ ($\omega_D = 1/2\, x_D$) the theoretical curve can be roughly approximated as $F_{2D}(\omega_D) = 0.12(\omega_D - 0.5)^n$ with $n = 5.7$. The Stanford experiment[6] gives $n = 6 \pm 0.5$. Note that quark counting rules give $n = 9$. A slow dependence from ω_D was predicted[4] in the composite quark model of the deuteron as a result of Fermi motion of quarks (due to the large average mo-

[x] We thank M.G.Ryskin who has drawn our attention to the relationship between the IMF approach and the dispersion approach.

mentum 0.4 GeV/c of quarks in hadrons). The threshold behaviour could be expected only at $\omega_D - 1/2 < 1/10$.

7. The invariant cross section of the reaction $D+p \to \pi^+ X$ studied in[8] $\left(\rho_D^\pi(x,p_\perp) = x \cdot \frac{d\sigma}{dx\, d^2p_\perp}\right)$ in the scaling limit for $N+N \to \pi+X$ has the form[x]:

$$\rho_D^\pi(x,p_\perp) = \int \left(\rho_p^\pi\left(\frac{x}{\alpha}, p_\perp - \kappa_\perp\right) + \rho_n^\pi\left(\frac{x}{\alpha}, p_\perp - \kappa_\perp\right)\right)\left(u^2(\kappa) + w^2(\kappa)\right) d^3\kappa \quad (3)$$

As a result of symmetry between the spectator and the interacting nucleon in DA the number of fast pions in the deuteron fragmentation region should be considerably larger than in the theoretical estimates[8,10].

8. Similar formulae can be written for reaction $D+p \to p+X$ in the cumulative region. This reaction is a way to measure directly the deuteron wave function. The reaction with polarized D is of special interest as S and D wave contributions can be separated here. In particular a large dependence from the deuteron polarization is expected at $K_N \sim 400$ MeV/c, where S wave contribution is negligible if the nuclear core hypothesis is valid.

9. The nuclear core seems to have a natural explanation in the quark model. Indeed it is known from deep inelastic lepton scattering that the average transverse momenta of quarks are limited. In the space-time representation it corresponds to suppression of the small inter-quark distances in the nucleon. The core corresponds to the configuration in which the quark density of overlapping nucleons is of the order of the maximal quark density in nucleon[4]: $2\rho_N^q(r_c/2) = \rho_N^q(0)$ $\left(\rho_N^q(r) \sim \rho_N^{charge}(r)\right.$ which is proportional to $exp(-\mu r)$ as determined from the charge nucleon form factor). As a result $r_c = 2\ ln\ 2/\mu \approx 0.35$ fm which is in agreement with nuclear physics estimates.

[x] The idea that this process in the cumulative region (i.e., at $x > 1/2$, $p_\perp \approx 0$) dominated small internucleon distances was put forward by Baldin[9].

REFERENCES

1. V.N.Gribov. Zh.Exp.Teor.Fiz., 57, 1306 (1969).
2. R.P.Feynman. Photon-Hadron Interactions, Benjamin, N.Y. (1972).
3. G.B.West. Phys.Lett., 37B, 509 (1971).
4. L.L.Frankfurt and M.I.Strikman. X LNPI Winter School, v. II, p. 449, Leningrad 1975; preprint LNPI No. 173, 1975.
5. L.L.Frankfurt and M.I.Strikman, preprint LNPI No. 238 (1976); report No. 265 to the Tbilisi conference.
6. B.Chertok talk, section A7.
7. T.Hamada, I.D.Johnston. Nucl.Phys., 34, 382 (1962).
8. A.M.Baldin et al. Sov.J.Nucl.Phys., 18, 79 (1973).
9. A.M.Baldin. JINR, P7-5769, Dubna, 1971.
10. G.A.Lobov et al. Pis'ma JETP, 23, 118 (1976).

О СПОНТАННЫХ ПЕРЕХОДАХ ЯДЕР В СВЕРХПЛОТНОЕ СОСТОЯНИЕ

В.И.Алешин, А.Я.Балыш, В.М.Галицкий, Ю.В.Козлов, В.И.Лебедев, В.П.Мартемьянов, Л.А.Микаэлян, В.Г.Тарасенков
Ордена Ленина институт атомной энергии им. И.В. Курчатова, Москва
А.А.Поманский
Институт ядерных исследований АН СССР, Москва

Рассмотрение π-мезонного поля в ядерном веществе, проведенное А.Б.Мигдалом[1], показывает, что одна из ветвей возбуждения этого поля может оказаться неустойчивой. Это явление, называемое обычно π-конденсацией, возникает при плотностях нуклонов n, превышающих некоторую критическую плотность n_0 и, возможно, приводит к появлению второго минимума, на кривой зависимости энергии ядра ε, отнесенной к одному изотопу, от его плотности. Наибольший интерес для дальнейшего обсуждения представляет случай существования стабильных сверхплотных ядер с плотностью n_s (возможность существования таких ядер по другой причине рассматривали Ли и Вик[2]). В этом случае обычные ядра метастабильны и могут спонтанно переходить в сверхплотное состояние.

То обстоятельство, что обычные ядра находятся в метастабильном, а не более выгодном сверхплотном состоянии, может объясняться тем, что процесс образования средних и тяжелых ядер из наиболее легких происходил путем реакции последовательного захвата, а для наиболее легких ядер сверхплотное состояние маловероятно, т.к. с уменьшением атомного веса критическая плотность растет[3].

Изложенные соображения послужили стимулом для поисков спонтанных переходов ядер в сверхплотное состояние. В эксперименте, проведенном на Нейтринной станции ИЯИ АН СССР на глубине 660 мвэ, использовались две сцинтилляционные установки, одна из которых содержала 25 кг иодистого натрия, а другая-3 кг сцинтилляционного фторбензола.

Для уменьшения внешнего фона применялась защита из вольфрама и система антисовпадений. В опыте регистрировались γ-кванты с энергией в диапазоне 3-10 МэВ. Такие кванты должны сопровождать переход в сверхплотное состояние, если выделяемая при этом энергия $\Delta\varepsilon$ превышает для исследованных ядер 0.05-1 МэВ/нуклон.

Измеренная скорость счета в установке с фторбензолом составляла 0.1 событие $кг^{-1}\cdot сутки^{-1}$, а в установке с иодистым натрием-2 события $кг^{-1}\cdot сутки^{-1}$. Приведенные скорости счета приписывались переходам в сверхплотное состояние, что с учетом эффективности регистрации и геометрии приводит к следующим нижним границам времени жизни τ ядер:

ядро	C	F	Na	I	W
τ, год	10^{22}	10^{22}	$3\cdot10^{20}$	$3\cdot10^{20}$	10^{21}

Эти значения позволяют оценить нижние границы для плотности n_s и величины энергетического барьера, отделяющего обычное состояние от сверхплотного. Зависимость энергии ядра на один нуклон, соответствующая существованию стабильных сверхплотных ядер, показана на рис.1.

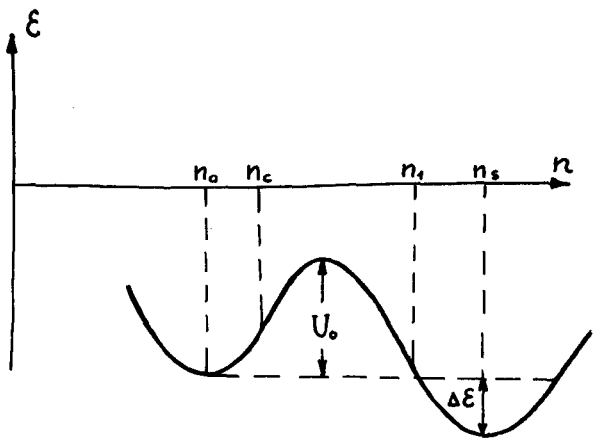


Рис. 1

Эта кривая может быть аппроксимирована выражением

$$\varepsilon=\varepsilon_0+\frac{k}{2}\left(\frac{n-n_0}{n_0}\right)^2+\frac{q}{6}\left(\frac{n-n_0}{n_0}\right)^3-\frac{\alpha}{2}\left(\frac{n-n_c}{n_0}\right)^2\theta(n-n_c), \quad (I)$$

в котором k есть известная величина, связанная с сжимаемостью ядерного вещества и равная $\cong 32$ МэВ*. Коэффициенты q, α и значение n_c являются варьируемыми параметрами. Последний член соответствует выигрышу энергии при появлении π-конденсата при $n>n_c$.

* Отметим, что в ряде работ, посвященных свойствам ядерного вещества, вводится величина, в 9 раз большая.

Вероятность перехода в сверхплотное состояние может быть найдена из обычной картины подбарьерного перехода

$$\frac{1}{\tau} = \omega \cdot \exp\left\{-\frac{2}{\hbar}\int_{r_0}^{r_1} dr\sqrt{2M_{эф}(U-E)}\right\}, \qquad (2)$$

где ω - частота попыток, равная по порядку величины отношению скорости звука к размеру ядра, что дает $\omega \simeq 10^{21}$ сек$^{-1}$, r_0 и r_1 - радиусы, соответствующие плотностям n_0 и n_1; $M_{эф}$- эффективная масса, равная для случая однородного сжатия 3/5 от массы ядра. В (2) следует перейти к величинам, отнесенным к одному нуклону, т.е. $U-E = A(\varepsilon-\varepsilon_0)$. Показатель экспоненты в (2) зависит, вообще говоря, от выделяемой в переходе энергии на один нуклон $\Delta\varepsilon$, однако при не очень больших $\Delta\varepsilon$ эта зависимость слабая, и в дальнейших оценках мы получаем $\Delta\varepsilon=0$. В результате, формула для вероятности перехода принимает вид

$$\frac{1}{\tau} = \omega \cdot \exp\left\{-const \cdot F\left(\frac{q}{k}, \frac{n_c}{n_0}\right) \cdot A^{4/3}\right\}. \qquad (3)$$

Приравнивая τ экспериментальному времени жизни, можно получить нижнюю границу $\frac{n_c}{n_0}$. Эта величина оказывается плавной функцией отношения $\frac{q}{k}$ (в интервале $\frac{q}{k} = 0{,}5 \div 2{,}0$). Приближенные значения $\frac{n_c}{n_0}$ и соответствующие им значения $\frac{n_s}{n}$ и U_0 приведены в таблице.

	^{23}Na	^{127}I	^{184}W
$\frac{n_c}{n_0}$	3,4	I,3	I,2
$\frac{n_s}{n_0}$	9,8	3,0	2,5
U_0 $\frac{МэВ}{нуклон}$	3I4	5,4	2,6

Из таблицы видно, что с уменьшением атомного номера нижняя граница $\frac{n_c}{n_0}$ и высота барьера на нуклон возрастают. Фтор и углерод не включены в таблицу; критические плотности и барьеры для них получаются еще более высокими, однако для таких легких ядер развиваемая здесь концепция может оказаться сомнительной. Более подробный анализ результатов и ограничений, накладываемых на коэффициенты разложения (I), будет проведен в дальнейшем.

Литература

I. А.Б.Мигдал. ЖЭТФ, 6I, 2209 (I97I).
А.Б.Мигдал, О.А.Маркин, И.Н.Мишустин. ЖЭТФ 66, 443 (I974).
2. T.D.Lee, G.C.Wick. Phys.Rev.D9,2291 (1974).
3. Э.Е.Саперштейн, С.В.Толоконников, С.А.Фаянс. Препринт ИАЭ им. И.В.Курчатова № 257I, Москва, I975.

PARALLEL SESSION ON ELECTROMAGNETIC INTERACTIONS OF HADRONS

ELASTIC AND INELASTIC ELECTRON SCATTERING FROM THE DEUTERON AT LARGE MOMENTUM TRANSFER

B.T.Chertok
American University, Washington, D.C., USA

The deuteron form factor $F_D(q^2)$ and inelastic structure function, $\nu W_{2D}(q^2,\nu)$, at threshold both provide excellent examples of the continuity between nuclear and particle physics at the microscopic level. The deuteron could be viewed as a very complex system at low and moderate q^2 ($\lesssim 1$ GeV^2). That is, this elementary two-body bound state at $q^2=0$ could become a complex system with increasing q^2 by the addition, for example, of isobar resonances ($\Delta\Delta$ and $N'N$) to the N-N ground state and with the increasing importance at the electromagnetic vertex of two-body meson-exchange currents.

However, the probing of the deuteron's electromagnetic structure at large q^2 ($\gtrsim 1$ GeV^2) appears to reveal a marvelous simplicity[1]. From a dimensional scaling quark model approach Brodsky had predicted that the deuteron form factor would diminish as $(q^2)^{-1}$ after the two-nucleon's structure was removed at reduced q^2[2], i.e.

$$F_D / F_p^2(q^2/4) \sim 1/q^2. \qquad (1)$$

This prediction has been confirmed in our experiment at SLAC[1] as seen in figs.1 and 2.

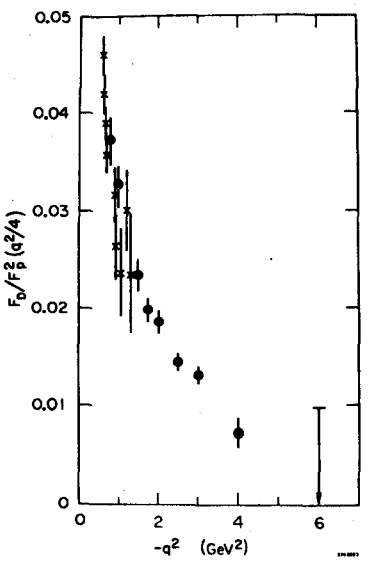


Fig.1

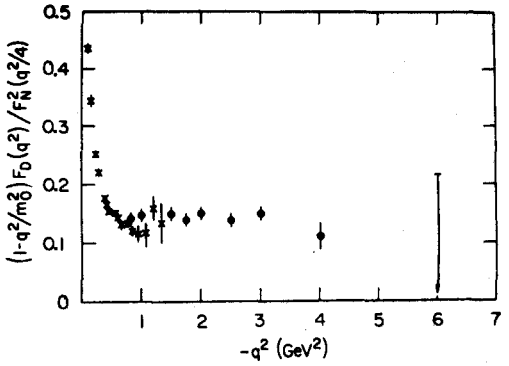


Fig.2

Thus, the underlying six-quark substructure of the deuteron is manifested in five powers of q^2; i.e., $F_p^2(\frac{q^2}{4})/q^2 \sim (q^2)^{-5}$ in agreement with quark counting, so that,

$$(q^2)^{n-1} F_n \longrightarrow \text{const}. \qquad (2)$$

This presentation will be divided into three sections:

1. The Asymptotic Elastic Form Factors of Hadrons and Nuclei, and the Continuity of Particle and Nuclear Dynamics;

2. Measurement of Inelastic e-D Scattering in the Threshold Region at large Momentum Transfer, and

3. Measurement of the Magnetic Form Factor of the Deuteron at $q^2=1$ GeV^2.

Professor Dally has presented our new measurement of the deuteron's magnetic form factor (section III) to this Conference.

I. The Asymptotic Elastic Form Factors

This study of the implications of the deuteron having an underlying six-quark substructure and the general connections between dimensional scaling and elastic form factors are summarized very briefly[3].

The large q^2 behaviour of the elastic form factor of a hadron or nucleus is related by dimensional counting to the number of its elementary constituents. Using the framework of a scale-invariant quark model, dimensional scaling

prediotions are derived for the $B(q^2)/A(q^2)$ ratio in the Rosenbluth formula, multiple photon exohange corrections, and the mass parameters whioh control the onset of the asymptotic power law in the meson, nucleon, and deuteron form factors. A simple "democratic chain" model predicts that for large q^2, $F(q^2) \sim (1-q^2/m_n^2)^{1-n}$ where m_n^2 is proportional to the number of constituents n as in Fig.3a. Quark interchange of Fig.3b is used to calculate F_D with the results already presented in Fig.2. In the case

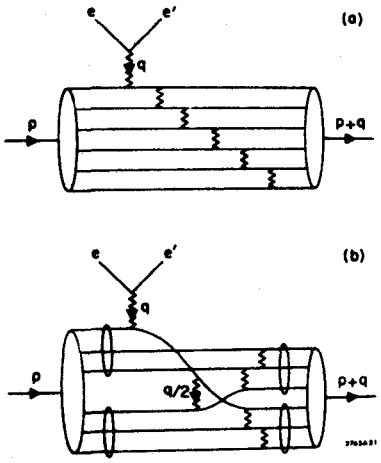


Fig.3

of nuclear targets (or systems with several scales of compositeness), we also define the "reduced" form factor $f_A(q^2)=F_A(q^2)/\prod_{a=1}^{A} F_a(q_a^2)$ in order to remove the minimal falloff of F_A due to the nucleon form factors at $q_a^2=(m_a^2/M_A^2)q^2$ Dimensional counting predicts $(q^2)^{A-1} f_A(q^2) \to const$ as summarized in Table I.

TABLE I

Compositeness of Matter

Bound State	$F_i\left(\frac{m_i^2}{m_A^2}t\right)$	A	$f_A(t)$
e, μ, γ, q	1	1	t^0
π, K	1	2	t^{-1}
p, n	1	3	t^{-2}
D	$F_p(t/4)$	2	t^{-1}
^{3}He	$F_p(t/9)$	3	t^{-2}
^{4}He	$F_p(t/16)$	4	t^{-3}

A systematic comparison of the data for π, p, n, and deuteron form factors with the dimensional scaling quark model predictions are given. We also relate the deuteron form factor to (off-shell) fixed angle n-p scattering, and show that the experimental results for $t^5 F_D(t)$ are consistent with the magnitude of the s-wave function $u'(0)$ obtained from soft-core potentials. The relation of the dynamics of an underlying six-quark state of the deuteron to the nuclear potential and exchange current contributions is discussed. The scaling of $q^2 f_D(q^2)$ implies that the nuclear potential (after removing the effects of nucleon structure) displays the scale-invariant behaviour of a theory without a fundamental length scale. Predictions are also given for the structure functions, fragmentation, and large angle scattering of a nucleus.

II. Inelastic e-D Soattering at Threshold

At squared momentum transfers $0.8 \leq q^2 \leq 6.0$ $(GeV/c)^2$, nine spectra of inelastic electron deuteron scattering were measured in the threshold region between 0 and 2.3% in $\Delta p/p$ below the elastic peak. The deuteron inelastic structure function νW_2 was extracted from these data. We found $\nu W_2(\omega')$ approaching a universal scaling curve and a close relation between νW_2 and the deuteron elastic structure function $A(q^2)/4$.

We report preliminary results of inelastic electron deuteron scattering in the threshold region at high momentum transfer q. The data were taken from a SLAC experiment[1] whose main purpose was to measure the elastic scattering cross sections and the deuteron struoture function $A(q^2)$ at nine values of q^2 in the region $0.8 \leq q^2 \leq 6.0$ $(GeV/c)^2$. The experimental conditions were such that we measured not only the elastic events, but also inelastic events from deuteron breakup and pion production between $0 \geq \Delta p/p_e \geq -2.3\%$, where p_e is the scattered electron momentum at the center of the elastic peak. The nine inelastic electron spectra span an unusual dynamic

region of large q^2 and small energy transfer $\nu = E_i - E_f$, the difference between initial and final electron energy. This region has not been explored before. Bjorken scaling is expected when both q^2 and ν are large compared with M_N^2, the square of the nucleon mass, as in deep inelastic electron scattering. The data presented here are on a scale where q^2 is expected to resolve the nucleons into fermion quark currents while ν is typical of excitation energies where nucleon-nucleon final state interaction effects may be significant.

We used the 20 GeV/c spectrometer of SLAC End Station A to detect scattered electrons at a fixed $\theta_e = 8^\circ$ from liquid deuterium, liquid hydrogen (for system calibration) and from a dummy target to determine the empty target background. To remove the elastic events out of the inelastic and background events, we used the 8 GeV/c spectrometer in coincidence with the 20 GeV/c spectrometer to detect the recoil deuterons with elastic kinematics.

Our results for the inelastic cross sections are the spectra of $d^2\sigma/d\Omega\, dE_f$ versus E_f. The error bars on the data points represent the statistical errors only. The systematical errors, mainly from uncertainties in $\Delta\Omega$ and the corrections, are estimated to $\pm 20\%$. The spectra rise almost exponentially with decreasing E_f, with a sharp rise from zero at the threshold.

For $q^2, \nu \to \infty$, it is observed that νW_2 becomes a function of the scaling variable ω' only, with $\omega' = 1 + W^2/q^2$ and $W^2 = M^2 + 2M\nu - q^2$, the square of the missing mass. Figure 4 shows a comparison of our data with data from Refs.5 and 7 on a νW_2 vs. ω' plot./6/. At q^2 below 2 $(\mathrm{GeV/c})^2$, we are not yet in the scaling region, but at $q^2 \geq 2$ $(\mathrm{GeV/c})^2$, our spectra merge with increasing q^2 into a universal $\nu W_2(\omega')$ curve. We find empirically that the spectra with $q^2 \geq 2$ $(\mathrm{GeV/c})^2$ can be described by the relation $\nu W_2 \sim (\omega' - 0.5)^n$, with $n = 6 \pm 0.5$. In an interesting paper presented to this Conference/8/,

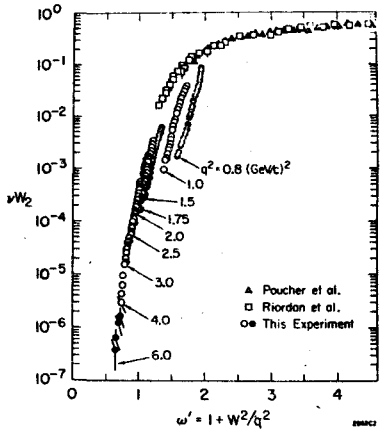


Fig. 4

Frankfurt and Strikman use a dispersion theory approach to the deuteron bound state and approximate their prediction for νW_{2D} as $.12\,(\omega' - \frac{1}{2})^{5.7}$ for $.55 \leq \omega' \leq 1$.

We find a close relation between the elastic $A(q^2)$ and W_2 at constant W^2. For W (Ref.6) close to M_d, we find empirically that our data follow the relation

$$W_2 \sim F_d^2(q^2) \cdot \varrho(W^2) \qquad (3)$$

with F_d given in Fig.5 and a function ϱ only depending on W^2 (see Fig.5).

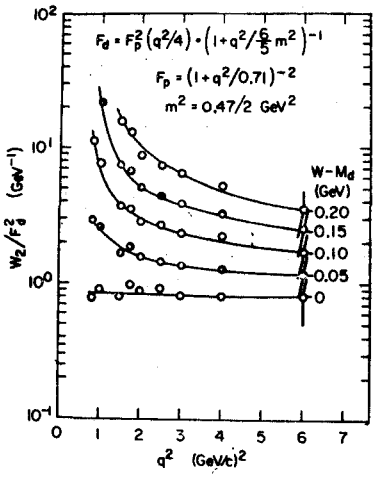


Fig.5

A connection between F and νW_2 near threshold has been given by Drell-Yan/9/ and West/10/ for the case of the proton:

$$\nu W_2 \sim x \cdot (1-x)^p, \quad F \sim (1/q^2)^{(p+1)/2}, \quad x = \frac{q^2}{2M\nu} - 1 \qquad (4)$$

If we extend this prediction to the deuteron, we postulate $p=9$, since $F\sim(1/q^2)^{-5}$. From our data, we could not get a reasonable fit within $4\leq p\leq 11$. So, we do not have any evidence that this connection works for the deuteron. However, we seem to be at too small q^2, ν -values to observe scaling in X.

If $G(q^2)$ is the excitation form factor of a resonance at $M=M_R$,

$$\nu W_2 = (M_R^2 - M_d^2 + q^2)\cdot\left[G(q^2)\right]^2\cdot\delta(W^2-M_R^2) \quad (5)$$

is its contribution to νW_2 in the narrow resonance approximation. This has been shown by Bloom and Gilman[11]. Our data indicate that this relation works in our case ($M_R\approx M_d$); i.e., $\nu W_2\sim q^2\cdot F_d^2\cdot\rho(W^2)$, similar to eqn. (3). Thus, our measurements indicate that νW_2 at threshold behaves like a resonance with $G(q^2)\sim F_d(q^2)$. This leads, in the language of the quark model, to be conclusion that, like in the elastic case, all six quarks participate in the threshold inelastic scattering process.

III. Measurement of Magnetic Structure Function of the Deuteron

At a momentum transfer squared of 1.0 $(GeV/c)^2$ the elastic scattering of electrons on deuterons has been measured at electron scattering angles of 8°, 60° and 82°. From these data we have extracted a value of $B(q^2)=1.55\pm.10\times10^{-5}$ for the deuteron. This measurement extends the range in momentum transfer by almost a factor of two over the previous measurements[12].

Large angle elastic eD scattering permits testing the dynamics of the deuteron's magnetic dipole moment, and large q^2 probes the short distance structure of these nuclear electromagnetic currents. Previous measurements of the deuteron's magnetic structure function $B(q^2)$ in the interval $0\leq q^2\leq 14\ F^{-2}$ (0.55 GeV^2) appear to be fully consistent with calculations using the impulse approximation[13]. These calculations use standard deuteron wave functions from N-N phenomenology and the measured nucleon form factors to compute $B(q^2)$. This approach appears to describe adequately any interaction effects in the deuteron at larger q^2 but leaves unexplained a discrepancy of 1-2% for the static magnetic dipole moment.

Our $A(q^2)$ is measured by scattering electrons at 8°, detecting the electron in the SLAC 20-GeV/c spectrometer and detecting, in coincidence with the electron, the deuteron in the SLAC 8-GeV/c spectrometer. The large angle data were taken at 60° and 82° where the electron was detected in the SLAC 1.6-GeV/c spectrometer, and the deuteron was detected as before. In order to calibrate the double-arm acceptances of these spectrometers, we also measured electron-proton scattering under the same conditions as those of the deuteron.

While it is not possible to rule out small contributions from exchange currents, our measurements are entirely consistent with the impulse approximation using empirical fits to the nucleon form factors. Thus, our measurement reaffirms the earlier observation made in Ref.[13] at lower q^2 to the same effect. Moreover, the impulse approximation for $B(q^2)$ is sensitive to the values for the nucleon form factors; in particular, the IJL form factors[14] yield a value of B which is 40% lower at $q^2=30\ f^{-2}$ than that using best fit to the data for G_{Mn}. We have also examined the effect of using different potential models for the deuteron with varying amounts of "D" state and find that the value of B is sensitive to these. For example, the Hamada-Johnson model with our most realistic nucleon form factors and a 7%D state wave function are estimated to produce a value of B approximately 30% higher at $q^2=1.0\ GeV/c^2$ than the Reid soft-core model we have used for our calculations. These uncertainties lead to considerable ambiguity in ascertaining the contribution - if any - of meson exchange currents in the magnetic structure of the deuteron.

Summary

Measurements of eD scattering at large values of q^2 as presented and discussed here, should enrich both nuclear and particle physics. In particular, the data[1,4,12] should provide important guidenoe for connecting the two fields of physics at the microscopic level. The constraints of quark-fermion currents and normal hadronic states must be simultaneously imposed and consistently satisfied. Measurement of elastic electromagnetic form factors to even larger q^2 will continue to play a unique role in physics.

References

1. R.Arnold, B.Chertok, E.Dally, A.Grigorian, C.Jordan, W.Schütz, R.Zdarko, F.Martin, B.Meoking. Phys.Rev.Lett., 35, 776 (1975); SLAC-PUB, 1596.
2. S.Brodsky. In "Proc. Int. Conf. on Few Body Problems in Nuclear and Particle Physics", edited by R.Slobodrian, B.Cujec, R.Ramavataram, p. 676, Les Presse de l'Univ. Laval, Quebec (1975), SLAC-PUB, 1497.
3. S.Brodsky, B.Chertok. SLAC-PUB. 1757 and 1759, submitted for publication.
4. W.Schütz and Collaboration of ref.1,submitted for publication.
5. J.S.Poucher et al. Phys.Rev.Lett., 32, 118 (1974).
6. For comparison with refs. 5 and 7, we calculated W^2 with M_N=.938 GeV. Our data are then in the range $-2.12 \leq W^2 \leq 0.76$ GeV^2. For comparison of νW_2 with F_d we defined W^2 with M_d = = 1.876 GeV ($3.52 \leq W^2 \leq 5.02$ GeV^2).
7. E.M.Riordan. Thesis, MIT Report No. COO-3069-176.
8. L.Frankfurt,M.Strikman.This Conference,265/B2
9. S.D.Drell, T.M.Yan. Phys.Rev.Lett., 24, 181 (1970).
10. G.B.West. Phys.Rev.Letters 24, 1206 (1970).
11. E.D.Bloom and F.J.Gilman. Phys.Rev.Letters 25, 1140 (1970).
12. F.Martin and collaboration of ref. 1, submitted for publication.
13. R.Rand et al., Phys.Rev., D8, 3229 (1973).
14. F.Iachello, A.Jackson and A.Lande.Phys.Lett., 43B, 191 (1973).

THE MEASUREMENT OF THE NUCLEON AND PION FORM FACTORS IN THE REGION OF TIME-LIKE 4-MOMENTUM TRANSFERS FROM 1.5 F^{-2} TO 3.0 F^{-2}

S.F.Berezhnev, T.D.Blokhintseva, A.V.Demyanov, A.V.Kuptsov, V.P.Kurochkin, L.L.Nemenov, G.I.Smirnov, D.M.Khazins

Joint Institute for Nuclear Research, Dubna

The experimental investigations[1-3] of the reaction of inverse electroproduction of pions (IEP)

$$\pi^- + p \to e^+ + e^- + n \qquad (1)$$

have been made at the pion energy of 275 MeV. The study [4] of reaction (1) was continued by means of a new experimental device, that permitted to detect 1043±46 events. The cross section of that part of the reaction which is determined by the geometry of the experimental device with the additional restriction $E_1, E_2 > 50$ MeV ($E_{1,2}$ is electron energy) is

$$\Delta\sigma = (4.80 \pm 0.43).10^{-33} \text{ cm}^2.$$

All events were separated into 5 groups according to the kinematic variable K^2, the average values of K^2 in each interval is 0.058, 0.073, 0.088, 0.103 and 0.119 (GeV/c)^2. The distributions of events as the function of $\cos\theta^*_{\pi N}$ between the pion and photon momenta (c.m.s.) were plotted for each group.

To analyse the experimental data the dispersion[6] model has been used. The formfactors $F_1^V(K^2)$ and $F_\pi(K^2)$ were taken as varying parameters upon which the differential cross sections are greatly dependent. The remaining form factors F_1^S, F_2^S, F_2^V and G_M^* affecting weakly the differential cross sections were calculated by means of the dipole formula. All the parameters were considered real. When determining the formfactors $F_1^V(K^2)$ and $F_\pi(K^2)$ the experimental cross sections $d\sigma/d\cos\theta^*$ were fitted by theoretical ones calculated under the assumption that the formfactors should be equal.

Calculations performed by using the dispersion model describe very well all the experimental data. The results of determining the form

factor $F_1^V(K^2)$ and $F_\pi(K^2)$ under the condition of their equality are presented in Table 1.

Table 1

$K^2\left(\frac{GeV}{c}\right)^2$	0.058	0.073	0.088	0.103	0.119
Dispersion Model	0.90 ± 0.07	1.00 ± 0.05	1.06 ± 0.05	1.12 ± 0.05	1.26 ± 0.04

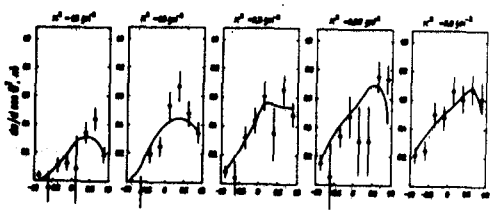


Fig.1 shows the distribution of experimental events as the functions of the $Cos\theta^\gamma$ variable. Theoretical curves have been obtained when determining the form factors $F_1^V(K^2)$ and $F_\pi(K^2)$ (see Table 1) by using the dispersion model.

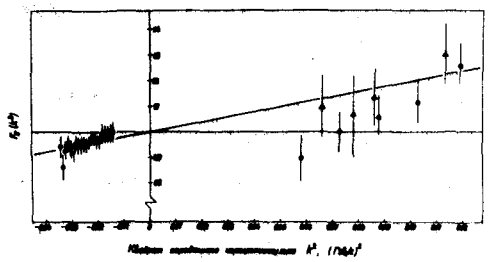


Fig.2. Results of pion formfactor measurements /8/ in experiments on pion scattering on electrons ($K^2<0$) and in the experimental studies of the $\pi^-p\to e^+e^-n$ process ($K^2>0$): ▲ –/27/, Δ –/3/, ● – the present investigation. Solid curve is the result of calculations in the superpropagator model /9/.

The data were ($\chi^2=13.7$ with $\overline{\chi^2}=4$) approximated by the function $F_1^V(K^2)=1+1/6\,\xi^2K^2$ with $\xi=\xi_\pi=0.75\pm 0.09$ f.

For the part of statistics the phenomenological analysis of data on reaction (1) is presented. It allowed to determine the contributions of states with various photon polarizations to the IEP differential cross section. In one-photon approximation the IEP cross section is written as /5/

$$\frac{d\sigma}{d\Omega_\gamma\, d\Omega_e\, dK^2}=\sum_{i=1}^{4}R_i T_i=\sum_i \sigma_i , \qquad (2)$$

where K^2 is the square of the 4-momentum transferred, Ω_e, Ω_γ are solid angles of gamma-quantum and electron scattering, i is the index determining photon polarization, T_1 describes the process

$$\pi^-p\to\gamma^*+n \qquad (3)$$

with transverse nonpolarized virtual gamma-quanta, T_2 corresponds to processes with transversely polarized photons, T_4 corresponds to processes with longitudinally polarized photons, T_3 describes interference longitudinally and transversely polarized photons, σ_i corresponding differential cross section, the coefficient R_i is the known functions of variables K^2, $Cos\varphi$, and $Cos\theta_e$.

The particular form of the parameter T_{1-4} depends upon the applied theoretical model. In the phenomenological analysis the two-dimensional distribution of IEP events of the variables $Cos\varphi$ and $Cos\theta_e$ was approximated by function (2) with varied parameters T; the coefficients R_i as functions of variable $Cos\varphi$ and $Cos\theta_e$ were calculated by the Monte-Carlo method with the account of real experimental conditions. All the experimental statistics was distributed into five groups on K^2 with average values of equal to 1.48 f^{-2}, 1.88 f^{-2}, 2.26 f^{-2}, 2.65 f^{-2}, 3.05 f^{-2}. For each group the phenomenological analysis was performed. The obtained evaluations are shown in Fig.3 (a,b,c). The same Figs. show the results of theoretical calculations (solid curve). It is seen that the model /6/ well des-

cribes the behaviour of cross sections corresponding to the radiation of tne transverse nonpolarized and longitudinal photons.

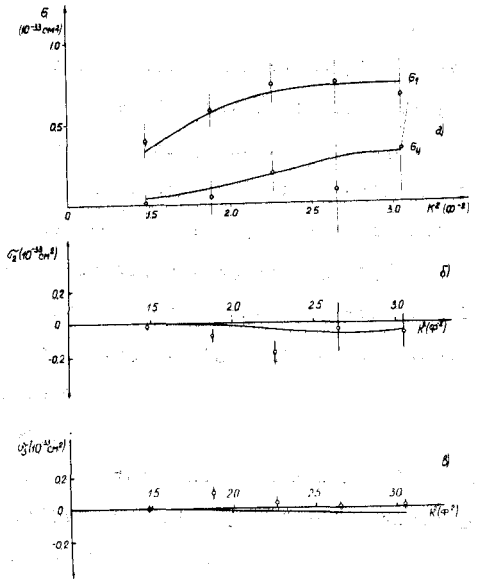


Fig.3

As has been shown by calculations, the σ_1 cross section depends equally on the Dirac isovector formfactor F_1^V of the nucleon and the pion formfactor F_π. The value of σ_4 depends, mainly, upon F_1^V: the variation of F_1^V within 10% changes σ_4 by 14%,2%, while a 10% change of F_π changes σ_4 only by 3.8%. Thus if the value of σ_4 is known with a small error, F_1^V can be determined with a good accuracy even when a rough estimation of the formfactor F_π is used. Since σ_4 is determined only by Born terms[6], the obtained value is not dependent upon model uncertainties.

References

1. Yu.K.Akimov, L.S.Vertogradov, A.V.Demyanov et al. Yad.Phys., 13, 748 (1971).
2. S.F.Berezhnev, L.S.Vertogradov, A.V.Demyanov et al. Yad.Phys., 16, 185 (1972).
3. S.F.Berezhnev, A.V.Demyanov, A.V.Kulikov et al. Yad.Phys., 18, 102 (1973).
4. S.F.Berezhnev, T.D.Blokhintseva, A.V.Demyanov et al. JINR, P1-9575, Dubna, 1976.
5. Yu.S.Surovtsev, F.G.Tkebuchava. JINR,P2-4524, Dubna, 1969.
6. T.D.Blokhintseva, Yu.S.Surovtsev, F.G.Tkebuchava. Yad.Phys., 21, 850 (1975).
7. G.Adylov, F.Aliev, D.Bardin et al. Phys.Lett., 51B, 402 (1974).
8. M.K.Volkov, V.N.Pervushin. Nuovo Cim., 27A, 277 (1975).

MEASUREMENT OF THE PION FORM FACTOR*

E.Dally, J.Hauptman, C.May, D.Stork
University of California at Los Angeles

J.Poirier, C.Rey, R.Wojslaw
University of Notre Dame

P.Shepard
University of Pittsburgh

A.Lennox, J.Tompkins, T.Toohig, A.Wehmann
Fermi National Accelerator Laboratory

I.Ioan, T.Nigmanov, E.Tsyganov, A.Vodopianov
Joint Institute for Nuclear Research, Dubna

The pion form factor has been measured in the momentum transfer range $0.03 \leq q^2 \leq 0.07$ $(GeV/c)^2$ by scattering pions from atomic electrons in a liquid hydrogen target. The pion form factor is defined to be the elastic scattering cross section divided by that predicted for a point pion. When it is expanded in powers of q^2, the mean-square radius of the pion electromagnetic charge distribution appears in the first coefficient:

$$\frac{d\sigma}{dq^2} = \left(\frac{d\sigma}{dq^2}\right)_{\substack{\text{POINT}\\ \text{PION}}} |F(q^2)|^2$$

The experiment was performed in a 100 GeV/c negative pion beam incident on a 50 cm liquid hydrogen target at Fermilab. The maximum recoil electron energy is 84.0 GeV which corresponds to a maximum momentum transfer squared in the elastic reaction of $q^2 = 2m_e(E_e - m_e) = 0.086$ $(GeV/c)^2$. These small momentum transfers give laboratory scattering angles which are typically a few milliradians within our acceptance. The trajectories of the incident pion and of the scattered pion and electron are measured with proportional wire chamber stations, each having four planes with 2 mm wire spacing staggered by 1 mm. The scattered particles are bent through two BM109 magnets with a total field integral of 70.35 Kg-m, and their trajectories beyond the magnets are measured by six magnetostrictive wire spark chambers.

Downstream of the spark chambers is a two particle trigger hodoscope. The geometric efficiency for triggering is nearly 100% for the range $0.03 \leq q^2 \leq 0.07$ $(GeV/c)^2$. An array of ten lead-glass shower counters 14 radiation lengths long served to reduce background triggers during the run and to aid in the subsequent identification of elastic pion-electron events. Scattered muons were identified with a segmented steel filter.

An event trigger required conditions of two distinct types: the first was a beam monitor signal defining the incident pions. The beam logic was composed of information from scintillation counters and the proportional chambers upstream of the hydrogen target. A portion of the beam logic required one and only one beam particle incident on the hydrogen target. This logic demanded a 1 microsecond spacing between usable particles; it vetoed beam counts with two particles in one r.f. bucket or with a particle in the following bucket. These requirements limited the amount of usable beam per machine pulse (typically, 300 K particles through the spectrometer of which about 100K were usable for the experiment), but created a clean environment for spectrometer operation which removed serious ambiguities and inefficiencies from the trackfinding procedure.

The second trigger logic condition defined the pion-electron scatter: a two particle signature from the proportional chambers downstream of the target, a two particle signal from a scintillation counter array behind the spark chambers, and a Čerenkov pulse height consistent with that expected from the scattered electron. The trigger rate during data taking was about 1.4×10^{-4} per incident pion, and about 15 events were recorded during the 1 second machine spill.

The geometrical event reconstruction was done by finding tracks in the horizontal and vertical planes, and matching them in rotated chambers. The efficiency of pion-electron event finding has been tested both by Monte Carlo simulation of the experiment and by a second, independent program, and found to be 99.0 ± 1.0 % in this sample of data. A distribution of the reconstructed vertex position for elastic events is shown in Figure 1.

* Supported in part by U.S.Energy Research and Development Administration and the National Science Foundation.

The pion-electron elastic scatters are separated from the large hadronic background by employing four constraints of energy-momentum conservation, and by requiring that the energy deposited in the leadglass shower counters be consistent with the momentum measured in the spectrometer of the showering particle. Constrained chi-squared fits were performed on the spectrometer data for the pion-electron elastic reaction with an additional external bremsstrahlung photon assumed to be along the electron direction. The χ^2 distribution for this three-constraint reaction hypothesis on the present sample of data is shown in Figure 2; the tail on this distribution has contributions both from strong interaction background and from real pion-electron elastic scatters. A relatively large number of pion electron elastic events (about 3%) in this sample exceeds the statistical 1 % confidence level (at χ^2=11.5 for three constraints), and these are accounted for by vertex associated radiative effects, pions which nuclear elastic scatter in the target or the spectrometer matter, pions which decay inside the spectrometer, the non-gaussian distributions associated with plural scattering in thin absorbers, and systematics of the geometrical event reconstruction. The fitted bremsstrahlung spectrum is shown in Figure 3; the insert shows the spectrum near zero photon energy. The normalized and calibrated Čerenkov pulse height spectrum for kinematically identified elastic events is displayed in Figure 4.

The final separation of the elastic events from the background employs the geometry of event reconstruction in the target, the kinematic χ^2 from the constrained fit to elastic kinematics, a cut on the fitted bremsstrahlung energy at 4 GeV, and a minimum shower counter pulse height for electron identification. Specifically, we demand that the confidence level of the kinematic fit exceed the 10^{-6} level, that the shower counter pulse height exceed 50% of that expected for the electron, that the reconstructed vertex position be within 30 cm of the target ends, and that the kinematically fitted photon energy be between -2.0 and 4.0 GeV.

To obtain the form factor from the measured distribution in q^2 of elastic events, corrections for many physical and instrumental effects must be made. The principal corrections affecting the incident pion flux are pion attenuation in the target and spectrometer matter (2.87%), beam momentum cut from 96 to 102 GeV/c (3.02%), and muon contamination (0.40%). Principal corrections affecting the elastic sample of events are bremsstrahlung of the electrons (15% to 20%), pion attenuation (4.63%), and radiative corrections[1] (7.9% to 9.3%). The pion decay, muon-electron scattering, and strong interaction background corrections are less than 1%. Track finding efficiency was found to be 99%, and geometrical efficiency varied from 95.25% to 99.47%.

The corrected form factor is shown in Figure 5. At the present time a simple least squares fit which neglects error correlations has been carried out on this sample of data in order to provide a preliminary value for the pion radius. The fit is constrained in overall normalization to correspond to a 2 percent uncertainty in the absolute cross section. We find

$$\langle r_\pi^2 \rangle = 0.33 \pm 0.06 \text{ f}^2.$$

For comparison, vector dominance predicts 0.40 f^2, and the size of the proton is 0.66 f^2. The first direct experimental determination[2] obtained 0.61 $\pm$ .15 f^2.

We express our appreciation to the staff of Fermilab for their assistance throughout this experiment. Dr. Charles Buchanan contributed to the preparation for the experiment, and Mr. Jonathan Kubic and Mr. Jim Volk were of great help. We are grateful for the support and encouragement of Dr. E. Goldwasser and Dr. A. Baldin.

References
1. D.Yu.Bardin, G.V.Micelmacher, N.M.Shumaiko. JINR E2-6235 (1972).
2. Adylov et al., Physics Letters 51B, 402 (1974).

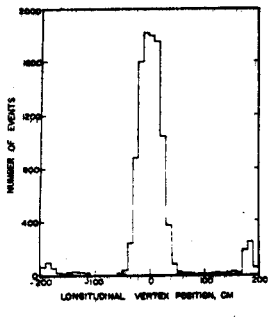


Fig.1. The reconstructed vertex position in 10-cm bins of identified elastic scatters in the neighborhood of the 50-cm liquid hydrogen target. The ends of the vacuum region and the PWC stations 2 and 3 are visible.

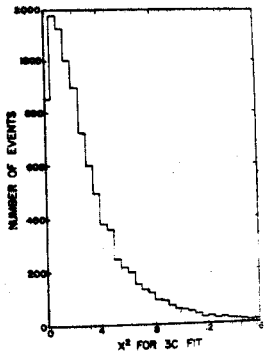


Fig.2. The three-constraint chi-squared distribution for constrained chi-squared fits to the elastic reaction with an assumed bremsstrahlung photon along the electron direction .

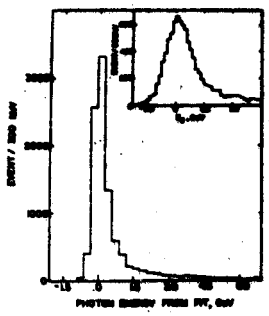


Fig.3. The fitted bremsstrahlung spectrum for elastic events, with an insert showing this distribution near zero photon energy. The mean of this distribution is consistent with the known amount of matter which the scattered electron tranverses.

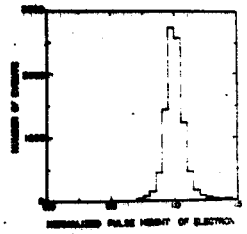


Fig.4. The momentum normalized shower counter pulse height spectrum for elastic events.

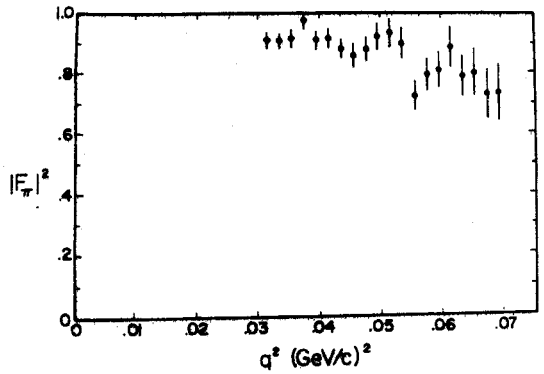


Fig.5. The pion form factor.

PHENOMENOLOGICAL ANALYSIS AND THE MODELS OF THE ELECTROMAGNETIC FORM FACTORS OF HADRONS

N.B.Skachkov
Joint Institute for Nuclear Research,Dubna

Nowadays the center of the interests in studying the structure of elementary particles has removed to studying the information which is contained in the experimentally observed behaviour of the structure functions of inelastic processes. But it does not mean that the problem of understanding the physics controlling the elastic form factors fall off is solved. This problem remains to be still interesting and it is the subject of a number of papers presented at this conference.

In /1/ a new formula was obtained for the proton form factor (f.f.)

$$F_p(t) = \frac{y}{\sinh y} \cdot \sum_{V=\rho,\omega,\varphi,\rho''(1650)} \frac{a_V}{\mu^2 - t} \qquad (1)$$

(y - is the rapidity, corresponding to the square of the 4-momentum transfer $t=(p-k)^2$: $y = Ar\cosh\left(\frac{2M^2-t}{2M^2}\right)$, M - proton mass). Formula (1) gives the correct, almost dipole asymptotical behaviour of the proton f.f.

$$F_p(t) \approx \frac{2M^2 \ln\frac{|t|}{2M^2}}{t^2}; \quad -t \gg 4M^2 \qquad (2)$$

The factor $y/\sinh y$ in (1) takes into account the contribution of the central part of the proton (with $R = 1/M$), because, as it was established in /1/, by passing to the relativistic configurational representation (RCR), the $\rho,\omega,\varphi,\rho''(1650)$ mesons produce the proton structure only at distances beyond the proton Compton wave length. The relativistic configurational representation was introduced in /2/ by using instead of the conventional Fourier analysis the expansion on the Lorentz group. For the form factor this transition looks like /1/

$$F(t) = 4\pi \int_0^\infty \frac{\sin rMy}{rM\sinh y} F(r) r^2 dr. \qquad (3)$$

The group parameter r in (3) enumerates the eigenvalues of the Casimir operator of the Lorentz group $\hat{C}_L = \frac{1}{4} M_{\mu\nu} M^{\mu\nu}$ ($M_{\mu\nu}$ generators of the Lorentz group)

$$\hat{C}_L \left(\frac{\sin rMy}{rM\sinh y}\right) = \left(\frac{1}{M^2} + r^2\right)\left(\frac{\sin rMy}{rM\sinh y}\right)$$

In (3) the parameter r plays the role of the relativistic generalisation of the relative coordinate.

Due to the modulus of the new coordinate r is the relativistic invariant and the expansion (3) holds in any reference frame,the distribution function $F(r)$ in this new coordinate space is also invariant and describes the particle structure in any reference frame(and not necessarily in the Breit frame as usual).

The relation that expresses the mean-square radius through a new coordinate plays an important role for the model. Let us mention first that to give the interpretation to the formal definition of the invariant mean-square radius $\langle r_0^2\rangle \equiv 6\frac{\partial F(t)}{\partial t}\Big/_{t=0}$ one usually passes to the Breit frame $(\vec{p} = -\vec{k};\ t = -(\vec{p}-\vec{k})^2 = -2\vec{p}^2)$, where it coincides with the eigenvalue of the Casimir operator $\hat{C}_E$ of the motions group of the three dimensional Euclidean momentum space $\hat{C}_E = \left(i\frac{\partial}{\partial q}\right)^2$: $\hat{C}_E e^{i\vec{q}\vec{r}} = r^2 e^{i\vec{q}\vec{r}}$

$$\langle r_0^2\rangle_{Br.fr.} \equiv -6\frac{\partial F(t)}{\partial \vec{q}^2}\Big/_{\vec{q}^2=0} = \left\{\hat{C}_E F(t)\right\}\Big/_{\vec{q}^2=0}$$

In /1/ it was shown that the invariant mean-square radius also has the group-theoretical meaning namely, it is the eigenvalue of the Casimir operator of the Lorentz group

$$\langle r_0^2\rangle \equiv 6\frac{\partial F(t)}{\partial t}\Big/_{t=0} = \left\{\hat{C}_L F(t)\right\}\Big/_{t=0}. \qquad (4)$$

From (3) and (4) the expression follows for an invariant mean-square radius through the invariant distribution $F(r)$ in a new coordinate space:

$$\langle r_0^2\rangle \equiv 6\frac{\partial F(t)}{\partial t}\Big/_{t=0} = \frac{1}{M^2} + \frac{\int r^2 F(r)\, d^3\vec{r}}{\int F(r)\, d\vec{r}}. \qquad (5)$$

We see that when the distribution $F(r)$ is of constant sign, a new coordinate r and $F(r)$ describe only the distance beyond the Compton wave length $\frac{1}{M}$ $(\hbar = c = 1)$.

If we analyze the VDM model of the electromagnetic form factors in terms of a new coordinate space then we shall find that in this space the transform $F(r)$ of a meson propagator $\frac{1}{\mu_V^2 - (p-k)^2}$ essentially depends on the relation between the mass M of the particle itself and that of the intermediate vector meson μ_V: $F(r)$ is the function of the constant sign when $\mu_V^2 < 4M^2$ and alternative function when $\mu_V^2 > 4M^2$ /2/. The recently discovered vector mesons ϱ, ω, φ and ϱ'' (1650) satisfy the first relation $\mu^2_{\varrho,\omega,\varphi,\varrho''} < 4M_p^2$, thus they contribute the proton structure only at distances beyond its Compton wave length $1/M_p$. So, to reflect the whole proton structure in the momentum space, we need to add the contribution of the central part with $\langle r_0^2 \rangle = 1/M_p^2$. From (5) it follows that to the central sphere with $\langle r_0^2 \rangle = 1/M^2$ there corresponds the spatial distribution $F(r) = \frac{\delta(r)}{4\pi r^2}$. According to (3) it provides the contribution to the form factor $F(t)|_{r_0 = 1/M} = y/\sinh y$ that modifies the VDM for the proton f.f. by formula (1).

From the view-point of quark models the obtained picture may be interpreted as follows. According to the estimate by these models /3/, the relative motion of three quarks constituting a proton is within the region of the proton Compton wave length order. Consequently, they produce the contribution of the central part of a proton, while the quark-antiquark pairs compose the vector mesons, responsible at $\mu_V^2 < 4M_p^2$ for the distribution at distances beyond $1/M_p$.

The results of fitting of experimental data by formula (1) are given in /4/. In /4/ at account of 84 data points with approximately equal number of data points at $-t < 1$ GeV^2 and $-t > 1$ GeV^2 the obtained value of χ^2 per degree of freedom was $\chi^2_{deg.fr.} = 1.04$. The fitting of the whole world experimental data (299 points) performed in /5/ gave $\chi^2_{deg.fr.} = 1.21$ with the confidence level C.L.=1%, while in this case the usual VDM gives C.L.=0.03–0.1%. Besides formula (1), that was obtained in 1974 /1/ when "the measured form factor seems to fall faster than $1/q^4$ " /6/, predicted that at asymptotical $-t \gg 4M_p^2$ the decrease of the f.f. should be more slow than t^{-2} up to the factor $\ln \frac{|t|}{M^2}$ in /2/. The quark counting rules /7/ also give the proton decrease as t^{-2}. The last experiments in 1975 have shown that really at $-t > 25$ GeV^2 the decrease becomes slower than t^{-2} (see Fig.1

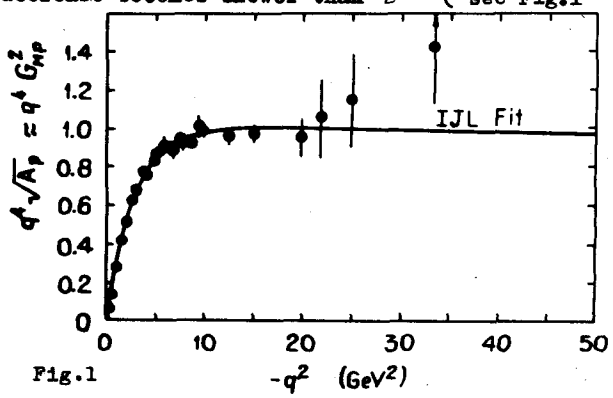


Fig.1

and prof.Chertok's talk also).

The problem of description of electromagnetic form factors in the framework of the dispersion approach was discussed in /8/. The authors also took into account the $\pi\omega$ state beside the $\pi\pi$ intermediate state. The analyticity and unitarity lead to the following system of equations (see Fig.2).

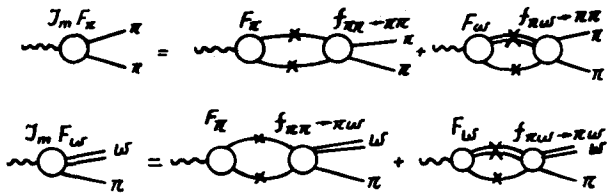


Fig.2

These relations allow to determine by a model independent way the F_π and f.f. F_ω of $\gamma \to \pi^0\omega$ transition by phase of $\pi\pi$ and $\pi\omega$ scattering and inelasticity. The relation obtained enables with the use of the data to conclude that the phase shift of $\pi\omega$-scatter-

ing goes through $\pi/2$ in the region of the ρ' (1250) resonance. By taking into account the ρ and ρ' with $\frac{g_{\rho'\omega\pi}}{g_{\rho\gamma}} \cdot \frac{g_{\rho\gamma}}{g_{\rho\omega\pi}} \approx \frac{1}{2}$ the authors succeded in the description of data on F_ω (fig. 3.) and F_π (fig. 4.) the $\Gamma_{\rho' \to 2\pi}$ being approximately close to zero.

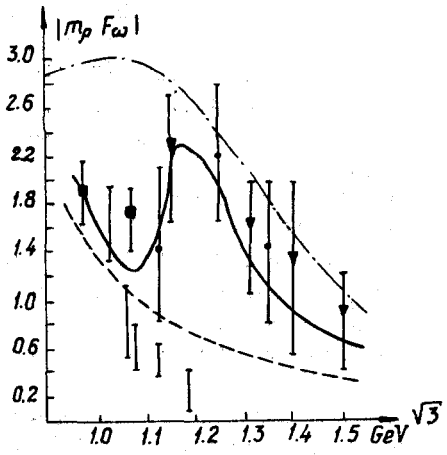


Fig.3

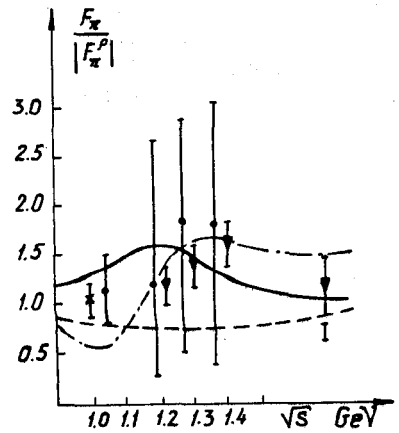


Fig.4

The remarkable property of these relations is that the data on $F_\pi(s)$ at $t > 0$ are satisfactory described too (fig.5).

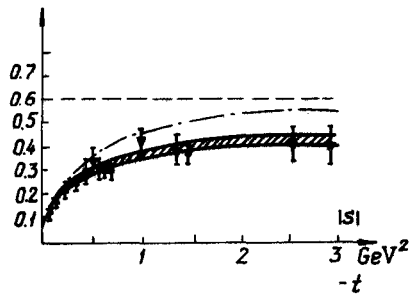


Fig.5

The authors of /9/ have analyzed the pion f.f. data in the time-like region to find out the possibly existing ρ' and ρ'' resonance structures in these data. They have shown that with the restriction $\chi^2_{deg.fr.} = 0.5$ 3 resonance structures can be distinguished in the Argand diagram at 1280 MeV (ρ' - meson region), 1510 MeV (ρ'' meson region) and at 1920 MeV. But with $\chi^2_{ireg.fr.}$ increasing up to $\chi^2_{deg.fr.} = 0.6$ only one resonating structure at 1510 MeV remains. So they conclude that the only feature that can be clearly extracted from nowadays data is a resonance at ρ'' 1500-1600 MeV region.

The problem to describe electromagnetic properties of hadrons on the basis of strong interaction data is also dealt within paper /10/. In this paper an integral representation is used expressing form factors of two-particle systems in terms of phase shifts of strong interaction between the constituent particles and their f.f.. Such an approach is manifestly covariant and is shown to yield the results usually obtained with the use of phenomenological potentials in the nonrelativistic limit. As example the authors present the deuteron's charge form factor. Their method when applied to the nucleon form factors shows that the magnetic f.f. should decrease faster than the electric one at large $-q^2$:

$$G_{E_{n,p}}(q^2) \sim G_E^V(q^2) \sim \frac{F_\pi(-q^2)}{\sqrt{-q^2}} \cdot \sin\delta_{11}(-q^2)$$

$$G_{M_{n,p}}(q^2) \sim G_M^V(q^2) \sim \frac{F_\pi(-q^2)}{(-q^2)\sqrt{-q^2}} \cdot \sin\delta_{11}(-q^2)$$

δ_{11} is the phase shift of the πN - scattering.

In paper /11/ it was shown that the measurements of asymmetries in the elastic scattering of longitudinally polarized leptons on a polarized proton target at high $-q^2$ makes it possible to distinguish between two possible relations for the proton f.f.

$$F_1(q^2) \sim F_2(q^2) \qquad \text{I}$$

or

$$G_E(q^2) \sim G_M(q^2) \qquad \text{II}$$

at large $-t$. The I case is realized in composed model based on the Bethe-Salpeter equation, the case II follows from standard parton model, asymptotically free theories and, as it was shown in /12/, also holds in theories with γ_5, or chirality invariance, proposed in /13/. In /11/ it is shown that in I case, that still cannot be excluded by available experimental data at high $-q^2$, the longitudinal $A_{\parallel}$ and transverse $A_{\perp}$ asymmetries behave similarly (fig.6) $A_{\parallel} \sim A_{\perp}$ while in the II case (fig.7)

$$|A_{\parallel}| \gg A_{\perp}$$

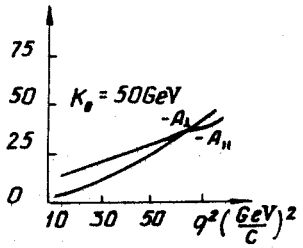


Fig.6

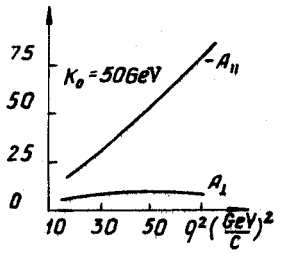


Fig.7

The experimental check of these relations will be a very powerful test of our understanding of proton structure.

The electroproduction of baryon resonances in the first, second and third resonance regions are analysed in /14/ within the framework of the relativistic quark model. Current matrix elements are constructed on the three-dimensional surphase, defined by Markov-Yukawa conditions. The obtained results are in good agreement with experiment in a wide range of transfer momentum.

References:

1. N.B.Skachkov. JINR preprints E2-7890; E2-8424, Dubna, 1974; E2-8857, Dubna, 1975; Soviet Journal Theor.and Math.Phys. 23, N3. (translation of Theor.i Mat.Fiz. 23, N.3 (1975) 313).
2. V.G.Kadyshevsky, R.M.Mir-Kasimov, N.B.Skachkov. Nuovo Cim. 55A (1968) 233; Soviet Journal of Particles and Nuclei (translation) 2, N.3 (1972) 69.
3. S.B.Gerasimov. JINR preprint P-2439, Dubna, 1965; P-2619, Dubna, 1966. A.D.Licht, A.Pagnaments. Phys.Rev. D2, 1150 (1970).
4. N.B.Skachkov, I.L.Solovtsov. JINR preprint E2-9504, Dubna, 1976.
5. S.I.Bilenkaya, N.B.Skachkov, I.L.Solovtsev, Contribution 602/A7-13 at this Conference.
6. P.N.Kirk et al. Phys.Rev. D8, 63 (1973).
7. V.A.Matveev, R.M.Muradyan, A.N.Tavkhelidze. Nuovo Cim. 7,719 (1973); S.J.Brodsky, G.R.Farrar. Phys.Rev.Lett. 31, 1153 (1973).
8. N.M.Budnev, V.M.Budnev, V.V.Serebryakov. Novosibirsk Math.Inst. preprints T - 88, T - 89 (1976).
9. C.B.Lang, I.Sabba-Stefanescu. Univ.of Karlsruhe TKP 14/75 (1975).
10. A.I.Kirillov, V.E.Troitski, Yu.M.Shirokov. Contribution 597/A7-31 at this section.
11. S.I.Bilenkaya, S.M.Bilenky, A.Frenkel, E.H.Hristova. JINR preprint E2-8678, Dubna (1975).
12. B.L.Ioffe. ITEF-preprint ITEP-50, Moscow, 1976.
13. A.A.Logunov, V.A.Meshcheryakov, A.N.Tavkhelidze, Dokl.Acad.Nauk SSSR 142, 317 (1962).
14. A.P.Kobushkin, Yu.M.Sinjukov. Contributions 596/C4-6; 598/C4-8 at this conference. V.F.Dushenko, A.P.Kobushkin, Y.M.Sinjukov. Soviet Journal Nucl.Phys. 24, 434 (1976).

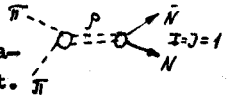
VECTOR MESON-NUCLEON COUPLING CONSTANTS

G. Höhler

Institute for Theoretical Nuclear Physics, Karlsruhe University, FRG

1. ρ NN Coupling Constants (Ref. [1]).

An investigation of the $I=J=1$ $\pi\pi NN$ partial waves offers the best possibility for a determination of the properties of the ρNN vertex. Following Frazer and Fulco [2] one has to perform two analytic continuations in order to obtain from πN amplitudes the partial waves in the region of interest.



i) The partial waves $\Gamma_i(t)$ at $t<0$ $(i=1,2)$ follow from a projection of πN amplitudes which are continued at fixed t to the region between the s- and u-channels in the Mandelstam diagram. The continuation is trivial, since we have used Pietarinen's new phase shift analysis [3] which incorporates fixed-t analyticity from the beginning.

ii) Continuation of the partial waves $\Gamma_i(t)$ to the t-region of the ρ-peak. A reliable continuation is possible only, because the phase of $\Gamma_i(t)$ can be taken from the p-wave $\pi\pi$-phase shift and also from a fit to the data for the pion form factor $F_\pi(t)$.

It is assumed that the 4π contribution to the extended unitarity relation can be ignored up to the $\omega\pi$ threshold, because 4π-production in $\pi+\pi$ and $e^+ + e^-$ is negligible in this range.

Because of the large ρ-width the value of the coupling constant depends to some extent on its definition (Ref. [1]). Results for the vector and tensor ρNN coupling constants in Sakurai's convention:

$$f_V^2(\rho)/4\pi = 2.2. \qquad f_T(\rho)/f_V(\rho) = 6.6$$

The error is estimated to be of the order of 10% for f_V, f_T.

f_V is near to the usual value, f_T/f_V is much larger than the value 3.7 obtained with the simplest VDM model for the nucleon form factor. We believe that other methods have a larger uncertainty.

2. Other VNN Coupling Constants

In order to determine further VNN coupling constants we have used the dispersion method for a new analysis of the electron-nucleon scattering data [4,5] . The dispersion relation for the Dirac and Pauli form factors reads $(i=1,2)$

$$F_i(t) = \frac{1}{\pi}\int_{4\mu^2}^{\infty} \frac{\mathrm{Im}\, F_i(t')}{t'-t}\, dt' \qquad (2.1)$$

According to Frazer and Fulco the ρ-contribution to $\mathrm{Im}\, F_{iV}$ follows easily from the result of the calculation described in sect. 1.

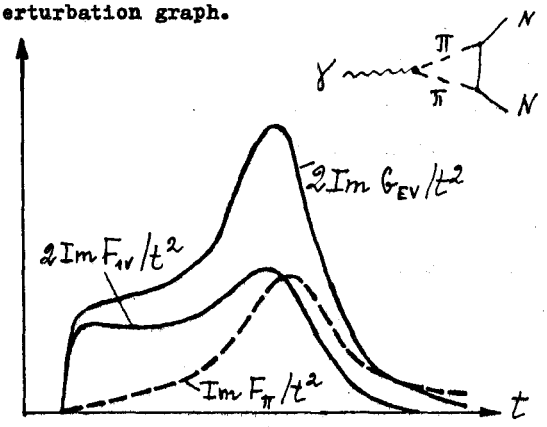
$$\mathrm{Im}\, F_{iV}(t) = \frac{q_t^3}{\sqrt{t}} F_\pi^*(t)\Gamma_i(t); \quad q_t^2 = \frac{t}{4} - \mu^2 \qquad (2.2)$$
$$t \le 50\mu^2$$

All other contributions are described by pole terms

$$\mathrm{Im}\, F_{iV} = \mathrm{Im}\, F_{iV}^{\rho} + \pi \sum_V a_i(V)\,\delta(t-t_V); \quad V=\rho',\rho''\ldots \qquad (2.3)$$

$$\mathrm{Im}\, F_{is} = \pi \sum_V a_i(V)\,\delta(t-t_V); \quad V=\omega,\phi,\omega'\ldots$$

In order to demonstrate that the accurate result for $\mathrm{Im}\, F_{iV}$ differs significantly from a pole approximation, we show a figure for the integrand of the dispersion integral for $F'(0)$, from which the isovector nucleon radius is determined [4] . The enhancement just above $t = 4\mu^2$ is caused by a logarithmic singularity of $F_{iV}(t)$ in the 2nd sheet at $t = 3.98\mu^2$, which belongs to the contribution of the perturbation graph.



The enhancement is not present in the pion form factor. Therefore its t-dependence must be different from that of F_{1V}, contrary to the assumption in several papers.

The VNN coupling constants $g_i(V)$ follow immediately from the results for the residues

$$a_i(V) = \frac{m_V^2}{f_V} g_i(V) \quad (2.4) \qquad \frac{m_V^2}{f_V} = \frac{1}{\tau_{V\cdot t}} g_i(V)$$

since the γV coupling constants are known from $e^+e^- \to V$ experiments. In order to have a simple notation, we are using now half of the earlier $\rho\bar{N}N$ coupling constants: $g_i(\rho) = f_i(\rho)/2$.

Input Data: all accurate $ep \to ep$ cross sections, $en \to en$ cross sections from ed-data, $e^+e^- \leftrightarrow \bar{p}p$ data. $G_{En}'(0)$ from the scattering of slow neutrons against atomic electrons (New data: [16]). Our result is consistent with the $\pi^- p \to e^+e^- n$ data of the Dubna group [17]. Since it is difficult to determine the Dirac isovector form factor and the pion form factor separately, it would be useful to analyse the data with the constraint that the difference $Re\,2F_{1V} - Re\,F_\pi$ and the imaginary parts are taken from our results.

Adjustable Parameters: all $a_i(V)$, the masses of the pole terms (except ω, ϕ). These masses were restricted to lie beyond 1 GeV. The normalizations of the eN-scattering data (in general within the errors given by the authors).

The problem is not well defined without a simplicity condition. We restricted the oscillations by demanding that $\sum_V |a_i(V)|$ should not be much larger than the minimum value necessary for a good fit $(\chi^2_{DF} \approx 1)$

Results

1. $ep \to ep$ data only

It is interesting to find the number of parameters which can be determined in a reliable way

Usual dipole fit, normalization of data as published 11.6
the same, but normalizations adjusted . . . 4.3

Best fit (298 data points, 5 parameters in the ansatz, normalizations adjusted) 0.9

2. All Data

In this case our best fit has $\chi^2_{DF} = 1.3$, the number of adjustable parameters in the ansatz being 8.

The main effects are large bump-dip structures in $Im\,F_{1S}$ and $Im\,F_{2V}$. $Im\,F_{1V}$ is not far from ρ-dominance, $Im\,F_{2S}$ is small.

F_{2V}. The large ρ-peak is followed by a dip of almost the same area. Its position is near to the mass of the first daughter $\rho'(1250)$ of the ρ according to the Veneziano model. Part of the dip could be due to the tail of the ρ and the effective pole could be a description of a broad structure. If one attempts to shift the dip to the 1600 MeV mass region, the fit develops huge oscillations at larger t and becomes unacceptable. It was reported at this Conference that $\rho'(1250)$ is not seen in $e^+e^- \to \pi^0\pi^0\pi^+\pi^-$ up to 1.3 GeV Ref. [18] . This point deserves a further study, taking into account the results of Budnev et al. [19] .

A crude estimate of the $\rho'NN$ tensor coupling constant gives $g_2^2(\rho') \approx 0.5\, g_2^2(\rho)$. There is no evidence for a structure at 1600 MeV, but this might change when better $e^+e^- \to \bar{p}p$ data give stronger restrictions for the spectral functions in the unphysical region.

F_{1S}. Since the OZI rule predicts a decoupling of ϕ from $\bar{N}N$, we started with an

ω – pole + 2 poles with adjustable masses. It turned out that one of the poles chose a mass near to the ϕ-mass. So we fixed this pole at m_ϕ. Our best solution has a fairly large vector coupling

$$g_1^2(\omega)/4\pi = 24 \pm 5 \pm 7.$$

The errors belong to f_ω and $a_1(\omega)$ respectively. Our results: $a_1(\phi)/a_1(\omega) = -0.9$, $g_1(\phi)/g_1(\omega) = -0.5$ clearly violate the OZI-rule. Therefore we have looked for other acceptable solutions.

It is easy to reduce the ϕ NN coupling by adding another pole in the 1200 MeV mass region. Up to now there is no evidence for a meson resonance $\omega'(1250)$, but it might be difficult to detect because of the large width due to $\omega' \to \rho\pi$ decay.

Since some symmetry predictions want a much smaller value of $g_1(\omega)$ (see below: $g_1^2(\omega)/4\pi = 3 g_1^2(\rho)/4\pi \approx 5$), we have tried to find acceptable solutions with a smaller $a_1(\omega)$. It turns out that the fit wants to retain the magnitude of the bump. If we enforce a smaller $a_1(\omega)$ one obtains a large positive $a_1(\phi)$. The solution becomes unacceptable because of large oscillations at larger t, if we demand that both $a_1(\omega)$ and $a_1(\phi)$ are small.

3. SU(3) Relations Between VNN Coupling Constants (Ref. /10/)

SU(3) gives a relation between $g_i(\rho)$ and all other $V\bar{N}N$ coupling constants of the octet $(\rho, K^*, \bar{K}^*, \phi_8)$. In particular

$$g_i(\phi_8) = \frac{1}{\sqrt{3}} (4\alpha_i - 1) g_i(\rho). \qquad (3.1)$$

α_i is the $F/(F+D)$ ratio which is not determined by SU(3). $i = 1,2$ denotes vector and tensor coupling. The relation (3.1) is also valid for $i = E, M$, where

$$g_E = g_1 + \frac{m_V^2}{4m^2} g_2, \quad g_M = g_1 + g_2, \qquad (3.2)$$

m denotes the nucleon mass. In the VDM g_1, g_2 belong to the Dirac and Pauli form factors and g_E, g_M to the electric and magnetic Sachs form factors.

In order to obtain a relation for the physical couplings $g_i(\omega)$, $g_i(\phi)$ we insert the mixing relation

$$|\phi_8\rangle = \cos\theta |\phi\rangle + \sin\theta |\omega\rangle. \qquad (3.3)$$

The mixing angle is $\theta = 40^\circ$ if calculated from the Gell-Mann-Okubo mass formula. $\theta = 35.2^\circ$ is the quark model prediction ("ideal mixing").

We obtain for $i = 1, 2, E, M$

$$\frac{1}{\sqrt{3}\sin\theta} (4\alpha_i - 1) \frac{g_i(\rho)}{g_i(\omega)} - 1 = \cot\theta \frac{g_i(\phi)}{g_i(\omega)}. \qquad (3.4)$$

If the OZI-rule is fulfilled ($g_i(\phi) = 0$) and the mixing is ideal, we have $(4\alpha_i - 1) g_i(\rho) = g_i(\omega)$, i.e., $3 g_i(\rho) = g_i(\omega)$ for pure F-coupling. If we compare our results with eq. (3.4), there are two simple possibilities for the assumption on the $F/(F+D)$ ratios:

i) We assume a pure F-type vector coupling, $\alpha_1 = 1$, as it follows, for instance, from Sakurai's conjecture that the interaction term in the Lagrangian is a product of the ρ-field and the isospin current ("ρ-universality"). Then eq. (3.4) agrees well with the $V\bar{N}N$ couplings of our best fit which violate the OZI-rule. The violation follows already from our large value of $g_1(\omega)$ as a SU(3) prediction from eq. (3.4). A possible $\omega'(1250)$ contribution must be small.

Another argument for a pure F-vector coupling starts from the fact that SU(3) leads to a pure F-coupling at t=0 for the matrix element of the electromagnetic current. Since ρ-dominance seems to be approximately valid for F_{1V}, there is a chance that this property remains valid up to $t = m_V^2$.

ii) Sugawara and von Hippel /11/ proposed that SU(3) should be applied to the couplings g_E and g_M and that the result for the $F/(F+D)$

ratios at t=0 remain valid up to $t = m_V^2$. Additional arguments were presented in a recent preprint by Gustafson [12]. Our results for g_E and g_M read

$$g_E(\rho)=5.5,\ g_M(\rho)=19.8;\ g_E(\omega)=16.9,\ g_M(\omega)=14.7$$

The assumption $\alpha_E = 1$ (pure F-coupling) is consistent with our values and the validity of the OZI rule ($g_E(\phi)=0$), since $g_E(\omega)=3g_E(\rho)$ There must be a large contribution from $\omega'(1250)$ exchange.

If we assume that ϕ decouples also in the magnetic case, we have for ideal mixing

$$(4\alpha_M - 1) = \frac{g_M(\omega)}{g_M(\rho)}$$

which gives $\alpha_M = 0.44$. The agreement with the SU(6) prediction 0.40 is good.

Aside from the fact that one needs a large contribution from ω' which has not been discovered, one would like to see a better justification, why the $F/(F+D)$ ratio at t=0 should remain valid up to $t = m_V^2$. The difficulty is that two exchanges ρ and ρ' give large contributions to $G_{EV}(0)$ and $G_{MV}(0)$. Furthermore the SU(6) prediction $G_{En}(t)=0$ is wrong for small t, whereas $F_{En}(t)=0$ is much nearer to the data.

Another possibility for a test of the OZI-rule was proposed by Gerasimov [13]. He studied relations between baryon form factors, in particular magnetic moments, taking into account SU(3) breaking but using unbroken SU(3) for the matrix element $\langle V | B\bar{B} \rangle$. The sign of the violation differs from ours.

4. Comparison with Other Determinations

Kravtsov et al. [14] used the optimal conformal method in order to determine new values for the nucleon radii. For the imput they used published form factors, taking into account normalisation errors. The result is not much different from that of Ref.[15], deviations being probably due to the fact that the authors of Ref.[14] ignored the information on the spectral functions $\mathrm{Im}\, F_{iV}$ from unitarity and also to the use of form factors instead of ep-cross section for the imput.

The information from unitarity has also been ignored in the work of Bilenkaja et al.[15] It will be interesting to compare the short range part of their spectral function with that of Ref. [15].

If our results for the VNN coupling constants are compared with those from other determinations, it is important to check whether the definitions of the coupling constants are the same. For instance authors working in NN-scattering give "$\bar{V}NN$ couplings at $t=0$", a notion which needs a more detailed explanations, since coupling constants are usually defined at $t = m_V^2$ (Ref.[16]).

In a paper presented by N.Zovko [17] the kaon radius was calculated in a low energy approximation to the unitarity relation for the $\pi\pi \to \pi\pi$ and $\pi\pi \to \bar{K}K$ amplitudes. The result is

$$F_K^V(q^2) = F_\pi(q^2).$$

References:

1. G.Höhler and E.Pietarinen, Nucl.Phys., B95 210 (1975).
2. W.R.Frazer and J.R.Fulco. Phys.Rev., 117, 1603 (1960).
3. E.Pietarinen, Nucl.Phys., B107, 21 (1976); preprint TKP 75/4 Un.of Karlsruhe, See also the talk of G.Oacles at this Conference.
4. G.Höhler and E.Pietarinen. Phys.Lett. 53B, 471 (1975).
5. G.Höhler et al. Preprint TKP 76/1. Papers 483 and I. Sabba-Stefanescu paper 104.
6. L. Koester et al. Phys.Rev.Lett., 36,1021 (1976).
7. S.F.Berezhnev et al. Yad.Fiz. 16, 185 (1972). and papers 1143,1144.
8. V.A.Sidorov , paper 639.
9. N.M.Budnev et al. Novosibirsk preprint TF 88.
10. H.Genz and G.Höhler. Phys.Lett. 61B, 389 (1976).
11. H.Sugawara and F.von Hippel . Phys.Rev. 145 1331, (1966); 172,1764 (1968).
12. G.Gustafson. Lund preprint (July, 1976).

13. S.B.Gerasimov, Paper 592.
14. A.V.Kravtsov and L.L. Nemenov, paper 1029.
15. S.I.Bilenkaya et al. Paper 602.
16. M.M.Nagels et al. Compilation of Coupling Constants and Low Energy Parameters, 1976.
17. N.Zovko, paper 364.

EFFECTS OF THE SU(3)-BREAKING IN MASSES AND ELECTROMAGNETIC DECAYS OF VECTOR MESONS

S.B.Gerasimov
Joint Institute for Nuclear Research,Dubna

Introduction

The breaking of the SU(3)-symmetry results in the mass shifts, modification of the interaction amplitudes and mixing of states belonging to different representations of the SU(3)-group. Various implications of the symmetry breaking in the vector meson sector came into focus of a particular attention when new data on the meson radiative decays have been obtained /1/ .

Mass relations and mixing angles

From the conventional assumptions on the octet breaking of the SU(3)-symmetry and the singlet-octet configuration of the ω and φ meson

$$\omega = \omega_8 \sin\theta_V + \omega_1 \cos\theta_V$$
$$\varphi = \omega_8 \cos\theta_V - \omega_1 \sin\theta_V \qquad (1)$$

the GMO formula

$$4m^n_{K^*} - m^n_\rho = 3\left(m^n_\varphi \cdot \cos^2\theta_V + m^n_\omega \cdot \sin^2\theta_V\right) \qquad (2)$$

follows. From the linear mass formula (n=1) one obtains $\theta_V \simeq 37^0$, while the quadratic one gives $\theta_V \simeq 39^0$. Introduoing the symmetry breaking and the singlet-octet mixing into the "kinetic" rather than "mass" term of the Lagrangian results in the "current-mixing" scheme and the Coleman-Schnitzer /2/ mass formula, corresponding to $n = -2$ in Eq. (2) and $\theta_V \simeq 28^0$. So, it is necessary to refer to other sources of information to choose between different mass formulas and mixing angles.

Spectral function sum rules and the mixing angles

The spectral function sum rules (s.r.) follow from rather general assumptions on the unitary structure of the current commutators /3-5/ . It was known for a long time that

the saturation of the 1-st Weinberg s.r. for the coserved vector currents (isospin I_μ^3 , hypercharge Y_μ and baryonic B_μ) by the ρ^0 , ω and φ - contributions gives the relation characteristic to the "current mixing" model /5/

$$tg\theta_B / tg\theta_Y = m_\omega^2 / m_\varphi^2 \qquad (3)$$

between angles θ_B and θ_Y , which define the vacuum-vector-meson matrix elements of the baryonic and hypercharge currents and related to θ_V in Eq. (1) via

$$tg^2\theta_V = tg\theta_B \cdot tg\theta_Y \quad . \qquad (4)$$

However, the lowest pole dominance assumption for the 1-st Weinberg s.r. within the SU(3)-symmetry appears to be too strong, as a sizeable deviation of the Das, Mathur and Okubo sum rule /4/ from experiment suggests. To have more reliable information on properties of the lowest vector mesons, it was proposed to consider a modified system of the spectral function sum rules in the broken nonet symmetry /6/

$$\rho_{-1}^{I_3 I_3} - \frac{3}{4}\rho_{-1}^{YY} = \frac{3}{2}\rho_{-1}^{BY} \quad , \qquad (5)$$

$$2\rho_{-1}^{BB} - \rho_{-1}^{YY} = \rho_{-1}^{BY} \quad , \qquad (6)$$

where

$$\rho_{-1}^{\alpha\beta} \equiv \int \frac{dm^2}{m^2}\rho^{\alpha\beta}(m^2) \quad , \qquad (7)$$

and, by construction, the integrals of the current spectral functions $\rho^{\alpha\beta}(m^2)$ over the high energy region are cancelled in Eqs. (5) and (6). Applying then (hopefully, more justified) the pole saturation to system (5) and (6) and using the (finite-width correcteed) g_V -coupling constants ($V = \rho^0, \omega, \varphi$) /7/ we find two solutions:

$$tg\theta_B / tg\theta_Y \simeq \begin{cases} 1 & (8) \\ 0.3 & (9) \end{cases}$$

with the uncertainty of ± 0.1 for each value. The first solution (8) leads to single, universal, mixing angle $\theta_V = \theta_B = \theta_Y = 39^\circ \div 40^\circ$ which is in excellent accord with the quadratic GMO mass formula. The second solution results, via Eq. (4) and definition $tg^2\theta_Y = g_\varphi^2/g_\omega^2$ in $\theta_V \simeq 23^\circ$, which is closer to 28° , given by the Coleman-Schnitzer mass relation. We should emphasize, however, that the conventional "current mixing" model gives relation (3) which does not coincide with either (8) or (9). We conclude therefore that the solution (9) might be connected with some different not yet well-recognized mixing scheme.

Radiative decays

Recent measurements of the meson radiative widths present serious difficulties for a number of popular theoretical models.

A. Quark model

The quark model description of the decays $V \to P\gamma$, $P \to V\gamma$ and (through the VDM) $P \to 2\gamma$, etc., has been discussed repeatedly /8/ . We add two remarks. First, assuming the universal SU(3)-breaking in the "strange" quark magnetic moment one can relate the established symmetry breaking in the Λ -hyperon magnetic moment to possible SU(3)-violation effects in the decays $K^* \to K\gamma$, $\varphi \to \eta\gamma$, $\eta(\eta') \to 2\gamma$. /9,10/. Note also that decrease in the transition magnetic moment $\mu(K^{*0}K^0)$ is accompanied by the increase of $\mu(K^{*\pm}K^\pm)$. Therefore, the comparison of the widths $\Gamma(K^{*0} \to K^0\gamma)$ and $\Gamma(K^{*\pm} \to K^\pm\gamma)$ should provide a critical check of the model.

The second remark refers to a possible strong breaking of the nonet symmetry for the pseudoscalar mesons. This effect can develop in a strong deviation from unity of the overlap radial integral $I_1 \equiv \langle 1|8\rangle_{rad.}$, when the singlet state is ths pseudoscalar one. The numerical estimate of the I_1 can be obtained from the Schwinger mass formula /11/ . If

$\eta' = X(958)$, then $|\theta_p| \simeq 10^\circ$ and $L \simeq 0.5$. Alternatively, if we identify $\eta' = E(1420)$ /12/, then $|\theta_p| \simeq 6^\circ$ and $L \simeq 1$. As far as $(L \cdot \sin\theta_p)_{\eta'=X} \simeq (L \cdot \sin\theta_p)_{\eta'=E}$ both hypotheses result in approximately the same value of $\Gamma(\eta \to 2\gamma)$. Clearly, $L < 1$ gives smaller values for the radiative widths of $\eta' = X(958)$. Some representative results of the quark model are given in Table 1 for the following set of parameters: $x = \mu(s)/\mu(d) = 2\mu(\Lambda)/\mu(N) \simeq 0.7$, $\theta_V = 39^\circ$, $\theta_p = -10^\circ$, $L = 0.5$. The widths of the $\rho \to \pi\gamma$ and $K^{*0} \to K^0\gamma$ decays may present difficulty for the model.

Table 1

Radiative decays of mesons

Decay mode	Theoretical models					Experiment
	1	2	3	4	5	
$\omega \to \pi^0\gamma$	input	790	850	870	824	870 ± 80 kev
$\rho \to \pi\gamma$	96 ± 7	83	73	35	73	35 ± 10 kev
$K^{*0} \to K^0\gamma$	150 ± 12	190	75	78	141	75 ± 35 kev
$K^{*+} \to K^+\gamma$	87 ± 7	46	180	19	59	< 80 kev
$\varphi \to \eta\gamma$	100 ± 8	150	70	70	82	70 ± 16 kev
$\varphi \to \pi^0\gamma$	8.4 ± 4.5	0.04	7.0	5.9	6.9 (input)	5.9 ± 2.1 kev
$\pi^0 \to 2\gamma$	input	7.2	6.3	3.0	6.7	7.92 ± 0.42 ev
$\eta \to 2\gamma$	0.36 ± 0.02	0.36	0.0036	0.28	0.49	0.324 ± 0.046 kev
$X^0 \to 2\gamma$	1.3 ± 0.1	6.0	5.3	12	–	< 19 kev
$X^0 \to \rho^0\gamma$	23 ± 2	100	150	220	–	< 270 kev

1. The quark model ($\theta_V = 39^\circ$; $\theta_p = -10^\circ$; $L = 0{,}5$; $x = 0.7$).
2. The nonet symmetry ($\theta_V = 35^\circ$; $\theta_p = -10^\circ$) /13/.
3. The nonet symmetry and the octet breaking of the SU(3) ($\theta_V = 35^\circ$; $\theta_p = -10^\circ$) /13/.
4. The broken nonet symmetry ($\theta_V = 24^\circ$; $\theta_p = -10^\circ$) /15/.
5. The generalized VDM and dynamical model of the SU(3) breaking ($\theta_V = 39^\circ$; $\theta_p = -10^\circ$) /16/.

B. Phenomenological models

Within these models a certain unitary structure is assumed for corresponding vertices and free parameters are then found by fitting to available data /13–15/.

a) Nonet symmetry and octet breaking of SU(3). The nonet symmetry dictates the following unitary structure for the $VP\gamma$ vertex

$$g(V^m P^i \gamma) = g_0 d_{min} \left(\delta_{n3} + \frac{1}{\sqrt{3}} \delta_{n8}\right), \quad (10)$$

where $m, i = 0, 1, 2, \ldots 8$. A general feature of all models using $\theta_V = 35 \div 40^\circ$ is a strong disagreement of the $\rho\pi\gamma$-width with experiment /13–16/ while the different models meet a different degree of success in describing the $K^* \to K\gamma$ decays. Taking account of the SU(3)-breaking via inclusion of the λ_8-spurion into Eq. (10), and using the "standard" angles $\theta_V = 35^\circ$ and $|\theta_p| = 10^\circ$ results in a very large value of the $K^{*+} \to K^+\gamma$ width /13/, while a model, based on the generalized vector meson dominance, is somewhat hampered by the $K^{*0} \to K^0\gamma$ decay /16/.

b) Broken nonet symmetry.

If only the nonet symmetry and not the SU(3) is broken, then three independent amplitudes describe all radiative transitions. In ref. /15/ the value $\theta_p = -10^\circ$ was fixed, but θ_V was taken as a free parameter to be fitted by comparison with data. The value $\theta_V = 24^\circ$ was obtained, which is surprisingly close to that, resulting from solution (9) of the spectral function s.r. (5) and (6). This model gives satisfactory agreement with all the $V \to P\gamma$ decays /15/ with an exception of the $\pi^0 \to 2\gamma$

width (assuming for the latter, as usual, the VDM model).

So, the $\varrho \to \pi\gamma$ decay appears like a key point in choosing between the symmetry breaking schemes. The accurate measurement of the $K^* \to K\gamma$ decays should be very important to check the SU(3). One can add also, that a useful information concerning the ω-φ mixing results from the $\omega\varphi$ - interference pattern in processes like $e^+e^- \to 3\pi, \pi^0\gamma$ /17/. The recent Orsay data /18/ seems to agree better with the mass-mixing models (i.e. when $\theta_V > 35^\circ$).

In conclusion, one cannot help stressing the extreme importance of (hopefully, soon and improved) new measurements of the $\varrho \to \pi\gamma$ and $K^* \to K\gamma$ decay widths.

REFERENCES:

1. C.Bemporad, in Proc. of 1975 Lepton-Photon Symposium, Ed. W.T.Kirk, Stanford, 1975, p.113. B.Gobbi et al., Phys.Rev.Lett., 33, 1450 (1974). W.C.Carithers et al. Phys.Rev.Lett., 35, 349 (1975).
2. S.Coleman, H.J.Schnitzer, Phys.Rev.,134, B 863 (1964).
3. S.Weinberg, Phys.Rev.Lett., 18, 507 (1967).
4. T.Das, V.S.Mathur, S.Okubo. Phys.Rev.Lett., 19, 470 (1967).
5. R.J.Oakes, J.J.Sakurai. Phys.Rev.Lett., 19, 1266 (1967).
6. S.B.Gerasimov. Communications of JINR P2-9020 (1975), and Paper No. 672.
7. J.LeFrancois, in Proc. of 1972 Leton-Photon Symposium, Cornell University, 1972.
8. G.Morpurgo, in Theory and Phenemenology in Particle Physics, Ed. A.Zichichi, Academic Press, N.Y. 1969.
9. S.B.Gerasimov, JETP 50, 1559 (1966).
10. N.Isgur, Phys.Rev.Lett., 36, 1262 (1976).
11. J.Schwinger. Phys.Rev. 135, B 816 (1964).
12. V.I.Ogievetsky. These proceedings.
13. B.J.Edwards, A.N.Kamal, Phys.Rev.Lett., 36, 241 (1976). Papers No 701 and 948.
14. P.J.O'Donnell. Phys.Rev.Lett., 36, 177 (1976). Paper No 882.
15. D.H.Boal et al. Phys.Rev.Lett., 36, 714 (1976), see also E.A.Ivanov, JINR E2-9430 (1975).
16. G.J.Gounaris. Paper No 981.
17. N.N.Achasov et al. ZhETP Pis'ma, 21, 497 (1975).
18. G.Parrour et al. Preprint LAL 1280,Orsay (1975).

THE NUCLEON AXIAL VECTOR FORM FACTOR FROM THRESHOLD π^+-ELECTROPRODUCTION

P.R.Norton

Daresbury Laboratory, United Kingdom

In this talk I shall review two papers.

307 A.Del Guerra, A.Giazotto, M.A.Giorgi, A.Stefanini, Pisa; D.R.Bottterill, H.E.Montgomery, P.R.Norton, Daresbury; G.Matone, Frascati.

504 A.S.Esaulov, A.S.Omelaenko, A.M.Pilipenko, Yu.I.Titov, Kharkov Inst.

1. G_A AND THRESHOLD π^+ ELECTROPRODUCTION

For massless pions one may use PCAC and current algebra to derive the transverse and scalar multipoles for π^+ electroproduction at threshold /1/.

For real pions a method is needed to extrapolate the unphysical $m_\pi = 0$ results to the physical pion mass. Specific models using different techniques have been used to derive the axial vector form factor from the measured cross sections /2-4/. Since there are small differences in detail between these models, we shall for consistency use that of Benfatto, Nicolo and Rossi to deduce G_A.

2. DATA OF DARESBURY-PISA-FRASCATI (#307)

The experiment was performed at momentum transfers of 0.45, 0.58 and 0.88 $(GeV/c)^2$. The electron was detected in a small-aperture focusing spectrometer and, in coincidence. The neutron in a 2x2 m^2 array of 145 blocks of plastic scintillator. Neutrons and protons were identified by additional thin scintillators in front of the array. A further counter telescope identified protons from radiative elastic scattering.

The cross section, measured up to W=1.13 GeV, was written as

$$\frac{1}{\Gamma_t}\,\frac{4\pi K_L}{q^*}\,\frac{d^3\sigma}{dE'd\Omega_e dl_z} = A_1 + Bq^{*2} + Cq^{*4},$$

where q^* is the π^+ c.m. momentum. The threshold cross section slope is

$$A_1 \sim |E_{0+}|^2 + \epsilon\,|k^2|\,|S_{0+}|^2 .$$

In this experiment the virtual photon polarization ϵ was ~ 0.94 and E_0^+ and S_0^+ could not be separated.

The results for A_1, together with some previous experimental measurements[5,6], are shown in Fig.1. The solid line is the prediction of the Devenish-Lyth fixed-t dispersion relation model[8], which is in excellent agreement with the data.

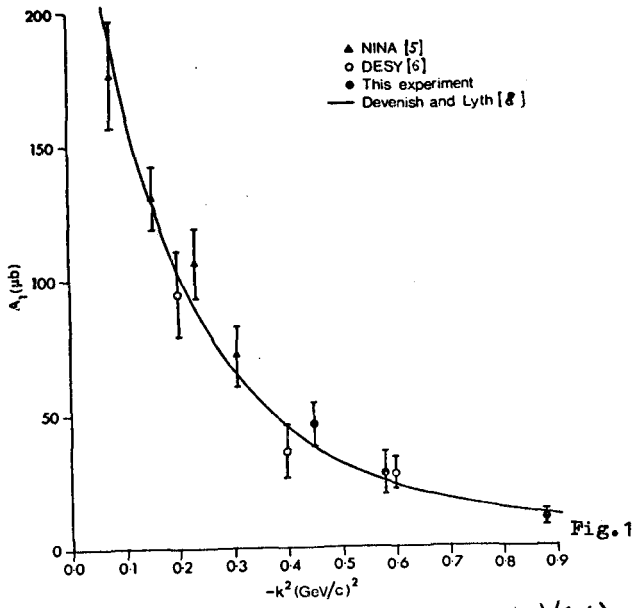


Fig.1

In Fig.2 are shown the values of $G_A(k^2)/G_A(0)$ deduced using the model of Benfatto, Nicolo and Rossi[2]. Assuming the dipole expression $G_A(k^2)/G_A(0) = \left(1 + \frac{|k^2|}{M_A^2}\right)^{-2}$ the best fit to all the data shown is $M_A = 0.96 \pm 0.03$ GeV. The dipole fit is preferred over the monopole. Using the parametrisation $G_A(k^2)/G_A(0) = 1/\left(1 + 2C_A|k^2| + C_B^2|k^2|^2\right)$ which is the monopole for $C_B = 0$, the dipole for $C_A = C_B$ we find the χ^2 contours shown in Fig.3. The dipole hypothesis is an excellent fit, but the data is within 2σ of the monopole.

This result, $M_A = 0.96 \pm 0.03$ GeV, is in excellent agreement with quasi-elastic neutrino scattering[9] which gives $M_A = 0.84 \pm 0.11$ GeV from the differential cross section and $M_A = 0.98 \pm 0.13$ GeV from the total cross section.

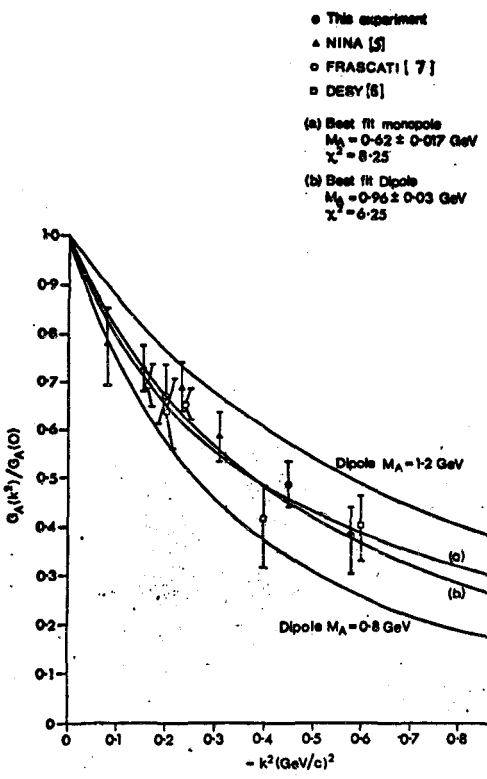


Fig.2

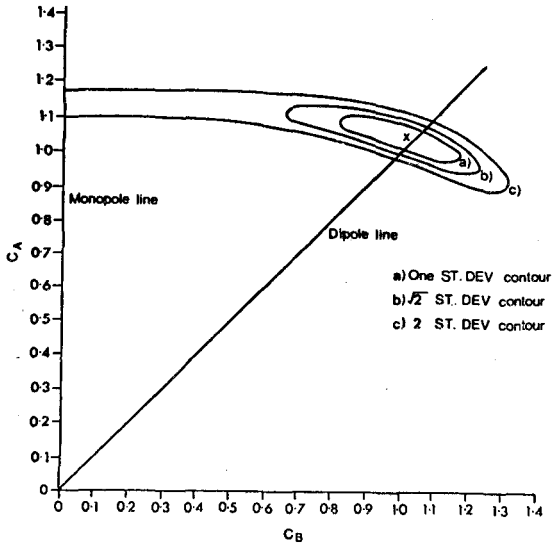


Fig.3

3. Data from Kharkov Inst. (# 504)

New data have been presented by the Kharkov Institute on a single-arm experiment at $|k^2| = 3.5$, 5.0 and 8.0 F^{-2}, in which the longitudinal and transverse contributions to the threshold cross section slope were separated by varying ϵ. Fig.4 shows the slope $\sum_1$, the sum of π^+ and π^0, defined by

$$\lim_{q^* \to 0}\left(\frac{1}{\Gamma_t}\frac{K_L}{q^*}\frac{M}{4\pi W}\frac{d^2\sigma}{dE'd\Omega_\epsilon}\right) = |E_{0+}|^2 + \epsilon\,|k^2|\,|S_{0+}|^2$$

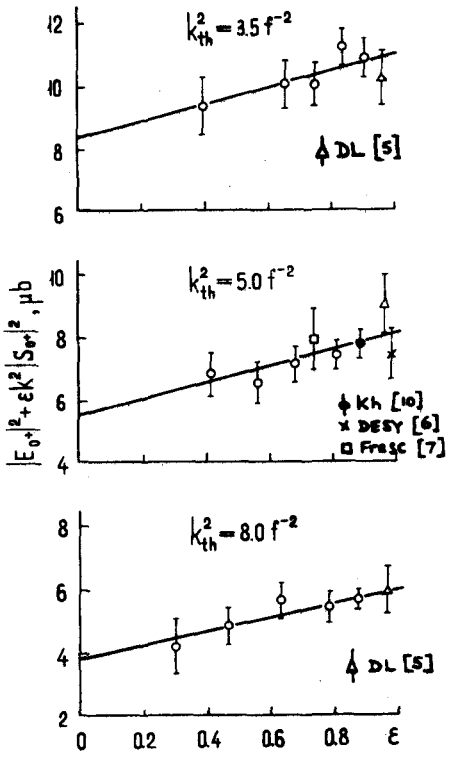


Fig.4

as a function of ϵ . The data are in agreement with previous measurements[5-7,10] (to whioh have been added a computed[2] π^0 contribution). The separated cross sections are shown in fig.5. The solid curve represents the BNR model with M_A=1 GeV, the dash-dot line the π^0 contribution (caloulated) and the dashed line the PVBA without dispersion corrections[4].

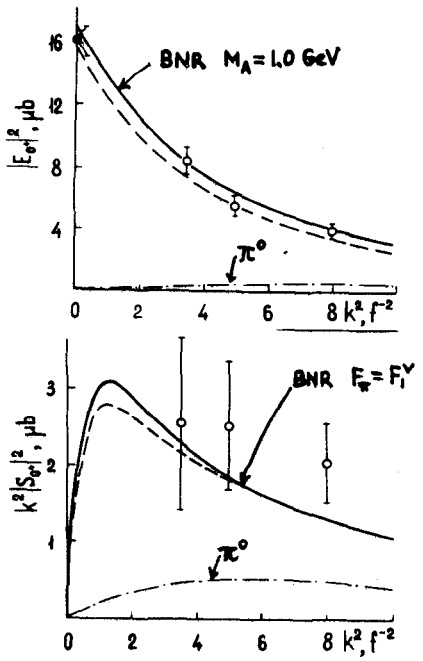


Fig.5

The values of $G_A(k^2)/G_A(0)$ deduced from the transverse cross section using the BNR model (0.78±0.03, 0.66±0.03, 0.57±0.03) are in excellent agreement with previous coincidence data. The pion form factor F_π deduced from $|S_{0+}|^2$ is oonsistent with previous determinations.

References

1. See ref.[5] for an extensive bibliography.
2. G.Benfatto, F.Nicolo and G.C.Rossi. Nucl.Phys., B50 (1972), 205, Nuovo Cimento 14A(1973)425.
3. G.Furlan et al. Nuovo Cimento 62A (1969)519.
4. N.Dombey and B.J.Read. Nucl.Phys., B60 (1973) 65.
   Yu.V.Kulish. Yader. Fiz. 13 (1971)1301.
5. A. Del Guerra et al. Nucl.Phys., B99 (1975) 253.
6. P.Brauel et al. Phys.Lett., 45B (1973)389; 50B (1974) 407.
7. E.Amaldi et al. Phys.Lett., 41B (1972) 216.
8. R.C.E.Devenish and D.H.Lyth. Nucl.Phys., B93 (1975) 109.
9. S.J.Barish et al. Talk by D.H.Perkins, Stanford Conf. 1975.
10. Yu.I.Titov et al. Pisma v. ZHETF 12 (1970)186.

SHADOWING EFFECT IN INELASTIC ELECTRON SCATTERING ON ^{12}C AND ^{27}Al NUCLEI AT SMALL FOUR MOMENTUM TRANSFER

S.Hartwig, F.H.Heimlich, G.Huber, E.Rössle, J.Bleckwenn, M.Köbberling, J.Moritz, K.H.Schmidt, D.Wegener, D.Zeller, P.David, H.Mommsen

DESY, FRG

The inelastic electron scattering on nucleons and nuclei can be described as an absorption process of virtual photons by hadronic matter, characterized by the absorption cross section

$$\sigma = \sigma_t + \varepsilon \sigma_l = \frac{1}{\Gamma_t} \frac{d^2\sigma}{d\Omega dE}$$

Γ_t is the flux of virtual photons, $\frac{d^2\sigma}{d\Omega dE}$ is the measured twofold electron scattering cross section[1]. For real high energetic photons it was shown that the number of effective nucleons A_{eff} of a nucleus is smaller than its atomic number A[2]. This effect, well known for absorption processes where hadrons are involved[3], has been explained by the vector meson dominance model to be due to a hadronic component of the photon[4,5]. On the other side it is known from deep inelastic electron scattering that at four momentum transfers $q^2 \geq 1$ (GeV/c)^2 the interaction between the virtual photon and the hadron has a point-like structure. Therefore it is of interest to study the damping of the photons hadronic component by increasing the mass q^2 of the virtual photon[5]. Foregoing experiments have found weak evidence for shadowing effects, which influence the absorption of virtual photons on nuclei[6]. In order to study this effect in more detail we have measured the inelastic electron scattering cross section on hydrogen, deuterium, ^{12}C and ^{27}Al nuclei for $0.075\,(\mathrm{GeV/c})^2 \leq q^2 \leq 1\,(\mathrm{GeV/c})^2$ and energies of the virtual photon $\nu < 6.2$ GeV at the DESY synchrotron[7].

The scattered electrons have been detected by a spectrometer consisting of a bending magnet, four wire spark chambers, trigger and particle identifying counters[7,8]. The typical statistical error of the data is 2% to 4% and the systematical error of the data is 3.5%.

The main corrections, which had to be applied to the raw data, were due to radiative processes. The calculations have been performed using the formulae of Mo and Tsai[9] for the radiative tail of the elastic electron scattering and the formula of Tsai[10] for the elastic electron scattering. We have used the formfactors of Hofstadter[11] to determine the radiative tail of elastic electron scattering on ^{12}C and ^{27}Al. If necessary the parametrization of the nucleus formfactor has been extrapolated to regions of the data four momentum transfer where no experimental data were available.

The influence of different sources of the radiative corrections has been studied by comparing the measured absorption cross section $\sigma_{\gamma A}$ on a nucleus with the corresponding one on nucleons:

$$\tau = \frac{A_{eff}}{A} = \frac{\sigma_{\gamma A}}{A(1-\frac{N}{\omega})\sigma_{\gamma p}}$$

$\sigma_{\gamma p}$ absorption cross section for virtual photons on protons,

$$\omega = \frac{2M\nu + M^2}{q^2}$$

M = nucleon mass, N number of neutrons. If the radiative process is not modified by the fact, that in a nucleus part of the possible final states, accessible to the scattered nucleon, are occupied by spectator nucleons, the radiative tail due to the contribution of (quasi-) elastic electron nucleon scattering should factorize in the measured inelastic electron nucleus scattering and this contribution to radiative corrections should cancel in the ratio $\tau = A_{eff}/A$. Under this assumption the only corrections which have to be taken into account are due to the radiative tail from elastic electron-nucleus scattering. In Fig. 1a typical results of the present experiment are plotted for the case that the factorization assumption holds. The data show clear evidence for a shadowing effect at small four momentum transfers

At small q^2, where the momentum of the struck nucleon after the scattering process is small, the occupation of possible final states by spectator nucleons will be of influence. Because of the Pauli principle the contribution of the

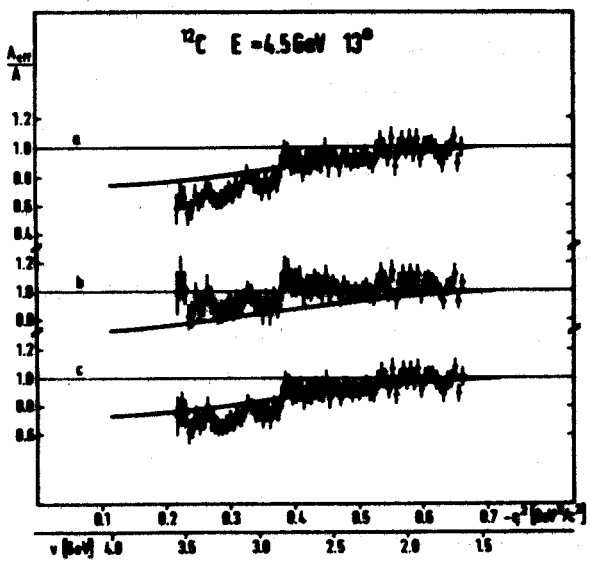


Fig. 1. Ratio A_{eff}/A for ^{12}C Primary electron energy E_e=4.5GeV, electron scattering θ_e = 13°. The figures a,b,c are for different treatments of the radiative corrections (see text).

quasi-elastic radiative tail should decrease compared to the radiative tail of elastic electron nucleon scattering. In the extreme the radiative tail contributes to the measured cross section only for free electron-nucleon scattering, while the electron doesn't radiate for electron-bound state nucleon scattering, because all possible final states are occupied. This extreme case is handled, if one applies only radiative corrections due to elastic electron proton scattering, but no corrections due to electron-bound state nucleon scattering. The result of this procedure is shown in fig . 1b, The shadowing effect nearly disappears. A realistic correction should yield results for the ratio $\tau = A_{eff}/A$ between the two extreme cases of fig. 1a and fig . 1b respectively.

An approach to the realistic computation of radiative corrections due to the radiative tail of electron-bound state nucleon scattering was given by Bernabeu[12]. He has described the influence of the Pauli principle to the quasi-elastic electron nucleon scattering by an effective nucleon formfactor. We have used this effective formfactor to compute the radiative correction of quasi-elastic scattered electrons. The results of this analysis are given in fig. 1c, showing clear evidence for a shadowing effect on both nuclei.

In fig. 2 the ratio $\tau: A_{eff}/A$ for ^{27}Al is plotted as a function of the scaling variable $x = q^2/(2M\nu)$ together with data of Stein et al.[6]. In both cases radiative corrections, using the method of fig. 1c have been applied. The general agreement between the two data sets is quite satisfying. The sharp increase of the shadowing at low values of q^2 in our data is due to the neglection of the Pauli principle effect discussed above. The full curve in fig. 2 is the prediction of the generalized vector dominance model[5] for ^{207}Pb

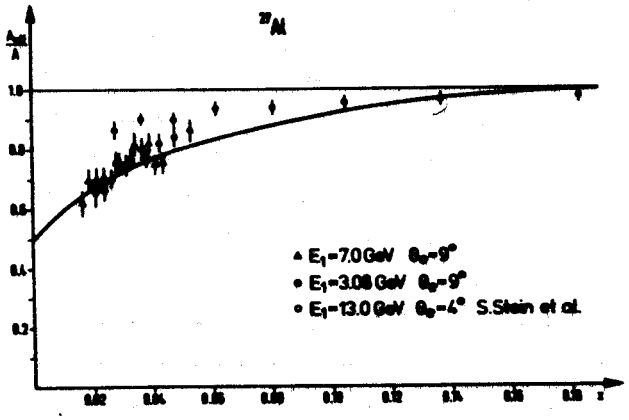


Fig. 2. Ratio A_{eff}/A for ^{27}Al as a function of the scaling variable x. The full curve is the theoretical prediction of the generalized vector meson dominance model for ^{207}Pb. [5].

In conclusion we have shown that a shadowing effect exists for the absorption cross section of virtual photons. It increases with decreasing values of the scaling variable x. For comparison with theoretical predictions one has to take into account the differences of the radiative tails of electron scattering on free and bound state nucleons respectively.

Theoretical prediction of improved version of the generalized vector dominance model[13] are in agreement with the data of the present experiment.

We acknowledge the untiring help of H.Sindt during all stages of the experiment. this work has been supported by the Bundesministerium für Forschung und Technologie.

REFERENCES

1. L.Hand. Phys.Rev., 129, 1834 (1963).
2. V.Heyne, H.Meyer, B.Naroska, D.Notz. Phys.Lett., 34B, 651 (1971).
3. G. Belletini et al. Nucl.Phys., 79, 609 (1966).
4. S.Brodsky, J.Pumplin. Phys.Rev., 182, 1794 (1969).
5. D.Schildknecht. Nucl.Phys., B66, 398 (1973).
6. S.Stein, W.B.Atwood, E.D.Bloom, R.L.A.Cottrell, H. De Staebler, C.L.Jordan, H.G.Piel, C.Y.Prescott, R.Siemarn, R.E.Taylor. Phys.Rev., D12, 1884 (1975). W.R.Ditzler et al. Phys.Lett., 57B, 201 (1975).
7. G.Huber, Thesis, Friberg University, 1976 and DESY Internal Report F23/76-1.
8. S.Galster, G.Hartwig, H.Klein, J.Moritz, K.H.Schmidt, W.Schmidt-Parzefall, D.Wegener, J.Bleckwenn. Phys.Rev., D5, 519 (1972).
9. L.W.Mo, Y.S.Tsai. Rev.Mod.Phys., 41, 205 (1969).
10. Y.S.Tsai. Phys.Rev., 122, 1898 (1961).
11. R.Hofstadter. Ann. Rev.Nucl.Sci., 7, 231 (1957).
12. J.Bernabeu. Nucl.Phys., 186 (1972).
13. Paper No. 487, 490, 491.

SMALL-ANGLE COMPTON SCATTERING ON HYDROGEN AND DEUTERIUM

L.Criegee, G.Franke, A.Ciese, Th.Kahl, G.Poelz, U.Timm, H.Werner, W.Zimmermann

(Presented by D.Wegener, University of Karlsruhe)

We have measured Compton scattering on hydrogen at 6 GeV, and in a second, slightly modified experiment on hydrogen and deuterium at 5 GeV, both at particularly small momentum transfers ranging from -0.004 to -0.08 $(GeV/c)^2$ at 6 GeV and from -0.002 to -0.06 $(GeV/c)^2$ at 5 GeV.

The experimental set up and the analysis procedure is described in paper No. 1016 on this conference.

The differential cross sections determined in this way are shown in Fig. 1. Only statistical errors are shown. Systematic errors result mainly from the uncertainty of the background $\pi^0+\eta$ ($\pm$1%) of the converter position ($\pm$1.5%), and in the case of the 6 GeV data from the error in the telescope efficiencies ($\pm$1.5%). By quadratic addition to the normalization error we obtain a total systematic error of $\pm$2.5% at 5 GeV and $\pm$3.6% at 6 GeV.

Fig. 2. shows the data of this experiment together with those of other DESY and SLAC experiments[1,2].

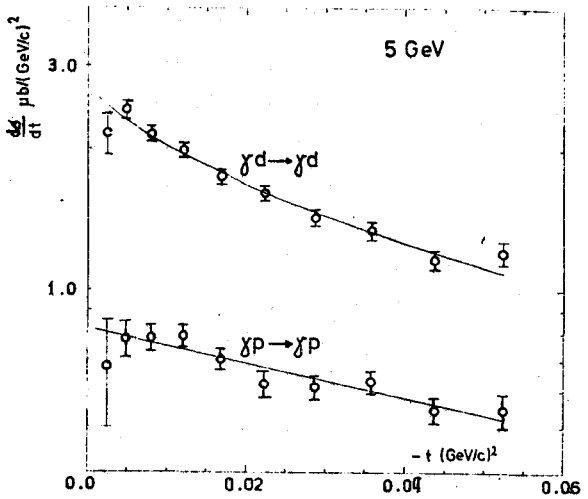


Fig. 1. Compton scattering on hydrogen and deuterium.

A fit to our data of the form $\frac{d\sigma}{dt} = A\, e^{bt}$ as suggested by diffraction theory, yields the results shown in Table 1. The errors include statistical errors as well as the total systematic error.

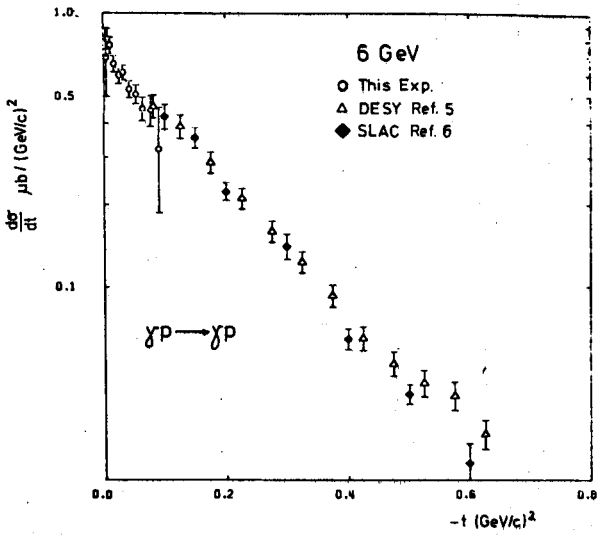


Fig. 2. Differential Compton cross section on hydrogen.

Table 1

	Photon energy GeV	$(GeV/c)^2$	$(GeV/c)^{-2}$
This experiment	5	0.82±0.04	8.5±1.5
	6	0.79±0.04	8.6±1.2
DESY/5/	4–6.2	0.84±0.08	5.7±0.35
SLAC/7/	8	0.82±0.04	7.7±0.5
VDM Prediction (see text)	5	0.46±0.05	-
	6	0.44±0.04	-

The extrapolated forward cross sections are shown as a function of energy in Fig. 3 together with those from other experiments/1-3/. The curve shows the contribution of the spin-independent amplitude f_1 in the standard decomposition

$$\frac{d\sigma}{dt}(0) = \frac{\pi}{k^2}\left(|f_1|^2 + |f_2|^2\right),$$

where f_2 is the spin-dependent amplitude, and k the photon energy, f_1 was calculated from the total cross section via optical theorem and dispersion relation/4/. Our extrapolated forward cross sections are 10% smaller than the predictions, but consistent within the errors. They are compatible with a vanishing spin dependent amplitude f_2 at both energies.

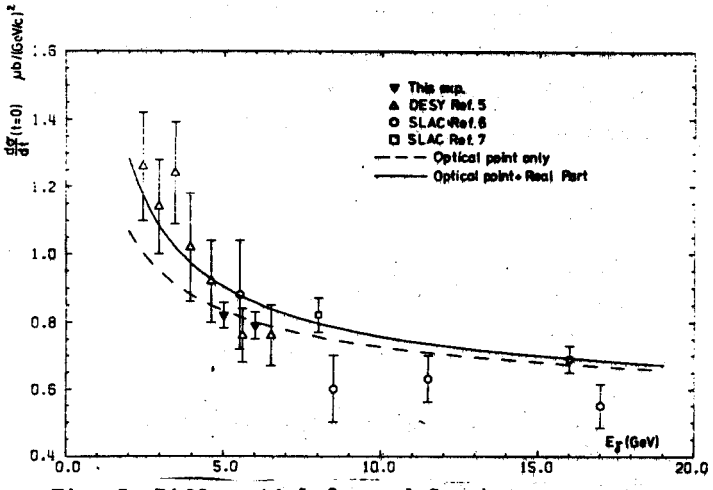


Fig. 3. Differential forward Compton cross section on hydrogen.

For comparison with the predictions of the vector dominance model, VDM, the forward cross sections have been calculated using the sum rule

$$\frac{d\sigma}{dt}(\gamma p \to \gamma p) = \left[\sum_V \frac{\alpha}{4}\frac{4\pi}{\gamma_V^2}\left(\frac{d\sigma}{dt}(\gamma p \to V p)\right)^{1/2}\right]^2$$

with recent values for the vector meson cross sections/5/ and the Orsay values for the coupling constants $\frac{\alpha}{4}\frac{4\pi}{\gamma_V^2}$ /6/. Table 1 demonstrates the well known discrepancy: The data are higher by about 40% than the VDM predictions. This discrepancy can be removed by including the higher vector mesons $\varphi'(1600)$, $\psi(3100)$ and $\psi(3700)$ and by extending the VDM to the GVDM/7/.

The differential cross section for the deuteron (Fig. 1) shows the transition from coherent scattering at low $|t|$ to incoherent scattering at higher $|t|$ values. Neglecting spin effects the cross section can be written in closure approximation as

$$\left(\frac{d\sigma}{dt}\right)_d = \frac{2\pi}{k^2}\left[|a_0|^2(1+F(t)) + |a_1|^2(1-F(t))\right] G(t)$$

where is the proton energy. $F(t)$ and $G(t)$ denote the deuteron form factor and the Glauber correction factor/8/. a_0 and a_1 are the amplitudes of isospin 0 and 1 exchange. The influence of the Fermi motion/9/ is smaller than the Glauber correction, according to our own calculations/10/. The corresponding differential proton cross section is given by

$$\left(\frac{d\sigma}{dt}\right)_p = \frac{\pi}{k^2}\left(|a_0|^2 + |a_1|^2 + 2\,\mathrm{Re}\,(a_0 a_1^*)\right)$$

From the deuteron and the proton cross sections

one can deduce the two isospin ratios $|a_1|^2/|a_0+a_1|^2$ and $Re(a_0 a_1^*)/|a_0+a_1|^2$. By a fit to our experimental data we obtain the values listed in Table 2. Systematic errors resulting mainly from the uncertainty in the $\pi^0\eta$ background component and in the precise converter position, amount to about half of the statistical errors, while normalization errors common to both targets should have no effect.

The isospin ratios depend however sensitively on the assumed shape of $F(t)$ and $G(t)$. We have used a deuteron wave function following Reid and calculated $G(t)$ in the ρ-dominance approxi-

Table 2

Ratios of isospin amplitudes with statistical errors. *Calculation with Hulthen wave function. ** Analysis of the data from Ref.[3] using a deuteron wave function by Reid[10,11]

	$\frac{\lvert a_1\rvert^2}{\lvert a_0+a_1\rvert^2}$	$\frac{Re(a_0 a_1^*)}{\lvert a_0+a_1\rvert^2}$
This experiment, 5 GeV	0.13±0.09 (0.08±0.10	0. ±0.03 0.02±0.03)*
SLAC[7]		
8 and 16 GeV	0.03±0.10 (0.04±0.11)	-0.049±0.012 (0.007±0.018)**
DESY[17] $\frac{Im\,a_1}{Im\,a_0}$	= 0.042±0.008	

mation. If we analyse the data starting from a Hulthen wave function[12], we obtain consistent, although numerically different ratios. For comparison we have also calculated these parameters from the data[3] using our Glauber corrections. The values are then changed slightly in Table 2.

All the ratios are compatible with a vanishing or at least small isospin 1 exchange contribution to photon nucleon interaction. They are also compatible with the measured[13] ratio

$$\frac{Im\,a_1}{Im\,a_0} = \frac{\sigma(\gamma p)-\sigma(\gamma n)}{\sigma(\gamma p)+\sigma(\gamma n)}$$

as listed in Table 2, if one assumes equal real to imaginary part of the a_1 amplitude as predicted for A_2 Regge exchange.

We are indebted to the technicians and to the members of the Hallendienst who made the experiment possible. We are grateful to the scientific directors of DESY for their interest into our experiment.

REFERENCES

1. G.Buschhorn et al. Phys.Lett., 37B, 207 (1971).
2. R.L.Anderson et al. Phys.Rev.Lett., 25, 1218 (1970).
3. A.M.Boyarski et al. Phys.Rev.Lett., 26, 1600 (1971); 30, 1098 (1973).
4. M.Damashek, F.J.Gilman. Phys.Rev., 1D, 1319 (1970).
5. J.Ballam et al. Phys.Rev., 7D, 3150 (1973).
6. J.Perez-Y-Jorba. In Proc. 4th Int. Symp. on El amd Phot. Int. at High En., Liverpool (1970).
7. J.J.Sakurai, D.Schildknecht. Phys.Lett., 42B, 216 (1972) and literature cited there.
8. V.Franco, R.J.Glauber. Phys.Rev., 142, 1195 (1966).
9. W.B.Atwood and G.B.West. Phys.Rev., D7, 773 (1973).
   A.Bodek. Phys.Rev., D8, 2331 (1973).
10. G.Poelz. Private communication.
11. R.V.Reid. Ann.Phys., 50, 411 (1968).
12. G.F.Chew, H.W.Lewis. Phys.Rev., 84, 779 (1951).
13. See e.g., G.Wolf. In Proc. 5th Int.Symp. on El and Phot. Int. at High En., Cornell University, 1971.

DETECTION OF $\pi\text{-}\mu$ COULOMB BOUND STATES

R.Coombes, R.Flexer, A.Hall, R.Kennelly,
J.Kirkby, R.Piccioni, D.Porat, M.Schwartz,
R.Spitzer, J.Toraskar, S.Wiesner
Stanford University, Stanford, California
B.Budick, J.W.Kast
New York University, New York, N.Y.

We report herewith the detection of hydrogen-like atoms consisting of a negative (or positive) pion and a positive (or negative) muon in a Coulomb bound state. These $\pi\text{-}\mu$ atoms are formed when the π and μ from the decay have sufficiently small relative momentum to bind. We have observed these atoms, produced at relativistic velocities, in the course of an experimental program at the Brookhaven A.G.S.

The basic properties of these atoms are calculated by the formalism used to describe the hydrogen atom. The reduced mass of the system is 60.2 MeV/c^2, its Bohr radius is 4.5×10^{-11}cm and the binding energy of the $1S$ state is 1.6 keV. To our knowledge, the first calculation of the branching ratio $R = \frac{K_L \to (\pi\mu)_{Atom}^{+} \nu}{K_L \to ALL}$ was carried out by Nemenov[1], who found that $R \sim 10^{-7}$, with the precise value depending upon the form factors of K_L^0 decay. We will present our results on R in a subsequent paper; only the evidence related to the detection of these atoms is discussed herein.

The prime motivations for the experiment are twofold. First, the value R is proportional to the square of the $\pi\text{-}\mu$ wave function at very small distances and so an anomaly in its value may be indicative of an anomaly in the $\pi\text{-}\mu$ interaction. Secondly, by passing the atoms through a magnetic field at high velocity the 2s states should be depopulated through stark mixing with the 2P states and consequent decay to the $1S$ states. The extent of this depopulation will be highly dependent upon the vacuum polarization shift (Lamb shift) of the $2P$ states relative to the $2S$ states and may, if measured with some accuracy lead to a determination of the pion charge radius.

The K_L^0 particles which give rise to our "atomic beam" are produced by a 30 GeV proton beam striking a 10 cm beryllium target (see Figure 1). A large vacuum tank and a connecting evacuated beam channel lead out to the detection equipment. A 4 ft steel collimator prevents any direct line of sight from the detector system to the target. This is to prevent background particles, in particular K_L^0's from approaching the neighborhood of our detectors.

Those K_L^0's which decay within the shaded area in the vacuum tank give rise to decay products which may, if properly oriented in their direction of motion, travel down the channel. In order to remove charged particles, we have interposed two magnets along this channel. The first of these, labeled the "sweeping magnet" bends horizontally and has an integrated field strength of 8 kilogauss meters. The second magnet, (originally intended to induce transitions between the 2s and 1s states of these atoms) is called the "transition magnet" and bends vertically with an integrated field strength of 36 kilogauss-meters. Those charged particles which survive have very high momenta or are given a significant deflection before entering the detector region.

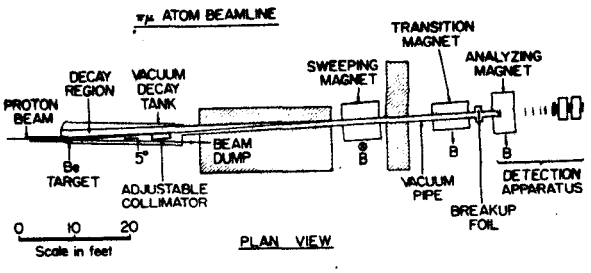


Fig. 1. Experimental arrangement at the A.G.S.

We have then a beam consisting largely of γ rays (resulting from π^0's which are in turn the products of kaon decays), highly energetic pions and muons, and occasional atoms. The momentum spectrum of the atoms coming down the channel has no appreciable contribution about 5 GeV/c.

To dissociate the atoms and make their detection possible, we interpose a thin aluminium foil before the end of the vacuum channel (see Fig. 2). Ionization of an atom takes place through a series of sequential transitions through the states having highest angular momentum for any given principal quantum number. We have calculated the thickness of foil required to break up a π-μ atom to be 0.025 cm of aluminium. In the course of the experiment, data was taken with foil thickness of 0.075 cm and 0.625 cm of aliminium.

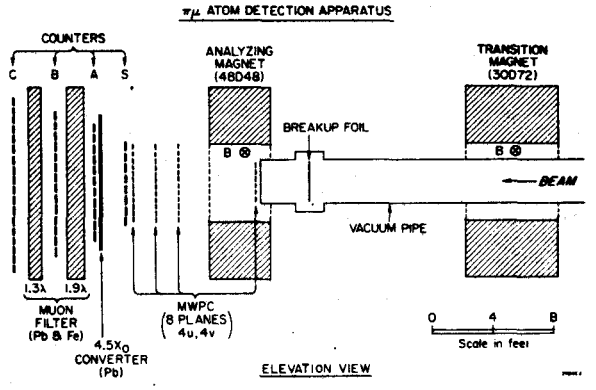


Fig. 2. Detection Apparatus.

The pion and the muon, now uncoupled, exit the foil at the same velocity (with momenta in the ratio of their rest masses) and in almost perfect spatial coincidence. The opening angle between them at a typical atomic momentum of 3 GeV/c, neglecting the multiple scattering in the foil, should be less than 0.5 milliradians. The projected multiple scattering of each particle in a 0.030'' aluminium foil is about (1.3/p (GeV)) milliradians. Thus the angle between pion and muon upon emerging from a 0.075 cm foil should be about two milliradians. The angle between them in the case of a 0.625 cm aluminium foil is about 5 miliradians.

We next introduce these two coincident particles into a horizontal field which serves to separate them vertically. We terminate the vacuum channel with a thin mylar window where the separation between the pion and muon is about a centimeter for a typical atom. Just beyond the window we place a multiwire proportional chamber made of two planes (planes 1 and 2) to allow the reconstruction of the vertical and horizontal coordinate of each of the particles. Each of these planes is constructed of a set of wires inclined at 60° to the vertical. At the point where the pion and the muon traverse these planes they are directly above one another and separated by a vertical distance Δ which is closely correlated to the sum of their momenta.

After leaving the analyzing magnet the pion and the muon continue through a series of three further pairs of proportional chambers, each constructed of wires at $\pm 60^\circ$ to the vertical. In each of these planes the x and y coordinates of each track can be localized to about $\pm$ 1 mm. Following the last of these chambers, we have, in sequence: a bank of 11 counters (S bank), a sheet of 1'' thick lead to induce showering of electrons, a bank of 15 counters (A bank), a lead and steel wall embodying 1.9 mean free paths of absorber, another bank of 19 counters (B bank), a wall comprising 1.3 free paths of absorber and a final bank of 23 counters (C bank). The absorber removes muons below a momentum of 0.9 GeV/c and about 90% of the pions. The first crude indication that an event of interest has passed through the detector comes when we obtain a trigger indicating simultaneous counts in two S counters, two non-adjacent A counters, one or more B counters and one or more C counters. We next examine planes 1 and 2 to determine rapidly whether two tracks passed directly above one another within the experimental reso-

lution and with Δ lying between .8 and 3.5 centimeters. We then remove, through the use of our on-line computer, all events in which more than four tracks passed through the first plane. The residual events are logged for further study. The information recorded includes the timing of all counters, the pulse height on each of the A counters and the positions of the tracks as they pass through the eight planes.

We carry forth the analysis of the data by subjecting each event to a sequence of tests, each of which must be passed before it can be considered a valid candidate for a π-μ atom. The geometrical characteristics of these tests have been determined through a study of the e^+-e^- pairs which are created by γ rays impinging on the foil and the muons which come down the vacuum channel when the sweeping and transition magnets are turned off. The tests are as follows:

1. All counters involved in a trigger must be time coincident within ± 2 nanoseconds after correction for flight times of the various particles.

2. The four counters which define the muon track must lie on a straight line within the limits of Coulomb scattering in the absorber. Only one track may penetrate to the C bank.

3. The pulse height on each of the counters must be less than 2.5 times that produced by a minimum ionizing particle.

4. Each of the tracks must have a momentum not less than 0.9 GeV/c.

5. After the two tracks are reconstructed back through the magnet, we can determine the x and y projections of their apparent separation and the apparent angle between them as they left the foil.

The cuts are as follows:

a) The vertical separation at the foil must be less than 1.35 cm.

b) The horizontal separation at the foil must be less than 0.50 cm.

c) The measured vertical angle between the two tracks as they leave the foil must be less than 0.025 radians.

d) The measured horizontal angle between the two tracks as they leave the foil must be less than 0.004 radians.

6. Our study of the e^+e^- pairs indicates that the vertical spacing, Δ between the two tracks in planes 1 and 2 is predictable to a wire spacing given the momenta of the two particles. We reject all candidates which do not conform to this constraint within ± 2 wire spacings.

7. By studying the e^+e^- pairs we have ascertained that we can project our tracks back to the vicinity of the collimator with a horizontal spatial resolution of ± 2.5 cm. We insist then that all of our tracks of interest point back to 22.5 cm wide fidicial region near the collimator, missing both the collimator itself and the walls of the vacuum channel.

8. Finally, we insist that the sum of the pion and muon momenta be no more than 5 GeV/c.

Having subjected all of the recorded data to these tests, we arrive at a residue of 33 events. For each of these events we plot (in Fig. 3) the parameter $\alpha = \frac{P_\pi - P_\mu}{P_\pi + P_\mu}$ where P_π is the pion momentum and P_μ is the muon momentum. A study of this parameter through an examination of e^+e^- pairs indicates that the acceptance of our apparatus, modified by the abovementioned

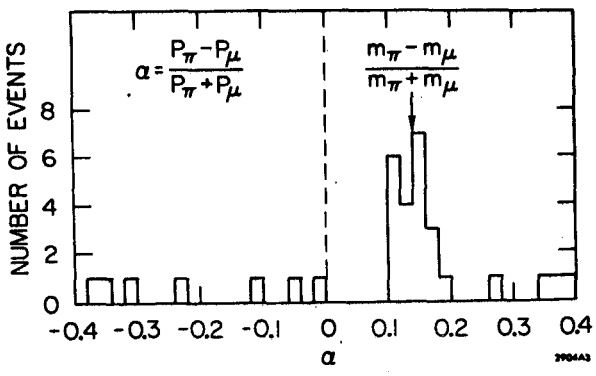


Fig. 3. A plot of the parameter α indicating the detection of $\pi\mu$ atoms.

tests, is flat within 30% from $\alpha = -0.4$) to $\alpha = +0.4$. None of our acceptance tests bias us toward one or another sign of α. Hence, any bump in this plot would indicate a strong correlation between pion and muon momenta; in particular the atoms should be characterized by a value of $\alpha = \frac{m_\pi - m_\mu}{m_\pi + m_\mu} = 0.14$ The data shows a clear peak at the predicted point containing a total of 21 events with an estimated background of 3 events. The width of the peak is consistant with that expected from measurement errors.

We conclude that we have observed Coulomb bound states of pions and muons.

We would like to express our appreciation to the Brookhaven A.G.S. staff and to L.Birkwood, J.Bjorken, S.Drell, G.Donaldson, M.Faessler, M.K.Gaillard, D.Hitlin, B.Kincaid, D.Ouimette, M.Prasad, C.Rasmussen, A.M.Rushton, J.Tannis, A.Tilgham, J.D.Walecka, S.Wojcicki and C.Zupancic for valuable assistance.

REFERENCES

1. L.L.Nemenov. Sov. Journ. of Nucl.Phys., 16, 67 (1973).

PARALLEL SESSION ON MESON SPECTROSCOPY

THE $\delta(970)$ RESONANCE AND OTHER 0^+ EFFECTS

S.O.Holmgren – CERN, Switzerland

Much experimental and theoretical effort has been devoted to the understanding of 0^+ resonances during at least 10 years. There has been a great deal of progress and it is possible today, as has been shown by Morgan[1], to fit the 0^+ candidates into an $SU(3)$ nonet:

I=1	I=1/2	I=0	I=0
$\delta^0(970)$	$\varkappa(1250)$	$\rho^*(993)$	$\varepsilon(1100\text{–}1300)$

The establishment of these states is however complicated by very drastic threshold effects and in a critical examination it is possible to cast some doubts on each one of them. This is especially true for S^+ [2], $\varkappa$ and ε for which most of the evidence comes from phase shift analysis of $\pi\pi$ and $K\pi$ scattering. The evidence for $\delta^0(970)$ comes from formation experiments and this kind of information will be the topic for this note.

The $\delta(970)$ Resonance

Two contributions to this conference present data for $\delta(970)\to\eta\pi$.

a). The Aachen-Berlin-Bonn-CERN-Cracow-Heidelberg-Warsaw Collaboration presents inclusive $\delta^{\pm}(970)$ production from bubble chamber data at 16 GeV/c[3]. The reactions studied are:
$\pi^{\pm}p\to p\pi^{\pm}\pi^+\pi^-\pi^-\pi^0$ (24902 events).
Making the selection they find a peak which gives M_δ=980±7 MeV and Γ=46±23 MeV when fitted to a simple Breit-Wigner with a handdrawn background. (Fig.1). They also observe a threshold enhancement in the $K\pi$ system when considering 5-body reactions with kaons in the final state. The absence of the δ in $\rho\pi$ final states is used as a support for $J^P=0^+$ assignment.

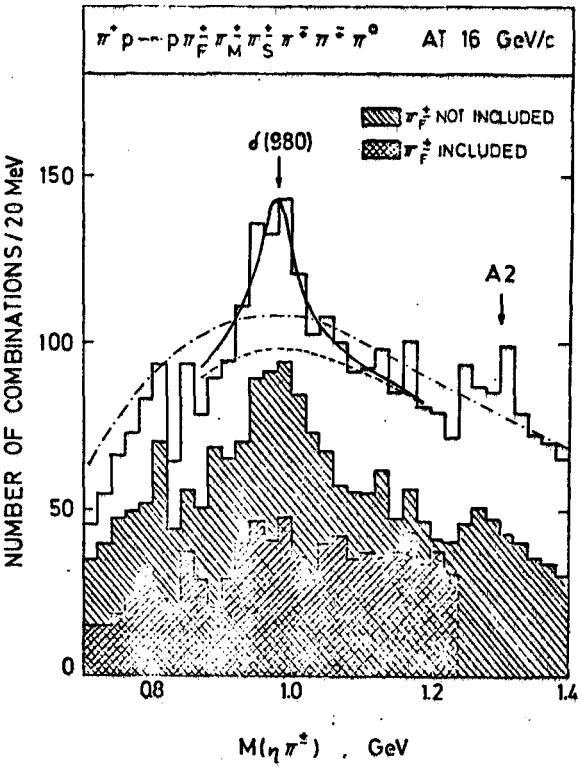


Fig.1.

b). The Amsterdam-CERN-Nijmegen-Oxford Collaboration (ACNO) studies $\delta^-(970)$ production in the reactions

$$K^-p\to\Sigma^+(1325)\,\eta\pi^- \qquad (1)$$

$$K^-p\to\Sigma^+(1325)K^0K^- \qquad (2)$$

resulting from a bubble chamber experiment with a sensitivity of 80 ev/mb[4]. When the appropriate cuts to isolate reaction (1) are applied a clear $\delta^-(970)$ peak is observed in the mass distribution (Fig.2a). For the subsequent analyses a weighting technique is used to isolate reaction (1) (Fig.2b). This approach also gives an estimate of the background. A simple Breit-Wigner fit to the mass distribution yields the parameters M=981± 6 MeV and Γ=55±5 MeV and a cross section of 6.2±1.3 mb. A coupled channel fit allowing for $\delta\to K\bar{K}$ was also attempted with the relative coupling ratio $g^2_{\eta\pi}/g^2_{K\bar{K}}$ fixed to the $SU(3)$ value 2/3. The result of this fit is M=974±9 MeV and Γ=72±51 MeV (Fig.2b and 2d). These values are not very far from the values obtained using a simple Breit-Wigner except for the error in Γ which becomes considerably larger. The properties of the decay angular distributions lend good support for the $J^P=0^+$ assignment.

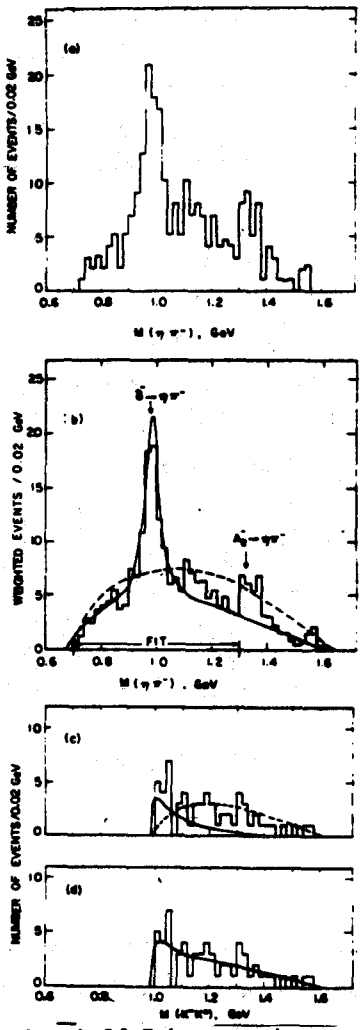


Fig.2.

$K^0_S K^0_S$ Threshold Enhancement

In a contributed paper[5] the ACHO Collaboration presents the Dalitz plots for the reactions

$$K^- p \to \Lambda K^0_S K^0_S \qquad (3)$$

$$K^- p \to \Sigma^0 K^0_S K^0_S \qquad (4)$$

In the reaction (3) a clear threshold enhancement is observed in the $K^0_S K^0_S$ mass distribution (Fig.3a). In contrast the corresponding distribution for the Σ^0 reaction shows no effect (Fig.3b). In the study of vector meson production together with Σ^0 and Λ it is found that Σ^0 couples almost entirely to natural parity exchange while Λ has a sizable coupling to both natural and unnatural exchange. This ties very well together with the above observation and indicates that the threshold enhancement is really due to the process $K\bar{K} \to K\bar{K}$.

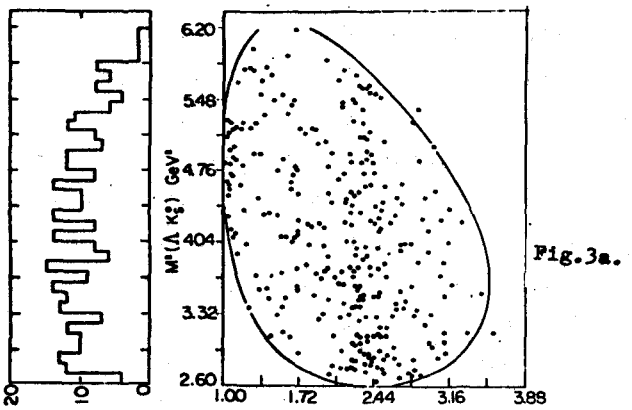
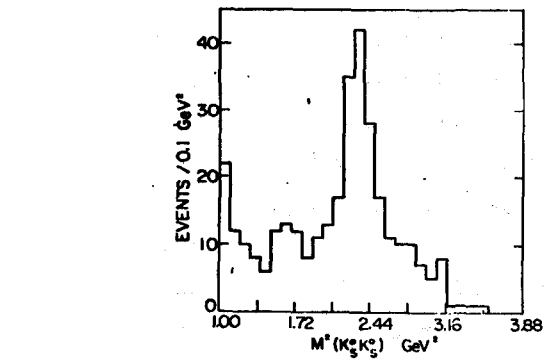
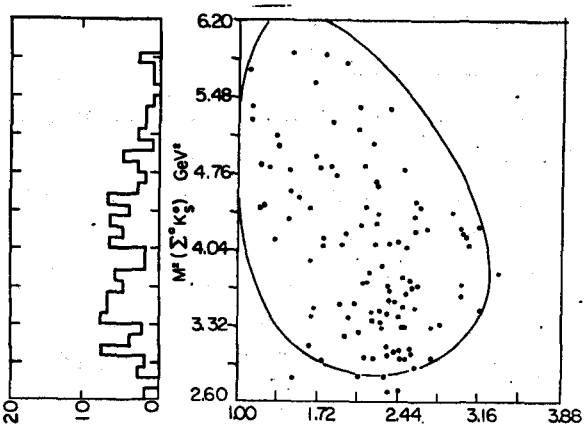


Fig.3a.





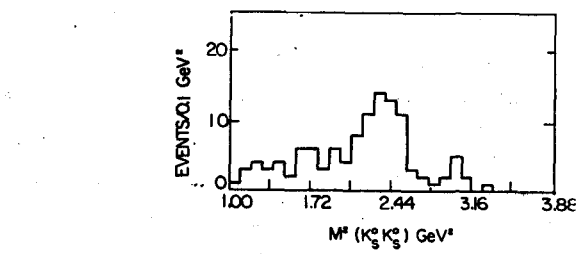


Fig.3b.

Brandenburg et al.[6] presents data from a spectrometer experiment on 13 GeV $K^- p$. They study the reaction

$$K^- p \to \pi^+ \pi^- (\Lambda, \Sigma)$$

and when they subtract the effect of ρ-ω they find an enhancement in the S^* mass region which within the quite large errors is in agreement with the predictions from various phase shift analyses of $\pi\pi$ scattering (Fig.4).

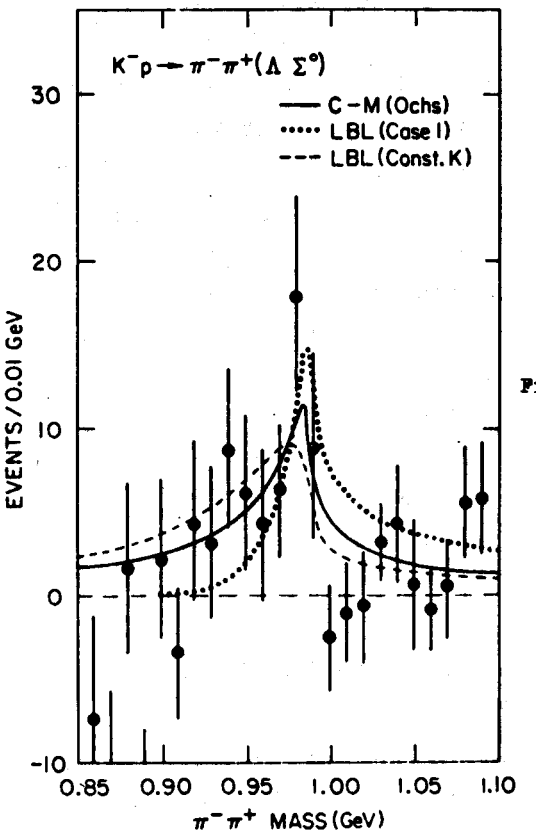


Fig.4.

An Alternative to Narrow Resonance Interpretation

In two contributions to the conference[7] Flatte presents a further investigation of $\delta(970)$ and $S^*(990)$ in terms of a coupled channel formalism. The formalism used is equivalent to the one used in the previously discussed ACNO-paper. In this analysis however the coupling ratios $g_{\pi\eta}/g_{K\bar{K}}$ and g_K/g_π for the δ and S^* respectively are treated as free parameters. In the χ^2-fits to the ACNO-data for the parameters at the minimum is found to be close to those given in the experimental report. The minimum is however found to be quite shallow and a fair discription of the data is found even with a large value for $\Gamma_{\eta\pi}$. The narrow mass distribution is then described by a cusp effect due to a large $K\bar{K}$ coupling. The situation is similar in the case of S^*. The author concludes from this that the 0^+ mesons may all be wide objects or in the extreme alternative that they may be so wide that one may doubt their interpretation as simple $SU(3)$ resonances.

New 0^+ States

Cason et al.[8] presents evidence for a new 0^+ resonance found in the process

$$\pi^- p \to n K_S^0 K_S^0$$

obtained in a streamer chamber experiment at 6-7 GeV/c. By an amplitude analysis in terms of S and D waves a peak in the S-wave is found at 1255±5 MeV and a width of 79±10 MeV (Fig.5).

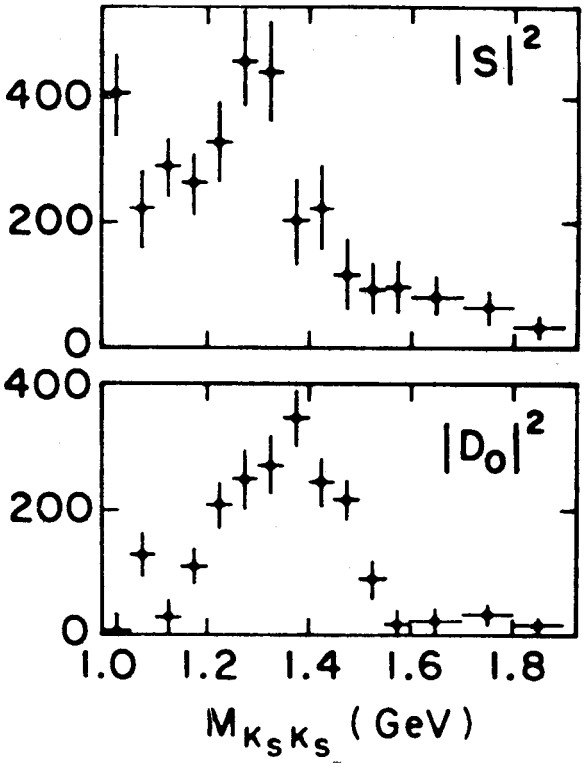


Fig.5.

By interpreting the D-wave as due to f-f' interference they find a solution with rapid S-wave phase variation in the resonance region. The preferred isospin assignment is $I^G = 1^-$ but another experiment (see review by A.B.Wicklund) observes a similar bump in $I=0$ but not in $I=1$.

Conclusions

New experimental information supports the

existence of a "narrow" $\delta(970)$ compatible with the $SU(3)$ predicted coupling to $K\bar{K}$. However the possibility that the small width may be caused by a wide object with strong $K\bar{K}$ coupling has been pointed out. A possible new 0^+ resonance has been reported. The confirmation and settlement of its isospin assignment is urgent.

References

1. D.Morgan. Phys.Letters 51B (1974) 71.
2. M.Cerrada et al., Madrid preprint J.E.N. 76/1.
3. CERN/EP/DRON, contributed paper 1041.
4. CERN/EP/ Phys/ 76-7, contributed paper 297.
5. CERN/EP/ Phys.76-26, contributed paper 298.
6. SLAC-PUB-1974, contributed paper 720.
7. CERN/EP/Phys. 76-8 and CERN/EP/Phys. 76-9, contributed papers 1132-1133.
8. Phys.Rev.Letters 36, 1485 (1976), contributed paper 1025.

$\eta'(958)$ SPIN-PARITY PROBLEM

V.I.Ogievetsky – JINR, Dubna

"Particle Data Group" (1976) states[1] "From the Dalitz plot analysis of $\eta' \to \eta\pi\pi$ and $\eta' \to \pi\pi\gamma$ and from the observation of $\eta' \to \gamma\gamma$ all assignments except $J^{PC}=0^{-+}$ and 2^{-+} are excluded. The Dalitz plot analysis favours spin zero but cannot rule out spin 2. Indication of anisotropy in the decay of very forward produced η' (Kalbfleisch 73) are not being confirmed by Baltay 74 thus favouring strongly spin 0".

This talk comments these statements and the present status of the η' spin-parity problem. The main comments are:

1. The Dalitz plot analysis does not distinguish between 0^- and 2^-. The statement "favours" is a matter of taste.

2. In fact the Batlay's data are in agreement with the 2^- hypothesis.

So all the data cited above are consistent with the 2^- assignment.

However the data of Amsterdam-CERN-Nijmegen-Oxford Collaboration (ACNO)[3] submitted to this Conference are the first data which really do not confirm the BNL-Michigan[4] ones.

The 0^- assignment is more natural and accepted widely. The 2^- assignment is more interesting and tempting.

The η' (or X)-meson has several mysterious properties, it is extreme narrow ($\Gamma < 1$ MeV), it has unnaturally large ratio of electromagnetic, to strong decays, $\frac{\pi^+\pi^-)}{\pi^+\pi^-\eta} = 0.87 \pm 0.06$, etc. Among these properties one can also mention that every time when it was stated that some analyses contradicted to the 2^- assignment the reanalyses revealed an agreement with this assignment. Note also that JP were 2^- the corresponding Regge trajectory would have the intercept 1 leading to the spin-spin amplitudes in the p-p elastic scattering which would survive at high energies[5]

When η' was discovered in 1964[6] it was claimed to be 0^-, the ninth pseudoscalar meson. Since 1967 it became clear that the 2^- assignment is also in agreement with the Dalitz plot[7] and the necessity of new measurements of its spin-parity was stressed. For the 2^- case the best fit of the world data on $\eta\pi\pi$ decay is given by some mixture of $(\ell_{\eta\pi}=0, \ell_\eta=2)$, $(\ell_{\pi\pi}=2, \ell_\eta=0)$ and $(\ell_{\eta\pi}=\ell_\eta=2)$ amplitudes, the last being very important.

The only way to establish the η' spin is to study production-decay correlations. However for 2^- these correlations can be masked in wide region of the production angles. So the Adair analysis is of great importance for η' (or X) produced in the extreme forward direction[8]. If the spin-parity of this meson were 2^- then in the forward direction it could not have the spin-projections ± 2 (because $\ell_z=0$) and therefore the anisotropies of predicted form must appear due to the spin-assignment (the spin-density matrix element $\rho_{22}=0$). For a long time no deviations from isotropy were observed at momenta 2-5 GeV/c in the distributions over angles between the incident momentum and any decay analysers. A considerable statistics became available in 72 of $K^-p\to\Lambda\eta'$ events at 2.18 GeV/c [9]. The authors[9] stated "no t-outs or out on Λ-direction was found to produce a plot with any anisotropy". Nevertheless after reanalysis of the same data with an appropriate t-cut some anisotropies were observed[4]. The correlations were pronounced for very small C.M. angles $\theta^*>0.2$ were absent for $\theta^*\lesssim 0.2$. The results for the polar-equatorial ratios P/E are

	$\eta'\to\pi^+\pi^-\eta$		$\eta'\to\pi^+\pi^-\gamma$
	$\frac{P}{E}(\vec{n}\vec{K})$	$\frac{P}{E}(\vec{\eta}\vec{K})$	$\frac{P}{E}(\vec{\gamma}\vec{K})$
$0.98\le\cos\theta^*\le 1$	0.54 ± 0.14	1.44 ± 0.36	0.35 ± 0.31
$0.94\le\cos\theta^*\le 1$	0.97 ± 0.16	0.97 ± 0.16	1.00 ± 0.34

where $(\vec{n}\vec{K})$, $(\vec{\eta}\vec{K})$ and $(\vec{\gamma}\vec{K})$ are the cosines angles of the incident beam momentum $\vec{K}$ relative to the normal of the $\pi^+\pi^-\eta$ decay plane $\vec{n}$ and to the momenta of η and γ in the η' rest frame correspondingly; P and E are the numbers of events cosines $>\frac{1}{2}$ and $<\frac{1}{2}$, respectively.

All the three one dimensional correlations observed agree with the 2^- predictions (see Fig.1).

Stress once more the importance of the cut. A natural Adair estimate is $\theta^*<\frac{1}{p r_0}$ or the transversal CM momentum $p_\perp=p\theta^*$, where p is the outgoing momentum in the CM frame. Correlations are only at $p_\perp\le 100$ MeV/c (but the statistics is poor, only 66 events remain). One can confirm or do not confirm these correlations only using the same (or more severe) cut in $p_\perp$. For example, for $K^-p\to\Lambda\eta'$ one must use $\cos\theta^*\gtrsim 0.92$ at $p_K=1.75$ GeV/c, $\cos\theta^*>0.996$ at $p_K=4.2$ GeV/c, etc. Baltay et al.[2] at 1.75 GeV/c used $\cos\theta^*\gtrsim 0.6$ (instead of 0.92) and observed some small deviations from isotropy which did not confirm the above correlations. It is quite natural because for these events $p_\perp\sim 200$ MeV/c and the nonzero ρ_{22} can be expected. It is remarkable that all the Baltay's data agree with the $\bar{\rho}_{22}=0.3$ (see Fig.1). Note moreover that in the range $0.5\le\cos\theta^*\le 0.8$ in this case one might expect an increase of deviations from isotropy due to the increase of $\bar{\rho}_{22}$.

So all the existing data are consistent with the 2^- assignment. Note also that there are some resources to explicit the existing experimental data more thoroughly. Only 3 out of 6 natural analysers were used. There exists also the best analyser[10]. The multidimensional analysis[11,12] is much more informative than the one-dimensional one.

Now to this Conference are submitted the new data of ACNO[3] on the $K^-p\to\Lambda\eta'$ at 4.2 GeV/c. Their statistics is 690 $\eta'\to\eta\pi\pi$ events. They state that the overall fit in different t-intervals is much better for 0^- than for 2^- and if one allows the both the ratio $\ell(2^-)/\ell(0^-)$ becomes smaller. We emphasize however that in this fit they have used the decay distribution without the admixture of the $\ell_{\pi\pi}=\ell_\eta=2$ part which turns out to be very

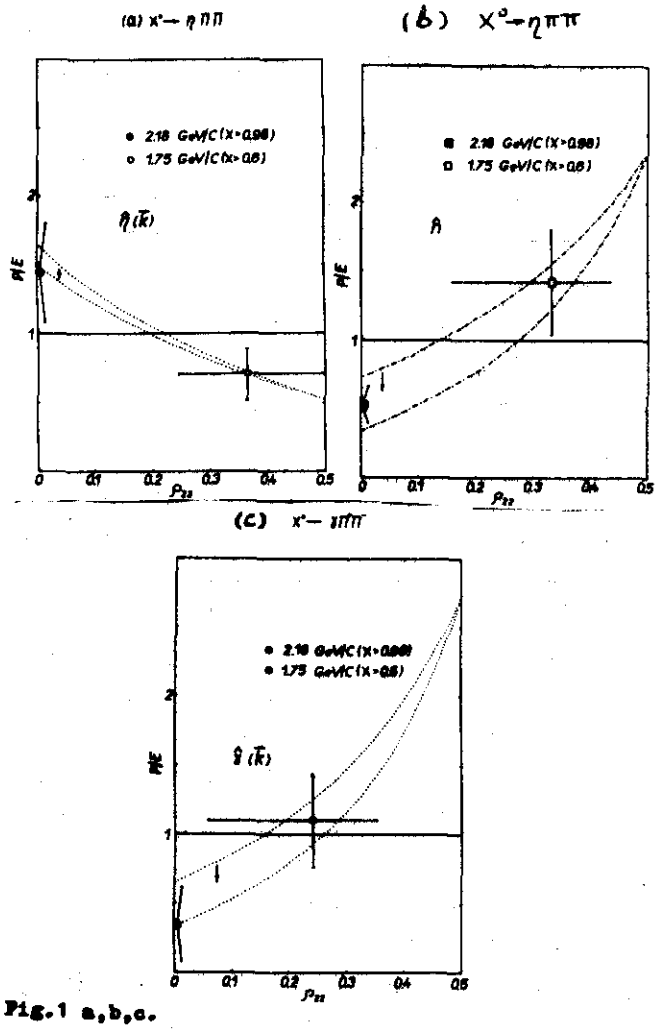


Fig.1 a,b,c.
Polar-equatorial ratios for different analysers ((a,b) in $\eta\pi^+\pi^-$ decays, (c) in $\pi^+\pi^-\gamma$ decay versus the spin-density matrix element ρ_{22}. The bounds correspond to the extreme ρ_{00} values 0 and $1-2\rho_{22}$. For the 2.18 GeV/c data the value $\rho_{22}=0$ is adopted.

essential in the world decay data analysis[11] increasing considerably the confidence level for 2^-. So the reanalysis have to be performed. It is more interesting that they have 56 events with $\cos\theta^* \geq 0.995$ or $P_\perp \leq 110$ MeV/c (Brookhaven-Michigan had[6] 66 events with $P_\perp \leq 100$ MeV/c). ACNO do not observe any anisotropy. Their results in comparison with the BNL-Michigan ones are

	P/E (ACNO)	P/E (BNL-Michigan)
π^-	28/28	23/43
η^-	30/26	39/27
$\varphi(\pi\hat{\pi})$	26/30	-

The overall fit of this extreme forward sample is not given. An analysis of the world data seems to be desirable. The only way to increase the confidence level against or in favour of 2^- is to perform the overall multidimensional (instead of one-dimensional) analysis of production and decay amplitudes[11,12] of very forward events with the cut $P_\perp \leq 100$ MeV/c (or a more severe one). For the estimation of the efficiency of the multi-dimensional analysis Lednicki[11] had generated the collinear $\eta\pi\pi$ events by Monte-Carlo using the experimental decay parameters. For 66 $\eta\pi\pi$ events (an imitation of the 2.18 GeV/c data) he obtained $\log P(0^-/2^-) \leq -3.1 \pm 1.0$ (integrating over the Λ -decay) provided $J^P = 2^-$. So in this case one can expect the likelihood ratio $P(0^-/2^-) \simeq 10^{-3}$. Note that $\log P(0^-/2^-)$ and its dispersion are additive quantities and one can collect information from different experiments. Compare that the one-dimensional analysis of $P/E(\pi\vec{K})$ gives in this case $\log P(0^-/2^-) = -1.8 \pm 0.9$. The multidimensional analysis of 58 events at 1.75 GeV/c might yield $P(0^-/2^-) \leq 10^{-1}$ provided $\rho_{22}=0.3$ and so on. So there is a hope that the multidimensional analysis of very forward events can help to determine the η' spin. Zaslavsky et al[13] pointed out that the photoproduction of $\eta'(X^0)$ and other resonances on the spinless nucleus He^4 may be useful for establishing their spin-particles. It is interesting to study the Adair distributions with the aid of electronics to obtain considerably larger statistics. Lednicki and Shafranov[14] discussed an experiment of this kind, $\pi^- p \to n\eta'$ with $\eta' \to \gamma\gamma$ where no uncertainties with the decay distributions occur.

In conclusion we stress once more that the η'-spin problem remains unsolved.

References

1. T.G.Trippe, A.Barbaro-Galtieri, A.L.Kelley et al. Rev.Mod.Phys., 48, N 2, 51 (1976).
2. C.Baltay et al. Phys.Rev., D9, 2999 (1974).
3. A Measurement of the η' Spin-Parity. Amsterdam-CERN-Nijmegen-Oxford Coll., this Conf.

4. G.R.Kalbfleisch et al. Phys.Rev.Lett.,31,33 (1975); Y.S.Danburg et al. Phys.Rev.,D8,3744 (1973).
5. A.Bujak et al. YaF, 13, 894 (1973).
6. G.R.Kalbfleisch et al. Phys.Rev.Lett.,12, 527 (1964); 13, 349 (1964); M.Goldberg et al.Phys.Rev.Lett.,12,546(1964); 13,249(1964).
7. A.N.Zaslavsky et al.Letters to JETP 6, 604 (1967); YaF 9, 852(1969); Phys.Lett., 35B, 69(1971).
8. S.Giler et al. Acta Phys.Pol.A37,475(1970). V.Ogievetsky et al.Phys.Lett.,35B,69(1971).
9. Y.S.Danburg et al. In Experimental Meson Spectroscopy-72, p.91, New York,1972.
10. R.Lednicki. Preprint JINR E2-7801 (1974).
11. R.Lednicki. Preprint JINR E2-8652 (1975).
12. Doncel. Preprint UAB FT-9, Barcelona,1975.
13. A.N.Zaslavsky et al. YaF 23, 1085 (1976).
14. R.Lednicki and M.D.Shafranov, YaF 22, 837(1975).

RECENT RESULTS ON THE $\bar{K}K$ SYSTEM AND ON $\rho-\omega$ INTERFERENCE

A.B.Wicklund - (ANL), USA

The $\bar{K}K$ System

The $\bar{K}K$ decay mode selects meson states of natural spin-parity having $I=0$ or 1 and $G=\pm1$. A high statistical study of $K\bar{K}^+$ production at 6 GeV/c has been carried out with the Argonne Effective Mass Spectrometer (E.M.S.) in the reactions[1]

$$\pi^-p\to K^-K^+n \qquad \text{(110,000 events)} \quad (1)$$

$$\pi^+n\to K^-K^+p \qquad \text{(50,000 events)} \quad (2)$$

These reactions are related to $K\bar{K}^0$ final states by charge symmetry; the $\bar{K}K$ channels can be decomposed into states of definite isospin as follows:

$$\sigma(\pi^-p\to K^-K^+n)=\sigma(\pi^+n\to\bar{K}^0K^0p)=|I=0+I=1|^2 \quad (3)$$

$$\sigma(\pi^+n\to K^-K^+p)=\sigma(\pi^-p\to\bar{K}^0K^0n)=|I=0-I=1|^2 \quad (4)$$

The reaction $\pi^-p\to K_SK_Sn$ at 6 and 7 GeV/c has been analyzed by the Notre Dame group[2]; K_SK_S is the same as $\bar{K}^0K^0$ except that odd partial waves are excluded in K_SK_S. Both the E.M.S. and Notre Dame experiments indicate a large $\bar{K}K$ S-wave cross section with a possible resonant enhancement under the $f(1270)$. The E.M.S. experiment having both isospin combinations, attempts to disentangle the $J^{PC}=2^{++}$ $\bar{K}K$ production amplitudes.

With the E.M.S. data on reactions (1) and (2), the dominant 2^{++} contributions can be isolated by projecting out the angular distribution moments corresponding to $J\geq2$, schematically:

$$\langle Y_4^0\rangle[\sigma(\pi^-p)+\sigma(\pi^+n)]=|f+f'|^2+|A_2^0|^2 \quad (5)$$

$$\langle Y_4^0\rangle[\sigma(\pi^-p)-\sigma(\pi^+n)]=2\,\mathrm{Re}\,A_2^{0*}(f+f') \quad (6)$$

For $-t<0.4$ GeV^2 the Y_4^1 and Y_4^2 moments are small and O.P.E. produced $f(1270)$ dominates the cross sections; A_2^0 and $f'(1514)$ are detectable mainly as interference effects. Fig.1 shows the projections in different t intervals for reactions

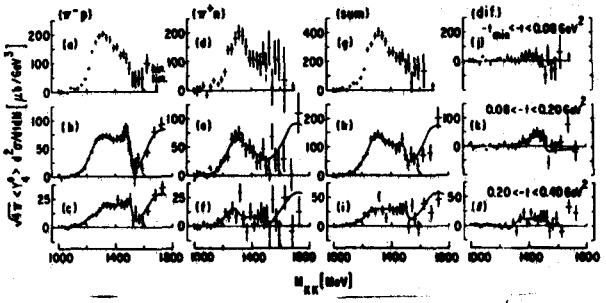


Fig.1. $\delta\langle Y_4^0\rangle$ projections for three t intervals, for $\pi^-p\to K^-K^+n$ (a-c), $\pi^+n\to K^-K^+p$ (d-f), ($\pi^-p+\pi^+n$) summed (g-i) and ($\pi^-p-\pi^+n$) difference (i-e).

1 and 2 as well as the sums and differences defined in Eqs. 5 and 6. The following conclusions follow from fits to the data of Fig.1:

1. $f'(1514)$ can be seen by its interference with f and A_2^0 productions (Fig.1b,1c). Assuming the f-f' interference term is dominated by exchange, both the sign and magnitude of the $f'\to\pi\pi$ coupling can be deduced. The sign corresponds to a nonet mixing angle less than the ideal value 35.3°; the magnitude corresponds to a branching ratio $f'\to\pi\pi/f'\to$ all $= 0.017\pm 0.005$.

2. f'-A_2^0 is generally larger than f-A_2^0 interference, implying that unlike the f, the f' and A_2^0 production amplitudes are not dominated by π or B exchange.

S-WAVE CROSS SECTION

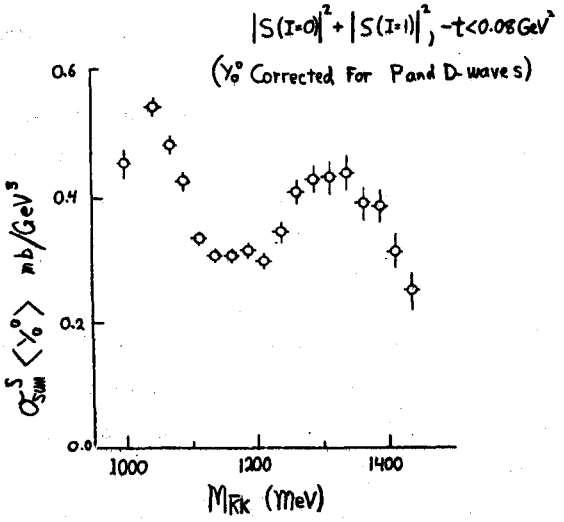


Fig.2. Corrected S-wave cross section for $-t<0.08$ GeV^2 from the $\delta\langle Y_0^0\rangle$ sum over ($\pi^-p+\pi^+n$) initial states.

3. The following branching ratios can be deduced $f\to\bar{K}K/f\to$ all $=0.038\pm0.007$, and $g(1700)\to\bar{K}K/g(1700)\to\omega\ell\ell=0.029\pm0.010$. Having determined the D-wave production properties, the $J=1$ and 2 waves (f, A_2^0, f' and the $I=1$ P-wave) can be explicity substracted to obtained the S-wave cross section of Fig.2. Besides the $S^*(980)$ threshold enhancement, a second peak occurs around 1300 MeV, suggesting a possible S-wave resonance. The Notre Dame analysis of K_SK_S indicates a similar enhancement. Fixing the D-wave phases as obtained from the E.M.S. data, they determine the magnitude and phase of the S-wave from an amplitude analysis of the Y_0, Y_2 and Y_4 moments. The Y_2^0 and Y_4^0 moments are shown in Figs,3a and 3b. Y_2^0 has a

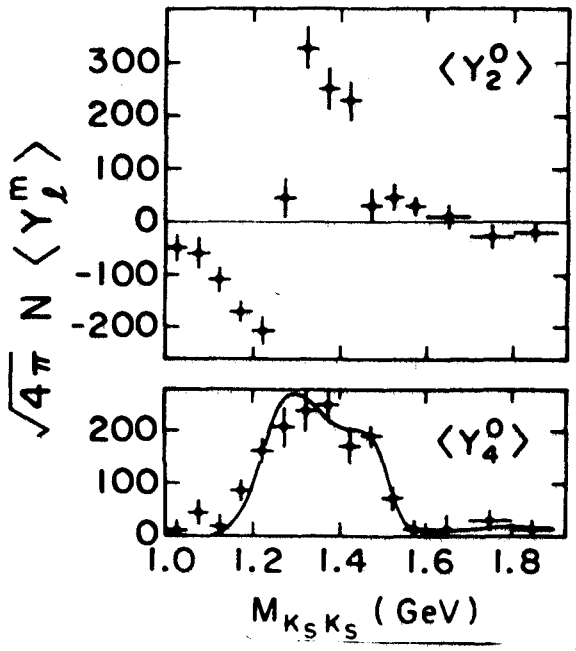


Fig.3. $\delta\langle Y_2^0\rangle$ and $\delta\langle Y_4^0\rangle$ for $\pi^-p\to K_SK_Sn$ at 6.7 GeV/c.

cross-over zero around 1255 MeV, indicating an S-D relative phase $\sim 90°$ near the f resonance; the S-wave must be approximately real in this region. The variation of the S-wave phase with mass is determined by Y_2^0; the two possible S-wave phase solutions (Fig,4b) derived using the D-wave phase of Fig.4a include a Breit-

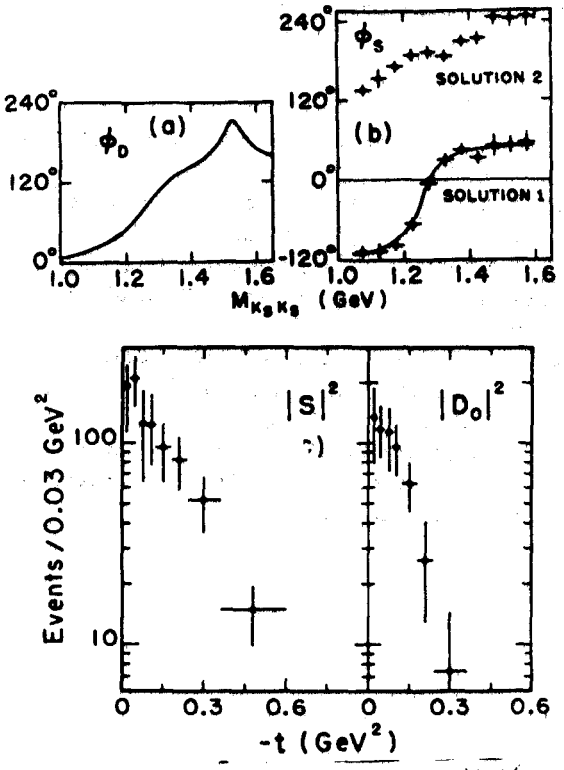


Fig.4. (a) D wave phase for $\pi^- p \to K_S K_S n$; (b) S-wave $K_S K_S$ phase solutions; (c) t distributions for S and D wave intensities.

Wigner solution (1) and a slowly varying solution (2). The S and D wave intensities are shown in Fig.5; the S-wave peak under the f is similar to that in Fig.2. The isospin of

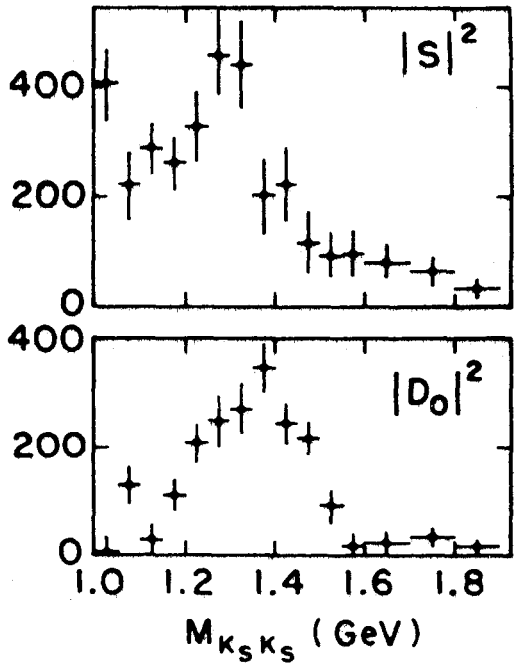


Fig.5. S and D wave intensities versus $K_S K_S$ mass.

S(1300) is ambiguous. The Notre Dame analysis shows that $|S|^2$ is much less peripheral in t than $|D|^2$ (Fig.4c). Furthermore, if S(1300) is truly resonant, its production phase must be 90° in order to explain the fact that the production + decay phase must be nearly real around f(1270). These two observations make β exchange an attractive production mechanism, in which case only $I = 1$ $\bar{K}K$ S waves are allowed.

However, the nature of the S-D interference manifested by the large Y_2^0 moment of Fig.3a can be elucidated with the E.M.S. data. Fig.6a shows the interference of $I = 0$ S wave with f(1270) from the $(\pi^- p + \pi^+ n)$ sum, while Fig.6b shows the

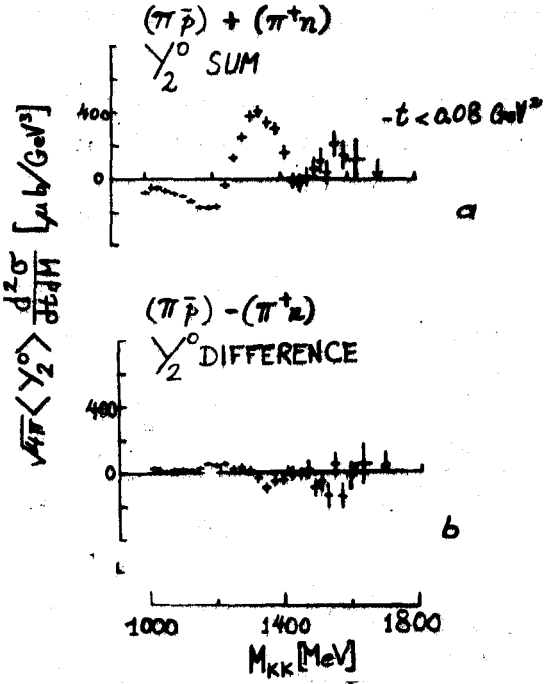


Fig.6. $\sqrt{4\pi}\langle Y_2^0\rangle$ for $-t < 0.08$ GeV^2, (a) for sum of $\pi^- p \to K^- K^+ n$ and $\pi^+ n \to K^- K^+ p$; (b) for difference of $(\pi^- p - \pi^+ n)$ initial states.

$I = 1$ S-wave contribution from the $(\pi^- p - \pi^+ n)$ difference. It is clear that most of the $\bar{K}K$ Y_2^0 interference moment arises from $I = 0$ S wave, which must account for the bulk of the S-wave intensity peak around f(1270).

Note that the nonresonant phase variation of solution 2 is not ruled out. However, the peaking in S-wave intensity under the f still remains to be explained.

ρ-ω Interference

ρ-ω interference measurements provide tests of SU(3) and quark-model predictions involving relative ρ and ω production phases. The non-strange exchange reactions $\pi^- p \to \rho(\omega)n$ and $K^{\pm}N \to K^{*0}N$ have been analyzed using E.M.S. data from 3 to 6 GeV/c[3]. The relations between $K^{*0} - \bar{K}^{*0}$ cross section differences and ρ-ω interference phases satisfy SU(3) rather well, and the systematics of higher energy data can be understood.

For K^*K^{**} exchange processes, ρ-ω interference measurements have been reported by the A.C.N.O. group[4] (4.2 GeV/c) and the SLAC group (13 GeV/c)[5]. Fig.7 shows the $\pi\pi$ mass spectrum at 13 GeV/c for the reaction $K^- p \to \pi^-\pi^+\Lambda(\Sigma^0)$ together with allowed quark diagrams. The quark model predicts the production amplitude relations

$$A_\omega = A_\rho = A_\phi/\sqrt{2} \qquad (7)$$

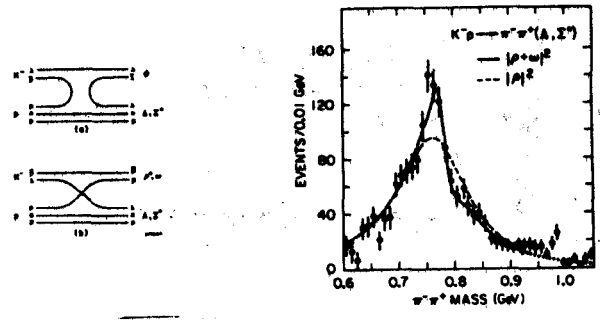


Fig.7. $\pi\pi$ Mass spectrum for $K^- p \to \pi^+\pi^-(\Lambda,\Sigma^0)$ at 13 GeV/c.

The ρ-ω interference phase is consistent with Eq.7; $Arg(A_\omega/A_\rho) = -4 \pm 11^0$. With the P.D.G. $\omega \to \pi\pi$ branching ratio of 0.013, $|A_\omega|/|A_\rho| = 1.5 \pm 0.4$. The relation between ρ and φ production in the dominant natural-parity exchange state is satisfied within statistical errors of $\sim 5\%$.

In summary, high statistics resonance production data have revealed new phenomena such as $f' \to \pi\pi$, f-f' and f-A_2^0 interference, and a possible new S wave $K\bar{K}$ state; previously observed phenomena such as ρ-ω interference have been better measured, allowing detailed tests of symmetry predictions for production amplitudes.

References

1. A.J.Pawlicki et al. f, f' and A_2^0 Interference in $\pi N \to K^-K^+N$ at 6 GeV/c, paper 173.
2. N.M.Cason et al. Production of Tensor Mesons in the $K\bar{K}$ System, paper 1025.
3. A.B.Wicklund et al. Systematic Study of Charge Exchange Vector Meson Production, paper 63.
4. Amsterdam-CERN-Nijmegen-Oxford Collaboration, ρ-ω Interference in Reactions $K^-p \to \pi^-\pi^+(\Lambda,\Sigma)$ at 4.2 GeV/c, paper 301.
5. G.B.Brandenburg et al. Analysis of $K\bar{K}^+$ and $\pi^-\pi^+$ Final States in 13 GeV/c K^-p Interactions, paper 720.

THE A_1 MESON PROBLEM

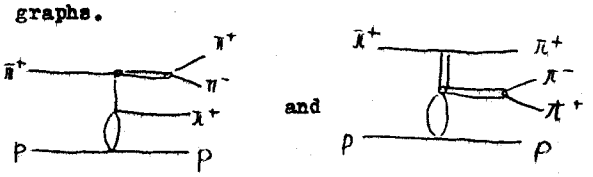
A.Markytan

(Institut fur Hochenergiephysik der Osterreichischen Akademie der Wissenschaften, Vienna)

The A_1 is currently seen as a threshold enhancement of the $(\rho^0\pi^\pm)$system in the reactions

$$\pi^\pm p \to \rho^0 \pi^\pm p \qquad (1)$$

The production cross section of this signal is almost energy independent and proportional to $p_{LAB}^{-0.2}$. The production mechanism and the nature of A_1 can be described by the Deck model. Kamalov and Ponomarev[1] described data of reaction (1) at 13.1 GeV /c, obtained in an experiment by Gaidos et al.[2], with the following Deck model graphs.



and obtained good agreement with $M_{\pi^+\rho^0}$, $t_{\pi^+\pi^+}$, $t_{\pi^+\rho^0}$, $\Delta t = |t_{\pi^+\pi^+}| - |t_{\pi^+\rho^0}|$, φ (Treiman-Yang), Ψ (Toller) and $\cos\theta_{GJ}$ distributions of A_1 production.

Ascoli, Wyld, Weinstein and Coll have already compared the results of their partial wave analysis (PWA) of Serpukhov data generated with the weight of the complete Deck amplitude squared. Otter[4] has performed a PWA of a large collection of data of reaction (1), and the mutually confirmed results are:

a) The $M(3\pi)$ distributions of the spin-parity amplitudes and of the phases between different spin-parity states as obtained from the experimental data are in good agreement with those obtained from the Deck model (except for the states);

b) No rapidly varying phases of the dominant $1^+S(\rho\pi)$ state with respect to the $2^-P(\rho\pi)$, $1^+P(\varepsilon\pi)$ and $0^-S(\varepsilon\pi)$ states. Therefore evidence accumulates that the phase variation is flat in the A_1 region, and that the A_1 ought not to be considered as a resonance. The question arises whether the Weinberg sum rules bading to the well satisfied relation $M(A_1)=\sqrt{2}\,M(\rho)$ require by necessity the A_1 being a resonance.

In order to establish experimentally the existence of a narrow width ($\sim$ 80 MeV) resonance A_1, other reaction mechanisms than diffractive production on the basis of the Deck model have to be considered.

I. Charge Exchange

Edwards et al.[5] performed an experiment on the search for A_1^0 and H^0 in the reaction

$$\pi^- p \to n\pi^+\pi^-\pi^0 \qquad (2)$$

at 8.4 GeV/c. The apparatus of this experiment consisted of spark chambers, a magnet, a spectrometer, shower spark chambers and lead glass. The $\pi^0\to\gamma\gamma$ decay is detected. The $M(\pi^+\pi^-\pi^0)$ distribution is shown in fig.1. The ω gives the mass resolution of this experiment. In the A_1 region appears a shoulder

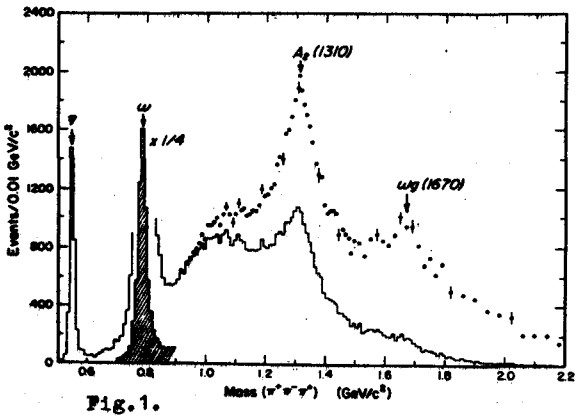
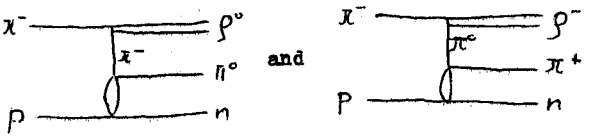


Fig.1.

in the distribution which has been obtained after correction for acceptance. It only becomes more pronounced when the $(\pi^-\pi^0)$system is required to be ρ^- (Fig.2), and can be attributed to the following graphs:



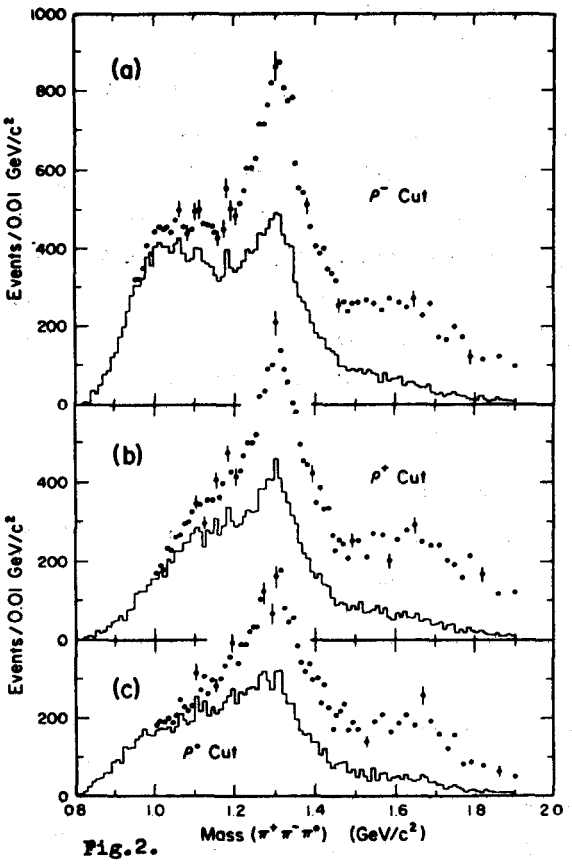


Fig.2.

The conclusion, based on 45% of the data, is that-no narrow structure shows up in the A_1 mass region so that it would infer the A_1 to be a resonance.

II. Annihilation-type Mechanisms

1) Backward Production of A_1.

Chapman et al./6/ obtained data of reaction (1) at 4 GeV/c in a streamer chamber experiment with spark chambers and a Cerenkov detector in the foward direction for triggering on the proton. Their analysis is based on 50% of their data. On account of a theoretical estimation by Kane (see ref.6) of the (A_1NN) and $(A_1N\Delta)$ coupling constants to 8/12 and 16/25 times the (ωNN) and $(\rho N\Delta)$ coupling constants respectively, one expects an A_1 signal in the backward direction whose production cross section is of the same order of magnitude as for vector meson backward production. Fig.3 shows no signal of a narrow width A_1 or A_2 in reaction (1), and only a statistically insignificant indication of in the reaction $\pi^-p \to p\pi^+\pi^-\pi^-\pi^0$. The upper

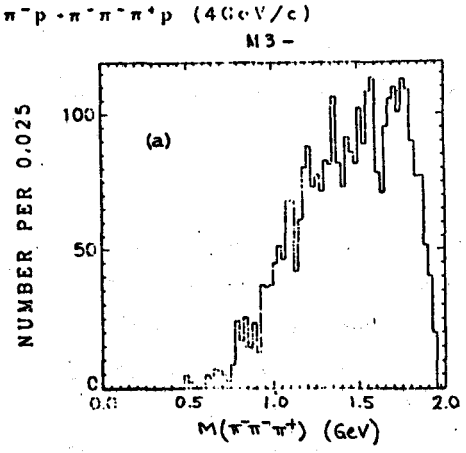


Fig.3a.

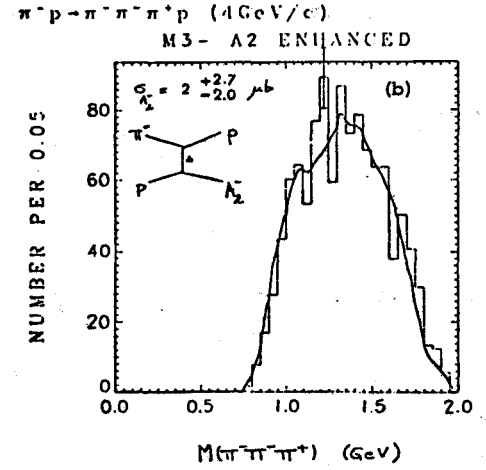


Fig.3b.

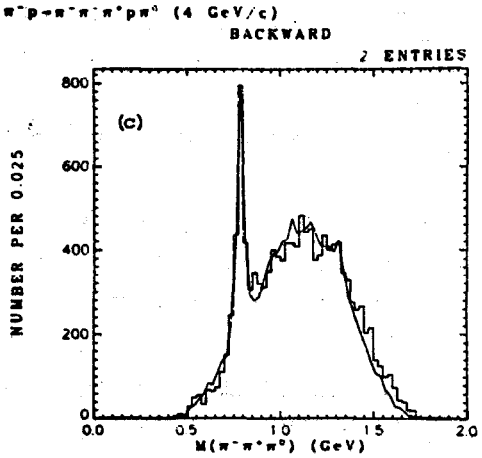


Fig.3c.

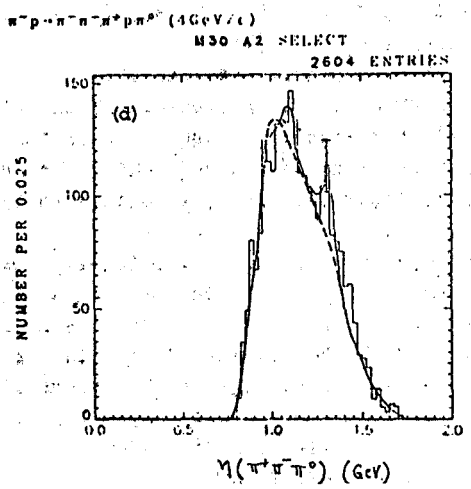


Fig.3d.

limits of cross sections in reaction (1) are:

$\sigma_{A_1^-} < 4\,\mu b$, $\sigma_{A_2^-} < 7.4\,\mu b$

A compilation of data for backward production of A_1 and A_2 (from ref./6/) is shown in fig.4.

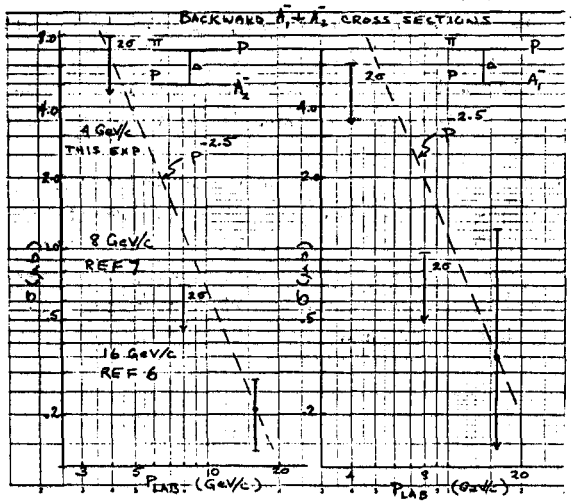


Fig.4.

2). $\bar{p}p$ Annihilation

The reaction $\bar{p}p \to 2\pi^+ 2\pi^-$ has been analysed at 2.5, 4.6 and 9.2 GeV/c, and the mass distributions of the three pion system recoiling to the most longitudinal pion are given in ref./7/.

No A_1 signal is apparent .

3). $\bar{B}p$ and $K^-(K^+, K^{*+}_{890}, K^{*++}_{1400})$ Off-Shell Annihilation.

In the reaction $K^-p \to \Lambda$ +anything , a great part of the particle system recoiling to the Λ consists only of pions and is produced by either baryon number or strangeness annihilation. Fig.5 shows the $M(X)$ distribution of this reaction at 4.2 GeV/c/8/, in which are appearent as narrow signals the η, ω, ϕ and A_2, but not the A_1 .

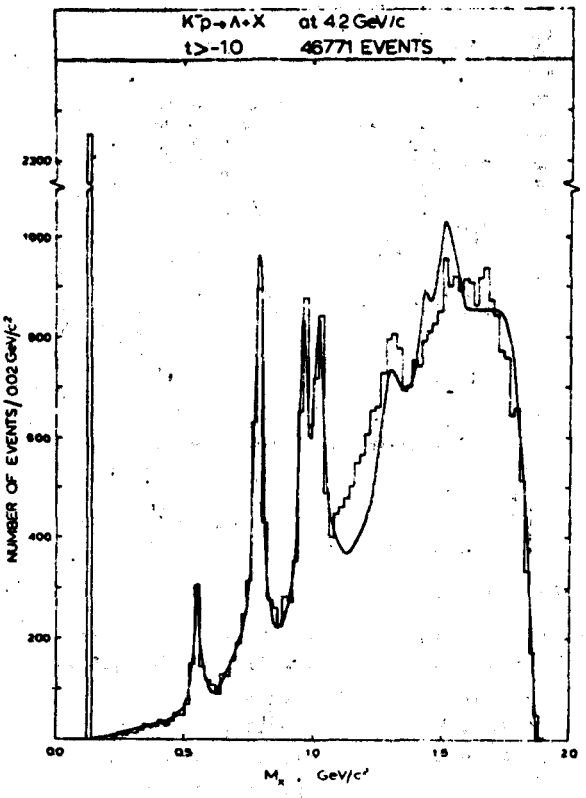


Fig.5.

The results of a PWA of the $(3\pi)^\circ$ system produced in the reaction

$$K^-p \to \Lambda\pi^+\pi^-\pi^\circ \qquad (3)$$

at 4.2 GeV/c/9/ show no indication for a narrow width enhancement in the A_1 region in the $J^P = 1^+(\rho\pi)$, $I = 0$ and 1, and in the $J^P = 1^+(\varepsilon\pi)$, $I = 1$ states (fig.6).

The $(\pi^+\pi^-\pi^\circ)$ mass distribution of reaction (3) at 8,25 GeV/c/10/ does not show a significant A_1 signal either.

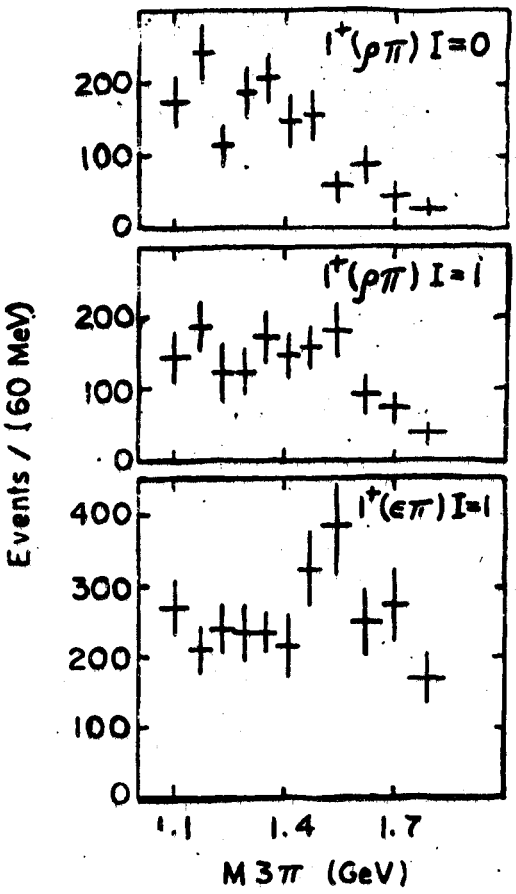


Fig.6.

Conclusions

1. The A_1, as a $J^P=1^+, I^G=1^-$ state of the $(\rho\pi)$ system was only found in the charged mode in hadronic interactions.
2. It is produced diffractively, and its production mechanism can well be explained by the Deck model which implies the A_1 not being a resonance, but a $(\rho\pi)$ threshold enhancement.
3. In cluster analyses (Berlin analysis[11] and prism plot analysis) the A_1 is found to be a low mass cluster which is characterized by the strong pion exchange coupling within the $(3\pi)^\pm$ systems.
4. The A_1 has not been seen in:
   a) Charge exchange reactions,
   b) Annihilation-type reactions,
   c) Reactions of the type $\pi p \to \pi A_1 p$, $Kp \to K A_1 p$

References

1. A.N.Kamalov, L.A.Ponomarev."Analysis of the $\pi^\pm$-Meson Diffraction Dissociation Region in the Reaction $\pi^+p\to(\pi^+p^o)p$", paper 32(A1-32), submitted to this conference.
2. J.A.Gaidos, C.R.Ezell, J.W.Lamza, R.B.Williams. Purdue University Preprint, COO-14 -28--231,1970.
3. Yu.M.Antipov et al.Nucl.Phys.,B63(1973)141, Nucl.Phys.,B63(1973)153.
4. G.Otter et al.Nucl.Phys.,B80(1974)1.
5. K.W.Edwards et al.(Carlton-McGill-Ohio-Toronto Collaboration): "A High Statistics Search for A_1^o and H^o in $\pi^-p\to\pi^+\pi^-\pi^o n$ at 8.4 GeV/c", paper 755(C1-58) submitted to this conference).
6. J.Chapman, R.Ely, G.Gidal,W.Michael,P.Oddone, D.Scharre (LBL) "A Search for Backward A_1 and A_2Production in 4 GeV/c π^-p Interactions", paper 318(C1- 76) submitted to this conference.
7. H.Muirhead. Proceedings of the International Symposium on $\bar{p}p$ -Interactions, Loma-Koli, Finland, June 11-19, 1975, p.300.
8. Amsterdam-CERN-Nijmegen-Oxford Collaboration, private communication by W.Kittel.
9. Amsterdam-CERN-Nijmegen-Oxford Collaboration: "A Partial Wave Analysis of the $(3\pi)^o$System in the Reaction $K^-p\to\Lambda\pi^+\pi^-\pi^o$ at 4.2 GeV/c", paper 303 (C1/2-29) submitted to this conference.
10. Athens-Demokritos-Liverpool-Vienna Collaboration: "A Comparison of ρ^o, ω^o and ϕ^o Production in K^-p Interactions at 8.25 GeV/c", paper 120 (A1-83), submitted to this conference.
11. Aachen-Berlin-Bonn-CERN-Cracow-Heidelberg-Warsaw Collaboration: "A Multidimensional Study of Clustering in the Reactions $\pi^\pm p\to p\pi^+\pi^\pm\pi^-$ at 16 GeV/c using Yang Variables", paper 1156 (A1-156) submitted to this conference.

REVIEW OF $K^*(1400)$ - $K^*(1800)$ S=1 MESON SPECTROSCOPY

V.P.Kenney

University of Notre Dame, USA

Speculation about charmed particles, together with considerable new data of high statistical quality, has given rise to a small renaissance of interest in meson spectroscopy. The situation as of the 1974 London Conference is shown in Fig.1. Only the $J^{PC}=0^{-+}, 1^{--}$, and 2^{++} nonets

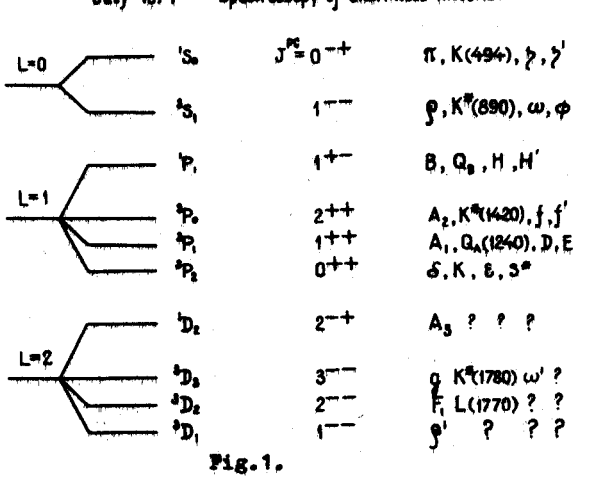


Fig.1.

were filled with established particles. S=1 counter - parts to the B and g in the 1^{+-} and 3^{--} nonets awaited confirmation. The 1^{++} and 2^{-+} nonets even appeared more poorly understood than in previous years, and the 0^{++} remained a mystery. The 2^{--} L(1770) was not well established, and the 1^{--} state, as well as all $L \geq 3$ $q\bar{q}$ states, awaited qualified candidates.

New data reported to this Conference shed light on the Q_A and Q_B mesons, establish definitively an $S=1$ $J^P=3^-$ counterpart to the g meson, and provide enough new bumps and squiggles in various partial waves to give new hope and encouragement to those who believe in the viability of constituent-quark spectroscopy. Space permits only a brief discussion of the highlights of a few of the many very interesting papers submitted.

Problem of the Q_A and Q_B Mesons. The SLAC group (1) have carried out a partial wave analysis of their 13 GeV/c $K^\pm p \to K^\pm \pi^+ \pi^- p$ spectrometer data and obtain results shown[x] in Figs.2 and 3. The 1^+ $K^*\pi$ data (Fig.2) show structure at $M(K\pi\pi) \simeq 1200$ and 1400 MeV, while $K\rho$ the 1^+ data (Fig.3) shows a pronounced peak around 1300 MeV. The authors interpret their data in terms

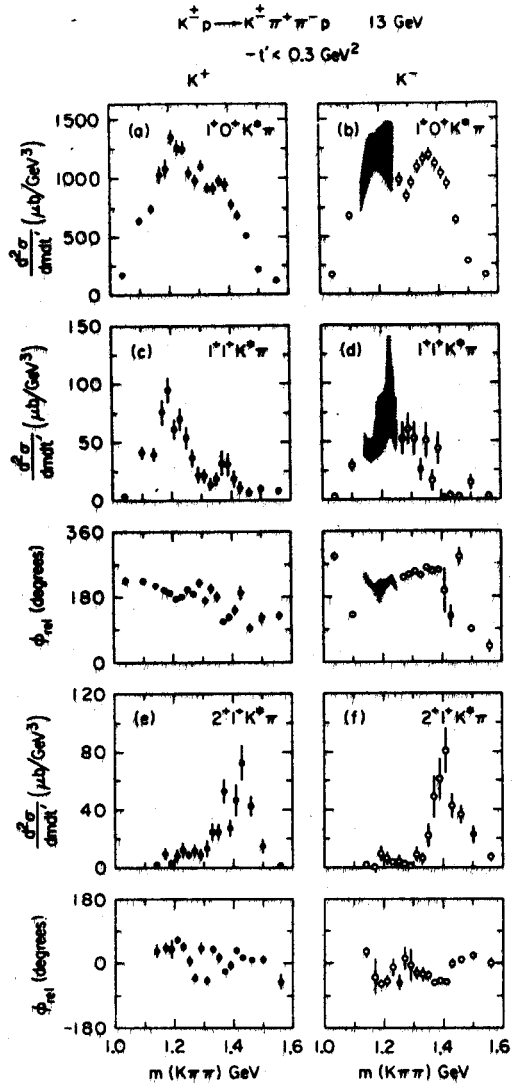


Fig.2.

of two 1^+ resonances plus a Deck background, the resonance Q_1 ($M \simeq 1300$ MeV, $\Gamma \simeq 200$ MeV) coupling to $K\rho$ and the resonance Q_2 ($M \simeq 1400$ MeV, $\Gamma \simeq 160$ MeV) coupling to $K^*\pi$. It is suggested that Q_1 and Q_2 are mixtures of Q_A and Q_B, the octet partners of the A_1 and B.

x/ As discussed elsewhere by Dr.Otter, the ABCLV/EPRS collaborations (2) obtain similar experimental results.

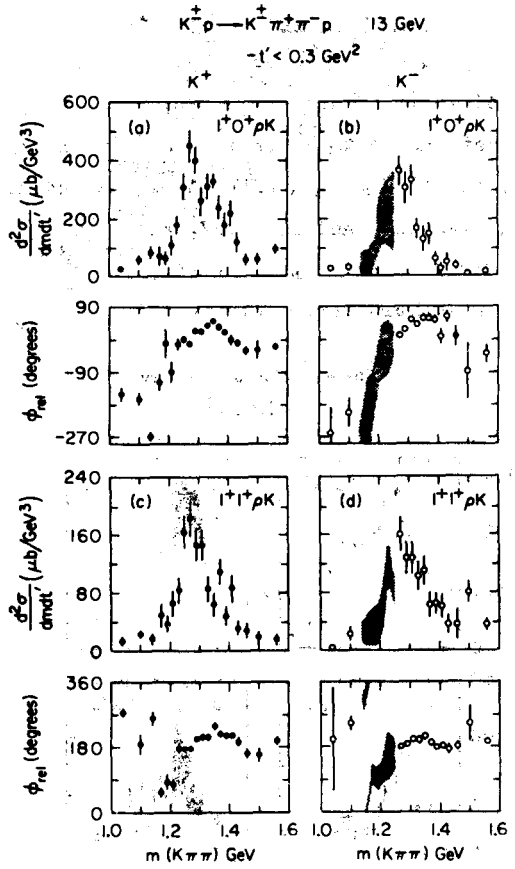


Fig..3.

A very different interpretation of R some SLAC data has been suggested by Basdevant and GBerger (3). Noting that the peak of the $K\rho$ distribution coincides with the valley in the $K^*\pi$ distribution and/or the $K^*\pi$ dip is at the $K\rho$ threshold, Basdevant and Berger suggest that the dip may be interpreted in terms of the interference of a single 1^+ Q resonance (coupling to both $K^*\pi$ and $K\rho$) with a non-resonant 1^+ Deck background which subtracts in the $K^*\pi$ channel and adds in the $K\rho$ channel. To obtain the dip in the $K^*\pi$ distribution, the ratio f/g of the $K\rho/K^*\pi$ coupling constants must be negative, indicating that the resonance has odd C relative to the K. Fig.4 shows their fits to the Deck alone (dashed) and Deck-plus-resonance, with the fit parameters. The resonance must be the 1^{+-} Q_B, with $M \approx 1340$ MeV and $\Gamma \approx 150$ MeV, $f/g = -1.5$. No Q_A resonance with width $\Gamma < 500$ MeV can be tolerated in this framework. If Basdevant and Berger's interpretation of the SLAC data

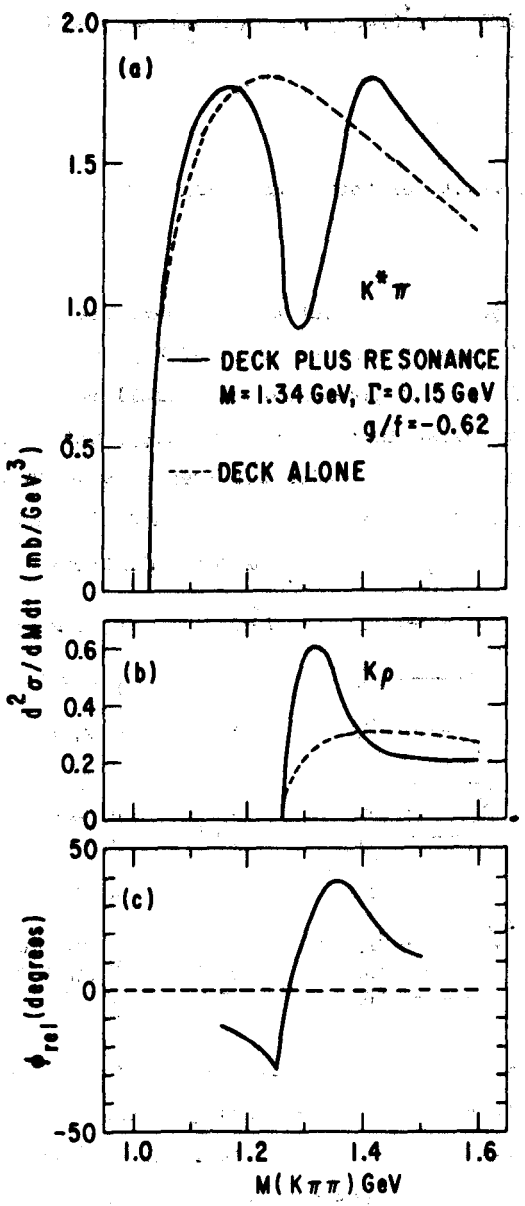


Fig.4.

is accepted, the 1^{+-} nonet has a second established member and the 1^{++} A_1 nonet remains obscure.

$J^P = 3^-$ Resonance at 1780 MeV is Confirmed.

The results of a CERN experiment by the Geneva University spectrometer group on the reaction $K^+p \to K^0_S\pi^+p$ at 10 GeV/c with $|t| < 1.0$ GeV/c have been reported to this conference (4). Their $M(K^0_S\pi^+)$ distribution, Fig.5 shows a pronounced peak, fit with the resonance parameters

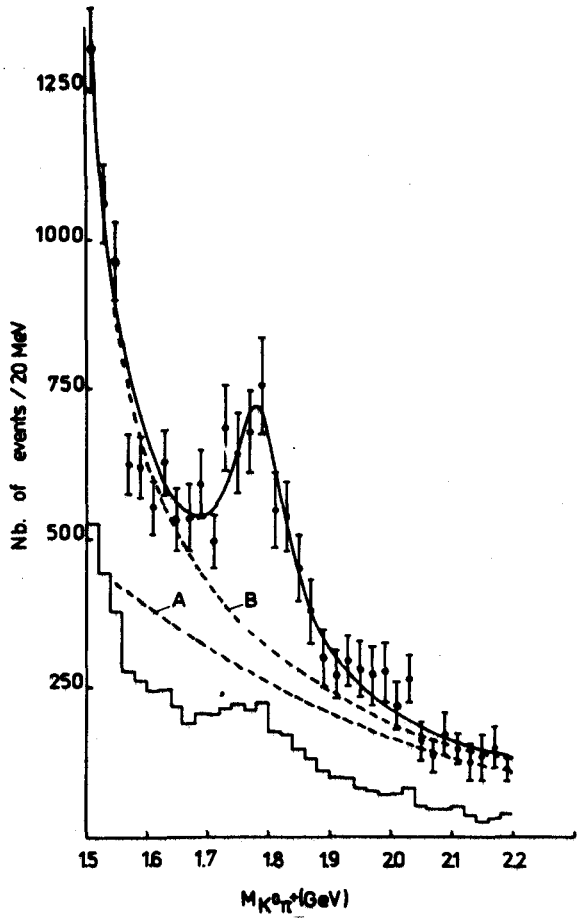


Fig.5.

M =1783±6 MeV, Γ =105±16 MeV. Their moments analysis of $K\pi$ decay, Fig.6, shows a peaking in $\langle Y_6^2 \rangle$ with M=1779 ± 11 MeV, Γ =135± 22 MeV, and $\langle Y_5^2 \rangle$ shows the expected p, f wave interference, confirming the 3^- assignment.

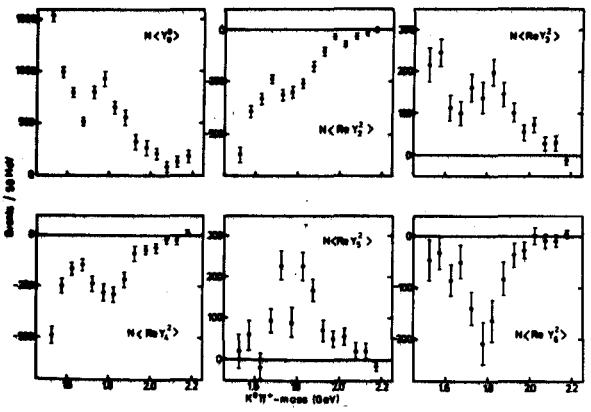


Fig.6.

The $K^+p \to K^+\pi^-\Delta^{++}$ and $K^-p \to K^-\pi^+n$ spectrometer data of the SLAC group (5) confirm the 3^- $K^*(1780)$. Fig.7 shows a rather broad

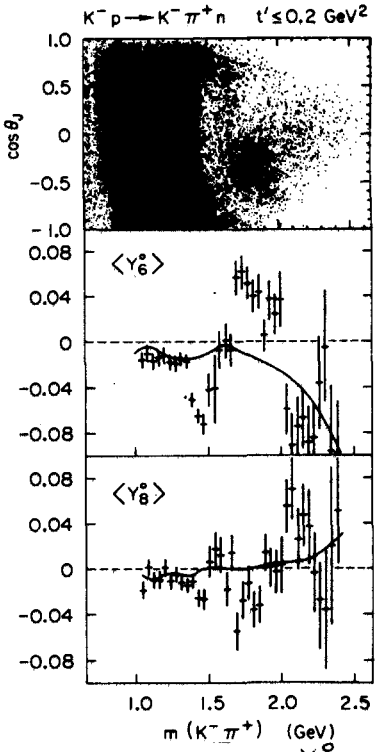


Fig.7.

(200-300 MeV) signal in the $\langle Y_6^0 \rangle$ moment at ~ 1800 MeV ($\langle Y_5^0 \rangle$, not shown, also indicates the expected f, d wave interference), and the scatter plot of $M(K^-\pi^+)$ vs. $\cos\theta_J$, shows a clustering consistent with $K^*(1780)$ production, with the backward peak and events with $\cos\theta_J < 0.7$ cancelled by interference. It is interesting that the scatterplot hints at a similar clustering at ~ 2100 MeV, where the pronounced rise of the $\langle Y_8^0 \rangle$ moment suggest that a broad $J^P = 4^+$ resonance is being produced. The acceptance of the spectrometer begins to restrict the data severely in this region.

New Structures Reported. Enhancements in effective mass plots have been reported to this Conference, including a broad peak in the ABCLV 10 and 16 GeV/c $K^-p \to K^-\pi^+n$ data (6) at $M(K^-\pi^+)$=1871±10 MeV, Γ =285±40 MeV. Absence of a corresponding enhancement in $K^-p \to (K\pi)^-p$ channels is consistent with pion exchange. A moments analysis of the $K^-\pi^+$ decay angular

distribution to determine the spin of this presumed object was inconclusive. The BNL multiparticle spectrometer group (7) report a surprisingly narrow "bump" in their 6 GeV/c $K^-p \to \bar{K}^0\pi^+\pi^-n$ data, with $M(\bar{K}^0\pi^+\pi^-) = 1692 \pm 6$ MeV, and $\Gamma = 26^{+24}_{-17}$ MeV, according to the fit.

The lack of new structures reported is sometimes even more interesting. There have been searches for the 0^+ Kappa meson; the SMBP collaboration, studying $K^+n \to K^+\pi^-p$ at 4.6, 8.25 and 12 GeV/c (8) observe no significant structure, only a very broad smooth enhancement centered about 1250 MeV. This suggests that despite the observation of a new narrow 0^{++} meson in the Notre Dame streamer chamber data (9) which gives new hope for the 0^{++} $q\bar{q}$ nonet, the more pessimistic conjectures of Flatte(10) may eventually prove correct. There is no new information reported on the suggested 2^{--} L(1770)meson.

It is reasonable to expect that further progress in this area will depend more on careful partial wave analysis than on fortuitous bump-hunting. Useful contributions toward understanding the production mechanisms of the established resonances have been made by the 4.2 GeV/c K^-p collaboration (11) and by the BBCM Collaboration with 5,8.25, and 16 GeV/c K^+p data (12). It is particularly encouraging that newly-available high statistics spectrometer data from $K^\pm p$ experiments at SLAC and ANL have been incorporated into the beginnings of a major program to analyze $K\pi$ phase shifts, similar to the effort which proved as successful in the $\pi\pi$ case. In a paper reported to the conference by P.Estabrooks et al. (13), new resonance values for the $J^P = 2^+$ K^* with $M = 1433 \pm 4$ MeV, $\Gamma = 94 \pm 10$ MeV are obtained. It is particularly interesting that the $K^-\pi^+$ partial waves are so similar as regards both amplitude and phase variation of all partial waves to the corresponding $\pi^-\pi^+$ solutions, particularly at high mass.

References

1. G.W.Brandenburg et al. SLAC paper 827.Phys. Rev.Lett.,36 ,703 (1976).
2. Aachen-Berlin-CERN-London-Vienna and Ecole Polytechnique-Rutherford-Saclay Collaboration, paper 170.
3. J.L.Basdevant and E.L.Berger, ANL-HEP-PR 76-24 and FNAL-Pub-76/39 THY (1976).
4. R.Baldi et al. Geneva University, paper 729.
5. G.W.Brandenburg et al. SLAC paper 119.
6. H.Grassler, Aachen-Berlin-CERN-London(I.C.)-Vienna Collaboration, paper 176.
7. A.Etkin et al., BNL-CUNY Collaboration, paper 182; Phys.Rev.Lett.,36, 1482 (1976).
8. D.Vignand et al. Saclay-Mons-Brussels-Paris, paper 180.
9. N.M.Cason et al. Notre Dame -ANL, paper 1075.
10. S.M.Flatte, CERN, paper 1132.
11. Amsterdam-CERN-Nijmegen-Oxford Collaboration, paper 280.
12. Birmingham, Brussels, CERN, Mons Collaboration, paper 881.
13. P.Estabrooks et al. McGill-Carleton-Durham-SLAC, paper 286.

NEW PHENOMENA IN THE Q-REGION

G.Otter, TH, Aachen

The Q-mass region has been studied by two high statistics experiments which have allowed a partial wave analysis (PWA) to be performed in small $(K\pi\pi)$ -mass intervals. The experiments were carried out by the SLAC spectrometer group who investigated the diffractive reactions

$$K^-p \to K^-\pi^+\pi^-p \qquad (1)$$

(56 K events for $1.0 \leq M(K\pi\pi) \leq 1.6$ GeV)

$$K^+p \to K^+\pi^+\pi^-p \qquad (2)$$

(72 K events for $1.0 \leq M(K\pi\pi) \leq 1.6$ GeV) at 13 GeV/c[1,2] and also by the A-B-C-L-V-E.P.-R-S bubble chamber collaboration who combined data from the reactions

$$K^-p \to K^-\pi^+\pi^-p \qquad (3)$$

(35 K events; for $1.0 \leq M(K\pi\pi) \leq 1.6$ GeV 10 K events)

$$K^-p \to \overline{K}^0\pi^-\pi^0p \qquad (4)$$

(8 K events; for $1.0 \leq M(K\pi\pi) \leq 1.6$ GeV 3.5 K events) at 10,14 and 16 GeV/c[3].

The PWA results for the various reactions considered essentially agree. In this report I shall mainly dicies the dominant 1^+ states, i.e. the $1^+S\ (K^*\pi)$ and $1^+S(K\rho)$. The main results are:

1) The $1^+S\ (K^*\pi)$ intensity as a function of $(K\pi\pi)$ mass shows a two-peaked structure with peaks in the region gof 1200 to 1270 MeV and near 1370 MeV. On the other hand the $1^+S\ (K\rho)$ spectrum has only a single peak at the $(K\rho)$-threshold near 1270 MeV(see fig.1 for the results from reactions (1) and (3)).

2) The two states, $1^+S\ (K^*\pi)$ and $1^+S\ (K\rho)$, are produced by different production mechanisms. Whereas the $1^+S\ (K^*\pi)$ fulfills approximately t-channels-helicity-conservation (TCHC), the

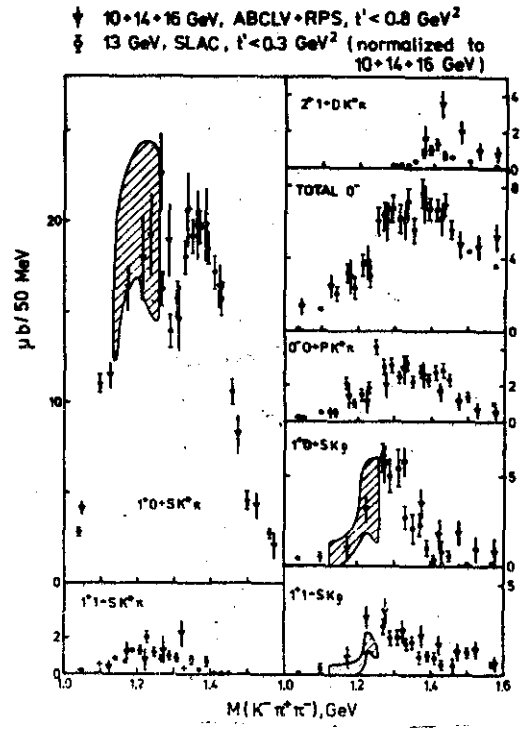


Fig.1. Mass dependence of various states for the reactions (1) and (3), calculated in the Gottfried-Jackson system. The shaded area indicates the range of the ambiguous solutions in reaction (1).

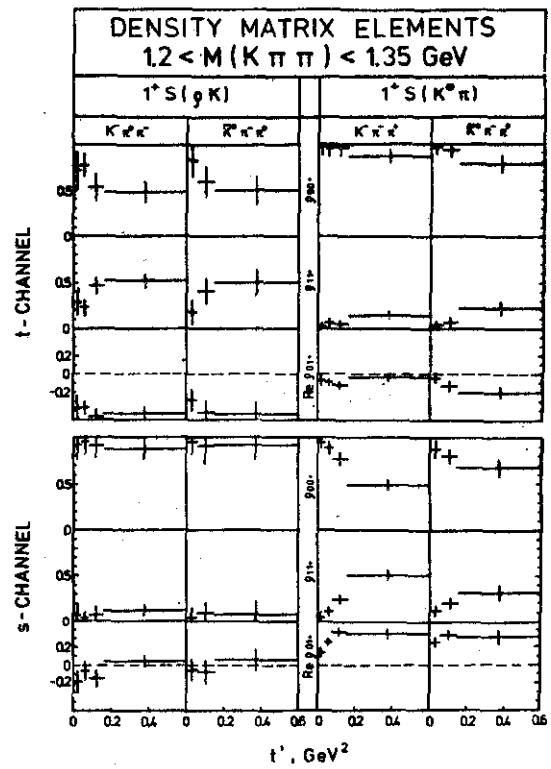


Fig.2. Density matrix elements for the states $1^+S\ (K\rho)$ and $1^+S\ (K^*\pi)$, calculated in the Gottfried-Jackson and S-channel-helicity frames for reactions (3) and (4).

$1^+S(K\rho)$ state shows approximately s-channel - helicity-conservation (SCHC). Data confirming this as a function of t' are shown in fig.2, where the density matrix elements for the two states are displayed for reactions (3) and (4) in the Gottfried-Jackson- and helicity frames respectively.

3) The $1^+S(K\rho)$ phase increases with respect to the $1^+S(K^*\pi)$ phase up to $M(K\pi\pi) \sim 1400$ MeV and then decreases for higher $(K\pi\pi)$ -masses. This is seen in fig.3. Two possible interpretations of these results have been proposed:

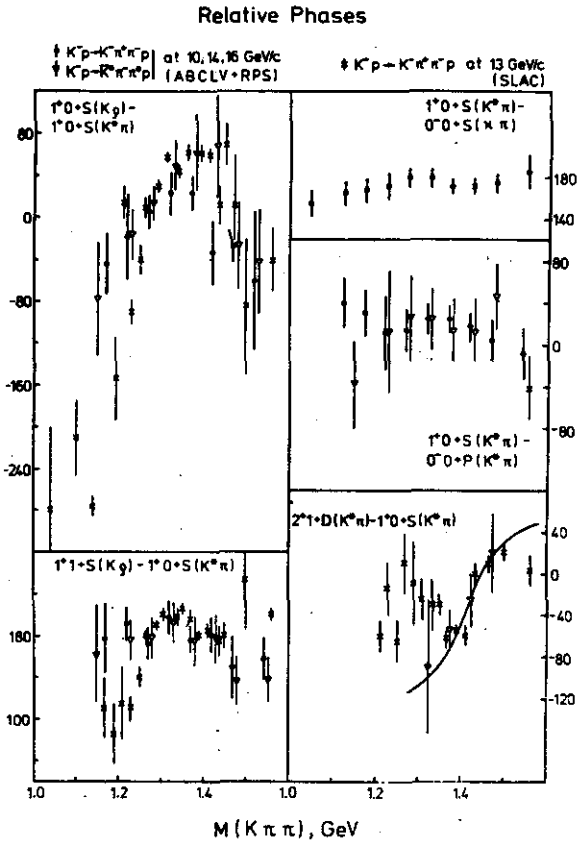


Fig.3 Mon dependence of relative phases between the dominant states for reactions (1), (3) and (4).

1. The SLAC group propoees the existence of two $J^P = 1^+$ resonances (Q_1 and Q_2), with the Q_2 on top of a Deck background. They have fitted the data with two resonances and a Deck-like background which is assumed to have a Gaussian mass dependence and a nonvarying phase as a function of $(K\pi\pi)$-mass. They obtained for the Q_1 [4]

M =1289±25 MeV
Γ = 150±70 MeV

and found that this resonance is produced by approximate SCHC (note, that other diffractive two-body reactions, as elastic scattering and photoproduction of vector mesons, are produced in the same way). It decays almost entirely to $K\rho$ and the peak in the $1^+S(K\rho)$ mass distribution corresponds to this decay mode. No $K^*\pi$ decay is observed, some $\varkappa\pi$ decay is possibly seen. The Q_2 with

M =1404±10 MeV
Γ = 142±15 MeV

is produced by approximate TCHC and decays essentially into $K^*\pi$, possibly also into some $K\epsilon$. There is no evidence for any $K\rho$ decay. The second peak in the $1^+S(K^*\pi)$ mass distribution corresponds to the $K^*\pi$ decay mode.

The first peak in the $1^+S(K^*\pi)$ mass distribution is ascribed to the background (the width of the fitted background is much too small for a Deck background). The relative $1^+S(K\rho)/1^+S(K^*\pi)$ phase variation is explained by the phase variation of the Q_1 and Q_2 resonances in the corresponding $(K\pi\pi)$ mass regions.

2. Another qualitative explanation of the experimental results has been proposed by Basdevant and Berger [5]. They explain the results with a unitary Deck model with coupled $K^*\pi$ and $K\rho$ - channels and a single 1^+ resonance ($M \simeq$ 1340 MeV, $\Gamma \simeq$ 150 MeV) decaying into $K\rho$ and $K^*\pi$. The interference of the two types of reactions explains the dip in the $K^*\pi$ mass spectrum (giving the two-peak structure) at the same $(K\pi\pi)$ mass as the increase of the $K\rho$ intensity. The correct $1^+S(K\rho)/1^+S(K^*\pi)$ phase variation is obtained. It is not clear to me whether SCHC for $K\rho$ and TCHC for $K^*\pi$ can be explained by this model.

Conclusion: There exists good evidence for at least one strangeness-1 resonance with $J^P = 1^+$ which decays mainly into $K\rho$ and which is produced

by a different mechanism (SCHC) than all the other states. Its mass has to be in the $\sim$1300 MeV region.

To search for other decay modes of this resonance the A-B-C-L-V-B-B-C-M-S collaboration has investigated the low mass $K\omega$-system[6]. This shows a peak near threshold which is diffractively produced in the same way as the $K\rho$-spectrum [7]. APWA gives SCHC for the lowest $K\omega$-mass region. If this region is attributed to the Q_1 resonance, they find a branching ratio

$$\frac{Q_1 \to K\omega}{Q_1 \to K\rho} = 0.8 \pm 0.2.$$

This number however depends strongly on the resonance parameters chosen.

I would like to emphasise that of all diffrastive meson systems investigated, only $K\rho$ and $K\omega$ show the unusual features of SCHC and of a mass peak near threshold[8].

One other interesting result concerning the $(K\pi\pi)$ system is reported by the SLAC group who claim the existence of a new strangeness 1 $J^P=0^-$ resonance in addition to the two 1^+ resonances. The resonance parameters are: $M \sim 1400$ MeV, $\Gamma \sim 250$ MeV. It decays mainly into $K\varepsilon$[9]. The existence of this resonance is however not confirmed by the bubble chamber experiment[10].

References

1. G.W.Brandenburg et al. PRL 36, 703 (1976).
2. G.W.Brandenburg et al. PRL 36, 706 (1976).
3. Aachen-Berlin-CERN-London-Vienna-Ecole Plytechnique-Rutherford-Saclay Collaboration G.Otter et al., N.P. B106, 77 (1976).
4. SLAC prepriat, SLAC-PUB-1767, June 1976. R.K.Carnejie et al. (A quantative description of the diffractively produced mass spectra) and paper to the Conference, 1131/61-81.
5. J.L.Basdevant and E.L.Berger. Argonne Preprint Argenne-ANL-HEP-PR-76-24 (Unitary coupled channel Deck model and the Q meson resonance region).
6. Aachen-Berlin-CERN-London-Vienna-Birmingham-Brussels-CERN-Mons-Serpukhov Collaboration, CERN-preprint CERN/EP/Phys 76,9 June 1976 (D.Hrarti, On dissociation and resonances in the $(K\omega)$ system produced in the reaction $K^\pm p \to (K^\pm\omega)p$.
7. G.Otter et al., NP B87, 189 (1975).
8. Aachen-Berlin-Benn-Heidelberg-London-Vienna Collaboration, P.Besotii et al. N.P. B101, 304 (1975).
9. G.W.Brandenbrug et al. PRL 36, 1239 (1976).
10. G.Otter and G.Rudolph, Aachen-nste, April 1976 (Comments on a new strangeness - one $J^P=0^-$ resonance claimed by SLAC).

THE D(1285) AND E(1420) MESONS

H. Böttcher – IHEP, Zeuthen, DDR

1. Introduction

The D(1285) and E(1420) mesons are known since 1965 and 1967 respectively. The D-meson was first seen in $\bar{p}p$ intsractions at 1.2 GeV/c while the E-meson was disoovered in $\bar{p}p$ annihilations at rest. However, up to now we know very little about these resonances. Their branching ratios are still not well determined. Both have isospin $I=0$ and $G=C=+1$. Spin and parity are only determined to belong to the unnatural series $J^P=0^-,1^+,2^-\ldots$ with 1^+ favoured for both. Clearly more experimental information is needed. At this conference there were four contributions dealing with the D(1285) and partly also with the E(1420).

2. The D(1285) Meson

The Bombay-CERN-College de Franoe-Madrid Collaboration (BCCM-Coll)[1] has represented evidenoe for D(1285) deoaying into $(K\bar{K}\pi)^0$ in $\bar{p}p$ annihilations at 0.76 GeV/o. The experiment performed in the 81 cm Saolay HBC at CERN yielded 22 events/μb . Adding data of a previous $\bar{p}p$ experiment at 0.7 GeV/c a total sample with 28 events/μb resulted. The following ohannele have been etudies.

$$\bar{p}+p\to K^0_{\text{seen}}K^{\pm}\pi^{\mp}\pi^{+}\pi^{-} \quad (1000\text{ events}) \quad (1)$$

$$\bar{p}+p\to K^0_{\text{seen}}K^0_{\text{seen}}\pi^{+}\pi^{-}\pi^0 \quad (1000\text{ events}) \quad (2)$$

$$\bar{p}+p\to K^0_{\text{seen}}K^{\pm}\pi^{\mp}+MM \quad (1000\text{ events}) \quad (3)$$

$$\bar{p}+p\to K^0_{\text{seen}}K^{\pm}\pi^{\mp}\pi^0 \quad (7000\text{ events}) \quad (4)$$

A D(1285) eignal is clearly observed in the $(K\bar{K}\pi)^0$ mass for the reactions (1), (2), (3). In reaction (4) only an indication is seen. As the most significant evidence the $(\text{mass})^2$ distribution for the $(K^0K^{\pm}\pi^{\mp})$ combinations of the reaction (1) is shown in fig.1.

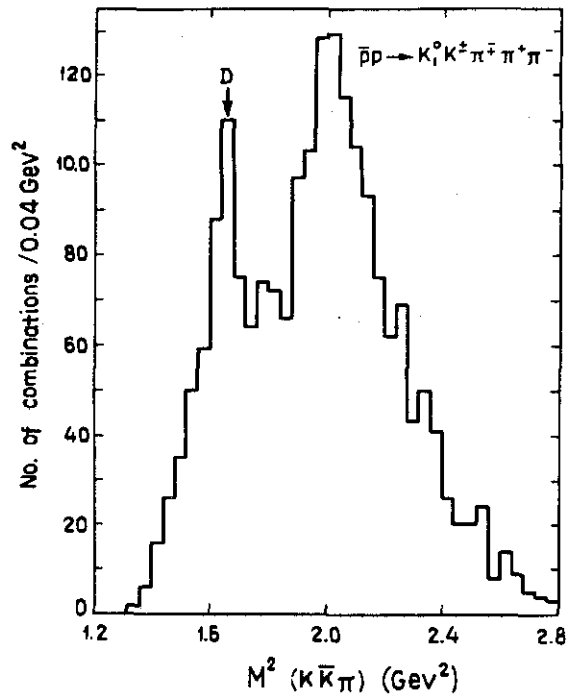


Fig.1.

Fitting the $(K\bar{K}\pi)^0_{(\text{mass})^2}$ distributions in the reactions (1)-(3) with a Breit-Wigner and a polynomial baokground unfolding the experimental resolution average values for the mass and width of the D are given $M_D=(1281\pm2)$ MeV, $\Gamma_D=(32\pm5)$ MeV. The Ottawa-Monreal-Ohio-Toronto Collaboration (OMOT-Coll)[2] has analyzed the reaction

$$\pi^-p\to\eta\pi^+\pi^-n \qquad \text{with } \eta\to\gamma\gamma \quad (5)$$

at 8.4 GeV/c. The experiment was performed using the charged and neutral spectrometer at the Argonne ZGS, where both charged particlee and both γ's are measured. The results presented are preliminary obtained from a first-pass analysis of 45% of the whole sample. Mass resolution and background rejection are not yet fully optimized. The aoceptanoe calculation has been done only crudely. Fig.2 a shows the $(\eta\pi^+\pi^-)$ effeotive mass whers a clear D(1285) signal containing 240 events is visible.

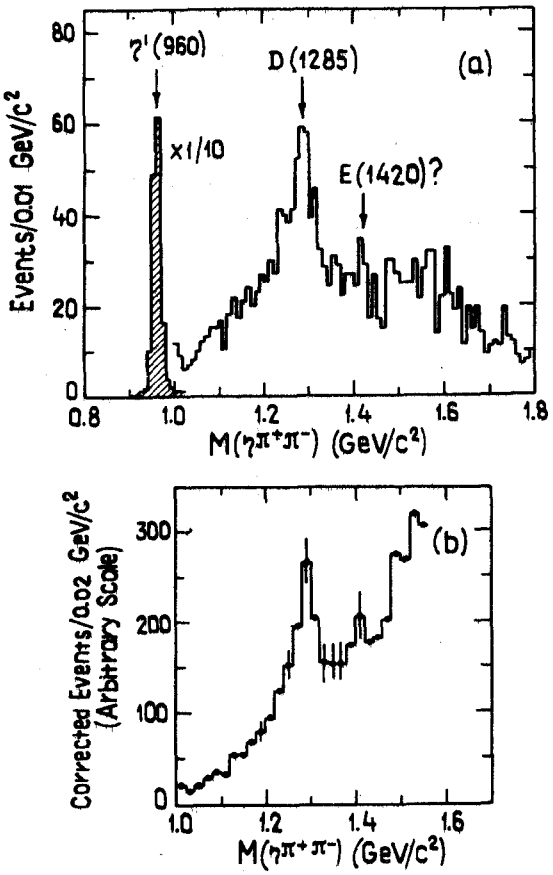


Fig.2.

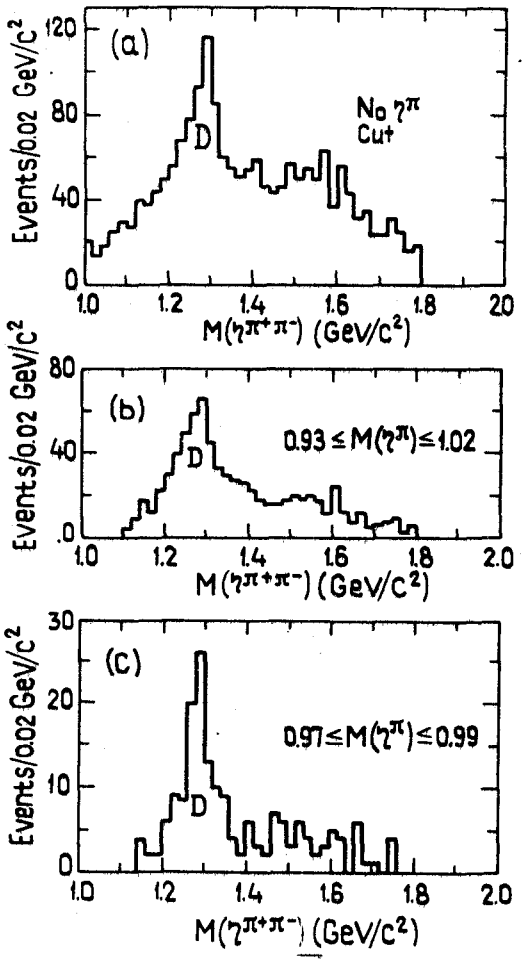


Fig.3.

The same spectrum is replotted in fig.2 b with the approximation acceptance calculation. Values for the mass and width of the D are not given. Evidence for the decay chain $D(1285) \to \delta(980)\pi$ is found. Fig.3 shows the $(\eta\pi^+\pi^-)$ mass for different cuts of the $(\eta\pi)$ mass around the $\delta(980)$ region. In fig.3c the D peak is virtually background free. A quantitative estimate revealed that about half of the $D \to \eta\pi^+\pi^-$ goes through $\delta\pi$, a ratio which has to be taken as preliminary. The Birmingham-Rutherford Laboratory-Tel-Aviv-London (Westfield College) Collaboration (BRTL-Coll)/3/ has studied the D in the reaction

$$\pi^- p \to \pi^+\pi^+\pi^-\pi^-\pi^0 n \qquad (6)$$

at 12 GeV/c. The data were recorded in an experiment using the Omega multiparticle spectrometer at CERN triggered by a neutron detector in an unseparated secondary negative beam (98.5% pions).

From part of the 2.7 million triggers in total 5400 events for the 1c-reaction (6) were found. Fig.4 shows the $(\eta\pi^+\pi^-)$ effective mass distribution.

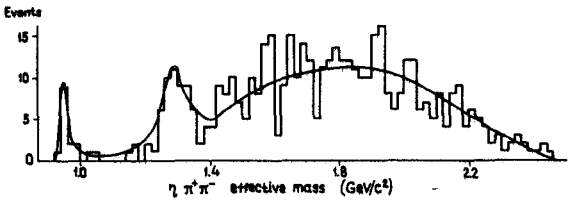


Fig.4.

At clear D(1285) signal is visible on a smooth background. A fit to this mass distribution using Breit-Wigner and a polynomial background (solid line) gave a mass of M_D=1283 MeV and a width of Γ_D=43 MeV. The experimental resolution has not been unfolded. Evidence for the decay chain $D \to \delta\pi \to \eta\pi\pi$ is given by investigating the Dalitz plot of $(\eta\pi^+\pi^-)$ masses in the

D-meson region. A simple fit yielded 0.42±0.14 for the $\delta(980)\pi$ branching fraction (not corrected for the background) as a preliminary value.

The Aachen-Berlin-Bonn-CERN-Cracow-Heidelberg-Warsaw Collaboration (ABBCCHW-Coll)[4] has studied the D in $\pi^{\pm}p$ interactions at 16 GeV/c. The experiments performed in the 2m HBC at CERN were combined representing ~20 events/mb for the π^+p and ~5 events/mb for the π^-p experiment. The following reactions have been used

$\pi^{\pm}p \to p\pi^{\pm}\pi^+\pi^+\pi^-\pi^-$ ($^+$: 8505 events, $^-$: 1214 events) (7)

$\pi^{\pm}p \to p\pi^{\pm}\pi^+\pi^+\pi^-\pi^-\pi^0$ ($^+$: 21496 events, $^-$: 3406 events) (8)

$\pi^+p \to p\pi^+K^+\bar{K}^0_{seen}\pi^-$ (309 events) (9)

$\pi^+p \to p\pi^+K^-K^0_{seen}\pi^+$ (205 events) (10)

In fig.5 the effective mass distributions $M(2\pi^+2\pi^-)$ and $M(\rho^0\pi^+\pi^-)$ (hatched histogram) for

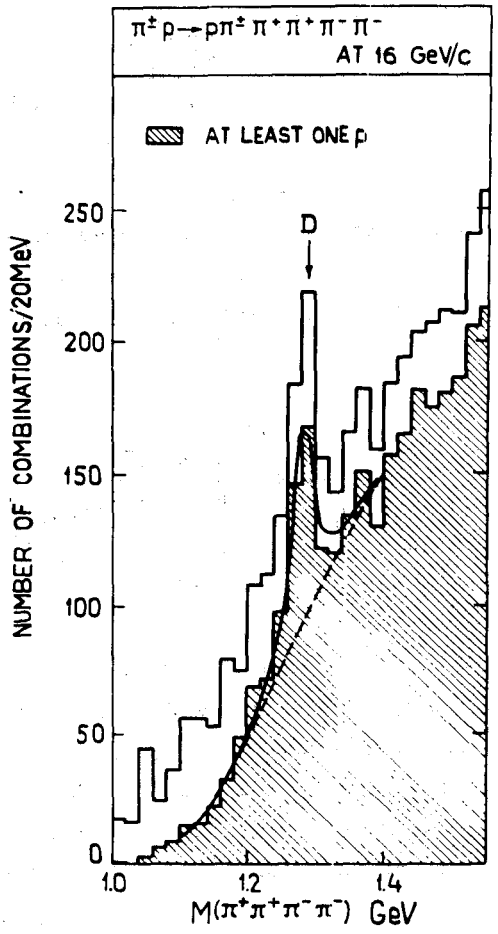


Fig.5.

the reactions (7) are presented. The clear peak visible at around 1280 MeV is interpreted as evidence for the $(\rho^0\pi^+\pi^-)$ decay of the D.

Fig.6 shows the mass distributions $M(\eta\pi^+\pi^-)$ and $M(\delta^{\pm}(980)\pi^{\mp})$ (hatched histogram). Clear evidence for the $(\eta\pi^+\pi^-)$ decay of the D is seen which proceeds mainly via the chain $D \to (\delta^{\pm}\pi^{\mp}) \to (\eta\pi^+\pi^-)$

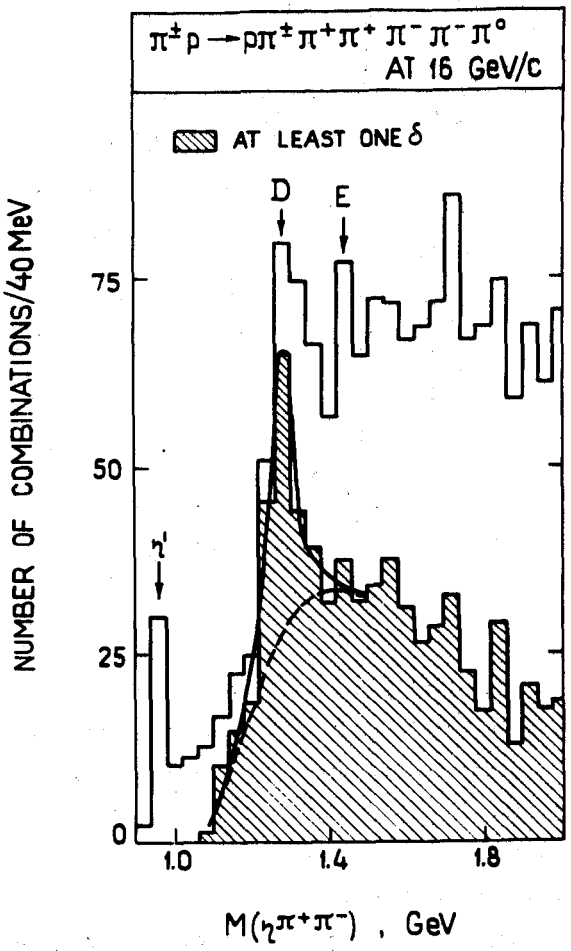


Fig.6.

In fig.7 showing the $(K\bar{K}\pi)^0$ mass distribution for the reactions (9) and (10) only an indication for the D(1285) is present. From the $(\rho^0\pi^+\pi^-)$ and $(\delta^{\pm}\pi^{\mp})$ mass distributions fitted with a Breit-Wigner and hand-drawn background (folding in the experimental resolution and taking into account the $(2\pi^+2\pi^-)$ decay of the f (1270) average value for the mass and width of the D are obtained M_D = (1279±5) MeV and

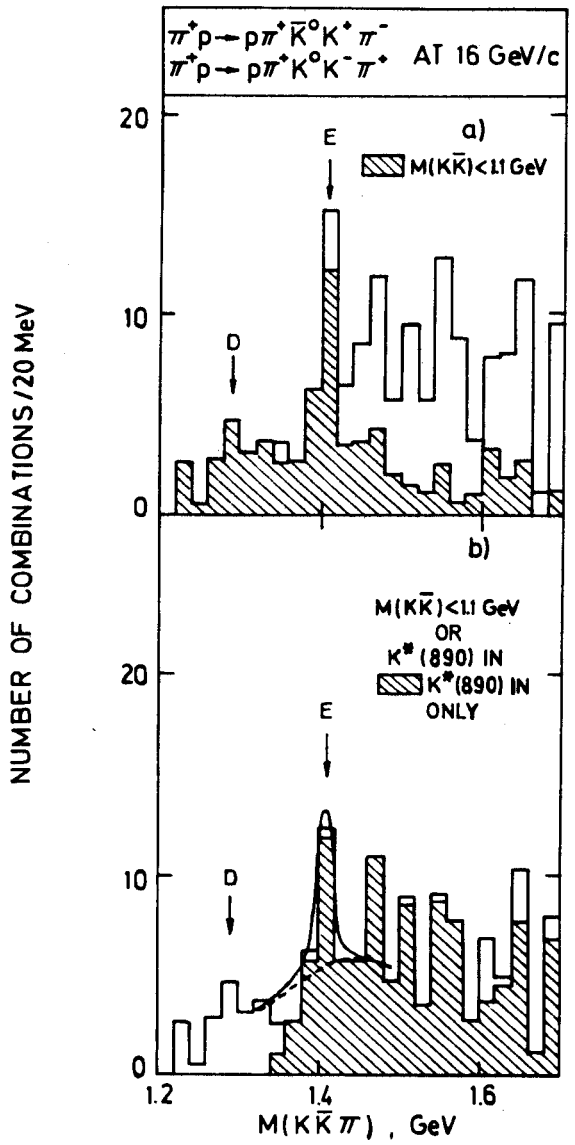


Fig.7.

Γ_D=(24±18) MeV. The branching ratios $(D\to\rho\pi\pi)/(D\to\eta\pi\pi)$ =0.93± 0.30 and $(D\to K\bar{K}\pi)/(D\to\eta\pi\pi) <$ 0.26 are found. The $(\delta\pi)$ branching fraction for $D\to\delta\pi\to\eta\pi\pi$ was determined to be 1.0±0.3. Ordering the beam-like pions according to their cms longitudinal momenta the D(1285) is dominantly produced in those mass combinations not including the fast pion. Analysing the angular distributions for the quasitwo-body decay $D\to\delta\pi$ its spin and parity could not be established.

3. The E(1420) Meson

For the E-meson there are no exciting news. The BCCM-Coll. attributed the second peak in fig.1 to the $(K\bar{K}\pi)$ decay of the E and took this peak into account to fit the mass spectrum. However, no information is given.

The OMOT-Coll. presented in fig.2a suggestion of the E(1420) with out giving further details.

The ABBCCHW-Coll. reported indications for the $(\eta\pi\pi)$ decay (fig.6) and weak evidence for $(K\bar{K}\pi)$ decay of the E. Fiting the $(K\bar{K}\pi)$ mass spectrum with a Breit-Wigner and a hand-drawn background a mass of M_E=(1407±10) MeV and a width of Γ_E =(10^{+15}_{-10}) MeV were obtained.

The evidence for the E(1420) presented at this conference is very weak and rather evidence against the existence of this resonance at all.

4. Summary

i. Evidence is presented for the D(1285) meson in its $(K\bar{K}\pi)$, $(\rho\pi\pi)$ and $(\eta\pi\pi)$ decay mode.

ii. The decay of the D into $(\eta\pi\pi)$ proceeds mainly via to the chain $D\to\delta\pi\to\eta\pi\pi$. The branching fraction ranges from about 0.5 te 1.0.

iii. New values for the mass and width of the D(1285) are given.

iv. A new value for the branching ratio $(D\to\rho\pi\pi)/(D\to\eta\pi\pi)$ and upper limit for $(D\to K\bar{K}\pi)/(D\to\eta\pi\pi)$ are derived.

v. Spin and parity of the D meson are not yet established.

vi. The evidence for the E(1420) is very weak. Its existence is questionable.

5. References

1. Submitted paper No. 1751.
2. Submitted paper No. 1075.
3. Submitted paper No. 188.
4. Submitted paper No. 1041.

A SEARCH FOR EXOTIC MESONS $X^{--} \to p\bar{p}\pi^-\pi^-$ IN THE C.E.R.N. OMEGA SPECTROMETER

C.E.R.N.-College de France - Ecole Polytechnique - Orsay Collaboration

Presented by A. Rouge

Up to now neither exotic baryons nor mesons have been undoubtedly observed. The existence of such mesons, coupled to baryons-antibaryon only, is required by the two-components duality theory[1]. They are expected to be narrow resonances decaying mainly into baryon-antibaryon systems. Their production via baryon-exchange is favoured with cross sections similar to other baryon-exchange reactions.

In the experiment reported here we have looked for I=2 exotic mesons X^{--} in the reaction $\pi^- n \to p_{forward} + X^{--}$ (X^{--} decaying into $p\bar{p}\pi^-\pi^-$) with a 12 GeV/c beam. The experimental layout, schematically shown in Fig.1, is the same as in

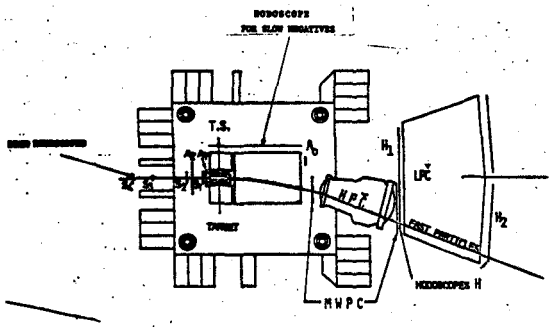


Fig.1.

the Omega-fast proton experiment[2]. The 60 cm length target was filled with deuterium.

The trigger was the coincidence of the two following requirements:

- Presence of a fast forward proton 7 GeV/c < p < 10 GeV/c[2].
- Presence of at least two negative particles detected by the large scintillation counters shown in Fig.1.

770000 triggers have been recorded, corresponding to an overall sensitivity of 7700 events/microbarn/ nuclear without acceptance and efficiency corrections.

After processing in the Omega pattern recognition and geometry program ROMEO 26600 candidates to reaction

$$\pi^- d \to \text{invisible} + p_{spectrator} + p_{fast} + p\bar{p}\pi^-\pi^-$$

have been found (3 charged prongs one of the two positive having a momentum greater than 6 GeV/c). All these candidates have been processed in the CERN KOMEGA program. 2C fits were attempted assuming the spectrator momentum to be given by the Hulthen distribution and equal to 45±30 MeV/c. 375 events with a probability

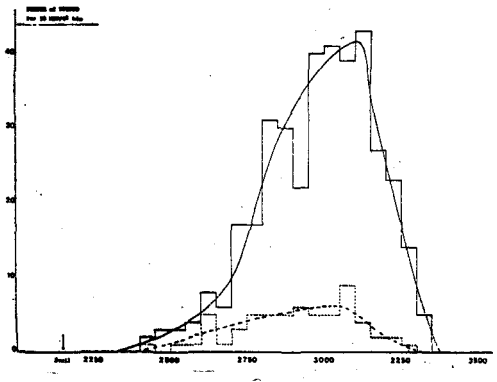


Fig.2.

better than 4% and a fitted spectator momentum less than 100 MeV/c remained. 24 ambiguous events were excluded from the analysis.

Fig.2 shows the $\bar{p}p\pi^-\pi^-$ invariant mass distribution for these events. In order to reduce contributions from diffraction-dissociation, a cut on the direction of the slow proton in the X^{--} rest system has been performed leaving us with 61 events (dotted histogram). Both spectra are well fitted by low-order polynomials and show no peak.

After correction for the acceptance and efficiency of the apparatus evaluated from a Monte-carlo method[3] we can set the following upper limits for the production of narrow ($\Gamma < 50$MeV/c) X^{--} resonances decaying into $p\bar{p}\pi^-\pi^-$.

Mass MeV/c	Mx 2500	2500<Mx<2600	2600<Mx<2800	Mx>2800
σ_{up}, nb	7	15	32	80

References

1. M.Jacob, J.Weyers N.C. 69 A(1970)521,NC 70A (1970) 285.
2. D.Treille et al. Proceedings of the International Conference, Palermo, 1975.
3. CERN-College de France-Ecole Polytechnique-Orsay Collaboration Backword elastic scattering $\pi^- p \to p\pi^-$ at 9 and 12 GeV/c (to be published).

NUCLEON POLARIZATION IN THE REACTION $\pi^- p \to n\pi^+\pi^-$

H.Becker, W.Blum, V.Chabaud, H.de Groot, H.Dietl, J.Gallisn, B.Gotteschalk, G.Hentschel, B.Hyams, E.Lorenz, G.Lutjens, G.Lutz, W.Manner, B.Niczyporuk, D.Notz, T.Papadoculou, R.Richter, K.Rybicki, U.Stierlin, B.Stringfellow, M.Turala, P.Weilhammer, A.Zalewska

CERN-Munich Collaboration

Presented by G.Lutz

Preliminary results from a high statistics measurements (1M events) of the reaction $\pi^- p \to n\pi^+\pi^-$ on a polarised target at 17.2 GeV show unexpected strong nucleon polarization effects which must be attributed to amplitudes corresponding to A_1 exchange. The evidence is

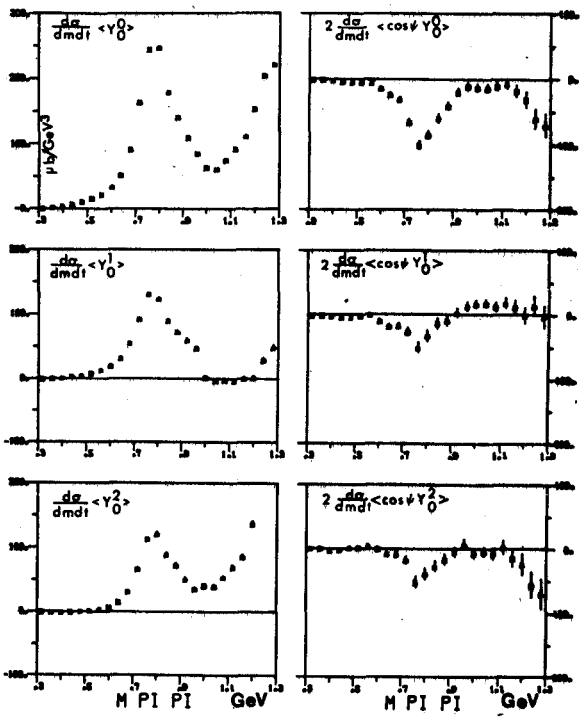


Fig.1. Mass dependence of Unnormalised moments $\frac{d\sigma}{dmdt}\langle Y_0^l\rangle$ and $\frac{d\sigma}{dmdt}\langle \cos\psi\, Y_0^l\rangle$ in the low t region ($0.01 < |t| < .2$ GeV^2)

shown in fig.1, where the helicity zero moments of angular distribution for 100% transversely polarized protons are given as function of the mass of the pion pair. Small four momentum transfer to the nucleons ($0.01 < |t| < 0.2$ GeV^2) has been selected. The spherical harmonics Y_0^1 are

expressed in the t channel (or Gottfried-Jackson) angles of the π^-. ψ is the angle between the normale to the production plane ($\vec{P}_n \times \vec{P}_{Beam}$) and the (transverse) polarisation direction of the target. There is a preliminary uncertainty of 25% between the polarisation dependent moments $\langle \cos\psi \, Re Y^1_m \rangle$ obtained in this experiment and the polarisation independent moments $\langle Re\, Y^1_m \rangle$ taken from the hydrogen experiment /1/.

Supprising is the large size of the polarisation dependent moments in this t-range which was supposed to be dominated by one pion exchange and should therefore show little or no nucleon polarization effect. For the left-right-asymmetry which is given by the ratio of the moments

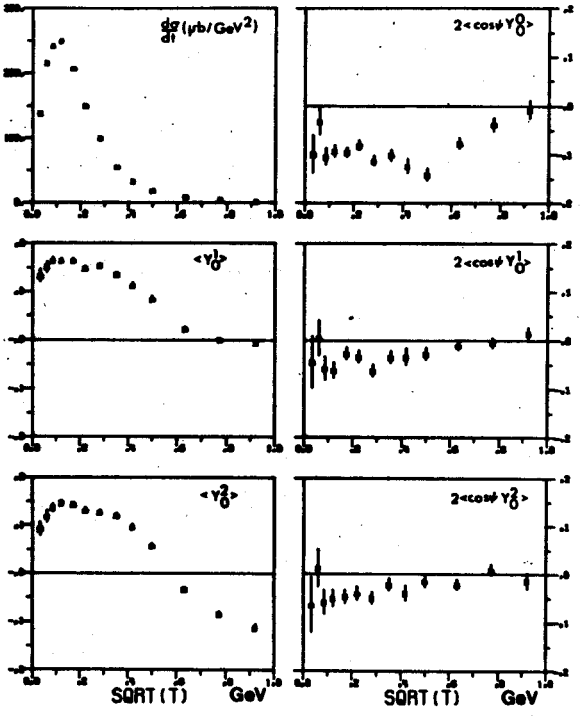


Fig.2. t-dependence of Cross section $\frac{d\sigma}{dt}$ and normalized moments $\langle Y^i_0 \rangle$ and $\langle \cos\psi Y^i_0 \rangle$ for the ρ-mass region ($.71 < m_{\pi\pi} < .83$) $2\langle\cos\psi\, Y^1_0\rangle / \langle Y^1_0\rangle$ one obtains 0.35 in the ρ mass region.

The occurence of $\langle \cos\psi \, Re\, Y^1_m \rangle$ moments requires the simultaneous presence of nucleon spin flip and nonflip amplitudes for equal naturality of the exchange. The moment $\langle \cos\psi \, Y^1_0 \rangle$ for example is given by the interference of the (unnatural) S wave and P wave helicity zero amplitudes (assuming absence of D and higher waves) with different nucleon spin flip.
$[2\langle \cos\psi\, Y^1_0 \rangle = Im(n_0 f_s - n_s f_0)\ f..\ f(p),\ n..\ nonf(p)]$
The corresponding moments $Re\langle Y^1_m \rangle$ combine flip with flip and nonflip amplitudes

The $\langle \cos\psi \, Re\, Y^1_m \rangle$ moments resemble (with opposite sign) the $\langle Re\, Y^1_m \rangle$ moments in the low t region where natural parity exchange is small. Earlier investigations of the density matrix /2/ showed the vanishing of one unnatural eigenvalue in the ρ mass region. This in turn gives a relation between nonflip and flip amplitudes $\eta = c f$ with the complex constant c independent of spin and helisity of the π-pair system. One then obtains a constant ratio

$$R = \frac{2\langle \cos\psi \, Re\, Y^1_m \rangle}{\langle Re\, Y^1_m \rangle} = \frac{2\, Im\, c}{1 + |c|^2}$$

for all moments or moments combinations which contain only unnatural parity exchange amplitudes. The relation seems to work in the limited region where it be has been tested. R decreases with m and has no strong variation with t in the ρ mass region. The minimum nonflip amplitude is obtained by assuming c pure imaginary. In the mass region this assumption holds to A_1-exchange (unnatural parity exchange nucleon spin nonflip) amplitude of roughly 20% of the corresponding flip amplitudes.

Amplitude analysis

A model independent determination of nucleon spin flip and nonflip amplitudes is not possible from this experiment since the polarization of the recoiling neutrons is not measured. One can however determine two sets of "transversity" amplitudes g and h corresponding to a polarization of the neutron perpendicular to the production plane $[g^u = \frac{1}{\sqrt{2}}(n^u + i f^u),\ h^u = \frac{1}{\sqrt{2}}(n^u - i f^u),\ g^N = \frac{1}{\sqrt{2}}(n^N - i f^N),$ $h^N = \frac{1}{\sqrt{2}}(n^N + i f^N)$, n and f-nonflip, flip, indeos N, u - natural, unnatural parity exchange. The relative phase between the set of g and the set of h - amplitudes remains unmeasurable.

Up to the ρ mass region where only s and P waves have to be considered 14 real quantities (8 amplitudes and 6 relative phases) are determined by 15 moments ($6\langle Re\, Y_m^l\rangle$, $6\langle \cos\psi\, Re\, Y_m^l\rangle$ and $3\langle \sin\psi\, Im\, Y_m^l\rangle$ moments) giving one constraint Suitable combination of the moments allows a splitting of the set of 15 equations into 4 subsets which can be solved analytically. The analysis has been performed in the ρ mass region ($.71 < m < .83$) for several bins in t. The analytical solution were taken as starting values for a χ^2 minimalization to satisfy the constraint. In most cases only one unique result for the magnitude of the amplitudes was obtained. The question of phase ambiguities is still under investigation.

The solutions for the transversity amplitudes of the S-wave (g_S, h_S), the helicity zero P_0 - wave (g_α, h_α - the helicity one unnatural parity exchange P_- - wave (g_U, h_U) and the natural parity exchange P_+-wave (g_N, h_N) are shown in fig.3. The solid curves are obtained from a fit

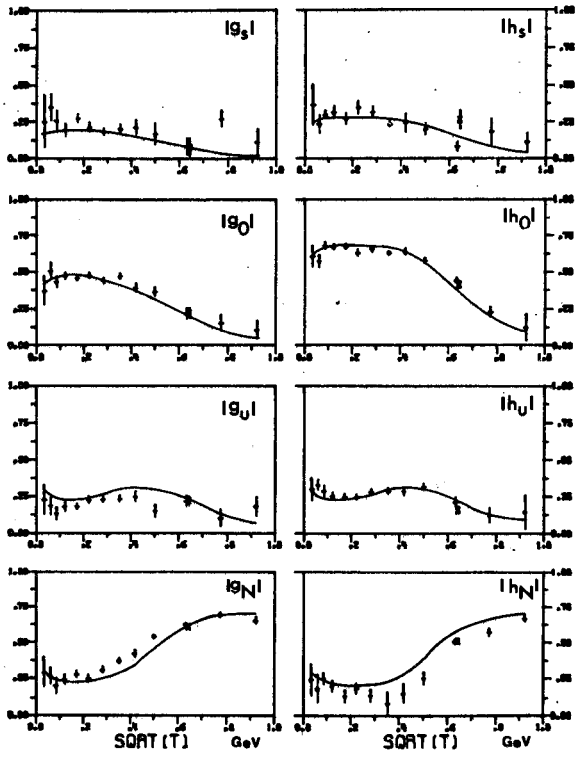


Fig.3. t-dependence of "nucleon transversity" amplitudes in the ρ-mass region ($.71 < m_{\pi\pi} < .83$).

of the moments by adding A_1 and A_2 exchange to the "poor man s absorbtion"model[3,4]. The amplitudes are normalised so that the squares enter with equal weight in the cross section.

Without the presence of nonflip amplitudes g and corresponding h amplitude would have the same magnitude. A lower limit for the nonflip amplitude is given by relation

$$|n| > |\,|g| - |h|\,|/\sqrt{2}\,.$$

The knowledge of the transversity amplitudes allows a determination of the intensity

$$|n|^2 + |f|^2 = |g|^2 + |h|^2$$

for each partial wave separately (fig.4) and

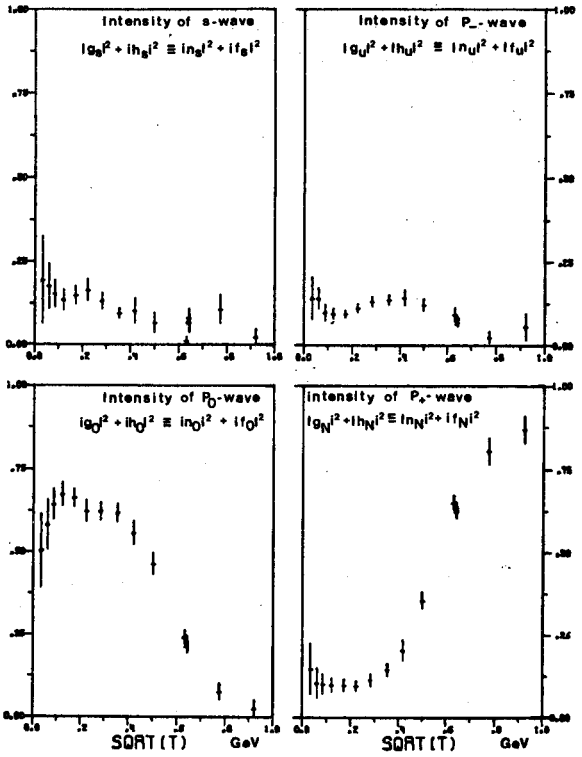


Fig.4. Intensities of the partial waves calculated from the transversity amplitudes.

therefore a exact splitting of the cross section into natural and unnatural parity exchange contributions.

Conclusions

The strong nucleon polarization effect found in a kinematic region which was supposed to be dominated by one pion exchange was completely unexpected. If it is due to the exchange of an addi-

tional particle this object has the quantum number of the A_1. Possibly it can also be explained-similarity to the helicity one moments in one pion exchange - by final state interaction. The problem is of particular interest for $\pi\pi$ scattering as A_1 exchange has been assumed to be absent in all $\pi\pi$ phase hift analysis. A continuation of the unfinished analysis will hopefully clarify the situation.

Referenoes

1. G.Grayer et al.Nucl.Phys.,B75(1974)189.
2. G.Grayer et al.Nucl.Phys.,B50(1972)29.
3. P.K.Williams,Phys.Rev.D1(1970)1312.
4. B.Hyams et al.Nucl.Phys.,B100 (1975) 205.

PARALLEL SESSION ON BARYON SPECTROSCOPY

RESONANCES AND RESONANCE PARAMETERS FROM A πN PARTIAL WAVE ANALYSIS BETWEEN 0.8 AND 2.0 GeV/c

R.E.Cutkosky, R.E.Hendrick
Carnegie-Mellon University, Pittsburgh,

R.L.Kelly
Lawrence Berkeley Laboratory, Berkeley, California

Phenomenological models of baryon structure have been studied with increasing interest in recent years. The SU(6)xO(3) harmonic oscillator model proposed by Greenberg, and its relativistic[2] and diquark[3] variations, have had notable success in reproducing the observed baryon mass spectrum. More recent developments such as the "dual string"[4] and "bag"[5] models of baryons have again focused attention on the spectrum of baryon resonances.

The primary source of information to test such models comes from partial wave analyses. For distinguishing among models, resonances on non-leading trajectories are of critical importance. It is hard to study such resonances, because they occur in partial waves which have low statistical weights and which are strongly affected by phase ambiguities. They also have small inelasticities and tend to overlap.For the unbiased determination of resonances in low partial waves, accurate data and sophisticated partial wave analysis methods are necessary.

We have analyzed amalgamated pion proton scattering data at 26 momenta in the range $0.8 \leq P_{lab} \leq 2.0$ GeV/c using the accelerated convergence expansion (ACE) method, in which higher partial waves are not required to vanish, but are determined by particle exchange processes and by extrapolation from lower partial waves. Dispersion relations along curves which lie within the physical region for scattering were used to remove ambiguities and to generate predicted amplitudes at each energy.

Refitting at each energy checked, these predictions and provided more precise fits.

Using some supplementary partial wave amplitude outside our energy range, the energy dependence of the partial waves was parametrized for I = 3/2 and I = 1/2. We confirm the existence of several resonances which have not been seen clearly in previous analyses. Resonance parameters have been determined. For the first time, positions (W) and residues (R) of poles have been determined for resonances in our energy region from EPWA. The SU(6)xO(3) assignment of these resonances is, in general, consistent with conventional baryon models[6]. The D35(1925 MeV) resonance, which we confirm, is not readily accomodated by standard harmonic oscillator quark models. We identify this resonanee as a member of a $(56,1^-)$ multiplet, and present a new phenomenological baryon model in which this multiplet is nearly degenerate with the $(56,2^+)$ multiplet.

To summarize, the main feature of our method is that we make extensive use of analyticity properties in both t and ν, which makes it possible for us to obtain a unique fit[7]. The fit is better determined for I = 3/2 than for I = 1/2, because the present π^+p data is more precise than the π^-p data, and because there is no much charge exchange data. At all stages of the analysis, strenuous efforts are made to keep track of errors and to propagate them correctly into the final results.

Resonances in partial waves are parametrized by the product of unitary factors: $S = S_R S_B$, where S_R is a modified Breit-Wigner resonance formula, in which the energy dependence of the width is given by elastic and quasi-two-body phase space factors. The background factor S_B includes resonances at higher and lower energies as fixed factors.

Table 1 gives the parameters for a number of well determined resonances which lie entirely within the energy region of our analysis.

TABLE 1

Resonances from CMU-LBL Analysis

Mass, Width, and Pole Parameters

Unit = MeV

Errors Listed Below Entry

	M	Γ	x	W_{re}	$-W_{im}$	R_{re}	R_{im}
P_{33}	1690	360	.135	1610	127	11	-22
	28	100	20	23	10	6	7
P_{31}	1940	380	.225	1863	125	-4	-27
	30	130	25	15	17	5	5
F_{35}	1885	310	.140	1825	125	13.5	-11
	27	90	8	12	18	3.5	5
F_{37}	1945	305	.396	1895	130	50	-25
	7	40	10	10	12	6	9
D_{33}	1695	275	.130	1645	115	11	-10
	20	70	7	23	24	4	4
D_{35}	1925	350	.133	1860	138	12	-15
	20	100	13	15	20	3	4
D_{13}	1658	75	.130	1657	38	4	-3
	10	35	20	12	17	2	2
D_{15}	1678	168	.428	1657	74	29	-14
	4	14	10	4	5	4	3
F_{15}	1684	129	.628	1672	61	37	-10
	4	8	12	4	4	4	4

These have all been considered well established, except for the P33(1960), D35(1925), and D13 (1660). The partial wave amplitudes for these three are shown on the figures; the results of energy independent fitting are shown as data points and the curves show the fit. The fit is also shown in the Argand plot, with arrows at miltiples of 50 MeV.

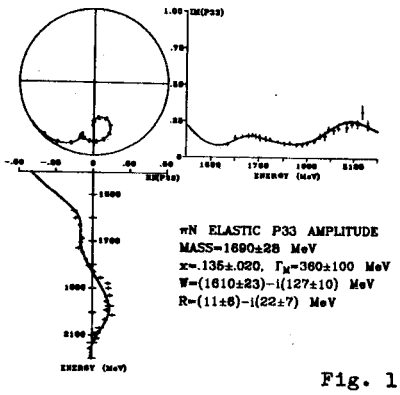


Fig. 1

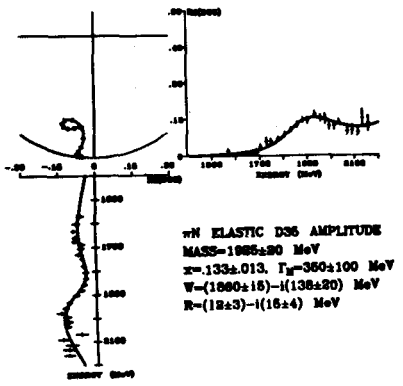


Fig. 2

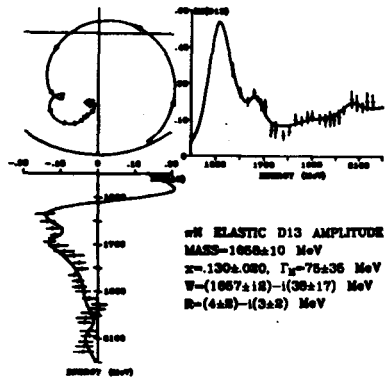


Fig. 3

Table 2

SU(6) x O(3) States Observed in πN Scattering

CMU-LBL Analysis

Multiplet $[N_{SU(6)}\ L^P]$	I = 1/2 States	I = 3/2 States
$[56,0^+]$	P_{11} 938$^+$ P^*_{11} 1467$^+$ P^{**}_{11} 1810$^\xi$	P_{33} 1233$^+$ P^*_{33} 1690$^\#$
$[56,2^+]$	P_{13} 1860$^\xi$ F_{15} 1684$^\#$ F^*_{15} 1965$^\xi$	P_{31} 1940 P_{33} 2130$^\xi$ F_{35} 1885$^\#$ F_{37} 1945$^\#$
$[56,4^+]$	F_{17} 1965$^\xi$ H_{19} 2260$^+$	F_{35} – F_{37} – H_{39} – $H_{3,11}$ –
$[79,1^-]$	S_{11} 1550$^+$ D_{13} 1520$^+$ 1624$^+$ 1661$^\#$ D_{15} 1678$^\#$	S_{31} 1634$^+$ D_{33} 1695$^\#$
$[70,3^-]$	D_{13} 2065$^\xi$ D_{15} – 2300$^\xi$ G_{17} 1995$^\xi$ 2191$^+$ G_{19} 2220$^+$	D_{35} 2300$^{+\xi}$ G_{37} 2200$^{+\xi}$
$[56,1^-]$	S_{11} D_{13} 1920$^\xi$	S_{31} 2070$^\xi$ D_{33} 2070$^\xi$ D_{35} 1925$^\#$

* Radial excitation.

$^+$ Uses some additional partial wave data.

$^\xi$ Resonance parameters not definite.

$^\#$ Uncertainties on parameters given in Table 1.

The P33 (1690) was seen by Almehed and Lovelace[8] but not by Ayed et al.[9] or Pietarinen[10]. However the Argand plots are not very different; at issue is the method of determining resonances. The P33 (1690) has a rapidly moving background from the tails of the P33 (1230) and of a third resonance at a higher energy. The resonance loop has turned into a cycloid with a "speed" minimum at the resonance energy. The D35(1925) was reported by Ayed, et al. and several other groups. In our analysis this shows up very clearly. Because of the importance of this state for the evaluation of models, we made many tests to check that it is required by the data. The D13(1660) was also reported by Ayed et al. However, our mass value is some what less and the resonance is narrower.

Our suggested SU(6)xO(3) assignments for these resonances are presented in Table 2. Resonances which lie entirely or in part outside our data region (but parametrized by us) are also listed. We have also listed a number of additional resonances from our analysis for which we do not get have reliable estimates of resonance parameters or errors. The P33(1690) and D13(1660) are needed to fill out SU(6)x xO(3) multiplets. However, we assign the D35(1925) to a new multiplet, $(56,1^-)$. We consider the mass to be too low for the alternative $(70,3^-)$ assignment (there is also some evidence for a second D35). There is some indication of S31, D13 and D33 resonances which could be either in this $(56,1^-)$ or in a second $(70,1^-)$.

The familiar 3-quark harmonic oscillator model does not predict a $(56,1^-)$ multiplet in the 1900 MeV region. Dual string models, however, suggest the existence of additional daughter states degenerate with those on leading trajectories. To pursue this idea in

a phenomenological model, we consider baryons as made up of 4 massless partons: 3 valence quarks and a neutral, colorness, scalar "monad" which represents the energy and momentum carried by gluon fields or non-valence quarks. The leading term in the potential energy is proportional to the minimum possible length of "colored strings" required to join the partons. This potential energy favours configurations in which the partons lie along a line, and also configurations with a quark-diquark structure. For configurations in which the partons form two clusters, an approximate calculation gives

$$M \approx 8\kappa T\left[L + \tfrac{1}{2} + \sqrt{2}\,(N+\tfrac{1}{2})\right] + const.$$

where L is the orbital angular momentum, N is the number of radial nodes, T is the tension, and K is the number of strings required to join the clusters. If all quarks are in one cluster separated from the monad, $K=2$; otherwise $K=1$. For $K=1$ we have the usual quark-diquark states $(56, L^{+}_{even})$, and $(70, L^{-}_{odd})$ while $K=2$ gives $(56, L^{\pm})$; the ground atate $(56, 0^{+})$ is identified with both sequences. The new multiplet $(56, 1^{-})_2$ is nearly degenerate with the $(56, 2^{+})_1$, while the radially excited $(56, 0^{+})_{1*}$ has a lower energy, in agreement with the observed masses of the P11 and P33 resonances.

References

1. O.W.Greenberg, Phys.Rev.Lett., 13, 598 (1964); O.W.Greenberg and M.Resnikoff, Phys.Rev., 163, 1844 (1967).
2. R.P.Feynman, M.Kislinger and F.Ravndal, Phys.Rev., D3, 2706 (1971).
3. A.N.Mitra and D.L.Katyal. Nucl.Phys., B5, 308 (1968); D.B.Lichtenberg. Phys.Rev., 178, 2197 (1969).
4. S.Mandelstam. Phys.Rev., 13C, 260 (1970). I.Bars and A.J.Hanson. Phys.Rev., D13, 1744 (1976).
5. A.Chodes et al. Phys.Rev., D9, 3471 (1974), Phys.Rev., D10, 2599 (1974); W.A.Bardeen et al. Phys.Rev., D11, 1094 (1975).
6. R.Horgan and R.A.Dalitz. Nucl.Phys., B66, 135 (1973).
7. For further details, see R.F.Cutkosky et al. Oxford Baryon Resonance Conference (July, 1976), Proceedings (to be Publ.).
8. S.Almehed and C.Lovelace. Nucl.Phys., B40, 157 (1972).
9. R.Ayed and P.Bareyre, private communication to the particle data group, 1974.
10. E.Pietarinen. Oxford Baryon Resonance Conference (July, 1976) Proceedings (to be published).

A π^+PROTON PARTIAL WAVE AMPLITUDE ANALYSIS FOR P_{lab}= 1.6 UP TO 10 GEV/C*

Archibald W.Hendry

Indiana Univ. Bloomington IN 47401

This paper reports on a partial wave amplitude analysis of π^+p elastic scattering over a large energy range, extending from p_{lab} =1.6 GeV/c up to 10 GeV/c. The aim of the analysis is to try to determine the contributions of at least the dominant resonanoes, and thereby obtain a olearer understanding of particle interactions in this region.

Because many partial waves are important, a standard type of analysis, in which each p.w. is parametrized separately, was not used. Instead, a method which inoorporates some aocepted physical ideas - diffraotion and peripheral scattering - was employed. The real and imaginary parts of the p.w. amplitudes were first parametrized in terms of distributions in b, the impact parameter, eaoh part containing a diffractive pieoe (main contribution from low b) and a peripheral piece (main contribution from partial waves centered around $b=\tau$, where τ is allowed to be energy dependent). Good fits oan be obtained to the data with this simple parametrization, though our final fits were achieved by subsequently letting the individual p.w. amplitudes vary freely.

Our p.w. amplitudes have the desirable feature of being close to those of previous analyses[1] at the lower momenta, and close to the Regge solutions[2] at the higher energies. We might also mention that the experimental data for π^+p polarization near the backward direction (which has pronounced structure that oscillates in a very definite way as p_{lab} increases) was particularly helpful in the analysis.

The analysis was carried out at 14 energies. The resulting Argand diagrams for the p.w. amplitudes $kf_{l\pm}$ show interesting loop structures from whioh one can extract resonance parameters (mass, elasticity x and full width Γ).

A very striking pattern emerges for these high mass, high spin resonances. To illustrate this, we have plotted in Fig.1 the spin j of the resonances against the corresponding c.m. momentum k in the pion-nucleon system; the dominant resonances that we observe seem to lie on two straight line trajectories whose equations are

$$j + \tfrac{1}{2} = kR \qquad \text{for the } f_{l+} \text{ resonances}$$
$$j + \tfrac{3}{2} = kR \qquad \text{for the } f_{l-} \text{ resonances}$$

with R is approximately 1.1 Fermi for both trajectories. Elasticity x decreases with higher spin, while the total width Γ increases. As shown in Fig.2, an interesting feature appears when we calculate the $N\pi$ partial widths - the event parity states consistently have greater $N\pi$ partial widths than the odd parity states of the same spin.

We have started to examine how these resonances can be accommodated in quark excitation schemes[3]. If one allows for radial excitations etc., the allocation of these high spin resonances is not unique. However a detailed calculation of the $N\pi$ decay rates should provide some strong clues about the higher lying 56 and 70 representations (L=3,4,...10).

References

1. Ayed et al., quoted by Particle Data Group, Rev.Mod.Phys., 48 (1976).
2. V.Barger and R.J.N.Phillips. Phys.Rev., 187 2210 (1969).
3. O.W.Greenberg. Phys.Rev.Lett.,13, 597 (1964). R.H.Dalitz. Proc.Irvine Conf.(1967). D.Faiman and A.W.Hendry. Phys.Rev., 173, 1720 (1968) and 180, 1572 (1969).

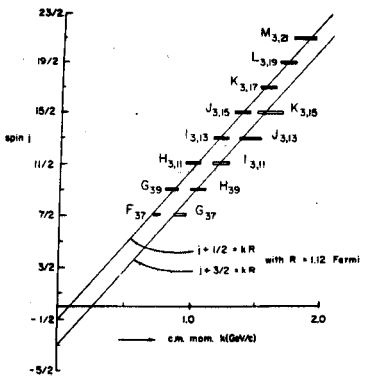


Fig.1. Spin j of resonances plotted against k, the πN c.m. momentum.

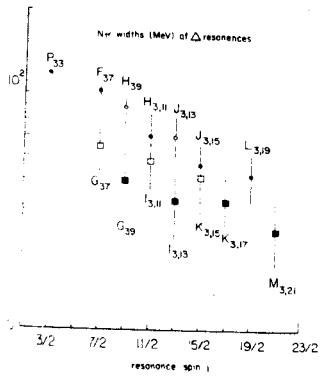


Fig.2. $N\pi$ widths plotted against resonance spin j.

INVESTIGATION OF THE NATURE OF ENHANCEMENTS OBSERVED IN Λp EFFECTIVE MASS SPECTRA

B.A.Shahbazian, P.P.Temnikov, A.A.Timonina, A.M.Rozhdestvensky
JINR, Dubna

The inclusive Λp effective mass spectrum from the interactions of 7 GeV/c average momentum neutrons with carbon nuclei has been investigated. Four enhancements have been discovered in it.

The comparison of physical and experimental conditions at which these peaks have been observed in this and other experiments /1-3/, suggests that they should be the manifestations of peculiarities of the Λp elastic scattering and $\Lambda\Sigma^-$ and $\Sigma\Lambda^-$ conversion effective cross sections.

To analyze this hypothesis, a model of creation and interactions of Λ^- and Σ^- hyperons in carbon nuclei, bombarded with 7 GeV/c average momentum neutrons, has been developed.

The model proposed is based on impulse approximation, which is valid in our case firstly because the neutron energy considerably exceeds the nucleon binding energy in the carbon nucleus and secondly because we consider only the low mass part (2053.859-- 2553.859) MeV/c^2 (or the relative momentum interval p_Λ = 0. - 2.0 GeV/c) of the whole Λp effective mass spectrum which extends in this experiment up to ~ 4800 MeV/c^2.

The most important intranuclear cascade processes resulting in the Λp + (Anything) and Λpp + (Anything) final states, which form the statistical sample of this experiment, have been modelled. For this purpose all known experimental data on Λ^- and Σ^- hyperon production, their two-body interactions with nucleons and decay processes /1,4/ have been used. The geometrical and kinematical restrictions imposed by this experiment have been accounted for.

The expected smallness of the ratio of resonance widths to the difference of their masses permitted us to use the isolated resonances approximation [5] . For the same reasons and what is more, because the low energy and potential scattering amplitudes vary with the Λp effective mass in opposite ways, it turned out possible to neglect all interference terms.

Thus the Λp elastic scattering effective cross section has been expressed as a sum of four cross sections corresponding to the low energy scattering with scattering parameters $a_s = a_t = a$ and $r_s = r_t = r$, elastic resonance scattering with parameters M_2, Γ_2 and M_3, Γ_3 and of the potential scattering. The last cross section has been assumed to be proportional to the two-body Λp phase space volume $R_2(M_{\Lambda p})$. Namely, $\sigma_{pot}^{\Lambda p}(M_{\Lambda p}) = \pi R^2 R_2(M_{\Lambda p})$, where R is an average range of the Λp interaction forces. This experiment did not permit us to account for the elastic Λp scattering and $\Sigma\Lambda$ - conversion channels coupling effects. So the $\Lambda\Sigma$ - and $\Sigma\Lambda$ - conversion processes contributed independently of the elastic scattering. The least square analysis resulted in all above mentioned parameters and moreover the contributions A,B,C,D of the elastic Λp scattering, $\Lambda\Sigma$ - and $\Sigma\Lambda$ conversion processes as well as of the independent Λ and proton creation in intranuclear cascade processes. The results of fits presented in table I clearly show that the best fit parameters for the Λp effective mass spectrum fit $(M_{\Lambda p} - fit)$ do not differ significantly from those for simultaneous Λp effective mass spectrum and elastic scattering effective cross section fit $((M_{\Lambda p} + \sigma_{\Lambda p}^{el}) - fit)$. We come to the following conclusions.

1. The analysis, performed in the frame of this model, permitted us to sucessfully describe not only the Λp effective mass spectrum with its enhancements, i.e., the results of the Λp enhancement production experiment but also the behaviour of the Λp elastic scattering effective cross section in the Λ - hyperon relative momentum interval P_Λ = (0.1–2.0) GeV/c, i.e., the results of the Λp enhancement formation experiments. This is demonstrated in Figs.1 and 2.

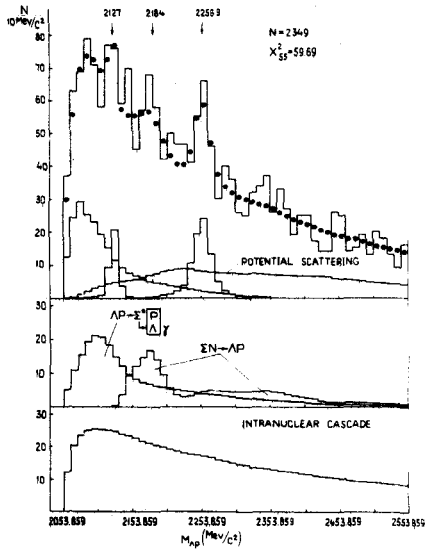


Fig. 1

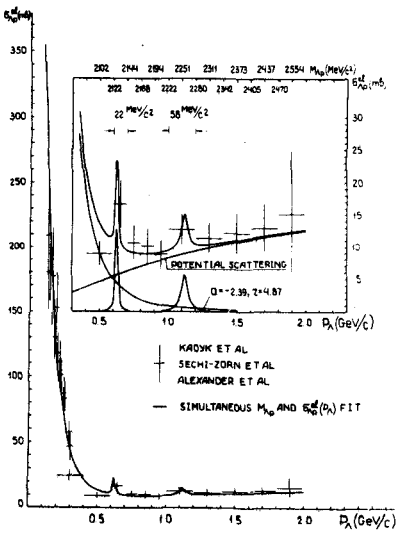


Fig. 2

2. The peak near the Λp threshold is due to the negative sign Λp scattering length effect at low energy. The negative scattering length excludes the possibility of the existence of (Λp) bound states. The unsuccessful up to now search for the Λ - hyperdeuteron confirms this result.

3. The peaks at 2127 MeV/c^2 and 2257 MeV/c^2 are due to the Λp elastic narrow resonances at 620 MeV/c and 1120 MeV/c of relative Λ hyperon momenta, respectively (fig.2).

4. The enhancement near 2184 MeV/c^2 is of kinematical origin and is due to the two-step process $n\,{}^{12}C \to (\Sigma N)$ +(Anything), $\Sigma N \to \Lambda p$.

5. The average range of the Λp interaction forces is about 0.66 fm.

6. The components of the average polarization of Λ- hyperons, presumed to be daughters of Λp - systems along the beam direction P_z, normal to the Λp -production plane - P_y and normal to both these directions - P_x, are zero within the limits of errors.

7. It is shown that all these results are very stable with respect to considerable changes of the Λp - and ΣN- c.m.s. angular distributions used to model various processes.

The neglect of interference terms in the expressions for the Λp scattering effective cross section, as well as the assumption $\Gamma_{tot} \approx \Gamma_{el} \approx \Gamma_R$ and the use of the isolated resonance approximation, are justified due to the narrowness of the resonance widths and the total precision of this experiment (Table 1, IVth col.).

8. It is shown that light nuclei, carbon nucleus at least, could be used as high density nucleon targets to study low energy scattering of unstable particles on nucleons in the absence of monoenergetic beams of such particles.

9. With the increase of the atomic number of nuclei one can expect the wearing perhaps even disapearing of enhancements because of the increasing probability of rescattering in heavy nuclei.

10. The effective cross sections of the observed Λp resonances have been estimated: $\sigma^{el}_{\Lambda p}(620)=12.80$ mb, $\sigma^{el}_{\Lambda p}(1120)=5.61$ mb (fig.2).

The authors are indebted to prof.A.M.Baldin for the continious interest and support of this work.

Table 1
The results of fitting

	$M_{\Lambda p}$ -fit	$(M_{\Lambda p}+\sigma^{el}_{\Lambda p})$ -fit	$(M_{\Lambda p}+\sigma^{el}_{\Lambda p})$ -fit for isotropic c.m.s. distributions over $\cos\theta_{\Lambda\Lambda}, \cos\theta_{\Lambda\Sigma}, \cos\theta_{\Sigma\Lambda}$
χ^2_n	$\chi^2_{34}=34.39$	$\chi^2_{55}=59.69$	$\chi^2_{55}=59.57$
C.L.(%)	44.92	31.56	31.92
a (fm)	-2.30±0.35	-2.39±0.04	-2.38±0.05
r (fm)	4.73±0.50	4.87±0.05	4.82±0.06
M_2(MeV/c^2)	2126.30±1.66	2127.00±3.38	2127.60±2.29
Γ_2 (MeV/c^2)	3.78±0.92	3.76±0.96	3.94±1.00
M_3(MeV/c^2)	2256.40±3.12	2256.90±1.33	2256.80±2.86
Γ_3 (MeV/c^2)	15.97±4.40	15.55±4.20	17.05±4.55
A($\Lambda p \to \Lambda p$)	0.332±0.008	0.336±0.005	0.345±0.018
B($\Lambda p \to \Sigma p$)	0.117±0.005	0.109±0.003	0.099±0.021
C($\Sigma\Lambda$)	0.081±0.004	0.083±0.004	0.083±0.023
D(i.c.b.)*	0.469±0.004	0.471±0.005	0.471±0.026
R (fm)	0.656±0.020	0.664±0.015	0.666±0.025

*i.c.b. - intranuclear cascade background.

REFERENCES

1. B.A.Shahbazian et al. Physics of Elementary Particles and Atomic Nuclei, v.4, part 3, 811(1973);
Nucl.Phys., B53, 19 (1973); Lett. Nuovo Cim., 6, 63 (1973); JINR, Dubna, E1-7669, 1974.
2. Tai Ho Tan. Phys.Rev.Lett., 23, 395 (1969);
D.T.Cline et al. Phys.Rev.Lett., 20, 1452 (1968);
D.Eastwood et al. Phys.Rev.,D3, 2603 (1971).

3. J.T.Read et al. Phys.Rev.,165, 1495 (1968).
4. J.A.Kadyk et al. Nucl.Phys., B27, 13 (1971);
G.Alexander et al. Phys.Rev., 173, 1452 (1968);
B.Sechi-Zorn et al. Phys.Rev., 175, 1735 (1968);
O.Benary et al. A Compilation of YN Reactions, UCRL-20000 YN (1970).
5. G.Breit. Theory of Resonance Reactions and Allied Topics Handbuch der Physik, Band XL 1/1 S.1, Springer-Verlag, 1959.

KN SCATTERING AND THE PROBLEM OF THE S=+1 BARYON RESONANCES

G. Giacomelli

Istituto di Fisica dell'Università di Bologna, Italy
Istituto Nazionale di Fisica Nucleare, Sezione di Bologna

1. Introduction

This report will summarize the present situation on low energy KN scattering and will discuss in particular the following contributions to this conference:

1. BCRT coll.: Quasi two-body K^+N interactions below 1.5 GeV/c[1];
2. BCRT coll.: Phase shift analysis of $K^+p \to K^*\Delta$ below 1.5 GeV/c[2];
3. BEGPR coll.: Study of $K^0_L p \to K^0_S p$ in $1490 < E_{cm} < 1700$ MeV[3];
4. BP coll.: Angular distribution for the $K^0_L p \to K^0_S p$ in 1600 E_{cm} 1900 MeV;
5. PNL Measurement of $K^+n \to K^0p$ at 0.7, 0.8 and 0.9 GeV/c[5].

Low energy KN scattering data have been discussed in terms of phase shift analysis of various complexity. We shall limit our considerations to the simplest ones, using the phase shift analyses as a method for searching for resonant states and/or for the parametrization of the experimental data.

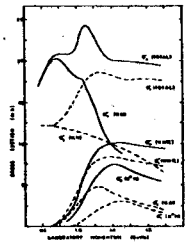


Fig. 1. Total, elastic and inelastic cross sections in I = 1 and I = 0 [1]. The curves are hand drawn through the experimental points.

Fig. 1 [1] illustrates the present knowledge on low energy K^+N scattering in both I = 1 and I = 0 states: the K^+p total cross section has an asymmetric structure at a lab. momentum of 1.25 GeV/c. The structure arises from a slowly varying elastic cross section and the opening up of inelastic channels, dominated by the $K^+p \to K^0\Delta^{++}$. The structure may thus be thought to be a threshold effect for the $K\Delta$ channel.

The K^+N, I = 0 total cross section has a shoulder at 0.8 GeV/c and a peak at 1.15 GeV/c. The shoulder corresponds to a peak in the elastic cross section, while the peak at 1.15 GeV/c is connected to the opening up of the $K^*(890)N$ channel.

The isospin structure of the various elastic channels is:

$$K^+p \to K^+p \qquad Z_1 \qquad (1)$$
$$K^+n \to K^+n \qquad \tfrac{1}{2}(Z_1 - Z_0) \qquad (2)$$
$$K^+n \to K^0p \qquad \tfrac{1}{2}(Z_1 + Z_0) \qquad (3)$$
$$K^0_L p \to K^0_S p \qquad \tfrac{1}{4}(Z_0 + Z_1 - 2Y_1) \qquad (4)$$

where Z_1, Z_0 denote the strangeness + 1, isospin 1 and 0 amplitudes, while Y_1 denotes the strangeness − 1, isospin 1 amplitude.

2. $K^+p \to K^+p$

The amount of data available on K^+p elastic scattering is quite large and of good accuracy[6]. No new data have been presented at this conference. It would be nice to have measurements of the P-parameter at 0.5 ÷ 0.8 GeV/c and some measurements of the A and R parameters.

The most recent phase shift analyses[7] go to 2.5 GeV/c and use many theoretical refinements. The analyses agree qualitatively, but there are quantitative disagreements. For instance at 0.8 GeV/c there are differences of up to a factor of two on the contribution of the $P_{3/2}$ cross section; the behaviour of the S-wave is not too well determined at high momenta.

It has been remarked long time ago [8] that the K^+p amplitudes are very similar to the background amplitudes in π^+p after the resonance contribution has been removed. In particular the behaviour of the $P_{3/2}$ amplitude, which has an appearance similar to a small resonance loop, is approximately reproduced in the π^+p amplitudes.

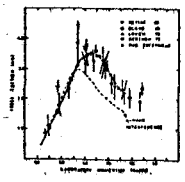
3. $K^+p \to K^0\Delta$

One of the difficulties connected with the study of the 1.25 GeV/c structure via the elastic scattering is its large inelasticity. One may thus hope to obtain new information from the study of the main enelastic channel in this energy region

$$K^+p \to K^0\Delta^{++}(1232) \quad \text{(}\hookrightarrow \pi^+p\text{)} \qquad (5)$$

The detailed analysis of (5) involves considerable difficulties of practical and theoretical nature: the amount of data for reaction (5) is neither as abundant nor as accurate as that for the elastic reaction. All data come from bubble chamber experiments and have typical statistics of 500 events per angular distribution. Fig. 2 shows the integrated cross sections computed with the empirical interference model and with the P-wave interference model; the two calculations differ by about 30% at the higher energies.

Fig. 2. Integrated cross sections for $K^+p \to K^0\Delta^{++}(1232)$ computed with the interference model (data points and solid line)[1]. The dashed line represents an eyeball fit through the cross sections computed with the P-wave interference model.



The phase shift analysis presented at this conference uses the formalism of Brody and Kernan and is energy dependent. The waves used are : SD1, PP1, PP3, DS3, DD3 and DD5. For each wave the following parametrization for the partial wave amplitude was used (for K > b):

$$F = \left[a(K-b) + c(K-b)^2\right] + i\left[d(K-b) + e(K-b)^2\right] \qquad (6)$$

a,b,c,d and e are parameters to be determined and K is the c.m.momentum. The parametrization involves 30 parameters, which is somewhat large as compared with the total of 481 data points used. On the other hand tests made with a smaller number of parameters (for instance fixing the b-threshold values) or changing the parametrization did not change appreciably the results.

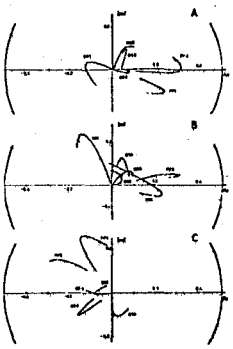


FIG. 3

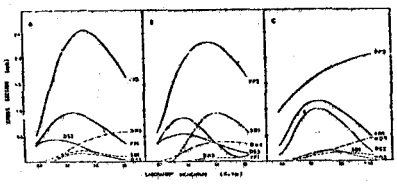


FIG. 4

Contributions of the partial waves to the $K^+p \to K\Delta$ integrated cross sections, for solutions A, B and C respectively.[2]

Argand diagrams for solutions A, B and C. The $K^+p \to K\Delta$ amplitudes are plotted in steps of 100 MeV/c, from 0,9 to 1.5 GeV/c.[2]

Fig. 3 shows the Argand diagrams for the three types of solutions found, while Fig.4 shows the contributions of the various partial waves to the integrated cross sections. The A and B solutions are favoured compared to the C solution. Both A and B show that the $K^+p \to K\Delta$ reaction is dominated by P-waves. S-waves are important, while the information on the higher waves is not significant.

In the solutions obtained there is no clear evidence for the formation of an exotic s-channel resonance. The solutions tend to explain the structure at 1.25 GeV/c as due to the superposition of various partial cross sections, the most prominent of which is the PP3 wave.

4. $K^+N \to KN$, I = 0

The amount of data available for the study of the $K^+N \to KN$, I = 0 channel is neither as abundant nor as accurate as for the $K^+p \to K^+p$. The data concern integrated cross sections and angular distributions. There is only one measurement, of limited statistics, of the P-parameter for charge exchange scattering at 600 MeV/c. One would clearly like to see more polarization measurements for both reactions (2) and (3), which until now have all been performed in deuterium bubble chambers. The uncertainties involved in deuterium reactions and the lack of polarization information have complicated all the analyses of the I = 0 channel.

At this conference new data on the charge exchange reaction (2) have been presented by a Brookhaven group[5].

A couple of years ago the BGRT collaboration performed a variety of phase shift analyses [9]. Three families of solutions were found: solution A, characterized by large S_1 and P_1 waves and solutions C, D characterised by a large P_1 wave. Solutions C and D are indistinguishable below 1 GeV/c; in solution D the $P_{\frac{3}{2}}$ wave has a resonant-like behaviour. Although the polarization data at 6 GeV/c and various other arguments favoured the C,D types of solutions, it is nice to have better indications in this sense, by other methods. One such method is offered by the study of the $K^0_L p \to K^0_S p$ channel [10].

5. $K^0_L p \to K^0_S p$

The results of two formation experiments with monochromatic/dichromatic K^0_L beams have been presented at this conference. The first experiment covers the K^0 lab. momentum from 0.32 to 0.79 GeV/c [3] and the second from 0.66 to 1.2 GeV/c [7]. Both have been performed with the CERN 2m bubble chamber; the K^0_L beam obtained from the associated production reactions $\pi^- p \to K^0\Lambda^0, K^+\Sigma^-$. Fig. 5, which shows the distribution of K^0_L momenta at six π^- beam momenta [3] indicates that the quality of the beam is good.

The absolute values of the integrated $K^0_L p \to K^0_S p$ cross sections are shown in fig. 6 [3]. These values have been mainly obtained from the knowledge of the $K^-p \to \Lambda^0\pi^0$ cross sections (which should be equal to those of the $K^0_L p \to \Lambda^0\pi^+$) and from the number of $\Lambda\pi^+$ events. This normalization procedure was sometimes checked experimentally using the number of τ -decays. Fig. 6 indicates that there are some fluctuations and some differences among the results of various groups.

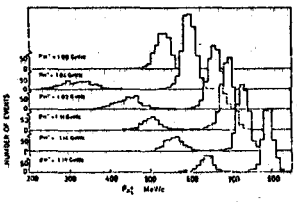


FIG. 5.

Distribution of K^0_L momenta for the 4-C fits events at six π^--beam momenta.[3]

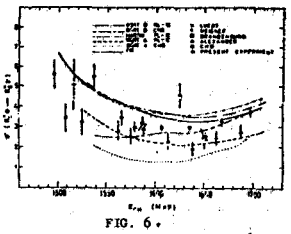


FIG. 6.

Integrated cross sections for $K^0_L p \to K^0_S p$. The curves are predictions from the combination of the amplitudes from different phase shift analyses.

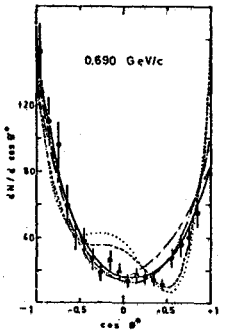


Fig. 7.

Unnormalized $K^0p \to K^0p$ angular distribution at 0.69 GeV/c compared with the predictions of previous phase shift analyses[3]. The notation is the same as in Fig.6.

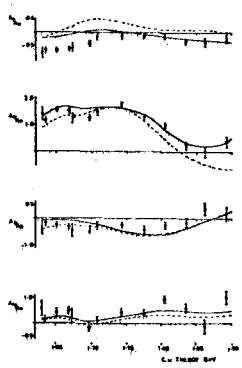


Fig. 8.

A_1/A_0 coefficients of the Legendre polynomial expansion.[7] The lines are the predictions of previous phase shift analyses: ... BGRT, A, ---- BGRT, C, BGRT, D, all with RL/IC solution for Y_1.

Fig. 7 shows a sample angular distribution at 0.69 GeV/c [3], while Fig. 8 shows the A_1/A_0 coefficients of the Legendre polynomial expansion [7].

Integrated cross sections, angular distributions and coefficients of the Legendre polynomial expansion have been compared with various predictions obtained using the amplitudes according to (1-4). For each combination of Z_0 and Z_1 amplitudes from the BGRT analyses a Y_1 amplitude has been taken, either from the RL/IC [11] or from the CH collaboration [12]. The various predictions are compared with the data in Figs. 6, 7 and 8. The angular distributions are sensitive to the choice of the Z_0 amplitude, while the integrated cross sections are equally sensitive to the choice of the Y_1 amplitude. The predictions of the angular distributions at 0.69 GeV/c (Fig.7) show that solution A gives a shape which is not seen in the data. This feature is seen at all energies, as indicated by the coefficients of the Legendre polynomial expansion (Fig.8, see in particular the A_2/A_0 coefficients). Thus the angular distributions prefer a C/D type of solution over the A-type. The same preference tends to be shown by the momentum dependence of the integrated cross sections, though their larger fluctuations and their sensitivity to the low partial waves in Y_1 solutions make the situation less clear.

From the results of these two new experiments we may conclude that the A-solution can be rejected. This is in agreement with the analysis of Cho et al. [13] and disagrees with that of Alexander et al. [14]. The data are not able to distinguish between solutions C and D.

6. Conclusion

The phenomenological knowledge of low energy KN scattering has improved further, in particular with the large amount of new data on the $K^0_S p \to K^0_S p$ channel. Correspondingly the number of acceptable phase shift solutions has decreased in number. Nevertheless there still is no unique answer on the problem of the existence of exotic resonances.

The I=1 structure at 1.25 GeV/c seems to be explained as due to the opening up of the $K\Delta$ channel, which in turn is due to a superposition of waves, tha most prominent of which is the PP3. The I = 0 structure at 1.15 GeV/c may have a similar explanation in connection with the opening up of the K^*N channel, but here the information is more scanty.

The best candidate for an exotic state remains the I=0 structure at 0.8 GeV/c. All analyses agree that the interaction is strongly attractive. The phase shift solution is either of the C or D type or something in between. Even if the final solution turns out to be the D-solution, one may be faced with the semantic definition of what is a resonance . It may be instructive to conclude this discussion comparing the properties expected for a Breit-Wigner resonance with those found for tha $P_{\frac{3}{2}}$ wave in the D-type solution:

Counterclockwise circle in Argand diagram	almost
Peak in partial cross section	yes
Phase δ goes through 0° or 90°	yes
absorption coefficient η = 1 or minimum	yes
speed goes through a maximum	probably no

I would like to thank many colleagues for useful discussions.

References
1. G. Giacomelli et al., Paper 1243/C2-15.
2. G. Giacomelli et al., Paper 1244/C2-16.
3. A. Bigi et al., Paper 1071/C2-12.
4. M.J. Corden et al., Paper presented at the Topical Conf. on Baryon resonances, Oxford 1976.
5. M. Sakitt et al., Paper 1066/C2-6.
6. G. Giacomelli et al., CERN-HERA 75-1 (1975).
7. R.E. Cutkosky et al., Nucl. Phys. B102 (1976) 139.
8. Litchfield, Proceedings of the 17th Int.Conf. on High Energy Physics, London (1974)
9. G. Giacomelli et al., Nucl. Phys., B71 (1974) 138.
10. G.W. London, Phys. Rev., D9 (1974) 1569.
11. Rutherford Report RL-75-182 (1975).
12. R. Armenteros et al., Nucl. Phys. B14 (1969) 91.
13. Y. Cho et al., Phys. Letters, 60B (1976) 293.
14. G. Alexander et al., Phys. Letters 58B (1975) 484.

PRODUCTION OF BARYON RESONANCES IN K^-p INTERACTIONS AT 4.2 GEV/C

W.Kittel

Amsterdam - CERN - Nijmegen - Oxford Collaboration

The Ξ^* resonances and the Ω^- observed in our high statistics K^-p bubble chamber experiment at 4.2 GeV/c are presented in the review by Barloutaud[1] in this session. I shall therefore restrict myself to the production of $\Sigma(1660)$ and of a $p\omega$ enhancement[3,4].

The reaction $K^-p \to \Sigma^+(1660)\pi^-$ was studied in a 65 event/μb sample of $\Sigma\pi\pi(\pi)$, $\Lambda\pi\pi(\pi)$ and $p\bar{K}^0\pi^-$ final states. As examples, the $\Sigma\pi\pi$ mass distributions are given in Fig. 1.

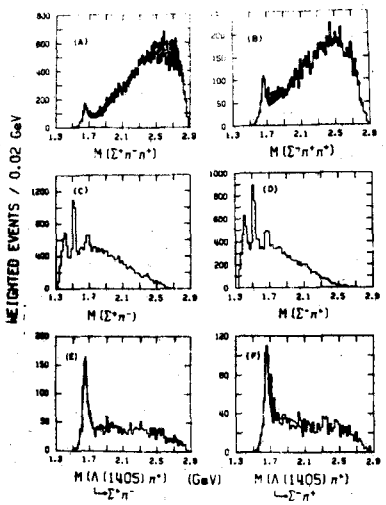


Fig. 1. Invariant mass distributions; (A) $M(\Sigma^+\pi^-\pi^+)$ from final state $\Sigma^+\pi^-\pi^+\pi^-$; (B) $M(\Sigma^-\pi^+\pi^+)$ from final state $\Sigma^-\pi^+\pi^+\pi^-$; (C) $M(\Sigma^+\pi^-)$ from final state $\Sigma^+\pi^-\pi^+\pi^-$; (D) $M(\Sigma^-\pi^+)$ from final state $\Sigma^-\pi^+\pi^+\pi^-$; (E) $M(\Sigma^+\pi^-\pi^+)$ from final state $\Sigma^+\pi^-\pi^+\pi^-$, where $1.34 < M(\Sigma^+\pi^-) \leq 1.44$ GeV; (F) $M(\Sigma^-\pi^+\pi^+)$ from final state $\Sigma^-\pi^+\pi^+\pi^-$ where $1.34 < M(\Sigma^-\pi^+) \leq 1.44$ GeV. The shaded areas correspond to events in the $\Lambda(1520)$.

We have confirmed the result of previous experiments that the $\Sigma(1660)$ produced in the decay mode $\Sigma\pi$ differs greatly in its production angular distribution from that produced in the mode $\Lambda(1405)\pi$ (see Fig. 2). The $\Sigma(1660) \to \Sigma\pi$

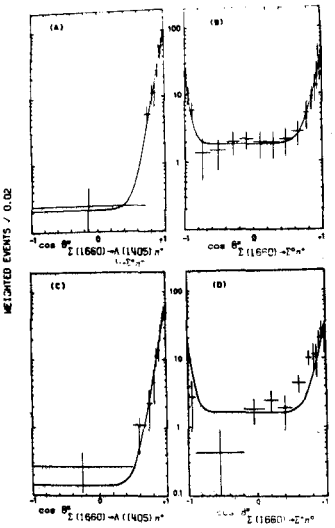


Fig. 2. Production angular distribution in the overall c.m.s. with background subtracted: (A) for $\Sigma(1660)\to\Lambda(1405)\pi^+\to\Sigma^-\pi^+\pi^+$ from final state $\Sigma^+\pi^-\pi^+\pi^-$; (B) for $\Sigma(1660)\to\Sigma^0\pi^+$ from final state $\Sigma^0\pi^+\pi^-$; (C) for $\Sigma(1660)\to\Lambda(1405)\pi^+\to\Sigma^-\pi^+\pi^+$ from final state $\Sigma^-\pi^+\pi^+\pi^-$; (D) for $\Sigma(1660)\to\Sigma^+\pi^0$ from final state $\Sigma^+\pi^0\pi^-$. The curves are the results of fits.

has a large forward peak, a small backward peak, and some production at intermediate angles; the $\Sigma(1660)\to\Lambda(1405)\pi$ is produced in the forward region only. This effect has been observed in experiments from 2.5 to 4.5 GeV/c. The simplest explanation is the existence of two $\Sigma(1660)$ resonances.

A moments analysis of the decay angle spherical harmonics of $\Sigma^+(1660)\to\Lambda(1405)\pi^+$ yields - by maximum complexity arguments - that the spin of the $\Sigma(1660)\to\Lambda(1405)\pi$ is $J\geq 3/2$. An Adair analysis suggests 3/2 for this spin. The absence of significantly non-zero odd-L moments makes the extended Byers-Fenster analysis inconclusive. However, the use of the rank condition plus the assumption that moments consistent with zero are identically zero suggests the result $J = 3/2$. Moreover, a Dalitz-Miller analysis on the $\Sigma^+(1660)\to\Sigma^-\pi^+\pi^+$ Dalitz plot gives a strong preference for $J^P = 3/2^-$.

For the $\Sigma(1660)\to\Sigma^0\pi^+$, the consistency of the branching fractions in all $\cos\theta^*$ intervals suggests that it is the same resonance in each interval. A moments analysis again yields that $J\geq 3/2$. Also for the $\Sigma(1660)\to\Sigma^0\pi^+$, the extended Byers-Fenster analysis yields no conclusion because of the absence of non-zero odd-L moments in all production angular regions. In the forward region the presence of background prevents the application of the test based on the rank condition and the assumption that only $L = 2$ moments are non-zero. In the backward region, however, this test shows that the data are consistent with $J = 3/2$.

We conclude that both production $\Sigma(1660)$'s are confirmed as $J\geq 3/2$ states with $J = 3/2$ preferred, particularly for $\Sigma(1660)\to\Lambda(1405)\pi$.

The branching ratios determined here are, with the exception of the $\Lambda(1405)\pi$ mode, in agreement with those found in formation experiments. It thus seems that the $\Sigma(1660)\to\Sigma\pi$ is the same resonance as the $J^P = 3/2^-$ formation $\Sigma(1660)$ and that the $\Sigma(1660)\to\Lambda(1405)\pi$ is a different resonance also having $J^P = 3/2^-$. Further, the branching ratios of the $\Sigma(1660)$ produced in $\Sigma\pi$ agree well with those of the formation $\Sigma(1660)$ and with those of the $\alpha = 0.625$ octet of the $(70,1^-)$ multiplet of $SU(6)_w$. The $\Sigma(1660)$ produced in $\Lambda(1405)\pi$ can be the other $J^P = 3/2^-$ octet-Σ of the $(70,1^-)$ only if one allows strong configuration maxing.

The reaction $K^-p\to K^-p\omega$ was studied in the $K^-\pi^+\pi^-\pi^0p$ final state with a (preliminary) sample of 21 ev/μb. We observe a $p\omega$ enhancement of mass 1815 MeV and width about 125 MeV (see Fig. 3) produced peripherally with no significant anisotropy in its decay. These results are in agreement with those found[4] in $\pi^\pm p\to\pi^\pm p\omega$ and in $\bar{p}p\to\bar{p}p\omega$. The narrowness of the width found in all of these experiments is in contrast to the much broader width normally associated with Deck-type enhancements, suggesting that this enhancement could well be a genuine resonance.

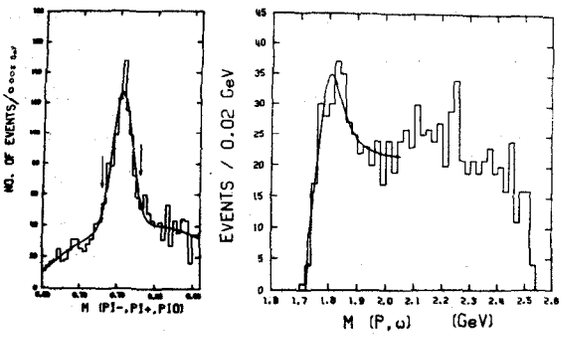


Fig. 3. a) $M(\pi^+\pi^-\pi^0)$ for events with $t'_{p\to p3\pi} <$ 0.35 GeV^2; b) $M(p\omega)$ for events with $t'_{p\to p3\pi} \leq 0.35$ GeV^2 and the ω defined by $0.76 < M(\pi^+\pi^-\pi^0) < 0.81$ GeV. The curve is the result of a fit to a S-wave Breit-Wigner plus phase space.

References

1. R.Barlotaud, "Ω^- and Ξ^* Production in K^-p Interactions, Session Baryon Spectroscopy", this Conference.
2. Amsterdam - CERN- Nijmegen - Oxford Collaboration. J.J.Timmermans et al."Production of $\Sigma(1660)$ in K^-p Interactions at 4.2 GeV/c". Paper 274, this Conference.
3. Amsterdam - CERN - Nijmegen - Oxford Collaboration,"Observation of a $p\omega$ Enhancement near Threshold in $K^-p \to K^-\pi^+\pi^-\pi^0 p$ at 4.2 GeV/c. Paper 275, this Conference.
4. V.Davidsen et al. Phys.Rev.Lett., 32, 855 (1974); D.Liglin et al., paper submitted to the XVII International Conference on High Energy Physics (London, 1974); H.W.Atherton et al. Nuovo Cimento., 30A, 505 (1975).

Ω^- AND Ξ^* PRODUCTION IN K^-p INTERACTIONS

R.Barloutaud

CEN Saclay, France

Three papers on this topic have been submitted to this Conference. The first one (paper 292/C2-13) deals with the Ω^--production studied in K^-p interactions at 4.2 GeV/c by the Amsterdam - CERN - Nijmegen - Oxford Collaboration (ACNO) in the CERN 2-meter hydrogen bubble chamber. The main results based on 32 events decaying into $\Lambda K^-(23)$, $\Xi^0\pi^-(7)$ and $\Xi^-\pi^0(2)$- are summarized in table 1, where a comparison is done with the present PDG values of the mass, the lifetime and the decay parameter. The second quantity shows a significant difference with the P.D.G. tables

Table 1

	Mass (GeV)	Mean life (sec)	Decay parameter
ACNO	$1.6718\pm.0008$	$(0.75\pm0.15)10^{-10}$	0.01 ± 0.58
P.D.G.	$1.6722\pm.0004$	$(1.3^{+0.3}_{-0.2})10^{-10}$	$-0.66^{+0.36}_{-0.30}$

Two papers on Ξ^* production have been submitted to the Conference. The first paper comes again from the ACNO Collaboration (299/C2-5). It presents the results of Ξ^* production in the 2 body reaction $K^-p \to \Xi^{*-}K^+$ followed by the decay of the Ξ^* into ΛK^-, Σ^0K^- or Σ^-K^-, $\Xi^-\pi^0$ and $\Xi^-\pi^+\pi^-$. Three significant peaks have been found in the various mass distributions shown in Fig. 1. The first one at 1.82 GeV was already reported in this experiment at the Palermo Conference (1975). The $\Xi^*(2030)$ was a candidate previously reported by other groups; but its evidence seems now quite good. Finally it is the first evidence for $\Xi^*(2120)$. The mass, width and partial cross section in the various final states of these resonances are summarized in table 2. The spin of $\Xi^*(1820)$ has been found to be larger than 1/2.

Finally a search for Ξ^* resonances in the K^-p interactions at 14.3 GeV/c has been reported by the Ecole Polytechnique, Rutherford, Saclay

Table 2

Mass (MeV)	Width (MeV)	Cross sections			
		ΛK^-	$(\Sigma\bar{K})^-$	$(\Xi\pi)^-$	$(\Xi^*_{1530}\pi)^-$
1823±2	21±7	2.5 ±0.3	0.6 ±0.2	<0.85	2.5 ±0.5
2025±3	28±8	0.53 ±0.18	2.2 ±0.28	<0.84	
2126±4	27±8	1.3 ±0.3			

Collaboration (paper 178/C2-3). At this incident momentum, the Ξ^* production in two-body reactions is so low that there is no hope to find them in a bubble chamber experiment. An inclusive search has then been carried out in the following reactions:

1) $K^-p \to \Xi^-\pi^+ +$ anything

2) $K^-p \to \Xi^{*0}_{1530}\pi^+ +$ anything

3) $K^-p \to \Xi^-\pi^+\pi^- +$ anything (with the $\Xi^-\pi^+$ mass outside Ξ^*_{1530})

4) $K^-p \to Y K^- +$ anything

that is the 4C or 1C reactions

$K^-p \to \Lambda(\Sigma^+)K^-K^+ +$ anything

$K^-p \to \Lambda(\Sigma^+)K^-K^{0} +$ anything

$K^-p \to \Lambda(\Sigma^-)\bar{K}^{0}K^+ +$ anything

where both Λ and K^0 are required to be seen in the chamber.

The inclusive mass distributions of the various mass combinations $\Xi^-\pi^+$, $\Xi^-\pi^+\pi^-$, YK^- show some structures which are more or less significant. Figs. 2 and 3 present as an example the $\Xi^-\pi^+$ and $\bar{Y}K$ distributions. In order to obtain more quantitative information on these peaks, a fit of these distributions has been performed by means of Breit-Wigner functions and a smooth parametrized background (full line on Figs. 2 and 3). The results which have been obtained are summarized in table 3 where only the enhancements with more than ~ 3 s.d. are reported. Most of these peaks are found in the decay mode and at a mass where evidence have already been found for Ξ^* resonances. Four of them however have not yet been reported and should be considered as new candidates waiting for confirmation.

Table 3

Mass (MeV)	Width (MeV)	Decay Mode	Previous Evidences
1534±2	16±2	$\Xi^-\pi^+$	$\Xi^*(1530)$
1632±4	≲ 20	$\Xi^-\pi^+$	$\Xi^-\pi^+$ between 1600 and 1635MeV
1825±10	98±4	$Y\bar{K}$	much broader than ; probably more than one resonance
1853±11	64±44	$\Xi^*_{1530}\pi$	
1977±9	67±30	$Y\bar{K}$	$\Xi^*(2020)$?
2119±5	24±12	$\Xi^-\pi^+$	$\Xi^*(2120)$ seen in ΛK
2272±14	90±29	$\Xi^-\pi^+\pi^-$	Peaks reported between 2240 and 2270 MeV in $\Xi\pi\pi$ and $Y\bar{K}\pi$
2392±14	41±7	$Y\bar{K}$	Peaks reported between 2390 and 2430 MeV in $\Xi\pi\pi$ and $Y\bar{K}$
1758±12	40±20		
1874±4	17±4		
2203±5	≲ 20		
2604±25	150±60		

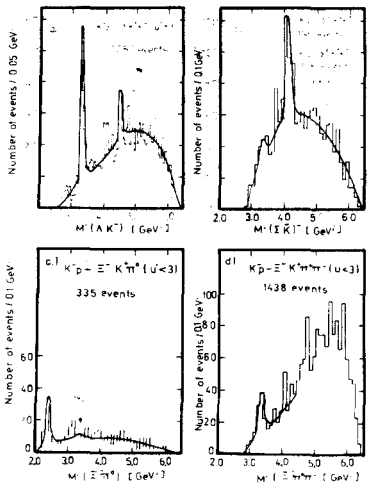


Fig. 1. a) $M^+(\Lambda K^-)$ for the reaction $K^-p \to \Lambda K^+K^-$ with $u' < 3$ (GeV/c)^2 and $\phi(1020)$ excluded. b) $M^+(\Sigma\bar{K})^-$ for the reactions $K^-p \to \Sigma^+K^+K^-$ with $u' < 3$ (GeV/c)^2 and $\phi(1020)$ excluded, together with $K^-p \to \Sigma^-K^+\bar{K}^0$ with $u' < 3$ (GeV/c)^2. c) $M^+(\Xi^-\pi^0)$ for the reaction $K^-p \to \Xi^-K^+\pi^0$ with $u' < 3$ (GeV/c)^2, d) $M^+(\Xi^-\pi^+\pi^-)$ for the reaction $K^-p \to \Xi^-\pi^+\pi^-K^+$ with $u' < 3$ (GeV/c)^2.

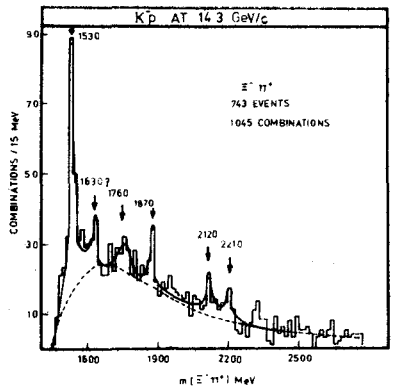


Fig. 2. $\Xi^-\pi^+$ effective mass distribution. The dashed curve is an estimate of the background, and the full curve results from the fit to Breit-Wigner functions superposed on the background.

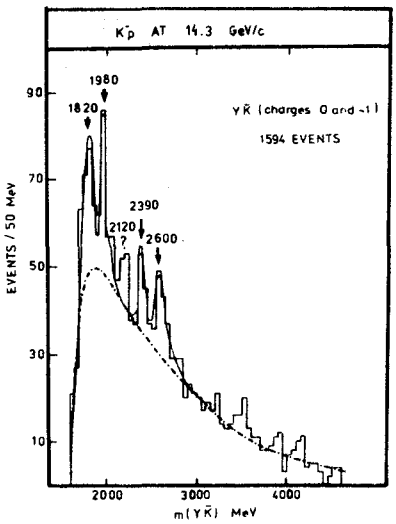


Fig. 3. $\Lambda\bar{K}$ and $\Sigma\bar{K}$ effective mass distribution. The dashed and full curve represents the background and the fit respectively.

PLENARY REPORT
MESON AND BARYON SPECTROSCOPY

K. Lanius*

* Permanent adress after 1 August 1976: Institut für Hochenergiephysik der Akademie der Wissenschaften der DDR. 1615 Zeuthen/Berlin Platanenallee 6.

1 Introduction

In a few words of introduction let me say that in spite of the enthusiasm over the new hadron spectroscopy, experimental work in the field of the old hadron spectroscopy has been carried on with some success since the XVIII International Conference on High Energy Physics in London 1974.

As you very well know the days of quick successes are long in the past. The progress obtained is achieved with enormous experimental and analytical expense in the study of selected channels.

In my report I have summarized some of the essential results in the old hadron spectroscopy, which have been obtained in the last two years.

I will take the naive quark model as a guide. With this quark (q) antiquark ($\bar{q}$) model for mesons and the qqq model for baryons, it is natural to expect that there should be excited states corresponding to rotational excitation (L) and radial excitation (n) of the internal motions of the quarks.

The parity of a $q\bar{q}$ system with an orbital angular momentum L is

$$P = (-1)^{L+1}$$

and of a qqq system

$$P = (-1)^{L}$$

The total angular momentum is

$$J = L + S$$

where S is the quark spin (S = 0,1 for mesons and S = $\frac{1}{2}$, $\frac{3}{2}$ for baryons). Mesons and baryons then must have well - defined J^P determined by L and S.

2 Mesons

If you look in the 1976 edition of the Meson Table of the Particle Data Group /1/ you find the following table of established nonets.

Table 1

The established nonets.

(J^P) Cn	Nonet Members	θ lin.	θ quadr
(0^-) +	π, K, η; η' (958)	$-24\pm1^\circ$	$-11\pm1^\circ$
(1^-) -	ϱ (773), K^* (892), ϕ (1020); ω (783)	$37\pm1^\circ$	$40\pm1^\circ$
(2^+) +	A_2(1310), K^*(1421), f'(1516); f (1271)	$29\pm2^\circ$	$31\pm2^\circ$

That also means that the pseudoscalar nonet is now well established. There have been two candidates for the ninth isoscalar meson the η' (958) - (or X^0) - Meson and the E (1420) - Meson.

From the Dalitz-Plot analyses of the $\eta' \longrightarrow \pi^+\pi^-\eta$ and $\eta' \longrightarrow \pi^+\pi^-\gamma$ decays, and from the observation of a $\eta' \longrightarrow \gamma\gamma$ decay mode the spin and parity of this particle have been restricted to the values 0^- and 2^-, with 0^- favoured. Three years ago in the high statistics BNL - Michigan experiment /2/ at 2.18 GeV/c on the reaction $K^-p \longrightarrow \Lambda\,\eta'$ evidence was presented for possible anisotropies in the production - dependent decay angular distribution of the η' implying $J^P = 2^-$. Following the suggestion of Ogievetsky et al. /3/ they have investigated the decay angular distribution of very forward produced η' - mesons.

Baltay et al. /4/ have carried out a study of the η' meson in the reaction

$$K^- p \longrightarrow \Lambda\,\eta'$$

at 1.75 GeV/c. They do not find any evidence for the existence of such anisotropies in the decay angular distributions of forward produced η mesons with statistics comparable to those of the Brookhaven-Michigan collaboration.

In a paper submitted to this conference Lednicky and Ogievetsky /5/ have shown, however, that the 1.75 GeV/c data are not in

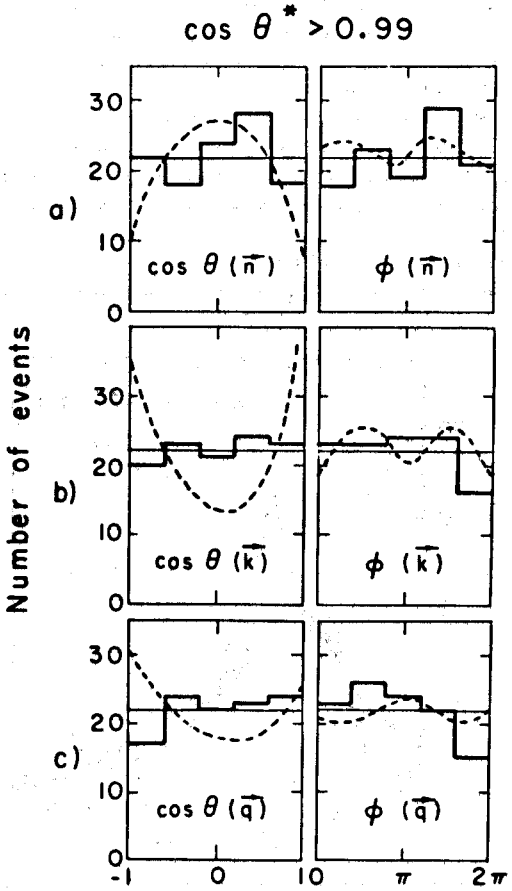


Fig. 1 Some experimental distributions. The curves are the projections of the fits (continuous line 0^- best fit, broken line 2^- best fit). θ and ϕ are polar and azimuthal angles of:
(a) normal to the $\eta\pi\pi$ plane
(b) η momentum in η' rest frame
(c) π^+ momentum in $\pi^+\pi^-$ rest frame.

contradiction with the 2^- hypothesis and, moreover, they slightly favour this assignment.

The Amsterdam-CERN-Nijmegen-Oxford collaboration has submitted a study of the spin parity of the η' in the same reaction at 4.2 GeV/c [6] using bubble chamber data with a statistical sensitivity of ~ 100 events/μb. The analysis used the Λ polarization as well as the η' decay angular distribution and the Dalitz plot population. They have also investigated the decay angular distribution of very forward produced η' - mesons. As you see from fig. 1 there is no indication of an anisotropy, thus definitely establishing the η' spin parity as 0^-.

The only motivation for keeping $J^P = 2^-$ could be that in general higher spins cannet be ruled out but this is true for many meson resonances listed in the Tables of Particle Properties [1]

An interesting tool which can be useful in hadron spectroscopy is the interference between resonances which have a common decay mode. The ϱ and ω are examples of states which are nearly degenerated in mass and for which interesting interference effects have already been observed. These particles have no common strong decay mode and the interference is observable only through the small electromagnetic contribution to the $\omega \longrightarrow 2\pi$ decay.

The $\varrho - \omega$ interference has been studied in the reaction

$$K^- p \longrightarrow (\Sigma^0, \Lambda)\, \pi^+\pi^-$$

at 4.2 GeV/c by the Amsterdam-CERN-Nijmegen-Oxford collaboration[7] and at 13 GeV/c using the SLAC wire chamber spectrometer [8]. From quark model predictions it follows that the ϱ^0 and ω production amplitudes should be equal in magnitude and phase in this reaction [9, 10]

The experimental $\pi^-\pi^+$ mass distribution of Brandenburg et al. [8] shows a clear peak - dip $\varrho^0 - \omega$ interference pattern (fig. 2).

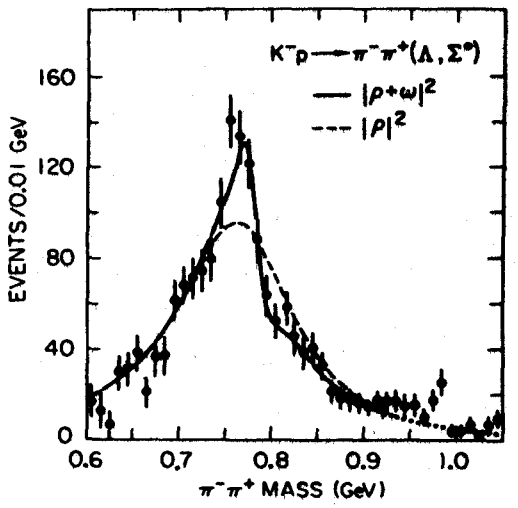


Fig. 2 Obeerved $\pi\pi'$ mass distribution with the background events from $K^-p \rightarrow K^-\pi^+ X^0$ subtracted. The solid curve is the result of a fit to these data of a coherent sum of acceptance corrected ϱ^0 and ω Breit-Wigner amplitudes (χ^2=31/29 DF). The dashed curve gives the best fit when only the ϱ amplitude is present (χ^2=81/31 DF). The dotted line is the extrapolation of the $\varrho^0 - \omega$ fit above 0.92 GeV^2.

The solid curve in this figure is the result of a fit to the experimental data of a coherent sum of acceptance corrected ϱ^0 and ω Breit-Wigner amplitudes. The dashed curve gives the best fit when only the ϱ amplitude is present.

In both studies the ϱ^0 and ω production amplitudes are found to be in phase and consistent with equality.

The Argonne Effective Mass Spectrometer has been used for a high statistics study of the reactions

$$\pi^- p \longrightarrow K^- K^+ n$$
$$\pi^+ p \longrightarrow K^- K^+ p$$

at 6 GeV/c [11].

Comparison of the two reactions allows isolation of interference between different tensor mesons of differing isospin. The mass dependence of the measured $\langle Y_4^0 \rangle$ moment which exhibits the behaviour of the D - wave in three different intervals of momentum transfer is shown in fig. 3.

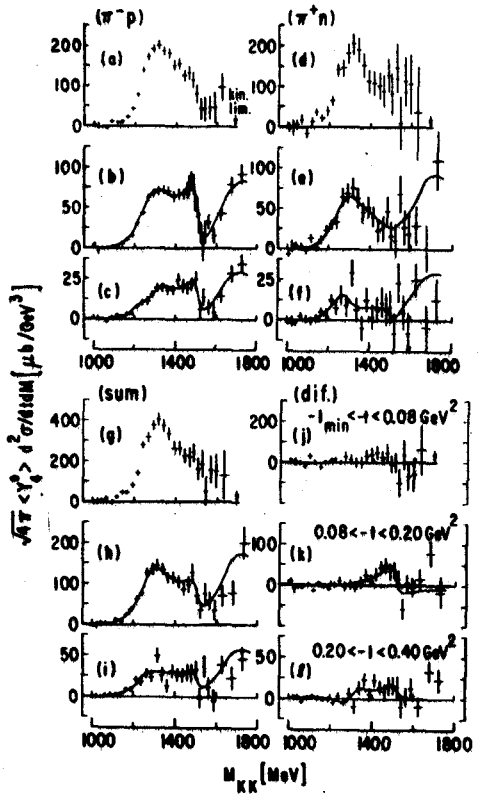


Fig. 3 $\sigma\langle Y_4^0\rangle$ in three t intervals for reactions (1) and (2), their sum and difference. The curves are the result of the fits described in the text. For $-t < 0.08$ GeV^2, the arrow at 1600 MeV indicates the point at which $t_{min} = -0.08$ GeV^2. The moments are calculated in the t-channel frame.

The results can be summarized as follows:

- $\sigma(\pi^- p)\ \langle Y_4^0 \rangle$ exhibits a striking interference pattern near 1500 MeV due to interference of the narrow f'(1514) with the slowly varying high mass tails of the f and A_2^0. The fit gives $M_{f'} = 1506 \pm 5$ MeV and $\Gamma_{f'} = 66 \pm 10$ MeV.
- A large f' - A_2^0 interference exists for $-t > 0.08$ GeV^2.
- f - A_2^0 interference is significant only for $-t > 0.20$ GeV^2.

- f - f' interference is significant for $-t < 0.40$ GeV^2.

Within the scope of the naive quark model the pseudoscalar nonet and the vector nonet correspond to configuration of the ground state of a quark (q) antiquark ($\bar{q}$) system with the radial excitation n = 1 and the orbital angular momentum L = 0.

For orbital angular momentum L = 1 of the $\bar{q}q$ system we have to expect four nonets. At the International Conference on High Energy Physics in Palermo last year French in his invited talk on Mesons - 1975 has shown the optimistic and pessimistic approaches to the status of L = 1 multiplets [12], (table 2). After discussing some results he was tending more to the pessimistic version of table 2.

Table 2

Status of L = 1 meson multiplet
(a) Optimistic (b) Pessimistic



J^{PC}	I = 1	I = 1/2	I = 0	I = 0
2^{++}	A_2	K^{**}	f	f'
1^{++}	A_1	Q_A	D	E
0^{++}	δ	κ	ε	S*
1^{+-}	B	Q_B		



J^{PC}	I = 1	I = 1/2	I = 0	I = 0
2^{++}	A_2	K^{**}_{1420}	f	f'
1^{++}				
0^{++}				
1^{+-}	B			

2.1 The Axial Vector Nonets

After many years of studies of the A and Q enhancements real progress was achieved with the help of partial wave analysis, p.w.a., as developed by the Illinois group [13]. The three - meson p.w.a. program assumes a quasi two-body production of the three meson system; i.e. the three meson system is always produced via an isobar and a bachelor meson (fig. 4).

A three meson system with spin - parity J^P and t-channel helicity M = 0,1 is produced via the exchanged naturality $\eta = \pm 1$. It decays via an l - wave into an isobar with spin j and a meson.

The majority of analyses done up to now except that of the Berkeley group [14] uses the Illinois p.w.a. program. In comparison with the Illinois program the Berkelsy analysis fits coherent amplitudes, not density matrix elements, and makes different assumptions about decay amplitudes of J^P states into various isobars.

A program which also parametrizes the 3π production amplitude in terms of amplitudes rather than a density matrix was used by the Bologna-Florence-Genoa-Milan-Oxford-Pavia collaboration [15]

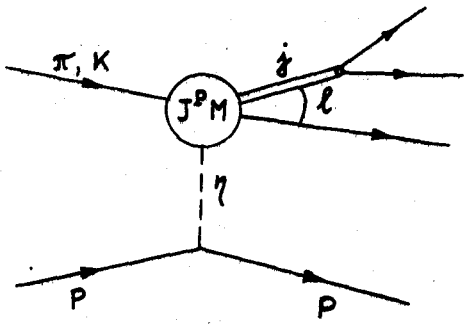


Fig. 4 The Isobar model. A three meson system with spin parity J^P and t-channel helicity M=0,1 is produced via the exchanged naturality $\eta = \pm 1$. It decays via an l-wave into a isobar with spin j and a meson.

All the different partial wave analyses of the diffractively produced $(3\pi)^{\pm}$ system done until now agree that the A_1 is produced predominantly in a $J^P = 1^+$ state via natural parity exchange and decays into $\pi\varrho^0$.

All analyses agree also that the A_1 phase measured with respect to other waves does not vary by more than $\sim 40^0$ over the whole A_1 region (see for example fig. 5 [15]).

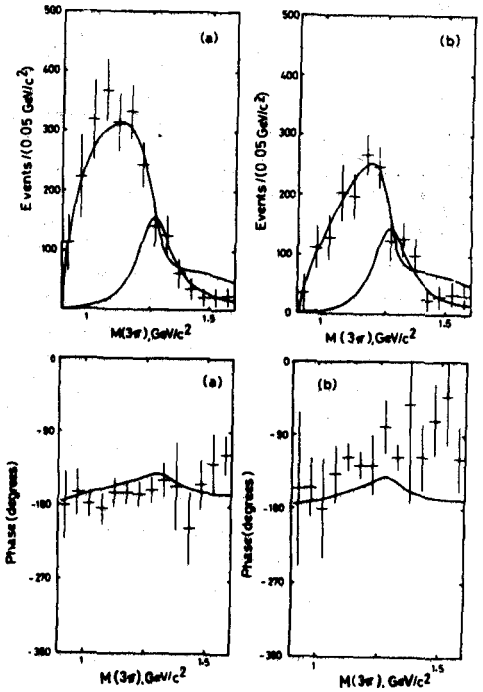


Fig. 5 The 1^+S intensity and phase with respect to 0^-S for (a) $0.0 < |t'| < 0.1$ (b) $0.1 < |t'| < 0.6$ (GeV/c)^2, the smooth lines are the result of a simultaneous fit to both t' regions, and the corresponding contribution from the pure resonance part.

It would seem therefore that the A_1 bump is a composite system rather than a single resonance.

In this connection I would like to remind you of a comment of A Rosenfeld at the 1974 - Conference in Experimental Meson Spectroscopy [16] We are dealing with an inelastic reaction known to

be dominated by background due to Deck effect or whatever you want to call the bump in the A_1 region. So we are trying to see a small resonant signal on top of a large energy-dependent but nonresonant background. In such cases it is known from $N\pi$ p.w.a. that the phase does not go through 90°. In fig. 6 are shown two $N\pi$ Argand plots - for D_{15} and F_{35} - and the corresponding plots for elasticity η and phase δ. The δ plots do not give a clue of these resonances, although they are clear on the Argand diagrams.

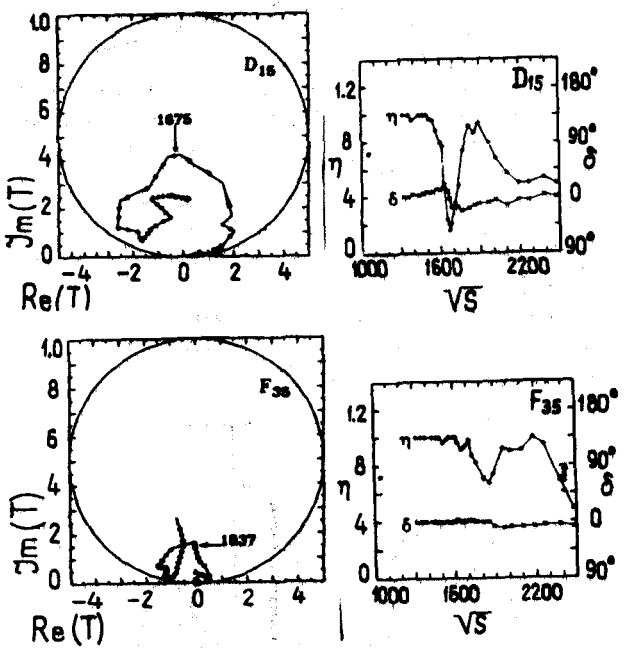


Fig. 6 Two illustrative $N\pi$ Argand plots, for D_{15} and F_{35}, and the corresponding plots for elasticity η and phase δ.

It seems to me that it will be very difficult to draw a negative conclusion about the existence of the A_1 meson from looking at diffractive reactions.

A partial wave analysis of the $(3\pi)^0$ system has been performed by Wagner et al. /17/, based on the charge exchange reaction

$$\pi^+ p \longrightarrow (\pi^+\pi^-\pi^0)\,\Delta^{++}(1236)$$

at 7.1 GeV/c. In this LBL-analysis the $I = 1$ $J^P = 1^+$ wave remains small. For a width $\Gamma < 150$ MeV Wagner et al. give $\sigma(A_1) < 2$ μb. Using A_1 couplings from typical models gives an expected cross section of 36 μb and $\sigma(A_1) = 4.5$ μb for the minimum cross section for any coupling /18/.

A p.w.a. of the $(3\pi)^0$ system from the charge exchange reaction

$$\pi^+ n \longrightarrow (\pi^+\pi^-\pi^0)\,p$$

at 4 GeV/c was done by a Birmingham-Durham-Rutherford collaboration /19/.

From this analysis the unnatural parity series can be explained reasonably well by the Reggeized Deck model with the exception of the 1^+ partial wave decaying into $\rho\pi$ with $I = 1$, where an excess of events is found around 0.9 GeV and from 1.4 to 1.7 GeV. The results do not suggest the production of an A_1 meson at 1.1 GeV (see fig. 7).

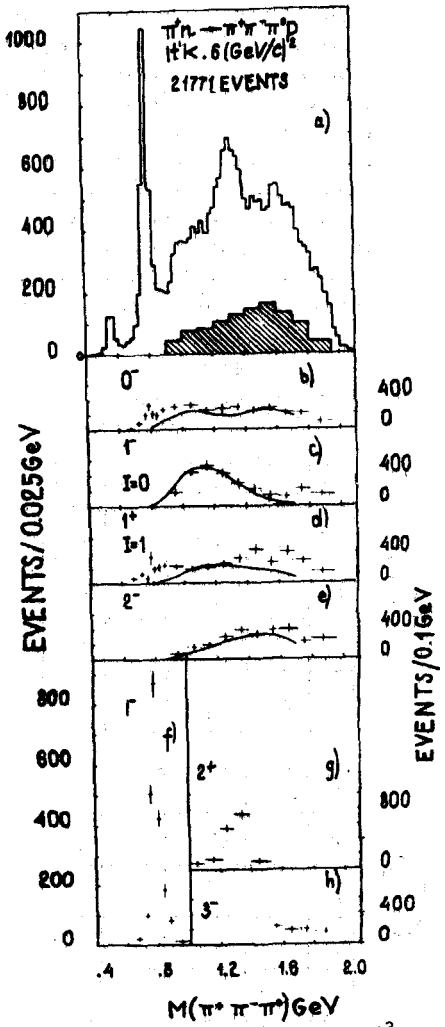


Fig. 7 a) $\pi^+\pi^-\pi^+$ effective mass for $|t'| < 0.6(\mathrm{GeV/c})^2$ with events from the reactions $\pi^+ n \longrightarrow \Delta^{++}\pi^-$ shaded.

b), c), d), e), f), g) & h). Contributions from the $J^P = 0^-$ $1^+(I=0,1)$, 2^-, 1^-, 2^+ and 3^- partial waves respectively. The scale is the same as that for a). The curves in b), c), d) and e) are the predictions of the Reggeized Deck model.

The Ottawa-Montreal-Ohio-Toronto collaboration submitted its preliminary results of a study of the reaction

$$\pi^- p \longrightarrow (\pi^+\pi^-\pi^0)\,n, \qquad \pi^0 \longrightarrow \gamma\gamma$$

at 8.4 GeV/c /20/. Both charged pions and both γ's are measured in the Charged and Neutral Spectrometer at the Argonne ZGS. The $(3\pi)^0$ spectrum shown in fig. 8 is dominated by strong peaks at the η, ω, A_2 and $\omega^*(1675)$ masses. Raw spectra uncorrected for acceptance are shown as histograms. Spectra with a very crude fir order acceptance correction are shown as heavy dots with statistical error flags.

Except for the η and ω no narrow structures in fig. 8 have

statistical significance above ~ 3 standard deviations. The present sensitivity to such effects is about 0.8 μbarn.

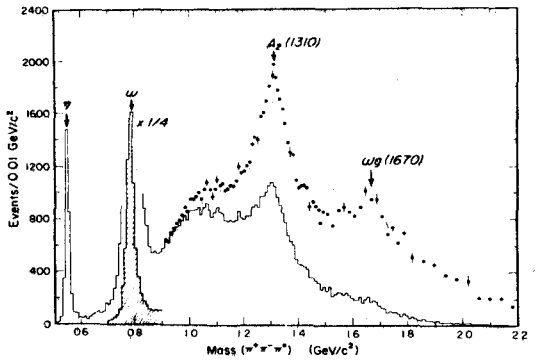


Fig. 8 $\pi^+\pi^-\pi^0$ mass spectrum. Raw events are shown by the histogram, and acceptance-corrected events (arbitrarily normalized at 0.9 GeV/c^2) by large dots with statistical error flags.

In order to exploit fully these high statistics data a partial wave analysis must be performed.

Observation of a backward produced A_1 meson would show that the A_1 exists. Already seven years ago Anderson et al. /21/ observed both backward A_1 and A_2 peaks.

In order to clarify this observation Chapman et al. /22/ searched for backward A_1 production in the reactions

$$\pi^- p \longrightarrow p_{fast}\ \pi^+\pi^-\pi^- \qquad (1)$$
$$\longrightarrow p_{fast}\ \pi^+\pi^-\pi^-\pi^0 \qquad (2)$$

at 4 GeV/c with a streamer chamber spectrometer. No evidence for the backward production of either A_1^- or A_2^- is observed in reaction (1). The upper limit of the cross section was determined to be $\sigma(A_1^-) < 4$ μb within 2 σ limits.

In a similar experiment an Illinois-Argonne collaboration /23/ gives a limit $\sigma(A_1^-) < 0.95$ μb at 8 GeV/c for reaction (1).

The Amsterdam-CERN-Nijmegen-Oxford collaboration /24/ has done a p.w.a. of the reaction

$$K^- p \longrightarrow (\pi^+\pi^-\pi^0)\,\Lambda^0$$

at 4.2 GeV/c. In this reaction the Λ polarization information is available from the $\Lambda \longrightarrow p\pi^-$ decay. Apart from two phases, all transversity amplitudes can be determined without any further assumption beyond the isobar model Ansatz.

The partial wave decomposition of the 3π system integrated over the region $|t_{min}| < |t| < 1$ GeV^2 is shown in fig. 9. Resonant shapes are evident for the 2^+ wave in the A_2 region and for the 3^- wave in the $\omega^*(1675)$ region. The 1^+ wave gives the largest contribution to the $(3\pi)^0$ system but no evidence for a resonance - like behaviour is found. The authors estimated $\sigma(A_1) < 2$ μb.

The A_1 can be produced by π-exchange in photon induced reactions. Therefore the expected cross section can be estimated more reliably by pole extrapolation than for the other charge exchange reactions /25/. Failure to observe the A_1 in photoproduction

$$\gamma p \longrightarrow (\pi^+\pi^-\pi^+)\,n$$

would be unambiguous evidence against the existence of an A_1 meson.

For both the A_1 nonet with $J^{PC} = 1^{++}$ and the B nonet with $J^{PC} = 1^{+-}$ we had until recently no evidence for the existence of two strange axial vector mesons, Q_1 and Q_2. Previous partial wave analyses of $(K\pi\pi)$ data have revealed no structure characteristic of resonance production. Some interesting results have been found but the statistics of the various experiments were not large enough to study these effects in detail.

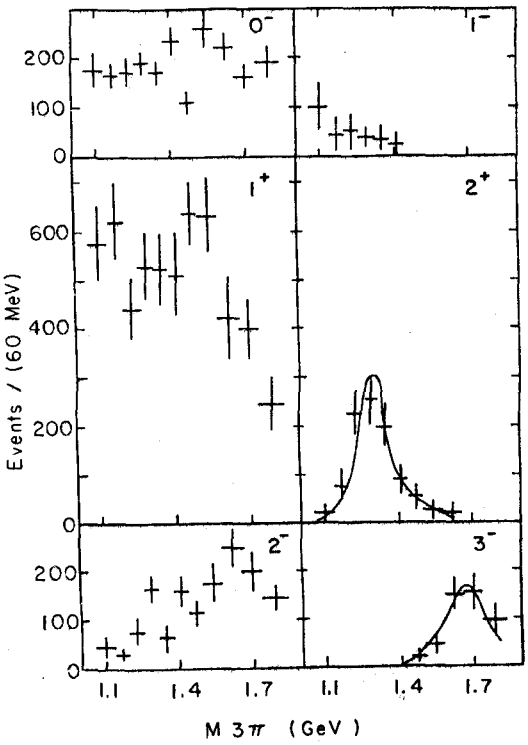


Fig. 9 Spin parity content of the (3π) system as a function of mass for $|t| < 1.0$ GeV^2.

The Aachen-Berlin-CERN-London-Vienna collaboration and the Ecole-Polytechnique-Rutherford-Saclay collaboration combined three experiments at 10, 14 and 16 GeV/c incident momentum /26/. They have performed a p.w.a. of the mainly diffractively produced low mass $(K\pi\pi)$ system in the reactions

$$K^- p \longrightarrow (K^-\pi^+\pi^-)\,p \qquad (1)$$
$$K^- p \longrightarrow (\bar{K}^0\pi^-\pi^0)\,p \qquad (2)$$

In this analysis the two dominant 1^+ S states, $K^*\pi$ and $K\varrho$, were treated as independent states. The degree of coherence between 1^+ S $(K^*\pi)$ and 1^+ S $(K\varrho)$ has been found to be significantly smaller than one.

The dominant 1^+ S $(K^*\pi)$ states possibly has a two - peak structure with peaks at 1.27 GeV and 1.37 GeV seen in both channels. The 1^+ S $(K\varrho)$ state shows one peak near threshold ($\sim$ 1.27 GeV) (fig. 10). The relative phases between different waves are shown in figs. 11, 12. There is no significant variation of the phases between 1^+ 0 + S $(K^*\pi)$ and 0^-0+ states. Otter et al. conclude therefore that 1^+ S $(K^*\pi)$ is mainly non-resonant.

The relative phase of the 1^+ $(K\varrho)$ wave shows a strong rise near threshold. This property and the observation that 1^+ S $(K\varrho)$ agrees at low $(K\pi\pi)$ - masses with s-channel helicity conservation favour the interpretation of the 1^+ S $(K\varrho)$ as a resonance below $K\varrho$ - threshold. The lower mass peak of 1^+ S $(K^*\pi)$ could be part-

ly due to the ($K^{\pm}\pi$) decay mode of this meson. The C-meson, found in $\bar{p}p$ -annihilation at rest, has similar properties: a dominant ($K\varrho$) - decay mode and a mass below ($K\varrho$) - threshold [27].

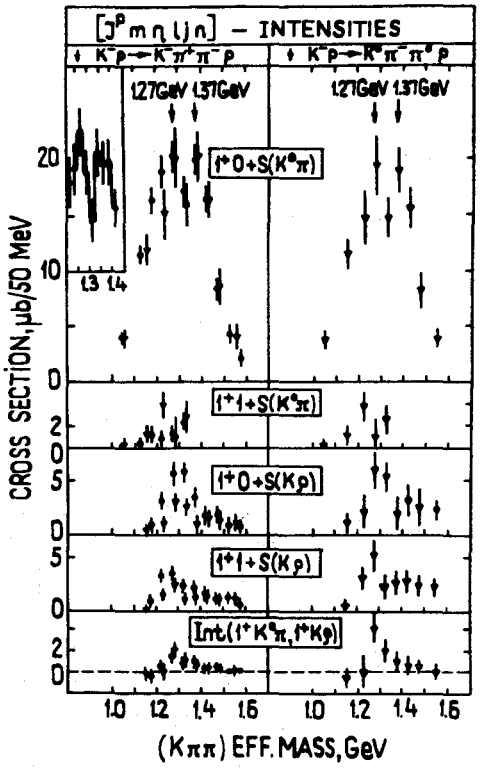


Fig.10 Cross sections of [$J^P m\eta l j n$] as function of the ($K\pi\pi$)-mass for reactions (1) and (2). Errors are statistical only. The triangles in the left hand part represent predictions from reaction (2) fnr reaction (1) based on I = 1/2 of the ($K\pi\varsigma$)-system. The insert shows the results of fits for $1^+0+S(K^*\pi)$ in 25 MeV wide ($K\pi\pi$)-mass bins for reaction (1).

The interpretation of the higher mass peak in 1^+ 0 + S ($K^{\pm}\pi$) also as a resonance decaying mainly into ($K^{\pm}\pi$) seems to be supported by the decreasing $K\varrho$ phase in this mass region. The following observations speak against this interpretation: The 1^+ S($K^{\pm}\pi$) wave vs. 0^- S ($K^{\pm}\pi$) does not vary. The variation of the relative phase 2^+ 1^+ ($K^{\pm}\pi$) vs. 1^+ 0 + ($K^{\pm}\pi$) in reaction (2) is consistent with a Breit-Wigner phase for $K^{\pm}$ (1420) varying against a constant 1^+ 0 + S ($K^{\pm}\pi$) phase. There is no significant violation of t-channel helicity conservation in this mass region contrary to what one might expect for diffractive resonance production.

At the same time a SLAC-group has performed a large statistics study using a wire spark chamber spectrometer system [28]. The partial wave analysis was done on the ($K^{\pm}\pi^+\pi^-$) system in the reaction

$$K^{\pm} p \longrightarrow (K^{\pm}\pi^+\pi^-)\, p$$

at 13 GeV/c.

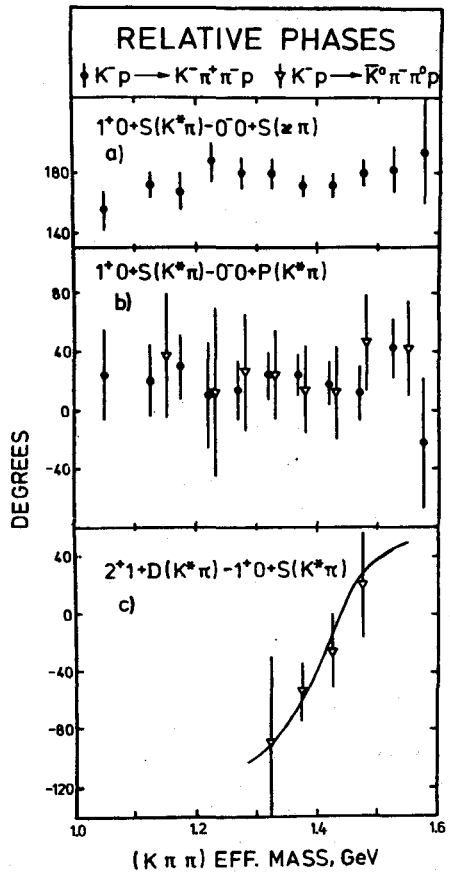


Fig.11 Relative phases of a) $1^+0+S(K\varrho)$ vs. $0^-0+S(K\pi)$, b) $1^+0+S(K^*\pi)$ vs. $0^-0+P(K^*\pi)$, c) $2^+1+D(K^*\pi)$ vs. $1^+0+S(K^*\pi)$ measured in the Gottfried-Jackson frame. The values of the latter phase are determined using a simpler hypothesis. The curve drawn represents the phase variation which is expected if the 2^+ is the $K^*(1420)$ resonance.

In the 1^+ 0 + ($K^{\pm}\pi$) waves (fig. 13), there are two peaks in the K^- data but only a peak-shoulder structure in the K^+ data. In the 1^+ (ϱ K) system (fig. 14), peaks are observed at ~ 1.28 GeV. There are pronounced phase variations: a forward motion of ~ 70° for 1.20 < m ($K\pi\pi$) < 1.35 GeV and a backward motion of ~ 50° for 1.35 < m ($K\pi\pi$) < 1.45 GeV. The measured coherence between the ϱ K and 1^+ 0 + ($K^{\pm}\pi$) statee is smaller than one. Furthermore, the production of the 1^+ (ϱ K) system obeys approximate s-channel helicity conservation [29].

Brandenburg et al. [28] explain these features qualitatively in terms if two 1^+ mesons, Q_1 at 1.3 GeV ($\Gamma \sim 0.20$ GeV) coupling principally to ϱ K and Q_2 at ~ 1.4 GeV ($\Gamma \sim 0.16$ GeV) coupling principally to $K^{\pm}\pi$, and a Deck background peaking at ~ 1.20 GeV in the 1^+ ($K^{\pm}\pi$) system.

The argument of the authors for the interpretation of the Q_2 as a resonance is the suppressed phase variation of the $K^{\pm}$ (1420) meson relative to 1^+ 0 + ($K^{\pm}\pi$) (fig. 13e and 13f) indicating that this reference state is also executing a Breit-Wigner phase variation in the region of 1400 MeV.

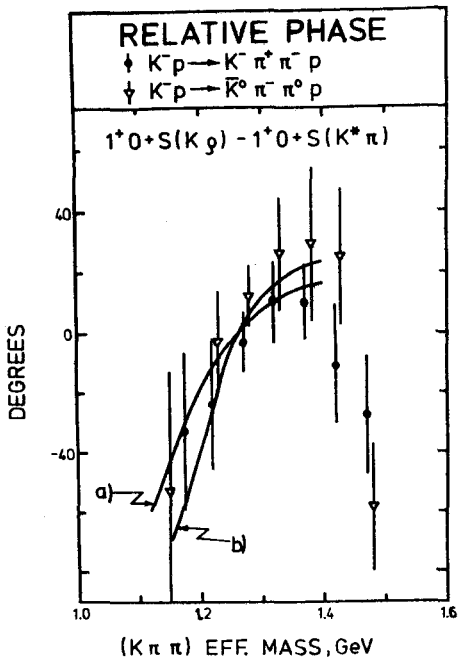


Fig.12 Relative phase of $1^+0^+S(K\rho)$ vs. $1^+0^+S(K^*\pi)$ measured in the s-channel helicity frame. The curves refer to phase variations which are expected if $1^+0^+S(K\rho)$ is resonant. The resonance parameters are:
a) M = 1150 MeV, Γ = 200 MeV
b) M = 1200 MeV, Γ = 150 MeV.

To me this argumentation does not seem to be well justified. I have put together the relative phase of $2^+\,1^+ + D$ ($K^{\pm}\pi$) vs. $1^+\,0^+ + (K^{\pm}\pi)$ of the two experiments in the following fig. 15. Both results are in agreement within errors. Brandenburg et al. consider this result as no phase variation around 1420 MeV. Otter et al. consider the phase variation as consistent with the existence of the $K^{\pm}$ (1420) resonance.

Before claiming the Q_2 as established it would be desirable to check the phase variation in the $(\bar{K}^0\pi^-\pi^0)$ p reaction channel.

In the differential cross section Brandenburg et al. /29/ observed a clear K^+, K^- cross-over at $t' \sim 0.18$ GeV^2 in the Q_2 - region and for the production of the Q_2, t-channel helicity conservation becomes a better approximation. Those features are inconsistent with the predictions of a π- exchange Deck mechanism /30/. They are more probably associated with the fact that in the Q_2-mass region, the $K^{\pm}\pi$ amplitude involves both Q_2 and Deck contributions.

In a study of the low mass ($K\omega$) system in the reaction

$$K^{\pm} p \longrightarrow (K^{\pm}\omega)\, p$$

at 8.25, 10 and 16 GeV/n the Aachen-Berlin-CERN-London-Vienna collaboration and Birmingham-Brussels-CERN-Mons-Serpukhov collaboration /31/ observed a peak at about 1.3 GeV in the ($K\omega$) mass distribution. Looking at its position, its spin parity and its production properties this peak seems to be a decay mode of the Q_1 resonance (see fig. 16).

Like in the A_1 case the charge exchange reaction

$$K^- p \longrightarrow (\bar{K}^0\pi^+\pi^-)\, n$$

shows no evidence for the Q bump in the $(\bar{K}^0\pi^+\pi^-)$ mass spectrum. The Aachen-Berlin-CERN-London-Vienna collaboration and Athens-Democritus-Liverpool-Vienna collaboration made a p.w.a. in the mass range $1.04 < M\,(K\pi\pi)^0 < 1.56$ GeV combining data at 8, 10 and 16 GeV/c /32/. The Ecole Polytechnique-Saclay-Rutherford collaboration made a p.w.a. for this charge exchange reaction in the mass range $1.0 < M\,(K\pi\pi)^0 < 1.56$ GeV /33/.

Due to the poor statistics in both experiments, these mass intervalls were not split into smaller bins. From the two analyses the production cross section of the 1^+ ($K\rho$) states comes out to be $\sim 1.5 - 2\ \mu$b. This can be compared with the $\sim$ x 20 larger diffractively produced 1^+ ($K\rho$) states in which the Q_1 was observed /26/.

In a contribution to this conference the Amsterdam-CERN-Nijmegen-Oxford collaboration /34/ presented a differential partial wave analysis of the $\bar{K}^0\pi^+\pi^-$ system, produced in a high statistics experiment at 4.2 GeV/c. The results of the analysis are shown in figs. 17-19.

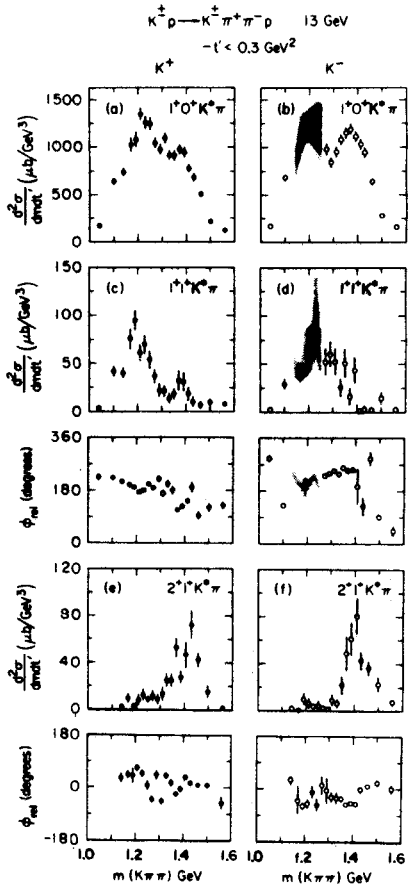


Fig.13 Mass dependence of the 1^+0^+, 1^+1^+, and $2^+1^+(K^*\pi)$ waves. The phase, ϕ_{rel}, is measured with respect to $1^+0^+(K^*\pi)$. The shaded area indicates the range of ambiguity.

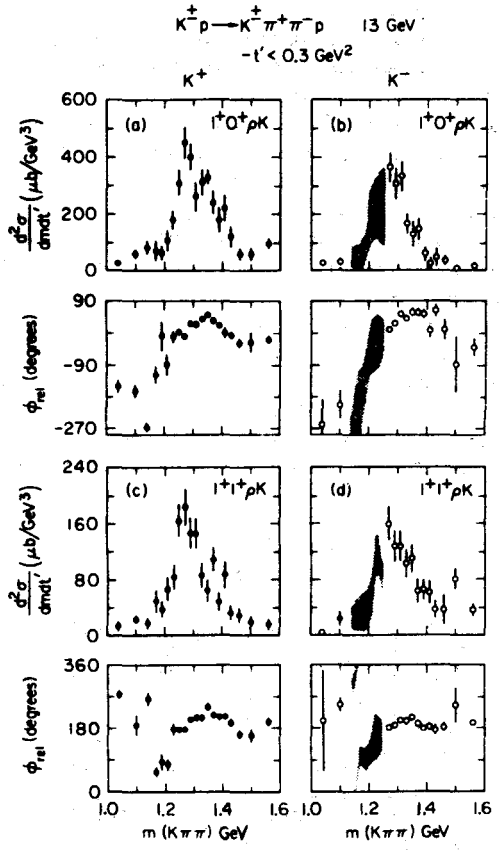


Fig.14 Mass dependence of the 1^+0^+ and $1^+1^+(\rho K)$ waves. The phase, ϕ_{rel}, is measured with respect to $1^+0^+(K^*\pi)$. The shaded area indicates the range of ambiguity.

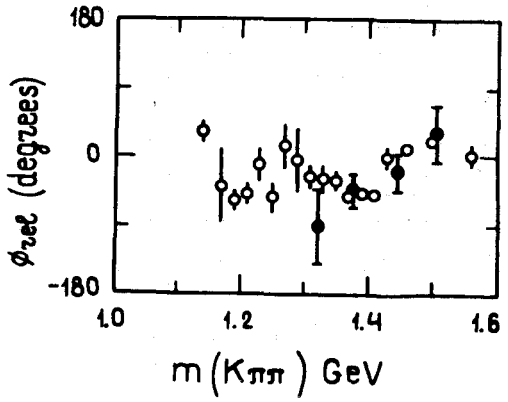


Fig.15 Relative phase of $2^+1^+D(K^*\pi)$ vs. $1^+0^+S(K^*\pi)$ measured in the Gottfried-Jackson frame.
I from /26/
I from /27/

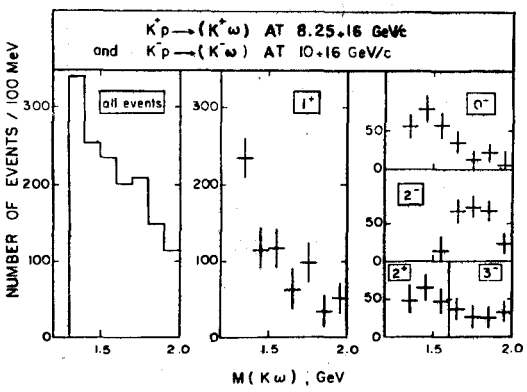


Fig.16 Mass distribution and spin-parity decomposition of ($K\omega$) systems for the combined data of all four experiments.

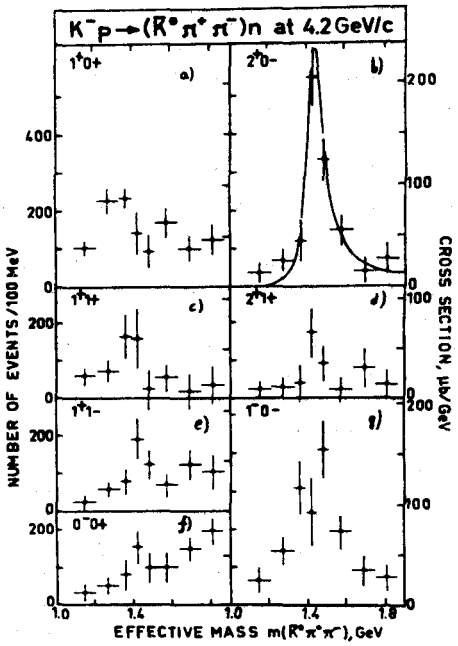


Fig.17 Partial wave content (denoted by $J^P M\eta$) of the $\bar{K}^*\pi^+\pi^-$ system as a function of mass for $t' < 0.5$ GeV^2. The numbers of events are corrected for the $n\pi^+$ and $n\bar{K}^*$ mass cuts and for K^0_S detection efficiency. The cross-sections are in addition corrected for unseen K^0 decay modes.

The 1^+ 0 + state peaks at roughly the same mass as does the Q_1 in diffractive production (fig. 17a). However, the 1^+ S ($K^{*}\pi$) wave has a maximum at ~ 1.4 GeV/c, while there is no peak in the 1^+ S ($K\varrho$) wave (figs. 18a, b). The relative $K^{*}\pi$ and $K\varrho$ intensities and polarization properties of the 1^+ wave differ from those in diffractive 1^+ production (fig. 18). $1^+0+(K^{*}\pi)$ vs. $0^-\,0+(\varrho\pi)$ shows a possible phase variation, while $1^+\,0+(K\varrho)$ vs. $0^-\,0+(\varrho\pi)$ does not (figs. 19g, h). These results suggest a resonance contribution to 1^+ S ($K^{*}\pi$) but not to 1^+ S ($K\varrho$).

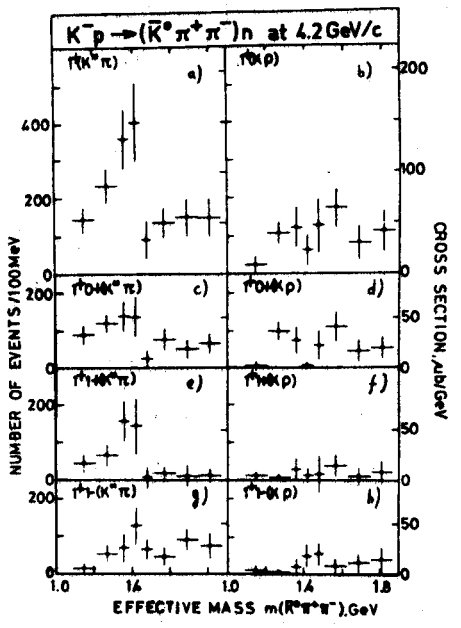


Fig.18 Decomposition of the 1^+ wave into the $K^{*}\pi$ and $K\varrho$ decay modes as a function of $(\bar{K}^{*}\pi^{+}\pi^{-})$ mass for $t' < 0.5$ GeV^2. The waves are denoted by $J^P n$ or $J^P M_\eta n$. The corrections made for the cross sections and numbers of events are the same as for fig. 17.

The Q_1 and Q_2 are mixed states of a Q_A and Q_B being the strangeness ona components of the two $J^{PC} = 1^{++}$ and $J^{PC} = 1^{+-}$ nonets. B. Conforto and G. Conforto /35/ discussed the decay modes of the Q_1 meson and estimated the $Q_A - Q_B$ mixing angle to be in the range from 20 to 35 degrees, with the Q_1 being the "mainly A - like" particle.

About the candidates of the isoscalar states of the axial vector nonets four contributions were submitted to this conference.

Very preliminary results concerning the D (1285) meson came from a study of the reaction

$$\pi^- p \longrightarrow \eta\,\pi^+\pi^- n, \qquad \eta \longrightarrow 2\gamma$$

at 8.4 GeV/c, using the Charged and Neutral Spectrometer at the Argonne ZGS /36/. The measured $\eta\pi^+\pi^-$ spectrum is shown in figure 20a and the same data is replotted in figure 20b with the approximate acceptance calculation.

The D (1285) resonance was studied in six and seven body final states in $\pi^{\pm}$ p interactions at 16 GeV/c by tha Aachen-Berlin-

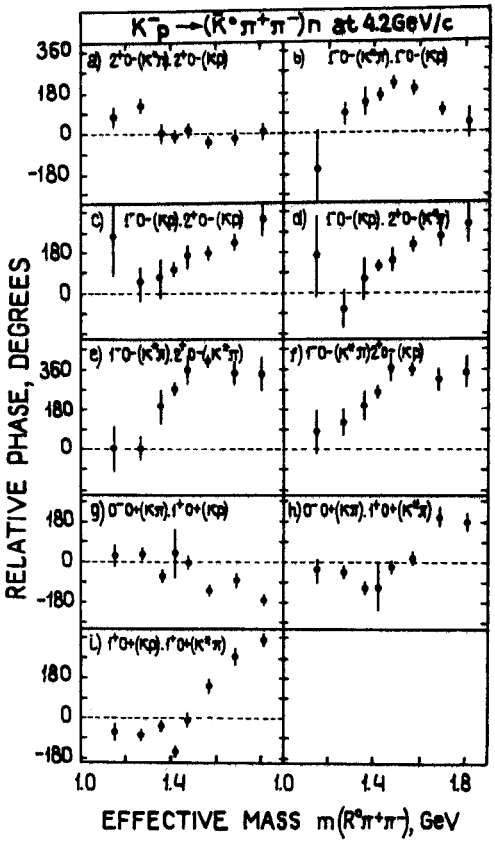


Fig.19 Relative phases between partial wave contributions (denoted by $J^P M_\eta n$, $J'^{P'} M'_{\eta'} n'$) as a function of $(\bar{K}^{*}\pi^{+}\pi^{-})$ mass for $t' < 0.5$ GeV^2.

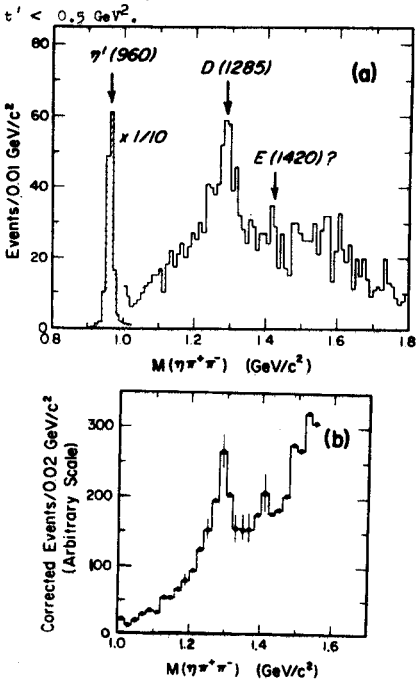


Fig.20 $\eta\pi^+\pi^-$ mass spectra, (a) uncorrected, and (b) with approximate

acceptance correction. The events shown here survive $\gamma\gamma$ and nucleon mass cuts.

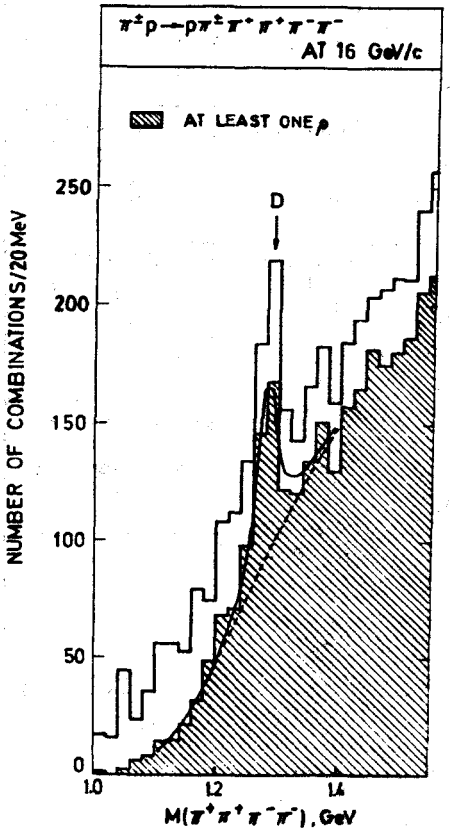


Fig.21 Effective mass distributions $M(\pi^{+}\pi^{+}\pi^{-}\pi^{-})$ for the reactions $\pi^{\pm}p \to p\,\pi^{\pm}\pi^{+}\pi^{+}\pi^{-}\pi^{-}$ combined. The hatched histogram shows the $(\pi^{+}\pi^{+}\pi^{-}\pi^{-})$ mass for events with at least one $(\pi^{+}\pi^{-})$ mass in the ρ mass region (0.66 - 0.86 GeV) together with a fitted Breit-Wigner curve and hand-drawn background.

Bonn-CERN-Cracow-Heidelberg-Warsaw collaboration /37/. The D meson was observed to decay to $\rho\pi\pi$ and to $\eta\pi\pi$ (see fig. 21). The branching ratios

$$\frac{(D \to \rho\pi\pi)}{(D \to \eta\pi\pi)} = 0.93 \pm 0.30 \text{ and } \frac{(D \to K\bar{K}\pi)}{(D \to \eta\pi\pi)} < 0.26 \pm 0.07$$

were found.

The Bombay-CERN-CdF-Madrid collaboration /38/ studied the properties of the D-meson observed in $\bar{p}p$ annihilations at 0.76 GeV/c. The D-signal in the $K\bar{K}\pi$ mass distribution is shown in figure 22.

Preliminary results concerning the D meson came from a study of the reaction

$$\pi^{-}p \to \pi^{+}\pi^{+}\pi^{-}\pi^{-}\pi^{0}n$$

at 12 GeV/c using the Omega spectrometer at CERN /39/.

As far as resonance parameters were measured the results of these studies are summarized in table 3.

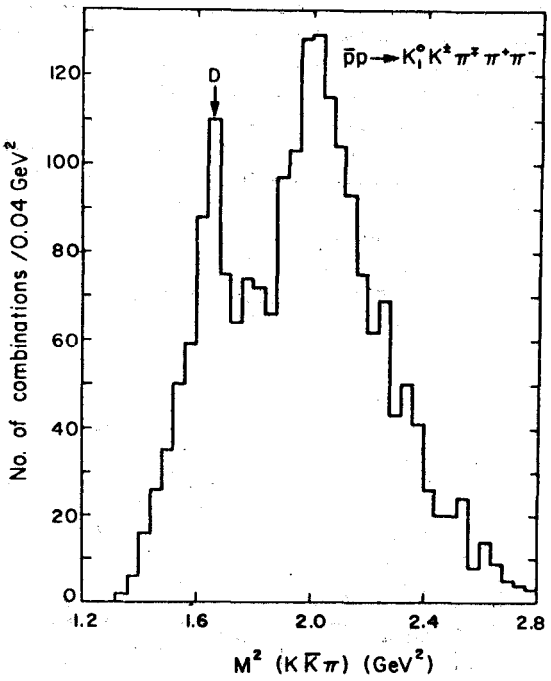


Fig.22 The(mass)^2 distribution of the $(K_1^{\circ}K^{\pm}\pi^{\mp})$ in the reaction $\bar{p}p \to K_1^{\circ}K^{\pm}\pi^{\mp}\pi^{+}\pi^{-}$.

Table 3

New results of the D (1285) meson

Reaction	Mass [MeV]	Width [MeV]	J^P	Reference
$\pi^{\pm}p \to p\pi^{\pm}D^{\circ}$ $D^{\circ} \to \rho^{\circ}\pi^{+}\pi^{-}$ $D^{\circ} \to \delta^{\pm}\pi^{\mp}$ $\quad\hookrightarrow \eta^{\circ}\pi^{\pm}$	1280 ± 3 1273 ± 8	26 ± 15 29 ± 22	0^{-}; 1^{+}; 2^{-}	/37/
$\bar{p}p \to D^{\circ}\pi^{+}\pi^{-}$ D° + MM $\quad\hookrightarrow K_s^{\circ}K^{\pm}\pi^{\mp}$	1281 ± 2	32 ± 5	-	/38/
$\pi^{-}p \to Dn$ $D \to \eta\pi^{+}\pi^{-}$ $D \to \delta^{\pm}\pi^{\mp}$	1283	43	-	/39/

From a point of view which I would like to call the realistic one, I shall include in the group of well established states of the axial vector nonets the B (1235) meson and the Q_1 (1280) meson.

2.2 The Scalar Nonet

Concerning the pessimistic view point none of the resonances of the scalar nonet could be considered as established. What is the news?

Concerning the isovector of the scalar nonet clearly more experimental data was needed in order to clarify the properties and perhaps even the existence of the δ(976) meson.

New evidence was presented for δ production in the reactions

$$K^- p \longrightarrow \Sigma^+(1385)\,\delta^- \;;\; \delta^- \longrightarrow \eta^0 \pi^- \;;$$
$$K^- p \longrightarrow \Lambda\,\delta^+ \pi^- \;;\; \delta^+ \longrightarrow \eta^0 \pi^+ \;;$$
$$\eta^0 \longleftarrow \text{neutrals}, \quad \pi^+\pi^-\pi^0$$

in a bubble chamber experiment with beam momentum in the range 3.1 to 3.6 GeV/c /40/.

Data were also presented to this conference on the reactions

$$\pi^\pm p \longrightarrow p\,\pi^\pm D;\; D \longrightarrow \delta^\pm \pi^\mp;\; \delta^\pm \longrightarrow \eta\,\pi^\pm;\; \eta \longrightarrow \pi^+\pi^-\pi^0$$

at 16 GeV/c by the Aachen-Berlin-Bonn-CERN-Cracow-Heidelberg-Warsaw collaboration /37/. A very clear $\delta^\pm$ signal is visible in the $(\eta\pi)^\pm$ mass spectrum.

The decay angular distributions of the $\delta^\pm \longrightarrow \eta^0 \pi^\pm$ do not contradict the $J^P = 0^+$ assignment for the δ(976) meson. The strongest evidence for 0^+ comes from the fact that no indication was observed for a $(\varrho\pi)$ decay mode of the δ meson.

Additional results came from a paper presented to this conference on the reactions

$$K^- p \longrightarrow \Sigma^+(1385)\,\delta^- \;;\; \delta^- \longrightarrow \eta^0 \pi^- \;;\; \eta^0 \longrightarrow \pi^+\pi^-\pi^0$$
$$\longrightarrow \Sigma^+(1385)\,K^0 K^-$$

at 4.2 GeV/c by the CERN-Amsterdam-Nijmegen collaboration /41/.

As you can see from figure 23b, the δ^-(976) peak is clearly significant. The decay angular distributions of the forward produced δ^-(976), $[\cos(\vec{K}_{inc}, \vec{\delta}^-)_{cms} > 0.8]$ are consistent with the assignment $J^P = 0^+$ (fig. 24). However, the limited statistics do not allow to exclude other natural spin parity assignments.

All the new results from these three experiments are summarized in table 4. In this table the full widths are given after allowing for experimental resolutions.

Table 4

New results of the δ(976) meson.

Reaction	Mass [MeV]	Width [MeV]	J^P	Reference
$K^- p \longrightarrow \Sigma^+(1385)\,\delta^-$	989 ± 4	16^{+25}_{-16}	-	/40/
$\pi^\pm p \longrightarrow p\pi^\pm D$, $D \longrightarrow \delta^\pm \pi^\mp$	980 ± 7	46 ± 23	0^+ preferred	/37/
$K^- p \longrightarrow \Sigma^+(1385)\,\delta^-$	981 ± 6	55 ± 5	0^+ preferred	/41/

As it was shown by Flatte /42/, the narrowness of the $\eta\pi$ peak can be explained by the action of unitarity and analyticity at $K\bar{K}$ threshold. It does not necessarily imply that the underlying resonance is narrow, only that it must have a relatively strong coupling to the $K\bar{K}$ channel.

A refit of the $\eta\pi^-$ mass spectrum using a two channel resonance parametrization /42/ reproduces equally well the $\eta\pi^-$ mass spectrum shown in fig. 23b and yields a mass of (974 ± 51) MeV. The coupled channel parametrization allows, after unseen decay mode corrections, a prediction for the $K^0 K^-$ mass spectrum. This is shown by the solid curve in fig. 23c.

From the different studies of the S-wave $K\pi$ phase shift δ^1_0 around 1300 MeV the results were contradictory. Some groups supported a resonant S-wave interpretation. Some other groups agreed that the S-wave is important but not necessarily resonant.

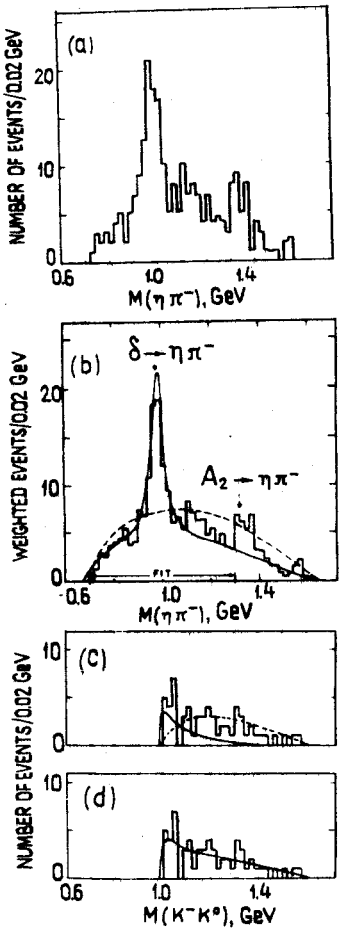


Fig.23 Effective mass distributions for systems recoiling off the Σ^+ (1185) in 4.2 GeV/c K^-p interactions.

a) $\eta\pi^-$ distribution for events of the reaction $K^-p \rightarrow \Sigma^+(1385)\,\eta\pi^-$ (contents = 245).

b) $\eta\pi^-$ distribution obtained for events of the reaction $K^-p \rightarrow \Lambda\pi^+\pi^-\eta$ weighted by the probability of the events belonging to the reaction $K^-p \rightarrow \Sigma^+(1385)\eta\pi^-$. The dashed curve is the expected distribution from the channel-likelihood fit to the reaction $K^-p \rightarrow \Lambda\pi^+\pi^-\eta$ without inclusion of δ^-(970). The full curve has included the δ^-(970) channel.

c) K^0K^- distribution for events of the reaction $K^-p \rightarrow \Sigma^+(1385)\,K^0K^-$. The dashed curve represents the phase space contribution. The full line is the KK threshold contribution as described in the text.

d) K^0K^- distribution for events of the reaction $K^-p \rightarrow \Sigma^+(1385)\,K^0K^-$. The full curve normalized to the number of events (59 events) represents $K\bar{K}$ threshold contribution plus phase space.

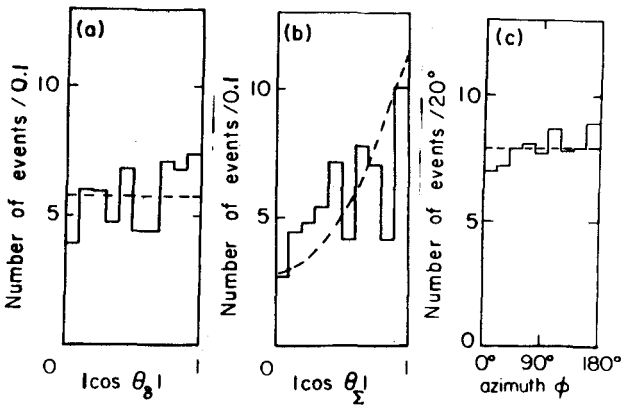


Fig.24 Decay angle distributions for $K^- p \to \Sigma^+(1385)\delta^-$ events with weight as described in the text

a) distribution of $|\cos\theta_\delta|$ where θ_δ is the angle between the incident K^- and the η in the δ^- rest frame.

b) Distribution of $|\cos\theta_\Sigma|$ where θ_Σ is the angle between the incident proton and the Λ in the $\Sigma^+(1385)$ rest frame.

c) Treiman-Yang distribution (ϕ) for the decay of the δ^-

The dotted curves on a) and b) are the expectations for a spin zero δ^- and an aligned spin $3/2^-$ $\Sigma^+(1385)$ respectively.

Published after the London Conference was only the spin-parity analysis of the $(K^- \pi^+)$ system produced in the reaction

$$K^- p \to (K^- \pi^+) n$$

at 10 and 16 GeV/c for $M(K\pi) < 1.68$ GeV and $|t_{pn}| < 0.2$ GeV^2 by the Aachen-Berlin-CERN-London-Vienna collaboration /43/. For this analysis a modified version of the Illinois p.w.a. program was used.

The mass and phase variations support the existence of a broad $I = 1/2$, S-wave resonance in the $(K\pi)$ system. Assuming a Breit-Wigner shape, the mass and width of the $\varkappa$ - meson are found to be $M_\varkappa = 1245 \pm 30$ MeV $\Gamma_\varkappa = 485 \pm 80$ MeV, respectively.

A partial wave analysis, similar to the one of Lauscher et al. /43/, of the $K^+\pi^-$ system produced by charge exchange in the reaction

$$K^+ n \to K^+ \pi^- p$$

was performed at 4.6, 8.25 and 12 GeV/c by the Saclay-Mons-Brussels-LPNHE (Paris) collaboration /44/. The S-wave $J^P = 0^+$ represents the major contribution for $M(K\pi) < 1.6$ GeV. It appears as a broad and smooth bump centered around 1250 MeV.

A study of $K\pi$ scattering using the reactions

$$K^\pm p \to K^\pm \pi^+ n$$
$$\to K^\pm \pi^- \Delta^{++}$$

at 13 GeV/c has been performed by Estabrooks et al. /45/ The data have been obtained in a spectrometer experiment performed at SLAC. Preliminary results of a p.w.a. indicate that the $I = 1/2$ S-wave rises smoothly to a maximum near 1400 MeV, followed by a fairly rapid drop. The S-wave phase also increases reasonably rapidly in the 1.4 to 1.6 GeV region suggesting the existence of a broad S-wave resonance in the 1500 MeV region.

Information about the isoscalars of the scalar nonet strongly depend on the results of $\pi\pi$- and to some extent of $K\bar{K}$ - phase shift analysis.

The large statistics 17.2 GeV/c CERN-Munich experiment /46/ on the reaction

$$\pi^- p \to \pi^+ \pi^- n$$

has opened up the energy range up to $M_{\pi\pi} \lesssim 1.9$ GeV for the study of the $\pi\pi$ phase shift. Using extrapolated $\pi^+\pi^-$ moments of the angular distribution to the pion exchange pole, during the last two years several attempts have been made to reconstruct these phase shifts /47/.

After the determination of the dominating resonances ρ, f, g the remaining problem was the study of the lower-lying partial-waves.

It is not possible to determine the position and the couplings to the $\pi\pi$ channel of the ε or other non-leading resonances in a unique and reliable way. The question of the existence of daughter resonances can only be settled after an unambiguous set of phase shifts is found. To determine this one has to wait for further experimental data. In order to select the physical solution from the different possible solutions it is necessary to use information obtained from other reaction channels as for example:

$$\pi^- p \to \pi^0 \pi^0 n$$
$$\pi^- p \to \pi^- \pi^0 p$$

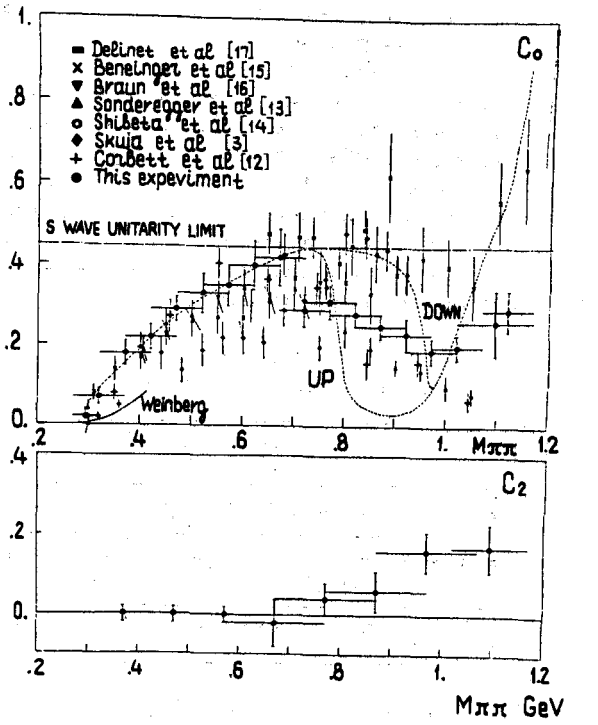


Fig.25 $C_0(\pi^+\pi^- \to \pi^0\pi^0)$ data from this experiment /48/ and from others. The solid curve shows Weinberg's scattering length prediction. The dashed curves show the phase shift analysis prediction for up and down solutions

Results of $\pi^+\pi^- \to \pi^0\pi^0$ total and differential cross sections from threshold to $M_{\pi\pi} = 1.1$ GeV have been obtained from studying the reaction

$$\pi^- p \to \pi^0 \pi^0 n$$

with Chew-Low extrapolation by David et al. /48/. In fig. 25 is shown the variation of

$$C_0 = \frac{\sigma(\pi^+\pi^- \to \pi^0\pi^0)}{2\pi\lambda^2} \quad \text{vs. } M_{\pi\pi}$$

compared with other experimental results. Especially above 620 MeV it appears that for a given experimental technique the behaviour of C_0 is similar in different experiments but in complete disagreement with the other results.

In a subsequent paper the same Saclay group /49/ has presented results of an energy independent phase shift analysis of the four measurable elastic scattering channels ($\pi^\pm\pi^\pm$, $\pi^\pm\pi^0$, $\pi^+\pi^-$, $\pi^0\pi^0$). An analysis of the four channels together makes it possible to use the constraints provided by charge independence. This model independent analysis covers the energy range from threshold to $M_{\pi\pi}$ = 1.2 GeV.

A unique solution is obtained in which the S_0 partial wave has a fast rise above threshold corresponding to a high value of the scattering length a_0^0 m_π = (0.50 ± 0.09). It crosses 90° near 720 MeV and has a fast variation between 970 and 1020 MeV. The speed plot of the partial amplitude exhibits the effect of the pole around 710 MeV and of the S^* pole at 994 MeV (see fig. 26).

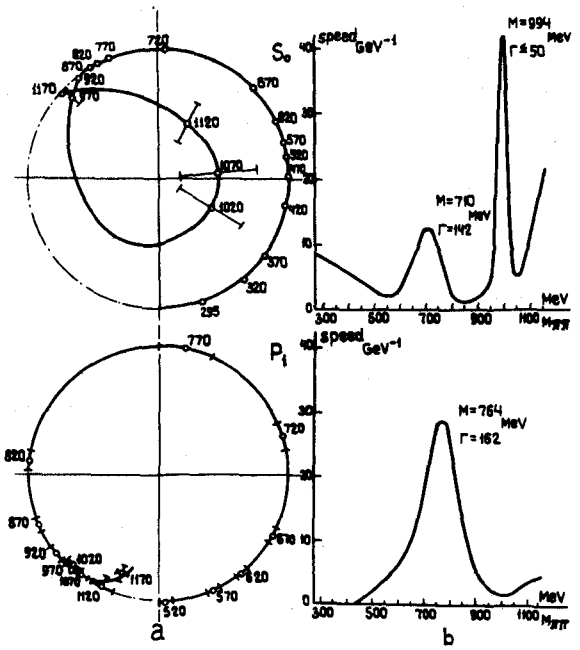


Fig.26 Argand plots and speeds for S_0 and P_1 waves. Curves results from a smoothening of δ and ρ versus $M_{\pi\pi}$ allowing the computation of the speed every 25. MeV

I should like to add a word of caution. You have seen the contradictory results of different experiments in fig. 25 on $\sigma(\pi^+\pi^- \to \pi^0\pi^0)$. The results in the other 3 channels are also only partly in agreement. Therefore the unique solution of Villet et al. /49/ depends on the selected set of experiments in the four channels.

So far good statistics experiments have been made using unpolarized targets. But a complete measurement needs more information. About one year ago the CERN-MPI (München) collaboration started to measure the reaction

$$\pi^- p_\uparrow \to n\pi^+\pi^-$$

with a transversely polarized target at 17.2 GeV/c.

Preliminary results /50/ presented to this conference show strong nucleon polarization dependent moments even at low four momentum transfer. They are due to the presence of s-channel nucleon spin non-flip amplitudes for unnatural spin parity exchange. This is in contradiction to the assumption of absence of the exchange of an object with the quantum numbers of the A_1. This assumption has been used in all pion pole extrapolations until now. The importance of this result in view of the $\pi\pi$ phase shift analyses cannot be overemphasized.

Regarding the S^*, new experimental results came from the study of the reaction

$$K^- p \to \pi^+\pi^- (\Lambda, \Sigma^0)$$

at 13 GeV using the SLAC wire chamber spectrometer /8/. In this reaction one can study the inverse process $\bar{K}K \to \pi\pi$ via K exchange. Since the S^* resonance is located just at or below the $K^- K^+$ threshold, only this reaction permits direct observation of the entire S^* line shape.

Brandenburg et al. /8/ observe in the $\pi^+\pi^-$ mass spectrum a S^* peak containing 35 ± 10 events above background in the mass interval 0.965 - 0.995 GeV. The S^* line shape appears to be significantly distorted in these data (see fig. 27).

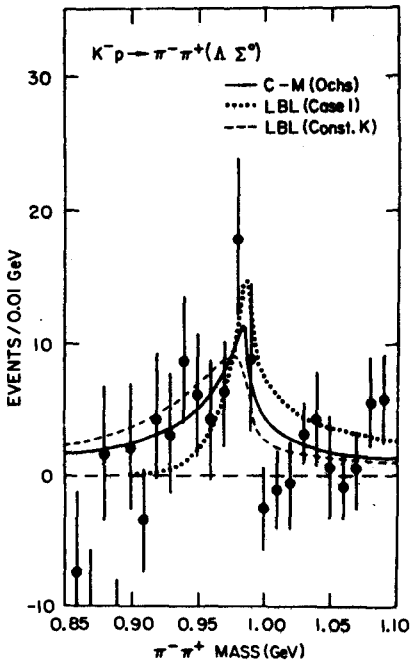


Fig.27 Observed $\pi^-\pi^+$ mass distribution in the S^* meson mass region with both the $K^-p \to K^-\pi^+X^0$ background and $K^-p \to (\rho^0,\omega)(\Lambda,\Sigma^0)$ events subtracted. The curves are the predicted S^* line shape normalized to this data obtained from three different solutions for the S^* parameters given by previous scattering analyses.

In order to check that the effect is in fact due to the S^*, they have computed the expected $\pi\pi$ mass dependence from the K matrix parameters determined in previous experiments. The three cur-

ves in fig. 27 correspond to the S^{**} parameters given in table 5 with the χ^2 obtained for each fit.

TABLE 5

Resonance parameters associated with the curves shown in fig 27

Curve	Pole (MeV)	δ_π	δ_K	χ^2 (9 bins)
C-M (Ochs)	$(1006 - i15)_{II}$	$0.28 \exp(i76^\circ)$	$0.55 \exp(-i29^\circ)$	7.4
LBL (Case 1)	$(997 - i27)_{II}$	$0.30 \exp(-i84^\circ)$	$0.47 \exp(i11^\circ)$	16.0
	$(930 - i18)_{III}$	$0.19 \exp(-i65^\circ)$	$0.63 \exp(i18^\circ)$	
LBL (Const. K)	$(1002 - i33)_{II}$	$0.35 \exp(-i89^\circ)$	$0.73 \exp(-i31^\circ)$	7.0

The other new result came from the study of the reaction

$$\pi^- p \longrightarrow \pi^+ \pi^- n$$

at 1.98 GeV/c by Buttram et al. /51/. The events were required to have a slow recoil neutron which restricted the allowed range of four - momentum transfer to $|t - t_{min}| < 0.003$ (GeV/c)^2 in the S^{**} region. The differential cross section for ϱ production dips near $t = t_{min}$. As a result the authors observe very little ϱ production and the S^{**} becomes the dominant feature of the data. The parameters of the S^{**} pole [(970 ± 5) - i (22 ± 5) MeV] were found by fitting the dimeson mass spectra to a Breit-Wigner resonance formula with a coherent background.

After this short survey of the different candidates for the scalar nonet I feel that only the δ (976) can be considered as an established resonanne with an acceptable pole position.

From the realistic point of view I will include in the L = 1 multiplet the following states as established:

Table 6

L = 1 multiplet

J^{PC}	I = 1	I = ½	I = 0	I = 0
2^{++}	A_2 (1310)	K^{**} (1420)	f (1270)	f' (1514)
1^{++}		Q_1 (1280)		
1^{+-}	B (1235)			
0^{++}	δ (976)			

2.3 The L = 2 Multiplet

If the orbital angular momentum of the quark and antiquark is L = 2 we might expect the four nonets $J^{PC} = 3^{--}$, 2^{-+}, 2^{--} and 1^{--}

Up to the London Conference only the quantum numbers of the g - meson were established to be $J^P = 3^-$

Progress about an isoscalar member of this nonet has come from the partial wave analysis of the reaction

$$\pi^+ p \longrightarrow \pi^+ \pi^- \pi^0 \Delta^{++}$$

at 7 GeV/c by Wagner et al. /17/. In this already mentioned LBL-analysis the experimental mass distributions show two significant peaks at $M_{3\pi} \sim 1.3$ GeV and $M_{3\pi} \sim 1.7$ GeV, respectively (fig. 28).

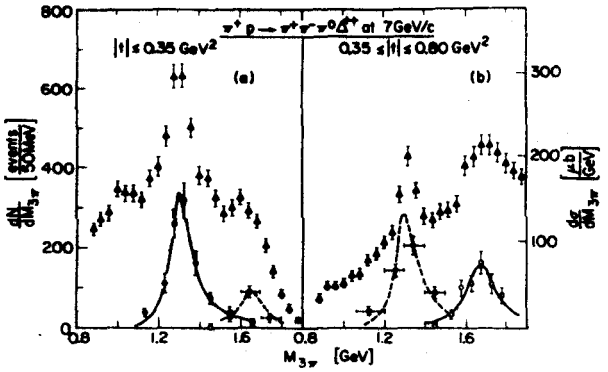


Fig.28 The experimental 3π mass spectrum for $\pi^+ p \to (3\pi)^0 \Delta^{++}$ as function of $M_{3\pi}(\phi)$, left hand scale in Events/30 MeV right hand scale in μb/GeV, Fig. 28a for $|t| \le 0.35$ GeV^2 and Fig. 28b for $0.35 \le |t| \le 0.80$ GeV^2. The total intensity going into $1(2^+ D_0 \pi)$ (ϕ) and into $0(3^- F_0 \pi)(\phi)$ are also given. Solid curves are Breit-Wigner fits to the 2^+ intensity at low |t| and to the 3^- intensity at high |t|. Dashed curves are the same fits normalized to the number of events in that |t| -bin.

The fitted total contribution of the 3^- F ($\varrho\pi$) wave shows that the second peak is caused by this amplitude. The authors identify this peak with the ω^{**} (1675).

The phase variation is more difficult to obtain but most of the solutions are compatible with a phase increase of 100° for $1.625 \le M(3\pi)^0 \le 1.725$ GeV.

This fact and the observed Breit-Wigner shape of the wave make a resonance interpretation very likely (see also fig. 9).

Several groups have presented evidence for structures in the $K\pi$ mass spectrum near 1.8 GeV and have interpreted them in terms of a new K^{**} (1800) resonance /52/.

Progress comes from a SLAC wire chamber spectrometer experiment which studies the charge exchange reactions

$$K^- p \longrightarrow K^- \pi^+ n$$

$$K^+ p \longrightarrow K^+ \pi^- \Delta^{++}$$

at 13 GeV /53/.

The combined data of the unnormalized spherical harmonic moments shown in fig. 29 indicate the existence of a rather broad $J^P = 3^- K^{**}$ resonance in the region of 1.8 GeV. The moments $\langle Y_{70} \rangle$ and $\langle Y_{80} \rangle$ were found to be zero within the errors below 2.0 GeV.

The Saclay-Rutherford-Ecole Polytechnique collaboration /54/ has studied the K^{**} (1800) production in the non-charge-exchange and in the charge-exchange reaction channels

$$K^- p \longrightarrow \bar{K}^0 \pi^- p$$

$$K^- p \longrightarrow K^- \pi^+ n$$

at 14.3 GeV/c. They find evidence for narrow K^{**} (1800) production in both reactions. From the decay angular distribution of the K^{**} and with plausible assumptions about the production mechanism, the $J^P = 3^-$ spin parity assignment is favoured.

In a paper submitted to this conference the Aachen-Berlin-CERN-London-Vienna collaboration presented data showing evidence for a rather broad K^{**} (1800) enhancement in the reaction

$$K^- p \longrightarrow K^- \pi^+ n$$

at 10 and 16 GeV/c [55].

In the non-charge-exchange reaction

$$K^- p \longrightarrow \bar{K}^0 \pi^- p$$

no K^* (1800) signal was seen. In contradiction to Brandenburg et al. [53] they do not see structure in $\langle Y_{60} \rangle$ in the peak region in the charge-exchange reaction.

$K^+ p \to K^+ \pi^- \Delta^{++}$ at 13 GeV/c ($|t'| \leq 0.2$ GeV^2).

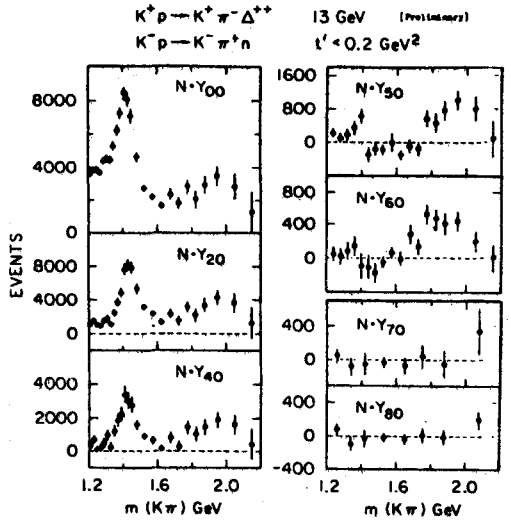


Fig.29 Spherical harmonic moments of the $K\pi$ system in the charge-exchange reactions $K^+p \to K^+\pi^-\Delta^{++}$ and $K^-p \to K^-\pi^+n$ at 13 GeV/c.

The results of the new experiments are summarized in table 7.

Table 2

New results of the K^* (1800) meson.

Reaction	Cuts	Mass [MeV]	Width [MeV]	J^P	Reference
$K^+p \to K^+\pi^-\Delta^{++}$ $K^-p \to K^-\pi^+ n$	$\lvert t'\rvert < 0.2$ (GeV/c)^2 $-0.77 < \cos\theta_J < 0$	1776±20	270±70	3⁻ favoured	/53/
$K^-p \to \bar{K}^0\pi^- p$ $\to K^-\pi^+ n$	$\lvert t\rvert < 0.2$ (GeV/c)^2 $\lvert t\rvert < 0.3$ (GeV/c)^2 $M_{n\pi} > 1.3$ GeV	1780±30 1840±30	120±40 100±40	3⁻ favoured	/54/
$K^-p \to K^-\pi^+ n$ $\to \bar{K}^0\pi^0 p$	$\cos\theta_J < 0$	1871±10 not seen	285±40 -		/55/
$K^+p \to K^0_S\pi^+ p$	$0.05 < \lvert t\rvert < 1.0$ $M_{p\pi} > 1.4$ GeV	1783±16		3⁻	/56/

There seems to be a difference between measured widths obtained by experiments using different cuts in order to reduce background.

In my opinion the most important contribution comes from a spectrometer study of the reaction

$$K^+ p \longrightarrow K^0_S \pi^+ p$$

at 10 GeV/c by Baldi et al. [56]. Figure 30 shows the observed (histogram) and the acceptance corrected (points) $K^0\pi^+$ mass spectrum. The fit parameters of the K^* (1800) are given in table 7. The results of a moment analysis of the $K\pi$ decay angular distribution are shown in fig. 31. A significant signal at the K^* (1800) is seen in all moments with M = 2 up to L = 6. A Breit-Wigner fit to the moment $N \langle \mathrm{Re}\, Y^2_6 \rangle$ gives M = 1779 ± 11 MeV and Γ = 135 ± 22 MeV.

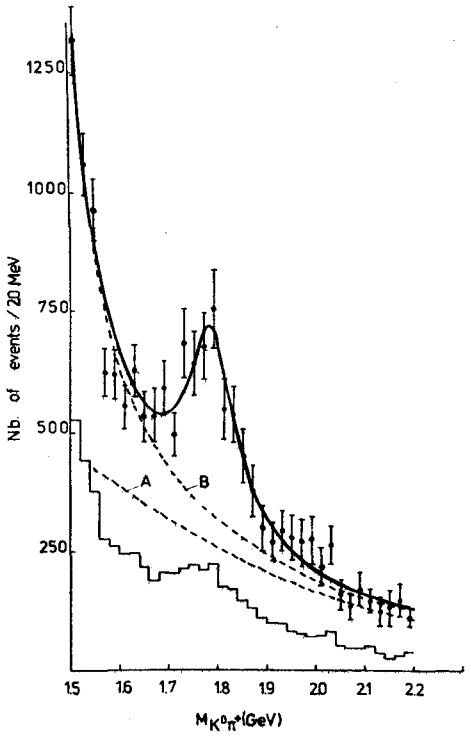


Fig.30 $K^0_S\pi^+$ mass distribution without (histogram) and with (points) acceptance correction. The fit includes a Breit-Wigner (full line) above a background compesed of a polynomial shape (broken line A) and the tail of the K^*(1420) (B).

I come to the conclusion that we have now clear evidence for a K^* (1780) meson with the parameters:

$$M \approx 1780 \text{ MeV} \; ; \; \Gamma \approx 100 \text{ MeV} \; ; \; J^P = 3^- \; .$$

Another possible candidate for a L = 2 multiplet is the F_1 (1540). Aguilar - Benitez [57] reported evidence for this state from a study of the reaction channel

$$\bar{p}p \longrightarrow K^0_S K^0 \pi^+ \pi^-$$

at 0.70 GeV/c.

In a paper contributed to this conference the Bombay-Madrid-CERN-College de France collaboration [58] looked for the $F_1 \longrightarrow K^0 K^\pm \pi^\mp$ in the same reaction channel from $\bar{p}p$ annihilations at 0.76 GeV/c. The sample was approximately 4 times the sample of that in which it was found first.

In fig. 32 the $(K\bar{K}\pi)^\pm$ mass spectrum is shown. The dashed histogram shows the expectation which is based on the previous result.

The experimental statement is that the F_1 (1540) disappeared at this slightly different beam momentum.

Let us now consider the table of L = 2 states. I will include in the table the new states K^{**} (1780) and ω^{**} (1675) which in my view are well established.

Table 8

The L = 2 multiplet

J^{PC}	I = 1	I = ½	I = 0	I = 0
3^{--} 2^{++} 2^{--} 1^{--}	ρ (1690)	K^{**} (1780)	ω^{**} (1675)	

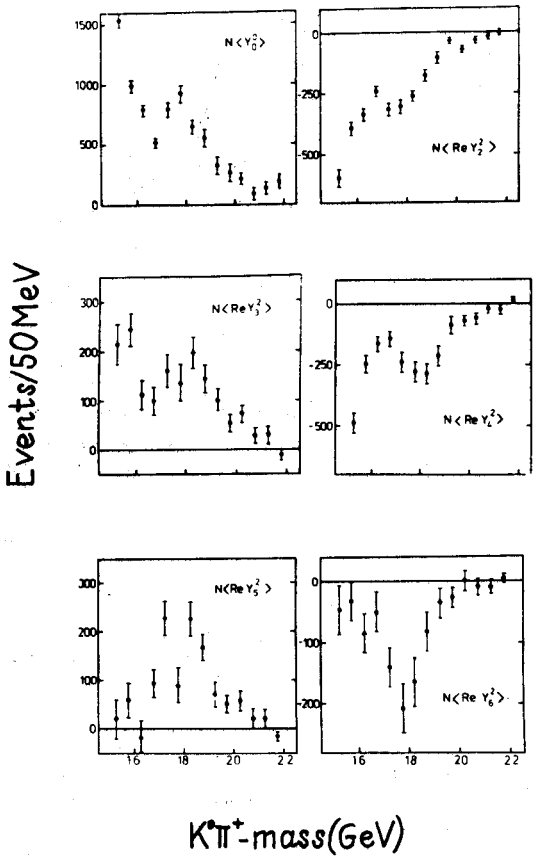


Fig.31 Spherical harmonics moments $N\langle \mathrm{Re}\, Y_L^M \rangle$ of the $K\pi$-decay angular distribution in the Gottfried-Jackson frame.

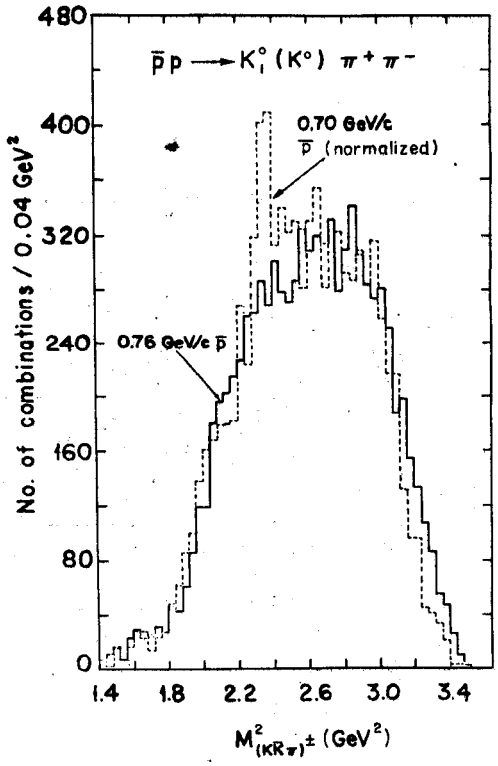


Fig.32 The $(K^0\bar{K}^0\pi)^{\pm}$ mass^2 distribution in reactions $\bar{p}p \to K_1^0(K^0)\pi^+\pi^-$. Solid lines refer to the present work while the dashed lines give the expectation based on the previous result /57/.

2.4 The L = 3 Multiplet

The only resonance which belongs to a L = 3 multiplet, the h (2040) - meson, has been established in two independent studies in the last year.

The reaction

$$\pi^- p \longrightarrow \pi^0 \pi^0 n$$

at 40 GeV/c has been studied with a scintillation counter hodoscope at Serpukhov by the CERN-Karlsruhe-Pisa-Serpukhov-Vienna collaboration /59/. Figs. 33a and 33b show the mass distributions for three and four γ's. From the decay angular distribution it follows that J = 4 for the spin of the h - meson.

The reaction

$$\pi^- p \longrightarrow K^+ K^- n$$

at 18.4 GeV/c has been studied with the CERN-Munich wire spark chamber spectrometer /60/ Fig. 34 shows the mass dependence of the moments $N\langle Y_L^M \rangle$ and the result of fit. In the mass region above 2 GeV only the moments Y_L^0 for $L \leq 8$ are significantly different from zero.

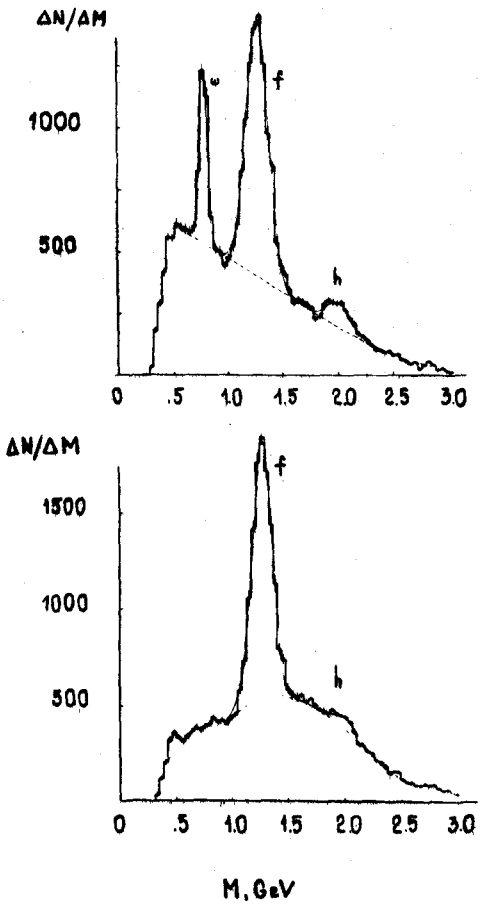


Fig.33 a) Invariant mass spectrum of three-shower events, i.e. $\pi^0\gamma$ of ($\pi^+\pi^-$) asymmetric decay from the reaction $\pi^-p \to \pi^+\pi^-n$ at 40 GeV/c.

b) Invariant mass spectrum of four-shower events, i.e. $\pi^+\pi^-$ from $\pi^-p \to \pi^+\pi^-n$ at 40 GeV/c.

The results of both experiments are summarized in table 9.

Table 9

New results of the h (2020) meson.

Reaction	Mass [MeV]	Width [MeV]	I^G	J^{PC}	Reference
$\pi^- p \to \pi^0\pi^0 n$	2020 ± 30	180 ± 60	0 or 2	4^+	/59/
$\pi^- p \to K^+ K^- n$	2050 ± 25	225^{+120}_{-70}	0^+	4^{++}	/60/

In the study of the $K\pi$ system in which Brandenburg et al. /53/ reported evidence for the K^* (1800), $J^P = 3^-$ state evidence was given also for the existence of a broad $J^P = 4^+$ K^* of mass ~ 2.1 GeV. In fig. 35c the uncorrected $\langle Y_8^0 \rangle$ moment is clearly positive and peaks at ~ 2.1 GeV.

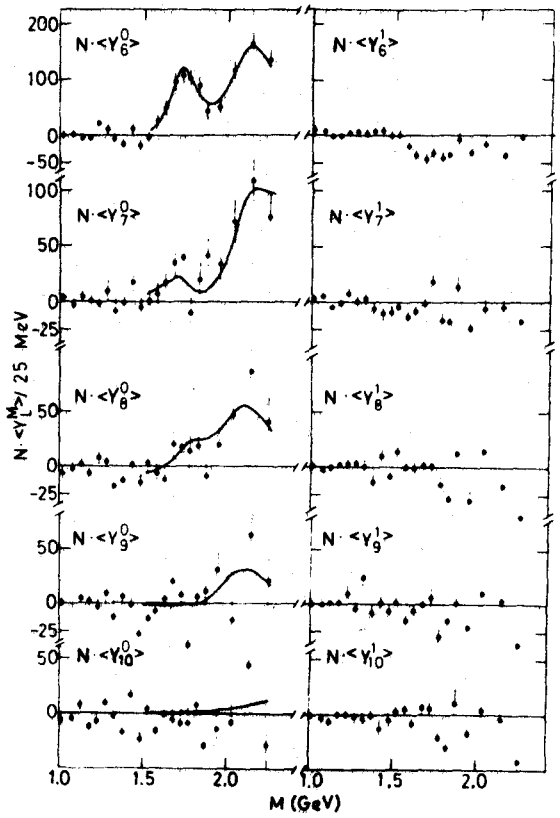


Fig.34 Mass dependence of the moments $N^*\langle Y_L^M \rangle$ for $6 \leq L \leq 10$; $0.025 < |t| < 0.25$ GeV^2.

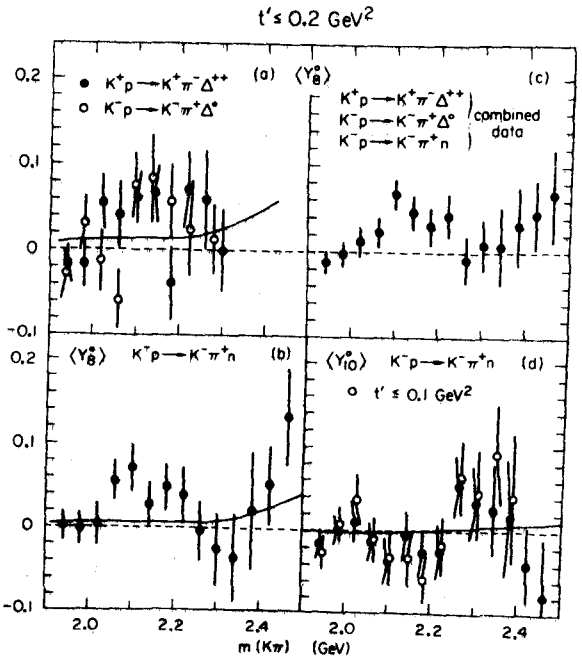


Fig.35 a) – c) Uncorrected $\langle Y_8^0 \rangle$ moment and

d) uncorrected $\langle Y_{10}^0 \rangle$ moment in the region $m > 1.92$ GeV.

2.5 The n = 2 States

After discussing the evidence for mesonic ($q\bar{q}$) states with orbital excitations L = 0, 1, 2 let us check whether or not we have any evidence for radial excitation.

Possible evidence for radial excitation in the meson sytem is provided by the ϱ' (1600) and the ψ' (3684).

In the 1974 edition of the meson table of the Particle Data Group /61/ the ϱ' (1600) $\longrightarrow \varrho\,\pi^+\pi^-$ was underlined as established. In the 1976 edition a remark was added that it is not a well established resonance. It has been seen in both electron-positron colliding beams which establishes its quantum oumbers as $J^P = 1^{--}$, and in photoproduction.

But there are some uncertainties which have to be checked.

Fig. 36a shows the exclusive cross section for the reaction

$$e^+e^- \longrightarrow \pi^+\pi^+\pi^-\pi^-$$

as a function of the c.m. energy /62/. This shows characteristic threshold behaviour of the cross section in exclusive channel production. The data are consistent with a smooth exponential fall-off above threshold. Certainly, a resonance interpretation is not definitively established by tha peak at threshold.

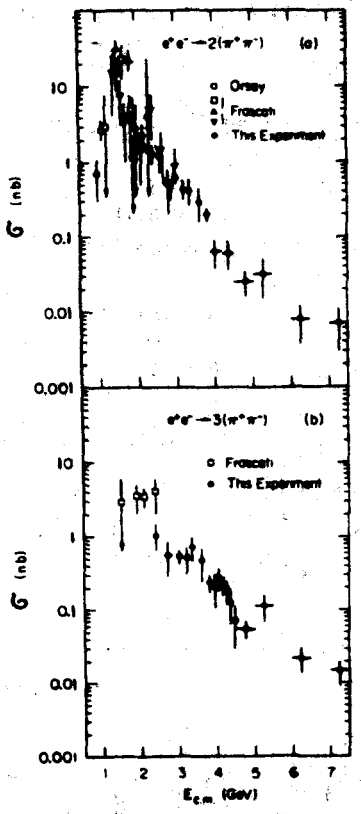


Fig.36 Total cross section for a) $e^+e^- \to 2(\pi^+\pi^-)$ and b) $e^+e^- \to 3(\pi^+\pi^-)$ vs $E_{c.m.}$

We have to expect that the ϱ' (1600) couples strongly to two pions. As already mentioned, from all $\pi\pi$ phase shift analyses which have been carried through up to now it was not possible to decide whether or not broad daughter resoaances like the ϱ' (1600) exist /47/.

As was shown by Ferbel and Slattery /63/ the enhancement seen in the four-pion mass spectrum in photoproduction can be described by a Deck - type mechanism.

Therefore one can consider the ϱ' (1600) to be in a similar state of evidence like the A_1 (1100) or the A_3 (1640).

Very recently Brandenburg et al. /64/ presented results which suggest the existence of a pseudoscalar, strangeness - one resonance, the K^- (1400) which in the $q\bar{q}$ model would result from a radial excitation of the L = 0, $q\bar{q}$ system.

The data on which these results are based were obtained with the SLAC wire spark chamber spectrometer studying the reaction

$$K^\pm p \longrightarrow K^\pm\pi^+\pi^- p$$

at 13 GeV. In figs. 37a, b are shown the $0^-\,0^+$ (ε K) cross section and relative phase as measured with respect to $1^+\,0^+$ (ϱ K). The corresponding results for the K^* (1420) are shown in figs. 37c, d.

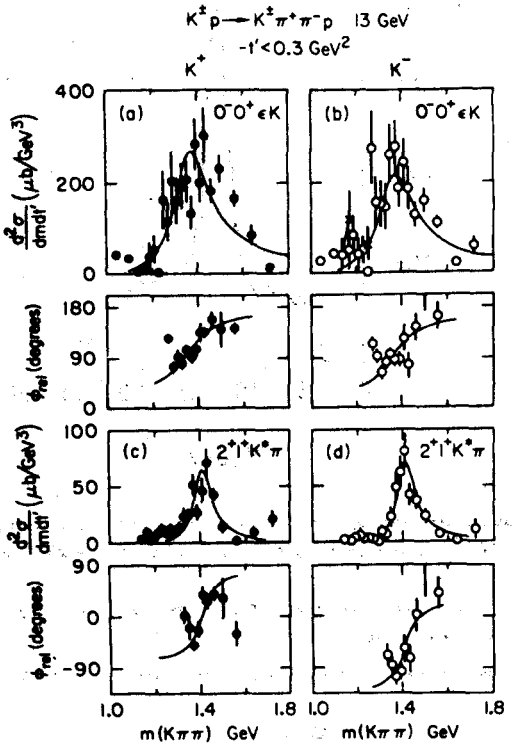


Fig.37 The mass dependenne of the $0^-0^+(\varepsilon K)$ and the $2^+1^+(K^*\pi)$ waves. Crosses correspond to ambiguous solutions, and ϕ_{rel} is measured with respect to the $1^+0^+(\varrho K)$ wave. The curves correspond to simple Breit-Wigner parametrizations.

Both the $0^-\,0^+$ (ε K) and the $2^+\,1^+$ ($K^*\pi$) waves are well described by Breit-Wigner parametrization. This is suggestive of a resonance interpretation for the $0^-\,0^+$ (ε K) wave with

$M_{K'} \approx 1.40$ GeV $\quad \Gamma_{K'} \approx 0.25$ GeV and $J^P = 0^-$.

This evidence is based in the assumption that the $1^+\,0^+$ (K ϱ) phase is constant around $M(K\pi\pi) \sim 1.4$ GeV.

As I already mentioned, Brandenburg et al. /28/ concluded that all the $1^+\,0^+$ ($K^*\pi$) in the 1400 MeV region is resonant. Therefore the $1^+\,0^+$ (K ϱ) vs. $1^+\,0^+$ ($K^*\pi$) phase motion was attributed to a variation of the $1^+\,0^+$ ($K^*\pi$) phase.

Otter et al. /26/, who do not claim a Q_2 resonance, attribute the phase motion of 1^+ 0 + (K ϱ) vs. 1^+ 0 + ($K^*\pi$) to a variation of the 1^+ 0 + (K ϱ).

Cason et al. /65/ have performed a study of the reaction

$$\pi^- p \longrightarrow n K^0_S K^0_S$$

at 6 and 7 GeV/c using a streamer chamber facility. The results of an amplitude analysis are shown in fig. 38. The S-wave intensity is large at threshold (the S^*), decreases, and then goes through a second maximum in the region near 1270 MeV. The shape is suggestive of an S-wave resonance on a smoothly falling S-wave background. The D-wave amplitude can be explained in terms of f (1270) and f' (1514) production. The authors used the corresponding D-wave phase ϕ_D to calculate ϕ_S and came to the conclusion that the S-wave amplitude and phase are both observed to have Breit-Wigner behaviour. The properties of this possible new δ' (1255) resonance are

$$M_{\delta'} \simeq 1255 \text{ MeV} \; ; \; \Gamma_{\delta'} \simeq 80 \text{ MeV} \; ; \; J^{PC} = 0^{++} \; .$$

It seems to me necessary to wait for additional experimental confirmation before one of these candidates ϱ' (1660); K' (1400) and δ' (1255) can be considered as established.

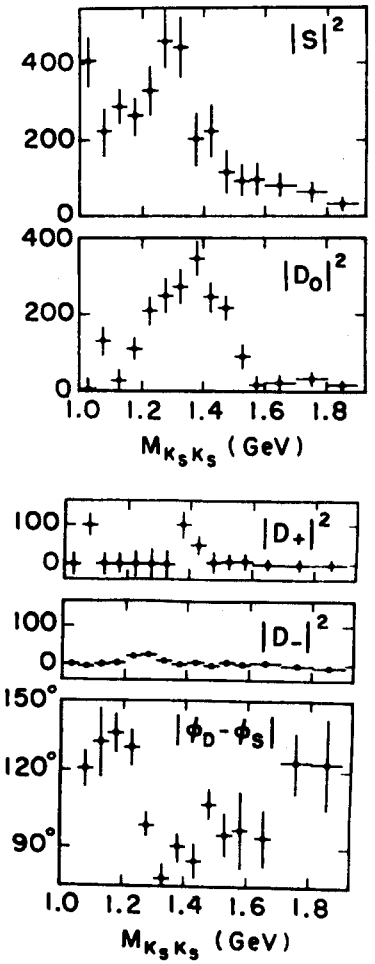


Fig.38 Fitted parameters of the amplitude analysis as a functinn of M_{KK} using data with $|t| < 0.2$ GeV^2.

2.6 The Heavy Mesons

Theoretical models predict a great profusion of mesonic states at high mass values. No strong evidence exists for higher levels because of the absence of reliable spin parity analyses. $\bar{p}p$ elastic scattering and annihilation into meson pairs is beginning to show some evidence.

From this broad field of studies I am taking the S-region as an example.

A measurement of $\bar{p}p$ and $\bar{p}d$ cross sections by Caroll et al. /66/ indicated the presence of a 18 mb bump at 1932 MeV c.m. energy with a width of 9 MeV. Two experiments have been recently performed to investigate the S-region further.

A measurement of the $\bar{p}p$ charge exchange cross section by Alston Garnjost et al. /67/ with high statistical precision found no indication for a 9 MeV wide resonance at 1932 MeV ($\sigma = 0.33 \pm 0.28$ mb).

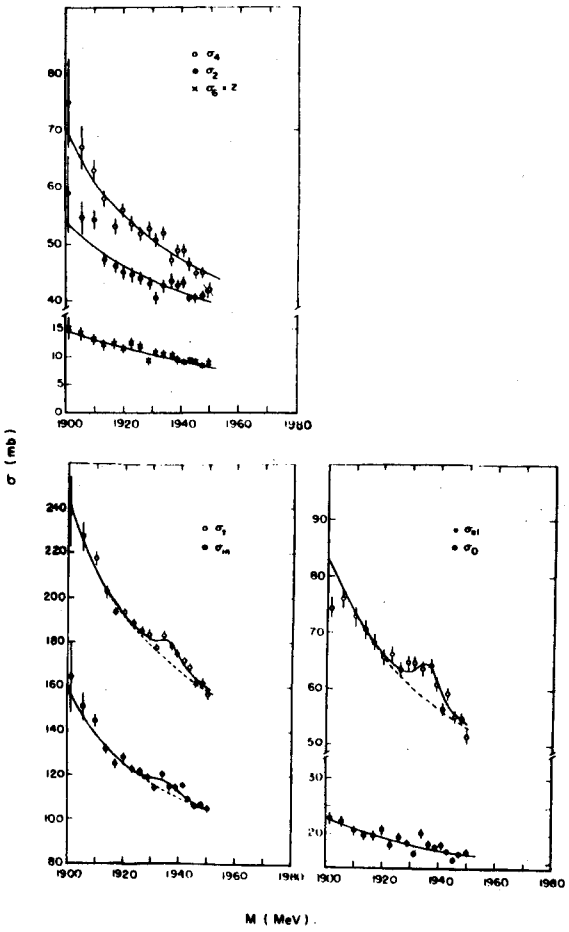


Fig.39 Total, inelastic (0 + 2 + 4 + 6 prongs), elastic and 0, 2, 4, 6 prong cross sections as functions of the total $\bar{p}p$ cm energy. The solid curves on the total, inelastic and elastic cross sections are the results of the fits to background plus resonance. The dashed curves are the polynomial background. The solid curves on the other cross sections are the fits to a polynomial background alone.

A measurement of the $\bar{p}p$ total, alastic and topological crosa sections between 1901 and 1950 MeV, with a resolution of ± 2 MeV, by the CERN-Liverpool-Mons-Padova-Roma-Trieste collaboration /68/, confirmed the existence of the structure in the total cross sections. The parameters are:

$M = 1936 \pm 1$ MeV ; $\Gamma = 9^{+4}_{-3}$; $\sigma = 10.6 \pm 2{,}4$ mb.

On the other hand the measurements also confirm the absance of the signal in the charge exchange cross section and give evidence for a strong contribution to the bump in the total cross section by the elastic channel (fig. 39).

These experimental facts make it difficult to interpret the data as due to the presence of a single, non interfering resonance of dafinite isnspin.

I would be necessary to investigate the S - region with larger s atistics. The same applies to the other regions lika T and U which can be studiad in $\bar{p}p$ formati: ı.

This leads us to the conclusion that the S, T, U structures observed up tn now in $\bar{p}p$ total and elastic cross section cannot be interpreted in terms of single resonances. Intarferences between degenerate resonances of diffarent isospin and interference effects with the background have to be introduced to interpret simultaneously the observations made on total, elastic and charge exchange $\bar{p}p$ reactions.

2.7 The Exotic Mesons

Exotic mesons were last reviewed at the Conference on Experimental Meson Spectroscopy - 1974 by Cohen /69/. From the search of both meson exchange and baryon exchange reactions upper limits on exotic production cross sections were typically in the order 2-9 μb.

By an exotic meson I mean, as usual, a mesonic state that cannot be formed by simple $q\bar{q}$ couplings.

Recently searches have been centred around the backwards produced exotic mesons. The motivation for looking at baryon exchange reactions arises from theoretical arguments /70/ that the baryon - antibaryon system requires exotics in order to satisfy two component duality. Thus exotics might be expected to couple more favourably to a baryon - antibaryon vertex then to a meson vertex. An important prediction from these theoretical ideas is that the cross sections for backwards produced exotic mesons should be of the same order as the cross sections for backwards produced mesons.

I will restrict myself in this report to experiments in which the upper limits on the exotic meson production are low enough to violate the duality requirement.

The CERN-Freiburg-Saclay collaboration /71/ has studied the reaction

$$\pi^+ p \longrightarrow K^{*++} + \Lambda^0_{forward}$$

at 12 GeV/c, using the CERN Ω- spactrometer. No effect of exotic production is visible with a production cross section equal to the non - exotic baryon - exchange cross section for the reaction

$$\pi^- p \longrightarrow \Lambda\ K^{*0}$$

The Indiana-Purdue-SLAC-Vanderbilt collaboration /72/ has studied the reaction

$$\pi^+ p \longrightarrow X^{++} + n_{forward}$$

at 8.4 GeV/c with the SLAC rapid cycling bubble chamber.

The Orsay-CERN-Collage de France-Ecole Polytechnique collaboration /73/ submitted preliminary results on backward production of exotic mesons in the reaction

$$\pi^- n \longrightarrow p_{forward} + X^{---}$$

at 12 GeV/c using the Omega spectrometer. They have searched for tha decay channel

$$X^{---} \longrightarrow \Delta^0\ (\bar{\Delta})^{--} \longrightarrow p\bar{p}\,\pi^-\pi^-$$

The $(p\bar{p}\,\pi^-\pi^-)$ effective mass spectrum shows no peak.

The upper limits on the production cross sections of the different experiments are summarized in table 10. These limits are given as 95% C. L. ones, assuming narrow resonances ($\Gamma \leq 100$ MeV or $\Gamma \leq 50$ MeV).

Table 10

New results of exotic meaons.

Reaction	σ(exotics) [μb]	σ(non-exotics) [μb]	Mass Interval [GeV/c^2]	Reference
$\pi^+p \longrightarrow K^{*++} + \Lambda^0_f$	< 0.060 <0.150	0.160	1.0 - 2.6 2.6 - 3.6	/71/
$\pi^+p \longrightarrow X^{++} + n_f$	< 1 - 2	0.5 - 1.9	<3.0	/72/
$\pi^-n \longrightarrow X^{---} + p_f$, $X^{---} \to p\bar{p}\,\pi^-\pi^-$	< 0.007	0.015	<2.5	/73/
	<0.015	0.038	2.5 - 2.6	
	<0.032	0.10	2.6 - 2.8	
	<0.080	0.32	>2.8	

A comparison with the cross sections for backwards-produced non-exotic mesons shows, aspecially in tha last axperiment, that the limit for backwards-produced exotic mesons is substantially lower. This result is in contradiction with two component duality.

2.8 Summary on Meson Resonances

The progress in meson spectroscopy in the last two years originates in high atatistics, systematic experiments and in the extensive use of partial wave analyses. These studies include both the analyses in elastic andinelastic exclusive reaction channels.

Now we are in a position to look how the established resonances fill the major meson multiplets. This multiplet structure is summarized in figure 40. The L = 0 multiplet is complete. With regard to the gaps in the 1^{++} and 1^{+-} nonets of the L = 1 multiplet we have some good candidates like the Q_2 (1400) and the D (1285). The clarification of the A_1 problem is urgently needed. Forthcomming studies of $\pi\pi$ scattering shnuld improve the isoscalar situation in the 0^{++} nonet.

Concerning the L = 2 and 3 multiplets we have until only very few established states. They were mostly identified with the present generation of magnet spectrometers. The reactions which we have to study in searching for the missing states of fig. 40 are exclusive channels with multiparticle final states. Typical decay modes which have to be studied are $\delta\pi$, $\omega\eta$, πA_2, $K\bar{K}^*$ etc. In order to identify the resonances and to determine their properties high statistics experiments with sensitivities $\geq$ 1000 events/μbarn are required.

Both the new evidence about meson resonances and the non evi-

dence for exotic states which cannot be represented as a bound $q\bar{q}$ pair show that the general pattern of meson states is in agreement with the naive nonrelativistic quark model.

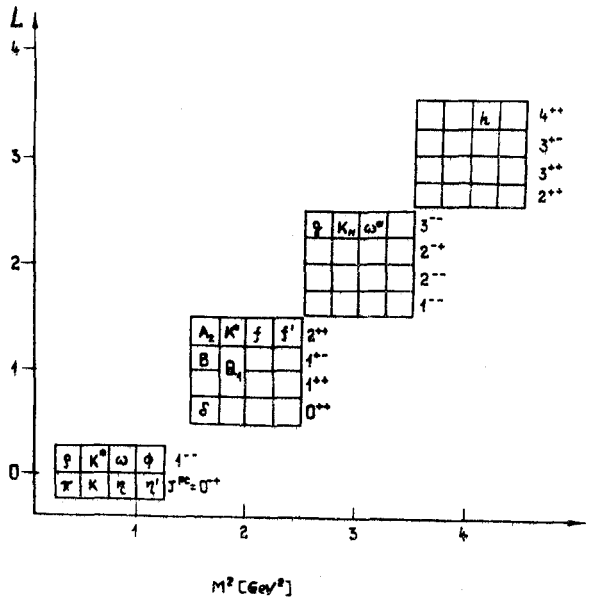


Fig.40 The multiplet structure of meson resonances.

3. Baryons

As you well know the data from formation experiments are far more extensive and complete than from production experiments. This results in the healthier state of baryon spectroscopy compared with meson spectroscopy.

The known baryon states belong to a decuplet [10], an octet [8] or a singlet [1] representation of SU(3). Like for the meson states this is a strong evidence for a constituent quark model.

Combining three quarks with spin ½ to make a baryon state yields

$$6 \otimes 6 \otimes 6 = [56] \oplus [70] \oplus [70] \oplus [20]$$

Combining the internal symmetry and the spin variables with the orbital excitation one could form the symmetry SU(6) ⊗ O(3) and produce multiplets of the type $[R, L^P]$. R denotes the dimensionality under SU(6), L, the orbital angular momentum and P the parity of the state.

These multiplets decompose as follows into components $[^{2S+1}R', J^P]$ where R' denotes the SU(3) representation, (2S + 1) the quark spin multiplicity and J^P the total angular momentum and parity of the stste.

$$\begin{aligned}
[56,0^+] &= [^4 10, 3/2^+] + [^2 8, 1/2^+] \\
[70,1^-] &= [^4 8, 5/2^-] + [^4 8, 3/2^-] + [^4 8, 1/2^-] + \\
&+ [^2 10, 3/2^-] + [^2 10, 1/2^-] + [^2 8, 3/2^-] + \\
&+ [^2 8, 1/2^-] + [^2 1, 3/2^-] + [^2 1, 1/2^-] \\
[56,2^+] &= [^4 10, 7/2^+] + [^4 10, 5/2^+] + [^4 10, 3/2^+] + \\
&+ [^4 10, 1/2^+] + [^2 8, 5/2^+] + [^2 8, 3/2^+]
\end{aligned}$$

etc.

The stable baryon $J^P = 1/2^+$ octet and the $J^P = 2^+$ decuplet can clearly be identified as belonging to the $[56,0^+]$ multiplet. Since L = 0 only the $1/2^+$ octet and the $3/2^+$ decuplet are present.

Concerning the SU(6) ⊗ O(3) multiplets Litchfield /74/ in his rapporteur talk on baryon resonances at the XVII International Conference on High Energy Physics, London 1974, came to the following conclusions:

(i) The $[70,1^-]$ and $[56,2^+]$ multiplets are nearly complete not taking into account the Ξ's and Ω's.

(ii) The $[56,0^+]$ n = 2, $[70,3^-]$ and $[56,4^+]$ are gradually getting filled. The second $[56,0^+]$ n = 2 is a radial excitation of $[56,0^+]$.

(iii) There are possible indications of a third $[56,0^+]$, a second $[70,1^-]$ and either a second $[56,2^+]$ or a $[70,2^+]$.

In order to illustrate the situation better in fig.41 are shown the $[70,1^-]$ and $[56,2^+]$ multiplets. The established resonances are given in full points. The assignments are taken from Litchfield's /74/ rapporteur talk. Open circles belong to states in the multiplets which were not established. Only resonances with a three or four star status are included. Here and in the following I use the PDG classification:

- ■■■■ Good, clear and unmistakable
- ■■■ Good, but in need of clarification, or not absolutely certain
- ■■ Needs confirmation
- ■ Weak

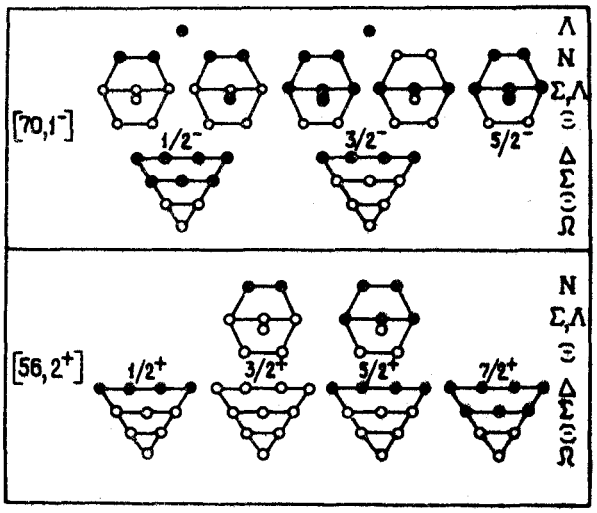


Fig.41 Baryon multiplets in SU(6). Open circles belong to states which were not established in 1974. Only resonances with a three or four star status are included.

3.1 Strangeness 0 Baryon States

Our knowledge about the S = 0 baryon states comes mainly from the study of the reactions

$$N \longrightarrow N_{1/2}^{*} \quad \text{or} \quad N_{2}^{*} \longrightarrow \pi N;\ \eta N;\ \Lambda K;\ \Sigma K;\ \pi\pi N;\ \ldots$$

The best source of information on baryon resonances is the experimental data on differential cross sections and polarizations in

two body reactions

$$0^- + 1/2^+ \longrightarrow 0^- + 1/2^+ .$$

They are analysed with the help of partial wave expansions. There are three distinct methods of doing this:

- The phase shift analysis is carried through at each energy separately. Partial waves with angular momentum above some cut-off value are mostly assumed to be negligible. A choice is made among the different indistinguishable or nearby solutions usually on the basis of energy continuity. A popular criterion for making this choice is the shortest path technique. Instead of this technique some recent analyses have imposed fixed t analyticity or hyperbolic dispersion relation as a constraint.
- In the energy dependent analysis the data at different energies are fitted at once. The partial wave amplitudes are usually chosen to include both resonances and non-resonant background.
- It was shown by Barrelet [75] that zeros near the physical region of the $0 + 1/2 \longrightarrow 0 + 1/2$ amplitudes can be systematically determined from differential cross sections and polarization. The resolution of the discrete ambiguity (related to the Minami ambiguity) can be achieved by the requirements that zero trajectories are analytic functions of energy and that causality demands negative imaginary parts for pole positions in the complex energy plane.

All the different methods are to some extent model dependent. Also in the last method one assumes that the amplitudes have only a minimum number of zeros. Starting from the Saclay (1974) phase shift analysis Atkinson et al. [76] construct continuum ambiguities that leave the total cross section, the differential cross section and the polarization unchanged. The existence of this ambiguity is a consequence of the fact that one can change both the spin-flip and the non-spin-flip amplitudes by multiplying each by the same angle dependent phase factor without changing σ_T, $d\sigma/d\Omega$ and P. Disagreements between different groups concerning the existence of weak resonances, or concerning the masses and widths of stronger ones, may be caused by the existence of the continuum ambiguity. They can be reduced by exploiting fixed t analyticity.

Before discussing new $\pi N \longrightarrow \pi N$ partial wave analyses I would like to mention some important experimental data which were published recently.

A sonic spark chamber system has been used by the Bristol-Rutherford-Southampton collaboration [77] to measure the $\pi^\pm p$ elastic differential cross section at 51 momenta from 0.4 to 2.15 GeV/c. In this high precision experiment a complete coverage was made of all centre of mass scattering angles except those for the extreme forward direction.

With these new data the $\pi^- p$ situation is greatly improved for purposes of partial wave analyses. Up to now the $\pi^+ p$ have been in a much better shape because they had more uniform angular coverage.

The comparison between $\pi^+ p$ and $\pi^- p$ elastic polarization experiments is even worse. Martin et al. [78] made polarization measurements in a very high statistics $\pi^+ p$ elastic scattering experiment in the momentum range from 0.60 to 2.65 GeV/c. There are no $\pi^- p$ elastic polarization data of comparable quality.

Charge exchange data are from the experimental point view much more difficult to obtain and hence more sparse than elastic data. Therefore another important new contribution of the RHEL is the measurement of the polarization and the differential cross section in the reaction

$$\pi^- p \longrightarrow \pi^0 n \; ; \; \pi^0 \longrightarrow 2\gamma$$

in a counter arrangement which covered almost the full range of centre of mass scattering angles [79]. The polarization parameter P has been measured at 22 momenta between 0.62 and 2.27 GeV/c and the differential cross section at 22 momenta in the range from 0.62 to 2.37 GeV/c. Fig. 42 shows for example measurements of the differential cross section and the polarization at four momenta. The statistical accuracy is substantially improved in comparison with previous experiments. The superimposed curves are predictions from the Saclay (1974) phase shift solutions. The agreement is poor for the new polarization measurements. Therefore the data should substantially constrain any future phase shift analysis.

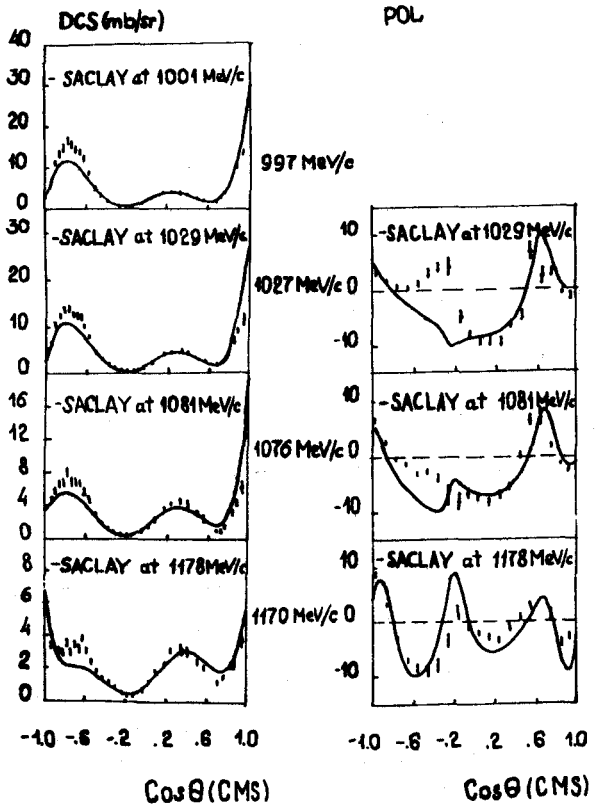


Fig.42 Measurement of differential cross section and polarization in $\pi^- p \rightarrow \pi^0 n$ reaction. The curves are predictions from the Saclay (1974) phase shift analysis.

At present we have four comprehensive partial wave analyses in the resonance region:

- The CERN (1972) energy - independent analysis [80].
- The Saclay (1974) energy - independent analysis [81].

Both of them used the shortest path method to connect solutions at different energies.

- In the Karlsruhe (1976) energy - independent analysis [82] fixed t ($0 \geq t \geq -1.5$ GeV^2), fixed angle and backward disper-

sion relations have been used as a constraint. The cut-off in L of the partial waves has been performed by the convergence test function method. Coulomb corrections have been carried out as proposed recently by Hamilton and Tromberg[83].

The partial waves were determined from threshold up to 10 GeV/c pion lab. momenta. The fixed t amplitudes for $t < 1.5$ GeV^2 use all the data up to the highest energies available. The backward amplitudes were separately determined from backward $d\sigma/d\Omega(\pi^{\pm}p \to \pi N)$ as well as from $d\sigma/d\Omega(\bar{p}p \to \pi^{+}\pi^{-})$. Amalgamation of data in the p.w.a. was avoided as far as possible. A small part of very contradictory data was removed.

- In the CMU - LBL (1976) energy - independent analysis[84] at each energy the data were analysed with the help of an accelerated convergence expansion in which higher partial waves are not required to vanish, but are determined in part by particle exchange processes and in part by extrapolation from lower partial waves. Energy smoothing of single energy fits is accomplished by using dispersion relations along hyperbolic curves in the s - t plane.

Amalgamated pion proton scattering data at 26 momenta in the range from 0.8 to 2.0 GeV/c have been used. The amalgamation includes

a) compilation (undating and correction)
b) fitting (normalization and momentum callibration errors, resolution of beam momenta, electromagnetic corrections and inconsistent data)
c) interpolation
d) statistical averaging.

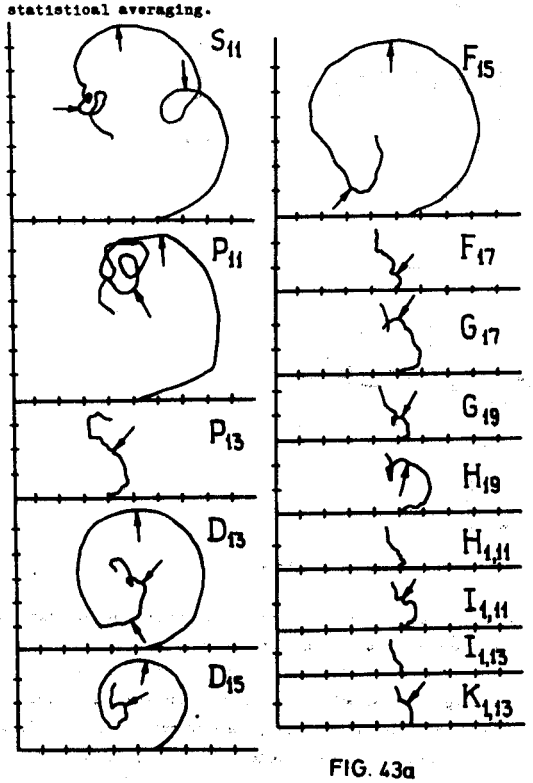


FIG. 43a

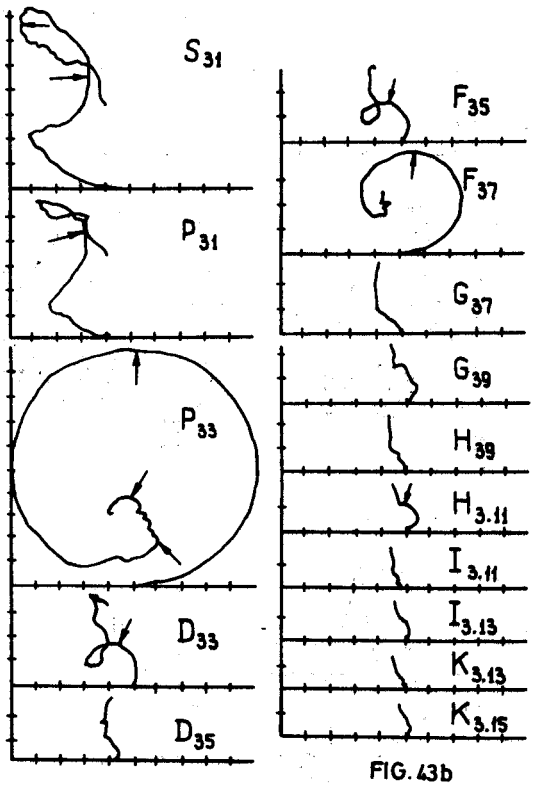


FIG. 43b

Fig.43a. Argand diagrams of I=1/2 πN partial waves. Triangles denote positions of resonances or speed maxima. b) Argand diagrams of I=3/2 πN partial waves. Triangles denote positions of resonances or speed maxima.

The results of the four different partial wave analyses on resonances are summarised in table 11a,b. The Argand diagrams of I=1/2 and I=3/2 πN partial waves of the last two analyses are shown in figs. 43a,b and 44 a-d.

The number of stars without brackets given to each of the states in table 11a,b are taken from the Tables of Particle Properties (April 1976)[1]. These assignments have to be confronted with the results of the two new analyses[82,84]. Some speed maxima have been excluded from the Karlsruhe (1976) data. This means only those resonances are included which can be considered at least as two star states. In addition to the confirmation of the already accepted three and four star states the Karlsruhe (1976) analysis presented strong evidence for states which, in the opinion of the authors, can now be considered as three star resonances:
I=1/2 states: $S_{11}(2100)$; $D_{15}(2100)$, $F_{17}(1990)$, $G_{19}(2140)$
I=3/2 states: $S_{31}(1900)$.
The splitting of the Roper resonance ($P_{11}'(1470)$) claimed by the Saclay (1974)[85] analysis was neither confirmed by the Karlsruhe (1976) nor by the CMU-LBL (1976) results.

Concerning the confirmation of well established three and four star resonances the results of the CMU-LBL (1976) analysis are in good agreement with the older data and with the Karlsruhe (1976) results. The D_{13} partial wave (fig.44a) shows a second resonance at about 1655 MeV and indicates a higher resonance at about 2070MeV. Fig.44a shows a fit to the G_{17} partial wave with two resonances. In

fitting G_{17} data from Saclay (1974) for $P_{LAB} > 2.0$ GeV/c have also been used.

The fit to the P_{33} partial wave includes the P_{33} (1232), a resonance at 1690 MeV and a third resonance near 2100 MeV. A comparison of the Argand diagram of the P_{33} partial wave in the CMU-LBL analysis and in the Karlsruhe analysis shows a good agreement.

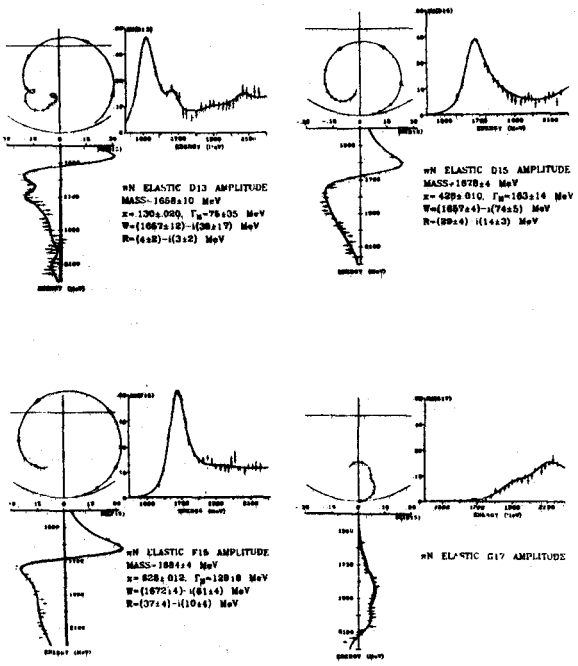


FIG. 44a

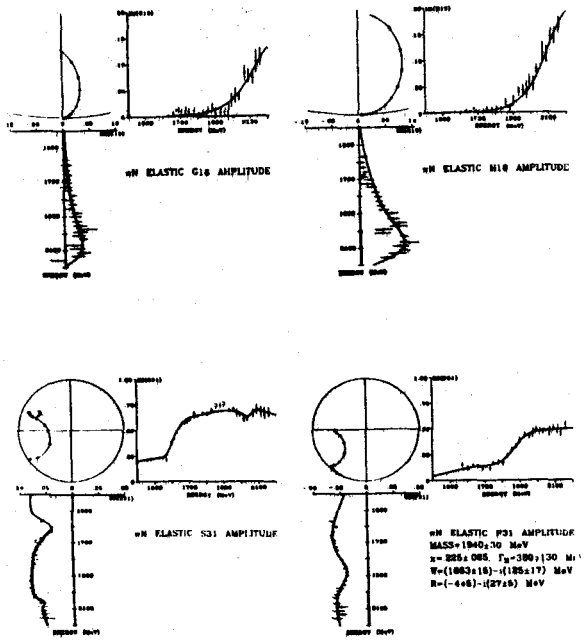
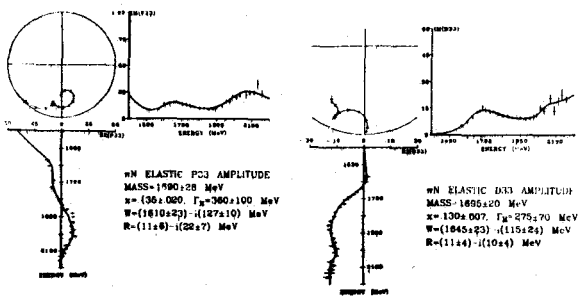


FIG. 44b



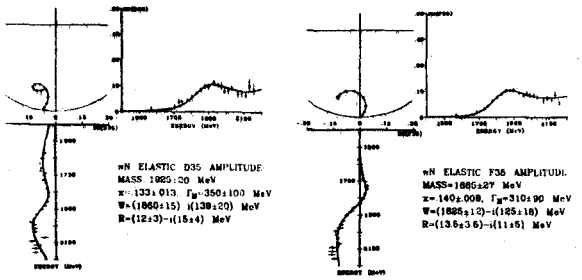
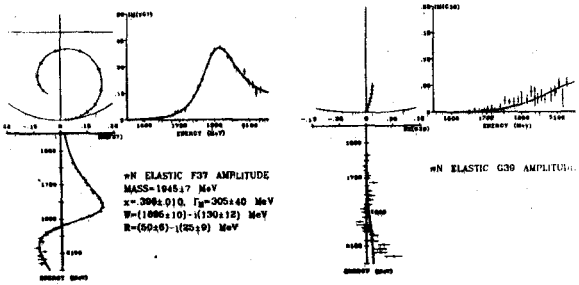


FIG. 44c



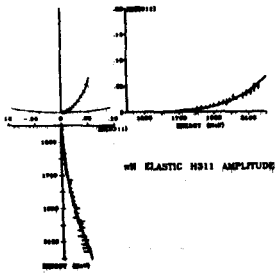


FIG. 44d

Fig. 44a–d p.w. amplitudes. Results of energy independent fitting are shown as data points; the curves show an energy dependent fit. The fit is also shown on the Argand plot, with arrows at multiples of 50 MeV. The errors on the real and imaginary parts are correlated; also, data at neighboring energies have an estimated average correlation coefficient of 0.3.

A significant result of the CMU-LBL analysis is the confirmation of a D_{35} state at 1925 MeV (see Fig. 44c). Unfortunately it was not found in the Karlsruhe (1976) analysis. A $[70,3^-]$ assignment for the D_{35} (1960) is unlikely, because the mass of the observed state seems to be too low. Therefore the D_{35} (1960) can be considered as a member of a $[56,1^-]$ multiplet.

Table IIa

S=0, I=1/2 resonance results of different phase shift analyses

	CERN(1972)			Saclay(1974)			Karlsruhe(1976)			CMU-LBL(1976)		
$L_{2I,2J}$	Mass [MeV]	Γ MeV	x_1	Mass [MeV]	Γ [MeV]	x_1	Mass [MeV]	Γ [MeV]	x_1	Mass [MeV]	Γ [MeV]	x_1
$S_{11}(1536)$	1500	50	0.25	1520	80	0.36	1517	108	0.38	1549†	162	0.321
$S_{11}(1700)$	1670	120	0.50	1672	179	0.586	1690	160	0.54	1624†	203	0.984
$S_{11}(2100)$	2100	200	0.50	2283	310	0.14	2055	205	0.16	above 1800 not solved		
$P_{11}(1470)$	1470	220	0.65	1413 1532	187 89	0.549 0.123	1447	190	0.55	1467†	311	0.683
$P_{11}(1780)$	1720	160	0.21	1729	217	0.188	1745	155	0.19	1810‡	225	0.444
$P_{13}(1810)$	1850	300	0.25	1696	117	0.145	1788	224	0.17	1859‡	302	0.159
$D_{13}(1520)$	1520	120	0.58	1525	122	0.558	1517	128	0.56	1521†	134	0.549
$D_{13}(1700)$				1710	100	0.089	1800	218	0.08	1658	75	0.130
$D_{13}(2040)$	2075	150	0.31	2029	116	0.10	2078	283	0.11	2066‡	118	0.096
$D_{15}(1670)$	1683	150	0.45	1660	146	0.415	1660	172	0.38	1678	163	0.428
$D_{15}(2100)$	2100	150	0.2	2100	220	0.08	2171	280	0.09	2296‡	385	0.115
$F_{15}(1688)$	1688	140	0.65	1680	126	0.593	1684	146	0.66	1684	129	0.628
$F_{15}(2000)$	2175	150	0.25	1989	179	0.08	2067	310	0.12	1965‡	416	0.084
$F_{17}(1990)$	2000	200	0.15	2049	119	0.064	1962	260	0.05	1966‡	184	0.055
$G_{17}(2000)$										1994‡	408	0.089
$G_{17}(2190)$	2225	150	0.35	2141	243	0.161	2123	250	0.1	2191†	483	0.177
$G_{19}(2140)$				2133	193	0.095	2150	400	0.08	2220†	362	0.081
$H_{19}(2220)$				2249	347	0.140	2116	380	0.19	2260†	489	0.188
$I_{1,11}(2650)$							2650					

†Uses some additional partial waves ‡Resonance parameters not definite

After this short discussion of the results of both the Karlsruhe (1976) and the CMU-LBL (1976) phase shift analyses it seems to me reasonable to change the assignments of stars of the S = 0 baryon resonances into those indicated in table IIa, b in brackets.

Table IIb

S=0, I=3/2 resonance results of different phase shift analyses

	CERN(1972)			Saclay(1974)			Karlsruhe(1976)			CMU-LBL(1976)		
$L_{2I,2J}$	Mass [MeV]	Γ MeV	x_1	Mass [MeV]	Γ MeV	x_1	Mass [MeV]	Γ MeV	x_1	Mass [MeV]	Γ MeV	x_1
$S_{31}(1650)$	1620	140	0.35	1623	161	0.315	1616	160	0.310	1634†	187	0.279
$S_{31}(1900)$				2001	307	0.08	1920	228	0.17	2070‡	100	0.122
$P_{31}(1910)$	1900			1786			1932	285	0.22	1940	380	0.225
$P_{33}(1232)$	1235	129	1.0	1234	120	1.0	1232		1.0	1233	122	1.0
$P_{33}(1690)$	1680	220	0.1	1904	204	0.194				1690	360	0.135
$P_{33}(2050)$							1955	200	0.1	2130‡	424	0.222
$D_{33}(1670)$	1700	260	0.16	1723	192	0.166	1660	236	0.21	1695	275	0.130
$D_{35}(1960)$	2200‡	600	0.25	1889	121	0.081				1925	350	0.133
$D_{35}(2430)$										2300‡	608	0.169
$F_{35}(1890)$	1875	250	0.18	1869	255	0.144	1860	307	0.13	1885	310	0.140
$F_{37}(1950)$	1925	200	0.4	1928	237	0.405	1910	259	0.41	1945	305	0.396
$G_{37}(2200)$										2200‡	293	0.045
$H_{3,11}(2420)$				2392	289	0.109	2420		0.1			
$K_{3,15}(2850)$							2850					

†Uses some additional partial waves ‡Resonance parameters not definite

Chew and Urban[85] submitted to this conference the first partial wave analysis using the method of Barrelet zeros[75] for elastic π^+p scattering data between 1.2 and 2.2 GeV c.m. energies.

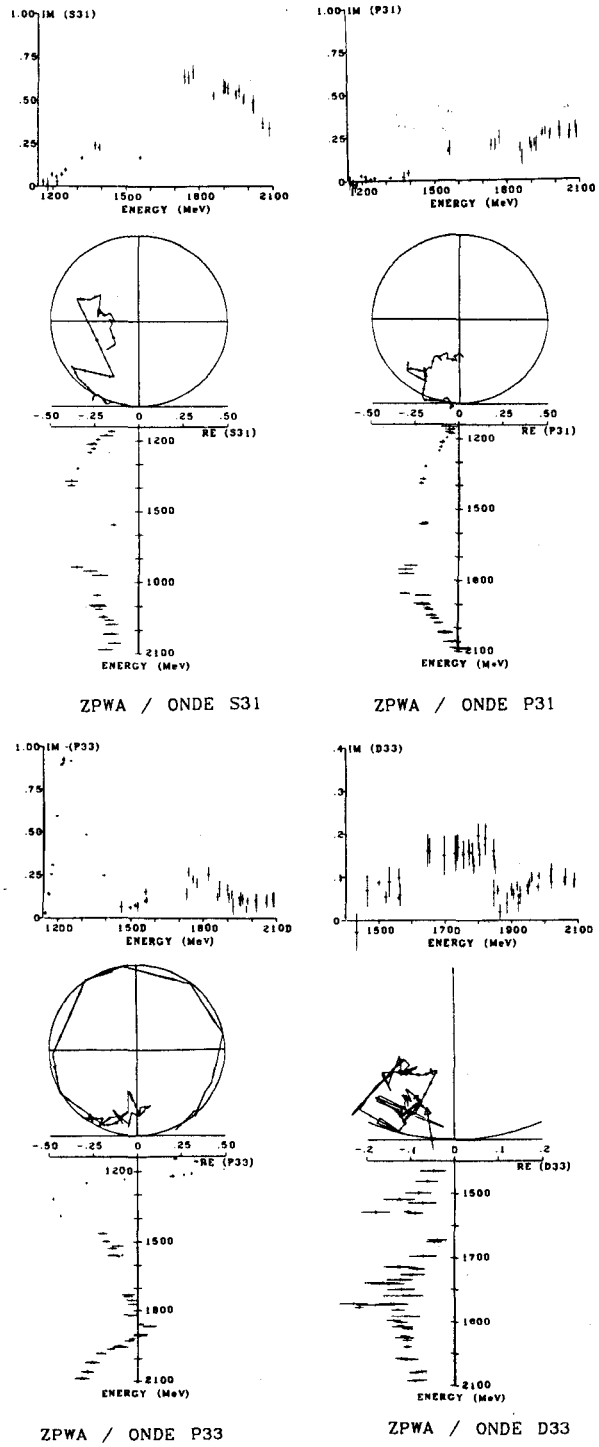
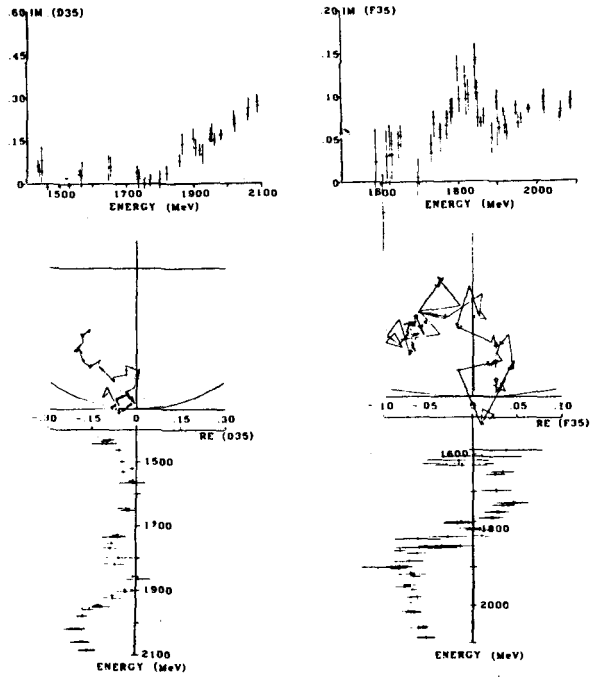
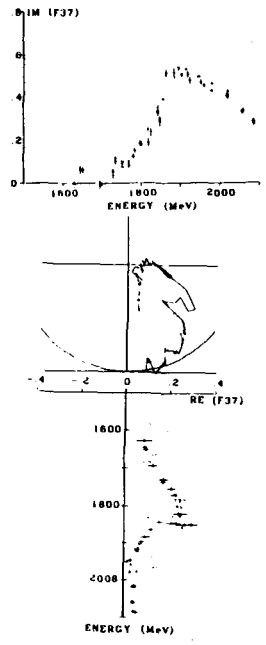


FIG. 45a



ZPWA / ONDE D35

ZPWA / ONDE F35



ZPWA / ONDE F37

FIG. 45b

Fig.45a,b. Partial - wave amplitudes without any cut: a)S31,b)P31,c)P33,d)D33,e)D35,f)F35,g)F37.

Fig.45a,b shows the results for their partial waves. In certain energy regions the partial wave errors are so large that it is impossible to make accurate deductions of resonance positions and widths. One can see structures in the Argand diagrams for all the three or four star states given in table 11b. Only in the region near 1910 where the table lists a three star P_{11} state no structure is observed (see fig.45a).

Chew and Urban found a structure in the D_{35} partial wave near 1900 MeV that may be related to the $\Delta(1960)$.

Another contribution submitted to this conference by Hendry /86/ is a π^+p phase shift analysis at energies above the existing phase shift region. In a first step an approximate solution is obtained by expressing the partial wave amplitudes $f_{\ell t}$ in terms of the impact parameter, such as to incorporate the diffractive and peripheral nature of the scattering. In the second step the final fit to the data is achieved by letting the real and imaginary parts of $f_{\ell t}$ vary freely.

Altogether, 14 momenta were selected for the analysis of p elastic scattering for laboratory beam momenta from 1.6 to 10GeV/c. Fig.46 shows the Argand diagram of D_{35} and F_{37} waves as examples.

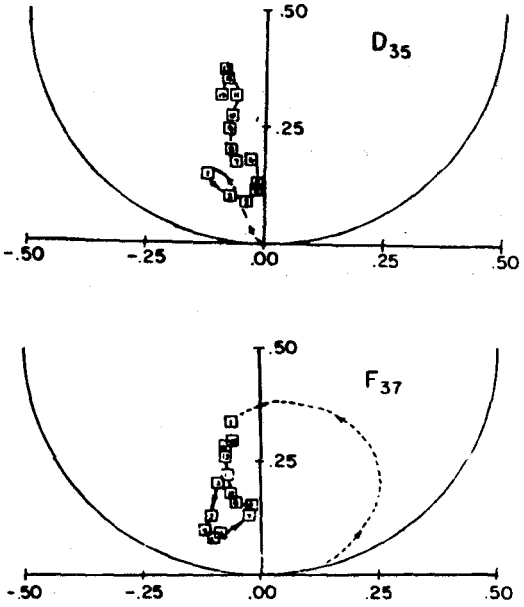


Fig.46: Argand diagrams for the $f_{\ell t}$ amplitudes D_{35} and F_{37}. (The dashed lines indicate the trends at lower energies, Ref. /85/).

The numbers 1 ... 14 correspond to the momenta that were fitted. Table 12 summarizes the resonance parameters.

Besides confirming the already accepted $H_{3,11}(2420)$ resonance Hendry presents evidence for an additional Δ resonance which is included table 11b (the $G_{37}(2200)$).

In addition there is a first indication of nine additional resonances with masses up to 4 GeV. It would be useful to discuss the relation between the Argand plots for these resonances to the Schmidcircles which have been derived from smooth invariant amplitudes.

From the partial wave analyses of the elastic N interaction we do not have any information how the N^* states couple to the other channels. Especially states with weak coupling to the πN channel have to be investigated in experiments where they may be

formed in a more favourable channel. The signs of the coupling constant and the branching ratio into the various decay modes are necessary for the classification of these states into the various multiplets.

Table 12

Table of resonance parameters

		Mass [GeV]	Elasticity x_1	Γ_2 [GeV]
f_{ℓ^+}	$G_{3,9}(2180)$	2.15±.05	0.09±.02	0.22±.05
	$H_{3,11}(2420)$	2.42±.06	0.12±.01	0.25±.05
	$I_{3,13}(2800)$	2.80±.10	0.05±.01	0.33±.06
	$K_{3,15}(3100)$	3.10±.10	0.04a±.008	0.48±.08
	$L_{3,17}(3450)$	3.45±.10	0.030±.005	0.55±.10
	$M_{3,19}(3750)$	3.75±.10	0.030±.006	0.70±.10
	$N_{3,21}(4000)$	4.00±.16	0.018±.006	0.70±.10
f_{ℓ^-}	$O_{3,7}(2200)$	2.27±.10	0.11±.01	0.25±.05
	$H_{3,9}(2490)$	2.49±.10	0.12±.01	0.33±.03
	$I_{3,11}(2800)$	2.80±.10	0.06±.01	0.40±.05
	$K_{3,13}(3200)$	3.20±.15	0.054±.005	0.55±.05
	$L_{3,15}(3500)$	3.50±.20	0.035±.010	0.60±.10

The largest analysis of the inelastic N scattering up to now is that of the LBL - SLAC collaboration /87/ who have analysed 200 K events of the reaction

$$\pi^- p \to \pi^- \pi^0 p \quad ; \quad \pi^+ p \to \pi^+ \pi^0 p$$
$$\pi^- p \to \pi^+ \pi^- n \quad ; \quad \pi^+ p \to \pi^+ \pi^+ n$$

in the centre of mass energy range from 1.3 to 2.0 GeV using the isobar model. There the presence of overlapping resonances in the final state and the interferences between the specific amplitudes were taken into account.

This partial wave analysis was already fully described in the rapporteur talk of Litohfield/74/ in London.

Two new experimental studies of the reaction

$$K^- p \to K^0 \Lambda^0$$

were contributed to the Topical Conference on Baryon Resonances which took place about two weeks ago in Oxford and to this conference.

In a spark chamber experiment Baker et al./88/ measured the differential cross section and the polarization at nine incident K^- momenta between 0.9 and 1.4 GeV/c. These data have been combined with existing data to make a Barrelet zero phase shift analysis from threshold to 2350 MeV. Barrelet ambiguities were resolved on the basis of the χ^2 of a fit of (resonance+background) to partial waves, using well established resonances in the three lowest waves.

Baton et al./89/ included in their partial wave analysis 13.5 K,Λ,K events measured at Saclay in a hydrogen bubble chamber at 12 separate momenta between 0.93 and 1.41 GeV/c.

A combining of several methods has been used in the analysis
- an energy independent search for partial wave amplitudes and a link in energy by means of the Barrelet zero trajectories.
- a fit to the resulting amplitudes with a model including resonances and background
- an overall energy-dependent fit over the entire range of energy.

From the first two methods Baton et al.were left with eight possible solutions. From an energy-dependent fit to the eight possible sets of amplitudes the authors got finally four distinct solutions.

The couplings $\sqrt{x_i \, x_i}$ from the final preferred solution of Baker et al. /88/ and from the four solutions of Baton et al. /89/ are shown in fig. 47. Both results are in general agreement and correspond also to the predictions of $SU(6)_w$.

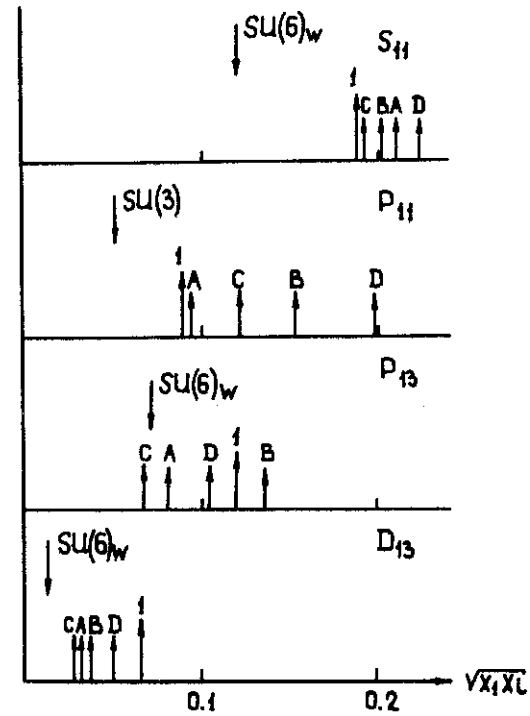


Fig.47 Comparison of resonance couplings to $K^0\Lambda$ from Baker et al./92/ (solution 1), from Baton et al./93/ (solution A,B,C,O) and from the predictions of SU(6)w.

Concerning the production experiments on S = 0 baryon states I should like to mention only a few new results submitted to this conference. They show that from high statistics production data you can get some qualitatively new information about N^* states.

The Birmingham-Brussels-CERN-Mons collaboration /90/ has studied the low mass $p\pi^+\pi^-$ system produced in the reaction

$$K^+ p \longrightarrow K^+ p \pi^+ \pi^-$$

between 7.3 and 16 GeV/c, and the Amsterdam-CERN-Nijmegen-Oxford collaboration /91/ in the reaction

$$K^- p \longrightarrow K^- p \pi^+ \pi^-$$

at 4.2 GeV/c. In both experiments a partial wave analysis of the $(p\pi^+\pi^-)$ system was carried out using an isobar model formalism.

The result of both analyses is that the peak in the $(p\pi^+\pi^-)$ mass spectrum near 1.7 GeV consists of mainly $\Delta\pi$ and $p\varepsilon$. The ACNO collaboration /91/ come to the conclusion that the main contributions are the $1/2^+$ wave decaying into $\Delta^{++}\pi^-$ and the $3/2^-$ wave decaying into $p\varepsilon$. The $K^+ p$ analysis finds also in the $3/2^-$ wave a $\Delta\pi$ contribution at 1.7 GeV. Both analyses agree with the result that the $5/2^+$ wave is not strong and shows no distinct structure, i.e. the peak cannot be caused by the F_{15} (1688).

Some papers reporting observations of a Δ resonance at about 1890 MeV in meson proton production experiments /92, 93/ are contributed to this conference. This state was found to be produced in association with the ϱ and ω resonances.

From an analysis of the moments Chung et al. /94/ got $9/2^+$ as most probable spin parity assignment.

If we assume that the number of hadron levels keeps increasing at high masses, we come to the point that higher mass resonances are not individually detectable because they overlap even in individual partial waves. Therefore their existence must be inferred more indirectly.

For the overlapping levels quantum mechanical interference begins to occur. That means that both the amplitudes of the overlapping states, and their phases, will determine their effects on cross sections. Due to the random phase, the observed cross sections fluctuate by factors which may be much larger than one would produce only fluctuations in the level density itself. This is the region of Ericson fluctuations.

Indications for such narrow structure in the energy dependence of π^+ p elastic scattering in the 5.0 GeV/c region was reported by Schmidt et al. /95/

In a new experiment /96/ which was designed to look for Ericson fluctuation in π^- and π^+ large angle elastic scattering in the momentum range from 2 to 9 GeV/c no indication was seen of large variations in the differential cross section occuring over very small closely spaced increments in c.m. energy. There is no indication for very narrow structures in the region of 5 GeV/c incident momentum.

Dixon et al. /97/ have performed a systematic study of backward elastic scattering from 3.0 to 5.5 GeV/c. They find no evidence for narrow structures in the energy dependence as would be expected for Ericson fluctuations or narrow resonances ($\Gamma \leq 30$ MeV).

3.2 Strangeness - 1 Baryon States

During the last two years data from several high statistics $\bar{K}N$ bubble chamber experiments have become available. In addition much new experimental data were submitted to the Topical Conference on Baryon Spectroscopy in Oxford, July 1976, and to this conference. These most recent experimental data are summarized in table 13.

As can be seen from the table the new experimental data not only cover a wider c.m. energy region than the data known before 1975 but the data are also at a higher statistical level ($\sim$ 1 event /μb/ 25 MeV/c beam momentum).

In the reactions

$$K^- n \longrightarrow (\Sigma \pi)^-$$

and $$\bar{K}^0 p \longrightarrow (\Sigma \pi)^+$$

a discrepancy is observed between the cross sections, comparing the experiments from Hepp et al. /103/ and Armenteros et al. /115/ on the first reaction with the experiments from Bertanza et al. /111/ and Chu et al. /112/ on the second reaction. Both I = 1 cross sections should be equal, but experiments with deuterium targets find cross sections which are about two times smaller than the measurements in K_L^0 p experiments.

After a study of possible systematic errors Hepp /116/ comes to the conclusion that both K^- n experiments are completely consistent with each other and the same is true for both K_L^0 p experiments. I see does not want to attack charge invariance, more experiments have to be performed. As it was shown by Hepp, specific channels of the K^- d interaction are appreciably modified by final state interactions. The effect of $\Sigma N \rightarrow \Lambda N$ conversion in the deuteron is clearly demonstrated in fig. 48. The effective (Λ p) mass in the reaction K^- d shows a pronounced peak at the Σ^+ n threshold. Therfore a part of the discrepancy between the K^- n and K_L^0 p cross sections can be attributed to final state Y-N interactions in deuterium /117/.

Table 13
Experiments on two body $\bar{K}N$ reactions.

Reaction	C.M. Energy Range [MeV]	No. of Momentum Intervals	Data Type	No. of Events/μb	Reference
$K^-p \rightarrow K^-p$ $\rightarrow \bar{K}^0n$ $\rightarrow A\pi^0$ $\rightarrow \Sigma^0\pi^0$	1775 - 1975	11	$\frac{d\sigma}{d\Omega}$, P	14.7	/98/
$K^-p \rightarrow K^-p$ $\rightarrow \bar{K}^0n$ $A\pi^0$ $\rightarrow \Sigma^+\pi^-$ $\rightarrow A\omega$	2200 - 2436	7	A_ℓ, B_ℓ	10	/99, 100/
$K^-p \rightarrow \bar{K}^0n$ $\rightarrow A\pi^0$ $\rightarrow \Sigma^0\pi^0$	1729 - 1794	9	$\frac{d\sigma}{d\Omega}$, P A_ℓ, B_ℓ	6	/101/
$K^-p \rightarrow K^-p$ $\rightarrow \bar{K}^0n$	1858 - 2150	23	A_ℓ		/102/
$K^-n \rightarrow \Sigma^0\pi^-$ $\rightarrow A\pi^-$	1600 - 1748	4	$\frac{d\sigma}{d\Omega}$, P A_ℓ, B_ℓ	5.2	/103/
$K^-n \rightarrow \pi^-\Lambda$	2050 - 2175	8	A_ℓ, B_ℓ	6.2	/104/
$K^-n \rightarrow \pi^-\Lambda$	1750 - 1980	12	A_ℓ, B_ℓ		/105/
$K^-n \rightarrow K^-n$	1850 - 2300	9	$\frac{d\sigma}{d\Omega}$		/106/
$K^-p \rightarrow \bar{K}^0n$	1570 - 1670	48	$\frac{d\sigma}{d\Omega}$	~500	/107/
$K^-n \rightarrow \pi^-\Sigma^+$	1780 - 2280	19	A_ℓ, B_ℓ	~1	/108/
$K^-p \rightarrow K^-p$ $\rightarrow \bar{K}^0n$ $\rightarrow A\pi^0$ $\rightarrow \Sigma^0\pi^0$	1858 - 1993	13	$\frac{d\sigma}{d\Omega}$, P	2	/109/
$K^-p \rightarrow K^-p$	1610 - 1765	14	$\frac{d\sigma}{d\Omega}$, A_ℓ		/110/
$K_L^0p \rightarrow A\pi^+$ $\Sigma^0\pi^+$	1495 - 1700	11	$\frac{d\sigma}{d\Omega}$, A_ℓ, B_ℓ		/111/
$K_L^0p \rightarrow A\pi^0$ $\rightarrow \Sigma^+\pi^-$	1600 - 1900	7 6	A_ℓ, B_ℓ A_ℓ		/112/
$K_L^0p \rightarrow A\pi^+$ $\rightarrow \Sigma^0\pi^+$	1588	1	$\frac{d\sigma}{d\Omega}$, A_ℓ, B_ℓ		/113/
$K_S^0p \rightarrow A^{0*}$ $\rightarrow K^0\pi^+$	1965 - 1605	10	A_ℓ, B_ℓ		/114/

Table 13 includes also two new counter experiments. The CERN-Cambridge collaboration /106/ measured the K^- n $\rightarrow K^-$ n elastic cross section for most of the c.m. angular range and for a c.m. energy range from 1.85 to 2.3 GeV. In fig 49 the measured elastic K^- n differential cross section is compared with the prediction of the RL-IC partial wave analysis /118/. At higher energy the RL-IC (76) analysis predicted oscillations which are not seen in the experimental data.

The second very high precision counter experiment was performed by Alston-Garnjost et al. /107/. They measured the cross section of the charge exchange reaction K^- p $\rightarrow \bar{K}^0$ n at 48 momenta between 515 and 1066 MeV/c. The enormous progress which the counter experiments bring is illustrated in the next two figures. In fig. 50 is shown σ_T (K^- p $\rightarrow \bar{K}^0$ n) from different bubble chamber experiments in comparison with the predictions of some partial wave analyses. Fig. 51 illustrates the high precision of the new data. The agreement with the prediction of the RL-IC partial wave analysis is fairly good.

These two new experiments mark the beginning of a new generation of experiments in the study of the S = -1 baryonic states.

Partial wave analyses have been performed on all the channels given in table 13.

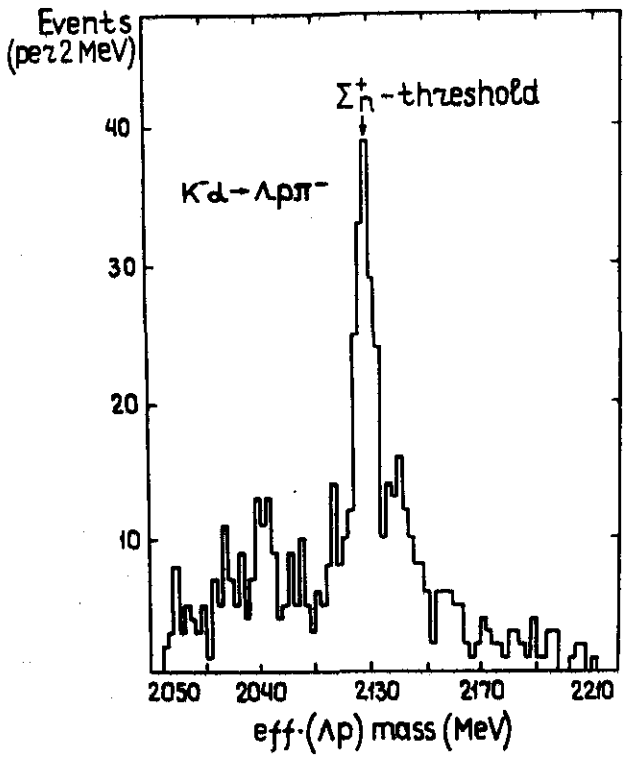


Fig.48 The Λ p effective mass distribution in $K^- d \to \Lambda p \pi^-$.

The $\bar{K}N$ system has superior data and so it is much easier to make use of additional theoretical constraints for $\bar{K}N$ partial wave analyses than it is for $\bar{K}N$ analyses. Therefore in the $\bar{K}N$ analyses a larger amount of extra input is required.

In most of the analyses the required constraints are realised by the input of a minimum number of dominant Breit-Wigner resonances. This method is used in $\bar{K}N$ partial wave analyses whether they are energy dependent, or use K-matrix or Barrelet zeros methods. Experience has shown that only a small number of resonances need to be imposed in order to reduce drastically the number of ambiguous solutions. With this input one finds some agreement between the different solutions.

Another method in order to supply the extra constraints is the usual approach for $\bar{K}N$ analyses, i.e. to take the theoretical constraints from fixed t dispersion relations. Such an energy independent phase shift analysis was applied to $\bar{K}N$ elastic and charge exchange scattering for the first time in a contribution to this conference by Hansen et al.[119].

Only two of the new analyses attempted an approach in which data were used on the three two body reaction channels $\bar{K}N$, $\Lambda\pi$ and $\Sigma\pi$ in parallel.

The advantage of the multi-channel fit is in the determination of the resonance parameters since they are fitted simultaneously to the data in all three reaction channels.

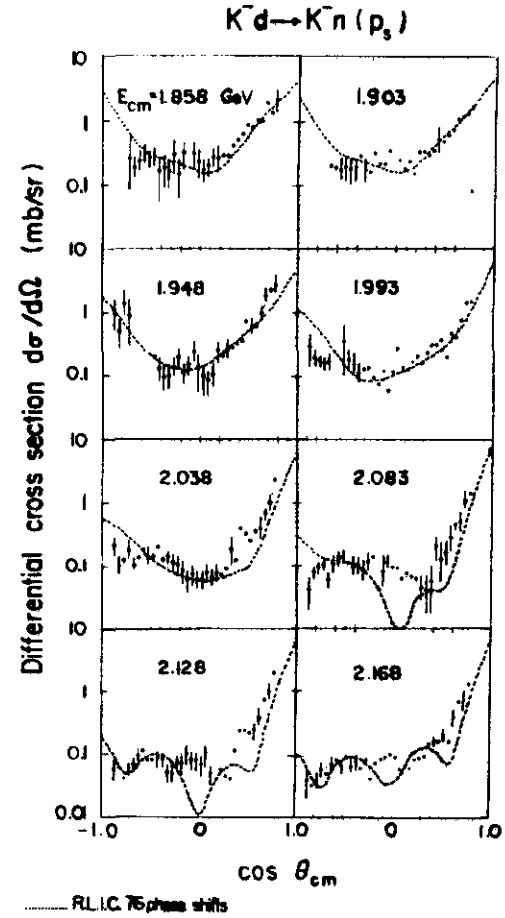


Fig.49 The $K^- n$ differential cross section compared to RL-IC(76) phase shifts.

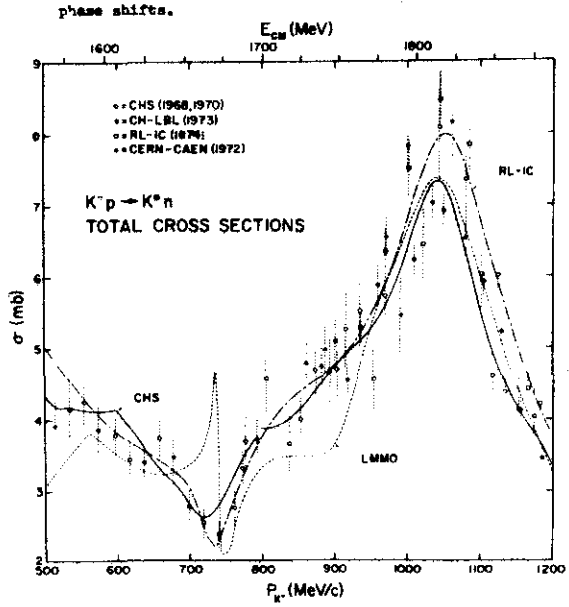


Fig.50 $(K^- p \to \bar{K}^0 n)$ from different bubble chamber experiments in comparison with the predictions of some p.w.a.

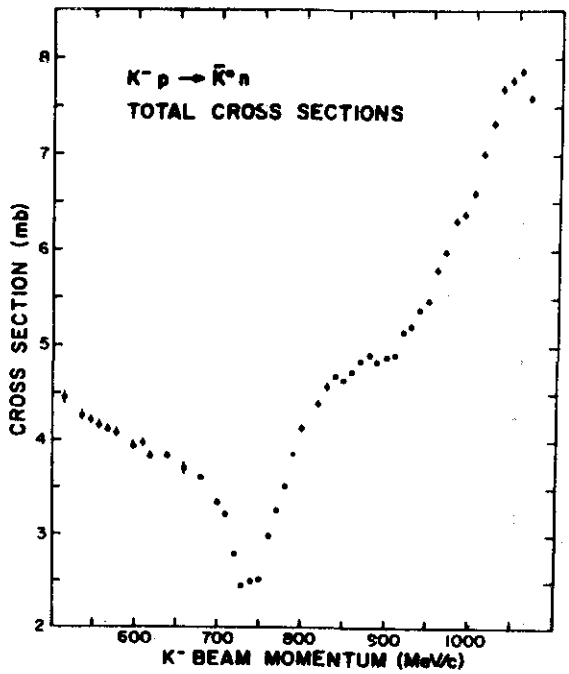


Fig.51 $\sigma_t(K^- p \to \bar{K}^0 n)$ from Alston-Garnjost et al. /107/.

The RL-IC collaboration /118/ has performed an energy dependent partial wave analysis in which the three reaction channels

$$\bar{K}\ N \longrightarrow \bar{K}\ N$$
$$K^- p \longrightarrow \Lambda^0 \pi^0$$
$$K^- p \longrightarrow \Sigma \pi$$

have been treated in parallel using data from 1480 to 2170 MeV c.m. energy. Good fits to the data over this broad energy range have been obtained by parametrising the partial waves as a sum of resonance and background contributions. The pure I = 1 data from the reaction channel

$$K^0_L p \longrightarrow \Sigma^0 \pi^+$$

has proved to be very useful in constraining the partial wave analysis of the $\Sigma\pi$ system /111/.
The resonance parameters are given in table 14 a, b.

The analysis of Martin et al. /120/ is a multi-channel energy dependent partial wave analysis with parametrised K-matrix elements, covering a c.m. energy region from 1540 to 2020 MeV. This is an extension of previous work /121/ which analysed a smaller data set in the region below 1880 MeV. In addition the new work incorporates improvements in both the parametrization and the method of extracting resonance parameters. Preliminary results for the multi-channel solution are given in table 14a, b.

3.2.1 The $\Lambda\pi$ Channel

The $\Lambda\pi$ channel is, in principle, the easiest inelastic channel to handle, because only one isospin has to be considered. Partial wave analyses for this reaction channel have been performed in the following new contributions:

- The RL-IC collaboration /118/ in the c.m. energy region from 1480 to 2170 MeV.

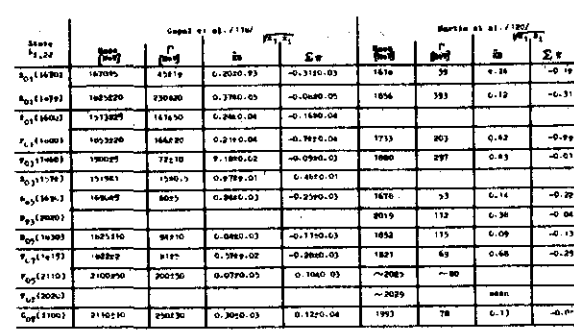


Table 14a

($\sqrt{x_i x_j}\,\sigma_{ij}/\Gamma_{tot}$ and $\sqrt{x_i}$ being the partial widths of the elastic and the specific inelastic channel, - indicates state not found in that channel)

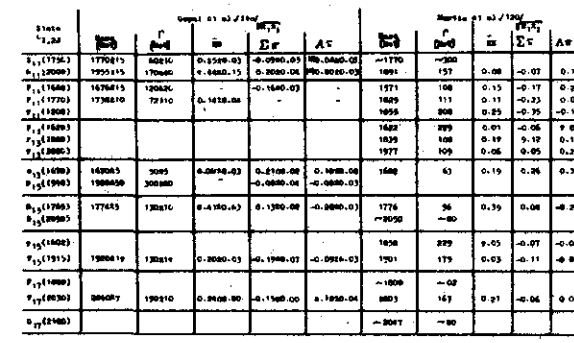


Table 14b

($\sqrt{x_i x_j}\,\sigma_{ij}/\Gamma_{tot}$, $\sqrt{x_i}$ being the partial widths of the elastic and the specific inelastic channel, - indicates state not found in that channel)

- The UC (London) - CERN collaboration /120/ in the c.m. energy region from 1540 to 2020 MeV.

The resonance parameters of these two analyses are included in table 14 b.

- Bailloo and Litchfield /122/ carried out a semi-energy independent analysis in the c.m. energy region from 1540 to 2140 MeV using two independent methods to provide energy continuity. Between 1750 and 2060 MeV the solution is believed to be unique under the assumption of the dominance of the two leading resonances, the D_{15} (1765) and F_{17} (2030), and smoothness of the Barrelet zeros. Below 1750 MeV there are two ambiguous solutions. One of them (solution 1) is somewhat preferred on the basis of the behaviour of the S and P waves for very low masses (around 1580 MeV). Final fits have been made to the amplitudes found in the energy independent analyses employing expressions of the type used in the energy dependent analyses, i.e. resonance plus background terms. The parameters of the resonances of solution 1 are given in table 15.
- De Bellefon and Berthon /100, 123/ applied the technique of Barrelet zeros to perform a phase shift analysis in the reaction

channel $\Lambda^0\pi^0$ in the c.m. energy range from 1540 to 2450 MeV. With the assumption of the existence of the well established states D_{15} (1765) and F_{17} (2030) an almost unique solution is presented. Its resonance parameters are included in table 15.

State $L_{I,2J}$	Baillon and Litchfield /122/ $K^-p \to \Lambda\pi^0$ Mass [MeV]	Γ [MeV]	$\sqrt{x_1 x_1}$	De Bellefon and Berthon /123/ $K^-p \to \Lambda\pi^0$ Mass [MeV]	Γ [MeV]	$\sqrt{x_1 x_1}$
$S_{11}(1750)$	1780±30	140±30	-0.12±0.02	1730	110	-0.12
$S_{11}(2000)$						
$P_{11}(1660)$	1660±30	80±40	-0.04±0.02			
$P_{11}(1770)$	1770±20	80±30	-0.08±0.02			
$P_{11}(1880)$	1960±30	260±40	-0.12±0.02			
$P_{13}(1620)$	1720±30	120±30	0.11±0.02			
$P_{13}(1840)$						
$P_{13}(2080)$	2120±40	240±50	-0.13±0.04	~2100	100	-0.10
$D_{13}(1670)$	1685±20	85±25	0.06±0.02	1650	80	0.05
$D_{13}(1940)$	1950±30	150±75	-0.04±0.02			
$D_{15}(1765)$	1775±10	125±15	-0.25±0.02	[1765]	[120]	[-0.30]
$D_{15}(2260)$				2260	100	0.11
$F_{15}(1860)$						
$F_{15}(1915)$	1920±30	70±20	-0.06±0.02	1915	60	-0.10
$F_{15}(2250)$						
$F_{17}(2030)$	2035±15	180±15	0.18±0.02	[2030]	[160]	[0.20]
$G_{19}(2215)$				2215	140	-0.10

Table 15 - Σ resonance parameters

In addition I should like to mention the energy dependent partial wave analysis in the $\Lambda\pi$ channel made by Corden et al. /104/ in the c.m. energy range from 1875 to 2175 MeV. The well established states F_{15} (1915) and F_{17} (2030) were included in the fits. The authors prefer a solution in which the only additional state included is the P_{13} (2080) resonance with the parameters:

M = 2091 ± 7 MeV; Γ = 186 ± 48 MeV; $\sqrt{x_1 x_1}$ = -0.10 ± 0.03.

No evidence has been found for any other resonance in the energy region covered.

If one compares the solutions of the different analyses of the $\Lambda\pi$ channel there is general agreement within the limits of error with the possible exception of the low partial waves of Martin et al. /120/. But we have to take into account that the results of Martin et al. are preliminary. Therefore I shall not include this analysis in the following discussions of results.

1.2.2 The $\bar{K}N$ Channel

Single-channel energy dependent analyses in the reaction channels

$K^- p \to K^- p$

$\to \bar{K}^0 n$

have been performed in the following contributions to the Topical Conference on Baryon Resonances and to this conference:

- The RL-IC collaboration /118/ in the c.m. energy region from 1480 to 2170 MeV.
- The UC (London) - CERN collaboration /120/ in the c.m. energy range from 1540 to 2020 MeV.

The resonance parameters of these two analyses are included in table 14 a, b.

- Alston-Garnjost et al. /107/ in the c.m. energy region from 1480 to 1900 MeV. The results included in table 16a, b, are from a preliminary analysis.
- The CERN-Caen collaboration /106/ in the c.m. energy region from 1480 to 1900 MeV.
- The energy independant phase shift analysis of $\bar{K}N$ elastic and charge exchange scattering in the c.m. energy range from 1540 to 2230 MeV performed by Hansen et al. /119/.
- The College de France-Saclay collaboration /100/ in the c.m. energy region from 2070 to 2450 MeV. The well established resonances F_{17} (2030) and G_{07} (2100) were introduced in the fits. Moreover, duality and s-helicity conservation constraints have been explicitly imposed on the imaginary parts of the amplitudes.

The resonance parameters of these four analyses are summarized in table 16.

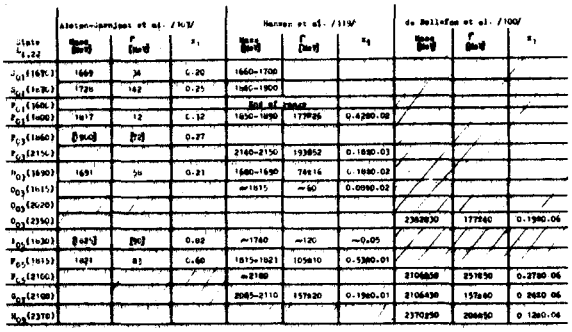


Table 16a

A- resonance parameters of different p.w.a. for the $\bar{K}N$ reaction channel.

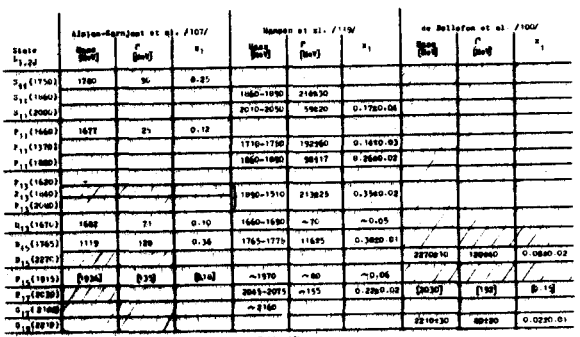


Table 16b

Σ- resonance parameters of different p.w.a. for the $\bar{K}N$ reaction channel.

Concerning $\bar{K}N$ channel there seems to be general agreement on the form of the Argand diagrams up to a c.m. energy of about 1800 MeV but above this energy there is more uncertainty. For example the higher energy analysis of de Bellefon et al./100/ does not seem to join on to the RL-IC analysis but is similar to the top end of the Hansen et al./119/ analysis. One particular example of interest to quark model fits is the second $F_{05}(2110)$ which RL-IC find to have only a small coupling to KN whereas both de Bellefon et al. and Hansen et al. see a much larger loop in the Argand diagram.

3.2.3. The $\Sigma\pi$-Channel

Five new energy dependent partial wave analyses of the $\Sigma\pi$ channel have been carried out and contributed to the Topical Conference on Baryon Resonances and to this conference:

- The RL-IC collaboration/118/ in the c.m. energy region from 1480 to 2170 MeV.
- The UC (London)-CERN collaboration/120/ in the c.m. energy region from 1540 to 2020 MeV.

The resonance parameters resulting from these two analyses are included in table 14.

- The CERN-Heidelberg-Munchen collaboration/103/ on the reaction $K^- n \to (\Sigma\pi)^-$ in the c.m. energy range from 1520 to 1745MeV.

The parameters of the well established states $D_{03}(1520)$, $D_{05}(1830)$, $F_{05}(1815)$ and $D_{15}(1765)$ were introduced in the analysis. In the search for acceptable solutions the authors tried to keep the number of resonances as small as possible.

- The College de France - Saclay collaboration/99/ on the reaction $K^- p \to (\Sigma\pi)^0$ in the c.m. energy range from 2070 to 2430 MeV.

The well established resonances $F_{17}(2030)$ and $G_{07}(2100)$ are introduced with fixed parameters.

- Corden et al./108/ on the reaction $K^- n \to (\Sigma\pi)^-$ in the c.m. energy range from 1750 to 2200 MeV. The analysis resulted in two alternative fits with similar parameters

The resonance parameters of these three analyses are summarised in table 17.

State $L_{I,2J}$	Hepp et al. /103/ $K^- N \to \Sigma\pi$ Mass [MeV]	Γ [MeV]	$\sqrt{x_1 x_1}$	De Bellefon et al./99,100/ $K^- N \to \Sigma\pi$ Mass [MeV]	Γ [MeV]	$\sqrt{x_1 x_1}$	Corden et al. /108/ $K^- N \to \Sigma\pi$ Mass [MeV]	Γ [MeV]	$\sqrt{x_1 x_1}$
$D_{13}(1670)$	1669±6	95±3	0.20±0.01						
$D_{13}(1940)$									
$D_{15}(1765)$		[123]	[0.10]				[1765]	[120]	[0.06-0.09]
$D_{15}(2270)$				2275±20	70±20	-0.06±0.02			
$F_{15}(1860)$									
$F_{15}(1915)$							1884±5 or 1909±5	107±14 or 85±13	-0.17±0.01 or -0.13±0.02
$F_{15}(2070)$				[2070]	[140]	+0.12±0.02			
$F_{17}(2030)$				[2030]	[160]	[-0.10]	[2020-2040]	[120-170]	-0.09±0.01 or -0.06±0.01
$G_{19}(2210)$				2215±20	60±20	-0.03±0.02			

Table 17b

Σ- resonance parameters of single channel $\Sigma\pi$ p.w.a.

State $L_{I,2J}$	Hepp et al. /103/ $K^- N \to \Sigma\pi$ Mass [MeV]	Γ [MeV]	$\sqrt{x_1 x_1}$	De Bellefon et al./99,100/ $K^- N \to \Sigma\pi$ Mass [MeV]	Γ [MeV]	$\sqrt{x_1 x_1}$
$S_{01}(1670)$	1676±2	43±5	-0.29±0.03			
$D_{03}(1520)$	[1519]	[16]	[0.44]			
$D_{03}(1690)$	1688±3	76±8	-0.30±0.03			
$D_{05}(1830)$	[1825]	[90]	[-0.15]			
$F_{05}(1815)$	[1820]	[123]	[0.10]			
$F_{05}(2110)$				2160±20	160±20	-0.14±0.02
$G_{07}(2100)$				[2100]	[140]	[+0.15]
$H_{09}(2350)$				2365±20	210±20	-0.11±0.02

Table 17a

A- resonance parameters of single channel $\Sigma\pi$ p.w.a.

In the discussion of the experimental data I mentioned already the discrepancy between the K^- d data and the K^0_L p data. As far as the c.m. energy regions in the different analyses overlapp there is a general agreement in position of amplitudes on Argand diagrams.

The biggest discrepancy in comparison of the RL-IC data with the results of the CERN-Heidelberg-München collaboration concerns the P_{11} (1660). In the last analysis it was not observed.

3.2.4 The Quasi Two Body Reactions

The College de France - Saclay collaboration /100/ also performed partial wave analyses of the quasi two body reaction channel

$$K^- p \longrightarrow \Lambda\omega$$

A quasi energy independent p.w.a. has been carried out in parallel with a standard energy dependent analysis. The coupling of the G_{07} (2100) to $\Lambda\omega$ was confirmed and evidence for a resonant D_{03} (2350) state was found. This state was also observed in the $\bar{K}N$ channel.

As it was shown before, formation experiments observe one Σ (1670) resonance with $J^P = 2^-$ and decaying primarily to $\bar{K}N$, $\Lambda\pi$, and $\Sigma\pi$ (see tables 14 - 17). On the other hand, production experiments since 1969 /124/ have found evidence suggestive of two resonances in this mass region with comparable values of mass and width.

The Amsterdam-CERN-Nijmegen-Oxford collaboration /125/ has studied the Σ (1660) in the reaction

$$K^- p \longrightarrow \Sigma^+ (1660)\, \pi^-$$

at 4.2 GeV/c in a high statistics experiment (~ 65 events/μb). The Σ (1660) is observed in the $\Sigma^\pm \pi^\mp \pi^+$ mass distributions and in the $\Sigma^0 \pi^\pm$ mass distributions. It appears that the Σ (1660) $\longrightarrow \Sigma\pi\pi$ decay could occur entirely via Λ (1405)π.

Fig. 52 shows the production angular distribution of the Σ (1660) in the two final states. The difference between the distributions is striking. Whereas Σ^+ (1660) $\longrightarrow \Lambda$(1405)π^+ shows only a sharp forward peak (fig. 53 A,J), Σ^+ (1660) $\longrightarrow \Sigma^0\pi^+$ has not only a forward peak (fig. 53 B, D), but is produced at all angles and in addition shows a significant backward peak.

It is this marked difference in production angular distribution that indicates that the Σ (1660)'s are not the same states.

A Dalitz - Miller analysis on the Σ (1660) $\longrightarrow \Sigma^-\pi^+\pi^+$ Dalitz plot gives a strong preference for $J^P = 3/2^-$. For the Σ^+ (1660) $\longrightarrow \Sigma^0\pi^+$ a momentum analysis suggests $J = 3/2$. It thus seems that the Σ (1660) $\longrightarrow \Sigma\pi$ is the same resonance as the

D_{13} (1670) state observed in formation experiments and the Σ (1660) $\longrightarrow \Lambda(1405)\pi$ is a different resonance also having $J^P = 3/2^-$.

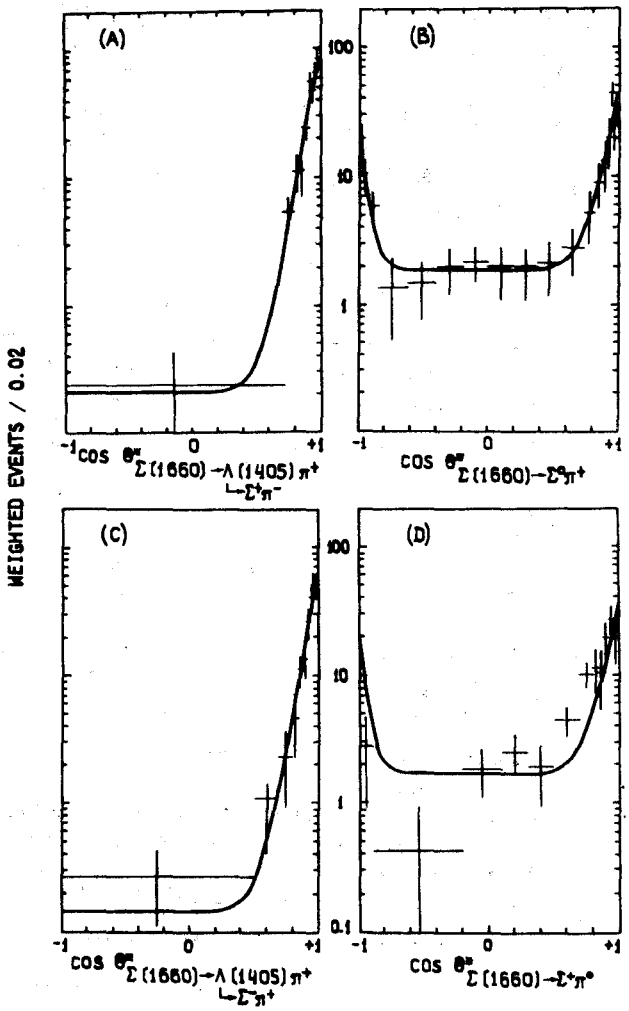


Fig.52 Production angular distribution in the overall c.m.s. with background subtracted: (A) for $\Sigma(1660)\to\Lambda(1405)\pi^+\to\pi^+\pi^-\Sigma^+$, (B) for $\Sigma(1660)\to\Sigma^0\pi^+$, (C) for $\Sigma(1660)\to\Lambda(1405)\pi^+\to\Sigma^-\pi^+\pi^+$, (D) for $\Sigma(1660)\to\Sigma^+\pi^0$. The curves are the results of fits.

3.2.5 Summary of S = -1 States

With the usual constraints the RL-IC analysis seems to be an acceptable solution. The other analyses generally agree though with detailed differences in structure. Comparing the results of different analyses it is important to look at the Argand diagrams and not only at the quoted resonance parameters which may differ considerably according to the method used for their extraction.

Because the 1976 PDG tables include the RL-IC analysis there will not be many changes. Possible suggestions are summarized in table 18:

Table 18

Summary of the progress on Y^* resonances.

PDG (76)	Tbilisi (76)	Comment
P_{03}^* (1860)	P_{03}^* (1860)	
Λ^* (2350)	D_{03}^* (2340)	fit into a four star bump
	H_{09}^* (2370)	
F_{05}^* (2110)	F_{05}^* (2110)	
S_{11}^* (1620)	S_{11}^* (1620)	
S_{11}^* (2000)	S_{11}^* (2000)	
Σ^* (2250)	D_{15}^* (2270)	fit into a four star bump
	G_{19}^* (2210)	

3.3 Strangeness +1 Exotic Baryon States

Three quarks cannot produce S = +1 baryon resonances (Z^*'s). Therefore the study of KN two body amplitudes at low energies have been of considerable interest.

Until now there is no final conclusion of the Z^*_1 problem because the phase shift analyses based on data of the K^+ p elastic differential cross section and polarization have not presented a unique solution. The most likely candidate of such an exotic state has long been considered to be the P_{13} wave around 1900 MeV, but the new partial wave analyses of Cutkosky et al. /126/ failed to observe the effect.

This non-observation of a Z^*_1 agrees with the result of the new simultaneous energy dependent phase shift analysis of Martin /127/ of both isospin channels, i.e. of K^+ p and K^+ d data.

Spin rotation measurements are needed. They will help to decide between existing solutions.

For the K^+ N, I = 0 channel the BGRT-collaboration /128/ found three possible classes of solutions:

Class A solutions have non resonant P_{01} amplitudes.

In class C solutions resonant behaviour of P_{01} cannot be ruled out but it is not required.

Indications of a highly elastic P_{01} resonance at about 1800 MeV exists in the class D solutions.

Regarding the Z^*_0 the new solution of Martin /127/ is similar to the class C and D solutions.

K^0_L p $\longrightarrow K^0_s$ p is a mixed strangeness channel and provides another way to study the Z^* problem. The amplitude for this reaction is given by

$$A(K^0_L p \longrightarrow K^0_s p) = \tfrac{1}{4}(Z_0 + Z_1) - \tfrac{1}{2} Y_1$$

where Z_0 and Z_1 are the S = +1, I = 0 and I = 1 amplitudes and Y_1 is the S = -1 amplitude.

In a contribution to this conference the HEGPR collaboration /129/ analysed their new experimental data of the reaction

$$K^0_L p \longrightarrow K^0_s p$$

with the specific aim to see if ons can discriminate among the

various classes of solutions. Their data are compatible with the predictions based on the C and D solutions for the I = 0 scattering, within the uncertainties of the various amplitudes. This conclusion agrees with the K^0_L p analysis of Cho et al. /113/ and disagrees with that of Alexander et al. /130/, who favour the A class solution.

Sakitt et al. /131/ measured the differential cross section of the reaction

$$K^+ n \longrightarrow K^0 p$$

at K^+ momenta of 0.7, 0.8 and 0.9 GeV/c. A comparison between the experimental data and the predictions of the three solutions does not yield a definitive choice.

3.4 Strangeness -2 Baryon States

Until now only two S = -2 baryon states can be considered as well established; the ground state Ξ (1320) and the Ξ^* (1530) resonance with $J^P = 2^+$. This is because

- they can be observed only in K^- p production experiments
- they are typically produced with cross sections of a few tens of microbarns.

Therefore an improvement of the situation can be expected only from a new generation of K^- p experiments on the level of $\gtrsim$ 100 events/μb exposures.

The Amsterdam-CERN-Nijmegen-Oxford collaboration /132/ has performed a study of Ξ^* production in a 80 events/μb K^-p experiment at 4.2 GeV/c. They have studied the following reaction channels:

$$K^- p \longrightarrow \Lambda K^+ K^- \quad (1)$$
$$\longrightarrow (\Sigma \bar{K})^- K^+ \quad (2)$$
$$\longrightarrow \Xi^- \pi^0 K^+ \quad (3)$$
$$\longrightarrow \Xi^- \pi^+ \pi^- K^+ \quad (4)$$

In channel (1) a statietically significant peak at 1823 MeV is observed in the ΛK^- mase distribution (see fig. 53). The dominant feature of the $(\Sigma \bar{K})^-$ spedtrum (fig. 53b) is the production of the Ξ^* (2030) first reported by Alitti et al. /133/. The $(\Xi^- \pi^+ \pi^-)$ spectrum (fig. 53d) shows the production of Ξ^* (1820). The decay plot for the events in this peak indicates the entire effect to be due to Ξ^{*0} (1530)π^-.

Spin parity tests allow elimination of J = 1/2 of thie I = 1/2, Ξ^* (1820) resonance, but do not allow discrimination among other possibilities.

The Ecole Polytechnique-Saclay-Rutherford collaboration /134/ submitted to this conference preliminary results of a search for Ξ^* production in K^- p interactions at 14.3 GeV/c.

Besides the prominent peak of the Ξ^0 (1530) other non significant peaks are seen.

The quality of the present world data is illustrated in fig. 54. From this diagram it follows that one can make the following changes to the 1976 PDG table 19:

Table 19

Summary of the progress en Ξ^* resonances.

PDG (76)	Tbilisi (76)
$\Xi^{*[illegible]}$ (1820)	$\Xi^{*[illegible]}$ (1820)
$\Xi^{*[illegible]}$ (2030)	$\Xi^{*[illegible]}$ (2030)
-	Ξ^* (2120)

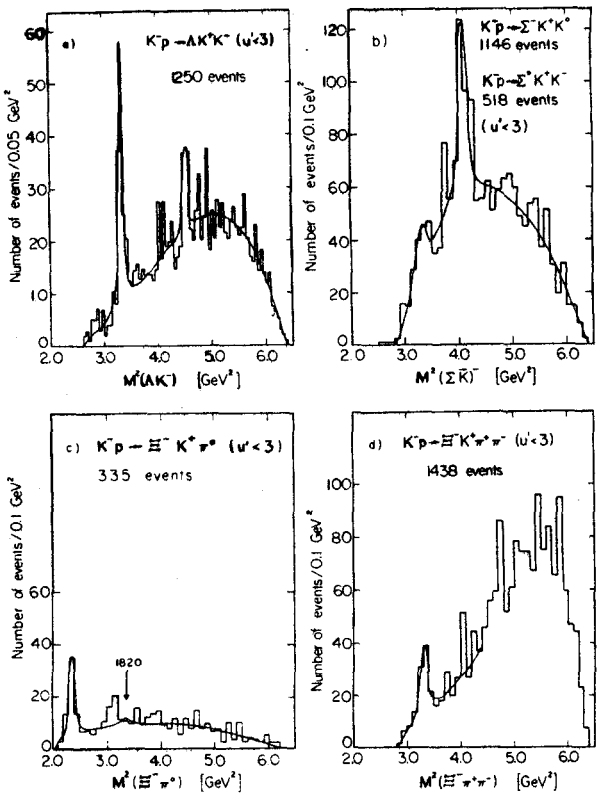


Fig.53a) $M^2(\Lambda K^-)$ for the reaction $K^-p \to \Lambda K^+ K^-$ with $u' < 3$ (GeV/c)^2 and $\phi(1020)$ excluded.
b) $M^2(\Sigma \bar{K})^-$ for the reactions $K^-p \to \Sigma^0 K^+ K^-$ with $u' < 3$(GeV/c)^2 and $\phi(1020)$ excluded together with $K^-p \to \bar{\Sigma}^- K^+ K^0$ with $u' < 3$(GeV/c)^2.
c) $M^2(\Xi^- \pi^0)$ for the reaction $K^-p \to \Xi^- K^+ \pi^0$ with $u' < 3$ (GeV/c)^2.
d) $M^2(\Xi^- \pi^+ \pi^-)$ for the reaction $K^-p \to \Xi^- K^+ \pi^+ \pi^-$ with $u' < 3$(GeV/c)^2.

The quoted number of events refer to weighted events.

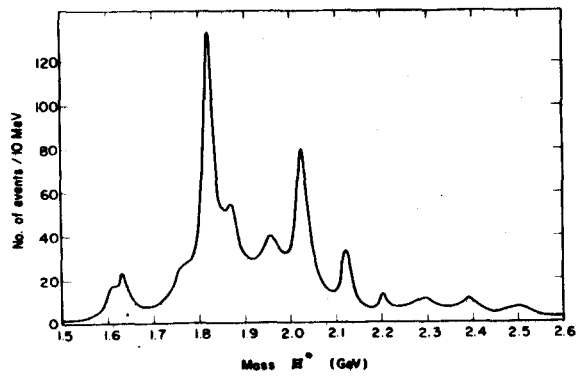


Fig.54. Summary of Ξ^* masses of all known experimental studies (diagram prepared by the Amsterdam-CERN-Nijmegen-Oxford collaboration).

3.5 Summary of Baryon Resonances

The progress in baryon spectroscopy originates as well in new high statistics experiments as in improved methods to analyse the data.

The classification of baryon resonances in terms of levels in a harmonic oscillator quark model and the analyses of decay rates in terms of $SU(6)_w$ schemes have been discussed in detail in recent publications (e.g. refs. /135/, /136/). Until now it is not clear which one of these schemes fits best the experimental results. Therefore the summary of $SU(6) \otimes O(3)$ multiplets given in table 20 as far as it belongs to the distribution of the observed resonances among the different multiplets can be changed in future. Only the $[56,0^+]$ can be considered as well established concerning the distribution of the states.

As far as it belongs to the $[56,1^-]$, $[70,2^+]$ and the second $[56,2^+]$ additional confirmations are necessary.

Table 20

Summary of the $SU(6) \otimes O(3)$ multiplets.

Multiplet in SU(6)	Comment
$[56,0^+]$	established, all states observed
$[56,0^+]$ radial exitation	established, few states observed
$[56,2^+]$	established, many states observed
$[56,4^+]$	established, few states observed
$[70,1^-]$	estsblished, many states observed
$[70,3^-]$	established, few states observed
$[56,1^-]$	possible, depends on $\Delta\, D_{35}^{***}$ (1960)
$[70,2^+]$	possible, depends on $\Lambda\, F_{05}^{***}$ (2100)
$[56,2^+]$ radial exitation	possible, depends on $N F_{15}^{***}$ (2000)

I would like to thank H. Burkhardt, R. Cutkosky, G. Höhler, R. Kelly, G. Oades, P. Schmid and R. Tripp for many discussions and constructive comments in preparing this review. I also thank the scientific secretaries N. G. Fadejev and G. S. Shabratova for helpful cooperation.

References

/1/ Particle Data Group, Review of Particle Properties, April 1976.

/2/ G. R. Kalbfleisch et al., Phys. Rev. Letters 31, 333 (1973).

/3/ V. I. Ogievetzki et al., Phys. Letters 35B, 69 (1971).

/4/ C. Baltay et al., Phys. Rev. D 9, 2999 (1974).

/5/ R. Lednicky and V. I. Ogievetsky, About X^0 (958) spin determination, paper submitted to the XVIII International Conference on High Energy Physics, Tbilisi, July 1976.

/6/ Amsterdam-CERN-Nijmegen-Oxford collaboration, A measurement of the η' spin - parity, paper submitted to the XVIII International Conference on High Energy Physics, Tbilisi, July 1976.

/7/ Amsterdam-CERN-Nijmegen-Oxford collaboration, $\varrho - \omega$ interference in the reaction $K^- p \longrightarrow (\Lambda, \Sigma^0)\pi^+\pi^-$ at 4.2 GeV/c, paper submitted to the XVIII International Conference on High Energy Physics, Tbilisi, July 1976.

/8/ G. W. Brandenburg et al., Analysis of $K^- K^+$ and $\pi^-\pi^+$ final states in 13 GeV K^- p interactions, paper submitted to the XVIII International Conference on High Energy Physics, Tbilisi, July 1976.

/9/ H. T. Lipkin, Nucl. Phys. 87, 321 (1968).

/10/ A. S. Goldhaber et al., Phys. Letters 30b, 249 (1969).

/11/ A. T. Pawlicki et al., f, f' and A_2^0 interference in $\pi N \longrightarrow K^- K^+ N$ at 6 GeV/c, paper submitted to the XVIII International Conference on High Energy Physics, Tbilisi, July 1976.

/12/ B. Preach, Meson - 1975, CERN/D PH. II/Phys. 75-38.

/13/ G. Ascoli et al., Phys. Rev. Letters 25, 926 (1970); Phys. Rev. Letters 26, 929 (1971); Phys. Rev. D 7, 669 (1973).

/14/ M. Tabak et al., in Experimental Meson Spectroscopy - 1974, p. 46.

/15/ G. Thompson et al., Nucl. Phys. B 101, 285 (1975).

/16/ A. Rosenfeld, in Experimental Meson Spectroscopy - 1974, p. 10.

/17/ F. Wagner et al., Phys. Rev. Letters 58 B, 201 (1975).

/18/ G. L. Kane, in New Directions in Hadron Spectroscopy, Argonne 1974, p. 39.

/19/ M. J. Emms et al., Phys. Letters 60 B, 109 (1976).

/20/ K. W. Edwards et al., A high statistics search for A_1^0 and H^0 in $\pi^- p \longrightarrow \pi^+\pi^-\pi^0 n$ at 8.4 GeV/c, paper submitted to the XVIII International Conference on High Energy Physics, Tbilisi, July 1976.

/21/ E. W. Anderson et al., Phys. Rev. Letters 22, 1390 (1969).

/22/ J. Chapman et al., A esarch for backward A_1 and A_2 production in 4 GeV/c π^- p interactions, paper submitted to the XVIII International Conference on High Energy Physics, Tbilisi, July 1976.

/23/ A. Abashian et al., Phys. Rev. D 13, 5 (1976).

/24/ Amsterdam-CERN-Nijmegen-Oxford collaboration, A partial wave analysis of the $(3\pi)^0$ system in the reaction $K^- p \longrightarrow \pi^+\pi^-\pi^0\Lambda$ at 4.2 GeV/c, paper submitted to the XVIII International Conference on High Energy Physics, Tbilisi, July 1976.

/25/ G. C. Fox and A. S. G. Hey, Nucl. Phys. B 56, 38 b (1973).

/26/ G. Otter et al., Nucl. Phys. B 106, 77 (1976).

/27/ A. Astier et al., Nucl. Phys. B 10, 65 (1069).

/28/ G. W. Brandenburg et al., Phys. Rev. Letters 36, 703 (1976).

/29/ G. W. Brandenburg et al., Phys. Rev. Letters 36, 706 (1976).

/30/ E. Berger, Phys. Rev. D 11, 3214 (1975).

/31/ Aachen-Berlin-CERN-London-Vienna collaboration and Birmingham-Brussels-CERN-Mons-Serpukhov collaboration, Diffraction dissociation and resonances in the $K\omega$ system produced in the reaction $K^{\pm} p \longrightarrow (K^{\pm}\omega) p$, paper submitted to the XVIII International Conference on High Energy Physics, Tbilisi, July 1976.

/32/ G. Otter et al., Nucl. Phys. B 84, 333 (1975).

/33/ B. Drevillon et al., Partial wave analysis of the low mass $\bar{K}^0\pi^+\pi^-$ system produced in the reaction $K^- p \to \bar{K}^0\pi^+\pi^- n$ at 3.95 and 14.3 GeV/c, preprint LPNHE /X/ 75.

/34/ J. S. M. Vergeest et al., Spin - parity structure of the $(\bar{K}\pi\pi)^0$ system produced in the charge - exchange reaction $K^- p \longrightarrow (\bar{K}^0\pi^+\pi^-) n$ at 4.2 GeV/c, paper submitted to the XVIII International Conference on High Energy Physics, Tbilisi, July 1976.

/35/ B. Conforto and G. Conforto, The Q region in non - K - induced reactions, paper submitted to the XVIII International Conference on High Energy Physics, Tbilisi, July 1976.

/36/ K. W. Edwards et al., Production of η', D and E mesons in $\pi^- p \longrightarrow \eta\pi^+\pi^- n$ at 8.4 GeV/c, paper submitted to the XVIII International Conference on High Energy Physics, Tbilisi, July 1976.

/37/ H. Grässler et al., Production and decay of the δ (980) and D (1280) in $\pi^{\pm}$ p interactions at 16 GeV/c, paper submitted to the XVIII International Conference on High Energy Physics, Tbilisi, July 1976.

/38/ Ch. Defoix et al., Properties of the D-meson observed in $\bar{p}p$ annihilations at 0.76 GeV/c, paper submitted to the XVIII International Conference on High Energy Physics, Tbilisi, July 1976.

/39/ M. Corden et al., A study of the D (1285) meson produced in the reaction $\pi^- p \longrightarrow \pi^+\pi^+\pi^-\pi^-\pi^0 n$ at 12 GeV/c beam momentum, paper submitted to the XVIII International Conference on High Energy Physics, Tbilisi, July 1976.

/40/ S. Wells et al., Nucl. Phys. B 101, 333 (1975).

/41/ J. B. Gay et al., Production and decay properties of the δ (970) meson, paper submitted to the XVIII International Conference on High Energy Physics, Tbilisi, July 1976.

/42/ S. M. Flatté, Coupled channel analysis of the $\pi\eta$ and $K\bar{K}$ systems near $K\bar{K}$ threshold, paper submitted to the XVIII International Conference on High Energy Physics, Tbilisi, July 1976.

/43/ P. Lauscher et al., Nucl. Phys. B 86, 189 (1975).

/44/ D. Vignaud et al., Partial wave analysis of the $K^+\pi^-$ system produced in $K^+ n \longrightarrow K^+\pi^- p$ at 4.6, 8.25 and 12 GeV/c, paper submitted to the XVIII International Conference on High Energy Physics, Tbilisi, July 1976.

/45/ P. Estabrooks et al., Study of $K\pi$ scattering using the reactions $K^+ p \longrightarrow K^+\pi^+ n$ at 13 GeV, paper submitted to the XVIII International Conference on High Energy Physics, Tbilisi, July 1976.

/46/ G. Grayer et al., Nucl. Phys. B 75, 189 (1974).

/47/ B. Hyams et al., Nucl. Phys. B 100, 205 (1975).
T. Shimada, Nucl. Phys. B 100, 225 (1975).
P. Estabrooks and D. Martin, $\pi\pi$ partial waves from 0.6 to 1.8 GeV, Durham preprint, March 1975.
A. K. Common, Nucl. Phys. B 103, 109 (1976).

/48/ M. David et al., Results on $\pi^+\pi^- \longrightarrow \pi^0\pi^0$ cross section from peripheral dipion production in the reaction $\pi^- p \longrightarrow \pi^0\pi^0 n$ at 2.01 GeV/c, Saclay preprint, D Ph PE 76 - 08.

/49/ G. Villet et al., A simultaneous phase shift analysis of the $\pi^+\pi^+$, $\pi^-\pi^0$, $\pi^+\pi^-$ and $\pi^0\pi^0$ final states from threshold to 1200 MeV $\pi\pi$ mass, Saclay preprint, D Ph PE 76 - 09.

/50/ H. Becker et al., Measurement of the reaction $\pi^- p \to \pi^+\pi^- n$ on a transversely polarized target at 17 GeV, paper submitted to the XVIII International Conference on High Energy Physics, Tbilisi, July 1976.

/51/ M. Buttram et al., Phys. Rev. D 13, 1153 (1976).

/52/ D. D. Carmony et al., Phys. Rev. Letters 27, 1160 (1971).
A. Firestone et al., Phys. Letters 36 B, 513 (1971).
M. Aguilar-Benitez et al., Phys. Rev. Letters 30, 672 (1973).

/53/ G. W. Brandenburg et al., Phys. Letters 60 B, 478 (1976).
G. W. Brandenburg et al., The $K\pi$ system in the reactions $K^+ p \longrightarrow K^+\pi^- \Delta^{++}$ and $K^- p \longrightarrow K^-\pi^+ n$ at 13 GeV, paper submitted to the XVIII International Conference on High Energy Physics, Tbilisi, July 1976.

/54/ M. Spiro et al., New evidence for K^{**} (1780) production, Saclay preprint, D Ph PE 75 - 12.

/55/ H. Grässler et al., Evidence for K^{**} (1850) production in the reaction $K^- p \longrightarrow K^-\pi^+ n$ at 10 and 16 GeV/c, paper submitted to the XVIII International Conference on High Energy Physics, Tbilisi, July 1976.

/56/ R. Baldi et al., Observation of the K^{**} (1780) in the reaction $K^+ p \longrightarrow K_s^0\pi^+ p$ at 10 GeV/c, paper submitted to the XVIII International Conference on High Energy Physics, Tbilisi, July 1976.

/57/ M. Aguilar-Benitez et al., Phys. Letters 29 B, 379 (1969).

/58/ A. M. Cooper et al., Search for the F_1 (1540) meson in $\bar{p}p$ annihilations at 0.76 GeV/c, paper submitted to the XVIII International Conference on High Energy Physics, Tbilisi, July 1976.

/59/ W. D. Apel et al., Phys. Letters 57 B, 398 (1975).

/60/ W. Blum et al., Phys. Letters 57 B, 403 (1975).

/61/ Particle Data Group, Rev. Mod. Phys. 47, 535 (1975).

/62/ W. Tanenbaum, Recent results from SPEAR, SLAC - PUB - 1722, February 1976.

/63/ T. Ferbel and P. Slattery, Phys. Rev. D 9, 824 (1974).

/64/ G. W. Brandenburg et al., Evidence for a new strangeness-one pseudoscalar meson, paper submitted to the XVIII International Conference on High Energy Physics, Tbilisi, July 1976 and Phys. Rev. Letters 36, 1239 (1976).

/65/ N. M. Cason et al., Production of scalar and tensor mesons in the $K\bar{K}$ system, paper submitted to the XVIII International Conference on High Energy Physics, Tbilisi, July 1976.

/66/ A. S. Caroll et al., Phys. Rev. Letters 32, 247 (1974).

/67/ M. Alston - Garnjost et al., Phys. Rev. Letters 35, 1685 (1975).

/68/ V. Chaloupka et al., submitted to Phys. Letters B (1976).

/69/ D. Cohen, in Experimental Meson Spectroscopy - 1974, p.79.

/70/ J. L. Rosner, Phys. Rev. Letters 21, 950 (1968).

/71/ H. Brundiers et al., Search for exotic mesons produced by baryon exchange in the reaction $\pi^+ p \longrightarrow \Lambda + X^{++}$ at 12 GeV/c, paper submitted to the XVIII International Conference on High Energy Physics, Tbilisi, July 1976.

/72/ P. Bonamy et al., Search for exotic mesons at SLAC, paper submitted to the XVIII International Conference on High Energy Physics, Tbilisi, July 1976.

/73/ J. Boucrot et al., Exotic search $X^{--} \longrightarrow p\bar{p}\,\pi^-\pi^-$ in the omega spectrometer, paper submitted to the XVIII International Conference on High Energy Physics, Tbilisi, July 1976.

/74/ P. J. Litchfield, in Proceedings of the XVII International Conference on High Energy Physics, London 1974, p. II-65.

/75/ E. Barrelet, Nuovo Cimento 8 A, 331 (1972).

/76/ D. Atkinson et al., Construction of a unitary analytic scattering amplitude V. $\pi^+ p$ scattering, paper submitted to the Topical Conference on Baryon Resonances, Oxford, July 1976.

/77/ D. J. Bradsley et al., Measurements of $\pi^+ p$ and $\pi^- p$ elastic differential cross sections from 0.4 to 2.15 GeV/c, paper submitted to the Topical Conference on Baryon Resonances, Oxford, July 1976.

/78/ J. F. Martin et al., Nucl. Phys. B 89, 253 (1975).

/79/ R. M. Brown et al., Measurements of the polarization parameter P and the differential cross section for the reaction $\pi^- p \longrightarrow \pi^0 n$ in the resonance region, paper submitted to the Topical Conference on Baryon Resonances, Oxford, July 1976.

/80/ S. Almehed and C. Lovelace, Nucl. Phys. B 40, 157 (1972).

/81/ R. Ayed and P. Bareyre, private communication to Particle Data Group, 1974, results are given in /1/.

/82/ E. Pietarinen, πN phase shift analysis using dispersion relations, paper submitted to the Topical Conference on Baryon Resonances, Oxford, July 1976.

/83/ J. Hamilton, Fortschritte der Physik 23, 211 (1975).

/84/ R. E. Cutkosky et al., Pion nucleon partial wave analysis from 0.8 to 2.0 GeV/c, paper submitted to the Topical Conference on Baryon Resonances, Oxford, July 1976.

/85/ D. M. Chaw and M. Urban, Barrelet zeros and elastic $\pi^+ p$ partial waves, paper submitted to the XVIII International Conference on High Energy Physics, Tbilisi, July 1976.

/86/ A. W. Hendry, A π^+ proton partial wave amplitude analysis up to 10 GeV/c, paper submitted to the XVIII International Conference on High Energy Physics, Tbilisi, July 1976.

/87/ D. J. Herndorf et al., Phys. Rev. D 11, 3183 (1975).
R. S. Longacre et al., Phys. Letters 55 B, 415 (1975).

/88/ R. D. Baker et al., A study of the reaction $\pi^- p \longrightarrow K^0 \Lambda^0$ in the resonance region, paper submitted to the XVIII International Conference on High Energy Physics, Tbilisi, July 1976.

/89/ J. P. Baton et al., Partial wave analysis of the reaction $\pi^- p \longrightarrow \Lambda K$ between threshold and 1.89 GeV in the centre of mass, paper submitted to the XVIII International Conference on High Energy Physics, Tbilisi, July 1976.

/90/ J. N. Carney et al., A study of the low mass $p\pi^+\pi^-$ system produced in the reaction $K^+ p \longrightarrow K^+ p \pi^+\pi^-$ between 7.3 and 16 GeV/c, paper submitted to the XVIII International Conference on High Energy Physics, Tbilisi, July 1976.

/91/ Amsterdam-CERN-Nijmegen-Oxford collaboration, Partial wave analysis of low-mass ($\pi^+\pi^-$ p) systems produced in K^- p interactions at 4. 2 GeV/c, paper submitted to the Topical Confsrence on Baryon Rsonancss, Oxford, July 1976.

/92/ J. Bartke et al., The effect of resonance production observed in angular correlations, paper submittsd to the XVIII International Confsrence on High Energy Physics, Tbilisi, July 1976.

/93/ Aachen-Berlin-Bonn-CERN-Cracow-Heidelberg-Warsaw collaboration, A multidimensional study of clustering in the reactions $\pi^\pm p \longrightarrow p\,\pi^+\pi^\pm\pi^-$ at 16 GeV/c using the Yang variables, paper submitted to the XVIII International Conference on High Energy Physics, Tbilisi, July 1976.

/94/ S. U. Chung et al., Observation of a high-mass Δ^{++} produced in association with K^*, ϱ and ω, BNL - 20176.

/95/ F. H. Schmidt et al., Phys. Letters 45B, 157 (1973).

/96/ R. Klem et al., Fluctuations in large-angle elastic scattering, preprint 1976.

/97/ R. L. Dixon et al., Measurement of the energy depsndence of backward $\pi^- p$ elastic scattering from 3.0 to 5.5 GeV/c, paper submitted to the Topical Conference on Baryon Resonances, Oxford, July 1976.

/98/ B. Conforto et al., Nucl. Phys. B 105, 189 (1976).

/99/ A. de Bellefon et al., Nucl. Phys. B 90, 1 (1975).
A. de Bellefon et al., New data on the reaction $K^- p \longrightarrow \Sigma^\pm \pi^\mp$ from 1.934 to 2.516 GeV/c and partial wave analysis for these reactions, between 2070 MeV and 2436 MeV cms energy , paper submitted to the Topical Conference on Baryon Resonances, Oxford, July 1976.

/100/ College de France-Saclay collaboration, K^- p formation experiment around 2 GeV/c, paper submitted to the XVIII International Conference on High Energy Physics, Tbilisi, July 1976.

/101/ M. Jones et al., Nucl. Phys. B 90, 349 (1975).

/102/ R. J. Hemingway et al., Nucl. Phys. B 91, 12 (1975).

/103/ V. Hepp et al., New data on the reaction $K^- n \longrightarrow (\Sigma \pi)^-$ and a partial wave analysis in the energy range 1520 - 1745 MeV, paper submitted to the Topical Conference on Baryon Resonances, Oxford, July 1976.

/104/ M. J. Cordes et al., Nucl. Phys. B 104, 382 (1976).

/105/ M. J. Corden et al., New measurements of the reaction $K^- n \longrightarrow \pi^- \Lambda$ in the c.m. energy range 1.75 to 2.0 GeV, paper submitted to the XVIII International Conference on High Energy Physics, Tbilisi, July 1976.

/106/ P. Baillon et al., Determination of the K^- n elastic differential cross section between 1.2 and 2.2 GeV/c, paper submitted to the Topical Conference on Baryon Resonances, Oxford, July 1976.

/107/ M. Alston - Garnjost et al., Study of the reaction $K^- p \longrightarrow \bar{K}^0 n$ at 48 momenta between 515 and 1066 MeV/c, paper submitted to the Topical Conference on Baryon Resonances, Oxford, July 1976.

/108/ M. J. Cordes et al., New experimental results on the reactions $K^- n \longrightarrow \pi^- \Sigma^0$ and $K^- n \longrightarrow \pi^0 \Sigma^-$ and a partial wave analysis of these data between 1750 and 2200 MeV, paper submitted to the Topical Conference on Baryon Resonances, Oxford, July 1976.

/109/ J. Griselin et al., Nucl. Phys. B 93, 189 (1975).

/110/ C. J. Adams et al., Nucl. Phys. B 96, 54 (1975).

/111/ L. Bertanza et al., A study of the reactions $K_L^0 p \longrightarrow \Lambda \pi^+$, $\Lambda \pi^+ \pi^0$, $\Sigma^0 \pi^+$ in the c.m. energy range 1490 - 1700 MeV, paper submitted to the XVIII International Conference on High Energy Physics, Tbilisi, July 1976.

/112/ M. J. Cordes et al., An experimental study of the reactions $K_L^0 p \longrightarrow \Lambda^n \pi^+$ and $K_L^0 p \longrightarrow \Sigma^0 \pi^+$ between 1630 and 1900 MeV c.m. energy, paper submitted to the Topical Conference on Baryon Resonances, Oxford, July 1976.

/113/ Y. Cho et al., Phys. Letters 60 B, 293 (1976).

/114/ B. E. C. P. H. collaboration, Results from a $K_L^0 p \longrightarrow \Lambda \pi^+$ experiment in the region of the narrow Σ^* (1580) (D13) resonance, paper submitted to the Topical Conference on Baryon Resonances, Oxford, July 1976.

/115/ B. Armenteros et al., Nucl. Phys. B 18, 233 (1968).

/116/ V. Hepp, private communication.

/117/ Already some years ago a narrow peak at 2127 MeV in the (Λ p) mass spectrum was observed by Shabanian et al., Nucl. Phys. B 53, 19 (1973), and interpreted as a final state Σ N interaction with the subsequent Σ N $\longrightarrow$ Λ p conversion.

/118/ G. P. Gopal et al., Partial wave analyses of $\bar{K}N$ two - body reactions between 1480 and 2170 MeV, paper submitted to the Topical Conference on Baryon Resonances, Oxford, July 1976.

/119/ P. N. Hansen et al., An energy independent $\bar{K}N$ phase shift analysis, paper submitted to the XVIII International Conference on High Energy Physics, Tbilisi, July 1976.

/120/ B. R. Martin et al., $\bar{K}N$ interactions in the resonance region, paper submitted to the XVIII International Conference on High Energy Physics, Tbilisi, July 1976.

/121/ A. T. Lea et al., Nucl. Phys. B 56, 77 (1973).

/122/ P. Bailloa and P. J. Litchfield, Nucl. Phys. B 94, 39 (1975).

/123/ A. de Bellefon and A. Berthon, The reaction $K^- p \longrightarrow \Lambda \pi^0$ zero and partial waves from 1.54 to 2.5 GeV/c, paper submitted to the Topical Conference on Baryon Resonances, Oxford, July 1976.

/124/ P. Eberhard et al., Phys. Rev. Letters 22, 200 (1969).

/125/ J. J. M. Timmermans et al., Production of Σ^*(1660) in $K^- p$ interactions at 4.2 GeV/c, paper submitted to the XVIII International Conference on High Energy Physics, Tbilisi, July 1976.

/126/ R. E. Cutkosky et al., Nucl. Physics B 102, 139 (1976).

/127/ B. R. Martin, Nucl. Phys. B 94, 413 (1975).

/128/ G. Giacomelli et al., Nucl. Phys. B 71, 138 (1974).

/129/ A. Bigi et al., Study of the reaction $K_L^0 p \longrightarrow K_S^0 p$ in the c.m. energy range 1490 - 1700 MeV, paper submitted to the XVIII International Conference on High Energy Physics, Tbilisi, July 1976.

/130/ G. Alexander et al., Phys. Letters 58 B, 484 (1975).

/131/ M. Sakitt et al., Measurement of the differential cross section of $K^+ n \longrightarrow K^0 p$ at K^+ momenta of 0.7, 0.8 and 0.9 GeV/c, paper submitted to the XVIII International Conference on High Energy Physics, Tbilisi, July 1976.

/132/ J. B. Cay et al., Production and decay of Ξ^* (1820) in $K^- p$ reactions at 4.2 GeV/c, paper submitted to the XVIII International Conference on High Energy Physics, Tbilisi, July 1976.

/133/ J. Alitti et al., Phys. Rev. Letters 22, 79 (1969).

/134/ J. M. Gago et al., Ξ^* production in $K^- p$ interactions at 14.3 GeV/c, paper submitted to the XVIII International Conference on High Energy Physics, Tbilisi, July 1976.

/135/ M. Jones et al., Nuovo Cimento 19 A, 365 (1974).
R. Horgan, Nucl. Phys. B 71, 514 (1974).

/136/ A. J. G. Hey et al., Nucl. Phys. B 95, 516 (1975).

PARALLEL SESSION ON INTERACTION MECHANISM IN THE RESONANCE REGION

REGGE AMPLITUDES WITH CROSSING AND UNITARITY

D.Atkinson

University of Groningen, The Netherlands

In 1968 I proved that there exist infinitely many amplitudes that satisfy the Mandelstam representation with the crossing symmetry appropriate to the pion-pion amplitude, elastic unitarity below the inelastic threshold and the inelastic unitarity inequality above it. It was never shown, however, that all these properties are consistent with Regge theory, at least if the leading trajectory rises beyond unity, although of course this assumption is tacitly made in Regge analysis.

Earlier attempts to combine Regge theory with unitarity and crossing have been made by Khuri and by Chew and Jones, among others; but in no case were all the above listed properties satisfied. I wish to report a new crossing symmetric Sommerfeld-Watson transformation that produces such an amplitude, which moreover has the expected Regge asymptotic behaviour and the correct support of the Mandelstam double spectral functions[1-4].

The major difficulty in a crossing symmetric Regge theory is the analytic continuation in the energy variable. We solve this problem by writing an unsubtracted fixed-t dispersion relation for the elastic part of the absorptive part of the amplitude, and the final representation for the amplitude, A(s,t), has the form

$$A(s,t) = B(s,t) + R(s,t) \tag{1}$$

where

$$B(s,t) = \bar{B}(s,t) + \bar{B}(t,u) + \bar{B}(u,s)$$

$$\bar{B}(s,t) = \frac{1}{\pi^2}\int_4^\infty ds' \int_4^\infty dt' \frac{\rho_B(s',t')}{(s'-s)(t'-t)} \tag{2}$$

$$\rho_B(s,t) = \theta\left(t-\frac{16s}{s-4}\right)\rho_B^{el}(s,t) + \theta\left(s-\frac{16t}{t-4}\right)\rho_B^{el}(t,s) + \theta(s-16)\theta(t-16)\nu(s,t) \tag{3}$$

$$\rho_B^{el}(s,t) = \frac{q_s}{4\pi}\int_\Gamma d\ell\,(2\ell+1)P_\ell\left(1+\frac{2t}{s-4}\right)A_\ell(s)\,A_\ell(s) \tag{4}$$

$$R(s,t) = \hat{R}(s,t) + \bar{R}(t,u) + \bar{R}(u,s) \tag{5}$$

$$\bar{R}(s,t) = \hat{R}(s,t) + \hat{R}(t,s) \tag{6}$$

$$\hat{R}(s,t) = \frac{1}{\pi}\int_4^\Lambda \frac{ds'}{s'-s}\hat{R}_s(s;t) \tag{7}$$

$$\hat{R}_s(s,t) = \frac{1}{4}\left\{\bar{\beta}(s_+)\left[\frac{\pi}{\sin\pi\alpha(s_+)}P_{\alpha(s_+)}\left(-1-\frac{2t}{s-4}\right) + \int_0^{\frac{16s}{s-4}}\frac{dt'}{t'-t}P_{\alpha(s_+)}\left(1+\frac{2t'}{s-4}\right)\right] + \right.$$
$$\left. -\bar{\beta}(s_-)\left[\frac{\pi}{\sin\pi\alpha(s_-)}P_{\alpha(s_-)}\left(-1-\frac{2t}{s-4}\right) + \int_0^{\frac{16s}{s-4}}\frac{dt'}{t'-t}P_{\alpha(s_-)}\left(1+\frac{2t'}{s-4}\right)\right]\right\} \tag{8}$$

Here we have assumed, for simplicity, that there is only one Regge pole, at $\ell=\alpha(s)$ with residue $\bar{\beta}(s)/[2\alpha(s)+1]$. The background contour in (5) is defined by $\ell=-\frac{1}{2}+\varepsilon+iy$, $-\infty<y<\infty$; and $\nu(s,t)$ in (4) is an arbitrary crossing symmetric inelastic function.

We have demonstrated the following properties of the above representation: (a) There do exist amplitudes that satisfy the above representation: this is proved by using fixed-point theorems in a Banach space of Hölder continuous functions. (b) Mandelstam analyticity and crossing symmetry are observed. (c) Elastic unitarity is satisfied for $4\le s\le 16$ (d) As $s\to\infty$ in any direction, at fixed t , the expected Regge behaviour is observed, namely

$$A(s,t) = -\frac{\pi\bar{\beta}(t)}{2\sin\pi\alpha(t)}\left\{P_{\alpha(t)}\left(1+\frac{2s}{t-4}\right) + P_{\alpha(t)}\left(-1-\frac{2s}{t-4}\right)\right\} + O\left(|s|^{\alpha(t)+\varepsilon}\right) \tag{10}$$

(e) The physical partial wave amplitudes remain bounded as $s\to\infty$. Properties (d) and (e) are proved by a careful consideration of the analytic properties of the Legendre functions with respect both to index and argument. This allows a crucial contour distortion in (8) (see ref. 3).

A point of especial interest, and perhaps surprise, is that we need no ℓ -plane cuts to guarantee the properties (a)-(e). Moreover, it seems that the possibility of the absorptive parts can be guaranteed in certain artificial cases, and probably arranged numerically in more realistic situations. The above representation should be of use in numerical and theoretical applications, and perhaps also in a dynamical model of Regge poles. We do not expect a bootstrap solution, however, but rather an amplitude that is specified by an externally imposed spectrum of CDD poles, which themselves might come from a harmonic oscillator quark model.

REFERENCES

1. D.Atkinson, J.S. Frederiksen. Comm.Math. Phys., 40, 55 (1975); 43, 1 (1975). References to earlier work may be found in these papers.
2. J.S.Frederiksen, P.W.Johnson, R.L.Warnock. J.Math.Phys., 16, 1886 (1975).
3. D.Atkinson, J.S.Frederiksen, P.W.Johnson, M.Kaekebeke, to be published in Comm.Math. Phys., vol.48 (1976).
4. D.Atkinson, M.Kaekebeke, Crossing Symmetric Amplitude with Regge Poles, Groningen preprint (1976).

HADRON PHYSICS IN QUANTUM CHIRAL THEORY

M.K.Volkov
JINR, Dubna, USSR

As it is known, the field theory with the chiral symmetric Lagrangian describes the low-energy hadron physics in the "tree" approximation rather well. However, in this approximation it is impossible to describe such fundamental properties of hadrons as, e.g., scattering lengths of higher partial waves, form factors and e.m. polarizabilities of mesons, decay structure constants, etc. To get information on all these quantities, one should consider the next, one-loop approximation. This is the subject of the report.

The chiral theory contains the internal energy scale $4\pi F_\pi \approx 1.2$ GeV (F_π=92 MeV is pion decay constant). All the processes will be analysed at energies much lower than that scale.

In the case of meson-meson interactions for the perturbation theory we have the following expansion parameters

$$\left(\frac{m_\pi}{4\pi F_\pi}\right)^2 \approx 0.015\,;\ \left(\frac{m_K}{4\pi F_\pi}\right)^2 \approx 0.17\,;\ \frac{q^2}{(4\pi F_\pi)^2} \ll 1,$$

i.e., the use of the perturbation theory is justified. However, there is another difficulty because of ultraviolet divergences which cannot be removed by the conventional renormalization. Therefore one should emply here the superpropagator method which is valid for field theories with non-polynomial Lagrangians[1].

In the case of meson-baryon interaction the ultraviolet divergences in the one-loop approximation are eliminated by the conventional renormalization if one keeps also the gauge inv. of the theory and uses the low-energy theorems of current algebra and PCAC (excluding πN scattering where one should employ the s.p. method again). But here the expansion parameter is no longer small: $\left(M_N/4\pi F_\pi\right)^2 \approx 0.66$. However, the strong vertices in baryon loops at low energies of meson lines appear to be in the same energy regime like in tree diagrams. Thus, by the low-energy theorems, these diagrams should essentially

c) NN scattering[5] (Contr, paper C3/914-2). There is discussed the role of 4-fermion interaction for NN scattering in the frame of $SU_2 \times SU_2$ inv. Lagrangian. Variant $g_S = g_P = g_V = g_A = 0$, $g_T = -85$ (only tensor coupling) gives correct behaviour of partial waves in energy region $\leq$ 400 MeV.

II. ELECTROMAGNETIC INTERACTIONS

(Contr. paper C3/915-3)

a) Form factors. The pion form factor behaviour[3] is consistent with electromagnetic data of Dubna and Batavia[6]. The pion radius is found to be equal to

$$\sqrt{\langle r^2 \rangle_{\pi^\pm}} = \sqrt{\langle r^2 \rangle_{\pi}^{(\pi)} + \langle r^2 \rangle_{\pi}^{(B)}} \approx 0.65 (fm),$$

where $\langle r^2 \rangle_{\pi}^{(\pi)} \approx 0.065$ (fm)^2 is the pion loop contribution, $\langle r^2 \rangle_{\pi}^{(B)} \approx 0.36$ (fm)^2 - the baryon loop. This result is in good agreement with the result of the ρ dominance model.

For the kaons we have [7]: $\sqrt{\langle r^2 \rangle_{K^\pm}} = 0.61$(fm), $\sqrt{\langle r^2 \rangle_{K^0}} = 0.28$ (fm) in good agreement with the recent experiment[8].

b) Meson polarizabilities[3]. One may obtain an interesting information on pion polarizabilities, calculating the Compton effect on a pion in the one-loop approximation. In this appr. the electric and magnetic pion polarizabilities are equal in magnitude and opposite in sign

$$V_{int.} = \frac{\alpha_\pi}{2} (\vec{E}^2 - \vec{H}^2),$$

$$\alpha_{\pi^\pm} = \frac{e}{m_\pi} (\beta_\pi^{(\pi)}(q_1 q_2) + \beta_\pi^{(B)}), \quad \alpha_{\pi^0} = 2 \frac{e}{m_\pi} \beta^{(\pi)}(q_1 q_2).$$

$\beta_\pi^{(\pi)}(q_1 q_2)$, $\beta_\pi^{(B)}$ - meson and baryon loop contributions. The $\beta_\pi^{(\pi)}(q_1 q_2)$ is rapidly varying in the threshold region! As a result, we have (q_1, q_2 are the photon momenta)

$$\begin{cases} \alpha_{\pi^\pm}(0) = 7 \cdot 10^{-3} (fm)^3, \\ \alpha_{\pi^0}(0) = -8 \cdot 10^{-4} (fm)^3 \end{cases}$$

$$\begin{cases} \alpha_{\pi^\pm}(2m_\pi^2) = 11 \cdot 10^{-3} (fm)^3, \\ \alpha_{\pi^0}(2m_\pi^2) = 7.4 \cdot 10^{-3} (fm)^3 \end{cases} \quad (1)$$

contribute to the corresponding lower order of the the amplitude expansion in energy.

We shall use three known parameters: 1) F_π, 2) mixing parameter of f and d coupling of SU_3 theory, $\alpha \approx \frac{2}{3}$, 3) axial current coupling constant $g_A \approx 1.25$ ($g \approx g_A \frac{M_N}{F_\pi}$ is the strong int. coupl. const.).

$SU_2 \times SU_2$ Lagrangian is represented in the form

$$\mathcal{L}(\psi, \pi) = i \bar{\psi} \hat{\partial} \psi - M_N \bar{\psi} U(\tfrac{\pi}{F_\pi}) \psi + \frac{F_\pi^2}{4} Sp \{ \partial_\mu U(\tfrac{\pi}{F_\pi}) \partial^\mu U^+(\tfrac{\pi}{F_\pi}) \},$$

where the matrix $U(\frac{\pi}{F_\pi})$ in the exponential parametrization has the form: $U^{exp}(\frac{\pi}{F_\pi}) = exp\{ i \gamma_5 \frac{\vec{\tau} \vec{\pi}}{F_\pi} \}$. ψ and π are the nucleon and meson fields, $\vec{\tau}$ and γ_i -Pauli and Dirac matrices. $SU_3 \times SU_3$ generalization can be found in ref.[2].

I. STRONG INTERACTIONS

a) $\pi\pi$ scattering[3] (Contr. paper C3/915-3). A good behaviour of the $\pi\pi$ phases δ_0^0, δ_0^2, δ_1^1 in the region $\sqrt{s} < 1$ GeV are obtained. There is ρ -resonance in P-wave at energy $m_\rho \approx 800$ MeV with width $\Gamma_\rho \approx 150$ MeV. For the $\pi\pi$ scattering lengths of the S, P, D waves we have obtained the values: $a_0^0 = 0.15$; $a_0^2 = -0.042$; $a_1^1 = 0.031$; $a_2^0 = 1.85 \times 10^{-3}$; $a_2^2 = 2.6 \times 10^{-4}$. For $\ell \geq 3$ we have general expressions

$$a_\ell^0 = (2\ell + 1)(4\ell + 7) Z_\ell;$$

$$a_\ell^1 = \tfrac{1}{3}(4\ell^2 - 2\ell - 1) Z_\ell;$$

$$a_\ell^2 = (4\ell^2 + 3\ell + 8) Z_\ell.$$

$$Z_\ell = \frac{\pi}{3} \left(\frac{m_\pi}{4\pi F_\pi} \right)^{4\ell+1} \frac{(\ell!)^3 (\ell - 3)!}{[(2\ell + 1)!]^2}.$$

Note, that in the report of Orlov I. and Parfenov Y. (Contr. paper C3/917-16) also the relations between the scattering lengths have been obtained from the low-energy interaction equations. Their values: $a_0^0 = 0.15$; $a_2^0 = 3.8 \times 10^{-3}$,

b) πN scattering[4] (Contr. paper C3/913-1). A behaviour of the πN phases δ_1 and δ_3 in the region $E_\pi < 400$ MeV are obtained. There are ρ and σ meson resonances: $m_\rho^2 = m_\sigma^2 = 30 m_\pi^2$ and $\omega_{33} \sim 2.6 m_\pi$, $\omega_{11} \sim 3 m_\pi$ ($\omega_{33}^{exp} \sim 2 m_\pi$, $\omega_{11}^{exp} \sim 3.7 m_\pi$).

Analogously, for kaons we have obtained[7]

$$\alpha_{K^\pm}(0) = 1.6 \cdot 10^{-3} (fm)^3, \qquad \alpha_{K^0}(0) = 0.$$

III. WEAK INTERACTIONS[9]

(Contr. paper C3/915-3)

The one-loop appr. for the decay $\pi^\pm \to \mu^\pm \nu (e^\pm \nu)$ leads to finite result which gives only a small (1.5%) correction to F_π : $F_\pi(m_\pi) \approx 93$ MeV. The calculation of the one-loop appr. for the process $\pi^\pm \to \mu^\pm \nu \gamma$ allows one to obtain the values of these decay structure constants which satisfy current algebra relations. The form factor of the decay $\pi^+ \to \pi^0 e^+ \nu$ coincides with elsctromagnetic one.

Finally, the one-loop appr. leads to the following values of the K_{e3} form factors[10] : $\lambda_+ = 0.025$; $\lambda_0 = -0.03$; $\xi = \frac{f_-(0)}{f_+(0)} = -0.7$ that are also in satisfactory agreement with experiment[11].

IV. INFORMATION ON THE CHIRAL SU(2)xSU(2) SYMMETRY BREAKING FROM THE ANALYSIS OF THE EXP. DATA ON $\pi N \to \pi\pi N$ (THREE-APPROXIMATION)

a) There is considered the symmetry breaking (s.b.) term

$$\Delta\mathcal{L}^{(a)} = \frac{1}{8F_\pi^2}\left(1 - \frac{\xi}{2}\right)^2 m_\pi^2 (\vec{\pi}^2)^2 - \frac{m_\pi^2}{2}\vec{\pi}^2 .$$

Two variants are discussed: 1) $\xi = 0$ (Weinberg); 2) $\xi = -1.4$ (fit $\pi^- p \to \pi^+ \pi^- n$ near threshold). Both variants give an unsatifactory description of exp. data on total cross sections (Contr. paper C3/820-48/); b) the s.b. terms are considered $\Delta\mathcal{L}^{(b)} = -\frac{m_\pi^2}{2}\vec{\pi}^2 + A(\vec{\pi}^2)^2 + \frac{C_1}{m_\pi^4}(\partial_\mu \vec{\pi}\partial^\mu\vec{\pi})^2 + \frac{C_2}{m_\pi^4}(\partial_\mu \vec{\pi}\,\partial_\nu\vec{\pi})^2$. The free parameters are determinated from the exp. data: 1) on total cross sections of $\pi N \to \pi\pi N$; 2) on differential cross section of $\pi^- p \to \pi^+\pi^- n$; 3) on total and differential cross section. All variants give an unsatisfactory description of exp, data (Contr. paper C3/841-4).

Therefore it is impossible to define the chiral symmetry breaking term from $\pi N \to \pi\pi N$ without consideration of the one-loop appr. or the contributions of resonances.

REFERENCES

1. M.K.Volkov. Ann.Phys.,49,202 (1968).
2. M.Gell-Mann,R.J.Oakes,B.Renner.Phys.Rev., 175,2195 (1968).
3. M.K.Volkov, V.N.Pervushin.Nuovo Cim.,27A, 277 (1975).
4. M.Haysak, V.Lengyel. JETP Lett.,19,772(1974), 22,598 (1975).
5. M.Haysak, V.Lengyel, M.Salak.Preprint ITP-76-41P, K., 1976.
6. S.F.Berezhnev et al. Yad.Fiz.,18,102(1973). C.A.Adylov et al. Phys.Lett., 51B, 402 (1974).
7. V.N.Pervushin, M.K.Volkov. Phys.Lett.,58B, 177 (1975).
8. F.Dydak et al. Nucl.Phys.,B102,253(1976).
9. M.K.Volkov, V.N.Pervushin.Yad.Fiz.,22,366 (1975).
10. D.I.Kazakov, V.N.Pervushin, M.K.Volkov. Phys.Lett., 64B,210 (1976).
11. H.Braun et al. Nucl.Phys.,B89,210(1975).

AMPLITUDE AND PHASE SHIFT ANALYSIS OF BINARY REACTIONS IN THE RESONANCE REGION

G.C.Oades, Institute of Physics, Aarhus Univ., Aarhus, Denmark

In this report I will attempt to put into perspective recent work in the field of amplitude and phase shift analysis. I will concentrate on the methods rather than the results since these will be covered by Prof. Lanius in his report on Baryon and Meson Spectrosoopy.

Let us start by considering a typical first generation phase shift analysis where a finite number of unitary partial wave amplitudes are fitted to the experimental scattering data. The work of Gersten[1] and Barrelet[2] tell us how from one solution we can construct other solutions which give identical fits to the experimental data. The method is simplest for spin 0-spin 0 scattering where with L+1 partial waves the scattering amplitude will have L complex zeroes in the cos θ plane. Any one of these zeroes can be switched to its complex conjugate position without changing the differential cross section. It must be checked that the new scattering amplitude gives partial waves which are still unitary but in general we expect to be left with several acceptable solutions at this one energy.

The task is now to find how many physically reasonable paths there are joining the solutions at the different energies. Typically the individual partial waves are required to be "smooth" functions of energy either by eye, by shortest path techniques or by using a particular energy dependent parametrization. The last method is used in two new multichannel $\bar{K}N$ analyses where the partial waves are parametrized as a sum of resonances plus background[3] or by a factorizing K-matrix form[4].

While such energy dependent fits necessary give smooth zero trajectories as functions of energy it is not clear whether alternative solutions with equally smooth trajectories may exist. Other methods may give less smooth trajectories or may even show sudden jumps to the complex conjugate position thus indicating troubles with the solution. Barrelet has pointed out that there are advantages with extracting the zeroes directly from the data since the error analysis is then easier. There have been recent studies of this form for $K^+p \to K^+p$ [5], $\pi^+p \to \pi^+p$ [6] and $\pi^-p \to K^0\Lambda$ [7,8] as well as other studies working with zeroes reconstructed from the partial wave amplitudes for $\pi N \to \pi N$ [9], $K^+p \to K^+p$ [10], $K^\pm p \to K^\pm p$ [11] and $K^-p \to \pi^0\Lambda$ [12]. The general conclusion is that $\pi^-p \to K^0\Lambda$ has four solutions but that may be only one is consistent with a resonance plus background form. For $K^+p \to K^+p$ and $\pi N \to \pi N$ there seem to be no ambiguities at least for $p_{Lab} \leq 2$ GeV/c while for both $K^-p \to K^-p$ and $K^-p \to \pi^0\Lambda$ there are two possible solutions although in each case there are reasons to prefer one of the two.

So far we have considered the case of a finite number of partial waves. Removing this unphysical restriction gives rise to a continuum ambiguity which has been studied by Atkinson et al.[13]. They have constructed a method of producing an identicial fit to the data with low partial waves plus a "tail" of unitary high partial waves with the correct exponential falloff. They then examine the effect of the high partial wave tail on the original low partial waves which, at a given energy, develop "ambiguity patches". The size of these patches has been examined for $\pi^+p \to \pi^+p$ [14] and $K^+p \to K^+p$ [15]. For π^+p they reach conclusions about which resonances are at risk and for K^+p they suggest that the continuum ambiguity allows transition from the amplitudes of Fich et al.[16] to those of Cutkosky et al.[17].

Now I turn from ways of producing ambiguites to attempts to remove them. There are two main lines of attack due to Cutkosky and to Pietarinen. Both methods use dispersion relations as a weapon with which to attack the continuum phase problem. In their K^+p analysis Cutkosky et al.[17] use

the ACE (accelerated convergence expansion) method to avoid a sudden cut-off in the partial wave expansion and they subject each partial wave to a smoothness constraint via partial wave dispersion relations. In their πN work[18] they make use of hyperbolic dispersion relations rather than partial wave dispersion relations as a smoothness constrain on their invariant amplitudes.

The work of Pietarinen is rather different in that he starts with a fixed-t amplitude analysis. Using a suitable mapping he expands the invariant amplitudes in a way which ensures the correct fixed-t analyticity and which gives a suitable high energy behaviour. The coefficients of the expansions are then determined by fitting to all available data. Such analysis have been made for πN[19] and for $K^{\pm}p$[20]. The question of the uniqueness of such a fit has also been considered[21] and Pietarinen has shown that possible ambiguites should be rather limited.

These fixed-t analyses are limited to $t \gtrsim -1.5$ (GeV/c)^2 due to double spectral function problems so direct projection of the partial waves is only possible for $p_{Lab} \lesssim 1$ GeV/c. To proceed to higher energies the fixed-t amplitudes are used as constraints on partial wave analyses of πN[22], of $K^+p \to K^+p$[16] and of $K^-p \to K^-p$[23]. These analyses produce partial waves which fit the experimental data and which reproduce the fixed-t invariant amplitudes. In practice the fixed-t and phase shift analyses are iterated a few times and in addition the partial waves are subjected to smoothness constraints via partial wave or fixed-angle dispersion relations. I should mention that similar techniques have been used in $\pi\pi$ analyses[24,25] where the conclusion is that dispersion relations favour a solution which shows the $\rho''(1600)$.

Finally I should point out that new data can influence all of these analyses. For example in πN there is new $\pi^-p \to \pi^0 n$ d.c.s. and polarization data from Thresher et al.[26] as well as new low energy measurements of $\pi^{\pm}p \to \pi^{\pm}p$[27] and of forward $\pi^-p \to \pi^0 n$[28] submitted to this conference. I should also mention the attempts of Cottingham et al.,[29] to understand the KN-KN system via t and u channel exchanges. This is similar in spirit to the studies of the NN potentials via meson exchanges where much progress has been made. These NN studies will no doubt be helped by new measurements of the pp spin correlation parameters at 610 and 630 MeV submitted to this conference[30].

REFERENCES

1. A.Gersten. Nucl.Phys.,B12, 537(1969).
2. E.Barrelet. Nuovo Cimento 8A,331 (1972).
3. Gopal et al., Proceedings of the 1976 Oxford Baryon Resonance Conference.
4. B.R.Martin et al. paper C3-21 (919).
5. M.Urban.Phys.Letters 60B,77(1975).
6. E.Barrelet et al.LBL-4644 (1976).
7. J.P.Baton et al.,paper C3-17 (346).
8. K.W.Abbott et al.,paper C3-33 (976).
9. F.A.Berends.Nucl.Phys.,B64,236(1973).
10. F.A.Berends, private communication.
11. N.O.Pederson. Aarhus thesis (1976).
12. P.Baillon and P.J.Litchfield. Nucl.Phys., B94,39(1975).
13. D.Atkinson et al.Nuol.Phys.,B66,429(1973).
14. D.Atkinson et al., Nuol.Phys (to be published).
15. J. vanDriel, Groningen report 106 (1976).
16. O.Fich et al.,Proceedings of the 1974 London Conf.
17. R.E.Cutkosky et al.Nucl.Phys.,B102,139(1976).
18. R.E.Cutkosky et al.,Proceedings of the 1976 Oxford Baryon Resonance Conference.
19. E.Pietarinen, paper C3-32(1008) and Nucl. Phys.,B107,21(1976).
20. E.Pietarinen.Nuol.Phys.,B76,231(1974).
21. E.Pietarinen,Helsinki preprint 27-75(1975).
22. E.Pietarinen et al.,to be published.
23. P.N.Hansen et al.,paper C3-23 (281).
24. C.D.Froggatt and J.L.Petersen.Nucl.Phys., B91,454 (1975).
25. R.C.Johnson et al., CERN preprint TH-2153 (1976).
26. J.Thresher et al.Proceedings of the 1976 Oxford Baryon Resonanoe Conference.
27. V.A.Gordeev et al.,paper C3-28 (840).
28. V.A.Krevtsev et al.paper C3-27(920).
29. A.C.Davis et al.,paper C3-34(978).
30. N.S.Borisov et al.,paper C3-61(822).

FINAL STATES OF K^-N REACTIONS

W.Kittel,
University of Nijmegen, Netherland

The papers to be reviewed in this report have little in common. I shall therefore give a short summary of each individually.

Corden et al.[1] give a good statistics formation measurement of K^-n cross sections in the energy range 1750-2200 MeV. The $K^-d \to p\Lambda^0\pi^-$ shows a sharp fall between 1750 and 1950 MeV and has a bump around 2000 MeV. It agrees well with previous experiments on the same reaction and on $K^-_L p \to \Lambda^0\pi^+$. The energy dependence agrees with that of the reaction $K^-p \to \Lambda^0\pi^0$. The $K^-n \to \Sigma^0\pi^0$ cross sections fall between 1750 and 2000 MeV and have indication for a maximum at 2100 MeV.

The isospin $I=3/2$ $K^-\pi^-$ inelastic scattering cross section is determined by the Amsterdam-CERN-Nijmegen-Oxford Collaboration from the reactions $K^-p \to \Delta^{++}(K^+p)$ at 4.2 GeV/c incident K^- momentum, using a Chew-Low extrapolation method[2]. The total inelastic $K^-\pi^-$ scattering cross section (shown in fig. 1) is found to increase almost linearly with the $K^-\pi^-$ mass from <0.1 mb at 0.9 GeV to 2.3 mb at 1.5 GeV. The available statistics also allowed a determination of the cross sections for individual reactions by this method. Below 1.3 GeV only the reactions $K^-\pi^- \to (K\pi\pi)^-$ contribute to the inelastic cross section; higher multiplicity $K^-\pi^-$ interactions start to play a role above this mass. A comparison to elastic $K^-\pi^-$ scattering gives an elasticity falling from > 0.97 at 900 MeV to 0.51 ± 0.08 at 1500 MeV.

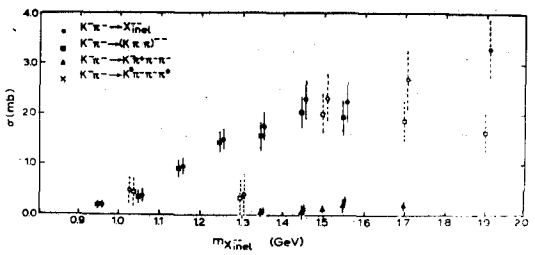


Fig. 1. The $K^-\pi^-$ inelastic cross section as a function of mass. The errors are statistical. Where several points occur at the same X^-_{inel} mass, they have been displaced for clarity. The open points with dashed error-bars refer to the corresponding values from the 14.3 GeV/c K^-p experiment[3].

Spin-parity content and production mechanism of $(\pi^+\pi^-)$ -systems in the reaction $\pi^+p \to (\pi^+\pi^-)\Delta^{++}$ at 16 GeV/c are studied[4] as functions of the $(\pi\pi)$ mass and of the four-momentum transfer $t'_{p\Delta}$. A substantial amount of S -wave is found both in the ρ - and f -meson regions. The production of these $(\pi\pi)$ systems is dominated by pion exchange. Natural parity exchange contributions are comparable to unnatural ones in the ρ -region for $t'_{p\Delta} > 0.3$ GeV^2. Relative to pion exchange they decrease in the production of higher mass $(\pi\pi)$ -systems.

Transversity amplitudes and spin density matrix elements for the similar process $K^-p \to (\pi^+\pi^-)_{S\text{-wave}}\Sigma^0(1385)$ are determined[5] from an amplitude analysis. The analysis is done in 8 variables (effective masses and decay angles). Contribution from S- and P -wave and their interference is assumed for the $(\pi^+\pi^-)$ system, $J^P = 1/2^-$ and $3/2^+$ for the $(\Lambda^0\pi^+)$ system.

Prediotions of the additive quark model and of duality diagrams are tested for the first time in a prooess where a scalar object is produced at the mesonio vertex. The predictions are found to be consistent with the data.

A partial wave analysis of the low-mass $(\pi^+\pi^-p)$ system produced in the reaction $K^-p \to K^-(\pi^+\pi^-p)$ at 4.2 GeV/c[6] shows that the low-mass $(\pi^+\pi^-p)$ system can be described using the spin-parity states $J^P = \frac{1}{2}^+$, $\frac{3}{2}^-$ and $\frac{5}{2}^+$. In the 1500 MeV region a contribution was observed from the $\frac{1}{2}^+$ wave decaying into $p\varepsilon$ and the $\frac{3}{2}^-$ wave decaying into $\Delta^{++}\pi^-$; in the 1700 MeV region we found contributions from the $\frac{1}{2}^+$ wave decaying into $\Delta^{++}\pi^-$, the $\frac{3}{2}^-$ wave decaying into $p\varepsilon$, and the

$\frac{5}{2}^+$ wave decaying into $p\varepsilon$. The pp decay mode was found to be small but its interference with the other modes makes its inclusion necessary.

A socalled "multi-channel" analysis considering simultaneously all contributions to a final state in full dimensional phase space has been applied to the reaction $K^-p \to \bar{K}^0\pi^-p$ at 4.2 GeV/c[7]. The channels introduced at the beginning of and during this analysis are well separated after a few iterations. The $(\bar{K}\pi)$ system contains s-, p-, d-and f-waves. The s-wave is wide and interferes in particular with the p- and d-waves. The p-, d-and f-waves are produced from both natural and unnatural exchanges. The $(p\pi)$ system can be best described by $1/2^-$, $3/2^+$, $3/2^-$, $5/2^+$ and $5/2^-$ contributions and interferences. Because of relatively low cross section and the large overlap with the $(\bar{K}\pi)$ system, in particular the interferences would be diffucult to study with simple mass cuts. The $(p\bar{K})$ system contains a $\Sigma^+(1765)$ produced both in the forward and backward direction.

Indication is found for an interference of the Δ^0 with both $K^*(1420)$ and $(K\pi)_S$ waves. From the phases extractable from this kind of interference one can expect to obtain more information about production mechanisms than from squared amplitudes alone.

REFERENCES

1. M.J.Corden et al. Contributed paper, 1115/C3-41.
2. Amsterdam-CERN-Nijmegen-Oxford Collab. Contributed paper, 277/C3-24.
3. M.Bardadin-Otwinowska et al. Nucl.Phys., B72, 1 (1974).
4. Aachen-Berlin-Bonn-CERN Collab. Contributed paper 51/A1-50.
5. Amsterdam-CERN-Nijmegen-Oxford Collab. Contributed paper 295/C3-35.
6. Amsterdam-CERN-Nijmegen-Oxford Collab. Contributed paper, 273/C3-26.
7. Amsterdam-CERN-Nijmegen-Oxford Collab. Contributed paper, 328/C3-25.

RECENT RESULTS FROM MINA

J.Allison, University of Manchester, England

I. PHOTOPRODUCTION

1. Nuclear Photoproduction of ρ,ω Mesons[1,2]

Targets of Be, C, Al, Cu, Ag, Au were exposed by a LANCASTER group to a tagged photon beam in the energy range 2.75 to 4.35 GeV, using a large solid angle heavy-plate optical spark chamber apparatus sensitive to both charged particles and γ-rays. Total cross sections for $\gamma A \to \rho A$ relative to Be are shown in fig. 1. They give $\sigma_{\rho N}$ = (20±3) mb and $\gamma_\rho^2/4\pi$ = 0.55±0.2 for $\alpha_{\rho N}$ = -0.2, slightly lower than previous results.

This group also present results on ω production from deuterium[2].

2. Backward Photoproduction of ρ^0 and f.

A DARESBURY-SHEFFIELD group have studied the reaction $\gamma p \to p\pi^+\pi^-$ with a tagged photon beam of energy between 2.8 and 4.8 GeV, covering backward angles of production of the $\pi^+\pi^-$ system ($0 < |u| < 1.4$ GeV^2). The forward going protons were detected and identified in a spectrometer with a Cerenkov counter. Other charged particles were detected in spark chambers surrounding the target.

Both ρ^0 and f production is prominent (see fig. 2), being 2 and 3 times higher than backward π^0 production respectively. This is in strong contrast to forward dipion production where ρ^0 is skew and f has never been seen. Instead, it closely resembles backward dipion production by pions apart from an overall scale factor of about 300.

These results on ρ^0 production require substantial I = 3/2 exchange in the u-channel near $u = 0$.

3. Polarization Parameters in Pseudoscalar Meson Photoproduction[4,5]

A series of single and double polarization experiments has been made by the Glasgow-Liverpool-Sheffield collaboration on the reactions

$\gamma p \to \pi^+ n$, $\gamma p \to \pi^0 p$ and $\gamma p \to \eta p$ at various incident beam energies between 0.6 and 3 GeV. They use a polarized photon beam of coherent bremsstrahlung from a diamond target. For the double polarization experiments they use a ^3He cooled butanol polarized target polarized in various directions.

Various polarization parameters have been measured:

Σ, the polarized photon asymmetry,

T, the polarized target asymmetry,

P, the recoil nucleon polarization,

H and G, double polarization parameters.

P, H and G are obtained from meaeurements with a polarized beam incident on a polarized target, polarized perpendicular to the reaction plane (P), in the reaction plane and perpendicular to the beam (H) and in the reaction plane and parallel to the beam (G). The reader is refarred to Fisher[6] for further explanations of these parameters.

The following data have been collected:

(a) Σ for $\gamma p \to \pi^0 p$, $E_\gamma = 1.2 - 2.8$ GeV, $\theta^*_\pi = 30^\circ - 100^\circ$[4]

The measurements agree quite well with predictions of fixed-t dispersion relation analyses of Knies, Moorhouse and Oberlack and Metcalf and Walker, except for a rapid excursion to negative values of Σ over the energy range 1.5-1.9 GeV for $|t|$ in the region of 0.6-0.7 GeV^2.

(b) Σ for $\gamma p \to \eta p$, $E_\gamma = 2.5$ and 3.0 GeV, $|t| = 0.2$-1.2 GeV^2[5]

The data strongly disagree with Regge predictions

(c) Σ for $\gamma p \to \pi^0 p$, $E_\gamma = 1.25$-2.15 GeV, $\theta^*_\pi = 30^\circ - 100^\circ$

These results are still preliminary and exist as in the SLAC 1975 conference report[6]. The measurements also contain information on P and T.

(d) Σ, P and T for $\gamma p \to \pi^+ n$, $E_\gamma = 0.5$-2.25 GeV, $\theta^*_\pi = 30^\circ - 115^\circ$

Preliminary results are shown in fig. 3 for a centre of mass angla of 105°. The curves show predictions of Metcalf and Walker (MW), Barbour and Crawford (BC) and Knies, Moorhouse, Oberlack and Rosenfeld (KMOR). There is substantial agreement below 1 GeV, but some departures above this, indicating the different high energy parametrizations of the models.

(e) H for $\gamma p \to \pi^+ n$, $E_\gamma = 0.6$-1.5 GeV, $\theta^*_\pi = 30^\circ - 100^\circ$

This is the first part of an experiment to measure G and H over this range. Preliminary data for H for $\theta^*_\pi = 60^\circ - 100^\circ$ is shown in fig. 4. Some of the data contain a small admixture of G and Σ because the target had to be rotated by about 7° to avoid obstructing the aperture, but this is unlikely to change the data by more than one standard deviation. The curves show predictions of Barbour and Crawford. Substantial agreement is obtained except at the higher energies, indicating that the resonance region is now fairly well understood. It is hoped that these data will allow a better determination of the couplings of higher resonances and place important constraints on high energy models.

II. ELECTROPRODUCTION

1. Threshold π^+ Electroproduction[7,8]

$\pi^+ n$ coincidence data have recently been published by a DARESBURY-PISA-ROME group. The threshold behaviour has been compared with fixed-t dispersion relation models and interpreted in terms of the axial-vector form factor G_A shown in fig. 5. They determine characteristic masses of 0.62 GeV on a monopole model and 0.96 GeV on a dipole model. The world data marginally prefers a dipole parametrization. This data is being reviewed by Norton at this conference.

2. Inclusive Neutron Spectra in Electroproduction above the Resonance Region[9]

This data from a DARESBURY-PISA-ROME collaboration is at momentum transfers of 0.3, 0.6 and 0.9 GeV^2 and a centre of mass energy of 2.3 GeV. They find a yield of neutrons significantly greater than that of protons.

REFERENCES

1. P.Coddington, M.Atkins, T.J.Brodbeck, D.H.Locke, J.V.Morris, D.Newton and T.Sloan. Nucl.Phys., B95, 249 (1975).
2. J.V.Morris, T.J.Brodbeck, P.Coddington, D.Newton, T.Sloan. Daresbury Lab., preprint DL/P264 (Submitted to Nucl.Phys.B).
3. R.W.Clift, J.B.Dainton, E.Gabathuler, L.S.Littenberg, R.Marshall, S.E.Rock, J.C.Thompson, D.L.Ward, G.R.Brookes. Daresbury Lab. preprint (to be published), (to be submitted to Phys.Rev.).
4. P.J.Bussey, C.Raine, J.G.Rutherglen, P.S.L.Booth, L.J.Carrol, P.R.Daniel, C.J.Hardwick, J.R.Holt, L.N.Jackson, J.Norem, W.H.Range, F.H.Combley, W.Galbraith, B.H.Rajaratnam, S.Sutton, M.C.Thorne, P.Waller. Nucl.Phys., B104, 253 (1976).
5. P.S.Bussey, C.Raine, J.G.Rutherglen, P.S.L.Booth, L.J.Carrol, P.R.Daniel, A.W.Edwards, C.J.Hardwick, J.R.Holt, J.N.Jackson, J.Norem, W.H.Range, W.Galbraith, V.H.Rajaratnam, C.Sutton, M.C.Thorne, P.Waller. Phys.Lett., 61B, 479 (1976).
6. H.M.Fischer. SLAC canference, 413 (1975).
7. A. Del Guerra, A.Giazotto, M.A.Giorgi, A.Stefanini, D.R.Botterill, D.W.Braben, D.Clarke, P.R.Norton. Nucl.Phys., B99, 253 (1975).
8. A.Del Guerra, A.Giazotto, M.Giorgi, A.Stefanini, D.R.Botterill , H.E.Montgomery, P.R.Norton and G.Matone, Nucl.Phys., B107, 65 (1976).
9. J.Bailey, D.R.Botterill , D.W.Braben, D.Clarke, H.E.Montgomery, P.R.Norton, G.Matone, A. Del Guerra, A.Giazotto, M.A.Giorgi, A.Stefanini. Nucl.Phys., B106, 385 (1976).

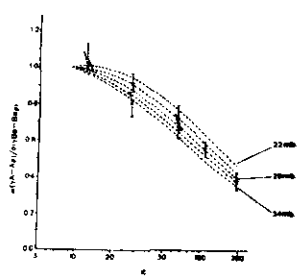


Fig. 1

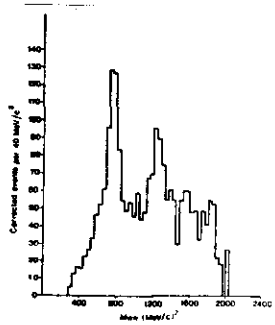


Fig. 2

Fig. 1. The measured total cross section for ρ^0 photoproduction relative to beryllium. The curves are predictions of the Trefil model for various $\sigma_{\rho N}$.

Fig. 2. Backward di-pion mass spectrum for $\gamma p \to p\pi^+\pi^-$. The spectrum has been corrected for acceptance variation.

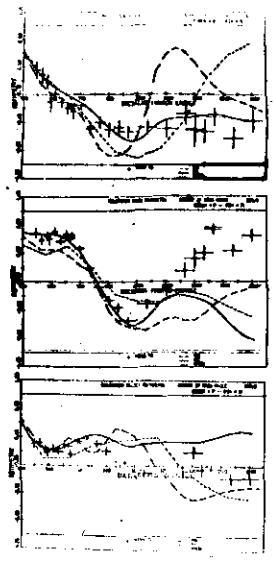


Fig. 3. Preliminary measurements of Σ, P and T for π^+ photoproduction from the Glasgow-Liverpool-Sheffield double polarization experiment, compared with predictions of Metcalf and Walker (MW), Barbour and Crawford (BC) and Knies, Moorhouse, Oberlack and Rosenfeld (KMOR).

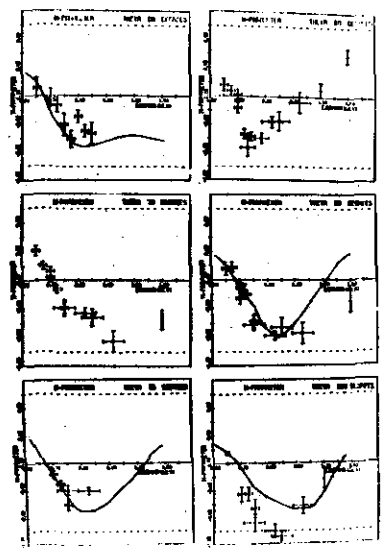


Fig. 4. Preliminary measurements of H for π^+ photoproduction from the Glasgow-Liverpool-Sheffield double polarization experiment compared with predictions of Barbour and Crawford.

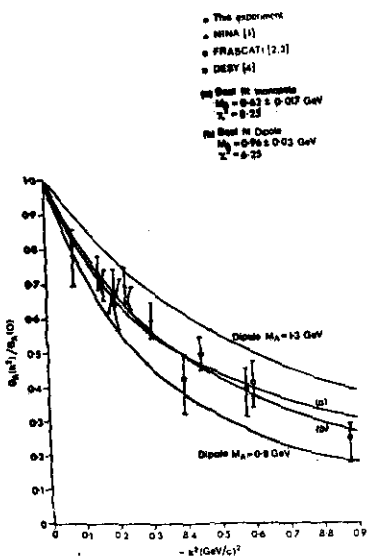


Fig. 5. Axial vector Form Factor measurements from NINA, FRASCATI and DESY. This figure is taken from ref. 7.

ФОТО- И ЭЛЕКТРОРОЖДЕНИЕ ПИОНОВ В ОБЛАСТИ ПЕРВОГО πN-РЕЗОНАНСА

П.В.Сорокин
Харьковский физико-технический институт, СССР

Исследованию процессов фото- и электророждения пионов на нуклонах в области энергий до 500 МэВ уделяется заметное внимание, т.к. здесь легче всего можно определить амплитуды процесса $\gamma N \to \pi N$ и с их помощью проверять различные предсказания теории и, используя пороговые теоремы, изучать электромагнитные свойства пионов, нуклонов.

Последние обзоры экспериментальных данных по этим вопросам были сделаны на Стэнфордском симпозиуме в августе 1975 г. На настоящую конференцию представлены три работы /1,2,3/, посвященные фоторождению, и одна /4/ - электророждению пионов на нуклонах.

Новый мультипольный анализ имеющихся экспериментальных данных представлен в работе /5/.

В работе /1/ приведены предварительные результаты первого эксперимента по измерению поляризации протона отдачи в реакции $\gamma p \to \pi^0 p$ на линейно поляризованном пучке фотонов. В таком эксперименте наряду с ранее измеренными наблюдаемыми Σ, T_y, P_y могут быть получены сведения о двух независимых и ранее неизмерявшихся величинах P_x и P_z - проекциях вектора поляризации протона отдачи, лежащих в плоскости реакции. Эксперимент проведен на Харьковском линейном ускорителе электронов.

Линейно поляризованные фотоны получались при когерентном тормозном излучении электронов в кристалле алмаза. Поляризация протонов измерялась с помощью искровой камеры с графитовыми электродами.

Результаты измерений параметров из двойного поляризационного эксперимента Σ, T_y, P_y хорошо согласуются с соответствующими величинами, полученными ранее.

Т.к. в эксперименте использовался магнитный спектрометр, то из-за прецессии спина могла быть измерена лишь величина $P_{xy} = P_x \cos\alpha + P_y \sin\alpha$,

где α – угол прецессии. Результаты эксперимента показаны на рис. I.

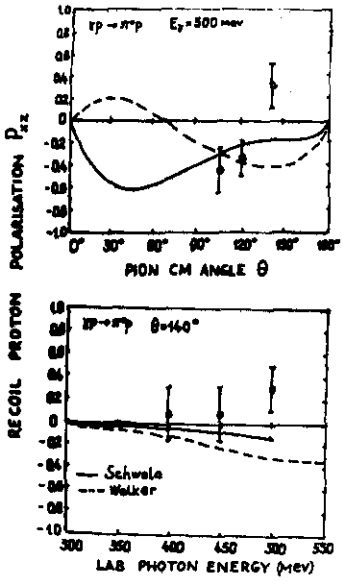


Рис. I

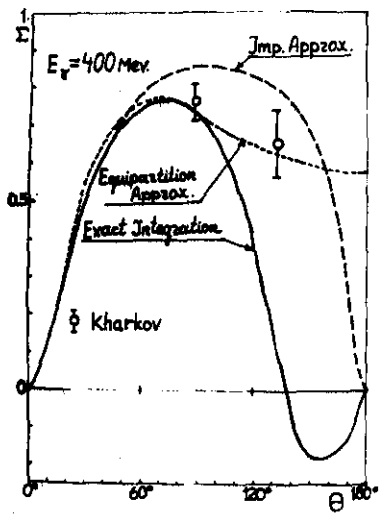


Рис. 2

В работе[2] приведены новые данные об асимметрии сечения реакции $\gamma d \to \pi^0 d$ на линейно поляризованных фотонах. Результаты приведены в таблице :

E_γ / θ_{π^0}	350 МэВ	400 МэВ	450 МэВ	500 МэВ
90°	0.73 ± 0.03	0.75 ± 0.05	0.63 ± 0.06	0.85 ± 0.07
I35°	0.44 ± 0.06	0.63 ± 0.09	$0.54\pm0.II$	$0.83\pm0.I5$

Сравнение с результатами расчета[6] показано на рис. 2.

Странно, что в случае EQUIPARTION – приближении расчетная асимметрия не равна нулю при угле I80°.

Новые теоретические расчеты процесса $\gamma d \to \pi^+ 2N$ приведены в работе[3] и дано сравнение с экспериментом.

На рис. 3 показано отношение сечений фоторождения π^+ мезонов на дейтерии и водороде. Экспериментальные точки взяты из работы[7]; сплошная кривая – расчет в импульсном приближении, штрих-пунктирная – расчет с учетом NN – взаимодействия, штрих-расчет согласно работе[8].

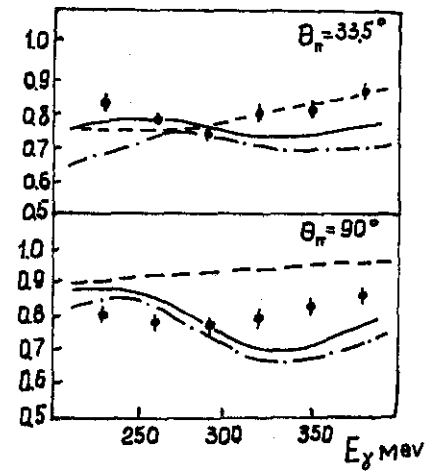


Рис. 3.

Отсюда видно, что в рамках существующих теорий, повидимому, трудно извлечь из опытов на дейтерии данные о сечении на нейтроне с точностью, лучшей ~I0%.

Новый энерго-независимый мультипольный анализ реакций $\gamma p \to \pi^+ n$, $\gamma p \to \pi^0 p$, $\gamma n \to \pi^- p$ был выполнен в работе[5].

Процедура анализа включает исследование неоднозначности решений, классификацию решений по принадлежности к траекториям минимума функционала, выбор решений на основе критерия "кратчайшего пути", исследование устойчивости решений к вариациям экспериментальных данных, предположениям об амплитудах с $\ell \geq 2$ и фазах πN рассеяния. Определены все S и P-изоспиновые мультипольные амплитуды. Сравнение этих амплитуд с результатами ранее выполненных анализов[9] и теорией показывает, что точность определения мультиполей в данной работе лучше, чем в[9]; в оценках малых амплитуд наблюдается существенное различие; тео-

рия неудовлетворительно описывает полученные решения. Показано, что для устранения аномалий, скачков в оценках амплитуд необходимы новые экспериментальные данные о поляризационных эффектах.

Определена фаза φ резонансной амплитуды $M_{1+}^{3/2}$, что дало возможность проверить Т-инвариантность. Различие фаз $\Phi_{33}=\varphi-\delta_{33}=(0,93\pm2,96)$, где δ_{33} – фаза πN-рассеяния. Последние результаты из анализов процессов $\gamma p\to\pi^+ n$ /I0/ и $\pi^- p\rightleftarrows\gamma n$ /II/ дают $\Phi_{33}<2$ и $(2,5\pm1^0)$, соответственно.

Получены значения массы $m_{\Delta^+}=(1237,5\pm1,0)$ МэВ [$m_{\Delta^+}=(1231,8\pm?)$ из работы /I2/, $m_{\Delta^0}=(1232,9\pm0,6)$ МэВ, $m_{\Delta^{++}}=(1230,3\pm0,6)$ из πN-рассеяния /I3/] и радиационной ширины $\Gamma_\gamma=(0,53\pm\pm0,01)$ МэВ (кварковая модель дает $\Gamma_\gamma=0,4$ МэВ, в /I4/ получено $\Gamma_\gamma=(0,64\pm0,03)$ МэВ).

Так же, как и в анализе /I2/, мультипольные амплитуды $M_{1-}^{1/2}$ для нейтрона и протона хорошо определены, и это позволяет исследовать возбуждение P_{11} (1470)-резонанса. Однако, для окончательного решения этого вопроса необходим энергонезависимый анализ в более широкой области энергий. Результаты первой попытки такого анализа были представлены в Стэнфорде в прошлом году, где $P_{11}(1470)$ был найден наряду с резонансами $D_{13}(1570)$ и $S_{11}(1535)$. Результаты энергозависимых анализов дают довольно надежную оценку константы радиационного распада $P_{11}(1470)\to\gamma p$, равную $A_{1-}^{\text{протон}}=(70\div80)\pm20$, в то время как кварковая модель дает $A_{1-}=27$.

В работе /4/ впервые определены поперечные и продольные мультиполи E_{0+} и S_{0+} из сечения электрообразования пионов на протоне у порога в эксперименте „одного плеча" при $k^2=3,5$; 5,0 и 8,0 F^{-2}. Результаты показаны на рис. 4. Сплошные кривые – расчеты по модели алгебры токов с дисперсионной поправкой /I5/; пунктирные – в псевдовекторном борновском приближении /I6/. В расчетах полагалось $M_A=1$ ГэВ, $F_\pi=F_1^v$. Из E_{0+} получены значения аксиально-векторного формфактора нуклона, а из S_{0+} – формфакторы пиона.

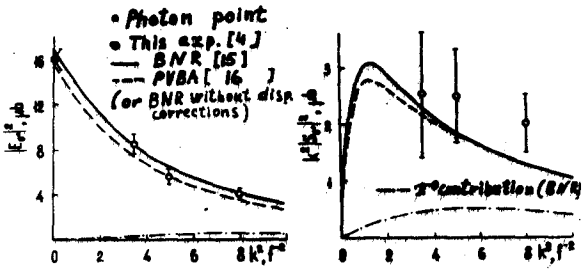


Рис. 4.

Результаты определения формфакторов не противоречат данным, полученным другими способами.

Интересно отметить, что в пороге псевдовекторное борновское приближение /I6/ и модель алгебры токов /I5/ (без учета дисперсионной поправки) дают одинаковые результаты. Поэтому можно надеяться, что результаты определения F_A и F_π имеют малую модельную неопределенность.

Литература

I. В.Г.Горбенко и др. ХФТИ, работа 501/С3-49.
2. В.Б.Ганенко и др. ХФТИ, работа 502/С3-52.
3. А.В.Шебеко, В.Б.Ганенко. ХФТИ, работа 1013/С3-60.
4. А.С.Всаулов и др. ХФТИ, работа 504/С3-19.
5. И.И.Мирошниченко и др. ХФТИ, работа 1011/С-59.
6. C.Lasard, Z.Maric. Preprint IPNO/TH 75-39.
7. Yu.Aleksandrov, V.B.Ganenko, V.V.Grushin et al. Yadern.Fiz., 20, 915, 1974.
8. G.F.Chew, H.W.Lewis. Phys.Rev., 84, 779, 1951.
9. P.Noele, W.Pfeil and D.Shwela. Nucl.Phys., B26, 461 (1971).
   W.Pfeil and D.Shwela. Nucl.Phys., B45, 379 (1972).
   S.Suzuki, S.Kurokawa, K.Kondo. Nucl.Phys., B68, 413 (1974).
10. Yu.M.Aleksandrov, V.F.Grushin, E.M.Leikin, A.Ya.Rotvain. Nucl.Phys., B45, 589 (1972).
    Yu.M.Aleksandrov, V.F.Grushin, E.M.Leikin, A.Ya.Rotvain. Preprint 116, FIAN SSSR, Moscow.
11. I.S.Comiso et al. Phys.Rev., D12, 719, 1975.
12. F.A.Berends, A.Donnachie. Nucl.Phys., B84, 342 (1975).
13. I.R.Carter, D.V.Bugg, A.A.Carfer. Nucl. Phys., B58, 378 (1973).
14. P.Feller et al. Nucl.Phys., B104, 219 (1976).
15. G.Bentaffo et al. Nuovo Cim., 14A, 425 (1973).
16. Yu.V.Kylish. Yadern Fiz., 13, 1301, 1971; N.Dombey and B.J.Read. Nucl.Phys., B60, 65, 1973; B.J.Read. Nucl.Phys., B74, 482 (1974).

РЕЗУЛЬТАТЫ ПОЛЯРИЗАЦИОННЫХ ЭКСПЕРИМЕНТОВ ПО ФОТОРОЖДЕНИЮ π И η МЕЗОНОВ В ОБЛАСТИ 0,7-1,8 ГЭВ

Г.А. Вартапетян
ЕрФИ, Ереван, СССР

За последние годы получили большое развитие эксперименты по фоторождению π-мезонов, а также теоретические исследования на основе различных феноменологических анализов, которые позволяют определить константы связи нуклонных резонансов $N^*N\gamma$ и сравнить их с предсказаниями кварковых моделей и различных схем симметрии.

На конференцию группой из Еревана /1/ представлен новый анализ фоторождения π^0-мезонов от порога до 1,2 ГэВ, основанный на применении дисперсионных соотношений при фиксированном t. Преимущество этого анализа заключается в сведении к минимуму неопределенностей, связанных с высокоэнергетическими вкладами в дисперсионные интегралы (по области $E_\gamma > 2$ ГэВ), что позволяет более точно учесть нерезонансный фон.

Наряду с совершенствованием феноменологических анализов необходимо дальнейшее накопление экспериментальной информации, особенно по поляризационным величинам в области энергий 1-2 ГэВ.

1. Фоторождение π -мезонов (E_γ=0,5-1,7 ГэВ)

На конференцию представлены результаты, полученные двумя группами:

Ереванской группой /2/, которой измерена асимметрия Σ в реакции фоторождения π^0-мезонов поляризованными фотонами;

Японской группой /3/, измерившей асимметрию T для процесса фоторождения π^+-мезонов на поляризованной мишени.

Полученные данные сравниваются в основном с 4 последними феноменологическими анализами /1,4-6/.

а) Асимметрия Σ в реакции $\gamma p \to \pi^0 p$

Измерения выполнены в интервале энергий E_γ = =0,8-1,3 при угле $\theta^{ц.м.}_{\pi^0}=60^0$. Протон отдачи регистрировался системой пробежного телескопа с проволочными искровыми камерами. Распадный γ-квант от π^0-мезона детектировался большим кристаллом NaJ.

Результаты измерений и их сравнение с различными анализами представлены на рис.I. Видно, что новые данные по асимметрии хорошо согласуются с анализами Азнаурян и др.[I] и Феллера и др.[4] и расходятся с предсказаниями, следующими из анализа Меткалфа и Уокера[5] и Муржауза и др.[6]. Рост асимметрии Σ при малых углах, полученный в[I] и [4], хорошо согласуется с экспериментом и виден на рис.2.

б) Асимметрия T в реакции $\gamma p \to \pi^+ n$.

Измерения выполнены в интервале энергий E_γ = =0,5-0,8 ГэВ при $\theta_\pi^{ц.м.}$=40°-I60° [3]. Регистрация π^+-мезона производилась магнитным спектрометром. Мишень создана на основе бутанола со средней поляризацией 63%. Результаты представлены на рис.3 и демонстрируют хорошее согласие с предсказаниями Феллера и др.[4]. В этом случае также имеется расхождение с анализом Меткалфа и Уокера, особенно при больших углах. Отметим, что расхождение с анализом Меткалфа и Уокера проявляется также при E_γ>I,2 ГэВ для Σ в реакции $\gamma p \to \pi^0 p$ [7] и для Σ в реакции $\gamma p \to \pi^+ n$ в интервале энергий 0,9-I,2 ГэВ[8]. Это можно объяснить недостатком экспериментального материала по поляризационным величинам, использованного в этом анализе. Из результатов анализа, проведенного в [I], важно отметить следующее:

I. Константы связи, полученные для резонансов S_{31}(I660), F_{15}(I690), P_{31}(I850) и F_{35}(I880), значительно отличаются от значений, полученных в других работах, и находятся в лучшем согласии с предсказаниями кварковой модели (см. таблицу).

2. Для резонансов P_{11}(I430) и P_{33}(I640), входящих в мультиплет $[56,0^+]$ с радиальным возбуждением, наблюдается существенное расхождение с предсказаниями кварковой модели, что подтверждается результатами всех анализов.

Константы связи, полученные в работе[I] для резонансов P_{33}(I233), S_{11}(I530), D_{13}(I5I0), D_{33}(I680), S_{11}(I700), D_{13}(I730), D_{15}(I650), P_{13}(I670), P_{33}(I900), хорошо согласуются с результатами других анализов.

В заключение этого раздела отметим важность дальнейшего накопления экспериментальных данных, а также проведения новых анализов, особенно в области энергий выше I,2 ГэВ.

2. Фоторождение η-мезонов

а) Асимметрия Σ в реакции фоторождения η-мезонов поляризованными фотонами $\gamma p \to \eta p$.

В Ереване[9] впервые получены экспериментальные результаты по этой асимметрии в резонансной области. Измерения проводились при E_γ=I,39; I,53; I,78 ГэВ и угле $\theta_\eta^{ц.м.}$=45°. η-мезон регистрируется системой 2-х черенковских счетчиков полного поглощения, протон отдачи - пробежной системой. Выход η-мезона для перпендикулярной и параллельной ориентаций получен путем сравнения спектров эффективных масс системы двух γ-квантов для нормальной и нарушенной кинематики (рис.4,5). На рис.6 показаны результаты Ереванской группы[9] вместе с данными, полученными недавно на ускорителе NINA[I0] при энергии фотонов E_γ=2,5; 3 ГэВ.

Если принять, что вблизи I,4 ГэВ доминирующими вкладами в амплитуду процесса $\gamma p \to \eta p$ являются вклады резонансов S_{11}(I700) (с возбуждением E_{0+}), P_{11}(I750) (возбуждение M_{1-}) и P_{13}(I860) (с основным возбуждением M_{1+}), то отличие асимметрии Σ от 0 определяет величину вклада резонанса P_{13}(I860). Полученные в[9], значения (см.рис.6) указывают на существенный вклад резонанса P_{13}(I860).

Сравнение результатов по асимметрии при энергии I,78 ГэВ ($|t| \sim 0{,}3$ (ГэВ/с)^2)[9], с данными Дарсбери при E_γ=2,5 и 3 ГэВ ($|t|$~0,2-0,4 (ГэВ/с)^2)[I0](рис.6) показывает, что амплитуда фоторождения η-мезона уже при энергии I,8 ГэВ имеет по-видимому реджевское поведение, как это предсказывалось в работе Донначи[II].

Литература

I. И.Г.Азнаурян и др., Работа 5I2/С3-55.
2. Р.О.Авакян и др., Работа 5I6/С3-5I.
3. M.Fukushima et al. Работа I236/С3-62.
4. P.Feller et al. Nucl.Phys., B104,219,1976.
5. W.J.Metcalf, R.L.Walker.Nucl.Phys.,B76,253, 1974.

6. G.Knies,R.G.Moorhouse,H.Oberlack.Phys.Rev., D9,2680,1974.
7. L.O.Abrahamian et al.Preprint EFI 71-74. Л.О.Абрамян и др. Письма ЖЭТФ, 23,415,1976.
8. L.O.Abrahamian et al.Preprint EFI-136(75).
9. Л.О.Абрамян и др., Работа 515/С3-50.
10. P.J.Bussey et al. Daresbury preprint DL/P 254, 1976.
11. A.Donnachie. Proc. 5th Int. Symposium of Electron and Photon Interaction, Cornell, 1971.

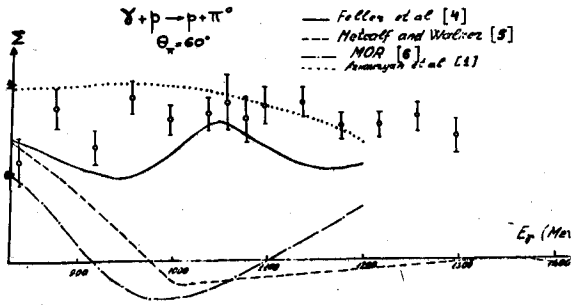


Рис. I

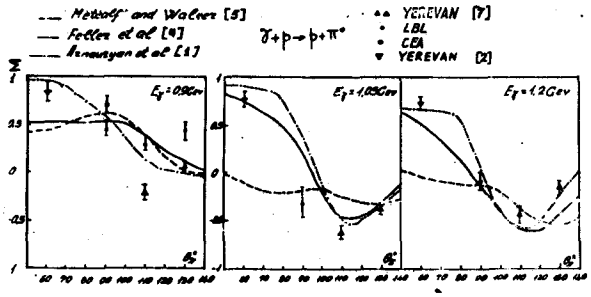


Рис. 2

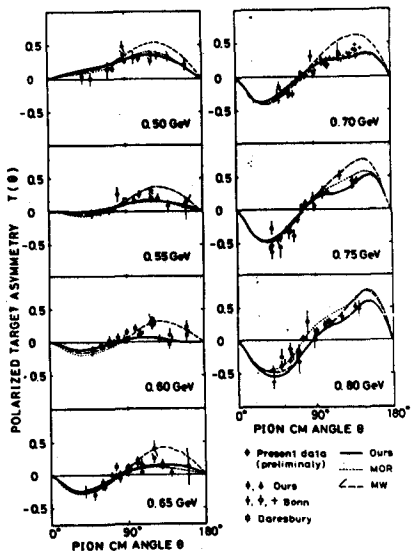


Рис. 3

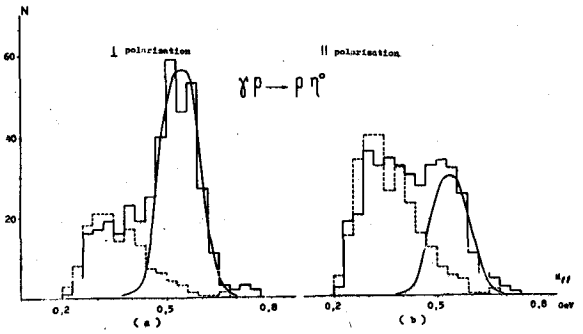


Рис. 4

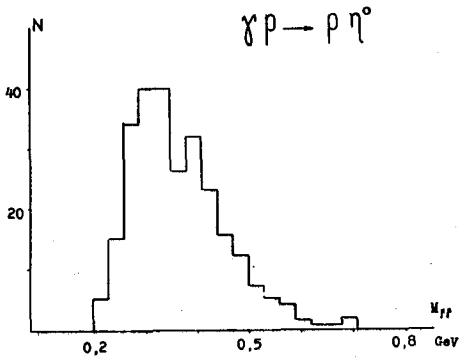


Рис. 5

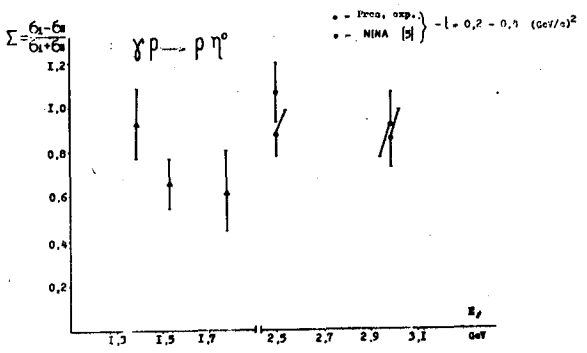


Рис. 6

Таблица

Амплитуда	Резонанс	Компоненты	Амальян	M Ф	Feller	NLR	KMD	Кварки
$/70,1^-/^2P_{1/2}$	$P_{31}(1660)$	$\Delta^3_{1/2}$	29 ± 14	105±38	-5±16	-16±17	33±15	47
$/56,2^+/^2P_{3/2}$	$P_{13}(1690)$	$\Delta^1_{1/2}$	-3 ± 6	-8±11	-9±2	27±19	-16±14	-10
		$\Delta^3_{3/2}$	79 ± 6	129±16	121±10	163±11	97±7	60
$/56,2^+/^4P_{1/2}$	$P_{31}(1850)$	$\Delta^1_{1/2}$	52 ± 16	-32±65		0±25	10±12	30
$/56,2^+/^4P_{3/2}$	$P_{33}(1880)$	$\Delta^3_{1/2}$	-8 ± 44	47±67		19±27	42±26	-20
		$\Delta^3_{3/2}$	-79±53	-88±66		78±30	-22±20	-90
$/56,0^+/^2S_{1/2}$	$S_{11}(1430)$	$\Delta^1_{1/2}$	-49±15	-70±23	-87±6	-79±12	-66±12	87
$/56,0^+/^4P_{3/2}$	$S_{33}(1640)$	$\Delta^1_{1/2}$	-105±28	0±38	0±20		5±15	34
		$\Delta^3_{3/2}$	-67±30	0±33	0±15		-34±22	20

PARALLEL SESSION ON COMPOSITE MODELS AND RELATIVISTIC BOUND STATES

MODELS OF QUARK BAGS AND THEIR CONSEQUENCES

P.N.Bogolubov
Institute for Nuclear Research of the USSR
Academy of Sciences, Moscow, USSR

The idea of the Quark Bags[1] was proposed less than in a half year after the appearance of the notion of Quarks. By means of this idea the main troubles of first naive quark models were avoided. It was realized in the works of the big group of Dubna theorists.

In this talk I would like to say about the developing of the first Dubna Quark Bag and the results obtained in this way. I shall not discuss the modern Quark Bag Theory because we have heard the beautiful talks of Weisskopf and Kuti about this matter at this conference.

In a few words the idea of the first Dubna Quark Bag is as follows: baryons are constructed of three quarks, mesons are constructed of two quarks and each quark is interpreted as a Dirac particle which moves in a scalar square well. Using this simple assumption it was shown that the quark magnetic moment depends on the bound state energy, i.e. on the effective mass of the quark rather than on the free quark mass. Hence there is no more troubles with magnetic moments of the composite particles, we recall that if one wanted to calculate these magnetic moments and inserted free quark mass (5 or more GeV) into calculations, then the quark magnetic moment is too small and one could not construct the magnetic moments of the known particles.

Further, the next trouble was connected to the quark statistics. In the quark model for baryons one must have the wave function of three quarks to be the symmetric function of the quark variables. But one can not construct symmetric wave function for three Dirac particles without introducing the new quantum number. This new quantum number which is now called colour, was introduced in the works of Dubna group[2].

By the way, from the fact that three quark wave function must be symmetric it automatically follows that all baryon states must be colour singlets and there is no more need to prove it somehow.

Consider now the so-called quasiindependent quark model[3]. It is a simple quark model based on an analogy with the shell model for nuclei. The quarks are considered as moving in an arbitrary radially-symmetric field, and their one-particle wave function satisfies the usual Dirac equation. The main results of this model are; the magnetic moments of proton

$$\mu_p = 3(1-\delta)$$

and neutron

$$\mu_N = -2(1-\delta)$$

the ratio of the coupling constants is

$$G_A/G_V = \frac{5}{3}(1-2\delta) .$$

Here, the quantity δ is the relativistic correction and it describes the contribution of the quark orbital momentum to the nucleons spin. More explicitly, it is the mean value of the quark orbital momentum Z -component, i.e.

$$\delta = \langle L_z \rangle \uparrow$$

One can calculate δ in two ways:

1. Assuming some special form of the potential, which allows the calculation of the value δ. For instance, assuming the potential to be the simple square well:

$$V(r) = -M , \quad r < r_0$$

$$V(r) = 0 , \quad r > r_0$$

After simple calculations we get $\delta = 0{,}17$. Then, for instance, $G_A/G_V = 1{,}1$; $\mu_p = 2{,}5$.

2. If we don't fix any form of the potential, then we cannot calculate δ from the Dirac equation. In this case we can get the value of δ, in particular, from the experimental data for the proton magnetic moment, $\mu_p = 2{,}79$,

then $\delta = 0{,}15$ and $G_A/G_V = 1{,}19$. Naturally, in the same manner one can get the other properties of the low-lying baryons. As it is seen such a simple-minded quark model can give us at least the same results as the modern relativistic bag model does. One can find the list of such results in paper[4].

Besides the afore-cited results there exists a possibility[5] to improve the results of the relativistic quark model with the oscillator interaction between quarks[6]. In this model there were received a number of good results concerning the decay widths of mesons and baryons. These results were obtained at the cost of using three parameters. By means of the quasiindependent quark model notions, namely considering the current matrix elements from this model, one can receive all the results of the ref.[6] using only one parameter.

At last I would like to say a few words about the mass spectrum. In the quasiindependent quark model there exists the mass spectrum for the low-lying baryons which is good whithin 10% accuracy. As regards the meson mass spectrum here I must give one short comment on the masses of the new heavy mesons.

Irrespective of the nature of this new mesons, if one makes a usual assumption that the state (3.1) is the lowest bound state of two heavy quarks, say $(C, \bar{C})$, then from the quasiindependent quark model it automatically follows that the first radial excitation in this system will have the mass (3.65) and the second excitation - (4.1). The last remark I shall say on the coincidence of the results of the MIT-Bag model and the quasiindependent quark model.

It is clear that this coincidence is due to the use of the same boundary conditions for the quark system in both models. This coincidence is absolute when one calculates some internal properties of baryons and mesons other than masses. In case of mass formulae the coincidence is inexact due to the presence in the MIT-Bag formula the term B which is absent in the quasiindependent quark model.

References

1. N.N.Bogolubov, B.V.Struminsky, A.N.Tavkhelidze. JINR, D-1968, Dubna, 1965.
2. N.N.Bogolubov et al. JINR, D-2075, P-2141, Dubna, 1965.
3. P.N.Bogolubov. Ann. Inst.Henri Poincaré, 8, 163 (1968).
4. P.N.Bogolubov. Soviet Phys.Particles and Nuclei. V.3, N 1 (1972).
5. P.N.Bogolubov. JINR, P2-6181, Dubna, 1971.
6. R.P.Feynman et al. Phys.Rev. D3, 2706 (1971).

THE BUDAPEST BAG MODEL

Julius KUTI

High Energy Physics Department
Central Research Institute for Physics, p.f.49,
Budapest 1525

This mini-rapporteur talk is a short review of our work on the Budapest bag model over the last eighteen months in collaboration with P.Gnädig, P.Hasenfratz and A.S.Szalay[1]. We have been impressed by the pioneering work of Dirac[2] on the first extended particle model of geometric variety, though our model would not exist without the ingenuity of the M.I.T. group[3] in this field. Nevertheless the Budapest bag model differs from the M.I.T. bag in some important aspects, most importantly in the description of surface dynamics for extended hadrons. Only satisfactory practical calculations can decide between the two different descriptions.

We shall assume that the physical vacuum is characterized by some microscopic structure. The normal phase of the vacuum outside hadrons cannot support the propagation of hadronic constituent fields which are identified with quarks and gluons here. In the abnormal phase of the vacuum - the hadron phase - quark and gluon fields can propagate in the usual manner. We picture the hadron as a closed domain of abnormal phase inside the normal phase of the physical vacuum. This is the bag. Inside the bag the quark and gluon fields are governed by the field equations of Quantum Chromodynamics.

The boundary surface of the bag is impenetrable against the non-Abelian vector gluon fields, since they cannot propagate in normal phase. The gluon E -fileds are tangential and the B-fields are normal to the surface in the instantaneous rest frame of the surface element. As a consequence, there is no gluon field energy or momentum flux through the surface. The field pressure associated with the impermeability of the surface against the gauge fields is balanced out by the surface energy σ per unit surface element.

We do not attempt to derive σ from some microscopic structure of the physical vacuum in gauge theories, though it did not escape our attention that the origin of surface energy may be related to instantons[4] or other vacuum phenomena[5].

Only colorless bags of finite energy can exist in the model, since the color electric flux of the gluon fields is zero across the surface. The boundary is transparent against the electromagnetic and weak interactions which can propagate in both phases of the vacuum in the normal manner.

In practical calculations we introduce the quarks as quantum mechanical point particles, only the gauge fields and the surface are treated field-theoretically in continuum fashion. There is a hint from deep inelastic scattering and hadron spectroscopy that three valence quarks dominate the nucleon with very little of additional $q\bar{q}$-pairs. It seems reasonable to conjecture that the bag with a fixed number of point-like valence quarks is perhaps a shortcut to the full quantum field theory of the model just as the two-body Bethe-Salpeter equation for positronium is a shortcut to the complete problem in quantum electrodynamics. Though pair creation is ignored at a firs stage of applications, quark fields can be introduced in our model to accomplish general field-theoretic description.

Although the field equations for quarks and gluons inside the bag are identical with those of an asymptotically free non-Abelian gauge theory, the bag approach is different. In an asymptotically free gauge theory higher order infrared quantum effects are conjectured to lead to quark confinement[6] together with an explanation for the hadronic scale. In our approach, which is more phenomenological, the finite size of the bag represents an infrared cut-off. Quark confinement exists already at the classical level, and the fundamental scale for hadrons is set

by the strength of the tension type force as described by σ.

In a four-dimensional relativistic picture the boundary of the hadron phase (bag) appears as a tube with a three-dimensional surface. The action W is written as

$$W = W_0 + W_S ,$$

where W_0 is a four-dimensional integral extended over the Minkowski space inside the tube. W_0 describes the quarks and gluons including their coupling.

Since we want W_S to lead to forces like a surface tension, we take it as a constant times the three-dimensional area of the tube swept out by the bag'surface in the four-dimensional Minkowski space:

$$W_S = -\sigma \int (\det g_{\alpha\beta})^{1/2} dx^0 dx^2 dx^3 .$$

Here $g_{\alpha\beta}$ is the induced metric on the surface, x^0 is a time-like parameter and x^2, x^3 are space-like coordinates on the surface (α, β take on the values 0,2,3). The strength of surface tension is determined by the positive constant σ of dimension (length)$^{-3}$.

The variational principle leads to the field equations of Quantum Chromodynamics inside the bag. When the non-Abelian gauge fields are varying on the boundary we get the above mentioned boundary conditions for the tangential components of the color electric fileds and for the normal components of the color magnetic fields.

Variation of the boundary yields the dynamical equation of motion for the surface

$$\frac{1}{4} F_i^{\mu\nu} F_{i\mu\nu} = 2\sigma \cdot (\text{mean curvature})$$

where a summation over the color index i of the gauge field-strength tensor is understood. The mean curvature on the right-hand side is expected from the theory of differential geometry[7]. It contains the velocity of the surface point, and its first time derivative. The equation of motion reflects that the surface moves according to the balance of gluon pressure from inside and vacuum pressure from outside.

In our model the quantized quark fields (or point quarks) are always coupled to color gauge fields. There is always a repulsive force between the quark and the surface and the boundary condition

$$q(x) = 0$$

for quark fields is a natural choice as a consequence of quark-gluon dynamics[1].

Our results are summarized as follows:

1. The surface in our model is described by independent dynamical variables and the complete Hamiltonian formulation is available.

2. We have worked out the Hamiltonian method in Coulomb gauge which is particularly useful in practical calculations.

3. The quantization of a color electric vertex is worked out in the model.

4. The model is applied to charmonium spectroscopy in adiabatic approximation.

5. The string limit for large angular momentum excitations is described.

6. The surface of the nucleon carries a significant fraction of the nucleon's momentum in our parton picture. This may be a very desirable feature of deep inelastic phenomena in the bag model.

7. Work is in progress for a detailed description of the nucleon in our bag model.

References

1. P.Gnädig, P.Hasenfratz, J.Kuti, A.S.Szalay. Paper submitted to this Conference; see also the proceedings of the Neutrino'75 IUPAP Conference Volume II, p.251, and Physics Letters B, in print.
2. P.A.M.Dirac. Proc. Roy.Soc. 268A, 57 (1962).
3. A.Chodos et al. Phys.Rev., D9, 3471 (1974).
4. A.Polyakov. Physics Letters 59B,85 (1975).
5. Physics Reports 23C, No 3 (1976).
6. See, for example, Ref.5.
7. L.P.Eisenhart. Riemannian Geometry, Princeton University Press (1949).

RELATIVISTIC EFFECTS IN THE CONSTITUENT QUARK MODEL

B.V.Struminsky

Institute of Theoretical Physics,

Ukrainian Academy of Sciences,Kiev,USSR

Considerable progress has been achieved in the classification of the hadron states and the predictions of the hadren properties in the quark model. An important and unselved problem of the quark model is: how one can take into account the relastivistic effects in a systematic way. The essential preperties ef the relativistic effects can be studied in the framework at a highly simplified medel in which the quark motion is considered in an external potential and the interactions between the quarks supposed being weak. Such a model was called the quasi-independent quarks medel.

One of the first effects discovered in this model was the enhancement of the quark magnetic moment in the scalar field /1/ . It was shown that involving the relativistic effects ene can ebtain the correct ratio g_A/g_V and find the relation between g_A/g_V and the proton magnetic moment /2/ . The similar results were also obtained in the so-called "bag" model.

In this report I consider some other quantities for which we must take into account the relativistic effects. Let us show that taking into account the relativistic motion of quarks we can obtain the relation between the decay constants for the processes $\pi \to \ell\nu$ and $\rho \to e^+e^-$ /3/ . If we consider these decays an annihilation processes of quarks at rest, we can obtain the following expressions for decay rates:

$$W(\pi\to\ell\nu)=\frac{g^2\cos^2\theta}{2\pi}|\Psi(0)|^2 m_\ell^2\left(1-\frac{m_\ell^2}{m_\pi^2}\right)^2, \quad (1)$$

$$W(\rho\to e^+e^-)=\frac{8\pi\alpha^2}{3m_\rho^2}|\Psi(0)|^2, \quad (2)$$

where $\Psi(0)$ is the value of the wave funotion in the origin of coordinates. Comparing the expressiens (1),(2) with the standard expressions for these decay rates and using SU(6) symmetry we obtain the relation between decay constants f_π and $g_{\rho\pi}$

$$g_{\rho\pi}=\frac{f_\pi m}{\sqrt{2}}. \quad (3)$$

Another relation between constants f_π and $g_{\rho\pi}$ has been obtained by current algebra methods:

$$g_{\rho\pi}=f_\pi m. \quad (4)$$

This relation is known as Kawarabayashi-Suzuki relatien and is better from the experimental point of view. Let us show that relation (4) can be obtained in the quark medel, if we take into acceunt the relativistic motion of quarks.

Let us consider bound states of quarks in the scalar petential, which we take in the form

$$V(r)=\begin{cases}0, & r>r_0,\\ -M, & r\le r_0,\end{cases} \quad (5)$$

where M is quark mass which we tend te infinity later. The solution of Dirac equatien with this potential has the form:

$$\Psi=\begin{pmatrix}\varphi\\ i\frac{\vec{\sigma}\vec{r}}{\varepsilon r}\varphi'\end{pmatrix} \quad (6)$$

where $\varphi = A r^{-1}\sin\varepsilon r$, $r\le r_0$;

$\varphi = 0$, $r>r_0$.

It is useful te separate centributiens ef upper and lower components in the normalization condition:

$$N_+=\frac{2\varepsilon r_0-1}{4(\varepsilon r_0-1)}, \quad N_-=\frac{2\varepsilon r_0-3}{4(\varepsilon r_0-1)} \quad (7)$$

The value εr_0 has been found from the spectrum equatien

$$ctg\,\varepsilon r_0=\frac{1-\varepsilon r_0}{\varepsilon r_0} \quad (8)$$

The lowest level corresponds $\varepsilon r_0 = 2.04$.

Further we calculate matrix elements of vector and axial-vector currents between the solution (6).

The expressions (1),(2) for the decay rates are replaced by the following ones:

$$W(\pi\to e\nu)=\frac{g^2\cos^2\theta}{2\pi}m_e^2\left(1-\frac{m_e^2}{m_\pi^2}\right)^2|\Psi(0)|^2(N_+-N_-)^2 \quad (9)$$

$$W(\rho\to e^+e^-)=\frac{8\pi\alpha^2}{3m_\rho^2}|\Psi(0)|^2\left(N_+-\frac{1}{3}N_-\right)^2 \quad (10)$$

From the expressions (9),(10) we find

$$\rho_{\rho\gamma}=f_\pi m\,\frac{\sqrt{2}\,\varepsilon r_0}{3} \quad (11)$$

This relation is close te Kawarabayashi-Suzuki relation. Now I shall consider SU(3) symmetry breaking. As usual, let us suppose that SU(3) symmetry breaking is caused by the mass ef strange λ quark. We choose the confining potential fer the strange quarks in the form

$$V(r)=\begin{cases}0, & r>r_0\\ -M+m, & r\le r_0\end{cases} \quad (12)$$

The solution of Dirac equation with this potential has the form

$$\Psi=N\begin{pmatrix}\dfrac{\sin r\sqrt{E^2-m^2}}{r}\,\chi\\ i\,\dfrac{(\vec\sigma\vec r)}{(E+m)r}\,\dfrac{d}{dr}\,\dfrac{\sin r\sqrt{E^2-m^2}}{r}\,\chi\end{pmatrix} \quad (13)$$

The energy spectrum is determined by the equation

$$\sqrt{\frac{E-m}{E+m}}\,\mathrm{ctg}\,r_0\sqrt{E^2-m^2}-\frac{1}{r_0(E+m)}=-1 \quad (14)$$

The magnetic moment of the strange quark is

$$\mu_s=\frac{e r_0}{6}\,\frac{4Er_0+2mr_0-3}{2(Er_0)^2-2Er_0+mr_0}\,. \quad (15)$$

The semileptonic decays with the change of strangeness in this model are described by the matrix elements of the vector and axial-vector currents between the solutions (6) and (13). The vector and axial vector constants can be expressed as follows:

$$g_V=I_++I_-=\sqrt{\frac{\varepsilon(E^2-m^2)}{2(\varepsilon r_0-1)[2E(Er_0-1)+m]}}\cdot\frac{2m}{E^2-\varepsilon^2-m^2} \quad (16)$$

$$g_A=I_+-\frac{1}{3}I_-=\sqrt{\frac{\varepsilon(E^2-m^2)}{2(\varepsilon r_0-1)[2E(Er_0-1)+m]}}\cdot\frac{4(E-\varepsilon)+2m}{3[E^2-\varepsilon^2-m^2]} \quad (17)$$

Differentiating (16) we obtain $\frac{dg_A}{dm}|_{m=0}=0$ that means that vector constant is different from 1 only in the second order in the symmetry breaking parameter m . It is analog of the Ademollo-Gatto theorem. Now I give some numerical results. The effective mass of p , n quarks is $m_N/3$. From this we can find the well radius r_0 . From the eq. (11) we find $\frac{1}{3}m_N r_0=2.04$. The effective mass of the λ quark we determine from the Λ hyperons mass $E=m_\Lambda-\frac{2}{3}m_N=488$ MeV, $Er_0=3.18$. From the equation (17) we find $mr_0=1.85$, $m=284$ MeV. The magnetic moment of the Λ hyperen in the quark model is equal to the magnetic moment of the λ quark. The expression (20) gives us $\mu_\Lambda=-e/2M_N\cdot 0.58$ (experimental value is 0.67 ± 0.06).

The analogous results are valid for another potentials. We have considered the potential $V(r)=im\omega\vec r\vec\alpha$ where $\vec\alpha$ is known Dirac matrices. This potential is one of the few potentials for which the Dirac equation is solved exactly. An interesting property of this potential is that it leads to the linear Regge trajectories. The axial-vector constant for the quark

$$g_A=\frac{E+2m}{3E} \quad (18)$$

where $E=\sqrt{m^2+6m\omega}$ is the energy of the bound state. The axial-vector constant for the neutron β-decay is $g_A=\frac{5}{3}g_A$. From the experiment $g_A=1.18$ and we find $\frac{m}{E}=0.562$ The Kawarabayashi-Suzuki relation in this model

$$g_{\rho\gamma} = f_\pi \bar{m}\, \frac{E+2m}{3\sqrt{2}\,m} = 0.89\, f_\pi \bar{m} \qquad (20)$$

The SU(3) symmetry breaking can be introduced through the λ quark mass $m = m + \Delta$ If we demand that the Regge trajectories for strange particle have the same slope as for unstrange ones, it is necessary to impose. the condition

$$mw = (m+\Delta)\Delta$$

By a simple caloulation we can verify that the vector constant is different from 1 only in the second order in Δ .

Another approach to describing the relativistic effects in the quark model was proposed by Melosh, who introduced the transformation between constituent and current quarks. Unfortunately, the explicit form of the transformation was found only in the model of free quarks. But it is easy to see that not only the explicit form of the transformation between the current and the constituent quarks, but also its algebraic structure depends on the dynamics of quark interactions.

References

1. N.N.Bogolubov, B.V.Struminsky, A.N. Tavkhelidze. Preprint JINR D-1968, 1965.
2. P.N.Bogolubov. Ann.Inst.Henri Poincare, 8, 163 (1968).
3. B.V.Struminsky. Preprint ITP-68-48, Kiev, 1968.
4. A.P.Kobushkin, B.V.Struminsky. Preprint ITP-75-102E, UFJ, v.21, No.4, 640 (1976).

RADIAL EXCITED MESONS IN THE M.I.T. BAG MODEL

I.Yu.Kobsarev, V.Yu.Matv'ev, M.G.Schepkin
ITEP, Moscow, USSR

The M.I.T. bag model /1-4/ describes rather successfully statical properties of light hadrons. The hadrons are described as a system of quarks, $q\bar{q}$ or qqq , confined inside a finite region of space. The quarks are supposed to be in a ground state, which corresponds to the lowest value of radial quantum number. The SU(3) x SU(3) scheme (3 quarks + color) is assumed to be valid in the first approximation, the physical particles being singlets under SU(3)' - transformations. The SU(3) x SU(3)' symmetry is assumed to be broken by nonzero mass of strange quark.

We present here the results of calculations of the masses of the radial excited mesons. Since the detailed description of the model is given in /1-4/ , we shall list here only the main assumptions of the model.

1) Quarks interact with colored, massless gauge vector gluons.

2) Quark confinement is provided by the requirement that quark current vanishes on the surface of the bag.

3) The colored gluon field is also assumed to be confined inside the bag. The main part of its energy is proportional to the bag volume $V = 4/3\,\pi R^3$. There is also a correction proportional to I/R. So the energy E_B , contained in the bag is equal to $E_B = B \cdot V - Z/R$

4) The masses of u,d. quarks are put equal to zero, $m_u = m_d = 0$. The fit to the experimental data gives for s-quark the mass about 300 MeV.

5) There exists some residual interaction between quarks due to quark - gluon coupling. The properties of this interaction will be discussed below.

It follows from assumptions 1)-5), that a meson is three-body object, the third body being the bag itself. As it was pointed by L.B. Okun and A.I.Vainshtein /5/ this means, that

there must exist a lot of excited states of different nature. We shall describe here only spherically symmetric ground and radial excited states. Radial excitations of ρ-type and their masses in the "naive" bag where $m_u = m_d = m_s = 0$, $Z_0 = 0$ and no residual quark interaction is taken into account were discussed in [6,7].

To describe all known hadrons one should take into account mass - splittings between states with different spins and SU(3)-symmetry breaking. The first is provided by spin-dependent short-range forces due to the one-gluon exchange diagram.

To illustrate the properties of the model we shall write here the symmetric wave function of the massless quark inside the bag

$$\Psi = \frac{N}{\sqrt{4\pi}} \begin{pmatrix} i \dfrac{\sin(\varepsilon r)}{\varepsilon r}\, \varphi \\ \dfrac{1}{\varepsilon r}\left[\cos(\varepsilon r) - \dfrac{\sin \varepsilon r}{\varepsilon r}\right](\vec{\sigma}\cdot\vec{n})\varphi \end{pmatrix} \qquad (1)$$

$$N = \left[\varepsilon^3 / 2(x-1)\sin^2 x\right]^{1/2}$$

for $K=-1$ and

$$\Psi = \frac{N'}{\sqrt{4\pi}} \begin{pmatrix} -\dfrac{i}{\varepsilon r}\left[\cos(\varepsilon r) - \dfrac{\sin(\varepsilon r)}{\varepsilon r}\right](\vec{\sigma}\cdot\vec{n})\varphi \\ \dfrac{\sin(\varepsilon r)}{\varepsilon r}\, \varphi \end{pmatrix} \qquad (2)$$

$$N' = \left[\varepsilon^3 / 2(x+1)\sin^2 x\right]^{1/2}$$

for $K=+1$, where $K = \pm(j+1/2) = \pm 1$ corresponds to the solutions with different parity; $\varepsilon = x/R$ is the energy of the quark, and R is the radius of the bag.

Boundary condition for the quark current to vanish on the surface of the bag leads to the equation:

$$\tan x = x/(1+Kx), \quad K = \pm 1. \qquad (3)$$

Positive roots of this equation characterize different radial excited states of quarks inside the bag. Hadronic mass can be expressed in the following form:

$$M = \sum_{i=1}^{N_q} \frac{x_i}{R} + \frac{4}{3}\pi B R^3 - \frac{Z_0}{R} + \frac{g^2}{4\pi}\frac{C}{R} \qquad (4)$$

N_q is the number of quarks. The first term in this expression is the energy of quarks, the second and third describe the energy of the bag, and the last one arises from the "magnetic" moments interaction [3,4]. Minimizing expression (4) upon R one obtains:

$$M = \frac{4}{3}(4\pi B)^{1/4}\left(\sum_{i=1}^{N_q} x_i - Z_0 + \frac{g^2}{4\pi}C\right)^{3/4} \qquad (5)$$

These simple formulas are valid for massless quarks. Similar expressions for general case are more complicated and given in [4].

We shall discuss now correction to the hadronic mass, which comes from "magnetic" moments interaction. Concerning this point our assumptions are different from those adopted in the M.I.T. bag model. In particular, we assume, that the long-range interaction due to gluon exchange gives corresponding contribution to the bag energy and is included in constant B. Short-range forces, violating SU(6)-symmetry, can be obtained from one-gluon exchange diagram. This is provided by asymptotic freedom of the theory, which makes it possible to use perturbative approach at small distances. The effective potential $\hat{V}$, corresponding to the first-order diagram, depends on quarks positions $\vec{r}_1$ and $\vec{r}_2$, momentum operators $\vec{p}_{1,2} = -i\dfrac{\partial}{\partial \vec{r}_{1,2}} = -i\vec{\nabla}_{1,2}$ spin and color variables. The correction to the hadronic mass is

$$\Delta M = \frac{g^2}{4\pi}\sum_{i\neq k}\int d\vec{r}_i\, d\vec{r}_k\, \Psi^+(\vec{r}_i,\vec{r}_k)\,\hat{V}\,\Psi(\vec{r}_i,\vec{r}_k). \qquad (6)$$

As we are interested now in the contribution of the short-range part of $\hat{V}$, we should integrate in (6) only over the region, where $|\vec{r}_1 - \vec{r}_2| < r$ being small with respect to the radius of the bag, $r \ll R$. Perturbation theory is supposed to be applicable in this

region. As in the model no parameters of the dimension of length besides R are known we shall take into account only those terms in $\hat{V}$, which survive when z is put equal to zero. If such assumption is made, then the effective potential is

$$\hat{V} = -\frac{8\pi}{3}\frac{\delta(\vec{r}_i-\vec{r}_k)}{\varepsilon_i\varepsilon_k}(\vec{\sigma}_i\vec{\sigma}_k-3/2)\vec{\lambda}_i\vec{\lambda}_k \qquad (7)$$

$$+\frac{4\pi}{3}\frac{\delta(\vec{r}_i-\vec{r}_k)}{\varepsilon_i^2\varepsilon_k^2}\left[(\vec{\sigma}_i\vec{p}_k)(\vec{\sigma}_k\vec{p}_i)-\right.$$

$$\left.-(\vec{\sigma}_i\vec{\sigma}_k)(\vec{p}_i\vec{p}_k)+(\vec{p}_i\vec{p}_k)\right]\vec{\lambda}_i\vec{\lambda}_k$$

After integration one obtains:

$$\Delta M = -\frac{g^2}{4\pi}\sum_{i\neq k}(\vec{\sigma}_i\vec{\sigma}_k-3/2)\vec{\lambda}_i\vec{\lambda}_k\frac{I_{ik}}{R} \qquad (8)$$

For massless quarks $I_{ik} = 0.1717$.

The masses of light hadrons, calculated in the framework of this assumptions, are presented in the Table I.

Table I

Baryons (masses in GeV)

Particle	Σ	Λ	Ξ	Σ^*	Ξ^*
Model predictions	1.191	1.122	1.337	1.383	1.530
Experiment	1.192	1.116	1.320	1.385	1.530

Mesons (masses in GeV)

Particle	π	K	K^*	ϕ
Model predictions	0.264	0.567	0.919	1.06
Experiment	0.140	0.494	0.890	1.020

$B^{1/4} = 0.169$ GeV, $m_s = 0.239$ GeV, $g^2/4\pi = 0.230$, $Z_0 = 1.651$

The masses of ρ, p, Δ and Ω were used to determine model parameters. Notice that the model predicts rather good value for Σ-Λ mass difference.

Let us discuss now the radial excited mesons. We use the following notation to fix radial quantum numbers of q and $\bar{q}$: $(n_q, n_{\bar{q}}, K)$, $K = "+"$ or $"-"$. Then the ground state is (1,1,-). Considering the first radial excitation one realizes, that there are three states with approximately equal masses. They are (1,2,-), (2,1,-) and (1,1+). One gluon exchange provides transitions between them, the effective potential responsible for these transitions having the following form:

$$V = -\frac{4\pi}{3}\frac{\delta(\vec{r}_i-\vec{r}_k)}{\varepsilon_i\varepsilon_k}\vec{\sigma}_i\vec{\sigma}_k\vec{\lambda}_i\vec{\lambda}_k +$$

$$+\frac{8\pi}{3}\frac{\delta(\vec{r}_i-\vec{r}_k)}{\varepsilon_i^2\varepsilon_k^2}\left[(\vec{p}_i\vec{p}_k)+(\vec{\sigma}_i\vec{p}_k)(\vec{\sigma}_k\vec{p}_i)\right. \qquad (9)$$

$$\left.-(\sigma_i\sigma_k)(\vec{p}_i\vec{p}_k)-\frac{3}{2}(\vec{\sigma}_i\vec{p}_i)(\vec{\sigma}_k\vec{p}_k)\right]\vec{\lambda}_i\vec{\lambda}_k$$

If the wave functions of states (1,2,-), (2,1,-), (1,1,+) are φ_1, φ_2, φ_3, respectively, then the wave functions of the diagonal states are

$$\psi_1 = \frac{\alpha}{\sqrt{2}}(\varphi_1+\varphi_2)+\beta\varphi_3,\ \psi_2 = \frac{\gamma}{\sqrt{2}}(\varphi_1+\varphi_2)+\delta\varphi_3 \qquad (10)$$

$$\psi_3 = \frac{(\varphi_1-\varphi_2)}{\sqrt{2}};\ \alpha^2+\beta^2=\gamma^2+\delta^2=1$$

For the nonstrange mesons $q\bar{q}$ and $s\bar{s}$ two of these states, namely ψ_1 and ψ_2 have the same quantum numbers $I^G(J^P)C$ as the ground state, and ψ_3 possesses opposite C and G parity. The masses of the first radial excited states are listed in Table 2.

Table 3 contains the model predictions for the masses of the first radial excited strange mesons.

Among experimentally observed particles there are only two which can be identified as radial excitation in light mesons. They are $\rho'(1250)$ and $\rho'(1600)$ with quantum numbers $I^G(J^P)C = 1^+(1^-)-$. The model predicts two particles with masses 1550 MeV and 1610 MeV (see Table 2) with quantum numbers $1^+(1^-)-$, which corresponds to the first radial excitation of ρ-type.

Table 2

Nonstrange mesons (masses in GeV)

Particle \ Wave function	Ψ_1	Ψ_2	Ψ_3
$(q\bar{q})_{J=1} = \rho$	1.623	1.572	1.578
$(q\bar{q})_{J=0} = \pi$	1.484	1.289	1.578
$(s\bar{s})_{J=1} = \phi$	1.753	1.710	1.765
$(s\bar{s})_{J=0}$	1.653	1.522	1.765

Table 3

Strange mesons (masses in GeV)

$(q\bar{s})_{J=0} = K$	1.560	1.417	1.66
$(q\bar{s})_{J=1} = K^*$	1.670	1.637	1.67

So there is no place for $\rho'(1250)$ in the bag model proposed here, as distinct from the "naive" bag model which had been used in /7/ . However, the existence of $\rho'(1250)$ is not firmly established and needs further experimental check.

References

1. A.Chodos, R.L.Jaffe, K.Johnson, C.B.Thorn, V.F.Weisskopf. Phys.Rev., D9, 3471, 1974.
2. A.Chodos, R.L.Jaffe, K.Johnson, C.B.Thorn. Phys.Rev., D10, 2599, 1974.
3. V.F.Weisskopf. Preprint CERN, TH. 2068, 1975.
4. T. DeGrand, R.L.Jaffe, K.Johnson, J.Kiskis. Phys.Rev., D12, 2060, 1975.
5. A.I.Vainshtein, L.B.Okun. Yadern.Fiz., 23, 1347, 1976.
6. P.Vinciarelli. Preprint CERN, TH. 1981, 1975.
7. I.Yu.Kobzarev, V.Yu.Mat'ev, A.S.Rubinov, M.G.Schepkin. Yadern.Fiz., 23, 1348, 1976.

THE POTENTIAL AND QUASIPOTENTIAL MODELS FOR BOUND QUARKS

R.M.Mir-Kasimov

Joint Institute for Nuclear Research, Dubna

The idea that quarks "inside" the hadrons are bounded by a simple potential is as old as the idea about quarks themselves. It is based on simple and conventional physical concepts and is attractive to many physicists. This viewpoint was first used by N.N.Bogolubov et al./1,2/.

The disoovery of new particles and their interpretation as bound states of the charmed quarks/3/ stimulated the creation of a "new wave" of papers, in which different simple potentials describing the interaction between quarks are used. The most popular is the linear potential

$$V = gr - V_0 \qquad (1)$$

where r is a relative distance between quarks.

This potential is suggested by gauge theories of quark confinement and by exact soluble models in the 2-dimensional quantum electrodynamics.

The spectroscopy which arises here is in satisfactory agreement with the experimental data on the mesonic (and baryonic) masses. Of course, all such models are the only first approximation to the real picture. The consistent solution of this problem should comprise both the quantum effects and all other attributes of the interaction of quarks.

The main part of this talk is devoted to the application of the quasipotential (q.p.) approach/4/. It is connected directly with quantum field theory and it is strictly relativistic. In fact, we shall employ the version of the q.p. approach given by Kadyshevsky/5/. But before passing to the q.p. analysis of hadronic spectra we should mention the papers devoted to investigation of this spectra on the basis of linear and other simple potentials/6/.

The q.p. equations for the wave function and the scattering amplitude given in [5] are absolute with respect to the geometry of the momentum space and could be obtained from the non-relativistic Schroedinger and Lippmann-Schwinger equations by changing the non-relativistic (Euclidean) expressions for energy, volume element, etc., by their relativistic (non-Euclidean) analogs. This fact allows us to pass to the relativistic r-representation using the expansion over matrix elements of the unitary irreducible representations of the Lorentz group [7]. The kernel of this relativistic Fourier transformation has the form[x]

$$\xi(\vec{q},\vec{r}) = (ch\chi_q - (\vec{n}\cdot\vec{n}_q)sh\chi_q)^{-1-ir} \qquad (2)$$

$\vec{r}=r\cdot\vec{n}$, $\vec{q}=\vec{n}_q\cdot q$ (the relative momentum of quarks in the c.m.s.) $\vec{n}^2=\vec{n}_q^2=1$. Here r is the eigenvalue of the Casimir operator of the Lorentz group $(0<r<\infty)$.

In the nonrelativistic limit

$$\xi(\vec{q},\vec{r}) \to e^{i\vec{q}\vec{r}} \qquad (3)$$

where $\vec{r}$ is a usual 3-vector.

The equation for the relativistic wave function $\Psi_q(\vec{r})$ in $\vec{r}$ representation is the finite-difference equation

$$[H_0 - 2E_q + V(\vec{r},E_q)]\Psi_q(\vec{r}) = 0 \qquad (4)$$

where $V(\vec{r},E_q)$ is the quasipotential and H_0 has the form

$$H_0 = 2chi\frac{\partial}{\partial r} + \frac{2i}{r}sh\,i\frac{\partial}{\partial r} - \frac{\Delta_{\vartheta,\varphi}}{r^2}e^{i\frac{\partial}{\partial r}}. \qquad (5)$$

This equation was successfully applied to the analysis of the $c\bar{c}$ system (ψ-particle) in the case of linear potential in paper [8]. The supplementary series of the Lorentz group representation was used in [9].

There is a number of difficulties connected with the finite-difference character of the q.p. equation. The main of them is the problem of boundary conditions.

We suggest a version of q.p. equation which corresponds to the second order differential equation in $\vec{r}$-representation [10]. We write the denominator in the Lippman-Schwinger equation in the form

$$\frac{1}{E_q - E_k + i\varepsilon} = \frac{1}{\frac{s^2(q,0)}{2} - \frac{s^2(k,0)}{2} + i\varepsilon} \qquad (6)$$

where $s(q,0)$ is the Euclidean distance between the point $\vec{q}$ and the origin in the flat non-relativistic momentum space. Passing now to the relativistic q.p. equation we must change

$$s(q,0) = \sqrt{\vec{q}^2} \to \chi_q = \ln\left(E_q + \sqrt{E_q^2 - 1}\right) \qquad (7)$$

where χ_q is the distance in the Lobachevsky momentum space, or rapidity.

The q.p. equation is

$$A(\vec{p},\vec{q}) = -\frac{1}{4\pi}V(\vec{p},\vec{q};E_q) + \frac{1}{2\pi}\frac{\chi_q}{sh\chi_q}\int\frac{V(\vec{p},\vec{k})\,d\Omega_k\,A(\vec{k},\vec{q})}{\chi_q^2 - \chi_k^2 + i\varepsilon} \qquad (8)$$

The equation for the radial wave function in $\vec{r}$-representation is

$$\left[\frac{d^2}{dr^2} + \chi_q^2 - R_\ell(r,\chi_q) + V(r,\chi_q)\right]\varphi_{q\ell}(r) = 0 \qquad (9)$$

where $R_\ell(r,\chi_q)$ is a specific centrifugal term [10] which in the non-relativistic limit goes over to the usual one

$$R_\ell(r,\chi_q) \to \frac{\ell(\ell+1)}{r^2} \qquad (10)$$

$$R_0 = 0. \qquad (11)$$

For linear potential (1) and $\ell=0$ the solution is the Airy function:

$$\varphi_{n0}(r) = \left(\frac{g\chi_n}{sh\chi_n}\right)Ai\left[\left(\frac{g\chi_n}{sh\chi_n}\right)^{1/3}\left(r - \frac{V_0}{g} - \frac{\chi_n sh\chi_n}{g}\right)\right] \qquad (12)$$

n is the principal quantum number. The spectrum of rapidities is given by the condition $\varphi_n(0)=0$, i.e., by zeros of Airy function. For $\ell\neq 0$ we have no analytic solutions.

Using the lowest mesonic masses and leptonic width (the colour is taken into account) as an input parameter, we made the computer calculations of radial and orbital excitations in $p\bar{p}$, $h\bar{h}$, $\lambda\bar{\lambda}$ and $c\bar{c}$ systems. The results are in good agreement with the data on mesonic spectroscopy [10]. For example the first radial excitations in the $c\bar{c}$ system take the following values:

$3.09 \sim \psi(3.095)$; $3.68 \sim \psi'(3.68)$;
$4.16 \sim \psi''(4.15)$; $4.57 \sim \psi'''(4.41)$.

The detailed results of computations are presented in [10].

We investigated also the case of extremely heavy quarks, which is suggested by the field-

[x] In what follows we consider the system $q\bar{q}$ i.e., the system of particles with equal masses. We employ the system of units in which $\hbar=m=c=1$, where m is the mass of quark.

theoretical scheme in which the momenta of quanta off the mass shell belong to the de-Sitter space[11-13]:

$$\frac{1}{\ell_0^2} p_4^2 + p_0^2 - \vec{p}^2 = \frac{1}{\ell_0^2} \qquad (13)$$

Following paper[14] we identify ℓ_0 with the length scale arising in the weak interaction theory:

$$\ell_0 = \sqrt{\frac{G_F}{\hbar c}} \cong 6 \cdot 10^{-4} \text{ fm}$$
$$M = \frac{\hbar}{\ell_0 c} \cong 300 \text{ Gev} \qquad (14)$$

The quanta with the mass M (the maximons), play in the theory with the de-Sitter momentum space the principal role[x].

The attractive idea is to identify the quark with maximon. In such a case these particles, originating due to the properties of the geometry of the momentum space, are at the same time the fundamental constituents of hadrons.

We consider the model of Ψ-mesons represented as the bound states of the quarks C and $\bar{C}$ with mass M. With slight modifications of the arguments of ref.[12] we obtain the q.p. equation which does not differ in form from (9), but includes the rapidity χ_q of another geometrical nature:

$$q_4 = Mc \operatorname{ch} \chi_q \qquad (15)$$

The masses μ of all known resonances are much smaller than M, that is $\chi_q \cong i\frac{\pi}{2}$ for low-laying excitations. It is easy to see that $V_0 \cong \frac{\pi}{2} M$, and the absolute value $2|\vec{p}|$ of the relative momentum equals

$$2|\vec{p}| \cong 2Mc \left(\mu/M\right)^2 \qquad (16)$$

within the accuracy $(\mu/M)^2$. Thus, the quarks motion has the relativistic character in this case.

Taking masses of Ψ (3.095) and Ψ' (3.686) as input parameters we obtain in this case also the higher excitations in the $C\bar{C}$ system, which could be identified with known Ψ'' (4.15) and Ψ''' (4.40) states.

The knowledge of the relativistic bound state wave function permits one to obtain further information about its structure. For example, the computation of the values of mean-square radius $\langle r^2 \rangle^{1/2}$ of the composite system $\Psi(c\bar{c})$ yields

$$\langle r^2 \rangle^{1/2} \cong 0.05 \text{ fm} \qquad (17)$$

It is remarkable that uncertainty relation in the relativistic $\vec{r}$-space[x]

$$\langle r^2 \rangle^{1/2} \langle \Delta\chi \rangle \cong \ell_0 \qquad (18)$$

results in the correct estimate for $\langle r^2 \rangle^{1/2}$.

It follows from (16) that the mean value of rapidity equals $i\pi/2$ within accurate of $(\mu/M)^2$. Hence

$$\mu/M = \operatorname{ch} i\left(\pi/2 - \Delta\chi\right) = \sin \Delta\chi \cong \Delta\chi \qquad (19)$$

Substituting (19) into (18) we obtain the estimation

$$\langle r^2 \rangle^{1/2} \cong \ell_0 \frac{M}{\mu} \cong 0.06 \qquad (20)$$

References

1. N.N.Bogolubov, B.V.Struminsky, A.N.Tavkhelidze. JINR Preprints D-1968, Dubna, 1965; P-2141, Dubna, 1965.
2. P.N.Bogolubov. Ann.Ins.Henri Poincare, VIII, 2 (1968).
3. T.Appelquist. H.D.Politzer. Phys.Rev.Lett., 34, 43 (1975).
   A. De Rujula and S.L.Glashow. ibid., 34, 46 (1975).
4. A.A.Logunov and A.N.Tavkhelidze. Nuovo Cimento, 29, 380 (1963).
5. V.G.Kadyshevsky. Nucl.Phys., B6, 125 (1968).
   V.G.Kadyshevsky and M.D.Mateev. Nuovo Cimento, 55A, 275 (1967).
6. B.J.Harrington, S.Y.Park, A.Yildiz. Phys.Rev.Lett., 34, 168 and 706 (1975).
   J.Kogut, L.Susskind. Phys.Rev.Lett., 34, 767 (1975).
   T.P.Chen and P.B.James. Phys.Rev.Lett., 34, 917 (1975).
   E.Eichten et al. Phys.Rev.Lett., 36, 369 (1975).
   J.F.Gunion and R.S.Willey.Phys.Rev., D12, 174 (1975).

[x] The mass M is the limiting mass of the virtual quanta[11-13]. The term "maximon" is taken from paper[15].

[x] The rapidity χ and the relativistic relative distance r are canonically conjugated in the sense of the relativistic Fourier transformation[7]. This relation is essentially used in the relativistic scheme describing the data on high energy hadron-hadron scattering[16].

J.S.Kang and H.J.Schnitzer. Phys.Rev., D12, 841 and 2791 (1975).
R.Barbieri, R.Kögerler, Z.Kunst and R.Gatto. CERN Preprint TH-2036 (1975).
J.F.Gunion and L.F.Li. Phys.Rev., D12, 3583 (1975); Phys.Rev., D12, 82 (1976).
7. V.G.Kadyshevsky, R.M.Mir-Kasimov, N.B.Skachkov. Nuovo Cim., 55A, 233 (1968).
8. K.S.Jhung, K.H.Chung and R.S.Willey. Phys. Rev., D12, 1999 (1975).
9. N.B.Skachkov. Sovjet Physics JETP, 23, 713, 1976.
10. I.V.Amirkhanov, G.V.Grusha and R.M.Mir-Kasimov. Dubna Preprints, E2-9767 and E2-9868 (See papers submitted to this Conference).
11. V.G.Kadyshevsky. In "Problems of Theoretical Physics", a memorial volume dedicated to memory of I.E.Tamm, Nauka, Moscow, 1972.
12. A.D.Donkov, V.G.Kadyshevsky, M.D.Mateev, R.M.Mir-Kasimov. In Proc. of the Int. Conf. on Nonlocal Quantum Field Theory, D2-9788, Dubna, 1975. (In this review the more complete list of refs. on this topic is presented).
13. V.G.Kadyshevsky. Talk presented to this conference.
14. V.G.Kadyshevsky. Dokl. Akad.Nauk SSSR, 136, 70 (1961).
15. M.A.Markov. Suppl. of Progress of Theor. Phys., Commemoration Issue for 30-th anniversary of meson theory by Dr. H.Yukawa, p. 85, 1965.
16. S.Cht.Mavrodiev. JINR Communications, E2-7910, Dubna, 1974; P2-8897, Dubna, 1975.

NULL-PLANE QUANTIZATION AND QUASIPOTENTIAL EQUATION FOR COMPOSITE PARTICLES

A.A.Khelashvili

Department of Physics, Tbilisi State University, Tbilisi, USSR

Methods of investigation of relativistic bound systems are known from the time of creation of quantum field theory. At present, (as always, of course) the problem is to develop more simpler and economical ways for dealing with bound states.

We are inclined to think that the null-plane /1/ quantum field theory is to be more adapted to the problems under consideration because, if we eliminate the $p^+ = 0$ modes, null-plane canonical commutation relations have simplest, Fock, representation even in the presence of interaction /2/ . Bound state wave functions at the equal $\tau = x^0 + x^3$ "times" for constituents are maximally close to nonrelativistic expressions without the transition to the infinite momentum frame /3,4/.

Bound state problem for two spinless particles on the one null-plane was considered in /5/ using Tamm-Dancoff approximation and in /6/ - on the basis of DGS spectral representation.

From our point of view, the most successive approach to the bound state problem in relativistic quantum field theory is a quasipotential method /7/ . Equal-time quasipotential method had been successfully applied in many investigations /8/ . Null-plane quasipotential equation was considered in papers /9/ for spinless particles and in /10,11/ - for spinorial particles.

In this report we shall discuss the main features of null-plane quasipotential approach and give an application to the asymptotic behaviour of composite particle form factors at large $\vec{p}_\perp$.

Taking into account that the $p^+=0$ modes may be eliminated /12/ from the Fock-space with the help of second class constraints /13/ it

is possible to prove /14/ the formal equivalence of S-matrix in null-plane and ordinary covariant field theories.

For the illustration of quasipotential method let us consider first the sector $a^+b^+|0\rangle$ of the Fock-space which consists of one quark and one antiquark. In coordinate space the meson wave function with momentum P and helicity h has the form /15,16/

$$\langle 0|q_+^\beta(y)\,q_+^\alpha(x)|P,h\rangle = e^{-\frac{i}{2}P(x+y)}\,\psi_+^{\alpha\beta}(z,P,h)\Big|_{z=x-y,\ z^+=0} \quad (1)$$

The module of this wave function is related to the probability for finding quark and antiquark inside the meson. Definning the covariant wave function

$$\langle 0|\bar q^\beta(y)\,q^\alpha(x)|P,h\rangle = e^{-\frac{i}{2}P(x+y)}\,\psi^{\alpha\beta}(z,P,h) \quad (2)$$

we have

$$\psi_+(z,P,h) = \Gamma_+\,\psi(z,P,h)\,\gamma^0\Gamma_+,\quad \Gamma_+ = \frac{1}{2}(1+\alpha_3) \quad (3)$$

Wave functions $\psi^{\alpha\beta}(z)$ may be connected apparently with very important characteristics such as the bilocal current matrix elements, weak and electromagnetic decay constants , etc. It is evident that in composite quark model these wave functions contain full dynamical information on the hadron structure, hence it is much desirable to have for them dynamical equations.

In the case of null-plane quantization the start point is the null-plane Bethe-Salpeter (BS) amplitude

$$\chi_{P,h}(x,y) = \langle 0|T_+(\bar q(x)\,q(y))|P,h\rangle$$

Since the anticommutators of "good" operators q_+ and q_+^+ are C-numbers the projected BS amplitude, $\Gamma_+\chi_{P,h}(x,y)\gamma_0\Gamma_+\big|_{x^+=y^+}$ coincides with Tamm-Dankoff wave function.

This formalism can be generalized to the arbitrary numbers of constituents and to the full operators /10,11/ . We shall give the main results underlining the advantages of general quasipotential approach in null-plane QFT. Let the hadron consists out of the N pointlike spinorial particles with 4-momenta $p_1, p_2, \dots, p_N$. Let $P=\sum_{i=1}^N p_i$, $p_i^+ = x_i P^+$, $\sum_{i=1}^N x_i = 1$, $0<x_i<1$ (as the spectrum of P^+ generator is positive-defined).

We introduce a momentum-space quasipotential wave function $\psi_{P\alpha}$ /9-11/

$$(P^+)^{N-1}\prod_{i=1}^N x_i^{-1}\psi_{P\alpha}(\{x_i,p_{i\perp}\}) = \int_{-\infty}^{\infty}\prod_{i=1}^N dp_i^-\,\delta\Big(P^- - \sum_{i=1}^N p_i^-\Big)\chi_{P\alpha} \quad (4)$$

This wave function satisfies the equation /10,11/

$$\Big(P^2 - \sum_{i=1}^N \frac{(\vec p_{i\perp} - x_i\vec P_\perp)^2 + m_i^2}{x_i}\Big)\prod_{i=1}^N\otimes(\bar p_i + m_i)\,\psi_{P\alpha}(\{x_i,\vec p_{i\perp}\})$$
$$= \int\prod_{i=1}^N d\vec p_{i\perp}'\,\delta^{(2)}\Big(\vec P_\perp - \sum_{i=1}^N \vec p_{i\perp}'\Big)\int_0^1\prod_{i=1}^N\frac{dx_i'}{x_i'}\,\delta\Big(1-\sum_{i=1}^N x_i'\Big)\cdot$$
$$\cdot\prod_{i=1}^N\otimes(\bar p_i' + m)\,V_P\big(\{x_i,\vec p_{i\perp}\},\{x_i',p_{i\perp}'\}\big)\cdot$$
$$\cdot\prod_{i=1}^N\otimes(\bar p_i' + m_i)\,\psi_{P\alpha}(\{x_i',p_{i\perp}'\}) \quad (5)$$

Here V_P is a quasipotential matrix defined according to the known recept /10,11/ with the aid of T-matrix , and $\bar P = (P^+, P_\perp, (\vec P_\perp^{\,2}+m^2)/P^+)$. We can easily reconstruct an eq. (5) to Faddeev form in the case of $N \geq 3$ /11/ .

The main features of eq. (5) are: maximal proximity to nonrelativistic expressions, invariance under the group isomorphic to the Galilean one, similarity to the quark-parton picture. On the other hand no reference frame is fixed and no approximation is made, i.e., full information of relativistic QFT is preserved. For these reasons our formalism may be successfully applied in any multiparticle problems. Quasipotential equation on the null-plane had been applied in studying of composite particle scattering /17/ , inclusive processes /18/ as well as in composite particle form factors /19/ at large transverse momenta.

Composite particle form factors are defined by the matrix elements of local operator (current) /9-11/

$$\langle p'\alpha' | J_n(0) | p\alpha \rangle = \int \prod_{i=1}^{N} d^2 p_{i\perp}' \, \delta^{(2)}\Big(\vec{p}_\perp' - \sum_{i=1}^{N} \vec{p}_{i\perp}'\Big) \cdot \int_0^1 \prod_{i=1}^{N} \frac{dx_i'}{x_i} \, \delta\Big(1 - \sum_{i=1}^{N} x_i'\Big) \int \prod_{i=1}^{N} d^2 p_{i\perp} \, \delta^{(2)}\Big(\vec{p}_\perp - \sum_{i=1}^{N} \vec{p}_{i\perp}\Big)$$

$$\int_0^1 \prod_{i=1}^{N} \frac{dx_i}{x_i} \, \delta\Big(1 - \sum_{i=1}^{N} x_i\Big) \, \bar{\Psi}_{p'\alpha'}(\{x_i', \vec{p}_{i\perp}'\})$$

$$\prod_{i=1}^{N} \otimes (\hat{\vec{p}}_i' + m) \, \tilde{J}_n(p'\{x_i', \vec{p}_{i\perp}'\}; p\{x_i, \vec{p}_{i\perp}\})$$

$$\prod_{i=1}^{N} \otimes (\hat{\vec{p}}_i + m) \, \Psi_{p\alpha}(\{x_i, \vec{p}_{i\perp}\})$$

Asymptotic behaviour of composite particle form factors at $|\vec{p}_\perp - \vec{p}_\perp'| \to \infty$ was studied in papers /20/ on the basis of various dynamical equations. In our equations (5),(6) the variables x_i (x_i') having the meaning of portions of total momentum p^+ are confined in the region (0,1). Moreover for every spinorial constituent there are corresponding projective operators $(\hat{\vec{p}}_i + m)$. (Note that the projective properties follow automatically in Kadyshevsky quasipotential approach as well /22/). These projective properties simplify the derivation of the automodel counting rule /22/ (up to logarithms) in the frame of perturbation theory for any renormalizable models with dimensionless coupling constants.

In conclusion we may note that it is easy to include internal symmetries (light-cone algebra, $SU_w(6)$ and etc.) in our approach. Then after the lightlike kinematical decompositions /15,16/ there remain equations for dynamical structure functions. There are wide classes of dynamical problems (lightlike quark symmetries, $\vec{p}_\perp$ phenomena, nuclear and atomic bound states , etc.) in which the application of null-plane quasipotential equations seems powerful.

References:

1. P.A.M.Dirac, Rev.Mod.Phys., 21, 392 (1949).
2. J.Jersak, J.Stern. Nuovo Cim., 59, 315 (1969).
   J.R.Klauder, H.Leutwyler, L.Streit.
   Nuovo Cim., 66A, 536 (1970).
3. S.Weinberg. Phys.Rev., 150, 1313 (1966).
4. J.Gunion, S.Brodsky, R.Blankenbecler. Phys. Rev., D8, 287 (1973).
5. G.Feldman, T.Fulton, J.Townsend. Phys.Rev., D7, 1814 (1973).
   H.Rothe, IFUSP/P39 (1975).
6. T.Jaroszewicz. Lett. Nuovo Cim., 8, 900 (1973); INF preprint, No 844/PH, Cracow (1973).
7. A.A.Logunov, A.N.Tavkhelidze. Nuovo Cim., 29, 38 (1963).
8. V.G.Kadyshevsky. Nucl.Phys., B6, 125 (1968).
   A.A.Logunov et al. TMF, 6, 157 (1971).
   R.N.Faustov. Ann.of Phys., 78, 176 (1973).
9. V.R.Garsevanishvili et al. TMF, 23, 310 (1975); 24, 3 (1975); JETP Lett., 23, 58 (1976).
10. A.A.Khelashvili. Proc. of JINR, P2-8750, Dubna (1975).
11. A.A.Khelashvili et al. Preprint JINR, D2-9540 (1976) Dubna.
12. T.Suzuki et al. Progr.Theor.Phys., 55, 922 (1976).
    T.Maskawa, K.Yamawaki. Preprint RIFP-242 (1975).
    M.Ida. Preprint RIFP-236 (1975).
13. P.A.M.Dirac. Lectures on Quantum Mechanics, New York, 1964.
14. J.Kogut, D.Soper. Phys.Rev., D1, 2901 (1970).
    S-.J.Chang, T.-M.Yan. Phys.Rev., D7, 1147 (1973).
    T.-M.Yan. Phys.Rev., D7, 1760; 1780 (1973).
    E.Tomboulis. Phys.Rev., D8, 2736 (1973);
    J.H.Ten Eyck, F.Rohlich. Phys.Rev., D9, 2237 (1974).
15. H.Leutwyler. Nucl.Phys., B76, 413 (1974).
    M.Ida. Progr.Theor.Phys., 54, 1519 (1975).
16. M.Ida, H.Yabuki. Preprint RIMS-195; RIFP-246 (1976).
17. R.N.Faustov et al. TMF, 25, 37 (1975).
18. A.N.Tavkhelidze. Invited report on Sec.A4 (this Conference).
19. A.A.Khelashvili, A.N.Kvinikhidze, (this conference). No. 658/C4-19.
20. C.Alabiso, G.Schirholz. Phys.Rev., D10, 960 (1974).
    SLAC-PUB-1509 (1974).
    S.Brodsky, G.Farrar. Phys.Rev., D11, 1309 (1975).
21. N.M.Atakishiev et al., this Conference, No 443/T4-26.
22. V.A.Matveev, R.N.Muradyan, A.N.Tavkhelidze. Lett. Nuovo Cim., 7, 719 (1973).
    S.Brodsky, G. Farrar. Phys.Rev.Lett., 31, 1153 (1973).

A NEW PARTICLE WITH THE MASS M=1110 MeV AND VECTOR MESON SPECTRUM IN THE RELATIVISTIC MODEL OF QUARK CONFINEMENT.

N.B.Skachkov

Joint Institute for Nuclear Research, Dubna

These notes concern the proposed several months ago a theoretical model[1] that predicts the existence, in the spectrum of the vector mesons, of a particle with mass equal to that of the particle discovered experimentally in July 1976 at DESY (the communication about this experiment is presented by DESY group at the section "New particle production in hadron collisions"*).

The main feature of the model (I) is the use of the new type of the potential that binds two quarks inside a meson (M-quark mass):

$$V(\rho) = \frac{I}{4\pi\rho} ctg\pi\rho M; \quad 0 < \rho < \frac{I}{M}. \qquad (I)$$

The parameter ρ in (I) is connected with the squared relative distance X^2 between two quarks by formula $X^2 = \frac{I}{M^2} - \rho^2$ and varies in the interval $0 < \rho < I/M$. The potential(I) confines quarks inside a shere of the radius equal to the Compton wave length (see Fig.I)

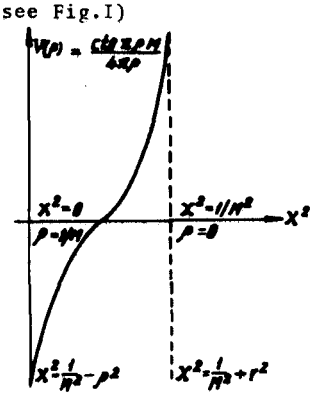


Fig.I

We shall consider the problem of the quark-antiquark bound states in the framework of the relativistic three- dimensional two-body equation of the quasipotential type[3], namely, the Kadyshevsky equation for the wave function of a two-particle relative motion. In c.m.s. this equation is

$$(E_p - E_q)\,\psi_q(\vec{p}) = \int \frac{d\vec{k}}{E_k} V(\vec{p},\vec{k},E_q)\,\psi_q(\vec{k}) \qquad (2)$$

$$E_p = p = \sqrt{M^2 + \vec{p}^2}; \quad E_p \neq E_k$$

(Here, $\vec{p}$ is the quark momentum in the c.m.s. $\vec{p}_1 = -\vec{p}_2 = \vec{p}$ and the quasipotential $V(\vec{p},\vec{k};Eq)$ is constructed from the Feynman diagrams). In the quasipotential equations, in contrast to the Bethe-Salpeter equation, the momenta of all the particles are on the mass shell $\vec{k}_o - \vec{k}^2 = M^2$. Therefore it is natural to use here the expansion on the Lorentz group, i.e. the system of functions[5]

*See also Denisov's rapporteur talk.

$$\xi(\vec{k},\vec{r}) = \left(\frac{k^o - \vec{k}\,\vec{n}}{M}\right)^{-1+irM}; \quad \vec{r} = r\,\vec{n}; \quad \vec{n}^2 = I \qquad (3)$$

complete with the volume element $d\Omega_k = \frac{d\vec{k}}{k^o}$ on the hyperboloid $k_o^2 - \vec{k}^2 = M^2$.

In[3] the transform with the functions

$$\psi(\vec{r}) = \frac{I}{2\pi^3} \int \xi(\vec{p},\vec{r})\,\psi(\vec{p})\,\frac{d\vec{p}}{p^o} \qquad (4)$$

was considered as a transform to a new relativistic configurational representation (RCR). It was shown that after this transformation eq.(2) takes the form

$$(\hat{H}_o + V(\vec{r},Eq))\,\psi_q(\vec{r}) = 2\,Eq\,\psi_q(\vec{r}), \qquad (5)$$

where the free Hamiltonian $\hat{H}_o$ ($H_o\,\xi(\vec{p},\vec{r}) = 2E_p\,\xi(\vec{p},\vec{r})$) is the differential-difference operator

$$H_o = 2M\,ch\,\frac{i}{M}\frac{\partial}{\partial r} + \frac{2}{r}\,sh\,\frac{i}{M}\frac{\partial}{\partial r} - \frac{\Delta_{\Omega}}{M\,r^2}\,e^{\frac{i}{M}\frac{\partial}{\partial r}} \qquad (6)$$

with the step proportional to the Compton wave length I/M. Eq.(5) can be solved exactly for a class of potential, e.g. for the relativistic Coulomb potential[6]

$$V(r) = -\frac{I}{4\pi r}\,\coth\frac{\pi}{2} r M,$$

V(r) is the transform of the quasipotential $V(\vec{p},\vec{k}) = \frac{-I}{(p-k)^2}$ corresponding to the massless gluon exchange propagator (the sign "minus" corresponds to an abstractive potential)**.

The transformation (4) has the group-theoretical meaning of the expansion in principal series (PS) of the unitary representations of SO(3.I). In the non-relativistic limit $\xi(\vec{p},\vec{r}) \to e^{i\vec{p}\vec{r}}$ and (4) is reduced to the ordinary Fourier transformation. Owing to (4) the group parameter r stands for a relativistic generalization of the relative distance between two particles. It is connected to the eigenvalue χ^2 of the invariant Casimir operator of SO(3.I) $\hat{C}_L = \frac{1}{2} M_{\mu\nu} M^{\mu\nu}$ (here, $M_{\mu\nu}$ are the generators of SO(3.I) derived by formula

$$\hat{C}_L\,\xi(\vec{p},\vec{r}) = \chi^2(\vec{p},\vec{r}); \quad \chi^2 = \frac{I}{M^2} + r^2, \quad 0 < r < \infty \qquad (7)$$

Thus, the modulus of the relativistic relative coordinate r is invariant. It was shown in[8] that the invariant mean-square radius definition $\langle r_o^2 \rangle \equiv \frac{\partial F(t)}{\partial t}/t=0$ has also the group-theoretical meaning of the eigenvalue of the Lorentz group Casimir operator for the invariant form factor of the system F(t):

$$\langle r_o^2 \rangle \equiv \frac{\partial F(t)}{\partial t}\Big/ t=0 = \{\hat{C}_L F(t)\}_{/t=0} \qquad (8)$$

So, if we describe the particle strusture in terms of the relativistic coordinate r, i.e. if we perform

** The solution of this equation and the energy spectrum in case of the confinement potential $V(r) = \lambda r$ was obtained in[7]. See also mini-report by Mir-Kasimov.

the transformation (4) of the form factor F(t), then due to (8) and (7) it follows that the distance from the center of the system is measured in terms of eigenvalue χ^2 of the Casimir operator $\hat{C}_L$. In case when the transform of the form factor F(r) in RCR is the function of the constant sign the new coordinate r specifies only the distances beyond the Compton wave lenght $^1/_M$ as is shown in[8] (see also mini-report by Skachkov at section A7).

Following [8] the transition to the distances smaller than the Compton wave lenght $\chi^2 < \frac{1}{M^2}$ may be achieved by including the supplementary series (SS) of SO(3.I) into the wave function expansion (4). The supplementary series are realized by functions

$$\zeta(\vec{p},\vec{\rho}) = \left(\frac{p_0 - \vec{p}\vec{n}}{M}\right)^{-1-\rho M} \qquad (9)$$

that can be formally obtained from the "plane waves" for PS $\xi(\vec{p},\vec{r})$ by changing $r \to i\rho$. The eigenvalue of the Casimir operator for the supplementary series, i.e. the square of the distance from the center, take the following values:

$$C_L \zeta(\vec{p},\vec{\rho}) = \chi^2(\vec{p},\vec{\rho}); \quad \chi^2 = \frac{1}{M^2} - \rho^2, \quad 0 < \rho < \frac{1}{M} \qquad (9)$$

The group parameter ρ may be then interpreted as a coordinate reckoned from the boundary of the sphere $R^2 = \chi^2 = \frac{1}{M^2}$ to its center, so that $\rho = {}^1/_M$ corresponds to the origin of the coordinates $\chi^2 = 0$.

In[1] the quasipotential equation was written for the wave function $\psi(\vec{\rho})$ describing the relative motion of the quark-antiquark in the range of the relative distances $0 < \chi^2 < \frac{1}{M^2}$ (no nonrelativistic analogue!):

$$(H_0 + V(\rho))\ \psi_q(\vec{\rho}) = 2E_q \psi_q(\vec{\rho}) \qquad (10)$$

where the free Hamiltonian $H_0\left(H_0\zeta(\vec{p},\vec{\rho}) = 2E_p\zeta(\vec{p},\vec{\rho})\right)$ is the differential-difference operator (as in case of r-space)

$$H_0 = 2M \cosh \frac{1}{M}\frac{\partial}{\partial\rho} + \frac{2M}{\rho}\sinh\frac{1}{M}\frac{\partial}{\partial\rho} + \frac{\Delta_{\rho\varphi}}{M\rho^2}\cosh\frac{1}{M}\frac{\partial}{\partial\rho} \qquad (11)$$

Now let us consider the analogue of the relativistic Coulomb potential (6) for the distances smaller than $\frac{1}{M}$. (We choose this potential because the Coulomb potential contains the maximal symmetry, and therefore the equation can be exactly solved). Since the transition to the distances $\chi^2 < \frac{1}{M^2}$ may be realized by passing to the supplementary series, we shall make use of the group-theoretical meaning of the modulus of the relativistic coordinate r and we shall obtain the potential $V(\rho)$ for $\chi^2 < \frac{1}{M}$ by changing $r \to i\rho$ in (6). Thus we arrive to the potential (I) which confines quarks inside the sphere $R^2 = \chi^2 = {}^1/_{M^2}$.

In [1] an exact solution for eq.(10) has been obtained in case of the potential (I). It was found that there may exist only three energy levels in the quark-antiquark system which moves with $\ell = 0$ in the field of the potential (I). The latter may be identified with masses of excited states of one particle:

$$M^I_{bound} \equiv 2Eq^I = 1.39798\ Mq; \quad M^{II}_{bound} \equiv 2Eq^{II} = 2Mq$$
$$M^{III}_{bound} \equiv 2Eq^{III} = 2.96750\ Mq \qquad (12)$$

(M_q is the quark mass).

Let us consider the ρ-meson excited state spectrum. Taking $M^I = M_\rho = 773 \pm 3$MeV we obtain from (12) the value of the quark mass $M_q = 553 \pm 2$MeV. It gives the following masses of the second and third radial excitations $M_{\rho'} = M^{II}_\rho = 1106 \pm 4$MeV; $M_{\rho''} = M^{III}_\rho = 1645 \pm 6$MeV.

At the time when the spectrum was obtained in [1] only the second excited state of ρ with $M^{III}_\rho = 1645 \pm 6$MeV could be identified with the previously observed ρ'' (1650) meson ($\Gamma_{\rho''} > 200$ MeV), and there was no experimentally found candidate for our first radial excitation of the ρ-meson with $M^{II}_\rho = 1106 \pm 4$MeV. The discovery at DESY of a new vector meson with the mass M=1110 MeV ($\Gamma \sim 20$-30 MeV) shows that all three particles appearing in the mass spectrum of our model exist in nature provided that the quantum numbers (isospin, parity, etc) of this vector meson coincide with the quantum numbers of the rho-meson as our model predicts.

Now let us apply this model to the J/ψ particle mass spectrum. Equating $M^I = M_{\psi(3095)}$ we obtain the heavy quark Q with the mass $M_Q = 2216$ MeV. For the radial excitations $\psi(3095)$ it gives the masses $M^{II}_\psi = 4432$ MeV, $M^{III}_\psi = 6576$ MeV with the help of (12). It is seen that in case of our confinement potential (I) the first radial excitation of the $\psi(3095)$ is not $\psi'(3685)$ but is close to $\psi(4414)$. Then the $\psi'(3685)$ should be interpreted as a bound state of other two heavy quarks Q' with mass $M_{Q'} = 2635$ MeV. With the help of (12) the values $M^{II}_\psi = 5270$ MeV and $M^{III}_\psi = 7820$ Mev may be given for the masses of the $\psi'(3585)$ possible excitations. Thus our model requires more than one (charmed) heavy quark in order to describe the J/ψ particle spectrum. This is consistent with other schemes including five or six quarks. Note that the mass of the heavy quark $M_Q = 2216$ appearing in our spectroscopy is in agreement with that obtained from the e^+e^- data analysis in the framework of 6 quark model with the account of heavy leptons.[10].

I express my sincere gratitude to Profs. Schopper and Höhler for the information about the DESY experiment at the beginning of the Conference.

R e f e r e n c e s:

I. N.B.Skachkov. JETP Letters,23,No I2,7I3(I976); Preprint JINR E2-9748,Dubna,I976.
2. S.Bartalucci et al. Contributed paper I258/N I, Preprint DESY 76/43,I976.
3. A.A.Logunov,A.N.Tavkhelidze,Nuovo Cimento,29, 380(I963); V.G.Kadyshevsky,Nucl.Phys.B6,I25(I968)
4. V.G.Kadyshevsky,R.M.Mir-Kasimov,N.B.Skachkov, Nuovo Cimento,55A,233(I968); Journ.of Particles and Nuclei,2,No 3,69(I972) Translation from Russian.
5. I.S.Shapiro. Doklady Akad.Nauk USSR,I06,647, (I965); Soviet Phys.Doklady,I,9I(I956).
6. M.D.Mateev,R.M.Mir-Kasimov,M.Freeman,Nucl.Phys. B12, 107 (1969).
7. K.S.Jhung,K.H.Chung,R.S.Willey,Phys.Rev.DI2, I999(I975).
8. N.B.Skachkov.Teor.i Mat.Fizika,23,3I3(I975); Soviet Jour.Theot.and Math.Phys.23,No 3(I975); preprint JINR E2-8857,Dubna,I975.
9. S.Ström. Arkiv f.Physic,Bd.38,No 22,373(I968).
I0.A.De Rujula,H.Georgi,Phys.Rev.DI3,I296(I976).

SCATTERING PROCESSES IN RELATIVISTIC COMPOSITE MODELS

A.N.Kvinikhidze

Institute of Mathematics,Georgian Academy of Sciences,Tbilisi,USSR

The successes in study of particle structure make us te believe in compositness of hadrons. Therefore the investigation even of twe hadren system represents in fact the many-body relativistic problem.

In this talk we present the three dimensional appreach to many-body problem in quantum field theory /1/ . This approach allows one in particular to construct exact expressions for relativistic scattering amplitudes corresponding te any precess of composite system collisien. Some simplest appreximations repreduce the well-known expressions obtained in naive quark parten model.

We perform our consideration in the null plane quantum field theory, taking into account the fact that it is very useful to avoid some specific many-body problem difficulties existing in usual quantum field theory.

Following to /2,3,4/ let us start with "two-time" Green function of n-particles

$$G^n(x^+;y^+;x,y)=(0|T\psi_1(x_1)\cdots\psi_m(x_m)\bar\psi_1(y_1)\cdots\bar\psi_n(y_n)|0)\Big|_{\substack{x_i^+=x^+\\ y_i^+=y^+}} \quad (1)$$

where $x^\pm=\frac{x^\pm}{\sqrt{2}}(x^0\pm x^3)$, $x=(x^-,x_\perp)$

T_+ is x^+ "time" ordering operator $\psi_i(x)$, $\bar\psi_i(x)$ are conjugate to each other Heisenberg field operators of i-th particle.

It is convenient to introduce in the momentum space the following notations

$p^\pm=p^0\pm p^3$, $\underline{p}=(p^+,p_\perp)$ then

$$px=p^-x^+ + p^+x^- - p_\perp x_\perp = p^-x^+ + \underline{p}\,\underline{x}$$

Determine the Fourier transform of the "two-time" Green function

$$G^n(x^+;x,y)=\frac{i}{(2\pi)^{3n+1}}\int e^{-ip^-x^+-i\sum_{j=1}^n(\underline{p}_j\underline{x}_j-\underline{q}_j\underline{y}_j)}$$

$$dp^-\prod_j d\underline{p}_j\,d\underline{q}_j\,\delta(\underline{p}-\underline{q})(p^+)^{2-2n}\,g^n(p;p,q) \quad (2)$$

The function has the following important properties:

a) Spectral representation

$$g^n(p;p,q)=\int_0^\infty \frac{G^n(s;p,q)}{p^2-s+i\varepsilon}\,ds \qquad (3)$$

Spectral density can be expressed by quasipotential wave functions

$$G^n(s;p,q)=(2\pi)^{3n}\sum_m' \rho^+\delta(s-P_m^2)\cdot$$
$$\{\Phi^n_{om}(p)\times\bar\Phi^u_{om}(q)\mp\Phi^n_{mo}(p)\times\bar\Phi^u_{mo}(q)\} \qquad (4)$$
$$\langle 0|T_+\psi_1(x_1)\cdots\psi_n(x_n)|m\rangle\big|_{x_i^+=0}=$$
$$=\int e^{-i\sum_1^n p_j x_j}\prod_1^n d^3p_j\,\delta(p-p_m)(p^+)^{1-u}\Phi^u_{om}(p)$$

b) Projection properties in scale variables $\xi_i=p_i^+/p^+$, $\eta_i=q_i^+/p^+$

$$g^n(p;p,q)=g^n(p;p,q)\prod_1^n\theta(\xi_i)\theta(\eta_i) \qquad (5)$$

c) Projection properties in spin struoture

$$g^n(p;p,q)=U_1(p_1)\cdots U_n(p_n)\times A_1\times\bar U_1(q_1)\cdots\bar U_n(q_n)$$
$$+V_1(p_1)\cdots V_n(p_n)\times A_2\times\bar V_1(q_1)\cdots\bar V_n(q_n) \qquad (6)$$

where $U_i(p)=\langle 0|\psi_i(0)|p\rangle$; $V_i(p)=\langle -p|\psi_i(0)|0\rangle$

d) Transformation properties

$$g^n(p;p,q)=S_p\,g^n(p;\xi_i,p_{i\perp}-\xi_i p_\perp,\eta_i,q_{i\perp}-\eta_i q_\perp)S_p^{-1}$$

where S_p - is the known transformation matrix acting only on the spin indices.

The most important fact is that the "two-time" Green function (2) has a complete information on all possible scattering processes in n-particle system. It is shown that the function (2) has different poles corresponding to the contribution of any initial or final state and the residues determine the corresponding relativistic scattering amplitudes. In particular, near the pole corresponding to two composite particle initial state and 1-particle final state we have

$$g^n(p;p,q)\sim i[2(2\pi)^3]^{n+c+3}\frac{\Phi_1^{n_1}(p)\cdots\Phi_c^{n_c}(p)\times}{\chi_1^{n_1}\cdots\chi_c^{n_c}}$$
$$\times\frac{T(p_1\cdots p_c;q_A,q_B)\times\bar\Phi_A^{n_A}(q)\,\bar\Phi_B^{n_B}(q)}{\left(p^2-\sum_1^c\frac{p_{i\perp}^2+M_i^2}{\chi_i}\right)\chi_A^{n_A}\chi_B^{n_B}\left(p^2-\frac{q_{A\perp}^2+M_A^2}{\chi_A}-\frac{q_{B\perp}^2+M_B^2}{\chi_B}\right)}$$
$$\chi_i=p_i^+/p^+$$

where $\Phi_1^{n_1}\cdots\Phi_c^{n_c}$, $\Phi_A^{n_A}$, $\Phi_B^{n_B}$ are the quasipotential wave functions of the $1\cdots c$, A, B composite states respectively; T is the physical scattering amplitude of the process $A+B\to 1+\cdots+c$

To construct an expression for this scattering amplitude, we introduce transition operators $M_{\alpha\beta}$ in the following way

$$g^n=R_{\alpha\beta}+g_\alpha^n M_{\alpha\beta}\,g_\beta^n \qquad (9)$$

where $\alpha(\beta)$ label the initial (final) states, $g_{\alpha(\beta)}$ - Green function in which interaction only inside some subsystems is taken into account. For α corresponding to the state of c composite particles arising in c subsystems g_α in n-particle Green function when interaction between this subsystems is excluded. $R_{\alpha\beta}$ is some term regular at the poles corresponding to initial (β) or final (α) states.

Using definition (9) and the pole structure (8) one gets the following expression for scattering amplitude:

$$iT_{\alpha\beta}=[2(2\pi)^3]^{n-1}\int\bar\Phi_1^{n_1}\cdots\bar\Phi_c^{n_c}M_{\alpha\beta}\,\Phi_A^{n_A}\Phi_B^{n_B} \qquad (10)$$

Using the equation for n-particle "two-time" Green function

$$g^n=g_0^n+g_0^n V^n g^n \qquad (11)$$

a set of three-dimensional equations for the transition operators are obtained. Taking into account the decomposition of quasipotential V^n on the sum of pair interaction, three,- four,- ... - forces terms (following from spectral representation (3)) these equations can be reconstructed to Faddeev form. Therefore the general representations for some distributions obtained in our approach depend crucially an the properties of constituent wave function and their scattering amplitudes /5,6/ .

Note that there are also the equations and normalisation conditions for the wave functions entering in (10) /7/ .

References:

1. A.N.Kvinikhidze, A.N.Sissakian, L.A.Slepchenko and A.N.Tavkhelidze. Large transverse momentum inclusive processes in composite particle approach, paper 1081/A4--31 contributed to the Conference; to be published in Particles and Nucleus, Atomizdat, Moscow (1976).
2. A.A.Logunov, A.N.Tavkhelidze. Nuovo Cim., 29, 380 (1963).
3. A.N.Kvinikhidze, D.Ts.Stoyanov. International School, Sukhumi, JINR P2-8667 (1972) Dubna.
4. A.A.Khelashvili, A.N.Kvinikhidze, V.A. Matveev, A.N.Tavkhelidze. JINR Preprint D2-9540, Dubna, 1976.
5. A.N.Tavkhelidze, High transverse momentum processes in composite models, invited talk on the Conference, Tbilisi (1976).
6. L.A.Slepchenko, Large $P_\perp$ inclusive distributions in composite models, invited talk on the conference, Tbilisi (1976).
7. A.A.Khelashvili. Null-plane quantisation and quasipotential equation for composite particles (this Conference).

INVESTIGATION OF THE SOLUTIONS OF QUASIPOTENTIAL EQUATIONS

V.Sh.Gogokhia, D.P.Mavlo, A.T.Filippov

JINR, Dubna

Quasipotential equations (QE) /1/ in quantum field theory are a convenient method for investigating relativistic bound state problems /2,3/ . In connection with possible applications of QE to the quark models it is necessary to note that there are many forms of QE and therefore it is not clear a priori which form is preferable on general grounds. On the other hand this fact is an advantage when it comes to possible applications /2,3,4/. Different physical problems may require different forms of QE.

Let us consider QE for the scattering amplitude of the equal mass (m) scalar particles (quarks):

$$T(\vec{p},\vec{p}') = V[(\vec{p}-\vec{p}')^2] + \int \frac{d^3q\,(K^2+m^2)^{\frac{\nu-1}{2}}}{(q^2+m^2)^{\nu/2}} \cdot \frac{V[(\vec{p}-\vec{q})^2]\,T(\vec{q},\vec{p}')}{K^2-q^2}, \quad (1)$$

where $\nu=1$ corresponds to the ordinary Logunov-Tavkhelidze quasipotential equation (LTQE), $\nu=2$ - to the modified LTQE (MLTQE). Let $V_0(p,p')$ be the S-wave quasipotential, corresponding in the coordinate representation to the quasipotential of the form $V(r)=-g r^{-1}$. Then eq. (1) can be reduced to the differential boundary value problem of the second order in momentum representation /2/ :

$$\frac{d^2 f(x)}{dx^2} + \lambda^2 V^{(\nu)}_{(x,E)} f(x) = 0, \quad V^{(\nu)}_{(x,E)} = (1+x^2)^{-\nu/2}(x^2+E^2)^{-1} \quad (2)$$

$$f(x) \underset{x\to 0}{\sim} x\,; \quad f(x) \underset{x\to\infty}{\sim} const, \quad (3)$$

where $x = pm^{-1}$, $\lambda^2 = gm^{-1}(1-E^2)^{\frac{\nu-1}{2}}$, $E^2 = -\kappa^2 m^{-2}$, $x \in X \equiv [0,\infty)$, $E \in \mathcal{E} \equiv [0,1]$.

We have investigated in detail the case $\nu = 1,2$. Let us recall now one of the Sturm-Liouville theorems:

THEOREM: If the non-negative function

$V(x,E)$ is incremented in its domain $x \in X$ $E \in \mathcal{E}$ then positive eigenvalues λ^2 will always decrease and negative ones increase.

To apply this theorem to our boundary value problem (2)–(3) it is necessary to find such functions $V_<^{(\nu)}(x,E)$ and $V_>^{(\nu)}(x,E)$, which satisfy the inequality

$$V_>^{(\nu)}(x,E) \geq V^{(\nu)}(x,E) = (1+x^2)^{-\nu/2}(x^2+E^2)^{-1} \geq V_<^{(\nu)}(x,E) \quad (4)$$

and which, when inserted instead of $V^{(\nu)}(x,E)$ make eq. (2) solvable in terms of known special functions. Then, using the mentioned theorem, we can derive exact upper and lower spectral bounds for the original problem (2)–(3):

$$|\lambda_<^2| \geq |\lambda_{exact}^2| \geq |\lambda_>^2| . \quad (5)$$

For the LTQE we use the following approximations:

$$V_<^{(1)}(x,E) = (1+x)^{-1}(x+E)^{-2} \quad (6)$$

$$V_>^{(1)}(x,E) = \begin{cases} (x^2+E^2)^{-1}, & x<1 \quad (7a) \\ x^{-3}, & x \geq 1 \quad (7b) \end{cases}$$

The eigenvalue problem (2)–(3) with potential (6) has the following solution (upper spectral condition):

$$(-1)^{1-2\alpha}\frac{\Gamma(\alpha^*)\Gamma(\alpha^*+1)\Gamma(2\alpha)}{\Gamma(\alpha)\Gamma(\alpha+1)\Gamma(2\alpha^*)} = \frac{F(\alpha,-\alpha^*;2\alpha;\frac{E}{E-1})}{F(\alpha^*,-\alpha;2\alpha^*;\frac{E}{E-1})}\left(\frac{E}{E-1}\right)^{2\alpha-1} \quad (8)$$

where $\alpha = \frac{1}{2} + i\left[\lambda_<^2(1-E)^{-1} - \frac{1}{4}\right]^{1/2}$.

For the function (7) the corresponding (lower) spectral condition is

$$\frac{1}{2} + \lambda_>\frac{J_1'(2\lambda_>)}{J_1(2\lambda_>)} = \frac{\lambda_>^2}{3}\cdot\frac{A(a)E^{2a}F(1+a,-a^*;2a+\frac{1}{2};-E^2)+c.c.}{B(a)E^{2a}F(a,-a^*;2a+\frac{1}{2};-E^2)+c.c.} \quad (9)$$

where $a = \frac{1}{4} + i\frac{1}{2}(\lambda_>^2 - \frac{1}{4})^{1/2}$,

$$A(a) = \frac{\Gamma(\frac{5}{2})\Gamma(\frac{1}{2}-2a)}{\Gamma^2(\frac{3}{2}-a)} ,$$

$$B(a) = \frac{\Gamma(\frac{3}{2})\Gamma(\frac{1}{2}-2a)}{\Gamma(\frac{1}{2}-a)\Gamma(\frac{3}{2}-a)} .$$

For the MLTQE we choose the following approximations:

$$V_<^{(2)}(x,E) = (1+x)^{-2}(x+E)^{-2} \quad (10)$$

$$V_>^{(2)}(x,E) = \begin{cases} (x^2+E^2)^{-1}, & x<1 \quad (11a) \\ x^{-4}, & x \geq 1 \quad (11b) \end{cases}$$

These as well as (6)–(7) accomodate properly the analytic and asymptotic properties of the original potentials. The eigenvalue problem (2)–(3) with potential (10) has the solution:

$$\lambda_{n,<}^2(E) = \frac{1}{4}(1-E)^2 + \left[n\pi\frac{1-E}{\ln E}\right]^2, \quad n=1,2,3,... \quad (12)$$

Taking into account, that $V_>^{(2)}(x,E) \equiv V_>^{(1)}(x,E)$ for $x \in [0,1)$, we obtain the solution of eigenvalue problem (2)–(3) with function (11) from the spectral condition (9) with the help of the substitution:

$$\frac{1}{2} + \lambda_>\frac{J_1'(2\lambda_>)}{J_1(2\lambda_>)} \Longrightarrow \lambda_> ctg\,\lambda_> \quad (13)$$

Consider now the limit of strongly bounded states ($E=1$). The analytic results for eigenvalues $\lambda_{n,\mu}^{2(\nu)}(1)$ ($\nu = 1,2$; $\mu = >, <$, exact) are:

$$\lambda_{n,<}^{2(1)}(1) = \frac{1}{4}\mathcal{Z}_n^2 ; \quad \lambda_{n,<}^{2(2)}(1) = \pi^2 n^2 ; \quad \lambda_{ex.,n}^{2(2)}(1) = 4n^2 - 1 , \quad (14)$$

where $n = 1,2,3,...$ and $\mathcal{Z}_n$ is the n-th root of the Bessel function $J_1(z)$.

Numerically: $\lambda_{1,>}^{2(1)} = 1.155$, $\lambda_{2,>}^{2(1)} = 5.759$, $\lambda_{1,>}^{2(2)} = 1.632$, $\lambda_{2,>}^{2(2)} = 11.162$. These results satisfy the main restriction (5).

In the weak-binding limit ($E \to 0$) we obtained from (8), (9), (13) the following behaviour of the energy eigenvalues:

$$E_{n,\mu}^{(\nu)}(\lambda) = \exp\left\{-\frac{n\pi}{\sqrt{\lambda^2-\frac{1}{4}}} + K_\mu^{(\nu)} + O(\sqrt{\lambda^2-\tfrac{1}{4}})\right\}, \quad (15)$$

where $K_{>}^{(1)}=K_{>}^{(2)}=1.65$, $K_{<}^{(1)}=0.77$, $K_{<}^{(2)}=0$ and $\mu=$ $=>,<$, $n=1,2,3,...$

Therefore, using the main inequality (5), we proved, that the behaviour of the exact energy eigenvalues in this limit must be of the type (15)

$$E_{n,ex.}^{(\nu)}(\lambda)=\exp\left\{-\frac{n\pi}{\sqrt{\lambda^2-1/4}}+K_{ex.}^{(\nu)}+O(\sqrt{\lambda^2-1/4})\right\} \quad (16)$$

with $K_{<}^{(\nu)}\le K_{ex.}^{(\nu)}\le K_{>}^{(\nu)}$. In connection with this formula we point out that the original eigenvalue problem (2)–(3) cannot be solved in terms of known special functions even if the E is small, and it is the Sturm–Lieuville upper and lower spectral bounds technique which renders the problem solvable. The spectral bounds considered make it possible to prove, that:
1) there exists the limit point of the spectrum $E_n(\lambda)$ for $E\to 0$; 2) the dependence $E_{n,ex.}^{(\nu)}(\lambda)$ is nonanalytic, namely of the type (16);
3) there are no energy eigenvalues in the interval $0\le\lambda^2\le 1/4$. Note, here that boundary value problem (2)–(3) for $\nu=1$ has been solved formerly /2/ by the (asymptotic) comparison equation method (CEM) /3/ with the following result for eigenvalues ($0\le E^2\le 1$):

$$\sqrt{\lambda_n^2(E)-1/4}=\frac{2\pi n}{B(1/4,1/2)\,F(1/2,1/4;3/4;1-E^2)} \quad (17)$$

which for $E\to 0$ reads

$$E_n(\lambda)=\exp\left\{-\frac{\pi n}{\sqrt{\lambda^2-1/4}}+\Psi(1)-\frac{1}{2}\Psi(\tfrac{1}{2})-\frac{1}{2}\Psi(\tfrac{1}{4})+O(\sqrt{\lambda^2-1/4})\right\}. \quad (18)$$

Then, the Sturm–Lieuville upper and lower spectral bounds method as well as CEM may be of great use for solving the broad class of linear differential boundary value problems often met with in different branches of theoretical physics.

In conclusion we note that in the nonrelativistic limit the quasipotential $V(r)=-gr^{-1}$ corresponds to the potential $V(r)=-g'r^{-2}$ in the Schrödinger radial equation, but in our case there is no problem of collapse into scattering centre.

References

1. A.A.Logunov, A.N.Tavkhelidze. Nuovo Cim., 29, 380 (1963).
A.N.Tavkhelidze. Lectures on Quasipotential Method in Field Theory, Bombay, Tata Institute of Fundamental Research, 1964.
2. V.Sh.Gogokhia, D.P.Mavlo, A.T.Filippov. TMP, 27, 323 (1976).
3. R.N.Faustov, Physics of Elementary Particles and Atomic Nuclei, 3, 238 (1972).
4. V.R.Garsevanishvili, V.A.Matveev, L.A.Slepchenko. Phys.of Elem. Part. and Atom.Nuclei, 1 (1970), 91, V.G.Kadyshevsky, R.M.Mir-Kasimov, N.B.Skachkov. Phys.of Elem.Part. and Atom.Nuclei, 2, 635 (1972); V.A.Rizov, I.T. Todorov, Phys.of Elem.Part. and Atom.Nuclei, 6, 669 (1975).
5. R.Langer. Trans.Am. Math.Soc., 67, 461 (1949), T.M.Cherry, Trans.Am.Math.Soc., 68, 224 (1950); R.B.Dingle, App.Sci.Res. B5, 345 (1956); F.W.J.Olver. Phil.Trans. Roy.Soc., A247, 307 (1954); ibid A249, 65 (1956); ibid. A250, 479 (1958).

LOCAL GAUGE SYMMETRY AND CONFINEMENT IN QUANTUM CHROMODYNAMICS

William A.Bardeen,
Robert B.Pearson

FNAL,Batavia,Illinois,USA

A nonabelian color gauge theory of quarks and gluons has been proposed as the basis for a fundamental theory of hadrons. We would like to focus on those features of this theory , quantum chromodynamics,which lead to confinement /1/ . We will also discuss a transverse lattice formulation of the theory which we use as a basis for calculation of properties of the hadronic bound states.

Quantum chromodynamics is a theory based on local gauge invariance. In order to define the quantum theory we must make a choice of gauge as not all degrees of freedom of the gauge fields are dynamical. Physics may appear much different for gauge dependent quantities but there exist a oemmen physical subspace for all choices of gauge. We note that a confinement picture of hadrons is necessarily gauge dependent.

In order to focus on physical quantities we must eliminate two of the four components of the vector potentials. This is most convenient in an axial gauge where the vector potentials $\vec{A}_z = 0$ and $\vec{A}_t$ is dependent. $\vec{A}_x$ and $\vec{A}_y$ are the two indepednent degrees of freedom.

The lagrangian for a nonabelian gauge theory is given by

$$\mathcal{L} = -\frac{1}{4}\vec{G}_{\mu\nu}^2 \qquad (1)$$

where

$$\vec{G}_{\mu\nu} = \partial_\mu \vec{A}_\nu - \partial_\nu \vec{A}_\mu + g\vec{A}_\mu \times \vec{A}_\nu .$$

In the axial gauge, canonical quantization leads to the hamiltonian density

$$\mathcal{H} = \frac{1}{2}\vec{P}_\alpha^2 + \frac{1}{2}(\partial_z \vec{A}_\alpha)^2 + \frac{1}{4}\vec{G}_{\alpha\beta}^2 + \frac{1}{2}g^2 \vec{J}_0 \frac{1}{\partial_z^2}\vec{J}_0 \qquad (2)$$

where $\alpha = x, y$. P_α is the conjugate momentum and J_0 is the color charge density

$$\vec{J}_0 = \frac{1}{g}\vec{D}_\alpha \vec{P}_\alpha = \frac{1}{g}\partial_\alpha \vec{P}_\alpha + \vec{A}_\alpha \times \vec{P}_\alpha . \qquad (3)$$

We note that there exists a linear longitudinal potential between the color charge densities in this gauge. The hamiltonian of Eq. (2) has a residual transverse gauge symmetry generated by the conserved charges

$$Q(\Lambda) = \int dz \int dx_\perp \, \vec{P}_\alpha (\vec{D}_\alpha \Lambda) \qquad (4)$$

where

$$\Lambda = \Lambda(x_\perp).$$

The question of color confinement depends duextly how this residual symmetry is realized. If the transverse gauge symmetry is spontaneously broken, the global charge "color" is not confined and the colored gluons emerge as "plasma" exoitations. The linear "coulomb" potential in E(2) is screened to a I/r potential, etc. Hence perturbation theory calculation assume a broken symmetry ground state. If a second symmetric phase could also exist, the linear longitudinal potential would confine the transverse color and only color singlet states would result. In either case, the matrix elements of gauge charges between physical states is zero. We note that either phase could, in principle, result dynamically as there exists nontrivial longitudinal dynamics /2/ .

As the residual symmetry is local in $x_\perp$ we do not know how to study the symmetry phase directly in the continuum theory. Hence, we have reformulated the gauge theory on a transverse lattice where the gauge charges become the color charge at each site. The transverse gauge fields $M_{n\alpha}$ are associated with links on the lattice /3/ . The longitudinal gauge fields $A_{n\beta}$ and the quarks are associated with sites on the lattice. We note that only x and y are made discrete while z and t remain continuous.

THe lagrangian of eq. (1) becomes

$$\mathcal{L} = \sum_{n\mu\nu} \left[-\frac{1}{4} \vec{G}_{\mu\nu}^{\,2} \right] + \sum_{n\alpha} TR \left[D_\mu M_{n\hat{\alpha}} D_\mu M^{+}_{n\hat{\alpha}} \right]$$

$$+ \sum_{n\alpha\beta} \frac{g^2}{a^2} TR \left[M_{n\hat{\alpha}} M_{n+\hat{\alpha},\beta} M^{+}_{n+\hat{\beta},\hat{\alpha}} M^{+}_{n\hat{\beta}} \right] \quad (5)$$

$$+ \sum_{n\alpha} V(M_{n\alpha})$$

where D_μ is the longitudinal covariant derivative with coupling strength, g/a and $V(M_{n\alpha})$ is a local potential chosen such that $M_{n\alpha} M^{+}_{n\alpha} = 1/g^2$ in the continuous limit. We have chosen to write the lagrangian in terms of linear degrees of freedom for the transverse gluons as we expect these to be generated in any oase in the symmetrical phase [4].

We again quantize the theory by eliminating the longitudinal degrees of freedom in favour of coulomb potential. Hadrons are formed as bound states of quarks and the symmetric phase gluons.

With E.Rabinovich we are using the transverse lattice theory to compute properties of the hadronic bound states. We hope in the near future to report the results of these calculations.

References

1. W.A.Bardeen and R.B.Pearson. Phys.Rev., July 1976 and references therein.
2. W.A.Bardeen and Myron Bander. Phys.Rev. (to be published).
3. K.Wilson. Phys.Rev D10, 2445 (1974), J.Kogut and L.Susskind. Phys.Rev., D11, 399 (1975).
4. W.A.Bardeen, D.L.Lee, R.Schrock. Phys. Rev. (to be published).

BOUND AND RESONANT STATES IN THE NUCLEON-ANTINUCLEON SYSTEM

I.S.Shapiro
ITEP,Moscow,USSR

A possibility of existence of relatively long living quasinuclear states of the $N\bar{N}$ system was shown theoretically in 1969-1970 (L.N.Bogdanova, O.D.Dalkarov et al., see references in reviews [1-3]). Later the same authors have considered production of NN systems in interactions of antiprotons ($\bar{p}$) with deuterium and the electromagnetic transitions of $p\bar{p}$ atoms to the levels of the NN quasinuclear system accompanied by hard (the average energy of about 100 MeV) γ radiation with a discrete spectrum.

The starting points of the theory of quasinuclear states are a) the choise of the interaction potential of nonrelativistic N and $\bar{N}$ and b) use of the faot that the $N\bar{N}$ annihilation distances are of the order of the nucleon Compton wave-length, whereas the mean radius of the $N\bar{N}$ quasinuclear state must be of the order of the nuclear range, i.e. about 1 fm.

The $N\bar{N}$ potential for euristical calculations was represented by one of the OBEP versions satisfactory fitting the nucleon-nucleon soattering at nonrelativistic energies. The NN channel was transformed into $N\bar{N}$ channel by G oonjugation. The change of the sign of the forces is determined by G-parity of the light meson which is exchanged between the interacting fermions. In the OBEP version used the π, η, δ and ω meson exchanges are taken into account as well as the exchange by two "effeotive" scalar bosons (pseudosoalar and isovector) introduced in order to substitute the two and three-pion exchange disgrams.

The ω -meson exchange plays a special role in the $N\bar{N}$ interaotion. The dimensionless constant of $N\bar{N}$ interaotion is large (about 20). So, the sign of the $N\bar{N}$ forces corresponds to attraction, the NN forces being repulsive. The

strong attractive $N\bar{N}$ interaction arising from the ω exchange produces a rather rich spectrum: the spectrum of NN states expected in such model involve about 20 levels (as a contrast to the deuteron which has the only discrete spectrum state - the ground state). The variety of $N\bar{N}$ discrete levels is due to the strong spin-orbit forces produced by the ω exchange. The results have shown that all quasinuclear $N\bar{N}$ states have no radial knots. The space dimensions of these states (as it was expected) has appeared to be relatively large- about 1 fm. Therefore, the total spectrum is in some sense stable against the variation of the potential at small distances and, particularly, (due to the point (b)) against annihilation corrections.

It should be emphasized that the calculation results are quite euristical because the data on NN scattering phases obtained with available accuracy are insufficient for unambiguous reconstruction of the $N\bar{N}$ potential even in the OBE model. Therefore, the inverse problem is more interesting: to understand the nature of NN forces studying the $N\bar{N}$ spectrum (at nonrelativistic energies of particles).

The annihilation widths of the quasinuclear states are proportional to the square of the modulus of the wave function at distances of the order of the nucleon Compton wavelength. At such distances the $N\bar{N}$ forces are not known and cannot be described in familiar OBEP models. However, the following two points should be noted: if there is no repulsion between N and N at small distances then the annihilation widths may reach the values of the order of 100-150 MeV. When the repulsion is due to the centrifugal barrier only, the annihilation widths for p, d and f states are expected to be of 10 MeV, 1 MeV and 100 keV, respectively. Since the nearthreshold states in the $N\bar{N}$ spectrum must have nonzero orbital momenta, the above statement means that the quasinuclear mesons of about 2 GeV masses must be "narrow".

A characteristic signature for the decay of a meson resonance is a relatively large partial width into $N\bar{N}$ channel (real if it is energy allowed and virtual for bound $N\bar{N}$ states). By the order of magnitude $\Gamma_{N\bar{N}} \simeq 1/mR$ with R being the radius of the state. For $R = 1/\mu$ where μ is the pion mass, $\Gamma_{N\bar{N}} \simeq 10$ MeV. Thus, the "elasticity" of the resonance $x = \Gamma_{N\bar{N}} / \Gamma_t$ (Γ_t is the total width) is expected to be large (from 0.1 to 1).

The above said means that the most effective way to generate quasinuclear mesons (bound and resonant $N\bar{N}$ states) is to make experiments with slow or stopped antiproton beams.

The experimental data giving evidence for existence of the quasinuclear NN systems begin to appear in 1971-1972. The data fall into three categories: observation of the above mentioned hard γ radiation accompanying the $N\bar{N}$ annihilation into pions; anomalies in the annihilation of slow $\bar{p}$ in hydrogen and deuterium (d); direct discovery of heavy mesons with the mass of about two nucleon masses strongly coupled to $N\bar{N}$ channal i.e. having a considerable (of the order of 10% or higher) partial decay (real or virtual for bound states) width.

The purpose of this talk is to review the modern status of the problem (mostly of the available data). The resume is the following.

1. γ radiation accompanying the annihilation of antiprotons. This radiation (with the average energy of about 100 MeV) was found in $\bar{p}d$ annihilation at RNL. by T.Kalogeropoulos and his collaborators. The radiation intensity turned out to be extremely high: (0.75 ± 0.08) quanta per an annihilation act (theoretically the the intensity may equal from 10^{-2} to 2/3).

This result has not been confirmed yet. The bubble chamber data on the γ- radiation spectrum show a disorete struoture (some lines having the intensity of about 10% and the of 10 MeV) /4-5/ . The statistics of these data is quite poor (about $4.4.10^3$ events). On the other side, the results of the scintillation speotrometer experiment where a great number of γ quanta (about 10^5) has been found and no discrete line has been seen (at 3.3% confidence level for lines with natural width much lower than 10 MeV) are difficult for interpretation beoause of bad resolution of the speotrometer (which, in particular, oannot show the known spectrum produoed in the decay of neutral pions /5,6/). Experiments being in progress now in various laboratories will, probably, give more definite data in the near future.

2. Anomalies in annihilation of slow antiprotons. Rather intensive annihilation from triplet P states of $\bar{p}p$ and $\bar{p}d$ atoms (40 and 70% of all annihilations, respectively) is observed, as well as deviation from the $1/v$ law for slow $\bar{p}$ (see /1-3,5/). These facts oan be understood in the scheme of $N\bar{N}$ quasinuclear states and would be difficult to explain if such states did not exist.

3. Direct disoovery of heavy "quasinuclear" $N\bar{N}$ mesons. Resonant $N\bar{N}$ states are seen in the energy behaviour of the pp and pd total oross seotions and in the large angle ("baokward") pp elastic scattering oross seotions. Bound states oan be found in the annihilation $\bar{p}d \to \chi + p$ or by the mixing or effeotive mass χ spectrum, or by p energy spectrum (in the same way suffioiently narrow $N\bar{N}$ states can be studied). Various experimental groups have used the above methods /3,5,7,8/ to observe the $N\bar{N}$ bound and resonant states with the following masses and widths (MeV, the widths are given in parantheses): 1794(7), 1873(10), 1900(20), 1932(9), 1940(60),200(200), 2150(95), 2335(110). The resonance 2000 observed in the prooess $\bar{p}p \to K^0 K^{\pm} \pi^{\pm}$ possibly ooinoides with the " h meson" found in the $2\pi^0$ channel in Serpukhov experiments and in the K^+K^- channel in CERN (see the list of referenoes in /7/). If this interpretation is valid, then almost all width of the " h meson" should be associated with the elastic channel. (See /9,10/). Not all quantum numbers of the observed quasinuclear mesons are known as yet. Isospins and G particles are known; however, the available data do not allow an unambigous ohoice for spin and P parity.

If the further investigations oonfirm the existence of $N\bar{N}$ quasinuclear states and give their energy speotrum and quantum oharaoteristios, then it will be the most important source of information on nuclear forces beoause $N\bar{N}$ and NN two-body interactions are direotly related (similarly to the case of electron--electron and eleotron-positron oase). One may say that nuclear physios would obtain "its own hydrogen atom" - the two-particle (or "almost two-particle") system with a reach spectrum of states-instead of the available one-level deuteron. On the other side, formation of $N\bar{N}$ quasinuclear states (as well as of $Y\bar{N}$ or $Y\bar{Y}$, where Y is a hyperon) may be essential for explanation of a number of phenomena in high energy particle interactions (see /3/). If it is so, then the "low energy" nuolear physios and the elementary partiole physics will turn to be related in some aspects much stronger and muoh more directly then we used to think. In partioular, nuolear forces having the same physioal nature must explain not only the states of the lightest nuclei (deuteron, tritium, helium) but as well the speotrum of heavy mesons (with their masses near 2 GeV) x) .

References

1. I.S.Shapiro, Ucp.Fiz.Nauk, 109, 431 (1973) (Sov.Phys.Usp., 16, 173 (1973)).
2. L.N.Bogdanova, O.D.Dalkarov and I.S.Shapiro. Ann.Phys. (N.Y.)., 84, 261 (1974).
3. L.N.Bogdanova, O.D.Dalkarov, B.O.Kerbikov and I.S.Shapiro. Narrow NN resonance. Preprint ITEP-27, Moscow, 1975 and in Proceedings of the IY International Symposium on Nucleon-Antinucleon Interactions, Editors T.E.Kalogeropoulos, K.C.Wali, Syracuse University, 1975, v.2, pp.VIII, 1-36.
4. T.E.Kalogeropoulos, A.Vayaki, G.Grammatikakis et al., Phys.Rev.Lett., 33, 1635 (1974).
5. T.E.Kalogeropoulos. The Antinucleon-Nucleon System at Non-Relativistic Energies, in Proceedings of the VI International Conference on High Energy Physics and Nuclear Structure, Santa-Fe, June 1975, AIP, 1975, p.155.
6. T.E.Kalogeropoulos et al. Phys.Rev.Lett., 35, 824 (1975).
7. B.French, Meson- 1975, Preprint CERN/D.PH. 11/Phys., 75-38 August 1975.
8. Chaloupka, H.Dreverman, F.Marzano et al. Measurement of the Total and Partial pp Cross Section between 1901 and 1950 MeV. Preprint CERN/EP/Phys., 76-5, 13 February 1976.
9. L.N.Bogdanova, O.D.Dalkarov, B.O.Kerbikov and I.S.Shapiro. Pisma v JETP 23, 76 (1976).
10. L.N.Bogdanova, O.D.Dalkarov, B.O.Kerbikov and I.S.Shapiro. Preprint ITEP-16, Moscow, 1976.
11. E.S.Birger, B.O.Kerbikov, N.B.Konyukhova, and I.S.Shapiro. Yad.Fiz., 17, 178 (1973). Sov.J.Nucl.Phys., 17, 92 (1973).
12. O.D.Dalkarov, B.O.Kerbikov, I.A.Rumyantsev and I.S.Shapiro. Yad.Fiz., 17, 1321 (1973). Sov.Hourn.Nucl.Phys., 17, 688 (1973).
13. G.Alexander et al. Nucl.Phys., B45, 29 (1972).

x) In this connection, one should as well mention the theoretically possible states $2N2\bar{N}$ /11/ and the baryon systems $2N\bar{N}$ /12/ having been not searched for as yet. (Some of the data /13/ may be considered as giving evidence in favour of the quasinuclear mesons $2N2\bar{N}$).

BILOCAL FUNCTIONAL APPROACH TO DYNAMICAL SYMMETRY-BREAKING

D.Ebert and V.N.Pervushin
JINR, Dubna

Let us consider an Abelian gauge theory of massless fermions("quarks") ψ interacting with a massless neutral vector ("gluon") field A_μ. The generating functional of all Green's functions including the disconnected ones, is given by the pathintegral

$$Z(J,\eta,\bar{\eta}) = N\int \mathcal{D}A_\mu \mathcal{D}\psi \mathcal{D}\bar{\psi}\,\delta[\partial_\mu A_\mu] \times$$
$$\times \exp\Big\{ i\int d^4x \Big[\bar{\psi} i\hat{\partial}\psi - \frac{1}{4}F_{\mu\nu}^2 + g\bar{\psi}\hat{A}\psi + J_\mu A_\mu + \bar{\psi}\eta + \bar{\eta}\psi\Big]\Big\} \qquad (1)$$
$$F_{\mu\nu} = \partial_\mu A_\nu - \partial_\nu A_\mu\,, \quad \hat{A} = \gamma_\mu A_\mu$$

Here J_μ, $\bar{\eta}$, η are the external sources of the fields $A_\mu, \psi, \bar{\psi}$ and N is a normalization factor chosen such that $Z(0,0,0) = 1$. Note that the Lagrangian appearing in eq. (1) is invariant under chiral transformations $\psi \to \exp(i\gamma_5\lambda)\psi$. If we first integrate over A_μ we get a factor with the exponent ($\psi, \bar{\psi}$ are anticommuting Grassman variables)

$$\frac{i}{2}g^2\int d^4x_1 d^4y_1 d^4x_2 d^4y_2 \Big[\bar{\psi}_{\alpha_1}(x_1)\psi_{\beta_1}(y_1)\Big] K^{(x_1y_1;x_2y_2)}_{(\alpha_1\beta_1;\alpha_2\beta_2)} \times \Big[\bar{\psi}_{\alpha_2}(x_2)\psi_{\beta_2}(y_2)\Big] \qquad (2)$$
$$= \frac{i}{2}g^2\, tr\big[(\bar{\psi}\times\psi)K(\bar{\psi}\times\psi)\big]$$

where

$$K^{(x_1y_1;x_2y_2)}_{(\alpha_1\beta_1,\alpha_2\beta_2)} = (\gamma_\mu)_{\alpha_1\beta_2} D_{\mu\nu}(x_1-x_2)(\gamma_\nu)_{\alpha_2\beta_1} \times \delta(x_1-y_2)\delta(y_1-x_2) \qquad (3)$$

Here $D_{\mu\nu}(x)$ is the propagator of a massless vector meson in the transverse Landau gauge (see ref. /1/ for its definition). We now linearize eq. (2) by a (bilocal) Gauss integration x)

x) In ref. /2/ an analogous technique has been used for a nonrelativistic system of interacting fermions and bosons.

$$\exp\tfrac{i}{2}g^2 \mathrm{tr}\left[(\bar\eta\times\eta)K(\bar\eta\times\eta)\right] = \left[\det K^{-1}\right]^{1/2} \times \qquad (4)$$
$$\times \int \mathcal{D}\chi(x,y)\exp\left\{-\tfrac{i}{2}\mathrm{tr}\,\chi K^{-1}\chi - i\,\bar\eta_a\eta_b\,g\chi_{ab}\right\}$$
$$a\equiv(\alpha,x)$$

Performing the integration over the quark field and using eq. (4) the generating functional (1) reads finally

$$Z(J,\bar\eta,\eta) = N'\int \mathcal{D}\chi\, e^{iS(\chi)} Z(J,\bar\eta,\eta|\chi) \qquad (5)$$

with

$$S(\chi) = \mathrm{tr}\left[-\tfrac{1}{2}\chi K^{-1}\chi - i\ln(1+gG_0\chi)\right]$$
$$Z(J,\bar\eta,\eta|\chi) = \exp\left[-\tfrac{i}{2}J_\mu\cdot D_{\mu\nu}\cdot J_\nu + i\bar\eta G(g\chi-g\hat A_{ext})\eta\right. \qquad (6)$$
$$\left. + \mathrm{tr}\ln(1-gG(g\chi)\hat A_{ext})\right]$$

The Green's functions $G(g\chi-g\hat A_{ext})$ and G_0 are defined as follows $i\partial_x G_0(x-y) = -\delta(x-y)$ and

$$(i\hat\partial_x + g\hat A_{ext})G(x,y|g\chi-g\hat A_{ext}) - g\int dz\,\chi(x,z)\times \qquad (7)$$
$$\times G(z,y|g\chi-g\hat A_{ext}) = -\delta(x-y)$$

where $\hat A_{ext}$ is the external field associated to J_μ.

The functional $S(\chi)$ that appears as a weight factor in the funotional integral (5) may be naturally interpreted as the effective action of the bilocal field $\chi(x,y)$. The "classical" field M is then determined from the action principle by

$$g\frac{\delta S(\chi)}{\delta\chi}\Big|_{g\chi=M} = -K^{-1}M - ig^2\Gamma(M) = 0 \qquad (8)$$

or, multiplying from the left by K,

$$M_{\alpha\beta}(x,y) = -ig^2 D_{\mu\nu}(x-y)\left[\gamma_\mu G(x,y|M)\gamma_\nu\right]_{\alpha\beta} \qquad (9)$$

Here $G(x,y|M)$ is given by an equation like eq. (7) but without the term $g\hat A_{ext}$. This equation and eq. (9) do not involve the external sources. It is therefore natural to assume translational invariance of the solutions, i.e. $M(x,y) = M(x-y)$ and $G(x,y|M) = G(x-y|M)$. Eq. (9) is just the Schwinger-Dyson gap equation for the quark propagator in the lowest non-trivial approximation of perturbation theory. It was years ago the starting point of the finite QED of Baker, Johnson and Willey /3/ who have shown that it admits a nontrivial γ_5-symmetry violating solution.

Let us now calculate corrections to the symmetry breaking solution of eq. (9) by expanding the integrand of eq. (5) around the "classical" solution $M(x-y)$. If we shift

$$g\chi(x,y) = M(x-y) + g\phi(x,y) \qquad (10)$$

we obtain

$$Z(J,\bar\eta,\eta) = N\int \mathcal{D}\phi\, e^{-\frac{i}{2}\mathrm{tr}\,\phi S^{(2)}(M)\phi}\left[e^{iS_{int}(\phi)}\right]_\times \qquad (11)$$
$$\times Z(J,\bar\eta,\eta|M+g\phi)\Big]$$

with

$$S_{int}(\phi) = i\sum_{n=3}^{\infty}\frac{(-g)^n}{n}\mathrm{tr}\left[G(M)\phi\right]^n \qquad (12)$$

$$S^{(2)}_{(\alpha_1\beta_1;\alpha_2\beta_2)}(M) = K^{-1}_{(\alpha_1\beta_1\alpha_2\beta_2)}\left[\delta_{(\alpha_3\beta_3;\alpha_4\beta_2)} - ig^2 K_{(\alpha_3\beta_3;\kappa\epsilon)}G^{(M)}_{\kappa\alpha_2}G^{(M)}_{\beta_2\epsilon}\right]$$

Moreover, we define the propagator $D^{\phi}_{(\alpha\alpha;\gamma\delta)}(xy;x'y')$ of the bilocal field $\phi_{\alpha\beta}(x,y)$ by

$$D^{\phi}_{(\alpha\beta\gamma\delta)}(xy;x'y') \equiv i\langle\phi_{\alpha\beta}(x,y)\phi_{\gamma\delta}(x'y')\rangle_\phi = \left[S^{(2)}(M)\right]^{-1}_{(\alpha\beta;\delta\delta)}(xy;x'y') \qquad (13)$$

where $\langle\ldots\rangle_\phi$ means a functional average with the weight factor $\exp -\frac{i}{2}\mathrm{tr}\,\phi S^{(2)}(M)\phi$ (a normalization factor is suppressed). Using a Wick theorem we may also evaluate the functional averages of higher order produots of bilocal fields. We computated the two-particle Green's functions G, Δ of the quarks and vector gluons defined by

$$G_{\alpha\beta}(x,y) = \frac{1}{iZ}\frac{\delta}{\delta\eta_\alpha(y)}\frac{\delta Z}{\delta\bar\eta_\alpha(x)}\Big|_{\eta=\bar\eta=0};\quad \Delta_{\mu\nu} = i\frac{\delta}{\delta J_\nu(y)}\frac{\delta\ln Z}{\delta J_\mu(x)}\Big|_{\eta=\bar\eta=0}$$

In fig.1 and 2 we give the graphical expression of the bilocal propagator and of different terms in the expansion of the pathintegrals for G and Δ. The dashed lines represent the bilocal propagator. On the right-hand side the associated classes of Feynman diagrams are shown.

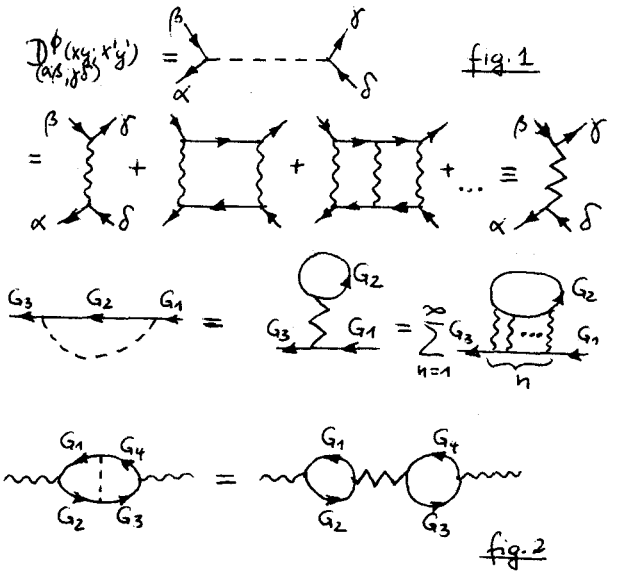


fig.1

fig.2

Acknowledgement

The authors would like to express their sincere thanks to D.I.Blokhintsev, A.T.Filippov, A.M.Polyakov, D.V.Volkov and M.K.Volkov for useful discussions.

Note Added

H.Kleinert has informed us that he has obtained similar results using bilocal techniques [4] (see also the contributions to this conference).

References

1. N.N.Bogolubov and D.V.Shirkov. Introduction in the Theory of Quantized Fields, Moscow 1971 (in Russian).
2. M.A.Braun. Works of the International Seminar of functional methods, FIAN SSSR, No.140, Moscow 1971.
E.S.Fradkin and O.K.Kalashnikov, ibida.
3. K. Johnson, M.Baker and R.Willey. Phys.Rev., 136, B1111 (1974).
M.Baker and K. Johnson. Phys.Rev., D8, 1110 (1973).
4. H.Kleinert. Univ. de Geneve prepr. (1976). and prepr. Freie Univ. Berlin (1976).

HADRONIZATION OF QUARK THEORIES AND BILOCAL QED

H.Kleinert

Institut für Theoretische Physik,
Freie Universität Berlin,Berlin,F R G

There are two approaches to strong interactions: Colored quark gluon theory (QCD) and the dual model. Either approach is powerful where the other has its weaknesses. In QCD, currents, their light cone properties, and their conservation laws (CVC,PCAC) can be studied without much effect. The spectrum, on the other hand, is very hard to calculate [1]. The opposite holds for dual models. Here the spectrum is obvious while proper currents have not yet been constructed.

Much work could be saved if the two approaches were, in fact, equivalent. Then one or the other could be used depending on whether long or short-range questions are to be answered.

We have been able to establish an equivalence of this type [2,3] for the simplified situation where gluons are color singlets with an arbitrary mass μ. Since quarks may have several flavours, this theory might be called quantum flavour dynamics (QFD). Using functional methods, we have transformed QFD into an equivalent bilocal field theory whose bare quanta propagate and interact just like hadrons in dual diagrams (only the dynamical property of duality itself is missing due to the absence of colour). Photons interact with hadrons via a current field identity. The bare quanta are quark-antiquark bound states as they arise from ladder exchange of gluons.

Since QFD contains a spontaneously broken chiral symmetry it gives naturally rise to massless π, K, etc.,mesons. The small physical masses of these mesons are obtained by introducing a small bare mass term.

In the limit of a large gluon mass, hadronized QFD simplifies considerably. The bilocal fields become local and describe π, ρ, σ, A, mesons in the standard σ model

Lagrangian [4,5,3] . This special case of hadronization is the four-dimensional analogue of the transition from the Thirring model to the sine-Gordon equation [6] . In solid-state physics it corresponds to the derivation of the Ginsburg-Landau equation from an electron Hamiltonian.

The σ model is known to account reasonably well for low-energy meson physics. Our derivation [5,3] yields additional connections between quark - and meson-properties. For example, the spontaneous breakdown of chiral symmetry generates a dynamical quark mass M which becomes related to the vector and axial-vector masses via

$$m_{A_1}^2 - m_\rho^2 = 6M^2.$$

From this one finds

$$M \approx 312 \text{ MeV}$$

The scalar mass is predicted:

$$m_\sigma = 2M \approx 624 \text{ MeV}.$$

The pseudoscalar masses vanish due to their Goldstone nature. If they are to have their proper physical values, bare quark masses $-\bar{\Psi} m \Psi$ have to be added to the Lagrangian with $m \approx \begin{pmatrix} 15 & & \\ & 15 & \\ & & 435 \end{pmatrix}$. This splits the dynamically generated mass M which now becomes a matrix

$$M \approx \begin{pmatrix} 312 & & \\ & 312 & \\ & & 432 \end{pmatrix}.$$

The masses M determine the vacuum expectations of scalar densities

$$\langle 0 | \bar{\Psi} \frac{\lambda^a}{2} \Psi | 0 \rangle = f_\pi^2 \, tr(\lambda^a M)$$

from which one finds an SU(3) violation in the vacuum of -16%.

I thank Dr.D.P.Mavlo for an interesting discussion.

References

1. A.A.Migdal, Czernogolovka preprint 1976.
2. H.Kleinert. Phys.Lett., 63 B (in press).
3. H.Kleinert, Erice Lectures 1976; Freie Universität Berlin, Preprint, June, 1976.
4. T.Eguchi and H. Sugawara. Phys.Rev., D10, 4257 (1974); H.Kleinert. Phys.Lett., 59B, 163 (1975).
5. H.Kleinert. Phys.Lett., 62B, 77 (1976).
6. For references see L.D.Fadeev's contribution to this conference.

P L E N A R Y R E P O R T

COMPOSITE MODELS OF HADRONS AND RELATIVISTIC BOUND STATES

A.T.Filippov

JINR, Dubna

1. Introduction

The main problems to be considered in this report are the following: 1) What are the constituents of the hadrons, what are their quantum numbers, and what are their broken and unbroken symmetries? 2) What is the dynamics of the constituents (equations, binding forces and the origin of symmetry violations)? The most puzzling question is: why the constituents "escape from freedom" and are confined inside the hadrons? 3) What experimentalists can tell us about the hadron constituents and their dynamics, if not finding them?

There are no final answers to all these questions. Today we can only give more or less plausible answers demonstrating that the questions are sensible.

Due to a great complexity of the matter, this review is by no means impartial. Nevertheless, the attempt is made to present also alternative views on the same problems. Many people have been thinking of these problems for years and it would be proper to remind their results having to do with the present-day concerns. "Those who do not remember the Past are condemned to repeat it" (Jaspers).

2. Constituents

2.1. A way to "Colour-ado"

The first model of composite hadrons was constructed by Fermi and Yang (1949) (F-Y). The constituents were the proton and the neutron, the pions being composed of them: $\pi^+ = p\bar{n}$, $\pi^\circ = \frac{p\bar{p} - n\bar{n}}{\sqrt{2}}$. The main difficulty of the model was the absence of $\pi_0^\circ = \frac{p\bar{p} + n\bar{n}}{\sqrt{2}}$ with mass roughly equal to that of the pion (Baldin et al.). The F-Y model was treated by physics community without any enthusiasm, but, as strange particles were being discovered, the attitude to composite models was becoming more friendly. In 1953 Goldhaber tried to compose all particles from p, n, K°, K^- (more symmetric form of this model was given by Frisch (1960), with constituents $\Lambda, K^\circ, K^+, \bar{K}^\circ, K^-$. A more natural extension of the F-Y model was proposed by Sakata (1956). All particles were assumed to be made of p,n and Λ (F-Y-S). This model successfully explained many facts of strong, electromagnetic and weak interactions, and in terms of it the SU(3) symmetry was first formulated (Markov, Okun, Ikeda, Ogawa, Ohnuki, Yamaguchi, Zeldovich et al.). With proper modifications, it still can be applied to the mesonic states. However, it could not naturally explain the baryon spectrum, and after the success of the eight fold-way approach to the SU(3)-symmetry (Gell-Mann and Ne'eman) it made the way to the quark model (QM) (Gell-Mann and Zweig). The essential difference of QM from F-Y-S model lies in the three-fermion structure of the baryons. The elementary particles in QM are the three spin-1/2 fermions(quarks) q: $u\ (Q=2/3, I=1/2, I_3=1/2)$, $d\ (Q=-1/3, I=1/2, I_3=-1/2)$ and $s\ (Q=-1/3, I=0)$, mesons being $\bar{q}q$ and baryons — qqq.

This model enables us to formulate the SU(6) spin-unitary spin symmetry (Gursey, Radicati, Sakita, Pais, B.Lee, Beg et al.) which, if properly formulated and used, gives qualitative understanding of hadron spectroscopy as well as collinear decays and scattering processes. The successes of this approach to hadron dynamics were summarized at the London conference /1/ and they are really impressive. Most impressive is the remarkable simplicity of the quark dynamics to be discussed below.

But let us turn to the difficulties. The main difficulty lies in understanding the baryon spectrum. In terms of the $SU(6) \times O(3)_L$ symmetry (L is the total orbital momentum of the quarks) the observed baryons are classified (see e.g. /2/) into the (mult. SU(6), L^P)

multiplets $(\underline{5}^6, 0^+), (\underline{70}, 1^-), (\underline{56}, 2^+), (\underline{56}, 0^+)_R$ ... with no candidates for $(\underline{20}, L^P), (\underline{56}, 1^-), (\underline{70}, 0^+)$ etc. Here eight $J^P = 1/2^+$ baryons and ten $3/2^+$ resonances nicely complete $(\underline{56}, 0^+) = (\underline{8}, 1/2^+) + (\underline{10}, 3/2^+)$ But why do they belong to $(\underline{56}, 0^+)$?

With Fermi statistics for quarks, it is extremely difficult, if not impossible, to construct a petential which gives a large mass for antisymmetric in spin and unitary spin $\underline{20}$ and the mentioned peculiar correlation of the SU(6)-structure to L^P (Instead , it is easily understandable with Bose-quarks). Even worse, the nonexistence of exotic states $qq\bar{q}$, $qqq\bar{q}$ (the triality puzzle) and qq (the diquark puzzle) says us that something essentially new must be added to the Gell-Mann -Zweig model. In view of these difficulties a new degree of freedom was introduced in 1965 by Bogolubov, Struminsky, Tavkhelidze et al. /3/ and by Han and Nambu /4/ . Each quark was supplied by a new quantum number (now called the "colour"), and it was postulated that the lowest baryon multiplets are made of quarks of different colours(i.e., "colourless"). The difficulty with the statistics was immediately resolved while the triality and diquark puzzles were reformulated in terms of the problem that coloured states must be much heavier than colourless ones.

Now we have three families of quarks (u_R, d_R, s_R), (u_B, d_B, s_B) and (u_G, d_G, s_G) (red, blue and green). There are two essentially different possibilities for prescribing to these quarks the usual quantum numbers (now called the "flaveurs"). It is most natural to introduce a symmetry in the colour space, say $SU(3)^C$ (the other possibilities were also discussed). Then, if the electric charge Q is the colour--singlet, the quarks of all coleurs have identical flavour quantum numbers (fractional charges) and the SU(3) - symmetry must be unbroken. Alternatively, if we assume Q to be colour non-singlet, the quarks may have integer charges and the $SU(3)^C$ need not be the exact symmetry. Other approaches to the statistics paradox (e.g. Greenberg /5/) are generally connected with violations of the spin-statistics theorem for quarks and, hence, require a revision of the foundations of the quantum field theory.

2.2. Charmed Colour-ado. How many flavours?

The primary motivation for introducing new flavours (charmed quarks) was simple: why not have a higher flavour symmetry, say SU(4) (Tarjanne, Teplitz; Hara; Maki, Ohnuki; Vladimirsky; Gerstein, Whippman; Bjorken, Glashow, Amati et al.; Okun et al., for refs. see eg./6/).

Later it became clear that the fourth quark (c) is indeed useful for making weak interactions internally consistent (Glashow, Illiopoulos, Miani). Without extra quarks and/or leptons all usual formulations of weak interactions badly violate universality and cannot survive. With the charmed quark we can also restore the lepton-quark universality. Finally, the existence of strangeness - conserving neutral weak current and the absence of the strangeness-changing ones is easily explained only in the theories with extra quarks. Thus we have very good reasons to believe in the fourth quark.

The discovery of J/ψ family (Ψ) tells us that we are on a right track interpreting them as $c\bar{c}$ /7/ . Of course, there are more exotic explanations of the Ψ - particles but we can say that in general the charmonium $(c\bar{c})$ spectrosoopy is today in a good shape (see esp. the talk given by De Rujula at this conference). As we have heard at this conference there is a reason to believe that a particle $D = u\bar{c}$ (c is the charmed quark), was discovered at SLAC. If confirmed, this would give the c - quark the same status as the older, uncharmed quarks (being necessary though invisible). But are we in need of more quarks?

The experiments, much discussed at this conference, seem to tell us that the introduction of one or two extra quarks ("t" and "b", e.g.) would be harmless and even agreable. The large R in e^+e^- annihilation into hadrons, dilepton events, anomalies in ν - reactions, etc., are most naturally understood with five or six flavours of quarks and some new leptons [8] . Such new flavours were discussed as soon as ψ was born (Barnett; Harari; P.Bogolubov, Matveev, Kuz'min, Tavkhelidze et al.; Mohapatra, Pati; Fritzsch, Minkowski; Wilczek et al. [9,10]). Later it was suggested that more than three quark flavours are required in unified theories of the weak, electromagnetic, and strong interactions based on a single gauge group, if one wants to avoid the introduction of extremely heavy gauge bosons ($\gtrsim 10^{15}$GeV). The minimal number of quark flavours in this approach is six (for a detailed explanation and references see: Fritzsch [10]). Introduction of new quarks and leptons allows one to construct beautiful vector- like theories of weak interaction (for refs. see [10]) ; unfortunately they are in a bad shape at this conference. However, there exist other (less symmetric) theories of weak interactions with extra quarks and leptons [11],[12] which do not contradict present experiments [8] .

There exists an entirely different approach to the problem of the flavour degrees of freedom which attempts to give the internal symmetry space a geometric meaning. As has been argued by Arbuzov and Filippov [13] for weak interactions, and by Ne'eman [14] for strong interactions, giving a geometric meaning to the elementary particle interactions (i.e., connecting them with a curvature of the space-time) requires an embedding of the space-time into some N-dimensional space. The minimum value of N is 10, as we can locally embed any curved 4-dimensional space into some 10-dimensional space ($g_{\mu\nu}$ has 10 independent components). Hence, the dimension of the compact internal space must be not less than 6. The corresponding symmetry group according to [13,14] must be SO(6) which is locally isomorphic to SU(4). It should be stressed that this is not the final answer. In fact, in a geometric theory of this type the dimension and the structure of the internal space is dependent of the interaction which, in turn, has to be deduced from geometric constraints (see [13]). The solution of all such constraints is a challenge, very little known as yet even how to approach this problem.

The geometric approach was recently revived in an attempt to construct a consistent dual theory of hadrons in the four-dimensional space-time. As has been earlier suggested by Fubini and Veneziano [15] , the extra dimensions (26-4 or 10-4) required by consistency of dual models can be ascribed to the "internal" space ("flavour space"). Then for a large enough dimension of the flavour space the dual theory could be realized in the 4-dimensional space-time . This idea combined with the geometric approach to the origin of symmetries is being investigated by Scherk, Schwartz et al. [16] . As the most difficult problem of solving geometric constraints is not yet clarified, it is premature to deduce from their results any predictions concerning flavour symmetries. The only firm prediction is that the flavour space must be large enough; the larger is the dimension, the easier is the solution of the geometric constraints.

To my mind, the most unsatisfactory feature of all above mentioned approaches to flavours is their inability to explain colours. Usually one asks the questions: how many quarks are there? and what is the flavour symmetry group? Probably these questions are unfair to Nature as stressed by Salam at this conference. Our primary concern must better be not the number of

quarks and leptons but the number of conserved charges and the nature of fundamental laws, controlling the "elementary" particle phenomena. We think that a "colour-blind" person cannot find such laws.

2.3. Confining colours give birth to flavours

What is the most fundamental thing in hadrodynamics? We cannot answer this question, but we know the most puzzling thing: coloured particles (quarks, diquarks e.a.) do not occur in the physical spectrum. If this is not merely the low energy phenomenon, then the colour, being exactly conserved, has a chance to be the most fundamental property of quarks, and the colour conservation has to be considered as one of the most fundamental laws of Nature. With permanently frozen (confined) colour degress of freedom, we face the novel feature of particle dynamics, probably requiring a revision of some basic ideas. Some people proposed that the phenomenon of confinement is "simply" reduced to disappearing the quark pole from the quark propagator in nonperturbative solutions of quark field theory. It is possible, but our task is much more ambitious: to construct colourless bound states and to prove that coloured states never appear in the physical world. There might be some analogy with quantum electrodynamics, where the longitudinal and "time-like" photons play a significant role in intermediate states but completely decouple from all asymptotic physical states (in modern usage they are "confined gluons" . For quantum description of this decoupling it is necessary to supply the Hilbert space with indefinite metrics. This simple trick does not help to confine much more complicated colour degrees of freedom, and it is quite possible that a more radical modification of the physical laws is necessary for describing coloured quarks.

The most radical approach to colour was proposed by Gursey /17/ et al. He suggested that the matrix elements of the quark field operators are octoniens (Cayley numbers) instead of being complex numbers. The octonien can be written as $\gamma_0 + \sum_{A=1}^{7} \gamma_A e_A$ where γ are real (or complex) numbers and e_A are "imaginary units": $e_A^2 = -1$. The multiplication law of e_A is non-commutative and non-associative (generally $(ab)c \neq a(bc)$). Like real and complex numbers, and quaterniens, which can be used for describing the spin, the octoniens form a normed algebra $\mathcal{O}$ having a unit element (in fact $\mathcal{O}$ is the highest dimensional algebra having such properties). Replacing complex numbers by octoniens we are forced to replace the i ($i^2=-1$) in the translation operator $e^{-ip_\mu x_\mu}$ by one of the new imaginary units, say e_7. It appears that the subalgebra of $\mathcal{O}$ which commutes with translations $e^{-e_7 p_\mu x_\mu}$ is isomorphic to the algebra of SU(3). This is identified with $SU(3)^c$ and the quark fields are represented by $q_\alpha^n u_n$ where $u_n \in SU(3)^c$ and α is the flavour index. Due to the non-associativity of octoniens, only colourless operators can be observable quantities.

With octonionic quarks the nightmarish quark-parton paradox can be resolved. It can be formulated as follows /18/ : the m.e. $\langle p|\bar{\Psi}_1(x)\Psi_2(0)|p\rangle$ has vanishing Fourier components if p_0 is below the colour-production threshold (∞ for permanently confined colour) and this is inconsistent with the early scaling in deep inelastic processes. In other words, how can one explain scaling with zero imaginary part of the quark propagator? The proof is based on inserting $I = \sum |n\rangle\langle n|$ between quark fields Ψ_1 and Ψ_2 and on using the translations. For octonions $\langle\alpha|[(\sum_n |n\rangle\langle n|)|\beta\rangle] \neq \neq \sum_n (\langle\alpha|n\rangle)(\langle n|\beta\rangle)$ and the proof is no longer

valid. This simple example is given to dramatize the difference between the usual and octonionic quark theory, the novel aspects of which deserve a careful investigation.

The octonionic approach also brings a new light on the choice of flavour groups. Octoniens are associated with representations of exceptional Lie algebras (e.g. G_2 is the automorphism group of the octonion algebra, for other groups the relation is more complex). For all exceptional simple Lie algebras the representations cannot be constructed in terms of usual matrices. To construct the representations of the exceptional groups G_2, F_4, E_6, E_7, E_8 the octonionic matrices (Jordan algebras) or their direct products (B.A.Rosenfeld algebras) must be used. For example the fundamental 27 dimensional representaion of E_6 can be realized in terms of the Jordan matrices which are 3x3 hermitian matrices with octonionic entries, etc. All exceptional groups contain G_2 as a subgroup which, as we have seen above, contain $SU(3)^C$. The group structure is as follows:

$F_4 \supset SU_3^C \times SU(3)$;

$E_6 \supset SU_3^C \times SU(3) \times SU(3)$;

$E_7 \supset SU_3^C \times SU(6)$;

$E_8 \supset SU_3^C \times SU(3) \times SU(3) \times SU(3)$.

Remark that all $G_{(flavour)}$ have no abelian part. The fundamental representations of the most interesting group E_7 are:

$$\underline{56} = (\underline{20},\underline{1}) + (\underline{6},\underline{3}) + (\underline{6},\underline{3}) \;/(SU_6, SU_3^C)\text{-classification/}$$
leptons quarks

As Q is the colour singlet, $Q \subset SU_6$ and we have $\sum_{\text{quarks}} Q = \sum_{\text{lept.}} Q = 0$. The charges of quarks are naturally fractional If we suppose that there is the usual SU(3)-triplet of quarks u, d, s with $Q_u - Q_d = +1$, $Q_d = Q_s$, then the charges of all quarks are uniquely determined $Q_q = (\frac{2}{3}, \frac{1}{3}, \frac{1}{3}, \frac{2}{3}, \frac{1}{3}, \frac{1}{3})$ and similarly the charges of leptons $\left((\text{lept.})\widetilde{SU_6}\ (6\times 6\times 6)\ (_{\text{antisymm.}})\right)$ must be $(\pm 1 \pm 1 \pm 1 \pm 1$; 12 neutrals). If we introduce gauge bosons (which is by no means necessary) we have the adjoint representation

$$\underline{133} = (\underline{35},\underline{1}) + (\underline{1},\underline{8}) + (\underline{15},\underline{3}) + (\underline{15},\underline{3})$$
gauge bosons; gluons; leptoquark bosons

It can be shown that theories based on exceptional groups /12/ are welcomed by recent experimental discoveries /8/ , but we will not dwell upon this. We only stress that among "simple" (mathematical term!) exceptional groups only E_7 is a plausible candidate (giving more than 3 quarks and large enough number of leptons, but not containing colour octet quarks). Hence, there must be six and only six quakrs -NO MORE QUARKS!

2.4. Alternatives

There are other approaches to the flavour symmetries not considering the colour conservation as a fundamental law. Pati and Salam /19/ introduce the following fundamental fermions: $\ell = (\nu_e, e^-, \mu^-, \nu_\mu$; $L=1, B=0)$ $\mathcal{C} = C_R^0, C_B^-, C_G^-$ ($L=1$, $B=1$, coloured) and S^0 ($B=1$, $L=0$, colourless). The quarks are made of leptons ℓ and prequarks $\mathcal{C}$, S^0: $u_R = \nu_e \bar{C}_R^0 S^0$, $d_R = e^- \bar{C}_R^0 S^0$, $S_R = \mu^- \bar{C}_R^0 S^0$, $C_R = \nu_\mu \bar{C}_R^0 S^0$ etc. Their integer-charge quarks are unconfined and unstable, with the lifetime $\sim 10^{-11}$ - 10^{-12} sec and hence can be found in emulsion experiments. This scheme is rich enough and flexible enough to be compatible with present experiments.

There exist suggestions to revive the Goldhaber model (Lipkin /20/) and F-Y-S model (Tyapkin /21/) which are not yet elaborated to be confronted with experiment. Finally, we note that some dualists propose the infinity of quarks and the corresponding

additive quantum numbers (D.V.Volkov [22]). Others, however, insist on finite number of quakrs [16] . We cannot go into discussion of these ideas.

3. Dynamics of quakrs

3.1. Independent quarks

As has been mentioned above, the simplest versions of the quark dynamics in which quarks are supposed to be almost freely moving inside a sphere gives very good quantitative results. Essential ingredients of this dynamics ("quasi-independent quark" model, which we now call the "Dubna bag") proposed by N.N.Bogolubov e.a. (see [3]) and further developed and improved by P.N.Bogolubov [23] are as follows. The quark mass outside the sphere (bag) is very large (or infinite) and it is very small inside the bag ($\sim \frac{m_M}{2}$ for mesons M and $\sim \frac{m_B}{3}$ for baryons B). The magnetic moments of baryons are explained by small effective masses of quarks inside the bag. The important new results which could not be obtained in the phenomenological SU(6) approach are: the magnitude of μ_p , the correct results for G_A/G_V , and $\langle r_p^2 \rangle_{e.m.}$ [23] . Of special importance is the good result for G_A/G_V (instead of 5/3 from SU(6)). At this point the relativistic corrections of the order of $\frac{\langle \vec{p}_q^2 \rangle}{m_q^2}$ or the contribution of the orbital motion of quarks inside the bag are crucial. The explicit expressions are roughly the following $G_A/G_V = \frac{5}{3}\langle \sigma_z \rangle$, $\mu_p = 3\left(\frac{e}{2m_p}\right)\langle \sigma_z + L_z \rangle$. As $\langle J_z \rangle = \langle \frac{1}{2}\sigma_z + L_z \rangle = \frac{1}{2}$ we can express G_A/G_V and μ_p in terms of $\langle L_z \rangle$. Describing the bag by a scalar spherical well potential (the cavity) and finding the Dirac wave functions of quarks moving inside the bag, it can be found that $G_A/G_V \approx 1.1$, $\mu_p \approx 2.5$, $\langle r_p^2 \rangle \approx 0.43/m_\pi^2$ [23] . We do not discuss the applications of this approach to mass formulae where the results are similar to other models (e.g., the nonrelativistic models with the oscillator potential [24]). For further discussion see papers by P.Bogolubov and B.Struminsky (these proceedings).

Relativistic corrections are also of importance in weak and electromagnetic decays of hadrons involving the annihilation of quarks ($\rho \to \ell\nu$, $\nu \to e\bar{e}$). The naive non-relativistic treatment of such processes has led to a rather paradoxical conclusion that e.g. $\left|\frac{\Psi_{q\bar{q},\pi}(0)}{\Psi_{q\bar{q},K}(0)}\right| \sim \frac{m_\pi}{m_K}$ in contrast to the supposed SU(3) symmetry of the $q\bar{q}$ potential. These processes were first treated by Matveev, Struminsky and Tavkhelidze [25] , very clear and comprehensive representation of the quark model results for different decays was given by Van Royen and Weisskopf [26] . The resolution of this paradox lies also in relativistic corrections (Struminsky, Llewellyn-Smith [27]). In relativistic theory, based e.g. on the Bethe-Salpeter equation, there are no apparent paradoxes with SU(3)-symmetry. The main idea of calculating the processes

$$h \to h'(e^+e^-),\ h \to h'(\ell\nu),\ h \to h'\pi(K)$$

consists in taking into account only one-quark transitions. This assumption is a generalization of the well-known Okubo-Zweig-Iizuka (OZI) rule and it was successfully applied for the mentioned hadronic decays. The calculations of L.Soloviev, Anisovitch et al.; Thirring, Becchi Morpurgo et al. used non-relativistic approximation. For a very clear and comprehensive presentation of these and other results of N.R.Q.M. see [28] .

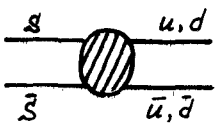
The consistent relativistic approach based on the Logunov-Tavkhelidze quasipotential equations for relativistic bound states was developed by N.Bogolubov, Matveev and Tavkhelidze [29] . The essence of their approach is the calculating of the moments of the currents V_μ^i, A_μ^i between bound states. With this aim they introduce external field v_μ^i, a_μ^i

interacting with corresponding currents and consider the case of small, slowly varying external fields. Then the variations of the energy of the bound state with respect to external field gives the matrix elements of the currents. This method enables one to reproduce all the nice results of the model of quasiindependent quarks and to obtain more general results. For example,

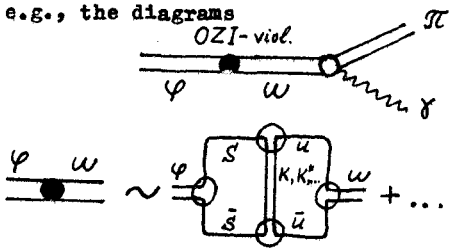
$$\frac{G_A}{G_V}=\frac{5}{3}\left(1-\frac{\langle \bar{p}_q^2\rangle}{3m_q^2}+\dots\right),\quad \mu_p=\frac{e}{2m_q}\left(1-\frac{\langle \bar{p}_q^2\rangle}{6m_q^2}+\dots\right).$$

Similar results were derived by Gell-Mann, using the algebra of "good" components of currents in the $P_z\to\infty$ frame [30] and by Shelest et al. [31] in the framework of relativistic bound-state equations supplemented by the Markov-Yukawa condition [55]. Using PCAC one can calculate the processes $h\to h'\pi$ etc. With different binding "potentials" (e.g., square well, oscillator) the more detailed predictions can be obtained. However, it is difficult (if not impossible)to describe all existing data by a single potential, and the introduction of some phenomenological parameters is necessary. This is the essence of the so-called current -constituent quarks approach to hadronic decays summarized at the London conference [1] .

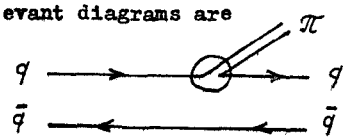
The essential ingredient of all these calculations is the OZI-rule, used to describe the different construction of the PS-multiplet and V (or T) multiplets. For the vector (tensor) mesons it is supposed that the process



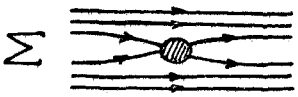
is very small while for PS-mesons it is appreciable. Then φ, f' are almost pure $s\bar{s}$-states, ω, f almost pure $\frac{u\bar{u}+d\bar{d}}{\sqrt{2}}$ states, while η and η' are certain mixtures of $s\bar{s}$ and $\frac{u\bar{u}+d\bar{d}}{\sqrt{2}}$. The effect of mixing is easily taken into account by considering e.g., the diagrams



For pure hadronic decays the only relevant diagrams are



If we consider the scattering process then, as first suggested by Levin and Frankfurt [32] the process is described by the sum of the diagrams with one-quark transition.



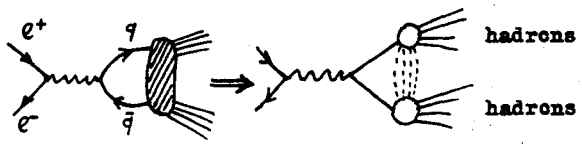
This is a generalization of OZI-rule for scattering processes. The predictions of the model are in reasonable agreement with experiment but show systematic deviations which can be naively interpreted as the result of somewhat smaller radius of the strange mesons [33], we will discuss some related considerations in meson spectroscopy in what follows.

The simple-minded approach of independent quarks moving inside a cavity is supported by ideas of quark-parton models of Feynman, Bjorken, Weisskopf, Kuti et al. [34] giving very clear and good description of all existing data on deep inelastic scattering of leptons on nucleons. The only cloud in this clear picture is the fact that the quarks are carrying only a half of the total momentum of the nucleon. The missing momentum is usually attributed to fashionable "gluons", but this is only another way of stating our essentially incomplete understanding of the quark-parton structure of the hadrons. The results of comparison of $\gamma N\to\dots$ and $eN\to\dots$ are in good agreement with the fractionally charged quarks. However, as was argued by Salam, Pati, Roy and Rajakes-

ran (see [35]) in theories with unconfined colour there exists a possibility that the quark charge sum rule is also consistent with integrally charge quarks.

Still ether very impressive prediction of simple quark model is the quark counting rule for exclusive processes with high transverse momentum (Matveev, Muradyan, Tavkhelidze; Brodsky, Farrar [36]). Not going into discussion of its nature we only mention that it rests on the assumption that the wave function of constituent quarks is finite when all quarks are at the same point, i.e., $\Psi(x=0) = \int d^4k\, \tilde{\Psi}(k) < \infty$. Hence, in such processes the short-distance behaviour of the bound-state wave function is directly proved. An interesting problem is to extract from the scattering data some information concerning the wave functions.

Remind finally the application of the quark-parton model to the reaction $e^+e^- \to$ hadrons

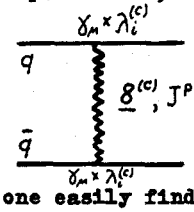


with clearly visible in SLAC experiment " jet structure", corresponding to $q\bar{q}$ pair. This dramatizes the mechanism of hadron production through the intermediate state of two quarks.

3.2. Dynamical role of colour: confining independent quarks.

Here we discuss some ether ideas about the dynamical role of colour. The radical ectonion approach is attractive, but, even if it is correct, it only gives a new frame for dynamics. It is also probable that there are different ways leading colour to confinement, and we are free to choose one that provides us with the simplest understanding of the hadron phenomenology.

The main facts of baryon spectroscopy can be explained in remarkably simple terms. Considering the SU(3)-invariant potential, corresponding to the exchange of colour-octet vector mesons (Nambu; O.Greenberg and Zwanziger; Lipkin [37])



$$\mathcal{L}_{int} = g\bar{q}\gamma_\mu \lambda_i^{(c)} q V_\mu^i$$

one easily finds that the effective coupling constants in different channels are

channel	qq	qq	$q\bar{q}$	$q\bar{q}$	qqq	...
SU(3)	$\underline{3}^c$	$\underline{6}^c$	$\underline{1}^c$	$\underline{8}^c$	$\underline{1}^c$	
$g^2_{eff.}$ (arb.units)	−4	+2	−8	+1	−12	

If the free quarks are heavy ($m_q \to \infty$) then the coleurless states are, on this scale, massless, i.e., "confined". From the above table one can infer that the mass of the colour-triplet diquark state is of the order of the quark mass. This makes the successful quark-diquark picture of the baryon [125] quite naturally emerging in this approach.

The colour-exchange vector potential was originally used for integrally charged quarks. If we take the colour-singlet charge operator (hence, fractionally charged quarks) and suppose that coleured vector mesons are massless Yang-Mills mesons, corresponding to the exactly conserved SU(3) gauge group, we arrive at "Quantum Chromodynamics" QCD (for refs. see e.g., [10]) (Gell-Mann, Weinberg et al.). As is by now well-known, such theories enjoy asymptotic (ultraviolet, U.V.) freedom (A.F.), i.e., the effective coupling constant $g(p^2)$ is vanishing for $p^2 \to \infty$.

It is generally believed that in asymptotically free theories there is a good reason to rely upon perturbation theory. Even if this is true for the estimate of the small-distance behaviour of the coupling constant,

the perturbative results for quark scattering amplitudes and bound states cannot be trusted. For example, consider the Logunov-Tavkhelidze or B.-S. equation with asymptotically-free potential. It is not difficult to demonstrate that for small r it can be reduced to a Sohrödinger-type equation with the potential of the form $V(r) \underset{r\to 0}{\approx} g^2 r^{-2}\left(1+g\ln\frac{r_0}{r}\right)^{-\alpha}$, $\alpha>0$ /38/ . The solutions of this equation have an essential singularity in the g-plane for which cannot be traced in perturbation theory. In addition, the scattering amplitude has an essential singularity in the ℓ-plane ($\ell=0$ for spinless particles). In the non-relativistic theory the singularity in the ℓ-plane has later been investigated by Oehme et al./39), who treated the simpler potentials: $V(r)=$ $=g^2 r^{-2}\left(\ln\frac{r_0}{r}\right)^{-\alpha}$, $\alpha=1,2$. Some general arguments in favour of the existence of the g-plane essential singularity were recently given by Shirkov /40/ who considered the theories with the Landau-Pomeranchuk null-charge phenomenon, using the renormalization group equations and a spectral representation for the invariant charge. It would be of great interest to extend his analysis to A.F. theoreis. The moral of this discussion is: using perturbation theory arguments for investigating U.V. behaviour in A.F. theories requires some caution.

The attitude of the QCD proponents to the infra-red (I.R.) behaviour of the theory with massless gluons is strikingly different. In fact, it is proposed to entirely disbelieve perturbation theory and to search for some peculiar non-perturbative solutions. The reason for this lies in the fact that the QCD can make sense only if coloured states are confined. So it is supposed that the effective interaction constant $g(p^2)$ which tends to 0 for $p^2\to\infty$ (small distance), infinitely grows for $p^2\to 0$ (large distance) providing the desirable confinement. Hence, the slogan of chromodynamists (Wilson, Susskind, Kogut; A.A.Migdal, Polyakov et al., for review and refs. see e.g. /41/): "Ultraviolet Freedom is Infrared Slavery".

The existence of the confined phase was demonstrated for some lattice theories as long as the lattice constant R was kept finite. The principal questions are; 1) is confinement preserved when $R\to 0$; 2) is the confined phase stable against external perturbation? 3) does the confinement work for all sectors of the Hilbert space and for all energies? (remind that the structure of the Hilbert space and observables in such a theory would be very unusual). Up to now there are no convincing answers to these questions. The recent progress in understanding the confinement of quarks in lattice gauge theories has been reviewed at this conference by Wilson /41/ . An attempt to construct a theory of composite hadrons in such a theory is presented at this conference by Bardeen /42/ . The light-front formulation (to be discussed below) of the QCD is used with a transition to the lattice variables in the transverse direction. Supposing the existence of a new phase of the theory (not realized in the usual perturbative solution), in which the transverse gauge invariance is exact, an attractive theory of composite hadrons can be formulated. However, the proof of the existence of such a phase is still lacking, the proof probably could be given for the finite lattice constant but there is no idea how to pass to the continuum limit.

The main difficulty of the confinement theories lies in that the perturbatien theory exhibits no hints for finding the confinement mechanism (Appelquist et al. /43/). The I.R.behaviour in nonabelian gauge theories seems to be very similar to that of QED. Alternative calculations were performed by Cornwall and

Tiktopoules. They claim that the summation of leading logarithms gives confinement, i.e., $\lim_{\mu\to 0}\sigma(\mu)=\lim_{\mu\to 0}\sum_{\text{leading}}\sigma^{(n)}(\mu)$ is zero for some matrix elements $\sigma(\mu)$ with colour creation. Even if these (very difficult) calculations are technically correct, we cannot rely upon this result. Some time ago it was shown (Arbuzov et al. /44/) that when you sum up a logarithmic series which in this case is almost certainly not convergent (most probably it is the asymptotic series) the summation of the leading logarithms usually gives a result which has very little in common with the exact sum. Therefore, unlike the U.V.freedom, the I.R.slavery is not in good position.

Concluding this discussion we stress that the QCD is a very promising theory of hadrons composed of confined coloured quarks, even if we forget the most ambitious attempts to unify all the interactions /10/ and some interesting phenomenological applications to be discussed below. However, it can be regarded as a real theory (not merely a new "religion" of theorists) only after having answered the fundamental questions discussed above.

3.3. Relativistic bound states

A) Now we turn to equations describing relativistic bound states. The systematic approach to this problem has been developed by Fock and Podolsky in 1932 (F.-P). It is based on a three-dimensional one-time formulation of the bound-state equations. In the alternative approach (Dirac, Fock, Podolsky, 1932, D-F-P) an individual time variable is assigned to each particle (for further details and refs. see /45/). The first is not covariant while the second is obviously covariant. Both approaches have given many fruits. The F-P approach in the formulation of Tamm and Dancoff was applied to meson theory (Dyson, Low) and for nucleon-nucleon interaction (Klein, Levy, Macke). The development of the D-F-P approach resulted in covariant equations for bound states (Nambu; Salpeter, Bethe, Schwinger, Gell-Mann, Low) /47/ (Some relations between both approaches have been investigated by Zimmermann /46/ .

However, in both approaches serious difficulties were found. After having found the rules for calculating matrix elements of currents between bound states and the normalization conditions (Nishijima; Mandelstam) and with some exact solutions in the ladder approximation (Wick, Cutkosky; Okubo, Feldman; Goldstein; Nakanishi; Kummer, et al.) it became clear that the price for covariance was quite high-physical interpretation of the bound state solution is unclear /47/ . There exist solutions of the Bethe-Salpeter equation with negative norm (violating unitarity) and solutions with exotic J^{PC} not occuring in the nonrelativistic limit, e.g. for $N\bar{N}$ or $q\bar{q}$ system $J^{PC}=0^{--},0^{+-},1^{-+},2^{+-},\ldots$ are exotic and we never saw such states. Both phenomena have a common source - the presence of the relative time in the bound state equations. The states with negative parity with respect to the relative-time reflection may have negative norm and/or exotic J^{PC} /47/ . For example, the solutions of the B-S equation for the pion are of the two types: the normal solution $F_\pi \cong \gamma_5 f(p^2,(pk)^2)$ and the anomalous solution $F_\pi \cong \gamma_5 (pk) f(p^2,(pk)^2)$. Due to a factor $(pk)=p_0 k_0$ for $\vec{k}=0$ the last solution has $J^{PC}=0^{--}$. All such anomalous states disappear in the nonrelativistic limit or in the equal time limit. However, as we have argued earlier, any reasonable theory of $q\bar{q}$ bound states must be relativistic. Besides this, the old equal-time formulations were extremely complicated in contrast to the relatively simple B-S equations.

B) The escape from these difficulties was found by Logunov and Tavkhelidze /48,45/ who proposed the quasipotential approach to quantum

field theory which unifies the physical simplicity of the equal time formulation and the mathematical simplicity of the covariant formulation. The main idea is that only the on-mass-shell scattering amplitudes are relevant for calculating bound states, and the potentials are expressed in terms of these amplitudes. The simplest example of such an equation for equal-mass spinless constituents is, in coordinate space,

$$(\Delta + K^2)\,\Psi_{\bar k}(\bar r) = (m^2-\Delta)^{-1/2}\, g\, \frac{V(r,K^2)}{r}\, \Psi_{\bar k}(\bar r)$$

where $\bar K^2 = \frac{1}{4}M^2 - m^2$, m – the constituent mass, M — the bound state mass $(s = M^2)$ $\bar r$ – the three dimensional relative coordinate, $\bar r = (\bar r_q - \bar r_{\bar q})$ in the CMS. This is the Fourier transform of the momentum-space equation of the form

$$\varphi_{\bar k}(\bar p) = \int \frac{d^3q}{\sqrt{m^2+q^2}}\, \frac{g\, \sigma((\bar p-\bar q)^2, K^2)\, \varphi_{\bar k}(q)}{\bar k^2 - \bar q^2 + i0}$$

Formally it can be derived from Lippman-Schwinger (L-S) equation by substitution $d^3q \to \frac{d^3q}{\sqrt{m^2+q^2}}$

This equation was generalized for unequal-mass case and for bound states of particles with spin 1/2, and was successfully applied to numerous problems in elementary particle /45/ and nuclear physics /49/ . Mathematically, the Logunov-Tavkhelidze (L-T) equation is somewhat more complicated than the non-relativistic Schrödinger equation. Nevertheless for large classes of the potentials different mathematical methods can be successfully employed for solving bound-state problems /50,51/ . The L-T equation has the correct small distance behaviour in the sense that it correctly reproduces the small distance behaviour of the wave function and the singularities of the scattering amplitude in the l-plane (poles and cuts) obtained in the corresponding field theories. For example, if we calculate the quasipotential in any given quantum field theory by using the perturbative expansion, the resulting L-T equation for the scattering amplitude $M(s,t)$ correctly reproduces each order of perturbation theory, and the asymptotic behaviour of $M(s,t)$ for $s<0, t\to\infty$ coincides with that of the sum of the corresponding ladder diagrams /52/ . Moreover, the differential formulation of the L-T equation /50,51/ can be used for finding scattering amplitudes and bound states in non-renormalizable theories when perturbation theory is inapplicable /51,53/.

A large class of other quasi-potential equations can be obtained by substitution

$$(m^2-\Delta)^{-1/2} \to f\left((m^2-\Delta)^{1/2}, (m^2+K^2)^{1/2}\right)(m^2+K^2)^{-1/2},$$

where $f(x,x) \equiv 1$. All these equations, like L-T equation, satisfy two-particle unitarity and, with energy-dependent potential $V(r,K^2)$ can incorporate many-particle unitarity. A rather simple equation useful for the description of tightly bound states can be obtained with $f = \frac{m^2+K^2}{m^2-\Delta}$ (Filippov, see also /50/). Then the bound state equation

$$(m^2-\Delta)(\Delta+K^2)\Psi_K(r) = \sqrt{m^2+K^2}\, g\, \frac{V(r,K^2)}{r}\, \Psi_K(r),$$
$$\sqrt{m^2+K^2} \equiv M/2$$

is of the fourth order (with four boundary conditions) and in it the effective potential automatically vanishes for $M \to 0$ (Correspondingly, for not very singular potentials there are no $M=0$ bound states). Most of other formulations of quasipotential equations as well as of the B-S equation have the difficulty that with any deep enough attractive potential the mass of the bound state is imaginary.

Another variation on this theme is the equation proposed by Todorov /45/

$$(\Delta + K^2)\,\Psi_K(r) = (m^2+K^2)^{-1/2}\, g\, \frac{V(r)}{r}\, \Psi_K(r).$$

This equation is useful in calculating high-energy ($K^2 \to \infty$) behaviour of the elastic scattering in $\lambda\varphi^3$- type theories but it is singular for $K^2 \to -m^2 (M \to 0)$ and the potential $V(r)$ is more singular for $r \to 0$ than in the L-T equation (in the above case of the fourth-order equation the potential is effectively less singular). These modifications are mathematically simpler, than the L-T equation, and there are rather general methods allowing one to obtain some analytical solutions for more or less simple potentials /50,51/ .

There have been proposed many other modifications of the original L-T equations (Kadyshevsky, Gross, Thompson, Fronsdal, Todorov, Yaes, Klein et al.) /45,49/ . They all differ either in the choice of the f - function or in the choice of the propagator: $(\Delta+K^2)^{-1} \to \ldots$ A freedom in the choice of the quasipotential equation (QPE) corresponds to a freedom in extrapolating the scattering amplitude off the mass shell.

C) The quasipotential equation can be also rewritten in an explicitely covariant form (Matveev, et al. /54/ , see also /29/):

$$\varphi_k(p) = \int d^4q\, \delta(n\cdot q)\, \frac{g\, \sigma(p,q;k^2)}{k^2/4 + p^2 - m^2}\, \varphi_k(q);$$

$$k\cdot p = 0, \quad n_\mu \equiv k_\mu/\sqrt{k^2}.$$

The condition $k\cdot q = 0$ was earlier used by Markov and later by Yukawa (M-Y) /55/ for excluding from the theory the dependence on relative time. (It can also be used for choosing the solutions of B-S equations having a finite nonrelativistic limit). The M-Y condition was originally invented as a mathematical device for a consistent treatment of a bilocal theory of composite particles. These ideas were recently revived by several authors (see e.g. /56/). The physical consequences of a bilocal quark theory of hadrons, based on equations somewhat intermediate between quasipotential and bag equations, are most detailly elaborated by Preparata /57/ . The main idea of the Preparata approach is to entirely exclude the quark variables from the physical quantities, the only dynamical trace of the quark structure being supposed the bilocal nature of the hadron fields. This is in parallel with attempts to use the bilocal current algebra instead of more specific assumptions of the parton model (see e.g., /34/). It is well known, that the predictive power of the bilocal current algebra is somewhat weaker than that of the parton model /34/ . Similarly, the bilocal quark theory of hadrons, reproducing many nice results of the constituent quark models, fails to give any definite prediction in several important points (e.g., for $R = \frac{\sigma(e^+e^- \to \text{hadrons})}{\sigma(e^+e^- \to \mu^+\mu^-)}$ /58/, it is also difficult to imagine a simple explanation of the jet structure in $e^+e^- \to$ hadrons). The main advantage of the bilocal theories over constituent theories lies in avoiding the quark-parton paradox (also in parallel with the bilocal current algebra). Our point of view is that a resolution of the paradox can only be found on a more fundamental level (octonions?) and that the quarks, while not existing as free particles, can otherwise be regarded as real particles of which the hadrons are composed. For these reasons we concentrate in what follows on the quasipotential quark models and on bags.

Return now to the covariant quasipotential equation. Generalizing the M-Y condition we can replace K_μ by some vector λ_μ . If this vector is light-like ($\lambda^2 = 0$, $\lambda = (1, 0, 0, \pm 1)$) we arrive at the simplest light-front (L-F) formulation of the QP equation. Several forms of such an equation are presented to this conference /59/ (see also /60,61/). There also exists an extensive literature on closely related approach of infinite-momentum-limit bound-state equation (see e.g. /63/). Here the people depart from Weinberg's formulation of the

quasipotential equation in the infinite momentum system [63] . The common feature of all these approaches is to describe the bound states in the light-front system (or in the infinite-momentum system).

D) Why the LIGHT-FRONT?

The L-F dynamics has been discovered by Dirac (1949) but until recently it was practically unknown to physics community. Later Fubini and Furlan [64] realized that the current algebraist's life is much more comfortable in the infinite momentum "frame" which essentially coincides with the L-F "frame". As the partons can live only in such a system, it is now most popular among theorists. The experimentalists gradually approach this system with growing available energies in CMS.

If we boost any Lorentz system in Z - direction then for $p_z \to \infty$ the most natural variables are the light-front variables $t+z, t-z, x, y$ Denote them as

$$x_+ = \frac{t+z}{2}, \quad x_- = \frac{t-z}{2}, \quad x_\perp^1 = x, \quad x_\perp^2 = y$$

and consider the variable x_+ as a substitute for the time variable t . The classical dynamics in such variables is not simple.

E.g. $(\Box + m^2)\varphi = 0 \Rightarrow (2\partial_+\partial_- - \partial_\perp^2 + m^2)\varphi = 0$

and the initial value problem on the surface $x_+ = 0$ is known by mathematicians as being "incorrect" (infinitely many solutions). However, if we require that these solutions correspond to the finite energy, there would be no ambiguity in finding such solutions [65].

The L-F quantum theory for finite degrees of freedom is not much different from usual (as realized by Dirac). However, for infinite degrees of freedom (QFT) the new theory is radically different. Due to the existence of the positively definite conserved operator $p_0 + p_z$ (for particles with $m \neq 0$, $p_0 = \sum\sqrt{\vec{p}^2+m^2} > \sum p_z$ the interactions do not produce particle-anti-particle pairs, and one can hope to avoid such frightening theorems as Haag's theorem and Coleman's theorem [65,61] . Let us explain this point in some detail (for details and refs. see [66]):

1) For systems with finite degrees of freedom we have very nice von Neumann's theorem that all irreducible representations of the commutation relations $[a_i(\vec{p}), a_j^\dagger(\vec{p}')] = \delta_{ij}\delta(\vec{p}-\vec{p}')$ are unitary equivalent, and so we can define the physical vacuum such that $a_i(\vec{p})|0\rangle_{ph} = a_i(p)|0\rangle_{bare} = 0$.

2) For systems with infinite degrees of freedom, according to Haag's theorem $|0\rangle_{ph.} = |0\rangle_{bare}$, and even free fields with different masses are unitary inequivalent! Stated in other way, this means that $S(t,-\infty)|0\rangle_{bare}$ does not exist, due to the pair production from the bare vacuum. In contrast, $S(t+z,-\infty)|0\rangle_{bare}$ probably may exist, due to the conservation of $p_0 + p_z$ forbidding the pair production.

Similarly, Coleman's theorem ("the invariance of the vacuum is the invariance of the world") is not true in the L-F variables, as the vacuum is stable under the action of any charge operator: $Q_i|0\rangle = \lambda_i|0\rangle$ If the charge is not conserved, then $\lambda_i = 0$ and Q_i annihilates the vacuum. We see that the vacuum is always automatically invariant. This fact is especially useful in considering dynamical realization of chiral symmetries [67]. These and other conceptual advantages of the L-F variables give us all the reasons for using the L-F dynamics in relativistic bound state theory. There are also several practical advantages of these variables: 1) The stability group (the little group) of the light-like system, $(E_2 \times \mathcal{D}) \times T_3$, is larger than the corresponding stability group of "space-like" systems, $SO_3 \times T_3$, and the first has the Galilei group as a subgroup. For this reason the dynamics in L-F system is (somewhat paradoxically!) very similar to nonrelativistic

dynamics [68] . 2) It follows that the bound state equations in this system must be of the three-dimensional quasipotential nature [63] . 3) The concept of the L-F variables proved to be very useful in parton model, in the light-cone current algebra, and it revealed its practical advantages in treating deep-inelastic processes. To unify these semiphenomenological approaches with quark-bound-state models is hardly possible without using the L-F formalism.

Some preliminary attempts in this direction were presented to this conference. For example, the quark-counting rules are naturally emerging from the quasipotential equations in LFV (Garsevanishvili et al. [69] , Brodsky et al. [70] , Khelashvili [71] , Kvinikhidze [72]). A connection of large and small momentum behaviour of meson form factors is discussed by Terent'ev [73] . An interesting field of application of light-front formalism is in high-energy hadron-nucleus reactions where the constituents (nucleons) are unconfined. For example, by considering $pd \to ppn$



one can directly measure the deuteron wave function $\Psi_d(x, \bar{p}_\perp^{sp})$, as the differential cross section is of the form [74]

$$\frac{d^2\sigma}{d\,p_\perp^{sp} dx} \sim \sigma_{el}(pp) \left| \Psi_d(x, \bar{p}_\perp^{sp}) \right|^2$$

In such a way the equations describing bound states of nucleons in extremely nonrelativistic situations can be confronted with experiment. Similar equations can be used for other relativistic bound states (e.g., for positronium, Faustov et al. [75]). Relativistic nuclear physics and atomic physics provide us a very promising field for applications of the described formalism. Here we know the constituents and have a very good knowledge of the binding forces. Confronting theoretical results with experiment we can probe our ideas on relativistic bound states.

E) Some other approaches to relativistic bound states are based on the Kadyshevsky formulation of the relativistic Hamiltonian quantum field theory which elegantly generalizes the non-covariant perturbation theory [76]. Starting from this formulation a class of quasipotential equations was derived. The simplest one can be obtained (formally!) from the Lippman-Schwinger equation by substitutions

$$E_p = m + \frac{\bar{p}^2}{2} \to E_p = \sqrt{\bar{p}^2 + m^2}; \quad d^3q \to \frac{d^3q}{\sqrt{m^2+q^2}}$$

and reads

$$\varphi_k(\bar{p}) = \frac{1}{2} \int \frac{V(\bar{p}, \bar{q}, k^2)\, \varphi_k(\bar{q})}{E_k - E_q + i0} \cdot \frac{d^3q}{\sqrt{m^2+q^2}}$$

By means of a transition to the relativistic coordinate space it can be transformed into a differential-difference equation. The relativistic coordinate space [76] is related to the momentum space through the Shapiro [77] transformation

$$\varphi_k(\bar{p}) = \int d^3\tau \left(\frac{p_0 - \bar{p}\bar{n}}{m} \right)^{-1 - i\tau M} \Psi_k(\bar{\tau}), \quad \bar{n} \equiv \frac{\bar{\tau}}{\tau}$$

This is the natural generalization of the usual Fourier transformation used in nonrelativistic quantum mechanics. In fact, the function entering this expression is the relativistic form of $e^{i\bar{p}\bar{\tau}}$ and its limit for $m \to \infty$ is exactly $e^{i(\bar{p}\bar{n})\tau} = e^{i\bar{p}\bar{\tau}}$.

An interesting variation of this theme is presented at this conference by Mir-Kasimov et al. [78] . It is suggested to use the rapidity variable instead of E_q: $\chi_q = \ln(E_q + \sqrt{E_q^2 - m^2})$. Then $(E_k - E_q)^{-1} \to \frac{\chi_q}{sh\,\chi_q} (\chi_q^2 - \chi_k^2)^{-1}$ and the resulting equation in the coordinate space is a second order differential equation similar to the Schrödinger equation. For the S-wave it reads

$$\frac{d^2\Psi_k(\tau)}{d\tau^2} + \chi_k^2 \Psi_k(\tau) = \frac{\chi_k}{sh\,\chi_k} V(\tau) \Psi_k(\tau)$$

This equation is as simple as the Schrödinger equation. The extension of this approach to

spinor particles and to the unequal-mass problems is very desirable .

Starting from the Kadyshevsky Hamiltonian formulation of quantum field theories a somewhat different approach to relativistic equations for bound states can be developed. In this formulation momenta of all particles belong to the mass shell (as in nonrelativistic theory). The formalism is particularly convenient for constructing the Fock space in the light-front variables. The corresponding equations for n-particle bound states were considered by Karmanov /79/ . It would be interesting to investigate such equations in detail and to extend them to spiner particles. A new feature of this equation is a dependence of the Fock amplitudes on a unit vector which is somehow related to $\bar{P}/|\bar{P}|$, $|\bar{P}| \to \infty$. However, the necessity of these new parameters and their meaning is not completely clarified. The consideration of some physical problems would be most instructive.

A simpler approach to the relativistic two-particle bound states without extra variables is applied by Terent'ev /73/ to different problems of the relativistic quark model, especially to radiative decays of mesons. Equations used by him are similar to quasipotential equations, constructed earlier by Sokolov /60/ , who starts from Dirac's formulation of the relativistic Hamiltonian theory. This approach avoids using the quantum field theory and only deals with the generators of the Poincare group. The quasipotential is introduced phenomenologically, the theory is only giving us a prescription for doing this in a covariant way. Sokolov's method can also be applied to many-particle bound-state problem /60/ , however, the practical realization of this possibility is not yet elaborated.

The methods described above do not allow one to specify the binding potential, and it should be extracted from some field theory or be somehow guessed. We discuss several popular potentials in the next section. Here we mention a possibility of constructing the two-particle relativistic bound-state theory, in which the "potential" is completely defined by the physical scattering matrix of the constituents. As proposed by Logunov, Khrustalev et al. /80/ the relativistic generalization of the Heitler-Sokolov-Wilson equation /81/ can be obtained in the framework of the equal time formulation of the relativistic two-body problem in QFT. The corresponding "quasipotential" is expressed in terms of the elastic and inelastic cross sections of the two constituent particles. This method has been successfully applied to the description of the high-energy two-particle scattering. It is potentially useful for describing the two-particle bound states. In relativistic atomic and nuclear physics and in hadron phenomenology it allows one to take phenomenologically into account many-particle contributions to scattering and to bound-state energy. In the quark theory of hadrons its application is less justified as some knowledge of the quark scattering amplitudes is required.

F) We have mostly reviewed above the quasipotential type formulations of the relativistic bound-state problem. There are presented to this conference a few more conventional treatment of the problem. Cung et al. /82/ summarize the results of their investigations of the two-fermion B-S equation with the kernel restricted to the zero relative time (static interaction). The approach is essentially equivalent to the quasipotential approach of Faustov and Todorov /45/ . In the paper presented by Ladanyi /83/ the small distance behaviour of the B-S equation for bound states of a fermion with a massive vector meson is investigated (see also Ciafaloni and Ferrara /83/). For similar (but more relevant to the quark model) investigations see e.g. /84,85/.

Note that the authors of ref. /85/ start from the B-S equation but subsequently reduce it to the Logunov-Tavkhelidze equation to simplify the calculation of the asymptotic behaviour of the bound-state form factors. (Compare to /68-72/). Some other calculations of this behaviour appear to a related method of summing the "leading" contributions of Feynman diagrams /86,87/ . In this case the bound state is conveniently defined in terms of a pole in the angular-momentum plane. (See especially Efremov et al. /87/ , where the method is consistently used for investigating the asymptotic behaviour of form factors, and the validity of the quark counting rules. Finally we mention some diverse results in the theory of the B-S equation which are related to the problems discussed above. New exact solutions of spinor-spinor B-S equations are obtained in references /88/ . In ref. /89/ exact upper and lower bounds for the sum of scalar ladder diagrams are found. Glimm and Jaffe /90/ have given a rigorous proof of existence of two-particle and three-particle B-S kernels in the Euclidean region for a wide class of two--dimensional scalar theories. The structure of the three-quark B-S equation is poorly known. An investigation of the general spinor structure of the bound-state wave functions is attempted in /91/ (see also /61/).

Concluding this rather lenghthy and by no means complete disoussion of present trends in the relativistic theory of bound states it is to be emphasized that up to now there is no formulation of the theory which is adequate for solving all problems, occuring in physical applications. For different problems we have to use different methods. In general, the L-F quasipotential equations seem to be most appropriate for describing relativistic bound system. However, the B-S equation is better suited for extremely tightly bound states (e.g., for zero mass bound states to be discussed in section 3.5).

3.4. Interquark forces

Once the equation is chosen the next question is: What is the (quasi)potential acting between quarks. The symmetry properties with respect to the colour and flavour groups have been discussed earlier: 1) The potential corresponds to the exchange of the colour-gauge bosons and most probably is colour-conserving. 2) It either is flavour-conserving or has a small symmetry violating term. The main flavour-symmetry violation is assumed to be attributed to the different masses of quarks. 3) As is argued in the next section it probably involves a piece corresponding to the exchange of flavour-gauge bosons. Such terms are desirable for spontaneously generating quark mass differences. As to the spatial dependence of the potential, the choice between different possibilities is much more difficult. We summarize here the most popular potentials together with new ones presented at this conference.

1) The "good old" oscillator potential (see e.g. /2,5,24,31/ $V(r) = \alpha r^2$ or the "bag-like" oscillator potential $V_{osc} = -V_0 + \alpha r^2$ (e.g. /73,92/). These are most popular due to availability of the exact analytic solutions for some of the bound-state equations mentioned above. The Regge-trajectories for these potentials are linearly growing with M^2 (or S). However, the form factors $F(q^2)$ of bound states have a pathological dependence on the momentum transfer q^2 and the predictions for excited states are unrealistic. Thus the oscillator potential can be considered only as an approximation to the "realistic" potential, which is only adequate for describing some properties of low-lying states of composite hadrons.

2) The QCD-potential $V_{QCD}(r)$ /10/

$V_{QCD} \underset{r\to 0}{\sim} \frac{\beta(r)}{r}$, $V_{QCD} \underset{r\to\infty}{\sim} \alpha r$

Here $\beta(r) \underset{r\to 0}{\sim} [\ln(r/r_0)]^{-\alpha}$, $\alpha > 0$. This potential has a singularity at infinity. For $r \to 0$ it is singular if $\alpha < 1$ and regular if $\alpha \geq 1$ /38/. Such potentials have been applied to a description of the $q\bar{q}$ states and especially to the charmonium spectroscopy. For a summary of the corresponding calculations see the invited paper of Mir-Kasimov /93/ (see also /94/). In all these calculations either Schrödinger or some quasipotential equations have been used. As many questions to theory and experiment are yet to be answered, it would be premature to draw from these calculations any definite conclusion.

3) Some other confining potentials are discussed at this conference. Skachkov /95/, generalizing Kadyshevsky approach /76/, obtaines a quasipotential equation for the $q\bar{q}$-system with the potential $V_s(r) = (4\pi r)^{-1} c\,tg(\pi m r)$ where m is the mass of the quark. m is the only free parameter in the equation, and fixing it, say, by the requirement that the lowest state is the ρ-meson one can predict a sequence of the excited states ($M_{\rho'} = 1100$ MeV, $M_{\rho''} = 1465$ MeV etc.). Unfortunately, the quarks are supposed to be scalars and so the spin effects have not been discussed. Another attempt to confine quarks is presented by Guenin /96/, who "simply" changes the sign of the mass of the gluon ($\mu \to -\mu$) in the space-like part of the gluon propagator, thus arriving at the potential $V_q(r) \underset{r\to\infty}{\sim} r^{-1} e^{\mu r}$ (the quark propagator is not modyfied). It is not clear at the moment whether the corresponding theory remains causal. The phenomenological applications are not discussed.

4) Dolgov /97/ gives some arguments in favour of a double-well structure of the $q\bar{q}$-potential. He starts from the Blokhintsev et al. /98/ quasipotential equation and observes that the structure of the equation itself dictates a double-well form of the effective potential in the radial equation. It is possibly true for other quasipotential equations for spinor particles. This idea is attempted to be applied to explaining Ψ-particles without new quarks.

5) It is known for long that a spherically symmetric well potential gives nice phenomenological results in the quark model /23/. Such potentials naturally arise in an approximation to MIT-bag model (see sect. 3.1 and 3.6). Another source of similar potentials is the exchange of infinite number of resonances with an exponentially growing mass spectrum $\sigma(\mu) \sim e^{\mu a}$ /99/. As the exchange of one particle results in the Yukawa potential $r^{-1} e^{-\mu r}$, the exchange of $\int d\mu\, \sigma(\mu)$ particles gives rise to the potential

$$V(r) \sim \int d\mu\, \sigma(\mu) \frac{e^{-\mu r}}{r} \underset{r\to a}{\sim} (r-a)^{-1}$$

having a singularity at the finite distance from the origin (FDS-potential). Such potentials can be obtained in a non-polynomial field theory /99/, or in theories with infinite-component fields /100/. Properties of the pion have been investigated in the model, suppesing the quark motion can be described by the Euclidean B-S equation with the kernel (potential) $V(r) = g^2 (r^2 - a^2)^{-1}$. The parameter a is fixed ($a = 3 \div 4$ GeV) by considering the empirical mass spectrum which in fact is exponentially growing up to 2 GeV. The remaining two parameters g and m_q are determined from the eigenvalue condition for the pion and from $\Gamma(\pi \to \mu\nu)$. The predictions for $\Gamma(\pi \to \gamma\gamma)$, $\langle r^2 \rangle_\pi$ and for the slope of the pion Regge-trajectory α'_π are in good agreement with experiment. The most remarkable prediction is the presence of oscillating terms $\sim t^{-6} \cos\left(\frac{a\sqrt{t}}{2}\right)$ (in form factors $F_\pi(t)$ and elastic cross sections $\frac{d\sigma}{dt}(pp)$

for large space-like t . The period of the oscillations is predicted to be $\Delta\sqrt{t} \simeq \frac{4\pi}{a} \sim 3 \div 4\,GeV^{-1}$ in a striking agreement with the observation of Schrempp and Schrempp /101/ . We are not aware of any other natural explanation of the oscillations in $\frac{d\sigma}{dt}(pp)_{el}$ found in /101/ . Note that the Regge trajectories for the FDS--potential are approximately linearly growing with mass M (not M^2!). It is assumed that a faster (linear in M^2) behaviour will result from the contributions of inelastic channels opening for large M . The theory with energy independent potentials is supposed to be applicable only to low-mass hadron states. Finally, the FDS potential strongly confines quarks but the confinement is only partial /99/ .

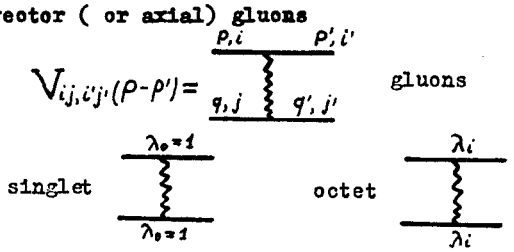
We discussed deverse coordinate dependences of the interquark potential for $q\bar{q}$-system. For choosing the most realistic one it is, first of all, necessary to consider the corresponding three quark potentials and to investigate the radially excited bound states of the three quarks. Very little has been done along this line (except for non-relativistic and simplest relativistic equations with $V_{osc}(r)$). To probe the radial dependence of the $q\bar{q}$- potential the decays and the radially excited states of mesons should be carefully investigated. Due to opening inelastic channels ($(q\bar{q}) \to (q\bar{q})(q\bar{q})$ etc) this is (at least!) a many channel problem which has not been discussed in detail. In addition, the experimental status of excited mesons is rather unclear. We discuss a possibility to by-pass these difficulties in sect. 4.

3.5. Chiral symmetry and quark masses

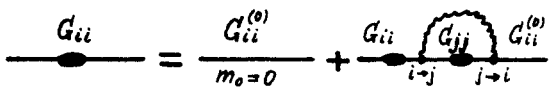
There are other difficult problems of the quark dynamics which have not been discussed above. 1) What is the origin of the flavour-symmetry violation (assuming the fundamental interaction is symmetry preserving)? 2) What is the origin of the approximate chiral symmetries (e.g. $SU(2)_R \times SU(2)_L$, $SU(3)_R \times SU(3)_L$ ...)? 3) What is the origin of the quark masses and of their differences? All these questions are obviously interdependent. In semi-phenomenological theories it is usually assumed that the strong interaction of quarks is $SU(3)$ and $SU(3)_R \times SU(3)_L$ symmetric, and the observed symmetry-breaking effects are ascribed to the quark-masses. At a more fundamental level we have to investigate seriously the third question. One promising approach to this problem is based on the unified gauge theories of all interactions (see e.g. /10/ and Slavnov's talk at this conference). Another, less ambitious one, is formulated within a semiphenomenological scheme of quark-quark interaction which simultaneously gives two apparently different effects: binding quarks and providing them with masses and mass splittings. This approach uses the mechanism of dynamical realization of symmetries which first has emerged in Bogolubov's theory of superfluidity /102/ and subsequently has been applied to ferromagnetism, superconductivity, etc. The main idea is that the invariance of the Hamiltonian needs not to be the invariance of the ground state. To obtain such a solution we have first to remove the degeneracy of the Hamiltonian by adding some symmetry-breaking term. This symmetry breaking is switched off only after finding the desired solution. If there exists such a symmetry-breaking solution then, generally, there appear some zero-mass excitations (quasiparticles) which, in a sense, restore the original symmetry. The ground state contains an infinity of such quasiparticles (magnons, Cooper pair, etc.). These ideas in the statistical physics were first formulated by Bogolubov /103/. Their relevance to problems of elementary particle physics was discovered by Nambu and Goldstone /104/ . We will call this approach

the Bogolubov-Nambu-Goldstone realization of symmetry (BNG). Nambu also suggested to treat the pion as the massless particle corresponding to BNG-realization of the chiral symmetry $SU(2)_R \times SU(2)_L$. Examples of the quantum field theories with BNG-realization of the chiral symmetry $U(1)_R \times U(1)_L$ were first treated by Arbuzov et al. /105/ (two-dimensional) and by Nambu and Jona - Lasinio /106/ (four-dimensional).

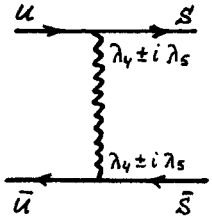
Following this line of thinking consider /107/ the $U(n)_R \times U(n)_L$ symmetric theory (for definiteness consider n=3) of n massless quarks interacting through exchange of vector (or axial) gluons



We treat this interaction as an effective potential (propagator). As we are not talking about three quark states we can be temporally "colour-blind". Then the equations for the propagator of quarks are of the form



For different potentials (e.g., for FDS-potential) these equations have solutions corresponding to $m_i = m \neq 0$. If there is only the SU(3)-singlet interaction, then there are 9 massless pseudoscalar bosons. If there is also the SU(3)-octet interaction, then different possibilities arise due to strong mixing of the quark configurations



A very preliminary statement is that in this case only one pseudoscalar state remains massless, others can acquire a mass. One can also hope to arrange the relative singlet-octet coupling strengths so as to split the masses of quarks. This has been done in some simple models with factorizable partial wave potentials $V_\ell(p,q)$ (V_ℓ is the angular-momentum projection of $V(p-q)$) /107/ . This probably opens new way for solving the three distinguished problems. Unfortunately, "Things Take Time" . To demonstrate the consistency of this approach we have to do a lot of job: 1) to find a non-trivial symmetry-breaking quark propagators by solving the system of nonlinear equations with a realistic potential; 2) to find the solutions of the corresponding linear equations for pseudoscalar meson bound states (the B-S equations with the "exact" non-symmetric quark propagators); 3) to demonstrate that the $q\bar{q} \to q\bar{q}$ Green's function has corresponding poles and/or to incorporate in this scheme a confinement mechanism.

These problems are essentially unsolved even in the technically simpler "finite quantum electrodynamics" of Johnson et al. /108/ (for new results and refs. see /109/). In the paper presented at this conference Fukuda and Kuge /110/ attempt to solve the non-linear equation for the electron propagator introduced in refs. /108,111/ . They claim the propagator to have in the time-like region neither poles nor cuts for arbitrary e^2 and interprete this as a "confinement". The absence of the pole can be proved quite convincingly, but they give no proof of the absence of a branch-point singularity. As a matter of fact, expanding the self-energy part $\sigma(p^2)$ of their electron propagator in a series of powers of $\alpha = e^2/4\pi$ (which is convergent for small enough values of α) one can easily demonstrate that any approxima-

tion to $\sigma(p^2)$ has a branch point at $p^2 = -\sigma(0)$ It is rather difficult to understand why this singularity could completely disappear in the sum of the series. This sum most probably has a branch point either in the time-like region or in the complex p^2- plane (in a vicinity of $p^2 = -\sigma(0)$ for small α). Remark in passing that there exist suggestions (Dubničkova, Efimov [112]) to describe confined particles by "propagators" having no singularities in the complex p^2- plane except infinity (an integer function of p^2). An interesting question is: can such "integer" propagator naturally emerge in any quantum field theory? We think this problem has something to do with colour-confinement mechanism but a more serious discussion of this point is impossible at this moment. The propagator of ref.[110] is almost certainly not an integer function.

Some other aspects of the BNG-realization of chiral symmetries are discussed at this conference. N.N.Bogolubov (Jr.) et al. [113] investigate in detail the structure of the vacuum in the four-fermion theory of ref.[106] by using Bogolubov's transformation. Kleinert [114] and Pervushin and Ebert [116] try to avoid the detailed discussion of the quark dynamics and to construct (without really solving the dynamical equations) a semiphenomenological theory which can be confronted with the usual $SU(3)_R \times SU(3)_L$ algebra of fields. This is achieved by "hadronizing" the quark interactions, i.e., by excluding the quark fields from the dynamics. This approach looks interesting but the important things must be clarified before we can reach some definite conclusions. Without solving dynamical equations the meaning of such approaches is not clear. In addition, some intriguing problems of the chiral quark theory - the η-η' mixing, the problem of the BNG-nature of pseudoscalar mesons (the so-called U(1) problem)are not touched upon in this approach. The U(1) problem can be formulated as follows. In any quark-gluon theory the chiral symmetry is $U(3)_R \times U(3)_L$, instead of the phenomenological $SU(3)_R \times SU(3)_L$. In the simplest models this results in obtaining 9 pseudoscalar massless mesons instead of desired 8 ones. This is reflected in some unpleasant features of the corresponding current algebra which can not be discussed here. The approach based on the nonlinear equations for the quark propagator probably offer a new possibility for the solution of this problem. An alternative approach based on the unified field theories is developed by Weinberg [116]. The present status of chiral phenomenology has been recently summarized by Pagels (see[117] where further references can be found).

3.6. Attempt of synthesis in bags

The modern fashionable bags contain the quarks and gluons and pretend to simultaneously incorperate the equations of motion as well as the forces keeping the quarks inside hadrons. There are different sorts of bags which I will not try to describe here. On the parallel session they were discussed in some detail by Weisskopf, Kuti, P.Bogolubov, Struminsky and Mat'ev and here I only summarize several important points (for further references and details see these Proceedings and [118-121] .

The M.I.T. bag is the most natural relativistic generalization of the Dubna bag. The new features are the following: 1) The external pressure B is intreduced to balance the internal pressure of quarks and gluons moving inside a sphere of the radius. 2) The radius R is not fixed and is determined by the condition of the minimum energy of the system. This energy is the sum of the three terms:

$$M = \left[n_u \left(m_u^2 + \frac{X_u^2}{R^2} \right)^{1/2} + n_s \left(m_s^2 + \frac{X_s^2}{R^2} \right)^{1/2} \right] +$$

$$+ \left[\frac{4}{3} \pi R^3 B - \frac{Z_0}{R} \right] + \Delta E_c \, .$$

Here n_u, n_s are the numbers of non-strange and strange quarks resp.; x/R is the momentum of the quark, which is derived by solving the Dirac equation in the infinitely deep spherical well. The second term represents a "renormalized zero-point fluctuation" energy, and the last term is the colour interaction energy which is responsible for spin-spin (hyperfine) splitting of hadron masses (this effect was first observed in the frame of QCD by De Rujula et al. /122/). 3) This expression was derived by using an analogy between massless colour gluons and photons, the colour playing the role of the electric charge. The colour gluons were confined by brute force inside the bag and the result of such a brutality is nice, only the colourless states can be stable. 4) The spectrum of excited states is exponentially growing in this model ($\sigma(M) \sim e^{MR}$). The Regge trajectories $\alpha(M^2)$ are also infinitely rising but for the spherically symmetric bag the dependence on M^2 is nonlinear.

We have just described a somewhat modified version of the M.I.T. bag. The main modification concerns the introduction of the quarks as point-like massive objects interacting with the coloured gluons. This modification of the original M.I.T. bag has been suggested by Kuti et al. /119/ and by De Grand et al./118/. When confined to a fixed sphere, the modified M.I.T. bag reproduces phenomenological results of the Dubna bag and, in addition, incorporates all good features of the QCD-approach/107,122/ to composite hadrons. Note that the confinement of the colourless bound states is in this approach an immediate consequence of the confinement of the gluons inside the bag. In general this bag picture is successful in qualitatively describing the lowest-lying states of baryons and mesons. However, further improvements are required if we wish to account for excited states and scattering processes.

First, the shape of the bag should be not fixed if we are to consider the processes of the fusion and fission of bags. As shown by Low /123/ the high-energy scattering of two bags can successfully reproduce the main features of elastic and inelastic processes of hadrons, provided that the bags are allowed to assume highly non-spherical shapes. With strongly deformed bags, we can also obtain a good description of hadrons with high values of the angular momentum of quarks and explain the linear growth of the Regge trajectories with M^2 /124/ . The diquark structure of the baryons /125/ is also naturally included in this picture /124/ . A variational approach to treating the static properties of deformed bags is presented at this conference by De Tar /126/ . A more radical modification of the bag model is suggested by the Budapest group /119/ . They supply the bag with an elastic skin (or "membrane") which enters into dynamical equations as a new variable, thus allowing for the canonical quantization of the whole system. The phenomenological motivation of this step is mainly in the fact that with the soft gluon-quark interaction (this hypothesis lies at the heart of the bag-phenomenology) it is difficult to explain the momentum sum rule in the deep-inelastic scattering (the missing momentum is ascribed to gluons, and yet the interaction of quarks with gluons is presumably weak). In the Budapest bag the missing momentum is possibly carried by the membrane. But now the question is: why the interaction of the membrane with quarks does not produce a large number of $q\bar{q}$? Being conceptually transparent the Budapest model is technically more complicated than the MIT model and phenomenological applications are still to be worked out. We hope that the relevant questions will be answered next year at the Budapest conference.

An interesting question to the bag-theory is: how to explain the nuclear structure? Without colour gluon exchange the lowest energy state of the 6 quarks would be a six quark bag and not a two-bag system representing a deuteron. With colour gluon exchange the six quark bag can be viewed as a system of two three-quark bags thus really representing the deuteron system [127]. For many-nucleon systems an interesting phenomenon is predicted [128]. At some quark density, higher than in nuclear matter, the "bag" will become the lowest state again, and a phase transition from nuclear matter to "quark matter" is possible. A simplified treatment of the deuteron as a six quark system is presented to this conference by Babutsidze and Machabeli [129]. They put all six coloured quarks in an effective potential well, described by an oscillator potential, and classify the colourless states by using the methods of the nuclear shell model. The phenomenological results seem to be satisfactory yet the physical motivation of the calculations is not convincing. There is no two-bag structure of the deuteron, and it is not clear why the energy, say, of twelve-quark systems is not lower than that of the "deuteron". In general, the bag approach to nuclear physics opens new ways for investigating the nuclear structure, but before a quantative approach is possible, many important points have to be clarified.

Recently, it has been realized that the bag-like models predict an essentially richer spectrum of hadrons than non-relativistic potential models (including the Dubna bag). In fact, all kinds of exotics are predicted to exist with masses comparable to masses of the usual hadrons: $(qq\bar{q}\bar{q})$ bound states, the mesons with exotic J^{PC}, excitations corresponding to center of mass motion, etc. [120]. These predictions are not in agreement with present experiment, as the empirical mass spectrum is rather sparse. In the contribution by Jaffe [120] an attempt is made to identify the predicted $(qq)(\bar{q}\bar{q})$ states ("cryptoexotic" mesons) with some more or less established resonances. However, this seriously aggravates the well-known difficulty of missing $q\bar{q}$ - states. We consider the whole problem as essentially unsettled both from the experimental and theoretical sides.

The most interesting alternative to the MIT bag is the Vinciarelli-SLAC bag [121] Unlike the MIT crew, the SLAC-crew starts from a field theory with a spontaneous symmetry breaking of the vacuum. Hence, the fundamental role of scalar fields in this approach. However, the surprising feature of the SLAC-bag is that the quarks concentrate near the surface of the bag which results in some not pleasant phenomenological predictions. The modern development of SLAC-bag is connected with solitons and is outside the scope of the present review. Some interrelations between SLAC and MIT-bags are discussed by Huang and Stump [130]. Using the variational approach to a model of quarks interacting with a scalar field, they obtain two solutions. One is similar to the MIT bag, either to the Vinciarelli-SLAC bag.

We have forgotten to mention two more problems of the bag theories. In the MIT-calculations it is supposed that the quark-gluon coupling is rather weak so as perturbation theory with respect to this interaction be sensible. In fact, the phenomenological applications require rather a large value for the coupling constant α_c ($\alpha_c \approx 2.2$) similar to the Sommerfeld constant $\alpha = 1/137$ (the authors of refs. [118,120] erroneously quote the value $\alpha_c \simeq 0.55$, see [119]); Kobzarev and Mat'ev [131] suggest a remedy to cure this desease at the price of the introducing new parameters in the theory (see these proceedings). We also have to note a difficulty

of the Vinciarelly-SLAC model in explaining the observed scaling in deep-inelastic scattering processes. As suggested by Giles [121], this difficulty can be resolved at the expense of supposing the surface of the bag to be extremely soft to deformations. Then the surface is considered as a dynamical object (like the Budapest membrane) and the theory becomes much more complicated than the original one. Only semiclassical solutions have been investigated up to now.

Concluding this rather sketchy discussion of bags we may generally state that the bag theories are successful phenomenological theories of hadrons made of coloured quarks and coloured gluons but they certainly do not constitute a fundamental theory of matter. The origin of the volume or surface tension, of symmetries and of their breaking and of quark masses is not explained. For example, bags are well suited for a description of the broken SU(6)-symmetry but not for the more fundamental $SU(3)_R \times SU(3)_L$ or at least $SU(2)_R \times SU(2)_L$ chiral symmetries. There are some attempts to incorporate PCAC in a bag-theory at a purely phenomenological level (see e.g. papers [132]). In these papers the pion is treated as an unconfined field interacting with a bag surface.

4. Quarks and Experiment. Conclusions.

Now we briefly consider some problems concerning the comparison of the quark model with experiment. The status of the baryon spectroscopy has not been significantly changed after the London conference [1] (see also [133]), and we will not discuss it here. As to the meson spectroscopy, there is a dramatic change due to discovery of the new heavy resonances which we identify with charmed particles. Here we will not touch upon the details of the charmonium spectroscopy as well as the new data on the "old" particles. Instead, we concentrate on some of long standing contradictions between the quark model and experiment 1) The masses of all well-established mesons (except pseudoscalars which require a special treatment) can be described by a remarkably simple formula [107] . The formula is obtained as follows. Consider some equation for the $q\bar{q}$ bound-state wave function Ψ_{ij} of the i-th and j-th quarks (i and j are the flavours of the quarks) which we write in a rather general form

$$[\hat{R}_{ij} - K^2(M, m_i, m_j)]\Psi_{ij} = 0$$

$$K^2(M, m_i, m_j) = \frac{M^2}{4} - \frac{m_i^2 + m_j^2}{2} + \frac{(m_i^2 - m_j^2)^2}{4M^2}$$

Here $\hat{R}_{ij}$ is assumed to be some operator which does not depend on the quark masses m_i and m_j . We suppose that R_{ij} has the eigenvalues r_{ij} depending on the orbital angular momentum $\vec{L}$ and on the total spin of the quarks as follows:

$$r_{ij} = \frac{m_0^2}{4} + \frac{\beta_{ij}}{4} L - \frac{m_i^2}{8} S(S+1) + \\ + \frac{m_i^2}{8}[J(J+1) - L(L+1) - S(S+1)]$$

where J is the total spin of the bound state. We introduce here the spin-spin and spin-orbital splittings and a linear dependence of the eigenvalue on L (this corresponds to linear Regge trajectories of mesons). The equation of such an abstract form can be obtained in different quasipotential formulations of the bound-state problem; the B-S equation for $M \gg m_i, m_j$ can also be approximately reduced to a similar equation [107] . However, our specific Ansatz for r_{ij} is of non-relativistic origin. We simply try to dramatize some problems concerning the meson mass spectrum. (Without using the above expression for r_{ij} , the mass relations for states with equal J, L, S can be obtained supposing r_{ij} is independent of i, j).

The expression for the meson masses is now obtained by setting $K^2(M, m_i, m_j) = r_{ij}$

The resulting mass formulae neglect the mixing of different quarks (say $u\bar{u} \leftrightarrow s\bar{s}$) in the isospin-zero $q\bar{q}$ - states. The mixing can be considered by writing the equations for these states

$$[\hat{R}_{ii} - K^2(M, m_i, m_i)]\Psi_{ii} = \varepsilon^2 \sum_j \Psi_{ji} \equiv$$

$$\equiv \varepsilon^2 \sum_j \Theta_{ij} \Psi_{ji} ; \qquad \Theta_{ij} \equiv 1$$

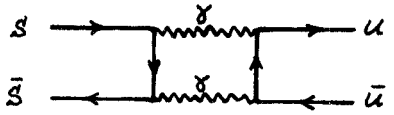
This mixing follows from the specific flavour-exchange mechanism discussed in Sect. 3.5. A similar form of the mixing matrix has been proposed by De Rujula et al. /122/ (mixing in the mass matrix) and by Fritzsch and Minkowsky (mixing in the mass-squared matrix, see /134/, where further references can be found). Our equations generalize the previous approaches, the quark dynamics is implicitly included in the dependence of K^2 on masses and in the eigenvalues τ_{ij} . Note that our mass formulae in general are neither linear nor quadratic in masses. For $L = 0$, with no quark-mixing ($\varepsilon = 0$) and with $m_u = m_d$ we obtain the linear mass formulae $m_\rho = m_\omega$, $M_{K^*} = \frac{1}{2}(M_\rho + M_\varphi)$ which are satisfied within 1%. To account for ω-ρ mixing, corresponding to $s\bar{s} \leftrightarrow u\bar{u}, d\bar{d}$ mixing in $I = 0, L = 0, S = 1, J = 1$ state consider the equations for Ψ_{uu}, Ψ_{dd} and Ψ_{ss} with some mixing parameter $\varepsilon^2_{\omega\varphi}$ By applying the Sohrödinger method of factorization (see e.g., /135/) one easily obtains the expressions for m_ω^2 and m_φ^2 in terms of one unknown parameter $\varepsilon^2_{\omega\varphi}$ (other parameters in this case are determined by the masses of K^* and ρ). The predicted mass of the φ- meson is in good agreement with the experimental value /139/ . The treatment of mixing the $I = 0, L = 1, S = 1, J = 2$ state requires some additional information on the coefficients β_{ij} .

These can be determined by fitting the general mass formulae (with mixing) to the masses of the well-established mesons. The result is rather interesting - the parameters $\beta_{uu}, \beta_{us}, \beta_{ss}$ ($\beta_{dd} = \beta_{uu}$, $\beta_{ds} = \beta_{us}$ - by isospin invariance) satisfy the relation $\beta_{us} = \frac{1}{2}(\beta_{uu} + \beta_{ss})$ As the differences between these parameters are in fact not large ($\beta_{uu} = 0.872$, $\beta_{us} = 0.942$, $\beta_{ss} = 1.015$) the multiplicative relation $\beta^2_{us} = \beta_{uu}\beta_{ss}$ is also very well satisfied. To our knowledge there are no arguments in favour of the additive relation but in the contribution to this conference by Pasupathy /136/ it was demonstrated that the multiplicative one probably follows from duality /137/ and from factorization property of the Regge-pole residues /138/ .

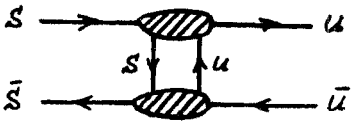
An interesting property of the Regge trajectories is that they seem to interseot in the same point of the L, m^2 plane. This fact for the J - trajectories was also observed by Becher and Böhm /147/ . It can be qualitatively explained by a somewhat smaller radius of the particles containing heavier quarks. Azimov, Frankfurt and Khoze also proposed that the radius of charmed particles is dramatically smaller than that of "usual" particles .

2) As was emphasized above the pseudoscalar mesons require a special treatment. Here we mention the most mysterious η-η' problem and the pion mass problem. It is now generally believed that any solution of both problems is possible only in a theory explaining the broken chiral symmetry. As discussed above there exist two approaches to the $\eta - \eta'$ problem. Both relate the large mass difference between η and π and the violation of both quadratic and linear relations $\eta' \neq K - \pi$ to a strong mixing of $s\bar{s}$ and $u\bar{u}$ (or $d\bar{d}$) in $I = 0, L = 0, S = 0$ channel.

In QCD this mixing is due to the diagram



where coloured gluons γ are exchanged in the S-channel.. A more phenomenological explanation is presented diagrammatically as



where strange (flavoured) bound states and resonances are exchanged in the t-channel (see Sect. 3.5).

For both mechanisms the mixing matrix can be written in the form $\mathcal{E}_{ij}=\mathcal{E}^2$ for all i and j . This mixing matrix was introduced above in the equation for Ψ_{ii} . The resulting expressions for the masses of η and η' are of the form

$$\eta^2 = m_\varphi^2 - 6\mathcal{E}^2 - 2\sqrt{9\mathcal{E}^4 + \Delta^2(\Delta^2+2\mathcal{E}^2)}$$

$$\eta'^2 = m_\varphi^2 - 6\mathcal{E}^2 + 2\sqrt{9\mathcal{E}^4 + \Delta^2(\Delta^2+2\mathcal{E}^2)}$$

Here $\Delta^2 = m_s^2 - m_u^2 = K^*(K^*-\rho) = 0.1064$, $m_\varphi^2 = K^2 + \Delta^2/K^2 = 0.2916$ the only unknown parameter being $\mathcal{E}^2$ .As $m_\varphi^2 \approx \eta^2 = 0.3012$, the approximate value of $\mathcal{E}^2$ is $\mathcal{E}^2 \approx \frac{\Delta^2}{2} = -0.053$. With this value of $\mathcal{E}^2$ the prediction for η' is $\eta' \simeq 0.963$ which is in very good agreement with the hypothesis that η' - meson is $X(958)$. However, in this approach the pion mass is defined by the relation $\pi^2 = m_p^2 - 2\Delta^2$ $(=\eta^2$ for $\mathcal{E}=0)$ and $\pi \simeq 0.280$ is two times as large than the experimental value. We conclude that the pion wave function cannot be described by this simple equation. The ideas described in Sect. 3.5 might be relevant to this problem but no successful model is available at this moment.

Fritzsch and Minkowsky /134/ used the same mixing matrix for the mass squared matrix. Their results can be obtained from our formulae if we write $m_\varphi^2 = K^2 = 0.2457$, $\Delta^2 = \frac{1}{2}(K^2-\pi^2) = 0.1134$ Note that this value of Δ^2 disagrees with that obtained from the vector and tensor meson masses: $\Delta_V^2 = (K^{*2}-\rho^2)/2 = 0.099$, $\Delta_T^2 = (K^{*2}-A_2^2)/2 = 0.150$. If we nevertheless, try to describe η and η' by their formulae with $\mathcal{E}^2$ defined by the η - mass, $\mathcal{E}_\eta^2 = -0.200$, the prediction for η' is $\eta' \simeq 1.61$. Alternatively, defining $\mathcal{E}^2$ from X-mass, we find $\mathcal{E}_X^2 \simeq -0.056$, $\eta \simeq 0.50$. This clearly shows that η and X do not satisfy the equations. A much better fit can be obtained with $\eta' = E(1.42)$. There are other schemes in which the mass of the η' is predicted to be close to the mass of the E-meson. For example, Caser and Testa /140/ came to this conclusion by using a variant of infinite momentum frame current algebra for describing the chiral symmetry breaking. They also suggest identifying the X(.958) with an almost pure glue state.

Attempts to preserve the identification $\eta' = X(.958)$ are based either on introducing some admixture of glue states in the η and η' /141/ or on using different mixing angles Θ_η, $\Theta_{\eta'}$ /142,122/ . To solve this long standing problem it is badly desirable to establish the J^P - quantum numbers of the X(.958) and E(1.42) and to obtain a more detailed and credible experimental information on radiative decays in which these mesons participate. In contrast with the statement of PDG /139/ , the present status of the quantum numbers of X(.958) is very controversial. This was clearly demonstrated at the Conference by Ogievetsky and Lednicky (see these Proceedings). Unfortunately, the state of the art in the meson radiative decays is also far from satisfactory (see e.g. /143/ and the invited paper by Gerasimov). In addition to defining the J^P - quantum numbers of the X and E the most important experimental problems are the measurements of $\Gamma(X\to\rho^0\gamma)$, $\Gamma(X\to\gamma\gamma)$, $\Gamma(\rho\to\pi\gamma)$

$\Gamma(K^{*0}\to K^0\gamma)$. New measurements of $\Gamma(\eta\to\gamma\gamma)$ and $\Gamma(\pi^0\to\gamma\gamma)$ not using the Primacoff effect would be also welcomed, in view of their utter importance for theory (esp. for quark models).

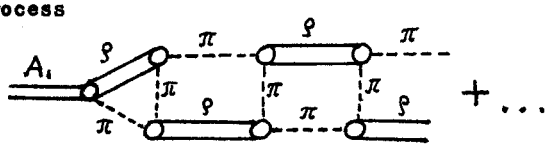
In recent paper /144/ Greco and Etim-Etim have constructed a model successfully describing all the known meson radiative widths expect $\Gamma(\rho\to\pi\gamma)$. Not judging their general reasoning, we only remark that the naive quadratice $\eta-\eta'$ mixing is used for calculating decays with η and η' . As must be clear from the above discussion, this unavoidably results in severe difficulties with mass formulae, which are not discussed in the paper.

Finally, consider the new particles. If we suppose that ψ is a pure $c\bar{c}$ state then our formulae immediately give the predictions $\mathcal{D}^*=\frac{1}{2}(\Psi+\rho)\approx 1.93$, $F^*=\frac{1}{2}(\psi+\varphi)\approx 2.06$. For the pseudoscalar mesons if we use the same m_ρ^2 as above, we will find $\mathcal{D}\approx 1.64$, $F\approx 1.87$, $X_{c\bar{c}}\approx 3.01$. If we use as the input $\mathcal{D}=1.87$, we find $X_{c\bar{c}}\approx 3.1$. Trying all possible modifications of our equations we never obtain the mass of the $X_{c\bar{c}}$ as low as 2.8 GeV. We think that the most plausible explanation of these discrepancies is the possibility of mixing the $c\bar{c}$ states with $t\bar{t}$ or $b\bar{b}$ states (the admixture of u,d quarks does not help). There exist good candidates for $L=1$ $c\bar{c}$ mesons (see Wilk's talk, these Proceedings). If we draw the straight-like L-trajectory for $c\bar{c}$ through the point in the L,m^2 plane in which $s\bar{s}$, $u\bar{u}$ and $u\bar{s}$ trajectories interseot, we find that the orbitally excited states of $c\bar{c}$ must lie near 3.6 GeV. More explicitly, we have obtained that

$$\frac{\beta_{ss}-\beta_{su}}{\Delta_{su}}\simeq\frac{\beta_{su}-\beta_{uu}}{\Delta_{su}}\approx 0.67 .$$

Let us suppose that the same is true if we replace the S-quark by the c-quark. Then we obtain $\beta_{cc}\approx 3.9$ which allows us to estimate the masses of $^3P_1$ and $^3P_2$ $c\bar{c}$ mesons. However, the SS and LS splittings for present candidates are difficult to explain in usual terms and this possibly tells us that we have no simple $c\bar{c}$ states but some more complicated mixtures of $c\bar{c}$ quarks with other new quarks.

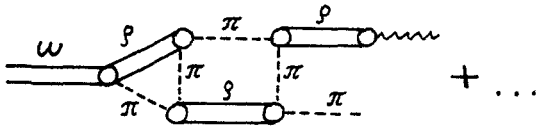
3) In conclusion we briefly discuss the problem of missing particles. A more detailed discussion of this problem can be found in Ref. /133/ . We mention here only the most notorious A_1-problem. Practically all variants of the quark model predict $J^{PC}=1^{++}$ particle with mass ~ 1.1 GeV. However, the latest very good experiments fail to confirm that the $A_1(1.1)$ bump can be interpreted as a resonance, and there are no other candidates for such a particle. A possible explanation of this phenomenon may be searched in the influence of the $(q\bar{q})(q\bar{q})$ channels. For example, in the decay the contribution of the rescattering process



is rather large (due to the large $\rho\pi\pi$ coupling and the large radius of the π-exchange interaction). In addition, there are other two-meson channels strongly coupled to A_1 and to each other. It is possible that the interaction of all these channels can spoil the simple quark model picture in which A_1 is regarded as the pure $q\bar{q}$-state. The detailed investigation of this problem would be very desirable. A preliminary discussion of some related ideas was attempted by Dashed and and Kane and by Badalyan, and Simonov /145/, see also /133/ .

A similar mechanism can spoil the quark model prediction for $\Gamma(\rho\to\pi\gamma)$ and $\Gamma(\omega\to\pi\gamma)$.

In the $\omega \to \pi\gamma$ decay the chain



may give a large contribution to the decay rate, and there is no similar contribution to the $\Gamma(\rho \to \pi\gamma)$. Such mechanisms could be relevant to $\mathcal{D}, \mathcal{D}^*$ interactions, as recently observed by Okun and Voloshin. They proposed the "hadronic molecules" made of $\mathcal{D}$ and $\mathcal{D}^*$ which are bound by the pion exchange.

The first discussion of the interaction in the exotic channels was given by Shapiro et al. /146/ who investigated the interactions in $N\bar{N}$ channels and demonstrated a possibility of existence of rather narrow $N\bar{N}$ resonances. The present state of arts in this field was summarized at the conference by Shapiro (these Proceedings). Additional information can be found in Rosner's review /133/.

The moral of this sketchy discussion is as follows. The naive two particle $(q\bar{q})$ model of massive meson resonances is certainly too naive. The exotic $(q\bar{q})(q\bar{q})$ channel cannot be neglected for large masses when many channels are open or almost open, and we face an unpleasant situation: with growing mass of the $q\bar{q}$ bound state, the $q\bar{q}$ interaction is becoming simpler (the exchange forces are dying away, the OZI-rule is becoming exact), but the influence of exotic $(q\bar{q})(q\bar{q})$ channels can spoil the usual quark model predictions. Fortunately, the existence of the new (charmed) particles provides us with the unique possibility of the pure $q\bar{q}$ high mass resonances which are not spoiled by $(q\bar{q})(q\bar{q})$ admixture.

In this brief discussion of the experimental status of the quark model we concentrated on some unsolved problems, leaving its numerous successful predictions aside. It must be stressed that there is no substitute today for the quark model in explaining diverse experimental facts in strong, weak, and electromagnetic interactions of hadrons. Despite the existence of some unsolved theoretical and experimental problems we may conclude that the quark model is in a very good shape in Tbilisi!

A preliminary version of this review was critically discussed by N.N.Bogolubov, A.A.Logunov, A.N.Tavkhelidze and they have given many suggestions about its general plan. Several topics were discussed with P.N.Bogolubov, A.De Rujula, A.D.Dolgov, A.V.Efremov, R.N.Faustov, S.B.Gerasimov, V.G.Kadyshevsky, O.A.Khrustalev, J.Kuti, R.Lednicky, V.A.Matveev, V.A.Meshcheryakov, R.Mir-Kasimov, R.M.Muradyan, V.I.Ogievetsky, G.Preparata, I.S.Shapiro, L.B.Okun, D.V.Shirkov, B.V.Struminsky, M.V.Terent'ev, I.T.Todorov, V.I.Zakharov, and many others. All these discussions and the help of the scientific secretaries D.P.Mavlo and I.L.Solovtsov are kindly acknowledged.

References

1. Proc. of the XVII Intern.Conf. on High Energy Physics, London, July, 1974, p.p.II, 101-II, 199 (see also /133/).
2. B.Feld. Models of Elementary Particles, Blaidell Pub.Company, Waltham, Massachusetts-Toronto-London, 1969.
3. N.N.Bogolubov et al. Preprints JINR, D-1968, D-2015, P-2141, Dubna, 1965. A.N.Tavkhelidze, in "High Energy Physics and Elementary Particles", IAEA, Vienna, 1965.
4. M.Y.Han, Y.Nambu. Phys.Rev., 139B, 1006 (1965).
5. O.W.Greenberg. Phys.Rev.Lett., 13, 598 (1964); A.B.Goworkov, Preprint JINR P-2756, E2-3003, Dubna, 1966.
6. M.Gaillard, B.Lee, J.Rosner. Phys.Mod. 47, 277 (1975). N.Cabibbo, Proc. of the EPS Intern. Conf. on HEP, Palermo, 1975.

7. G.Feldman, M.Perl. Phys.Rep., C 1975.
V.I.Zakharov et al. Usp.Fiz.Nauk, 117, 227 (1975).
8. M.Barnett, Phys.Rev.Lett., 36, 1163 (1976).
H.Georgi, H.Politzer. Phys.Rev.Lett., 36, 1281 (1976);
C.Albright et al. Preprint FERMILAB-Pub-76/40, 1976.
9. M.Barnett.Phys.Rev.Lett., 34, 41 (1975);
Phys.Rev., IID, 3246 (1975);
N.V.Krasnikov, V.A.Kuz'min. Pis'ma JETP, 21, 510 (1975);
N.V.Krasnikov et al., ibid. 22, 106 (1975).
10. H.Frtizsch. Fortschritte der Physik, to be published (Preprint CALT-68-524, Pasadena, 1975).
11. Y.Achiman et al. Phys.Lett., 59B, 261 (1975).
12. Gursey F. et al. Phys.Lett., 60B, 177 (1976);
F.Gursey, P.Sikivie. Phys.Rev.Lett., 36, 775 (1976);
P.Ramond. Preprint CALT-68-540, Pasadena, 1976.
13. B.A.Arbuzov, Zh.Exp.Teor.Fiz., 46, 1285 (1964);
B.A.Arbuzov, A.T.Filippov, ibid. 51, 1389 (1966).
14. Y.Ne'eman. Rev.Mod.Phys., 37, 227 (1965);
Phys.Lett., 14, 327 (1965).
15. S.Fubini, G.Veneziano. Ann.Phys., 63, 12 (1971).
16. J.Scherk, J.Schwartz. Phys.Lett., 57B, 463 (1975);
E.Cremmer, J.Scherk. Nucl.Phys., B103, 399 (1976).
17. F.Gursey. Proc. of the Intern.Symp. on Math.Probl., Kyoto, 1975;
M.Gunadin, F.Gursey. Lett. Nuovo Cim., 6, 401 (1973); Phys.Rev., D9, 3387 (1974);
J.Math.Phys., 14, 1651 (1973);
R.Casalbuoni et al. Nuovo Cim., 31A, 423 (1976); preprint CERN, TH 2150, Geneva, 1976.
18. H.Lipkin. Proc. of the Irvine Conf. on Particle Phys., Irvine, 1972.
19. J.Pati et al. Phys.Lett., 59B, 3, 265 (1975).
20. H.Lipkin. In "New Directions in Hadron Spectroscopy", Argonne, 1975.
21. A.A.Tyapkin. Preprint JINR, E2-9826, Dubna, 1976.
22. D.V.Volkov. Preprint JINR, P2-8765 (1975).
23. P.N.Bogolubov. Ann.Inst.H.Poincare, 8, 2 (1968); Phys. of Elem.Part. and Atomic Nucl., 3, 144 (1972).
24. R.Dalitz, in Elementary Particle Physics" (G.Takeda, A.Fujii, ed.) Tokyo, 1967;
in "New Directions in Hadron Spectroscopy", Argonne, 1975.
25. V.A.Matveev et al. Preprint JINR, P-2524, Dubna, 1965.
26. R. Van Royen, V.Weisskopf. Nuovo Cim., 50, 617 (1967); 51, 583 (1967).
27. B.V.Struminsky. Preprint ITP 68-48, Kiev, 1968;
C.Llewellyn-Smith. Ann.Phys. (N.Y.), 53, 521 (1969).
28. J.Kokkedee. "The Quark Model", Benjamin, N.-Y., 1969.
29. N.N.Bogolubov et al. Preprint JINR, P2-4050, Dubna, 1968;
A.N.Tavkhelidze. in "Fundamental Problems in Physics", Wiley, Lond., 1968.
30. M.Gell-Mann, Preprints CALT-68-102, 103 Pasadena, 1968.
31. V.P.Shelest, Preprints ITP, 67-47, 67-48, 67-51, Kiev, 1967;
A.P.Kobushkin, V.P.Shelest. Preprint JINR, E2-8594, Dubna, 1975.
32. E.M.Levin, L.L.Frankfurt. JETP Lett., 2, 65 (1965);
H.Lipkin, F.Scheck. Phys.Rev.Lett., 16, 71 (1966).
33. H.Lipkin. Phys.Rev. IID, 1827 (1975);
Phys.Lett., 56B, 76 (1975).
V.P.Gerdt, V.A.Meshcheryakov. Preprint JINR P2-9572, Dubna, 1976, N 1064/A5-30.
34. R.Feynman, Photon-Hadron Interactions, Benjamin, N.-Y. 1972;
B.Barish, Preprint CALT-68-535, Pasadena, 1975.
35. A.Salam. Preprint IC/76/21, Trieste, 1976.
36. V.A.Matveev et al. Lett. Nuovo Cim., 7, 719 (1973);
V.Garsevanishvili et al. Teor. Mat.Fiz., 25, 37 (1975);
S.Bredsky, G.Farrar. Phys.Rev.Lett., 31, 1153 (1973); Phys.Rev., IID, 1309 (1975).
37. Y.Nambu, in "Preludes in Theoretical Physics", North Holl., Amsterdam, 1966;
O. Greenberg, D.Zwanziger. Phys.Rev. 150, 1177 (1966);
H.Lipkin, Phys.Lett., 45B, 267 (1973).
38. A.T.Filippov. Preprint JINR, 2-4956, Dubna (1970);
V.Sh.Gogokhia, A.T.Filippov. Yadern.Fiz., 15, 1294 (1972).
39. D.Heckathorn, R.Oehme. Phys.Rev., 13D, 1003 (1976).
40. D.V.Shirkov. Preprint JINR, E2-9340, Dubna, 1975.
41. J.Kogut. "Problems and Prospects in Constituent Theories of Quarks", preprint CLNS, Ithaca, 1974;
K.Wilson, Phys.Rev., 10D, 2445 (1974);
K.Wilson, These proceedings.

42. W.Bardeen, R.Pearson, N 669/C4-20, preprint FERMILAB-PUB-76/24, THY, Batavia, 1976; (See also these Proceedings).
43. T.Appelquist et al., Preprint FERMILAB-PUB-76/16 THY, Batavia, 1976.
44. B.A.Arbuzov et al. Phys.Lett., 8, 205 (1964);
45. V.G.Kadyshevsky, A.N.Tavkhelidze, in "Problems of Theoretical Physics" (dedicated to N.N.Bogolubov), Moscow, Nauka, 1969.
I.Todorov, in "Properties of the Fundamental Interactions" (E.Majorana School), Bologna Ed. Compositori, 1973;
R.Faustov. Physics of Elementary Particles and Atomic Nucl., 3, 238 (1972);
V.Rizov, I.Todorov, ibid. 6, 669 (1975).
46. W.Zimmermann. Nuovo Cim.Suppl., 11, 43 (1954).
47. N.Nakanishi. Progr.Theor.Phys. Suppl., 43, 1 (1969).
48. A.A.Logunov, A.N.Tavkhelidze. Nuovo Cim., 29, 380 (1963).
49. K.Erkelenz. Phys.Rep., 130, 193 (1974).
50. V.Gogokhia et al., NN 657, 1123/C4-18, 31; (See also these Proceedings).
51. B.A.Arbuzov et al., Zh.Exp.Teor.Fiz., 46, 1266 (1964);
B.A.Arbuzov, A.T.Filippov. Phys.Lett., 13, 95 (1964);
V.Sh.Gogokhia et al. Teor.Mat.Fiz., 21, 37 (1974); 27, 323 (1976).
52. A.T.Filippov. Phys.Lett., 9, 78 (1964); preprint JINR P-1493, Dubna, 1963;
J.M.Charap, N.Dombey. Phys.Lett., 9, 210 (1964).
53. A.T.Filippov. Proc. of the Intern.Conf. on Math.Probl. of Quantum Fields and Quantum Stat., p.302, Nauka, Moscow, 1975; Preprint JINR D2-7161, Dubna, 1973; in "High Energy Phys. and Elem.Part.", IAEA , Vienna, 1965.
54. V.A.Matveev et al. Preprint JINR, E2-3498, 1967.
55. M.A.Markov. Journ.of Phys. USSR, 3, 452 (1940); H.Yukawa. Phys.Rev., 80, 1047 (1950); J.Rayski. Proc. Phys.Soc., 64A, 957 (1951).
56. I.Sogami. Proc.of the Alushta Symp. on Non-local Theories, preprint JINR, D2-97-88, Dubna, 1976;
J.Lukierski, Ibidem.
A.Capri, C.Chiang. Preprint MPI-PAE/Pth 39/75, Munchen, 1975.
57. G.Preparata. Preprint CERN TH 2180, Geneva, 1976.
58. H.Fritzsch, M.Gell-Mann. Proc. of 1971 Coral Gables Conf., N.-Y. (1971).
59. A.Khelashvili, A.Kvinikhidze. Invited papers, these Proceedings.
60. S.N.Sokolov. Preprints IHEP 75-93, 75-95, Serpukhov, 1975.
L.Bell, H.Ruegg. Preprint CERN, TH 2101, Geneva, 1975.
61. M.Ida, H.Yabuki. Preprints RIMS-195, TIFP--246, Kyoto, 1975.
62. J.Namyslovsky. Preprints IFT 19, 20,21, Warsaw, 1973.
A.Atanasov. Preprints JINR E2-6202, E2-7050, Dubna (1973).
S.Brodsky. Preprint SLAC-PUB-1328, Stanford, 1973.
63. S.Weinberg. Phys.Rev., 150, 1313 (1966).
64. S.Fubini, G.Furlan. Physics, 1, 229 (1965).
65. H.Leutwyller et al. Nuovo Cim., 66A, 536 (1970).
66. N.N.Bogolubov et al. Introduction to Axiomatic Quantum Field Theory, Benjamin, N.Y., 1975.
67. R.Carlitz et al. Preprint EFI 74/32, Chicago, 1974.
68. J.Kogut, L.Susskind. Phys.Rep. 8C, 75 (1973); J.Kogut, D.Soper. Phys.Rev., ID, 2901 (1970).
69. V.A.Garsevanishvili , V.A.Matveev, N 656/C4; Teor.Mat.Fiz., 24, 3 (1975);
V.A.Garsevanishvili et al. Ibid. 23, 310 (1975); Preprint JINR E2-9162, Dubna, 1975.
70. S.Brodsky. These Proceedings;
J.F.Gunion et al. Phys.Rev., 8D, 287 (1973) (see also ref. /36/).
71. A.A.Khelashvili et al. Preprint JINR D2-9540 Dubna (1976);
A.A.Khelashvili, Preprint JINR P2-8750, Dubna, 1975 (see also these Proceedings).
72. A.N.Kvinikhidze. N 658/C4 (see also these Proceedings).
73. M.V.Terent'ev. Preprints ITEP-5,6, Moscow, (1976).
74. A.N.Kvinikhidze, L.A.Slepchenko. Preprint JINR, P2-8273, Dubna, 1974.
V.A.Garsevanishvili, V.A.Matveev, N 656/C4.

B.S.Adadashvili et al. Preprints JINR E1-7304, P1-7646, Dubna, 1973; P1-8441, Dubna, 1974.
75. L.S.Dulyan et al. N 599/C4-9.
76. V.G.Kadyshevsky et al. Nucl.Phys. 6B, 125 (1968); Nuovo Cim., 55A, 233, 275 (1968); Phys.Rev.of Element.Part. and Atomic Nucl., 2, 635 (1972).
77. I.S.Shapiro. DAN SSSR 106, 647 (1956); Phys.Lett., 1, 253 (1962).
78. R.M.Mir-Kasimov. These Proceedings; I.V.Amirkhanov et al. N 606/C4-12.

79. V.A.Karmanov. Preprint ITEP-54, Moscow, (1976); Pis'ma JETP 23, 62 (1976).
80. A.A.Logunov et al. Teor.Mat.Fiz., 6, 157 (1971);
V.I.Savrin et al. Physics of Elem.Part. and Atomic Nucl., 7, 21 (1976).
81. A.A.Sokolov. J.Phys.USSR, 5, 231 (1941);
W.Heitler. Proc.Camb.Phil.Soc., 37, 291 (1941);
A.Wilson. ibid, 37, 301 (1941).
82. V.K.Cung et al. N 671/C4-30.
83. K.Ladanyi. N 703/C4-32.
M.Ciafaloni, S.Ferrara. Nucl.Phys., 88B, 365 (1975).
84. T.Appelquist, E.Peggio. Phys.Rev., 10, D1309 (1974);
C.Callan, D.Gross. Phys.Rev., IID, 2905 (1975);
A.Guth, D.Soper. Phys.Rev., 12D, 1143 (1975).
85. C.Alabise, G.Schierholz. Phys.Rev., 10D, 960 (1974)1; IID, 1905 (1975); preprint SLAC-PUB-1588 (1975).
86. A.M.Popova, Yu.V.Popov. N 608/C4-20.
87. A.V.Efremov, A.V.Radyushkin. Preprint JINR E2-9717, Dubna, 1976.
88. L.Suttorp. Nuovo Cim., 29A, 225 (1975);
K.Higashijima. Preprint UT-252, Tokyo, 1976;
A.Nishimura, K.Higashijima. Preprint UT-261, Tokyo, 1976.
89. G.Wanders. Preprints Univ. of Lausanne (1975).
90. J.Glimm, A.Jaffe. Preprint, Harward Univ., Cambridge (1975).
91. A.Henriques et al. Ann.Phys., 93, 125 (1975).
92. M.Böhm et al. Preprint DESY 73/20, Hamburg (1973).
93. R.M.Mir-Kasimov. These Proceedings;
I.V.Amirkanov et al. N 605/C4-11.
94. B.Harrington et al. Phys.Rev.Lett., 34, 168 (1975); 34, 706 (1975).

E.Eichten et al. ibid, 34, 369 (1975);
T.Cheng, P.James, ibid. 34, 917 (1975);
J.Gunion, R.Willey. Phys.Rev., 12D, 174 (1975);
J.Gunion, L.Li. Phys.Rev., 12D, 3583 (1975); 13D, 82 (1976).
J.Kang, H.Schnitzer. Ibid., 12D, 841 (1975); 12D, 2791 (1975);
K.Jhung et al. Ibid. 12D, 1999 (1975);
D.Lichtenberg, J.Wills. Phys.Rev.Lett., 35, 1055 (1975).
R.Barbieri et al. Preprint CERN TH 2036, Geneva, 1975.

95. N.B.Skachkov. N 604/C4-10; Pis'ma Zh. Expt.Teor.Fiz., 23, 713 (1976).
96. M.Guenin. N 412/C4, T4; Preprints Geneva Univ., 1976 / 06-112, 114, Geneva, 1976.
97. A.D.Dolgov. Pis'ma JETP 23, 127 (1976).
98. D.I.Blokhintsev et al. Preprint JINR P2-7719, Dubna (1974).
99. A.T.Filippov. Preprints JINR: E2-7563, Dubna, 1973; E2-7939, Dubna, 1974; D2-9788, Dubna, 1976; Phys.Lett., 51B, 379 (1974); see also ref. /1/, 153.
100. R.Rivers. Preprint, ICTP 73/47; ICTP 75/6, Imperial College, London.
101. F.Schrempp, B.Schrempp. Proc. of the EPS Intern.Conf. on HEP, Palermo (1975).
102. N.N.Bogolubov. Journ.of Phys. USSR, 9, 23 (1947).
103. N.N.Bogolubov. Physica, Suppl. to V.26, 1 (1960); Preprint JINR D-781, Dubna, 1961.
104. Y.Nambu. Phys.Rev.Lett., 4, 380 (1960); J.Goldstone. Nuovo Cim., 19, 154 (1960).
105. B.A.Arbuzov et al. DAN USSR, 139, 345 (1961).
106. Y.Nambu, G.Jona-Lasinio. Phys.Rev., 122, 345.
107. A.T.Filippov. In "Neutrino-75" (Proc. of the IUPAP Conf., Hungary, June, 1975). Budapest, 1975; Preprint JINR D2-97,98, Dubna, 1976.
108. K.Johnson et al. Phys.Rev., 136B, 1111 (1964); 163, 1699 (1967); 183, 1292 (1969); 3D, 2516, 2541 (1971); D8, 1110 (1973).
S.Adler. Phys.Rev., 5D, 3021 (1972).
109. K.Lane. Phys.Rev., 10, D2, 605 (1974); P.Mannheim. Ibid. 10D, 3311 (1974); P.Narayanaswamy. Ibid. 12D, 3296 (1975).
110. R.Fukuda, T.Kugo. Preprint KUNS 350, HE(TH), 76/05, Kyoto, 1976.
111. R.Haag, T.Maris. Phys.Rev., 132, 2325 (1963).
112. A.Z.Dubničkova, G.V.Efimov. N 610/C4-15.
113. N.N.Bogolubov (Jr) et al. N 611/C4-16.
114. H.Kleinert. NN 130/C4; Preprint FUB HEP Nov. 75/18, Berlin, (1975).
115. D.Ebert, V.N.Pervushin. Preprint JINR, E2-10020, (1976);
116. S.Weinberg. Phys.Rev., 11D, 3583 (1975); 13D, 974 (1976).
117. H.Pagels. Phys.Rep., 16C, 219 (1975).
118. A.Chodos et al. Phys.Rev., 9, D 3471 (1974); T.De Grand et al. Ibid., 12, D 2060 (1975). K.Johnson . Acta Phys.Polonica, B6, 865 (1975).
119. P.Gnadig et al. In "Neutrino-75" (Proc. of the IUPAP Conf., Hungary, June, 1975). Budapest, 1975;
P.Gnadig et al. N 983, 994/C4-39, 40.
J.Kuti. These Proceedings.
120. T.De Grand, R.Jaffe. Preprint MIT, Cambridge 1976;
R.Jaffe, N 1126/C4- 38;
R.Jaffe, K.Johnson. Phys.Lett., B60, 201 (1976).

121. P.Vinciareli. Lett. Nuovo Cim., 4, 905 (1972);Preprint CERN TH 1934, Geneva (1974). W.Bardeen et al. Phys.Rev., 11D, 1094 (1975); R.Giles. Preprint SLAC-PUB-1682, Stanford (1975).
122. A.De Rujula et al. Phys.Rev., 12D, 147 (1975).
123. F.Low. Phys.Rev., 12D, 163 (1975).
124. T.Eguchi. Phys.Lett., 59, B457 (1975); K.Johnson , C.Thorn. Phys.Rev., 13D, 1934 (1976).
125. D.Lichtenberg. Phys.Rev., 178, 2197 (1968); R.Capps. Phys.Rev.Lett., 33, 1637 (1974).
126. C.De Tar. N 668/C4.
127. G.Fairley, E.Squires. Nucl.Phys., B93, 56 (1975).
128. J.Collins, M.Perry. Phys.Rev.Lett., 34, 1353 (1975); B.Freedman, D.McLerran. N 750/C4.
129. T.D.Babutsidze, I.Z.Machabeli. N 607/C4.
130. K.Huang, R.Stump. N 947/C4-49.
131. I.Yu.Kobzarev et al. N 661/C4 (see also these Proceedings).
132. S.Chang et al. Phys.Rev., 11D, 3572 (1975); A.Chodos, B.Thorn. Ibid.D12, 2733 (1975).
133. "New Directions in Hadron Spectroscopy", Argonne, 1975.
134. H.Fritzsch, P.Minkovsky. Nuovo Cim., 30A, 393 (1975).
135. L.Infeld, T.Hull. Rev.Mod.Phys., 23, 21 (1951).
136. J.Pasupathy. N 957/N3.
137. C.Lovelace. Phys.Lett., 28B, 265 (1968); J.Shapiro. Phys.Rev., 179, 1345 (1969).
138. V.N.Gribov, I.Ya.Pomeranchuk. Phys.Rev.Lett., 8, 343 (1962); M.Gell-Mann. Ibid. 8, 263 (1962).
139. Particle Data Group. Rev.Mod.Phys., 48, N2, Part II, April (1976).
140. S.Caser, M.Testa. Preprints CALT-68-526, CALT-68-536 , Pasadena, 1976.
141. N.H.Fuchs. N 1094/C4.
142. T.Inami et al. Phys.Lett., 61, 60 (1976).
143. B.Edwards, A.Kamal. Phys.Rev.Lett., 36, 241 (1976); D.Boal et al. Ibid. 36, 714 (1976); A.Kazi et al. Preprint DESY 76/18, Hamburg (1976).
144. Etim-Etim, M.Greco. Preprint CERN TH.2174, Geneva, 1976.
145. R.Dashen, G.Kane. Phys.Rev., 11D, 136 (1975); A.M.Badalyan, Yu.A.Simonov. Preprint ITEP-65, Moscow, 1976.
146. L.N.Bogdanova et al. Ann.Phys. (N.Y.), 84, 261 (1974).
147. P.Becher, M.Böhm. Phys.Lett., 60B, 189 (1976).